Al-Mustansiriyah Journal of Science

ISSN 1814 - 635X

Vol. 21, No. 5, 2010

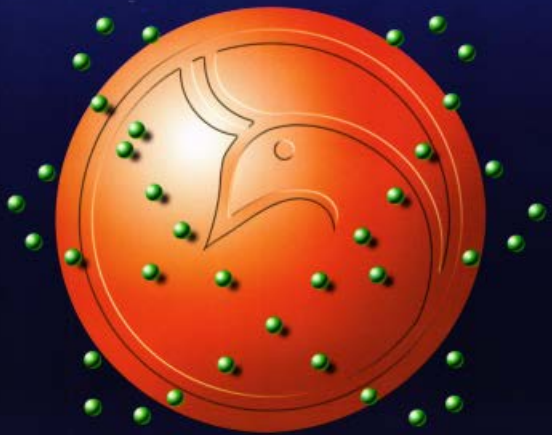

Issued by College of Science - Mustansiriyah University

Vol. 21
No. 5
2010

Al- Mustansiriyah Journal of Science

Issued by College of Science- Al- Mustansiriya University

Special Edition
Researchs of The 6th Conference College Of Science Al-Mustansiriyah University
From 9-10 February

Mobile: 07706289924
e-mail: must_sci@yahoo.com

INSTRUCTION FOR AUTHORS

1. The journal accepts manuscripts in Arabic and English languages. Which had not been published before.
2. Author (s) has to introduce an application requesting publication of his manuscript in the journal. Four copies (one original) of the manuscript should be submitted. Should be printed by on the computer by lasser printer and re produced on A4 white paper in three coppice with flopy disc should be also submitted.
3. The title of the manuscript together with the name and address of the author (s) should typed on a separate sheet in both Arabic and English. Only manuscript,s title to be typed again with the manuscript.
4. For manuscripts written in English, full name (S) of author (s) and only first letters of the words (except prepositions and auxiliaries) forming title of the manuscript should be written in capital letters. Author (s) address (es) to be written in small letters.
5. Both Arabic and English abstracts are required for each manuscript. They should be typed on two separate sheets (not more then 250 words each).
6. Figures and illustrations should be drawn using black China ink on tracing papers. Two photocopies (Plus original) of each diagram should be submitted. Captions to figures should be written on separate papers. The same information should not be repeated in tables unless it is necessary and required in the discussion.
7. References should be denoted by a number between two bracket on the same level of the line and directly at the end of the sentence. A list of references should be given on a separate sheet of paper, following the intemational style for names and abbreviations of journals.
8. Whenever possible, research papers should follow this pattem: INTRODUCTION, EXPERIMENTAL (MATERIALS AND METHODS), RESULTS, DISCUSSION and REFERENCES. All written in capital

letters at the middle of the page. Without numbers or underneath lines.

9. The following pattern should be followed upon writing the references on the reference sheet: Sumame (s), intials of author (s), title of the paper, name or abbreviation of the journal, volume, number, pages and (Year). For books give the author(s) name(s), the title, edition, pages, publisher, place of publication and (Year).

10. A publication fees in the amount of ID. 20 thousend is charged upon a Reciepet of the paper and 20 thousend upon the acceptance for publication for their ID. 40 thousend should be paid for the editorial board.

CONTENTS

Oxygen Pressure Effect on Optical Properties and FTIR Results of MgO Thin Films Prepared Using RPLD Technique

Evan T. Salem[1], Mukkaram. A Fakhry[2] and Frhan A. Mohammed[3]
[1]University of technology, applied science department
[2]University of Technology, Laser Engineering Department
[3]Ministry Of Science Dnd Technology

الخلاصة

في هذا البحث تم دراسة تاثير ضغط غاز الاوكسجين المستخدم كوسط ترسيب على الخصائص البصريه ونتائج تحويلات فورير للمنطقة تحت الحمراء لاغشية اوكسيد المغنيسيوم الشفافة الموصلة باستخدام تقنية الترسيب بالليزر النبضي الفعالة باستخدام ليزر الندميوم ياك والذي يعمل بامد نبضة (7nsec) على قاعدة من الزجاج عند ضغوط مختلفة لاوكسجين تمتد بين (150-350mbar) وعند درجة حرارة قاعدة (423K). اظهرت نتائج الخصائص البصرية لاوكسيد المغنيسيوم ان فجوة الطاقة عند افضل الشروط(200mbar) هي (5.01eV). كما ان نسبة النفاذية لاوكسيد المغنيسيوم كانت عالية وتصل الى (85%) ووجدت بانها تقل مع نقصان ضغط الاوكسجين المحيط .

ABSTRACT

In the present work, oxygen pressure effect on optical and FTIR spectrum of MgO dielectric oxide thin film has been carried out using Reactive Pulsed Laser as a Deposition technique (RPLD),werer (7nsec) Nd-YAG laser has been use to ablated pure Mg target and deposited on glass substrates. This has been done at different oxygen back ground pressure ranged from (150-300) mbar and constant substrate temperature of (423K).The result shows that the bond formation between Mg and oxygen atoms is directly depended on the back ground oxygen pressure. The optical properties of MgO films show that high transparency of about (80-85) % can be achieved with MgO film which it self decreases sharply with the decreasing of oxygen pressure. While the optical ban gap is 5.01eV at optimum oxygen pressure of (200) mbar.

INTRODUCTION

Oxide ceramics are probably among the oldest man made materials because of their excellent properties including abundance and easy availability of ingredients, mechanical strength and excellent durability against severe chemical and thermal environment. Thin films prepared from these oxide materials have been found to have wide applications in microelectronic device such as non-volatile Ferro electronic memories piezoelectric micro-actuators and sensors, superconducting quantum interference devices (SQUID) and microwave devices (1). One of these oxides is Magnesium oxide (MgO). It is a highly ionic crystalline solid which crystallized into a rock salt structure, it has ffc Mg^{+} and O^{-} sub lattice and low energy neutral (100) cleavage planes, viewed as an arrangement of hard sphere bound together by electrostatic forces. Magnesium oxide (MgO) has a very large band gab about 7.8ev and transparent in a wide spectral range from 300nm to 6000nm(2), MgO has refractive index 1.73. This found by the Stephens and Malitson from relation ship between refractive index and wave length (3).The optical absorption spectrum of the MgO films for the as- deposited films were recorded in the wave length range (200- 1500) nm, by many worker (4, 5). The absorption co-

efficient of the films were found to be of the order of $10^4 cm^{-1}$. The percentage of transmission(T%) value in the visible region is found to increase with increase in substrate temperature. Maximum transmission behavior is observed for the MgO films prepared at high temperature and comparatively lower transmission values are recorded for the films prepared at low temperature. The increase in T% is attributed to well adherent and crystalline nature of the film throughout the coated Area, which is obtained due to uniform oxidation and in provement in lattice arrangements (4). In order to confirm the nature of optical transition with this results, the optical data were analyzed using the classical equation

$$\alpha - \alpha_o \frac{(h\nu - Eg)^r}{h\nu} \qquad (1)$$

Where 'Eg' is the separation between the bottom of the conduction band and the top of valence band, '$h\upsilon$' the photon energy and 'r' is constant.

The band gap energy(Eg) of the MgO films increases at high temperature, while the films processed at low temperature decreased band gap energy of MgO may be due to varied extent of non- stoichiometry of the deposited layers. But, interestingly these observed band gap energies of MgO films are invariably lower than the band gap value of bulk MgO (7.8 ev) which may be due to the various lattice associated atomic interaction phenomena come into play from its ionic crystalline nature(6) beside that one of most important properties is the FTIR spectroscopic results which give an information about phase composition and the way in which Oxygen is bound to metal ions (4). The FTIR spectrum of MgO film deposited at high temperature, which indicated the complete thermal conversion of the precursor into oxide the sped rum compriser five transmission band at $407cm^{-1}(\upsilon_1)$, 533 $cm^{-1}(\upsilon_2)$, 966 $cm^{-1}(\upsilon_3)$,1228cm^{-1} (υ_4) and 3634 cm^{-1} (υ_5). The very small peak observed at $3634cm^{-1}$ can be assigred to hydrogen- bonded hydroxyl groups and $Mg(OH)_2$ (7) the broad peak at 1228 cm^{-1} and could be assigned to the deformation band in water and to the C-O stretching absorption in the bicarbonate and carbonate ions(8). The MgO absorption peak are expected in the (400- 600) cm^{-1} region the sharp peak seen at 533 and $482cm^{-1}$ are associated with the longitudinal optical(Lo) photon modes of MgO lattice.

The wave number of MgO desorption in pure ionic magnesium oxide is ~$425cm^{-1}$(9). MgO film prepared at lower temperature, exhibits additional intense peak in the FTIR spectrum and these peak could be due to absorption of more water on exposing the films to the atmosphere (4).

MATERIAL AND METHODS

Film deposition was typically performed in an ambient background gas (O_2) with a pressure up to 300 mbar. This background gas was let into the vacuum chamber through a needle valve. The thin film was achieved immediately after the laser beam hits the target resulting in the evaporation of

the target material, which itself mounted on rotating holder with 45° orientation from the substrate in order to ensure that the plasma plume is right-angled with respect to the substrate. The rotation of the target was employed to avoid the ablation of the same spot on the target the following figure (1) shows a schematic diagram of the PLD system used process. The distance between target and substrate is about 3 cm and it was found to be the optimum distance.

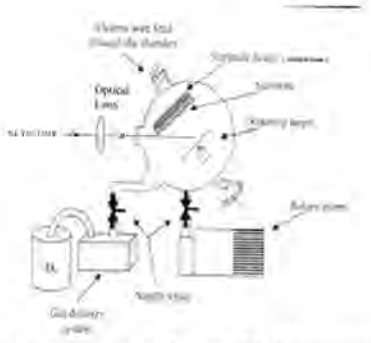

Figure -1: schematic diagram of the PLD system used(14)

(I) Optical microscopic measurement

The Film Topography of the MgO thin films surface prepared under various preparation conditions was investigated with two Optical microscope of 600X and 640X magnification power type OLUMPUS BH-2. A digital Camera was mounted on the microscope and connected to the computer in order to store the surface image of the prepared films.

(II) Optical properties measurements

1-Optical transition measurement: a double-beam UIR-210A spectrophotometer from Shimadzu was used in order to record the optical transmission spectra of the deposited films at different deposition conditions within the wavelength range (200-1100) nm. All films were deposited on glass substrates. The optical band gab was estimated graphically by applying the Tauce model, using equation 1.

2- Surface uniformity measurement: a two dimension square matrix are used to determind the surface uniformity of the sample, were 632.8nm wavelength He-Ne laser are transmitted throw each pixel in these matrex, and the transmited power are collimated using a power meter. The optend power as a function of the position on the film surface are plotted.

(III) FTIR measurment

Fourier Transform-Infrared Spectroscopy (FTIR) probes the molecular vibrations of molecules. Light of different energies (or frequency, represented by wavenumbers in the spectrum above) is directed through a sample. When a particular energy (or frequency) of light matches a vibrational frequency of the molecule, the molecule absorbs the light and vibrates. Peaks in an infrared spectrum are upsidedown compared to other forms of spectroscopy to convey that the peak is a decreased intensity, or absorbance of light. The

(SHIMADZU – 8400S) Scan of the FTIR measurments are performed over range between (400 – 4000) cm^{-1} for prepared sample .

RESULTS AND DISCUSSION

Figure (2), gives the optical micrographs of the films produced at room temperature in vacuum and different oxygen pressure, and at room temperature, to Mg target. At vacuum condition, the color of films tends to be dark (nearly black) which reflect the metallic nature of Mg, which typically has dark grey color as well as the high reflectivity of the obtained film.

It can clearly be noticed that the film color is the same as the physical color of the target metal, so, they look in dark grey (2-a) for Mg metal. At pressures as shown in figure (2-b) we can recognize the change in the deposited film color change from black to brown, which may be attributed to the fact that oxygen atoms have been fired rather than reacting with Mg atoms to form MgO. Droplets and particulates of submicron sizes are observed over the film surface at low O_2 pressure and they are sprayed randomly as dark regions on the film surface which explain its inhomogeneity.

At oxygen pressure of about (100 mbar) figure(2-c) where oxides particulates begin to form as the metal atoms that are still available in the film structure reflect. The incident light, so they appear as black dots in the microscope picture, while the oxides appear as white particulates for MgO molecules. This result is inconsistent with XRD result which will be given below. The obtained films at oxygen pressure of (200 mbar) for Mg target figure (2-e) display very smooth, uniform grain size and void free, i.e., no droplets were observed.

Also, they were free from cracks and corrugation. When the O_2 pressure is increased as shown in figure(2-f), the growth rate decreased due to the associated decrease in the atom mean free path caused by reaction between the source atoms ejected from the target and O_2 molecules in the environment of the substrate.

The best surface morphology of produced films which represents the optimum case was obtained at (200mbar) oxygen pressure for MgO film that appears to be white in color, which is consistent with the standard physical properties of the MgO films.

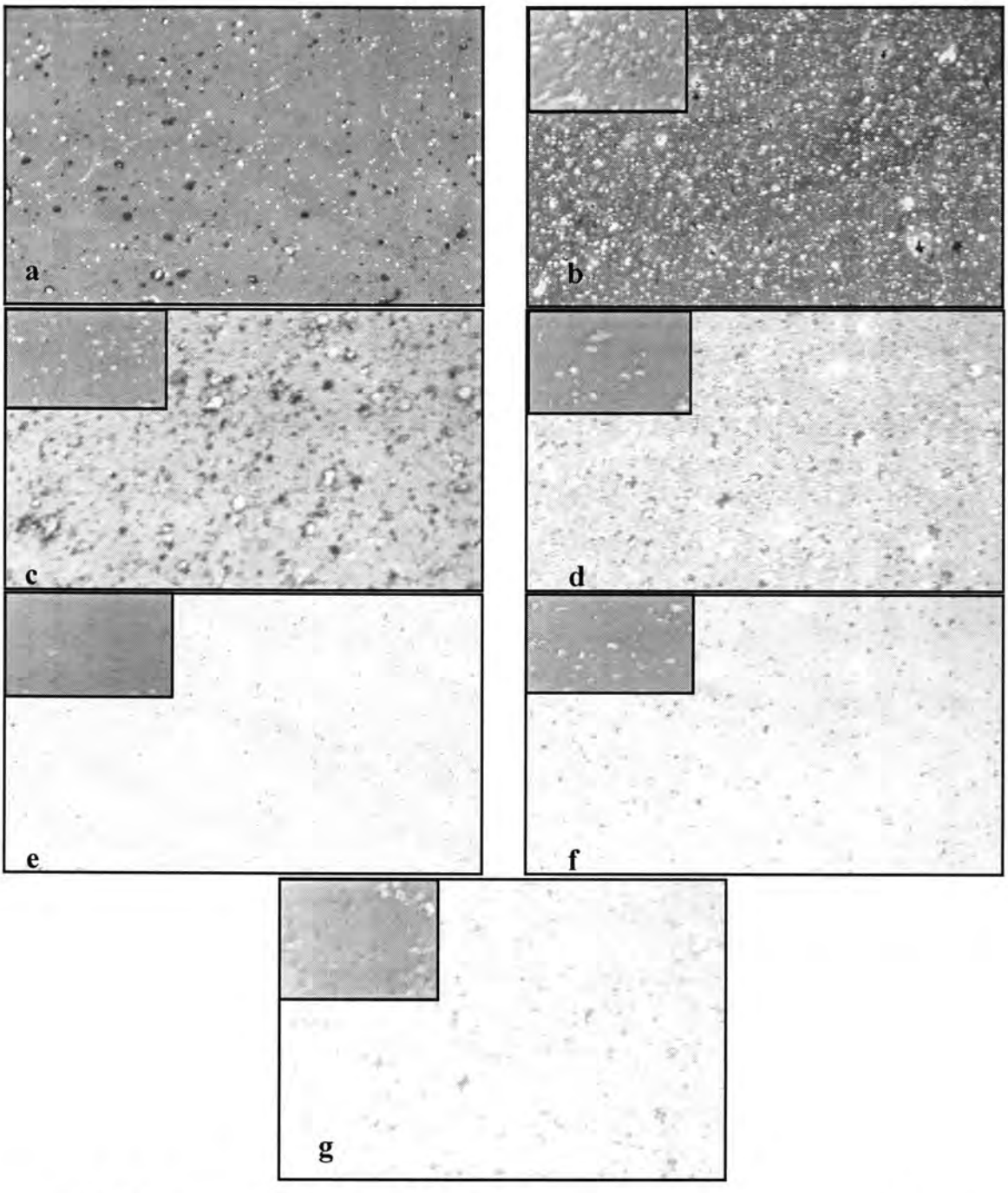

Figure -2: Surface morphology of MgO samples prepared at room tempreture and different oxgyen pressure (a- 0.001mbar b-50mbar c-100mbar d-150mbar e-200mbar f-250mbar g-300mbar) and laser fluence of (89.17)J /cm^2 ,x=640 for larg picture and 1050 for small one.

The influence of growth condition on optical properties of the MgO films is studied extensively, using the spectrophotometer, transmittance of deposited films on glass substrates was measured and plotted in figures (3) and for Mg sample. Transmittance spectra were recorded in the ultraviolet and visible, and NIR ranges for the films growth at different O_2 pressures and different substrate temperatures. In general, it has been found that the

transmittance of the films was improved when the oxygen pressure was increased. From this result at figure (3-a), films prepared in vacuum represented purely metal films that have high reflectivity in the visible and near-infrared regions. This justifies the low transmittance in vacuum deposition. The film deposited in vacuum were black in color and show low transmittance ,the coloration of the film is due to excessive Mg atom in the film structure .the low value of transmittance attributed to these excessive (Mg)ions existing at interstitial sites that probably absorb light. Figure (3-b) shows optical transmittance (200-1200)nm as a function of the wave length for MgO film prepared at different oxygen pressure ,high transmittance (>90%)was exhibited by films prepared at (200-300)mbar of oxygen pressure, however the reduction in the transmittance at the NIR wavelengths is related to the reflection of their photons due to the interaction with the plasma in the conduction band. The effect of substrate temperature on the optical properties of the film can be observed in figure (3-c). The results show an increase in the transmittance with substarte temperature (Tsub) at a given wavelength, which relates to the reduction in the film thickness and increasing the transmittance according to the Lambert's law. Low transmission at low substrate temperature is related to the increase in film thickness at these temperatures as shown in the figure (3) below.

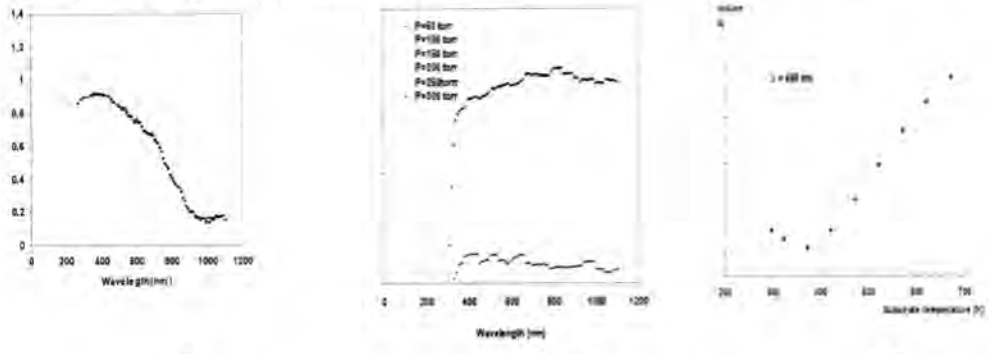

a b c

Figure -3: Optical Transmittance as a function of wavelength for thin films prepared from Mg target (a) vacuum (b) different pressure, and (c) different substrate temperatures

We have also calculated the optical band gap of the film depending on value of the transmittance for various wavelengths. The plots of $(\alpha h\upsilon)^2$ against $h\upsilon$ for MgO film prepared at optimum condition of (200mbar) oxygen pressure and (423k) substrate temperature are shown in figure (4) the nature of the plots suggests direct inter-band transition .The extrapolation of the straight-line portion to zero absorption co-efficient (α=0)leads to the estimation of band gap energy ,this band gap found to be about (5.01)eV. Generally ,it can be state that this reduced band gap energy of MgO may be due to varied extent of non-stoichiometry of the deposited layer. But, interesting these observed band gap energy of MgO film are invariably lower

than the band gap value of MgO (7.8 eV) which related to the various lattice associated atomic interaction phenomena came from its ionic crystalline nature. This result is conditional with many other workers (10,11,12).

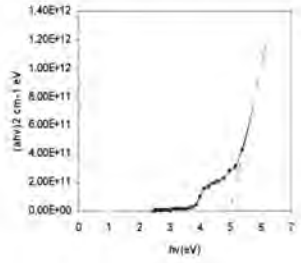

Figure -4: Energy band gap of the MgO at pressure (200 mbar) and T_{sub} (423k).

The optical transmittance as a function of deposition position upon the substrate surface is illustrated in figure (5). We can recognize that the transmittance of the incident (632.8mm) wave length decreases to its minimum value whenever we approach the center, where the lowest transmittance can be achieved. This relates to the film thickness, which is higher at the center and this reduces as we depart for in the radial direction.

This coincides with the theoretical concept that imposes the deposition or evaporating an atom from the target with a solid angle. This result also ensures the difference in the transmitted power that can be neglected for a limited area of about 1 cm^2, which found to have a uniform transmittance that attributed to the well adherent and crystalline nature of the film through out the coated area, which is obtained lattice arrangement, resulting in the better optical properties.

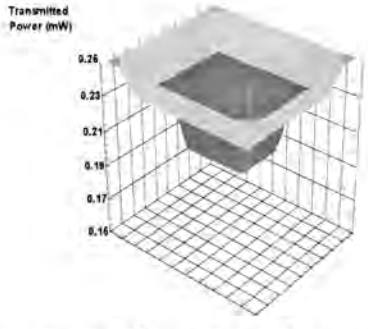

Figure -5: Transmitted power as a function of position at optimum condition oxygen pressure (200mbar) and substrate temperature (423k) for MgO samples.

Fourier transformation-Infrared spectroscopic results give information about phase composition and the way in which oxygen is bound to metal ions. The following figures show the FTIR spectra of both Mg film at (vacuum conditions)and MgO films deposited at different oxygen pressure .

At vacuum condition, figure (6) shows the absorption peak around (254-1974.29)cm^{-1}spectra which is related to the Mg metal atoms. These insure the formation of pure metal thin film at (10^{-3})mbar vacuum condition. At different oxygen pressure (50-300) mbar as a background gas, we can recognize the change in the deposited film composition.

Figure (7-a) gives the FTIR result for film prepared at oxygen pressure of (50) mbar, we can recognize the absorption peak at (1620.9,1041.49,786.9,725.18) cm^{-1} which related to the Mg metal atoms , beside (694.33,648.04) cm^{-1} absorption spectra which related to the formation of MgO molecule. An increasing the formation ability of the MgO molecule could be recognize obviously by increasing the oxygen pressure to(100)mbar, figure (7-b), where 94.33,609.46,408.88) cm^{-1} absorption peak could be found that belong to the formation of the MgO molecule beside that ,the presences of the (987.49,918.05,817.7) cm^{-1} peak which related to Mg atom that still unoxide sized.

The peaks at (1542, 1465.8, 1049.2, and 871.76,) cm^{-1} at low oxygen pressure in the last two cases (50-100)mbar is related to c-o stringing mode, which may attributed to the fact that Mg atoms are fired rather than react with O_2 atoms. At higher oxygen pressure about (150)mbar figure(7-c), we can recognize that the peak related to Mg atoms is eliminated to one peak at (918.05)cm^{-1} while higher no. of MgO molecules are formed, this could be obtained at (648.04, 466.03, 408.88)cm^{-1}.

At oxygen pressure of (200)mbar, figure (7-d), absorption spectra related to Mg atom is Cleary disappeared while that found at (655.75, 570.89,455.17, 408.88)cm^{-1} is related to the for mat ion of MgO molecules. For the case of the MgO formation ,the mean kinetic energy of the Mg atoms decreases through collision with oxygen ,formation of (O^{+2}) ions (through energetic charge collision of Mg with O_2 molecules) so chemical bonding like(Mg-O)produced, which could be recognized by the FTIR obtained result, show in the given figure, by increasing the oxygen pressure up to (250and 300)mbar figure (7-e,f) the peak at (655.75, 655.75, 632.61, 570.89, 470.60, 455.17, 408.88) cm^{-1} are related to the formation of MgO molecule.

In all above results we can recognize peaks at (599.03, 617.18, 879.48, 840.91, 1396.37, 1342.36, 1072.19, 1612.38, 1550.66,and 1296.08)cm^{-1}which are related to glass substrate .

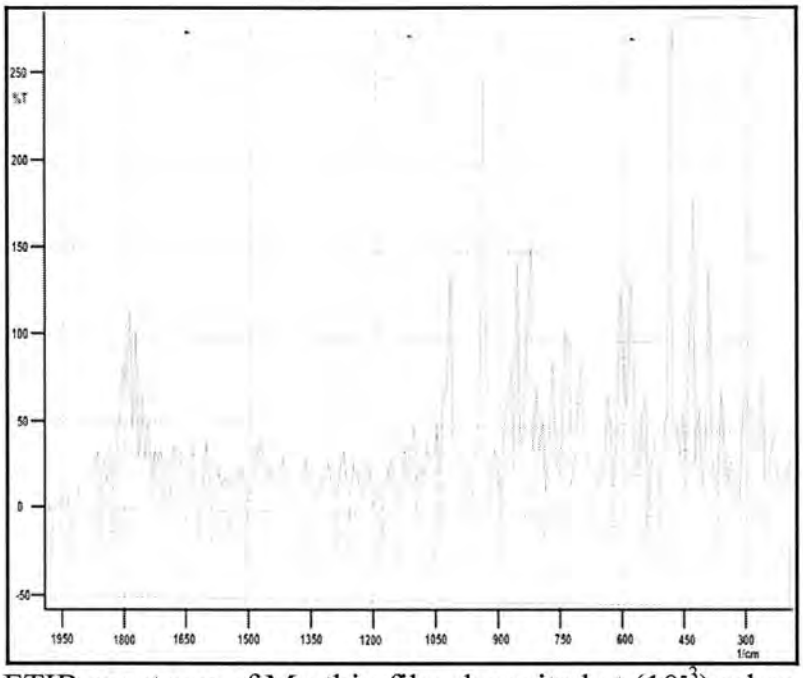

Figure -6: FTIR spectrum of Mg thin film deposited at (10^{-3}) mbar

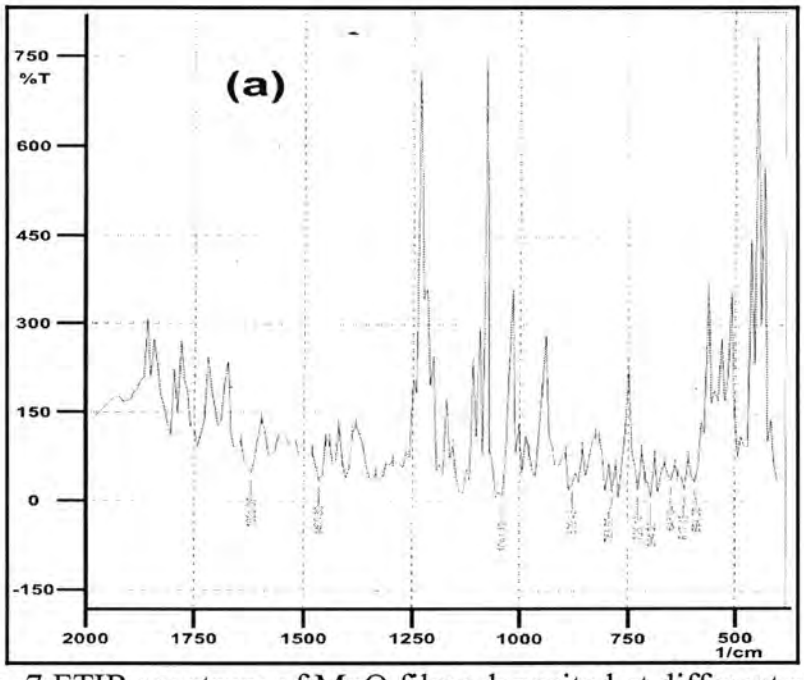

Figure -7:FTIR spectrum of MgO films deposited at different oxygen pressures and substrate temperature (423k)constant .(a)p=50 mbar ,(b) p=100mbar ,(c) p=150mbar,(d)p=200mbar ,(e) p=250mbar,(f)p=300mbar.

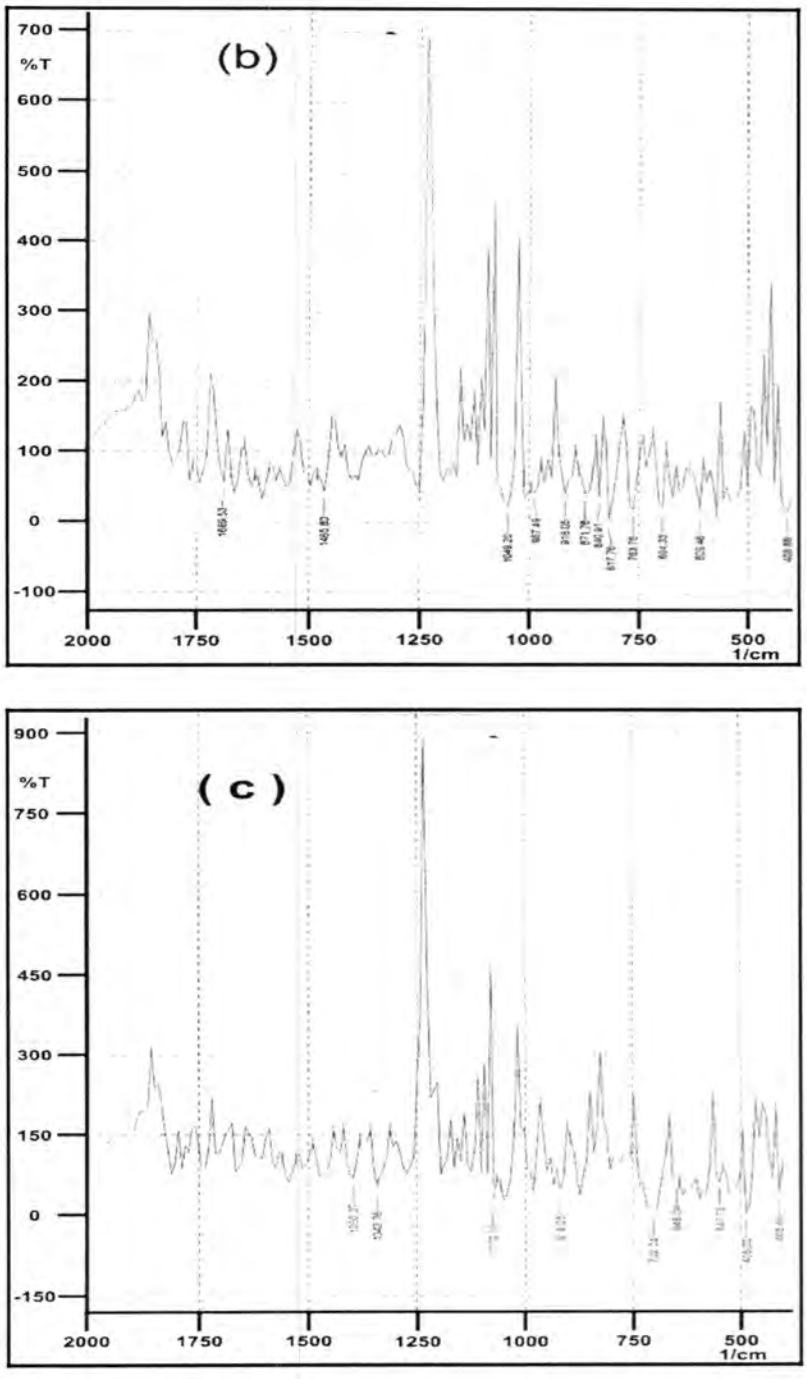

Figure -7 : continued

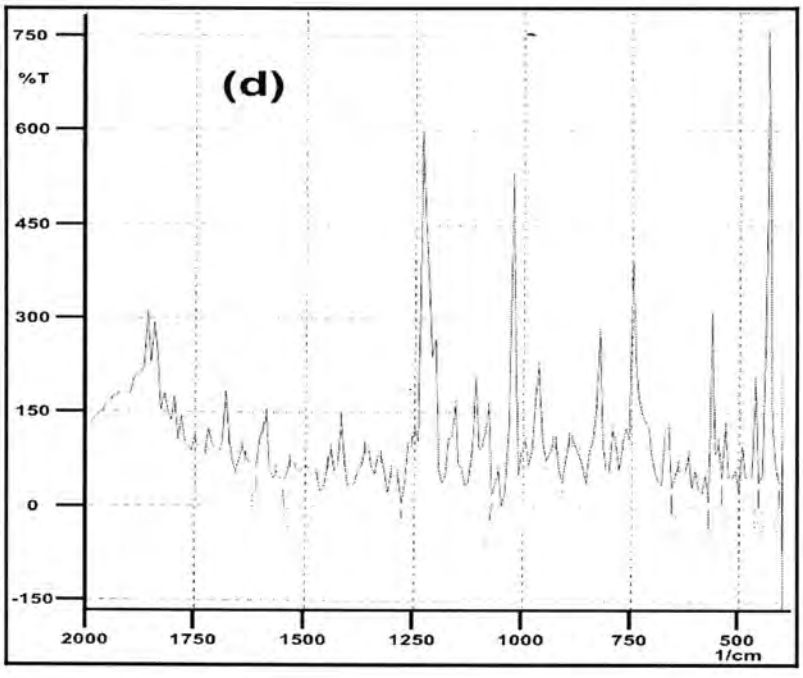

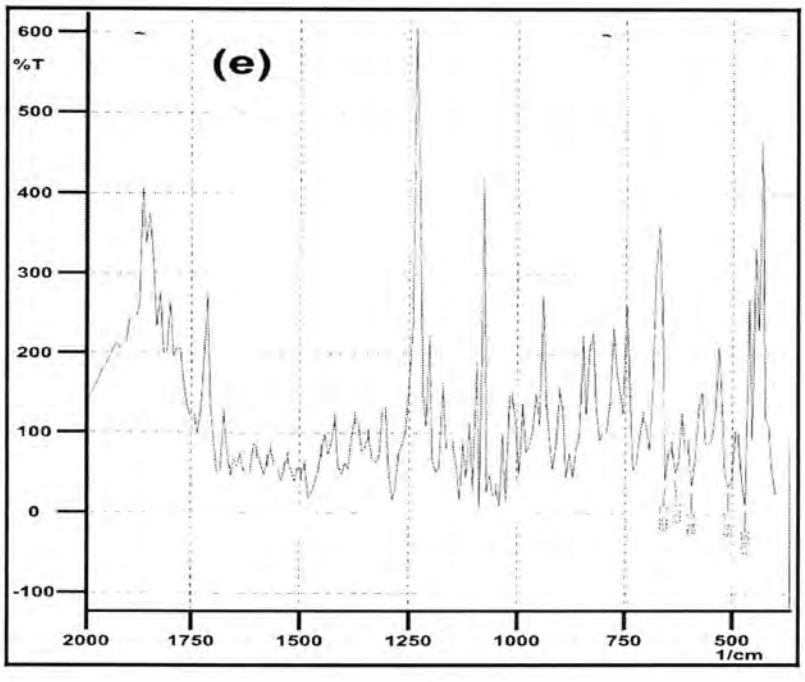

Figure -7 : continued

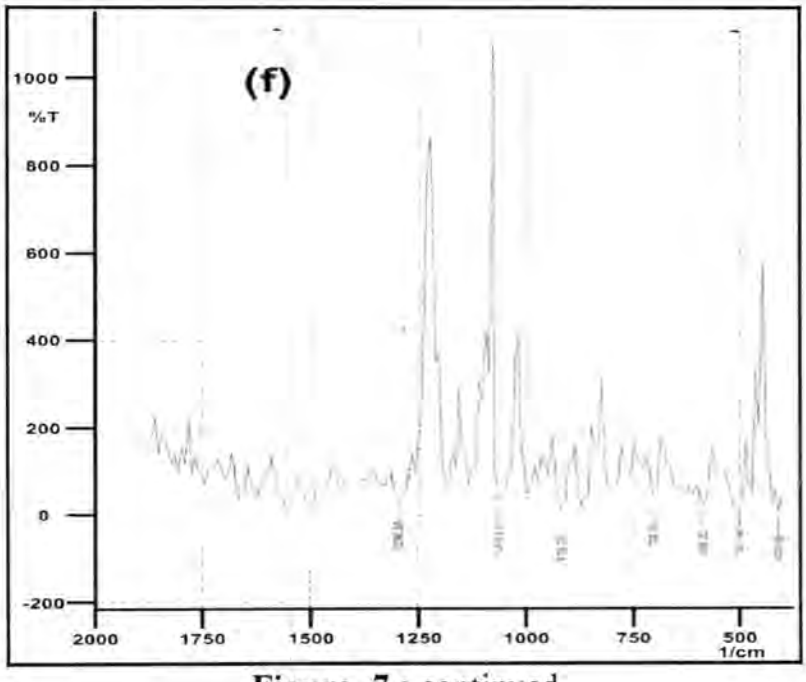

Figure -7 : continued

We can summarize from this research, that this work gives new trends towards the formation of high purity oxides from their high purity metals by laser ablation process. Several deposition conditions control the properties of the deposited oxide film, one of these are oxygen pressure where optimum oxygen pressure found to be about (200 mbar) for MgO thin film at substrate temperature of (473K), Surface morphology ensures the appearance of the metallic structure when the film is prepared at vacuum condition, while the white and brown homogenous film at optimum pressure insure the formation of the oxides. The optical properties results for prepared films show that it has a band gap of (5.1)eV at the optimum oxygen pressure. FTIR measurements show that the oxide formation probability directly depened on surrounding oxygen pressure.

REFERNCES

1. F. Hebard, "Oxygen – rich polycrystalline magnesium oxide – A high quality thin–film dielectric," Appl.Phys. Lett. **48** (8),24 February (1986).
2. T. J. Zhu, L. Lu, X.B. Zhao, "Orientation of MgO Thin films grown by pulsed laser deposition" Materials Science and Engineering B 129: 96-99, (2006).
3. Y.D. Kim, J. stultz, D. w. Goodman "Characterization of MgO (100) thin film growth on Mo (100)" Surface Science 509:228-243, (2002).
4. S. BABA and A. KINBARA "Internal stress and adhesion of R.F Sputtered MgO film on substrate" Thin Solid Film 164 :169 – 174 (1988).

5. S.SLEE Yong lee, "Use of a 3c–Sic Buffer layer and vicinal substrates for the Hetero Epitaxy growth of MgO films on Si (001) chem. vap. Deposition (6), 8 (2002).
6. S. Witanachchi, S. Patel. H.S Kwoke, D. T. Shaw,"Crystal structure of MgO thin films grown on Si by PLD, " Apply, Phys Lett. **54**. 578, (1989).
7. M. O. Aboelfotoh, "Crystal structure of evaporated MgO films on Amorphous and polycrystalline substrates" J. Vac. Sci. Techno1., 10, (5) Sept/ Oct, (1962).
8. G. F. Dionne and Janes F. "Effect of high – intensity electron bombardment on the secondary – emission characteristics of a MgO/ Au – carmet film). Journal of applied, vol. 48, No. 7, July (1977).
9. M.O.Abo elfotoh, "Infrared and high energy electron on diffraction analyses of electron-beam-evaporation MgO films" J.voc.sci. Technol. 10, 621 (1968)
10. G.S. Nadkarni and J.G.simmons," Crystal structure of MgO films on Pb substrate". Apply. phys. 41,545(1970).
11. P.Vuorist, T. Mantyla, in proceeding of the international workshop on fossil fuel fired MHD retrofit of existing power stations (1973).
12. M. O. Abo elfotoh, "Epltaxol growth of MgO on (001) Surface of silver single – crystal films substrate," Thin Solid Films, 33: 373- 379 (1976).
13. M.O. Aboelfotoh, K.C. Park, and W.A. Parkin, "Adhesion and structure of RF sputtered magnesium oxide coating on various metal substrate," J. Appl. Phys 48, 2910, (1977).
14. E.T. Salm, PhD. thesis, University of Technology ,Baghdad ,Iraq,(2006).

Bending Strength of Fibers - Hydroquinone Resin Composites

Faiza M. Salim[1], Bahjat B. Kadhim[2], and Ali Z. Manshad[2]
[1] Department of Physics Opened Educational College, Ministry of Education .
[2] Department of Physics, College of Science, University of AL-Mustansiriya.

الخلاصة

تم دراسة متانة الانحناء للهيدروكيونون المسلح بالالياف الزجاجية نوع E- glass والالياف الكاربونية بدلالة الخصائص الميكانيكية لمتغيرات الكسر الحجمي للاضافات .إن النماذج التي خضعت للاختبار كانت مادة الهيدروكيونون النقية كمادة اساس , متراكبات الهيدروكيونون المسلحة بالالياف الزجاجية والكاربونية بنسب 20% , 40% , 60% و 70% الحجمية . تم استخدام تقنية الكبس الحار لتحضير المتراكبات باستخدام القوالب المارقة وتحت الظروف القياسية .تم استخدام ماكنة(3- points bending strength mode Instron-) لحساب نقطة الخضوع , معامل يونك, ومتانة الأنحناء وحسب المواصفات القياسية ASTM D 790 .اظهرت نتائج قيم متانة الانحناء زيادة تعاقبية مع الكسر الحجمي للالياف المضافة. كما تبين ان متانةالانحناء تعتمد خطيا مع الكسر الحجمي للالياف , تلك العلاقة الخطية ذات تاثير قوي مع شرط التسليح وتساهم باستجابةالمتراكبات لشروط اختبار الانحناء , مثل هكذا استجابة قد تظهر كتشوه لدن مقترن مع التهدم الملاحظ. أن الملاحظات العملية لفشل النماذج كانت جيدة ومتفقة مع ميكانيكية الكسر والتي تتعلق بآلية الاقتلاع. كانت قيم الصلادة والكثافات وبالأقتران مع الصور المجهرية دليلا" على النتائج.

ABSTRACT

Bending strength for phenolic resin type (hydroquinone resin) reinforced E-glass and carbon fiber have been studied, in terms of mechanical properties, which are subject to changes in fiber volume fraction. The specimens candidates for this study were pure matrix hydroquinone, carbon fibers hydroquinone composites, and E-glass fibers hydroquinone composites with (20, 40, 60, and 70) Vol. % . Hot press technique was used to prepare the composites as well as hydroquinone specimens using flash mold at standard conditions. The bending testing machine type Instron was used in 3- points bending strength mode to calculate the yield point, Young modulus, and flexural strength according to standard ASTM D 790.

Bending strength results show that the strength values were increased progressively by succession of volume fraction of fibers in general. For E- glass mat composites, flexural strength results showed a linear dependence with the fibers volume fraction. These linear relationships are strongly influenced with the reinforced condition and they are attributed to the response of the composites to the bending test conditions. Such responses were appeared as plastic deformation associated with the damage observed. The experimental observation of the failure specimens are in good agreement with fracture mechanism, which concerned with pull out mechanism. Hardness and densities values coupled with optical microscopy were evidenced to the results.

Key word: Bending strength, Flexural strength, Carbon fibers, Glass fibers, and Hydroquinone composites.

INTRODUCTION

Intensive development of polymer engineering as well as specific capability of polymers to form new, synthetic structures with improved mechanical properties, led to expansion in usage of composite materials followed by continuous improvement of technology of their fabrication.

Development of technology of composites was speeded up also in the area of design and production of big structures which will have low price and adequate reliability. Due to good mechanical properties, low mass and relatively simple fabrication, composites represent main competition to classical constructional materials (1, 2).

There has been various rehabilitation techniques proposed for civil infrastructure to overcome problems associated with the aging process, increased traffic, change in use, and deterioration. Among these techniques, external strengthening provides a practical and cost effective solution when compared to other traditional repair methods. The first generation of external strengthening methods utilized steel plates bonded to the tension surface of the structure. The strengthening effectiveness was acceptable; however several problems, including durability, heavy weight, handling, and shoring, had to be resolved; thus the need for alternative materials aroused. The introduction of advanced composite materials, particularly fiber reinforced polymers (FRP), in structural engineering industries, as a second generation of externally bonded retrofit materials, has offered numerous benefits. Retrofits of structures using glass-FRP (GFRP) and carbon-FRP(CFRP) has been studied extensive over the past decade.

THEORETICAL APPROACH

The modulus measures the resistance of a material to elastic deformation, for linear elastic materials the stress σ is related to the strain ε by Young's modulus E (Hook's law).

$$E = \left(\frac{Mass}{Deflection}\right)\left(\frac{gL^3}{48I}\right) \quad \text{.....(1)}$$

$$I = \frac{dB^3}{12} \quad \text{.....(2)}$$

Where : I =Engineering bending momentum, d = width of samples, B = thickness of sample , g = gravity , L = sample length.

$\left(\frac{Mass}{Deflection}\right)$ Is the slope of linear part of mass deflection curve obtained from three point bending load tests (3).

The flexural test measures behavior of materials when subjected to simple beam loading. It is also called a transverse beam test with some materials. Maximum fiber stress and maximum strain are calculated for increments of load. Flexural strength is defined as the maximum stress in the outermost fiber. It is obtained when the ultimate flexibility of one

material is achieved before its proportional limit. Specimens are placed on two supports and a load is applied at the center, this test is known as three-point bending test. Flexural modulus is calculated from the slope of the stress against deflection curve [4]. Flexural test is often done on relatively flexible materials such as polymers, wood and composites. There are two types of the test: 3-point flexural test and 4-point flexural test. Three point bending test will be used in this project. In this test, the area of uniform stress is quite small and concentrated on the centre loading point.

Consider a rectangular beam, on which a simple concentrated force is exercised in the centre of the beam with a load of P. The equation used for calculating the flexural stress [5]:

$$\sigma_f = \frac{3PL}{2bh^2} \quad \text{.....(3)}$$

The equation used for calculating the flexural strain:

$$\varepsilon_f = \frac{6Dh}{L^2} \quad \text{.....(4)}$$

The equation used for calculating the Young's modulus:

$$E_B = \frac{L^3 m}{4bh^3} = \frac{Flexural, strength}{Flexural, strain} \quad \text{.....(5)}$$

where: σ_f: stress in outer fiber at midpoint, MPa;

ε_f: strain in the upper surface, %;

E_B: modulus of elasticity in bending, MPa;

P: load at a given point on the load deflection curve, N;

L: support span, mm;

b: width of test beam, mm;

h: depth of test beam, mm;

D: maximum deflection of the centre of the beam, mm;

m: slope of the tangent to the initial straight line portion of the load deflection curve, N/mm .

MATERIALS AND METHODS

Hydroquinone – formaldehyde resin material designated by (HQR) in form of liquid was used as a matrix in preparation of composite materials [6]. Fibers used as reinforcing materials for Hydroquinone resin composites. These fibers are glass fiber type, E- glass designated by (EGF) and carbon fiber designated by (CF). Hydroquinone in form of liquid was dried in an electric oven at (323 K) for 3hr. to obtain the

hydroquinone resin in form of solid, followed by milling to a desirable size suitable for molding operation.(HQF), which was prepared by this method, was used to prepare a reference specimens according to testing standard requirement. (HQR) in form of liquid was solved using ethanol to obtain a suitable matrix. At same time, fibers, which were used (EGF and CF), were dried in an electric oven at (393 K) for 3hr. to reduce humidity and activation its porosity. Then fibers were impregnated in matrix, which was prepared as above, followed by drying the mixture in air using dispersion method on a dry plate for 3hr. The mixture was pre-cured using an oven at (353 K) for 3hr. the mixture was poured in molds. The surfaces of molds were coated on the inside with oleic acid to avoid adhesion of the mixture and to allow easy removal of the composites. Hot–press technique was used in this work to prepare the composites specimens of HQR matrix, using flash mold. The numbers of specimen used for the determination of mechanical properties were nine and the tests were conducted at ambient laboratory conditions.

RESULTS AND DISCUSSION

Flexural Strength results were shown in Fig. 1. Influence of fibers Vol. % (EGF or CF) on the Flexural Strength of HQ matrix was shown in Fig. (1). Generally, reinforcement by fibers lead to increase flexural strength values with the increasing volume fraction. This increment was differentiated in HQ composites depending on capability of strength of fibers, which depend on type, length, and orientation of fibers, with respect to the load. According to the Fig. 1, flexural strength values were increased gradually with respect to increasing of volume fraction of fibers, Influence of interface between the matrix and the reinforcement materials was clearly observed on flexural strength. From the Figure, it can be seen that the behavior of Flexural Strength curves of Hydroquinone composites are similar to others and the failure is done by pullout mechanism as shown in Fig. 2. But the highest value it was for CFC group which was reached (270MPa), then EGC group (159.4 MPa), because the strength of CF is greater than strength of EGF. The flexural modulus and yield point values of all the composites are presented in Table (1). From Table (1) and Fig. 1, it is clear that the flexural strength and modulus (E) has improved over pure treated fibers hydroquinone composites.

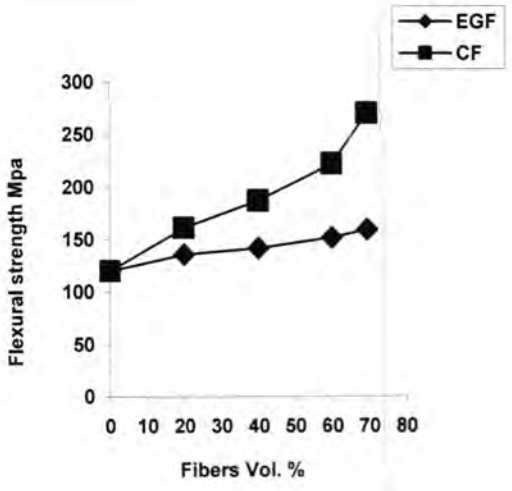

Fig. -1 : Influence of different fibers Vol. % on the flexureal strength of hydroquinone resin.

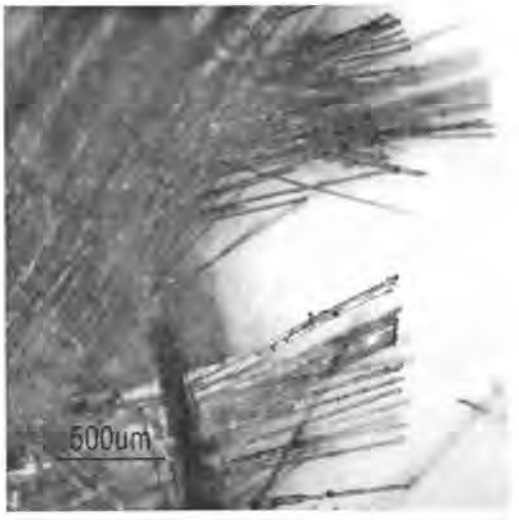

Fig. -2 : Optical microscopy of pullout of fibers.

Table- 1: The effect of fibers volume fraction on yield point and Young modulus of Hydroquinone resin.

Group symbol	Vol.%	E GPa	Y.S MPa
HQR	0	51.73	94.05
EGFC	20	62.86	109.29
	40	87.92	123.11
	60	106.74	137.41
	70	128	152.86
CFC	20	139.61	178.05
	40	147.13	202.16
	60	152.55	231.39
	70	169.14	262.86

From this study, the following remarkable points can be concluded:

1. Reinforcing hydroquinone resin with fibers (carbon and E-glass) has improved the, mechanical properties of composite in different percentages depending on difference factors; kind of fiber, direction of fibers, and nature of interface between the matrix and fibers.
2. Failure takes place by pull-out mechanism.

REFERENCES

1. K.K. Chawia, "Composite Materials", Springer-Verlag, New York, (1987).
2. M. F. Ashby, "Materials and Engineering Design", Institute of Metals, London, (1988).
3. Baltan W., Engineering Materials Technology, 3rd edition, John Wiley and Sons, Inc., New York (1998).
4. Smith, W F and Hashemir, J., "Foundations of Material Science and Engineering", McGraw-Hill, New York, : 523-525. (2006)
5. W. D. Callister, Jr., "Materials Science and Engineering an Introduction", 6th ed., John Wiley &Sons,Inc.New York:120-132 (2003).
6. Anusavice KJ., Recent developments in restorative dental ceramics, J Am Dent Ass, : 73-84 (1993).

Induced Potential for Proton Ions Moving Parallel to the Solid Surface

Khalid.A.Ahmad and Shadha J. Khalaf
Department of Phys., College of Science, Al- Mustansiriya University

الخلاصة

جهد الصورة والقوة المحتثة المتكونة نتيجة لحركة الجسيمات المشحونة وبصورة موازية للسطح الصلب قد تم بحثها والتحقق منها من خلال دراسة هيئة الوسط العازل (لمادة مشتتة صلبة شبه لا نهائية) (Semi-infinite dispersion media) وبمراعاة الأضمحلال.

ومن الممكن تعديل وتثبيت معلمات نموذج الوسط لتعطي نتائج منسجمة بشكل جيد مع (تكامل المعلومات الضوئية) (Optical-data integration) لحساب قوة الايقاف المعيقة (Stopping forces) والقوة الجانبية (Lateral forces) على شحنة متحركة او باخذ دالة العزل للطور العشوائي التقريبي.

هذا العمل دراسه جهد الحركة والقوى الموقفة والجانبية لحركة بروتون في السطوح الصلبة تم مقارنة النتائج التي حصلنا عليها مع المعلومات والنتائج التجريبية المتوفرة للثوابت الضوئية لمواد صلبة مختلفة مثل الالمنيوم (Al) والنحاس (Cu) والذهب (Ag) والفضة (Au) .

ABSTRACT

The image potential and ensuing forces induced by a charged particle moving parallel to a solid surface are investigated by using a dielectric formulation for a semi-infinite dispersive taking into the consideration a damping.

The model parameters may be adjusted to provide a very good agreement with the optical-data integrations of the stopping and lateral forces on the moving charge, or by taking dielectric of Random Phase Approximation. The wake potential, stopping and lateral forces of proton in Al, Cu, Ag, and Au solids are in good agreement with experimental previous work.

INTRODUCTION

A fast heavy ion moving in a solid target produces a charge polarization in the medium that acts back on the ion as an induced potential. This is called wake potential, gives the reaction of the medium to the motion of the ion, and through its gradient at the ion position defines the electric field that produces the slowing down of the projectile (1)

The interaction of charged particles with solid surfaces has been investigated theoretically and experimentally in recent literature as well as the application to relevant processes of electronic and atomic interactions with surface

The theoretical description of these processes is usually based on earlier studies of surface-plasmon excitation by Ritchie (2)

One of the interesting points in the present work is the calculation of the induced field or dynamical image potential and induced forces produced by a proton moving close to the surface investigations of the problem have been made by several authors (3,4) using the dielectric formalism for semi-infinite media and the electron gas Random-Phase Approximation (RPA) dielectric function.

In the present work theoretical study out the subject of a wake potential for the proton falling on the solid targets ,this investigation has dealt with using the real part to calculate the wake potential and using imaginary part to calculate the forces. The calculations were done for computer on the proton interaction with Al, Ag, Cu and Au solid surfaces by a program (Shathwake.f90) which was written in Fortran-90 using software Compaq visual Fortran 6.6 (CVF) for compiling, linking and exacting the program.

2. Theory

2.1 Real and Imaginary parts of dielectric function

The dielectric function plays an important rule in calculating the energy loss, wake potential and stopping and lateral forces for interaction of charged particles with solid material. The real and imaginary parts experiments values of $[\varepsilon(\omega)-1]/[\varepsilon(\omega)+1]$, versus photo energy $E(eV)=\hbar\omega$ for Al and Ag solid materials are taken from reference(5) which are shown in Fig(1), where ε is the dielectric function, $\hbar$ is blank constant and ω is the angular frequency.
Drude dielectric function is given by the fallowing eq. (6):

$$\varepsilon(\omega) = 1 - \frac{\omega_p^2}{\omega(\omega + i\gamma)} \qquad (1)$$

Where γ is the damping and ω_p is the plasmon frequency.

To find the real and imaginary part of $\frac{\varepsilon(\omega)-1}{\varepsilon(\omega)+1}$ follow the fallowing steps:

Start with eq. (1):

$$\frac{\varepsilon(\omega)-1}{\varepsilon(\omega)+1} = -\frac{\omega_p^2}{2\omega(\omega+i\gamma)-\omega_p^2},$$

$$= \frac{-\omega_p^2}{(2\omega^2-\omega_p^2)+i2\omega\gamma} * \frac{(2\omega^2-\omega_p^2)-i2\omega\gamma}{(2\omega^2-\omega_p^2)-i2\omega\gamma}$$

$$= \frac{-\omega_p^2(2\omega^2-\omega_p^2)}{(2\omega^2-\omega_p^2)+(2\omega\gamma)^2} + i\frac{\omega_p^2\,(2\omega\gamma)}{(2\omega^2-\omega_p^2)+(2\omega\gamma)^2}$$

(2)

This means that the real part of Eq. (2) is:

$$\varepsilon_r = \mathrm{Re}\left[\frac{\varepsilon(\omega)-1}{\varepsilon(\omega)+1}\right] = -\frac{\omega_p^2(2\omega^2-\omega_p^2)}{(2\omega^2-\omega_p^2)+i2\omega\gamma} \quad (2a)$$

And the imaginary part is:

$$\varepsilon_i = \mathrm{Im}\left[\frac{\varepsilon(\omega)-1}{\varepsilon(\omega)+1}\right] = \frac{\omega_p^2(2\omega\gamma)}{(2\omega^2-\omega_p^2)^2+(2\omega\gamma)^2} \quad (2b)$$

Where $\left[\frac{\varepsilon(\omega)-1}{\varepsilon(\omega)+1}\right] = \varepsilon_r + i\varepsilon_i$ (3)

In a single plasma resonance which describes the surface resonance, the surface-plasma poles are shifted to complex frequencies: $\mp \omega_s' - i\gamma/2$, where ω_s is the surface-plasmon frequency, γ is the damping and $\omega_s' = \sqrt{\omega_s^2 - \gamma^2/4}$ is the shifted surface-plasmon frequency. The surface-response function [ε (ω)-1]/ [ε (ω) +1] can be written as [7]

$$\frac{\epsilon(\omega)-1}{\epsilon(\omega)+1} = \frac{\omega_s^2}{2\omega_s'}\left[\frac{1}{\omega+\omega_s'+i\gamma/2} - \frac{1}{\omega-\omega_s'+i\gamma/2}\right] \quad (4)$$

Figs. (1(a) and 1(b) show the real and imaginary parts of the surface response function [ε(ω)-1]/ [ε(ω)+1] versus the energy $E=\hbar\omega$, for Cu and Ag. These values have been taken form Ref (5). The appropriate parameters in for the solid materials Al, Cu, Ag and Au are shown in table (1).

Table -1: of parameters: characteristic frequency ω_s and damping γ in a.u (8)

Element	ω_s	γ
Al	0.4	0.037
Cu	0.75	1.2
Ag	1.30	2.8
Au	1.41	2.5

2 Image potential:

Let us consider the interaction between a fast probe and a semi-infinite medium bounded by a planar surface. In the frame of classical electrodynamics, the interaction of a fast charge particle moving near a planar interface is given by the induced potential, i.e., the so-called image potential, which problem was first studied by Ritchie and Takimoto (9). Now we consider the simplest approach to this problem, where a probe of charge Z_P is traveling parallel to the surface at a constant distance b from the surface and with constant velocity v. Neglecting retardation effects, the total potential is the solution of Poisson equation: (10)

$$\nabla^2\phi = -\frac{4\pi}{\varepsilon(\omega)}\rho(r,\omega)$$

(5)

Where $\rho(r,\omega)$ stands for the ω-component of the charge density. Assuming that the probe is moving along the x-axis, the charge density is given by:(11)

$$\rho(r,\omega) = \frac{Z_P}{v} e^{i\omega x/v}\delta(y)\delta(z-b)$$

(6)

Then, in the region where the charge is traveling (z > 0), the Potential can be written as:

$$\phi_{ind}(r,\omega) =$$

$$-\frac{2Z_p}{v}K_0\left[\frac{|\omega|}{v}\sqrt{y^2+(z-b)^2}\right]e^{\frac{i\omega x}{v}} - 2\frac{Z}{v}g(\omega)K_\circ\left[\frac{|\omega|}{v}\sqrt{y^2+(z+b)}\right]e^{\frac{i\omega x}{v}}$$

(7)

Where x, y and z are the Cartesian coordinates of r, $K_0(x)$ stands for the modified Bessel function b is impact parameter, v velocity Z_p is atomic number for proton and g (ω) is the planar surface response function

$$g(\omega) = \frac{\varepsilon(\omega)-1}{\varepsilon(\omega)+1}$$

(8)

The first term in (7) is the ω -component of the Coulomb potential, while the second one is the surface induced potential. This last term can be understood as the ω -component of the image potential; the

potential created outside the medium by the dynamic image charge, i.e., a charge $q_{image}(\omega) = -Z_P\, g(\omega)$ placed in front of the probe and inside the medium at a distance b from the surface. Then, the induced potential is:

$$\phi_{ind}(r,t) = -\frac{Z_p}{\pi v}\int_{-\infty}^{\infty} d\omega\, g(\omega)\, K_o\left[\frac{|\omega|}{v}\sqrt{y^2+(z+b)^2}\right] e^{i\frac{\omega}{v}(x-vt)} \quad (9)$$

Because of the analytic properties of the dielectric function $\varepsilon(\omega)$ the response function satisfies $g(-\omega)=g^*(\omega)$, where z* stands for the complex conjugate of z. Therefore, one can write the former expression as an integral over positive values of ω :

$$\phi_{ind}(r,t) = -\frac{Z_p}{\pi v}\int_{-\infty}^{\infty} d\omega\; K_o\left[\frac{|\omega|}{v}\sqrt{y^2+(z+b)^2}\right]\left(\frac{\varepsilon(\omega)-1}{\varepsilon(\omega)+1}\right) e^{i\frac{\omega}{v}(x-vt)} \quad (10)$$

Although Eq. (10) explicitly exhibits the fact that the field find ϕ (r, t)
Choose y=0 , t=0

$$\phi_{ind}(r) = \frac{-2Z_p}{\pi v}\int_{-\infty}^{\infty} d\omega\, K_o\left[\frac{\omega}{v}(z+b)\right]\left(\frac{\varepsilon(\omega)-1}{\varepsilon(\omega)+1}\right) e^{\frac{i\omega x}{v}} \quad (11)$$

Substituting Eq. (3) into Eq. (11) one can get,

$$\phi_{ind}(r) = \frac{-Z_p}{\pi v}\int_0^{\infty} d\omega\, K_o\frac{\omega}{v}(z+b)(E_r+E_i)(\cos\frac{\omega x}{v}) + i\sin(\frac{\omega x}{v}) \quad (12)$$

$$= \left\{\frac{-Z}{\pi v}\int_0^{\infty} d\omega\, K_o\frac{\omega}{v}(z+b)\left[(E_r\cos(\frac{\omega x}{v}) + E_i\sin(\frac{\omega x}{v})\right] + i\left[E_r\sin(\frac{\omega x}{v}) + E_i\cos(\frac{\omega x}{v})\right]\right\} \quad (13)$$

Taking the real part,

$$\phi_{ind}(r) = \frac{-Z_p}{\pi v}\int_0^{\infty} d\omega\, k_o\frac{\omega}{v}(z+b)\left[(E_r\cos(\frac{\omega x}{v}) + E_i\sin(\frac{\omega x}{v})\right] \quad (14)$$

Let take some special cases:

(i) X=0 , z=b=0 and $\gamma\rightarrow 0$

$$\phi_{ind}(0,0) \cong \frac{Z_P \omega_p^2}{\pi \upsilon} \int_0^{\infty} \frac{d\omega}{(2\omega^2 - \omega_p^2)}$$

(15)

(ii) $\gamma \to 0$, z=b

$$\phi_{ind}(x,z) = \frac{-Z_P}{\pi v} \int_0^{\infty} \mathrm{d}\omega \, \mathrm{K}_{\circ}\left(\frac{2\omega b}{\upsilon}\right)\left\{\left[\frac{-\omega_p^2}{2\omega^2 - \omega_p^2}\right]\cos\left(\frac{\omega x}{\upsilon}\right)\lim_{\varepsilon \to 0}\frac{\omega_p^2 \varepsilon_0}{W^2 + \varepsilon_0^2}\sin\left(\frac{\omega x}{\upsilon}\right)\right\}$$

(16)

Where $W^2 = 2\omega^2 - \omega_p^2$, $\varepsilon_{\circ} = \omega\gamma$

From the properties Dirack-delta function [12]

$$\delta(x) = \frac{1}{\pi} \lim_{x_{\circ} \to 0} \frac{x_0}{x^2 + x_{\circ}^2}$$

$$\phi_{ind} = \frac{-Z_p}{\pi \upsilon} \int d\omega \, \mathrm{k}_{\circ}\left[\frac{2\omega b}{\upsilon}\right]\left\{\left(\frac{-\omega_p^2}{2\omega^2 - \omega_p^2}\right)\cos\left(\frac{\omega x}{\upsilon}\right) - \pi\delta(2\omega^2 - \omega_p^2)\sin\left(\frac{\omega x}{\upsilon}\right)\right\}$$

(17)

Also,

$$\delta(a^2 - x^2) = \frac{1}{2a}[\delta(x-a) + \delta(x+a)]$$

and

$$f(x_{\circ}) = \int_{-\infty}^{\infty} \delta(x - x_{\circ}) f(x) dx$$

Then the induced potential becomes:

$$\phi_{ind} = \frac{Z_P}{\pi \upsilon} \int d\omega K_{\circ}\left[\frac{2\omega b}{\upsilon}\right]\left\{\left(\frac{-\omega_p^2}{2\omega^2 - \omega_p^2}\right)\cos\left(\frac{\omega x}{\upsilon}\right) - \frac{\pi}{2\omega_p}\sin\left(\frac{\omega_p x}{\upsilon}\right)K_{\circ}\left(\frac{2\omega_p b}{\upsilon}\right)\right\}$$

(18)

Eqs. (14, 18) have been solved numerically using a program (Shathwake. f90). Figs. (2, 3, 4) show the variation of the induced potential ϕ_{ind} with x and z for interaction of proton with different values of velocities υ =0.5, 1.5 and 2.5 (a.u) with solid materials Al, Ag, Cu at distance b=5 (a.u).

When the probe particle is moving outside the solid the effect of the boundary is to cause energy loss at the surface-plasmon energy ω_s (11).

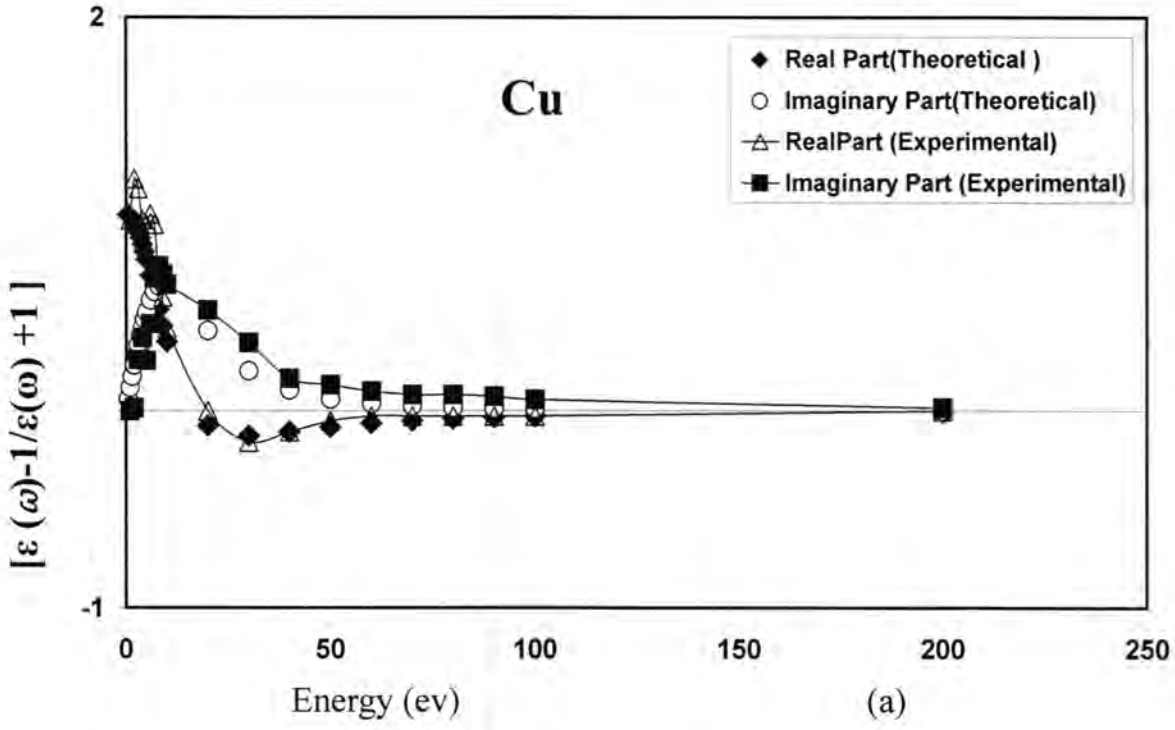

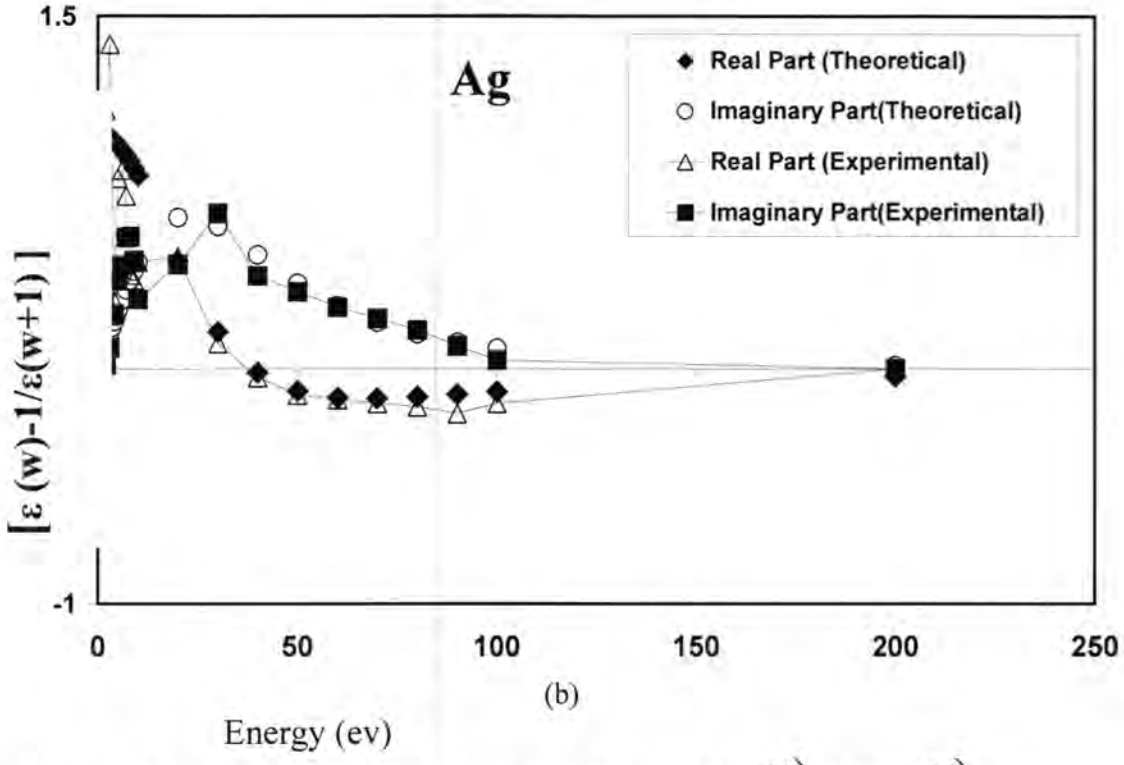

Fig- 1: Values of the surface response function $[\varepsilon(\omega)-1]/[\varepsilon(\omega)+1]$ versus energy $E=\hbar w$. The values of the real and imaginary parts are shows in (a)and (b) both Cu and Ag. [5]

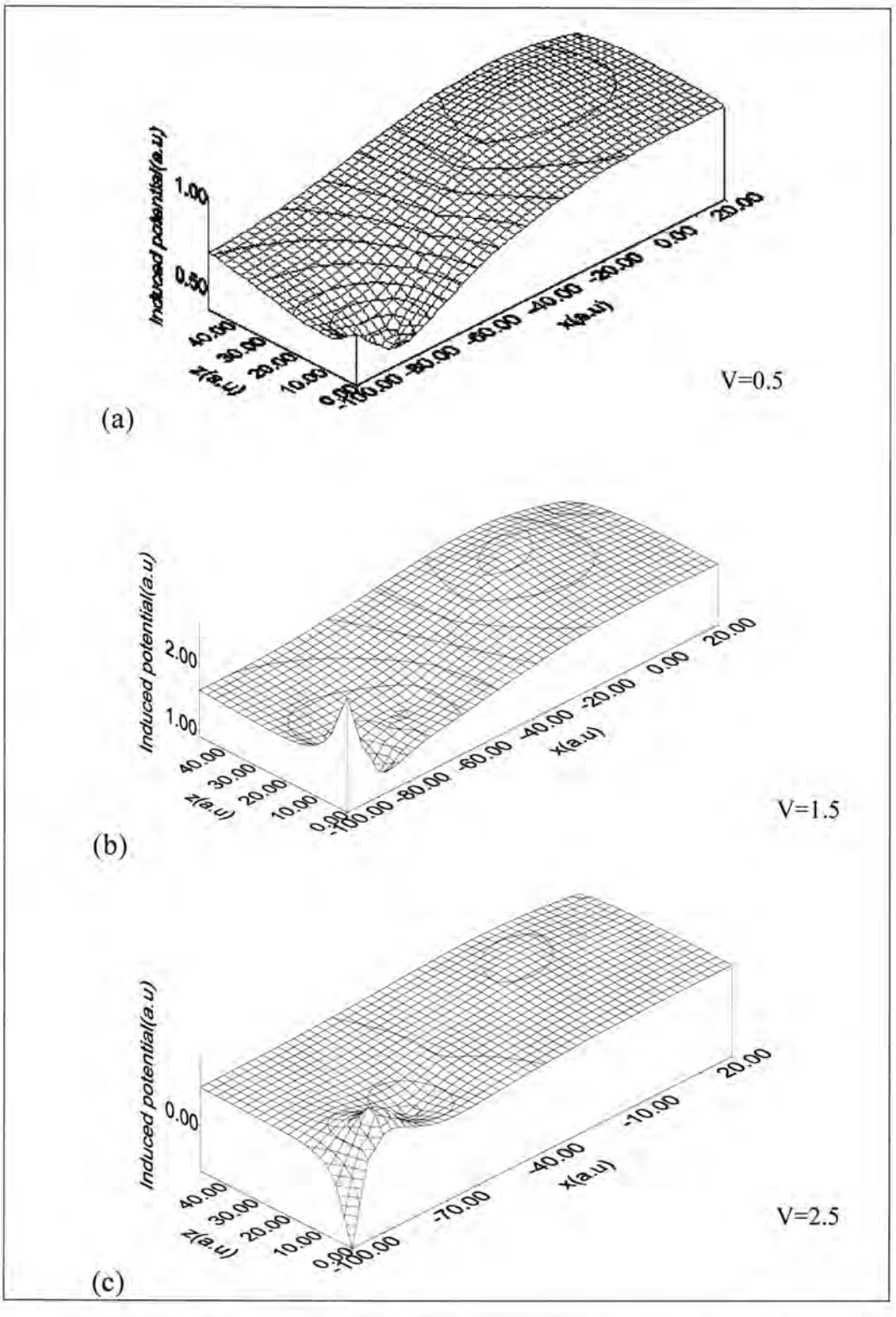

Figs-2: induced potential for Al at distant b=5(a.u) with velocity 0.5, 1.5, 2.5 (a.u)

γ=1.37, ω_s=0.45

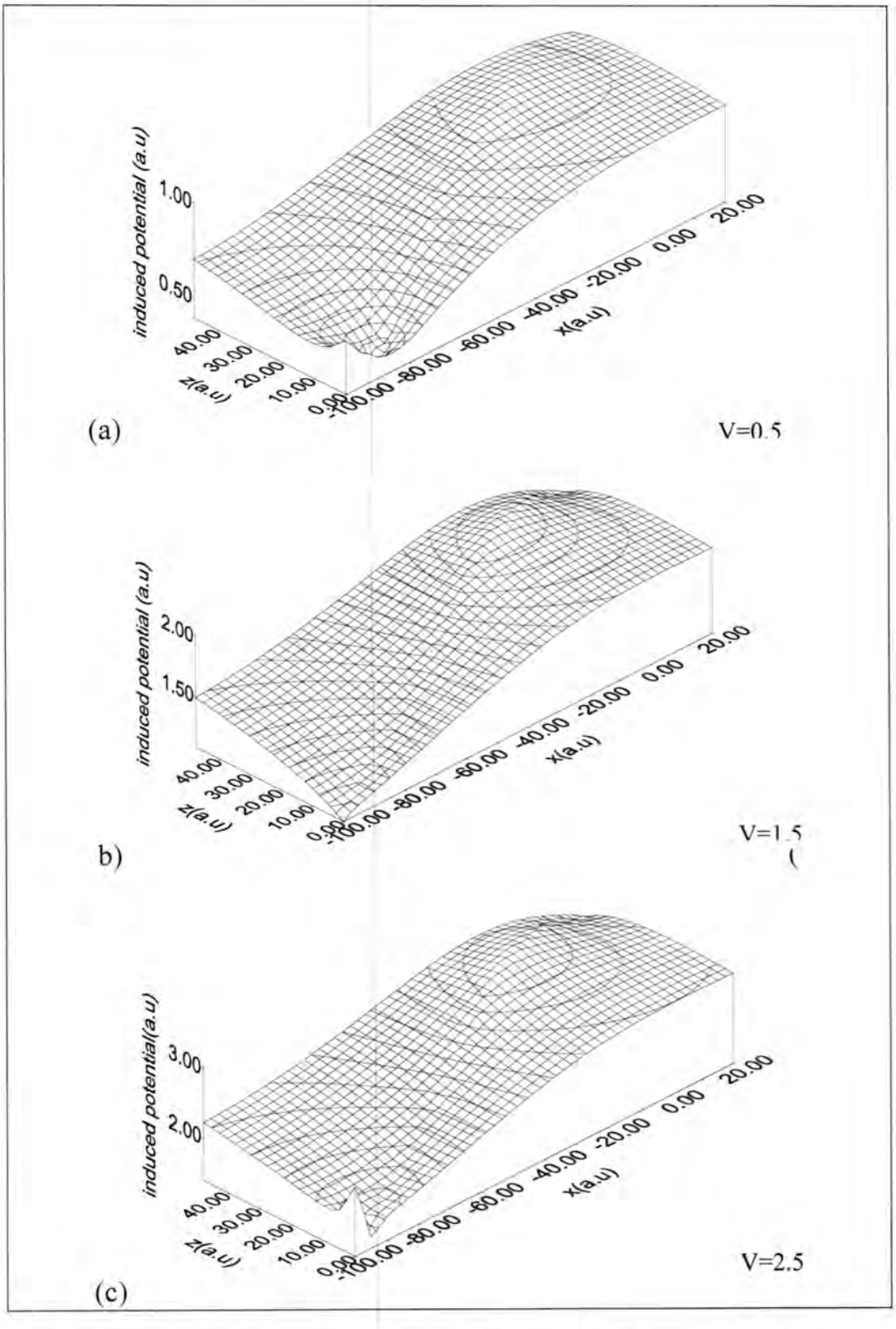

Figs-3: Induced potential for a particle moving parallel to an Ag surface at distance b=5 (a.u) with velocity v=0.5, 1.5, 2.5 (a.u) (γ=2.8, ω_s=1.3).

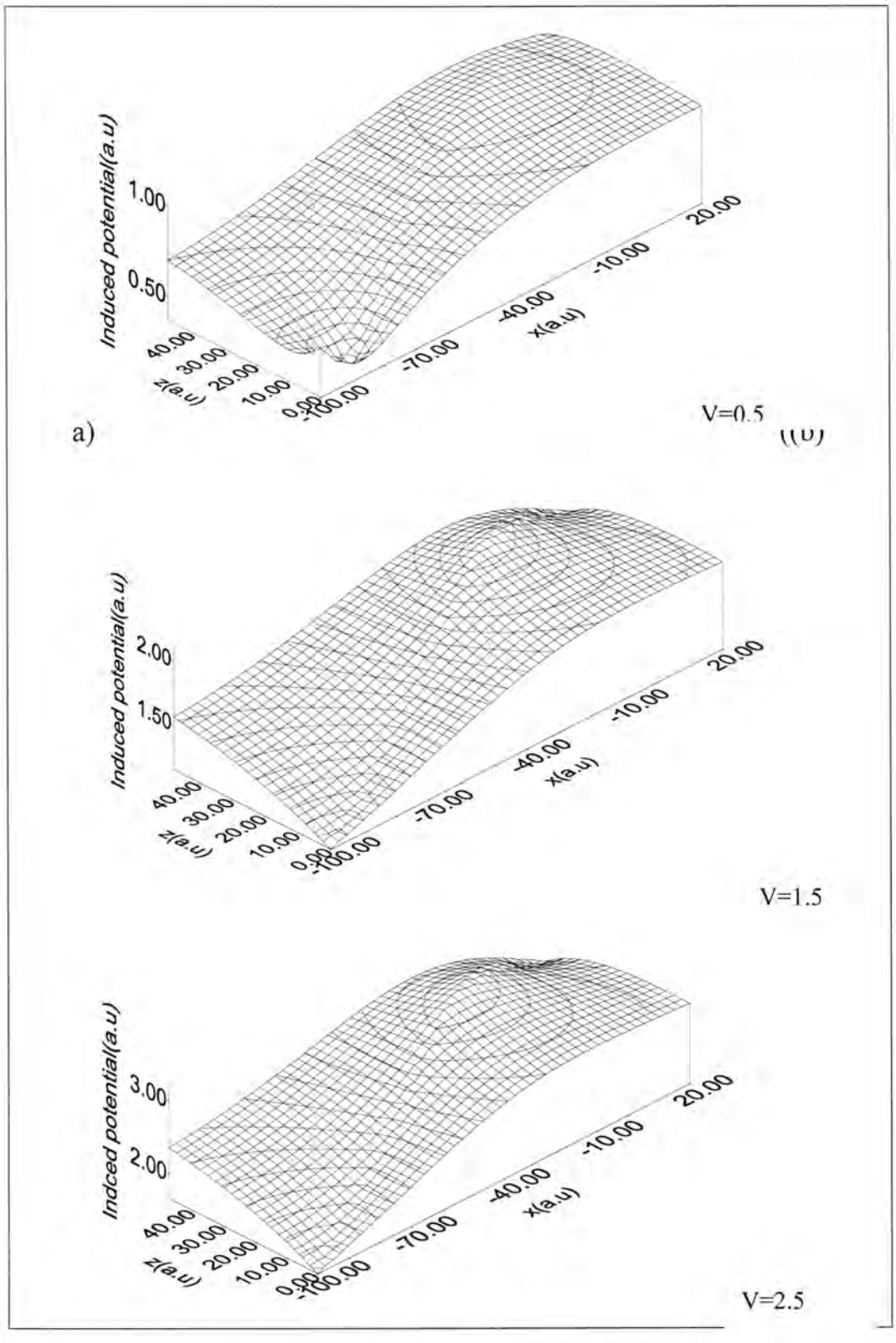

Figs-4: induced potential (Cu) for a particle moving at distance b=5 (a.u) and velocity $\gamma = 1.6, \omega_s = 2.07$ 0.5, 1.5 (a.u) and 2.5

Stopping and lateral forces:

The stopping power may be understood as a time average force on the projectile, directed opposite to the stopping to the velocity and originating in the response of the stopping medium to the electric field set up by the projectile (13) The response of the medium also includes a force component perpendicular to the direction of motion which contributes to lateral scattering of the projectile for penetration in the bulk there is no net deflection because of symmetry. (14) The stopping force reflected the response of target electrons to the electric field induced by the projectile. The same is true for the lateral force which is known to be related to the electrostatic image force and its significance in grazing-incident studies with ion beams has been pointed out (15,16)

The induced electric field is given by the following Eq:

$$E_{ind} = -\nabla V_{ind} \tag{19}$$

We separate the x and z components to obtain the expression for stopping and lateral force acting on the particle acting on the particle. This field takes following form:

1. Stopping force, F_x

$$F_x = -Q \left. \frac{\partial \phi_{ind}}{\partial x} \right|_{z=b},$$

$$= \frac{2QZ_p}{\pi \upsilon^2} \int_0^{\infty} \omega \, d\omega \, \mathrm{K}_{\circ}\left[\frac{2\omega b}{\upsilon}\right]\left[-E_r \sin\left(\frac{\omega x}{\upsilon}\right) - E_i \cos\left(\frac{\omega x}{\upsilon}\right)\right] \tag{20}$$

When x→0

$$F_x = \frac{2QZ_p}{\pi \upsilon^2} \int_0^{\infty} \omega \, d\omega \, \mathrm{K}_{\circ}\left[\frac{2\omega b}{\upsilon}\right]\left[\mathrm{Im}\left[\frac{\varepsilon(\omega)-1}{\varepsilon(\omega)+1}\right]\right] \tag{21}$$

Where ϕ_{ind} is given by Eq (9),

2. Lateral force, F_z

$$F_z = -Q\frac{\partial \phi_{ind}}{\partial z}\bigg|_{z=b}$$

$$= -\frac{2Qz}{\pi \upsilon^2}\int_0^\infty \omega\, d\omega\, K_1\left[\frac{2\omega b}{\upsilon}\right]\left[\mathrm{Re}\left[\frac{\varepsilon(\omega)-1}{\varepsilon(\omega)+1}\right]\right] \qquad (22)$$

Fig. (5) Shows the variation of stopping and lateral forces (F_X, F_Z) with velocity for proton interaction Al, Au, Ag and Cu at b=2 (a.u).

RESULTS AND DISCUSION

The plasma-resonance,it is interest to investigate the values of the dynamical potential and induced forces using more realistic representation of the dielectric function of various

For this purpose, we will now introduce into the formalism the experimental information on the dielectric function for various solids (Cu and Ag) using the results of the optical-data analysis derived from experimental determinations as shown in fig. (1).

The induced surface wake potential created by a proton which is moving an Al-vacuum (γ =1.37), (ω_s =0.45) in parallel direction to the surface. The RPA have been used. The particle velocity is (a) υ =0.5 a.u, (b) υ =1.5 a.u, (c) υ =2.5 a.u. The wake is plotted on grid z (a.u) and x (a.u) for distance b =5 (a.u) as shown in fig (2). The proton has been represented by a black circle.

Figs. (6,7)show the calculation of stopping and lateral forces (ev/A^0) as a function of velocity υ (a.u) using RPA model, Eq.(21, 22) with the calculations using full set of optical data. The calculations for the interaction of proton with solid targets Al, Cu, Ag and Au at b=5 a.u are a good agreement.

In the figs (5) we compare the values of parallel (stopping) and perpendicular (lateral)forces for proton moving close to (Al, Cu, Ag and Au surfaces. The distinct behavior of the stopping and lateral forces at low velocities and they are equal at velocity a.u) $\upsilon \geq 10$ (Al, Cu, Au, and Ag). This is clear in fig. (5) at low velocity the stopping force is related to the dynamic response of the medium and therefore it drops to zero for a static charge. In contrast, the lateral force has a finite limit given by the static image potential. Mathematically, this difference arises from Eqs. (21) and (22) where the two forces are determined by the imaginary and real parts of the response function.

(a)

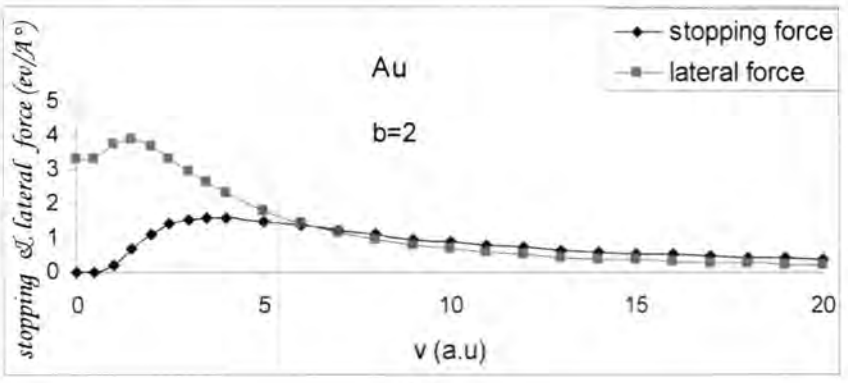

(b)

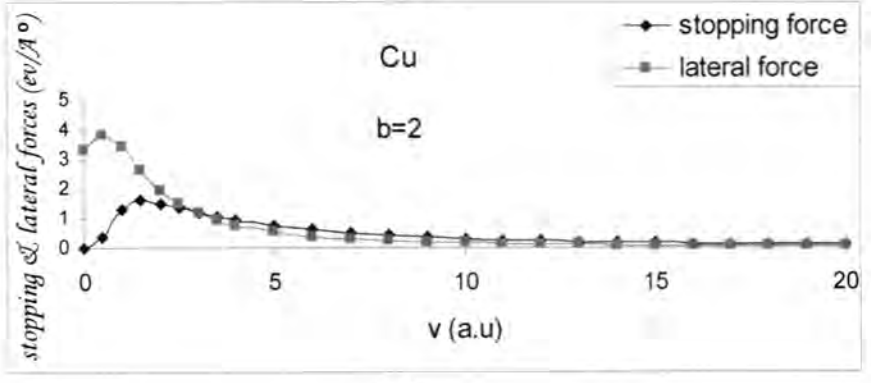

(c)

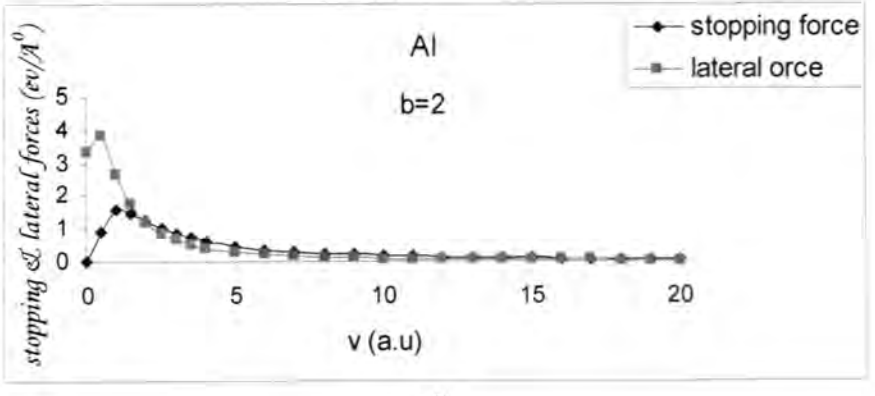

(d)

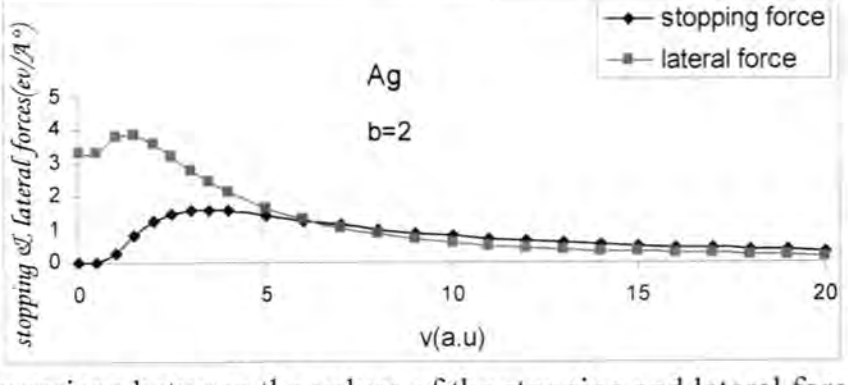

Fig-5: Comparison between the values of the stopping and lateral forces at b=5 a.u for Al, Au, Cu and Ag

REFERENCES

1. J. D. Fuhr, V. H. Ponce, F. J. Garcı´a de Abajo and Echenique Phys. Rev. B57(1998).
2. H. Ritchie and A.L. Marusak,"Interaction of charged particles with a degenerated fermi-Dirac electron gas" Surface Science.4 234(1966).
3. F. Flores and R.Garcia-Moliner, J.Phys.:solid state Phys.C14 (1979).
4. F. J. Garcı´a de Abajo and M. Echenique"Wake potential in the vicinity of a surface " Phys.Rev.B46 2663(1992).
5. H.J.Hagemann,W.Gudat&C.Kunz"Optical constant from the far infrared to the x-ray region:Mg,Al,Au,Bi,C & Al_2O_3"J.Opt.Soc.Am. 65, 442 (1975).
6. 6)J. M.Pitarke,V.M.Silkin,2E.V.Chulkov & P.M.Echenique arxiv: cond-mat / 0408683v1[con-mat.mtrl-sci]"Theory of surface plasmons and surface – plasmon polaritons".
7. 7). R. Arista, Phys.Rev.A49 1885(1994)
8. 8) J. I. Juaristi, F. J. Garcie de Abajo and P. M. Echenique, "Dynamical image potential and induced forces for charged particles moving parallel +va solid surface" Phys. Rev. B53 , 13839(1996-II).
9. A.Rivacoba,N.Zabala,J.Aizpurua,progress"Image potential in scanning transmission electron microscopy" 65 :1-64(2000).
10. A.Arnanu et al./surface science.Reports 27 ,113 239(1997).
11. INSTITUTE OF PHYSICS PUBLISHING REPORTS ON PROGRESS IN PHYSICS Rep. Prog. Phys. 70 :1–87(2007).
12. Handbook of mathematical function, Edited by Abramowitz and I. A. Stegun (Dever, New York,(1974)
13. P. Sigmund,"Charged – dependent electronic stopping of swift nonrelativistic heavy ions" Nuclear Instruments and Methods in Physics Research B 125:77-96(1997).
14. K.Dettmann,Z.Physik A272 227(1975).
15. H.Winter,ohys.Rev.46 R13(1992).
16. H.Winter,C.Auth,R.Schuchand E.Beeb,Phys.Rev.Lett,71(1993).

Longitudinal Development and the Inelasticity of Extensive Air Showers

Sarah Hussein Ali and Ahmed Aziz Ahmed
Al-Mustansiriyah University, college of science, department of physics

الخلاصه

في عملنا الحالي بعض خصائص وابل الجسيمات المشحونه تم مناقشتها و حسابها : عدد الجسيمات المشحونه كداله للطاقه الابتدائيه و التوسع الطولي لوابل من الجسيمات الناشئة في الغلاف الجوي ويعتبر أعلى عمق لوابل الجسيمات في الغلاف الجوي (X_{max}) احد خصائص هذا للتوسع و اخيرا عدم المرونه و الذي يعبر عنها بواسطه المعامل (k) .

ABSTRACT

In the present work some of properties for Extensive Air Showers are discussed. The number of charge particles (N) as a function of primary energy E_0 is estimated at the energy range (10^{13}-10^{16}) eV. In longitudinal developments of Extensive Air Showers, the depth of shower at maximum X_{max}, was calculated for electromagnetic and hadronioc cascade at the same energy range. The dependence of inelasticity, which is described by the parameter (k), is used for describing the variation of muons number.

INTRODUCTION

When high-energy cosmic ray particles penetrate the Earth atmosphere they interact with and generate a cascade of secondary particles, that is called Extensive Air Shower (EAS), which can be classified into three types elements, the hadronic, the electromagnetic and the muonic showers (1,2). The number of charged particles in EAS as a function of atmospheric depth, called longitudinal shower profile, is closely related to the primary particle type and energy. The atmospheric depth at which a shower exhibits its maximum of charged particles, X_{max}, is well correlated with the mass of the primary particle (3). In the hadronic cascade the important quantity that rules the shower development is the inelasticity. When two hadrons interact, an important fraction of the total energy is carried away by the main single secondary particle. The inelasticity of a single interaction which is described by a parameter k, can be defined as the fraction of the total energy directed into new pion production (both $\pi^{\pm}$ and π^{0}) (4). In this paper, we will calculate the number of charge particles ((muons, pions and electrons), and density of particles at maximum), the longitudinal development of air showers and its X_{max} for primary particles with the energy rang (10^{13}-10^{16} eV) for the hadronic and electromagnetic (EM) showers and the inelasticity affect on the number of muons in the hadronic shower.

Electromagnetic Cascade

An electron radiates a single photon after traveling one splitting length $d = \lambda_\gamma \ln 2$ (where d is the distance which an electron loses half its energy by radiation, λ_γ is the radiation wave length in the medium $\lambda_r = 37\, g/cm^2$ [5]. After traveling the same distance, a photon splits into an $e^{\pm}$ pair. In either instance, the energy of a particle (electron or photon) is assumed to be equally divided between two outgoing particles. After n splitting lengths, a distance of $x = n\lambda_\gamma \ln 2$, the total shower size (electrons and photons) is $N = 2^n = e^{x/\lambda_\gamma}$. Multiplication ceases when the energies of the particles are too low for pair production or bremsstrahlung. the energy to be critical energy ,ξ_c^e below which radiative energy loss becomes less than collision energy loss. In air,$\xi_c^e = 85\, g/cm^2$.Consider a shower initiated by a single photon with energy E_0. The cascade reaches maximum size $N = N_{max}$ when all particles have energy ξ_c^e so that

$$E = \xi_c^e N_{max}. \quad (1)$$

The penetration depth $X_{\max}$ at which the shower reaches maximum size is obtained by determining the number n_c of splitting lengths required for the energy per particle to be reduced to ξ_c^e Since $N_{max} = 2^{n_c}$ we obtain from Eq. 1 that

$$n_c = ln\left[\frac{E_0}{\xi_c^e} - 2\right]. \quad (2)$$

In atmosphere, the number of the generated electrons N_e is given as:

$$N_e = 10^6\left[\frac{E_0}{\xi_c^e}\right]^{1.03}. \quad (3)$$

The depth of electromagnetic shower maximum $X^{\gamma}_{\max}$ is given as:

$$x^{\gamma}_{max} - n_c\lambda_\gamma \ln 2 - \lambda_\gamma \ln\left(\frac{E_2}{\xi_c^e}\right) \quad (4)$$

Hadronic Cascade

Air showers initiated by hadrons interact after traversing one layer. The atmosphere is imagined in layers of fixed thickness $\lambda_p \ln 2$ where λ_p is the interaction length of strongly interacting particles where $\lambda_p = 120\ g/cm^2$. Hadrons interact after traversing one layer,

producing N_{ch} charged pions and $\frac{1}{2}N_{ch}$ neutral pions. A π^0 immediately decays to photons, initiating electromagnetic showers. Charged pions continue through another layer and interact. The process continues until the $\pi^{\pm}$ fall below the critical energy ξ_c^{π} where they then are all assumed to decay, yielding muons. ($\xi_c^{\pi} = 85\ g/cm^2$). Consider a single cosmic ray proton entering the atmosphere with energy E0. After n layers there are

$$N_{\pi} = (N_{ch})^n . \quad (5)$$

total charged pions. Assuming equal division of energy during particle production, these pions carry a total energy of $(2/3)^n E_0$. The remainder of the primary energy E_0 has goneinto electromagnetic showers from π^0 decays. The energy per charged pion in atmospheric layer n is therefore

$$E_{\pi} = \frac{E_0}{(3/2N_{ch})^n} \quad (6)$$

a certain number n_c of interactions, E_{π} becomes less than the critical energy of pions ξ_{π}^{e} therefore

$$n_c = \frac{ln(E_0/\xi_c^{\pi})}{ln(3/2N_{ch})} \quad (7)$$

where N_{ch} given as a constant value equal to 10 (6). The number of muons in the shower is obtained using $N_{\pi} = N_{\mu} = (N_{ch})^n$. Using Eq.6, the energy dependence of the muon size is shown through the relation:

$$N_{\pi} = \left[\frac{E_0}{\xi_c^{\pi}}\right]^{0.85} \quad (8)$$

The first interaction occurs at an atmospheric depth $X_0 = \lambda_p \ln 2 = 59\ g/cm$ Using Eqs. (4) and (7) we can find:

$$X_{max}^{p} = X_0 + \lambda_{\gamma} \ln E_0/3N_{ch}\ \xi_c^{\pi} \quad (9)$$

In Figure 1, one can see the number of charged particles in the shower for electrons; muons and pions in the energy range 10^{13}-10^{16} eV. In that

figure shown that, the number of particles will reach to maximum through the development of shower in atmosphere.

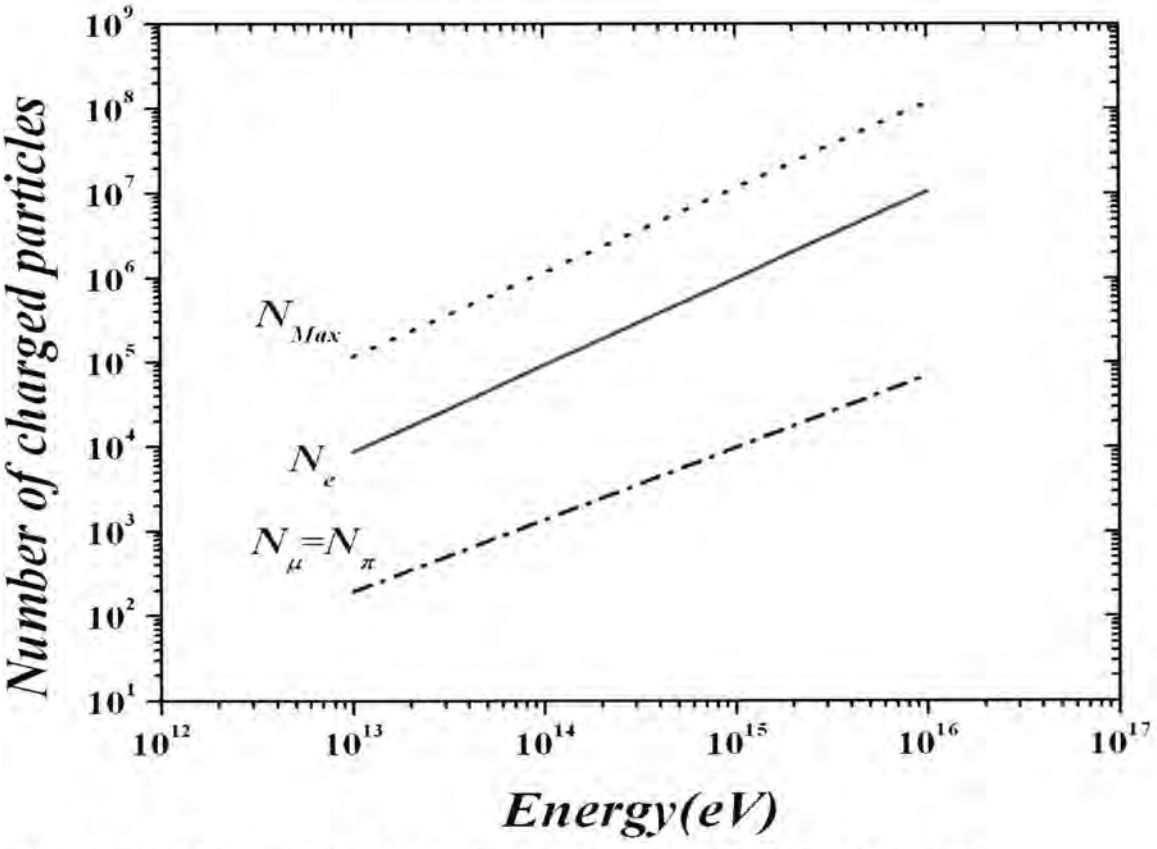

Figure - 1: The number of charged particles in atmosphere: Dashed dotted line for muons and pions (Eq. 8); solid line for electrons (Eq. 3); dotted line represent the number of particles at maximum (Eq. 1).

The Figure (2) bellow shows the depth of shower maximum for electromagnetic and hadronic cascades for photons, iron nuclei and protons initiated in the shower in the energy range 10^{13}-10^{16} eV.

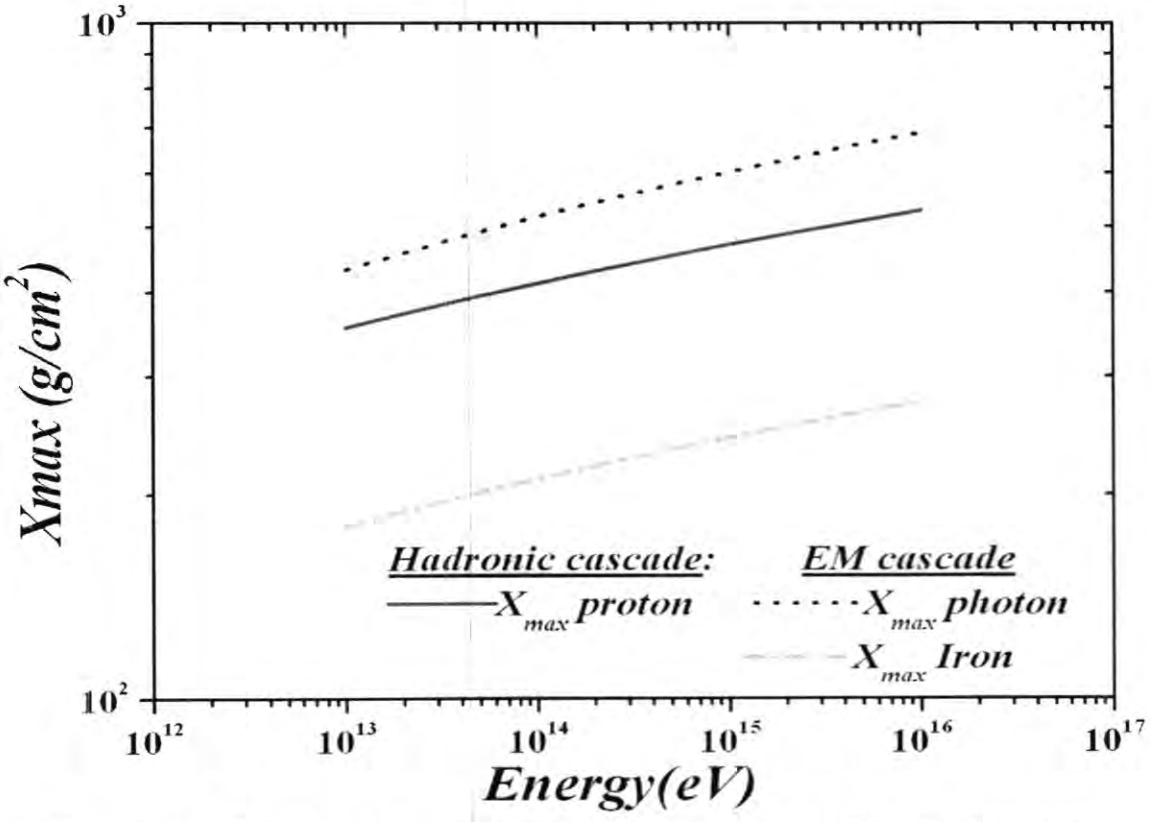

Figure - 2: Depth maximum versus primary energy for air showers. Dashed and Dashed Dotted lines: photon and iron induced electromagnetic showers; Solid: proton induced hadronic shower.

Inelasticity

The important quantity that rules the shower development is the inelasticity. This quantity combines the multiplicity and the energy of the secondaries, thus describing how much of the energy of the incoming particle is transferred onto secondary particles. Therefore it is more relevant than the particle multiplicity alone. High inelasticity means that the energy is dissipated quickly and the shower develops fast. Low inelasticity means that the leading particle carries off most of the energy, leading to slow developing and long showers (4). The inelasticity of a single interaction is described by a parameter k, defined as the fraction of the total energy directed into new pion production (both $\pi^{\pm}$ and π^{0}). The parameter k has value when its smaller than 1, i.e. its more effective in low energy, but is not well known at high energy, i.e. $K \geq 1$. In an interaction initiated by a particle with energy E_0 We develop in the same fashion as before, but adjusting the method to account for $k < 1$. We find that the muon size increases with energy as:

$$N_{\pi} = \left[\frac{E_0}{\xi_c^{\pi}}\right]^{\beta} . \quad (10)$$

And β will equal to:

$$\beta = \frac{ln[1+N_{ch}]}{ln\left[(1+N_{ch})/\left(1-\frac{1}{3}k\right)\right]} \cong$$

(11)

$$\approx 1 - \frac{k}{3\ln[N_{ch}]} = 1 - 0.14k$$

(14)

The muon size increases at a faster rate ($k < 1$) than ($k \geq 1$) as the Figure (3) shows [7].

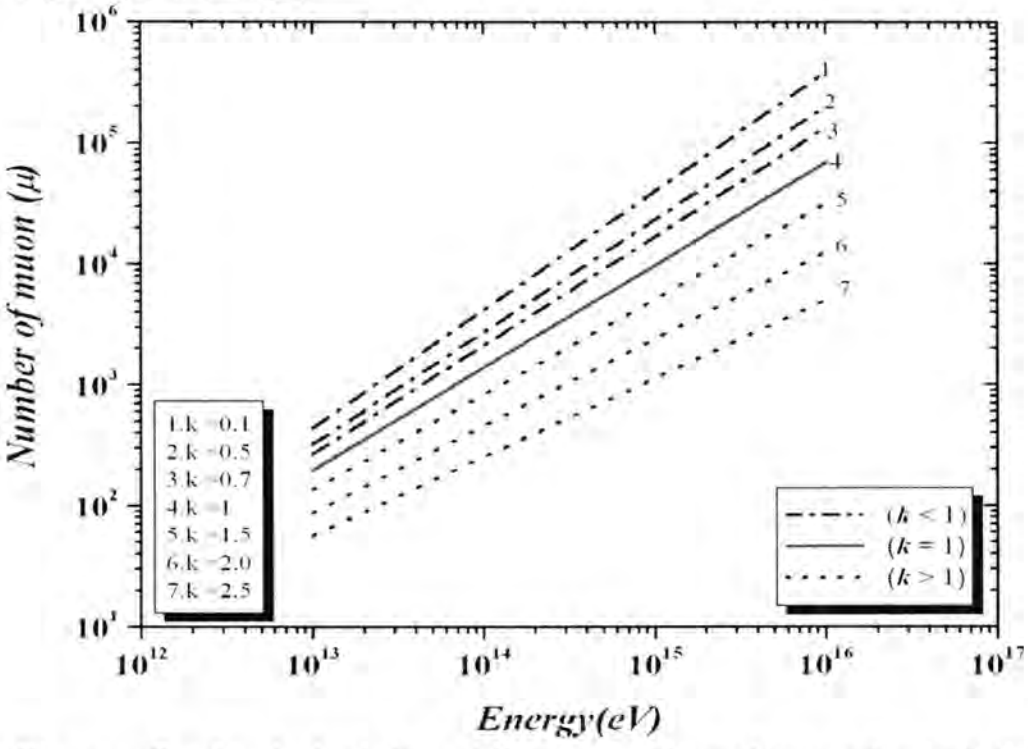

Figure – 3: the dashed dotted line is number of muon for k<1 the solid line is number of muon for k=1.the dotted line is the number of muon for k>1.

In this work, the number of secondary particles (muons, pions, electrons, and density of particles at maximum) in Extensive Air Shower have been calculated at energy range (10^{13}-10^{16}) *eV*. Also we obtained the depth of shower maximum, X_{max}, for electromagnetic and hadronic cascades for photon, iron nuclei and proton in the same energy range. The inelasticity, which is depends on the parameter (k) for hadronic showers, have been included. The results show that the number of muons will be increased when $k < 1$ and decreased when $k \geq 1$.

REFERENCES

1. Matthews, J.: Astropart, Phys .22: 385 (2005).
2. Giller, M.; Stojek, H.; Wieczorek, G.: Extensive air shower characteristics as functions of shower age. Int. J. Mod. Phys.A.20, (29) : 6821-6824 (2005).
3. Baltrusaitis R.M.et al.,Nucl. Instr.and Meth.in Phys.Res.A240, 410 (1985).
4. Antoni T. et al., (KASCADE Collaboration), J. Phys. G: Nucl. Part. Phys. 27, 1785 (2001).
5. W. Heitler, The Quantum Theory of Radiation, third ed.,Oxford University Press, London, (Section 38) : 386 (1954).
6. Matthews, J.: A Heitler model of extensive air showers. Astropart. Phys. , 22. : 387-397 (2005).
7. Alvarez-Muniz J., et al., Phys. Rev. D 66:033011 (2002) .

Influence of Co Doping on the Optical Properties of ZnO Thin Films

Nadir Fadhil Habubi, Reem Saadi Khaleel and Sami Salman Chiad
nadir_fadhil@yahoo.com, reem.saadi@yahoo.com, samichiad2003@yahoo.com
Al_Mustansiriyah University, College of Education, Physics Department

الخلاصة

حضرت نماذج من اوكسيد الخارصين النقي والمشوب بنسبتين مختلفتين (1%,3%) بتقنية التحلل الكيمياني الحراري.
تم دراسة تأثير التشويب بالكوبلت على طيف الامتصاص لأغشية ZnO, قيست النفاذية البصرية (T %) في مدى الاطوال الموجية nm (300-1100) للأغشية المرسبة على الزجاج, ابدى معامل الامتصاص اعتمادا اسيا على طاقة الفوتون محققا قانون اورباخ عند حافة الامتصاص وكان معتمدا على نسبة التشويب. الثوابت البصرية كمعامل الانكسار, معامل الخمود وثوابت العزل (ε_r),(ε_i) حسبت وربطت مع نسبة الاشابة.

ABSTRACT

Undoped and Co doped ZnO samples with two different percentage of Co content (1 %, 3 %) were prepared by a chemical spray deposition technique.

The effect of doping with cobalt on the absorption spectra of ZnO thin films has been studied. The optical transmission (T %) in the wavelength range (300-1100) nm of films deposited on glass was measured. The absorption coefficient exhibits exponential dependence on photon energy obeying Urbach's rule in the absorption edge, it was found to be doping dependent. Optical constants like refractive index, extinction coefficient and dielectric constants (ε_r),(ε_i) are calculated and correlated with sputtering time

INTRODUCTION

ZnO is one of the few metal oxides which can be used as a transparent conducting oxide. It has some advantages over other possible materials such as In_2O_3,Cd_2SnO_4 or SnO_2 due to its unique combination of interesting properties: non-toxicity, good electrical ,optical and piezoelectric behavior, and its low cost.**(1)** It is used as transparent conducting electrode material for various applications such as solar cells, organic light-emitting diodes, flat panel displays, blue and ultraviolet light emitters, gas sensors.(2).The device application of micro and nanostructure of ZnO is one of the major focuses among researchers to diminish the size of the device in order to achieve higher speeds in its electrical transport and also to study the effect of confinement on optical properties. The interest in doping ZnO is to explore the possibility of tailoring its electrical, magnetic and optical properties.**(3)**

Many techniques have been adopted to prepare ZnO thin films such as magnetron sputtering, thermal evaporation, low temperature chemical bath method, chemical spray pyrolysis.(4),electrochemical deposition.(5), hydrothermal method.(6), reactive plasma deposition.(7), pulsed enhanced chemical vapor deposition.(8), sol-gel (9), pulsed laser deposition.(10), RF- magnetron sputtering.(11).

The absorption spectra in the lower region (IR) are useful in studying the molecular vibrations. The higher energy region (UV) can be useful to manifest the electronic states of the atoms **(12)**

In the present investigation, some optical proprieties of ZnO films are studied as a function of cobalt concentration.

MATERIALS AND METHODS

ZnO and cobalt doped ZnO thin films were deposited using spray pyrolysis technique. An homogeneous was prepared by dissolving $ZnCl_2$ supplied from Fluka (99.99 % purity) of 0.1 M in distilled water. One to two drops of HCl was added to prevent the formation of zinc hydroxide. Similarly, aqueous solution of $CoCl_2.6H_2O$ was used to obtain Co doped films. Slide glass microscope were used as a substrate to support ZnO films. The substrate is then placed on the plate and heated progressively until the deposition temperature is reached. Prepared solution was sprayed with a glass nozzle on to the substrate, kept at 400 °C at a spraying rate of about 10 ml/min using air as a carrier gas. The nozzle was kept at a distance of 28 cm from substrate surface the observations were repeated with several films doped under identical conditions so as to be sure about the consistency of the results. The conditions mentioned above were found to be optimum so far as the qualities of the films are concerned.

Layer grown had good adhesion to their substrates. The average thickness of the film were measured by optical interference method and were found to be in the rang of 0.3 ± 0.05 nm. Optical transmission and absorption measurement were performed with a shimadzu UV-VIS-NIR spectrophotometer over the wavelength range (300-1100) nm

RESULTS AND DISCUSSION

For most applications, high transmission in the visible range is important. The transmittance spectra for undoped ZnO and different concentration of Co doped ZnO are shown in Figure (1).

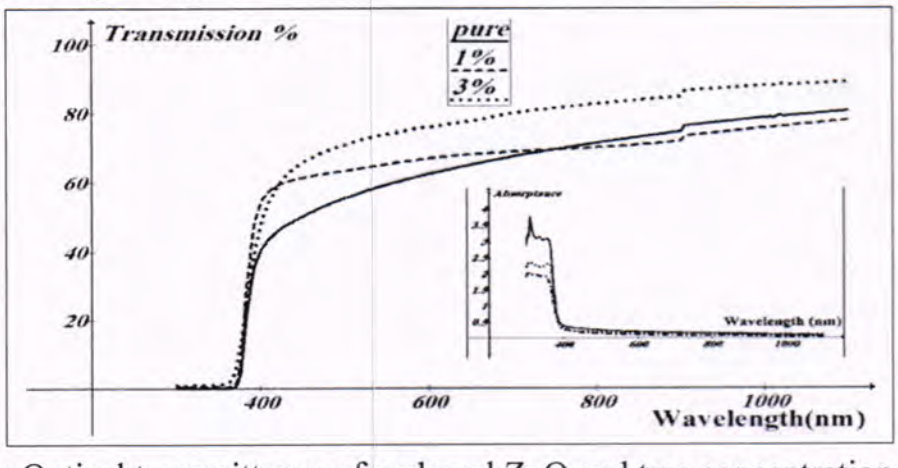

Figure -1: Optical transmittance of undoped ZnO and two concentration of Co doped ZnO, the inset illustrates the absorptance as a function of wavelength.

In general the transmittance increases when the doping concentration increases, the average transmittance of ZnO thin films in (400-1100) nm range increases "in average" from 60% for pure sample to about 80% for sample doped with 3% cobalt . Near the fundamental absorption edge all Films show a very sharp absorption edge. The transmittance is expected to depend mainly on three factors, (13) i.e., (1) oxygen

deficiency, (2) surface roughness; surface scattering reduces the transmittance which depends on the grain size, and (3) impurity centers. We can assume that the higher transmittance of the film with an increase of doping concentration is mainly due to the impurity centers.

The dependence of the absorption coefficient α, on photon energy is important in studying energy band structure and the type of transition; it was estimated by the transmittance data.

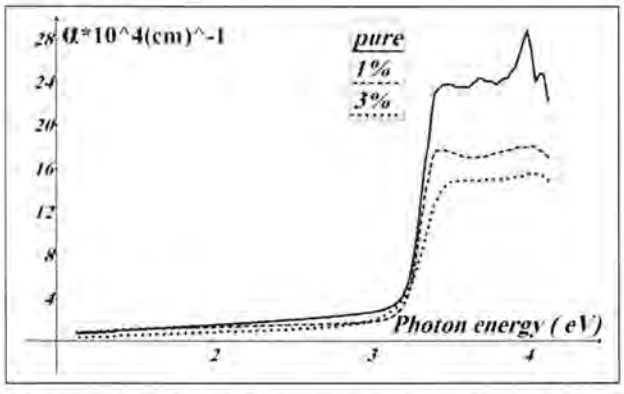

Figure -2: Absorption Coefficient as a function of Photon energy (eV) .

From figure (2) absorption coefficient decreases with concentration of doping, this behavior could be explained by the variation of the carrier concentration with respect to the doping concentration. At short wavelength (α) takes higher value ($\alpha \geq 10^4$) cm^{-1} and then decreases with increasing λ (decreasing photon energy), this might be attributed to the lattice absorption bonds correspond to the electronic transitions between highest filled energy bands to lowest empty band as well as transition through the defect centers such as impurities .

The optical absorption and particularly the absorption band edge is a good method for studying optically induced transition and gives information about the structure and optical energy gap in thin films. The absorption edge in many materials follows the Urbach rule:**(12)**

$$\alpha(f) = \alpha o \exp(\hbar f / E_e)$$

where, αo is a constant and (E_e) is the energy width of the tail of localized state in the normally forbidden band gap. E_e is often interpreted as the width of the localized states in the band gap of the material. E_e is estimated from the slopes of $\ln(\alpha)$ vs hf plots, figure(3) represents such dependence. The energy width of the tail (E_e) could be obtained by extrapolating the linear portions of these curves. The increasing of localized states with doping concentration from E_e (pure) = 0.093 eV to E_e (3%) = 0.161 eV refer to the increase in impurity concentrations, which in turn causes the increasing of energy gap as it was explained by Burstein-Moss effect.

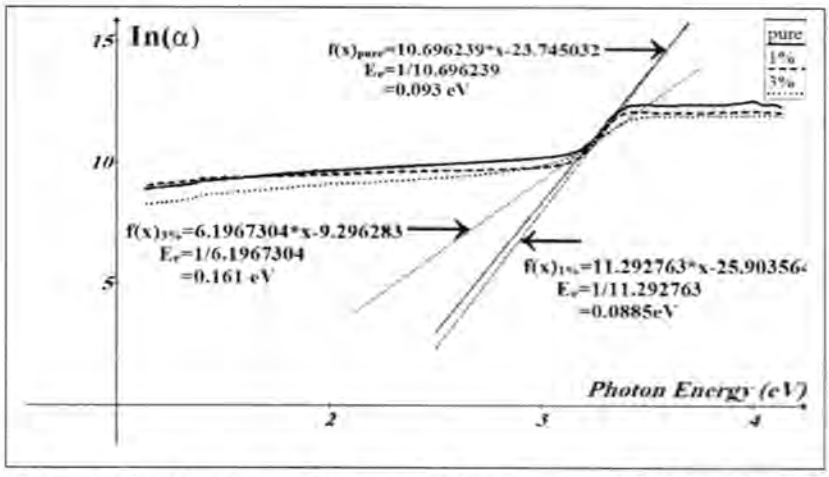

Figure-3: Relation between lnα and photon energy hf for ZnO:Co.

Refractive index is one of the fundamental properties for an optical material, because it is closely related to the electronic polarizability of ions and the local field inside materials. The evaluation of refractive index of optical material is important for many applications especially in optical devices. Figure (4) shows the variation of refractive index with photon energy, beyond fundamental edge toward higher photon energy (n_0) increases with doping concentration. Extinction Coefficient (K_0) represents the imaginary part of complex refractive index and it can be defined as the amount of energy losing as a result of interaction between the light and the charge of medium.**(13)** Figure (5) shows the extinction coefficient (k_0) as a function of photon energy, the behavior of (k_0) is corresponding to that for (α). In general (k_0) for all films decreases with increasing wavelength , and its have high values in spectral region with high absorption coefficients , but its values are small in "transparent" region where absorption coefficients are low ; this behavior refers to direct electronic transitions .**(14)**

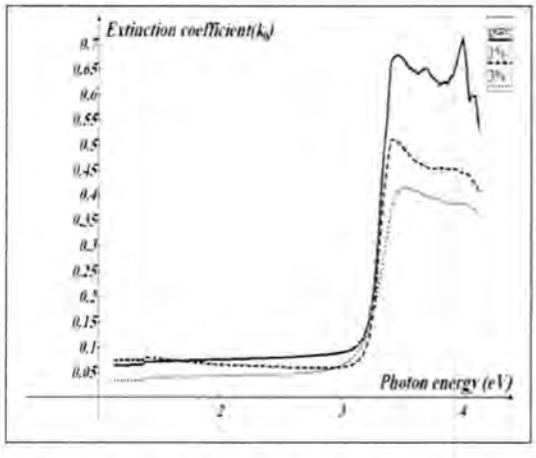

Figure -4: Refractive Index versus Photon energy.

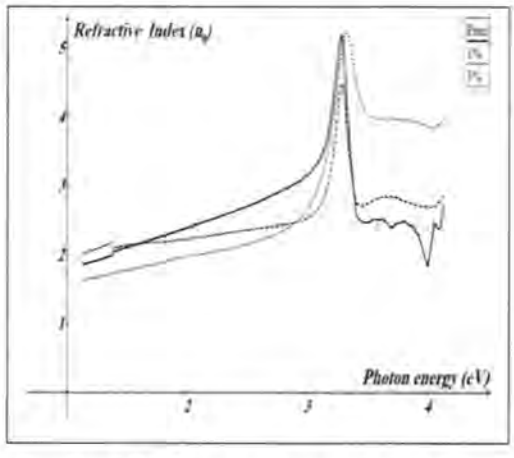

Figure-5: Extinction coefficient versus Photon energy

The dielectric constants consists of real part (ε_r) and imaginary part (ε_i) ,the variations of them with photon energy were determined and shown in figure (6) and(7).

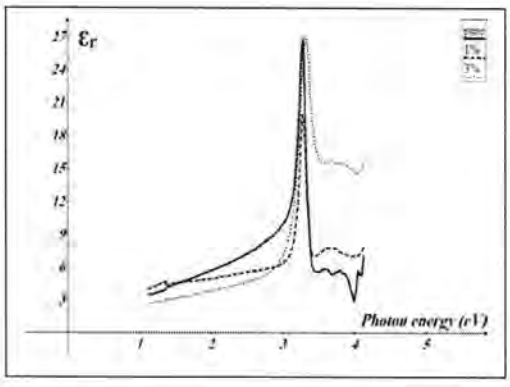

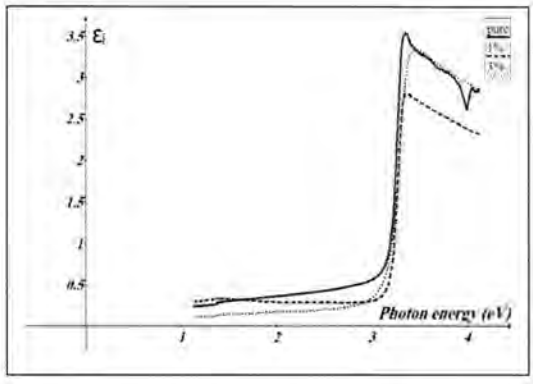

Figure-7: ε_i versus Photon energy. **Figure-6: ε_r versus Photon energy.**

It is useful to define a characteristic ''skin'' thickness that is subject to an appreciable density of optical energy. A convenient form used widely is simply the inverse of α, i.e. 1 / α. This skin depth is usually denoted by χ (**15**):

$$\chi = 1 / \alpha$$

In other words ,the electromagnetic wave will have amplitude reduced by a factor 'e' after traversing a thickness (called the skin depth) (**16**). In long wavelength greater than absorption edge, skin depth increases with doping concentration as shown in figure (8), this might be due to decrease the probability of absorption with doping concentration and the amplitude of the incident photons will be reduced by a factor 'e' through the short distance within the film thickness .

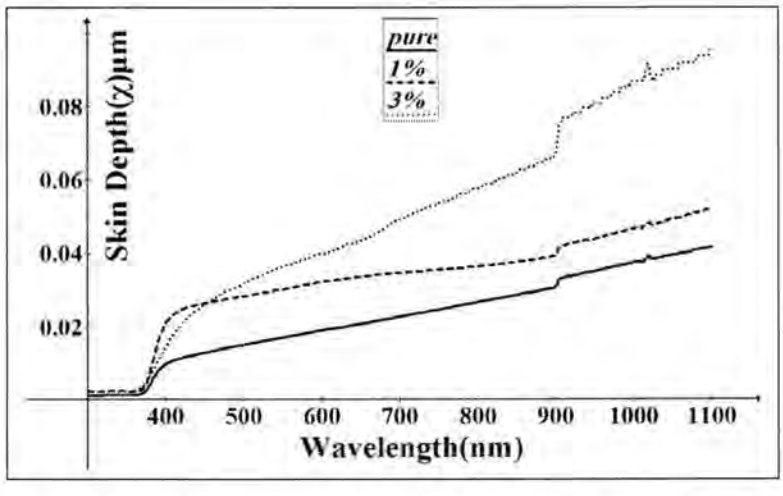

Figure -8: Skin depth (χ) as a function of wavelength.

The value of the absorption coefficient increase very fast at high photon energy region, this behavior support the assumption of using these thin films for fabrication of photodectors, and light emitting diode.

The transmition of 1 % cobalt doped ZnO remains approximately constant in the visible region which allow these material to be used as antireflection coating thin this region, the localized states were increase as the doping percentage increased.

It is clearly seen from the curve of skin depth versus wavelength is increased sharply in 3 % cobalt doped ZnO.

REFERENCES

1. Seeber W.T., Abou-Helal M.O., Barth S., Beil D., Hoe Che T., Afify H.H. and Demian S.E., Transparent semiconducting ZnO:Al Thin Films Prepared by Spray Pyrolysis, Materials Science in Semiconductor Processing,2:45-55, (1999).
2. Wang Y.G.,Lau S.P.,Lee H.W.,Yu S.F.,and Tay B.K., Comprehen -sive Study of ZnO Films Prepared by Filtered Cathodic Vacuum arc at Room Temperature,Journal of applied physics.94:31,(2003).
3. Major S., Banerjee A., and Chopra K. L., Highly Transparent and Conducting Indium-Doped Zinc Oxide Films by Spray Pyrolysis, Thin Solid Films, 108: 333-340, (1983).
4. Kadi Allah F.,Yapi Abe S.,Nunez C.M., Khelil A.,Cattin L.,Morsli M.,Bernede J.C.,Bougrine A.,del Valle M.A.and Dıaz F.R., Charac -terisation of Porous Doped ZnO Thin Films Deposited by Spray Pyrolysis Technique,Applied Surface Science,253:9241–9247, (2007).
5. Gur E., Asil H., Coskun C. Tuzemen S., Meral K., Onganer Y. and Serifoglu K., Optical and Structural Properties of ZnO Thin Films Effects of High Energy Electron Irradiation an Annealing, Nudear Instruments and Methods In Physics Research, 266: 2021, (2008).
6. Bai S. N., Tsai H. H. and Tseng T. Y., Structural and Optical Properties of Al – Doped ZnO Nanowires Synthesized by Hydrothermal Method, Thin Solid Films,516:155, (2007).
7. Yamada T., Nebiki T., Shimoto S. K., Makino H., Awa K., Narusawa T., and Yamamoto T., Dependence of Structural and Electrical Properties on Thickness of Polycrystalline Ga – Doped ZnO Thin Films Prepared by Reactive Plasma Deposition,Super lattices and Microstructures,42:68, (2007).
8. Zou W.Q, Mo Z. R., Lu Z. L., Lu Z. H., Zhang F. M. and Du Y. W., Magnetic And Optical Properties of Zn1-xCoxO Thin Films Prepared Yy Plasma Enhanced Chemical Vapor Deposition, Physica B, 403:3686, (2008).
9. Wang M., Kim E. J., Kim S., Chung J. S., Yoo I-K., Shin E. W., Hahn S. H. and Park C., Optical And Structural Properties of Sol- Gel Prepared MgZnO

Alloy Thin Films, Thin Solid Films, 516: 1124, (2008).

10. Zhu B. L., Sun X. H., Zhao X. Z., Li F. H., Wu X. G., Wu J., Wu R. and Liu J., The Effects of Substrate Temperature on The Structure Properties of ZnO Films Prepared by Pulsed Laser Deposition, Vacuum, 82: 495, (2008).
11. Wang X. H., Yao B., Shen Di Z., Zhang Z. Z., Li B. H., Wei Z. P., Lu Y. M., Zhao D. X., Zhang J. Y., Fan X. W., Guan L. X. and Cong C. X., Optical Properties of P- Type ZnO Doped By Lithium and Mtrogen, Solid Stste Communications, 141:600, (2007).
12. Abu El-Fadl A., El-Maghraby E. M., and Mohamad G. A., Influence of Gamma Radiation on the Absorption Spectra and Optical Energy Gap of Li-Doped ZnO Thin Films,.Cryst. Res. Technol, 39 (2): 143 – 150, (2004).
13. Jeong Ju-Hyun, Jeon Young-Sun, Jeon Kyung-Ok, Hwang Kyu-Seog and Kim Byung-Hoon, Preparation of Zinc Oxide Films by an Electrostatic Spray Deposition Process, Journal of Ceramic Processing Research, 7 (1): 70-74, (2006).
14. Ahmed F. H., A Studu of The Influence of Thermal Treatement on Optical and Electctrical Properties of (BaTiO3) Thin Films, Thesis, College of Science, AL-Mustansiriay University, (2003).
15. khaleel R.S., Fabrication of CdSe Detector Using Vacuum Evaporation Technique and Studing its Electro – Optical Properties, Thesis , College of Education for Women , University of Baghdad, (1998).
16. Eloy J. F. , Power Lasers , National School of Physics, Grenoble , France , John Wiley & Sons, :59 (1984).

Study of Optical Properties of (LiF) Thin Films Prepared by Thermal Evaporation

Wafaa M. Saleh , Abdulla A.Rasheed and Asaad M. Abbas
Al-Mustansiriyah University , College of Science, Department of Physics

الخلاصة

دُرست الخصائص البصرية لاغشية فلوريد الليثيوم (LiF) بسمكين مختلفين (300,400)nm.
وتم قياس طيف النفاذية والامتصاصية للاغشية في مدى الاطوال الموجية (200,1100)nm. وحساب فجوة الطاقة البصرية حيث وجد ان فجوة الطاقة تقل مع زيادة السمك. ودرس التغير في معامل الانكسار (n) ومعامل الخمود (K) لمعرفة الكفاءة البصرية لاغشية (LiF).

ABSTRACT

The optical properties of lithium fluoride (LiF) thin film have been studied for two thickness (300,400)nm. The transmittance and absorbance of thin film were measured in the wavelength range (200-1100)nm.The optical band gap has been calculated, it was found that the optical band gap decreases with the increasing of film thickness.The variation of refractive index (n)and extinction coefficient(K) with thicknss have been studied to analyze optical efficiency of (LiF) thin film.

INTRODUCTION

LiF thin films are extensively studied because of their interesting chemical, electrical and optical properties (high band gap, transparent to UV-visible light, low refractive index) which are considered for various optical applications such as windows, prism and lenses in the vacuum UV, visible and infrared (1,2). It is also very useful for x-ray monochromaters and for the study of fundamental properties and defect in crystal(3).

Also single crystal LiF has been base-lined as one of the optical materials for the Near-Infrared Camera (NIRCam) on the James Webb Space telescope (JWST) optically, this material is outstanding for use in the near IR(4).

LiF is one of the most widely used material for thermoluminescence dosimeters(TLD). The primary reason for this is that LiF has a near-tissue equivalent responsible radiation. This property makes it excellent for use in personal dosimeters or for diagnosis and therapy in Medicine. On the other hand, the sensitivity of LiF is considerably less than that of non-tissue equivalent material(5).

MATERIALS AND METHODS

The thin films of Lithium fluoride LiF were prepared by thermal evaporation system type Edwards coating unit model E306. On microscope glass slides as a substrates at room Temperatur. under low pressure. The thermal chamber was evacuated down to (10^{-5}mbar) by the diffusion pump.

The glass slides were sequentially cleaned in an ultrasonic both with acetone and ethanol. Finally they were rinsed with distilled water and dried, then molybdenum boat source is used for the deposition of LiF thin films, different thickness of LiF films were prepared by using theoretical formula given by:[6]

$$t = \frac{M}{2\pi\rho R^2} \qquad \text{.....(1)}$$

Where:

M=mass of material

ρ=density of material

R: distance between the substrate and the boat

In the present work the structure of the LiF thin films on glass substrates have been investigated by X-ray diffraction using the apparatus, (Philips X-ray Diffractometer) type Cuke (t=1.5456Å), I=20mA, V=40KV.

The transmission and absorption spectra of LiF thin films at different thickness, have been recording in the wave length range (200-1100) using double-beam spectrophotometer (UV-210Å Shimedza).

RESULTS AND DISCUSSION

A. Structure

Fig.(1) illustrate the X-ray diffraction patterns of LiF films which were as-deposited at R.T at thickness 400nm-500nm. From the Figure it was found that all films were crystalline and this satisfy agreement with reported research(7,8).

B. Optical Properties

Fig.(2) show the UV-VIS spectra LiF thin films for different thickness in wavelength range 200-1100nm.

Initially it has been observed that the transmittance is lowest the wavelength which are shorter than cut off wavelength λ_c, which is (210nm) of LiF. After that we observe increasement in the transmittance with wavelength. The maximum transmittance get was almost 95% at λ>250nm, i.e. in visible and the near infrared region .

Also we notice the thickness of the films don't effect on transmission spectral. This characteristic agree with published papers(9).

Fig.(3) show the change of the absorption coefficient of LiF films as a function of the change of the incident photon energy the absorption coefficient (α) has been calculated by using the equation[10]:

$$\alpha = \frac{2.303A}{d} \qquad \text{.....(2)}$$

Where

A: is the absorption at a cetain wavelength

d= is the thickness of the film.

It is observed that the absorption coefficient α increase slightly with the incident photon energy until 500nm. After that (α)increases roughly, and that value is greater than ($10^4 cm^{-1}$). Also it was noted α increases with increasing the thickness of the film this behaviour is attributed to the increasing of absorbance with thickness [10].

Fig.(4) show the allowed band gap by the plotting the variation of $(\alpha h\upsilon)^2$ with the photon energy (hυ) of LiF films by using the equation[11]:

$$\alpha h\upsilon=\beta(h\upsilon-eg)^r \quad \text{.....(3)}$$

The energy gap of the LiF films at thickness (400nm-500nm) has been found to be (5.3, 5.25)eV respectively by a straight line from the $(\alpha h\upsilon)^2$ and intersect with the photon axis (hυ) at [$(\alpha h\upsilon)^2$=0)] points.

The intersection point represents the value of the allowed direct band gap. It is noticed that the values of the band gap of LiF films decreases slightly with the increasing of thickness this satisfy with may authors.

Also Forbidden direct gap was calculated by plotting the relation $(\alpha h\upsilon)^{2/3}$ with the photon energy (hυ) of LiF films at thickness (400nm, 500nm as in fig (5), it has been noticed that the same case of direct allowed band gap.

Extinction coefficient was determined by using the relation(12):

$$K_o = \frac{\alpha\lambda}{4\pi} \quad \text{.....(4)}$$

Fig.(5) show that the extinction coefficient K_o changes with the change of the incident photon energy (hυ). The extinction coefficient values obtained in this work range between (0.01-0.06) for the wavelength (200-700nm).

Fig.(6) show the results of the calculation of the refractive index (n) for LiF thin films for different thickness. The refractive index have the value between (1.38-1.5) at wavelength 550 nm (hυ=2.55) .

Lithium fluoride thin films (LiF) good transmittance in the uv-visible region XRD technique showed a single crystal structure of LiF thin films.

The optical properties of LiF thin films showed it have low refractive index and extinction coefficient. LiF thin films have high energy gap value (5.3, 5.25) ev for thickness (400-500)nm respectively.

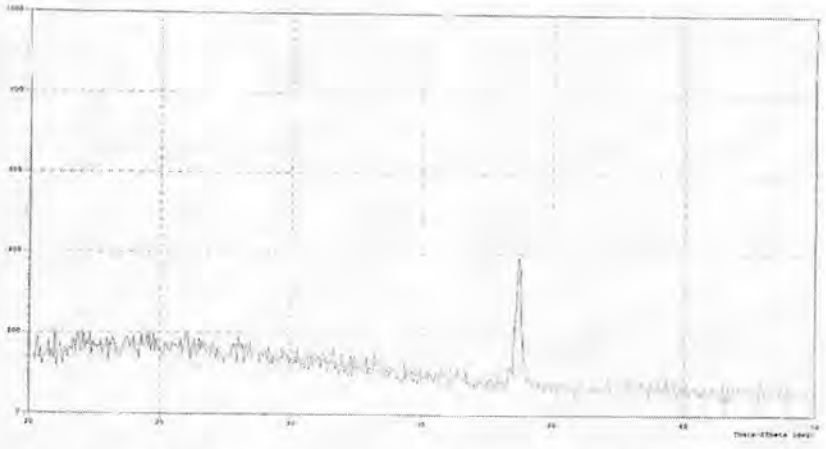

Fig.-1: Show the x-ray diffraction patterns of LiF films

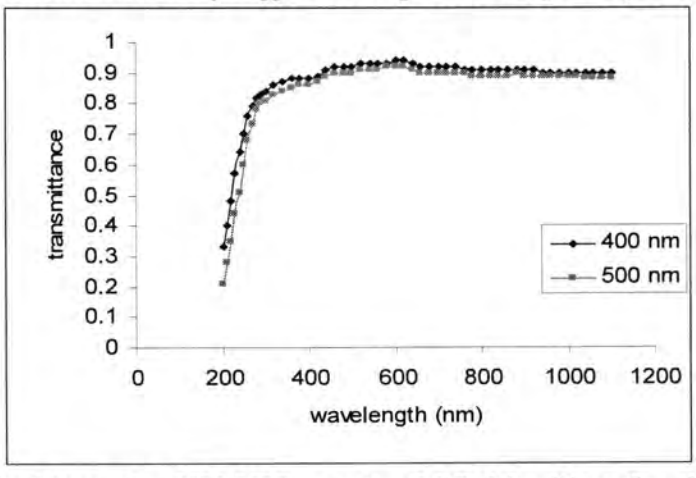

Fig.-2: Show the UV-VIS spectra LiF thin films for different thickness.

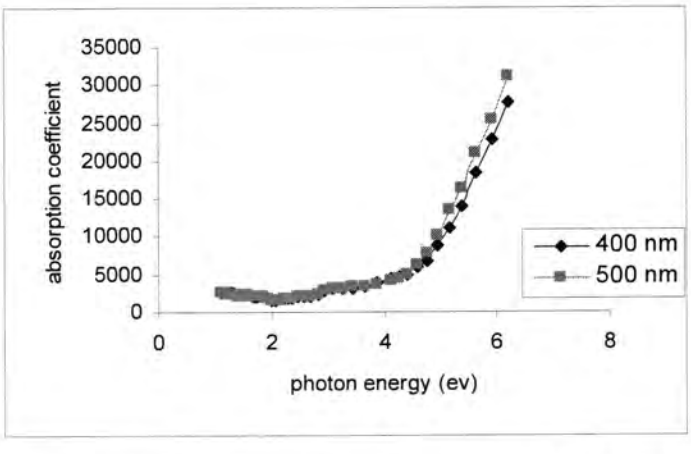

Fig.-3: show the change of the absorption coefficient of LiF films with photon energy

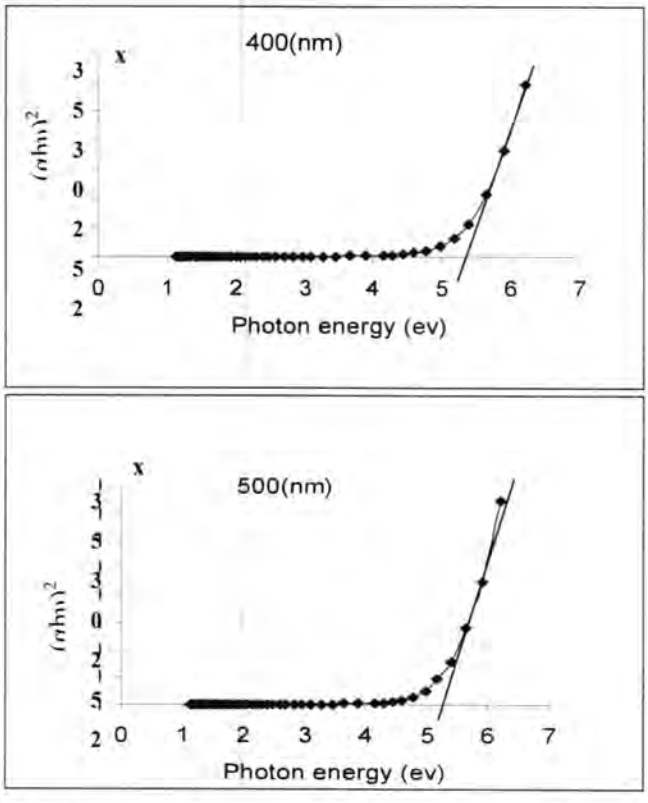

Fig.-4: Show the allowed direct band gap (a) t=400nm , (b) t=500nm

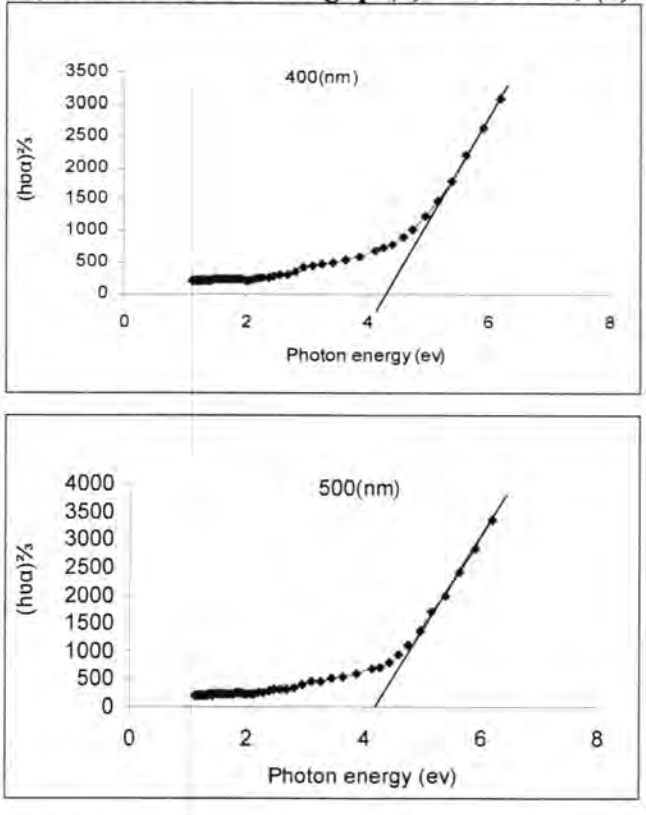

Fig.5: Show the forbidden direct band gap (a) t=400nm , (b) t=500nm

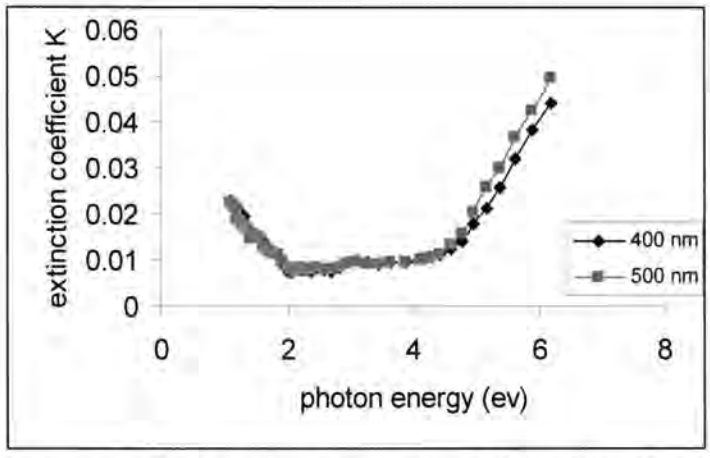

Fig.-6:change of extension coefficient (K_o) with photon energy

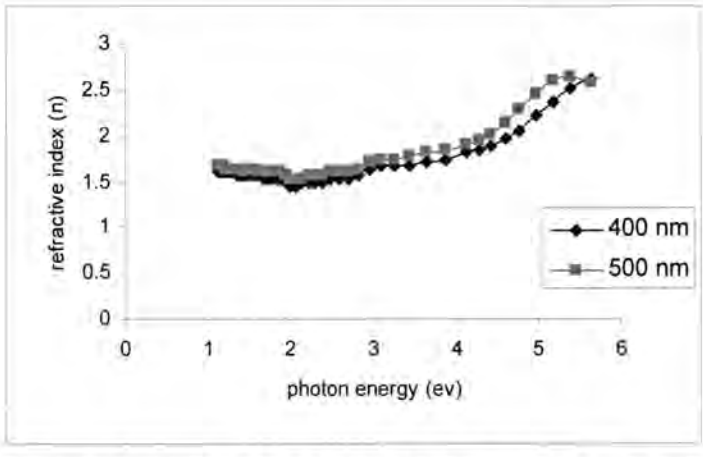

Fig.-7: show the results of the calculation of the refractive index (n) for LiF thin films for different thickness.

REFERENCES

1. P.Heath and P.Sacher, "Quality crystals and optics for laser application ",Applied opt, 15, 937(1986).
2. S.Scaglione and R.M.Montereali, "F-colour centers and lithium nano clusters in ion-beam assisted LiF thin films" journal of optoelectronics and advanced materials. 7.1(2005).
3. L. Reale, "X-Ray microscopy research and technique" ,(2008).
4. E. Todd Kvamme and J. C.Earthman, "lithium fluoride material properties as applied on the NIRCam instrument", nasa Goddard space flight center,(2006).
5. M.A.Forostiere and R.M.Montereali, "Leaky modes in lithium fluoride thick films thermally evaporated on glass",optics communication ,217 :249-256(2003).
6. B. Roitan, "Deposition technology for films and coatigs", Noyes publishing park ridge, New Jresey:170-237(1982).

7. L. Ekertova, "physics of thin films", plenum press. New York and London,(1977).
8. M. Montecchi and S. Baccaro, "point defects in lithium fluoride films induced by gamma irradiation" 7th international conference, advanced technology and particle physics, (2001).
9. A.Moses, "spray pyrolysis deposition and characterization of highly (100) oriented magnesium oxide thin films", Crystal Res.Technol .42.4,976 (2007).
10. J.Tanc, "Amorphous and liquid semiconductors" London, (1974).
11. J. I.Pankove "optical process in semiconductors", Prentice Hall Inc, (1971).
12. B. Sapoval, C. Hermang,"physics of semiconductor" verlag,Newyork,Inc. (1995).

High Lightness Image Enhancement Using Adaptive Histogram Equalization Algorithm

[1]Hazim G. dway , [2]Hana H. kareem, [3]Firaas K. Nsaif and [4]Baidaa K. Hamed
[1.4]Al-Mustansiriyah University /College of Science/ Department of Physics
[3]Baghdad University /College of Education-Ibn Alhaitham/ Department of Physics

الخلاصة

الهدف الرئيسي من تحسين الصورة هو معالجتها للحصول على صور افضل من الصورة الاصلية ولتطبيق محدد. في هذا البحث تم تقديم خوارزمية تحسين جديدة لتحسين الصور عالية الاضاءة هي خوارزمية تسوية الهستوغرام المقترحة بالاعتماد على فضاء YIQ عن طريق معالجة مركبة الاضاءة فقط ثم استخدام التحويل العكسي من هذا الفضاء الى الفضاء الاساسي RGB ثم صححت الالوان باستخدام نظرية تعتمد على نظام الرؤية للانسان. تمت مقارنة النتائج مع خوارزمية تسوية الهستوغرام عن طريق حساب معدل مربع الخطأ العياري بين الصورة الاصلية ذات الاضاءة الجيدة والصورة المعالجة كذلك المخططات التكرارية لكلا الطريقتين اخذت بنظر الاعتبار. الخوارزمية المقترحة اظهرة كفاءة افضل في تحسين الصور عالية الاضاء عند مقارنتها مع خوارزمية تسوية الهستو غرام.

ABSTRACT

The Principle objective of Images enhancement is to process an image so that result is more suitable than original image for specific application. This search describe a new image enhancement algorithm which is apply to enhance low lightness images called adaptive histogram equalization AHD algorithm dependent on YIQ color space via processed only lightness component then used inverse transformation from YIQ color space to basic color space and color correction dependent on retinex theory. The results was compared with Histogram Equalization HE algorithm by calculate normalize mean square error NMSR between processed images and original images with fair lightness, histogram of both method enhancement was a account. Adaptive algorithm has best efficiency in enhanced low lightness compared with HE algorithm.

Keywords: contrast, high lightness, Histogram Equalization, adaptive Histogram Equalization, color transformation.

INTRODUCTION

Producing digital images with good brightness/contrast and detail is a strong requirement in several areas including vision, remote sensing, biomedical image analysis, and fault detection. Producing visually natural images or transforming the image such as to enhance the visual information within is a primary requirement for almost all vision and image processing tasks. Methods that implement such transformations are called image enhancement techniques (1,2). Histogram equalization and its variations have traditionally been used to correct for uniform lighting and exposure problems. This technique is based on the idea of remapping the histogram of the scene to a histogram that has a near-uniform probability density function. This results in reassigning dark regions to brighter values and bright regions to darker values. Histogram equalization works well for scenes that have unimodal or weakly bi-modal histograms (i.e. very dark, or very bright), but not so well for those images with strongly bi-modal histograms (i.e. scenes that contain very dark and very bright regions) (3) there are number of studies as following:

1. D. J. Jobson, Z. Rahman, and G. A. Woodell 1996: introduced new algorithm to improve the brightness, contrast and sharpness of an image. It performs a non-linear spatial/spectral transform that provides simultaneous dynamic range compression (4).
2. B. V. Funt, K. Barnard, M. Brockington, and V.Cardei 1997: introduced investigations into Multi-Scale Retinex algorithm approach to image enhancement to explain the effect of the processing from a theoretical standpoint (5).
3. Mark Grundland and Neil A 2004. Dodgson presented an automated algorithm for global contrast enhancement of images with multimodal histograms. To locate modes and valleys, histogram analysis is performed by kernel density estimation, a robust nonparametric statistical method (6).
4. Osman Nuri & Capt. Ender 2007 proposed a new algorithm to enhance night scenes and under nonuniform lighting conditions, either the low intensity areas or the high intensity areas cannot be clearly seen dependent on non linear transform (7).
5. Nabeel M. Al Dalawy 2008: This research aimed to study the Quality of TV images and determined the type of the noise and the relationship between the mean and the standard deviation for regions illumination components of small rotating angles of the antenna. (8).

In this work, we introduce a new enhancement algorithm used to enhancement high lightness image called adaptive Histogram equalization (AHE) algorithm this algorithm dependent on traditional HE , processing lightness component in YIQ color space and logarithm function to correct color image. The outline of this paper is as follows: Section 2 shown histogram equalization. Section 3 describes the adaptive histogram equalization. Results and discussion are shown in Section 4, finally conclusion shown in Section 5

Histogram Equalization (HE)

A global technique that works well for a wide variety of images is histogram equalization (HE) If lightness levels are continuous quantities normalized to the range (0, 1), $p_r(r)$ denote the probability density function (PDF) of the lightness levels in a given image, where the subscript is use for differentiating between the PDFs of the input and output images. Suppose that is performed the following transformation on the input levels to obtain output (processed) intensity levels (9),

$$s = T(r) = \int_0^r p_r(w)dw \qquad \text{.....(1)}$$

Where w is a dummy variable of integration, that the probability density function of the output levels is uniform, that is[9]:

$$P_s(s) = \begin{cases} 1 & for \quad 0 \le s \le 1 \\ 0 & otherwise \end{cases} \quad \text{..... (2)}$$

When dealing with discrete quantities worked with histograms and called the preceding technique histogram equalization, where (4):

$$s_k = T(r_k) = \sum_{j=0}^{k} p_r(r_j) = \sum_{j=o}^{k} \frac{n_j}{n} \qquad k = 0.....L \qquad \text{..... (3)}$$

Where: r_k is normalized intensity level of the input image corresponding to the (un-normalized) intensity level k: $r_k = \frac{k}{L}$ (r_k=0..1) and (k =0.....L-1) and L =256 for lightness band with 8 bit/pixel), s_k corresponding normalized intensity level of the output image .The cumulative probability density function (CPDF) calculated by[9]:

$$p_c(r_k) = \sum_{j=0}^{k} p_r(r_j) = \sum_{j=0}^{k} \frac{n_j}{n} \quad \text{..... (4)}$$

r_j is normalized intensity level of the input image corresponding to the (un – normalized) intensity level j , and r_j given by :

$$r_j = \frac{j}{L} \quad , j = 0...L-1. \quad \text{..... (5)}$$

Where n_j being the number of pixel with intensity j and n is the total number of pixel of the image this algorithm done by using following steps:

1. Input color image $C(n,m,i)$, $i=1,2,3$ (red ,green& blue) components.
2. Normalize each component $r_j(i) = C(n,m,i)/ 255$ and calculated iteration of each gradual level $n_j(i)$, where $j=0,1,..255$.
3. Compute histogram from $P(r_j(i)) = n_j(i) /N$, where N being the size of image.
4. Calculate cumulative histogram by :

$$s_k(i) = \sum_{j=0}^{k} \frac{n_j(i)}{N} \quad \text{where } k=0,1,..255 .$$

5. *Replaced each normalized component $r_{j\,(i)}$ by value of $s_k(i)$ and we get out put image .*

3. Adaptive Histogram Equalization (AHE).

First step in the AHE is transform color image from basic RGB color space to YIQ color space and processing Y component only by using traditional HE algorithm, the forward transform given from following equations [10]:

$$\left.\begin{aligned} y &= 0.299r + 0.587g + 0.114b \\ i &= 0.596r - 0.27g + 0.322b \\ q &= 0.211r - 0.253g + 0.312b \end{aligned}\right\} \quad \text{..... (6)}$$

Where y is lightness component, i,q are chromatic components and r,g,b being red ,green and blue components of RGB color space respectively. And then inverse transformation used from YIQ to RGB given by (11):

$$\left.\begin{aligned} r &= y + 0.956i + 0.621q \\ g &= y - 0.272i - 0.647q \\ b &= y - 1.106i + 1.703q \end{aligned}\right\} \quad \ldots\ldots\ldots\ldots\ldots\ldots\ldots\ldots\ldots\ldots (7)$$

The lightness component has ratio of 80% from the data of image [10]. Second step is color correction or color restoration scheme that provides good color rendition for images that contain gray-world violations[12]. This method inspiration from retinex theory dependent on human visual perception from logarithm function given by(13):

$$In_i(x,y) = Ihe_i(x,y).I_i'(x,y,a) \quad \ldots\ldots\ldots\ldots\ldots\ldots\ldots\ldots\ldots\ldots (8)$$

Where

$$I_i'(x,y,a) = \log[1 + a\frac{I_i(x,y)}{\sum_{i=1}^{3} I_i(x,y)}] \quad \ldots\ldots\ldots\ldots\ldots\ldots\ldots\ldots\ldots\ldots (9)$$

Where $Ihe_i(x,y)$ is histogram equalization of the image results from inverse transformation from YIQ color space , $I_i(x,y)$ is original color image

(i=1,2,3 being red, green and blue bands) and a is default constant equal 120 in this work , we have taken the liberty to use $log(1+x)$ in place of log(x) to ensure a positive result.

The data results from equation (8) has negative value and its histogram has large tails, thus finely step is gain-offset by 0.35 and 056 respectively where:

$$Iahe_i(x,y) = 0.35(In_i(x,y) + 0.56) \quad \ldots\ldots\ldots\ldots\ldots\ldots\ldots\ldots\ldots\ldots (10)$$

AHE algorithm can be done from following steps:

1. Input color image $C(n,m)$.
2. Transform color image $C(n,m)$ from RGB space to YIQ space and estimated lightness component $Y(n,m)$.
3. Normalize lightness component $r_j = Y(n,m)/255$ and calculated iteration of each gray level n_j , where $j=0,1,..255$.
4. Compute histogram from $P(r_j)=n_j/N$, where N being the size of image.
5. Calculate cumulative histogram by :

$$s_k = \sum_{j=0}^{k} \frac{n_j}{N} \quad \text{, where } k=0,1,..255 .$$

High Lightness Image Enhancement Using Adaptive Histogram Equalization Algorithm

[1]Hazim G. dway , [2]Hana H. kareem, [3]Firaas K. Nsaif and [4]Baidaa K. Hamed
[1,4]Al-Mustansiriyah University /College of Science/ Department of Physics
[3]Baghdad University /College of Education-Ibn Alhaitham/ Department of Physics

الخلاصة

الهدف الرئيسي من تحسين الصورة هو معالجتها للحصول على صور افضل من الصورة الاصلية ولتطبيق محدد. في هذا البحث تم تقديم خوارزمية تحسين جديدة لتحسين الصور عالية الاضاءة هي خوارزمية تسوية الهستوغرام المقترحة بالاعتماد على فضاء YIQ عن طريق معالجة مركبة الاضاءة فقط ثم استخدام التحويل العكسي من هذا الفضاء الى الفضاء الاساسي RGB ثم صححت الالوان باستخدام نظرية تعتمد على نظام الرؤية للانسان. تمت مقارنة النتائج مع خوارزمية تسوية الهستوغرام عن طريق حساب معدل مربع الخطأ العياري بين الصورة الاصلية ذات الاضاءة الجيدة والصورة المعالجة كذلك المخططات التكرارية لكلا الطريقتين اخذت بنظر الاعتبار. الخوارزمية المقترحة اظهرة كفاءة افضل في تحسين الصور عالية الاضاء عند مقارنتها مع خوارزمية تسوية الهستو غرام.

ABSTRACT

The Principle objective of Images enhancement is to process an image so that result is more suitable than original image for specific application. This search describe a new image enhancement algorithm which is apply to enhance low lightness images called adaptive histogram equalization AHD algorithm dependent on YIQ color space via processed only lightness component then used inverse transformation from YIQ color space to basic color space and color correction dependent on retinex theory. The results was compared with Histogram Equalization HE algorithm by calculate normalize mean square error NMSR between processed images and original images with fair lightness, histogram of both method enhancement was a account. Adaptive algorithm has best efficiency in enhanced low lightness compared with HE algorithm.

Keywords: contrast, high lightness, Histogram Equalization, adaptive Histogram Equalization, color transformation.

INTRODUCTION

Producing digital images with good brightness/contrast and detail is a strong requirement in several areas including vision, remote sensing, biomedical image analysis, and fault detection. Producing visually natural images or transforming the image such as to enhance the visual information within is a primary requirement for almost all vision and image processing tasks. Methods that implement such transformations are called image enhancement techniques (1,2). Histogram equalization and its variations have traditionally been used to correct for uniform lighting and exposure problems. This technique is based on the idea of remapping the histogram of the scene to a histogram that has a near-uniform probability density function. This results in reassigning dark regions to brighter values and bright regions to darker values. Histogram equalization works well for scenes that have unimodal or weakly bi-modal histograms (i.e. very dark, or very bright), but not so well for those images with strongly bi-modal histograms (i.e. scenes that contain very dark and very bright regions) (3) there are number of studies as following:

Where y is lightness component, i,q are chromatic components and r,g,b being red ,green and blue components of RGB color space respectively. And then inverse transformation used from YIQ to RGB given by (11):

$$\left.\begin{aligned} r &= y + 0.956i + 0.621q \\ g &= y - 0.272i - 0.647q \\ b &= y - 1.106i + 1.703q \end{aligned}\right\} \quad \ldots\ldots\ldots\ldots\ldots\ldots\ldots\ldots\ldots\ldots (7)$$

The lightness component has ratio of 80% from the data of image [10]. Second step is color correction or color restoration scheme that provides good color rendition for images that contain gray-world violations[12]. This method inspiration from retinex theory dependent on human visual perception from logarithm function given by(13):

$$In_i(x,y) = Ihe_i(x,y).I_i'(x,y,a) \quad \ldots\ldots\ldots\ldots\ldots\ldots\ldots\ldots\ldots\ldots (8)$$

Where

$$I_i'(x,y,a) = \log[1 + a\frac{I_i(x,y)}{\sum_{i=1}^{3} I_i(x,y)}] \quad \ldots\ldots\ldots\ldots\ldots\ldots\ldots\ldots\ldots\ldots (9)$$

Where $Ihe_i(x,y)$ is histogram equalization of the image results from inverse transformation from YIQ color space , $I_i(x,y)$ is original color image

(i=1,2,3 being red, green and blue bands) and a is default constant equal 120 in this work , we have taken the liberty to use $log(1+x)$ in place of log(x) to ensure a positive result.

The data results from equation (8) has negative value and its histogram has large tails, thus finely step is gain-offset by 0.35 and 056 respectively where:

$$Iahe_i(x,y) = 0.35(In_i(x,y) + 0.56) \quad \ldots\ldots\ldots\ldots\ldots\ldots\ldots\ldots\ldots\ldots (10)$$

AHE algorithm can be done from following steps:

1. Input color image $C(n,m)$.
2. Transform color image $C(n,m)$ from RGB space to YIQ space and estimated lightness component $Y(n,m)$.
3. Normalize lightness component $r_j = Y(n,m)/255$ and calculated iteration of each gray level n_j , where $j=0,1,..255$.
4. Compute histogram from $P(r_j)=n_j/N$, where N being the size of image.
5. Calculate cumulative histogram by :

$$s_k = \sum_{j=0}^{k} \frac{n_j}{N} \quad \text{, where } k=0,1,..255 .$$

6. Replaced each normalized component r_j by value of s_k and we get processing lightness component $Y_p(n,m)$.
7. Transform image from Y_pIQ to RGB color space, we get $Ihe_i(x,y)$.
8.Calculate color correction from $In_i(x,y) = Ihe_i(x,y).I_i'(x,y,a)$,where $I_i'(x,y,a) = \log[1 + a\frac{I_i(x,y)}{\sum_{i=1}^{3} I_i(x,y)}]$, a=120 .
9. Computed gain-offset value of $I_i'(x,y,a)$ from $Iahe_i(x,y) = 0.35(In_i(x,y) + 0.56)$
Where $Iahe_i$(x,y) being output image.

RESULTS AND DISCUSSION

In this work we captured four images from (Sony digital camera) with size (320×240) bmp type, two image with high lightness and another with moderate lightness (fair or original images) as shown in figure(1) . Original images are used to compare with processing images by calculated normalized mean square error (NMSE) that given by[10]:

$$NMSE = \frac{1}{N \times M}\sum_{x=1}^{N}\sum_{y=1}^{M}(\frac{Io(x,y) - Ip(x,y)}{255})^2 \quad \text{..... (11)}$$

Where Io being the lightness of fair image captured with preparation lightness its size ($N \times M$) and Ip is the lightness of processing image resulted from HE, and AHE algorithm.
From figure (2-a , 2-c) we noted in AHE enhanced images were more obvious however, increased contrast and lightness compared with image enhancement by using HE as in figure (2-b, 2-d) .While in figure (2-e,f,g & h) shown histogram distribution of high lightness images and fair images, we noted in high lightness image the histogram nears from white region due to high lightness, however in enhancement images the histogram nears from histogram of fair images as in figure (2-e,f,g & h) with increasing in variance. The distribution of histogram in processing images reflected in NMSE as shown in table (1) appeared from these values the minimum value in image enhanced by AHE algorithm.

Table- 1: NMSE values for high lightness image and enhanced images resulted from HE , AHE algorithm.

Image	High lightness	HE	ADH
(a)	0.0952	0.0761	0.0742
(b)	0.0821	0.0607	0.0438

The AHE algorithm is efficiently method to enhance high lightness images compared HE Algorithm due to color correction that restorated in AHE. This

algorithm is restored many features that lost in high image because high illumination due to increase the lightness and decrease the contrast in high lightness images.

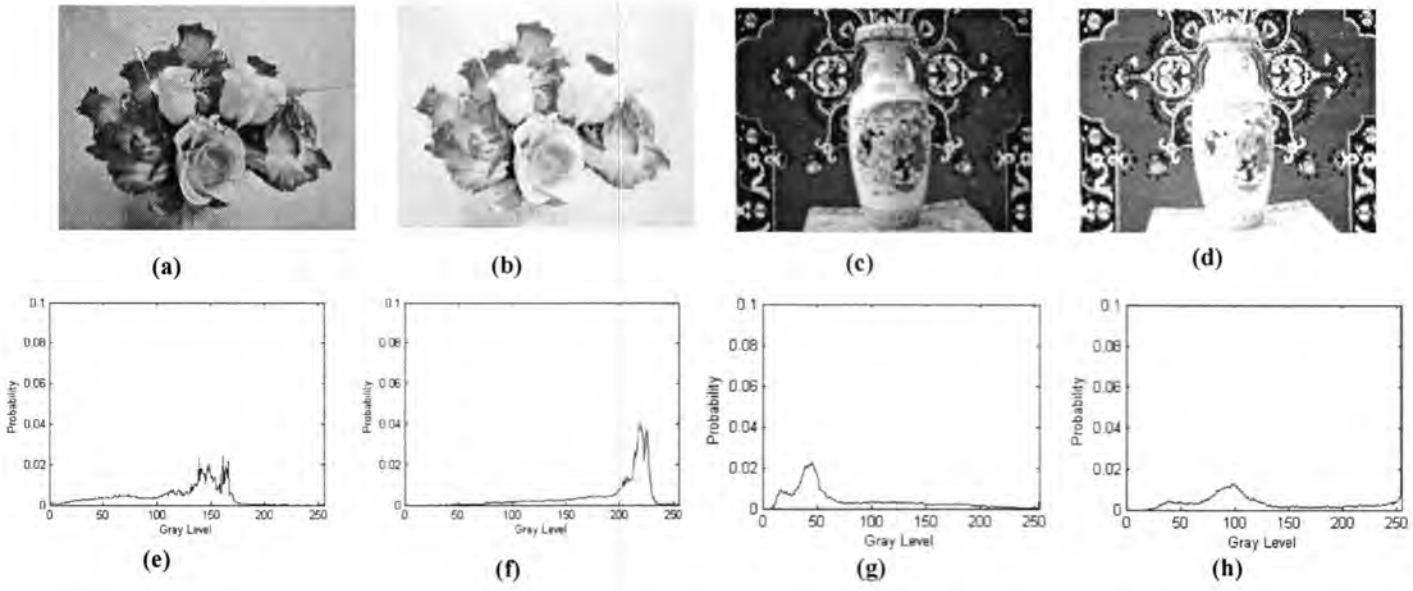

Figure -1: Upper row represent :
(a) Original image 1. (b) High lightness images 1. (c) Original images 2. (d) High lightness l images 2. Lower row represent: histogram of (a), (b) ,(c)and(d) images respectively.

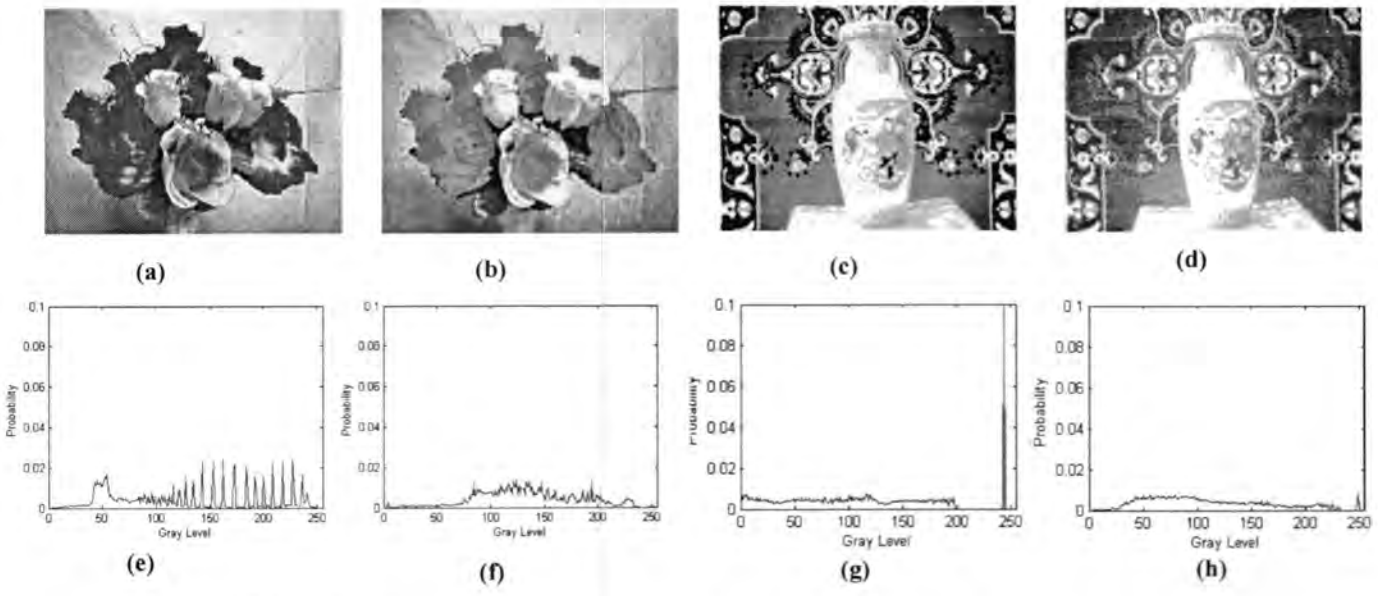

Figure -2:Upper row represent:
(a) Images 1 enhancement by using AHE . (b image 1 enhancement by using HE.
(c) Images 2 enhancement by using AHE. (d) Image 2 enhancement by using HE.
Lower row represent: histogram of (a), (b) ,(c)and(d) images respectively.

REFERENCES

1.R. C. Gonzalez, "Digital Image Processing Using MATLAB" , Prentice-Hal , (2004).
2. A. K. Jain," Fundamentals of Digital Image Processing". Englewood Cliffs, NJ: Prentice-Hall, (1991).
3. Z. Rahman, G. A. Woodell, and D. J. Jobson, "A Comparison of the Multiscale Retinex With Other Image Enhancement Techniques," Proceedings of the IS&T 50th Anniversary Conference, May (1997).
4. D. J. Jobson, Z. Rahman, and G. A. Woodell, "Properties and performance of a center/surround retinex," IEEE Trans. on Image Processing 6:451–462,March (1996).
5. B. V. Funt, K. Barnard, M. Brockington, and V.Cardei, "Luminance-based multi-scale Retinex",Proceedings AIC Color 97, Kyoto, Japan, (1997) .
6. Mark Grundland and Neil A. Dodgson ,"Automatic Contrast Enhancement by Histogram Warping ",Computational Imaging and Vision, 32 : 293-300, Springer. ISBN 1-4020-4178-0 , (2004).
7. Osman Nuri & Capt. Ender," A non-linear Technique for the enhancement of extremely non-uniform lighten images ", journal of aeronautics and space technologies, june,(2007).
8. Nabeel M. Al Dalawy, "TV Image Quality Study of Broadcasting Television Terrestrial Channels", M.Sc. Thesis, Physics Department, Al Mustansiriya University, 2008.
9. R. C. Gonzales and R. E. Woods," Digital Image Processing. Reading", MA: Addison-Wesley, (1987).
10. S.J. Sangwine and R. E.N. Horne" The color image processing Handbook", Chapman & Hall (1998).
11. Haim Levkowitz, "Color theory and modeling for computer graphics, visualization, and multimedia applications ", Kluwer Academic Publishers, (1997).
12. D.Jabson, Z.Rahman, and G.A. Woodel, "A multi-scale retinex for bridging the gap between color images and the human observation of scenes," IEEE Trans. Image Process. 6 : 965-976, July (1997).
13. Barnard, K. and Funt, B., "Analysis and Improvement of Multi-Scale Retinex," Proc. Fifth IS&T Color Imaging Conference," Scottsdale (1997).

Effect of Incident Photon Energy on the Optical Conductivity and Carrier Concentration of the Thermally Evaporated ZnO:Al Thin Film

Ali J. Mohammed ,Ibraheem R. Agool and Mohannad Sh. Kashkool
Department of Physics, College of Science, Al-Mustansiriya University.

الخلاصة

في هذا البحث تم تحضير غشاء اوكسيد الخارصين المشوب بالالمنيوم بتقنية التبخير الحراري .
تم دراسة تاثير طاقة الفوتون الساقط على بعض الخصائص البصرية (اعتمادا على قياس النفاذية) وبالذات على تركيز حاملات الشحن والتوصيلية الضوئية , وحساب معامل الامتصاص ومعامل الخمود .
الدراسة بينت زيادة حادة في تركيز حاملات الشحن والتوصيلية الضوئية خصوصا لطاقة الفوتون ضمن المنطقة القريبة من حافة الامتصاص وبحدود طاقة الفجوة , وبسبب حصول اعلى امتصاص في هذه المنطقة وكذلك فان ادنى مقدار للنفاذية هو في المنطقة ادنى من حافة الامتصاص.

ABSTRACT

All doped ZnO thin film was prepared by thermal vacuum evaporation technique. The effect of incident photon energy on the optical (carrier concentration and conductivity) of the prepared sample , depending on the transmission, absorption and extinction coefficient . Sharply increasing of carrier concentration and conductivity was recorded when the incident energy increased nearly the band gap region depending on the high absorption .

Keywords: *ZnO films , Thermal evaporation , TCO films*

INTRODUCTION

Transparent conducting oxide (TCO) films have found extensive applications in optoelectronic devices (for example, solar cells (1), liquid crystal displays, heat mirrors and multiplayer photo-thermal conversion system (2). Zinc oxide has attracted attention as a transparent conducting oxide because of its (i) large band gap (_3.3eV) , (ii) high conductivity, (iii) ease in doping, (iv) chemical stability in hydrogen plasma , (v) thermal stability when doped with III group elements , and (vi) abundance in nature and non toxicity (3). Zinc oxide can be applied in UV-emitting diodes, piezoelectric devices, electron field emitters, heterogeneous catalyst for methanol synthesis and short wavelength electrooptic devices (4).

Several deposition techniques are used to grow zinc oxide ZnO and aluminium-doped zinc oxide (AZO) thin films. These include chemical vapor deposition (CVD) (5), magnetron sputtering (6), spray pyrolysis (7,8), and pulsed laser deposition (PLD) (9). The optical properties of ZnO thin films were studied (10) .

MATERIALS AND METHODS

The film sample was prepared by using an alloy of zinc oxide doped with 3% aluminum The alloy prepared and then thermally evaporated on the glass substrate to produced a thin film of (272 nm) in thickness , the thickness of the film (t) was measured by using an (Optical Interference Fringes Method) employing the He-Ne laser (632nm) in wavelength , the thickness calculated from the relation

$$t = (\lambda / 2)\,(\Delta X / X) \quad \text{.....(1)}$$

where λ is the wavelength , ΔX is the dark fringe width and X is the distance between two neighboring fringes . In the measurements of transmittance of the film

at normal incidence was recorded wavelength range from 300 to 900 nm was detected using a double-beam spectrophotometer (Shimadzu UV 210A) operating in the UV/VIS .

RESULTS AND DISCUSSION

Transmittance is explained in Fig. (1) as a function of the incident photon energy for ZnO:Al thin film sample. The optical properties of the thermally evaporated film similar to those produced by using other methods. It is clear that the transmittance is continuously decreasing with increasing photon energy from 90% at about 1.5 eV to 30% at 3.4 eV .

Consequently, the absorption coefficient (α) is determined by the following relation:

$$\alpha = -(LnT)/t \quad \text{.....(2)}$$

Fig. (2) shows the calculated absorption coefficient rapidly increasing with the increasing

of incident energy .

This is a characteristic feature for all TCO thin films that they found many applications in

MIR optoelectronic devices. It is worth to mention that the absorption coefficient is necessarily determined by overall preparation conditions.

The extinction coefficient (*kex*) is determined by the following relation:

$$k_{ex} = \frac{\alpha\lambda}{4\pi} \quad \text{.....(3)}$$

So, its behaviour with energy shown in Fig. (3) is the same as for the absorption coefficient (α). The effect of the extinction coefficient on the refractive index, and hence

reflectance, is relatively higher than that of the real refractive index.

In order to determine the type of energy gap in the prepared ZnO:Al sample, $(\alpha h\nu)^n$ was plotted versus the incident photon energy, and the linear bahvior was obtained from the relation between $(\alpha h\nu)^2$ and $(h\nu)$ as shown in Fig. (4). It is explained that the prepared sample has a direct bandgap and the allowed absorption processes are the dominant.

Extrapolation of the linear portion of the plot to the energy axis yielded the bandgap value of about (3.12)eV,

The discrepancy between the obtained and reported values is attributed to the preparation

conditions of the samples as well as electron-electron and electron-impurity scattering.In all semiconductors, the optical properties are dependent of carrier concentration as these materials are mainly classified from conductors and insulators due to their properties. So, the relation between carrier concentration and incident photon energy for ZnO:Al thin film sample is shown in Fig. (5). As the carrier

concentration (*Ne*) is directly proportional to the plasma frequency (ω_p), which is in turn directly proportional to the absorption coefficient (α), as follows:

$$N_e = \frac{m_e \varepsilon_0}{e^2}\omega_p = \frac{m_e \varepsilon_0}{e^2}\left(\frac{\alpha c}{2}\right) \quad \text{.....(4)}$$

where *me* and *e* are electron mass and charge, respectively, and (ε_o)is the vacuum permittivity.

In highly n-doped semiconductor, the conduction band is shifted downwards by ΔE^{Ex}. The shift in absorption edge can be determined by:

$$\Delta E = E_g - E_{g0} = \Delta E^{BM} - \Delta E^{Ex} \quad \text{.....(5)}$$

Eg0 is the bandgap of intrinsic semiconductor.

Accordingly, as the photo-conductivity (σo) is a dynamic property of semiconductor, it is related to the carrier concentration (*Ne*) as[11]:

$$\sigma_o = \frac{2k_o e^2}{m_e} N_e \quad \text{..... (6)}$$

It is shown in Fig. (6) that the optical conductivity varies with incident photon energy just

same as the carrier concentration. So, the sample has high photoconductivity at the absorption edge of about (380 nm) due to the high absorption , then the ZnO:Al thin films highly efficient in the visible reign .

In order to determine the type of scattering contained in the ZnO structure . Free carrier absorption in an absorption spectrum is usually characterized by a monotonic . This spectrum expands with λ^p , where p varies between 1.5 to 3.5 and λ is the photon wavelength . The Drude theory for oscillasion of an electron driven by a periodic electric field in a metal leads to a dampening which increases as λ^2 . The oscillation with the semiconductor lattice , resulting in scattering by acoustic phonons , which leads to an absorption increase as $\lambda^{1.5}$. But scattering by optical phonons gives a dependence in $\lambda^{2.5}$, while scattering by ionized impurity will result on dependence of λ^3 or $\lambda^{3.5}$. A relation between Ln(λ)-Ln(α) is plotted, as shown in Fig. (7), to deduce the slope (p) as (12):

$$\boldsymbol{P = ln\ (\alpha) / ln\ (\lambda)} \quad \text{.....(7)}$$

The value of *p* is about 1.69 , this value means that the scattering caused by the acoustic phonons .

The optical parameters of the as deposited film were (4.5×10^4 cm^{-1}) absorption coefficient, (0.14) extinction coefficient, ($2 \times 10^{9} cm^{-3}$) carrier concentration which is directly depending on the band gap and sharply increased with the incident photon energy greater than band gap , (17 $F/cm^2.s$) maximum photo-conductivity, (3.12 eV) direct bandgap and the allowed absorption processes are the dominant , the optical scattering by the film is may be due to the annealing and non-doping contaminated impurities .

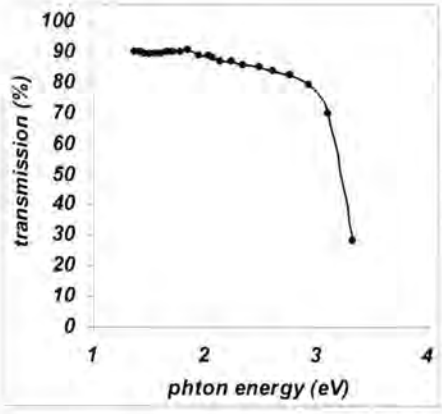

Fig. -1: T versus hv of prepared sample .

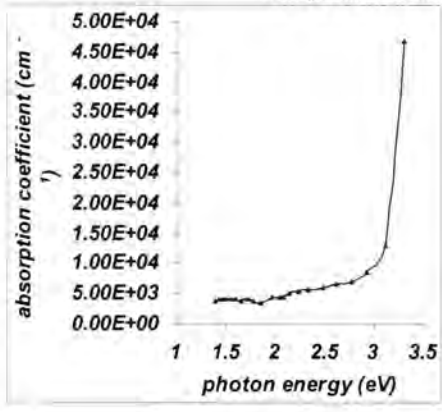

Fig. -2: α versus hv of prepared sample .

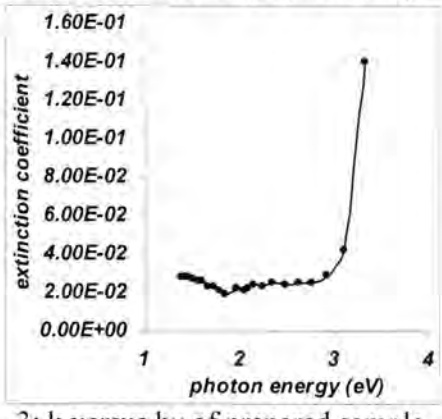

Fig. -3: k versus hv of prepared sample .

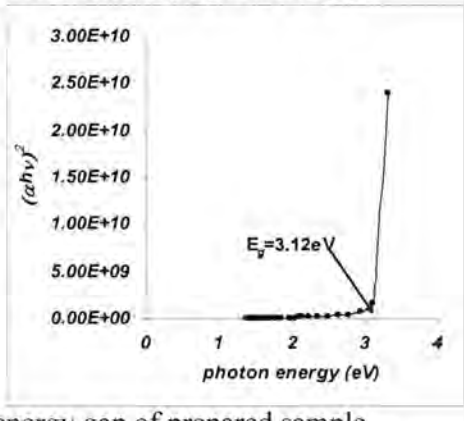

Fig. -4: energy gap of prepared sample .

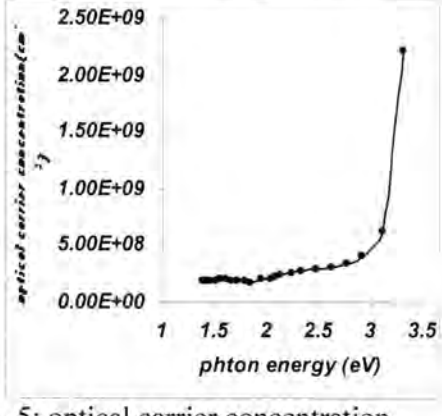

Fig. -5: optical carrier concentration .

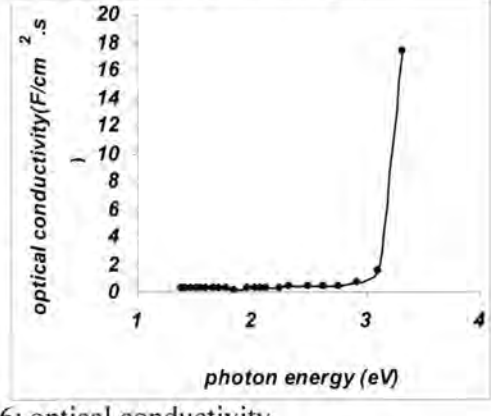

Fig. -6: optical conductivity

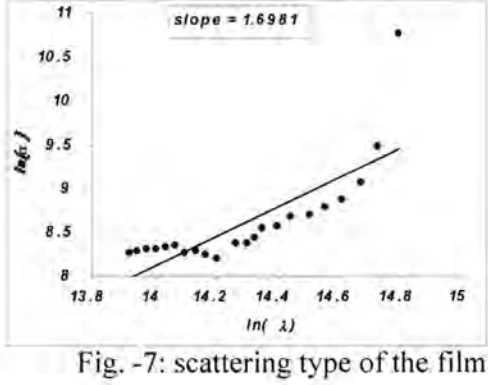

Fig. -7: scattering type of the film

REFERENCES

1. Kim T. Y. , Lee S. H. , Mo Y. H. , Nahm K. S. , Kim J. Y. , Suh E. K. , and Kim M. , " Growth Mechanism of Needle – Shaped ZnO Nano Structure Over NiO – Coated Si Substrates " , Korean J. Chem. Eng. , 21 , 733 , (2004) .
2. Haug F. J. , Geller Zs. , Zogg H. , and Tiwari A. N. , " Influence of Deposition Conditions on the Thermal Stability of ZnO : Al Films Grown by Magnetron Sputtering " , J. Vac. Sci. Technol. , A19 , 1 , 171 , (2001) .
3. Jeong S. H. , Park B. N. , Lee S. B. , and Boo J. H. , " Structural and Optical Properties of Silver Doped Zinc Oxide Sputtered Films " , Surf. Coat. Technol. , 193 , 340 , (2005) .
4. Zheng H. J. , Zhang L. D. , Li G. H. , and Shen W. Z. , " Fabrication and Optical Properties of Large – Scale Uniform Zinc Oxide Nanowire Array by One – Step Electrochemical Deposition Technique " Chem. Phys. Lett. , 363 , 123, (2002) .
5. Li X. , Yan Y. , Gessert T. A. , DeHart C. , Perkins C. L. , Young D. , and Coutts T. J. , " P- Type ZnO Thin Films by Formed by CVD Reaction of Diethylzinc and NO Gas " , Electrochemical of Solid – State Lett. , 6 , 4 , C56 , (2003) .
6. Jeong S. H. , Kho S. , Jung D. , Lee S. B. , and Boo J. H. , " Deposition of Al-Doped ZnO Films by RF Magnetron Sputtering and Study of their Surface Characteristics " , Surf. Coat. Technol. , 174 , 187(2003) .
7. Ronovich J. A. , Golompya D. , and Bube D. K. , " Preparation of ZnO – Doped Al Films by Spray Pyrolysis Technique " , J. Appl. Phys. , 51 , 4560 , (1980) .
8. Seeber W. T. , Abou – Helal M. O. , Barth s. , Beil D. , Hoche T. , Afify H. H. , and Demian S. E. , " Transparent Semiconducting ZnO : Al Thin Films Preparation by Spray Pyrolysis " , Mater. Sci. Semico. Proc. , 2 , 45 , (1999) .
9. Singh A. V. , Kumar M. , Mehra R. M. , Wakahara A. , and Yoshida A. , " Al – Doped Zinc Oxide Thin Film by Pulsed Laser Ablation " J. Indian Inst. Sci. , 81 , 527 , (2001) .
10. Mohammad A. J. , " Optical and Electrical Properties of ZnO Thin Films Prepared by Spray Pyrolysis Technique " , IJAP , 4 , 1 , 31 (2008).
11. Martin Von Allen and Andreas Blatter " Laser Beam Interaction with Materials , Physical Properties and Applications " , second edition , Springer , (1998) .
12. Smith, R.A, " Semiconductors " , Cambridge University Press, (1959).

Effect of Lithium Fluoride on Some Optical Properties of High Density Polyethylene

Asrar Abdul Muniam and Ahmed Hashim
Al-Mustansiriyah University, College of Science, Department of Physics

الخلاصة

في هذا البحث تم دراسة تأثير إضافة فلوريد الليثيوم على بعض الخواص البصرية للبولي اثيلين عالي الكثافة. ولهذا الغرض تم تحضير نماذج بإضافة فلوريد الليثيوم إلى البولي اثيلين عالي الكثافة وبنسب حجمية مختلفة من هذه الأملاح مع البوليمر وبسمك مختلف.تم تسجيل طيفي الامتصاص و النفاذية و لمدى الاطوال الموجية nm(300-1100). و حساب معامل الامتصاص و فجوة الطاقة للانتقال غير المباشر المسموح و الممنوع.

ABSTRACT

In the present work , effect of addition Lithium Fluoride on some optical properties of High Density Polyethylene has been studied . for that purpose , many samples has been prepared by adding Lithium Fluoride on the High Density Polyethylene by different volume percentages from these salts with polymer and by different thickness .The absorption and transmission spectra has been recorded in the wavelength range (300-1100)nm . The absorption coefficient and energy gap of the indirect, allowed, forbidden transition have been determined.

INTRODUCTION

Polymers have traditionally been considered as insulating materials by chemists and physicists alike . A conducting polymer is chewable and desirable . A light weight ready moldable , desirable conductive material has long been recognized as a worthwhile goal to work for(1,2).Researches, generally, have demonstrated that conductive polymers can be used as energy storage element in:(3,4)

1- Capacitors and Secondary batteries .
2- As semiconductor material in schottky diode.
3- Insulated gate field effect transitions (FET) and light emitting diodes.
4-As conductive layer for electromagnetic shelding (EMI) and electrostatic protection.

In the recent years conjugated conducting polymers have been the main focus of research throughout the world . Since the discovery led by 2000 chemistry Nobel winners, Shirakawa, MacDiarmid and Heeger , the perception that plastic could not conduct electricity has changed Nowadays, conducting polymers also known as conductive plastics are being developed for many uses such as corrosion inhibitors, compact capacitors, antistatic coating, electromagnetic shielding and smart windows; which capable to vary the amount of light to pass(5,6)

LiF material is extensively used because of interesting optical properties (high band gap, transparent to uv-visible light, low refractive index) which are considered for various optical applications such as windows, prism and lenses in the vacuum uv, visible and infrared here desired transmission in the 0.104μm-7μm range(7). It is also very useful for X-ray nonochromaters and for the study of fundamental properties and defect in crystal(8).

MATERIALS AND METHODS

The materials used in the papar is High Density Polyethylene as matrix and Lithium fluoride as a filler.

The electronic balanced of accuracy 10^{-4} have been used to obtain a weight amount of LiF powder and polymer powder .These mixed by Hand Lay up and the Microscopic Examination used to obtain homogenized mixture .The volume percentages of LiF which equivalent weight percentages are (0 , 19.73 , 35.1) vol%. The Hot Press method is used to press the powder mixture. The mixture of different LiF percentages have been compacted at temperature 110°C under a pressure 100 par for 10 minutes . Its cooled to room temperature , the samples were disc shap of a diameter about 30mm and thickness ranged between (1.85-2.2)mm. The transmission & absorption spectra of HDPE-LiF composites have been recording in the length range (300-1100) nm using double-beam spectrophotometer (UV-210°A shimedza).

RESULTS AND DISCUSSION

The absorption coefficient (α) was calculated in the fundamental absorption region from the following equation(9):

$$\alpha = 2.303\frac{A}{d} \quad \text{.....(1)}$$

Where : A absorbance , d the thickness of sample.

Figure (1) shows the relationship between the absorption coefficient and photon energy of the HDPE-LiF composites we note the change in the absorption coefficient is small at low energies this is indicates the possibility of electronic transitions is a low. At high energy , the change of absorption coefficient is large this is indicates the high Probability of electronic transitions are the absorption edge of the region (10). The absorption coefficient helps to conclude the nature of electronic transitions, when the high absorption coefficient values ($\alpha > 10^4 cm^{-1}$) at high energies we expected direct electronic transitions ,and the energy and momentum preserve of the electron and photon , when the values of absorption coefficient is low($\alpha < 10^4 cm^{-1}$) at low energies we expected in this case indirect electronic transitions, the momentum of the electron and photon preserves by phonon helps(11). The results showed that the values ofabsorption coefficient of the HDPE-LiF composites less than $10^4 cm^{-1}$ which indicates to the indirect electronic transition.

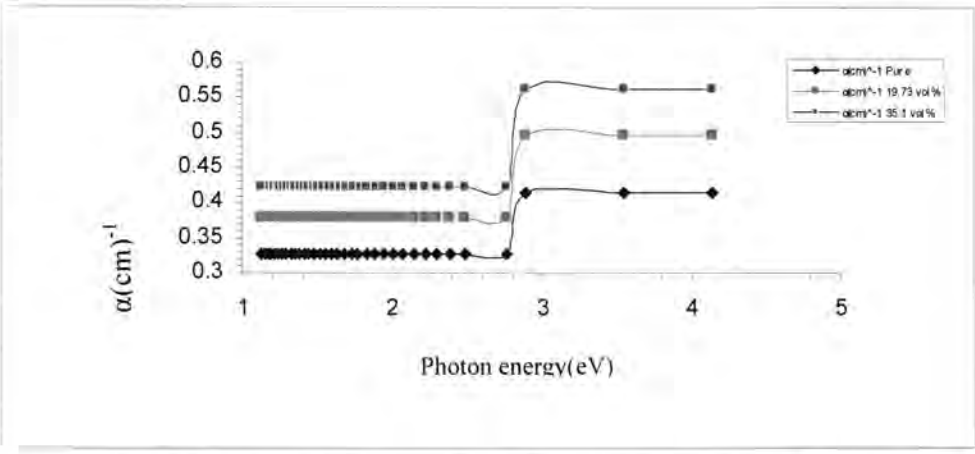

Figure -1: the relationship between the absorption coefficient and photon energy of the HDPE-LiF composites

The forbidden energy gap of indirect transition both allowed, forbidden calculated according to the relationship(12) :

$$\alpha h\nu = A(h\nu - E_g)^m \quad \text{.....(2)}$$

Where : hv the energy of photon , A proportionality constant, Eg forbidden energy gap of the indirect transition.

If the value of (m=2) indicates ton allowed indirect transition . when the value (m=3) indicates to forbidden indirect transition. Figure (2) shows the relationship between $(\alpha h\nu)^{1/2}$ $(cm^{-1}.eV)^{1/2}$ and the photon energy of pure polymer (HDPE) , with take over

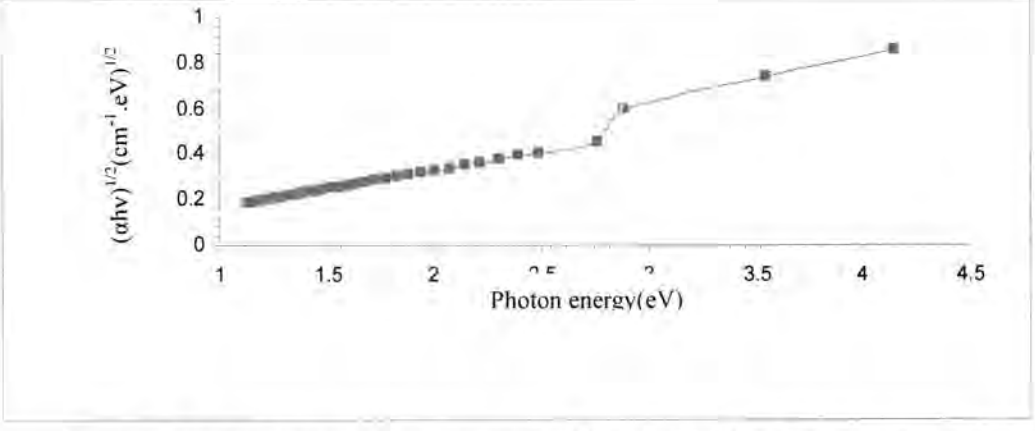

Figure -2: the relationship between $(\alpha h\nu)^{1/2}(cm^{-1}.eV)^{1/2}$ and photon energy of pure polymer (HDPE).

Part of the straight cut oriented axis at the point $(\alpha h\nu)^{1/2}=0$ will get the value of forbidden energy gap of the allowed indirect transition , which equal (2.64eV).Figure (3) and figure (4) represents the same relationship but to the polymer filled with (LiF) with volume percentages of LiF are(19.73 , 35.1) vol% ,the same way we can be

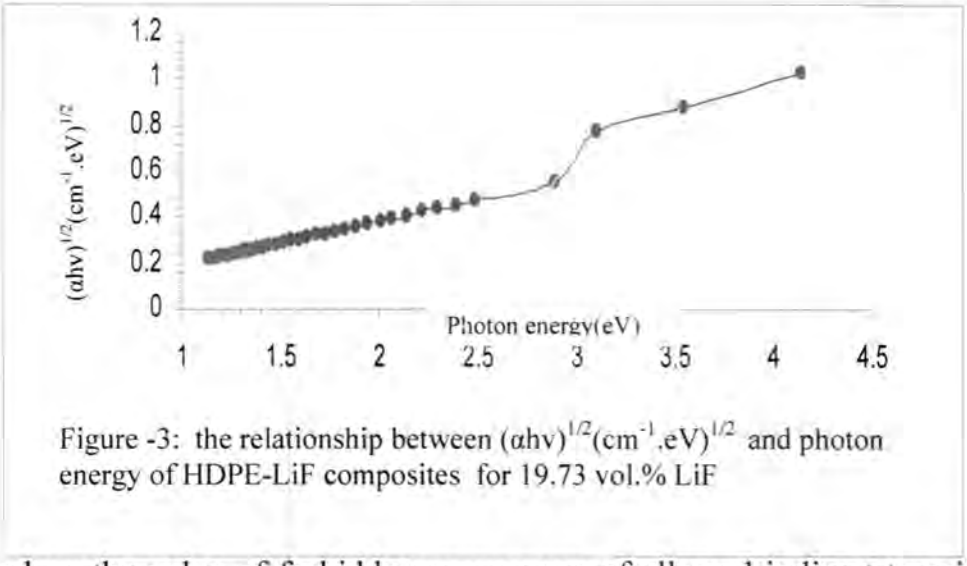

Figure -3: the relationship between $(\alpha hv)^{1/2}(cm^{-1}.eV)^{1/2}$ and photon energy of HDPE-LiF composites for 19.73 vol.% LiF

obtained on the value of forbidden energy gap of allowed indirect transition which equal (2.43eV) for 19.73 vol% LiF, and (2.1eV) for 35.1vol.% LiF .

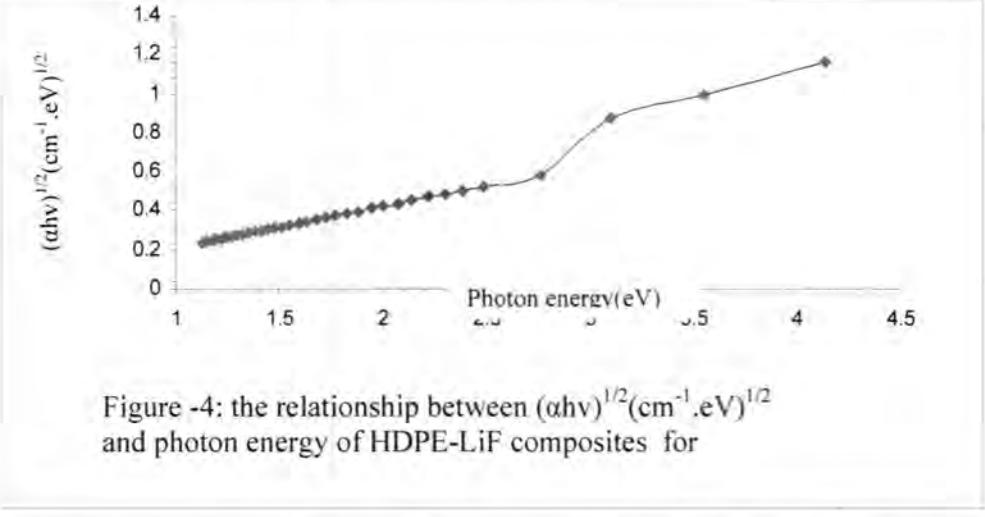

Figure -4: the relationship between $(\alpha hv)^{1/2}(cm^{-1}.eV)^{1/2}$ and photon energy of HDPE-LiF composites for

we note that the value of the forbidden energy gap decreases with increasing LiF concentration.. Figure(5) shows the relationship between the $(\alpha hv)^{1/3}$ $(cm^{-1}.eV)^{1/3}$ and photon energy of pure polymer (HDPE) , the same way we obtain to the forbidden

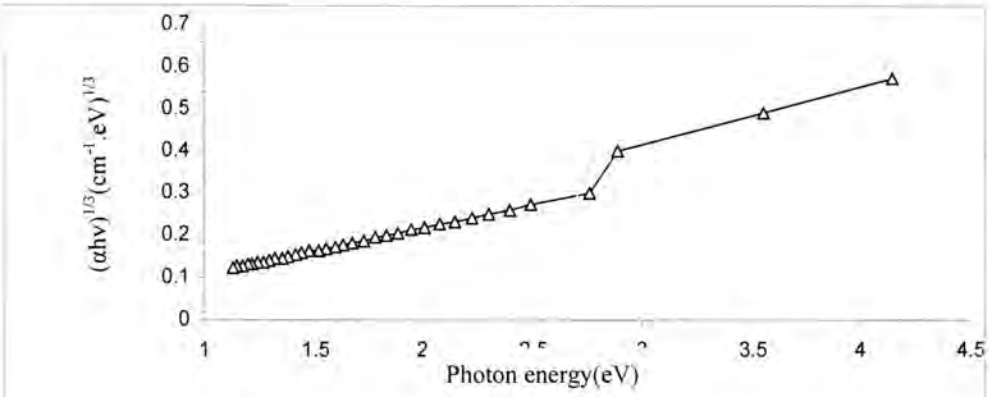

Figure -5: the relationship between $(\alpha hv)^{1/3}(cm^{-1}.eV)^{1/3}$ and photon energy of pure polymer (HDPE).

energy gap of forbidden indirect transition which equal (2.535eV). Figure (6) and figure (7) represents the same relationship but to the polymer filled with (LiF) with volume percentages of LiF are (19.73 ,35.1) vol% ,the same way we can be obtained on the value of the forbidden energy gap.

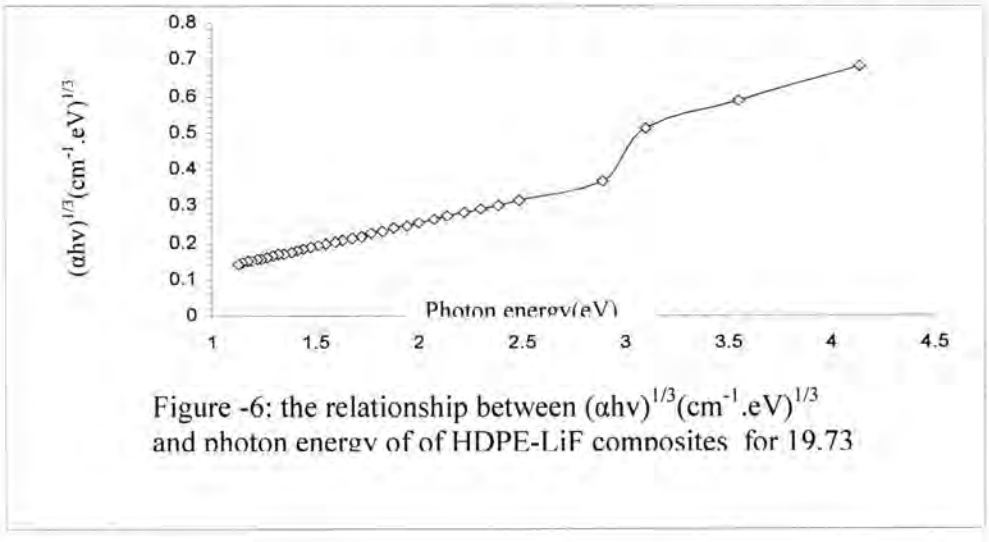

Figure -6: the relationship between $(\alpha hv)^{1/3}(cm^{-1}.eV)^{1/3}$ and photon energy of of HDPE-LiF composites for 19.73

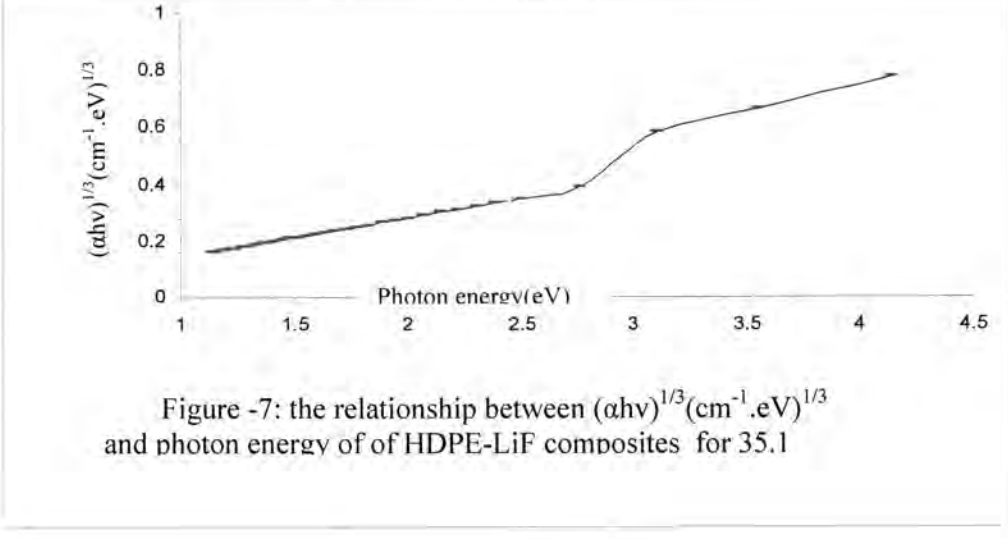

Figure -7: the relationship between $(\alpha hv)^{1/3}(cm^{-1}.eV)^{1/3}$ and photon energy of of HDPE-LiF composites for 35.1

of the forbidden indirect transition which equal (2.41eV) for 19.73vol.%LiF and (2.05eV) for 35.1 vol% we note that the value of the energy gap decreases with increasing LiF concentration(13).

We can conclude:

1.The absorption coefficient is increasing with increasing of the filler vol.% content.

2.The experimental results showed that the absorption coefficient less than $10^4 cm^{-1}$ this is indicates to forbidden and allowed indirect electronic transitions.

3.The LiF additive change not the nature of electronic transfers of HDPE samples.

4.The forbidden energy gap is decreasing with increasing of the filler vol.% content.

REFERENCES

1. Blyth A.R."Electrical properties of polymers",London-New York,., (1979).
2. Ramos M. V.," conductive polymer- copmposite Sensor for Gas Detection ", Newzeland, (2005).
3. Seanor D.A."Electrical properties of polymers", New York., (1982).
4. Alvarez M.P." Submicron Copper-Low-Density polyethylene conducting composites : Structural,Electrical and percolation Threshold",Chile, (2008).
5. 5-Harun M.H.,"Temperature dependence of A.C electrical conductivity of PVA-PY-$FeCl_3$ composite polymer flims",Malaysia Malaysian polymer Jounal (MPJ),3, (2) :24-31(2009).
6. Al-Ramadhan.Z.,"Effect of Nickel salt on electrical properties of polymethyl methacrylate" , Al-Mustansiriyah Uni.. , (2008).
7. Heath P.&Sacher P.,"Quality crystals and optics for laser applications"pplied opt. 15(937) (1986) .
8. Reale L.,"X-ray microscopy of plan cells by using LiF crystal", microscopy research and technique,(2008).
9. Hutagalwng.S.D.&Lee.B.Y.,Proceeding of the 2nd international conference Nano/ Micro Engineered and Molecular systems,January ,Bangkok, Thailand, (2007).
10. Scholz.S.M,Carrot.G&Hilborn.J"Optical properties of Gold-Containing poly (Acrylic Acid)composites",Lausanne, Switzerland,(2008).
11. Thangaraju B. , Kalianna P.,Cryst. Res. Techon.35(71)(2000).
12. Kathalingam A.,"Materials Chemistry and physics, 106 (215)(2007).
13. Soliman.L.I and Sayed.W.M,"Some physical properties of Vinylpyridine Carbon-Black composites", Cairo, Egypt,(2002).

Comparison between Square Loop Antenna and Fractal Minkowiski Island

Amer Basim Shaalan [1], Sami Salman Chiad [2] and Nadir Fadhil Habubi [2]
[1] Muthana University, College of Science, Physics Department
[2] Al_Mustansiriyah University, College of Education, Physics Department

الخلاصة

إن تصميم الهوائيات بالاستعانة بالهندسة الكسورية قد يؤدي الى تحسن خصائصها. تمت محاكاة خصائص الهوائي منكوسكي باستخدام البرنامج **NEC4WIN95VM** الذي يعتمد طريقة الفترات لحل معادلات ماكسويل. هذا النموذج تمت مقارنته مع الهوائي الكلاسيكي المربع. اظهرت النتائج ان مساحة الهوائي منكوسكي اصغر من مساحة الهوائي المربع وان هذا التقليص في المساحة لا يؤثر على كفاءة الهوائي. الجزء الاساس في هذا البحث هو توزيع التيارات على سطح الهوائي. وجدنا ان تطبيق مباديء الهندسة الكسورية على الهوائي الكلاسيكي المربع يحسن معظم خصائص الهوائي.

ABSTRACT

Antenna design with fractal geometry may improves the characteristic of the antenna. Minkowski Island was simulated using NEC4WIN95VM software based on the method of moments for solving Maxwell equations. This model was compared to classical square loop antenna. The result showed that the area of the Minkowski Island antenna was smaller than the area of square loop antenna and this reduction in area does not degrade the performance of the antenna. The main part of this research is the current distribution over the body of the antenna. We found that fractalizing classical square shape improves most of antenna parameters.

INTRODCUTION

Fractal is a term coined by Mandelbrot in 1975 while studying irregular shapes (1). Fractal objects have two common properties: self-similarity that means the object has many copies of itself at several scales, and fractal dimension, which represents the space-filling properties of the object (2,3).

The most important fractal application is fractal antenna design. Fractal antennas are very useful tools to solve two of the limitations of classical antennas, the single band performance and the dependence of antenna's size on the operating frequency (4).

The first one who worked in this field was Nathan Cohen at Boston University. He published his first article "Fractal Antennas" on 15August 1995 (5). Few months later, Carles Puente at University of Catalonia, Barcelona in Spain published papers about fractal antennas (6,7). Fractal electrodynamics is a research area connecting the fractal geometry and electromagnetic theory, the term was coined by Dwight L. Jaggard (8).

In this research we simulate Minkowski Island of indentation width equal 0.6. The previous study for this model done by Kutter (9) and Gianvittorio (10) focused on the area reduction, they used indentation width equal 0.8. Gianvittorio did not mention the shape of the far field, which make the antenna application unknown.

In this work we have made calculations for the most antenna parameters especially for the current distribution over the antenna structure, which represent the physical point of view for the antenna behavior.

Fractal Generation:

The starting shape of Minkowiski Island is a square loop. Each of the four sides of the square is replaced by the generator. The generator is a straight segment divided into three segments, each segment is equal to one third (1/3) the length of the starting one. The middle one is removed from its place and connected with two other segments (11), this is shown in figure (1). These two segments are tuned to adjust the overall perimeter of the fractal length. This tuning length is called the indentation width (12). Six representative widths were chosen, they include 1/5, 1/3, 1/2, 2/3, 4/5 and 9/10. The indentation widths are the widths of the second and fourth segments. The shape of the antenna for the zero, first and second iteration is shown in figure (2).

Simulation Method:

Method of Moments is a numerical method for solving integral equations. The general form of this equation is (13):

$$\int I(z')K(z,z')dz' = -E^{i}(z) \quad \text{.....(1)}$$

The kernel K(z, ź) depends on the specific integral equation formula. The procedure of moments' method is; reducing this integral equation to a system of linear algebraic equations in terms of the unknown current I(ź). Most electromagnetic radiation problems are expressed as integral equations with a source term on the right hand side and the unknown within the integral.

Total sharing of the electric field over the wire volume is (14):

$$\bar{E}_z = \frac{1}{j\omega\varepsilon_0}\iiint\left[\frac{\partial^2\psi(z,z')}{\partial z^2}+\beta^2\psi(z,z')\right]Jdv' \quad \text{.....(2)}$$

$$\beta^2 = \omega^2\mu_0\varepsilon_0$$

$\psi(z,z')$ is the free space green function (14)

If we assume the conductivity goes to infinity, then the current is confined to the surface of the wire and by considering the distribution of the current as uniform with respect to (φ), then equation (2) is reduced to a line integral of current (15).

$$\bar{E}_z = \frac{1}{j\omega\varepsilon_0}\int_{-L/2}^{L/2}\left[\frac{\partial^2\psi(z,z')}{\partial z^2}+\beta^2\psi(z,z')\right]I(z')dz' \quad \text{..... (3)}$$

where: L is the wire length.

We can set the quantity ($\bar{E}_z$) in equation (2) as the scattered field ($\bar{E}_z^s$) that is radiated by the equivalent current I(z'). There is also the incident field ($\bar{E}_z^i$) at the

surface of a perfectly conducting wire, and the sum of the scattered and incident fields must be zero, i.e., $\bar{E}_z^s = -\bar{E}_z^i$

Thus, equation (2) becomes (15):

$$\frac{1}{j\omega\varepsilon_0}\int_{-L/2}^{L/2} I(z')\left[\frac{\partial^2\psi(z,z')}{\partial z^2}+\beta^2\psi(z,z')\right]dz' = -\bar{E}_z^i(z) \quad \ldots\ldots\ldots\ldots\ldots (4)$$

This equation was derived by Pocklington (13) and it is equivalent to equation (1). The expansion functions are a stair step approximation to the current distribution on the wire(14):

$$\int_{-L/2}^{L/2} I(z')K(z_m,z')dz' \approx I_1 f(z_m,z_1') + I_2 f(z_m,z_2') + \ldots + I_n f(z_m,z_n') + \ldots + I_N f(z_m,z_N') \approx -E_z^i(z_m)$$

$\ldots\ldots\ldots\ldots\ldots\ldots$ (5)

The physical interpretation of this equation is illustrated in figure (3)

From the computed currents we can calculate the radiation pattern of the simulated antenna by using the standard far field approximations (15,16):

$$\bar{E} = -j\omega\bar{A} \quad \ldots\ldots\ldots\ldots\ldots\ldots (6)$$

$$\bar{H} = \frac{j\omega}{\eta}\times\bar{A} \quad \ldots\ldots\ldots\ldots\ldots\ldots (7)$$

where $\eta = \sqrt{\frac{\mu}{\varepsilon}}$ $\ldots\ldots\ldots\ldots\ldots\ldots (8)$

$$A(r) = \frac{\mu}{4\pi}\frac{e^{-j\beta r}}{r}\int_s J(r)e^{-j\beta r}ds \quad \ldots\ldots\ldots (9)$$

RESULTS AND DISCUSSION

Minkowiski Island was simulated at specific resonance frequency. That is required a scaling to the fractal antenna through iterations to resonate at the same frequency. Square loop antenna was designed with side length of 180 mm and diameter of 0.5 mm. The main results of calculations of square loop antenna are shown in Figures. (4) and (5).

From the figures, one observes that the square loop antenna is matched in the frequency 455MHz and the SWR equal to 2.62. The antenna gain is equal to 3.38 dB_i. Shape of the radiation pattern is two lobes, similar to the radiation pattern of the dipole.

Figure (6) and figure (7) show the results obtained from analyzing the first iteration of Minkowiski Island. It can be seen that this model is matching at the same frequency of the square antenna with SWR 1.34. The radiation pattern is similar to that of the square antenna and the gain is equal to 2.61 dB_i.

It is noticed that the second iteration of Minkowiski Island has a point of matching at the same frequency with SWR 1.14.

The shape of the radiation pattern is similar to the radiation pattern of the square loop and the first iteration. The gain of the antenna at this band is equal to 2.34 dB_i. These results are shown in figure (8) and (9).

The current distributions over the antenna structures are shown in figure (10), (11) and (12). From these distributions one can conclude the reason of the similar radiation pattern among models, this is because of the similar distribution of the currents over the antenna structure.

Summary of the antennas parameters are listed in table (1).

Figure - 1: The generator of Minkowiski Island.

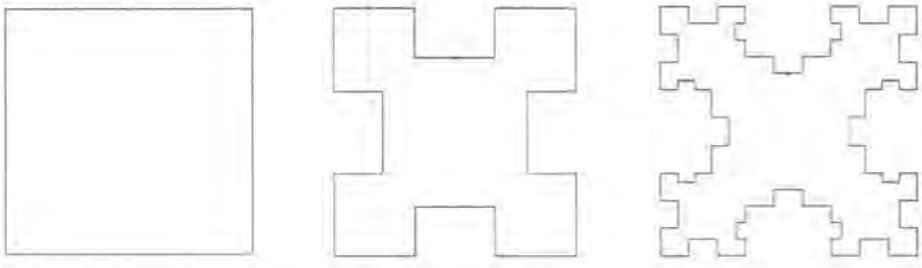

Figure -2: Shape of Minkowiski Island.

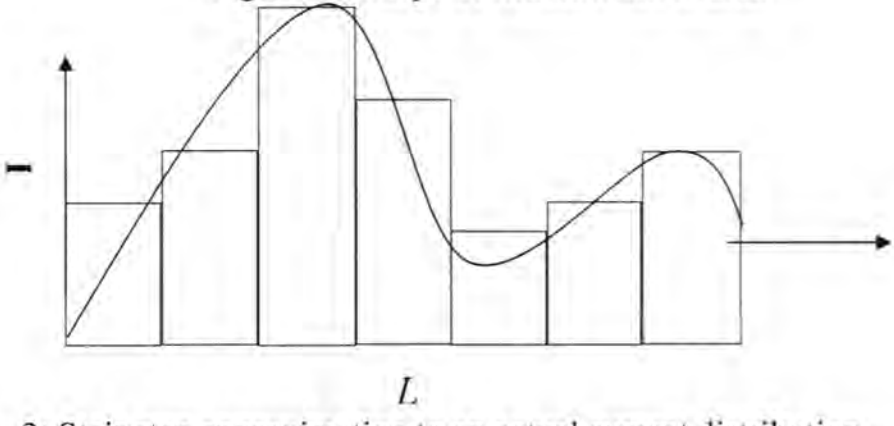

Figure -3: Stair step approximation to an actual current distribution.

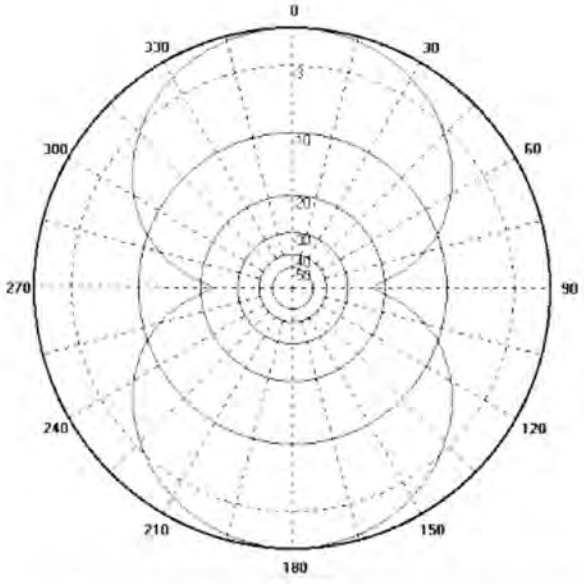

Figure -4: Radiation pattern of Square loop antenna.

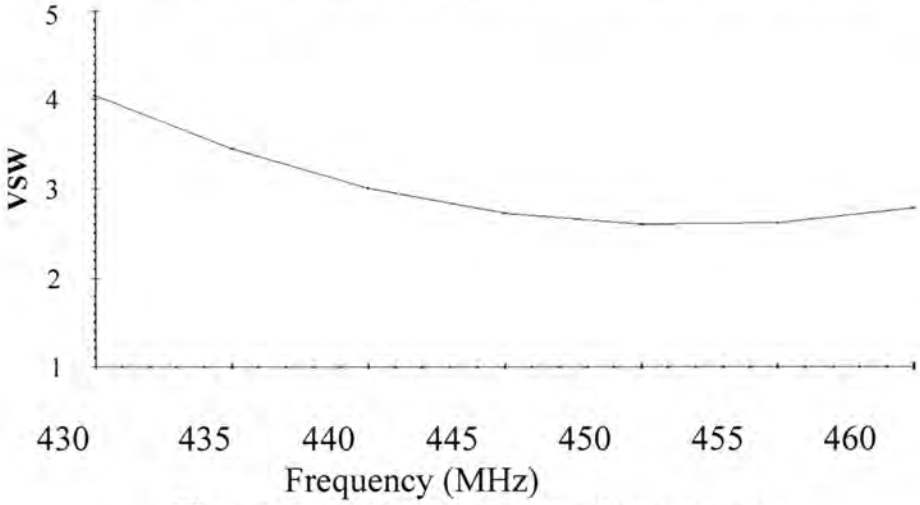

Figure -5: SWR of the Square loop antenna.

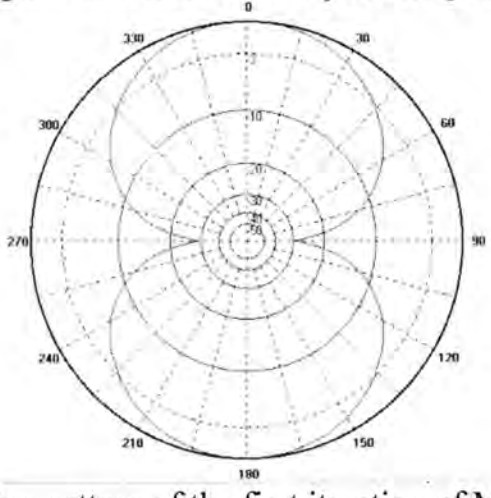

Figure -6: Radiation pattern of the first iteration of Minkowiski Island.

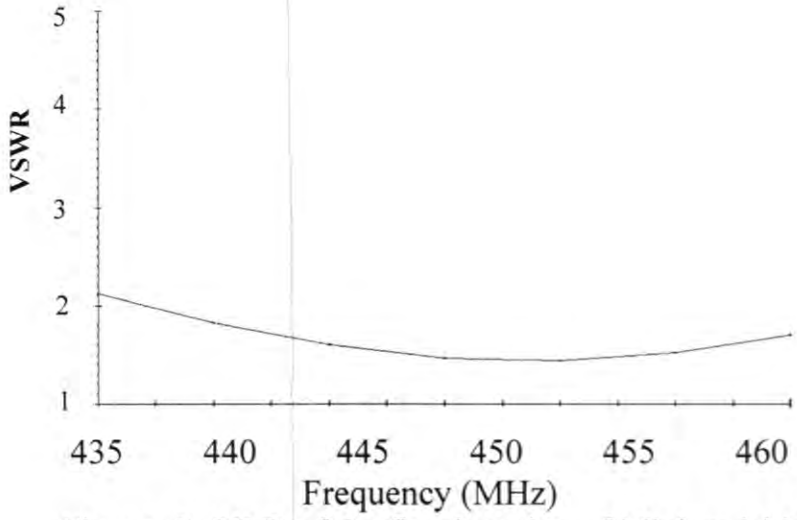

Figure -7: SWR of the first iteration of Minkowiski Island.

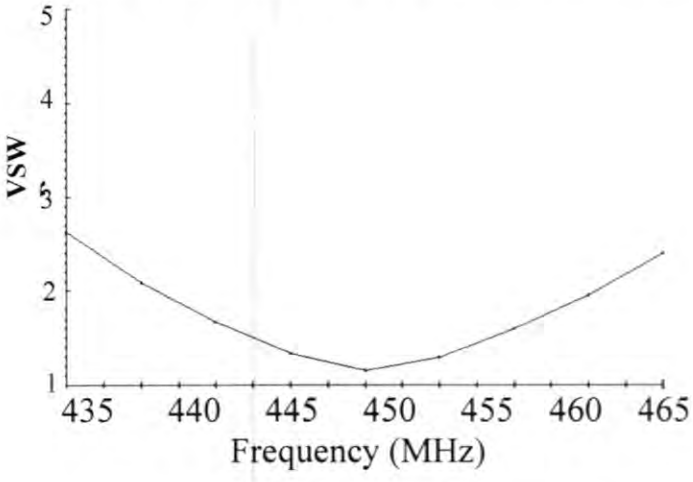

Figure -8: SWR of the second iteration of Minkowiski Island.

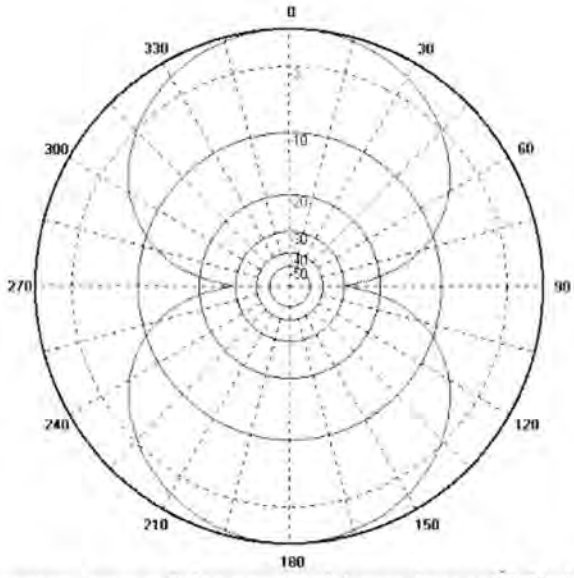

Figure -9: Radiation pattern of the second iteration of Minkowiski Island.

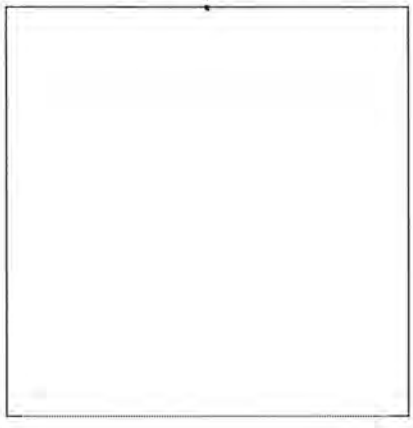

Figure -10: Current distribution over Square loop antenna.

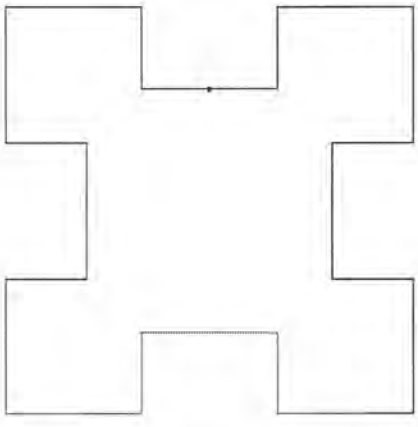

Figure -11: Current distribution over the first iteration of Minkowiski Island.

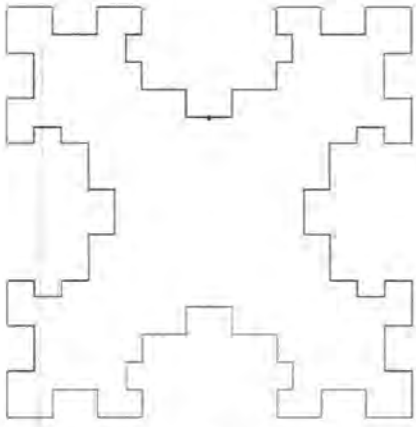

Figure-12: Current distribution over the second iteration of Minkowiski Island.

Table -1: Summary of antenna parameters.

Parameter	*Square*	*Minkowiski 1st iteration*	*Minkowiski 2nd iteration*
Gain (dB_i)	3.38	2.61	2.34
½ Power Beamwidth	86°	88°	88°
SWR	2.62	1.43	1.14
Area	324 cm^2	155.8 cm^2	152.7 cm^2
Reduction	-	51.9%	52.8%

1. The area of the fractal Minkowiski Island antenna is reduced to 51.9% for the first iteration and 52.8% for the second one from the area of the square loop antenna without affecting the antenna performance as shown in table (1).
2. The matching properties of the antenna which is represented by the SWR parameter is improved for the square loop by adding the fractalizing procedure to it, this results can be seen in figures (5,7,8).
3. There is a small decrease in the value of the gain for Minkowiski Island. This decrease is regarded as valueless compared to the advantages obtained from fractalizing Square loop antenna.
4. The current is distributed uniformly at the same side of the antennas structure. This distribution explain the similarity of the radiation pattern of square and Minkowiski Island antennas.

REFERENCES

1. Lee K. F., Principles of Antenna Theory, John Wiley & sons, (1984).
2. Tom Vernon, Fractal Antennas Offer Benefits, http//members, fortunecity. com/scienzatopazzo/fractarticle.htm, (1999).
3. Cohen N., Fractal Antennas: part 1, http://www.fractenna.com/ images/ comm-quarterly-article-3. jpg, (1995).
4. Puente C. and Claret J., Multiband Properties of a Fractal Tree Antenna Generated by Electrochemical Deposition, IEEE Electronics letters, 32,(25) :2298-2299, (1996).
5. Puente C., Romeu J., Perturbation of the Sierpinski Antenna to Allocate Operating Bands, IEE Electronics letters, 32, (24):2186-2188, (1996).
6. Jaggard D.L. and Kritikos H. N., On Fractal Electrodynamics, In Recent Advances in Electromagnetic theory, :183-224, Springer verlag, (1990).
7. Werner D.H., Fractal Antenna Engineering: The Theory and Design of Fractal Antenna Array, IEEE Antennas and Propagation magazine, 41(5):37-59, (1999).
8. Collejon J. et al, On the Application of Parametric Models to the Transient Analysis of Resonant and Multiband Antennas, IEEE Transections on Antenna and propagation,46(3):312 (1998).
9. Mandelbrot B. B., The Fractal Geometry of Nature, Freeman and company, New York, (1983).
10. Robert L.D.,Fractal Geometry of the Mandelbrot,http://math.bu.edu/ Dysys / fracgeom/ fracgeom.html, (2000).
11. Kutter R.E., Fractal Antenna Design, B. Sc. Honor Thesis, BEE, University of Dayton, (1996).
12. Gianvittorio J., Fractal Antennas: Design, Characterization and Applications, M.Sc. thesis, University of California, Los Angeles, (2000).
13. Stutzman, W. L., Antenna Theory and Design, John Wiley & Sons , 2nd edition, (1998).
14. EdminIster J. A, Electromagnetic, McGraw Hill Comp, (1993).
15. Harrington R. F., Field Computation by Moment Method, McMillan, New York, (1968).
16. Lorrain P. and Freeman W.H., Electromagnetic Fields and Waves, and Company, Sanfransisco, (1970).

Electronic Transitions For Polystyrene Filled With Lithium Fluoride Additive

Asrar Abdul Muniam and Ahmed Hashim
Al-Mustansiriyah University, College of Science, Department of Physics

الخلاصة

في هذا البحث تم دراسة تأثير إضافة فلوريد الليثيوم على بعض الخواص البصرية للبولي ستايرين. ولهذا الغرض تم تحضير نماذج بإضافة فلوريد الليثيوم إلى البولي ستايرين وبنسب حجمية مختلفة من هذه الأملاح مع البوليمر وبسمك مختلف.تم تسجيل طيفي الامتصاص و النفاذية و لمدى الاطوال الموجية nm(190-1100). و حساب معامل الامتصاص و فجوة الطاقة للانتقال غير المباشر المسموح و الممنوع.

ABSTRACT

In the present work , effect of addition Lithium Fluoride on some optical properties of polystyrene has been studied . for that purpose , many samples has been prepared by adding Lithium Fluoride on the polystyrene by different volume percentages from these salts with polymer and by different thickness .The absorption and transmission spectra has been recorded in the wavelength range (190-1100)nm . The absorption coefficient and energy gap of the indirect, allowed, forbidden transition have been determined.

INTRODUCTION

Polymers have traditionally been considered as insulating materials by chemists and physicists alike . A conducting polymer is chewable and desirable . A light weight ready moldable , desirable conductive material has long been recognized as a worthwhile goal to work for(1,2).Researches, generally, have demonstrated that conductive polymers can be used as energy storage element in:(3,4)

1-Capacitors and Secondary batteries .
2-As semiconductor material in schottky diode.
3-Insulated gate field effect transitions (FET) and light emitting diodes.
4-As conductive layer for electromagnetic shelding (EMI) and electrostatic protection.

In the recent years conjugated conducting polymers have been the main focus of research throughout the world . Since the discovery led by 2000 chemistry Nobel winners, Shirakawa, MacDiarmid and Heeger , the perception that plastic could not conduct electricity has changed Nowadays, conducting polymers also known as conductive plastics are being developed for many uses such as corrosion inhibitors, compact capacitors, antistatic coating, electromagnetic shielding and smart windows; which capable to vary the amount of light to pass(5,6)

LiF material is extensively used because of interesting optical properties (high band gap, transparent to uv-visible light, low refractive index) which are considered for various optical applications such as windows, prism and lenses in the vacuum uv, visible and infrared here desired transmission in the 0.104μm-7μm range(7). It is also very useful for X-ray nonochromaters and for the study of fundamental properties and defect in crystal(8).

MATERIALS AND METHODS

The materials used in the papar is polystyrene as matrix and Lithium florid as a filler.

The electronic balanced of accuracy 10^{-4} have been used to obtain a weight amount of LiF powder and polymer powder .These mixed by Hand Lay up and the Microscopic Examination used to obtain homogenized mixture .The volume percentages of LiF which equivalent weight percentages are (0 , 14.6 , 28.5) vol%. The Hot Press method is used to press the powder mixture. The mixture of different LiF percentages have been compacted at temperature 145°C under a pressure 100 par for 10 minutes . Its cooled to room temperature , the samples were disc shap of a diameter about 30mm and thickness ranged between (1.75-2.2). The transmission & absorption spectra of PS-LiF composites have been recording in the length range (190-1100) nm using double-beam spectrophotometer (UV-210°A shimedza).

RESULTS AND DISCUSSION

The absorption coefficient (α) was calculated in the fundamental absorption region from the following equation(9):

$$\alpha = 2.303\frac{A}{d} \quad \text{.....(1)}$$

Where : A absorbance , d the thickness of sample.

Figure (1) shows the relationship between the absorption coefficient and photon energy of the PS-LiF composites we note the change in the absorption coefficient is small at low energies this is indicates the possibility of electronic transitions is a few. At high energy , the change of absorption coefficient is large this is indicates the large Probability of electronic transitions are the absorption edge of the region (10). The absorption coefficient helps to conclude the nature of electronic transitions, when the high absorption coefficient values ($\alpha > 10^4 cm^{-1}$) at high energies we expected direct electronic transitions ,and the energy and momentum preserve of the electron and photon , when the values of absorption coefficient is low($\alpha < 10^4 cm^{-1}$) at low energies we expected in this case indirect electronic transitions, the momentum of the electron and photon preserves by phonon helps(11).

The results showed that the values of absorption coefficient of the PS-LiF composites less than $10^4 cm^{-1}$ which indicates to the indirect electronic transition

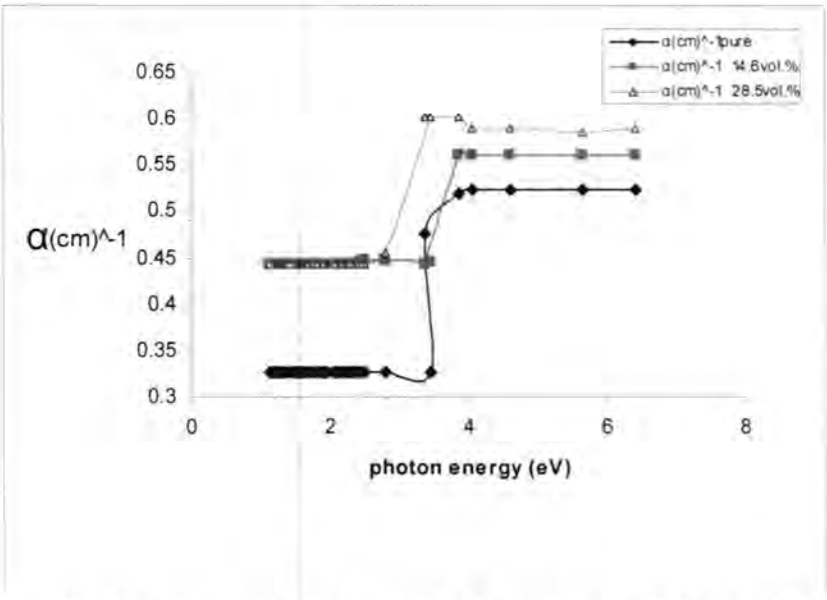

Figure -1: the relationship between the absorption coefficient and photon energy of the PS-LiF composites

The forbidden energy gap of indirect transition both allowed, forbidden calculated according to the relationship(12) :

$$\alpha h\nu = A\left(h\nu - E_g\right)^m \quad \text{.....(2)}$$

Where : hv the energy of photon , A proportionality constant, Eg forbidden energy gap of the indirect transition.

If the value of (m=2) indicates ton allowed indirect transition . when the value (m=3) indicates to forbidden indirect transition. Figure (2) shows the relationship between $(\alpha h\nu)^{1/2}$ $(cm^{-1}.eV)^{1/2}$ and the photon energy of pure polymer (PS) , with take over part

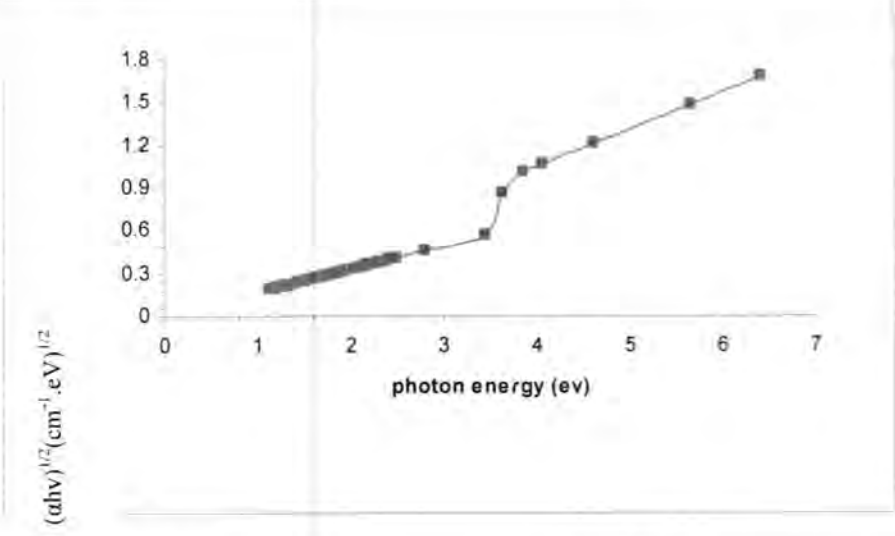

Figure -2 : the relationship between $(\alpha h\nu)^{1/2}(cm^{-1}.eV)^{1/2}$ and photon energy of pure polymer (PS).

of the straight cut oriented axis at the point $(\alpha h\nu)^{1/2} = 0$ will get the value of forbidden energy gap of the allowed indirect transition , which equal (3.2eV). Figure (3) and figure (4) represents the same relationship but to the polymer filled with (LiF) with volume percentages of LiF are(14.6 , 28.5) vol% ,the same way we can be obtained

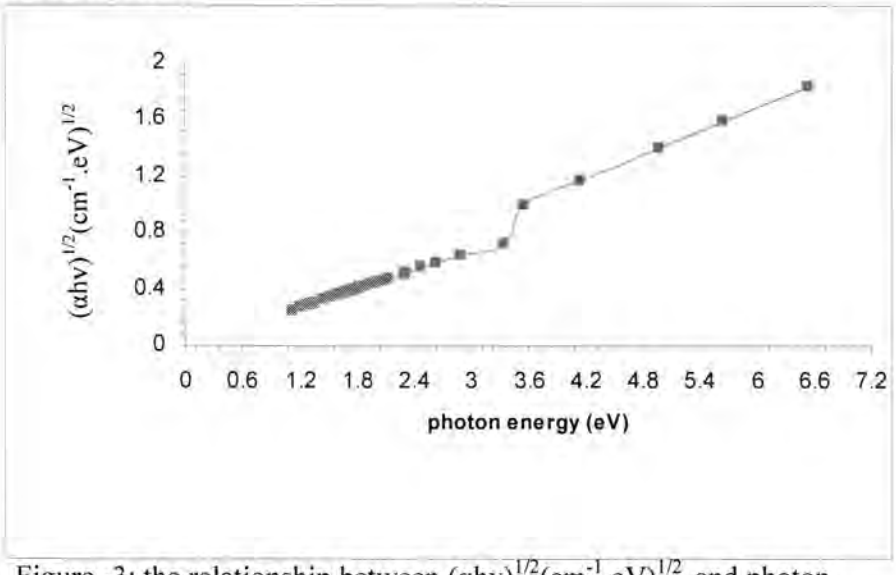

Figure -3: the relationship between $(\alpha h\nu)^{1/2}(cm^{-1}.eV)^{1/2}$ and photon energy of PS-LiF composites for 14.6 vol.% LiF

on the value of forbidden energy gap of allowed indirect transition which equal (2.9eV) for 14.6 vol% LiF, and (2.3eV) for 28.5 vol.% LiF .

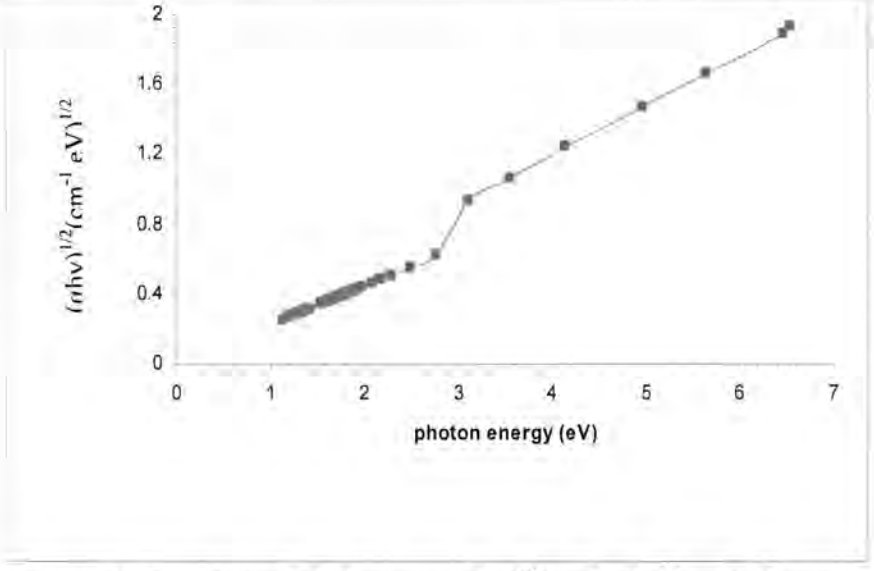

Figure -4: the relationship between $(\alpha h\nu)^{1/2}(cm^{-1}.eV)^{1/2}$ and photon energy of PS-LiF composites for 28.5 vol.% LiF

we note that the value of the forbidden energy gap decreases with increasing LiF concentration.. Figure(5) shows the relationship between the $(\alpha h\nu)^{1/3}(cm^{-1}.eV)^{1/3}$

and photon energy of pure polymer (PS) , the same way we obtain to the forbidden energy

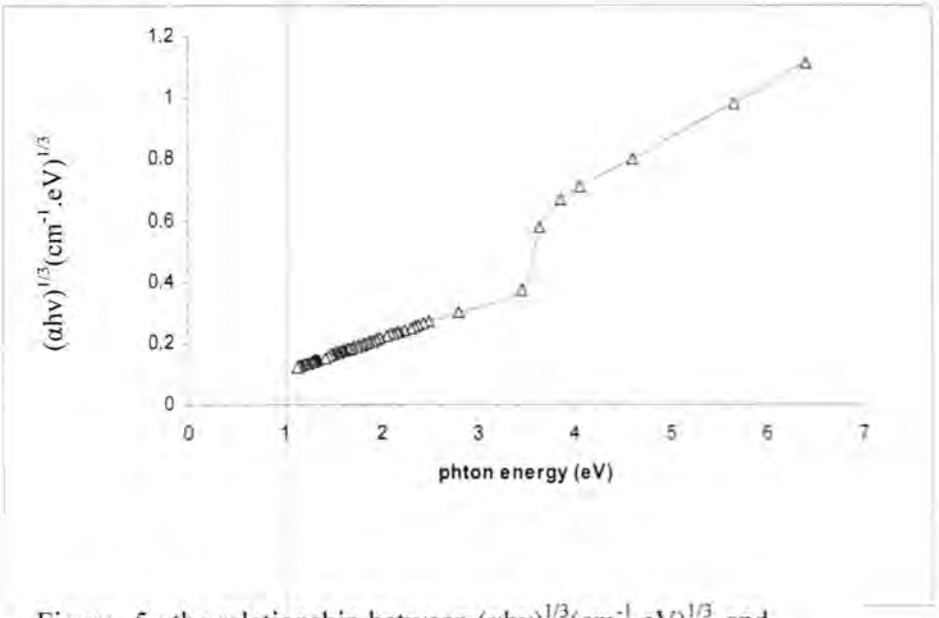

Figure -5 : the relationship between $(\alpha hv)^{1/3}(cm^{-1}.eV)^{1/3}$ and photon energy of pure polymer (PS).

gap of forbidden indirect transition which equal (3.03eV).

Figure (6) and figure (7) represents the same relationship but to the polymer filled with (LiF) with volume percentages of LiF are (14.6 , 28.5) vol% ,the same way we can be obtained on the value of the forbidden energy gap

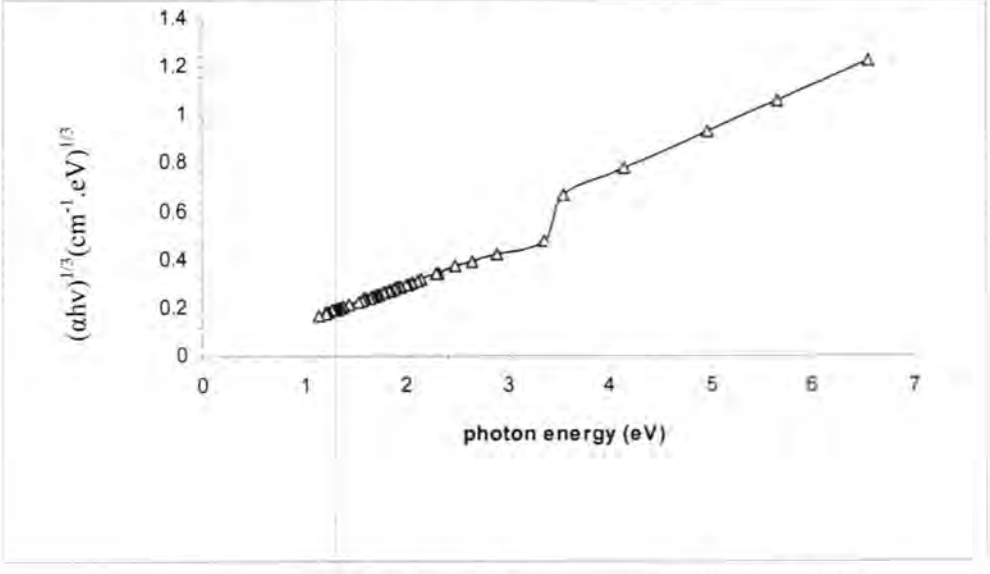

Figure -6: the relationship between $(\alpha hv)^{1/3}(cm^{-1}.eV)^{1/3}$ and photon energy of of PS-LiF composites for 14.6 vol.% LiF

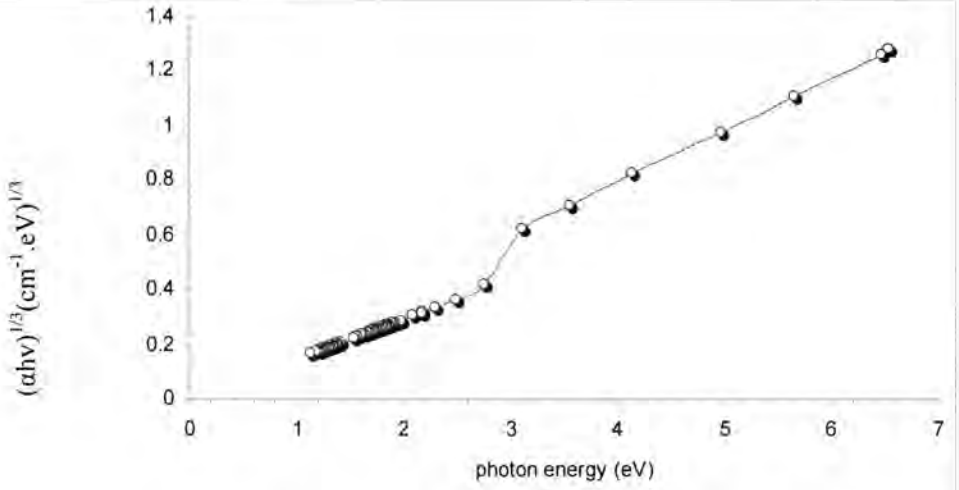

Figure -7 : the relationship between $(\alpha hv)^{1/3}(cm^{-1}.eV)^{1/3}$ and photon energy of of PS-LiF composites for 28.5 vol.% LiF

of the forbidden indirect transition which equal(2.82eV) for14.6vol.% LiF. And (2.19eV) for 28.5 vol%. we note that the value of the energy gap decreases with increasing LiF concentration(13).

We can conclude:

1. The absorption coefficient is increasing with increasing of the filler vol.% content.
2. The experimental results showed that the absorption coefficient less than $10^4 cm^{-1}$ this is indicates to forbidden and allowed indirect electronic transitions.
3. The LiF additive change not the nature of electronic transfers of PS samples.
4. The forbidden energy gap is decreasing with increasing of the filler vol.% content.

REFERENCES

1. 1-Blyth A. R,"Electrical properties of polymers", London-New York., (1979).
2. Ramos M. V.," conductive polymer- copmposite Sensor for Gas Detection ", Newzeland, (2005).
3. Seanor D.A, "Electrical properties of polymers", New York., (1982).
4. Alvarez M. P., " Submicron Copper-Low-Density polyethylene conducting composites : Structural, Electrical and percolation Threshold" ,Chile, (2008).
5. Harun M. H.,"Temperature dependence of A.C electrical conductivity of PVA-PPY-$FeCl_3$ composite polymer flims",Malaysia, Malaysian polymer Jounal (MPJ), 3 (2) :24-31(2009) .

6. Al-Ramadhan. Z.,"Effect of Nickel salt on electrical properties of polymethyl methacrylate" , Al-Mustansiriyah Uni. ,(2008).
7. Heath P. and Sacher P., "Quality crystals and optics for laser applications", Applied opt. , (15) 937 (1986) .
8. Reale L, "X-ray microscopy of plan cells by using LiF crystal", microscopy research and technique.,(2008).
9. Hutagalwng. S. D. and Lee. B. Y., Proceeding of the 2nd international conference Nano/Micro Engineered and Molecular systems, January ,Bangkok,Thailand,(2007).
10. Scholz. S.M, Carrot.G and Hilborn.J, "Optical properties of Gold-Containing poly (Acrylic Acid) composites" , Lausanne, Switzerland,2008.
11. Thangaraju B. , Kalianna P.,Cryst. Res. Techon., 35(71)(2000).
12. Kathalingam A, "Materials Chemistry and physics, .106,(215)(2007).
13. Soliman.L.I and Sayed.W. M,"Some physical properties of Vinylpyridine Carbon-Black composites", Cairo, Egypt. ,(2002).

X-ray Diffraction and FTIR Spectra of SnO_2 Thin Film Prepared Using RTO Method

[1]Evan T. Salem, [2]Ibrahim R. Agool and [2]Marwa A .Hassan
[1]School of Applied Sciences, University of Technology, Laser and Optoelectronic Branch
[2]Department of Physics, College of Science, Al Mustansiriyah University

الخلاصه

في هذا البحث تم تحضير اغشية اوكسيد القصدير وهو من الاكاسيد الشفافه الموصله على قواعد من الكوارتز عند ظروف مختافه باستخدام تقنية الاكسده الحراريه السريعه عند درجة حراره اكسده وازمان اكسده مختلفه وتم دراسة كل من حيود الاشعه السينيه وطيف ال FTIR . وجد ان اغشية اوكسيد القصدير متعددة التبلور ورباعية التركيب وتنمو عند درجة حرارة (873 K) وزمن اكسده (90 sec) وهذا ما تبينه ايضا نتائج ال FTIR.

ABSTRACT

Transparent conducting oxide thin films of SnO_2 has been prepared on quartz substrates at different oxidation conditions such as oxidation temperature and oxidation time using rapid thermal oxidation method. The films crystallize is a tetragonal structure and X-ray diffraction measurements have shown polycrystalline SnO_2 films prepared at 873 K, 90 sec with (101) orientation. The SnO_2 phase formation was also confirmed with the recorded Fourier Transform Infrared (FTIR) results.

INTRODUCTION

Transparent conducting oxide thin films are of great interest due to its variety of applications. Consequently, thin films with high optical transparency and electrical conductivity have been a subject of investigation since last century (1–2). Tin oxide (SnO_2), indium tin oxide (ITO), and zinc oxide (ZnO) were used in place of the metal electrode. Among these, SnO2 is chosen because of its high electrical conductivity and its transparency in the visible and infrared light, therefore it acts as a window for sunlight and heat reflectors in solar cells, various gas sensors, LCDs etc (3-4). Further, its refractive index lies in between 1.9 and 2.0. Now SnO_2 thin films have become an integral part of modern electronic technology. There are various methods such as spray pyrolysis, electron beam evaporation, chemical vapour deposition, magnetron sputtering and the Pechini method, etc., for the preparation of doped or undoped SnO_2 films. The SnO_2 films are n-type semiconductors with a direct optical band gap of about 3.87–4.3 eV (5-8). The valence band is closed shell of oxygen $2S^2$, $2P^6$ state mixed with some Sn states. The structure of the material in its bulk form is tetragonal rutile with lattice parameters $a = b = 4.737$ °A and $c = 3.816$ °A. However in thin film form, depending on the deposition technique its structure can be polycrystalline or amorphous. The grain size is typically200–400 °A, which is highly dependant on deposition

technique, temperature, doping level etc. SnO_2 films close to stoichiometric condition have low free carrier concentration and high resistivity, but non-stoichiometric SnO_2 films have high carrier concentration, conductivity and transparency. This comes about from an oxygen vacancy in the structure so that the formula for the thin film material is SnO_2-x, where x is the deviation from stoichiometry (2). .In this work , we have investigated the x-ray diffraction and FTIR properties of SnO_2 films deposited on to quartz substrates using the rapid thermal oxidation at different condition such as oxidation temperature and oxidation time.

MATERIALS AND METHODS

The thermal evaporation system type (Edwards) has been used to evaporate the high purity (99.9 %). Tin on quartz slides at room temperature under low pressure (about10^{-6}torr). Using a rapid thermal oxidation (RTO) of Sn film at different oxidation temperature and oxidation time. Ohmic contacts were fabricated by evaporating 99.999 purity aluminum wires. A boat of tungsten was used to include the evaporated source.

RESULTS AND DISCUSSION

a- X-ray diffraction

The crystalinity of the produced material characterized using x-ray diffraction (XRD). This technique was also employed by other group give an indication about the grain size and formation material type of the prepared thin film. The following figures show the XRD patterns for samples grown at different oxidation temperature and oxidation time. For Sn films depositing on quartz substrate, one peak could be recognized in figure (1), the film is single crystalline with a tetragonal structure according to the ASTM standards where (200) Sn, with lattice constant of (5.8285) respectively could be recognize, which related to the formation of tin thin film and such result indicate that no formation of the oxide film occurs on quartz substrate.

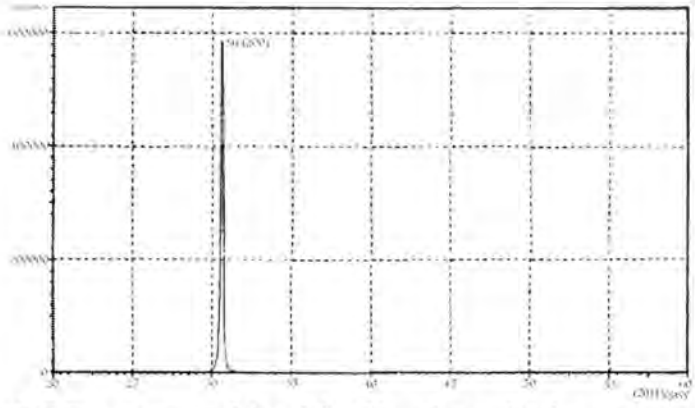

Figure -1: XRD pattern of Sn thin film deposited on quartz substrate

Figure (2) (a, b), prepared at (373,473 K) oxidation temperature and constant oxidation time. There is one sharp peak in this pattern at 2θ $=30.6402^0$ for Sn film correspond to diffraction from (200) plane. Where no formation of the oxide film and all the lines correspond to a single crystalline tetragonal Sn phase.

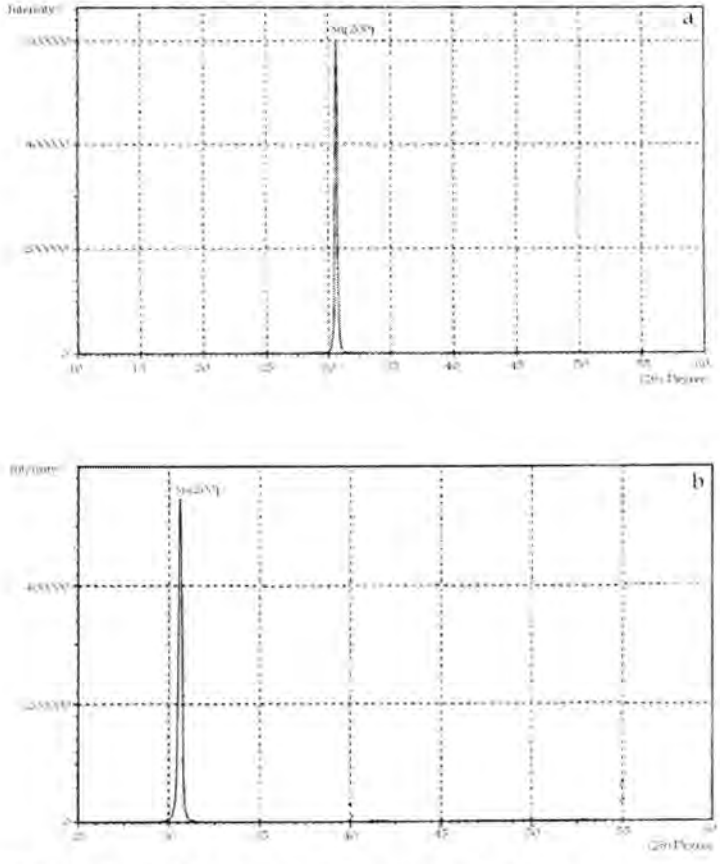

Figure-2: XRD pattern of Sn thin film deposited at (a) T =373 K and (b) T=473 K, oxidation time (60) sec

At farther increase in oxidation temperature up to (573,673 K), figure (3) (a, b). The XRD pattern consists of two sharp peaks at $2\theta = 30.1340^0$ and $2\theta = 30.7633^0$ which related to the formation of SnO film with orthorhombic structure. The intensity of the (101) peak show the formation of the SnO oxide and a polycrystalline in nature.

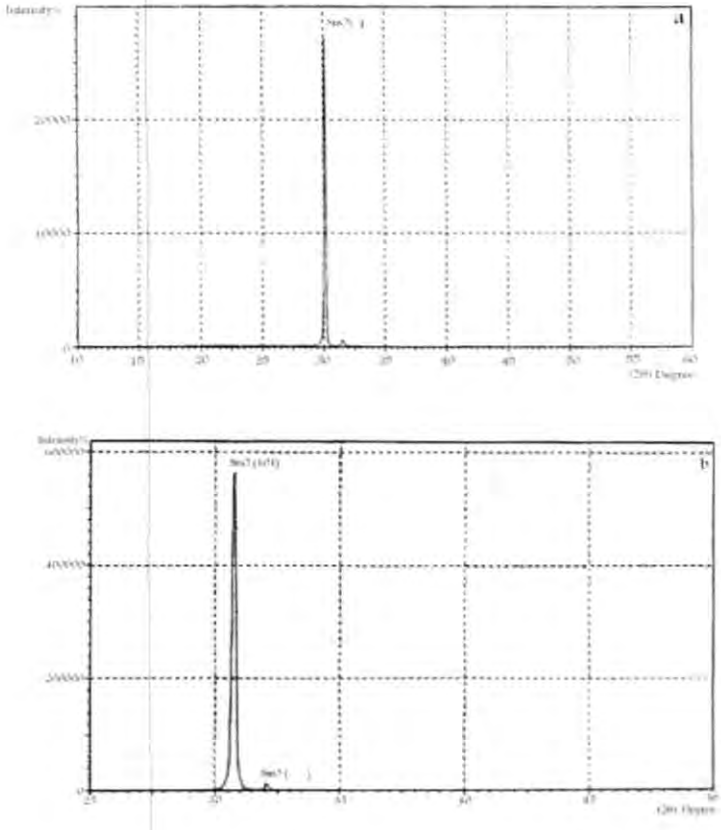

Figure -3: XRD pattern of Sn thin film oxidation at (a) T =573 K and (b) T =673 K, oxidation time 60 sec

Figure (4) (a, b) give the XRD pattern for sample prepared at (773, 873 K), where four peak could be recognized corresponding to the diffraction from (101) at $2\theta = 33.8436^0$ and $2\theta = 34.0896^0$ respectively which related to the formation of SnO_2.The XRD pattern at the oxidation time of 60 sec and increasing temperature about 973 K are shown in figure (5), we can recognize that the peaks appear at $2\theta = 26.7397^0$ and $2\theta = 34.0658^0$ in the spectra of the SnO_2 corresponding to the reflection from the planes (110) and (101), the intensities of this peaks increasing with increases of oxidation temperature can be attributed to the improvement in the crystallinity at higher temperature. This improvement in the structural order can also be attributed to the increase in the film density, which results in demonstrated of (101) SnO_2 peak rather than author peak.

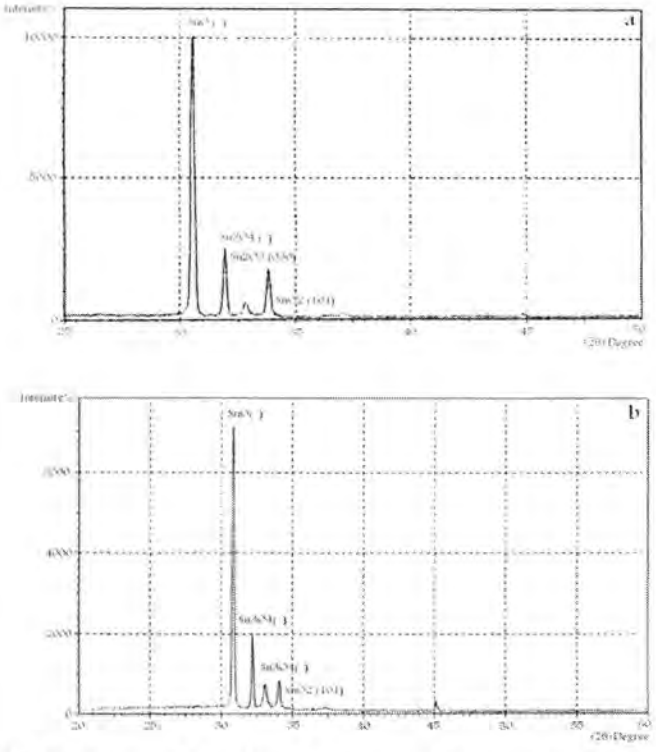

Figure -4: XRD pattern of Sn thin film oxidation at (a) T =773 K and (b) T =873 K at oxidation time 60 sec

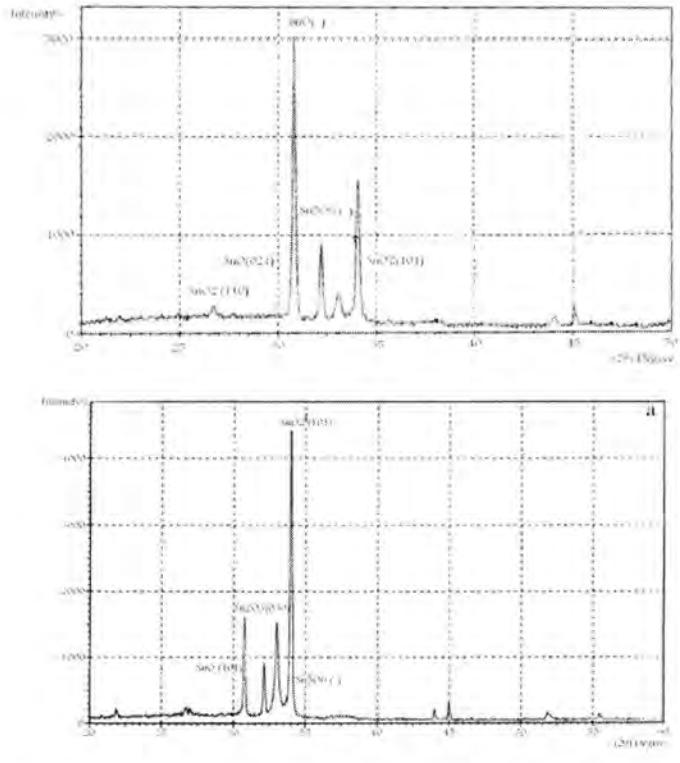

Figure -5: XRD pattern of Sn thin film oxidation at T =973 K at oxidation time 60 sec

Figure (6) (a, b, c) show the diffraction pattern for samples prepared at different oxidation time. At 90 sec oxidation time figure (a) show that the structures of films are clearly improved where a significant increase in peak intensity at (101) plane. This indicates the formation of nearly stoichometry SnO_2 films. The intensities of these peaks reduced with increasing oxidation time up to (120 sec) as shown in figure (b, c).

The results below ensure that the optimum value of oxidation temperature is 873 K and oxidation time is 90 sec. The deviation in XRD peak of the film with respect to the standard ASTM data is attributed to the mechanical micro stress produced by different recourses like impurities, defects and vacancies reside in the film structure. Results at higher oxidation time about (140 sec) and at same oxidation temperature is shown in figure (c), we can recognize that peaks appear at $2\theta=33.9813^0$ in the spectra of SnO_2 film corresponding to the reflection from (101) plane. The presences of sharp peak (in all deprogram) indicate that all films are polycrystalline in nature and inacordance with data reported in literature. These results are similar to that obtained by other workers (9-10). Table (1) shows the FWHM of the XRD and gives the value of the estimated grain size for the prepared films at different growth conditions. It appears clearly from the results that the enhancement the film morphology and smoothness with increasing the oxidation time up to (90 sec, 873 K). Here we can recognize the reduction in the FWHM reflect in the grain size. The dislocation density and the micro strain increased with increase oxidation temperature at oxidation time 60 sec and observed decrease the dislocation density and the micro strain at optimum condition (90 sec, 873 K) (11).

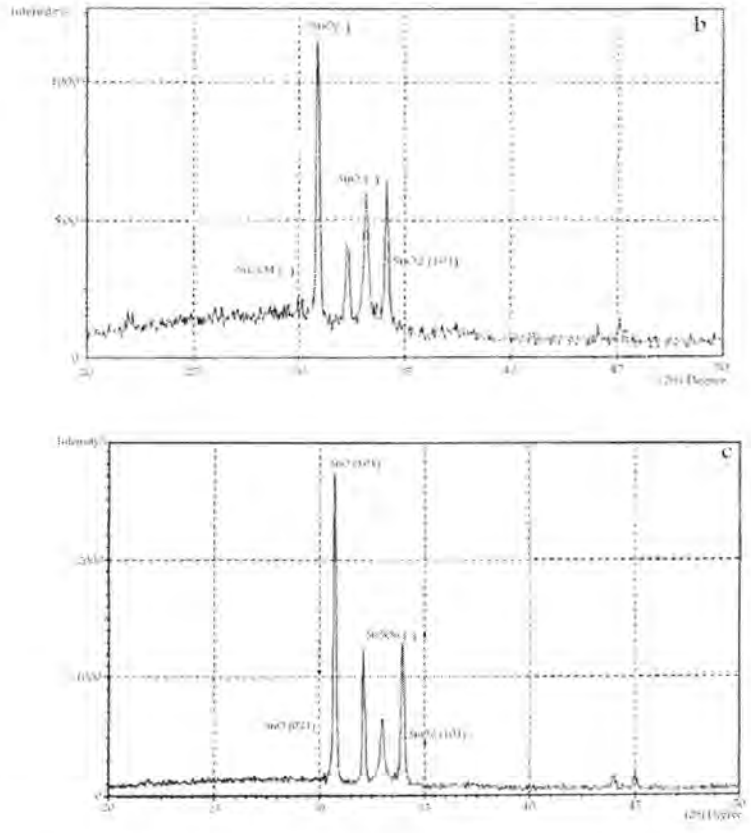

Figure-6:XRD pattern of Sn thin film oxidation at T =873 K at oxidation time (a) 90 sec , (b) 120 sec and (c) 140 sec

Table -1: FWHM for SnO_2 Samples at different condition

Deposition Conductions	hkl	FWHM Degree (SnO_2)	Grain size (nm)	dislocation density(δ) 10^{10}lines/cm^2	micro strain (ε) 10^{-4}
T=773K t=60 sec	(101)	0.1682	51.94	3.7	4.19
T=873K T=60 sec	(101)	0.1712	51.03	3.84	4.45
T=973K T=60 sec	(110)	0.2	42.78	5.46	4.3
	(101)	0.1948	44.85	4.97	4.72
T=873K t=90 sec	(101)	0.1544	56.58	3.12	3.21
T=873K t=120 sec	(101)	0.1945	44.92	4.95	4.9
T=873K t=140 sec	(101)	0.1557	56.11	3.17	3.46

b- FTIR Spectra measurement

Fourier transformation-Infrared spectroscopic results give information about phase composition and the way in which oxygen is bound to metal ions.

The following figures show the FTIR spectra of both Sn films deposited on quartz substrate and SnO_2 films prepare at different oxidation temperature and time.

Figure (7) shows the absorption peak around (216.01-3980.80) cm^{-1} spectra which is related to the Sn metal atoms. These insure the deposition of pure metal thin film on quartz substrate.

At different oxidation temperature (373-973 K) and constant oxidation time of 60 sec, we can recognize the change in the oxidation film composition as shown in figure (8) (a, b), we can recognize that all the absorption peaks which related to the Sn metal atoms.

At higher oxidation temperature of 573 K at the same oxidation time figure (8) (c) we can observed the absorption spectra at (725.18, 671.18, 401.17, and 277.73) cm^{-1} which are related to the formation of tin oxide molecules. Beside that, the presences of the absorption peak which related to Sn atom that still un oxidized. An increasing the formation ability of the tin oxide molecule could be recognize obviously by increasing the oxidation temperature to 673 K figure (8) (d) where (178.10, 1743.53, 1450.37, 979.77, 709.76, 694.33, 385.74) cm^{-1} absorption peak could be found that belong to the formation of the tin oxide molecule. Figure (8) (e) gives the FTIR results for films prepared at oxidation temperature of 773 K, we can recognize that the peak related the tin oxide is eliminated to three peaks at (1751.24, 1681.81, 948.91) cm^{-1}. At oxidation temperature of (873 and973 K) figure (8) (f, g) absorption spectra related to Sn atom is clearly disappeared while that found at (879.48, 686.61, 370.31, 308.59, 300.87, 208.30) cm^{-1} is related to the formation of tin oxide molecules. For the case of the tin oxide formation, the mean kinetic energy of the Sn atoms decrease through collision with oxygen, formation of (O^{+2}) ions (through energetic change reaction of Sn with O_2 molecules) so chemical bonding like (Sn-O) vibrational and O-Sn-O stretching modes are formed respectively (12). This could be recognize by the FTIR obtain result shown in the given figure. By increasing the oxidation time up to 90 sec figure (9) the peak at (686.61and316.30) cm^{-1} are related to the formation of tin oxide molecule. In all above result we can recognize peak at (331.73, 408.88, 432.03, 486.03, 609.46, 648.04, 740.61, 810.05, 864.05, 887.19, 941.20, 972.06, 1010.63, 1110.92, 1172.64, 1211.21, 1311.50, 1350.08, 1419.51, 1720.39, 1735.81, 1905.54, 1951.83, 12005.83) cm^{-1} is related to quartz substrate.

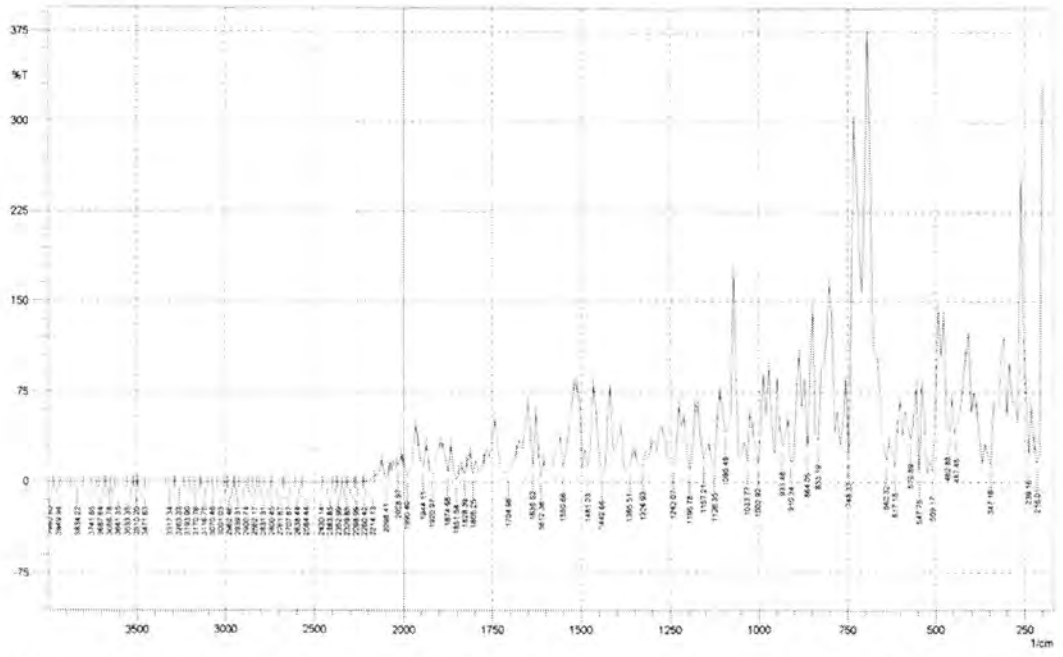

Figure -7: FTIR spectrum of Sn thin film deposited on quartz substrate

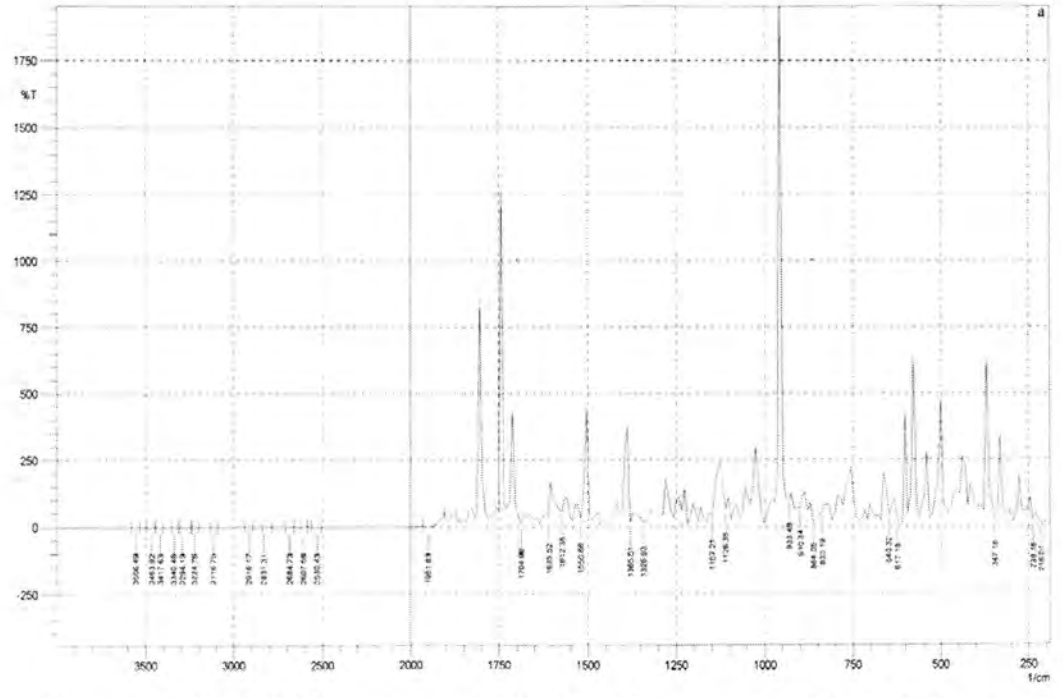

Figure -8: (a) FTIR spectrum of Sn thin film prepared at oxidation temperature T=373 K and oxidation time t=60 sec constant

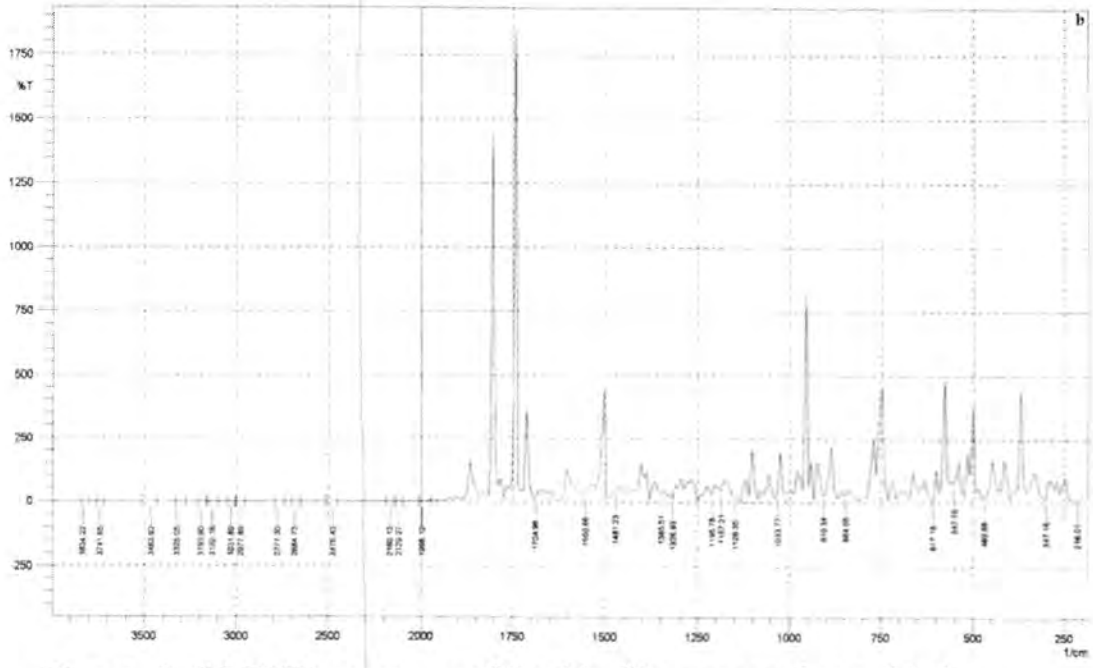

Figure -8: (b) FTIR spectrum of Sn thin film prepared at oxidation temperature T=473 K and oxidation time t=60 sec constant

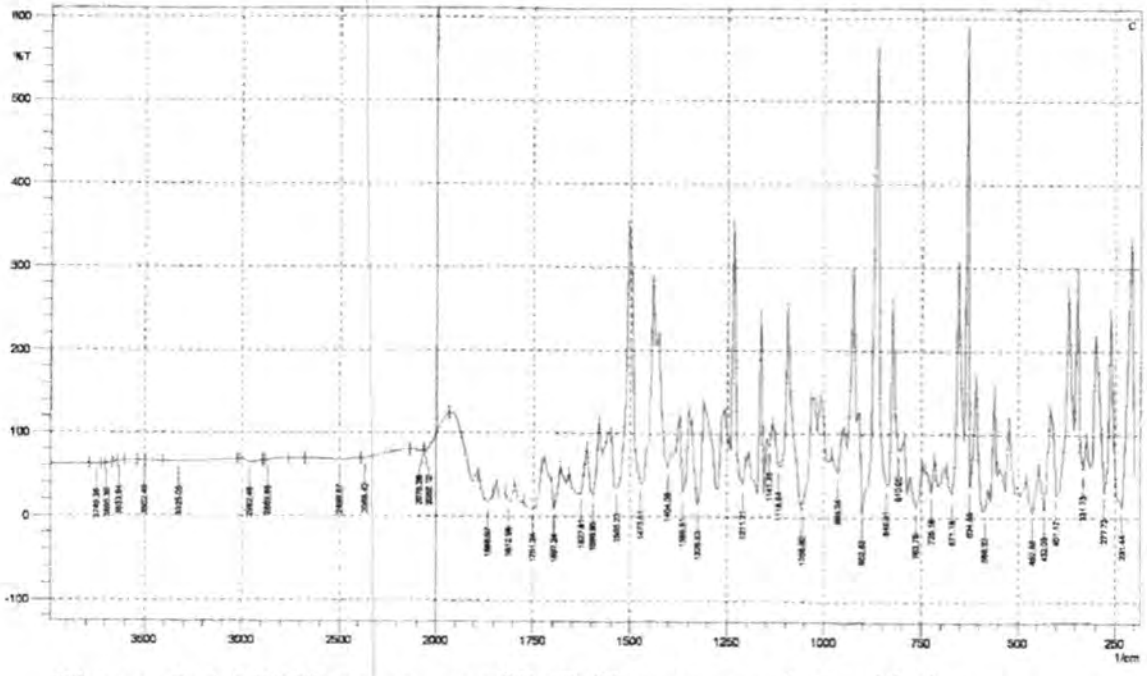

Figure -8: (c) FTIR spectrum of SnO films prepared at oxidation temperature T=573 K and oxidation time t=60 sec constant

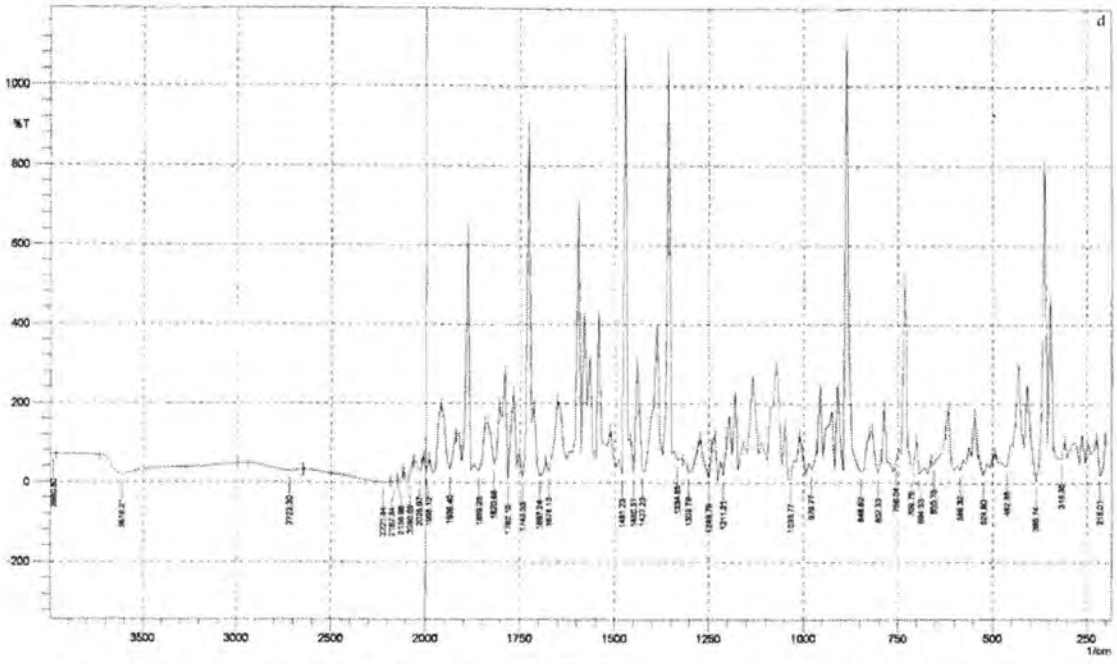

Figure -8: (d) FTIR spectrum of SnO films prepared at oxidation temperature T=673 K and oxidation time t=60 sec constant

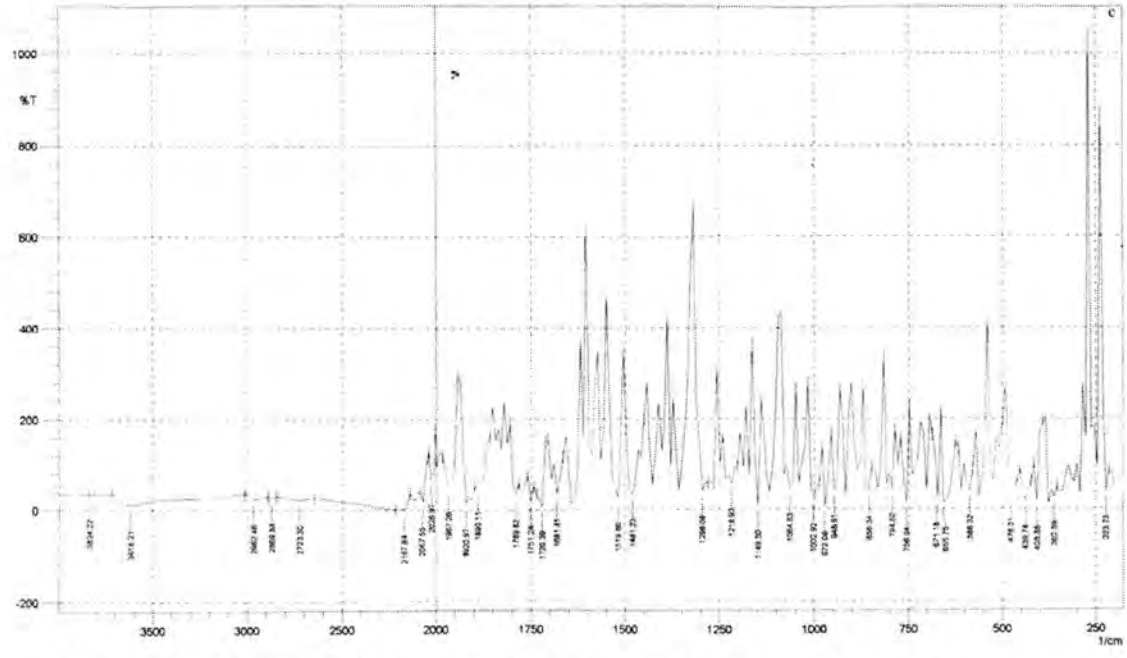

Figure -8: (e) FTIR spectrum of SnO_2 films prepared at oxidation temperature T=773 K and oxidation time t=60 sec constant

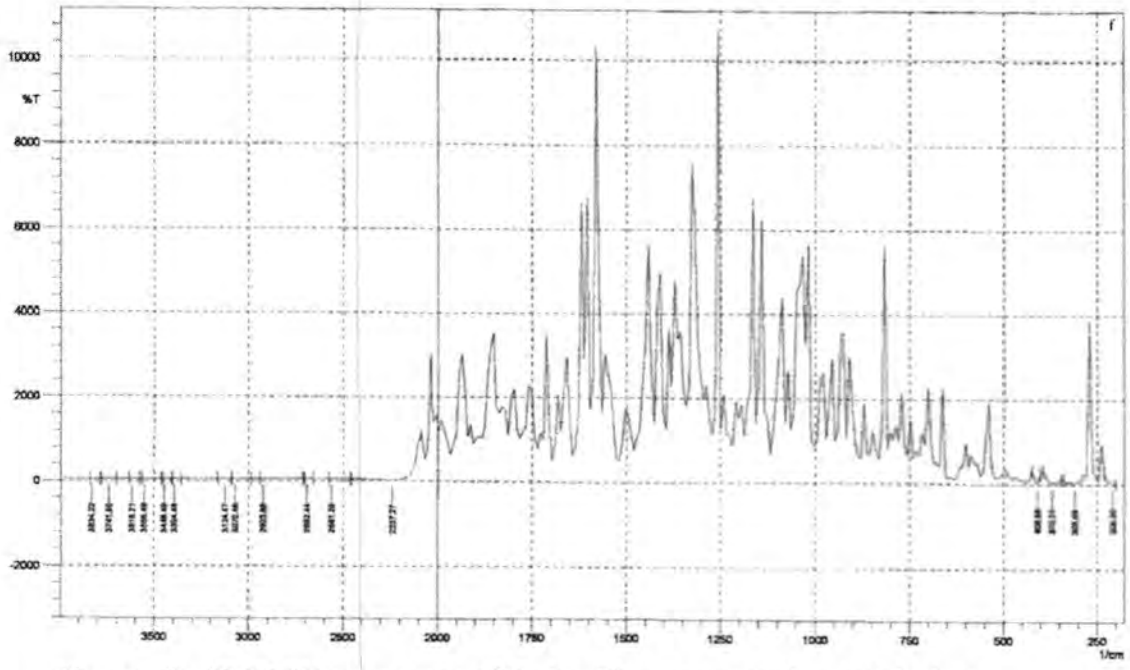

Figure -8: (f) FTIR spectrum of SnO_2 films prepared at oxidation temperature T=873 K and oxidation time t=60 sec constant

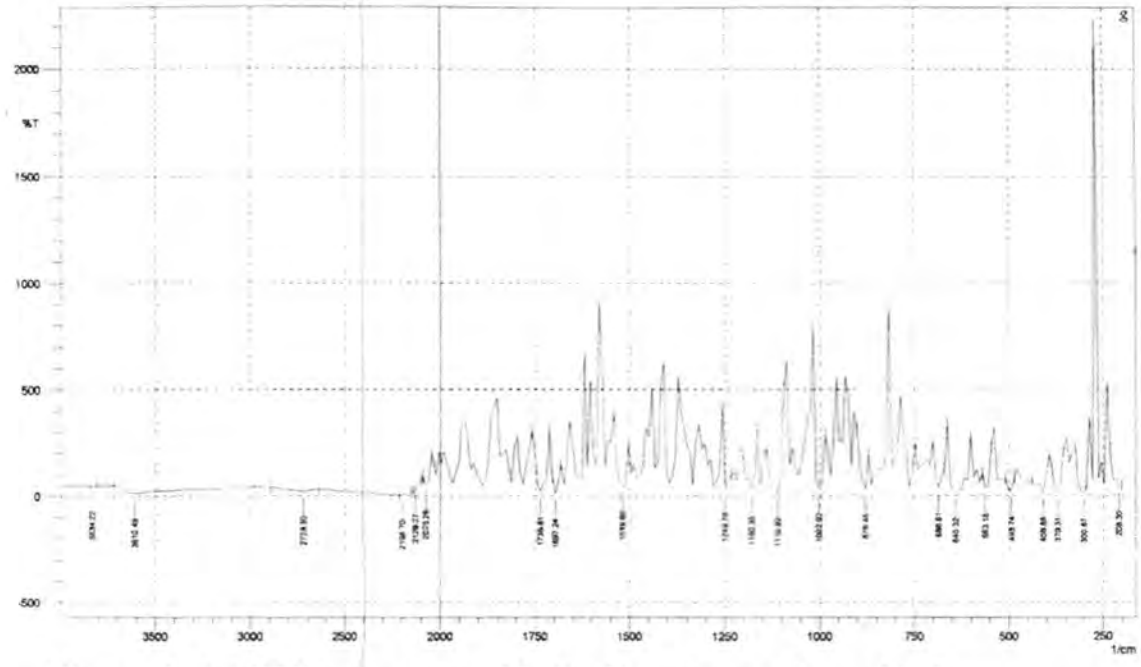

Figure -8: (g) FTIR spectrum of SnO_2 films prepared at oxidation temperature T=973 K and oxidation time t=60 sec constant

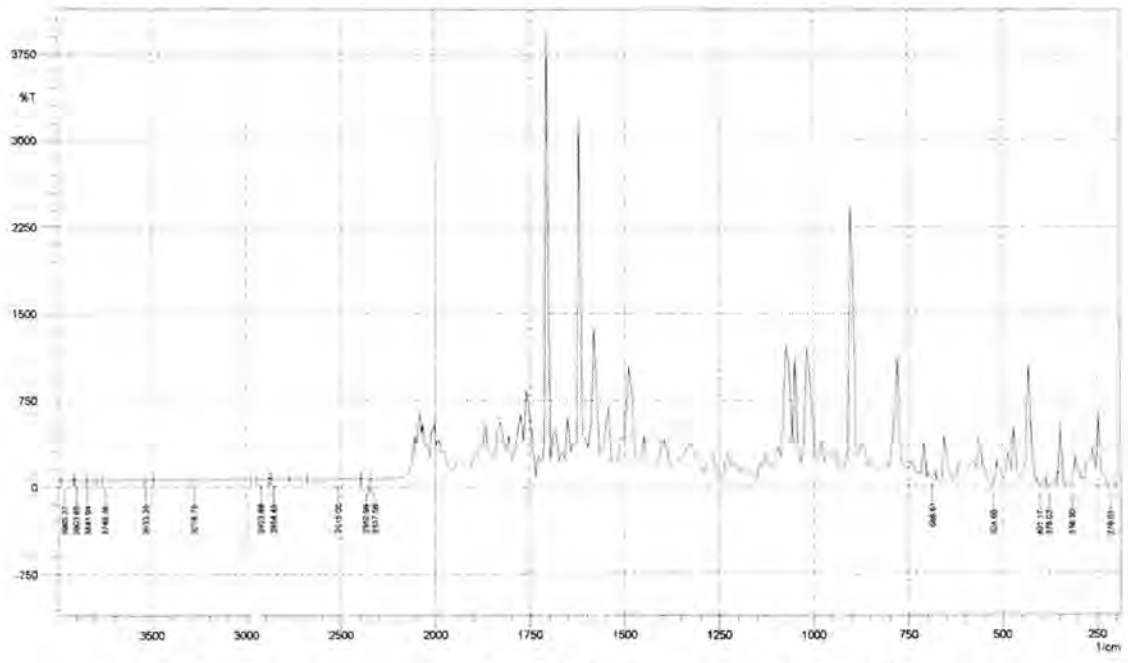

Figure -9: FTIR spectrum of SnO_2 films prepared at oxidation temperature T=873 K and oxidation time t=90 sec

SnO_2 films have been successfully prepared on quartz substrates at oxidation temperature 600 °C and oxidation time 90 sec by rapid thermal oxidation. SnO_2 film started to crystallize above 673 K and preferentially oriented in the (101) direction as the oxidation temperature increased to 873 and oxidation time 90 sec. The (Sn-O) vibrational and O-Sn-O phase's formations were identified from the FTIR results.

REFERENCES

1. K. Omura,[Z] P.Veluchamy,[*]M. Tsuji, T. Nishio, and. M. Murozono, Journal of the Electrochemical Society, 146 (6) :2113-2116 (1999).
2. Jochan Joseph,Varghese Mathew[1],Jacob Mathew[2],K.E. Abraham[2], Turk J Phys, 32: 1-11(2008).
3. L.S. Roman [A,*], R. Valaski [A], C.D. Canestraro[A], E.C.S.Magalhaes[B], C. Persson[C], R. Ahuja[D], E. F. Dasilvajr[e]. I. Pepe[B], A. Ferreira Dasilva, Applied Surface Science 252: 5361-5364, (2006)
4. K. L. Chopra, S. Major and D.K. pandya, Thin Solid Films, 102, 1-46 Electronics and Optics, (1983).
5. D. Hocine[*], M. S. Belkaïd and K. lagha, Revuedes Energies Renouvel Ables, 11 (3): 379-384, (2008).
6. M.Gökçen,A.Tataroğlu, Ş. Altindal,İ. Yücedağ, 24[TH]International Physics Congress of Turkish Physical Society,:28-31 August, Malatya - Turkye, (2007).

[7] R. Riveros*, E. Romero*, and G. Girdillo**, Brazillian Journal of Physics,.36, (3B), September, (2006).

[8] T. M. Uen, K. F. Huang, M. S. Chen* and Y. S. Gou, Thin Solid Films, 158 :69-80(1988).

[9] Jochan Joseph, Varghese Mathew, Jacob Mathew, K. E. Abraham " Studies on Physical Properties and Carrier Conversion of SnO2: Nd Thin Films" Turk J Phys, 33: 37 – 47, (2009).

[10] Yong-Sahm Choe, Jae-Ho Chung, Dae-Seung Kim, Gyeung-Ho Kim and Hong Koo Baik "Phase Transformation and Morphological Evolution of Ion-Beam Sputtered Tin Oxide Films on Silicon Substrate"Materials Research Bulletin,34,Issue9,:1473-1479, (1999).

[11] A. Moses Ezhi Raj, L. C. Nehru, M. Jayachandran, and C. Sanjeeviraja "Spray Pyrolysis Deposition and Characterization of Highly (100) Oriented Magnesium Oxide Thin Films" Cryst. Res. Technol. 42, (9) : 867 – 875 (2007).

[12] Wachirapunt Puntgrawee and Sutatip Siripaisarnpipat "Synthesis of Tin Oxide Nanoparticles by Sol-Gel Method Using Gelating Promoter"E-mail:g4764024@ku.ac.th.

The limitations and pitfalls in clinical implications of Bragg's peak: A theoretical SRIM – TRIM model of human breast tumor

Marwan S.M. Al-Nimer and Zainab Wahbee Abdul Lateef
Department of Pharmacology/College of Medicine/Al-Mustansiriya University
Department of Physiology/College of Medicine/Al-Mustansiriya University

الخلاصة

تعد معالجة حزمة البروتون فريدة لأنها تسمح بوضع طاقتها الأيونية في عمق محدد مع تبعثر ضئيل جدا في الطاقة والتي تعرف بقمة براك. هدفت الدراسة الى التقصي عن الهفوات التي يمكن ان تحصل عند تطبيق قمة براك لنموذج نظري لأورام الثدي في الانسان. تم استعمال برنامج سرم – ترم طبعة 1998 و2003 وتم تصميم نموذج لسرطان الثدي بحيث تخترق الايونات (الهيدروجين او الكاربون) وبطاقات مختلفة طبقات الجلد والشحم وانسجة الثدي الطبيعية ونسيج ورم في الثدي ذو كثافات مختلفة. اظهرت النتائج ان الطاقة المكبوحة للكاربون هي اكبر من الهيدروجين وتتناسب طرديا مع كثافة النسيج. وتناسب المدى الأفقي عند اختراق الأيونات مع الطاقة المسلطة وقد تدنى اقتحام ايونات الهيدروجين بزيادة كثافة نسيج الورم في حين كانت الطاقة المفقودة في الورم عالية مع تشعيع الكاربون. وقد تسبب التشعيع الأيوني الذي تناسب طرديا مع الطاقة المسلطة وعكسيا مع كتلة الورم في تلف الورم . نستنتج من هذه الدراسة انه بالأمكان الحصول على قمة براك وتطبيقه في معالجة اورام الثدي اذا ما اخذ بنظر الاعتبار كثافة او كتلة الورم ، و موضع الورم في النسيج الطبيعي و طبيعة الأيون المشع والطاقة المسلطة مجتمعة.

ABSTRACT

Proton beam therapy is unique because it allows for minimal scattering as particulate beam pass through tissue and deposing ionizing energy at precise depth i.e. Bragg peak. This study is aimed to investigate the limitations and pitfalls in clinical application of Bragg peak in theoretical model of human breast tumor. The Microsoft; "The Stopping and Range of Ions in Matter (SRIM)" version 1998, and 2003 was used. A model of breast tumor was designed and the projection of irradiated ions (hydrogen or carbon) crossed multi-layers including skin, adipose tissue, normal and abnormal breast tissues of different densities. The results showed that the stopping power of carbon ions was higher than corresponding hydrogen ions and proportionally increased with tissue density. The longitudinal range was directly correlated with acceleration potential energy for both hydrogen and carbon ions. The straggling of the hydrogen ions and to lesser extent the carbon ions tended to be declined, for each accelerated potential, with increment in density of breast tissue. The energy loss was higher with carbon ions compared with hydrogen ions. Irradiation with hydrogen or carbon ions resulted in breast tissue damage which was proportionally related to the accelerated potentials and inversely with target density. The damaging effect of carbon ions was inferior to that of hydrogen ions. It concludes that typical Bragg's peak can be achieved when the density of irradiated tissue , the localization of abnormal tissue , the type of ions radiation and the acceleration potentials are taken collectively in consideration.
Key words: Breast tumor, Bragg peak

INTRODUCTION

The concept of proton therapy was first developed by, the father of proton therapy, Dr. Robert Rathbun Wilson in 1946 (1). In 1954, the university of Berkeley began using proton technology after the construction of a cyclotron to treat cancer patient. In the United States there are few facilities offering proton therapy. The therapeutic use of protons (or helium ions) is produced by an accelerator; cyclotron, synchrotron, synchrocyclotron or linear (2). This type of

radiation is unique because it allows for minimal scattering as particulate beam pass through tissue and deposing ionizing energy at precise depth i.e. Bragg peak, which was described by William Bragg over 100 years (3,4). The heavy particles appear to continuously slow down gradually losing their energy along an unaltered linear path. Protons pass near orbiting electrons pulling them out of their orbits causing ionization (5). These processes end with the heating of the absorber (i.e. the target) through atom and of the molecule. The real advantages of proton therapy could not be realized until imaging systems; computerized tomography, magnetic resonance image, positron emission tomography were invented that could precisely located the tumor lesion (6).

The exact depth to which protons penetrate, and at which the Bragg peak occurs, is dependent on the energy of the proton beam. This energy can be very precisely controlled the place of the Bragg peak within a tumor or other tissue that are targeted to receive the radiation dose. The energy is inversely proportioned with stopping power. The other influencing factors include the electron mass, the charge and the target density. The electron is much faster than the alpha particles due to its smaller mass, therefore, the electron has less time to spread near orbital electrons. This reduces the effect of Coulomb interactions (hence stopping power) and increase range. The more charge or density, the more stopping power and the lower range. Protons have physical advantages over gamma rays and X-rays when it comes to sparing normal tissue and to treat irregular shaped lesions with awkward configurations near critical structures (7). The use of proton beam radiation therapy (PBRT) has been studied most extensively in terms of clinical effectiveness and safety for the treatment of uveal (ocular) melanoma, pituitary adenoma, and intracranial arterio-venous malformation where open surgery is not an option and conventional radiation therapy may not be appropriate (8,9). Also it is indicated for carcinoma of prostate, head and neck tumors etc.. (10,11).

This study is aimed to demonstrate the limitations and pitfalls in clinical application of Bragg peak in theoretical model of human breast tumor if the management of breast cancer is carried on by proton beams (hydrogen or carbon ions).

MATERIALS AND METHODS

This study was conducted in Department of Physiology/Medical Physics in cooperation with Department of Pharmacology, College of Medicine, Al-Mustansiriya University in Baghdad, Iraq during 2009. The Microsoft "The Stopping and Range of Ions in Matter (SRIM)" version 1998, and 2003 was used. A model of breast tumor located 27 mm from the skin was persumed. Therefore, projection of protons passed through skin (presumed as normal healthy skin of 2mm), subcutaneous and mammary adipose tissues (presumed 5 mm) and the pre-tumor healthy mammary tissues of 20 mm. The specifications

of each layer and the breast tumors of different densities were seen in table 1. The effectiveness of proton beam therapy was studied using fixed localization of tumors but differed in their densities (1.5, 2.0 and 2.5 g/cm^3) irradiated by acceleration potential of 60, 70, 80 and 90 MeV. The following variables were considered in assessment the effectiveness and the hazard of proton:

a. Hydrogen ion (1 amu) projected to the target tissue at 0 angle i.e. perpendicular to the tumor.

b. The transmitted ions, scattered ions, the range and the straggle of ions in longitudinal (X) lateral (Y), radial (Z) projections.

c. Vacancy/ion,

d. Percent of energy loss in ion ionization

e. A symmetrical distribution of energy losses of particles i.e. straggling

f. Phonens

g. Ion effective charge, fractional effective charge, vacancies energy loss and energy loss (eVA) for 25000 electrons were considered in assessment of proton beam therapy.

In another series of experiments , the carbon ions (for 10000 electrons) instead of hydrogen ions are delivered at acceleration potential of 600, 700, 800 and 900 MeV to the breast tissue of 0.99 g/cm^3 density.

The stopping power (S) is given by:

S= - dE/dx

The quantity of S (keV/μ) is referred to specific energy loss

E: charged particle kinetic energy

-dE: the energy increment lost in infinitesimal material thickness (dx)

The specific energy loss is expressed by Bethe-Bloch formula (12,13).

For heavy charged particle:

$$-\frac{dE}{dx} = \frac{4\pi e^4 z^2}{m_0 v^2} NB$$

Where

$$B = Z\left[\ln\frac{2m_0v^2}{I} - \ln\left(1-\frac{v^2}{c^2}\right) - \frac{v^2}{c^2}\right]$$

With the following definitions:

V velocity of the charged particle
ze charge of the charged particle
N number density of absorber atoms
Z atomic number of absorber atoms
m electron rest mass
e electron charge
I A parameter, treated as experimentally determined, representing average
excitation and ionization potential

B is known as the stopping number (atomic number scaled for stopping)

Bethe-Bloch formula for electrons :

$-dE/dx = (2\pi e^4 / m_e v^2)\, NB$

$B = Z\left[\ln \frac{m_e v^2 T}{2I^2(1-\beta^2)} - (\ln 2)\left(2\sqrt{1-\beta^2} - 1 + \beta^2\right) + 1 - \beta^2 + \frac{1}{8}\left(1 - \sqrt{1-\beta^2}\right)^2\right]$

Where $\beta = \frac{v}{c}$

The total stopping power for electron can be given as a combination of collisional (inelastic collision with atomic electrons) and radiative (inelastic collision with nucleous) types of interaction; (Bremsstrahlung)

[dE/dx] total = [dE/dx]collision + [dE/dx] radiative

For heavy particles, orbital electron interactions are only considered since the probability of nuclear interaction resulting in energy loss is much smaller.

$$-\left(\frac{dE}{dx}\right)_r = \frac{NTZ(Z+1)e^4}{137 m_0^2 c^4}\left(4\ln\frac{2T}{m_0 c^2} - \frac{4}{3}\right)$$

The percent of the energy loss goes to emitted rays is expressed by:

$$(\frac{dE}{dx})_r / (\frac{dE}{dx})\text{total} = EZ/1000$$

where E is in MeV, where Z is the atomic number of the absorber.

The range of a charged particle can be derived from stopping power formula:

$$R = \int_E^0 dx(cm) = \int_E^0 \frac{dE}{dE} dx = -\int_0^E \frac{1}{dE/dx} dE = \int_0^E \frac{dE}{S}$$

The summal distance elements as kinetic energy goes from E down to 0 is the total distance along the incident direction, or the range.

The lattice binding energy was 1.5 eV while the surface binding energy was 4.0 eV The displacement energy for each atom ; H (hydrogen), C (carbon), N (nitrogen), O (oxygen), Na (sodium), Mg (magnesium), P (phosphorus), S (sulphur), Cl (chloride), K (potassium), or Ca (calcium) or was 15 eV. The total target vacancies are depended on the accelerated potential and their energy loss was calculated by: Total target vacancies x binding energy (i.e. 1.5 eV). The Microsoft "The Stopping and Range of Ions in Matter (SRIM)" version 1998, and 2003 calculate the above variables and the lay out computerized data were obtained. Microsoft Excel 2003 was used for calculations and figures plotting.

RESULTS AND DISCUSSION

Figure 1 shows the stopping power of hydrogen ions in the skin and adipose tissue which differed from the stopping power of carbon ions. At the acceleration potential of 14 MeV, the stopping power of hydrogen at the distal end of the skin i.e. 2mm was 3.832 keV/μ while the stopping power of carbon ions was 927.4 keV/μ at longitudinal range of 5.61μ with acceleration potential of 4 MeV. Comparative results were obtained with adipose tissue. The stopping powers of hydrogen ions were 2.513 and 2.324 keV/μ for longitudinal ranges 4.39 and 5.21 mm at acceleration potentials of 20 and 22 MeV respectively. Again the stopping power of carbon ions was higher than corresponding hydrogen ions. It was 858.7 kev/ions at longitudinal range of 4.02μ with acceleration potential of 2.4 MeV.

In the breast tissue the stopping power of carbon ions were increased with increasing breast tissue density. It amounted 87.83, 1337, 1795, and 2244 kev/ion for breast tissue density of 0.99, 1.5, 2.0 and 2.5 g/cm^3 respectively [Fig.2].The stopping powers of hydrogen ions were 1.091, 1.653, 2.204 and 2.587 for corresponding breast mass density [Fig.2]. The longitudinal range was directly correlated with acceleration potential energy for both hydrogen and carbon ions but the depth tissue penetration was so lesser with carbon ions compared with than that observed with hydrogen ions [Fig 3]. From figure 3, the calculated energy for 1 micron and 1000 micron tissue penetration was 28.57 MeV and 32.50 MeV for carbon and hydrogen ions respectively. The interesting observation is the ability of hydrogen ions to deposit their energies in abnormal breast tissue (i.e. of different densities) that embedded in normal breast tissues with minimal effect of radiation to the normal breast tissue [Fig 4 A]. The energy deposited by carbon ions were superficial i.e. the Bragg's peak of abnormal breast tissue was shifted down to the normal breast tissue [Fig 4B].

The straggling of hydrogen ions whether longitudinal, radial, or lateral tended to be declined, for each accelerated potential, with increment in density of breast tissue [Tables 2-5], while the ion straggling was proportionally increased with increasing accelerated potential for each density [Tables 2-5].

The same finding was observed with carbon ions but to a lesser degree than that observed with hydrogen ions [Table 6]. For example the longitudinal straggling of hydrogen ion at 60 MeV acceleration potential was 1.269% (386μ/30.4 mm) compared with 0.32 (27.4 μ/7.48mm) at 600 MeV acceleration potential for carbon ions. The vacancies of the target was not differed for each accelerated potential when the tissue density was changed. In each breast tissue with specific density the vacancies were proportionally increased with high accelerated energy [Tables 2-6]. Table 7 shows the total energy loss in respect to the target vacancies. Taking in consideration the magnitude of accelerated potential and the counted electrons, the energy loss was higher with carbon ions compared with hydrogen ions. The shape of Bragg's peaks were statistically determined by the skewness and the kurtosis. Therefore, it is expected to find

several shapes according to the results of skewness and kurtosis listed in Tables2-6.

The electron stopping power of irradiated hydrogen to each atom of breast tissue was higher than that irradiated with carbon ions at all studied accelerated energies [Tables 8 and 9] while the picture is reversed with the nuclear stopping power. Moreover the ion effective charge as well as the fractional effective charge remained constant at different accelerated potentials with carbon ions but they fluctuated with hydrogen ions [Tables 8 & 9]. From the above data, the damaged breast tissue volume or mass were calculated. Table 10 shows that irradiation with hydrogen or carbon ions resulted in breast tissue damage which was proportionally related to the accelerated potentials and inversely with target density. The damaging effect of carbon ions was inferior to that of hydrogen ions.

The results of this study demonstrate that both hydrogen and carbon ions radiation produce ionization density in the Bragg region but their behaviors are differed. For the treatment purposes the position of Bragg peak needs to be spread out to cover the tumor volume and the production of such a spread out Bragg peak results in a build up in the spread out Bragg peak relative to the plateau (14). In this work the spread out Bragg peak is well demonstrated with hydrogen ions compared with carbon ions radiation (15). The width of Bragg peak for hydrogen and carbon ions in human tissues was less than the typical width of 8 mm for 177 MeV proton beam. In this study the Bragg curve of carbon ions radiation is differed from that of hydrogen ions radiation because carbon ions distribute in a considerably wider region beyond the Bragg-peak due to its strong penetrability (16). The scatter events as a result of energy lost through proton interaction with the nucleus rather than with atomic electrons were well demonstrated with the hydrogen ions radiation (17). These scatters events cause the proton's path to deviate from a straight line, and a lateral fall of 5-8 mm at 10 cm depth was known. The lateral and radial scatters reported in this study are much lower than reported by others (18). The width penetration of hydrogen ions radiation is increased with increasing the acceleration potentials i.e. radiation energy for fixed tissue density and it decreased as the tissue density is increased (19) . It is well known that women with a tumor size more than 1 cm were more likely to have dense breast in mammography compared with a tumor size less than 1 cm (20, 21). Therefore, it is necessary to use high acceleration potential for highly dense breast tissue (i.e. large tumor volume) in order to achieve the full blown Bragg peak. The differences in the skewness and kurtosis of Bragg peaks reflected on the deposition of ionized energy on the tissue as well as it gives a clue for the harmful effect of radiation on the normal tissue. The stopping power of hydrogen ions targeting the atoms in breast tissue is differed from that of carbon ion radiation in respect to the electrons or nuclear stopping power. This observation can explained the

multiple scatters that demonstrated in this study. The fact that the range straggling and multiple scattering are reduced from hydrogen to carbon increases the possibility to accurately deposit only the high linear energy transfer component in the tumor with negligible dose to organs at risk (22). The calculated volume and mass of damaged breast tissue pointed out that the carbon ion radiation is more suitable for superficial and tiny abnormal breast tissue with negligible effect on the normal tissue while the hydrogen ions radiation is suitable for large, deep seated tumors with less acceleration potentials. The relative biological effectiveness of the carbon ions dose (calculated as the ratio of ^{60}Co to proton doses which resulted in the same level of cell survival) deposited in tumor is higher than that reported with hydrogen ions but it carried a potential risk of later onset of secondary cancers (23-25). In this work the relative biological effectiveness of carbon ions is not achieved to the standard of the National Institute of Radiological Sciences which equivalent to 3 at a depth where the dose averaged is 80 keV/micron because the accelerated potentials that are used in this work are less (26). The rational for proton beams for breast tumor results in unparalleled homogeneous dose distributions within complex target volumes, while simultaneously sparing neighboring organs (27). The findings of this study confirmed the advantages of proton therapy for tiny tumors and metastases. It concludes that typical Bragg's peak can be achieved when the density of irradiated tissue , the localization of abnormal tissue , the type of ions radiation and the acceleration potentials are taken collectively in considerations.

Table - 1: Specification of target layers exposed to protons

Tissue			Atomic percent (mass percent)								
	Layer width (A)	Density g/cm^3 (atom/cm^3)	H	C	N	O	Na	S	Cl	K	P
Skin	2x10^7	1.09 (10.56x10^{22})	61.7 (10)	12.9 (25)	2.04 (4.6)	23.1 (59.4)	5.4 (0.199)	5.8 (0.299)	5.3 (0.302)	1.6 (0.100)	- -
Adipose tissue	5x10^7	0.92 (10.35x10^{22})	63.4 (11.9)	28.4 (63.8)	0.305 (0.801)	7.77 (23.2)	1.19 (5.15)	- -	1.79 0.119	- -	- -
Breast density (0.99 g/cm^3)	2x10^8	0.99 (10.39x10^{22})	61.9 (10.8)	24.1 (50.6)	0.941 (2.29)	12.8 (35.7)	0.025 (0.1)	0.018 (0.1)	0.016 (9.89)	-	0.019 (0.102)
Breast density (1.5 g/cm^3)	2x10^8	1.5 (15.75x10^{22})	61.9 (10.8)	24.1 (50.6)	0.941 (2.29)	12.8 (35.7)	0.025 (0.1)	0.018 (0.1)	0.016 (9.89)	-	0.019 (0.102)
Breast density (2.0 g/cm^3)	2x10^8	2.0 (21.0x10^{22})	61.9 (10.8)	24.1 (50.6)	0.941 (2.29)	12.8 (35.7)	0.025 (0.1)	0.018 (0.1)	0.016 (9.89)	-	0.019 (0.102)
Breast density (2.5 g/cm^3)	2x10^8	2.5 (26.25x10^{22})	61.9 (10.8)	24.1 (50.6)	0.941 (2.29)	12.8 (35.7)	0.025 (0.1)	0.018 (0.1)	0.016 (9.89)	-	0.019 (0.102)

A: Armstrong, H: hydrogen, C: carbon, N: nitrogen, O: oxygen, Na: sodium, S: sulphur, Cl: chloride, K: potassium, P: phosphorus

Table -2: The individual data of Bragg's peak generated by hydrogen ions in breast tissue ($0.99g/cm^3$) at different acceleration potential.

	Longitudinal	Lateral	Radial		Ionization	Vaccancies	Phonens
Breast tissue	Range (straggling)	Range (straggling)	Range (straggling)	Vaccancy ./ ion	Ions (recoil)	Ions (recoil)	Ions (recoil)
Density ($0.99g/cm^3$) 60 MeV	30.4mm (386 μ)	395 μ (575 μ)	621 μ (511 μ)	228.9	99.96 (0.02)	0 0	0 (0.02)
70 MeV	40.2mm (477 μ)	514 μ (712 μ)	814 μ (657 μ)	258.9	99.96	0 0	0 (0.02)
80 MeV	51.0mm (718 μ)	663 μ (1 mm)	1.04mm (949 μ)	285.9	99.96 (0.02)	0 0	0 (0.02)
90 Mev	63mm (772 μ)	812 μ (1.16mm)	1.26mm (1.04mm)	311.7	99.96 (0.02)	0 0	0 (0.02)

Table -3: The individual data of Bragg's peak generated by hydrogen ions in breast tissue ($1.5g/cm^3$) at different acceleration potential.

	Long.	Lateral	Radial		Ionization	Vaccancies	Phonens
Breast tissue	Range (straggling)	Range (straggling)	Range (straggling)	Vaccancy./ion	Ions (recoil)	Ions (recoil)	Ions (recoil)
Density ($1.5g/cm^3$) 60 MeV	26mm (286 μ)	308 μ (479 μ)	485 μ (463 μ)	230.5	99.96 (0.02)	0 0	0 (0.02)
70 MeV	32.4mm (327 μ)	373μ (532 μ)	589 μ (478 μ)	259	99.96	0 0	0 (0.02)
80 MeV	40.8mm (605 μ)	497 μ (727μ)	779 μ (674 μ)	283.9	99.96 (0.02)	0 0	0 (0.02)
90 Mev	40.1mm (672 μ)	715μ (989 μ)	14.6mm (6.41mm)	302.5	99.96 (0.02)	0 0	0 (0.01)

Table -4: The individual data of Bragg's peak generated by hydrogen ions in breast tissue (2 g/cm^3) at different acceleration potential.

	Long.	Lateral	Radial		ionization	vaccancies	phonens		
Mammary gland	Range (strag.)	Range (strag.)	Range (strag.)	Vac./ion	Ions (recoil)	Ions (recoil)	Ions (recoil)	Skewness	kurtosis
Density (2g/cm^3) 60 MeV	23.8mm (220 μ)	264 μ (421 μ)	416 μ (415 μ)	231.4	99.96 (0.02)	0 0	0 (0.02)	-14.2859	607.136
70 MeV	28.7mm (245 μ)	305μ (439 μ)	480 μ (393 μ)	259.7	99.96	0 0	0 (0.02)	-4.4113	132.549
80 MeV	34.1mm (299 μ)	366 μ (545μ)	572 μ (491 μ)	285.9	99.96 (0.02)	0 0	0 (0.02)	-2.0846	39.7743
90 Mev	35.5mm (288 μ)	356 μ (514 μ)	564 μ (473 μ)	313.4	99.96 (0.02)	0 0	0 (0.01)	-1.5526	25.5295

Table -5: The individual data of Bragg's peak generated by hydrogen ions in breast tissue (2.5g/cm^3) at different acceleration potential.

	Long.	Lateral	Radial		ionization	vaccancies	phonens		
Mammary gland	Range (strag.)	Range (strag.)	Range (strag.)	Vac./ion	Ions (recoil)	Ions (recoil)	Ions (recoil)	Skewness	kurtosis
Density (2.5g/cm^3) 60 MeV	22.6mm (182 μ)	238 μ (385 μ)	375 μ (387 μ)	231.9	99.96 (0.02)	0 0	0 (0.02)	-16.7621	775.1576
70 MeV	26.4mm (196 μ)	264μ (380 μ)	410 μ (344 μ)	260.3	99.96	0 0	0 (0.02)	-4.4113	133.1514
80 MeV	30.7mm (237 μ)	307 μ (451μ)	481 μ (402 μ)	286.2	99.96 (0.02)	0 0	0 (0.02)	-1.7378	33.0656
90 Mev	35.5mm (731 μ)	506 μ (723 μ)	794 μ (677 μ)	308.2	99.96 (0.02)	0 0	0 (0.01)	-2.3901	50.1785

Table -6: The individual data of Bragg's peak generated by carbon ions in breast tissue (0.99g/cm^3) at different acceleration potential.

	Long.	Lateral	Radial		ionization	vaccancies	phonens		
Mammary gland	Range (strag.)	Range (strag.)	Range (strag.)	Vac./ion	Ions (recoils)	Ions (recoils)	Ions (recoils)	Skewness	kurtosis
Density (0.99g/cm^3)									
600 MeV	7.48mm (27.4 μ)	31.8 μ (26 μ)	49.9 μ (40 μ)	2912.9	99.94 (0.03)	0 0	0 (0.03)	-4.7695	130.6926
700 MeV	9.83mm (70 μ)	40.2μ (58.8 μ)	63.2 μ (53.9 μ)	3225.3	99.94 (0.03)	0 0	0 (0.02)	-67.2618	5877.178
800 MeV	13mm (47.1 μ)	53.5 μ (79.1μ)	83.2 μ (67.2 μ)	3540	99.95 (0.03)	0 0	0 (0.02)	-0.929	13.0216
900 Mev	15.3mm (80.6 μ)	60.8 μ (85 μ)	95.1 μ (74.5 μ)	3801	99.94 (0.04)	0 0	0 (0.02)	-27.5539	1407.1163

Table- 7: the calculated energy loss of total target (breast tissue 0.99 g/cm^3 density) vacancies /ion irradiated with hydrogen ions (total electrons 25000) or carbon ions (total electrons 10000).

	Energy loss with hydrogen ions (keV)	Energy loss with carbon ions (keV)
Density (0.99g/cm^3) 60 MeV	343.35	
70 MeV	388.35	
80 MeV	428.85	
90 Mev	467.55	
Density (0.99g/cm^3) 600 MeV		4378.5
700 MeV		4837.95
800 MeV		5310
900 MeV		5701.5

Table-8: The stopping power of hydrogen ions targeted each atom in breast tissue at different accelerated potentials

Energy (keV)	Ion	Target	Stopping Electron (keV/μ)	Stopping Nuclear (keV/μ)	Stopping total (keV/μ)	Ion effective charge	Fractional effective charge
60000	H	H	$2.563x10^{5}$	$1.231x10^{-4}$	$2.563x10^{5}$	%1249.885	%1239.965
		C	$6.780x10^{5}$	$8.785x10^{-4}$	$6.780x10^{5}$	%557.293	%552.8697
		N	$2.647x10^{5}$	$3.946x10^{-4}$	$2.647x10^{5}$	519.110	%514.9903
		O	$3.221x10^{5}$	$5.423x10^{-4}$	$3.221x10^{5}$	%490.359	%486.4674
		S	$2.331x10^{5}$	$7.306x10^{-4}$	$2.331x10^{5}$	%362.689	%359.8104
		Cl	$1.932x10^{5}$	$6.144x10^{-4}$	$1.932x10^{5}$	%350.420	%347.6390
		Na	$1.525x10^{5}$	$3.275x10^{-4}$	$1.525x10^{5}$	%428.981	%425.5765
		K	$7.980x10^{4}$	$2.840x10^{-4}$	$7.980x10^{4}$	%334.263	%331.6099
		P	$3.060x10^{5}$	$1.539x10^{-3}$	$3.060x10^{5}$	%274.663	%272.4835
70000	H	H	$2.990x10^{5}$	$1.064x10^{-4}$	$2.990x10^{5}$	%1434.355	%1422.970
		C	$7.910x10^{5}$	$7.629x10^{-4}$	$7.910x10^{5}$	%639.507	%634.4317
		N	$3.088x10^{5}$	$3.428x10^{-4}$	$3.088x10^{5}$	%595.480	%590.7541
		O	$3.758x10^{5}$	4.711x10v	$3.758x10^{5}$	%562.492	%558.0275
		S	$2.720x10^{5}$	$6.354x10^{-4}$	$2.720x10^{5}$	%415.495	%412.1970
		Cl	$2.254x10^{5}$	$5.343x10^{-4}$	$2.254x10^{5}$	%401.668	%398.4798
		Na	$1.779x10^{5}$	$2.845x10^{-4}$	$1.779x10^{5}$	%492.161	%488.2552
		K	$9.310x10^{4}$	$2.471x10^{-4}$	$9.310x10^{4}$	%383.014	%379.9743
		P	$3.570x10^{5}$	$1.340x10^{-3}$	$3.570x10^{5}$	%314.459	%311.9632
80000	H	H	$3.417x10^{5}$	$9.438x10^{-4}$	$3.417x10^{5}$	%1615.052	%1602.2342
		C	$9.040x10^{5}$	$3.034x10^{-4}$	$9.040x10^{5}$	%719.880	%714.1668
		N	$3.529x10^{5}$	$3.034x10^{-4}$	$3.529x10^{5}$	%670.151	%664.8323
		O	$4.294x10^{5}$	$4.170x10^{-4}$	$4.294x10^{5}$	%633.002	%627.9781
		S	$3.108x10^{5}$	$5.628x10^{-4}$	$3.108x10^{5}$	%467.107	%463.3998
		Cl	$2.576x10^{5}$	$4.734x10^{-4}$	$2.576x10^{5}$	%451.736	%463.3998
		Na	$2.033x10^{5}$	$2.520x10^{-4}$	$2.033x10^{5}$	%553.867	%549.4716
		K	$1.064x10^{5}$	$2.189x10^{-4}$	$1.064x10^{6}$	%430.647	%427.2295
		P	$4.080x10^{5}$	$1.188x10^{-3}$	$4.080x10^{5}$	%353.308	%350.5037
90000	H	H	$3.844x10^{5}$	$8.463x10^{-4}$	$3.844x10^{5}$	%1792.253	%1778.0286
		C	$1.017x10^{6}$	$6.060x10^{-4}$	$1.017x10^{6}$	%798.550	%792.2123
		N	$3.970x10^{5}$	$2.723x10^{-4}$	$3.970x10^{5}$	%743.250	%737.3511
		O	$4.831x10^{5}$	$3.744x10^{-4}$	$4.831x10^{5}$	%702.012	%696.4403
		S	$3.497x10^{5}$	$5.057x10^{-4}$	$3.497x10^{5}$	%517.615	513.5071
		Cl	$2.898x10^{5}$	$4.254x10^{-4}$	$2.898x10^{5}$	%500.713	%496.7392
		Na	$2.287x10^{5}$	$2.263x10^{-4}$	$2.287x10^{5}$	%614.212	%609.2589
		K	$1.197x10^{5}$	$2.189x10^{-4}$	$1.197x10^{5}$	%477.247	%473.4589
		P	$4.590x10^{5}$	$1.068x10^{-3}$	$4.590x10^{5}$	%391.282	%388.1767

Table - 9:The stopping power of carbon ions targeted each atom in breast tissue at different accelerated potentials

Energy (keV)	Ion	Target	Stopping Electron (keV/μ)	Stopping Nuclear (keV/μ)	Stopping total (keV/μ)	Ion effective charge	Fractional effective charge
600000	C	H	6.782	4.570×10^{-3}	6.782	6	1
		C	9.031×10^{1}	3.617×10^{-2}	9.031×10^{1}	6	1
		N	4.059×10^{1}	1.634×10^{-2}	4.059×10^{1}	6	1
		O	5.536×10^{1}	2.256×10^{-2}	5.536×10^{1}	6	1
		S	7.299×10^{1}	3.102×10^{-2}	7.299×10^{1}	6	1
		Cl	6.491×10^{1}	2.615×10^{-2}	6.491×10^{1}	6	1
		Na	3.426×10^{1}	1.378×10^{-2}	3.426×10^{1}	6	1
		K	2.944×10^{1}	1.212×10^{-2}	2.944×10^{1}	6	1
		P	1.669×10^{2}	6.643×10^{-2}	1.669×10^{2}	6	1
700000	C	H	6	3.969×10^{-3}	6.004	6	1
		C	7.986×10^{1}	3.143×10^{-2}	7.989×10^{1}	6	1
		N	3.592×10^{1}	1.420×10^{-2}	3.594×10^{1}	6	1
		O	4.899×10^{1}	1.960×10^{-2}	4.901×10^{1}	6	1
		S	6.479×10^{1}	2.697×10^{-2}	6.482×10^{1}	6	1
		Cl	5.754×10^{1}	2.274×10^{-2}	5.746×10^{1}	6	1
		Na	3.030×10^{1}	1.197×10^{-2}	3.032×10^{1}	6	1
		K	2.612×10^{1}	1.054×10^{-2}	2.613×10^{1}	6	1
		P	1.483×10^{2}	5.781×10^{-2}	1.483×10^{1}	6	1
800000	C	H	5.401	3.513×10^{-3}	5.405	6	1
		C	7.188×10^{1}	2.782×10^{-2}	7.191×10^{1}	6	1
		N	3.236×10^{1}	1.257×10^{-2}	3.237×10^{1}	6	1
		O	4.413×10^{1}	1.735×10^{-2}	4.415×10^{1}	6	1
		S	5.850×10^{1}	2.389×10^{-2}	5.852×10^{1}	6	1
		Cl	5.189×10^{1}	2.014×10^{-2}	$5,191\times10^{1}$	6	1
		Na	2.729×10^{1}	1.060×10^{-2}	3.730×10^{1}	6	1
		K	2.357×10^{1}	9.336×10^{-3}	2.358×10^{1}	6	1
		P	1.340×10^{2}	5.124×10^{-2}	1.341×10^{2}	6	1
900000	C	H	4.927	3.154×10^{-3}	4.930	6	1
		C	6.559×10^{1}	2.497×10^{-2}	6.562×10^{1}	6	1
		N	2.954×10^{1}	1.128×10^{-2}	2.955×10^{1}	6	1
		O	4.029×10^{1}	1.558×10^{-2}	4.031×10^{1}	6	1
		S	5.351×10^{1}	2.147×10^{-2}	5.353×10^{1}	6	1
		Cl	4.743×10^{1}	1.810×10^{-2}	4.745×10^{1}	6	1
		Na	2.491×10^{1}	9.523×10^{-3}	2.492×10^{1}	6	1
		K	2.155×10^{1}	8.389×10^{-3}	2.156×10^{1}	6	1
		P	1.227×10^{2}	4.606×10^{-2}	1.228×10^{2}	6	1

Table – 10:Effect of proton beam radiation by hydrogen or carbon ions on the breast tissue volume and mass at different range of energies and tissue density.

	Density 1.5 g/cm^3				Density 2 g/cm^3				Density 2.5 g/cm^3			
	Hydrogen ion		Carbon ion		Hydrogen ion		Carbon ion		Hydrogen ion		Carbon ion	
MeV	Volume (cm^3)	Mass (g)	Volume (cm^3)	Mass (g)	Volume (cm^3)	Mass (g)	Volume (cm^3)	Mass (g)	Volume (cm^3)	Mass (g)	Volume (cm^3)	Mass (g)
1	$5.087x10^{-12}$	$7.631x10^{-12}$	$1.602x10^{-14}$	$2.4x\ 10^{-14}$	$2.147x10^{-12}$	$4.295x\ 10^{-12}$	$6.745x\ 10^{-15}$	$1.349x\ 10^{-14}$	$1.089x10^{-12}$	$2.745x10^{-12}$	$3.468x10^{-15}$	$8.670x\ 10^{-15}$
5	$1.377x10^{-8}$	$2.065x10^{-8}$	$1.147x10^{-13}$	$1.720x10^{-13}$	$5.812x10^{-9}$	$1.162x\ 10^{-8}$	$4.831x10^{-14}$	$9.663x\ 10^{-14}$	$2.971x10^{-9}$	$7.427x10^{-9}$	$2.478x10^{-14}$	$6.196x\ 10^{-14}$
10	$5.674x10^{-7}$	$8.512x10^{-7}$	$4.765x10^{-13}$	$7.148x10^{-13}$	$2.395x10^{-7}$	$4.79x\ 10^{-7}$	$2.009x10^{-13}$	$4.018x\ 10^{-13}$	$1.226x10^{-7}$	$3.065x10^{-7}$	$1.029x10^{-13}$	$2.574x\ 10^{-13}$
20	$2.073x10^{-5}$	$3.11x10^{-5}$	$2.899x10^{-12}$	$4.349x10^{-12}$	$8.727x10^{-6}$	$1.745x\ 10^{-5}$	$1.223x10^{-12}$	$2.446x\ 10^{-12}$	$4.468x10^{-6}$	$1.117x10^{-5}$	$6.233x10^{-13}$	$1.558x\ 10^{-12}$
30	$1.264x10^{-4}$	$1.897x10^{-4}$	$1.152x10^{-11}$	$1.728x10^{-11}$	$7.6x10^{-5}$	$1.520x\ 10^{-4}$	$4.861x10^{-12}$	$9.722x\ 10^{-12}$	$3.898x10^{-5}$	$9.745x10^{-5}$	$2.489x10^{-12}$	$6.222x\ 10^{-12}$
40	$9.086x10^{-4}$	$1.363x10^{-3}$	$3.815x10^{-11}$	$5.722x10^{-11}$	$3.836x10^{-4}$	$7.672x\ 10^{-4}$	$1.609x10^{-11}$	$3.218x\ 10^{-11}$	$1.962x10^{-4}$	$4.905x10^{-4}$	$8.258x10^{-12}$	$2.064x\ 10^{-11}$
50	$3.188x10^{-3}$	$4.782x10^{-3}$	$1.044x10^{-10}$	$1.566x10^{-10}$	$1.344x10^{-3}$	$2.688x\ 10^{-3}$	$4.399x10^{-11}$	$8.799x\ 10^{-11}$	$6.884x10^{-4}$	$1.721x10^{-3}$	$2.255x10^{-11}$	$5.637x\ 10^{-11}$
60	$8.269x10^{-3}$	$1.240x10^{-2}$	$2.314x10^{-10}$	$3.471x10^{-10}$	$3.489x10^{-3}$	$6.978x\ 10^{-3}$	$9.745x10^{-11}$	$1.949x\ 10^{-10}$	$1.786x10^{-3}$	$4.465x10^{-3}$	$5.003x10^{-11}$	$1.250x\ 10^{-10}$
70	$1.810x10^{-2}$	$2.715x10^{-2}$	$4.543x10^{-10}$	$6.815x10^{-10}$	$7.625x10^{-3}$	$1.525x\ 10^{-2}$	$1.912x10^{-10}$	$3.824x\ 10^{-10}$	$3.905x10^{-3}$	$9.762x10^{-3}$	$9.791x10^{-11}$	$2.447x\ 10^{-10}$
80	$4.008x10^{-2}$	$6.013x10^{-2}$	$9.348x10^{-10}$	$1.402x10^{-9}$	$1.695x10^{-2}$	$3.39x\ 10^{-2}$	$3.941x10^{-10}$	$7.882x\ 10^{-10}$	$8.664x10^{-3}$	$2.166x10^{-2}$	$2.020x10^{-10}$	$5.050x\ 10^{-10}$
90	$7.626x10^{-2}$	$1.143x10^{-2}$	$1.695x10^{-9}$	$2.543x10^{-9}$	$3.211x10^{-2}$	$6.422x\ 10^{-2}$	$7.104x10^{-10}$	$1.420x\ 10^{-9}$	$1.644x10^{-2}$	$4.11x10^{-2}$	$3.655x10^{-10}$	$9.138x\ 10^{-10}$

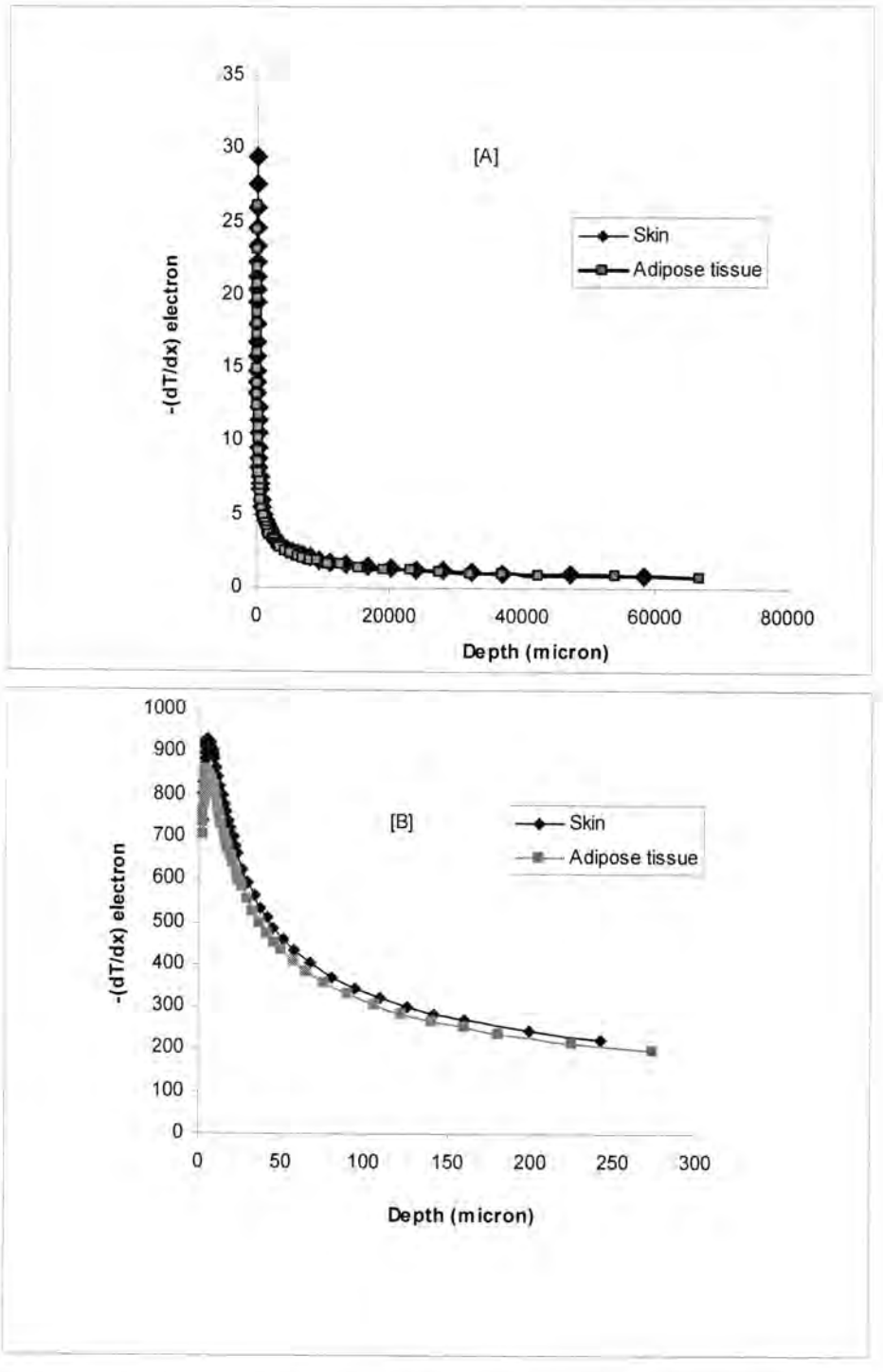

Fig - 1: The stopping power of hydrogen ions [A] and carbon ions [B] in the human skin and adipose tissue

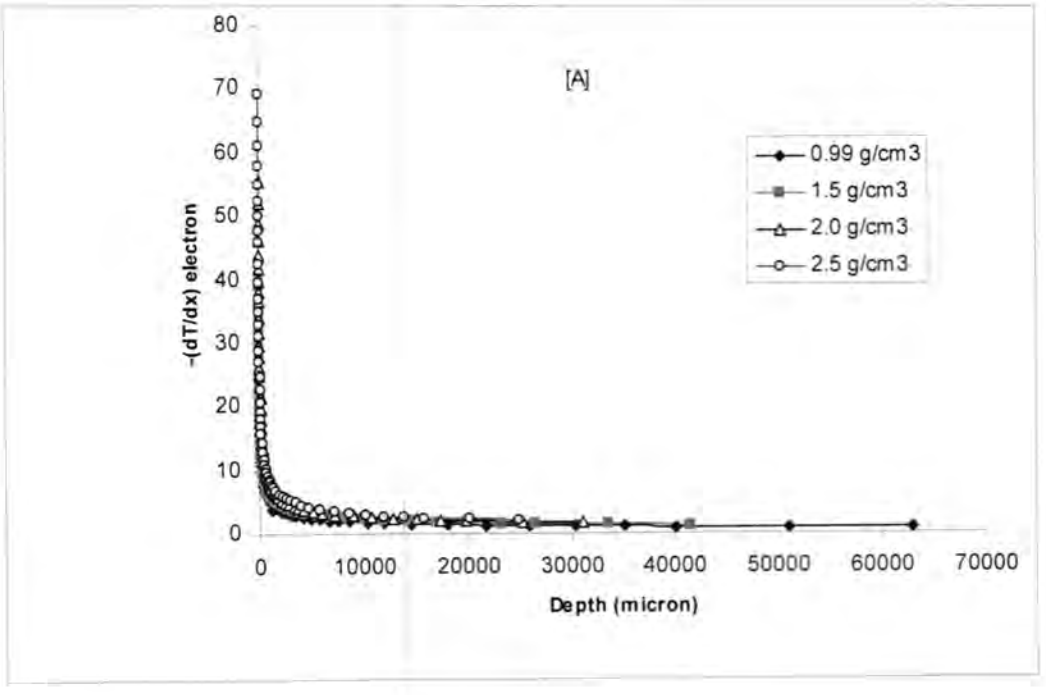

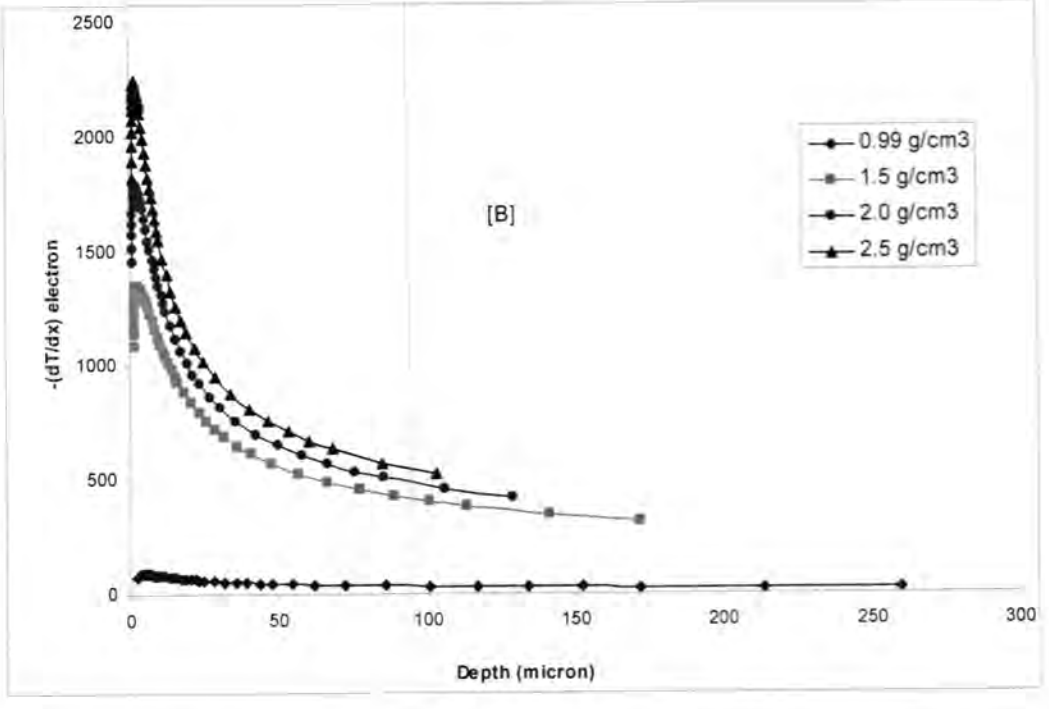

Fig- 2: The stopping power of hydrogen ions [A] and carbon ions [B] in the human breast tissue contained different densities of breast tissues.

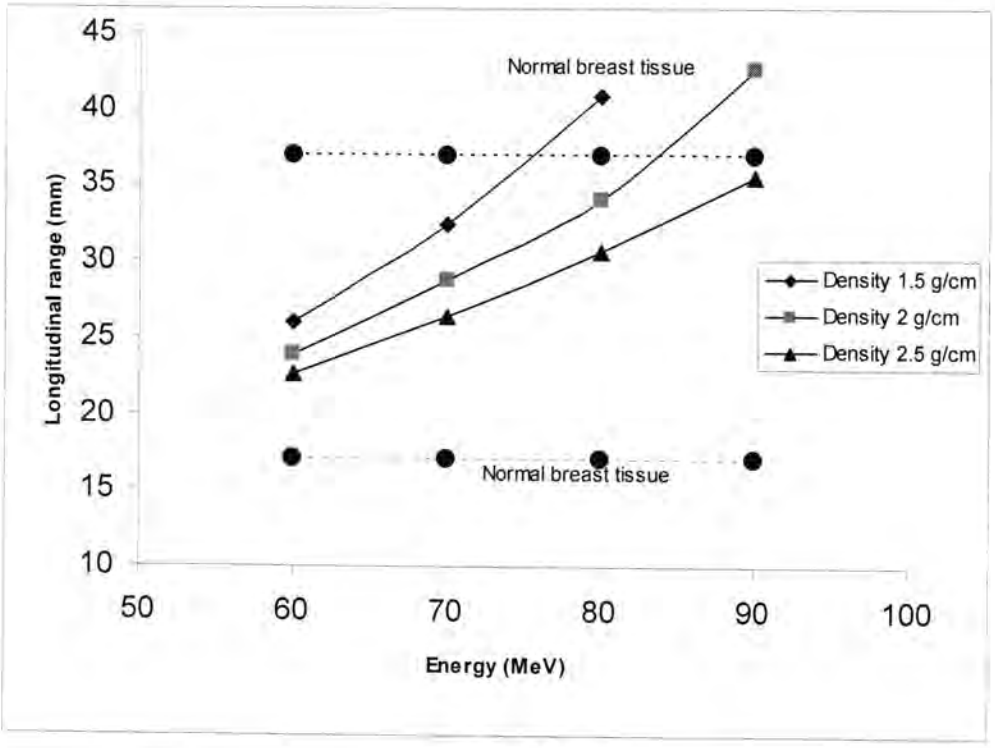
45
40
35
30
25
20
15
10
Longitudinal range (mm)
Normal breast tissue
Normal breast tissue
Density 1.5 g/cm
Density 2 g/cm
Density 2.5 g/cm
50
60
70
80
90
100
Energy (MeV)

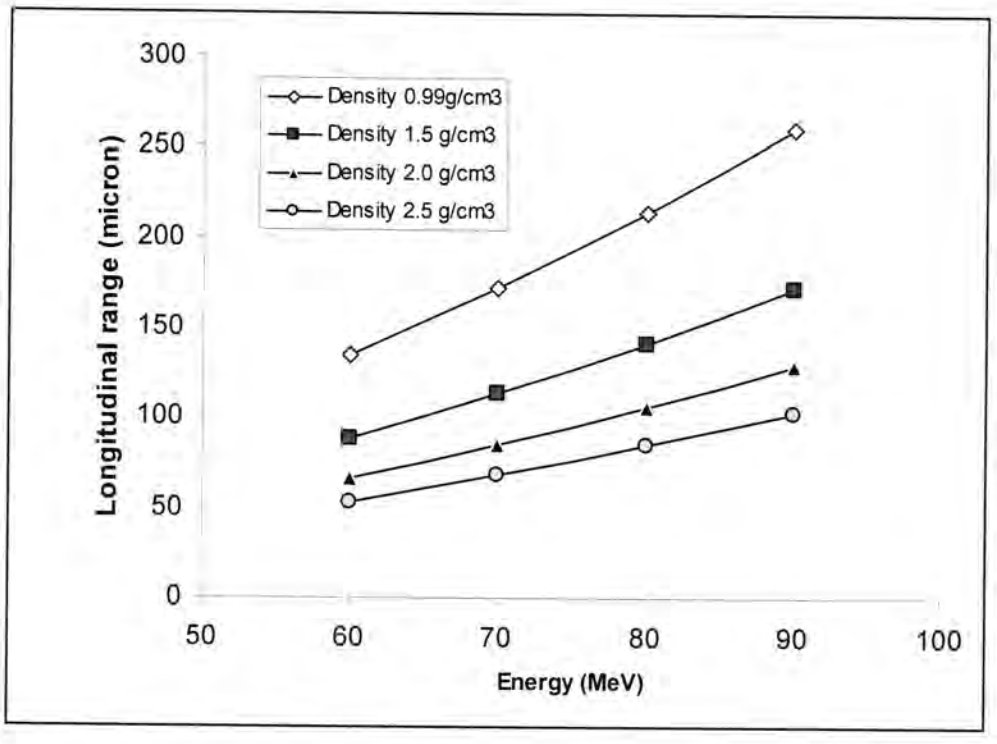
300
250
200
150
100
50
0
Longitudinal range (micron)
Density 0.99g/cm3
Density 1.5 g/cm3
Density 2.0 g/cm3
Density 2.5 g/cm3
50
60
70
80
90
100
Energy (MeV)

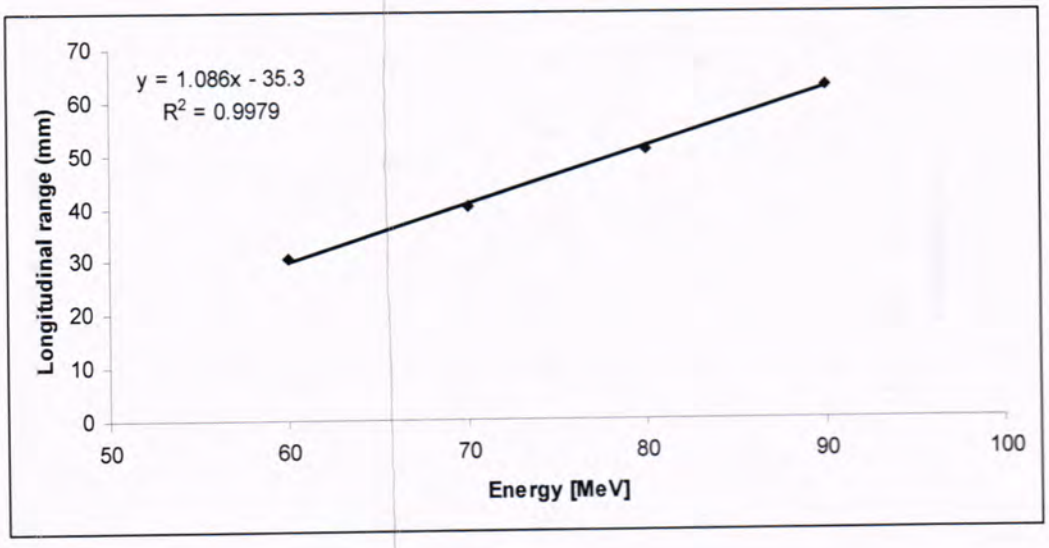

[A]

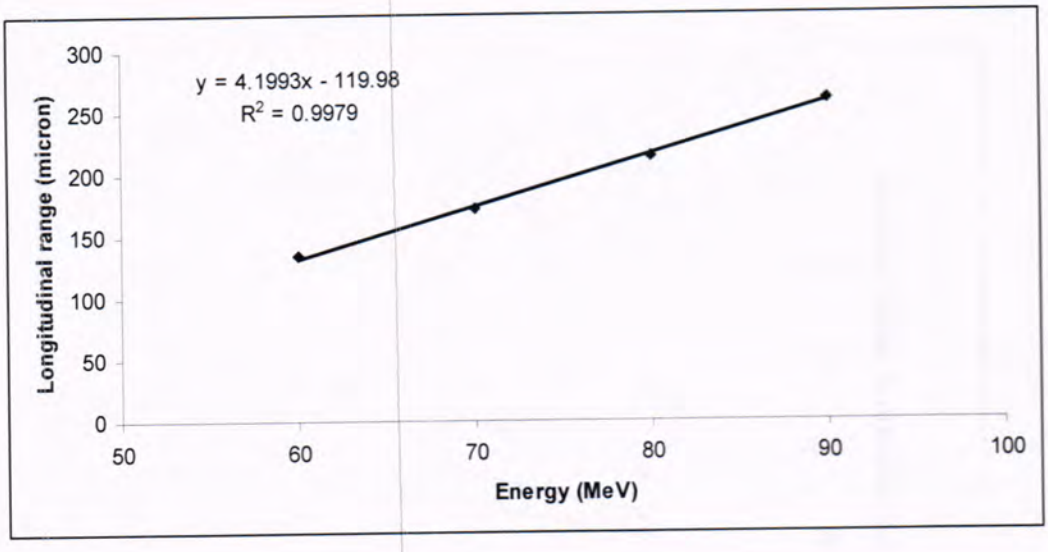

[B]

Fig- 3: Correlation between acceleration potential either with hydrogen ions [A] or carbon ions [B] and longitudinal range

REFERENCES

1. Wilson RR. Radiological use of fast protons. Radiology **47**:487- 491 (1946).
2. Coutrakon G, Bauman M, Lesyna D,Miller D,Nusbaum J,Slater J,Johanning J, Miranda J,DeLuca PM Jr, Siebers J, et al. A prototype beam delivery system for the proton medical accelerator at Loma Linda. Med Phys **18**:1093-1099 (1991).
3. Wagner MS.Automated range compensation for proton therapy.Med Phys **9**:749-752 (1982).
4. Goitein M, Chen F.Beam scanning for heavy charged particle radiotherapy. Med Phys **10**:831-840 (1983).
5. Schulz-Ertner D, Jäkel O, Schlegel W. Radiation therapy with charged particles. Semin Radiat Oncol **16:**249-259 (2006).
6. Fourkal E, Fan J, Veltchev I. Absolute dose reconstruction in proton therapy using PET imaging modality: feasibility study. Phys Med Biol **54**:N217-28(2009)
7. Andisheh B, Brahme A, Bitaraf MA, Mavroidis P, Lind BK.Clinical and radiobiological advantages of single-dose stereotactic light-ion radiation therapy for large intracranial arteriovenous malformations. J Neurosurg , Apr 24(2009).
8. Barker FG 2nd, Butler WE, Lyons S, Cascio E, Ogilvy CS, Loeffler JS, Chapman PH. Dose-volume prediction of radiation-related complications after proton beam radiosurgery for cerebral arteriovenous malformations. J Neurosurg **99**:254-263 (2003).
9. Noël G, Feuvret L, Ferrand R, Mazeron JJ. Treatment with charged particles beams: hydrogen therapy part I: physical basis and clinical experience of treatment with protons. Cancer Radiother **7**:321-339 (2003).
10. Coen JJ, Zietman AL. Proton radiation for localized prostate cancer.Nat Rev Urol **6**:324-330 (2009).
11. Truong MT, Kamat UR, Liebsch NJ, Curry WT, Lin DT, Barker FG 2nd, Loeffler JS, Chan AW. Proton radiation therapy for primary sphenoid sinus malignancies: Treatment outcome and prognostic factors. Head Neck. Jun 17(2009).
12. Bethe H und Ashkin J. In Experimental Nuclear Physics, ed: E. Segre, J Wiley, New York, p253(1953).
13. Wagenaar DJ. Charged particle interactions; Stopping power (1995) http://www.med.harvard.edu/JPNM/physics/nmltd/radprin/sect7/7.1/7_1.2html
14. Ishizaki A, Ishii K, Kanematsu N, Kanai T, Yonai S, Kase Y, Takei Y, Komori M.Development of an irradiation method with lateral modulation of SOBP width using a cone-type filter for carbon ion beams. Med Phys **36**:2222-2227 (2009)
15. Takiguchi Y, Miyamoto T, Nagao K, Kuriyama T. Assessment of the homogeneous efficacy of carbon ions in the spread-out Bragg peak for human lung cancer cell lines. Radiat Med **25**:272-277 (2007).
16. Iwase H, Gunzert-Marx K, Haettner E, Schardt D, Gutermuth F, Kraemer M, Kraft G. Experimental and theoretical study of the neutron dose produced by carbon ion therapy beams. Radiat Prot Dosimetry **126**(1-4):615-618 (2007).
17. Kundrát P. A semi-analytical radiobiological model may assist treatment planning in light ion radiotherapy. Phys Med Biol **52**:6813-6830 (2007).

18. Sawakuchi GO, Titt U, Mirkovic D, Mohan R. Density heterogeneities and the influence of multiple Coulomb and nuclear scatterings on the Bragg peak distal edge of proton therapy beams. Phys Med Biol **53**:4605-4619 (2008).
19. Patyal B. Dosimetry aspects of proton therapy. Technol Cancer Res Treat **6**(4 Suppl):17-23 (2007).
20. Aiello EJ, Buist DSM, White E, Porter PL. Association between mammographic breast density and breast cancer tumor characteristics. Cancer Epidemiol Biomarkers Prev **14**: 662-668 (2005).
21. Heine JJ, Carston MJ, Scott CG, Brandt KR, Wu FF, Pankratz VS, Sellers TA, Vachon CM. An automated approach for estimation of breast density. Cancer Epidemiol Biomarkers Prev **17**:3090-3097 (2008)
22. Kempe J, Gudowska I, Brahme A.Depth absorbed dose and LET distributions of therapeutic 1H, 4He, 7Li, and 12C beams. Med Phys **34**:183-192 (2007).
23. Imaoka T, Nishimura M, Kakinuma S, Hatano Y, Ohmachi Y, Yoshinaga S, Kawano A, Maekawa A, Shimada Y. High relative biologic effectiveness of carbon ion radiation on induction of rat mammary carcinoma and its lack of H-ras and Tp53 mutations. Int J Radiat Oncol Biol Phys **69**:194-203 (2007)
24. Hall EJ. Intensity modulated radiation therapy, protons and the risk of secondary cancer. Int J Radiat Oncol Biol Phys **65**: 1-7 (2006)
25. Weyrather WK, Kraft G. RBE of carbon ions: experimental data and the strategy of RBE calculation for treatment planning. Radiother Oncol **73**: S161-S169 (2004).
26. Matsufuji N, Kanai T, Kanematsu N, Miyamoto T, Baba M, Kamada T, Kato H, Yamada S, Mizoe JE, Tsujii H.Specification of Carbon Ion Dose at the National Institute of Radiological Sciences (NIRS). J Radiat Res (Tokyo) 48 **Suppl A**:A81-86 (2007).
27. Weber DC, Ares C, Lomax AJ, Kurtz JM.Radiation therapy planning with photons and protons for early and advanced breast cancer: an overview. Radiat Oncol **20**; 1:22 (2006).

Controlled Release of Vitamin (C) From Acrylamide Grafted Chitosan Hydrogel

Ahmed Jasim M. AL-Karawi ,Zyad Hussein J. AL-Qaisi and Ali Mohamad Ali A.A. AL-Mokaram
AL-Mustansiriya University,College Of Science,Dept. Of Chemistry

الخلاصة

تم تحوير الكيتوسان بتطعيمه الكيمياني بمونيمر الأكريل امايد من خلال بلمرة الجذور الحرة وبوجود بيرسلفات الصوديوم كبادىء . تم الحصول على نسب تطعيم مختلفة من خلال تغيير في تركيز المونيمر (الأكريل امايد). وتبين ان زيادة تركيز المونيمر يؤدي الى زيادة في النسبة المئوية للتطعيم. تم تشخيص البوليمرات المحضرة بأستخدام مطيافية الأشعة تحت الحمراء. تمت دراسة درجة الأنتفاخ لجميع البلوليمرات المحضرة من تطعيم الكيتوسان بالأكريل امايد وفي وسطين مختلفين (الماء المقطر و المحلول المشبع لكلوريد الصوديوم), وتبين ان لهذه البلوليمرات قابلية كبيرة لأمتصاص الماء. تم تحميل فيتامين (C) على الهلام المائي لجميع البوليمرات المحضرة وتم التحكم بنسب انطلاقه في وسطين مختلفين (الماء المقطر و المحلول المشبع لكلوريد الصوديوم) وبأستخدام تقنية الأشعة فوق البنفسجية لمتابعة كميات الفيتامين المنطلقة من البوليمرات. تبين من خلال التجارب التي اجريت ان كمية الفيتامين المنطلقة تتصاعد تدريجيا حتى تصل الى قيمة ثابتة.

ABSTRACT

Chitosan was modified through chemical grafted of acrylamide on the Chitosan polymer by free radical copolymerization in the presence of potassium persulfate as initiator. Various of grafting percentages have been obtained by changing the concentration of monomer (acrylamide). The percentage of grafting increases with the increasing of monomer concentration. The prepared polymers have been characterized by IR spectroscopy to identify the structure of the grafted polymer. The gelation of modified polymers (acrylamide grafted chitosan) according to the equilibrium swelling degree has been investigated in two different media (distilled water and n-saline). Acrylamide grafted chitosan shows high uptake of water, suggests its hydrophilicity. In vitro controlled release of vitamin (C) from hydrogel of prepared polymers was studied in two different media (distilled water and n-saline) using ultra violate absorption to follow quantities released at different times. The concentrations of vitamin (C) released increased gradually and then attain affixed value.

INTRODUCTION

Chitosan (poly -β - (1→4) – 2 – deoxy – D- glucose) is a biocompatible, biodegradable, non toxic and antithromboginic polymer (1,2). These properties made Chitosan widely applicable in the pharmaceutical and biomedical fields for controlled release of drugs, wound management and space filling implants (3 – 5). Chemical modification of chitosan is important for the production of bio functional materials with wide practical applications in many areas. Among various methods, graft copolymerization is most attractive because it is a useful technique for modifying the chemical and physical properties of natural polymers. Grafting of chitosan is a common way to improve its properties such as increasing chelating donors (6), complexation properties (7) and enhancing the adsorption properties (8). In this work we have focused on the modification of chitosan via chemical grafted of acrylamide and study the effect of acrylamide concentration on the graft copolymerization. Also we have studied the gelation of acrylamide grafted Chitosan in two different media (distilled water and n-saline) and Controlled release of Vitamin (C) from acrylamide grafted chitosan hydrogels in two different

media (distilled water and n-saline) using ultra violate absorption to follow quantities released at different times.

MATERIALS AND METHODS

All UV measurements were recorded at (R.T.) by using (UV–Vis) spectrophotometer type Shimadzu, 100. Infrared spectra were recorded as KBr discs using the (8400) (FTIR) Shimadzu spectrophotometer in the range (4000–500) cm^{-1}.

n-saline (aqueous solution of sodium chloride 9g/L) were used as Iraqi local product. All other reagents were commercially available and used without further purification.

Graft copolymerization of chitosan chitosan with acrylamide

Grafting reactions were carried out in 250ml polymerization flasks by first dissolving an exact amount of chitosan in 2% acetic acid solution followed by the addition of a solution of acrylamide. Finally a solution of potassium persulfate was added as initiator. The polymerization flask was closed and placed in a thermostated bath at desired temperature for 2hrs (Table 1).The reaction product was precipitated in acetone. The precipitated was filtered off and then dried in vacuum to constant weight. The dried products were extracted with acetone – water (volume ratio= 40:60) mixture for 24hrs to remove the homopolymer of acrylamide.

Swelling measurement

Acrylamide grafted chitosan, was accurately weighed in suitable closed thumb and placed in stoppered conical flask containing 100ml distilled water, which was left in a thermostated cabinet at 30±0.1°C for 6 days. After every 24hrs. excess water was poured off from the thumb, the gel is held for 10sec. Then dropped in a weighing bottle which is covered and weighed. The swelling number was calculated as follows (9):-

$$\alpha = \frac{W_1 - W_0}{W_0} \times 100$$

where α, is the percentage swelling number.

W_1, is the weight of equilibrium swelled sample.

W_0, is the original weight of the polymer.

This experiment was repeated again by using normal saline instead of distilled water.

U.V. Quanttative determination of vitamin (C)

1.76 mg of the pure Vitamin (C) was dissolved in 100mL distilled water. The maximum absorption wavelength was determined. Different concentrations of Vitamin (C) were prepared by transferring suitable volume of the mother solution into 10mL calibrated flask to cover the working range. The absorbance of the solution at the specific λ_{max} was measured against the blank. The absorbance was plotted against concentration to obtain a calibration graph. This experiment was repeated again by using n-saline instead of distilled water.

Drug release studied

In vitro studies: The release was performed by using acrylamide grafted Chitosan. 0.05g of acrylamide grafted Chitosan was accurately weighed in suitable closed thumb, and placed in stoppered vial containing 100mL distilled water. The vial was kept in a thermo stated cabinet at 30±0.1°C for 6 days (the time which required attaining maximum swelling). 1.76 mg of Vitamin C was dispensed in the swelled polymeric matrix by using horizontal shaker. The elution medium was sampled and the content of Vitamin (C) in the samples was measured spectrophotometrically at 265 nm. Sampling was almost carried out every 24 hrs, and the concentration of Vitamin C release was calculated from the calibration curve of drug. The above method was repeated again by using normal saline instead of distilled water.

RESULTS AND DISCUSSIONS

Chitosan was chemically modified by grafting with acrylamide in a homogenous aqueous phase by using potassium persulfate as initiator. The starting point of this work was to study the effect of monomer concentration on the grafting of acrylamide (AA) onto Chitosan. The percentage of grafting was calculated as follows:

$$P.G. = \frac{W_P}{W_A} \times 100$$

Where P.G. is the percentage of grafting% , W_P is the weight of product , W_A is the weight of Acrylamide.

Table -1: Grafting of vinyl monomer to chitosan (Reaction time, 2hrs at 70°C)

Polymers	Chitosan Wt/g	Acrylamide Wt/g	Acrylamide Grafted chitosan Wt/g	percentage of grafting %
AGC1	0.8	1.8	0.18	10.0
AGC2	0.8	2.6	0.69	26.54
AGC3	0.8	3.4	1.46	42.94

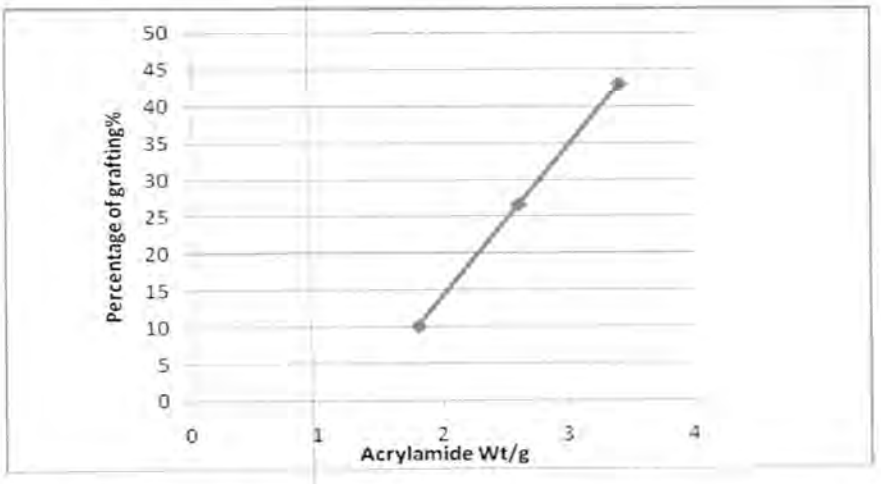

Fig -1: Effect of monomer concentration on percentage of grafting

It can be seen from Table (1) and Figure (1) that the percentage of grafting increases with the increasing of monomer concentration.

FTIR Spectra of polymers

FTIR spectroscopy was used for characterization of prepared polymers. The FTIR spectrum, of Acryl amide grafted Chitosan (AGC) Figure (2) - C , shows characteristic band at 1660 cm^{-1} , which could be assigned to the stretching vibration of amide carbonyl group in grafted chain. This band is located at 1674 cm^{-1} in the spectrum of acrylamide monomer Figure (2) - B. This shifting to lower frequency is may be due to inter and /or intra molecular interactions through hydrogen bonding

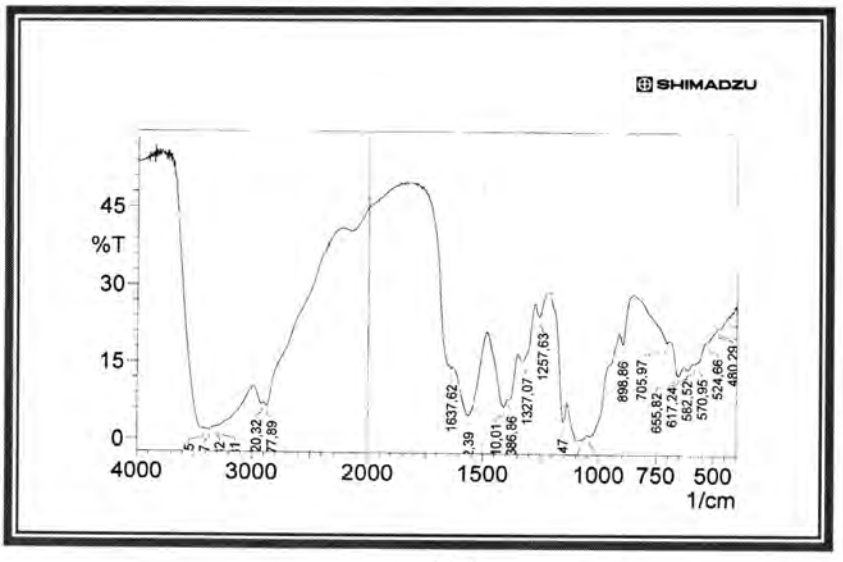

(A)

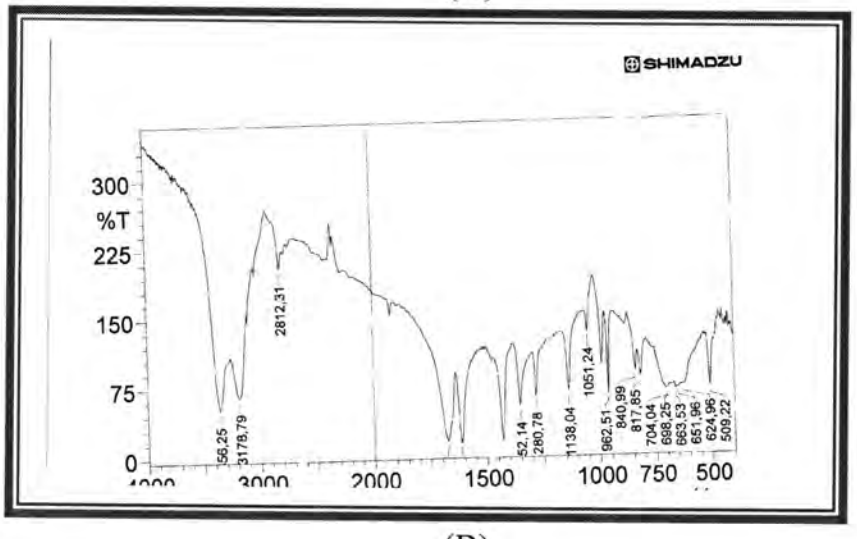

(B)

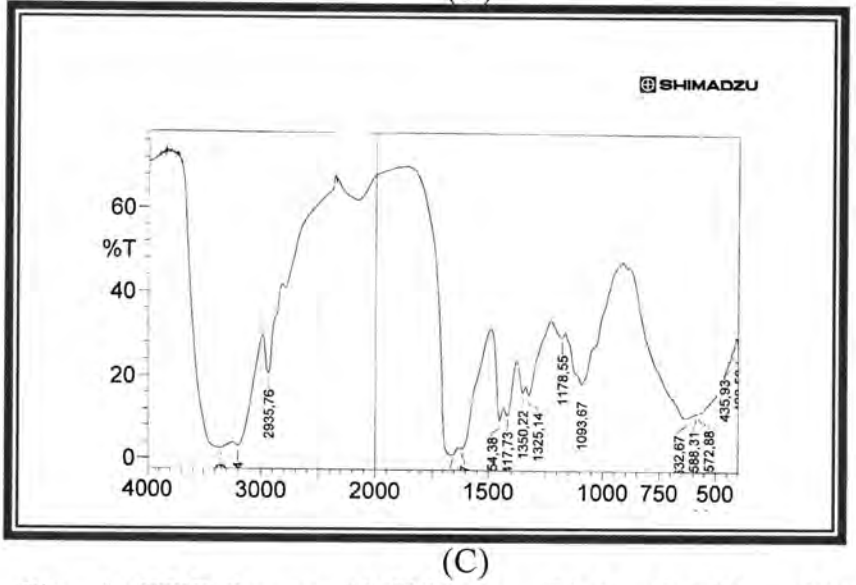

(C)

Fig – 2: FTIR Spectra A) Chitosan B) Acrylamide C)AGC
Gelation of acrylamide grafted chitosan (AGC)

Chitosan is a linear cationic biopolymer composed of glucosamine and *N*-acetyl-glucosamine that is only soluble in acidic aqueous solutions and precipitates when neutralized. However, it was recently discovered that chitosan dissolved in solutions containing glycerol phosphate was soluble at near neutral pH and produced a sol-gel transition when heated. Understanding this unique thermogelling system requires improved characterization of the ionization and solubility behaviors of chitosan (10). Therefore we have modified Chitosan with monomer containing hydrophilic group. This copolymeric material swell more in water and contain large amount of water, which is considered to be better for their biocompatibility for living tissues because the interfacial free energy between water-swollen gel and the aqueous biological environment is very small and the inner water provides good permeability to oxygen metal ions, and other metabolites (11).

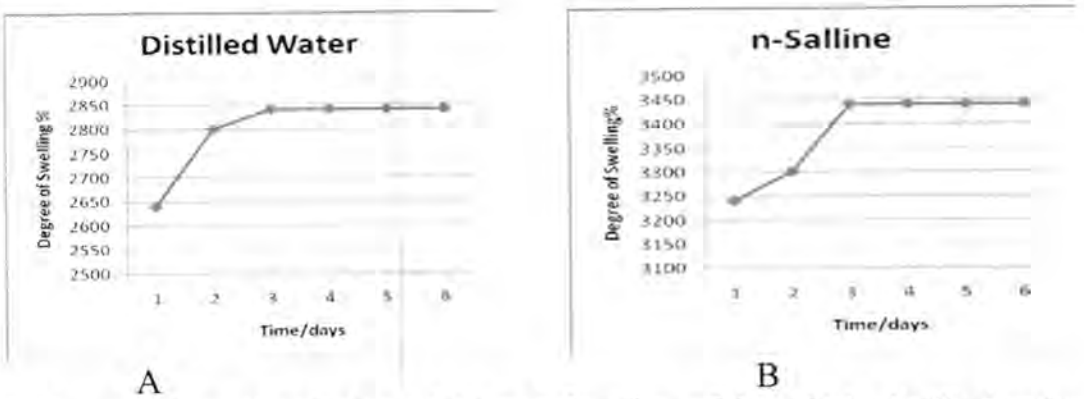

A B

Fig-3: Degree of swelling% for AGC1 as a function of time A) in distilled water B) in n-saline

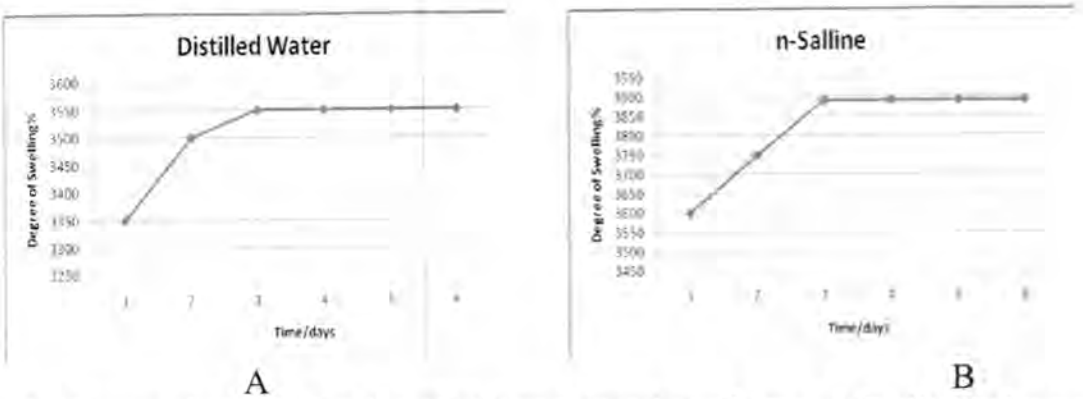

A B

Fig-4: Degree of swelling% for AGC2 as a function of time A) in distilled water B) in n-saline

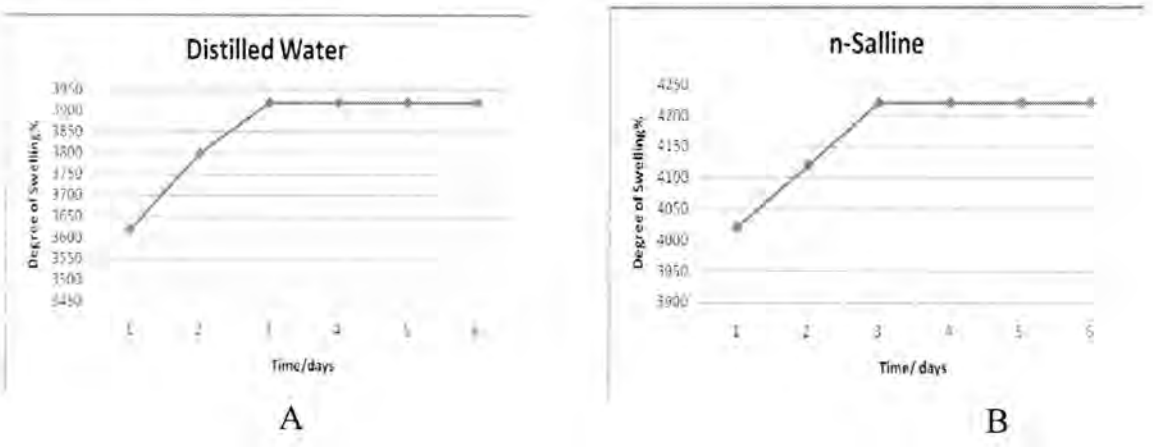

A B

Fig-5: Degree of swelling% for AGC3 as a function of time A) in distilled water B) in n-saline

The effect of water and normal saline on the swelling of modified Chitosan (AGC) have been reported. The process of swelling in aqueous media that is the interaction energy between aqueous media and chitosan needs to be sufficient to overcome the hydrogen bonding in the interior of Chitosan granule. The amorphous regions of the granules are solvated first and the granules swell rapidly, eventually many times its original size. In hydrophilic matrices consisting of drug with a water gelling polymer (usually polysaccharide) and in vitro drug release occurs by a combination of diffusion through the gel and erosion of the matrix. The proportion of drug released by each mechanism is determined by the properties of the gel and the solubility of the drug (12). The rate of swelling was the highest in normal saline and the lowest rate was in distilled water in all polymers. In n-saline there will be interference between hydrogen bonding and ionic species Na^+ and Cl^- which shield macromolecular chain and weakens hydrogen bonding. In addition n-saline will be more under its own osmotic pressure through pushing water from the aqueous solution of sodium chloride to the matrix, enhancing the extent of swelling than in the presence of water alone.

U.V. ANALYSIS

Generally, molecules that absorb in the U.V. region at a certain wavelength will contain suitable chromophor. The spectrum consisting of a plot of absorbance, percent transmittance, or log of absorbance as a function of wavelength is automatically obtained using scanning spectro-photometer. The absorptivity or molar absorptivity of many substances at specified wavelength is listed in various tables in literature. The U.V. spectrum of Vitamin (C) was determined and the molar absorpitivity of the drug was calculated.

Vitamin (C)
$A = \epsilon bc$
$1.49 = \epsilon$. 1 cm. 1×10^{-4}M
ϵ = 14900 L/ (mol.cm)

Calibration curve of vitamin (C)

In many but not all cases. Lambert-Beer's low is obeyed during ultraviolet-visible absorption by polyatomic substances. The most straightforward way to use Lambert-Beer's low for quantitative analysis is to measure the absorbance of the sample solution at a wavelength at which the species in solution is known to absorb radiation. A working curve of Vitamin (C) as a function of concentration is shown in Figures (6) and (7)

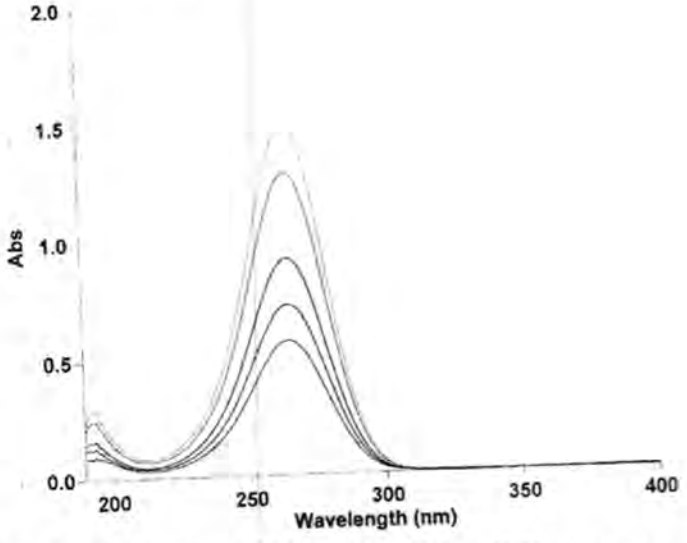

Fig-6: U.V spectra of Vitamin (C) at different concentrations

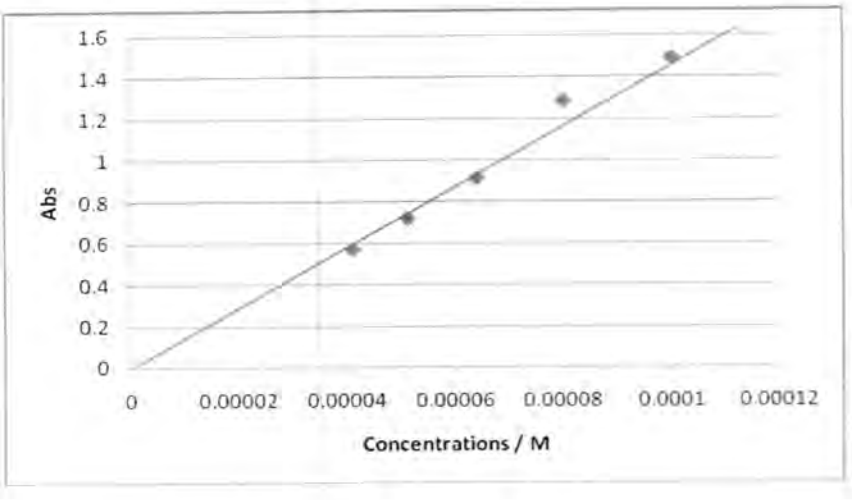

Fig -7: Calibration curve for the data of Vitamin (C). (The absorbance in 1 cm cell at λ_{max} 265 nm).

It is apparent that the slope of the plot should be the product of molar absorptivity and the cell path length. Because the working curve is linear and goes through the origin it can be used to determine concentrations from the measured absorption values (13).

Vitamin (C)

Vitamins are a group of organic nutrients in small quantities for a variety of biomedical functions and which generally, cannot be synthesized by the body and must therefore be supplied in the diet[14].Vitamin C or Ascorbic acid, is the enolic form of 3-oxo-L-gulofuranolacetone , Scheme (1).

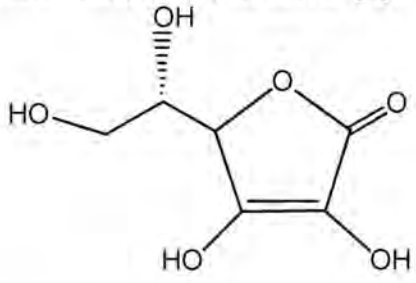

Scheme -1: Molecular structure of vitamin (C)

It can be prepared by synthesis from glucose or extracted from plant sources such as rose hips, blackcurrants or citrus fruit. It is easily oxidized in air. It is essential for the formation of collagen and intercellular material, bone and teeth and for the healing of wounds. It helps maintain elasticity of the skin, aid the absorption of iron and improves resistance to infection. It is used in the treatment of scurvy. Also it may prevent the occurrence and development of cancer (15). It has an absorption maximal in distilled water at 265 nm. The same λ_{max} was found in normal saline. After attaining maximum swelling at 30 ± 0.1°C, vitamin (C) load (1.76 mg) was dispensed and the elution medium was sampled every 24hrs., where absorptions were measured at 265 nm. The percentage of vitamin (C) released with time from acrylamide grafted Chitosan hydrogel are graphically represented in Figures (8) and (9).

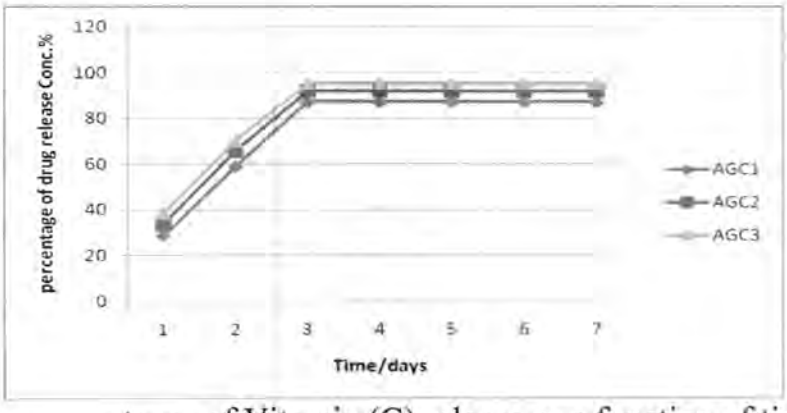

Fig - 8:The percentages of Vitamin (C) release as a function of time (load 1.76 mg/0.05g AGC) in distilled water medium.

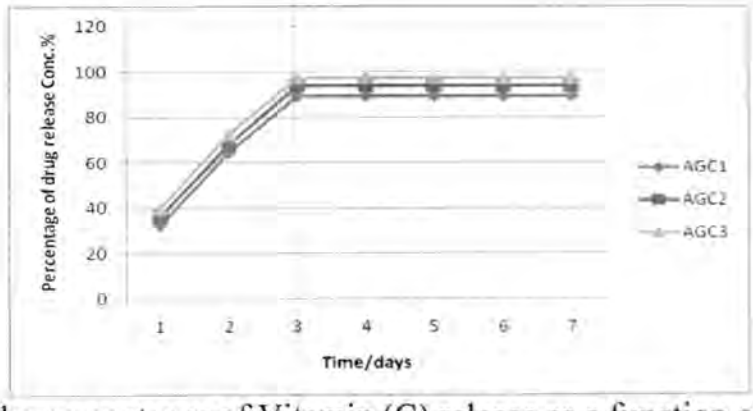

Fig - 9:The percentages of Vitamin (C) release as a function of time (load 1.76 mg/0.05g AGC) in n-saline medium.

In all examined media the amount of Vitamin (C) release is increased gradually and then attains equilibrium fixed value at certain concentration. This concentration depends on the medium in which Vitamin (C) release study was carried out (distilled water and n-saline). The rate and amount of Vitamin (C) release are increased with the increasing of grafting percentage. The grafting to an existing matrix provides a good way to modify matrix properties. Grafting take place especially in the amorphous parts of the films around crystalline domains and thus offer a great number of diffusion paths for the permeating molecules. The solubility of the penetrant in and its diffusion through the polymer matrix follow Henry's and Fick's Laws, respectively. Rate of diffusion is explained by Fick's law:

$$- J = - D \, d \, Cm/dx, \text{ where}$$

J: flux (g/Cm^2 sec).
D: Diffusion coefficient
Cm: concentration of the diffusing material
X: cross-sectional area, crossed by the drug
Release occurs by outflow of drug from the gel and inflow of water to the gel. Therefore the rate of passage of a permeating species through a polymer matrix is

governed by its solubility in the polymer and the relationship between the size of the penetrant molecule and interstices in the polymer.

REFERENCES

1. Tatjana R., Saulute B., Aurelija L., Irina G., Asta Z. and Gervydas D., Synthsis of chitosan graft poly (ethylene glycol) methyl ether methacrylate copolymer and its application for immobilization of maltogenase, CHEMIJA, 18,2, 33 (2007).
2. Radhakumary C., Prabaha D., Suresh M. and Reghunadhan C.,Biopolymer composite of chitosan and methyl methacrylate for medical application, Trends Biomater. Artif. Organs., 18,2,117 (2005).
3. Matsuyama H., Shiraishi H., Kitamur Y., "Effect of membrane preparation conditions on solute permeability in chitosn membrane",J.Appl. Polym.Sci., 73 ,2715 (1999).
4. Hubell J., Bio. Technol., 3, 565 (1998).
5. Aiedeh A., Gianasi E., Orienti I. , Zecchi V., J. Macroencapsul., 14,567 (1997).
6. Yang Z. and Yuam Y., "Studies on the synthesis and properties of hydroxyl azacrwon ether grafted chitosan" J. Appl. Polym. Sci., 82,1838 (2001).
7. Chen S. and Wang Y., "Study on β- cyclodextrin grafting with chitosan and slow release of its inclusion complex with radioactive iodine", J. Appl. Polym. Sci., 82,2414 (2001).
8. Kotze A., Lueben H.,De Leeuw B., De Boer A., Verhoef J. and Junginger H., Pharm. Res., 14, 1197 (1997).
9. Rabek J. F., "Experimental Methods in polymer Chemistry" Willy interscience, New York (1980).
10. Dominic Filion ,Marc Lavertu, and Michael D. Buschmann "Ionization and Solubility of Chitosan Solutions Related to Thermosensitive Chitosan/Glycerol-Phosphate Systems Biomacromolecules" , *8* (10), 3224 (2007).
11. Taylor N. W. and Bagley E. B., "Dispersions or solutions A mechanism for certain thickening agents" J. Appl. Polym. Sci.,18,2747 (1974).
12. Melia C.,Critical Rev's in therapeutic drugs carrier systems,8,395(1991).
13. Silverstein R., Webster F. and Kiemle D., "Spectrophotometric Identification of Organic Compounds" 7th Ed., John Willy and sons, New York (2005).
14. Gropper S., Smith J., Grodd J, . Advanced Nutrition and Human Metabolism. 4th Edn.. Thomson Wadsworth, Belmont, CA. USA.(2004).
15. Padayatty S, Katz A, Wang Y, Eck P, Kwon O, Lee J, Chen S, Corpe C, Dutta A, Dutta S and Levine M "Vitamin C as an Antioxidant: evaluation of its role in disease prevention", J. Am. Coll. Nutr. 22 (1): 18–35 (2003).

Synthesis of New N-Substituted Phenothiazine Derivatives

Suaad.M.Al.Araji., Mohammad.R.Ahamad and Luma S.Ahamed.
Dept of Chemistery, College of Science University of Baghdad.

الخلاصة

يتضمن البحث تحضير مشتقات جديدة من الفينوثايازين وهي مشتقات معوضة على ذرة النتروجين.
وقد اعتبرت المادة الاولية وهي الفينوثايازين (1) لتحضير هذه المشتقات والتي تم الحصول عليها من تسخين داي فنيل امين مع الكبريت بدرجة ^{O}270C وبوجود اليود كعامل مساعد .

عند معاملة الفينوثايزين (1) مع كلورو استيل كلورايد ليعطي N_{10} استيل فينوثايزين (2) الذي بدوره يتفاعل مع الهيدرازين المائي تحول الى مشتق الهايدرازين(3) والاخير يستعمل لتحضير نوعين من مشتقات الحلقات غير المتجانسة.
أ) المركب 4,2,1 ترايازين —4 فنيل —3 ثايول فينوثايازين(5)
ب) المركب 4,2,1 ترايازين —4 فنيل —3 هيدروكسيل فينوثايازين(11)
تحضير المشتق 4,2,1 —4 فنيل —3- ثايول(5) من الغلق في محيط قاعدي للثايوسيميكارباز ايد (4)
تحضير المشتق 4,2,1 4 فنيل —3 هيدروكسيل(11) فقد حضر بنفس الطريقة اعلاه ولكن باستعمال مشتق السيميكار بازايد(10) بدل المشتق الثايوسيميكارباز ايد
ج) الكلـه المركـب 4,2,1 ترايـزين–4- فنيـل–3-ثـايول فينوثـايزين(5) باسـتعمال هاليـدات الكيـل مختلفـة وهـي كلوروبروبان كلوروبيوتان بروموبنتان, بنزيل كلورايد)
د) الكله المركب 4,2,1 ترايزين–4- فنيل 3 هيدروكسيل فينوثايازين (11) باستعمال هاليدات الكيل مختلفة وهي (كلوروبروبان كلوروبيوتان بروموبنتان, بنزيل كلورايد)

ABSTRACT

The aim of the present work is synthesis of new phenothiazine derivatives containing N-substituted phenothiazine.

To obtain these derivatives,the diphenyl amine was chosen as the starting material, which was heated for 6hrs with sulfur. In the presence of iodine at 270C°,it gave the phenothiazine(1)

Treatment of phenothiazine (1) with (chloroacetyl chloride) gave the N_{10} acetyl phenothiazine (2), which was treated with hydrazine hydrate to give the hydrazine (3). The hydrazine (3) was used for synthesis of two types of heterocyclic derivatives: -

(a) N_{10} (4-phenyl – 1, 2, 4 - triazine – 3 – thiol) phenothiazine (5).

(b) N_{10} (4-phenyl – 1,2,4- triazine – 3 – o1) phenothiazine (11).

Compound (5) was synthesized by the intermolecular cyclization of thiosemicarbazide derivative (4), which was obtained from the reaction of the hydrazide (3) and phenyl isothiocynate.

Compound (11) was synthesized in similar manner that used for the preparation of (5), by using semicarbazide derivative instead of thiosemicarbazide derivative.

(c) Alkylation of N_{10} (4-phenyl–1,2,4-triazine–3–thio) phenothiazine (5) using different alkyl halides (chloro propane, bromo butane, chloro pentane, benzyl chloride) .

(d) Alkylation of N_{10} (4- phenyl – 1, 2, 4-triazine-3-ol) phenothiazine (11) using different alkylhalides (chloro propane, bromo butane, chloro pentane, benzyl chloride) in basic condition.

INTRODUCTION

During the past period phenothiazine and a number of its derivatives have been reported to posses various biological activities. So the importance of phenothiazine compounds as drugs have long been recognized (1). The pharmacological activities of phenothiazine have been attributed to the basic nitrogen of the ring, which donates electrons to the biological receptors, by a chargetransfer mechanism (2). Phenothiazines are an important group of neuroleptics used in treatment of moderate and severe mental and emotional conditions (3). Another types of its derivatives have been reported as antiseptic, insecticides .In additional to the biological activities phenothiazine and its derivatives have found numerous application in other fields, complexes such as methylene blue are well-known as dyes, bacteriological stains, or redox indicators, to mention a few of their many applications. They have also been successfully employed as antioxidants in industrial applications (4). Finally more than 100 compounds are derived from the fundamental phenothiazine skeleton have been synthesized and pharmacologically tested in the past four decades (5). Therefore, the present work was directed toward synthesis of new derivatives of N-substituted phenothiazine derivatives, which expected to have possible biological activity.

MATERIALS AND METHODS

Melting points were recorded using Gallen Kamp melting point apparatus and are uncorrected. Infrared spectra were recorded on a Pye-Unicam SP3-300, and on (FT-IR) infrared spectrophotometer as KBr disc by AL- Nahrain University. Chemistry Dept. and by Baghdad Univ., College of Science, Chemistry Dept. Thin layer chromatography (T.L.C) was performed on aluminum sheets precoated with silica gel F254.The biological activity were performed by the genetic engineering and biotechnology for post graduate institute Baghdad university .

General Experimental For The synthesis of New Compounds

Experimental:

1.Stnthesis of Phenothiazine (1).(6)

A mixture of diphenylamine (1.69g, 0.01 mole) , sulfur (0.64g ,0.02mole) and 0.01gm of iodine was heated in a sand bath maintained at 250 -260 °C for 6 hrs. The reaction mixture was cooled and dissolved in hot ethanol; the mixture was added to water. The formed yellow precipitate was filtered and recrystallized from ethanol m.p (181-182 °C) yield 70% purity of phenothiazine was checked by T.L.C using chloroform: ethanol (8:2) as eluent.

2. Stnthesis of N_{10} (Chloro acetyl) phenothiazine (2) .

To a solution of phenothiazine (5.8 g, 0.029 mole) in dry benzene 35 mL. containing triethyl amine (10 drops) chloro acetyl chloride was gradually added

with continuous stirring . The mixture was refluxed on water bath for 7hrs. T.L.C showed that the reaction was complete. The solvent was distilled, to give a residue which was washed with water to remove the acidic impurities .Then the solid was dissolved in hot ethanol, and was added to water, then the solid product was filtered. Finally the resulted solid was recrystallized from ethanol m.p. (111-113°C) yield 62% .

3. Stnthesis of N_{10} (Acetyl phenothiazine) Hydrazine (3)(7)

To a solution of (chloro acetyl) 10H phenothiazine (2,7 g, 0.01 mole) in ethanol (50 mL.) hydrazine hydrate (0.32g, 0.01 mole) was added and the resulting mixture was refluxed on water –bath for 5hrs. The formed precipitate was filtered and recrystallized from ethanol to give the hydrazine derivative (10) m.p. (170-173°C) yield 73%.

4. Stnthesis of N_{10} (Acetylphenothiazine) Thiosemicarbazide (4)(8)

To a solution of N10- acetyl phenothiazine hydrazine (0,281g, 0.001mole) in absolute ethanol (20 mL.) phenyl isothiocynate (0.135g , 0.001mole)was added with continuous stirring and the mixture was refluxed for 3- 4 hrs . The reaction mixture was cooled and the formed solid was recrystallized from benzene m.p. 160-162°C yield 55%.

5. Stnthesis of N_{10} (4- phenyl – 1,2,4 triazine – 3 –thiol) phenothiazine (5)(9)

N_{10} (acetyl phenothiazine) thiosemicarbazide (1g, 0,002 mole) was refluxed with 10% aqueous sodium hydroxide solution (25mL) for 3-4 hrs. the reaction mixture was filtered , cooled and neutralized by gradual addition with stirring of 10% acetic acid solution . The formed precipitate was filtered and recrystallized from ethanol , m.p. (215-217 °C) yield 52%.

6.Stnthesis of N_{10}(4–phenyl-1,2,5, triazine-3 alkyl thioether phenothiazine(6–9)(10)

To a stirred solution of N_{10} (4- phenyl-1,2,4, -triazine - 3 - thiol) phenothiazine (0.388g , 0 . 001 mole) in absolute ethanol (5 m L.) was added during 20 min KOH(0,056gm) with stirring , then (0.001 mole) of chloropropane / chlorobutane / Bromopentane / benzoylchloride was added drop wise and the reaction mixture was refluxed for 4hrs. T.L.C. (benzene: methanol 9:1) showed that the reaction was complete. The reaction mixture was filtered, cooled and filtrates were poured on to cold water then the resulting aqueous layer was extracted with chloroform (3 ×10 ml.). The combined chloroform layer was evaporated to give the desired compound. See table (1)

7. Stnthesis of N_{10}(Acetyl phenothiazine) semicarbazid (10)

Compound (10) was synthesis by the same method described for the synthesized of thiosemicarbazide using phenyl isocynate (1ml) . m.p (200- 202°C) yield 55%

8. Stnthesis of N_{10}(4- phenyl -1,2,4,triazine- 3-ol) phenothiozine (11)

Using the same method which was described for the synthesized of 4 - phenyl -1,2,4, triazine-3- thiol phenothiazine, the derivative 3- hydroxy triazine was obtained m. p. (212- 214°C) yield 46%.

9. Stnthesis of N_{10}(4- phenyl -alkyl -1,2,4-triazine–3-on) phenothiazine (12-15).

Using the same method for the preparation of N_{10} (4–phenyl 1,2,4-triazine – 3–alkyl thioether) phenothiazine using compound (11) with alkyl halide see table(4).

RESULTS AND DISCUSSION

N-substituted phenothiazine:

Literature survey showed that N-substituted phenothiazine is associated with range of biological and pharmacological properties.

chloro acetyl chloride in dry benzene was refluxed with 10H-phenothiazine it gave the corresponding N_{10}-chloro acetyl phenothiazine (2), IR spectrum showed strong stretching bands at 1690 and 1670cm^{-1} due to (C=O) .To prepare heterocyclic compound (triazine), the hydrazine (3) was seen suitable chosen for this synthetic approach. When the N_{10}-chloro acetyl phenothiazine was refluxed with 98% hydrazine hydrate, it gave the expected hydrazine (3)

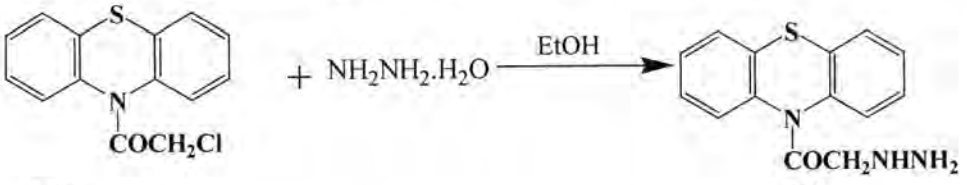

(2) **(3)**

Structure of compound (3) was confirmed by IR spectroscopy. IR spectrum showed a split broad at 3336 and 3200 cm^{-1} which was assigned to the asymmetric and symmetric stretching bands of NH_2 and NH groups, and anther band at 1670 cm^{-1} due to (C=O). The IR spectrum also showed a characteristics aromatic band at 3057cm^{-1}(C-H) , 1600 cm^{-1} (C=C)aromatic and two bands at 1590-1560 cm^{-1} characteristics of the phenothiazine nuclues .

Refluxing of hydrazide (3) with phenyl isothiocynate in ethanol gave the thiosemicarbazide (4). IR spectrum showed stretching band at 3211 cm^{-1} due to (NH) and 3111 cm^{-1} (amide NH group), 1630 cm^{-1} for (C=O) , 1600 cm^{-1} for (C=C) aromatic. IR spectrum also showed absorption bands at 1546(C=N), 1250 cm^{-1} (C=S) and 1506cm^{-1} corresponding to thioamide II and I for ($-\overset{\overset{S}{//}}{C}-NH-$) .

The titled compound (5) was synthesized according to reaction scheme (1).

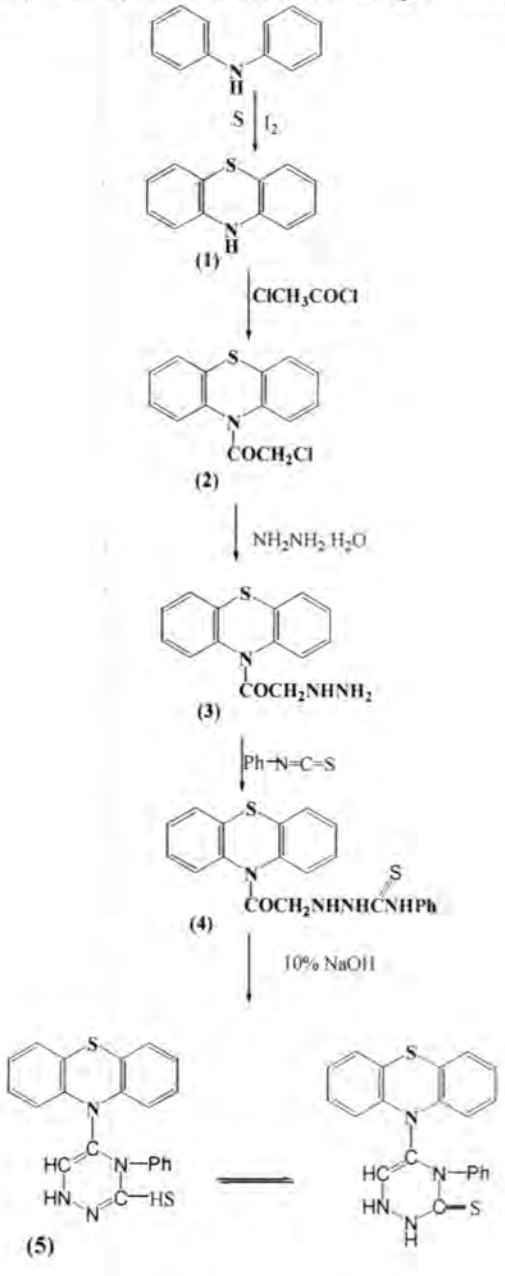

Scheme 1

The reaction of thiosemicarbazide (4) with 10% NaOH under refluxing condition affected intramolecular cyclization through the loss of H_2O giving the desired thiotriazine derivative (5), the formation of (5) may be visualized by the following mechanism:-

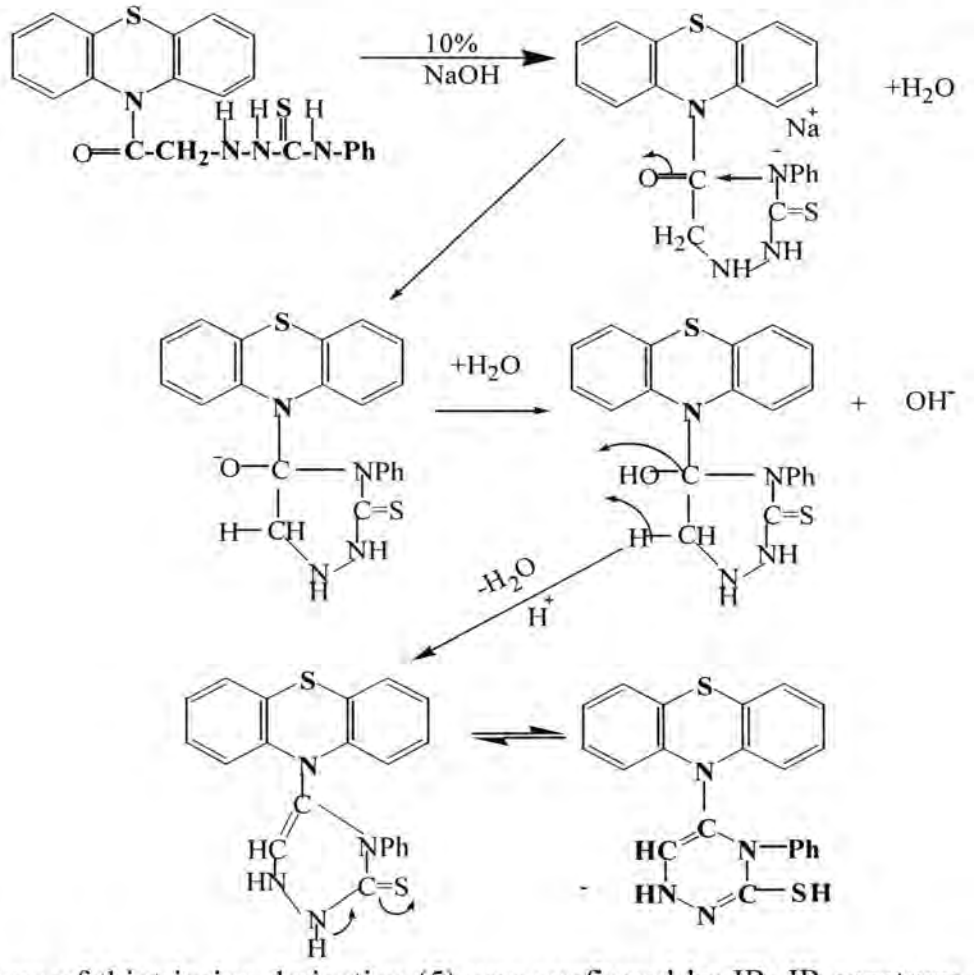

Structure of thiotriazine derivative (5) was confirmed by IR. IR spectrum showed bands at 3301 cm^{-1} and 3132 cm^{-1} (NH) and 1606cm^{-1} (C=N) also at 1323cm^{-1} (C=S) and at 1450 cm^{-1} corresponding to thioamide I and II ($-\overset{S}{\overset{\|}{C}}-NH-$).

The refluxing of thiotriazine derivative**(5)** with alkyl halides in the presence of KOH in ethanol gave thioalkyl**(6-9)**the alkyl halides were used chloropropane, chloro butane ,bromo pentane ,benzyl chloride. Compounds (6-9) were obtained respectively according to the steps out lined in scheme (1). Alkylation of thiotriazine (5) under basic condition using different alkyl halides gave the thio ether derivatives (6-8) and N-benzyl derivative (9).

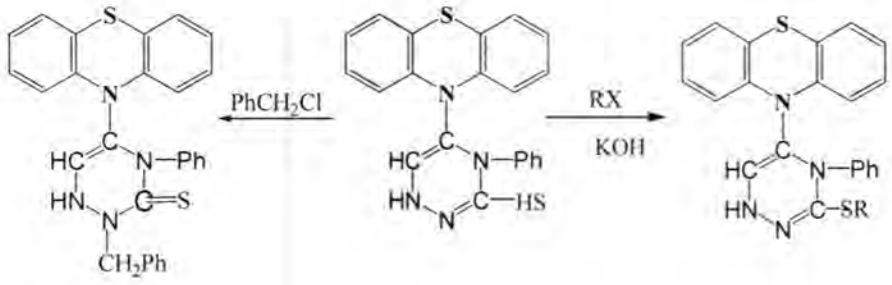

(9) (5) (6-8)

only difference from compound (5) was the disappearance (NH) and(C=S) at (3301cm^{-1} and1323 cm^{-1}) respectively with appearance of 1400cm^{-1} for the Alkyl derivative (6-8) also appearance (C-H) aliphatic at 2900-2990 cm^{-1} and ~1600 cm^{-1} for (C=N) see table3 , and appearance (C-H) aromatic at 3050 cm.$^{-1}$

Refluxing of hydrazide (3) with phenyl isocynate in ethanol gave the semicarbazide derivative (10).

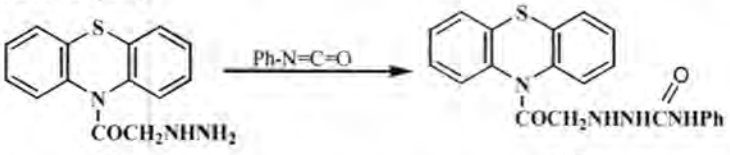

(3) (10)

This compound was characterized by IR spectral data. IR spectrum showed stretching bands at 3290 and 3210 cm^{-1} (amide NH) groups.Abroad band at 1670 cm^{-1} was appeared and other band at 1620 cm^{-1} which were attributed to amide I and amide II bands. The IR spectrum also showed characteristic aromatic band at 3020 cm^{-1} and1600 cm^{-1} (C=C).

The titled compound (11) was synthesized according to reaction scheme[2]

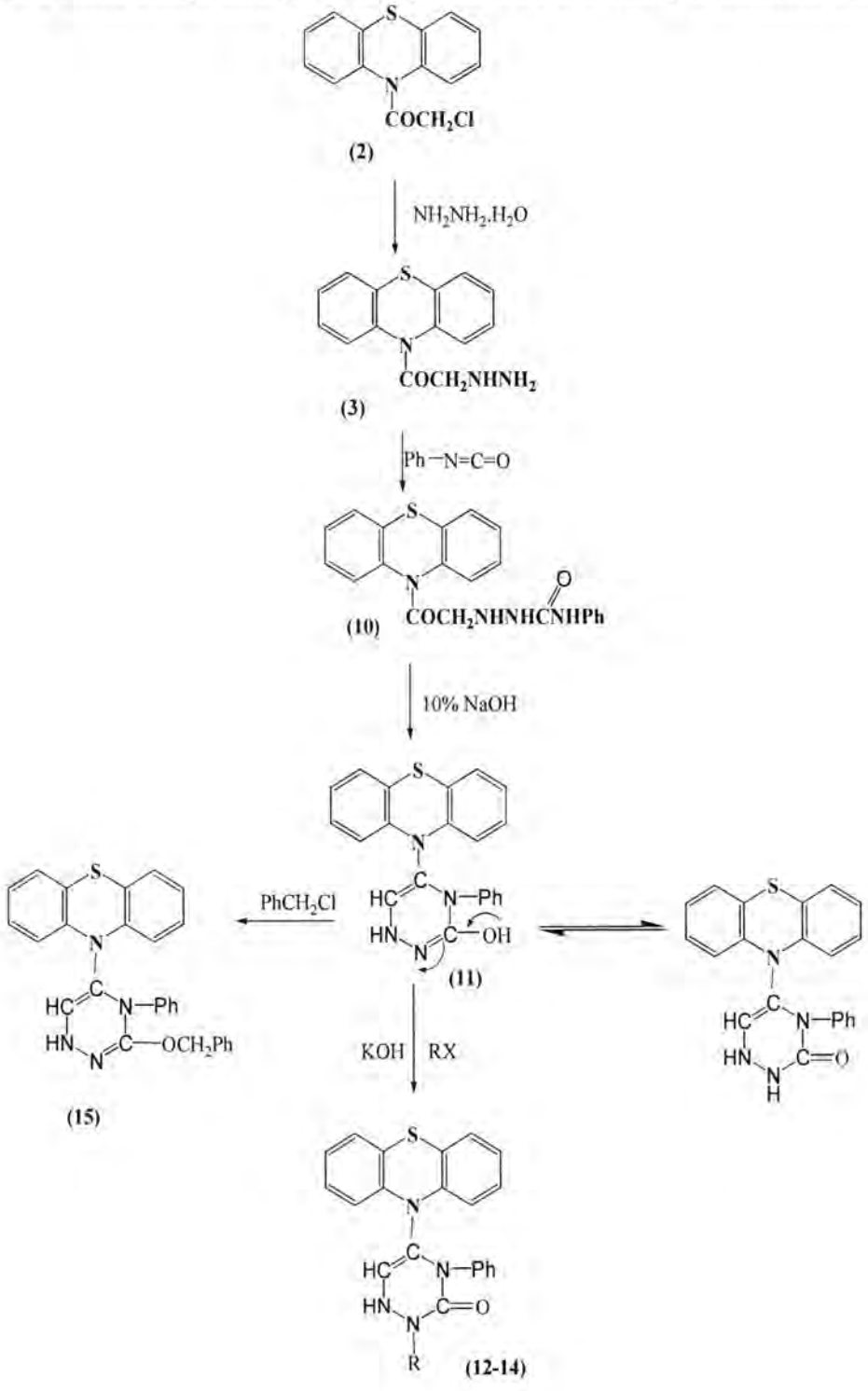

Scheme 2

The reaction of semicarbazide (10) with 10% NaOH under refluxing condition effected intramoleculare cyclization through the loss of H_2O giving The structure of hydroxytriazine derivative (11) was confirmed by IR spectra.

IR spectrum showed stretching bands at 3288 cm^{-1}(N-H). A broad band at 3436 cm^{-1} for (O-H) band and other bands at 1645 and 1700 cm^{-1} which were, attributed to amide I and amide II bands and 1566cm^{-1} (C=N)

Alkylation of hydroxyl triazine(11)with different alkyl halides under basic condition gave two different alkylated products (12-15)and the hydroxyl triazine (11) is considered as nucleophile under SN^2 mechanism, the alkyl halides(propane chloride, butane chloride ,pentane bromide)are attacked by the better nucleophile ,i.e.nitrogen atom to give the N-alkyl derivative while under SN^1 mechanism benzyl chloride is attacked by the more electronegative atom, i.e., oxygen to give ether derivative (15) .The N-alkyl derivative (15) showed the same general IR spectral features figs. the only difference from(11)was disappearance of (C=O) band.

Table -1: Physical properties of compounds (2-9)

Compd. No.	Structure	Chemical formula MWt	M. P.C°	% Yield	Colour of Cryst.
2	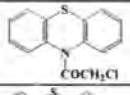	$C_{14}H_{10}N$ SOCl (275)	111-113	62	White
3	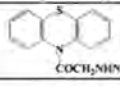	$C_{14}H_{13}N_3$ SO (271)	170-173	73	yellow
4	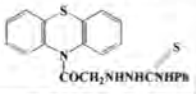	$C_{21}H_{18}N_4$ S $_2$O (406)	160	55	yellow
5	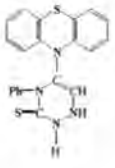	$C_{21}H_{16}N_4S_2$ (388)	215-217	52	White
6	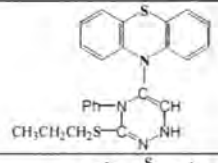	$C_{24}H_{22}N_4S_2$ (430)	186-188	75.3	White
7	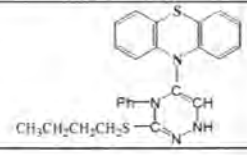	$C_{25}H_{24}N_4S_2$ (444)	168-170	73	White

Compd. No.	Structure	Chemical formula MWt	M. P.C°	% Yield	Colour of Cryst.
8	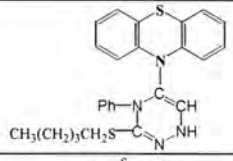	$C_{26}H_{26}N_4S_2$ (458)	118-120	73	White
9	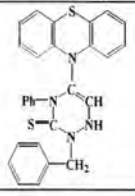	$C_{28}H_{22}N_4S_2$ (478)	113	65	Gray

Table - 2: Infrared data of compounds (2-5)

Compd. No.	Structure	υ N-H cm^{-1}	υ C-H Aromatic	υ C-H Aliphatic	υ C=O cm^{-1}	υ C=N cm^{-1}	υ C=C aromatic	Other band cm^{-1}
2	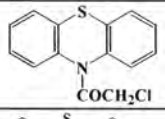	-	3060 W	2950 W	1690 VS 1970 VS	-	1580 M	C-Cl 610
3	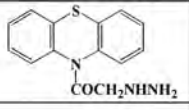	3336M 3200 VW	3057 VS	2900 VW	1670 S	-	1600 M	-
4	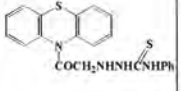	3211 3111M	3050 W	2939 M	1600 M	1546 S	1506 S	σ C=S 1190 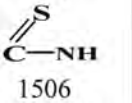 1506 S-H 2588
5	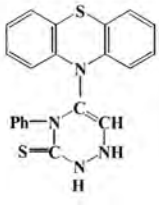	3301 M 3132 M	3020 VW	2927 VW	-	1606 S	1544 S	σ c=s 1323 S 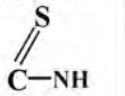 1450 S

Table -3: Infrared data of compounds (6-9) (continued)

Compd. No.	Alkyl halid	υ N-H cm^{-1}	υ C-H Aromatic	υ C-H Aliphatic	υ C=N cm^{-1}	υ C=C Aromatic	υ C=S cm^{-1}	Other band cm^{-1}
6	Chloropropane	3210 W	3060W	2990W	1630 S	1610 S	-	-
7	Chlorobutane	3182 M	3037M	2923 M	1604 S	1556 VS	-	-
8	Bromopentane	3200 W	3050 W	2920 W	1600 S	1550 S	-	-
9	benzylchloride	3200 M	3050 M	2900 W	1602 S	1500 VS	1321	-

Table-4: Physical properties of compounds (10-15)

Compd. No.	Structure	Chemical formula MWt	M. P.C°	% Yield	Colour of Cryst.
10	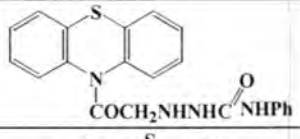	$C_{21}H_{18}N_4SO_2$ (446)	200-202	55	White
11	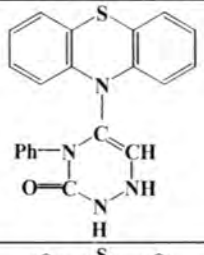	$C_{21}H_{16}N_4SO$ (372)	212-214	46	Gray
12	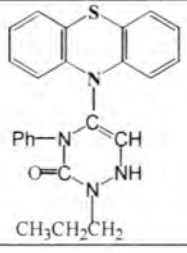	$C_{24}H_{22}N_4SO$ (414)	190	31	Beach

13	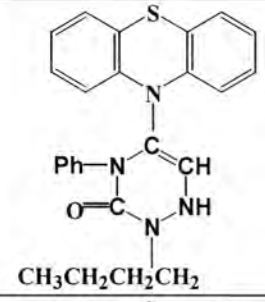	$C_{25}H_{24}N_4SO$ (428)	195-197	30	Beach
14	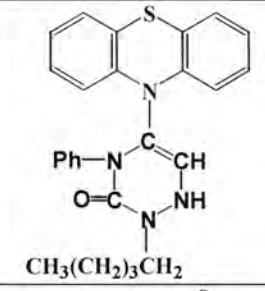	$C_{26}H_{26}N_4SO$ (442)	203	29	Beach
15	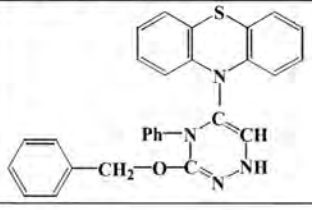	$C_{28}H_{22}N_4SO$ (462)	183-185	20	Beach

Table -5: Infrared data of compounds (10-11)

Comp. No.	Structure	υ N-H cm^{-1}	υ C-H Aromatic	υ C-H Aliphatic	υ C=O cm^{-1}	υ C=N cm^{-1}	υ C=C cm^{-1}	Other bands cm^{-1}
10	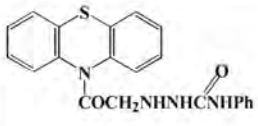	3290 3210	3020 W	2920 W	1670	1610	1600	Amid II 1650 Amid II 1600
11	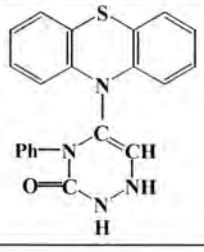	3436 W	3070 W	2990 W	1645 S	1566 S	1675 S	Broad O-H 3436

Table -6: Infrared data of compounds (12-15)

Comp. No.	RX	υ N-H cm^{-1}	υ C-H Aromatic	υ C-H Aliphatic	υ C=O	υ C=N cm^{-1}	υ C=C cm^{-1}	Other bands cm^{-1}
12	chloropropane	3436 M	3010 W	2870 W	1700 M	1571 S	1519 M	σ C-N 1020 ,1070 σ N-CH_2 2860
13	chlorobutane	3450 M	3100V W	2950 VS	1703 S	1610 M	1600 M	σ C-N 1028, 1095 σ N-CH_2 2852
14	bromopentane	3400 M	3005 W	2920 M	1710	1650	1580	σ C-N 1020, 1085
15	benzylchloride	3450 M	3050	2923	-	1664	1590	σ C-N 1026, 1100 σ N-CH_2 2854

REFERENCES

1. Zhong, j., Fan,C. and Matsuda,N., sensing phenothiazine Drugs at a Gold electrode Co-Modified with DNA and Gold Nanoparticales Analytical Sciences , 19,553 (2003).
2. Sharma,V.N.Pancholi. N.S. Phenothiarines as anticholinergics J. Pharm., Sci.,60 :t 262-t 264(1971).
3. Nagaraja,P.,Dinesh,N.D.,Gowda,N.M.M.,aSimple Spectrophoto metric Determina - tion of Some phenothiazine Drugs in Pharmaceutical samples Analytical Sciences ,16:1127-1130 (2000).
4. Mital R.L, Gupta C.I. Synthesis of some 11-substituted6-Chloro-12H –Benzo [a] phenothiazine -5-ols Ind.J.Chem.24B:551-552 (1985).

5. Usdin,L.E. & Efron,D.H."Psychotropis Drugs and related compounds" department of health. Education and welfare , Health service and mental Health, Washington, D.C(1992).
6. Barnes,B., Gore, R.C.,Stafford R.W. and Williams, V.Z.,Qualitative Organic Analysis and Infrared Spectrophotometry Anal. Chem 20, 402, (1948).
7. Singh,S.P. & Parmar,S.S.Synthesis of 10 (Substituted phenyl hydrazono acetyl) Phenothiazines as Possible Anticonvulsant J. Heterocyclic Chem.15,175(1978)
8. Hogale M.B. & Deshmukh,D.S. Synthesis of some New phenothiazine Derivatives J. Ind.Chem.Soc. 66:212 (1989).
9. Mamedov,V.A.,Nuretdinov,I.A. & Sibgatullina,F.G.Synthesis of novel thiazoles bearing hydrazine,thiosemicarbazide,thiazole, and thiazolidi -none moieties Russian Chemical Bulletin ,40,12:2470-2474, (1991).
10. Shah,S.T.,Khan,K.M.An alternative approach towards the syntheses of thioethers and thioesters using CsF–Celite in acetonitrile Tetrahedron Letters , 43,46:8281-8283 (2002).

Synthesis of Novel N-amino quinoline-2-one derivatives

Redha I. H.AL-Bayati and Mahdi F. Radi
Department of Chemistry , College of Sciences , Al-Mustansiriyah University

الخلاصة

يتضمن هذا البحث تحضير المشتق N-امينو كوينولين-2-اون (2) من تصعيد الكومارين(1) مع الهيدرازين المائي 99% في الايثانول لمدة 12 ساعة .

حضرت قواعد شف (3-8) من تكاثف الالديهايدات أو الكيتونات الاروماتية مع المركب (2) .اما المركبات (9-12) حضرت من تفاعل المركب (2) مع الانهيدريدات المناسبة .

كما تم تفاعل المركب (2) مع أريل أو الكيل ايزوسيانات ليعطي مشتقات اليوريا (13- 16) . ان تفاعل المركب (2) مع حامض الفورميك يؤدي الى تكوين المشتق (17) . تم معاملة المركب (1) مع السيمي كاربازايد هايدروكلورايد ليعطي المركب (18) . تم تشخيص المركبات المحضرة باستخدام بعض الطرائق الطيفية , الاشعة تحت الحمراء , الاشعة فوق البنفسجية والمرئية ومطيافية الرنين النووي المغناطيسي .

ABSTRACT

In this work, N-amino quinoline-2-one (2) has been synthesized by the reflux of coumarin (1) with hydrazine hydrate 99% in ethanol for 12 hr . The azomethines (3-8) were prepared from the corresponding aryl aldehydes and ketones . Imides derivatives (9-12) were prepared from the reaction of compound (2) with appropriate anhydrides .

However the reaction of compound (2) with aryl or alkyl isocyanate afforded the urea derivatives (13 -16,).Reaction of compound(2) with formic acid give the derivative (17) . Treatment of compound (1) with semicarbazide hydrochloride give the compound (18) The structure of the synthesized compounds deduced by using some spectroscopic methods, FT-IR, UV-Visible and NMR .

INTRODUCTION

Quinoline-2-one derivatives has been reported to possess wide rang of activities such as antitumor(1), antimalarial(2), antiplatelet3, antidepressant(4), antiulcer(5), plant virucides6, antifungal agents(7) , antioxidant activity(8) and herbicides(9) . Many substituted quinoline-2-one derivatives have recently craned great interest in chemotherapy as ant tumor drugs(10,11). Also a number of quinolones are excellent reservoir of bioactive substances (12).

In the present study, N-amino quinoline-2-one is allowed to react with aryl aldehydes and ketones, anhydrides, aryl and alkyl isocyanate, and formic acid . (scheme1) .

MATERIALS AND METHODS

Melting points were determined on GallenKamp (MFB-600) melting point apparatus and are uncorrected . The IR spectra of the compounds were recorded on a shimadzu FT-IR-8300 spectrometer as KBr disk . The UV spectra were performed on Cintra-5-Gbes scientific equipment . The ^{1}H-NMR and ^{13}C-NMR spectra

(solvent DMSO-d_6) were recorded on Bruker 400 MHz spectrophotometer using TMS as internal standard .

Synthesis of N-amino quinoline-2-one (2) :

Refluxing of coumarin (1.46 g , 0.01 mol) with excess hydrazine hydrate 99% (3.2 g , 0.1 mol) in absolute ethanol 25 ml for 12 hr , then cooled , the formed solid was collected and recrystallized from chloroform . (Table 1) .

Synthesis of Schiff bases (3-8) :

A mixture of compound 2 (0.8 g , 0.005 mol) and the appropriate aryl aldehyde or ketone (0.005 mol) was refluxed in absolute ethanol 25 ml for 6-8 hr . The reaction mixture was cooled and the product obtained was recrystallized from appropriate solvent (Table 1) .

Synthesis of compounds (9-12) :

A mixture of compound 2 (0.3 g , 0.0018 mol) and appropriate anhydride (0.0018 mol) was heated without solvent on an oil bath at 180-185 C° for 15 minutes . The reaction mixture was left to cool and the solid was separated out and recrystallized from the proper solvent (Table 1) .

Synthesis of compounds (13-14) :

A mixture of compound 1 (0.5 g , 0.003 mol) and appropriate alkyl and aryl isocyanate (0.003 mol) in absolute ethanol 25 ml was refluxed for 6hr . The precipitate thus obtained was filtered off and recrystallized from a suitable solvent , (Table 1)

Synthesis of compounds (15 -16) :

A mixture of compound 2 (0.5 g , 0.003 mol) and appropriate alkyl and aryl diisocyanate (0.0015 mol) in absolute ethanol 25 ml was refluxed for 6 hr . The precipitate thus obtained was filtered off and recrystallized from a suitable solvent , (Table 1) .

Synthesis of compound (17) :

The compound 2 (0.5 g , 0.003 mol) was refluxed with formic acid 10 ml for 2 hr . The solvent was evaporated and the solid was filtered and recystallized from ethanol , (Table 1) .

Synthesis of compound (18) :

To a solution of coumarin 1 (3.0 g , 0.02 mol) in 30 ml of pyridine , semicarbazide hydrochloride (3.3 g , 0.03 mol) was added and the reaction mixture was heated under reflux for 10 hr , left to cool , poured into cold water with stirring .

The solid product that separated out was filtered off by suction , washed with cold water , dried and recrystallized from the appropriate solvent , (Table 1) .

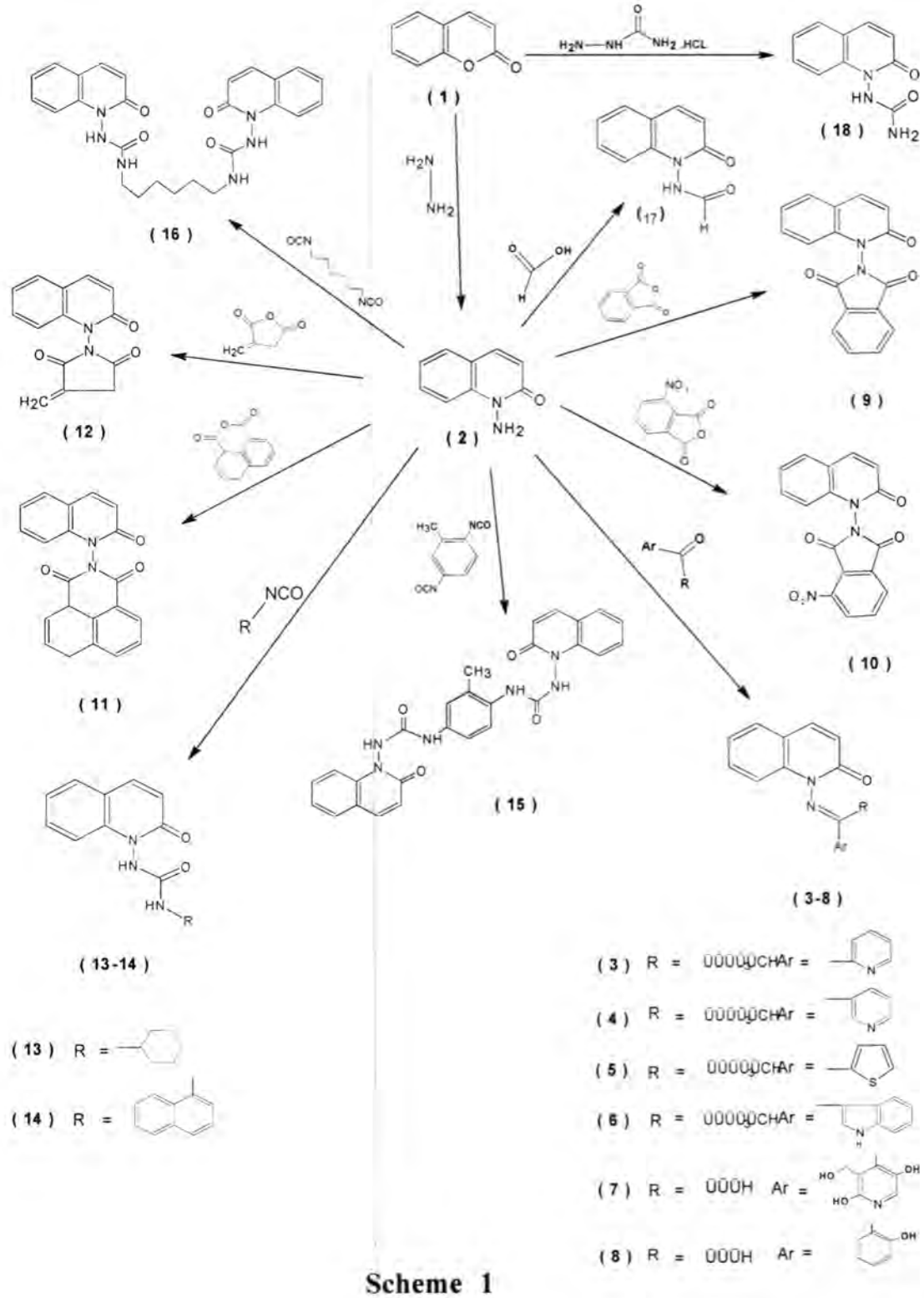

Scheme 1

RESULTS AND DISCUSSION

N-amino quinoline-2-one (2) was obtained by heating a mixture of coumarin with large excess of hydrazine hydrate in boiling absolute ethanol for 12 hr with yield 91 % . The structure of compound (2) was confirmed from its spectral data . The IR spectrum showed two strong absorption bands at 3290 – 3300 cm^{-1} and strong band at 1645 cm^{-1} corresponding to υNH_2 and $\upsilon C=O$ respectively (Table 2). ^{1}H-NMR : 4.1(s, 2H, $-NH_2$) , 6.7(t, Ar-H), 7.4(d, Ar-H), 7.1(d,Ar-H) . ^{13}C-NMR: 126,127,127.8,128,123.3,128.5,129,155,157 .

Reaction of compound (2) with aromatic aldehydes and ketones in boiling absolute ethanol afforded 3-arylidene derivatives (3-8) . IR spectra of 3-imino derivatives showed the disappearance of the absorption bands for NH_2 while showed bands due to C=O and C=N groups at 1662-1683 , 1583-1621 cm^{-1} respectively (Table 3) . ^{1}H-NMR of compound (5) show : 2.3(s, 3H, $-CH_3$), 7.6(d, Ar-H), 7.5(d,Ar-H), 7.1(t, Ar-H) , 7.9(d, -C=C-H), 7.97(d, -C=C-H) . ^{13}C-NMR : 15,23,126,128,128.2,129,129.8,130,131,131,133,135,143,144,157 . The ^{1}H-NMR of compound (8) show : 3.3(s,1H, Ar-OH), 9(s, 1H, N=C-H), 7.7(d, Ar-H), 7.4(d, Ar-H), 6.9(t, Ar-H) . ^{13}C-NMR : 60,117,118,120,126,131,133,159,163 .

Compound (2) was converted to the imide derivatives (9-12) by reaction with appropriate anhydrides without solvent , This reaction proceeds by attack of the nucleophile to the carbon of carbonyl group , causing ring opening , then recyclize to form the corresponding Imide derivatives . The IR spectrum of these compounds showed the disappearance of the absorption bands for NH_2 and showed bands due to $\upsilon C=O$ (Table 4) .

Compound (13,14) have been prepared by treatment of equimolar quantities of the corresponding 1-amino quinolone with appropriate aryl or alkyl isocyanate . This reaction is indicated by nucleophilic attack of the most nucleophilic nitrogen of hydrazide compound on the sp^2 carbon of isocyanate group . The IR spectrum of these derivatives showed the disappearance of the absorption bands for NH_2 and showed bands due to NH and two strong bands for $\upsilon C=O$ of the ring and urea (Table 5) .The ^{1}H-NMR of compound (13) show : 6.6(s,1H, NH-C=O), 4.4(s, 1H, NH-), 3.4(s, 1H, NH-CH-), 2.1(m, 2H, CH_2), 1.1(m, 2H, CH_2), 7-7.8(Ar-H) . ^{13}C-NMR : 25,33,33.5,119,119.2,126,127,128,128.4,154,155,157 .

Two moles of compound (2) were reacted with one mole of appropriate aryl and alkyl diisocyanate to afforded urea derivatives (15 , 16) . The IR spectrum of this compounds showed the disappearance of the absorption bands for NH_2 while showed bands due to NH and C=O groups at 3300 cm^{-1} and 1658 – 1670 cm^{-1} respectively (Table 6) . The ^{1}H-NMR of compound (16) show : 1.3(t, 2H, CH_2CH_2), 3.3(s, 1H, CONH), 3(s, 2H, $NHCH_2$), 6.3(s, 1H, NH), 6.9(t, Ar-H), 7.3(d,Ar-H),7.5(d,Ar-H)^{13}C-NMR:
19,26.5,26.6,30.2,30.5,57,119,126,128,129,129.5,152,157,159

Refluxing of compound (2) with formic acid for 2 hr afforded the formamide derivative (17) . The IR spectrum of this compound showed the disappearance of the absorption bands for NH_2 while showed bands due to NH and C=O and C—H aldehyde at 3115 cm^{-1} , 1703 cm^{-1} (2800 , 2700 cm^{-1}) respectively (Table 7)
Reaction of compound (1) with semicarbazidehydrochloride in dry pyridine for 10 hr give the compound (18) . The IR spectrum of this compound showed two strong absorption bands at 3402-3304 cm^{-1} corresponding to υ NH_2 and showed band at 3124 cm^{-1} due to υ NH and the absorption of carbonyl group was shift from 1740 to 1662 cm^{-1} because of the nucluphilic substitution of semicarbazide on the ring Table(8).^{1}H-NMR:3.3(s,2H,NH_2),6(s,1H,NH),7.1-7.9(m,Ar-H).

Table - 1 : Physical properties of synthesized compounds

Comp. No.	◦M . P C	Yield %	Recryst. Solvent
2	131-133	91	Chloroform
3	46-48	75	Ethanol
4	52-54	76	Ethanol
5	85-87	72	Ethanol
6	240 dec	55	Ethanol
7	74-76	88	Ethanol
8	216-218	60	Ethanol : water (1: 1)
9	340 dec	76	Ethanol
10	254 dec	72	Ethanol
11	206-208	85	Ethanol : water (1: 1)
12	96-98	72	Ethanol
13	118-120	80	Benzene
14	218-220	60	Dioxane
15	212-214	71	Benzene
16	248-250	72	Acetic acid
17	162-164	94	Ethanol
18	262-264	36	Dioxane

Comp. No.	U . V Ethanol		Characteristic bands of FT-IR spectrum (cm^{-1} , KBr disk)				
	λ_{max} (nm)	ϵ_{max} x 10^6	υ C═O	υ C═C_{ar}	υC—H_{ar}	υC—N	others
2	280 227	0. 93 1. 88	1645	1595 1452	3045	1242	υNH_2 3200 – 3300

Table – 2: U.V and IR spectral data for compound (2)

Table - 3 : U.V and IR spectral data for compounds (3 – 8)

Comp. No.	U . V Ethanol		Characteristic bands of FT-IR (cm^{-1} , KBr disk)					
	λ_{max}(nm)	ϵ_{max} x 10^6	υ C═O	υ C═C_{ar}	υ C—H_{ar}	υ C═N	υ C—N	Others
3	290 222	0.45 1.82	1670	1564 1456	3050	1583	1246	υC—H_{ali} 2924 2840
4	282 224 203	1.8 1.32 0.67	1670	1456	3050	1604	1244	υC—H_{ali} 2924 2840
5	339 268 221	1.18 0.72 0.27	1681	1425 1520	3076	1583	1232	2920 υC—H_{ali}2945
6	340 262 222	0.86 0.35 1.1	1683	1572 1523 1438	3060	1585	1244	υ C—H_{ali} 2950 υ N—H 3394 υC—H_{vinyl} 3132
7	358 281 206	1.18 0.62 1.46	1662	1550 1455	3070	1620	1215	υ OH 2800-3348 υ C—H_{ali} 2900 2872
8	356 289	0.86 0.28	1681	1573 1487	3046	1621	1271	υ OH 3200

Table - 4 : U.V and IR spectral data for compounds (9 – 12)

Comp. No.	U . V Ethanol		Characteristic bands of FT-IR (cm -1 , KBr)				
	λ_{max}(nm)	ϵ_{max} x 10^6	υ C=O	υ C=C ar	υC—H ar	υC—N	other
9	283 263 209	0.32 0.29 1.74	1661	1557 1490	3016	1261	
10	306 267 209	0.29 0.34 1.53	1665	1545 1600	3026	1296	υNO_2 1336 1542
11	331 236 211	0.31 0.93 0.7	1703 1653	1585 1618	3045	1238	
12	305 274 210	0.45 0.89 1.94	1705 1681	1604 1562 1454	3001	1259	υC—H ali 2925

Table - 5 : U.V and IR spectral data for compounds (13 , 14)

Comp. No.	U . V Ethanol		Characteristic bands of FT-IR (cm -1 , KBr disk)				
	λ_{max}(nm)	ϵ_{max} x 10^6	υ C=O	υ C=C ar	υC—H ar	υC—N	Others
13	274 213	0.64 2.1	1647 1660	1544 1452	3080	1253	υ C—H ali 2929 , 2852 υ N—H 3307
14	292 248	1.5 0.15	1660 1654 Interference	1608 1552	3049	1249	υ N—H 3271

Table - 6 : U.V and IR spectral data for compounds (15 , 16)

Comp. No.	U .V Ethanol		Characteristic bands of FT-IR (cm-1 , KBr disk)				
	λ_{max} (nm)	ϵ_{max} x 10^6	υ C=O	υ C=C ar	υC—H ar	υC—N	Others
15	218 280	1.6 0.67	1670 1658 Interf.	1602 1533	3020	1234	υ N—H 3307 υC—H ali 2850 , 2926
16	202 239	1.82 0.5	1664	1556 1458	3095	1265	υN—H 3300 υC—H ali 2931 , 2858

Table - 7 : U.V and IR spectral data for compound (17)

Comp. No.	U . V Water		Characteristic bands of FT-IR (cm^{-1} , KBr disk)				
	λ_{max} (nm)	ϵ_{max} x 10^6	υ C=O	υ C=C ar	υC—H ar	υC—N	Others
17	276 207	0.11 3.37	1703 1660 Interference	1616 1481	3050	1226	υN—H 3115 υC—H aldehyde 2800 2700

Table- 8 : U.V and IR spectral data for compound (18)

Comp. No.	U . V Acetic acid		Characteristic bands of FT-IR(cm^{-1} , KBr disk)			
	λ_{max} (nm)	ϵ_{max} x 10^6	υ C=O	υ C=C $_{ar}$	υC—H $_{ar}$	Others
18	260 204	2.01 0.54	1662 1687	1502 1510 1602	3057	υN—H 3124 υNH_2 3402 , 3304

REFERENCES

1.Joseph, B.; Darro, F., Behard, A., Lesur, B., Collignon, F., Decaestecker, C., Frydman, A., Guillaumet, G., Kiss, R. 3-Aryl-2-quinolone derivatives: synthesis and characterization of in vitro and in vivo anti-tumor effects with emphasis on a new therapeutical target connected with cell migration. J.Med.Chem, 45: 2534-2555, (2002).

2.Xiao, Z., Waters, N. C., Woodard, C. L., Li, p. K. Design and synthesis of pfmrk inhibitors as potential antimalarial agents. Bioorg. Med.Chem. Lett, 11: 2875-2878, (2001).

3.Nishi, T., Kimura, Y., Nakagawa, K. Research and development of cilostazol: An antiplatelet agent. Yaku-gaku. Zasshi, 120: 1247-1260, (2000).

4.Oshiro, Y., Sakurai, Y., Sato, S., Kurahashi, N., Tanaka, T., Kikuchi, T., Tottori, K., Uwahodo, Y., Miwa, T., Nishi, T. 3,4-Dihydro-2(1H) quinolinone as a novel antidepressant drug: synthesis and pharmacology of 1-[3-[4-(3-chlorophenyl)-1-piperazinyl]-3,4-dihydro-5-methoxy-2(1H)-quinolinone and Its Derivatives. J. Med. Chem, 43: 177-189, (2000).

5.Banno, K., Fujioka, T., Kikuchi, T., Oshiro, Y., Hiyama, T., Nakagawa, K. Studies on 2(1H)-uinolinonederivatives as neuroleptic agents I. Synthesis and biological activities of (4-phenyl-1-iperazinyl)-propoxy-2(1H)-quinolinone derivatives. Chem. Pharm. Bull, 36: 4377-4388. (1988).

6.Hung, R.Q ., Li,H.Y.,Ma,J.A., Qiu, Giu. D.W. Synthesis of O-(4-Quinazolinyl)oxime Ethers and Their Antiviral Activity. Chem. J. Chin. Univ.,17,57(1996).

7.Dandia, A., Singh, R., Sarawagi, P. Green chemical multicomponent one pot Synthesis of fluorinated 2,3-disubstituted qunazolin-4(3H)-ones under solvent-free conditions and their anti-fungal activity. J. fluorine Chem. 125, 1835-1840 (2004).

8.AL – Omar , M. A., EL-Azab , Adel S . EL-Obeid H. A . and Abdel Hamide Synthesis of som new 4-(3H)-quinazoline analogs as potential antioxidant agents. J. Sandi Chem. Soc , 10 , 113 (2006).

9.Khan, I. A., Hassan, G, Ihsanullah, khan, M. A., Efficacy of post-emergence Herbicides for controlling weeds in canola. Asian J. Plant Sci, 2 , 294 (2003).
10. Jin, Y., Li, H. Y. Lin, L. P,, Tan, J. Z ., Ding, J ., Luo,X.M. Long, Y. Q. Synthesis and antitumor evaluation of novel 5-substituted-4-hydroxy-8-nitroquinazolines as EGFR signaling-targeted inhibitors . Bioorg. Med. Chem. 13 , 5613 (2005).
11.Wissner, A., Berger, D.M., Boschelli, D. H. etal. 4-anilino-6,7-dialkoxyquinoline-3-carbonitrile inhibitors. J. Med.Chem.,43,3244 (2000)
12.AL-Bayati, R. F.H, Hassan,Y.K and Hameed S. M. Synthesis of novel N-substituted quinoline-2-one derivatives , AL- Qadisia J. for Pure Science , 10 , 90 (2004)

Spectrophotometric Determination of Dopamine in Pharmaceutical Formulations by Reaction with Tyramine .

Mohammed .J.M. Hassan
AL-Mustansiriya University-College of Science-Chemistry Department

الخلاصه

تم في هذه الدراسه تطوير طريقه طيفيه جديده لتقدير الدوبامين في المحاليل المائيه و المستحضرات الصيدلانيه.
استندت الطريقه على تفاعل الدوبامين مع التايرمين بوجود ميتا بريودات البوتاسيوم كمادة مؤكسده.قيست امتصاصيه الصبغه العضويه الناتجه الذائبه في الماء واعطت اقصى امتصاص عند الطول الموجي 472 نانوميتر .الخطيه كانت مابين0.5 الى20 مايكروغرام/مل ,اما حد الكشف فكان 0.25 مايكروغرام/مل .درست المتغيرات الكيميائيه والفيزيائيه واخذت افضل المتغيرات في الدراسه.طبقت الطريقه الجديدة بنجاح في تقدير المستحضرات الصيدلانيه للدوبامين على شكل امبولات

ABSTACT

A batch Spectrophotometric method have been developed for the determination of dopamine in aqueous solution and in pharmaceutical ampoules preparation .The methods are based on the reaction of dopamine with tyramine in presence of potassium metaperiodate as oxidizing agent .The water soluble orange color produced was measured at 472 nm .the range linearity was observed from 0. 5 – 20 $\mu g.ml^{-1}$ dopamine with quantification limits of 0.28 $\mu g.ml^{-1}$ dopamine. The effects of chemical and physical parameters have been carefully considered and the proposed methods were successfully applied to the determination of dopamine in ampoules formulation.

Keywords: catecholamine's, dopamine, tyramine, pharmaceutical formulations

INTRODUCTION

Dopamine (DA) [2– (3,4 – dihydroxy phenyl) ethyl amine] is one of the catecholamines drugs that discovered in 1960 and was used as anti Glucoma and agonist (1) . Various methods have been reported for the determination of (DA). Rami Reddy. N and et al(2) was developed spectrophotometric method for (DA) estimation based on the bromination of the (DA) with a solution of excess brominating mixture, after bromination, the excess brominating mixture is treated with potassium iodide to produce a yellow solution. Tayyebeh .M et al(3) determination of catecholamines based on their oxidation reaction followed by coupling with 4-aminobenzoic acid. Markovic (4) S and Amrain. S determined of (DA) with thiosemicarbazide .Nagaraja(5) P, determined (DA) by reaction with chloramind T,and many other spectro -photometric methods(6) .Wang and et al(7) determined (DA) Fluorimetrically in pharmaceutical products and urine by using ethylene -diamine as fluorigenic reagent. Flow-injection spectrophoto -metric method use for determining (DA), Berzas Nevado, and et al (8) used A

flow-injection spectrophotometric method for determining (DA) via reaction with metaperiodate. Nalewaja .E, and et al(9) determined (DA) by flow injection analysis coupled with luminol-hexacyanoferrate III via chemiluminescence detection.Al-Abachi9(10-11)M.Q. and Da,amy, determined Adrenaline and (DA) in pharmaceutical preparation via oxidative coupling reaction with thiourea and ferric nitrate .also determined of (DA) with 3-Amino pyridine and sodium periodate. (DA) Injection was determined using flow injection-spectrophotometric by reaction of (DA) with P-toluidine and sodium Periodate (12). Chromatog raphic methods have been reported for the determination of (DA) in Various matrices,(DA)could be determined by liquid chromatography(LC)(13-15)gas chromatography(GC)(16),C-Mass (17) and Capillary Electrophoresis-Mass Spectrometry(18-19).Electro-analyt ical Techniques have been used extendedly for the determination of (DA),Voltammetric(20),Electrochemical(21,24)and Amperometric(25) . In the objective of the investigation reported in this paper is to evaluate a spectrophotometric batch method for the determination of a (DA) based on its reaction with tyramine in the presence of potassium metaperiodate in neutral medium. A stable-soluble-orange color product was formed which can be measured at 475 nm .the method dose not required temperature control or solvent extraction step. no previous puplished reports on the reaction mechanism have been appeared ,the reaction scheme may be proposed for the (DA)-tyramine in the present potassium metaperiodate.The method was successfully applied to determination of (DA) in pharmaceutical formulations.

MATERIALS AND METHODS

The Dopamine pure drug was obtained from biological – Italy Company.

Dopamine stock solution (1000 $\mu g.ml^{-1}$):

0.1000 gm of Dopamine was dissolved in 10 ml of ethanol and completed the volume to 100 ml with deionized water in a volumetric flask of 100 ml.

Tyramine reagent (0.1 M):

Tyramine reagent standard was purchased from Samara Drug Company (Iraq).

Was prepared by dissolving 1.2108 gm in 100 ml of deionized water.

Potassium metaperiodate (0.1 M):

Potassium metaperiodate from Merck (Germany)

Solutions were prepared by dissolving 2.3000 gm of KIO_4 in 100 ml of deionized water. More dilute solutions were prepared by suitable dilutions.

Apparatus used

All spectral and absorbance measurements were carried out on a shimadzu UV– visible 260 digital double beam recording spectrophotometer using 1 cm silica cell.

Into a series of 25 ml calibrated flask, transfer increasing volumes of Dopamine (10 μg.ml^{-}). Add 1.5 ml of $1x10^{-1}$ M of potassium metaperiodate solution, flowed by 3.5 ml of $5x10^{-2}$ M of tyramine solution. Dilute the solution to the mark with deionized water and allow the reaction mixture to stand for 25 min at room temperature. Measure the absorbance at 472 nm against a reagent blank prepared in the same way but containing no Dopamine. The color of the formed dye is stable for about 120 min. For the optimization of conditions and in all subsequent experiments, a solution of 10 μg.ml^{-1} Dopamine was used and the final volume was 25 ml.

RESULTS AND DISCUSION

When a diluted aqueous solution of Dopamine and tyramine are mixed in the present of potassium metaperiodate in neutral medium, an intense orange color forms immediately and become stable after 25 min. The color has a maximum absorption at 472 nm. Fig (1) shows the spectra of the orange color formed and of the reagent blank. The above reaction can be utilized for the determination of Dopamine using spectrophotometric system. Initial studies were directed toward optimization of the experimental conditions, in order to establish the most favorable parameters for the determination of Dopamine. The influence of various reaction variables such as concentration of reactants, temperature, order of addition, and time of reaction were investigated. Experimental result showed that there was no effect in color intensity and stability on using different order of addition and the order of addition of reagents cited under recommended procedure was in further experiments. The effect of reagent (tyramine) concentration from $1x10^{-4}$ to $1x10^{-2}$ M was studied and found the concentration of $6x10^{-3}$M enough to developed the color to its full intensity and was chosen for subsequent studies. The effects of oxidant (potassium metaperiodate) concentration from $1x10^{-4}$ to $8x10^{-3}$ M was studied, the results obtained indicated that a concentration of $6x10^{-3}$ M gave the highest absorption and give a minimum blank value and was considered to be optimum for the further studies.

The effect of reaction time indicated that the color intensity reached a maximum after a mixture of Dopamine solution containing 10 μg.ml^{-1} in 0.0004 M potassium metaperiodate and 0.006 M tyramine in a neutral medium in final volume of 25 ml, had been reacted, the color develops during the first 25 min. and remains stable for more than 120 min.

The effect of temperature on the color intensity of the dye was studied, In practice , high absorbance was obtained when the color was developed at room temperature (25 C) than when the calibrated flask were placed in an ice – bath at (0° C) or in a water bath at (45°C). The calibration graph Fig(2) for the determination of Dopamine was constructed under the optimum conditions listed in Table (1) . The regression equation have been obtained from a series of Dopamine standards, the analytical figures of merit of this procedure are summarized in Table 2.

The stoichiometry of the reaction was investigated using molar ratio method. The result obtained (Fig. 3) show that a 1:1 product was formed between Dopamine and tyramine reagent at 472 nm. Therefore the formation of the product probably occurs as follows:

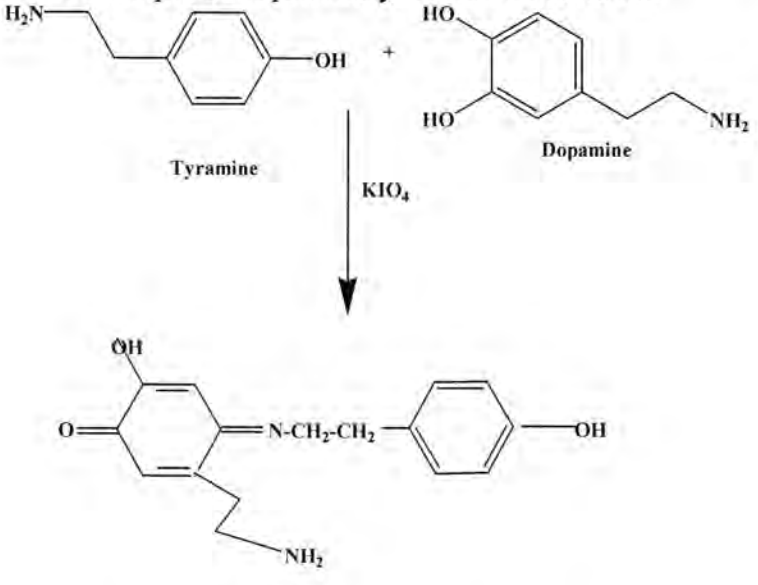

Orangic soluble dye

The product formed was soluble in water .the apparent stability constant was calculated by comparing the absorbance of a solution containing stoichiometric amount of Dopamine and tyramine in a neutral medium, With that of a solution containing a five-fold excess of tyramine reagent. The stability constant of the product in water under the describe experimental conditions were 3.177×10^3 L. mol^{-1}

Analytical application

The developed methodology is very adequate for the determination of Dopamine in aqueous solution and in pharmaceutical preparation samples at a concentration level of traces (ppm) ,and without requiring neither any previous separation step nor a temperature or pH control. Moreover the proposed procedures are very economical when compared to other methods such as those based on the use of another

instrumental analysis such as GC, HPLC and etc. Sample preparation was done by diluting the ampoules with deionized water.

Accuracy and precision

The accuracy and precision of the method was evaluated by analyzing pure sample of Dopamine. A good recovery was obtained (Table 3). Finally the proposed method was applied successfully to the analysis of some ampoules containing Dopamine. The results in Table 3 are in accordance with those obtained by the official method (26).

Table -1: Optimum conditions for the determination of Dopamine.

Parameters	*Value*
Conc. of tyramine	$6x10^{-3}$M
Conc. of potassium metaperiodate	$6x10^{-3}$ M
Time on the stability of complex	120 min.
Temperature	Room temp.
wavelength	472 nm

Table -2: Analytical feature of the procedures developed for the determination of Dopamine.

parameter	*Batch method*
Regression equation	**Y=0.0161X-0.001**
Linear range ($\mu g.ml^{-1}$)	**0. 5 – 20**
Correlation coefficient	**0.9999**
Limit of detection (s/n=3) ($\mu g.ml^{-1}$)	**0.28**
RSD% for 10 $\mu g.ml^{-1}$	**1.03**
Recovery % for 10 $\mu g.ml^{-1}$	**99.65**
Molar absorptive($L.mol^{-1}.cm^{-1}$)	$3.177x10^{3}$
λ_{max} (nm)	**472**

Table -3: Application of the proposed methods to the determination of Dopamine in ampoules

Drug sample	*Amount of drugs*	*Batch method*		*OFFICIAL Method*[26]
		Recovery* %	RSD* %	**Recovery* %**
Pure Dopamine	10 μg.ml^{-1}	98.84	1.09	
Ampoules Dopamine	10 μg.ml^{-1}	101.34	1.16	**100**
Ampoules Dopamine	25 μg.ml^{-1}	98.74	1.24	

* Average of five determination

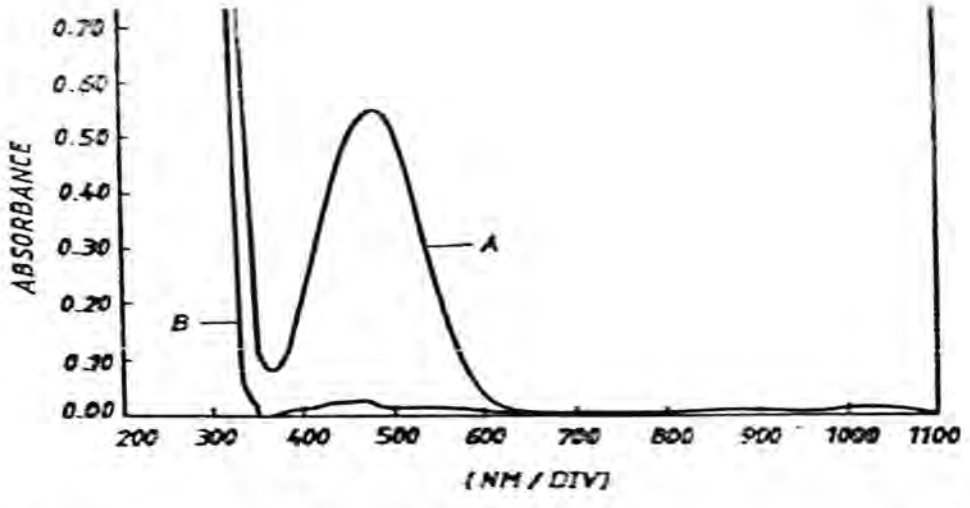

Fig -1: Absorption spectra of Dopamine treated as described under procedure and measured against reagent blank and B the reagent blank measured against deionized water.

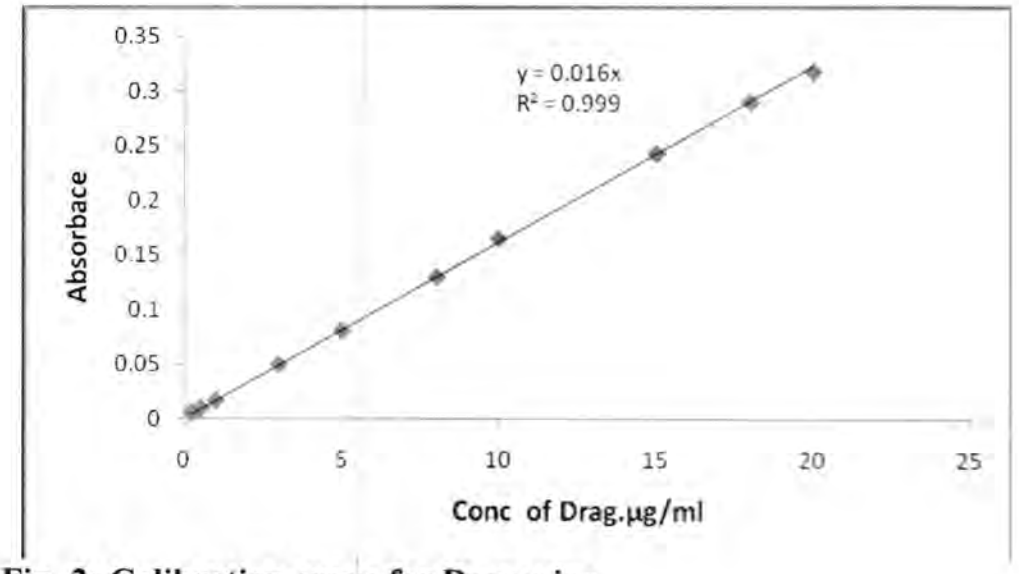

Fig -2: Calibration curve for Dopamine

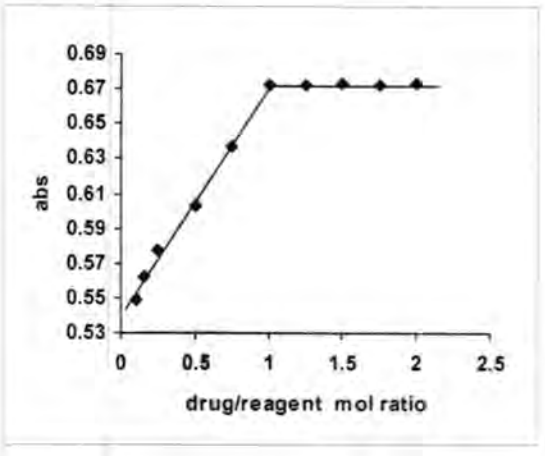

Fig -3: Molar ratio of Dopamine to reagent for the colored product

A Practical, reliable, Simple analytical procedures using Spectroph - otometer has been described for the quantitive determination of pharmaceutical injections contain (DA). The procedures described in This research no needs the elaborate treatment and tedious extraction or pH control.

REFERENCES

1. " British pharmacopoeia on CD-ROM", 3rd Ed., copyright by system simulation Ltd., The stationary office, LonDAn,(2000).
2. Rami Reddy.N.,Sreedevi.G.,Prabhavathi.K.&Chakravarthy.I. E.Spe ct-rophotometric determination of Dopamine in pharmaceutical formulations Journal of Analytical Chemistry, 60,(3) March, (2005)

3. Tayyebeh Madrakian , Abbas Afkhami; Lida Khalafi; Massoumeh Mohammad nejad Spectrophotometric determination of catecholamines based on their oxidation reaction followed by coupling with 4-aminobenzoic acid. Journal of the Brazilian Chemical Society .17 (7) So Paulo Nov./Dec.(2006).
4. Markovic S and Amrain S Spectrophotornetric determination of Dopamine with thiosemicarbazide. *DiePharmazie*, 45: 292-3(1990).
5. Nagaraja P, Murthy KCS, Yathirajan HS and Mohan BM Rapid spectro-photometric determination of Dopamine hydrochloride with chloramine T. *Indian J. Pharm. Sciences*, 60: 99-101(1998)..
6. Murthy .M SR, Sundaram .MS,Spectrophotometric determination of Dopamine hydrochloride. Indian Journal of Pharmaceutical Sciences, 58, (3) :124-126(1996).
7. Wang HY, Hui QS, Xu LX, Jiang JG and Sun Y Fluorimetric determination of Dopamine in pharmaceutical products and urine using ethylenediamine as fluorigenic reagent. *Anal. Chim. Acta.*, 497: 93-99, (2003).
8. Berzas NevaDA J. J. , Lemus Gallego J. M. and Buitrago LagunaA. P. flow-injection spectrophotometric method for determining Dopamine and methyldopa is described. It is based on the oxidation reaction with metaperiodate .Fresenius' Journal of Analytical Chemistry, 353 (2) January (1995).
9. Nalewaja E, Bort Ramirez R and Kojla A Determination of Dopamine by flow injection analysis coupled with luminol-hexacyanoferrate(III), chemiluminescence detection. *J. Pharm. Biomed. Anal.*, 36: 219-223 (2004)..
10. Al-Abachi M.Q.and Al-Da'amy M.A., FI-Specrophotometric determination of Catechol Amine drugs in pharmaceutical preparation via oxidative coupling reaction with3-Amino pyridine and sodium periodate ,National Journal. of Chemistry,16,485,2004.
11. Al-Abachi M.Q.and Al-Da'amy M.A., FI-Specrophotometric determination of methyledopa in pharmaceutical preparation via oxidative coupling reaction with thiourea and ferric nitrate National Journal of Chemistry,13, 47(2004).
12. Loay K.Abdulrahman,Anas M.Al-abachi,Mayada H.Al-Qaissy. Flow injection-Specrophotometric determination of some Catecholamine drugs in pharmaceutical preparation via oxidative coupling reaction with P-toluidine and sodium periodate. Aalytical Chimica Acta,538:331-335 (2005).

13. Bielavska M and Kassa J Simultaneousdetermination of Dopamine, serotonin and theirmetabolities in the rat brain by HPLC method withcoulometric detection, Coil. *Czechoslovak Chem.Commu.*, 65: 1677-1682 (2000).

14. Vander Hoorn FAJ, Boomsma F, Manin Tveld AJ and Schalekamp MADH Determination of catecholamines in human plasma by high performance liquid chromatography: Comparison between a new method with flourescence detection and an established method with eiectrochemical detection. *J. Chromatogr.*, 487: 17-28 (1989).

15. Wang H, Li J, Liu X, Yang TX and Zhang HS N hydroxyl succinimidyl fluorescein-o-acetate as a fluorescent derivatizing reagent for catecholamines in liquid chromatography. *Anal. Biochem.*, 281: 15-20 (2000).

16. Uchimura H and T. Matsumoto T, Highly sensitive determination of Dopamine and homovanillic acid by gas chromatography-mass spectrometry-application of reaction gas chromatography. *JEOL News, Anal Instrumentation*, 19A: 9-13 (1983).

17. Musshoff F, Schmidt P, Dettmeyer R, Priemer F, Jachau K and Madea B Determination of Dopamine and Dopamine derived (R)-/(S)-salsolinol and norsaisoiinoi in various human brain areas using solid phase extraction and gas chromatography – mass spectrometry. *Forensic Sci. International*. 113: 389-366. (2000).

18. Vuorensola K, Siren H and Karjalainen U. Determination of dopamine and methoxycatechoiamine in patients urine by liquid chromatography with electrochemical detection and by capillary electrophoresis coupled with spectrophotometric and mass spectrometry, *J. Chromatogr. B. Anal. Techn. Biomed. Life Sci.* 788: 277-282 (2003).

19. Katariina Vuorensola ,"ph.D Thesis", Capillary Electrophoresis and Capillary Electrophoresis.Mass Spectrometry in Catecholamine Studies University of Helsinki l, Finland .*November 8th,* (2002).

20. *L. G. Shaidarova, I. A. Chelnokova, A. V. Gedmina, and G. K. Budnikov* .Simultaneous Voltammetric Determination of Dopamine and Ascorbic Acid at an Electrode Modified with the Gold–Palladium Binary System , Journal of Analitical Chemistry 64, (1): 36 (2009).

21. *W. Hu, D. Sun and W. Ma.* Simultaneous electrochemical epinephrine with silver-doped determination of dopamine and poly(L-glutamic acid) modified electrode Chemia Analityczna, 53 :703(2008).

22. Mehmet Aslanoglu*, Sultan Abbasoglu,Serpil Karabulut,Aysegul Kutluay. Electrochemical Determination of dopamine in the

Presence of Ascorbic Acid Using a Poly(3-cetylthiophene) Modified Glassy Carbon Electrode *Acta Chim. Slov.* , *54:* 834-839 (2007).

23. Wang Z, Liu J, Liang Q, Wang Y and Luo G. Carbon nonotube-modified electrodes for the simultaneous determination of dopamine and ascorbric acid. *Analyst,* 127: 653-658(2002).
24. Zhang Y, Jin G, Yang Z and Zhao H. Determination of dopamine in the presence of ascorbic acid using a poly(amidosulfonic acid) modified glassy carbon electrode. *Microchim. Acta.,* 147: 225-230 (2004).
25. Zhang L, Wang Z and Chang J. Determination of dopamine in single rat pheochromocytoma cell by capillary electrophorresis with amperometric detection. *J. Chromatogr. B. Anal. Techn.Biomed.Life Sci.*,792: 381-85(2003).
26. British pharmacopoeia ,London Department of Health,Scottish home and Health Department, crownon copyright 1993.
27. iely and Sons Inc., New York. , (1993).

Synthesis Of Carbon Nanotubes By Electrochemical Deposition using Aluminum Substrate

Dhia H. Hussain[1] ,Abdul-jabbar I. Rasheed[1] and Abdul Qader D. Faisal[2]
[1]Department of Chemistry College of Science Almustansiriya University
[2]Department of Applied Sciences University of Technology

الخلاصة

استخدمت تقنية الترسيب الكهروكيميائي لأنتاج أنابيب الكربون النانوية وكانت الخلية الكهروكيميائية مكونة من قطب الأنود (الكرافيت) وقطب الكاثود (الألمنيوم) والألكتروليت المكون من محلول أسيتونيتريل في الماء اللاأيوني بنسبة (1% v/v) وقدرة مجهزة (24V). كان تصرف قطب الألمنيوم في الخلية بأتجاهين, الأول أرضية لتجميع ونمو أنابيب الكربون النانوية, والثاني مصدر لأنتاج حبيبات الألومينا المائية [Aluminum Oxide Hydroxide(AlOHO)] عالقة في الألكتروليت, هذه الحبيبات هي الأخرى تعمل على تجميع ونمو أنابيب الكربون النانوية. فحص العالق وأرضية الألمنيوم بأستخدام المجهر البصري والمجهر الماسح الالكتروني SEM و تقنيتي XRD و FTIR جميع هذه التقنيات أثبتت نمو الكربون بشكل أنابيب نانوية بقطر حوالي 100 nm على سطح الالمنيوم وقطر أقل من 20nm عالق في المحلول.

ABSTRACT

An electrochemical deposition technique has been employed to produce carbon nanotubes. The electrochemical deposition cell consists of graphite electrode as an anode, aluminum electrode as a cathode and an aqueous solution of organic material as an electrolyte. Carbon nanotube were grown on aluminum electrode using acetonitrile (1% v/v) and water as electrolyte at an applied d.c. potential (24V), The aluminum electrode acts as a deposition surface (substrate) to collect carbon nanotubes and as a source of aqueous alumina [aluminum oxide hydroxide (AlOHO)] particles suspend in the electrolyte which also deposit carbon nanotubes. The suspension and aluminum substrate were characterized by Optical Microscope, Scanning Electron Microscope (SEM), Fourier Transform Infra Red spectroscopy (FTIR) and X-Ray diffraction analysis, all these techniques show the nanotube finger print and the nanotube shape of the deposited carbon.

INTRODUCTION

There are a huge increasing in commercial applications in modern technologies of carbon nanotubes, for example, composite materials, electrochemical devices, hydrogen storage, field emission devices, and nanoscale electronic devices (1). Wide applications of carbon nanotubes are based on their unique physical and mechanical properties, which show the high electrical and thermal conductivities, and high mechanical strength along the tubular axis (2).

There are several methods for producing carbon nanotubes (CNTs) like carbon arc-discharge technique (3), laser ablation, pyrolysis, plasma enhanced, thermal and chemical vapor deposition (CVD) (4). All these synthesis techniques inherently produce carbon nanotubes along with various impurities in the form of amorphous carbon, metal catalysts and many carbonaceous particles, etc. It needed further purification to produce high quality CNTs for device applications (5).

In this study, we described for the first time to the best our knowledge an attempt to synthesis CNTs directly onto the aluminum electrode and in the

electrolyte by a simple electro deposition technique. Aluminum oxide hydroxide has never used yet as a catalyst for preparing CNTs by electrochemical deposition technique, here we used it and had a good results with it.

MATERIALS AND METHODS

Electrochemical deposition cell was fabricated to synthesize CNTs by electrolysis using acetonitrile/de-ionized water (1% v/v) as electrolyte. Electrolysis was carried out at atmospheric pressure and room temperature [6]. Carbon nanotubes were deposited onto cathode (Aluminum sheet Size (0.5x30x100mm)). Graphite was used as the counter electrode (anode). Before mounting the substrates on the cathode, they were thoroughly cleaned and rinsed with de-ionized water and ethanol, respectively. The electrodes were separated by a distance of ~10mm. The applied d.c. voltage between the electrodes was kept ~24 V using DC power supply (HEWLETT.PACKARD 6264B). The deposition was carried out for ~ (4-6) h. One step purification was applied to remove $Al(OH)_3$ from CNT`s, by dissolving impurities in a batch of row material in boiled 2.5N NaOH solution, pure CNT`s filtered and washed with boiled de-ionized water then dried in the oven.

The deposits were characterized by X-ray Diffraction (SHIMADZU XRD-6000), Fourier Transform Infra Red spectroscopy (FTIR) (Shimadzu 8400s), Microscope (NIKON ECLIPSE ME600), Scanning Electron Microscope (SEM).

RESULTS AND DISCUSSION

It should be possible to deposit carbon nanotube by electrochemical deposition technique by suitably choosing the electrolyte and the deposition parameters (7), the possibility of the formation of carbon nonotube structures by electrolysis at an applied voltage of ~24V using aluminum cathode, graphite anode and acetonitrile as the organic precursor at atmospheric pressure and room temperature is demonstrated in this communication (8).

The FTIR spectra of graphite, aluminum oxide hydroxide, untreated CNT and CNT after Sodium Hydroxide treatment are presented in Fig. 1. The FTIR spectrum for untreated CNT (Fig.1-C) indicates many peaks at 1070– 1653 cm^{-1}. The peak at about 1070 cm^{-1} is a characteristic to Al-O-Al stretching vibration. The other peaks 1404 - 1653 cm^{-1} may be attributed to the vibrational modes of carbon nanotubes (6). The broad band centered at about 3450 cm^{-1} could be attributed to the presence of –OH groups [Al-(OH)] (9). The FTIR spectrum for CNT after Sodium Hydroxide treatment (Fig. 1-D) indicates the disappearance of many peaks (1070, 3450 cm^{-1}) and appearance of new peaks which were covered or prevented by the impurities, 2850-3000 cm^{-1} which may be attributed to the C-H aliphatic symmetrical and asymmetrical vibrational modes(10), the peak at about 1456 cm^{-1} is a characteristic to CH_2 absorption, 1338, 3444 cm^{-1} could be attributed to the presence of C-N and N-H groups

respectively and that means the π bonds of acetonitrile was cracked during tailoring process of CNT, The peaks 1404 - 1745 cm^{-1} was appeared which attributed to the vibrational modes of carbon nanotubes (6).

In comparison between the band around 2360 cm^{-1} in Fig.1 (A and D) we found that the band changed from sharp strong absorption band (transparency 24%) for graphite (Fig.1-A) to sharp strong transmission band (transparency 90%) for CNT (Fig.1-D), thereto, the transparency of the IR spectra changed from less than 27% (Fig.1-A)to more than 75% (Fig.1-D) , this is a good argument for changing graphite to CNT(11).

Fig. 2(A-F) shows the reflection micrographs of prepared aluminum oxide hydroxide/CNT deposited on Aluminum sheet electrode with magnifications (A=50X, B=100X, C=200X, D=500X, E=1000X, F=1000X). The micrographs (E&F) clearly indicated the formation of carbon nanotube structures. The CNTs produced on the aluminum sheet seemed to be twisted and the diameter of nanotubes is of order of 100 nm.

Fig. 3(A&B) shows the scanning electron microscope of suspended aluminum oxide hydroxide/CNT after filtration from the electrolyte. The CNTs produced in the electrolyte seemed to be straight and the diameter of nanotubes is of order of less than 20 nm.

We expect that twisty CNTs are the results of very complex change of catalytic activity. The difference between diameters of CNTs on the electrode and CNTs in the electrolyte is due to the size of the catalyst particles.

The XRD spectra (Fig. 4, 5) of the suspension and the deposited film showed (002) (004) reflections which could be assigned to the hexagonal ring structure of the graphite sheets forming the carbon nanotube. Additional peaks for graphite carbon for the reflections from (102) and (105) planes could also be observed. All the peaks are slightly shifted to lower angle from that of graphite indicating the wider interlayer spacing. The (002) peak position of the CNT deposits on Al was located at $2\theta = 26.54^{o}$ while for the suspended CNT was located at 2θ-28.2^{o} (6, 9).

Using an electrochemical deposition method, carbon nanotubes have been synthesized from organic solutions at room temperature. The formation and growth of carbon nanotubes are catalyzed by aluminum oxide hydroxide catalyst formed immediately during electrochemical process on the aluminum electrode and in the electrolyte. SEM characterization shows that the diameter of nanotubes is of order of 100 nm deposited on the aluminum sheet and is of order less than 20 nm suspended in the electrolyte depending on the size of catalyst particles.

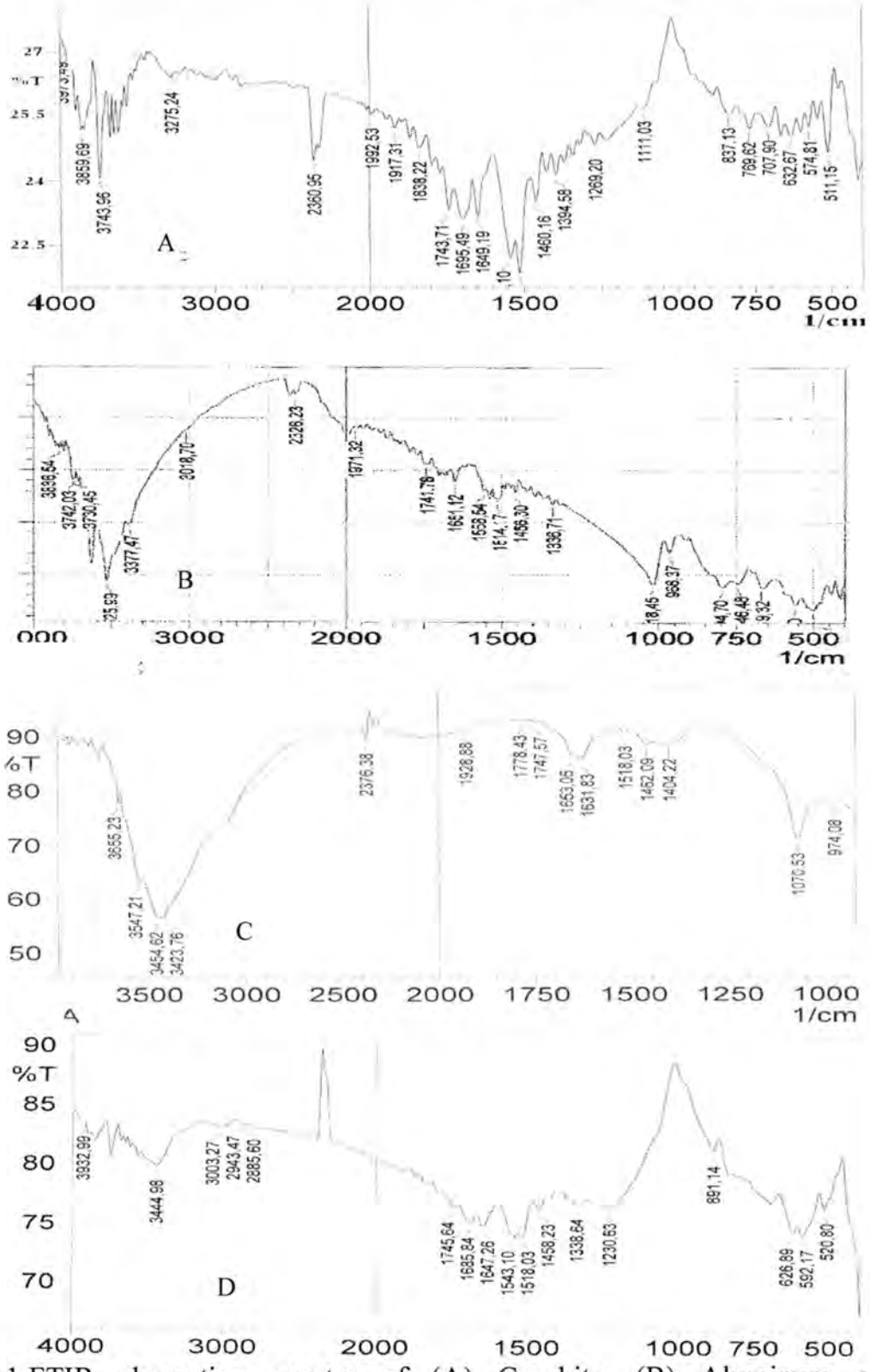

Fig.-1:FTIR absorption spectra of (A) Graphite, (B) Aluminum oxide hydroxide, (C) Untreated CNT and (D) CNT after Sodium Hydroxide treatment.

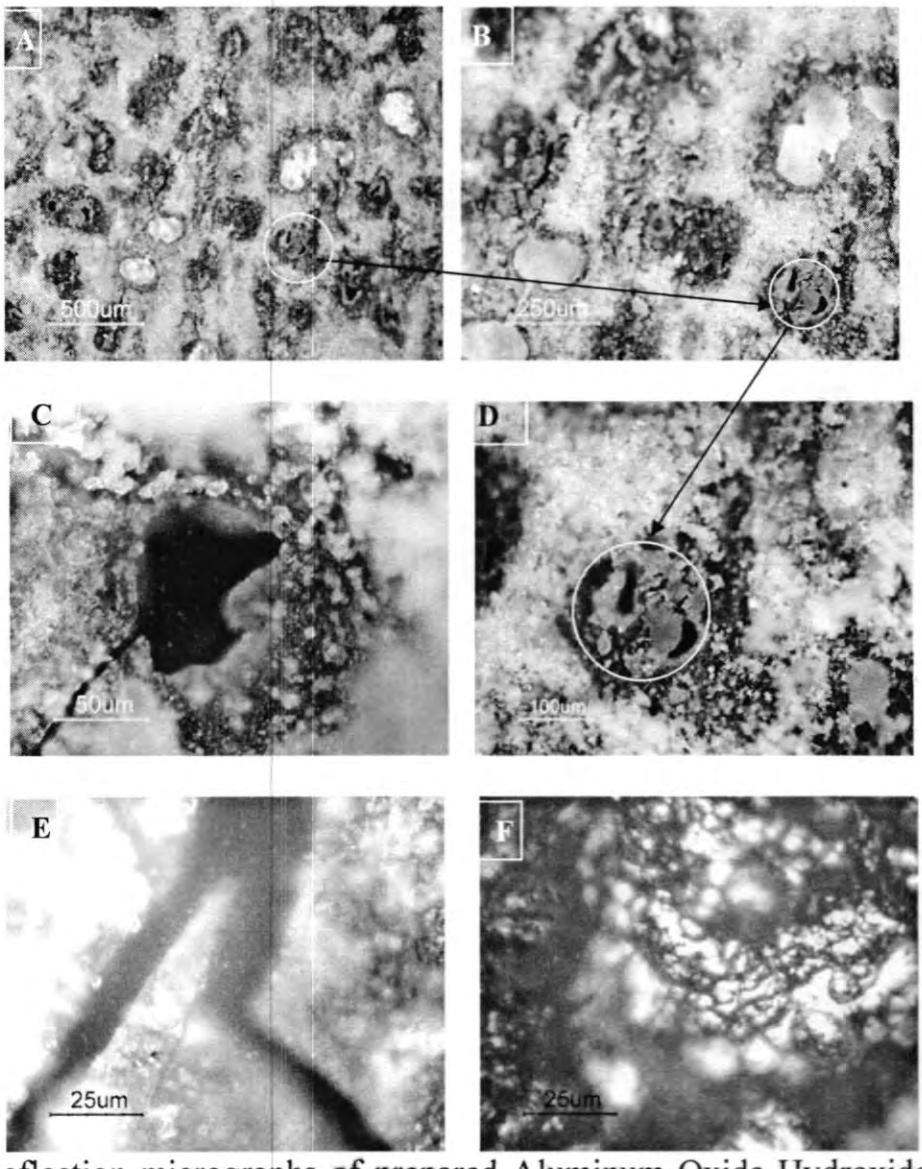

Fig.-2:Reflection micrographs of prepared Aluminum Oxide Hydroxide /CNT deposited on Aluminum electrode.

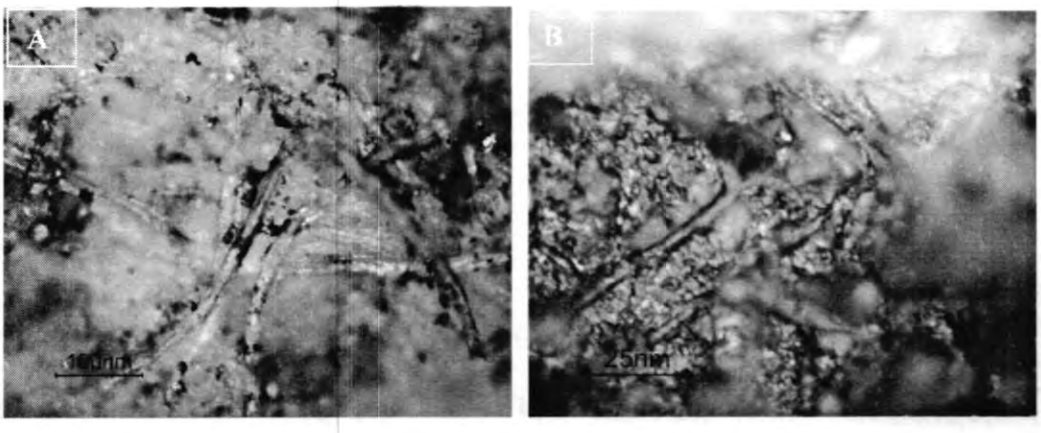

Fig.-3.SEM micrographs of suspended Aluminum Oxide Hydroxide /CNT after filtration from the electrolyte.

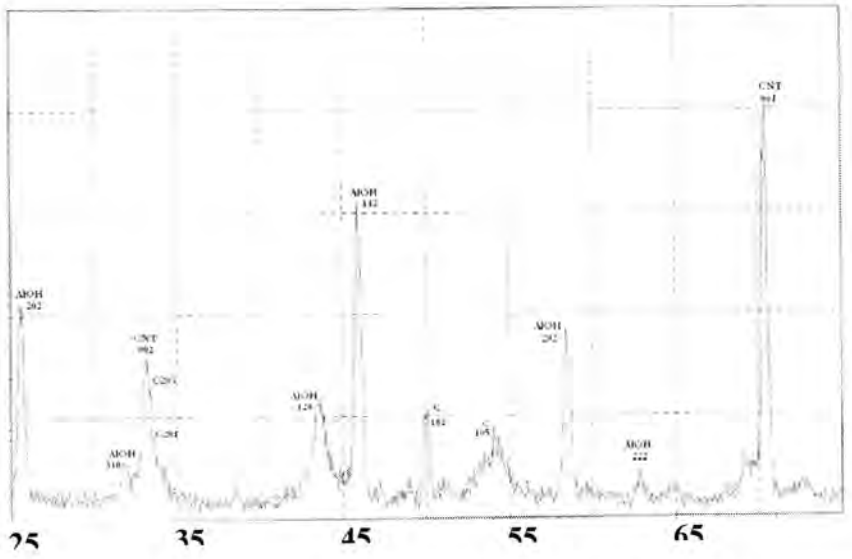

Fig.-4: XRD analysis of suspended Aluminum Oxide Hydroxide/CNT after filtration from the electrolyte.

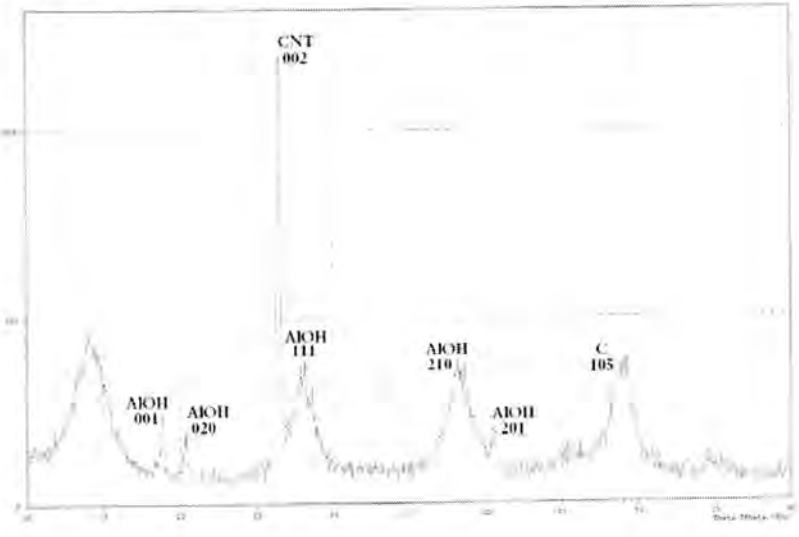

Fig.-5: XRD analysis of Aluminum Oxide Hydroxide/CNT deposited on Al sheet.

REFERENCES

1. Morinobu Endo, Takuaya Hayashi, Yoong Ahm Kim, Mauricio Terrones & Milred Dresselhaus,"Application of carbon nanotubes in the twenty-firstcentury", Phil. Trans. R. Soc. Land. A 362, 2223-2238, (2004).
2. Ray H.Baughman, Anvar A.Zakhidov & Walt A.de Heer,"Carbon nanotubes the route toward applications",Science,297,787 (2002).
3. Hyeon H. Kim & Hyeong J. Kim, " Preparation of carbon nanotubes by DC arc discharge process under reduced pressure in an air atmosphere",Materials Science and Engineering B 133, 241–244 (2006).

4. S. Karthikeyan, P. Mahalingam & M. Karthik, "Large scale synthesis of carbon nanotubes", E-Journal of Chemistry, **6(1),** 1-12 (2009).
5. L. A.Montoro & J. M. Rosolen," Step-by-step chemical purification of carbon nanotubes analyzed by high resolution electron microscopy" Carbon, 44, 3293-3301 (2006).
6. K. Pal, R. K. Roy, S. K. Mandal, S. Gupta & B. Deb, " Electrodeposited carbon nanotube thin films", Thin Solid Films 476, 288-294 (2005).
7. D. Zhou & L. Chow, "Electrochemical deposition of carbon nanoparticles from organic solutions", US Patent 6,758,957 B1 (2004).
8. D. Zhou, E. V. Anoshkina, L. chow & G. Chai, "Synthesis of carbon nanotubes by electrochemical deposition at room tamerature", Carbon, 44, 1013-1024 (2006).
9. C. B. Mo, S. I. Cha, K. T. Kim, K. H. Lee & S. H. Hong," Fabrication of carbon nanotube reinforced alumina matrix nanocomposite by sol-gel process", Material Science and Engineering A 395, 124-128 (2005).
10. Yeon S. Jung & Duk y. jeon, "Surface structure and field emission property of carbon nanotubes grown by radio-frequency plasma-enhanced chemical vapor deposition", Applied Surface Science 193, 129-137 (2002).
11. L. Hu, D. S. Hecht & G. Grüner, " Infrared transparent carbon nanotube thin films", Appl. Phys. Lett. **94**, 081103 (2009).

Determination of Diazinon Pesticide in Water Using Continuous Solvent Extraction - Steam Distillation

Salam A. H. Al-Ameri
Department of Chemistry, College of Science, Al-Mustansiriya University

الخلاصة

تم استخدام طريقة الاستخلاص المستمر - التقطير البخاري لاستخلاص المبيد ديازنون, المستخدم كثيرا" محليا, في العينات المائية متضمنة الظروف المثلى للاستخلاص باستعمال المذيبات العضوية الأثقل من الماء كلوريد المثلين أو الكلوروفورم. إن نسبة الاسترجاع للمبيد لمحلول تركيزه 10 ملغم / لتر كانت 100 % تقريبا بعد تعديل حامضية العينة المائية (الأس الهيدروجيني = 1.5- 2) وزمن استخلاص مستمر – تقطير بخاري 3.5ساعات لعينة مائية ذات حجم 500 مللتر باستعمال حجم 150 مللتر من الكلوروفورم أو كلوريد المثيلين. أعطى الاستخلاص بدفعة واحدة لعينة صغيرة من المبيد نسبة تراوحت بين 70 – 78 % لمدى تركيز 1 – 10 ملغم / لتر باستعمال الكلوروفورم أو كلوريد المثيلين . استخدمت طريقة امتصاص الأشعة فوق البنفسجية – المرئية لتقدير وتحليل المبيد ديازنون باستعمال خلايا مصنوعة من زجاج الكوارتز ذات سمك 1سم . تم حساب قيم الدقة والضبط لهذه الطريقة باستعمال عينات مائية قياسية محضرة مختبريا لمبيد ديازنون , وبأجراء المعالجات الإحصائية أظهرت النتائج وجود خطأ نسبي منوي %R.E يتراوح مابين ± 0.2 إلى 4.8 % وكان الانحراف المعياري النسبي R.S.D % لا يزيد على 8.19 % . هذه الطريقة بسيطة وطبقت باستعمال معدات بسيطة ورخيصة متوفرة في المختبرات الكيميائية لمدى واسع من العينات المائية.

ABSTRACT

A continuous solvent extraction-steam distillation method of water by heavier solvents was used for the extraction of diazinon pesticide, locally widely used, in aqueous samples involving the optimal conditions for extraction with chloroform or dichloromethane as extractor. The recovery for a concentration about 10 $mg.L^{-1}$ of diazinon approaches to 100% using acidification of the water sample (pH=1.5-2) and a extraction- distillation time of 3.5 hour for an aqueous sample 500 ml with 150 ml of chloroform or dichloromethane as extractor. One extraction with small volumes of chloroform or dichloromethane, diazinon could be recovered to the extent of 70-78 % in the range 1-10 $mg . L^{-1}$. A UV- spectrophotometric method has been used for the determination and analysis of diazinon using 1cm quartz cells. The accuracy and precision of the method were determined by preparing laboratory samples of diazinon , the results showed relative error ranging from ± 0.2 to 4.8 % and the Relative standard deviation did not exceed 8.19 %. This method is simple and could be implemented with relatively low-coast equipment which is already available in chemical laboratories and it may be applicable to a wide range of aqueous samples.

INTRODUCTION

It is important to determine small concentration of pesticides in aqueous samples such as waste streams, natural water used as raw water for drinking water supplies. The organophosphates are more soluble and have half lives in fresh water on the order of one to four weak (1) . Hunt J. W.et al (2) study organophosphates diazinon and chlorpyrifos in a central California watershed because of their high toxicity, their common usage and their previously reported association with biological effects. The concentration of diazinon, chlorpyrifos and malathion in

water was reported by using polyester foams, the sorption efficiency and the recovery were found to be up to 95.5%(3). Athanasius C. Kimbris et al (4) reported a method for analyzed organophosphates with FT-Raman spectroscopy which is simple, rapid and non-destructive for the sample. H. B. Mathur et al (5) found a method for analysis of organophosphates pesticides in soft drinks using methylene chloride as solvent. Methods for the determination of trace pesticides pollutants in aqueous samples generally include solvent extraction(6), continuous solvent extraction-steam distillation(7) and concentration step (8) or concentration on solid adsorbents by adsorption and subsequent elution from XAD resins(9,10). W. John et al(11) have reported a method for the determination of diazinon residues in sheep's wool using petroleum spirit as solvent and analysis using GC-Mass spectrometer. A. Neicheva et al. (12) reported good method for simultaneous determination of organophosphorus pesticides in plant products and water, the pesticides were extracted with acetonitrile or chloroform. A continuous liquid-liquid extraction apparatus based on mixed settling is described (13). The recovery of pesticides is 83-96% for different pesticides and different pump rates. Size Exclusion Chromatography SEC is used of extraction of pesticides with ethyl acetate , recoveries better than 90% are obtain for organophosphorus pesticides from fats, fish oils, vegetable, fruits, cereal and liver (14). V. Janda and K. Krijt (15) used continuous distillation- continuous liquid-liquid extraction for the isolation of phenols from water using diethyl ether as the extraction solvent, the recovery approaches 100% for a concentration range about 0.1-30 mg. L^{-1} at distillation- extraction time of 1.5 hour. Pesticides residue in raw wool wax were removed by continuous counter current extraction with hexane and DMF in mixer-settler contactor (16), the caffeinate wool wax produced by this process after conventional neutralization met all BP and USP specification for pharmaceutical lanolin. Hunt J. W.et al (17) found relationships between water quality and organophosphorus pesticides application rates in agricultural watersheds, to evaluate the usefulness of pesticides application data in regional monitoring sites. Nguyen Van Cong et al (18) were tested level from 0.008 to 0.52 mg. L^{-1} of diazinon to assess the effects on the brain cholinesterase activity of the snakehead fish.

This work was aimed to improve the analytical methodology for the determination of diazinon, widely used in Iraq, in polluted aqueous samples by optimization the continuous solvent extraction-steam distillation and analysis by a UV-spectrophotometer. It was also desirable to minimize the analysis time required by avoiding further clean-up steps and avoid time-consuming.

MATERIALS AND METHODS

Apparatus

A shimadzu-160 double beam UV- spectrophotometer was used for the determination and analysis of diazinon samples using 1 cm quartz cells.

Materials

All compounds were of high purity purchased and obtained from Fluka and BDH and no further purification was need. Diazinon commercially available were of technical purity (table-1). All glassware was cleaned with detergent and water, rinsed with distilled water, dried and rinsed with chloroform or dichloromethane several time before use.

Preparation of samples

Samples of different standard concentrations of diazinon were prepared by transferred accurately weighted amount of liquid standard diazinon pesticide into appropriates volumetric flasks and added distill water or organic solvents.

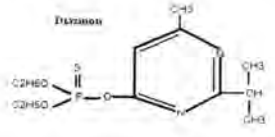

Phosphorothioic acid o,o-diethyl-o-(6-methyl-2-(1-methyl ethyl)-4-pyrimidinyl) ester

Extraction

The apparatus used for the continuous solvent extraction-steam distillation of diazinon in water by heavier solvents, chloroform or dichloromethane (table-2) is shown in (fig.1).

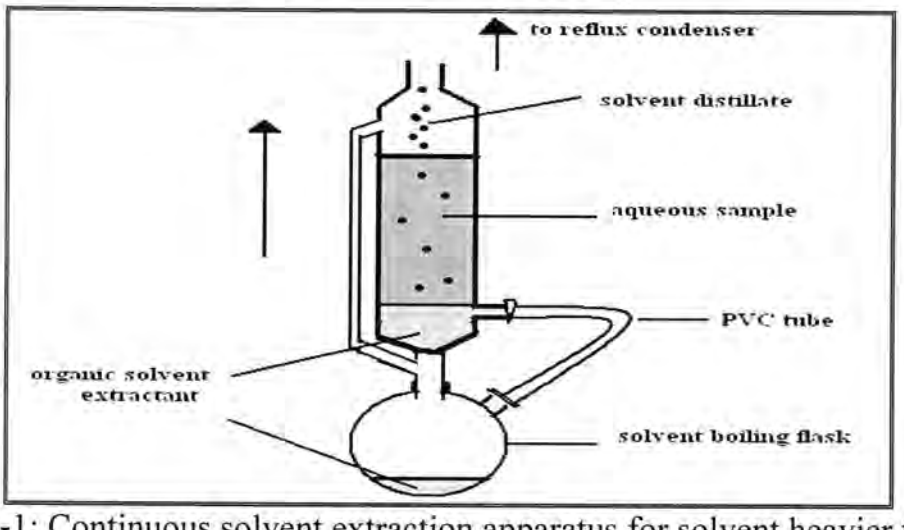

Fig. -1: Continuous solvent extraction apparatus for solvent heavier than water

Diazinon in chloroform or dichloromethane exhibit two maximum absorption peaks at 250, 270 nm, (fig-2) the absorption peak (λ_{max})at 250 nm having the highest absorption intensity, was selected for the determination of diazinon , construction of standard calibration graph, and %extraction using 1 cm quartz cells in acidic (pH=1.5-2) and basic (pH=12-13)aqueous samples using hydrochloric acid and sodium hydroxide to adjusted pH, and phase ratio organic to aqueous layer was 1:5 and 1:10 at extraction time 2 and 5 minutes .

Table-1: Physical and chemical properties of diazinon pesticide

Compound	M.Wt	Empirical Formula	LD50 mg/ kg	Solubility in water mg/L	Liquid density, gm/ml	B. P. ° C	TLV, g/m^3
Diazinon	304.34	$C_{12}H_{21}N_2O_3PS$	250m,285f	40	1.116-1.118	120	0.1

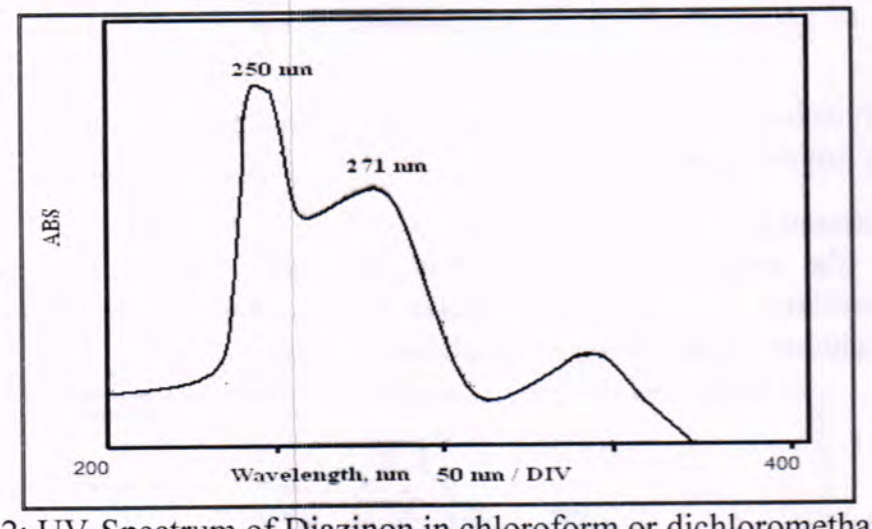

Fig. -2: UV-Spectrum of Diazinon in chloroform or dichloromethane

Table-2: Physical and chemical properties of organic solvents

Organic solvent	Chemical formula	density	B. p °C	Dielectric constant	Solubility in water , g\l
dichloromethane	CH_2Cl_2	1.144	40.1	9.1	20
Chloroform	$CHCl_3$	1.498	61.62	4.8	10

A 100 ml volume of dichloromethane was placed in 250 ml round bottom flask and a boiling chips was added. The extractor containing 50 ml of dichloromethane was placed above the flask. The aqueous sample, 500 ml was adjusted to pH=1.5-2.0 with hydrochloric acid and

poured into the extractor to form a layer above the dichloromethane which distilled and condensed and fell as small drops through the water column and returned to the boiling flask. The diazinon were continuously extracted with fresh portions of solvent. After 5 hour the extraction-steam distillation is finished, the extract was collected and dried with sodium sulfate . The sample was ready for analysis by UV-spectrophotometer.

Analysis

A 10 – 35 µL volumes of the diazinon solutions were diluted with appropriate solvent and analysis using UV-spectrophotometer. A standard calibration graph for diazinon (fig. -3) in the concentration range 0.5 to 20 $mg.L^{-1}$ were prepared and used to determine the amounts of diazinon using the Method of Least Squares (M.L.S)(19).

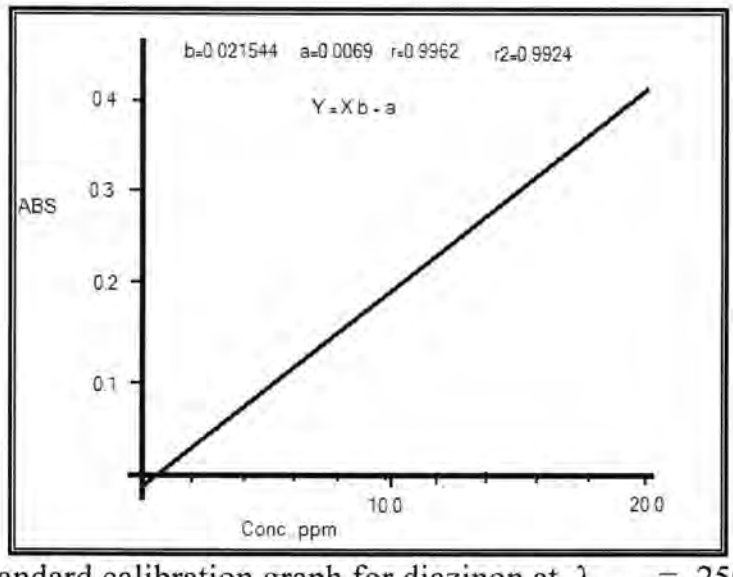

Fig.- 3: Standard calibration graph for diazinon at λ_{max} = 250 nm

The regression equation { Y= X b ± a , where Y is the sample absorbance , X is the calculated unknown concentration, b is the slope = 0.021544 , a is the intercept = 0.0069, r is the correlation coefficient = 0.9962} were utilized for the calculation of unknown concentration in polluted aqueous samples.

RESULTS AND DISCUSSION

In this paper describe a method for the determination of diazinon based on continuous solvent extraction-steam distillation. The method has been successfully applied to aqueous samples.

Dichloromethane was the solvent of choice because of its moderate polarity, higher density compared with water, lower tendency to form emulsion and ease to distillation (table-2). The extraction in acidic

aqueous samples give best results compared with basic which give emulsion. One extraction with small volumes of chloroform or dichloromethane, diazinon could be recovered to the extent of 70-78% in the range 1-10 $mg.L^{-1}$. The results showed that 2 minutes extraction time is sufficient to do and obtain higher extraction with phase ratio 1:5 or 1:10 organic to aqueous layer (table-3) .

Using a continuous solvent extraction-steam distillation apparatus, for an aqueous sample 500 ml with 150 ml of dichloromethane as extractor the diazinon were continuously extracted with fresh portions of solvent, after 3.5 hour the extraction-steam distillation is finished, the extract was collected and dried with sodium sulfate The recovery for a concentration about 10 $mg.L^{-1}$ approaches to 100% using acidification of the water sample (pH=1.5-2). The sample was analysis by UV-spectrophotometer by measured the absorbance at $\lambda_{max} = 250$ nm using 1 cm quartz cells. The validity of the regression equation was tested by analyzing standard samples of diazinon. Beers law is valid within the concentration ranges of diazinon. The results are summarized in(table-4) for standard samples , with chloroform or dichloromethane as extractor.

The accuracy and precision of the method were determined by preparing laboratory samples of diazinon , the results showed relative error ranging from ± 0.2 to 4.8 % and the Relative standard deviation did not exceed 8.19 %. This method proved to be simple and could be implemented with relatively low-coast equipment which is already available in chemical laboratories and it may be applicable to a wide range of aqueous samples .

Table-3: %Extraction of diazinon from acidic and basic aqueous samples using chloroform or dichloromethane

Organic solvent	pH aqueous layer	Phase Ratio Organic : Aqueous	% Extraction ± 3
Dichloromethane	1.5-2.0	1:5	73
Dichloromethane	1.5-2.0	1:10	73
Dichloromethane	12-13	1:5	21
Dichloromethane	12-13	1:10	22
chloroform	1.5-2.0	1:5	75
chloroform	1.5-2.0	1:10	75
chloroform	12-13	1:5	20
chloroform	12-13	1:10	18

Table-4: Analysis of standard diazinon samples

Sample No.	ABS	Diazinon Conc.,mg.L^{-1}	Absolute Error	Relative Error %	Average Conc. mg.L^{-1}	Standard Deviation	%Relative Standard Deviation
1	0.104	5.147	+0.147	2.94	5.025	0.412	8.19
2	0.106	5.24	+0.24	4.8			
3	0.101	5.01	+0.01	0.2			
4	0.103	5.10	+0.10	2.0			
5	0.098	4.87	-0.13	2.6			
6	0.096	4.78	-0.22	4.4			

REFERENCES

1. Bandarenko S. et al, " *Persistence of selected organophosphates And Carbamate insecticides in waters from a coastal watershed*",Environ. Toxicology &Chemistry, *23*, 2649, (2004).
2. Hunt J.W et al," *Ambient toxicity due to chlorpyrifos and diazinon in a central California watershed"* Environ.Monit. Assess. *82*, 83, (2003).
3. M.S.El-Shahawi et al,"The relation behavior and separation of some Water soluble organophosphorus insecticides on polyester-based Polyurethane foams " , Talanta , *24*, 1471, (1995).
4. Athanasius C.Kimbris et al,"Quantitative analysis of garlic oil unsaturated cyclic components using FT-Raman spectroscopy",Food Chemistry, *94*, 287, (2006).
5. H.B.Mathur et al,"Analysis of Pesticides in soft Drinks", (2003).
6. G.Bengtsson," A gas chromatographic micro method for trace determination of phenols" *J. of Chromatogr. Sci., 23* , 397, (1985).
7. G.Norwitz;N.Nataro;P.N.Keliher, *Anal. Chem., 58*, 639, (1986).
8. J.P.Mieure;M.W.Dietrich,*J.of Chromatogr. Sci., 11* , 559, (1973).
9. C.Borra, et al., *Anal. Chem., 58*, 2048, (1986).
10. A.Tateda; J.S. Fritz, *J. of Chromatogr. 152*, 329, (1978).
11. W.John,et al.,"Determination of propetamphos and diazinon residues in sheep's wool", *Analyst, 112*, 1761, (1987).
12. A.Neicheva et al."Determination of organophosphorus pesticides in apples and water by gas-liquid chromatography with electron-capture detection", *J. of Chromatogr. 437*, 2499, (1988).
13. Martin A.;Bjorn J.,"Simple apparatus for on-site continuous liquid-Liquid extraction of organic compounds from natural waters",*Anal.Chem.,46*,658, (1974).
14. A. H. Roos, et al.," Universal extraction/clean-up procedure for screening of pesticides by extraction with ethyl acetate & size exclusion chromatography " , *Anal. Chim. Acta. 196*, 95, (1987).

15. V. Janda & K. Krijt ," Recovery of phenols from water by continuous Steam distillation-extraction", *J. of Chromatogr. 283*, 309, (1984).
16. F.William Jones,"Removal of pesticides from wool wax by continuous countercurrent dual-solvent extraction"J.of Ameri.Oil Chemists Soci.,*74*, 1247, (1997).
17. Hunt J.W et al,"Spatial relationships between water quality & pesticide application rates in agricultural watersheds",Environ.Monit. Assess. 121,245, (2006).
18. Nguyen Van Cong et al," Sensitivity of brain cholinesterase activity to diazinon and fenobucarb insecticides in the air-breathing fish channa striata", Environmental Toxicology &Chemistry, 25, 1418, (2006).
19. James N.Miller & Jane C.Miller,"Statistics & Chemometric for Analytical Chemistry " , 4th Ed, (2000).

Copolymerization of Acrylonitrile with Some Allyl Monomers: Characterization and Determination of Reactivity Ratios.

Tariq S.Najim and Muntadhar S.Sultan.

Chemistry Department , College of Science,Al-Mustansiriya University

الخلاصه

تم اجراء البلمره المشتركه للاكريلونايتريل AN مع كحول الاليل AA وبنزوات الاليل AB وكلوريد الاليل AC بدرجة 60 درجة مئوية وباستخدام ايزوبس ايزوبيوترونايتريل AIBN كمادة بادئة . نسبة تحول المونمير الى البروليمر اجريت باوقات مخلفة وذلك لتحديد نسبة التحول اقل من 10 % دائما . اجريت كذلك بلمرة متجانسة للمونمرات AC,AB,AA,AN باستخدام نفس البادئ ونفس الظروف . استخدم ال FTIR وIR الاعتيادي لتحديد تركيز المونمرات في الكوبوليمر المحضر وذلك بالاعتماد على حزم الامتصاص مختارة مثل C=N في AN و OH– في AA و C=O في AB و C-Cl– في AC. تم حساب الفاعلية النسبية للمونمرات (r_1,r_2) لكل من AC,AB,AA,AN باستخدام طريقة فنمان وروس (F-R) وطريقة كلين- تثيودوس(K-T) وكذلك استخدام برنامج مايكروسوفت لحساب الفاعلية النسبية .

الفعالية النسبية للمونمرات AC , AA, AN تم تعينها نظريا بطريقة الفري-برايس او ما يسما Q-e scheme في كل الاحوال كان هناك توافق جيد بين القيم المحسوبة نظريا وعمليا والموجودة في الادبيات. تم حساب Q,e لبنزوات الاليل في البولي AN-Co-AB حيث تم حسابها من قيم الفعالية النسبية . وبالاعتماد على حاصل ضرب r_1 وr_2 فان البوليمرات الحضرة تتجه نحو التناوب كلما اصبحت قيم حاصل الضرب اقرب الى الصفر ولكل نظام كما ان الكوبوليمرات المحضرة دائما تكون غنية بوحدات الاكرونايتري وذلك بسبب استقرار الجزر الحر العملاق العائد لمونمرات الاليل بسبب الاقتران وكذلك بسبب المشاركة بتفاعلات انتقال السلسلة . تم تقيم تركيب الكوبوليمر وذلك برسم الكسر المولي لكل مونمر في التغذية وفي الكوبوليمر.

ABSTRACT

Free radical copolymerization of acrylonitrile (AN) with allyl alcohol (AA), allyl benzoate (AB) and allyl chloride (AC) were carried out at 60°C in Bulk . Azobisisobutyronitrile (AIBN) was used as an initiator. The conversion of the monomers to polymers at different intervals were carried out under the same conditions so as to maintain the conversion below 10%. Free radical homopolymerizations of AN, AA, AB and AC ware also performed using AIBN as initiator under the same conditions. Fourier transform infra-red (FTIR) and normal infra-red (IR) spectroscopy were used to evaluate the concentration of each monomer in the prepared copolymers using the absorption bands of a chosen group in each monomer which are (-C≡N) in acrylonitrile , (-OH) in allyl alcohol, (C=O) in allyl benzoate and (-C-Cl) in allyl chloride . Monomer reactivity ratios (r_1 and r_2) for AN, AA, AB and AC have been calculated utilizing Fineman-Ross (F-R) and Kelen-Tudos (K-T)equations, Microsoft quick basic program has also been used for estimating some of reactivity ratios. Reactivity ratios for AN, AA and AC monomers have also been calculated theoretically by using (Q-e) scheme of Alfrey-Price. In all cases, there were a good agreement between theoretical and experimental values of reactivity ratios and that found in literature. Q and e values of allyl benzoate in poly(AN-co-AB) were calculated from its reactivity ratio values. Depending on the multiplying result of r_1 and r_2, the prepared copolymers were random and getting close to alternative according to the product (r_1r_2) for each system and each copolymer system were rich in acrylonitrile monomer units, due to the stabilization by conjugation of maromolecular radical of allyl monomers,as well as, its participation in chain transfer reactions. The composition of each copolymer was evaluated by plotting the mole fraction of AN monomer in feed and in the copolymer.

INTRODUCTION

In many instances, the composition of a copolymer are found to be different to that of the copolymer feed from which it is produced. In other words , different monomers exhibit different tendencies towards copolymerization.Some monomers are more reactive in copolymerize -ation than indicated by their rate of homopolymerization(1).For example ,monomers like the maleic anhydride / stilbene pair, undergo copolymerization readily although they have little tendency to homopolymerize .Thus,the composition of a copolymer cannot be determined from the knowledge of homopolymerization rates of the two monomers .Several workers (2-4) determined copolymer composition by assuming the chemical reactivity of the propagating chain in a copolymerization to be dependent only on the monomer unit at the growing end and independent of the chain composition preceding the last monomer unit. Mayo et al (2) proposed that copolymer composition formed at any instant is dependent not only on the concentration of monomer species present in the system but also on the reactivity ratios. The reactivity ratios indicate whether a growing chain , carrying an active centre on a particular monomer unit, would prefer to add its own monomer or a co-monomer unit. The reactivity ratios will throw light on copolymerization behavior and also on type of copolymer obtained. The accurate estimation of copolymer composition and determination of reactivity ratios is significant for tailor making copolymers with required physico-chemical properties and evaluating the end application of copolymers .It is well known that physical properties and sequence length distribution are important characteristics of copolymers.

The most fundamental quantity characterizing a copolymer is its composition on a molar basis ,which eventnally used for determination of the relevant reactivity ratios.

Spectroscopic methods, preferably ^{1}H-NMR ,^{13}C-NMR (5,6), IR and Fourier transform IR (FTIR) (7) and UV (8) spectroscopy are probably the most widely used methods of analysis of copolymers , and determination of reactivity ratio of comonomers (r_1 and r_2) . In general FTIR spectroscopy can provide not only qualitative but also very good quantitative analysis (9). The present research paper reports the synthesis, characterization, copolymer composition and determination of reactivity ratios for the comonomers in copolymrization of acrylonitrile with some allyl monomers by using FTIR techniques.

MATERIALS AND METHODS

Materials

AN was freed from inhibitor by washing with sodium hydroxide solution and then with distilled water to remove traces of sodium hydroxide and dried over calicium chloride , then vaccum distilled, AIBN was purified by recrystalization from methanol and dried at room temperature .

Allyl alcohol and allyl chloride were distilled under vaccum .The other chemicals are used as received.

Preparation of Allyl benzoate

AB was synthesized by the reaction of benzoyl chloride with allyl alcohol as follows (10). 0.2 mol of benzoyl chloride was placed in round bottomed flask 0.2 mol of allyl alcohol was added drop wise at room temperature the mixture was then refluxed for 1 hour.

The product was collected and washed twice with 5% sodium bicarbonate solution then with distilled water to remove traces of HCl.The product was dried with calcium chloride.

Preparation of Homopolymers

Four types of homopolymers were prepared,polyacrylonitrile(PAN), polyallyl alcohol (PAA),poly allyl benzoate (PAB), and poly allyl chloride (PAC).

In separate polymerization tubes 6 gm of each monomer were placed with appropriate amount of intiator (AIBN) , the test tubes were bubbled with agron for five minutes , the mixture were heated at 60°C on a water bath type (HAAKE K15) for one hour , then the contents were pured into excess methanol , the produced polymers were filtered off and reprecipitated from dimethylforamide (DMF) solution using methanol and dried in a vaccum oven type (Gallen Kamp.Vacuum oven) at 50°C for 12 hrs

Copolymerization

Copolymer of AN with each of the following monomer (AA, AB, AC) were prepared in bulk,using AIBN as initiator at 60° C .

Appropriate amounts of each monomer were used in each copolymerization which were carried out in a polymerization tube in bulk using AIBN as initiator at 60°C, the tube was degassed with argon, and kept in a thermostated water bath for a predetermined period of time so as to maintain the conversion below 10%.

The contents were poured into excess methanol ,the precipitated copolymer was filtered off and purified by reprecipitation from dimethylforamide (DMF) solution using methanol and dried in a vacuum oven at 50C° for 12 hrs

Measurements

FTIR spectra of the samples were recorded with testcan shemadzo FTIR 8000 series spectrophotometer on solid samples as KBr pellets .The absorption band at 2241cm^{-1} corresponds to nitrile(-C≡N) group of acrylonitrile.The peak at 3504 cm^{-1} was due to hydroxyl group (-OH) in allyl alcohol,at 1716 cm^{-1} correspond to carbonyl(-C=O) group in allyl benzoate and the absorption band at 688 cm^{-1} was due to (-C-Cl) in allyl chloride.

RESULTS AND DISCUSSION

Copolymerization of AN with AA , AB,AC from different feed composition were carried out in bulk by free radical polymerization . The reaction time was selected to give low conversion (<10%) in order to make use of the instantaneous copolymer composition to the extent possible .

FTIR Spectrum

The FTIR spectrum of poly (allyl benzoate) shows peak at 3066.61cm^{-1}, corresponding to the aromatic C-H stretching.The asymmetrical and symmetric all stretching due to the methylene groups are observed at 2929.87 and 2667.95 cm^{-1}.The peak at 1716.53cm^{-1} is attributed to the ester carbonyl stretching ,the aromatic C=C stretching is observed at 1600.81cm^{-1}, 1500 and 1452.3 cm^{-1}.The C-O stretching due to ester group seen at 1274.88 and 1176.5 cm^{-1}.

The C-H out of plane bending vibrations of the aromatic nuclei is observed at 713.81 cm^{-1} . For poly (allyl alcohol) the broad peak at 3480 cm^{-1} is due to hydroxyl group .The asymmetrical and symmetrical stretching due to the methylene groups are observed at 2950 and 2880 cm^{-1}.The FTIR spectrum of poly(allyl chloride) shows the following main absorption bands .The peaks at 2989.46 and 2882.17 cm^{-1} are due to asymmetrical and symmetrical stretching of C-H of methylene groups.The C-Cl stretching seen at 688.5 cm^{-1}.The main characteristic band of PAN is the stretching vibration of (-C≡N) ,which is observed at 2241 cm^{-1}.

Copolymer composition

Molar fractions of comonomer units(F_1 and F_2) in each copolymer system using FTIR analysis data are calculated according to the following methods.

The first method

This method depend on the measurement of the absorbance of analytical band in each monomer unit and its molecular weight (g/mol) (11).

$$F_1 = \frac{\dfrac{\text{Absorbance of CN group}}{M_1}}{\dfrac{\text{Absorbance of CN group}}{M_1} + \dfrac{\text{Absorbance of choosen group}}{M_2}} \quad \ldots\ldots\ldots\ldots\ldots 1$$

$$F_2 = \frac{\dfrac{\text{Absorbance of Choosen group}}{M_2}}{\dfrac{\text{Absorbance of CN}}{M_1} + \dfrac{\text{Absorbance of choosen group}}{M_2}} \quad \text{.....2}$$

$$\frac{F_1}{F_2} = \frac{\text{Absorbance of CN group}/M_1}{\text{Absorbance of chosen group}/M_2} \quad \text{.....}$$

Where, F_1 is the molar fraction of acrylonitrile in the copolymer and F_2 is the molar fraction of AA or AB or AC monomers in the copolymer.

The second method

This method is almost similar to the first one except the absorbance of each group divided by a refrence band (The least changing absorbance band)(9) which is in poly (AN-co-AA) is 680 cm^{-1}, in poly(AN-co-AB) is 800cm^{-1} and poly(AN-co-AC) is 720 cm^{-1} .

$$\Delta A = \frac{A}{A_{ref}} \quad \text{.....4}$$

Where, A is the absorbance of a certain group in the monomer unit at certain wave number and A_{ref} is the Absorbance of the reference band, then the number of moles of each monomer unit in each copolymer is:

$$n = \frac{\Delta A}{M} \quad \text{.....5}$$

The molar fraction of each monomer unit in the copolymer.

$$F_1 = \frac{\dfrac{\Delta A_1}{M_1}}{\dfrac{\Delta A_1}{M_1} - \dfrac{\Delta A_2}{M_2}} \quad \text{.....6}$$

The FTIR spectrum of each copolymer system, poly (AN-CO-AA), poly (AN-CO-AB) and poly (AN-CO-AC) of various initial monomer ratios are illustrated in figures 1-3 .

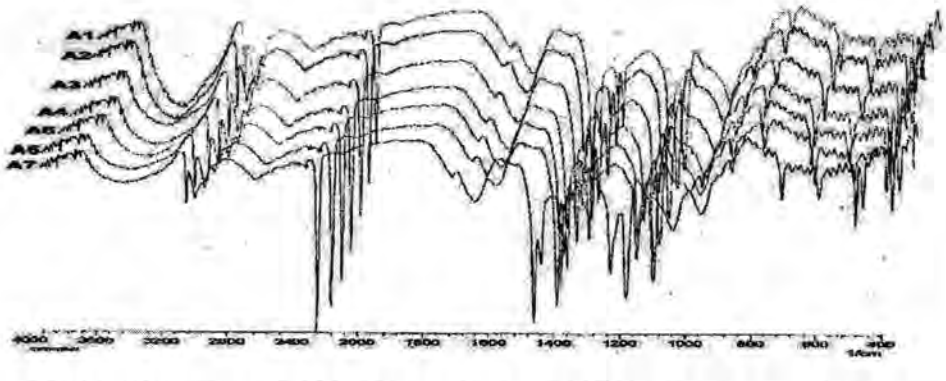

Fig.- 1: FTIR spectra of AN-AA copolymers of different compostion.

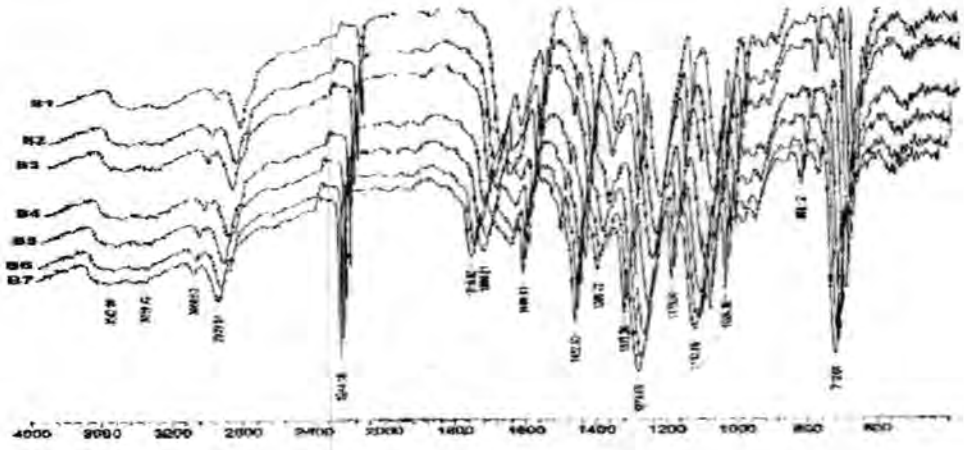

Fig. -2: FTIR spectra of AN-AB copolymers of different composition.

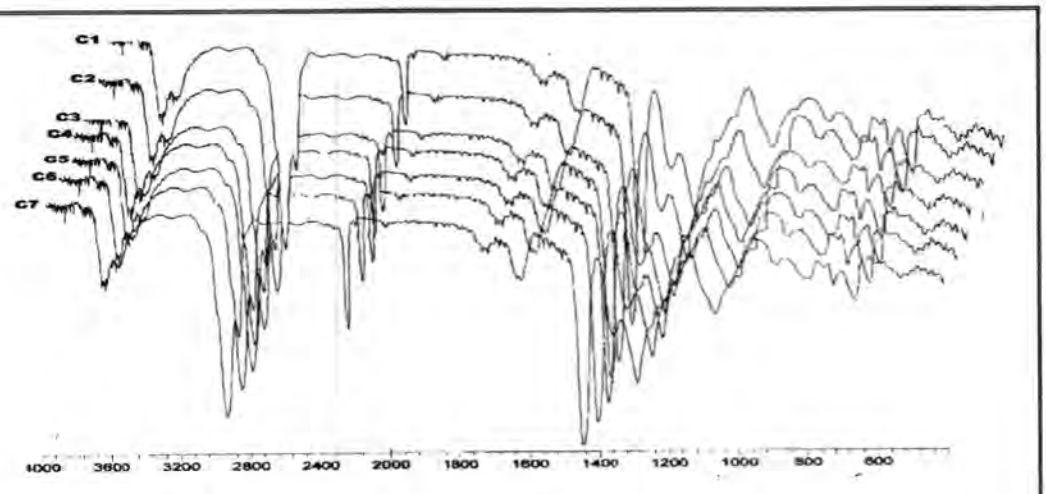

Fig.-3: FTIR spectra of AN-AC copolymers of different composition.

Determination of Monomer Reactivity Ratios

The monomer reactivity ratios for the copolymerization of AN with AA , AB , AC were determined from the monomer feed ratios and the copolymer composition.The Fineman-Ross (F-R) (12) and kelen –Tüdos (K-T) (13) methods were used to determine the monomer reactivity ratios. The parameters of K-T method were also determined using Microsoft program in Basic Lanquage (14).

The reactivity ratio of comonomers were evaluated by F-R equation 7 and K-T equation 8.

$$f(F-1)/F = r_1 - \frac{f^2}{F} r_2 \quad \ldots\ldots 7$$

$$\eta = (r_1 + r_2/\alpha)\,\zeta - \frac{r_2}{\alpha} \quad \ldots\ldots 8$$

Where:

$$\eta = \frac{f(F-1)F}{f^2/F+\alpha}$$

$$\zeta = \frac{f^2/F}{f^2/F+\alpha}$$

$$\alpha = \sqrt{(f^2/F)_{max}+(f^2/F)_{min}}$$

and $f = f_1 / f_2$ where f_1 is mole fraction of AN in the feed and f_2 is mole fraction of either AA , AB or AC in the feed. From equation 7 the plot of f(F-1)/F against f^2/F give straight line with slope = - r_2 and intercept = r_1. From equation 8 a plot of η against ξ give straight line with slope = $r_1 + r_2/\alpha$, and intercept= $-r_2/\alpha$. These results are presented in table 1, 2 and figures (4-9).

Table -1: The reactivity ratios of comonomers using K-T and F-R equations applying first and second methods.

Copolymer	$r_1(r_{AN})$				$r_2(r_{AA},r_{AB},r_{AC})$				average	r_2 average
	F-R		K-T							
	1st	2nd	1st	2nd	1st	2nd	1st	2nd		
Poly (AN-co-A	4.82	4.50	5.03	5.028	0.012	0.003	0.031	0.022	4.85	0.017
Poly	3.02	3.54	2.96	3.47	0.061	0.0714	0.044	0.041	3.25	0.054
Poly	2.25	2.57	2.02	2.25	0.087	0.089	0.061	0.055	2.27	0.073

Table -2: The reactivity ratios of comonomers by K-T equation using Microsoft program and applying first and second methods.

Copolymer	$r_1(r_{AN})$		$_A,r_{AB},r_{AC})$		average	average
	1st	2nd	1st	2nd		
Poly (AN-co-AA)	5.08	5.155	0.036	0.026	5.120	0.031
Poly(AN-co-AB)	3.18	3.51	0.090	0.010	3.34	0.050
Poly(AN-co-AC)	2.35	2.60	0.244	0.128	2.47	0.182

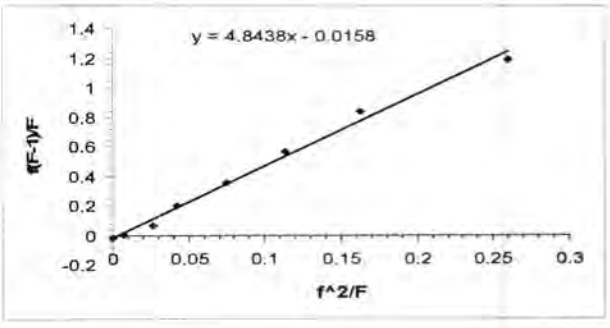

Fig. -4:Fineman – Ross Plot of poly (AN-CO-AA).

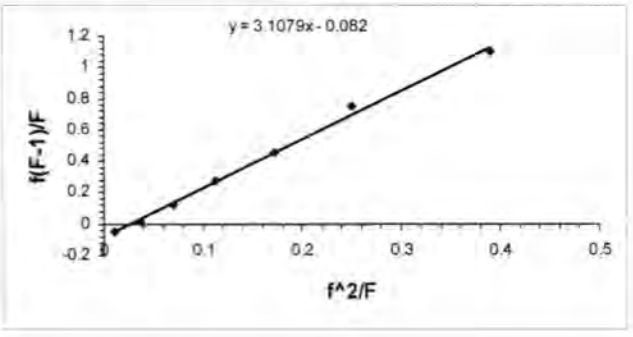

Fig.-5: Kelen-Tudos plot of poly (AN-CO-AB)

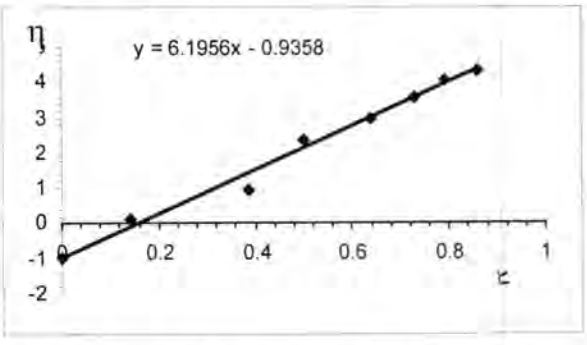

Fig. -6: Fineman-Ross plot of poly (AN-CO-AB)

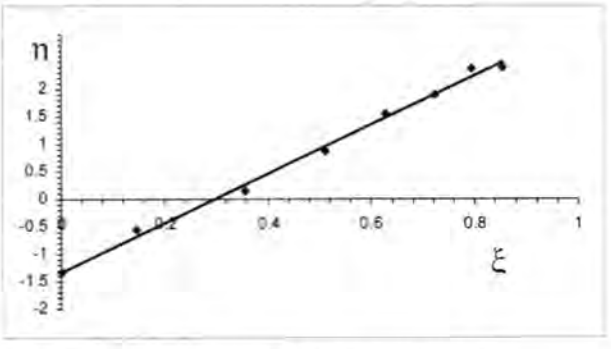

Fig.-7: Kelen-Tudos plot of poly (AN-CO-AB)

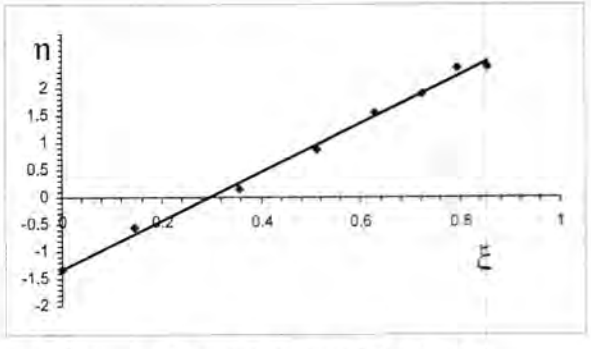

Fig.-8:Fineman-Ross plot of poly (AN-CO-AC)

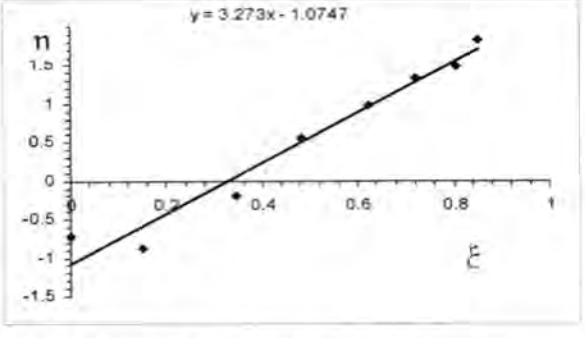

Fig.-9:Kelen-Tudos plot of poly (AN-CO-AC)

The reactivity ratios of acrylonitrile in all copolymers are higher than ally monomers indicating that higher level of acrylonitrile is incorporated in all copolymers . Furthermore , allyl monomers suffer from chain transfer reactions during radical polymerization, which make allyl radical to be stabilized by conjugation, for this reason some of allyl monomers have been used as transfer agents in radical polymerization (15,16) , on this basis the reactivity ratio of ally monomers used in this study are very low in agreement with other studies(17,18).

Theoretical evaluation of reactivity ratios of AN,AA and AC have been carried out depending on values of Q and e , from litreture(15). Q and e values are shown in table 3.The calculated values of r_1 and r_2 are summarized in table 4.

$$r_1 = \frac{Q_1}{Q_2}\exp[-e_1(e_1 - e_2)]\ldots\ldots \quad \ldots\ldots\ldots\ldots\ldots\ldots 9$$

$$r_2 = \frac{Q_2}{Q_1}\exp[-e_2(e_2 - e_1)]\ldots \quad \ldots\ldots\ldots\ldots\ldots\ldots 10$$

Table- 3: Values of Q and e.

Monomer	Q	e
AN	0.6	1.2
AA	0.005	-1.48
AC	0.026	-0.6

Table -4: Reactivity ratios of AN,AA,AC measured Theriotically.

System	r_1(AN)	r_2(AA,AC)
Poly(AN-co-AA)	4.8	0.0016
Poly(AN-co-AC)	2.66	0.015

From table 4, reactivity ratios obtained from Q and e values (threotical) were in good agreement with experimental values obtained by this study.

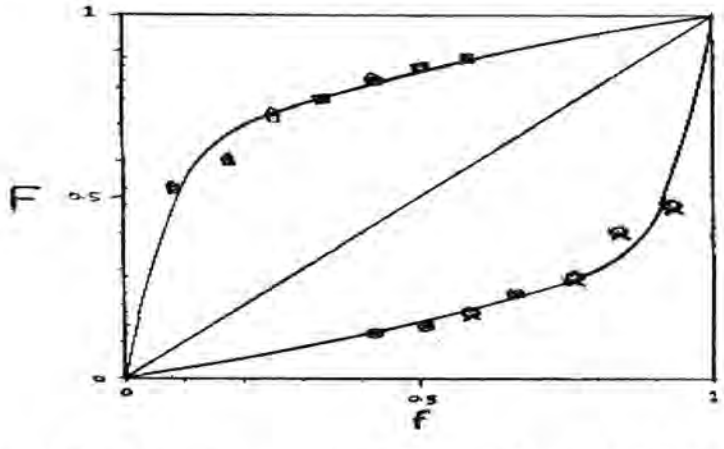

Figure -10: Copolymer composition diagram of poly (AN-Co-AA) system.

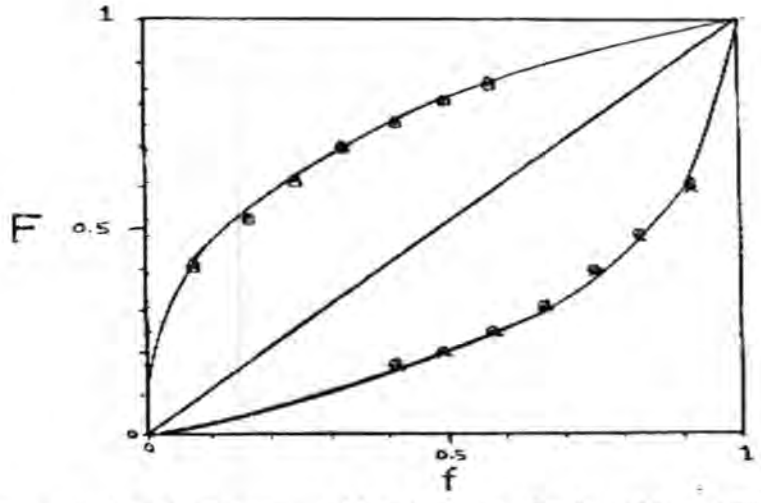

Figure -11: Copolymer composition diagram of poly (AN-co-AB) system

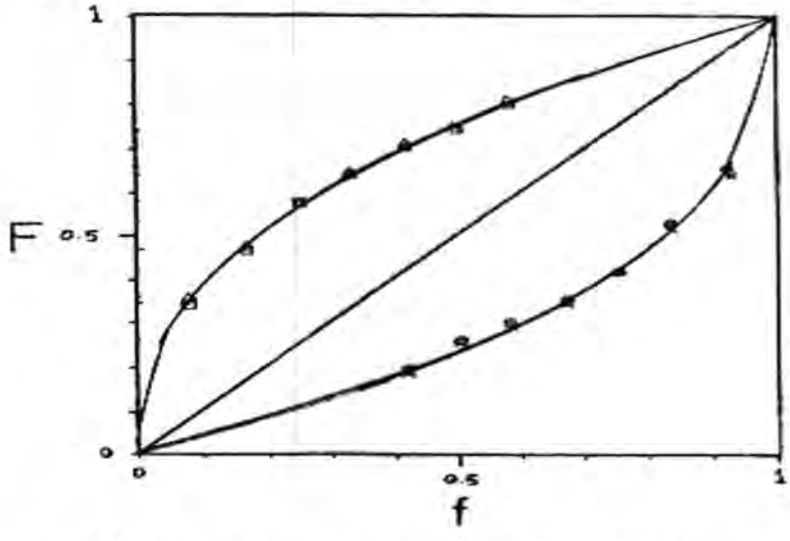

Figure- 12:Copolymer composition diagram of poly (AN-co-AC) system

The kinetic behaviour of the copolymerization was determined by plotting the mole fractions of AN in the feed (f_1) versus that in the copolymer (F_1) or allyl monomer in the feed and that in the copolymer.Figures(10-12) show the copolymer composition curves belong to the three systems. These figures indicate clearly that the AN content in the three copolymer system is always higher than that of allyl monomers.

REFERENCES

1. Alfrey,T.;Goldfinger,G.,J. The mechanism of copolymerization I.A basis for comparing the behavior of monomers in copolymerization ; the copolymerization of styrene and methylmethacrylate. J. Chem.Phys.,12:205-209, (1944)
2. Mayo,F.R.;Lewis,F.M. Copolymerization I. A basis for comparing the behavior of monomers in copolymerization ; the copolymerization of styrene and methyl methacrylate. J.Am.Chem.Soc., 66: 1594-1601, (1944).
3. Wall,F.T. The structure of vinyl copolymers. J.Am.Chem.Soc.,63(7): 1862-1866, (1941).
4. Wall,F.T, The structure of copolymers II. J.Am.Chem.Soc.,66 (12):2050-2051, (1944).
5. Shiomi,T.;Suzuki,M.;Tohyama,M.andImai,K. Dependence of miscibility on copolymer composition for blends of poly(vinyl chloride-co-vinyl acetate) and poly(butyl methacrylate-co-isobutyl methacrylate).Macromolecules 22:3578-3581, (1989).
6. Bednarski,R.;Braun,D.;Borbely, J. and Kelen,T. Copolymerization of styrene methylcyanocinnamate, I. Synthesis, NMR -assignment, reactivity ratios Makromol. Chem.,191:773-782,(1990).
7. Bastűrkmen,M.;Rzaev,Z.M.O.;Akoah,G and Kisakűrek,D. Complex-radical terpolymerization of phenanthrene,maleic anhydride,and trans-stilbene, J.polm.Sci.A,33:7-13,(1995).
8. Dionisio,J.M.and O,Driscoll,K.F. High conversion copolymerization of styrene and methyl methacrylate.J.polym.Sci.,polym.Lett. Ed., 17: 701-707 (1979).
9. Cengiz,S.;Ramazan,C.and Ali,D. Microbial screening of copolymers of N-vinyl imidiazole with phenancryl methacrylate: synthesis and monomer reactivity ratios. J. Macromol. Sci., Part A : Pure and Applied Chemistry, 42:1603-1619 (2005).
10. Arthur,I.V. "Practical organic chemistry" 3rd Ed . Longmans London :263 (1964).
11. Abdul Hussien K.Sharba,Tariq S.Najim and Nadia A.Butti. Copolymerization of acrylonitrile with butyl acrylate and determination of reactivity ratios. Iraqi.J.Polymers,11(2):141-152 (2007).
12. Fineman ,M. and Ross,S.D. Linear method for determining monomer reactivity ratios in copolymerization. J.polym.Sci., 5(2) :259-262 (1950).
13. Tűdős,F.Kelen,T.,Turcsanyi,B.,and Kennedy, J.P. Analysis of linear methods for determining copolymerization reactivity ratios.VI.A comprehensive critical re-examination of oxonium ion copolymerization. J. polym., Sci. Polym. Chem. Ed.,19: 1119-1132 (1981).

14. J.Brandrup,E.H.Imnerut, E.A.Gruke "Polymer Handbook " PII 288, 4th Ed . Willey Intorscience New York (1999).

15. Kudshhkin,V.O.;Vokhidova,N.R.,Bororov,N.I.Sidorenko,O.E.;Ruban,I.N.;Vorop a -eva ,N.L.; Rashidova,S.Sh. Use of allyl benzene and allyl phenyl ether as chain transfer agents in radical polymerization. Russian Journal of applied chemistry 77, 6: 994-997 (2004).

16. Kudyshkin,V.O.;Bozorov.,N.I.;Sidorenko,O.E.;Voropaeva. Polymerization of N-vinylcaprolactam in the presence of chain –transfer agents. Chem.Pap.,58,4:286-291 (2004).

17. Dilek Solpan, Olgun Güven. The copolymerization of allyl glycidyl ether with acrylonitrile initiated by gamma-rays.J.Polym.Sci.Part A: Polymer Chemistry , 34, 5: 833-838 (1995).

18. Volodina,V.I.;Tarasov,A.I.& Spasskii,SS. Russ.Chem.Rev.,39:140-155 (1970).

Synthesis, Structures and Antibacterial Activity of Some 2-Amino-5-(2-acetyloxyphenyl)-1,3,4-Thiadiazole complexes

Ahmed S. Majeed
Department of Chemistry, College of Science, Al-Nahrain University

الخلاصة:

تم تحضير معقدات لليكاند 2-أمينو -5-(2-اسيتوكسيفينيل)-1,3,4-ثايودايازول مع الايونات الفلزية التالية:الكروم(III)والحديد(III)والذهب(III) الكوبلت(II)والنحاس(II) في وسط كحولي مائي.

شخصت المعقدات المحضرة بتقنية الأطياف تحت الحمراء بتحويلات فورير(FTIR) والامتصاصات الأليكترونية وتحليل العناصر والتوصيلية الكهربائية والحساسية المغناطيسية. تم قياس النسب المولية والمتغيرة في المحلول فأعطت نتائج مطابقة مع تلك التي تم الحصول عليها في الحالة الصلبة.حيث تم اقتراح هندسة الوحدة الاساسية للمعقدات.

تم تقييم الفعالية البايولوجية للمعقدات الجديدة المحضرة ضد انواع منتجة من البكتيريا (خارج الجسم) وقد دلت النتائج المستحصلة بان لهذه المعقدات فعالية جيدة ضد البكتيريا.

ABSTRACT

New metal complexes of the ligand 2- Amino-5-(2-acetyloxyphenyl)-1,3,4-thiadiazole with the metal ion Cr(III), Fe(III), Au(III), Co(II) and Cu(II) were prepared in alcoholic water medium.

The prepared complexes were characterized by FTIR Spectroscopy, electronic spectroscopy, elemental analysis, conductivity and magnetic susceptibility measurement. Molar ratio and continuous variation studies in solution gave comparable result with those obtained from solid state study. From the spectral measurement, monomer structures for the complexes were proposed. The newly metal complexes were subjected to *in vitro* testing against pathogenic microorganisms. The results obtained revealed that these complexes showed measurable activity against bacteria.

INTRODUCTION

An important and versatile class of well established biologically active compound are those containing the –N-C=S moiety(1-3). This group is included in many basic structures of drugs either to be a part of an open chain,e.g.thiocarbamates,isothiocyanates and thiosemicarb - azides, or involved in heterocyclic ring, e. g. mercapto derivatives of thiodiazoles, triazoles and oxadiazole.

In particular, the 1,3,4-thiadiazole derivatives showed these activities(4-9). Metal complexes of 1,3,4-thiadiazole also have been used as antifungal(10), and other applications.

These complexes are suggested as a possible measure of drugs, since the action of many drugs is based on the ability of complex compound of metal ions to traverse biomembranes, whereas individual aqua-ions and ligands almost or completely lack this ability.

A case in point is antibiotics whose activity increase drastically in the presence of metal ions(11). Metal chelats differ in their mode of action and activity in biological system in accord with their structural

considerations, e.g., inert, highly stable metal chelats have a considerable activity against microorganisms, fungi and viruses and are used in controlling the speed of neoplastic tissue.
Later, it was found that certain copper and gold complexes appear to have antitumer activity(12).

MATERIALS AND METHODS

All chemical used were of reagent grade (supplied by either Merk or Fluka) and used as supplied. The FTIR spectra in the range (4000-200) cm^{-1} were recorded as CsI disc on ***FTIR 8300 Shimadzu*** Spectrophotometer. The electronic spectra of the complexes were obtained using ***Shimadzu Uv-Vis-160A*** Ultra-violet spectrophotometer at room temperature in the range (200-1000) nm. Magnetic susceptibility measurements for complexes were obtained at room temperature using (Magnetic Susceptibility Balance) ***Jhonson Mattey catalytic system division. Gallencamp M.F.B600.01F*** melting point apparatus were used to measure the melting point of all the prepared compounds. Conductivity measurement by using ***Coring Conductivity Meter 220***. Elemental microanalysis was carried out using elemental C, H, N and S analysis were carried out on ***afison EA 1108*** analyzer instruments (Malaysia).

The metal content of the complexes was measured using atomic absorption technique by ***Pye Unicam of Philips scientific*** instrument which employed the Hallow cathode lamp of Pye Unicam Ltd. Cambridge.

Synthesis of the ligand: 2-Amino-5-(2-acetyloxypheyl)-1, 3, 4-thiadiazole (L):

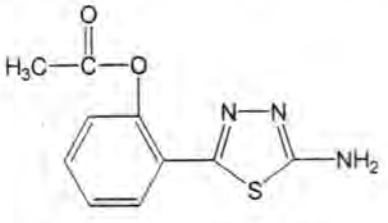

A mixture of 2-acetyl salicylic acid (0.01 mol), thiosemicarbazide (0.01mol), and phosphorus oxy chloride (5 ml). The mixture was refluxed for five hours. After cooling, water was added (25 ml).The mixture was refluxed for four hours and filtered. The solution was neutralized with potassium hydroxide. The precipitate was filtered and washed with distilled water and recrystallized from ethanol to give the ligand.

Preparation of complexes:

Ethanolic solution of (1 mmol) of the metal salts $CrCl_3.6H_2O$, $FeCl_3.9H_2O$, $HAuCl_3.H_2O$, $CoCl_2.6H_2O$ and $CuCl_2.2H_2O$ were added to (2 mmol) of (L) dissolve in ethanol. The mixture was stirred at room temperature for one hour. Fine precipitate was formed in all cases which was filtered on sintered glass crucible and recrystallized using ethanol/water mixture, then dried under vacuum at about 50°C.

RESULTS AND DISCUSSION

(A)Elemental analysis

The physical analytical data of (L) and its complexes are given in Table (1), in a satisfactory agreement with the calculated values. The suggested molecular which are
formulas also supported by subsequence spectral and molar ratio, as well as magnetic susceptibility.

Table -1: Physical data for L and its complexes

Symbol	Melting point, °C	Color	M% Found	M% Calc.	Elemental analysis Found (Calc.)%				Suggested Formula
					C	H	N	S	
L	208	White	-	-	50.90 (51.04)	3..35 (3.85)	17.00 (17.87)	13.81 (13.61)	$C_{10}H_9N_3SO_2$
CuL	(123)d	Blue	9.98	10.21	38.77 (38.56)	2.90 (2.89)	13.55 (13.49)	10.55 (10.28)	$[Cu(L)_2]Cl_2.H2O$
AuL	155	White	24.01	24.33	29.33 (29.65)	2.09 (2.22)	10.22 (10.38)	8.04 (7.91)	$[Au(L)_2]Cl_3.2H_2O$
CoL	(98-100)	Blue	11.22	10.59	39.00 (38.84)	2.88 (2.91)	13.70 (13.59)	10.22 (10.36)	$[Co(L)_2]Cl_2.H_2O$
CrL	(230)d	Deep Green	7.88	8.04	37.05 (37.13)	2.66 (2.78)	12.88 (12.99)	10.09 (9.90)	$[Cr(L)_2Cl_2]Cl.H_2O$
FeL	(>250)d	Brown	8.00	8.59	36.55 (36.91)	2.80 (2.77)	13.00 (12.91)	9.88 (9.84)	$[Fe(L)_2Cl_2]Cl.H_2O$

(B)-Electronic and Infrared Spectra

The bands are classified into the intermolecular transitions appear in the uv region, and d-d transitions appear in the visible region. These transitions are assigned in relevant to the structures of complexes. Table (2), show the position of electronic absorption band and its transitions, and also include the calculated value of Racah parameter (B), 10*D*q and nephelauxetic factor (β) for CoL, CrL and FeL.

The complex of CuL shows a broad band(13) at 15,780 cm^{-1} which can be assigned to $^2B_1g \rightarrow {}^2B_2g$ and $^2B_1g \rightarrow {}^2Eg$ transitions.

For AuL complex the charge transfer bands appear at longer wavelength, in the same time ligand field transition are expected to appear at shorter wave length. This result in an over lap between the two absorption bands, which make the interpretation of the spectra more difficalt (14,15). Only one band has been observed at 27,030cm^{-1}, which can be assigned to the transition $^1A_1g \rightarrow {}^1B_1g$ in the square planar geometry.

The CoL complex spectrum in DMF shows three bands.

The first two bands at 16,611 and 14,880 cm^{-1} were assigned to the transition $^4A_2 \rightarrow {}^4T_1{}^{(P)}$ (ν_3), since this transition is known to be a triplet in the range (14,000-17,500) cm^{-1} in divalent cobalt of tetrahedral geometry. This splitting is due to spin orbital coupling(16). Therefore ν_3 have been calculated as the average of these two bands.

The third band which appear as a weak band at 9,346 cm^{-1} was assigned to the transition of $^4A_2 \rightarrow {}^4T_1{}^{(F)}$ (ν_2), while ν_1 could not be observed since it is expected to appear in the range out of the instrument scale so it was calculated using Tanabe-sugano diagram for d^7 system(17) and found to be 6,265 cm^{-1}which belong to the transition $^4A_2 \rightarrow {}^4T_2{}^{(F)}$. The different ligand field parameters have been calculated using the same diagram, the results are found in Table (2). Comparison of the results obtained in this work with the literature data suggests high spin tetrahedral geometry around Cobalt (II) ion(18-20).

The relatively high value of 10Dq and the low value of nephelauxetic factor (β) indicate the covalent character between the Co (II) ion and the ligand.

The CrL complex spectrum in DMF shows three bands, the first two bands at 16,420 and 22,883 cm^{-1} were assigned as belonging to transitions $^4A_2g \rightarrow {}^4T_2g^{(F)}$ (ν_1 which is equal to $10Dq$) and $^4A_2g \rightarrow {}^4T_1g^{(F)}$ (ν_2)(17).

The third band could not be observed since it was expected to appear in the ligand or charge transfer absorption region, so it was calculated using the Tanabe-Sugano diagram(18) and was found to be at 35,568 $cm^{-1}$and assigned to the transition $^4A_2g \rightarrow {}^4T_1g^{(P)}$ (ν_3)(18).

The uv-vis spectrum of the FeL complex showed two transitions, the first transition at 28,517 cm^{-1} which assigned to $^6A_1g \rightarrow {}^4T_2g$ and the second at 20,000 cm^{-1} belong to $^6A_1g \rightarrow {}^4T_1g$ both as a shoulders. This complex and came in accordance to other available data so an octahedral geometry was suggested to the FeL complex (21). The value of the measured magnetic moment in accordance with the presumption of high-spin d^5 ferric ion in octahedral geometry(17).

From Tanabe-Sugano diagram for d^5 octahedral field(17) , the value of 10*D*q equal to 25,800cm^{-1} and the high value of nephelauxetic factor (β) (0.99) indicated the ionic character between iron (III) ion and the ligand.
The infrared data are shown in table (3).The Table lists the stretching frequency (ν) for some of the characteristic groups exhibited by the ligand and complexes.
The formations of these complexes were confirmed by monitoring the changes both in location and intensity of the certain bands.
In the free ligand, the band at 1614 cm^{-1} is assigned to the stretching of C=N (22). On complexation, this band is shifted to a lower frequency region. This shift is probably due to the lowering of bond order of the carbon-nitrogen bond resulted from complexation of the metal to the ligand through nitrogen. The frequencies for the ν (N-H) asm. and ν(N-H) sym. in the complex was not seen because it was covered by a broad band appear in the range (3400-3550) cm^{-1} assigned to –OH stretching of outer sphere water molecules.
Stretching of metal-nitrogen and metal-chloride bonds of the complexes appeared in low frequency regions (23), Table (3).
The molar ratio method and continues variation were followed to detect the ratio of metal ion to ligand of complex (24). Ethanol was used as a solvent. The M: L ratio was found 1:2 to all complexes. The values of magnetic moment and conductivity measurements in table (4) supported the suggested structures.

Table-2:Electronic spectra for L and its complexes in DMF solvent(cm^{-1})

Symbol	Absorption band (cm^{-1})	Transition	B	Dq/$\bar{B}$	$\bar{B}$	β	10Dq	15$\bar{B}$
L	35,715 37,735	$\pi \rightarrow \pi^*$ $n \rightarrow \pi^*$						
CuL	15,780	$^2B_1g \rightarrow {}^2B_2g$ $^2B_1g \rightarrow {}^2Eg$						
AuL	27,030	$^1A_1g \rightarrow {}^1B_1g$						
CoL	6,265 9,346 15,664	$(\upsilon_1)\ ^4A_2 \rightarrow {}^4T_2{}^{(F)}$ $(\upsilon_2)\ ^4A_2 \rightarrow {}^4T_1{}^{(F)}$ $(\upsilon_3)\ ^4A_2 \rightarrow {}^4T_1{}^{(P)}$	1,135	1.2	522	0.46	6,265	16,920
CrL	16,420 22,883 35,568	$(\upsilon_1)\ ^4A_2g \rightarrow {}^4T_2g^{(F)}$ $(\upsilon_2)\ ^4A_2g \rightarrow {}^4T_1g^{(F)}\ (\upsilon_3)$ $^4A_2g \rightarrow {}^4T_1g^{(P)}$	1,030	2.4	684	0.66	16,420	15,450
FeL	20,000 28,517	$^6A_1g \rightarrow {}^4T_1g$ $^6A_1g \rightarrow {}^4T_2g$	1300	2.0	1,290	0.99	25,800	19,350

Table -3:The absorption band in infrared spectrum for L and its complexes

Symbol	ν(C=N)	ν(N-H)asm	ν(N-H)sym	ν(O-H)	ν(M-N)	ν(M-Cl)
L	1614	3402	3288	-	-	-
CuL	1608	-	-	3300	483	-
AuL	1605	-	-	3313	480	-
CoL	1607	-	-	3374	480	-
CrL	1606	-	-	3390	480	395
FeL	1606	-	-	3380	483	399

Table -4:Magnetic moment, Conductivity and suggested structures for complexes

Complex	Magnetic moment μeff(B.M.)	Conductivity $\mu s.cm^{-1}$	Suggested structure
CuL	1.11	140	Square planar
AuL	0.99	155	Square planar
CoL	4.35	134	Tetrahedral
CrL	3.80	145	Octahedral
FeL	5.90	156	Octahedral

Antibacterial activity

With a view to explore the possibility of obtaining biologically useful compounds that contain 1,3,4-thiadiazole ring system (25-27), such biological activity prompt us to prepare some new series containing the above mentioned unite. The antimicrobial activity of these compounds was determined by the agar diffusion method [28] used were *Staphylococcus aureus* , *Escherishia coli* , *Pseudomonas aeroginosa and Candida albicans* .

In this method a slandered (5mm) diameter sterilized filter paper disc impregnated with the compound (1mg per 1 ml of acetone) was placed on an agar plate seeded with the test organism. The plate were incubated for 24 hours at 37 ˚C .

The zone of inhibition formed was measured in mm and are represented by (+), (++), (+++) depending upon the diameter and clarity, Table (5).

Table -5: Antibacterial activity for ligand and complexes at (conc. 1mg/ml)

Symbol	*Staphylococcus aureus*	*Escherishia coli*	*Pseudomonas aeroginosa*	*Candida albicans*
L	+	+++	-	-
CuL	+	+++	+	++
AuL	+	+++	++	+
CoL	++	++	++	++
CrL	+	+++	+++	+
FeL	++	+++	++	+

Note:
(-) = No Inhibition, (+) = Inhibition zone (6-8) mm, (++) = Inhibition zone (8-10) mm and
(+++) = Inhibition zone >10mm

On the basis of the preceding discussion, the structure of the complexes may be suggested as follow:

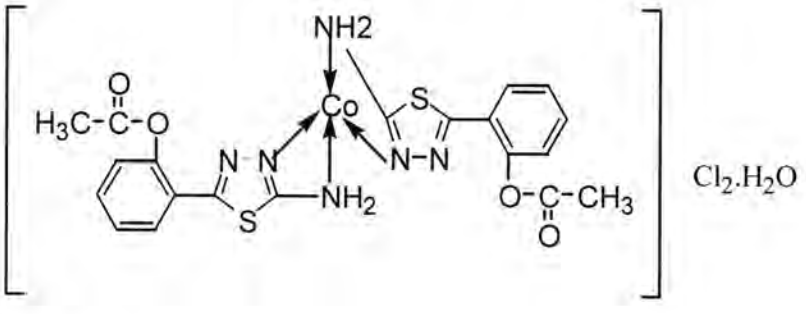

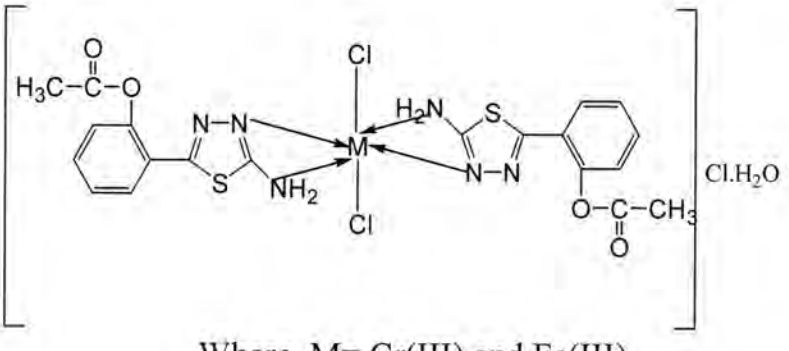

Where, M= Cr(III) and Fe(III)

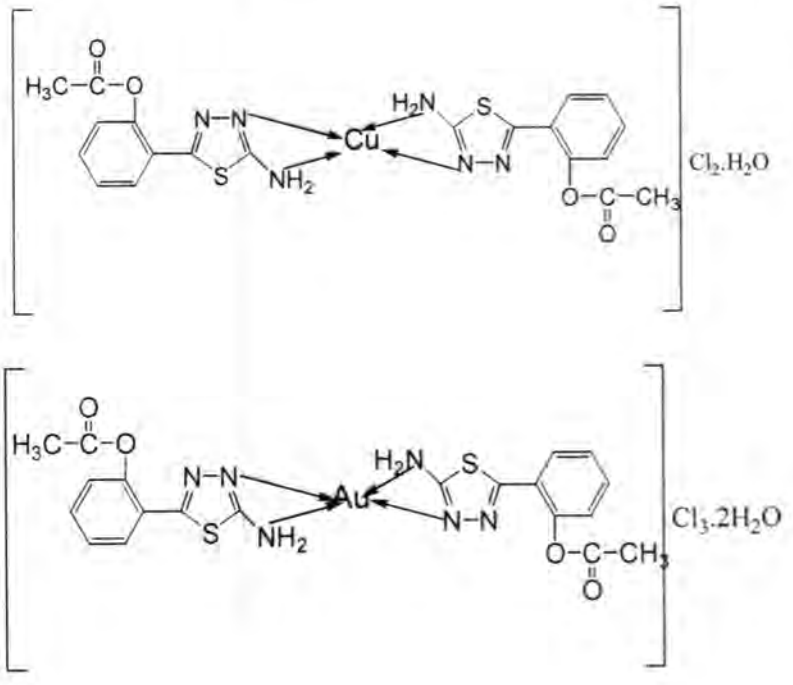

REFERENCES

1. F.Tellez, A.Pen˜a-Hueso, N.Barba-Behrens, R.Contreras & A. Flores-Parra" Coordination compounds in a pentacyclic aromatic system from 2-aminobenzothiazole derivatives and transition metals ions",***Polyh.*,25**:2363–2374 (2006).
2. S.Pinheiro,J.de Sousa, M. Santiago, I. Carvalho, A.Silva, A. Batista,E. Castellano,V.Ram,U.Singhab & P.Gurub ***Eur.J.Med.Chem*.25(6)**:533-538 (1990).
3. E. Marchesi, A. Marchi, L. Marvelli, M. Peruzzini, M. Brugnati and V. Bertolasi" Rhenium(III) and technetium(III) complexes with 2-mercapto-1,3-azole ligands and X-ray crystal structures", ***Inorg. Chem. Acta*. 358**: 352–362(2005).
4. N. Kahalil " N- and S-α-l-Arabinopyranosyl[1,2,4]triazolo[3,4-b][1,3,4] thiadiazoles ", ***Eur. J. Med. Chem.***, 2007,**42**,1193
5. Z. Li, X. Wang, & Y. da "Synthesis of 2-(5-(2-Chlorophenyl)-2-Furoylamido)-5-Aryloxymethyl-1,3,4-Thiadiazoles under Microwave Irradiation" , ***Synthetic Communications*, 31(12)**,1829(2001).
6. A. Gadad, M. Palkar, K. Anand, M. Noolvi, T. Boreddy and J. Wagwade, "Synthesis and biological evaluation of 2-trifluoromethyl /sulfonamido-5,6-diaryl substituted imidazo[2,1-*b*]-1,3,4-thiadiazoles: A novel class of cyclooxygenase-2 inhibitors", ***Bioorg. Med. Chem.*,16**, 276(2008).
7. C.Liao, Y. Wang, C. Huang, H. Shev, G. Lee and C. Lai, " Synthesis, crystal structures, mesomorphic and photo-luminescent properties of 1,3,4-

thia(oxa)diazole-based compounds with a terminal methoxy or methylthio group ", ***Tetrahedron*,63**, 12437, (2007).

8. R.C.Becker, C. M. Gibson, Lisa K. Jennings and david A. Morrow, "Antiplatlate Therapy in ACS : Applying New Science to Clinical Decisions", ***Farmaco*,60**,869-996,(2005).
9. R.Qiao,X.Hui and Z.Zhang, ***J. Biol. Chem.***, "Current Opinion in Clinical Nutrition and Metabolic Care ", **5**, 800, (2002).
10. W. Huang and G. Yang, "A General and Straightforward Method for the Synthesis of 2-Trifluoromethylbenzothiazoles ", ***Bioorg. Med. Chem.***, **14**, 8280., (2006).
11. A. H. Jassim, ***Ph.D. Thesis***, " Synthesis and study of transition metal Complexes of chelating hetrocyclic towards the design of Biologically active compounds", Al-Nahrain University, (1993).
12. P. Calamai ,S. Carottil, A. Guerri, T. Mazzeil, L. Messori, E. Minil, P. Orioli, and Gp.Speroni,"Structural characterization and cytostatic activity of chlorobis-cholylglycinatogold(III) ", ***Anti-Cancer Druug Design*, 13, (**1998).
13. Ahmed S. Majeed, ***M.Sc. Thesis***, "Synthesis and Characterization of Transition Metal Complexes of Mercapto Allyl Triazole Derivatives "Al-Nahrain University , Iraq (2000).
14. B.N.Figgis "***Ligand field theory and its applications***" Verlag GmbH, (2000)
15. C.K. Jorgensen " Optical spectra and chemical bonding in inorganic compounds ", sipringer, (2004).
16. N. K. Dutt & N. C. Chakder, "Complexes of cobalt(II) with some thiocarbazide derivatives ", J. Inorg. Nucl. Chem.,33, 393(1971).
17. N.N.Green Wood and A. Earnshow " Chemistry of the elements",2nd Ed, Elsevier Science Ltd., (2002).
18. D.K.Pastogi, K. C. Sharma S. K. Dua and M. P. Teotia, " Electronic spectral data vis-a-vis nephelauxetic effect-calculation and accuracy of the interelectronic repulsion parameter in some vanadium(II), chromium(III), cobalt(II) and nickel(II) complexes of amino ligands—V ", ***J.Inorg. Nucl. Chem.*, 37**, 685-693. ,(1975).
19. F. A. Cotton, D. M. L. Goodgame, "Spectrochemical and magnetic studies of cobalt(II) complexes of 1-substituted tetrazoline-5-thiones ", ***J. Am. Chem. Soc.***, 83, 4690, (1961).
20. R. L. Carlin ***Transition metal chemistry***, New Yourk (1965).
21. A. M. Fatta and R. L. Lintvedt, "Ligand field, electronic and solvent effects in the non-aqueous electrochemistry of tris(β-dionato) chromium(III) chelates", ***Inorg. Chem.***, **11**, (1972).
22. R.M.Silver Stein,G.C.Bassler and T.G.Morrill,"***Spectrometric Identification of organic Comopunde***",7thEd.,John-Wiely and Sons,Inc.,New York, London,(2005).
23. K.Nakamoto,"***Infrared of Inorganic and Coordination Compounda***",6th Ed. ,John-Wiely,Inc.,New Yourk,London,(1997)

24. D.Skoog,D.West and F.Holler,"***Fandamental of Analytical Chemistry***",8th Ed, Saunders College,New york(2004)
25. H. Dogan, A. Duran, S. rollas, G. Sener, M. Uysal and D. Gules, " Parallel Synthesis of Drug-like 5-Amino-Substituted 1,2,4-Thiadiazole,Libraries Using Cyclization Reactions of a Carboxamidine Dithiocarb –amate Linker ", ***Bioorg. Med. Chem.*** **10**, 2893, (2002).
26. J.Matysiiak, "Synthesis, pharmacological screening, quantum chemical and *in vitro* permeability studies of *N*-Mannich bases of benzimidazoles through bovine cornea", ***Eur. J. Med. Chem.***,**42**, 940(2007).
27. U.Goksen,N.Keleka,O.Gokas,Y.Koysal,E.Kilic,S.Esik,G.Aktay & Meral Ozalp" Synthesis and characterization of new pyrimidine-based 1,3,4-oxa(thia)diazoles, 1,2,4-triazoles and 4-thiazolidinones",***Bioorg. Med. Chem.*** **15**, 5738(2007).
28. M.Dutta and J.Kataky,"Bicyclic Compounds Derived from 4-Amino-3-Mercapto -1,2,4-Triazoles: Facile Routes To 1,2,4-Triazolo [3,4-b] [1,3,4] Thiadiazoles and 1,2,4-Triazolo[3,4-b][1,3,4]Thiadiazines",***J. Hetrocyclic Chem.*** ,**23**,1339(1996).

VO (IV), Mn (II), Fe (III) Co (II), Ni (II), Cu (II) and Zn(II) Complexes With Tetradentate Schiff Base[4-methyl-3,5-bis{(3-methyl-5- (4-phenyl-Thiosemicarbazonlidin) Pyrazoline-2yl)Pyrazoline

Rehab A.M. Al-Hasani
Al-Mustansirya University, College of Science, Department of Chemistry.

الخلاصة

تم في هذا البحث تحضير قاعدة شف جديدة:
[4-methyl-3,5-bis{(3-methyl-5- (4-phenyl-thiosemicarbazonlidine) pyrazoline-2yl)pyrazoline] [L] جرى تشخيص **(L)** بطرق تحليل طيف الاشعة تحت الحمراء (FT-IR) والتحليل الدقيق للعناصر (C.H.N) .استخدم **(L)** كليكاند في تحضير معقدات الايونات الفلزية الثنائية(II) (منغنيزوالكوبلت والنيكل والنحاس والخارصين) والثلاثية (III)(الحديد) والرباعية (الفناديوم) (IV).تم عزل المعقدات الجديدة وتشخيصها باستخدام طيف الاشعة تحت الحمراء وطيف الاشعة فوق البنفسجية-المرئية وتقنية (C.H.N) وتقنية الامتصاص الذري للعناصر اضافة الى قياسات الحساسية المغناطيسية والتوصيلية الكهربائية .وتم دراسة طبيعة المعقد المتكون في محلول الايثانول باتباع طريقة النسب المولية وقد اعطت هذه الدراسة نتائجا مطابقة مع تلك التي تم الحصول عليها في الحالة الصلبة،كما درست ثوابت الاستقرار للمعقدات المتكونة مع الزمن وكانت مدة ثبات اللون اكثر من (4)ساعات، فضلا عن ذلك تم حساب قيمة الممتصية المولارية للمعقدات. تمّ تقويم الفعالية المضادة للبكتريا لليكاند **(L)** ومعقداته وأختير نوعان من البكتريا (*Pseudonomous aerugionosa*) سالبة الصبغة و (*Bacillus Subtilis*) موجبة الصبغة لهذا الغرض ودراسة أقل تركيز يحدث عنده التثبيط (MIC) ومن ثم تمت مقارنة فعالية المركبات المحضرة مع المضاد الحيوي (Ampicillin) .
كما تم اجراء التقويم الحيوي لليكاند **(L)** ومعقداته ضد نوعين من الفطريات (*Penicillum Spp.* و *Aspergillus flavus*) وقد أظهرت نتائج التقويم زيادة كبيرة في فعالية المعقدات المحضرة منها.تم تفسير الفعالية المضادة للبكتريا و الفطريات إلى التأثير المتداوب للفعالية بين الفلز و الليكاند فضلاً عن الإختلاف في تراكيب المركبات المحضرة .

ABSTRACT

A new Schiff base [4-methyl-3,5-bis{(3-methyl-5- (4-phenyl-thiosemicarbazonlidine) pyrazoline-2yl)pyrazoline] **[L],** have been prepared and characterized by (FT-IR) Spectroscopy and elemental analysis (C.H.N) .(**L**) has been used as a chelating ligand to prepare some complexes of (V(IV) , Mn(II), Fe(III) ,Co(II), Ni(II), Cu(II), and Zn(II) ions .The prepared complexes were identified and their geometrical were suggested in solid state by using (FT-IR) and (UV-Vis) spectroscopy ,elemental analysis(C.H.N), Flame atomic absorption technique, in addition to magnetic susceptibility and conductivity measurements .The study of the nature of the complexes formed in ethanol following the mole ratio method, gave result which were compared successfully with those obtained from solid state studies . The apparent stability constant of the complexes have been studied with the time and their color were stable for more than (4hours), as well as the molar absorptivities have been calculated.

The antibacterial activity for free ligand **(L)** and their metal complexes were studied against two selected micro - organisms *[(Pseudonomous aerugionosa) as gram negative]* and*[(Bacillus Subtilis) as gram positive]*. The minimal inhibitory concentrations (MIC) have been also studied to determine the low concentration for inhibition. The antibiotic (Ampicillin) has been chosen to compare their activity with those of the new compounds. Further more the antifungal activity against two micro-organism *(Penicillum Spp.)* and *(Aspergillus flavus)* were studied for all compounds. The results showed great enhancement of activity of the complexes relative to that of their respective free ligand **(L)**. This was attributed top the synergetic effect between the metal ion and the ligand, in addition to the differences in the structural varieties.

INTRODUCTION

Schiff bases are an important class of ligands in coordination chemistry and find extensive application in different fields(1-3). Some of these bases exhibited antimicrobial and anticancer activities(4-6). The biological activities were attributed mainly to azomethine group(4). Some complexes of Schiff bases were found more active than the parent ligands against bacteria and fungi(6-8) and as herbicides(7). Complexes containing more than one metal center represent synthetic models of ferromagnetic interaction between metal centers which can explain oxidation-reduction process in biological systems in addition to their catalytic and biological activities(9,10).The coordination compounds quadridentate Schiff bases have been reported to act as inhibitors for enzymes(11,12) this gave us motives to synthesis new metal complexes of a new quadridentate Schiff base [4 – methyl - 3 ,5-bis{(3-methyl-5- (4-phenyl-thiosemicarbazonlidine) pyrazoline-2yl)pyrazoline] **[L]** to investigate the coordination behavior of the new ligand toward some metal ions, then compare the biological activities of ligand with their metal complexes .

MATERIALS AND METHODS

Physical measurements and analysis

Melting points were recorded on gallenkamp Melting point apparatus and were uncorrected. FT-IR spectra were recoded using FT-IR8300 Schimadzu in the range of (4000-200) cm^{-1}, samples were measured as (CsI disc).Electronic spectra were obtained using UV-1650PC Schimadzu Spectrophotometer at room temperature, the measurements were recorded using a concentration of (10^{-3})M of the complex in chloroform as a solvent. The metal content was estimated spectrophotometerically using atomic absorption Schimadzu AA670 Spectrophotometer. The elemental analyses (C.H.N.S) were obtained using EA-034.mth. Conductivity measurements were obtained using Corning conductivity meter 220, these measurements were obtained in DMF solvent using concentration of (10^{-3} M) at 25C°.Magnetic susceptibility measurements were obtained at 25C° on the solid state applying Faraday's method using Bruker BM6 instrument.

All chemicals were of highest purity and were used as received.

Preparation of the ligand {L}:-

(1)- Preparation [3,5-dihydrazide-4-methylpyrazoline] **[A] .**

A mixture of [3,5-dimercapto-4-methyl-pyrazoline] (0.01 mole,1.45gm) and hydrazine hydrate(0.02 mole,1.0gm)were refluxed for (7) hours . The precipitate which separated on cooling was filtered off, dried and recrystallized from ethanol, to give compound **(A)**.The physical data are given in Table (1).

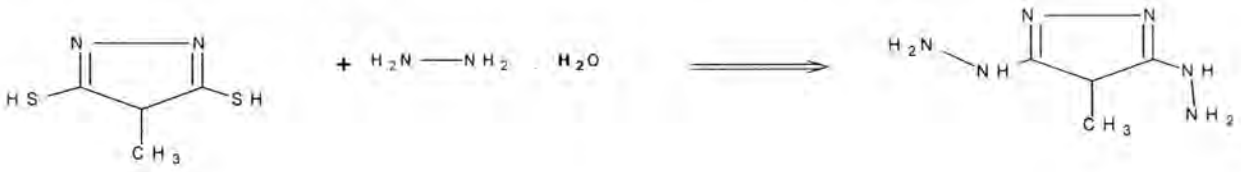

[A]

***(2)- Preparation [4-methyl-3,5-di(3-methyl-5-oxopyrazoline-2-yl pyrazoline]* [B] .**

To solution **(A)** (0.01 mole , 1.41gm) in ethanol was added ethyl acetyl acetone (0.02 mole, 5.2gm), the reaction mixture was refluxed for (6-7) hours . The volume was reduced and reaction mixture was kept at room temperature .The product so obtained was filtered off, dried and recrystallized from ethanol, the physical data are given in Table (1).

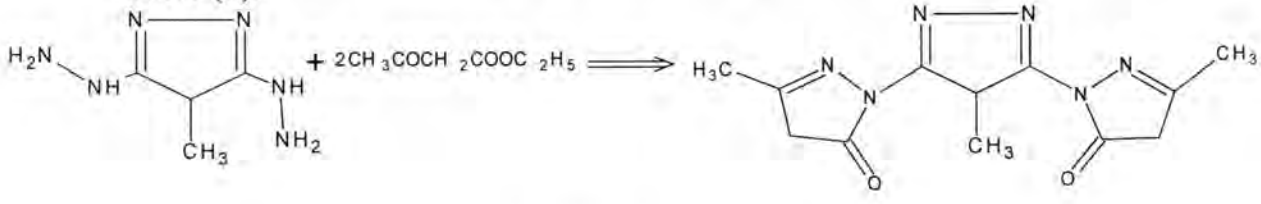

[B]

***(3)-Preparation[4-methyl-3,5-bis{(3-methyl-5-(4-phenyl-thiosemicar-bazonlidine) pyrazoline- 2yl)pyrazoline]* [L] .**

The Schiff base **[L]**was prepared by condensing the **[B]** (0.01 mole, 2.73gm) and (4-methyl thiosemicarbazide) (0.02 mole,6.68gm) in ethanol ,the reaction mixture was refluxed for (3) hours. On cooling the separated solid was filtered off, dried and recrystallized from ethanol, the physical data are given in Table (1).

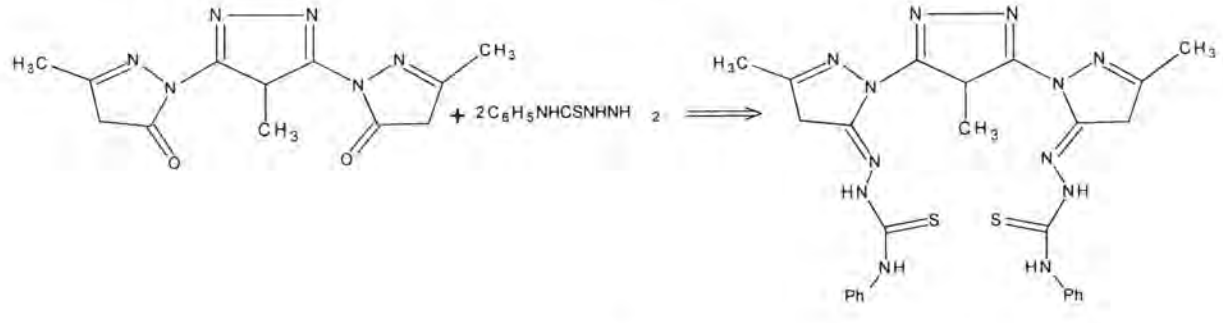

[L]

Preparation of Schiff base complexes:

Hot ethanolic solution of metal ion salts (0.01M) **[$VOSO_4.5H_2O$,$MnCl_2.4H_2O$,$FeCl_3.9H_2O$, $CoCl_2.6H_2O$, $NiCl_2.6H_2O$,$CuCl_2.2H_2O$ and $ZnCl_2.H_2O$]** (0.01M) of **[L]**, were mixed in stoichiometric ratio with continuous stirring and heated under reflux for one hour. The reaction mixture was then concentrated to half of its original volume when complexes precipitated. The complexes thus obtained were filtered and washed with hot water and finally washed well with hot ethanol. The complexes were dried under vacuum. The physical data of the prepared complexes are shown in Table (1).

Study of complex formation in solution:-

Complexes of **[L]** with metal ions were studied in solution using ethanol as a solvent, in order to determined [M: **L**] ratio in the complex following molar ratio method[13] . A series of solutions were prepared having a constant concentration [1×10^{-3}M] of the metal ion and **[L]**. The [M **/L**] ratio was determined from the relation ship between the absorption of the absorbed light and the mole ratio of [M: **L**].The results of complexes formation in solution were listed in Table(1).

Stability constant of Schiff base complexes:

The conditional (13,14) stability constant of the (1:1) [Metal: ligand] complex were evaluated as fallows:

Two sets of solutions were prepared, the first set of solution (As)were formulated to contain stoichiometric amount (1ml) of (10^{-3}M) ligand**[L]** to (1ml)of (10^{-3}M) of metal ion by placing in to a three series of (10ml) volumetric flasks. The solutions of the coloured complexes were diluted to the mark with ethanol. The second set (Am)were formulated to contain five fold excess (5ml) of (10^{-3}M) ligand**[L]**, by placing in to a three series of (10ml) volumetric flasks followed by addition of (1ml) of (10^{-3}M)of metal ion solution, the volumes were then completed to the mark with ethanol. The absorbance (As and Am) of the solutions were measured at (λ_{max}) of maximum absorption. The stability constant (k) and the molar absorptivity (ε_{max}) have been calculated.

Study of biological activities for [L] ligand and their metal complexes:-

The ***in vitro*** biological screening effects of the investigated compounds were tested against selected types of bacteria which include ***(Pseudonomous aerugionosa)*** as gram negative **and** ***(Bacillus Subtilis)*** as gram positive and the fungus, ***(Penicillum Spp.)*** and ***(Aspergillus flavus)*** by the well diffusion method using Nutrient agar as method(15). Stock solutions (10^{-3}M) were prepared by dissolving the compounds in DMSO solution. In a typical procedure, a well was made on the agar medium inoculated with microorganisms. The well was filled with the

test solution using a micropipette and the plat was incubated at 30 C° for 72 hours. During this period, the test solution diffused and the growth of the inoculated microorganisms was affected. The second technique was to get the sensitivity of each microorganism toward the new compounds by determining the minimal inhibitory concentration (MIC) which was a achieved by using Tube Dilution Method (16). The (MIC) of the new compounds for each micro-organism was measured at the lowest concentration of the compound required to inhibit the growth of this micro-organism, these tubes containing different concentrations of the new compounds were incubated at 37 °C for 45 hours and the antibiotic **(Ampicillin)** has been chosen to compare their activity with those of the new compounds.

RESULTS AND DISCUSSION

Part (I):- Synthesis and characterization of the isolated Schiff base derivatives and its metal complexes

(A)Elemental analysis:

The interaction of Schiff base **[L]** with appropriate metal salt under study in ethanol gave crystalline products with different colors depending on the metal ion. All complexes were readily soluble in chloroform, dimethylformamide and dimethylsulfoxide and were found to be stable toward air and moisture, as well as they were decomposed before melting. The physical and analytical data of [A], [B] and free ligand **[L]** and their metal complexes are given in Table (1).Results obtained from elemental analyses (C.H.N.S) and flam atomic absorption are in a satisfactory agreement with the calculated values .The suggested molecular formulas also supported by spectra(FT-IR) and (UV-Vis.) analyses , furthermore magnetic susceptibility and conductivity measurements.

Table -1: Physical data for [A], [B] and free ligand [L] and it's metal complexes

Comp. No.	*Color*	*Melting point*	*Yield %*	*Metal analyses found (calc.)*					*Suggested formula for isolated precipitate*
				C%	*H%*	*N%*	*S%*	*M%*	
[A]	Bright Yellow	143-146	88	34.22 (34.04)	6.92 (6.38)	59.46 (59.57)	-	-	$C_4 H_9N_6$
[B]	White	170-173	95	51.92 (52.74)	5.03 (4.76)	31.47 (30.77)	-	-	$C_{12} H_{13}N_6 O_2$
[L]	Pale Yellow	198-201	80	54.55 (54.64)	4.66 (4.73)	29.39 (29.42)	11.69 (11.21)	-	$C_{26}H_{27}N_{12} S_2$
VOL	Greeni sh blue	233	75	42.09 (42.51)	3.76 (3.68)	23.04 (22.89)	12.93 (13.08)	6.88 (6.94)	[VO **L**] SO_4
MnL	Brown	219	80	43.86 (44.77)	2.93 (3.87)	24.19 (24.11)	10.01 (9.18)	7.67 (7.88)	[Mn **L**Cl_2]
FeL	Dark brown	245	83	41.05 (40.56)	3.34 (4.03)	20.97 (21.84)	8.27 (8.32)	8.11 (7.25)	[Fe **L**Cl_2] Cl.$2H_2O$
CoL	Deep blue	232	90	44.18 (44.51)	3.48 (3.85)	23.39 (23.97)	10.03 (9.13)	8.23 (8.40)	[Co **L**] Cl_2
NiL	Orange	258	65	42.78 (43.41)	4.13 (4.04)	22.89 (23.38)	7.97 (8.90)	9.12 (8.17)	[Ni **L**] Cl_2. H_2O
CuL	Brown	273	82	43.46 (44.22)	2.95 (3.83)	23.54 (23.81)	9.13 (9.07)	8.96 (9.00)	[Cu **L**Cl_2]
ZnL	Off-white	250	90	44.09 (44.11)	3.33 (3.82)	22.82 (23.75)	8.89 (9.05)	10.02 (9.25)	[Zn **L**] Cl_2

Infrared Spectroscopic Study:-

All the recorded spectra were in the solid state using CsI .As expected, FT-IR gave a good information about the complexation behavior of the ligand**[L]** with various metal ions. The characteristic frequencies of free ligand**[L]** and its metal complexes were readily assigned based on comparison with literature values(17 -22).

The FT-IR of [3,5-dihydrazide-4-methylpyrazoline] **(A)** was confirmed by the disappearance of (-SH) group in the region (2600-2550) cm^{-1} and the appearance of hydrazine group which showed three bands at the regions [3360,3420 and 3165]cm^{-1} ,these can be assigned to [υNH_2 andυNH] vibrations(18,19).

Compound**[4-methyl-3,5-di(3-methyl-5-oxopyrazoline-2-yl pyrazoline] (B)** was confirmed from the disappearance of the three bands of hydrazine group **(-$NHNH_2$)** of compound **(A)** and appearance of a new band at (1700) cm^{-1} due to (C=O) stretching(19) .

The infrared spectra of the Schiff base ligand **(L)** has the important absorption bands in the regions (3100,1630 and 1335) cm^{-1} assignable to [υNH,C=N and υC=S] respectively .The ligand (L) has no absorption band at (1700) cm^{-1} which indicates that free carbonyl groups are absent and so the ketimine structure is ruled out . In the all complexes the Schiff base **[L]** ligand behave as a tetradentate coordinating to the

[VO(IV) ,Mn(II), Fe(III) , Co(II)), Cu(II) and Zn(II)]ions throw the nitrogen of azomethine and sulfer of the thiocarbonyl groups therefore the bands due to[υC=N and υC=S] were shifted to lower frequencies side on complexation, table(2).The behavior of **[L]** was further indicated by the newly formed bands in the regions (480-464),(440-400) and (370-350) cm^{-1} which are tentatively assigned to (M-N, M-S and M-Cl) bands stretching frequencies respectively (21,22), table (2) . Abroad band at (3400) cm^{-1} was observed in the spectra of [FeL and NiL] complexes assigned as (υO-H) suggested the presence of a water molecule (21).

Table -2: Characteristic stretching vibrational frequencies (cm^{-1}) located in the FT-IR spectra of free ligand [L] and itś metal complexes

Comp. No.	*υC=N*	*υC=S*	*υ M-N*	*υ M-S*	*υ M-Cl*	*Others*
[L]	1630(ms)	1335 (s)	-	-	-	-
VOL	1596(m)	1325(m)	478(mw)	422(mw)	-	975(s) (υV=0), 1015, 1260 and 1470 (υSO_4) a free anion
MnL	1598(m)	1322(m)	469(mw)	400(mw)	368(w)	-
FeL	1594(m)	1320(m)	480(mw)	440(mw)	370(w)	υ(O-H) 3400(b)
CoL	1596 (m)	1325(m)	464(mw)	435(mw)	-	-
NiL	1598 (m)	1322(m)	472(mw)	428(mw)	-	υ(O-H) 3400(b)
CuL	1594(m)	1324(m)	476(mw)	438(mw)	350(w)	-
ZnL	1598(m)	1322(m)	464(mw)	428(mw)	-	-

Where :- (s=strong, m=medium, mw=medium week, w =week, b=broad)

Electronic absorption Spectra, Magnetic susceptibility and Conductivity measurement:

Table (3) gives the electronic spectra of the metal complexes were recorded for their solution in chloroform, in the range (200-1100) nm, and magnetic moments at room temperature as well as the molar conductance values of the complexes in (DMF).

The **(L)** ligand exhibit two bands around 34000 and 30000 cm^{-1}, these intense bands are due to $\pi \rightarrow \pi^*$ and $n \rightarrow \pi^*$ transitions respectively[20].

[VOL]:- The spectrum of vanadyl (IV) complex show two main absorption bands, table (3), which are assigned to the two transition $^2B_2 \rightarrow {}^2E$ and $^2B_2 \rightarrow {}^2B_1$ respectively in a square pyramidal geometry(23,24) . The magnetic moment (2.01B.M) is higher than spin value of the vanadium metal only, this result indicate a higher orbital contribution (25-27) . Conductivity measurement in (DMF) showed that the complex was ionic, Table (3).

[MnL] :- Electronic spectra of Mn(II) complex showed very weak absorption bands at (12658,18348 and 26505) cm^{-1} , which are assigned to the transitions :
$^6A_1g \rightarrow {}^4T_1g$ (G), $^6A_1g \rightarrow {}^4T_2g$ (G) and $^6A_1g \rightarrow {}^4A_1g + {}^4Eg$ (G) respectively (23,28) . The values of racah parameters (10Dq,B',Dq/ B',15B' and β) have been calculated to be (9350,850,1.09,11742 and 0.98) respectively(23) .Magnetic moment of the solid complex was (5.0 B.M) showed the complex to be paramagnetic and five unpaired electrons indicating a high spin octahedral configuration (27). The conductivity measurement showed that the complex was non ionic, table (3).

[FeL]:- This complex showed three bands related to octahedral iron complex (23,28). They were observed at (11695,18518 and 26315) cm^{-1} that refer to $^6A_1g \rightarrow {}^4T_1g$ (G), $^6A_1g \rightarrow {}^4T_2g$ (G) and $^6A_1g \rightarrow {}^4A_1g + {}^4Eg$ (G) respectively (23,29,30). The ligand field (10Dq,B',Dq/ B',15B' and β) came out to (10030,771,1.29,10327 and 0.43) respectively. The magnetic moment is (5.31 B.M.) indicated a high spin octahedral complex (25,26,31-33). Conductivity in (DMF) showed that the complex was ionic, table (3).

[CoL]:- The blue cobalt(II) complex gave a magnetic moment value of (4.53B.M), which indicates a high-spin type complex(25,26,31) . Electronic spectrum in chloroform solvent exhibited a splitted band in the range of (17452-14184)cm^{-1} (23,34-39). These bands can be assigned to the transition $^4A_2 \rightarrow {}^4T_1$ (P) (ν_3) .

A broad band was observed at 3244cm^{-1} in infrared spectrum can be assigned to the $^4A_2 \rightarrow {}^4T_2$ (F) (ν_1) , while the transition of (ν_2) expected in the range (5000-6000)cm^{-1} can not be measured(39).The various ligand field parameters(10Dq, B' and ν_2) have been calculated by refer to Tanaba-Sugano diagram for (d^7) configuration (35,38,39) , to be (3244, 720.8 and 5453) respectively, as well as the calculation of the spin-orbit coupling constant (λ') was calculated .The resulting value (λ' = -198.4) show the present complex to be distorted tetrahedral(23) . The nephelauxetic factor (β) was calculated and found to be (0.64) indicating high degree of covalence in bonding of ligand donor atoms with cobalt (II) ion(23,40) .The molar conductance showed that the complex was electrolyte, table(3) .

[NiL]:- The diamagnetic Ni(II) complex exhibit a medium intensity band at 16673cm^{-1} and a high intensity band at 28810 cm^{-1} corresponding to transitions from $^1A_{1g} \rightarrow {}^1A_{2g}$, ^1E_g and the high intensity of the latter band may be due to over lap of L → Ni(II) charge transfer band respectively in square planar disposition(23,34-37). Conductivity measurement in Table (3) showed that the complex was highly conducting therefore the **(Cl)** ion wasn't considered to be coordinated with metal ion and is located outside the coordination zone.

[CuL]:- The UV-Vis spectrum of Cu (II) complex in ($CHCl_3$) solution displays a broad band at 16130 cm^{-1} ,can be assigned to $^2E_g \rightarrow {}^2T_{2g}$, transition and the other to a charge transfer band in distorted octahedral geometry(23,40,41). This is further supported by the magnetic susceptibility value (1.74B.M), which agree well with distorted octahedral structure (31-33).Conductivity in (DMF) solution, table (3) showed that the complex was non ionic.

[ZnL]:- The prepared complex is colorless and diamagnetic which is expected for d^{10} ion, since the spectra of this complex show some shifting and change in the shape of the bands were compared with those of the free ligand (L). The UV-Vis. spectrum of Zn(II) complex in ($CHCl_3$) solution show some transition found in the region (200- 443 nm),can be assigned as intra ligand transition(34,35,40,42) ,table (3). Conductivity showed that the complex was to be electrolyte, table (3).

Table -3: Electronic spectra ($CHCl_3$), Magnetic moment (B.M) and Conductance in (DMF) for metal complexes

Comp. No.	*Bands cm^{-1}*	*Assignment*	*10Dq*	*Molar cond. $\mu s.\ Cm^{-1}$*	*$\mu eff.$ B.M*	*Suggested structure*
[VOL]	11224 23975	$^2B_2 \rightarrow {}^2E$ $^2B_2 \rightarrow {}^2A_1$	-	72.68	2.01	Square Pyramidal
[MnL]	12658 11688(cal) 18348 26505	$^6A_1g \rightarrow {}^4T_1g(G)$ $^6A_1g \rightarrow {}^4T_2g\ (G)$ $^6A_1g \rightarrow {}^4A_1g + {}^4Eg(G)$	9350	21.07	5.03	Octahedral
[FeL]	11695 18518 26315	$^6A_1g \rightarrow {}^4T_1g(G)$ $^6A_1g \rightarrow {}^4T_2g\ (G)$ $^6A_1g \rightarrow {}^4A_1g + {}^4Eg(G)$	10030	87	5.31	Octahedral
[CoL]	3244 5453 (cal) 15733(av.)	$^4A_2 \rightarrow {}^4T_2\ (F)$ $^4A_2 \rightarrow {}^4T_1\ (F)$ $^4A_2 \rightarrow {}^4T_1\ (P)$	3244	182.18	4.53	Tetrahedral
[NiL]	16673 28810	$^1A_1g \rightarrow {}^1A_2g$, ^1Eg L $\rightarrow$Ni(II) (C.T)	-	179.63	0.0	Square planar
[CuL]	16130 30894	$^2E_g \rightarrow {}^2T_{2g}$ L$\rightarrow$Cu(II) (C.T)	-	14.03	1.74	Octahedral
[ZnL]	29200 27854 20989	Internal ligand charge transfer (L $\rightarrow$Zn(II) or Zn(II) $\rightarrow$ L)	-	187.24	0.0	Tetrahedral

Part (II):- Spectrophotometer study of complex formation in organic solvent

(1)-Molar ratio method:

The compositions of the (**VOL , MnL, FeL, CoL, NiL and CuL**) complexes have been studied by the molar ratio method. The results of complexes in ethanol as a solvent, suggest that the metal to ligand ratio was (1:1) for all complexes, which were comparable to those obtained from solid state study, table (4).

(2)-Stability constant of the Schiff base complexes:

The apparent stability constant of the (1:1) [Metal: Ligand] complexes was estimated, table (4).

The average of three measurements of the absorption of solution containing a stoichiomtetric amount of ligand and metal ions **(As)**, while the **(Am)** equal the average of three measurements of the absorption of solution containing the same amount of metal and five fold excess of ligand of the solutions, were measured at λmax of maximum absorption, as well as the degree of dissociation **(α)** and molar absorptivity **(ε_{max})** for all complexes were calculated (13,14), Table (4). The results indicate that (**VOL ,MnL, FeL, and CuL**) complexes yielded rather high stability in contrast to the other values obtained with (**, CoL and NiL**) , this refer to their structural geometric, table(4). Furthermore the (ε_{max}) of all complexes is rather high, table (4). The developed colors become stable after one hour, up to four hours.

Table-4: Molar ratio, Stability constant and molar absorptivities of Schiff base complexes at room temperature

Complex	*M:L Ratio*	*As*	*Am*	*α*	*K L.mol^{-1}*	*ε_{max} L.mol.cm^{-1}*	*λ max nm*
[VOL]	1:1	0.369	0.458	0.194	$6.144*10^5$	4580	751
[MnL]	1:1	0.496	0.585	0.089	$7.64*10^5$	5853	445
[FeL]	1:1	0.458	0.497	0.039	$8.06*10^5$	4976	498
[CoL]	1:1	0.217	0.354	0.137	$2.58*10^5$	3541	575
[NiL]	1:1	0.377	0.439	0.135	$6.09*10^5$	4396	457
[CuL]	1:1	0.441	0.496	0.111	$7.23*10^5$	4960	521

(As)= The average of three measurements of the absorption of solution containing a stoichiomtetric amount of ligand and metal ions.
(Am) = The average of three measurements of the absorption of solution containing the same amount of metal and five fold excess of ligand of the solutions.

Suggested Stereo Chemistry Structure for Schiff base complexes:

According to the results obtained from elemental and spectral analyses as well as magnetic moment and conductivity measurements, the suggested structure of the above mentioned complexes can be illustrated as follow:-

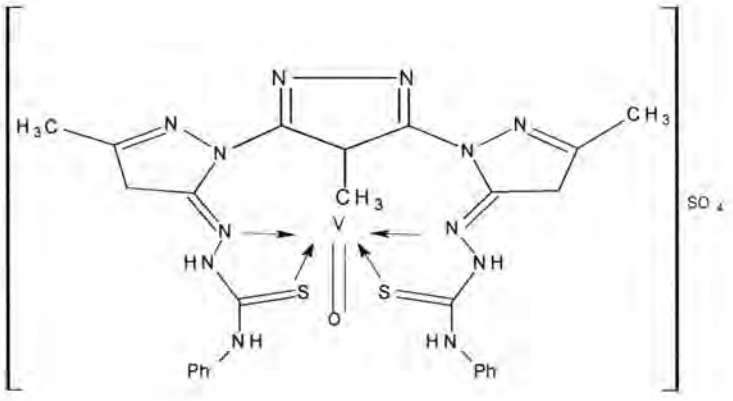
H3C
CH3
CH3
V
O
S
S
HN
NH
NH
HN
Ph
Ph
SO4

[VOL]

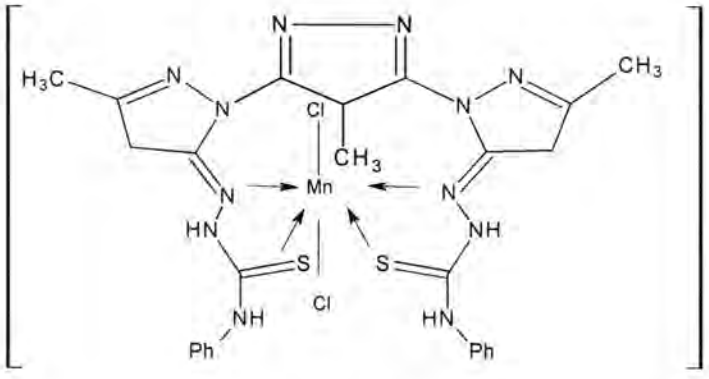
H3C
CH3
Cl
CH3
Mn
Cl
S
S
HN
NH
NH
HN
Ph
Ph

[MnL]

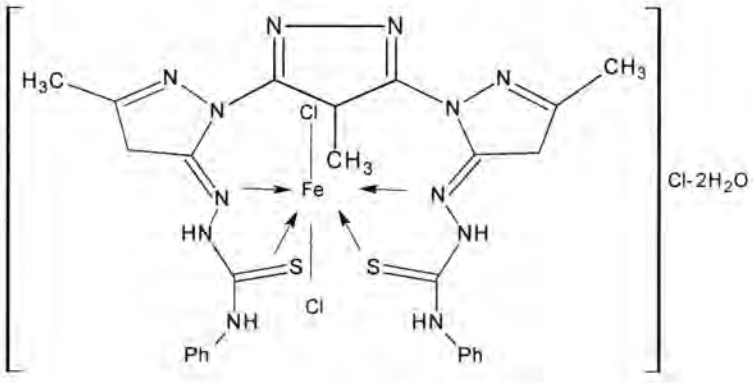
H3C
CH3
Cl
CH3
Fe
Cl
S
S
HN
NH
NH
HN
Ph
Ph
Cl-2H2O

[FeL]

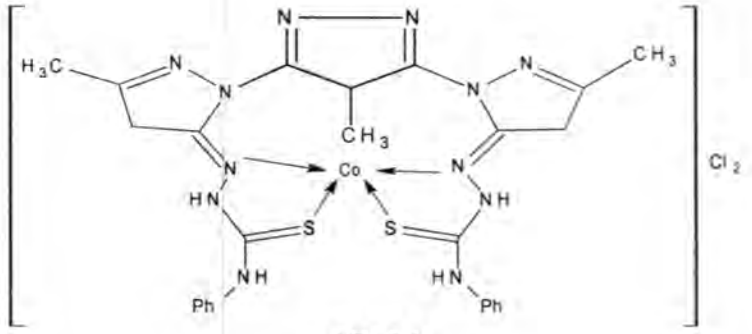

[CoL]

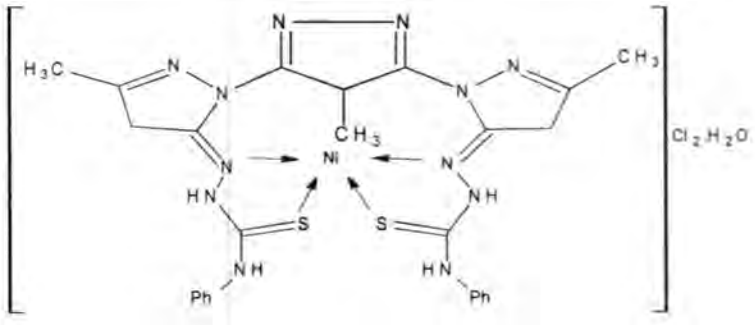

[NiL]

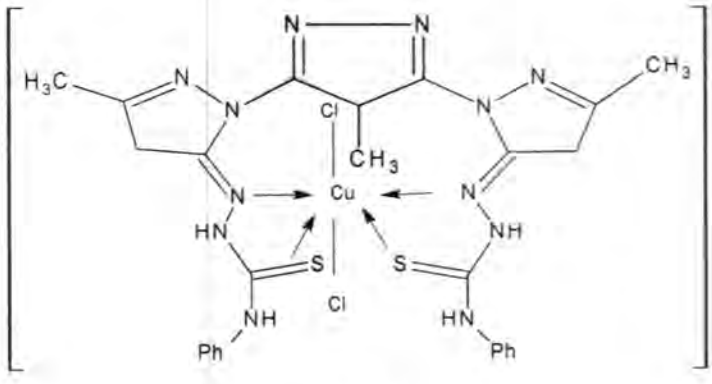

[CuL]

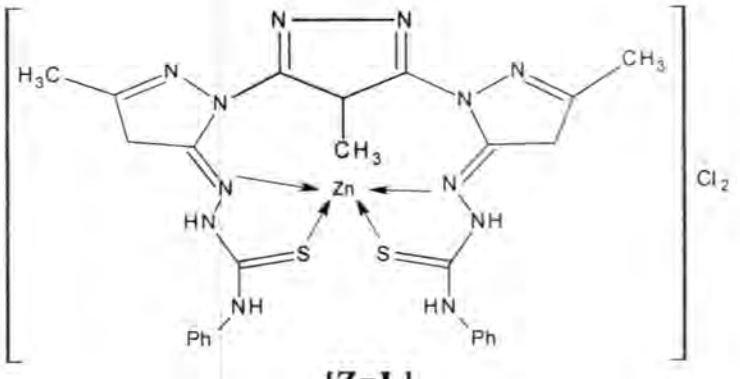

[ZnL]

Biological Studies:-

The new synthetic compounds were screened ***in vitro*** for their ability to inhibit the growth of representative [(***Pseudonomous aerugionosa***) as gram negative] and [(***Bacillus Subtilis***) as gram positive]. Also the study was done against ***(Candida albicans*** and ***Aspergillus flavus)*** fungus, in DMSO as a solvent at two different concentrations. The results showed that the **(A** and **B)** compounds are moderate activities against the studied bacteria and fungus as compared with their Schiff base ligand **[L]** against the same microorganisms and under the identical experimental conditions, Table(5),this difference attributed to effect of introducing the pharmacologically important Schiff base moiety in the structure of the prepared free ligand.

The complexes were found to be more toxic than the corresponding parent ligand **[L]** against all the types of the microorganisms Table(5), this was attributed to the synergetic effect(43) between the metal ion and the ligand. Furthermore the results of the **(MIC)** study for the **(A** and **B)** and**{L}** and their metal complexes are shown in table (6), these results indicate that some of the new compounds exhibited antibacterial activity against the studied bacteria at lower concentration, while they don't show such activity at higher concentration. As well as the all compounds were more active at lower concentration on comparison of these values with the antibiotic(44).

Table -5: Antibacterial and antifungal activities for (A), (B) and free ligand [L] and their Metal Complexes (mgm.ml^{-1})

Compo.	*Pseudonomous aerugionosa*		*Bacillus Subtilis*		*Penicillum Spp.*		*Aspergillus flavus*	
	100 ppm	**200 ppm**	**100 ppm**	**200 ppm**	**100 ppm**	**200 ppm**	**100 ppm**	**200 ppm**
Control (DMSO)	-	-	-	-	-	-	-	-
(A)	33	44	30	38	6	2	8	4
(B)	19	29	22	32	8	6	10	8
[L]	23	27	24	22	12	8	10	10
[VOL]	11	23	15	20	10	12	8	10
[MnL]	14	14	10	17	10	16	10	12
[FeL]	13	16	18	14	12	16	18	14
[CoL]	12	10	20	12	14	23	18	18
[NiL]	14	14	10	17	10	16	10	12
[CuL]	11	23	15	20	10	12	8	10
[ZnL]	25	12	10	13	12	18	8	16
Where :[6-8: (+),8-10: (++), >10: (+++)]					**30-40: (+++) , 20-30 :(++++) , 10-20: (+++++)**			

Table - 6:Minimal Inhibitory Concentration (MIC) for (A), (B) and free ligand [L] and their Metal Complexes(μgm. ml^{-1})

ompo.	*Pseudonomous aerugionosa*				*Bacillus Subtili*			
	0.05	**0.5**	**1.5**	**2**	**0.05**	**0.5**	**1.5**	**2**
(A)	+	+	MIC	-	+	+	+	MIC
(B)	+	+	MIC	-	+	+	MIC	-
[L]	+	MIC	-	-	+	+	MIC	-
[VOL]	MIC	-	-	-	+	MIC	-	-
[MnL]	+	MIC	-	-	MIC	-	-	-
[FeL]	MIC	-	-	-	MIC	-	-	-
[CoL]	MIC	-	-	-	MIC	-	-	-
[NiL]	+	+	MIC	-	+	MIC	-	-
[CuL]	MIC	-	-	-	MIC	-	-	-
[ZnL]	+	MIC	-	-	MIC	-	-	-
Ampicillin	+	+	MIC	-	+	+	+	MIC

REFERENCES

1. El-Sonbati A.Z., & El-Bindary A.A., "Stereochemistry of new Nitrogen containg Aldehydes.V.Novel synthesis & spectroscopic studies of some qunoline Schiff bases complexes", Polish J.Chem., 74, (2000).
2. Mitsunobu,N.L,and Akio,Y.E., "Crystal structure of 2,6-dihydroxy-4-methyl-pyrimidine copper(II)complexes",Anal.Sci., 21(6), (2005).
3. Peya,S.V.,Irena,K.O.,and Georgi,M.S., "Synthesis and in *vitro* screening of 2,6-dicarboxylic acids and its complexes with Samarium(III), Gadolinium(III) and Dysprosium(III) ions", J.Bio.Sci., 8(3), (2007).
4. Haghes,M.N, "The inorganic Chemistry of Biological Processes", 2nd Ed., (1988), John- Wiely and Sons ,Inc., New York, London.
5. Eichhorn, G.L., & Marzilli,L.G., "Advances in Inorganic Biochemistry, models in Inorganic Chemistry "PTR prentice – Hall, Inc, (1994).
6. Sahu K., Behera R. and Nayak A., "Synthesis and Fungitoxicity of complexes of the Schiff bases derived from 2- Hydroxyl – 1 – Naphthaldehyde and 2- amino thiazoles", Ind. J.Chem., 18 B, (1997).
7. Sinha A.I., Manjin B. and Scchnur I., "Metal Induced Hydroplysis of some Herbicidal Schiff bases and formation of mixed ligand complexes", Acta Sci. Ind.,14(1),(1988).
8. Mahapartra B.D. and Patanik R.C., "Fungicidal activities and mass spectral studies of some Schiff bases derived from p.Hydroxy benzaldehyde and their derivatives", J.Ind.Chem.Soc., LXI,(1984).

9. Zhang C.X. and Lippard S.J., "Current opinion in Chemical Biology", 7, (2003).
10. Dayagi S. and Degani Y., "The Chemistry of carbon – nitrogen double bond",S.Patai, John Wiley and Sons, Inter sciences, New York, (1970).
11. Cezar, S.and Angela , K., "Co (II), Ni (II) and Cu (II) complexes of Tetradentate Schiff bases", Acta Chim. Slov., 47(6),(2000).
12. 12) Saxena R.C., Jain C.L. and Sangal S.K., "Magnetic and spectral behaviour of Pd (II), Pt (IV) and Ru (III) complexes with some tetradentate substituted thiosemicarbazones",J.Ind.Chem.Soc.,LX III,(2008).
13. مؤيد قاسم العبايجي و ثابت الغبشة,(اسس الكيمياء التحليلية),مديرية جامعة الموصل,(1983)
14. Skooge, D.A. ,"Fundementals of analytical Chemistry", 5th Ed., New York ,London, (1988).
15. Collins C.H. and Lyne P.M., "Micribiological Methods", 3rd Ed. , Butter Worth and Co.Ltd. , (1970).
16. Atlas M.R., Alfres E.A and Lawrence C.N., "Laboratory Manual Experimental Microbiology",2nd Ed.,p.824,Mosby-Year book,Inc., (1995).
17. Kovaeic J.E., "The C=N stretching frequency in the infrared spectra of Schiff base complexes-Copper complexes of salicylidene anilines", Spectrochimica Acta, 23A, (1967) .
18. Parikh, V.M., "Absorption, Spectroscopy of organic Molecules" , Addison - Wesely Publishing Co- Inc. , (1974).
19. Shrma ,Y.R. , "Elementary Organic Absorption Spectroscopy", 1st Ed., S.Chand , New Delhi, (1980).
20. Silverstain,R.M.,Bassler, G.C., and Morrill, T.G., "Spectrometric Identification of Organic compound", 4th Ed., John-Wiely and Sons, Inc., New York, London , (1980).
21. Nakamoto K. , "Infrared and Raman Spectra of Inorganic and Coordination Compounds", 5th Ed., John Wiely and Sons Inc., New York,(1997).
22. Al-Mukhtar, S.E., and Mustafa, I.A., "Inorganic and Coordination Chemistry",Arabic Version,(1998).
23. Figgis,B.N., "Introduction to ligand field", John- Wiely and Sons, Inc., New York, London, (1966).
24. Singh C.P., and Mishra, L.K., "Ox vanadium (IV) complexes with thiohydrazide derivatives", J.Ind. Chem. Soc., LVll, (1998).
25. Mabbas F.E. and Machin D.J., "Magnetic and Transition Metal Complexes", London,(1973).
26. Carlin, R.L., and Van, A.J., "Magnetic properties of transition metal compounds", New York, London, (1977).
27. Datta ,R.L., and Syamal, A.S. ,"Elements of Magneto Chemistry",2nd Ed., Press,New Delhi, (1993).

28. Aly,M.M.,"Synthesis and Stability of chelate rings in coordination compounds of Co(II), Mn(II),Fe(II) and pd(II) with Vicinal Oxime-imine ligands", Trans.Met. Chem., 15(6),(1990).
29. Lever, A.B.P., "Inorganic electronic Spectroscopy", 2nd Ed., Elsevier, New York, (1968).
30. Pui,A.K.,Teodor M.T.,& Apostu, O.B.,"Synthesis and Characterization of new Fe(III) Schiff bases complexes",Inorg.Chime.Acta.,25A, (2005).
31. Burger, K.,"Magneto Chemistry",2nd Ed., Ins. Publishers, Ltd, London(1956).
32. M.Alaudeen,M.Y., & Prabhakaran,C.P.,"Synthesis and characterizea -tion of iron (III) complexes of N-(2-thienylidene)-N-isonicotinoylh -ydrazine and N-(2-furylidene)-N-Salicyloylhydrazine"Ind.J. Chem. ,35A,(1996).
33. Kopel, P.T., and Biler,M.K., "Iron (III) salen and saloph Schiff bases bridged by dicarboxylic acid" , Inorg. Chem., 41(22) (2002).
34. Sutton, D., "Electronic spectra of transition metal complexes", Mc-Graw-Hill Publishing Company litd, (1968).
35. 35)Bailer,I.C.,H.J.Emeleus,H.J.,and Nypholm,R.H."Comprehensive inorganic chemistry",Pergamon press,(1973).
36. Fredrick,F.C.,and Johnson, K.E.,"Composition and electronic spectra of some dimethyl sulfoxide complexes of Cr(II),Mn(II),Fe(III), Co(II), Ni(II) and Cu(II)"J.Inorg. Nucl. Chem., 43(11), (1981).
37. 37) Antipas A. and Gouterman M. "Electronic states of Co(II),Ni (II) ,Rh(III) and Pd(II) complexes", J.Am.Chem.Soc., 105(8)(1983).
38. Greenwood, N.N., and Earnchaw, A.I., "Chemistry of the Elements" .2nd Ed., Pergaman Press, (1998).
39. Ballhausen I.C.,"Introduction to Ligand Field Theory",New York, Toronto – London,(1962).
40. Nawar, N.N, Kattab ,M.U.,and Kaddah, A.R., "Synthesis and spectral studies of Mn(II), Co(II), Cu(II),Zn(II) , Cd(II) and Hg(II) complexes of μ-oxo-μH-1- benzopyran –3- carbox-aldehyde hydrazone derivatives", Ind. J. Chem., 35A, (1996).
41. Al-Hasani,R.A.M.,"Preparation,Characterization & Biological activities of some metal complexes of [N [2-(4,5–diphenyl-3-thion-1,2,4- triazole) methyl] diphenyl amine] ", J.of Al-Nahrain Univ.,9(20), (2006).
42. Nicholis D.,"Complexes & First–Row Transition Elements" ,Translated by Dr.W.I.Azeez, (1984).
43. Hogg,S.,"Essential microbiology", 4th Ed., John- Wiely and Sons, New York , England, (2005).
44. Johnson C.W and joyner J.W., "Antibiotics Chemotherapy", 2st Ed., John Wiely and Sons Inc., New York. , (1993).

Spectrophotometric Determination of Chloramphenicol in Pharmaceutical Preparations via Oxidative Coupling Reaction with Pyrocatechol

Raghad Sinan and Mouayed Q. Al-Abachi
Department of Chemistry, College of Science, University of Baghdad, Al-Jadiria,

الخلاصة

اقترحت طريقة طيفية حساسة لتقدير الكلورامفينيكول في المستحضرات الصيدلانية. تعتمد الطريقة على تفاعل الازدواج التأكسدي العضوي لدواء الكلورامفينيكول المختزل (بوساطة مسحوق الخارصين وحامض الهيدروكلوريك) مع البايروكاتيكول بوجود كبريتات الحديديك، إذ يتكون ناتج أحمر ذائب في الماء أظهر أقصى امتصاصية عند طول موجي 500 نانومترا. تم دراسة و تثبيت ظروف التفاعل الفضلى. كان مدى الخطية لتقدير الكلورامفينيكول بين 1 – 22 مايكروغرام مل$^{-1}$ و بحد كشف 0.520 مايكروغرام مل$^{-1}$. طبقت الطريقة بنجاح في تقدير الكلورامفينيكول في المستحضرات الصيدلانية، و تم مقارنة نتائجها إحصائياً باستعمال اختباري t و F مع نتائج طريقة دستور الأدوية البريطاني، و وجد أنه لا يوجد فرق معنوي في دقة و مصداقية الطريقة المقترحة مع طريقة دستور الأدوية البريطاني عند مستوى ثقة 95%.

الكلمات المفتاح: كلورامفينيكول، التقدير الطيفي، بايروكاتيكول، المستحضرات الصيدلانية.

ABSTRACT

A sensitive spectrophotometric method was proposed for the determination of chloramphenicol (CAP) in pharmaceutical preparations. The method was based on oxidative coupling organic reaction of reduced CAP with pyrocatechol in the presence of ferric sulfate to form red water soluble product with maximum absorbance at 500 nm. The reaction conditions were studied and optimized. The linear range for the determination of CAP, and the detection limit were 1 – 22 μg ml^{-1} and 0.520 μg ml^{-1}, respectively. The proposed method has been applied successfully for the determination of CAP in pharmaceutical preparations. A statistical comparison of these results with those obtained by the British pharmacopoeia procedure using the Student t-test and variance ratio F-test shows a good agreement and indicates no significant difference in accuracy and precision at the 95% confidence.

Keywords: Chloramphenicol; Spectrophotometric; Pyrocatechol; Pharmaceutical preparations.

INTRODUCTION

Chloramphenicol (CAP) is acetamide, 2,2-dichloro-N-[2-hydroxy-1-(hydroxymethyl)-2-(4-nitrophenyl)ethyl]-, [R-(R*, R*)]-, $C_{11}H_{12}Cl_2N_2O_5$(1).

CAP was first isolated in 1947s from cultures of Streptomyces venezuelae(2-3). It was synthetized in 1949s, becoming the first completely synthetic antibiotic of importance to be produced commercially(2).

CAP is a potent, potentially toxic, which should be reserved for the treatment of life-threatening infections(4), particularly those caused by Haemophilus influenzae(5). It is used topically in the treatment of bacterial conjunctivitis of the eyes because of its wide antibacterial spectrum(4, 5) and its penetration of ocular tissues and the aqueous humor(2).

Various methods have been reported for determining this drug in pharmaceutical preparations,including titrimetric(6-8),potentiometric titration(9),polarographic(10),voltammetric(11),capillary zone electrophoresis amperometric (12) , flow injection-biamperometric(13),reverse phase-high performance liquid chrom -atographic(14,15),flow injection-chemiluminescence (16-18), flame atomic absorption spectrophotometric (9, 19), spectrophotometric (20, 21).

Many colorimetric methods for the determination of CAP in pharmaceutical preparations are described in Table (1).

Table–1: Colorimetric methods for determination chloramphenicol in pharmaceutical preparations

Reagents	Comments	Colored species	λmax., nm	Linear range, $\mu g\ ml^{-1}$	Ref.
$NaIO_3$, Metol and sulfanilamide of pH 3	$NaIO_3$ produced from oxidation of acidic hydrolysis product of CAP with $NaIO_4$ and masking the excess of $NaIO_4$ with sodium molybdate	Charge transfer complex	520	4 – 28	22
Ethyl acetoacetate and NaOH	Reduction of CAP with Zn / HCl followed by diazotization	Diazotization and coupling	345	2 – 18	23
8-Hydroxyquinoline and NaOH	Reduction of CAP with Zn / HCl followed by diazotization	Diazotization and coupling	487	0.8 – 11.2	24
Promethazine.HCl with $Ca(OCl)_2$ in CH_3COOH medium	Reduction of CAP with Zn / HCl	Oxidative coupling	600	0.4 – 10	25
N,N-Diethyl-p-phenylenediamine with $K_2Cr_2O_7$ in H_2SO_4 medium	Reduction of CAP with Zn / HCl	Oxidative coupling	530	0.4 – 20	26
Fluoranil and borate buffer of pH 9	Reaction with reagents at 45°C for 40 min and 50 min respectively after reduction of CAP with Zn / HCl followed by neutralization with Na_2CO_3	Charge transfer complex	350	0.2 – 14	27
Chloranil and borate buffer of pH 9			342	0.4 – 14	
3-Methyl-2-benzothiazolinone hydrazone with $(NH_4)_2SO_4$. $Fe_2(SO_4)_3.24H_2O$ in ethanol medium	Reaction with reagents after reduction of CAP with Zn / HCl	Oxidative coupling	570	1 – 10	28
N-(1-Naphthyl)ethylene-diamine dihydrochloride	Reduction of CAP with $SnCl_2$ / HCl followed by diazotization and coupling with Bratton-Marshall reagent in a micellar medium of sodium dodecyl sulfate	Diazotization and coupling	561	0.65– 22.62	29

KIO_3, HCl, sodium chloroacetate buffer of pH 3 and KI	KIO_3 was produced from oxidation of CAP in NaOH medium with KIO_4 (Malaprad reaction) for 20 min and masking the excess of KIO_4 with sodium molybdate	Triiodide complex	355	0.2 – 2	30
Fe (III) in high acidic medium at pH 1 – 2	Reaction of CAP with hydroxylamine hydrochloride in high alkaline medium (3 M NaOH) at 60°C to yield a hydroxamic acid which was formed complex with reagent and was extracted by benzyl alcohol	Ferric hydroxamic complex	497	7 – 250	19

The BP recommends a spectrophotometric method for pharmaceutical preparations of CAP at 278 nm(31).

This search describes the development of simple and sensitive spectrophotometric method for the quantitative determination of CAP in pharmaceutical preparations. The proposed method was based on reduction of the nitro aromatic drug (CAP) to the corresponding primary aromatic amine followed by oxidative coupling reaction of the latter with pyrocatechol in the presence ferric sulfate and the measurement of the absorbance of the compounds thus, formed.

MATERIALS AND METHODS

A Shimadzu UV-VIS 260 digital double-beam recording spectrophotometer (Kyoto, Japan) was used for all spectral and absorbance measurements with matched 1-cm quartz cells.

Chemicals and reagents

Chemicals and reagents of analytical grade used in present study. The standard material of CAP was provided from the State Company for Drug Industries and Medical Appliances (SDI), Samarra-Iraq.

Pharmaceutical preparations

Pharmaceutical preparations were obtained from commercial sources.

Aphenicol Capsules: 250 mg Chloramphenicol for each capsule (Ajanta Pharma Limited, India).

Samaphenicol Eye Drops: 0.5% Chloramphenicol and 0.005% Cetrimide for each drop (10 ml) (SDI, Samarra-Iraq).

Ophtamycetine Eye Drops: 0.5% Chloramphenicol for each drop (10 ml) (Kahira Pharm. and Chem. Ind. Co., Cairo-Egypt).

Betaphenicol Sterile Ophthalmic Ointment: 0.2% Betamethasone and 0.5% Chloramphenicol for each ointment (5g) (Delta for medicaments, Ashrafieh and Co., Aleppo-Syria)

Solutions

Chloramphenicol (CAP) reduction solution (500 μg ml^{-1})(23)

This was prepared by dissolving 0.0500 g of CAP in ethanol. It was transferred into 50 ml volumetric flask, and diluted to the mark with the same solvent. The solution was transferred into beaker of 125 ml. A 20 ml of distilled water, 20 ml of hydrochloric acid (11.64 N), and 3 g of zinc powder were added. The beaker was allowed to stand for 15 min at room temperature, then the solution was filtered into 100 ml volumetric flask, washed the residues with distilled water, and diluted to the mark volume with distilled water to obtain 500 μg ml^{-1} of CAP reduction solution. More dilute solution was prepared daily by appropriate dilution using distilled water.

Pyrocatechol (PC) solution (5 mM)

This was freshly prepared by dissolving 0.1101 g of PC and diluting to 200 ml with distilled water in volumetric flask.

Ferric sulfate solutions (10 mM)

This was prepared by dissolving 0.5619 g of ferric sulfate and diluting to 100 ml with distilled water in volumetric flask.

Solutions of pharmaceutical preparations

Capsules samples: The contents of ten capsules were weighed and the powder was mixed. The accurately weighed portion of the powder equivalent to 50 mg of CAP was dissolved in 30 ml of ethanol. The solution was filtered into a 50 ml volumetric flask, the residue was washed with ethanol and diluted to volume with the same solvent to obtain 1000 μg ml^{-1} of CAP. This solution was transferred into 125 ml beaker and was reduced as described above.

Eye drops samples: The contents of three bottles of eye drops were mixed. An aliquot corresponding to 50 mg of CAP (10 ml) was diluted to 50 ml with ethanol in a volumetric flask to obtain 1000 μg ml^{-1}of CAP. This solution was transferred into 125 ml beaker and was reduced as described above.

Ointment samples: The contents of five tubes of ointment were mixed. The accurately weighed amount of ointment equivalent to 50 mg of CAP was extracted with three 10 ml of ethanol. The solution was filtered into a 50 ml volumetric flask, the residue was washed with ethanol and diluted to volume with the same solvent to obtain 1000 μg ml^{-1} of CAP. This solution was transferred into 125 ml beaker and was reduced as described above.

Analytical procedure

Into a series of 25 ml volumetric flasks an increasing volume of the reduced solution of drug (100 μg ml^{-1}) were transferred to cover the range of the calibration graph (1 – 22 μg ml^{-1}). To each of these were added 1 of PC (5 mM) and 1 ml of ferric sulfate (10 mM) and diluted to the mark with distilled water, mixed well and left for 20 min at room temperature (25°C). The absorbances were measured at 500 nm versus the reagent blanks, prepared in the same way but containing no drug.

RESULTS AND DISCUSSION

Absorption spectra of the colored product

When a solution of reduced CAP was mixed with PC reagent and oxidized with ferric sulfate, an intense red color forms immediately, which became stable after 20 min. The red solution has a maximum absorption at 500 nm. Fig. (1) shows the spectra of the red solution formed and of the reagent blank. The maximum absorption at 500 nm was used in all subsequent experiments.

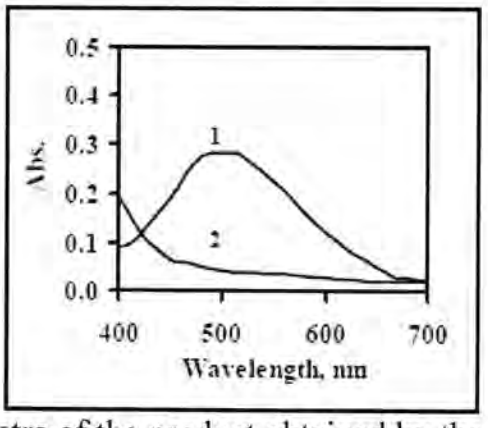

Fig. –1: Absorption spectra of the product obtained by the reaction of PC with 40 μg ml^{-1} of 1- reduced CAP in the presence of ferric sulfate versus reagent blank,
2- reagent blank versus distilled water

Optimum conditions for product formation

The effect of various variables on the color development was tested to establish the optimum conditions for the determination of CAP by oxidative coupling with PC reagent in the presence of ferric sulfate.

In the subsequent experiments, 500 μg of the reduced CAP was taken in 25 ml final volumes and the absorbances of a series of solutions were measured by varying one and fixing the other parameters at 500 nm versus reagent blank after 20 min from the beginning of the reaction.

Effect of oxidant

$Fe_2(SO_4)_3.9H_2O$ was found to be a useful oxidizing agent for oxidative coupling reaction, other oxidizing agents such as NBS, $K_2Cr_2O_7$, $K_2S_2O_8$, $NaIO_4$, KIO_4, and $NaIO_3$ have also been tested, but none offered real advantages over ferric sulfate.

The effect of the different volumes (0.3 – 2.0 ml) of 10 mM ferric sulfate solution was examined on the maximum absorbance of the colored product in the presence 1 ml of PC (5 mM). Fig. (2) shows that 1 ml of the solution was enough to obtain a maximum absorbance, and it was used in the subsequent experiments.

Effect of the coupling reagent

Pyrocatechol (PC) was found to be a useful coupling reagent for oxidative coupling reaction, because it produced stable oxidative coupling organic products rapidly. Moreover, this reagent is easily to obtain and solve in water. Other

coupling reagents such as resorcinol, phloroglucinol, phenol, 2-nitrophenol and 3-nitrophenol did not give product when tried in place of PC.

The effects of the different volumes (0.3 – 2.0 ml) of 5 mM PC solution were examined on the maximum formation of the colored product. Fig. (2) shows that 1 ml of the solution was optimum and was used in the subsequent experiments.

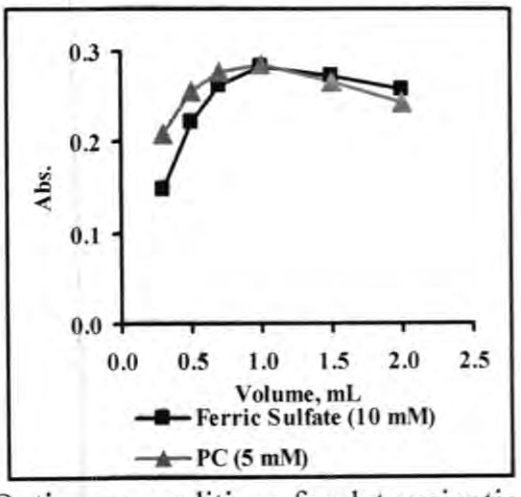

Fig. –2: Optimum conditions for determination of CAP

Effect of order of addition

To obtain optimum results the order of addition of reagents should be followed as given under the analytical procedure, otherwise a loss in color intensity and stability was observed. The order of addition of reagents cited under analytical procedure was used in all subsequent experiments.

Effect of temperature

The effect of temperature on the color intensity of the product was studied. In practice a maximum absorbance was obtained when the color was developed at room temperature (25°C), but when the color was developed in an ice-bath (5°C) or in a water-bath (45°C) a loss in color intensity and stability were observed. It is therefore recommended that the color reaction should be carried out at room temperature (25°C).

Effect of reaction time

The color intensity reached a maximum after reduced drug solution had been reacted immediately with PC and ferric sulfate in aqueous medium and became stable after 20 min and remained stable for at least 60 min. Therefore, 20 min development time was selected as optimum in the analytical procedure.

Structure of the product

Based on the mole ratio and continuous variation methods, it was found that reduced CAP reacted with PC in a ratio of 1:1 as shown in Fig. (3) and Fig. (4).

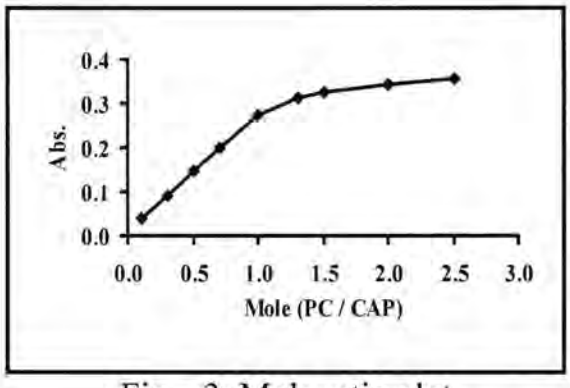

Fig. –3: Mole ratio plot

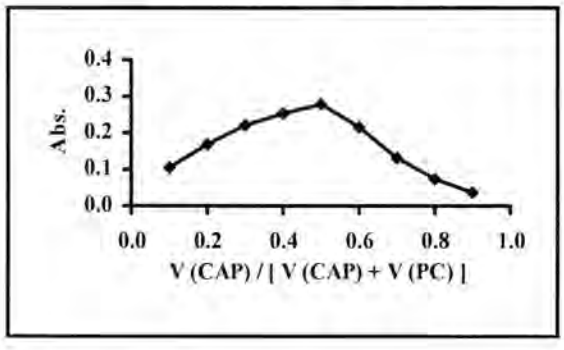

Fig. –4: Continuous variation plot

The reduced drug of CAP, by virtue of their strong electron donating ability, coupling with PC (oxidized to o-benzoquinone by ferric sulfate), leading to the formation of oxidative coupled products[32], as shown in Fig. (5).

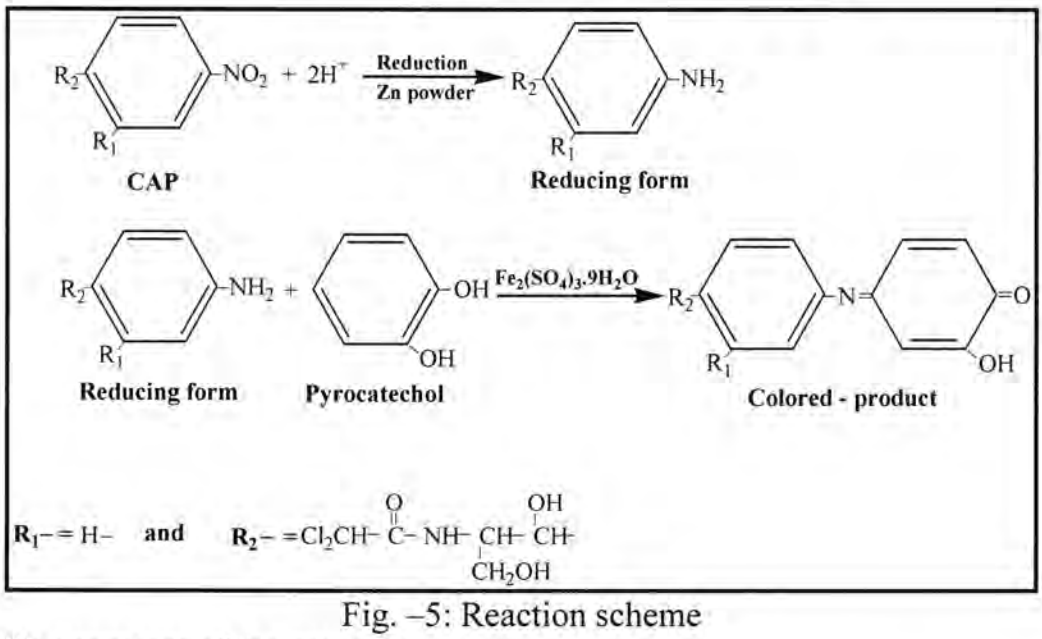

Fig. –5: Reaction scheme

Stability constant of the product

The product formed was soluble in water. The apparent stability constant was calculated by comparing the absorbance of a solution containing stoichiometric amount of CAP and PC (concentration of both CAP and PC are 2

mM) that of a solution containing a five-fold excess of PC reagent. The stability constant of the product in water under the described experimental of conditions was 7.297×10^4 L mol^{-1}.

Optical characteristics

Employing the conditions described under the analytical procedure, a calibration graph for CAP was studied. The linearity of calibration graph, molar absorptivity, Sandell's sensitivity, limit of detection, and limit of quantitative are summarized in Table (2). The slope, the intercept, the standard deviations for residuals, slope and intercept and the correlation coefficient were evaluated by a least-squares regression analysis[33], and are also included in the same Table. The obtained correlation coefficient value is highly significant.

Table–2: Analytical values of statistical treatments for the calibration graph

Parameter	Value
Correlation coefficient, r	9.997269×10^{-1}
Regression equation y = b x + a; y = absorbance, x = concentration (µg ml^{-1})	y = 0.013210 x + 0.019751
Slope, b (ml μg^{-1})	1.321048×10^{-2}
Intercept, a	1.975136×10^{-2}
Standard deviation of the residuals, $S_{y/x}$	2.291876×10^{-3}
Standard deviation of the slope, S_b	9.764513×10^{-5}
Standard deviation of the intercept, S_a	1.268440×10^{-3}
Linearity range (µg ml^{-1})	1 – 22
Molar absorptivity, ε (L mol^{-1} cm^{-1})	4.268306×10^3
Sandell's sensitivity, S (µg cm^{-2}) per 0.001 absorbance unit	7.569749×10^{-2}
Limit of detection, LOD (µg ml^{-1})	5.204678×10^{-1}
Limit of quantification, LOQ (µg ml^{-1})	1.734892

Accuracy and precision

The accuracy and precision of the determination of MPH was studied depending upon the value percentage of the relative error (E%), recovery (Rec.%), and relative standard deviation (RSD%), respectively. For five replicates of each concentration of MPH containing 8, 12, and 16 µg ml^{-1}. The results in Table (3) show a good accuracy and precision.

Table–3: Accuracy and precision of the proposed method

Concn., μg ml^{-1}		E%	Rec.%	RSD%
Present	Found			
8.000	7.956	– 0.550	99.450	1.296
12.000	12.030	+ 0.250	100.250	1.057
16.000	16.104	+ 0.650	100.650	0.806

Pharmaceutical applications

The proposed method was applied for the determination of CAP in capsules, eye drops, and ointment by the analysis of three different concentrations of each sample using the analytical procedure. The results obtained are summarized in Table (4).

Table–4: Application of the proposed method for determination of CAP in pharmaceutical preparations

Pharmaceutical preparation	Concn. of MPH, μg ml^{-1}		E%*	Rec.%*	RSD%*
	Present	Found			
Aphenicol Capsules	8.000 12.000 16.000	7.982 11.989 15.954	– 0.225 – 0.092 – 0.288	99.775 99.908 99.712	1.226 0.930 0.605
Samaphenicol Eye Drops	8.000 12.000 16.000	8.083 12.044 16.069	+ 1.038 + 0.367 + 0.431	101.038 100.367 100.431	0.938 0.596 0.482
Ophtamycetine Eye Drops	8.000 12.000 16.000	8.024 12.039 16.077	+ 0.300 + 0.325 + 0.481	100.300 100.325 100.481	1.169 1.041 0.885
Betaphenicol Steril Opthalmic Ointment	8.000 12.000 16.000	7.899 11.934 15.931	– 1.263 – 0.550 – 0.431	98.737 99.450 99.569	1.045 0.875 0.678

* Average of five determinations.

Evaluation of the proposed method

For evaluating the competence and the success of the proposed method, the results obtained were compared with those obtained by standard BP method(31).

The same pharmaceutical preparations for CAP were analyzed by standard BP method. The results obtained by the two different methods (Table (5)) were statistically compared, using the Student t-test and variance ratio F-test at 95% confidence level(33). In all cases, the calculated t- and F-values (Table (5)) did not exceed the theoretical values, which indicate that there is no significant difference between either methods in accuracy and precision in the determination of CAP in pharmaceutical preparations.

Table–5: The comparison of the proposed method with standard BP method using t- and F-statistical tests

Pharmaceutical preparation	Proposed method		BP method		s	Value	
	Rec.%* $(x_i)_1$	$(x_i-\bar{x})^2_1$	Rec.%* $(x_i)_2$	$(x_i-\bar{x})^2_2$		t (theor.)	F (theor.)
CAP pure	100.000	0.00004	100.000	0.00292	0.734	0.129 (2.306)	2.878 (9.605)
Aphenicol Capsules	99.798	0.04326	99.530	0.17306			
Samaphenicol Eye Drops	100.612	0.36724	100.930	0.96826			
Ophtamycetine Eye Drops	100.369	0.13177	100.600	0.42772			
Betaphenicol Steril Opthalmic Ointment	99.252	0.56852	98.670	1.62818			
	$\bar{x}_1$ = 100.006	Σ = 1.11083	$\bar{x}_2$ = 99.946	Σ = 3.20014	$(n_1 + n_2 - 2)$ = 8		$(n_1 - 1)$ = 4 $(n_2 - 1)$ = 4

* Average of five determinations.

From an analytical point of view, it is concluded that the described procedure allow for the determination of CAP in pharmaceutical preparations. Unlike the other procedures, the instrument is simple and inexpensive. Its importance lies in the chemical reaction upon which the procedure is based, rather than upon the sophistication of the instrument. This aspect of spectrophotometric analysis is of a major interest in analytical pharmacy, since it offers a distinct possibility in the assay of a particular component in complex pharmaceutical preparations. The reagents utilized in the proposed method are cheaper and readily available, and the procedure do not involve any critical reaction conditions, such as heating, extraction or removal of excipients, and hence could be used for routine quality

control in drug industries. The method was found to be simple, low cost, and fairly selective than some of the reported colorimetric methods (Table (1)).

The proposed method advantage over the standard BP method (spectrophotometric method) are more selective, as they depend on the presence of the nitro group, and less prone to interfere, which are normally encountered in single wavelength UV measurements.

The proposed method was applied to analysis of CAP in capsules, eye drops, and ointment solutions, suggesting that it used as a reliable and advantageous alternative to the other previously exported methods for routine analysis of CAP in these samples.

REFERENCES

1. Fleeger, C. A., "USAN and the USP Dictionary of Drug Names", United States Pharmacopeial Convention, Inc., USA, (1992).
2. Katzung, B. G., "Basic and Clinical Pharmacology", 8th Ed., McGraw-Hill, New York, (2001).
3. Negwer, M. and Scharnow, H. G., "Organic-Chemical Drugs and Their Synonyms", 8th Ed., Vol. 1, Wiley-VCH, New York, (2001).
4. Mycek, M. J., Harey, R. A. and Champe, P. C., "Lippincott's Illustrated Reviews: Pharmacology", 2nd Ed., Lippincott Williams and Wilkins, London, (2000).
5. "British National Formulary", No. 15, The British Medical Association and The Pharmaceutical Society of Great Britain, (1988).
6. Jayaram, B. and Mayanna, S. M., Oxidimetric estimation of chloramphenicol with aromatic sulphonyl monohaloamines. Talanta, 30 (10), 798-800, (1983).
7. Koka, I. P., Analysis of medicinal preparations containing chloromycetin [chloramphenicol] by iodimetric and cerimetric methods. Farmatsiya, 33 (4), 64-66, (1984); through Anal. Abstr., 47, 3E37, (1985).
8. Fedchenko, S. B., Determination of chloramphenicol in 0.25% solution. Farmatsiya, 34 (4), 65, (1985); through Anal. Abstr., 48, 4E24, (1986).
9. Lee, V. D., Bennekom,W. P. V. and De Jong, H. J., Determination of chloramphenicol at ultra-trace levels by high-performance differential pluse polarograph. Anal. Chim. Acta, 117 (6), 171-182, (1980).
10. Joshi, D. M. and Joshi, A. P., Polarographic determination of metronidazole and chloramphenicol. J. Indian Chem. Soc., 74 (7), 585, (1997).
11. Mena, M. L., Agui, L., Ruiz, P. M., Sedeno, P. Y., Reviejo, A. J. and Pingarron, J. M., Molecularly imprinted polymers for on-line clean up and preconcentration of chloramphenicol prior to its voltammetric determination. Anal. Bioanal. Chem., 376 (1), 18-25, (2003).
12. Wang, A. B., Zhang, L. and Fang, Y. Z., Determination and separation of chloramphenicol and its hydrolysate in eye-drops by capillary zone electrophoresis with amperometric detection. Anal. Chim. Acta, 394 (2-3), 309-316, (1999).
13. Bautista, J. A. G., Mateo, J. V. G. and Calatayud, J. M., Flow injection biamperometric determination of chloramphenicol and related nitro

compounds by on-line chemical photodegradation. Anal. Chim. Acta, 404 (1), 141-150, (2000).

14. Khalil, S. A. H., Shah, A. H. and Alshareef, A. H., A reverse phase HPLC method for the determination of chloramphenicol and its hydrolytic product in ophthalmic solutions. Anal. Lett., 26 (6), 1163-1179, (1993).
15. Rao, R. M., Al-Ashban, R. M. and Shah, A. H., J., Stabability-indicating liquid chromatographic assay method for ophthalmic solutions containing combination of dexamethasone and chloramphenicol. Saudi Chem. Soc., 8 (2), 223-232, (2004).
16. David, V., Saez, R. M. M., Mateo, J. V. G. and Calatayud, J. M., Enhanced chemiluminescent determination of chloramphenicol and related nitro compounds by 'on-line' photochemical reaction. Analyst, 125 (7), 1313 -1319, (2000).
17. Icardo, M. C., Misiewicz, M., Ciucu, A., Mateo, J. V. G. and Calatayud, J. M., FI-on line photochemical reaction for direct chemiluminescence determination of photodegradated chloramphenicol. Talanta, 60 (2-3), 405-414, (2003).
18. Lindino, C. A. and Bulhoes, L. O. S., Determination of chloramphenicol in tablets by electrogenerated chemiluminescence. J. Braz. Chem. Soc., 15 (2), 178-182, (2004).
19. Hassoon, B. A. K., Atomic and molecular spectrophotometric determination of the drugs atenolol, finastride, chloramphenicol, sulfacetamide, and paracetamol as derivatives of hydroxamic acide in some pharmaceutical preparations. Ph. D. Thesis, Baghdad University, Baghdad, (2005).
20. Abdel-Hamid, M. E. and Abuirjeie, M. A., Spectrophotometric determination of chloramphenicol using orthogonal polynomials. Analyst, 112 (6), 895-897, (1987).
21. Collado, M. S., Mantovani, V. E., Goicoechea, H. C. and Olivieri, A. C., Simultaneous spectrophotometric-multivariate calibration determination of several components of ophthalmic solutions: phenylephrine, chloramphenicol, antipyrine, methylparaben and thimerosal. Talanta, 52 (5), 909-920, (2000).
22. Sastry, C. S. P., Divakar, T. E. and Prasad, U. V., Indirect spectrophotometric methods for the determination of antibiotics with iodine or periodate, and metol and sulfanilamide. Talanta, 33 (2), 164-166, (1986).
23. Hassan, S. M., Belal, F., El-Din, M. S. and Sultan, M., Spectrophotometric determination of some pharmaceutically important nitro compounds in their dosage forms. Analyst, 113 (7), 1087-1089, (1988).
24. Shihab, Y. M., Development of new photometric methods to estimate manufactured chloramphenicol from samara factory of drug industries. M. Sc. Thesis, Mosul University, Mosul, (1990).
25. Al-Abachi, M. Q., Akrawi, B. A., Salih, E. S. and Shihab, Y. M., Spectrophotometric Determination of chloramphenicol in pharmaceutical preparations using promethazine hydrochloride. Mu'tah J. Res. Stud., 7 (1), 163-173, (1992).

26. Al-Abachi, M. Q., Al-Ghabsha, T. S. and Salih, E. S., Spectrophotometric assay of chloramphenicol in pharmaceutical by oxidative coupling. J. Edu. Sci., 25, 5-12, (1996).
27. Jarallah, S. M., Development of spectrophotometric methods for determination of drug nitrogen compounds. M. Sc. Thesis, Mosul University, Mosul, (1998).
28. Rafat, M., Colorimetric determination of chloramphenicol with 3-methylbenzathiazoline-2-one hydrazone. J. Edu. Sci., 32, 9-18, (1998).
29. Tena, I. E., Rodriguez, L. A., Romero, J. E. and Coque, M. C. G. A., Micellar modified spectrophotometric determination of nitrobenzenes based upon reduction with tin(II), diazotization and coupling with the Bratton-Marshall reagent. Talanta, 47 (1), 43-52, (1998).
30. Bakir, M. H., Applications of periodate oxidation reaction in selective organic analysis. Ph. D. Thesis, Baghdad University, Baghdad, (2004).
31. "British Pharmacopoeia on CD-ROM", Version 5, 3rd Ed., Vol. 1, Copyright by System Simulation Ltd, The Stationery Office Ltd., London, (2001).
32. Al-Abachi, M. Q. and Al-Abaidi, R. S., Spectrophotometric microdetermination of folic acid in pharmaceutical tablets via oxidative coupling with catechol and ferric nitrate. Iraqi J. of Chem., 29 (1), 41-49, (2003).
33. Miller, J. N. and Miller, J. C., "Statistics and Chemometrics for Analytical Chemistry", 4th Ed., Pearson Education Limited, London, (2000).

Study the Relationship Between Vitamin E and Some Biochemical Changes in Patients with Type 2 Diabetes Mellitus

Salwa H.N.Al-Rubae'I[1] and Najlaa Qasim Muftin[1]
[1]College of Science, Al-Mustansiriya University, Baghdad, Iraq.

الخلاصة

تضمنت الدراسة الحالية مقارنة مستويات فيتامين E وأنزيم كاما- كلوتامايل ترانس ببتيديز ومستوى البروتين المتفاعل من نوع سي والكوليسترول الكلي والسكر الصائم في امصال المرضى المصابين بداء السكري من النوع الثاني ومقارنة النتائج مع اشخاص سويين كمجموعة سيطرة . وايجاد العلاقة بين فيتامين E كمانع للتأكسد وبعض المتغيرات البايوكيميائية الاخرى.

تضمنت الدراسة 30 شخصا مصابا بداء السكري من النوع الثاني (18 ذكورا و12 اناثا) اللذين يراجعون مركز الكندي للغدد الصم والسكري في بغداد . وتضمنت مجموعة السيطرة 30 شخصا سويا (15 ذكورا و15 اناثا) كمجموعة سيطرة . تم قياس مستوى السكر الصائم (7.39 ±3.095 ملي مول / لتر) في امصال المرضى T2DM.

اشارت النتائج الى عدم وجود فروقات معنوية في العمر في المرضى المصابين T2DM مقارنة بمجموعة السيطرة بينت الدراسة الحالية بان هناك فروقات معنوية في مؤشر كتلة الجسم (20.13±1.79 كغم/م ^{2}) وأنزيم كاما- كلوتامايل ترانس ببتيديز(41.95 ± 6.012 وحدة دولية/لتر) والكوليسترول الكلي (201.36±38.17 ملي غرام / ديسيليتر) و فيتامين E (0.565 ±0.178 ملي غرام/ ديسيليتر) ونسبة فيتامين E الى الكولستيرول الكلي (0.003±0.001) في مرضى T2DM مقارنة بمجموعة السيطرة . واظهر البروتين المتفاعل من نوع سي مستوى سالبا (< من 0.6 ملغم /دسيلتر) في 12 مريضا ومستوى موجبا (> من 0.6 ملغم /دسيلتر) في 18 مريضا (2.07 ± 0.066 ملغم /دسيلتر) . علاوة على ذلك اظهرت الدراسة علاقة ايجابية معنوية بين فيتامين E ونسبة فيتامين E الى الكولستيرول الكلي وعلاقة سلبية معنوية بين فيتامين E مع كل من مؤشر كتلة الجسم والسكر الصائم وأنزيم كاما- كلوتامايل ترانس ببتيديز، بينما علاقة موجبة غير معنوية مع كل من العمر والكولستيرول الكلي و البروتين المتفاعل من نوع سي.

ABSTRACT

The present study is an attempt to assess the serum levels of vitamin E, γ- GGT.CRP, total cholesterol, and fasting glucose in patients with type 2 Diabetes Mellitus and compare the results obtained with healthy controls group, and to ascertain the relationship between the antioxidant vitamin E with some associated parameters.

Type 2 diabetes mellitus group include 30 patients (18 male and 12 female) who were selected from patients attending Specialist Center for Endocrine and Diabetes in AL-Kindy Hospital in Baghdad. The control group included 30 healthy subjects (15 male and 15 female). Fasting glucose level in patients with T2DM was (7.39±3.095 mmol/L).The results reveal there were no significant differences between T2DM and control in age.The present study shows that the means for BMI (20.13±1.79 kg/m^2), γ- GGT (41.95±6.012 U/L), cholesterol (201.36±38.17mg/dL), vitamin E (0.565±0.178 mg/dL), and vit.E/TC (0.003±0.001) were significantly differences in T2DM as compared to control group. CRP levels were negative (<0.6 mg/dL) in 12 patients and positive (>0.6 mg/dL) was (2.07±2.066 mg/dL)) in 18 patients.Furthermore, serum vitamin E concentrations showed significantly positive relationship with the ratio of vit.E/TC, and negative significant relationship found between vitamin E and BMI, fasting glucose, and γ- GGT. While non significant positive relationship found between vitamin E and both of cholesterol, age and CRP.

INTRODUCTION

Type 2 Diabetes Mellitus (T2DM) or non insulin-Dependent Diabetes Mellitus, is the most common form of diabetes, due to dietary habits and increasing obesity and sedentariness in both Western and developing countries, the prevalence of T2DM is growing at an exponential rate (1).It is a heterogeneous group of disorders usually characterized by variable degrees of insulin resistance, impaired insulin secretion, and increased glucose production. Insulin resistance develops from obesity and physical inactivity, acting on a substrate of genetic susceptibility (2, 3). Although the precise mechanism responsible for insulin resistance remains unclear, it would appear that a number of adipocyte-derived factors impair insulin activity and that the secretion of these factors is altered in the obese individual (4).

There has been currently great interest in the potential contribution of increased oxidative stress to the development of diabetes mellitus .An increase in oxidative stress may occur due to an increase in the production of free radicals. These reactive oxygen species (ROS) are capable of chemically altering all major classes of biomolecules (e.g. lipids, proteins and nucleic acid) by changing their structure and function, thus leading to cell damage in diabetes (5). These ROS are potentially harmful to cellular functions. To prevent these harmful effects, the cell has developed a complex antioxidant system to dispose of ROS. However, antioxidant concentrations are reduced in obese individuals, and the resulting imbalance between the production of ROS and antioxidant defenses results in oxidative stress (6).The biological effects of free radicals are normally controlled in vivo by a wide range of antioxidants such as vitamin A ,C ,E ,glutathione and antioxidant enzymes (7). Vitamin E is a generic term for a group of a compound known as tocopherols and tocotrienols, of which α-tocopherol has been shown to have the greatest biological activity (8). The antioxidant property of vitamin E is well established in the literature (9).

Vitamin E, blocks the chain reaction of lipid peroxidation by scavenging intermediate peroxy radicals. The α- tocopherol radical is much less reactive in attacking adjacent acid side chain and can be converted to α-tocopherol by vitamin C (5).

In longitudinal studies, gamma-glutamyl transferase (γ-GGT) predicts future risk of developing diabetes (10). γ-GGT is a cell- surface protein contributing to the extracellular catabolism of glutathione (11). In the serum, γ-GGT is carried primarily with lipoproteins and albumin (12). Serum levels of γ-GGT are determined by several factors: alcohol intake, body fat content, plasma lipid/lipoproteins, glucose levels, and various medications (11, 13). Systemic concentrations of hepatic enzymes reflect hepatocellular health. Raised levels in obese individuals probably reflect nonalcoholic fatty liver disease, which is itself a marker of insulin resistance (14).C-reactive protein (CRP) plays a key role in the host's defense against infection. CRP is predominantly made in the

liver and is secreted in increased amounts within six hours of an acute inflammatory stimulus. Some workers demonstrated later that diabetic individuals with stigmata of insulin resistance ,for example ,central obesity and hypertension had higher serum CRP levels .They regarded this as evidence that inflammation was related to insulin resistance (15).Cholesterols play key roles in controlling molecular fluidity in a biological membrane (16).Cholesterol is one of the major components of biological membranes, and it is known to influence various membrane properties such as elasticity, mechanical strength, and molecular fluidity. Diabetes mellitus is a common secondary cause of hyperlipidaemia, particularly, if glycaemic control is poor(17), which in-turn is an important risk factor for atherosclerosis and coronary heart disease(18).

MATERIALS AND METHODS

Sample Collection

A total of 30 (T2DM) patients were recruited from the diabetic center, in AL-Kindy Hospital (specialized center of endocrinology center and diabetes). Medical records were screened by specialist physicians. The mean age of the patients was 53.3±13 years with a range of 35-60 years. Body mass index of the corresponding patients was 29.76±7.5 Kg/m^2 .

Healthy control group consisted of 30 individuals. The mean age was 40.7±11 years and body mass index was 20.13 + 1.79 Kg/m^2 . All individuals were non smokers and none had taken vitamin supplements.

Preparation of Blood Samples

Six milliliters of blood samples were taken from patients and normal controls in the morning after 12 hours fasting .Blood sample were left for 20 minutes at room temperature, after blood coagulation, the sera were separated by centrifugation at 3000 xg for 15 minutes. Hemolyzed samples were discarded.

The concentration of serum glucose and cholesterol were measured by enzymatic colorimetric assay using kit supplied by Biomegrab. The concentration of vitamin E in the collected serum samples was determined according to the method of Hashim & Schuttriger (19) .Serum GGT activity was also determined using kit supplied by Szasz G.c . C-reactive protein was measured by rapid test for the qualitative and semiquantitative determination of CRP in serum by agglutination of latex particles on slide using a kit supplied by linear chemicals-Spain.

Statistical analysis

The data was analyzed on the computer statistical programme SPSS version10. The mean ±SD was also computed for the comparison of results. The comparison of mean between two groups was tested by Student's't' test. Results were considered statistically significant if P value is less than 0.05.

RESULTS AND DISCUSSION

The incidence of T2DM as well as its related morbidity and mortality has been well correlated with generalized Obesity measured by BMI. The body mass index was calculated as weight (in Kilograms) / height (in meter) squared shows significant changes in T2DM as compared to controls group Table (1). This different in the obesity might be explained the differences in the operation of the risk factors or the causal pathways leading to the disorder (20).

The mean age of the T2DM was 53. ±13 and the mean age of the control group were 40.7 ±11 years Table (1).The groups were not statistically different with respect to age ($p > 0.05$).

Table-1: Comparison of serum glucose, cholesterol, CRP ,GGT, vitamin E and BMI.

Parameters	Controls(Mean+SD) N=20	Diabetic patients (Mean+SD) N=20
Age (years)	40.7±11	53.3±13
BMI (kg/m^2)	20.13 ± 1.79	31.33±6.86**
FBG (mmol/L)	5.35±0.532	7.39±3.095*
Cholesterol (mg./dL)	169.45± 20.91	201.36±38.17*
GGT (U/L)	20.6±3.95	41.95±6.012**
CRP (mg/dL)	< 0.6	< 0.6 (N=12)
		2.07±2.06 (N=18)
Vitamin E (mg/dL)	0.847 ± 0.206	0.565±0.178**
Vit.E/cholesterol	0.005 ± 0.001	0.003±0.001**

Values significantly different from the controls *$p<0.01$, **$p<0.001$

In T2DM, fasting blood glucose (FBG) is the main parameter of glucose metabolism that is used to monitor and control hyperglycaemia (21). In this study, there is also a significant difference ($p<0.01$) in the mean FBG of the T2DM was 7.39 ±3.095 and the mean FBG of the control group were 5.35 ±0.532 mmol/L as shown in Table (1). Because sugar is not getting into the tissues, abnormally high levels of sugar build up in the blood. This is called hyperglycemia. Many people with insulin resistance have hyperglycemia and high blood insulin levels at the same time. People who are overweight have a higher risk of insulin resistance, because fat interferes with the body's ability to use insulin(22).

Cholesterols play key roles in controlling molecular fluidity in a biological membrane. There were, however, significant differences ($p<0.01$) in mean serum total cholesterol in T2DM 201.36±38.17 when compared to control group 169.45± 20.91 mg/dL as shown in Table (1).

In this study, we observed an increase in CRP levels in some diabetic patients table (1), and this study graded increment in CRP may predict for future diabetes but the cut-off point of CRP can not been determined .Pradhan *et al* (23)
showed in a retrospective study that there was a strong and graded association of CRP level with incident diabetes mellitus independent of established risk factors. The above findings support the hypothesis that diabetes mellitus has inflammatory aspects, but the causal pathway between diabetes mellitus and inflammation was not clear. It was possible that inflammation could be the primary disorder that leads to insulin resistance .Also it is possible that inflammation and diabetes mellitus arise from another yet unidentified common genetic antecedent.

Serum γ-GGT, a marker of oxidative stress, has been shown to be associated with diabetes mellitus in some population (24). We examined the association between serum γ-GGT and diabetes mellitus, we observed a highly significant increase ($p<0.001$) in the levels of γ-GGT in T2DM (41.95±6.012 U/L) as compared to control group (20.6±3.95 U/L) Table (1). γ-GGT retains a large part of its predictive power after adjusting for correlated risk factors such as obesity, fasting glucose, and insulin resistance. Our results are in good agreement with Sabanayagam *et al* who found higher serum γ-GGT levels were positively associated with diabetes mellitus, independent of, alcohol consumption, body mass index, hypertension and other confounders (24). The risk of T2DM increased with increasing levels of serum γ-GGT, and the γ-GGT is an important predictor for incident T2DM in men and women from the general population.(25, 26).

The reduction in fasting plasma insulin and glucose concentrations, during vitamin E supplementation suggests improved insulin sensitivity. Furthermore, the magnitude of this improvement in insulin sensitivity, as indicated by fasting insulin levels, depends on the magnitude of the increase in plasma vitamin E (10). In addition, increased vitamin E may enhance the endogenous cellular antioxidant defense system and reduce levels of ROS that are produced by mitochondria. In the present study, vitamin E was significantly reduced ($p<0.001$) in the levels in T2DM (0.565+0.178 mg/dL) as compared to control group (0.847±0.206 mg/dL) Table (1). This lower mean serum vitamin E value may reflect reduced dietary intake or increased consumption associated with increased oxidative stress in patients with diabetes mellitus (27).

Manning *et al* show in thier study that vitamin E improves insulin sensitivity and several of its associated parameters in overweight individuals, but the effect of treatment is not sustained. In addition, vitamin E decreased circulating levels of ALT, a risk factor for the development of T2DM, during entire study period. These results suggest that vitamin E could have a role to play in delaying the onset of diabetes in at-risk individuals (10). Other small

studies have shown improvements in insulin sensitivity in elderly subjects (28) and diabetic individuals receiving high-dose vitamin E therapy (29).

We observed significant decrease in the vitamin E/Total cholesterol (vit.E/TC) ratio in T2DM as compared to control groups (Table 1). Ziegler D. *et al* (30) concluded a significance decrease in vit. E/ TC and non significant change in the level of cholesterol in T2DM patients without polyneuropathy and cardiovascular autonomic neuropathy disease compared to control. In this study we observed non significance positive correlation between vitamin E and age in T2DM patients table (2).

Table-2: Correlation coefficients and the significance levels of different Chemical components in T2DM.

Component vs vitamin E	Slope	R_2	r
Age	0.008	0.146	0.383
BMI	-0.013	0.264	-0.514*
glucose	-0.0264	0.202	-0.449*
GGT	-0.016	0.281	-0.530*
Cholesterol	0.0022	0.145	0.381
CRP	0.077	0.2851	0.534
Vit.E/cholesterol	158.39	0.624	0.790**

* Correlation is significant at the level 0.05

**Correlation is significant at the level 0.01

Mobarhan M.G. et al (31), observed non significance correlation between age and either serum vitamin E or serum (vit.E/TC) ratio. Ford and Sowell (32) in the third National Health and Nutrition examination survey found that age directly related to serum vitamin E.

In this study significant negative correlation between vitamin E and BMI were observed table(2), These results consistent with other study done by Kimmons J E *et al* (33), who reported that low vitamin E levels among overweight and obese persons may result from the increased systemic and adipose tissue specific oxidative stress found in over weight persons ,which may leads to increased oxidative catabolism of these lipid soluble nutrients .Ford and Sowell(32) reported that mean serum vitamin E concentration was not related to BMI . Mobarhan M.G. etal(31), found non significante negative correlation between BMI and vitamin E in T2DM patients associated with dyslipidemia .Other studies done by Kardinaal etal, (34) which revealed a significant positive relationship between plasma vitamin E and BMI.

This study revealed a significant negative correlation between glucose and vitamin E table(2) and this result consistent with experimental studies suggested that oxidative stress impaired pancreatic B-cell insulin secretion

(35,36), interfered with glucose disposal in peripheral tissues ,and elicited systemic inflammation (37) ,there by accelerating the development and progression of T2DM (38) .In vitro studies indicated that vitamin E may improve insulin action and insulin secretion by protecting peripheral tissues and B- cells from free radical –mediated damage , leading to hypothesis that vitamin E may help delay development of T2DM (39).However ,in a large cohort of Finnish men and women those who self -selected for higher intake of dietary vitamin E experienced a significantly decreased incidence of T2DM(40).

In addition to these results ,this study found non significance positive correlation between cholesterol and vitamin E and a highly significant positive correlation between vitamin E and vit.E/TC ratio table(2). our results in agreement with Bouwstra R.J.(41), Mubarhan M.G. *et al* (31), and Ford and Sowell (32) who stated that the strongest positive unadjusted correlation was between serum vitamin E concentration and serum cholesterol.

Since vitamin E is mainly transported by plasma lipoproteins, this strong correlation suggested that changes in plasma vitamin E should be considered as epiphenomenon of altered plasma transport capacity.

In the present study, we observed a significant negative relationship between γ-GGT and vitamin E (Table 2).The decreases in vitamin E due to blocks the chain reaction of lipid peroxidation by scavenging intermediate peroxy radicals. Cellular γ-GGT is an ectoplasmic enzyme responsible for the extracellular catabolism of glutathione and is widely distributed in various cell with secretary or absorptive activities (42).So, the increase in γ-GGT levels with the decrease of vitamin E levels may be reflect the excess of ROS in T2DM . Our study were in a agreement with Mobarhan M.G. etal(31) who found non significance positive correlation between vitamin E and CRP table(2).

These results suggest that vitamin E can work as endogenous antioxidants to protect cells from oxidative stress and could have a role to play in delaying the onset of diabetes in at-risk individuals

REFERENCES

1.Ludwig D.S. and Ebbeling C.B.: Type 2 diabetes mellitus in children primary care and public health considerations. ***JAMA***, 286: 1427-1430,(2001).

2. Gerick J.E.: The genetic basis of type 2 diabetes mellitus: impaired insulin secretion versus impaired insulin sensitivity. ***Endocr Rev.***, 19:491-503, (1998).

3.Chisholm D.J.;Campbell L.V.; Kraegen E.W. **:** Pathogenesis of the insulin resistance syndrome (syndrome X). ***Clin Exp Pharmacol Physiol.***, 24:782-784, (1997).

4.Grenberg A.S.; McDaniel M.L.: Identifying the links between obesity, insulin resistance and beta cell function: potential roleof adipocyte-derived cytokines in thepathogenesis of type 2 diabetes. **Eur J Clin Invest.**, 32 (Suppl. 3): 24–34, (2002)

5. Therond P.; Bonnefont-Rousselot D.;Davit –spraul A.,Conti M. L.; Egrand A.: Biomarker of oxidative stress : an analytical approach. ***Curr. Opin. Clin. Nutr. Metabo. Care***. , 3:373-384. (2000).
6. Ford E.S.; Mokdad A.H.; Giles W.H.; Brown D.W.: The metabolic syndrome and antioxidant concentrations: findings from the Third National Health and Nutrition Examination Survey. ***Diabetes*** , 52: 2346–2352, (2003).
7. Merzouk S.;Hichami A.;Madani S.;Merzouk H.;Berrouiguet A.Y.; Prost J.; Moutairou K.; Chabane-Sari N.; Khan N.A.: Antioxidant Status andmjn;' levels of different vitamins by high performance liquid chromatography in diabetic subjects with multiple compli -cations. ***Gen.Physiol.Biophys.***,22:15-27, (2003).
8. Spanevello R .;Mazzanti C.M. ;Schmatz R. ;Bagatini M. ;Stefanello N.;Correa M. ;Kaizer R.;Maldononadao PN.;Mazzanti A.;Graca L.D.;Martins T.B.;Danesi C.;Morch V.;Schetinger M.R.C.: .Effect of vitamin E on endonnucleotidase activities in rat experimentally demyelinated. ***Brain Reseearch Bulltin***,80:45-51, (2009).
9. Kashif S.M. ;Zaidi R. ;Banu N. :Antioxidant potential of vitamin A,E and C in modulating oxidative stress in rat brain, ***Clin. Chim. Acta***.,340:229-233,(2004).
10. Manning P. J. ; Sutherland W. H.F.; walker R. J. ;Williams S.M. ;Anner S. D.; Ryalls B.E.A. :Effect of High-Dose Vitamin E on Insulin Resistance and Associated Parameters in Overweight Subjects. ***Diabetes Care***, 27:2166–2171, (2004).
11. Emdin M.;Pompella A.;Paolicchi A. :Gamma-glutamyltransferase, atheroscler -osis,and cardiovascular disease: triggering oxidative stress within the plaque. ***Circulation,*** 112: 2078 –2080,(2005).
12. Whitfield J.B. : Gamma-glutamyl transferase. ***Crit Rev Clin Lab Sci.***,38: 263–355, (2001).
13. Grundy S. M.: Gamma-Glutamyl Transferase:Another Biomarker for Metabolic Syndrome and Cardiovascular Risk.***Arterioscler Thromb Vasc Biol.***,27:4-7 ,(2007).
14. Angulo P: Nonalcoholic fatty liver disease.***N Engl J Med.***, 346, :1221–1231, (2002).
15. Reeves G.: C-reactive protein ***.Austr.Presc.***,30, 3, (2007).
16. Askawa H. and Fukuma T.:The moleculare –scale arrengment and mechanical strength of phospholipids /cholesterol mixed bilayers investigated by frequency modulation atomic force microscopy in liquid. ***Nanotechnology***, 20, 26400 :7, (2009).
17. Nathen D.M.; Buse J.B.;Davidson M.B.; Heine R.J.; Holman R.R.;Sherwin R. : Management of Hyperglycaemia in Type 2 Diabetes:A Consensus Algorithm for the Initiation and Adjustment of Therapy; A consensus statement from the American Diabetes Association and the European Association for the Study of Diabetes. ***Diabetes Care***, 29: 1963–72, (2006)

18.Ahmed N.; Khan J.; Siddiqui T.S.: Frequency of Dyslipidaemia in type 2 diabetes mellitus in patients of hazara division. ***J Ayub Med Coll Abbottabad.***, 20, 2,51-54, (2008).

19.Hashim S.A.; Schuttringer G.R. : Rapid determination of tocopherol in marco- and microquantities of plasma, results obtained in various nutrition and metabolic studies. ***Am. J. Clin. Nutr.***, 19,2: 137- 145, (1966).

20.Parikh P, Mani U, Iyer U. Abdominal adiposity and metabolic control in patients with type 2 diabetes mellitus. ***INT. J. DIAB. DEV. COUNTRIES***. 22: 28-34, (2002).

21. Singh N.; Rambiritch V.; Mayet L.:An evaluation of postprandial glucose excursions in type 2 diabetic mellitus subjects on Monotard® HM (ge) versus Humulin N® or Humulin L® insulin, each in combination with metformin. ***SA Fam Pract.***,49,5,14, (2007).

22.American Diabetes Association. Standards of medical care in diabetes 2008. ***Diabetes Care.***, 31: S12-S54,(2008).

23.Pradhan A.D.;Manson J. A.E.;Rifai N.etal.:C-reactive protein , intrlukin -6,and risk of developing type 2 diabtesmelltius ***.JAMA.,*** 286:327-334, (2001).

24.Sabanayagam C.;Shankar A. ;Li J.;Pollard C.;Ducatman A.:Serum gamma-glutamyl transferase level and diabetes mellitus among US adults ***European Journal of Epidemiology*** ,24, 7 ,July, (2009).

25.Meisinger C.,Lowel H.,Heier M.,Schneider A.;Thorand B.:Serum γ-glutamyl - transferase and risk of type 2 diabetes mellitus in men and women from the general population.***Journal of Internal Medicine***,258:527-535, (2005).

26.André P.; Balkau B.; Born C.; Charles M.A.; Eschwège E.:Three-year increase of gamma-glutamyltransferase level and development of type 2 diabetes in middle-aged men and women: the D.E.S.I.R. cohort.***Diabetologia,*** 49,11: 2599–2603, (2006).

27.Wen Y.; Sahni A.; Rea C.; Zhang X.;Khokher M .; Singh B. : Differential antioxidant status among Indo-Asian compared with Caucasians with and without diabetes. ***Diabetes care***, 23 , 2 : 254-255,(2000).

28.Paolisso G.;Di Maro G.;Galzerano D.; Cacciapuoti F.; Varicchio G.;Varricchio M.; D'Onofrio F: Pharmacological doses of vitamin E and insulin action in elderly subjects. ***Am J Clin Nutr***, 59:1291–1296, (1994).

29. Paolisso G.D.;Amore A.;Galzerano D.;Balbi V.; Giugliano D.; Varricchio M.; D'Onofrio F: Daily vitamin E supplements improve metabolic control but not insulin secretion in elderly type II diabetic patients. ***Diabetes Care*** ,16:1433–1437,(1993).

30.Ziegler D.; Sohr C. G.H. ; Nourooz-zadeh M.; Oxidative Stress and Antioxidant Defense in Relation to the Severity of Diabetic Polyneuropathy and Cardiovascular Autonomic Neuropathy. ***Diab -etes Care***,27:2178–2183,(2004).

31. Mobarhan M. G.; Sahebkar A. H.; Starkey B. ; Livingstone C. ; Wan T.: An Investigation of the Relationship between Serum Vitamin E Status and Coronary Risk Factors in Dyslipidaemic Patients. ***Iranian Journal of Basic Medical Sciences***.10, 4: 206 – 215,(2008).

32 .Ford E.S .and Sowell A.: Serum α-tocopherol status in the United States population: findings from the third national health nutrition examination survey. ***Am J Epidemiol,*** 150: 290-300, (1999).

33.Kimmons J.E.:Associations between body mass index and the prevalence of low micronutrient levels among US adults. ***MedGenMed.***,8,4,59,(2006).

34. Kardinaal A.F.;Veer P.V. ;Brants H.A. M and Berg H.: Relations between antioxidant vitamins in adipose tissue, plasma and diet. Am J Epidimiol, 141: 440-50,(1995).

35. Evans J.L. ;Goldfine I.D.; Maddux B.A.; Grodsky G.M.: Are oxidative stress activated signaling pathways mediators of insulin resistance and -cell dysfunction? ***Diabetes*** ,52:1– 8, (2003).

36. Bast A. ;Wolf G.;Oberbaumer I.; Walther R: Oxidative and nitrosative stress induces peroxiredoxins in pancreatic beta cells. ***Diabetologia.***, 45:867– 876, (2002).

37. Ceriello A.; Motz E.: Is oxidative stress the pathogenic mechanism underlying insulin resistance, diabetes, and cardiovascular disease? The commonsoil hypothesis revisited. ***Arterioscler Thromb Vasc Bio.***,24:816–823,(2004).

38.Singh U.; Devaraj S.; Jialal I: Vitamin E, oxidative stress, and inflammation. ***Annu Rev Nutr.***, 25:151–174, (2005).

39.Liu S.; Lee M. ; Song Y.; Denburgh M. V.; Cook N.R.;Manson J. E.; and Buring J. E.:Vitamin E and Risk of Type 2 Diabetes in the Women's Health Study Randomized Controlled Trial. ***Diabetes,*** 55:2856–2862, (2006).

40.Montonen J.; Knekt P. ;Jarvinen R.; Reunanen A: Dietary antioxidant intake and risk of type 2 diabetes. ***Diabetes Care,*** 27:362–366, (2004)

41.Bouwstra R.J.;Goselink R.M.A.; Dobbelaar P.;Nieln M.;Newbold R.J.;Werven T.:the relationship between oxidative damage and vitamin E concentration in blood ,milk ,and liver tissue from vitamin E supplemented and non supplemented periparturient heifers . **American Dairy science association** .,91:977-987,(2008).

42. Sun Lim J.; Lee, D.H.; Park J.Y. ; Soo-Hee Jin,1 and Jacobs D.R. :A Strong Interaction between Serum-Glutamyltransferase and Obesity on the Risk of Prevalent Type 2 Diabetes: Results from the Third National Health and Nutrition Examination Survey. ***Clinical Chemistry.***, 53,6: 1092–1098 ,(2007).

Synthesis of Thiazolidines, Oxadiazoles, Thiadiazoles and Triazoles derived from 6-nitro-2-quinolone

Abdul-Hussain K. Sharba, Redha I. AL-Bayati and Mazin J. Habib
Department of Chemistry, College of Science, AL-Mustansirya University,

الخلاصة

تم في هذا البحث تحضير 6-نايترو كومارين [1] وذلك بنيترة الكومارين ,ثم تحويل هذا المركب الى 6- نايترو-1-امينوكوينولين-2-اون.[2b]. حضر ايضا مركبات الازوميثان [3a-e]من تفاعل الالديهايدات او الكيتونات الاروماتية المقابلة مع المركب[2b]. مفاعلة المركبات [3a-e] مع مركبتو حامض الخليك اعطى مشتقات الثايازولدينون[4-5]. اضافة الى ذلك فأن مفاعلة المركب [1]مع الكلايسين اعطى مشتقات حامض الخليك ل 2-كوينولون[6] والتي حولت الى حامض الهايدرزايد [7]. ايضا معاملة المركب[7] مع ثاني كبريتيد الكاربون في محلول هيدروكسيد البوتاسيوم اعطى مشتق الاوكسوديازول[8]. اما تفاعل المركب[6] مع الثايوسميكارباز ايد فقد اعطى المركب [9].

كما تم مفاعلة المركب[9] مع هيدروكسيد الصوديوم والذي الى غلق حلقي للمركب ليعطي المركبات [10a-b]. اضافة لذلك فأن معاملة المركب[9] مع حامض الكبريتيك المركز ادى الى غلق حلقي ليعطي مشتق الثايا دايازول ل 6-نايترو-2-كوينولون [11].

ABSTRACT

In this work, 6-nitro coumarin **[1]** has been prepared by nitration of coumarin and then converted into 6-nitro-1-aminoquinoline-2-one **[2b].** The azomethines **[3a-e]** were prepared from the corresponding aryl aldehydes and ketones with **[2b].** Treatment of compounds **[3a-e]** with mercapto acetic acid gave the thiazolidinone derivatives **[4-5].** Moreover the reaction of compound **[1]** with glycine afforded the acetic acid derivative of 2-quinolone **[6],** which was converted into the acid hydrazide **[7].** Treatment of compound **[7]** with carbon disulfide in potassium hydroxide gave the oxadiazole derivative **[8]**. The reaction of compound **[6]** with thiosemicarbazide yielded 2-[(6-nitro-2-oxoquinolin-1(2H)-yl)acetyl] hydrazine carbothioamide **[9].** Reaction of compound **[9]** with NaOH leads to ring closure giving 1-[(5-mercapto-4H-1,2,4-triazol-3-yl)methyl]-6-nitro quinolin-2-(1H)-one **[10a-b].** In addition, treatment of compound **[9]** with H_2SO_4 leads to ring closure also giving the thiadiazole derivative of 6-nitro-2-quinolone **[11]**.

INTRODUCTION

Coumarin (benzo-α-pyrone) and its derivatives are naturally occuring substanes found in plant sources including sweet clover and tonka bean(1) in both free state or as glycosides . They are especially abundant in grasses , orchids , legumes and citrus fruits(2) . Moreover coumarins are well known as a photosensitizing agents in photobiology(3,4) .

The biological activity of coumarins varies according to the substituents on the benzopyran ring(5) . The 7-hydroxy-4-methyl coumarin could be used as cardioactive drug by inhibition of calcium influx(6) , and has anti – asthmatic activity (7) . Furthermore it is used as insect repellant (5) , insect anti-feeding and as plant regulator (8) . The 4- hydroxy coumarin behaves as a blood anticoagulant(9) , and is responsible for hemorrhagic sweet clover disease in cattles(7) . Coumarin-3-carboxylic acids are sedative in small doses and hypnotic in large doses(10) . Some of hydroxy coumarins possessing the power of absorbing utraviolet light are extensively used as medicinals in skin disease(1) .

Coumarin nucleus undergoes ring substitution e.g. nitration mainly at C-6 giving 6- nitro coumarin **[1]**. Moreover coumarin is easily attaked by nucleophilic reagents such as ammonia , amines or hydroxylamine(11) leading to ring opening and occasionally recyclized into another ring(12) , as in the equation below :

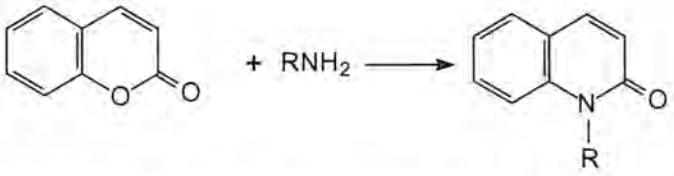

In this work coumarin or 6- nitro coumarin is allowed to react with hydrazine hydrate giving 1- amino quinoline-2-one **(2a-b)** (Scheme 1) and these latter compounds were used to prepare thiazolidine compounds **[4-5].**

The oxadiazole **[8]** , thiadiazole **[11]** and triazole **[10]** derivatives were also prepared (Scheme 3) .

MATERIALS AND METHODS

General

Melting points were determined in open capillary tubes in an electrically heated metal block apparatus and are uncorrected .

The IR spectra (KBr discs) were recorded with a Pye-Unicam SP3-100 spectrophotometer . UV spectra were recorded on cinta -5- Gbes scientific equipment , using absolute ethanol as solvent . ^{1}H- NMR spectra have been performed by spectral laboratories in Germany using a 400-MHZ .

Microanalyses have been performed by spectra laboratories in Jordan.

Preparation of 6-nitro-2H-chromen-2-one[1](13) .

This compound was prepared according to the method reported in the literature (10) , m.p 140-141°C .

Preparation of 1-amino-6-nitroquinolin -2(1H)-one [2] .

A solution of 6-nitro coumarin [1] (0.035 mole) and hydrazine hydrate (95%) (0.035 mole) in absolute ethanol was refluxed for (24 hrs.) . The solvent was concentrated and the separated solid product was filtered and washed with cold ethanol . The precipitate was recrystalized from ethanol-water . mp 166-168°C , 62% yield , IR(ν cm^{-1}) :
3450(NH_2) , 3060(C-Har) , 1670(C=O amide) , 1450,1550(C=C_{ar}) , 1510,1320(NO_2) , UV(λmax) : 282,211nm , ^{1}HNMR(δ ppm) : 6.3(d,1H,H_3) , 7.5(d,2H,H_4,H_8) , 7.7(d,2H,H_5,H_7), 7.2(dd,2H,NH_2).

General procedure for preparation of Schiff bases [3a-e]

To a solution of compound **[2]** (0.005mole) in (30ml) absolute ethanol , the appropriate aldehyde or ketone (0.005mole) was added .

The mixture was refluxed for (4 hrs.) , cooled , then the solid precipitate was filtered and recrystallized from the appropriate solvent . **[3a]**(R=H , Ar=C6H5) yield 65% , m.p. 271 dec. (benzene), IR(υ cm^{-1}) : 1630(C=N) , 1680(C=O) , 3050(C-H_{ar}) ; UV(λmax) : 251 , 491nm . **[3b]**(R=H) , Ar=2-NO_2 C_6H_4) m.p 233(dec) (EtOH :H_2O) , yield 56% , IR(υ cm^{-1}) 1620(C=N) , 1690(C=O) , 3050(C-H_{ar});UV, (λmax) : 267 , 350 nm ; ^{1}HNMR(δ ppm) : 6.6(d,1H,H_3) , 7.3(S,N=CH-Ar , 1H) , 7.5(d , 2H,H_4 , H_8) , 7.85(d ,2H, H_5 , H_7) . **[3C]**(R=H , Ar = 4-OHC_6H_4) m.p 203-205(EtOH:H_2O) , yield 63% , IR(υ cm^{-1}) : 1630(C=N) , 1690(C=O) , 3100(C-H_{ar}) , 3500)(OH) , UV;

(λmax): 205 , 335 nm , calculated for $C_{10}H_{11}N_3O_3$(%)C , 62.14 , H, 3.58 , N , 13.59 , found(%) C,61.91 , H,3.66 , N , 13.50 . [3d] (R=H , Ar = 2-furyl) m.p 212 – 214°C($CHCl_3$) , yield 42% , IR(υ cm^{-1}) 1610 (C=N) , 1700(C =O) , 3050(C-H_{ar}), 1150(C-O-C), UV; (λmax): 253 , 314 nm . **[3e]** (R = CH_3 , Ar = 2-ClC_6H_4) mp : 245-247° (benzene) , yield 48% , IR(υ cm^{-1}) : 1630(C=N) , 1690 (C=O) , 3020 (C-H_{ar}) , 1035(C-Cl) ; UV; (λmax) 266 , 491 nm .

General procedure for preparation of thiazolidine derivatives [4,5]

A solution of α – mercapto acetic acid (0.01 mole) in (15ml.) dry benzene , was added slowly with stirring to a solution of compounds **[3d,3e]** (0.01 mole) in (15ml) of dry benzene . The solution was concentrated and neutralized with sodium bicarbonate solution (10%) . The solid product was filtered and recrystallized from chloroform .

Compound **[4]** : m.p 202 – 204°C , yield 67% , IR(υ cm^{-1}): 1700 (C=O) , 3000(C-H_{ar}) , 2950 (C-$H_{al.}$) , 1515 , 1310(NO_2) , 720(C-S-C) , UV. (λmax) : 258 , 320nm .

Compound **[5]** : mp228 – 230°C , yield 56% , IR(υ cm^{-1}): 1695 (C =O) , 3050(C-H_{ar}) , 2900 (C-$H_{al.}$) , 1510(NO_2) , 800 , 620 (C-Cl) , UV. (λmax) : 231 , 317 nm ; calcd for $C_{19}H_{14}N_3O_4ClS$(%) C , 54.87 , H, 3.36 , N, 10.10 , found (%) C , 54.33 , H, 3.61 , N , 10.85 .

Preparation of (6- nitro-2-oxoquinolin -1 (2H)-yl) acetic acid [6]

A solution of 6-nitro coumarin **[1]** (0.02mole) and glycine (0.02 mole) in (20ml.) of absolute ethanol was refluxed for (24 hrs.) . After that the mixture was concentrated and cooled . The solid separated was filtered , then recrystallized from ethanol , a (45%) yield of pale – yellow crystals was obtained with melting point 180-182°C .

Preparation of 2-(6-nitro-2-oxoquinolin-1(2H)-yl) acetohydrazide [7]

To a solution of compound **[6]** (0.005mole) in (20ml) of ethanol , hydrazine hydrate (95%) (0.005mole)was added dropwise with stirring .

The mixture was refluxed for one hour , cooled then the solid formed was filtered and recrystallized from ethanol- water (1:1) to give (60%) yield of compound **[7]** as yellow precipitate with melting point (201-203°C) .

Preparation of 1-[5-mercapto-1,3,4-oxadiazol-2-yl] methyl]-6-nitro quinolin-2(1H)-one [8]

To a mixture of compound **[7]** (0.01 mole) in a solution of potassium hydroxide (0.01mole) , (100ml) of ethanol (96%) was added . To the above solution carbon disulfide (0.2mole) was added slowly with stirring . The mixture was refluxed for (5-6 hrs.) until the liberation of dihydrogen sulfide (H_2S) gas ceased . After that , the mixture was cooled and concentrated under vacuum , then poured slowly with stirring onto ice (60gm) .The solution was acidified with dilute hydrochloric acid (10%) to (pH = 5-6) , and the resulting precipitate was recrystallized from acetone to give (87%)yield of white precipitate , melting point (256-258°C) IR(υ cm^{-1}) : 1730(C=O) , 3200(N-H) , 1620(C = N) , 1520 , 1380(NO_2) , 2650(SH) ;

UV. (λmax) : 220 , 295 nm.

Calcd . for $C_{12}H_8N_2O_4S$(%) C, 47.37 ; H, 2.65 ; N, 18.41 ; found(%) C, 47.21 ; H,3.01 ; N,18.28 .

Preparation of 2-[(6-nitro-2-oxoquinolin -1(2H) – yl) acetyl] hydrazine carbothioamide [9]

To a solution of compound **[6]** (0.01mole) an excess of thionyl chloride (12ml) was added , then the mixture refluxed gently on a water bath at (70-80°C) in a hood for (2hrs.). Excess of thionyl chloride was removed under vacuum . Then to the resulting precipitate , (25ml) of dry benzene and thiosemicarbazide (0.02mole) were added . The mixture was refluxed for (3hrs). After cooling , the resulting precipitate was filtered and recrystallized from ethanol to give (61%) yield of compound **[9]** as brown precipitate , with melting point of (274 – 276°C).

Preparation of 1-[(5-mercapt-4H-1,2,4-triazol-3-yl)methyl]-6-nitro quinolin -2(1H)- one [10] .

A mixture of compound **[9]** (0.01mole) and (4%) aqueous sodium hydroxide solution (120ml) was refluxed with stirring for (4hrs). The mixture was decolorized with activated carbon , then filtered . The filtrate was acidified with dilute hydrochloric acid (10%) , and the resultant precipitate was filtered and recrystallized from ethanol – water (2:1) to give compound **[10]** as yellow precipitate : mp 305(dec); yield 35% ; IR(υ cm^{-1}) : 3200 (NH) , 3050 (C-H_{ar}) , 2590(SH), 1700(C =O) , 1640 (C =N) , 1580, 1350 (NO_2), 1220(C =S) ; UV (λmax) 212 , 239 , 340 nm. Calcd for $C_{12}H_9N_5O_3S$(%) C , 47.21 ; H , 3.63 , N , 22.94 ; found (%) C , 47.38 ; H , 3.05 , N, 22.46 .

RESULTS AND DISCUSSION

Coumarin is known to react with hydrazine or primary amines to give N-substituted quinolin-2-one **[2a]**(7) . The reaction involves ring opening of the pyron ring through nucleophilic attack at C-9 followed by recyclization (**scheme 1**) . Thus the reaction of coumarins with hydrazine hydrate afforded 1-amino-quinolin-2(1H)-one 2a or 1- amino- 6-nitro quinolin -2(1H)- one (2-b) .

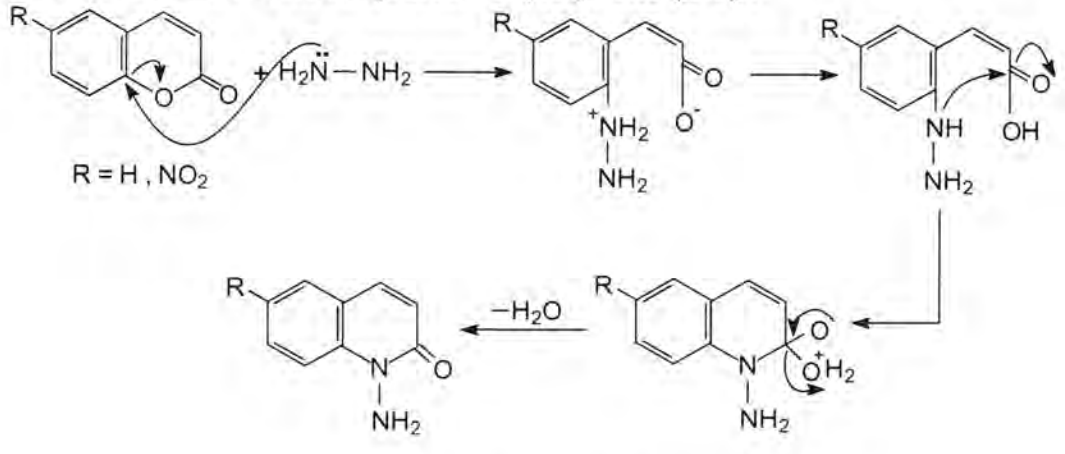

2a (R=H)
2b (R=NO2)

Scheme (1)

The IR spectrum of **[2]** indicated the presence of NH_2 group (3450 cm^{-1}) and amide carbonyl at (1670 cm^{-1}), and the NMR spectrum showed a double doublet at 7.2 ppm

due to NH_2 protons because of hydrogen bonding with carbonyl oxygen in addition to signals of the ring protons (see experimental) .

Condensation of compound **[2b]** with aryl aldehydes or ketones produced new Schiff bases **[3a-e]** in high yield as indicated by the presence of the azomethine (CH=N) stretching band at (1610-1630 cm^{-1}) with disappearance of NH_2 stretching band .

Treatment of the Schiff bases with mercapto acetic acid in dry benzene gave the thiozolidine derivatives **[4 and 5]** which displayed in their IR spectra the C-S-C stretching vibration at (700-740 cm^{-1})
(Scheme 2) .

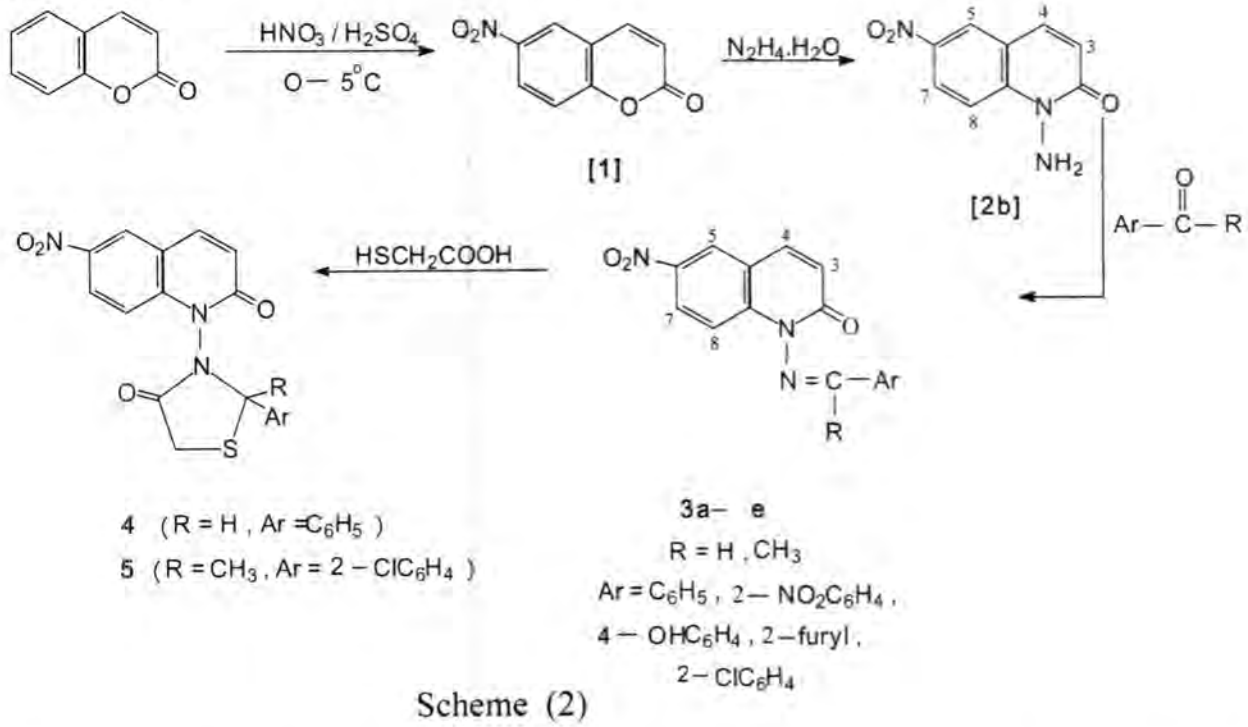

4 (R = H , Ar =C_6H_5)

5 (R = CH_3 , Ar = 2 – ClC_6H_4)

3a– e

R = H , CH_3

Ar = C_6H_5 , 2— $NO_2C_6H_4$,
4 — OHC_6H_4 , 2–furyl ,
2– ClC_6H_4

Scheme (2)

On the other hand the reaction of **[1]** with glycine afforded (6-nitro-2-oxoquinolin-1(2H)-yl) acetic acid **[6]** which gave the acid hydrazide **[7]** on treatment with hydrazine hydrate in absolute ethanol .

The IR spectrum of **[7]** showed NH_2 absorption at 3300-3400 cm^{-1} and the N-H stretching band at 3150 cm^{-1} in addition to the two bands at 1510 and 1320 cm^{-1} for the asymmetrical and symmetrical vibration of NO_2 group .

Furthermore , treatment of acid hydrazide **[7]** with carbon disulfide in alcoholic potassium hydroxide yielded the 1,3,4-oxadiazole-2-thiol **[8]** which displayed in the IR spectrum a band at 1620 cm^{-1} for C=N stretching vibration and another band at 2650 cm^{-1} for the S-H group(14) .

Reaction of compound **[6]** with thionyl chloride then with thiosemicarbazide in dry benzene produced the thiosemicarbazide derivative **[9]** which upon ring closure with NaOH gave 1-[(5-mercapto-4,5-dihydro-3H-1,2,4-triazol-3-yl) methyl] -6-nitro quinolin -2 (1H)-one **[10]** , which exists in two tautomeric forms the thiol [10a] and the thion **[10b]** as indicated by the presence of the characteristic S-H stretching at 2550 cm^{-1} **[10a]** or the C=S stretching at 1220cm^{-1} **[10b]** (14) .

Further,the reaction of **[9]** with concentrated sulfuric acid afforded compound **[11]** , 1-[(5-amino-1,3,4-thiadiazol-2-yl) methyl] -6-nitro quinolin -2(1H)- one (Scheme 3) .The IR spectrum of **[11]** displayed absorption band at 3250 cm^{-1} for the NH_2 fun - ction in addition to the bands at 1420 cm^{-1} and 1050 cm^{-1} which are due to C-S-C and N-N stretching vibrations respectively(14) .

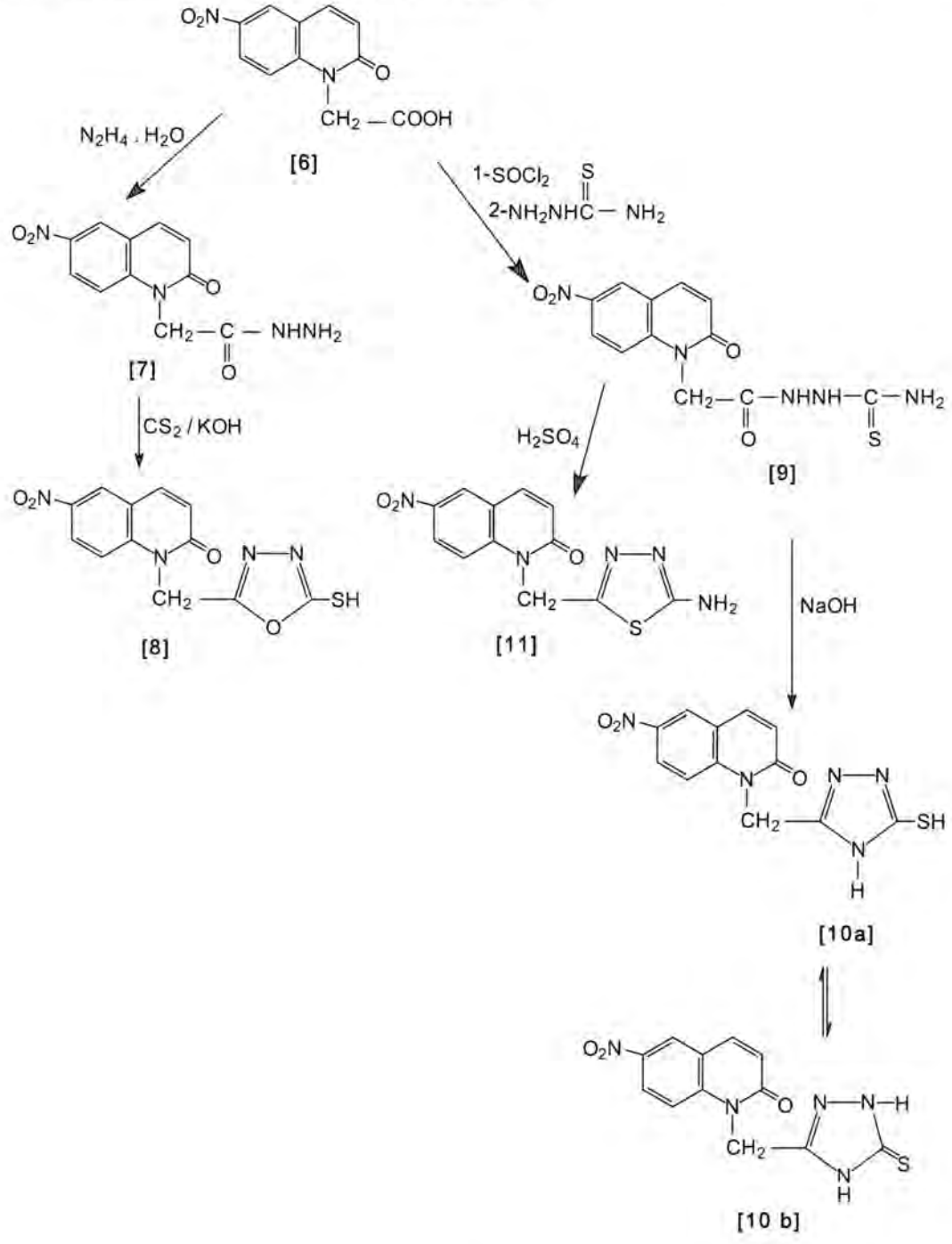

Scheme (3)

REFERENCES

1. Sentha S. M. " Synthesis of coumarin and 4 - methyl coumarin " Chem.Rev., 36 , 2 (1945) .
2. Heindel N.D. and Foster N. ,"Reduced quaternized psoralens as photp-activated therapeutics as photo-activated theraputics" J. Hetero . Chem., 22 , 73 (1985) .
3. Jabin I. and Heindel N.D.,"Direct fluorination of coumarin ,6-methyl-coumarin and 7-alkoxy-coumarins" J. Hetero . Chem., 37 , 31 (2000) .
4. Ray N.K.and Ahvja V.K.Ahvja,Photochemistry and photobiology,17,347 (1973).
5. Sentar S.S. , Org. Mag. Res. , 19(4) , 222 (1982) .
6. 6- Tavnco N. , " Studies on cardioactive crude drugs " , Plant Med. , 54(4) , 277(1986) , C.A., 109, 183238y (1988).
7. Nagesma M. and Rajn K.M. , J. Ind. Chem. Soc., 65 , 380 (1988) .
8. Chatterjce A. , Ganguly D. and Sen R.., Tetrahedron , 32 , 2407 (1976).
9. Foye A.H. " Principle in Medical Chemistry " Alea and Febiger Book U.S.A. : 393 (1995) .
10. Bary R.D. ,"Facoltit di medicina e veterinaria" Chem.Rev., 64 , 229 (1964) .
11. Spences E.Y. and Wright G.F. ,"A lignin –carbohydrate complex in wood" J. Am. Chem. Soc. , 63 , 2017 (1941).
12. Parkanyi C., Schmidt D.S. ,"Synthesis of ,3-dihydroquinazolin-4(1H)-ones" J. Hetero . Chem., 37 , 725 (2000) .
13. Nofal Z.M. , El-Zahar M.L and Abd El- Karim S.S., Molecules ,5:99-113 (2000) .

Photo Degradation of Poly Styrene and Poly (exo-Galactosene-co-Styrene

[1]Yousif Ali Al-Fattahi , [2]Salah M. Aliwi , and [3]Hammed H. Mohamed
[1] Department of Chemistry ,College of Science , University of Baghdad
[2] Ministry of Higher Education & Scientific Research
[3] Department of Chemistry , College of Science , University of Al-Mustansiriah

الخلاصة

تم دراسة التجزئة الضوئية للبوليمر poly (exo-galactosene-co-styrene) في الحالة الصلبة بأستخدام الأشعة فوق البنفسجية (U.V) عند طول موجي λ = 313 nm ومقارنته مع التجزئة الضوئية للبولي ستايرين, وقد تمت متابعة التجزئة الضوئية بالطرق الطيفية: (الأشعة تحت الحمراء (I.R) و الأشعة فوق البنفسجية (U.V.) وبأستخدام المتغيرات التالية :

1. استعمال نسب جزيئية مختلفة من الستايرين الداخل في تركيب البوليمر : (كوبوليمر I) سكر-ستايرين (1 مكافئ : 1 مكلفئ) و كوبوليمر (II) (1 مكافئ : 3 مكافئ)
2. محفزات التجزئة الضوئية مختلفة (الثنائي بنزويل بيروكساید و البنزوفينون) بتركيز (0.003 غرام/مل)
3. تراكيز مختلفة من الثنائي بنزويل بيروكساید (0.01 and 0.003 غرام/مل)

اظهرت البوليمرات تغيراً في اطياف امتصاص الأشعة فوق البنفسجية (U.V) و الأشعة تحت الحمراء (I.R , وخاصة في منطقة امتصاص مجموعة الكاربونيل عند التشعيع الضوئي, حيث اضهرت اطياف الأشعة تحت الحمراء (I.R) ان نسبة الأمتصاصية A_{co}/A_{1600} تزداد مع ازدياد زمن التشعيع , واظهر البوليمر المشترك المحضر زيادة سريعة في امتصاص مجموعة الكاربونيل مقارنة مع بولي ستايرين وهذا يعود الى الدور المهم لوحدات السكر في زيادة التجزئة الضوئية للبوليمر المحضر, التجزئة الضوئية للكوبوليمر مع البنزوفينون هي اسرع من التجزئة الضوئية للكوبوليمر مع الثنائي بنزويل بيروكساید كما ان سرعة التجزئة الضوئية تزداد مع ازدياد تركيز الثنائي بنزويل بيروكساید

ABSTRACT

The photodegradation of poly (exo-galactosene-co-styrene) was investigated in solid state using u.v.-radiation at λ = 313 nm and compared with polystyrene . The photodegradation rate is followed by U.V. and I.R spectrophotometry using either:

1. copolymer with different molar ratios of styrene : vinyl sugar : styrene (copolymer I) (1 mole : 1 mole) and (copolymer II) (1 mole : 3 mole)
2. Different photosensitizers (dibenzoyl peroxide and benzophenone) (0.003 g/mL).
3. Different concentrations of dibenzoyl peroxide (0.003 and 0.01 g/mL).

The copolymers showed a change in their I.R and U.V. absorption spectra, especially at the carbonyl absorption region. Upon photoirradiation, the I.R spectra showed that the absorbance ratios A_{co}/A_{1600} have increased with irradiation period, whereas the copolymer showed the most rapid increase in carbonyl group absorbance compared with polystyrene due to the sugar units which had on important role in increasing photodegradation of the copolymer. The rate of photodegradation of copolymers increases with benzophenone (BPH) and dibenzoyl peroxide (DBP) as photosensitizers, but the increase in the rate of photodegradation is higher with benzophenone (BPH) , also the rate of photodegradation is increased with increasing the concentration of dibenzoyl peroxide (DBP) photosensitizer . The aim of this work is study the effect of sugar molecule on the photodegradation of copolymer for styrene when compared with polystyrene

INTRODUCTION

During recent years there has been an increasing interest in the use of renewable resources as organic raw materials(1), especially the use of carbohydrates for the preparation of polymers(2). Large amounts of carbohydrates are commercially available and a substantial part of the surplus of their agricultural production may be spent in this way. One possibility to prepare macromolecules from sugars makes use of the preparation of vinyl sugars and their polymerization(3).

A new *exo*-glucopyranoide(4),*exo*-fructofuranoid(5),*exo*-fructopyranoid (6), glucono -δ- lactone (7,8) derivatives were synthesized and investigated in chain polymerization reaction. The corresponding saccharide polymers, homo-and copolymers, were synthesized under free radical conditions(4,8,9)

The application of polymerizable vinyl sugar molecules for the preparation of special polymers was investigated. In one research project, hydrophilic surface are generated on standard polymers after copolymerization with low amounts of protected vinyl sugars.

The polymers might then find use as thickners (10,11) (e.g. in the tertiary oil recovery),as flocculating agents (11), as polymeric detergents [10,11], or for surface modification of standard polymers (2,12). They might also be of interest as models for intercellular recognition processes.

Polymers are sensitive to u.v. radiation, however their sensitivities vary due to the difference in their chemical structure as well as the range of incident radiation(13-15). The physical processes involved in photodegradation include adsorption of light by the material leading to electronic excitation of the molecules, and eventually deactivation through radiative or radiationless transition, or by energy transfer to some acceptor.

Polymers may degrade by some sensitizers(16,17) through photooxidation mechanisms via decomposition formation of the hydroperoxide and carbonyl free radicals. Some of the photooxidation products incorporated in the polymer absorb U.V. light better than the original polymer. These chromophores may lead to intiation and acceleration of degradation reaction. The study and understanding of the photochemical and photodegradation processes caused by light could lead to the production of polymers with controlled service life. This could pave the route for reducing the permanent pollution of the environment caused by the increasing amount of waste plastics which is produced from disposal packaging. Controlled life time of plastics are also used in mulch films for the protection of important plants by covering the soil until the plant has grown and strengthened and the film disappears with the aid of sunlight(18).

MATERIALS AND METHODS

Polymers :

The copolymer poly(exo-galactosene-co-styrene) (1) was prepared as described previously[19]

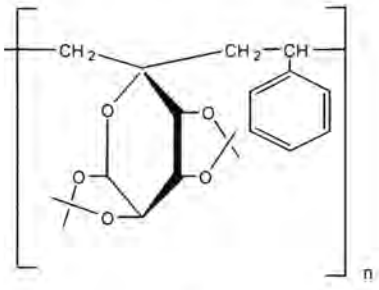

(1)

Techniques:

Film preparations

0.05 g/mL of poly (exo-galactosene-co-styrene) (1) and polystyrene in dichloromethane solvent with and without dibenzoyl peroxide (DBP) (0.003,0.01g/mL),benzophenone (BPH)(0.003g/mL) as photosensitizers are used to prepare polymer films (85 μm in thickness), casting on plate (from NaCl salt, 3.41mm thickness)at room temperature for 24 hr to remove the residual solvent. The film samples were further dried at room temperature .The film samples were fixed on a special holder for irradiation (which is an aluminum plate (0.6mm) in thickness supplied from (Q-panel) company U.S.A.)

Irradiation experiments:

Accelerated testing technique:

The accelerated weather-o-meter, Q.U.V. tester, (Q panel company, U.S.A), was used for irradiation of polymer films. The accelerated weathering tester contains stainless steel plate with two cavities in the front and rear sides.

Each side contains four lamps, type (U.V.B. 313), located horizontally, giving spectrum range of wavelength between (290 to 360)nm, and the maximum intensity is located at (313) nm .

The polymer film holders are fixed vertically and paralleled to the lamps, so that U.V radiation is vertically incident on the polymeric samples. The irradiated sample holders were changed in positions from time to time to ensure that all samples received the same intensity of light, the temperature of the tester chamber is constant at 50 °C for all samples .

During the irradiation process, the degree of photodegradation of the polymer films was monitored, by taking different exposure times.

Ultraviolet visible spectrophotometry (U.V)

The absorption spectra was recorded using the ultraviolet visible spectrophotometer using the Hitachi U-2000 and Cary 100 conc. to record the absorption spectra in the wavelength range between (200-600) nm.

Infrared spectrophotometry (IR)

A Pye-Unicam SP_3-100 infrared spectrophotometer was used to record the IR spectra between (600-4000) cm^{-1}.

Photodegradation measuring methods

A- Measuring the photodegradation rate of polymer film using infrared spectrophotometery.

The photodegradation of the polymer film was followed by I.R spectrophotometer. The absorption spectra of the film samples were recorded in the wavenumber ranged from 600 to 4000 cm^{-1}. The position and the growth of the carbonyl absorptions were monitored at (1720) cm^{-1}.

The photodegradation during different irradiation times was followed by recording changes in the carbonyl and benzene ring absorption peaks (1720 and 1600 cm^{-1}) respectively. To eliminate experimental errors, the carbonyl indices were calculated using the band index method , by comparing the (IR) absorption peaks at the specified positions, with a reference peak (i.e. at 1600 cm^{-1}) which refers to the (C=C) bond of aromatic bending vibration in polystyrene and poly (exo-galactosene-co-styrene).

$$I_S = \frac{A_S}{A_r} \qquad \text{.....(2-4)}$$

Where:

A_S = Absorbance of the peak under study.

A_r = Absorbance of the reference peak.

I_S = Index of the group under study.

The absorbance (A) is calculated from the recorded percentage transmittance using Beer's-Lambert law as shown in the following equation.

$$\left.\begin{aligned} A &= \log(100/T\%) \\ A &= \log(100) - \log(T\%) \\ A &= 2 - \log(T\%) \end{aligned}\right\} \qquad \text{.....(2-5)}$$

Actual absorbance, the difference between the absorbance of the base line and the top peak, ($A_{top\ peak} - A_{base\ line}$) is calculated using the base line method .

B- Photodegradation rate measurments of polymer films using ultraviolet-visible spectrophotometry.

The ultraviolet-visible spectrophotometer technique was used to measure the changes in the UV-visible spectrum during irradiation times for copolymers. The absorption spectra were recorded in the wavelength range from 200 to 600 nm and the (λ max) at each absorption peak was also recorded for different irradiation times.

RESULTS AND DISCUSSION

Photodegradation of poly (exo-galactosene-co-styrene) in solid state.

Photooxidative degradation of poly (exo-galactosene-co-styrene), and polystyrene occurs by irradiation in a broad spectral range between 254 to 400 nm. Initiation of the photo-oxidative degradation of copolymer and polystyrene is attributed to the absorption of U.V-light by different chromophoric impurities such as peroxide groups in the polymer chain formed during the polymerization process of styrene monomer, by reaction of oxygen with copolymer and polystyrene growing radicals.

The polystyrene and copolymers films (control) without photosensitizers was irradiated at different time intervals. The difference between irradiated and unirradiated spectra is given to show the newly produced species clearly (i.e. ketones compounds) . On photo- irradiation, the optical density of polystyrene at wavelength in the range 250-350 nm increases with the irradiation time. The increase in intensity is assigned to the formation of carbonyl groups by photooxidation of polymer.

Very small peaks at longer wavelength are attributed to the formation of conjugated double bonds in the polymer backbone. The elementary processes of photodegradation of polystyrene initiates from photoabsorption by polystyrene and formation polystyryl radical and then polyenes has been investigated .

On photoirradiation of copolymer, the absorption of longer wavelengths increases in its intensity, the presence of chemically combined oxygen in the form of, for example, carbonyl or peroxide function is almost totally precluded.

It must therefore be concluded that the chromophore responsible for absorbing at 313nm is a charger-transfer complex involving oxygen and the aromatic nuclei. The proposed mechanism has been investigated .

The absorption bands in the wavenumber 1730 cm^{-1} increase in intensity with the increase of the irradiation time which has been attributed to the creating of carbony groups of ketones compounds. In this time, the concentration of (OH) group in the polymers, in general, is smaller.

The carbonyl index (I_{co}) is used to follow the extent of photodegradation for polymers during irradiation. The values of the (I_{co}) indices of polystyrene, copolymer (I) and copolymer (II) are tabulated in table (1) and figure (1) shows the relationship between (I_{co}) and irradiation time for polymers.

Table -1: The carbonyl index (I_{co}) polystyrene, copolymer (I) and copolymer (II) (control) (85 μm in thickness) with irradiation time hr)

Polymers	Irradiation time (hr)				
	0	30	90	160	300
Polystyrene	0.220	0.252	0.397	0.495	0.633
Copolymer (I)	0.425	0.482	1.0	1.0	1.0
Copolymer (II)	0.119	0.137	0.470	0.716	0.837

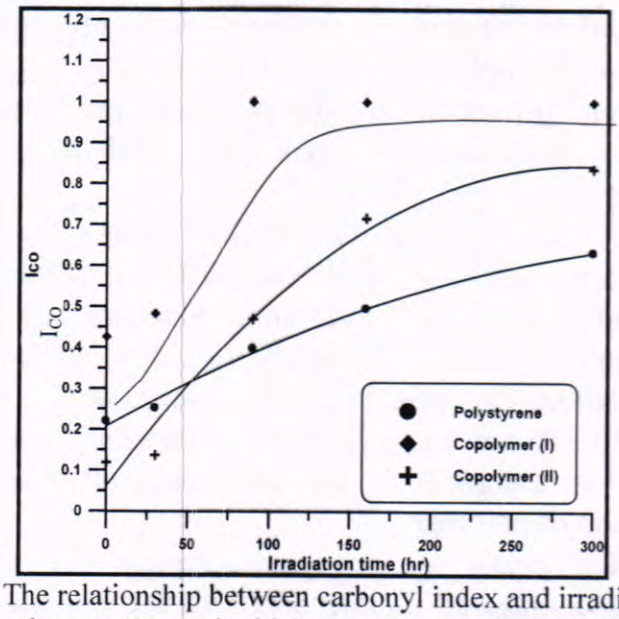

Figure -1: The relationship between carbonyl index and irradiation time for polymers (85 μm in thickness) without photosensitizer

From table (1) and figure (1), these polymers may be arranged in order to increase the rate of degradation depending on increase in the values of (I_{co}) index:

copolymer (I) > copolymer (II) > polystyrene.

The (Ico) indices data led us to the conclusion that ratio of vinyl sugar monomer in copolymer plays an important role in increasing the rate of photodegradation. From the reactivity ratio values, the composition of copolymers is random copolymer, and the vinyl sugar monomer units content decreases the stability of copolymers , hence the photodegradation of copolymers increased .

Effect of photosensitizers

The kind and concentration of photosensitizers play an important role in inducing the photodegradation of polymers. In the present work, the

degradation of polymers were examined with (i) different mole ratios of styrene in the feed (ii) different photosensitizers in the copolymer (II) , (iii) different concentrations from DBP photosensitizers in the copolymer (II)

(i) Different mole ratios of monomers in feed

In this work different mole ratios in feed of comonomer is used , with dibenzoyl peroxide (0.003 g/mL) as photosensitizer .

(A) Copolymer (I) from (vinyl sugar- styrene 1 mole : 1mole) in feed

(B) Copolymer (II) from (vinyl sugar- styrene 1 mole : 3 mole) in feed

The extent of photodegradation of the copolymer is followed by U.V and IR spectral changes and compared with polystyrene. The ultraviolet-visible spectral changes during photolysis of polystyrene, copolymer (I) and copolymer (II) with dibenzoyl peroxide (DBP) (0.003g/mL) as photosensitizer are shown in figures (2) to (4). It can be seen that the growth in absorption of carbonyl group at wavelength between 300 to 375 nm. The observed overall increase in U.V. absorption is probably taking place due to the generation of different types of other chromospheres in polystyrene and copolymer such aromatic ketones, hydro- peroxides, etc.

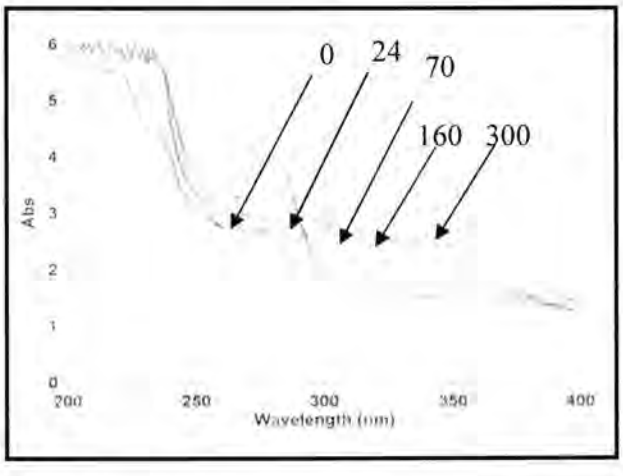

Figure-2:U.V. Visible spectral changes of polystyrene film (85 μm in thickness) with 0.003g/mL DBP. Numbers on the spectra are irradiation times in hours.

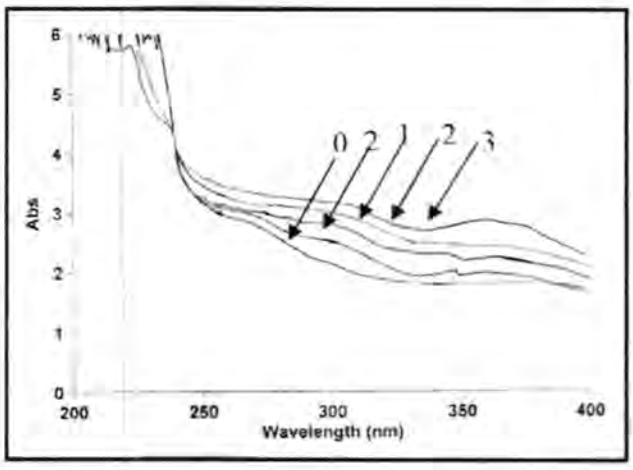

Figure-3:U.V. Visible spectral change of copolymer(I) film (85 μm in thickness) with 0.003g/mL DBP. Numbers on the spectra are irradiation times in hours

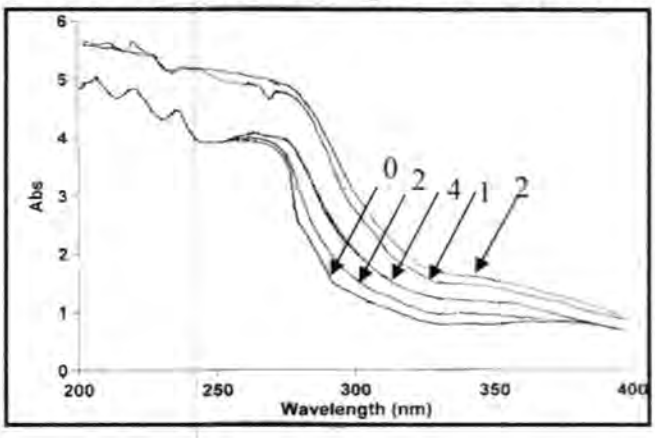

Figure-4:U.V. Visible spectral change of copolymer(II) film (85 μm in thickness) with 0.003g/mL DBP. Numbers on the spectra are irradiation times in hours

The physical properties of photosensitizers and polymers have a pronounced effect on the photodegradation efficiency of polymers. The most important property is the compatibility i.e. any type of photosensitizer (photodegradation inducer, photooxidant....etc) must be evenly distributed within the polymer matrix, which requires that it is compatible with polymer matrix[20,21]. Concerning the photosensitizers in this study, they are completely soluble in the polymers solvent (dichloromethane) that was used for casting polymers film samples . The photodegradation rate of polymers can be followed by (IR) spectra from growth of the carbonyl group (i.e. measuring the I_{co} index) while growth of the hydroxyl group was smaller.

In the (IR) spectra of photoirradiated polystyrene, copolymer (I) and copolymer (II) films, the intensity of the absorption band of carbonyl group appeared around 1700 cm^{-1} increases with the increase of the irradiation time. This is in agreement with the result obtained from the changes in the U.V-visible spectral where the increase in the absorbent

between (300-375) nm as shown in figure (2) to (4). The peak centered at 1730 cm^{-1} is assigned to a carbonyl vibration.

The carbonyl group formation was compared in this region (1730 cm^{-1}) by calculating the carbonyl index (I_{co}), and are used to follow the extent of polymer photodegradation during the irradiation process. The effect of dibenzoyl peroxide (DBP) on the rate of carbonyl formation (I_{CO}) are shown in table (2) and figure (5).

Table -2 :Calculated values of the carbonyl index (I_{co}) with irradiation time for polymers films (85 μm in thickness) containing DBP (0.003 g.mL) at 50 °C.

Polymers	Irradiation time (hr)				
	0	30	90	160	300
polystyrene	0.215	0.302	0.553	0.629	0.729
Copolymer(II)	0.15	0.671	0.764	0.831	0.921
Copolymer (I)	0.238	0.47	1.307	2.2	4.4

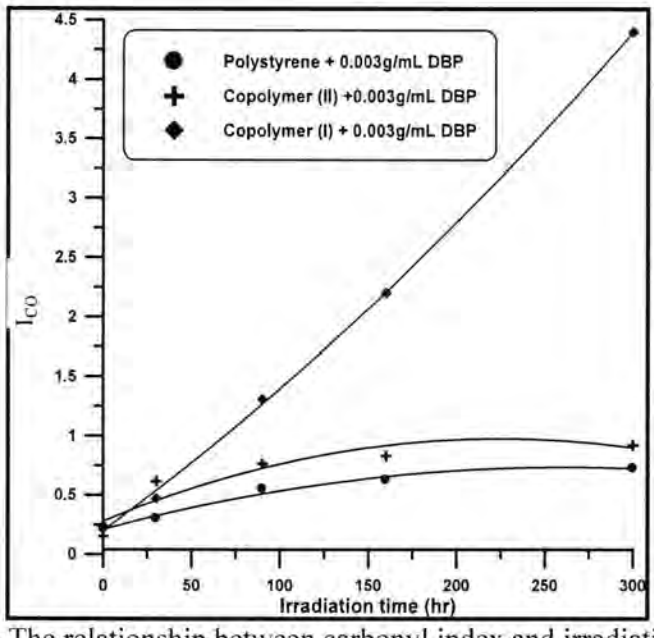

Figure -5: The relationship between carbonyl index and irradiation time for polymers (85 μm in thickness) with 0.003g/mL DBP

From the results obtained in table (2) and figure (5), it can be observed that the rate of carbonyl formation (I_{co}) with irradiation time follow the following trend :

Copolymer (I) > copolymer (II) > polystyrene

Therefore , the dibenzoyl peroxide is acting as photodegradation inducer for polystyrene and copolymers films .The growth of carbonyl index in the copolymers with the photosensitizer is higher than polystyrene & copolymer without photosensitizer (control), Also results shown in figure (5) indicate the increase in the moles ratio of vinyl sugar in copolymer cause the increases in the photodegradation compared with polystyrene, as the formation rates of carbonyl index (Ico) are much higher than for polystyrene (control) or polystyrene with photosensitizer.

Effect of dibenzoyl peroxide (DBP) and benzophenone (BPH) as photosensitizer

The photodegradation of copolymer (II) film (85 μm in thickness) was studied with different photosensitizers (0.003 g/mL) : a-) dibenzoyl peroxide (DBP) (I) , b-) benzopheone (BPH) (II).

The changes in the U.V-visible and IR spectra was adopted to follow photodegradation of copolymer. The spectral changes during photolysis of copolymer films with photosensitizers (I) and (II) are shown in figures (4) and (6). Fig.(6) shows a growth at absorption region (300-400)nm which could be attributed to the generation of different types of other chromophers in the copolymer such as kenotic derivatives. The degradation of copolymer in presence of DBP and BPH photosensitizers was also followed by the (IR) spectral changes of the carbonyl group absorption between the wavenumber (1680-1800)cm^{-1}.

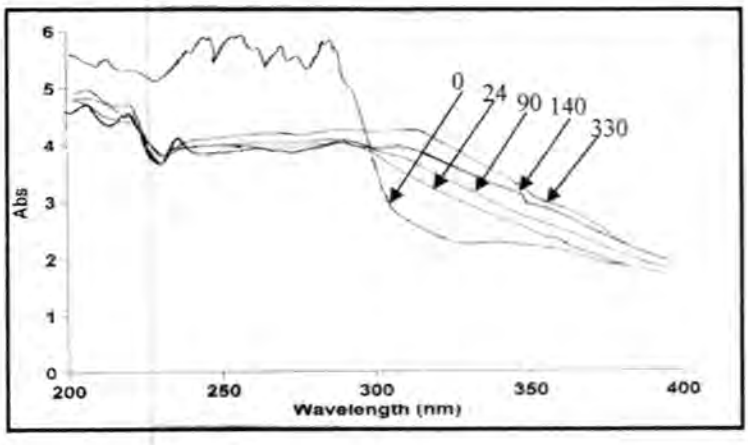

Figure-6: U.V. Visible spectral change of copolymer(II) film (85 μm in thickness) with 0.003g/mL BPH. Numbers on the spectra are irradiation times in hours

The carbonyl index (I_{co}) (from I.R spectra) is used to follow the extent of polymer degradation during irradiation.

The effect of these photosensitizers on the rate of carbonyl formation (I_{co}) is shown in table (3) and figure (7).

Table -3: Carbonyl index (I_{co}) of copolymers with photosensitizers and irradiation time (hr).

Copolymers	Irradiation time (hr)				
	0	30	90	160	300
Copolymer(II) with 0.003g/mL DBP	0.15	0.671	0.764	0.831	0.921
Copolymer(II) with 0.003g/mL BPH	0.263	0.908	1.052	1.302	1.302
Copolymer(II) (control)	0.119	0.137	0.470	0.716	0.837

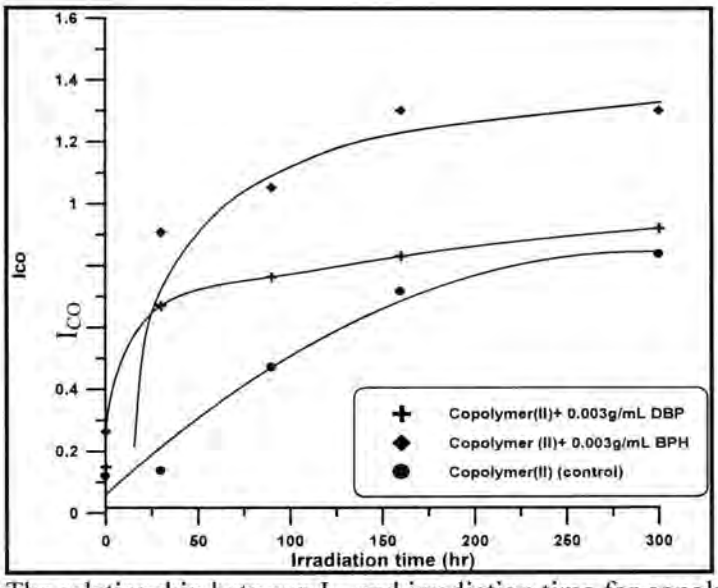

Figure -7:The relationship between I_{co} and irradiation time for copolymer(II) film (85 μm in thickness) with 0.003g/mL of photosensitizers at 50 °C.

From the results obtained in table (3) and figure (7). It can be observed that the rate of carbonyl formation (I_{co}) with BPH photosensitizer is higher than (I_{co}) with DBP photosensitizer . The above mentioned results illustrate that the affect of photosensitizers in photointiations of copolymer degradation depends upon their structure and surroundings of (C=O) group in DBP and BPH photosensitizers , these results are similar to other studies.[22]

The high activity of BPH is probably not only by its reaction with polymer molecule (PH) but also by reaction of polymeric radicals with oxygen and creation of active ($HO^{\bullet}$) and ($HOO^{\bullet}$) radicals[23].

These radicals are known as accelerators of photooxidative degradation of polymers. Dibenzoyl peroxide (DBP) under UV-irradiation undergoes decomposition to benzyl radicals, which are unstable and rapidly fragmentated to CO_2 molecule and creating phenyl radicals.

Effect of photosensitizer concentrations.

The degradation of copolymer (II) film (85 μm in thickness) was examined with two concentrations of dibenzoyl peroxide as photosensitizer : a-) 0.003 g/Ml b-) 0.01 g/mL

The U.V- visible spectra, figure (4) and (8) , shows the irradiated copolymer(II)films with 0.003 g/mL and 0.01 g/mL of DBP at different time intervals respectively.

Figure (8) shows the increase of intensity in the wavelength between 300 to 400 nm region are attributed to the increase of carbonyl chromospheres concentration. The effect of 0.003 g/mL and 0.01 g/mL of dibenzoyl peroxide (DBP) on the photodegradation process of copolymer films was followed by IR spectral changes using the growth of the absorbance bands at 1680-1740 cm^{-1} of carbonyl group.

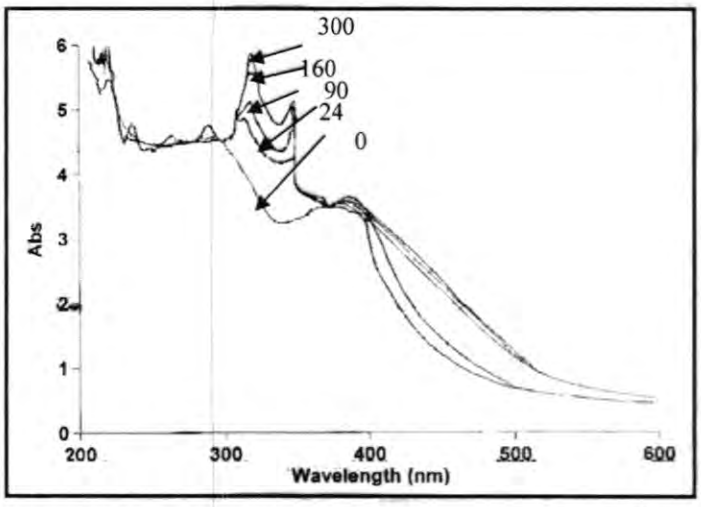

Figure- 8: U.V.-Visible spectral change of copolymer(II) film (85 μm in thickness) with 0.01 g/mL DBP. Numbers on the spectra are the irradiation times in hours

The carbonyl indices (I_{co}) are calculated and tabulated at different time of irradiation for copolymer (II) film contains 0.003 and 0.01g/mL of DBP and shown in table (4). The relationship between the carbonyl index (I_{co}) and irradiation time are shown in figure (9)

Table -4: Calculated values of the carbonyl index (I_{co}) with irradiation time for copolymer(II) containing 0.0030 and 0.01g/mL of DBP.

Copolymers with DBP	Irradiation time (hr)				
	0	30	90	160	300
Copolymer(II) with 0.003g/mL DBP	0.15	0.67	0.764	0.831	0.921
Copolymer(II) with 0.01g/mL DBP	0.25	1.22	1.23	1.93	2.83

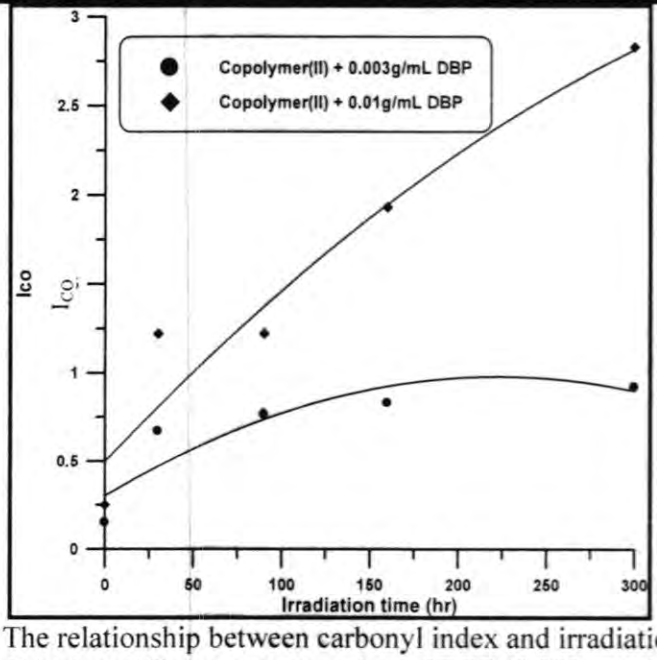

Figure -9: The relationship between carbonyl index and irradiation time for copolymer (II)using different concentration of DBP (0.003 and 0.01 g/mL)

The above mentioned results show that increasing the concentration of DBP in the copolymer, the carbonyl index (I_{co}) and the extent of degradation would obviously increase, these results are similar to other studies[22,24] .

During U.V. irradiation of polymers in solid state ,the concentration of functional groups in macromolecules (carbonyl groups) increases with and without photosensitizers. It is also well known that the efficient main chain scission in irradiation polymers causes their mechanical deterioration and breaking into small pieces.

The rate increase of degradation of the polymer may be arranged as following:

1. The copolymer (I) > copolymer (II) > polystyrene.
2. The copolymer (II) with benzophenone show higher degradation than same copolymer with dibenzoyl peroxide.
3. The degradation increases with increase of concentration of dibenzoyl peroxide.

The sugar units in the copolymer plays an important role in decreasing the stability of copolymer ,therefore photodegradation of copolymer increased .

REFERENCES

1. Deseotes G.,Ed.,"Carbohydrates as Organic Raw Materials II".VCH, Weinheim, (1993).
2. Wulff G.,Clarkson G.,Diderichs H.,Gunz S.,in"3 Symposium Nachwachsede Rohstoffe-Perspektiven für die chemie", Schrifteureihe des Bundesministeriums für Ernährung, landwirtschaftund Forsten, Reihe A, londwirtschaftsverlag, Münster, :187, (1994).
3. Wulff G., Schmid J. and Venhoff T.P., "The preparation of new types of polymerizable vinyl sugars with C-C bonds between sugar and double bond", Macromol. Chem.. phys., 197 , 259, (1996).
4. Yaacoub E.J.,Skeries B.and Buchholz K.,"Synthesis and polymerization of exo-glucal derivatives",Macromol.Chem. Phys., 198 , 899, (1997).
5. Wick S.and Yaacoub E.J.,"Synthesis and polymerization of a 5,6-unsat -urated fructofuranoid derivatives"Macromol.Chem.Phys.201,93(2000).
6. Glümer A.&Yaacoub E.J."Synthesis & polymerization of 1,2-unsaturated fructopyranoid derivatives"Macromol.Chem Phys.201,1521,(2000).
7. Glumer A.G.,Skeries B.,&Buchholz K."Synthesis and copolymerization of unsaturated Glucono–δ-lactone derivatives" Macromol.Chem.Phys .,205 ,73, (2004).
8. Boltres D.,Schmalbruch B.&Buchholz K."Copolymerization of unsaturated Glucono–δ-lactone derivatives"Macromol.Chem.Phys.205,1508, (2004).

9. Yaacoub E.J.,Wick S.,&Buchholz K."Synthesis&polymerization of met -hyl 5-deoxy-2,3-O-isopropylidene-β-D-erythro-pent-4-enofuranoside" Macromol .Chem.Phys., 196 , 3155, (1995).
10. Kunz M.,in"Nachwachsende Rohstoffe-Perspektiven für die chemie" M. Eggersdorfer,S.warvel,G.Wulff,Edes.,VCH,Weinheim:367(1993).
11. Klein J.Kunz M.,"Nachwachsende Rohstoffe:Polysaccharid Forschung" Edited in Commission of BMFT,Forschungszentrum Jülich.:198 (1993).
12. Kunz M., "in:Carbohydrates as Organic Raw Materials" , F.W. Lichten -fhler ,Ed.,VCH,Weinheim, :127, (1999).
13. Timoteo G.A.V., Fechine G.J.M. and Rabllo, "Stress cracking and photodegradation: the combination of two major causes of HIPS failure", Macromolecular Symposia, 258 , 162 , (2007).
14. Norrman K., Kingshott P., Kaeselev B. and Siahkali A.G., "Photodegradation of poly (ether sulphone) part 1. Atime – of – flight secondary ion mass spectrometry study", Surface and interface analysis, 36 , 1533, (2004) .
15. Janorkar A.V.,Mettere A.T.&Hirt D.E.,"Degradation of poly (L-lactide) films under ultraviolet-induced photografting and sterilization condit -ions ",J.of Applied Polymer Science,106,1042,(2007).
16. Saron C.,Felisberti M.I.,Zulli F.&Giordano M.,"Influence of diazo pigm -ent on polycarbonate photodegradation",J.of Applied Polymer Science, 107,1071(2007).
17. Chang J.,Y.J.Yu, J.H.Na,J.An, C.Im,D.H.Choi,J.L.Jin,S.H.Lee & Y.K. Kim , "Photodegradation-induced photoluminescence behaviors of π-conjugated polymers upon the doping of organometallic triplet emitters" J. of Polymer Science Part B: Polymer Physics, 46 , 2395(2008).
18. Scott G.,ICS-INDO Report."Environmental Degradable Plastics": 20-24 March, (2000).
19. Yousif A. Al-Fattahi ,Salah. M. A and Hamid. H. M., Ph.D Thesis , " Copolymerization of Vinylic Carbohydrate Monomer as Photo and Biodegradable Copolymer", University of Al-Mustansiriah, (2007) .
20. chai Z., Sun R. and karasz F., "Miscibility in blends of branched copolymers", Macromolecules, No. 7, 28 2297, (1999).
21. Utracki L. A., "Polymer blends and alloys", New yourk, (1990).
22. Salah M. A.,Tariq S. N. and Zainab.N.M., PhD .Thesis," Induced Photodegradation of Some Cellulose Derivatives", AL-Mustansiriah Univerisity ,(2006)
23. Rabek J.F."Mechanisms of Photo-physical Processes &Photochemical reactions in Polymers"(Theory&Applications)Wiely,Chichester (1987)
24. Zhang R., Chen H., Cao H., Huang C.M., Mallon P.E., Y.Li, Y.He, Sandreczki T.C., Y.C.Jean, Suzuki R. and Ohdaira T., "Degradation of polymer coating systems studied by positron annihilation spectroscopy. IV.oxygen effect of UV irradiation", J. of Polymer Science Part B: Polymer Physics, 39 , 2035, (2001) .

Adsorption–Desorption Studies Of One Of Antihypertensive Drug in Solution on Selected Clays Surfaces

Athraa. S. Ahmed.
Al- Mustansiriya University, College of Science, Chemistry Department

الخلاصة

يتضمن هذا البحث دراسة عملية امتزاز- ابتزاز احد الادوية المستخدمة في معالجة ارتفاع ضغط الدم (البيسوبرولول هيميفيوفاريت) باستخدام اطيان عراقية (الكاؤولين والاتابلكيت) وأجريت دراسة متكاملة لهذه الانظمة باستخدام مطيافية الاشعة فوق البنفسجية لتعين كمية الامتزاز على السطوح المذكورة (قبل وبعد الامتزاز) وبدرجات حرارية مختلفة. كما تم دراسة تأثير التغير في حامضية المحلول، القوة الايونية للمحلول. تحديد وقت الاتزان، ودراسة عملية ابتزاز الدواء من على السطوح المازة المستخدمة.

كذلك تم اختبار ايزوثيرمات الامتزاز ووجد انها تتبع ايزوثيرم فرندلش للامتزاز. كما تم استخراج الدوال الثرموديناميكية للامتزاز ووجد بان عملية الامتزاز هي عملية تلقائية باعثة للحرارة.

ان امتزاز (البيسوبرولول هيميفيوماريت) على السطوح الطينية في المحلول المتعادل اعلى منه في المحلول الحامضي. وكذلك وجد ان امتزاز الدواء على سطح الكاؤولين محدود التأثير بالقوة الايونية للمحلول بينما وجد ان امتزاز نفس الدواء على سطح طين الاتابلكيت يزداد بنقصان القوة الايونية للمحلول. كذلك تم دراسة فعالية السطوح المذكورة للابتزاز الدواء عند درجة حرارة ($37.5C^{o}$).

ABSTRACT

The experimental work cocern the studying of the adsorption- desorption systems of Bisoprelolhemifumarats by using two of Iraqi natural clays kaolin and attapulgite focused on determining the adsorption – desorption isotherms of the adsorbates employed in this study. The concentrations, both before and after the attainment of equilibrium; were determined with the aid of U.V. spectro photometric technique. The effect of initial drug concentration, temperature, contact time, solution pH, ionic strength and desoreption of the drug from the two surfaces was studied. The equilibrium sorption isotherms have been analysed by the Freundlich and langmuir models. The Freundlich isotherms had the highest correlation coefficients. The apparent thermodynamic parameters were calculated and the abtained values support the conclusion that the drug molecules sorbs by exothermic process. Drug adsorption was the highest at neutral pH value. The adsorbed amount of studied drug on attapulgite clay is decreased with increasing ionic strength, but adsorbed amount of the same drug on kaolin clay has of a limited influenced with increasing the ionic strength. In addition, kaolin, attapuglite clays were compared according to their efficiency of drug desorbing

INTRODUCTION

Solids have the property of holding the molecules at their surfaces, and this properly is quite marked in the case of porous and finely divided materials(1). Adsorption accurs on the surface of a solid because of the attractive forces of the atoms or molecules in the surface of the soild. Various forces are involved, ranging from those which are definitely physical in nature to those which are referred to as chemicals(2).

The medical importance of the active surface materials is based on its adsorptive property which has many applications like haemoperfusion for endo to xaemia (2,3), chromatography and extraction of drugs from urine or serum in order to be detected by

different methods in clinical Laboratories(4). Active surface materials may also be used as drugs, Kaolin, for example, acts as antidiarrheal and antiendotoxin agent in inflammatory bewel disease(5). The most important application of these materials (usually called adsorbents) in medicine is to use them as physical antidotes in the treatment of acute poisoning by toxic substances and drug overdosage (called adsorbates)(6,7)

Bisoprololhemifumarate is a cardio selective beta bloker. It is reported to be devoid of intrinsic sympathomimetic and membrance-stabilizing properties. Bisoprolol is given as the fumarate in the management of hypertension and angina pectoris. It is also used as in adjunct to standard therapy in patients with stable chronicheart failure(8,9).

The most common expected symptoms with overdosage of bisoprolol are bradycardia, hypotension, bronchospasm and hypogly - cemia. In the case of overdosage, bisoprolol treatment should be stopped and suportive and symptomatic treatment should be provided. One of the overdosage treatment is the resorption of bisoprolol in the gastrointestinel tract or administration of adsorbents. The use of standard adsorbents such as kaolin and attapulgite in the prevention of further absorption of drugs, are recognized in clinical practice. The safety, the high adsorptive capcity, there low density and the high specific surface, have been accepted for along time, and they account for most of the current uses of the two clays(10).

This study reports the experimental results for adsorption and desorption of Bisoprololhemifumarats drug. The adsorption date are tested for a number of isotherm equations. Moreover, the current study has been to visualize the pattern of adsorption of this drug on the two clays to various situations such as ionic strength,pH, temperature contact time and desorption.

MATERIALS AND METHODS

Materials

The drug used in this study was obtained from DSL chemicals. This drug is pure, and the melting point of this drug was measured practically (Digital melting point apparatus, GallenKamp, UK) 105 c^{o}.(structure 1). The empirical formula is ($C_{36}H_{64}N_2O_{12}$) with amolecular weight of (383.49) g/mol.(8.), and the maximum absorption for this drug was (224 nm).(11) the clay (attapulgite and kaolin) employed in this study were obtained from (The General company for Geological survey and mining.), Baghdad. The clays in powder forms were washed several times excessive amounts of distilled water. The two adsorbents were dried at (160C^{o}) in an oven (Hot Air oven, yamato Dp61, Japan) for 3h and then kept in airtight containers. The clays were

them ground and sieved (Electrical sieve, Retsoh Gmb & Co. KG Germany) by using test sieves (Retsoh Gmb &Co. KG, Germany) sieve. The partical size of 125 μm are used in further experiments.

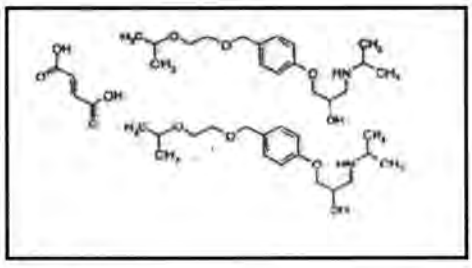

Figure -1: The structure of Bisoprolol hemifumarats drug

Method

Adsorption experiments were carried out by shaking 0.25 g from each clays samples with 12.5 ml aqueous solution of drug of desired concentration at various ionic strength (0.03,0.05M Nacl solution inwater), pH_s (pH of neutral medium, pH of stomach fluid which is equal to 1.2).(12) temperatures (17.5- 45 c^o) for 2 and ahalf hours (the required time for the drug to reach the equilibrium concentration). Athermostated shaker bath (BS. 11 degetal, JEIO TECH, Korea, (20-185) rpm (-10-120 c^o)$\pm$ 0.5 c^o), was used to keep the temperature constant. The initial concentration of drug solutes,C_o were in the range of ($2X10^{-5}$ – $9X10^{-5}$ mol/L). All adsorption experiments were preformed at 37.5 C^o and pH=6.0 except those in which the effects of temperature and pH of the solution were investigated. The pH of the solution was adjust with Hcl solution by using a (HM- 73, TDA Electronic Ltd. pH meter). At the end of the adsorption period. The solution was fillered by using double filter papers (Whatman No. 42, Germany). The concentration of the residual bisoprolol hemifumarat drug, Ce, was determined spectrophotometrically using a UV-visible recording spectrophotometer (100 Conc./ Varian, USA). The adsorbed amounts of drug were calculated from the concentrations in solutions before and after adsorption according to the equation (1) :-

$$Q_e = (C_o - C_e)\, V/W \qquad \ldots\ldots\ldots\ldots(1)$$

Where C_o and C_e were the initial and equilibrium liquid – phase concentration of drug solution (mgl/L), respectively, Q_e is equilibrium drug concentration on adsorbent (mg/L). V is the volume of drug solution (L), and W is the mass of clay sample used (g). For dsorption experiments, the remainder of the supernatant of the sorption flasks after setting was removed and (12.5ml) portions of eluent was added to the sorbent residue in each flask. The mixture was allowed to equilibrate for 1 hour in the shaker and the suspensions were centrifuged for 15 minutes (JANETZKI.T 130).

The concentration of the $\frac{C_e.V}{W}$ drug desorbed was determined in the

supernatant (13, 14).

The amount desorbed (mg\g)= .....(2)

Where C_e is the concentration of drug desorbed at equilibrium (mgIL), Vis the volume of eluent (L) and W represent the weight of adsorbent (g).

The percent of desorption was obtained from the following equation (3)

$$\text{Percent desorption} = \frac{amountofdrugdesorbed}{amountofdrugadesorbed} X100 \quad \text{.....(3)}$$

RESULTS AND DISCUSSION

In atwo – component system (sorbent and solution) a graph of the solute concentration in the solid phase Q_e (mglg)can be plotted as a function of the solute concentration in the liquid phase C_e (mg/L) at equilibrium. since the data for the curve are obtained at a single temperature, the curve is an isotherm.

In asolid – liquid system, positive sorption results in the removal of solute from the bulk solution and the concentration at the surface of the solid, until the remaining solute in the solution is in dynamic equilibrium with the solute on the solid surface.

At equilibrium there is a defined distribution of the solute between the liquid and the solid phase, which can generally be expressed by one or more isotherm (15). Figure(2) displays the istherms of adsorption related to bisoprolol hemifumarate drug from aqueous solution on kaolin and Attapulgite clays surfaces. It was seen that these isotherms fitted the Freundlich adsorption isotherm.

Experimental data were also applied to the Langmuir adsorption isotherm, but the linear state of the Langmuir adsorption isotherm was not obtained

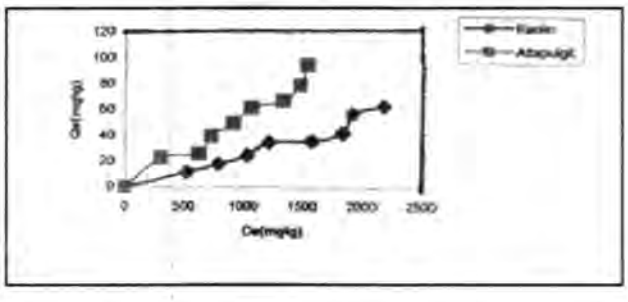

Figure - 2: Adsorption isotherms of Bisoprolol hemifumarat on the two clays surfaces from aqueous solution at (37.5 C°)

The R^2 values (goodness of fit criterion) computed by linear regression for the two types of isotherms are presented in table (1). For the two sorbets. This consistency is seen in freundlich linear adsorption isotherm drawn according to equation (4) (16).

$$\log Q_e = \log K + \frac{1}{n} \log C_e \quad \text{.....(4)}$$

Figure (3). k and n constants peculiar to adsorbent and adsorbate were determined from the intercept and slopes of freundlich linear adsorption isotherms (Table 2).

The k-constant is concerned with the ability of the adsorbent to adsorb, and the n-constant is concerned with tendency of the adsorbate to be adsorbed.

As can be seen in table (2), n-constants of the drug adsorbed on clay surface change in the order of attapulgite > kaolin.

It is seen that the n-constants obtained fit the Irving – Williams series because the stable system (adsorbent – adsorbate system) formed increases the ability of the adsorbate to be adsorbed and causes the n-constant to be high. This is compatible with our experimental results.

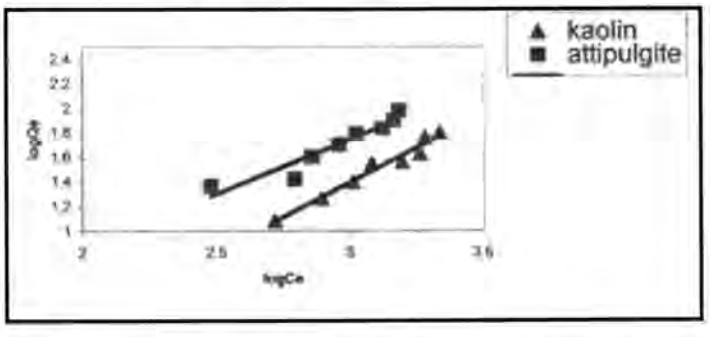

Figure - 3: Freundlich's linear isotherms related to adsorption of Bisoprolol hemifumarate drug from aqueous solution on the two clays surfaces.

Table - 1: Goodness of fit of the Freundlich and langmuir isotherm to the sorption experimental data-values corresponding to best fit isotherms.

Clays	R^2 values	
	Freundlich isotherm	Langmuir isotherm
Kaolin	**0.9655**	**0.463**
attapulgite	**0.9019**	**0.011**

Table - 2:Freundlich's constants related to adsorption of Bisprolol hemifumarate drug from aqueous solution by the two surface.

Adsorbent	**k**	**n**
Kaolin	0.010	0.8815
Attapulgite	0.119	1.125

Effect of pH

The adsorption of the drug extent is highly dependent on the pH of the solution, which affects the surface charge of the adsorbent, the degree of ionization, and specification of the adsorbate species. The adsorption isotherms at two various pH_s (pH of neutal solution and the other is equal to (pH=1.2) which is the value of the pH of stomach fluid are shown in figure (4) and (5). It is seen that the adsorbed amount of the drug on the two clays surfaces at 37.5 c^o has increased with increasing pH values. At low pH, a competition exerted by the hydronium ions is expected to cause a significant reduction in adsorption of the drug.In addition,the solubility of the adsorbate (drug molecules) may be effected by the changing of the pH value (from acidic to neutral) causing an increase in adsorption affinity towards the surface. On the other hand, the increase in adsorption uptake of the drug with increasing pH of solution could be attributed to the possible changes in properties of the surface.

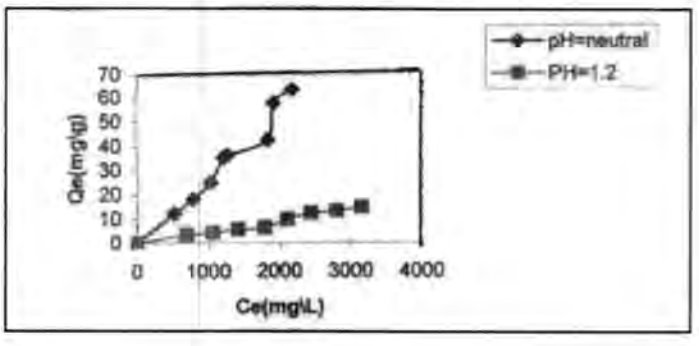

Figure - 4: The effect of pH on the adsorption of Bisoprolol-hemifumarate on kaolin surface at 37.5 c^o

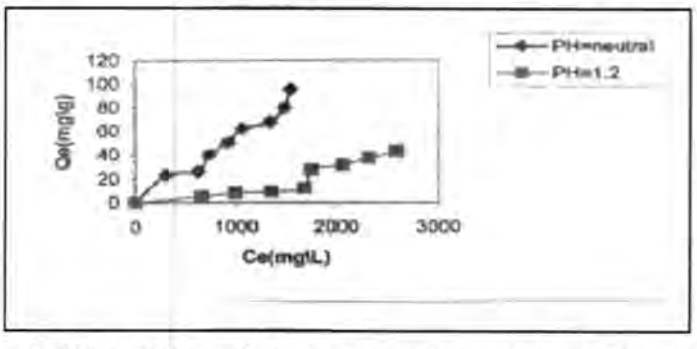

Figure - 5: The effect of pH on the adsorption of Bisoprolol - hemifumarate on attapulgite surface at 37.5 c^o

Effect of ionic strength

The effect of ionic strength on adsorption uptake of the drug on the two clays surface was studied at different salt concentration (0.03,0.05,M Nacl solution in water). As can be seen in figure (6,7),

there is no positive or negative correlation between the extent of adsorption of this drug on kaolin surface and the concentration of the salt used.

The result could be attributed to the nature of adsorbate – adsorbent binding.a type of electrostatic interaction may contribute to the binding between the negatively charged carboxylic group of the drug and the active sites of the surface, and that connection some what does not affect the presence of other ions in solution and this result is in agreement with those obtained by Terada et al., and A kintonwa et al(17) respectively. On the other hand, the adsorption extent of the same drug on attapulgite surface decreased with increasing the ionic strength. This behavior may due to the inhibition effect of salt used (Nacl) on adsorption extent.

Thus, the (Na^+),(cL^-) ions will compete drug molecules for the active sites which could be found on the surface. Moreover,the attraction between these ions and the surface is grater than the attraction between the drug molecules and the surface, therefore, the electrostatic attraction will decrease between the adsorbent and the adsorbate and that leads to decrease in the adsorption extant .

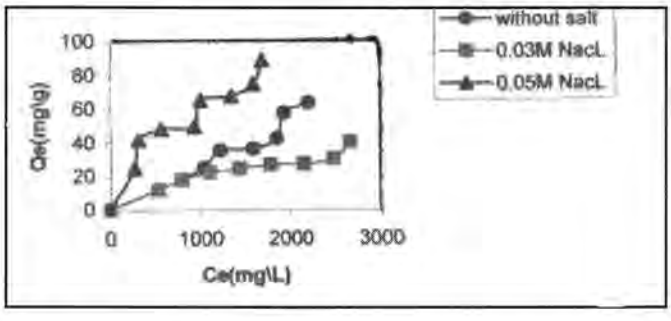

Figure - 6: The effect of ionic strength on the adsorption of Bisoprolol hemifumarate on kaolin surface at 37.5 c^o

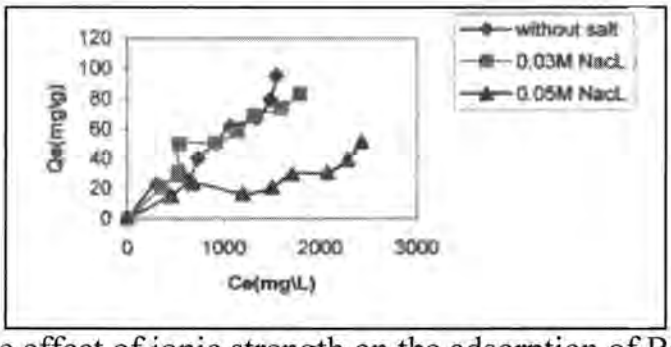

Figure - 7: The effect of ionic strength on the adsorption of Bisoprolol hemifumarate on attapulgite surface at 37.5 c^o

Effect of Temperature

The adsorption of Bisoprolol hemifumarate on kaolin and attapulgite clays at three different temperature has been carried out. The result are presented in figure (9,10)-variable temperatures study will help in evaluating the basic thermodynamical functions (Δ H, ΔG and Δ S) .

For the adsorption process. The adsorption values of bisoprolol on attapulgite clay surface showed asilight increase with decreasing temperature. This result agree with the general principles of adsorption process (18).

From the following equations (19,20), one can calculate the variations of apparent enthalpy (ΔH, Kj/mol), apparent free energy (ΔG, Kj/mol) and apparent entropy (ΔS, J/mol.k) of drug adsorption on attapulgite clay (table 4) according to equation (5-7), where R is the gas law constant and T is the absolute temperature.

$$\ln K = - \frac{\Delta H}{R.T} + \text{constant} \qquad \text{.....(5)}$$

$$\Delta G = - RT \ln k \qquad \text{.....(6)}$$

$$\Delta S = \frac{\Delta H - \Delta G}{T} \qquad \text{.....(7)}$$

Table - 3:The values (LnXm),(10^3\T) of Bisoprolol hemifumarate on attapulgite

tc^o	T(K)	10^3\T	Xm(mg\g)	LnXm
			Ce=250	
17.5	290.5	3.44	33	3.49
37.5	310.5	3.22	19	2.94
45	318	3.14	10	2.30

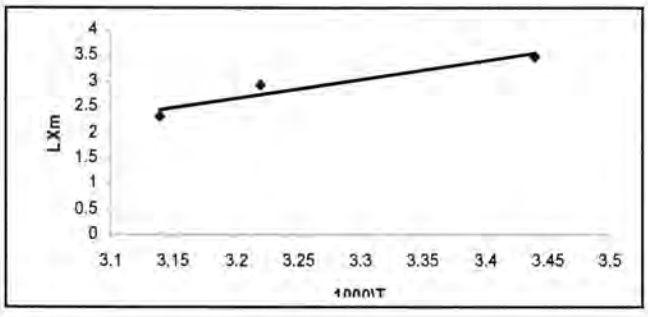

Figure - 8: (LnXm) plotted against,(10^3\T) for the adsorption of Bisoprolol hemifumarate on attapulgite

Table - 4: The apparent thermodynamic parameters of adsorption process of Bisoprolol hemifumarate on attapulgite surface at 37.5 c^o

Δ H Kj.mol^{-1}	Δ G Kj.mol^{-1}	ΔS J.mol^{-1}.k^{-1}
-33.25	-1.08	-103.60

Thermodynamic quantities of Bisoprolol – attapulgite system exhibited exothermic physical adsorption accompanied with the decrease in entropy as it shown in table (4) because of the fact that, the apparent (S) of the ordered constrained adsorbed layer is always less than that of dissolved solutes.Also, the negative value of (G) confirm that the reactive drug sorption on attapulgite clay is a spontaneous process. So all the basic thermodynamical function were found to possess negative values, and this result is agreement with previous studies (21).

On the other hand, the adsorption extent of this drug on kaolin has no significant differences found in the amount at the different temperatures.

It has been exhibited that the adsorption of this drug is of limited influenced with the increasing temperature in the studied range.

That can be explained depending on kaolin properties and the nature of the adsorbate indicating the possibility of formation strong interactive forces between the adsorbent and the adsorbate, as kaolin has a high colloids properties. Moreover,the possibility of the clay in saving solution inside its internal layers because of its highly plasticity and colloidlity would give diffusion property of materials in this surface. Therefore, the increasing in temperature in the selected rang showed a limit effect in this clay adsorption for this drug especially at higher concentration from solution (18).

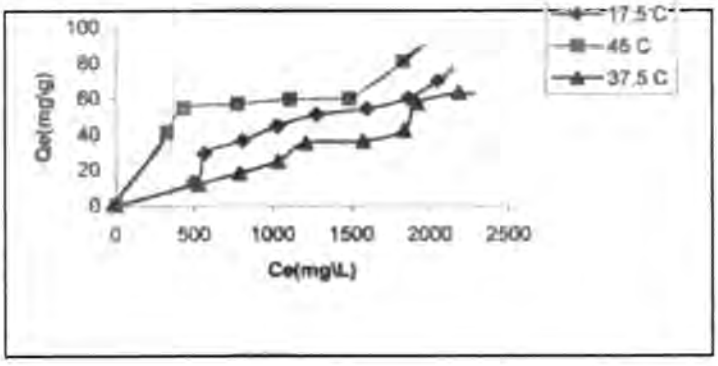

Figure -9: Adsorption isotherms of Bisoprolol hemifumarate on kaolin surface from aqueous solution at(17.5, 37.5 and 45 C°)

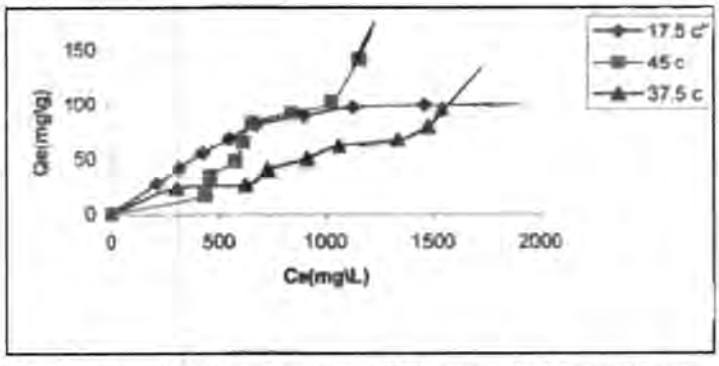

Figure -10: Adsorption isotherms of Bisoprolol hemifumarate on attapulgite surface from aqueous solution at(17.5, 37.5 and 45 c°

Desorption of the drug from the clays surfaces

The desorption is similar to adsorption process depending mainly on solution temperature, concentration of adsorptive, the condition of adsorptive and on the condition of the adsorbent surface. The possibility of desorption of the drug model (Bisoprolol hemifumarate) from the two clays surfaces (kaolin and at Attapulgite) was investigated using distilled water as an eluent to simulate in vivo conditions. The extent of drug desorption from the clays at (37.5 c°) increase as the concentration of the drug in its solution increase as its shown in (figure 11,12). This is due to the strong interaction of adsorbate – adsorbent system and the heterogeneity of the surface, which indicates the difficulty of the drug release at low concentrations.

The percent desorption after one washing procedure with distilled water was also determined. The results are summarized in table(5) by the amount of drug released in one elution step.

The release studies show the lowest percentage amount of drug desorbed from attapulgite which was equal to (31.7), while the same drug desorbed from kaolin clay has the higher percent which was about

(79.03) of the original amounts of bisoprolol hemifumarate drug. The little amounts of drug removed from attapulgite surface suggest the interaction of drug molecules with the surface may be specific and strong enough leading to a decrease in the quantity desorbed (22,23).

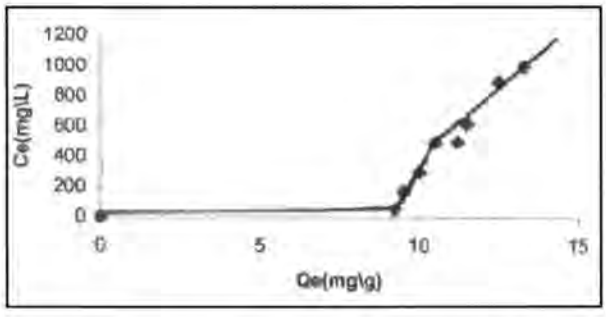

Figure -11 : Desorption isotherms of Bisoprolol hemifumarate drug from kaolin clay surface by distilled water at(37.5 c^{o})

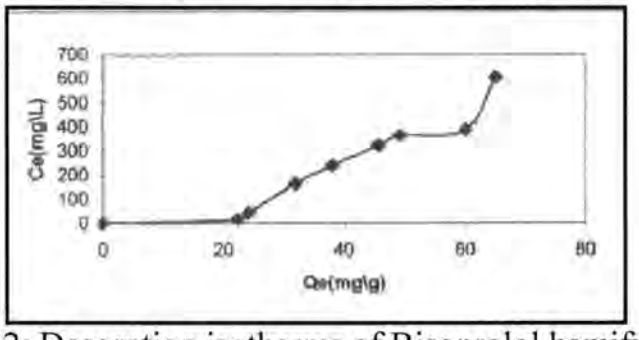

Figure - 12: Desorption isotherms of Bisoprolol hemifumarate drug from attapulgite clay surface by distilled water at(37.5° C)

Table -5: percent desorption of bisoprolol hemifumarate from clays surface with distilled water as an eluant at(37.5° C)

Adsorbent	Elution No.	Amount desorbed mglg	Percent desorption
Kaolin	1	50	79.03
attapulgite	1	30.33	31.70

We can conclude

- The experimental data correlated reasonably well with the Freundlinch adsorption isotherm and the isotherm parameters (k and n) were calculated.
- The contact time for the maximum adsorption required is nearly 2.5 hours.
- This study showed that at temperature of (37.5 c^{o}) the quantity of bisoprolol hemifumarate drug adsorbed by attapulgite clay is grater than that by kaolin clay.

- (bisoprolol- attapulgite) adsorption system exhibited exothermic process. While (bisoprolol-kaolin) adsorption system has of limited influence with increasing temperature in the studied rang.
- Both two clays adsorbed the mentioned drug poorly in acid medium as compared with neutral medium.
- The adsorbed amount of studied drug on attapulgite clay is decreased with increasing ionic strength, but adsorbed amount of the same drug on kaolin clay has of a limited influenced with increasing the ionic strength.
- The desorption abilities (the amount desorbed) of bisoprolol hemifumarats drug from clays surfaces at 37.5 c^{o} follow the order :

  Attapulgite < kaolin

REFERENCES

1. F.Daniels, "Experimental physical chemistry", (1970) .
2. F. Daniels and R-Alberty, " physical chemistry",(1961).
3. B.V.kirkin etal, Biomat Artif –cells – Artif –Organs. "Efficiency of hemosorption in treatment of patients with ulcerative colitis.",15 , :271-279,(1987).
4. M.Jhon , G, Thomas, Rosano, and Thomas, "Clinical Chemistry", 27(7),(1981).
5. K.R.Gardiner, etal, Gut. "Adsorbents as antiendotoxin agents in experimental colitis"., 34:51-55, (1993).
6. E-Chilvers,J.Hunter, and A.Nicholas,"Davidson's Priniciples and practice of Medicine ".,18th edition : 1110-1120,(1999).
7. B.Ditter,R.Urbaschek,and B. Urbaschek , Gastro enterology. "Ability of various adsorbents to bind endotoxins in vitro and to brevent orally induced endotoxemia in mice",84:1547-1552,(1982).
8. Heumann Pharma, Your Partner for outsoucing,http:// www. acdabs.com/ downlood/publ/2002/euml2002/Ce-methods.Pdf-microsoft-internet explorer.
9. Heible etal., α and ß –Adreno captors from the gene to the clinic -1-Molecular biology and adreno- captor sub classification., Med-chem. :38-3415,(1995).
10. R.H.S. Rebertson, "Industrialuses of clay minerals silic".. Silicate .Ind-38,33,43. (1973).
11. British Pharma copoeia CD-Rom-Monographs, Medicinal and pharmaceutical substances ,1,(2002).
12. T.Tsuchiya , and G.levy, "Relationship between effect of activated charcoal on crug absorption in man and its drug

adsorption characteristics in vitro".,J.pharm.Sci.61(4):586-589, (1972).

13. D.L. sorby , "Effect of adsorbents on drug adsorption".,J. Pharm . Sci, 54(5) : PP. :677-683(1965) .
14. E.Voudrias, K. Fytianos ,E. Bozani, "Sorption- desorption isotherms of dyes from aqueous solutions and wastewaters with different sorbent materials"., the int. J.4, (1):75-83,(2002).
15. A.Findon, G.Mckay ,and HS. Blair, "Transport studies for the sorption of copper ions by chitosan". J. of Environ. Sci. and Health A28(1): 173-185, (1993).
16. K.E. Noll, V. Gounaris and W.S. Hon, "Adsorption Technology for Air and water pollution control ", Lewis publishers, Inc., USA , (1992).
17. H. Terada, T.Miyoshi , and M. Imaki , Tokushima".Effect of several adsorbents on the gastronitinol absorption of paraquat" J.Exp. Med. , 41 (1-2) , PP. : 31-40, (1994) .
18. A.Adamson , physical chemistry of surfaces, wiley-Interscience pub., 4th ed.:369-398,(1984).
19. R.Qadeer, J. Hanif, "Temperature and concentration dependence of kineties of thorium adsorption on activated charcool from aqueos solutions" .,Journal of Islamic Academy of sciences , 7,1:56-60,(1994).
20. J.P. Divincezo, D.L. Sparks ,Arch ., "sorption of the neutral andcharged forms of pentachloro phenol on spil ; Evidenec fordifferent mechanisms"., Environ. Contam. Toxical 40: 445-450, (2001).
21. Y.C. Wu ,and copeland , l.E "Athermodynamic theory of adsorption chapter Book chepter" ., Adv- Chem. Ser., 33 : 348-356. (1961).
22. WF. Von – Ottingmen , Resent Research in Emergency Treatment of Acidental poisoning., In:A Guideto clinical Diagnosis and Treatment., Philadelphia WB sandos company 400, (1983).
23. OE., Orisakwe , A.oluboyo, Sofoefule, etal., "Adsorption studies of artesunate: evaluation of saline carthartics as additives in management of artesnate poisoning".,J.Health Sci, 47(5): 491-494(2001).

Photodegradation and Biodegradation of Poly(exo-Galactosene-co-styrene) and Poly (Exo-Galactosene-Co-Acrylonitrile

[1]Yousif Ali Al-Fattahi , [2]Salah M. Aliwi and [3]Hammed H. Mohamed
[1] Department of Chemistry ,College of Science . University of Baghdad
[2] Ministry of Higher Education & Scientific Research
[3]Department of Chemistry , College of Science , University of Al-Mustansiriah

الخلاصة

تم دراسة الأكسدة الضوئية للبوليمرات المشتركة :(poly (exo-galactosene-co-styrene و (poly (exo-galactosene-co-acrylonitrile في الحالة الصلبة بأستخدام الأشعة فوق البنفسجية (U.V) عند طول موجي λ = 313 nm , وقد تمت متابعة التجزئة الضوئية بالطرق الطيفية: (الأشعة تحت الحمراء (I.R) و الأشعة فوق البنفسجية (U.V. بأستخدام الثنائي بنزويل بيروكسايد 0.003 غرام/مل) اظهرت البوليمرات تغيرا في اطياف امتصاص الأشعة فوق البنفسجية (U.V) و الأشعة تحت الحمراء (I.R) , وخاصة في منطقة امتصاص مجموعة الكاربونيل عند التشعيع الضوئي, حيث اضهرت اطياف الأشعة تحت الحمراء (I.R) ان نسبة الأمتصاصية A_{co}/A_{1600} تزداد مع ازدياد زمن التشعيع , واظهر البوليمر المشترك المحضر زيادة سريعة في امتصاص مجموعة الكاربونيل . لقد وجد بأن التجزئة الضوئية للبوليمر poly(galactosene-co-styrene) هي اسرع من البوليمر poly (exo-galactosene-co-acrylonitrile) وهذا فسر بواسطة زيادة امتصاص الضوء في الطول الموجي المشع (313 نانوميتر).
تم دراسة التجزئة الحيوية للبوليمرات المتجزئة ضوئيا بواسطة البكتريا المعزولة من النفط (*Pseudomonas aeuroginosa RB-19*) , ان مصدر الكاربون هو البوليمر المتجزء , حيث ان البكتريا قادرة على استهلاك البوليمر المشترك المحضر.

ABSTRACT

The photodegradation of poly (exo-galactosene-co-styrene) copolymer in dichloromethane and in benzene solution was studied using dibenzoyl proxide as photosensitizer. It was observed that higher photodegradation rate of the copolymer in dichloromethane compared with benzene solution. Decreases in relative and specific viscosity were also observed in the irradiated polymers where the viscosity decreased in the presence of dibenzoyl peroxide and benzophenone photosensitizers , and also with increased concentration of dibenzoyl peroxide with irradiation time .
The photodegradation of poly (exo-galactosene-co-styrene) and poly (exo-galactosene-co-acrelonitrile) was investigated in solid state using u.v.-radiation at λ = 313 nm . The photodegradation rate is followed by U.V. and I.R spectrophotometry using dibenzoyl peroxide (0.003 g/mL). The copolymers showed a change in their I.R and U.V. absorption spectra, especially at the carbonyl absorption region. Upon photoirradiation, the I.R spectra showed that the absorbance ratios A_{co}/A_{1600} have increased with irradiation period, whereas the copolymer showed the most rapid increase in carbonyl group absorbance.
The rate of photodegradation of poly (exo-galactosene-co-styrene) is higher than the rate of photodegradation of poly (exo-galactosene-co-acrylonitrile) in solid state which was explained by the higher light absorption at the irradiated wavelength (313 nm).
The biodegradability of photodegradable polymers has been also studied using isolated bacteria from crude oil (*Pseudomonas aeuroginosaRB-19*).This type of bacteria is known to be capable of utilizing the degraded copolymers.

INTRODUCTION

Recently the critical discussion about the preservation of natural resources and recycling has led to the renewed interest concerning biomaterials with the focus on renewable raw materials because of increasing environmental consciousness and demands of legislative authorities. Biodegradable polymers have offered scientists a possible solution to waste-disposal problems associated with traditional petroleum-derived plastics(1). biodegradable polymers have currently attracted high interest as ideal carriers in drug delivery and tissue engineering applications. In situ forming devices based on these materials will synergistically provide the advantages of the customary prefabricated devices as well as ease of administration(2)

During UV-irradiation of polymers the concentration of functional groups on the chain ends and inside macromolecules (double bonds and carbonyl groups) increases. It probably makes polymers more susceptible to attack of bacteria in natural environment. It is also well known that the efficient main chain scission in irradiated polymers causes their mechanical deterioration and breaking on to small pieces. Thus, the access of oxygen and microorganisms is facilitated to the bulk of such destroyed products. In this way polymers become biodegradable(3).

The biological degradability is defined as the transformation and deterioration of polymers solely by living organisms (including microorganisms and /or enzymes excreted by microorganisms)(4) . The biochemical attack on polymers can occur at the side chain and /or directly at the backbone. In the first instance the properties are certainly altered, but basic polymeric structure may be retained and the material is not degraded. The reduction in molecular mass is an essential requirement for polymers in order to serve as nutrient for microorganisms because only low molecular substances can be transported into the cells and incorporated in internal cycles(4) .The aim of this work study the biodegradation of photodegraded copolymers, this type of copolymers have found useful applications: in medicine and industry. Study of their either UV-light degradation or biodegradation may give an understanding of their application as degradable saccharide-polymers .

MATERIALS AND METHODS

Polymers

The copolymers poly(exo-galactosene-co-styrene) **(I)** and poly(exo-galactosene-co-acrylonitrile) **(II)** was prepared and had been photodegraded as described previously(5)

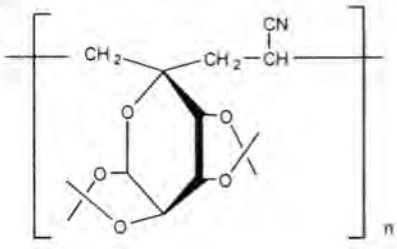

(II)

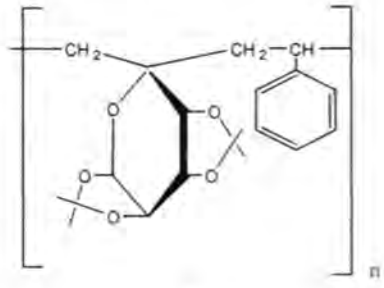

(I)

Experimental techniques:

Film preparations

0.05 g/mL of poly (exo-galactosene-co-acrylonitrile) (II) in dimethyl sulfoxide (DMSO), poly (exo-galactosene-co-styrene) (I) and polystyrene in dichloromethane solvent with and without dibenzoyl peroxide (DBP) (0.003 g/mL), as photosensitizers are used to prepare polymer films (85 μm in thickness), casting on plate (from NaCl salt, 3.41mm thickness)at room temperature for 24 hr to remove the residual solvent. The film samples were further dried at room temperature. The film samples were fixed on a special holder for irradiation (which is an aluminum plate (0.6mm) in thickness supplied from (Q-panel) company U.S.A.)

Irradiation experiments

Accelerated testing technique

The accelerated weather-o-meter, Q.U.V. tester, (Q panel company, U.S.A), was used for irradiation of polymer films. The accelerated weathering tester contains stainless steel plate with two cavities in the front and rear sides.

Each side contains four lamps, type (U.V.B. 313), located horizontally, giving spectrum range of wavelength between (290 to 360)nm, and the maximum intensity is located at (313) nm .

The polymer film holders are fixed vertically and paralleled to the lamps, so that U.V radiation is vertically incident on the polymeric samples. The irradiated sample holders were changed in positions from time to time to ensure that all samples received the same intensity of light, the temperature of the tester chamber is constant at 50 °C for all samples .

During the irradiation process, the degree of photodegradation of the polymer films was monitored, by taking different exposure times.

Photodegradation measuring methods

A- Measuring the photodegradation rate of polymer film using infrared spectrophotometery.

The photodegradation of the polymer film was followed by I.R spectrophotometer. The absorption spectra of the film samples were recorded in the wavenumber ranged from 600 to 4000 cm^{-1}. The position and the growth of the carbonyl absorptions for polymer (I) and polymer (II) were monitored at (1730 and 1790) cm^{-1} respectively. The photodegradation during different irradiation times was followed by recording changes in the carbonyl and benzene ring absorption peaks (1730 and 1600 cm^{-1}) respectively. To eliminate experimental errors, the carbonyl indices were calculated using the band index method , by comparing the (IR) absorption peaks at the specified positions, with a reference peak (i.e. at 1600 cm^{-1}) which refers to the (C=C) bond of aromatic bending vibration poly (exo-galactosene-co-styrene), at (2200 cm^{-1}) which refers to the cyanide stretching ($C \equiv N$) in poly (exo-galactosene-co-acrylonitrile)

$$I_S = \frac{A_S}{A_r} \qquad \text{.....(1)}$$

Where:

A_S = Absorbance of the peak under study.

A_r = Absorbance of the reference peak.

I_S = Index of the group under study.

The absorbance (A) is calculated from the recorded percentage transmittance using Beer's-Lambert law as shown in the following equation.

$$\left.\begin{aligned} A &= \log(100/T\%) \\ A &= \log(100) - \log(T\%) \\ A &= 2 - \log(T\%) \end{aligned}\right\} \qquad \text{.....(2)}$$

Actual absorbance, the difference between the absorbance of the base line and the top peak, ($A_{top\ peak} - A_{base\ line}$) is calculated using the base line method

B- Photodegradation rate measurments of polymer films using ultraviolet-visible spectrophotometry.

The ultraviolet-visible spectrophotometer technique was used to measure the changes in the UV-visible spectrum during irradiation times for copolymers. The absorption spectra were recorded in the wavelength range from 200 to 600 nm and the (λ max) at each absorption peak was also recorded for different irradiation times.

Biodegradation method

Bacteria isolated from crude oil, type *Pseudomonas aeuroginosa RB-19* was grown on irradiated polymers,poly (exo-galactosene-co-styrene) without and with photosensitizer (DBP),and poly(exo-galactosene-co-acrylonitrile) with photosensitizer (DBP) as a sole source of carbon and energy in order to ensure their ability to utilize them. Five milliliters of mineral salt medium (table 1) distributed in 25 mL tube. The tube was sterilized by autoclaving at 120 °C for 15 minute, then it was taken to the isolated bacteria. All the tubes were inoculated with 1% of fresh culture (18hrs.), then 1g/Lof polymer was added and incubated with shaking (180 rpm) at 37°C for two weeks.

Table -1: Mineral Salt Medium for growth bacteria type *Pseudomonas aeruginosa Rb-19(6)*

Salt	Weight(g)
K_2HPO_4	1.170
KH_2PO_4	0.121
$MgSO_4.7H_2O$	0.121
NH_4CL	2.140
$FeSO_4.7H_2O$	0.28
$MnSO_4.4H_2O$	0.06
H_3BO_3	0.005
$ZnSO_4.7H_2O$	0.01
$CuSO_4.5H_2O$	0.061
$Co(NO_3)_2.6H_2O$	0.06
$NiSO_4.7H_2O$	0.00006
Distilled water	1000 mL

The pH was adjusted to 7.5 by buffer solution (K_2HPO_4 1.17g and KH_2PO_4 0.121g in 100mL).

Bacteria strains

The bacteria strain used in this study is :

Bacterial strain	phenotype
Pseudomonas aeruginosa Rb-19	Neo^r., sm^s

Neo^r : neomycin resistant

sm^s : streptomycine resistant

RESULTS AND DISCUSSION

Photodegradation of poly (exo-galactosene-co-styrene) in solid state.

Photooxidative degradation of poly (exo-galactosene-co-styrene), occurs by irradiation in a broad spectral range between 254 to 400 nm at different time intervals. Initiation of the photo-oxidative degradation of copolymer is attributed to the absorption of U.V-light by different chromophoric impurities such as peroxide groups in the polymer chain formed during the polymerization process of monomers, by reaction of oxygen with copolymer growing radicals. It must therefore be concluded that the chromophore responsible for absorbing at 313nm is a charger-transfer complex involving oxygen and the aromatic nuclei. Aromatic molecules form such complexes absorbing in this region of the spectrum . The concentration of charge-transfer complex depends on two factors, the diffusion rate of oxygen in the polymer and the equilibrium constant for the reaction. The interplay of these two conditions explains the variation in amount of light absorbed at 313nm by different copolymers.

The difference between irradiated and unirradiated spectra is given to show the newly produced species clearly (i.e. ketones compounds). The increase in intensity above wavelength λ=300nm is assigned to the formation of carbonyl groups by photooxidation of polymer.

The production of hydroperoxides which themselves absorb at 313nm is the first step in the oxidative break down of the polymer. At some stage in the reaction, the concentration of hydroperoxidative reaches such a level that this functional group becomes the major absorber of incident radiation and the photo-induced decomposition of the hydroperoxide becomes the predominant reaction. It is proposed that in an immobile phase such as a polymer film .

In the IR spectrum of photoirradiated copolymer (I) films, the absorption bands in the wavenumber range (1690-1800) cm^{-1} increase in intensity with the increase of the irradiation time which has been attributed to the creating of carbony groups of ketones compounds. The peak centered at 1730 cm^{-1} is assigned to carbonyl vibration. In this time, the concentration of (OH) group in the polymers, in general, is smaller.

The U.V-visible and IR spectra of the poly (exo-galactosene-co-acrylonitrile) without photosensitizers show no change in the spectra.

When the photosensitizer DBP (0.003 g/mL) was added to the copolymers, the ultraviolet-visible spectral changes during photolysis of copolymers. For poly (exo-galactosene-co-styrene) the growth in absorption of carbonyl group at wavelength between 300 to 375 nm. The observed overall increase in U.V. absorption is probably taking

place due to the generation of different types of other chromospheres in copolymer (I) such aromatic ketones, hydro- peroxides, etc.
The U.V-visible spectral changes in poly (exo-galactosene-co-acrylonitrile) indicates a decrease in intensity of absorption band between 240 to 300 nm which might be attributed to the formation of hydroperoxide and ketones in the polymer backbone and also to break down in polymer chain. The physical properties of photosensitizers and polymers have a pronounced effect on the photodegradation efficiency of polymers. The most important property is the compatibility i.e. any type of photosensitizer (photodegradation inducer, photooxidant....etc) must be evenly distributed within the polymer matrix, which requires that it is compatible with polymer matrix(7,8).

The photodegradation rate of polymers can be followed by (IR) spectra from growth of the carbonyl group (i.e. measuring the I_{co} index) while growth of the hydroxyl group was smaller.

In the (IR) spectra of photoirradiated copolymer (I) films the intensity of the absorption band of carbonyl group appeared at 1730 cm^{-1} increases with the increase of the irradiation time. This is in agreement with the result obtained from the changes in the U.V-visible spectral where the increase in the absorbent between (300-375) nm .
In the IR spectrum of irradiated copolymer (II) ,the band located at 1790 cm^{-1} increased which could be assigned to carbonyl group absorption resulting from the attack of atmospheric oxygen on the free redicals formed on irradiation.

The carbonyl group formation was compared in this region (1730 and 1790 cm^{-1}) by calculating the carbonyl index (I_{co}), and are used to follow the extent of polymer photodegradation during the irradiation process. The effect of dibenzoyl peroxide (DBP) on the rate of carbonyl formation(I_{CO}) are shown in table (2) and figure (1).

Table -2 :Calculated values of the carbonyl index (I_{co}) with irradiation time for polymers films (85 μm in thickness) containing DBP (0.003 g.mL) at 50 °C.

Polymers	Irradiation time (hr)				
	0	50	90	170	300
Copolymer(I)	0.15	0.67	0.76	0.83	0.92
Copolymer (II)	0	0.50	0.11	0.15	0.18

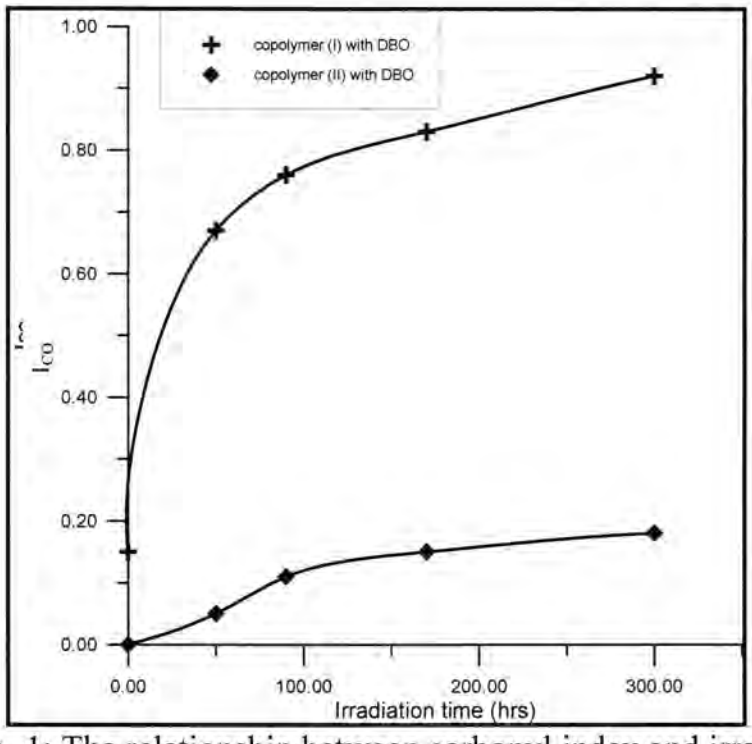

Figure -1: The relationship between carbonyl index and irradiation time for polymers (85 μm in thickness) with 0.003g/mL DBP

Therefore,the dibenzoyl peroxide is acting as photodegradation inducer for copolymers films .
Dibenzoyl peroxide (DBP) under UV-irradiation undergoes decomposition to benzyl radicals, which are unstable and rapidly fragmentated to CO_2 molecule and creating phenyl radicals.

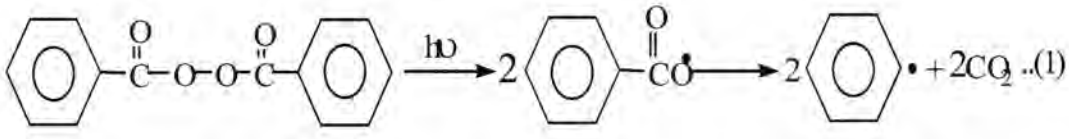

...(1)

These radicals in contact with polymer molecules form macroadicals and non- reactive benzene molecules. In this way, the action of this photoinitiator may be rapidly diminished.

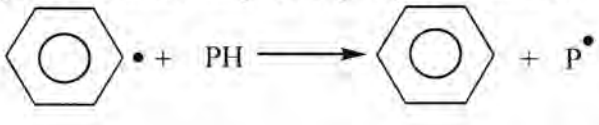

...(2)

The recombination of radicals generated from DBP with phenyl radicals leading to phenyl benzoate is also possible resulting of cage effect.

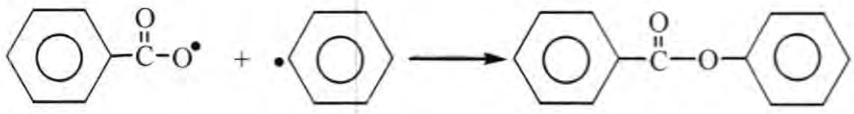

....(3)

When the rate of photodegradation between poly(exo-galactosene-co-styrene) and poly (exo-galactosene-co-acrylonitrile) is compared , it has found from carbonyl index results, the rate of photodegradation of poly (exo-galactosene-co-styrene) is higher than poly (exo-galactosene-co-acrylonitrile). This could be attributed to the most effective light absorption at the irradiated wave -length .

Acoording to the experimental results which are already discussed ,the following mechanism might be suggested for the photodegradation process of poly(exo-galactosene-co-styrene) and poly (exo-galactosen-co-acrylonitrile) in presence DBP photosensitizer(5).

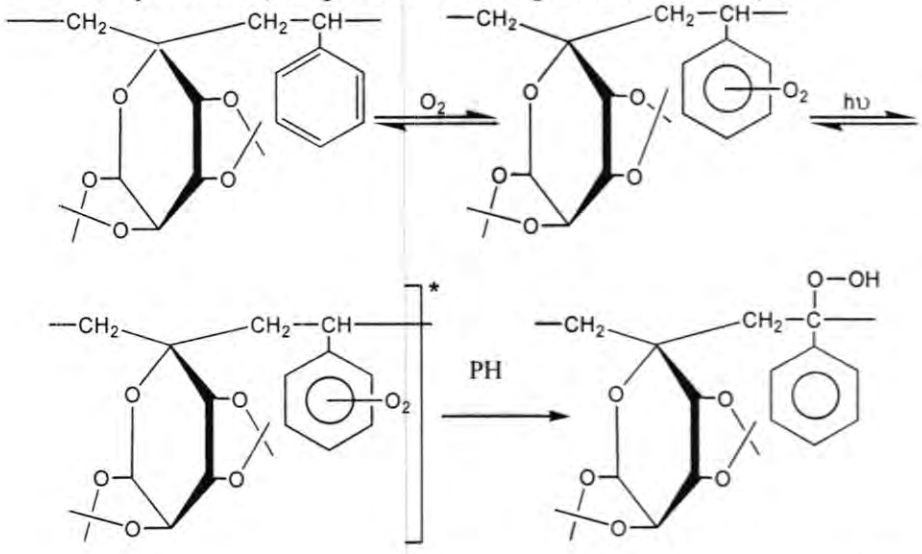

....(4)

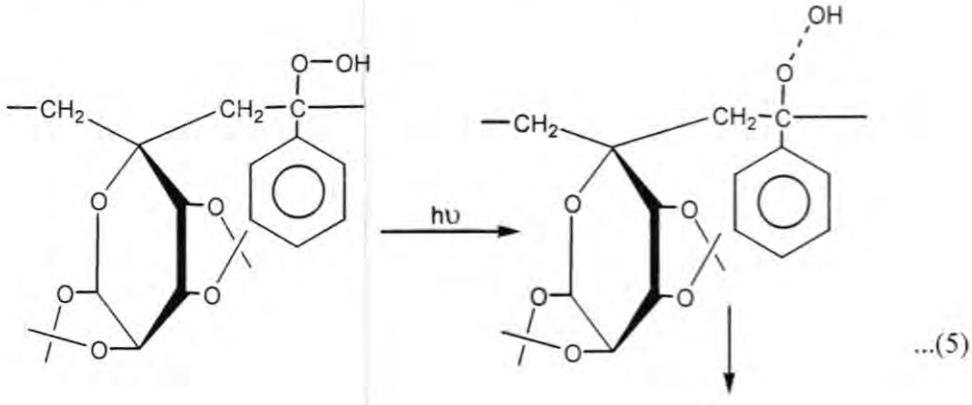

...(5)

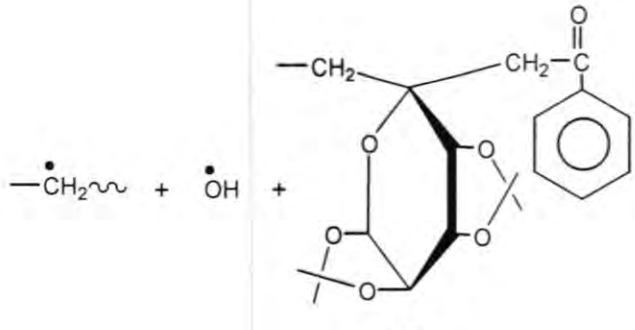

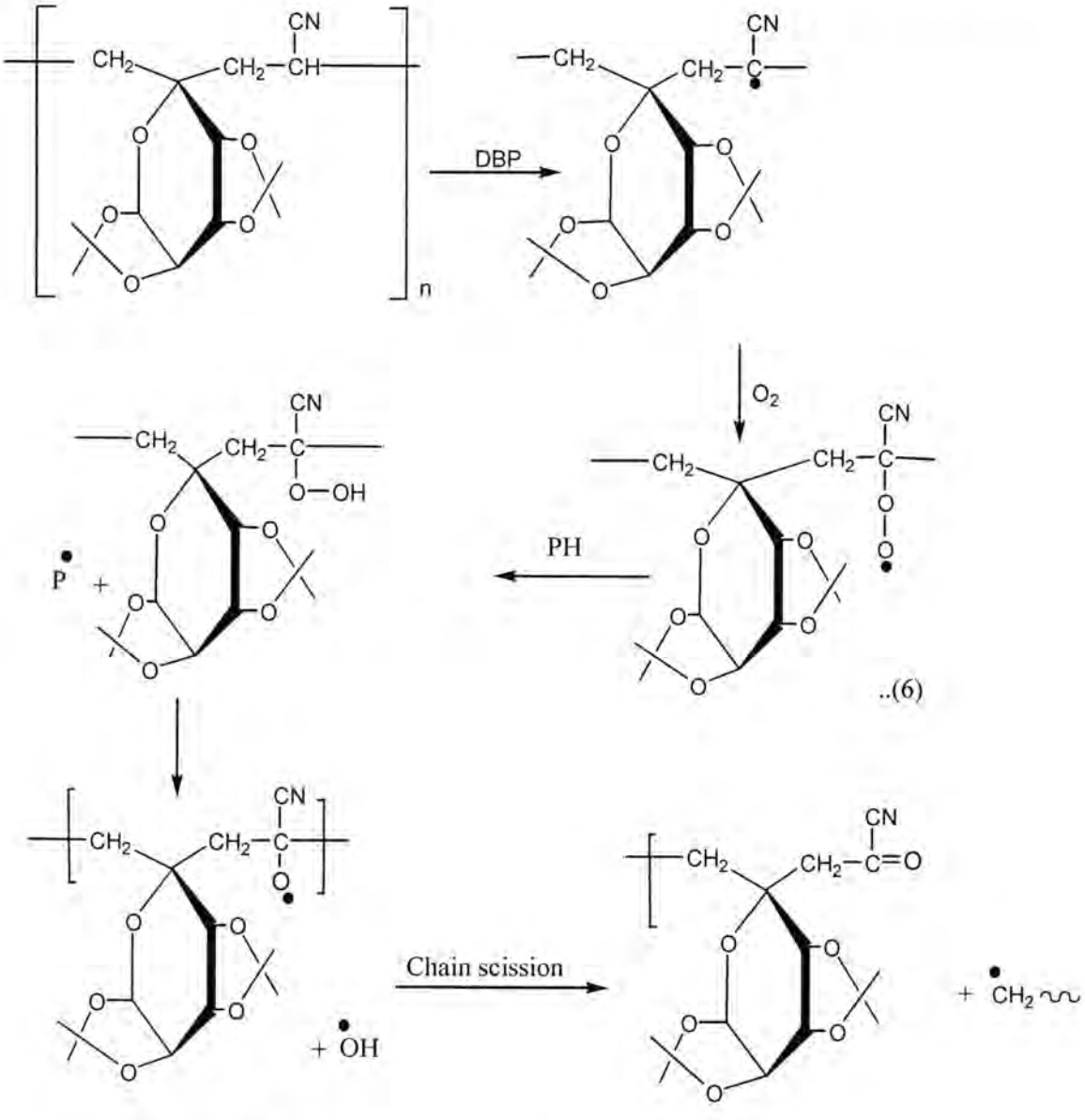

PH : polymer molecule

Scheme -1:Suggested mechanisms of photodegradation process for poly (exo-galactosene-co-styrene) and poly (exo-galactosen-co-acrylonitrile) in presence DBP photosensitizer

Biodegradation of polymers

The bacteria, *Pseudomonas aeuroginosa RB-19*, used in this work, was isolated from crude oil is utilizing aliphatic and aromatic hydrocarbons(such as phenol and n-hexane). In order to ensure that the isolated bacteria was indeed capable to growth in procure of irradiated polymers (as the sole available carbon source),a series of experiments were carried out in which the growth in the polymer environment was compared with that in control (mineral medium free of carbon source) , A typical result are shown in table (3)

Table – 3 :Growth of bacteria on polymers after 300 hours photolysis

Compounds	Bacterial growth	% loss weight
Vinyl sugar	3	50%
Polystyrene	1	10%
Poly (exo-galactosene-co-styrene) without DBP	1	10%
Poly (exo-galactosene-co-styrene) with DBP	4	80%
Poly (exo-galactosene-co-acrylonitrile) with DBP	4	75%

ASTM rating: (9)
(0) = no visible growth , (1) = 10% surface growth , (2) = 10-30% surface growth, (3) = 30-60% surface growth , (4) = 60-100% surface growth

It was concluded from such data that these bacteria were indeed capable of a significant amount of growth when the only carbon source present was the polymer.

Color changes from colorless solution to green solution indicate to microbial growth. The biodegradation are followed by percentage weight loss of polymer after biodegradation, where the polymer precipitated from bacterial solution by ethanol ,then dried under vacuum.

%loss weight = weight of polymer before biodegradation - weight of polymer after biodegradation

In general, during UV-irradiation of polymers the concentration of functional groups on the chain ends and inside macromolecules (double bonds and carbonyl groups) increases. It probably makes polymers more susceptible to attack by bacteria in natural environment. It is also well-known that the efficient main chain scission in irradiated polymers causes their mechanical deterioration and breaking on to small pieces. Thus, the access of oxygen and microorganisms is facilitated to the bulk of such destroyed products. In this way polymers become biodegradable.

From above results, the irradiation polymers contain dibenzoyl peroxide photosensitizer (DBP) was biodegradaded higher than irradiation polymer without sensitizer where sensitizer increases photodegradation of polymer into small species ,then the molecular weight was reduced. This results agreement with litertures10,11,12.The conclusion of this work that polymer fragments produced by photodegradation of certain plastic molecules indeed attacked and metabolized by soil microorganism. The vinyl sugar units increases the biodegradation of copolymer compared with polystyrene.

The use of biodegradation offers a cheap method for recycling nutrients efficiently and , when optimized, at a faster rate than under natural conditions. It would appear to be low in its energy requirements.

The photodegradation of poly (exo-galactosene-co-acrylonitrile) in presence dibenzoyl peroxide was studies in this work, and compared with degradation of poly (exo-galactosene-co-styrene) using carbonyl index values , where we found the rate of degradation of poly (exo-galactosene-co-styrene) is higher than the rate of degradation of poly (exo-galactosene-co-acrylonitrile) which is due to the effective light absorption at the irradiated wavelength.

By using repetitive transfer to mineral media in which the only carbon source is degraded polymer, some of the bacteria isolated are of genera which are known to attack both aliphatic and aromatic hydrocarbons. These results confirm that polymer fragments produced by photodegradation of certain plastic molecules indeed attacked and metabolized by soil microorganism. The vinyl sugar units increases the biodegradation of copolymer compared with polystyrene.

The use of biodegradation offers a cheap method for recycling nutrients efficiently and , when optimized, at a faster rate than under natural conditions. It would appear to be low in its energy requirements.

REFERENCES

1. Mohanty A.K., Misra M. and Hinrichsen G., "Biofibres, biodegradable polymers and biocomposites: An overview", Macromolecular Materials and Engineering, 1: 276-277 ,(2000)
2. Doulabi A.S.H., Mirzadeh H., Imani M., Shahriar S., Atai M. and Ataei S.M., "Synthesis and preparation of biodegradable and visible light crosslinkable unsaturated fumarate-based networks for biomedical applications", Polymers for advanced technologies, 19 , 1199, (2008) .
3. Scott G. , ICS- INDO Report. "Environmental Degradable Plastics". :20-24 March, (2000).
4. Fritz H.-G., Seidenstucker T., Bolz U., Juza M., Schroeter J. and Endres H.- J., " Study on Production of Thermolastics and Fibres Based Mainly on Biological Materials", Stuttgart, June (1994).
5. Yousif. A. Al-Fattahi ,Salah. M. A. and Hamid H. M., Ph.D Thesis , " Copolymerization of Vinylic Carbohydrate Monomer as Photo and Biodegradable Copolymer", University of Al-Mustansiriah, (2007) .
6. Unichiyama H. and Tabuchi T., "Aerobic degradation of trichloroethylene at high concentration by a methan utilizing mixed culture, Agric. Boil. Chem., 53 , 1019, (1988).
7. Chai Z., Sun R. and Karasz F., "Miscibility in blends of branched copolymers", Macromolecules, 7, (28) 2297, (1999).
8. L. Utracki A., "Polymer blends and alloys", New yourk, (1990).

9. Fritz H.-G., Seidenstucker T., Bolz U., Juza M., Schroeter J. and Endres H.- J., " Study on Production of Thermolastics and Fibres Based Mainly on Biological Materials", Stuttgart, June (1994).
10. H. Unichiyama and T. Tabuchi, "Aerobic degradation of trichloroethylene at high concentration by a methan utilizing mixed culture", Agric. Boil. Chem., 53 , 1019 (1988).
11.. Salah M. A., Tariq. S. N. and Zainab N. M., PhD .Thesis," Induced Photodegradation of Some Cellulose Derivatives" AL-Mustansiriah Univerisity ,(2006) .
12. T.Artham and M.Doble, "Biodegradation of aliphatic and aromatic polycarbonates", Macromolecular Bioscience, 8 , 14, (2007) .

Synthesis of 1, 2, 3-Triazole Compounds Derived from 4-Amino Benzoic Acid

Rafah F.Al-Smaisim[1]; Abdul Hussain K. Sharba[2] ; Redha I.Al-Bayati [2]
[1] Al-Mustansirya University of \College of Pharmacy
[2] Al-Mustansirya University \College of Science/ Chemistry Department

ABSTRACT

This work involves the synthesis of some 1,2,3-Triazoles derived from 4-aminobenzoic acid were synthesis 4-azido benzoic acid **[1]** synthesis by the action of sodium azide on the diazonium chloride salt, 4-(4-amino-5-cyano-1*H*-1,2,3-triazol-1-yl)benzoic acid **[2]** then 1-(4-carboxy-phenyl)-5-methyl-1-H-[1,2,3] triazole-4-carboxylic acid **[3]**by reaction of **[1]**with ethyacetoacetate and malonitrile; respectively in sodium ethoxide using absolute as a solvent. reaction of **[2]**with thionyl chloride to give acid chloride derivative **[4]**, followed by conversion into the corresponding acid hydrazide derivative**[5]**, carboxylic acid thiosemicarbazide **[12]**, esters **[15-17]**, thioesters **[18]**, **[19]**, and amides **[20-22]**, when treated hydrazine hydrate, thiosemicarbazide, alcohols, alkylthiol and secondary amines in dry benzene; respectively. Then compound **[5]** reflux with various aldehydes and ketons to give a number of Schiff's bases **[6-10]**. Furthermore, 1,2,4-triazole derivative **[13]** have been also prepared by refluxing thiosemicarbazide derivative **[12]** with sodium hydroxide solution (4%) then acidify with (10%)HCl . Moreover, a thiadiazole derivative **[14]** has been prepared by treatment of thiosemicarbazide derivative **[12]** with concentrated sulfuric acid as cyclyzing agent. Finally, oxadiazole derivative **[11]** has prepared by condensation of its acid hydrazide derivative **[5]** with carbon disulfide in basic medium.

الخلاصة

يتضمن هذا البحث تحضير بعض مركبات3,2,1-ترايازول مشتقة من 4-امينو حامض البنزويك.حيث تم تحضير المركب 4-ازيدو حاض البنزويك **[1]** من مفاعلة ازيد الصوديوم و ملح كلوريد الدايزونيوم للحصول على المركب 4-(4-امينو-فنيل)-5-سيانيد-1*H*-3,2,1-ترايازول) حامض البنزويك **[2]** و1-(4-كاربوكسي-فنيل)-5-مثيل-1*H*-3,2,1-ترايازول) حامض البنزويك [3] بالتفاعل مع اثيل اسيتو اسيتيت و مالونونايتريل على التوالي, في ايثوكسيد الصوديوم و الايثانول كمذيب.تضمن البحث مفاعلة المركب**[2]** مع كلوريد الثايونيل للحصول على مشتق حامض الكلوريد **[4]** و بعدها تم تحويل هذه المشتق الى مشتق الهايدرازيد **[5]**, ثايوسميكاربازايد حامض الكاربوكسيل **[12]** استرات **-[17]** **[15]** استرات الثايول **[18]**, **[19]** و الامايد **[20-22]**و بالمفاعلة مع الهايدرازين, الثايوسمي كاربازايد, الكحولات, ثايولات الالكيل, و الامايدات في البنزين الجاف, على التوالي.كذلك تضمن تحضير عدد من قواعد شف,**[6-10]** وذلك بمعاملة المركب **[5]**مع عدد من الاديهايدات و الكيتونات الاروماتية المختلفة,تم ايضا تحضير مشتقات 1,2,4-الترايازول عن طريق مفاعلة مشتقات الثايوسيميكاربازايد **[12]** و مع محلول هيدروكسيد الصوديوم (4%) ثم تحميض الناتج باستخدام حامض الهيدروكلوريك (10%) حيث حصلنا على المشتق **[13]** .و ضمن هذا المحور ايضا تم تحضير مشتق الثايادايزول **[14]** من معاملة مشتق الثايوسيميكاربازايد **[12]** و مع حامض الكبريتيك المركز. اخيرا و ضمن نفس الاطار تم تحضير مشتق الاوكسادايازول, حيث حضر المشتق **[11]** من تتصعيد مشتق هيدرازيد الحامض **[5]** مع CS_2 و KOH في الايثانول المطلق.

INTRODUCTION

The 1,2,3-triazole unit is an important element in a number of drugs and development candidates.

The triazole is a structural backbone of many therapeutic value as cytostatic (1), human (GABA) receptors antagonists (2) and antiproliferative agents (3). Also as synthetic intermediates for antibiotics agents (4), antihistaminic agent (5), muscarinic agonists for the treatment of Al-zheimers disease (6), anti human immunodeficiency virus (HIV) (7).4-Aminobenzoic acid was chosen as the starting material for the synthesis of 1,2,3-triazole

derivatives and their heterocyclic congeners such as 1,2,4-triazole, 1,3,4-thiadiazole, and 1,3,4-oxadiazole compounds. All the synthesized compounds have been identified via their physical properties and their spectroscopic data such as IR, U.V., and H^1 NMR spectroscopy for some compounds.

MATERIALS AND METHODS

Apparatus and Chemicals

Electrothermal 9100 melting point apparatus, Perkin-Elmer 1310 infrared spectrophotometer or a Shimadzu FTIR-800, as KBr discs or thin films, UV-Visible Varian UV-Cary-100 spectrophotometers were used in this work.^{1}H-NMR spectra was recorded on spectrometer (200MHz) at Silicone Research Center at Wisconsin University, USA. Tetramethylsilane was used as an internal reference and DMSO as solvent. All the chemicals used were supplied by Merck, Fluka and BDH chemicals. The solvents were purified by distillation and dried with calcium chloride.

Synthesis of compounds:

Synthesis of 4-Azidobenzoic acid[1](8):

4-Aminobenzoic acid (0.01 mole, 1.37g) is added to a solution of water (4 ml) and concentrated hydrochloric acid (2.25 ml). A solution of sodium nitrite (0.011 mole, 0.76 g) in water (2.5 ml) is added dropwise. Solution of sodium azide (0.012 mole, 0.78 g) in water (2.5 ml) is added dropwise then mixture was stirred for further 20 minutes. The resulting solid filtered and recrystalized from absolute ethanol.

Synthesis of 4-(5-amino-4-cyano-1H-1,2,3-triazol-1-yl)benzoic acid [2](9)

Sodium ethoxide solution (20 ml) was added dropwise to a stirred solution containing 4-azidobenzoic acid **[1]** (0.1 mole, 16.3 g) and malononitrile (0.1 mole, 6.60g) in absolute ethanol (25 ml), over 10 minutes, at room temperature. The buff pale-yellow solid quickly precipitated and was filtered and recrystallized from ethanol.

Synthesis of 1-(4-carboxyphenyl)-5-methyl-1H-1,2,3-triazole-4-carboxylic acid [3] (10,11)

To a cold solution of sodium ethoxide (7 ml) and ethyl acetoacetate (0.1 mole, 13.01 gm), 4-azidobezoic acid **[1]** (0.1 mole, 16.3 g) was cautiously added and the mixture was heated under reflux on a water bath for 2 hours. The product made alkaline with sodium hydroxide (4 %,10 ml). Water (75 ml) was added, the mixture was acidified with (5 ml) of concentrated hydrochloric acid. The resulting solid **[3]** recrystallized from ethanol.

Synthesis of 1-[4-(chlorocarbonyl)phenyl]-5-methyl-1H-1,2,3-triazole-4-carbonyl chloride [4]

To a solution of compound **[3]** (0.01 mole, 2.47 g) in excess thionyl chloride (15 ml, 0.2 mole) was added and the mixture was refluxed gently for 2 hours. After cooling excess of thionyl chloride was removed under vacuum, and the product was recrystallized from benzene.

Synthesis of 1-[4-(hydrazinocarbonyl)phenyl]-5-methyl-1H-1,2,3-triazole-4-carbohydrazide [5](12)

To a stirred solution of compound **[4]** (0.005 mole, 1.42 g) in dry benzene (15 ml), a mixture of hydrazine hydrate (95 %) (0.01 mole, 0.32 g) and benzene (10 ml) was added dropwise. The mixture was then refluxed for 3 hours. After cooling, excess of benzene was removed under reduced pressure. The product was collected and recrystallized from the appropriate solvent.

Synthesis of Schiff's bases compounds [6-10]: (13)

To a stirred solution of compound **[5]** (0.01 mole, 2.75 g) in absolute ethanol (30 ml), the appropriate aldehyde or ketone was added (0.02 mole). Mixture was refluxed for 3 hours ,cooled to room temperature. The precipitate was filtered and recrystallized from the appropriate solvent.

Synthesis of 5-{4-[4-(5-mercapto-1,3,4-oxadiazol-2-yl)-5-methyl-1H-1,2,3-triazol-1-yl]phenyl}-1,3,4-oxadiazole-2-thiol [11]

To a mixture of compound **[5]**, (0.005 mole, 2.75 g) in a solution of potassium hydroxide (0.01 mole, 0.56 g), in (100 ml) of ethanol (96 %) was added. To the above solution carbon disulfide (0.2 mole, 12 ml) was added slowly with stirring. The mixture was refluxed for (36 hours), cooled and concentrated, poured slowly with stirring into ice (60 g). The solution was acidified with dilute hydrochloric acid (10 %) to (pH 5-6); the resulting precipitate was filtered and recrystallized from the acetone.

Synthesis of 3-{4-[4-(3-amino-3-thioxopropanoyl)-5-methyl-1H-1,2,3-triazol-1-yl]phenyl}-3-oxopropanethioamide [12]

To a solution of **[4]** (0.01 mole, 2.84 g) in dry benzene (25 ml), thiosemicarbazide (0.02 mole 0.9 g) was added. Mixture refluxed for 3 hours, the resulting precipitate was filtered and recrystalized from benzene.

Synthesis of 5-{4-[4-(5-mercapto-4H-1,2,4-triazol-3-yl)-5-methyl-1H-1,2,3-triazol-1-yl]phenyl}-4H-1,2,4-triazole-3-thiol [13]

A mixture of **[12]** (0.001 mole, 0.35 g) and (4 %) aqueous sodium hydroxide solution (60 ml) was refluxed for 4 hours, cooled, poured into crushed ice, and acidified with dilute hydrochloric acid (10 %). The resulting precipitate was filtered, washed with water and recrystallized from ethanol.

Synthesis of 5-{4-[4-(5-amino-1,3,4-thiadiazol-2-yl)-5-methyl-1H-1,2,3-triazol -1-yl]phenyl}-1,3,4-thiadiazol-2-amine [14]

Compound **[12]** (0.001 mole, 0.35 g) was dissolved in cold concentrated sulfuric acid (10 ml) , stirred at room temperature for 24 hours, and poured into crushed ice. The filtered, washed with water, recrystalized from ethanol.

Estereification of 1-(4-Chlorocarbonyl-phenyl)-5-methyl-1H-[*1*,2,3] triazole -4-carbonyl chloride [15-17]

To a solution of compound **[4]** (0.005 mole, 1.24g) in dry benzene (25 ml), alkyl, phenyl alcohol (0.01 mole) was added, the mixture was refluxed for 6 hours. After that, excess benzene was removed under vacuum.

Synthesis of thiol derivatives of 1-(4-chlorocarbonyl-phenyl)-5-methyl-1H-[1,2,3]triazole-4-carbonyl chloride [18and 19]

To a solution of compound **[4]** (0.005 mole, 1.24 g) in dry benzene (25 ml), alkylthiol (0.01 mole) was added, Mixture was refluxed for 6 hours. The excess of benzene was removed under vacuum to give thiolester.

Synthesis of amide derivatives of 1-(4-chlorocarbonyl-phenyl)-5-methyl-1H-[1,2,3]triazole-4-carbonyl chloride [20-22](14)

To a solution of compound **[4]** (0.005 mole, 1.24 g) in dry benzene (25 ml), secondary amine (0.01 mole) was added, the mixture was refluxed for 4 hours. The excess of benzene was removed under vacuum.

Table -1: The physical properties of compounds [1-22]

Comp NO.	Mol. Formula	M.P / °C	Color	Yield (%)
1	$C_7H_5N_3O_2$	178-180	Pale-yellow	88
2	$C_{10}H_7N_5O_2$	284-286	Pale-yellow	86
3	$C_{11}H_9N_3O_4$	230-232	Brown	78
4	$C_{11}H_7C_{l2}N_3O_2$	190-191	Pale Yellow	83
5	$C_{11}H_{13}N_7O_2$	208-210	White	81
6	$C_{25}H_{19}N_9O_6$	290 dec.	Brown	89
7	$C_{25}H_{19}C_{l2}N_7O_2$	244-246	Yellow	82
8	$C_{25}H_{21}N_7O_4$	250-252	Pale- Green	68
9	$C_{27}H_{25}N_7O_2$	227-229	Brown	59
10	$C_{27}H_{27}N_9O_2$	268-270	Brown	72
11	$C_{13}H_9N_7O_2S_2$	238-240	Brown	68
12	$C_{13}H_{15}N_9O_2S_2$	260-262	Pale yellow	78
13	$C_{13}H_{11}N_9S_2$	218-220	Brownish-red	35
14	$C_{13}H_{11}N_9S_2$	305 dec.	Brown	81
15	$C_{17}H_{13}N_3O_4$	177 dec.	Yellow	70
16	$C_{25}H_{17}N_3O_6$	155-157	Pale-Brown	31
17	$C_{19}H_{25}N_3O_4$	139 dec.	Pale-Brown	72
18	$C_{25}H_{21}N_3O_2S_2$	300 dec.	Yellow	31
19	$C_{19}H_{25}N_3O_2S_2$	181 dec.	Brown	42
20	$C_{21}H_{27}N_5O_2$	150-152	Pale-Brown	70
21	$C_{19}H_{23}N_5O_4$	144-146	Brown	62
22	$C_{15}H_{19}N_5O_2$	135-137	ellow	56

RESULTS AND DISCUSSION

For the synthesis of the target 4-aminobenzoic acid derivatives in this work, the reaction sequences are outlined in schemes **(1 and 2)**

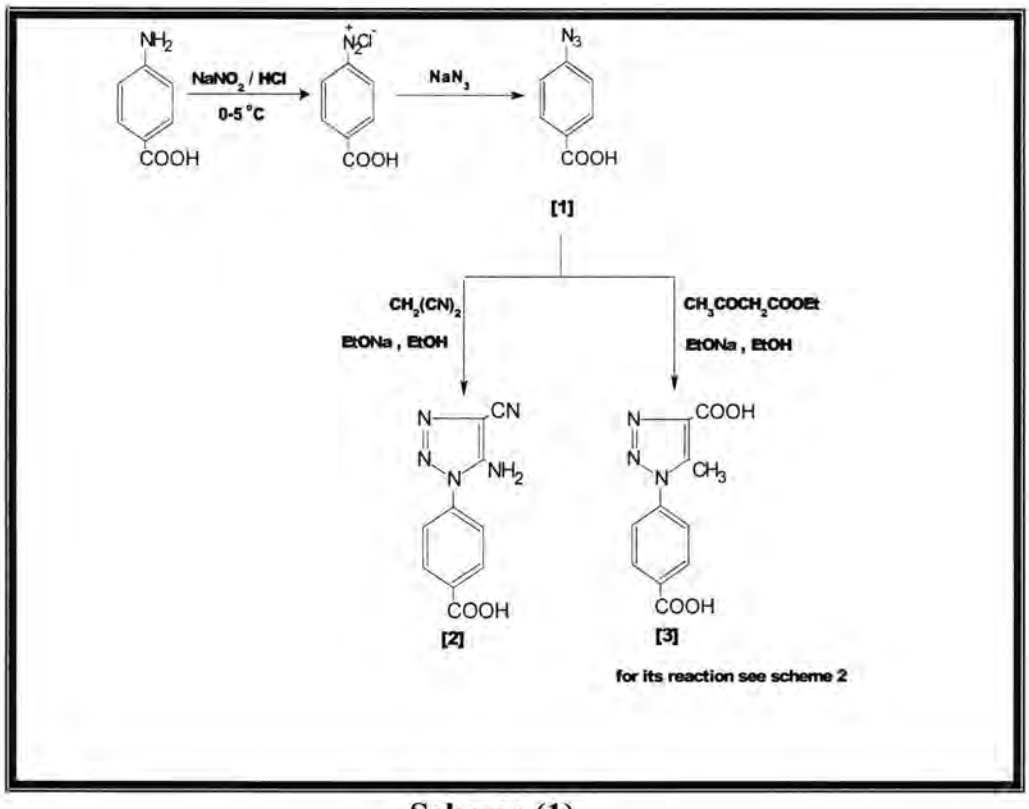

Scheme (1)

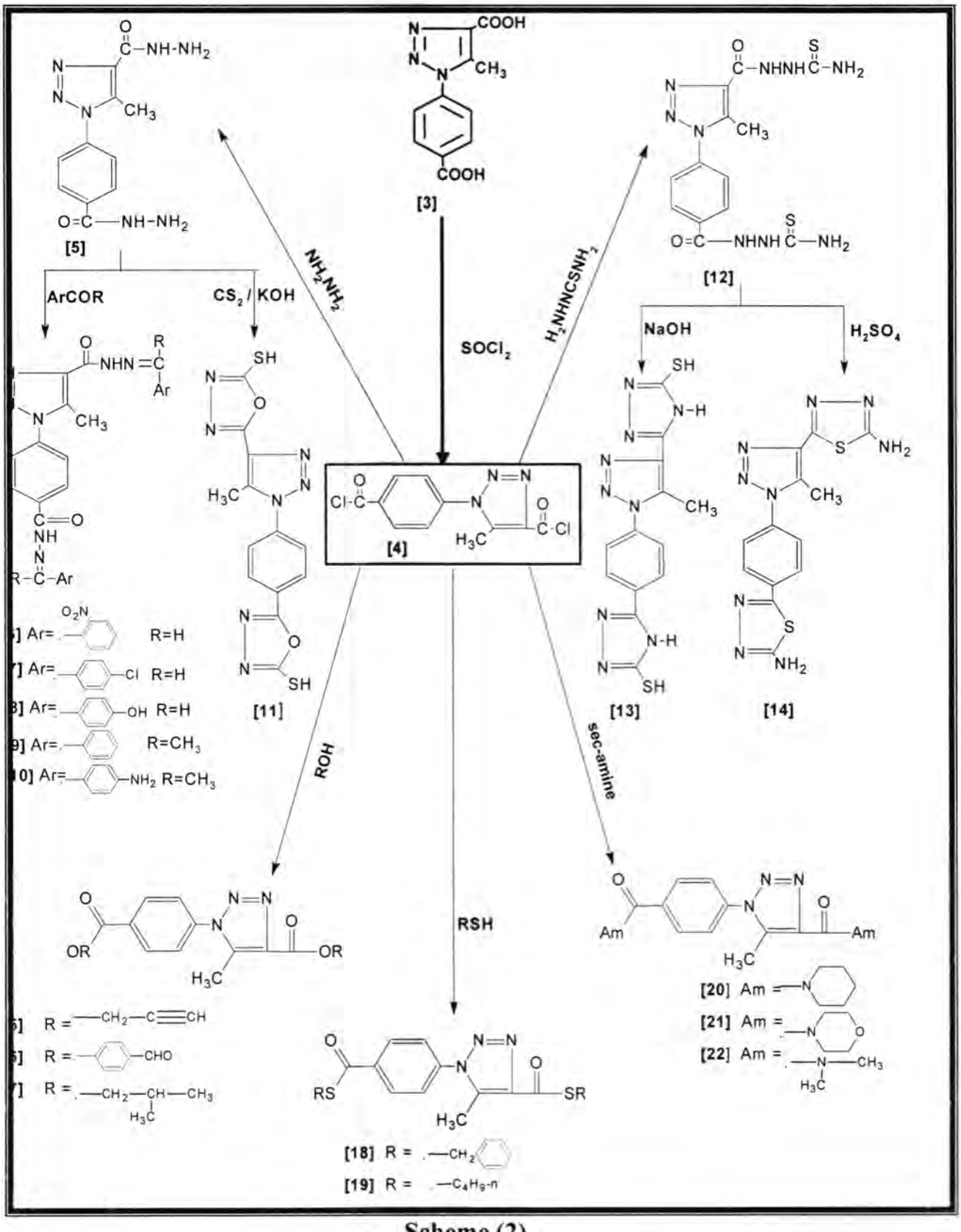

Scheme (2)

The action of sodium azide on diazonium chloride salt of 4-aminobenzoic acid give a 4-azidobenzoic acid **[1]** ,the formation of this compound was

indicated by presence in their FTIR spectrum that shows the disappearance of the absorption bands of the amine group in the starting material at (3470-3300 cm^{-1}) and the appearance of new absorption band for azide group (N_3) at (2108 cm^{-1})(15,16), The spectrum also shows absorptions bands at (3300-2553 cm^{-1}) and (1683 cm^{-1}) due to the stretching vibrations of (OH) and (C=O), respectively. The reaction of the azide **[1]** with active methylene compounds is an especially attractive route to the synthesis of heterocyclic derivatives (15). Compound **[2]** has been synthesized by the reaction of 4-azidobenzoic acid **[1]** with active nitrile namely malonitrile in sodium ethoxide, using absolute ethanol as solvent. The IR spectrum of this compound shows an absorption band at (2270 cm^{-1}) due to (C≡N) stretching vibration with disappearance of (N_3) band at (2108cm^{-1}). Also when the azide **[1]** reacted with ethyl acetoacetate compound **[3]** was obtained. The FTIIR spectrum of compound **[3]** clearly shows the disappearance of the band of azide group in starting material **[1]**, which is a good indication for successful condensation (1). The spectrum also shows absorption bands at (1687 cm^{-1}) referred to (C=O) stretching vibration of carboxylic acid, (3300-2500 cm^{-1}) due to (OH) stretching vibration, furthermore vibration bands of N-N=N occurred in the region of (949 cm^{-1}) for the 1,2,3-triazole ring which were in agreement with the values reported for triazole N-N=N in the region (940-1120 cm^{-1}) by Ykman and Hartzel (17) . The U.V. spectrum of this compound has λ_{max} (MeOH) of (303 nm) responsible for (n-π^*) transition and (224.0 nm) due to (π-π^*) transition. The ^{1}H-NMR spectrum of compound **[3]**, showed signals at δ (2.5 ppm) integrated for three protons of the methyl group. Multiple signal for the aromatic protons appeared as AB quartet at δ (7.7-8.1 ppm) integrated for four protons. A signal at δ (13.2 ppm) integrated for two protons, attributed for the proton of the two carboxylic acid group.

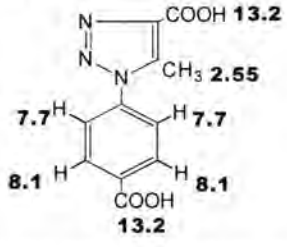

The proposed mechanism of the condensation of 4-azidobenzoic acid **[1]** with ethyl acetoacetate, shows that the (-CH_2-) group flanked by the two carbonyl functions is readily transformed into the nucleophilic anion.

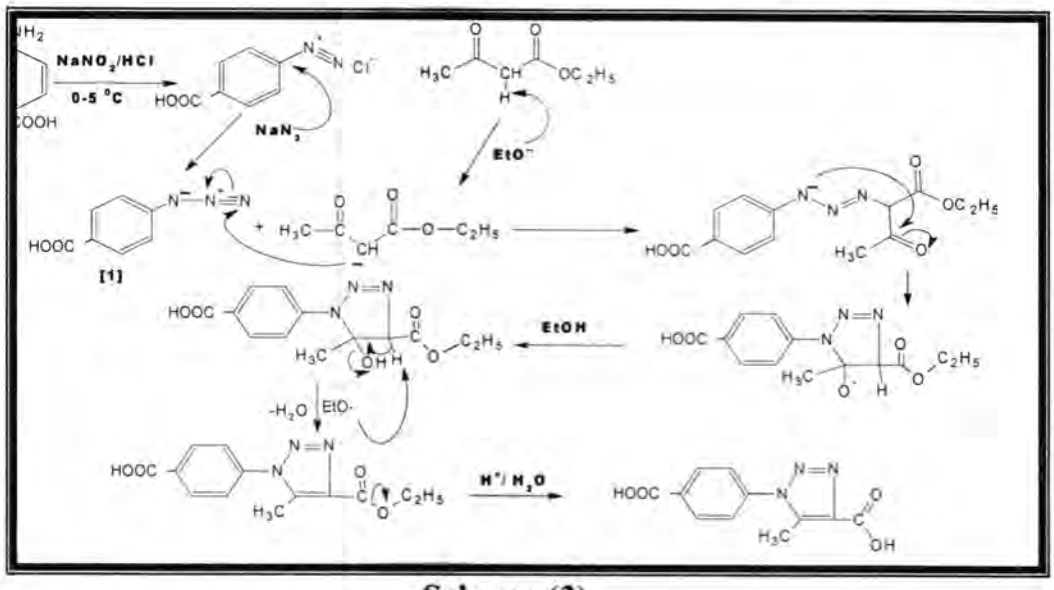

Scheme (3)

The IR spectrum of compound **[4]** shows the disappearance of the hydroxyl stretching vibration for the acid at (3300-2500) and appearance of the new $\upsilon_{C=O}$ at (1800 cm^{-1}). The spectrum also shows an absorption band at (720 cm^{-1}) referring to (C-Cl) band. The IR spectrum of compound **[5]** shows an absorption bands at (1700 cm^{-1}) for (C=O) stretching vibration, (3300-3450) for (NH_2) stretching vibration, (3100 cm^{-1}) for (N-H) stretching vibration. The ^{1}H-NMR spectrum of compound **[5]** showed a signal at δ (2.5) ppm integrated for three protons attributed to the methyl group. Protons of the two terminals (NH_2) groups showed signal at δ (3.3) ppm integrated for four protons. Aromatic protons appeared at the region δ (7.7-8.0) ppm as AB quartet integrated for four protons. The spectrum also showed two signals at δ (9.7 and 9.9) ppm, each integrated for one proton, which may be attributed to the proton of the hydrazide groups.

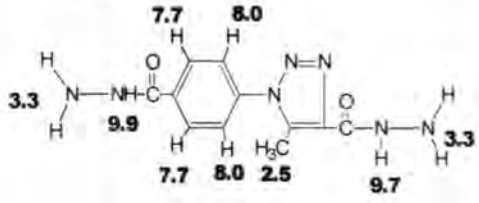

In the present work, the Schiff's bases **[6- 10]** have been synthesized by the condensation of **[5]** with appropriate aromatic aldehydes or ketones in the presence of appropriate solvent. The IR spectrum of compound **[8]** shows an absorption band at (1620 cm^{-1}) due to (C=N) stretching vibration, and a stretching band at (1675 cm^{-1}) due to (C=O) amide stretching vibration while the stretching band at (3300 cm^{-1}) is for (NH) which interfere with stretching vibration of (OH) band at (2800-3300 cm^{-1}). Other bands of the synthesized Schiff's bases **[6- 10]** are listed in **table(2).**

The IR spectrum of compound **[11]** shows absorption band at (3100 cm^{-1}) which corresponds to (NH) stretching vibration, the spectrum also shows a

band at (1625 cm^{-1}) due to (C=N) stretching vibration, and another band for (C-O-C) vibration at (1100 cm^{-1}). The IR spectra of compound **[12]** shows the main characteristic bands at (1240 cm^{-1}) referred to (C=S)stretching vibration,(3450cm^{-1} and 3300 cm^{-1}) due to (NH_2) assymetrical and symmetrical bands respectively, interfered with (NH) band at (3200 cm^{-1}), which is a good indication for success of reaction . In addition, the success of reaction has been confirmed by the disappearance of (C=O) band at (1800 cm^{-1}) in acid chloride, and appearance of (C=O) band at (1670 cm^{-1}) in the acid thiosemicarbazide. The synthesis of the corresponding triazole **[13]** was carried out by oxidative cyclization of the carboxylic acid thiosemicarbazide **[12]** in the presence of (4 %) of aqueous sodium hydroxide.The IR spectrum of compound**[13]** shows characteristic (S-H) stretching vibration (weak band) at (2700 cm^{-1}) and (C=S) stretching vibration at (1220 cm^{-1}) which confirmed the tautomerism between thion and thiol forms and an absorption band at (1630 cm^{-1}) due to (C=N) stretching vibration of triazole The IR spectrum of compound **[14]** shows absorption band at (620 cm^{-1}) due to (C-S-C) stretching vibration (1250 cm^{-1}) due to (N-N) stretching vibration and at (3350 cm^{-1}) due to (NH_2) symmetric stretching vibration (18).The ^{1}H-NMR spectrum of compound **[14]** showed a signals at δ (2.1) ppm integrated for three protons attributed to the methyl group. Protons of the two terminals (NH_2) group showed signal at δ (3.5) ppm integrated for four protons. Aromatic protons appeared as AB quartet (two doublets) at the region δ (7.4-7.9) ppm integrated for four protons.

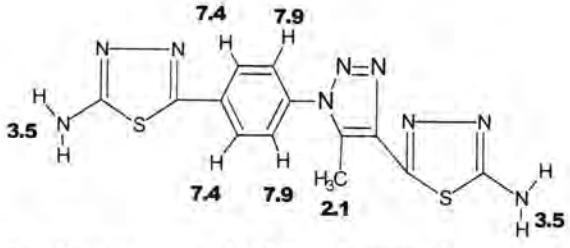

The IR spectrum of compound **[15]** shows the disappearance of (C-Cl) stretching band and appearance of absorption band at (1728 cm^{-1}) due to (C=O) stretching vibration, appearance of (C≡C-H) stretching band at (3250 cm^{-1}) and band at (2150 cm^{-1}) for (C≡C) assymetrical stretching vibration(18). The success of the reaction has been confirmed by the appearance of the triple bond of the acetylenic group. The IR spectrum of **[18]** shows band at (1690 cm^{-1}) due to (C=O) stretching vibration which had appeared at (1800 cm^{-1}) in acid chloride compound **[4],** band at (690cm^{-1}) due to (C-S) stretching vibration. The IR spectrum of compound **[21]**, shows the main characteristic bands at (1640 cm^{-1}) due to (C=O) of amide, and at (1150 cm^{-1}) due to (C-O-C) stretching vibration.

Table -2: Spectral data for compounds [1-22]

Comp. No.	UV λ_{max} (nm)	(C=O)	ν(C=C)	ν(C=N)	ν(C-H)$_{al}$	ν(C-H)$_{ar}$	ν others
1	293 261	1683	1610	-------	-------	3050	2108 $(N_3)_{st}$. 3300-2500(O-H)
2	267 215	1690	1605	-------	2950	3050	2270 (CN)st 3300-3400 (NH_2)st interfere with (OH)st. 3300-2600(O-H)st.
3	303 224	1687	1425 1605	-------	2850	3080	949(N-N=N)ring 3300-2500(O-H)st.
4	290	1800	1500 1600	---------	2950 asy 2800 sy	3080	720 ν(C-Cl)$_{ar}$
5	279	1700	1500 1600	---------	2970 asy	3050	3100 $(NH)_{st}$ 3300-3450 $(NH_2)_{st}$
6	289	1650	1495 1600	1620	2985 asy 2890 sy	3040	3250 $(N-H)_{st}$ 15020, 1320 (NO_2)st
7	301	1663	1460 1580	1610	2970 asy 2830 sy	3100	3340 (N-H)st 770(C-Cl)st 860 (p-substituted)
8	332 259	1675	1500 1610	1620 Interfere with C=C	2980 asy 2860 sy	3080	3300 $(N-H)_{st}$ interfere with 2800-3300 (OH)
9	321	1668	1500 1600	1620 Interfere with C=C	2985 asy 2880 sy	0730	3300 $(NH)_{st}$
10	295	1670	1500 1600	1620 Interfere with C=C	2960 asy 2900sy	3030	3290-3200 $(N-H_2)_{st}$ Interfere with (NH)st
11	300 240	-------	1550	1625	2970 asy 2880 sy	3060	1100 $(C-O-C)_{st}$ 2700$(SH)_{st}$ weak 1220 (C=S) 3100 $(N-H)_{st}$
12	330 250	1670	1600	--------	2950 asy 2850 sy	3050	1240 $(C=S)_{st}$ 3200 (NH) 3450-3300 $(NH_2)_{st}$
13	342	--------	1500 1600	1630 interfere with C=C	2975 asy 2830 sy	3050	1220 (C=S) 2700 weak $(SH)_{st}$ 3100$(N-H)_{st}$
14	306 351	-------	1425 1560	1620	2970 asy 2850 sy	3070	620 (C-S-C) 1250 (N-N) 3350 $(NH_2)_{st}$

15	325	1728	1600	--------	2980 asy 2840 sy	3050	3250 (C ≡CH)st 2150 (C≡C)st
16	275	1720	1580	---------	2965 asy 2850 sy	3050	1250 (C-O) 2735 (C-H)ald
17	218	1715	1600	---------	2970 asy 2860 sy	3080	1270 (C-O)
18	225	1690	1450 1580	----------	2980 asy 2850 sy	3100	690
19	230 207	1700	1500 1610	---------- -	2985 asy 2865 sy	3090	720
20	220	1635	1600	----------	2970 asy 2820 sy	3050	1620
21	234	1640	1510	1625 interfere with (C=O)	2970 asy 2820 sy	3050	1150(C-O-C)
22	229	1640	1560 1600	1620 interfere with (C=O)	2970 asy 2760 sy	3050	----------

REFERENCES

1. Y. S. Sanghvi, B. K. Bhattacharya, G. D. Kini, S. S. Matsumoto, S.B. Larson, W. B. Jolly, R. K. Robins and G. R. Revanker" Growth inhibition and induction of cellular differentiation of human myeloid leukemia cells in culture by carbamoyl congeners of ribavirin" J. Med. Chem., 33, 336(1990).
2. M. A. Alam, R. Kajiki, H. Hanatani, X. Kong, F. Ozoe, Y. Matsui, F. Matsumura and Y. Ozoe" Synthesis and Structure–Activity Relationships of 1-Phenyl-1H-1,2,3-triazoles as Selective Insect GABA Receptor Antagonists", J. Agric. Food Chem., 54 :1361-72(2006).
3. D. J. Hupe, R. Boltz, C.J. Cohen, J. Felix, E. Ham, D. Miller, D. Soderman, and D.V. Skiver" The inhibition of receptor-mediated and voltage-dependent calcium entry by the antiproliferative, J. Biology. Chem., 266, 10136(1991).
4. C. Peto, G. Batta, Z. Gyorgydeak, and F. Sztaricskai "Glycoside Synthesis with Anomeric 1-N-Glycobiosyl-1,2,3-triazoles",J.Carbohydrate Chem.15 465(1996).
5. D. R. Buckle, C. J. M. Rokell, H. Smith, and B. A. Spicer "Studies on 1,2,3-triazoles. 13. (Piperazinylalkoxy)-[1]benzopyrano[2,3-d]-1,2,3-triazol-9(1H)-ones with combined H1-antihistamine and mast cell stabilizing properties", J. Med. Chem., 29, 2252(1986).

6. C.Bruhlmann,F.Ooms,P.A.Carrupt, B. Testa, M.Catto, F.Leonetti, C. Altomar, A. Carotti "Coumarins Derivatives as Dual Inhibitors of Acetyl cholinesterase and Monoamine Oxidase", J. Med. Chem. 44 ,3195 (2001).
7. R.Alvarez,S.Velazqes,F.San,S.Aquaro,C.De,C.F.Perno,A.Karlsson,T.Balzarin -i,M.Camarasa" 1,2,3- Triazole- [2,5-Bis-O-(tert-butyldimethylsilyl) -.beta.-D-ribofuranosyl]-3'-spiro-5"-(4"-amino-1",2"-oxathiole 2",2"-dioxide) (TSAO) Analogs: Synthesis and Anti-HIV-1 Activity",J.Med.Chem.,37:4185-94 (1994).
8. L. Racane, V. T-Kulenovi, D. W. Boykin and G. K-Zamola "Synthesis of New Cyano-Substituted bis-Benzothiazolyl Arylfurans and Arylthiophenes", Molecules, 8 ,342- 49(2003).
9. E. M. Kamel, R. A. Ahmed and O. S. Moustafa "A Convenient and Efficient Conversion of 4-Aminobenzophenone intosome new 1,2,3-Triazole and Benzothiazole Derivatives", J. Chin. Chem. Soc., 52 149-53(2005).
10. H. El-khadem, H. A. R. Mansour, M. H. Meshreki "Some 1-aryl 1,2,3-triazoles", J. Chem. Soc.(c) 1329(1968).
11. H-S. Dong and B. Wang" Synthesis of Some Novel 3,6-Bis(1,2,3-triazolyl)-s-triazolo [3,4-b]-1,3,4-thiadiazole Derivatives", J. Chin. Chem. Soc., 52 103-8 (2005).
12. H.Shan,K.Wei,Q.Lian,B.Quan & Z.Zhang"Synthesis of 3-[5-methyl phenyl)-1,2,3-triazol-4-yl]-6-substituted-s-triazol[3,4-b]1,3,4-thiadiazoles,J.Chin. Chem.Soc. 47 :343-346(2000).
13. Y. Zhang, R-Z. Qiao, P-F. Xu, Z.Y. Zhang, Q. Wang, L-M. Mao and K-B. Yu "Synthesis and Antibacterial Activities of 2-(1-Aryl-5-methyl-1,2,3-triazol-4-yl) -1,3,4-oxadiazole Derivatives", J. Chin. Chem. Soc., 49 :369-73(2002).
14. S. T. Abo-Orabi "Review1,3-Dipolar Cycloaddition Reactions of Substituted Benzyl Azides with Acetylenic Compounds" ; Molecules, 7 :302-14(2002).
15. R. T. Morrison and R. N. Boyed ' Organic Chemistry' 5th Ed., Prenice-Hall of India, :976-81 (1989).
16. H-S. Dong and S-Q. Lin" the study on synthesis of some new 1,2,3-triazolurea and carbonyl amide derivatives", J. Chin. Chem. Soc., 50: 1215-19 (2003)
17. H-S. Dong, W. Jia, J-D. Cui and Q-L. Wang" the synthesis of some new N-[1-(2,5-dichlorophenyl)-5-methyl-1,2,3-triazol-4-yl]-carbamic acid ester derivatives", J. Chin. Chem. Soc., 50 :1209-13(2003).
18. V. M. Parikh, "Absorption Spectroscopic of Organic Molecules" Translated by A. H. Khuthier, J. M. A. Al-Rawi, M. A. Al-Iraqi, Mousul University (1985).

Lipid profile and FFA in Iraqi patients with Chronic Renal Failure after Renal Dialysis

[1]Salwa H.N.Al-Rubae'i, [2]Tariq H.Al-Khayat and [1]Najlaa Q. Muftin
[1]Chemistry Department, College of Science, Al-Mustansiriya University.
[2]College of Medicine, Babylon University, Babylon.
[1]Chemistry Department, College of Science, Al-Mustansiriya University.

الخلاصة

اجريت دراسة شملت 30 مريضاً (17 ذكراً و 13 انثى)مصابين بمرض الفشل الكلوي المزمن وتم أخذ عينات من الدم قبل الديلزة الدموية وبعدها لقياس مستوى صورة الدهون والاحماض الدهنية الحرة . قورنت النتائج مع نماذج دم 30 شخصاً (18 ذكراً و 12 انثى) اصحاء غير مصابين (مجموعة سيطرة) . اظهرت نتائج الدراسة وجود زيادة معنوية في مستويات TG وVLDL-C قبل وبعد الديلزة مقارنة بمجموعة السيطرة ، بينما كانت هناك تغيرات غير معنوية في مستوى LDL-C و TC لدى المرضى قبل الديلزة مقارنة مع مجموعة السيطرة ، بينما لوحظ هناك علاقة معنوية في مستوى TC بعد عملية الديلزة لاولئك المرضى مقارنة مع مجموعة السيطرة . اظهرت ايضاً هذه الدراسة بان هناك نقصان معنوي في مستوىHDL-C قبل عملية الديلزة مقارنة بمجموعة السيطرة وعدم تغير معنوي في مستوى LDL-C و HDL-C بعد عملية غسل الكلية مقارنة مع مجموعة السيطرة.اظهر مستوى FFA قبل وبعد عملية الديلزة زيادة معنوية مقارنة مع مجموعة السيطرة . أشارت النتائج الي ان هناك ارتباط ايجابي بين مستوى FFA ومستوى كل من TG وVLDL-C و LDL-Cوعلاقة موجبة غير معنوية مع TC وعلاقة سالبة معنوية مع مستوى HDL-C في مرضى الفشل الكلوي قبل عملية الديلزة .ولوحظ هناك علاقة موجبة معنوية بين مستوى FFA ومستوى كل من TC وLDL-C وعلاقة غيلر معنوية مع مستويات TG وVLDL-C وHDL-C في مرضى الفشل الكلوي بعد عملية الديلزة .

ABSTRACT

A study was carried out on 30 patients (17 male and 13 female) with chronic renal failure. Blood samples have been taken before and after hemodialysis to measure lipid profile and free fatty acids.

The results obtained have been compared with 30 (18male and 12 female) healthy subjects (control group). The results showed that there were significant increase in the level of TG, VLDL-C before and after hemodialysis , while there was non significant difference in the level of TC, LDL-C in pre-dialysis patients as compared to control group. The results also revealed a significant relation in the level of TC, in those patients after hemodialysis comparison with control group. This study also show a significant decrease in the level of HDL-C in pre dialysis patients as compared to control group and non significant changes in the levels of LDL-C and HDL-C in post-dialysis patients compared with control group. The level of FFA in patients before and after hemodialysis was significant increase as compared with control group. There is a significant positive correlation between serum FFA levels and TG, LDL-C, VLDL-C, whereas no significant positive correlation with TC and significant negative correlation with HDL-C levels in pre-dialysis patients. There is a significant positive correlation between serum FFA levels and TC, LDL-C, where as no significant correlation with HDL-C, TG, and VLDL-C in post- dialysis patients.

INTRODUCTION

Chronic renal failure (CRF) is defined as kidney damage for more than three months as evidenced by structural or functional abnormalities with or without decreased glomerular filtration rate (GFR) and manifested either as pathological abnormalities or kidney damage markers in blood or urine or in the imaging tests. Many people are unaware of the problem until more than 70% of kidney function has been lost (1, 2). Dialysis is a procedure that removes excess fluids and toxic end products of metabolism such as urea from the plasma and

corrects electrolytes balance by dialyzing the patients blood against fluid containing no urea but with appropriate concentrations of electrolytes ,free – ionized calcium and some other plasma constituents (3).

Hemodialysis relies on the principles of solute diffusion across a semi-permeable membrane. Movement of metabolic waste products takes place down a concentration gradient from the circulation into the dialysate, and in the reverse direction (4).

Patients with end-stage renal disease, whether or not they are undergoing dialysis therapy, frequently present evidence of dyslipoproteinemia (5,6) and have an increased risk of developing cardiovascular disease and of suffering from its complications. The frequent findings are increased concentrations of triacylglycerols and very low density lipoproteins (VLDL) and intermediate density lipoproteins (IDL) (7), and decreased concentrations of high density lipoproteins (HDL) (5). By contrast, total cholesterol and low density lipoproteins (LDL) appear to be little affected by renal disease, except in nephritic subjects (8) .Total serum free fatty acid (FFA) levels provide an important measure of the physiologic state (9). Low level of FFA occurs in all tissues but substantial amount can sometimes be found in the plasma, particularly during fasting or starvation. Plasma FFA (transport by serum albumin) is "en route" from their point of origin (triacylglycerol of adipose tissue or circulating lipoproteins) to their site of consumption (most tissues) (10).

Plasma concentrations of FFA are very variable, being influenced by hormonal, metabolic and nutritional status. Abnormally high plasma concentrations of FFA are implicated in increased risk ventricular fibrillation (10) and sudden cardiac death (11) and more controversially of coronary heart disease (12, 13). The important of FFA in renal disease seems to have been neglected in the last years; nevertheless, many studies have in the past, established that FFA concentrations in end stage renal failure patients are increased following treatment by hemodialysis (14, 9).

MATERIAL AND METHODS

Serum total cholesterol, triglyceride, HDL, were measured by colorimetric assay using kits supplied by Spinreact in spain. Free fatty acid was estimated by colorimetric assay using soap formation (15).

Calculations:

a- LDL-C was calculated according to Bairaktary *et al* equation (16):

$$\text{LDL-C} = 0.94 \times \text{Total cholesterol} - 0.94 \times \text{HDL-C} - 0.19 \times \text{TG}$$

This equation is more accurate than Friedewald equation because Friedewald's equation considerably inaccurate even at TG concentrations of 200-400 mg/dL (17) .

b- $\text{VLDL-C} = \text{TG}/5$

Sample Collection

Thirty patients (17 male and 13 female) were involved in this study. The patients were referred to Baghdad Teaching Hospital, Al-Kadhimiya Teaching Hospital, and Al -Hakeem Hospital, Baghdad, Iraq. All patients with CRF were diagnosed by clinical examination (urea & creatinine) in those medical centers. The mean age of the patients was 45±10 years. All those patients were treated with hemodialysis (twice in a week). Control group consisted of 30 healthy subjects (18 male and 12 female) with mean age (40±10).

Preparation of Blood Samples

Ten milliliters samples of venous blood were taken from all fasting patients before and after hemodialysis. Blood samples were left for 20 minutes at room temperature. After blood coagulation, the sera were separated by centrifugation at 3000 xg for 15 minutes and then sera stored at -20 °C. Hemolyzed samples were discarded.

Statistical Analysis

The data was analyzed on the computer statistical programme SPSS version10. The mean ±SD was also computed for the comparison of results. The comparison of mean between two groups was tested by Student's't' test. Results were considered statistically significant if P value is less than 0.05.

RESULTS AND DISCUSSION

The results in table 1 referred to non significant increased in the serum level of TC in pre-dialysis patients and significant increased in the serum level of TC in post-dialysis patients with CRF may be attributed to either a highly significant increase in FFA. The increase in the latter component leads to increased formation of acetyl-CoA with a subsequent increase of cholesterol synthesis . The increase in the level of cholesterol in post- dialysis patients with CRF as compared with pre- dialysis patients with CRF due to haemoconcentration and selective retention of high molecular weight compounds after hemodialysis (18).

Table - 1: Lipid profile and FFA levels in pre-and post dialysis patients and control group.

Parameters	Control	Pre-dialysis	Post-dialysis
TC (mmol/L)	4.327±0.235	4.575±1.216	4.772±1.013*
TG (mmol/L)	1.41 ± 0.127	2.45 ± 1.006***	2.267 ± 0.623***
HDL-C (mmol/L)	1.24 ± 0.168	1.08 ± 0.174***	1.27 ± 0.309
VLDL-C (mmol/L)	0.28 ± 0.025	0.49 ± 0.205***	0.453 ± 0.125***
LDL-C (mmol/L)	2.634 ± 0.124	2.822 ± 1.145	2.86 ± 1.027
FFA (mmol/L)	0.353 ± 0.08	1.016± 0.717***	1.514± 0.626***

Values significantly different from the controls *p<0.05, **p<0.01, ***p<0.001

The significant increased in the serum level of TG and VLDL-C in patients with CRF as compared to control group can be explained in reference to Klin M. etal (19), observations .Those investigators found that the downregulation of hepatic triglyceride lipase, and the VLDL receptor can, in part ,account for the associated hypertriglyceridemia, elevation of plasma VLDL-C, and impaired clearance of triglyceride-rich lipoproteins in CRF. Our results were in a good agreement with Ikewaki *et al* (20), Miida *et al* (21). Tzanatos *etal* (18), found non significant decrease in the serum levels of TG and VLDL-C in post- dialysis patients with CRF as compared with pre-dialysis patients with CRF . This decrease can be attributed to heparin given during dialysis activate endothelial lipoprotein lipase , leading to enhancement of hydrolysis of circulating TG (22).

The present study showed decreased in concentration of HDL-C in pre-dialysis patients with CRF as compared to control group. Fuh *et al* (23), found the decrease in HDL-C concentration in CRF patients is associated with decreases in both the fractional catabolic rate (FCR) and total synthetic rate of apoAI/HDL. Furthermore, it appears that the worse the renal function , as estimated by either blood urea nitrogen or creatinine , the slower the FCR and the lower the total synthetic rate of apo AI /HDL. Castelli *et al*, found that low levels of HDL-C are strongly associated with high risk of atherosclerotic heart disease (24) .Thus, cholesterol esterification by lecithin-cholesterol acyltransferase may play a key role in the prevention of cardiovascular disease, improving cholesterol exportation in biliary acids (25). AL- Rashidi *et al* (22) and Gillett *et al* (9), attributed the increase in the level of HDL after hemodialysis to haemoconcentration and changes in some chemical components of dialysate which lead to increased synthesis APoE ,APo cII, APoA.

The results in table 1 showed there was a non significant increase in the serum levels of LDL-C in pre- and post-dialysis patients with CRF as compared to control group. The alternative equation for LDL-C yield slightly better results than the Friedewald equation especialy in hypertriglyceridemia . The results of this equation is more accurate and nearest to the results ultercentrifugation procedure (16). In this study there was non significant increase in the level of LDL-C in post-dialysis patients in comparison with that of pre-dialysis .The changes in lipoproteins and their carrier protein (apoliproteins) could not have been due to solely to haemoconcentration caused by fluid withdrowal during maintaining hemodialysis , it would appeare that selective retention of high molecular weight apoliproteins by dialysis membranes caused the increase in apolipoprotein levels , which inturn , resulted in retention of lipoproteins (22). There was a highly significant increase in the serum levels of FFA in pre- and post-dialysis patients with CRF as compared to control group. The results also revealed highly significant increase in the levels of FFA in post - dialysis patients with CRF compared with pre- dialysis patients with CRF ($p< 0.001$).

The increase of FFA in blood may affect metabolic pathway and endocrine disturbance, it may lead to metabolic syndrome and insulin resistance

.It may also affect the levels of total different type of lipoproteins, is associated with increased risk of vascular disease (11). Gillett *et al*, explained this result by heparinization of patients during hemodialysis and the consequent release into the circulation of lipoproteins and hepatic lipases has been thought to cause raised level of FFA concentrations. Other factors such as carnitine deficiency and the presence of acetate in the dialysis buffer solutions may lead to those subsequent changes in FFA (9).

Table (2) shows a significant positive correlation between FFA and each of TG , VLDL-C and LDL-C in pre-dialysis patients and the same trend of significant were found in TC ,LDL-C in post-dialysis patients while there was a significant negative correlation between FFA and HDL-C in pre-dialysis patients.

Table – 2 : Correlation coefficients and the significance levels of different serum chemical components in patients with CRF.

Component *VS* FFA	Pre-Dialysis		Post-Dialysis	
	r	P	r	P
TC	0.317	0.088	0.397*	0. 03
TG	0.517**	0.003	-0.141	0.458
HDL-C	-0.487**	0. 006	0.061	0.750
VLDL-C	0.517**	0.003	-0.141	0.458
LDL-C	0. 366*	0.046	0.372*	0.043

* Correlation is significant at the level 0.05
**Correlation is significant at the level 0.01

FFA is one of the best indicators of metabolic changes (especially with lipid profile). FFA significantly increase in post-dialysis patients due to heparin infusion. This increase is an independent risk factor for CRF patients. Thus, regular determination of FFA in CRF patients is important for monitoring the treatment.

REFERENCES

1. Narula C.A.;Hooda C.A .: Conservative management of chronic renal failure. *MJAFI* , 63 : 56-61,(2007).
2. O'Shaughnessy D.:An introduction to haemodialysis. 1st ed., Fresenius Medical Care :5-7(2005).
3. Zilva F.;Pannall.; Mayne P.H.: Clinical chemistry in diagnosis and treatment, 6th ed., London, Arnold, (1994).
4. Braunwald E.;Fuaci A.;Kasper D.L.;Hauser S.L.;Longo D.;Hauser S.L.; Jameson J.L.:Harrison's Principles of Internal Medicine.16th ed.,NewYork, San Francisco, Toronto , London, 1664,(2005).

5. Wanner C. Importance of hyperlipidaemia and therapy in renal patients. *Nephrol Dial Transplant*, 15 (suppl 5): S92-96,(2000).
6. Gillett MP, Obineche EN, El-Rokhaimi M, Lakhani MS, Abdulle A, Sulaiman M. Lecithin: cholesterol acyltransfer dyslipoproteinaemia and membrane lipids in uraemia. *J Nephrol*, 14: 472-480, (2001).
7. Oi K, Hirano T, Sakai S, Kawaguchi Y, Hosaya T. Role of hepatic lipase in intermediate-density lipoprotein and small, dense low-density lipoprotein formation in hemodialysis patients. *Kidney Int*,56(suppl 71):S227-228, (1999).
8. Wheeler DC, Bernard DB Lipid abnormalities in the nephrotic syndrome: Causes, consequences and treatment. *Am J Kidney Dis* .,1994; 23: 331-346.
9. Gillett M.P. ; Obineche E.N.; Khan S. T.; Abdull A.M.: Plasma concentrations of non-esterified fattyacids in chronic renal failure in the United Arab Emirates. *Saudi Med J*, 25 (11): 1611-1616, 2004.
10. Oliver M.F.: Metabolic causes and prevention of ventricular fibrillation during acute coronary syndromes. *Am. J. Med.*, 112: 305- 311, (2002).
11. Jouven X.;Charles M.A.;Denos M.;Ducimetiere P.:Circulating nonstestrified fatty acid level as predictive risk factor for sudden death in the population. *Circulation*, 104: 756- 761, (2001).
12. Carlsson M.; Wessman Y.; Almgren P.; Group L.: High concentrations of nonestrified are associated with increased familial risk of cardiovascular disease. *Arterioscler. Thromb. Vasc. Biol.*, 20: 1588- 1594, (2000).
13. Charles M.A.;Fontbonne A.;Thibult N.;Claude J.R.;Warnet J.M.; Rosselin G.; Ducimetière P; Eschwège E.: High plasma nonestrified fatty acids are predictive of cancer mortality but not of coronary heart disease mortality: results from the paris prospective study.*Am.J.Epidimiol.*,153:292-298; (2001).
14. Pirro M.; Mauriège P.; Tchernof A.; Cantin B.; Dagenais G. R.; Després J. P. ; Lamarche B. .: Plasma free fatty acid concentrations and the risk of ischemic heart disease in men: prospective results from the Quebec cardiovascular study. *Atherosclerosis* ,160: 377- 384, 2002
15. Falholt K. ;Lund B.; Falfolt W.: An easy colorimetric micro method for routine determination of free fatty acids in plasma .*Clin. Chim.Acta.*,46(Issue 2):105-111,(1973).
16. Bairaktari E. T.; Tzallas C. ; Kalientzidou M. ; Tselepis A. D. ; Siamopoulos K. C ; Seferiadis K. I ; Elisaf M. S. : Evaluation of alternative calculation methods for determining low-density lipoprotein cholesterol in hemodialysis patients .*Clinical Biochemistry*, 37:937– 940, (2004).
17. Warnick G.R.; Knopp R.H.; Fitzpatrick V.; Branson L.: Estimating low density lipoprotein cholesterol by the Friedewald equation is adequate for classifying patients on the basis of nationally recommended cut points.*Clin. Chem.*,36:15–9. (1990).

18. Tzanatos H. A.; Agroyannis B.; Chondrose C.; Kapetanaki A.; Fourtounas C.; Soubassi L.; Kopelias I.: Cytokine release and serum lipoprotein(a)Alterations during hemodialysis *.Artif.Organs.*, 24(5):329-333,(2000).
19. Klin M.; Smogorzewski M.; Ni Z.; Zhang G. ;Massry S.G. : Abnormalities in hepatic lipase in chronic renal failure: role of excess parathyroid hormone. *J. Clin. Invest.*, 97: 2167–2173,(1996).
20. Ikewaki K.; Schaefer J . R.; Frischmann M. E.; Okubo K.; Hosoya T.; Mochizuki S.; Dieplinger B.; Trenkwalder E.; Schweer H.;Kronenberg F.; Koenig P.; Dieplinger H.: Delayed in vivo catabolism of intermediate-density lipoprotein and low-density lipoprotein in hemodialysis patients as potential cause of premature atherosclerosis. *Arterioscler .Thromb .Vasc . Biol.*, 25: 2615-2622. (2005).
21. Miida T.; Miyazaki O.; Hanyuo.; Nakamura Y.;Hirayama S.; Narita I.; Gejyo F.; EI.I.;Tasaki K.; Kohadi Y.;OhtaT.;Yatas.; Fukamachi I.;Okada M.: LCAT-Dependent conversion of Pre β1-HDL into α-migrating HDL is severely delayed in hemodialysis patients.*J.Am.Soc.Nephro.*,14:732–738, (2003).
22. Al-Rashidi M.; Hussain A.A.; Nampoory M. R.N.; Al-Ali J. H.; Akanji A. O. :Post-dialysis retention of blood lipoproteins and apolipoproteins in patients with end-stage renal disease on maintenance haemodialysis in Kuwait. *Clin. Chim. Acta* .,344: 149–154,(2004).
23. Fuh M.M.T.; Lee C.; Jeng C.; Shen D.; Shieh S.; Reaven G.; IdaChen Y. : Effect of chronic renal failure on high-density lipoprotein kinetics. *Kidney Int.*,37:1295–1300. (1990).
24. Castelli W.P.; Anderson K.; Wilson P.M.; Levy D.; Lipids and risk of coronary heart disease:the Framingham study *.Am. Epidemiol.* ,2:2308,(1991).
25. Mekki K.; Bouchenak M.; Lamri M.; Remaoun M.; Belleville J: Changes in plasma lecithin:cholesterol acyltransferase activity, HDL_2, HDL_3amounts and compositions in paitents with chronic renal failure after different times of hemodialysis *.Atherosclerosis* , 162:409-417,(2002).

Thermal and Ablative Properties of Some Phenolic Resin Derivatives and Composites

[1]Tariq S. Najim and [2]Amel M.Naji
[1]University of Mustansiriya, College of Science,Chemistry Department,
[2]Department of Applied Chemistry, School of Applied Science, University of Technology

الخلاصه

احد عشر مركبا من مركبات قواعد شف الفينوليه تم تحضيرها سابقا عن طريق تكثيف بارا-هيدروكسي بنزلديهايد او الفورمالديهايد مع عشرة من المركبات الامينيه ثم تحويل قواعد شف الفينوليه الى راتنجات الفينول فورمالديهايد بواسطة التكثيف مع زياده من الفورمالديهايد والتي تم تشخيصها بواسطة ال IR والتحليل الحراري. وكذلك تم تحضير راتنج الفينول –فورمالديهايد الحاوي على نسبه عاليه من من الاورثو عن طريق تكثيف الفينول والفورمالديهايد بوجود اوكسيد المغنيسيوم كعامل مساعد والذي تم تشخيصه ايضا بواسطة ال IR والتحليل الحراري . الاستقراريه الحراريه للراتنجات المقساة طبقا لمعيار ال 50% فقدان بالوزن تم تقييمها وكانت النتائج كالاتي:

XX >XIII , XII > XVI >XIX > XVII , XXI > XXII >XV > XXIII

الاستقراريه الحراريه العاليه لبعض الراتنجات يعود الى التركيب السلمي المتكون بعد التشابك وكذلك الى التركيب الخطي للسلاسل البوليمريه الحاويه على النتروجين والى الصفات الاروماتيه . النماذج المتراكبه تم تشكيلها باستخدام الياف الزجاج من نوع E والمشبعه بالبوليمرات السابق ذكرها . اما خصائص التعريه فقد تم تقييمها من خلال تعريض النماذج المتراكبه المقولبه الى الشعله الاوكسي استيلينيه طبقا لل ASTM E 285-8 معظم النماذج المعرضه للفحص اعطت عزل جيد من خلال السرعه الواطئه لتكوين الرماد وكذلك معامل التعريه

ABSTRACT

Eleven phenolic Schiff bases were prepared previously by condensation reaction of p-hydroxy benzaldehyde or furfuryldehyde with p-aminophenol, p-phenelene diamine, 1,2- phenelene diamine ,4,5-dimethyl 1,2-phenelene diamine, p-dianilino methane , p-dianilino ether , hydrazine, ethylene diamine, benzidene and aniline.These phenolic Schiff bases were converted to phenol formaldehyde,resole type resin, by polycondensation with excess formaldehyde, which were characterized by I.R and thermal analysis.

High ortho resole resin was also prepared previously by condensation of phenol with excess of formaldehyde in the presence of magnesium oxide as catalyst and characterized by infrared spectroscopy and thermogravemetric analysis. The thermal stability of the cured resins according to the 50% wt. loss was evaluated, and were in the following order XX > XIII, XII > XVI > XIX > XVII, XXI > XXII > XV > XXIII. The higher thermal stability is attributed to ladder structure which is expected to be formed in the cured resins as well as to the linear nitrogenous backbone structure and aromatic character. Composite samples were prepared by using chopped fiber glass type E as a reinforcing fiber impregnated with a polymeric matrix based on the above phenolic resin derivatives and high ortho resole resin. The ablative characteristics were investigated by subjecting the molded composite species to oxy- acetylene flame test according to ASTM E 285 - 80 .Most of the examined ablative samples showed good insulation properties in view of their low char rates and outstanding ablative indices.

INTRODUCTION

The outstanding advantage of phenolic resins as matrix materials for structural composites is their fire and heat resistance. These key properties add to their market growth and as a result of research, new products and applications continue to emerge, demonstrating its versatility and the potential to cope with the ever changing requirements and challenges of advanced technology.

Traditional applications of phenolics are in areas such as frictional materials (1), foundry binders (2), grinding and cutting equipment (3), foam insulation (4), coating and adhesives (5), construction (6), electrical purposes (7). Also it is used in the manufacturing of molding compounds with superior mechanical strength, heat resistance and dimensional stability (8), thermal insulation (9), flame ratardance and fire resistance insulation (10). A phenolic resin composite possesses excellent ablative properties and may be used for thermal protection in many high temperature applications. Consequently the knowledge of thermal properties of these materials is essential for designing process. By comparison with other resins, Phenolic Glass Reinforced Plastic (GRP) retains its structure integrity at high temperature. These characteristics make phenolic (GRP)

attractive for use in the construction industry, including spacecraft heat shields for atmospheric re-entry, rocket motor nozzle liners, missile magazine and plenum liners and blast deflectors for missile launching areas These ablative materials have found a significant application in aerospace (11), in solid fuel rockets where they are used for various components (12).
In the present work we aim to study the thermal and ablative properties of some phenolic resin derivatives and their composite.

MATERIALS AND METHODS

p-Hydroxy benzaldehyde ,p-Aminophenol ,4,4`-Diamino diphenyl ether ,4,4`-Diamino diphenyl methane , Benzidene , Calcium stearate , Magnesium oxide , Polyvinyl butyral , γ- aminopropyl – triethoxy silane , Benzene , Acetone (Merck) , 4,5-Dimethyl1,2-phenylene diamine , 1,2-phenylene diamine , Sodium hydroxide (BDH) , p-phenylene diamine , Hydrazine , 1,2-Ethylene diamine , Absolute ethanol , Chopped fiber glass type E-glass, length (3-5) cm (Fluka) , Aniline , Formaldehyde solution (37%) , Phosphoric acid (Riedel – De Haen) , Furfural, Purified by vacuum distillation (13) (Baker)

Synthesis and Characterization of Phenolic Schiff Base Resins

The phenolic schiff base resins and high ortho resol resin Fig (1) were synthesized and characterized by IR, UV spectroscopies and thermal analysis as described earlier (14,15)

Preperation of Cured Methylolic Phenolic Schiff Base and High Ortho Resol Resins

Methylolic phenolic Schiff bases resins (XII-XXII) and high ortho resol resin (XXIII) were cured by heating for 5 hours at 180°C and used in the thermogravemetric analysis, the (TGA, DTG) thermograms are shown in Figs.(2 – 11).

Preparation of the Polymeric Phenolic Composites

Composite samples were prepared by using chopped fiber glass type E as reinforcing fiber impregnated with a polymeric matrix based on the following resins:

Phenol - formaldehyde high ortho resol resin (XXIII).
3, 5- Dihydroxymethyl - 4 - hydroxybenzylidene - 3`, 5`-dihydroxymethyl - 4`-hydroxy aniline (XII)
Bis [3, 5 - dihydroxymethyl - 4, 4`-dihydroxybenzylidene]-p-phenylene diamine (XIII).
Bis [3, 5 - dihydroxymethyl - 4, 4`- dihydroxybenzylidene] - p-dianiline ether(XIV).
Bis [3, 5 - dihydroxymethyl - 4, 4`- dihydroxybenzylidene - p-dianiline methane (XV).
Bis [3, 5 - dihydroxymethyl - 4, 4`-dihydroxy benzylidene] hydrazine (XVI).
Bis [3, 5 - dihydroxymethyl - 4, 4`- dihydroxy benzylidene] - 1, 2 - phenylene diamine (XVII).
Bis [3, 5 - dihydroxymethyl - 4, 4` - dihydroxy benzylidene] - 4, 5 - dimethyl - 1, 2 - phenylene diamine (XVIII).
Bis [3, 5 -dihydroxymethyl - 4, 4`- dihydroxy benzylidene] ethylene diamine (XIX).
Bis [3, 5 - dihydroxymethyl - 4,4`- dihydroxybenzylidene]-p-biphenylene diamine (XX).
3, 5 -Dihydroxymethyl - 4 - hydroxy benzylidene aniline (XXI).
Furfurylidene - 5, 3 - dihydroxymethyl - p-hydroxyaniline (XXII).

The chopped fiber-glass type E was treated [16] with 2.0% by weight of γ-aminopropyltriethoxysilane as coupling agent in aqueous solution at pH 5 and dried in air for one day. Subsequently, the fibers were dried under vacuum at 50°C for an additional ten hrs. The polymeric matrix was prepared by mixing the resins under study with the 12% by weight of poly(vinyl butyral) [17] and 2% by

weight of calcium stearate as a release agent, by using mechanical stirrer for about 15 min. at room temperature. Then the viscosity of the polymeric matrix was measured by using (German Standard) (DIN-4) cup. The viscosity can be adjusted by adding absolute ethanol in order to achieve a viscosity range of about (45-50) s. Which is suitable for the impregnation of the fiber glass. The silane treated chopped fiber-glass was then impregnated in the polymeric matrix. The fiber glass form about 60% of the composite weight. The prepared wet polymeric composite samples were dried in an oven for (4-5) hrs at 50°C. The humidity content which should not exceed 4-5%. The polymeric composites were molded by using hot hydraulic press.

Measurements and techniques

Thermal Analysis

The thermal stability of the prepared high ortho resol and methylolic schiff base resins were tested by thermogravimetric technique (TGA and DTG). Thermo Haak, S11 was used in this study by taking (2.9-1.5) mg of the cured resins and exposed under programmed heating rate of 20°C/min from (25-800°C) under inert atmosphere (N_2 gas),so the weight loss vs. temperature thermograms were recorded (Figures 2-11) and analyzed table(1).

Ablative Testing

The ablative tests were carried out according to ASTM E 285-80, by this test, composite burn through time, erosion rate, char rate and insulation indices were determined. The set up consists of a welding torch, equipped with a mixture of oxygen – acetylene gases (1:20 by volume). The insulation index was calculated by dividing the time by original thickness of the specimen in (mm) The char rate was also determined as reciprocal of the insulating index (ablative index) × 1000.The erosion rate was calculated by dividing the original thickness of the specimen by the time to burn through. the ablative parameters obtained were listed in table 2.

RESULTS AND DISCUSSION

Phenolic composites consisting of reinforced fiberglass were prepared in this study by impregnating the chopped short fiber glass type E in the modified phenolic resin in order to improve the adhesion characteristics of the phenolic resin to produce a flexibilized film, (10-12) part of poly (vinyl butyral) (17) was mixed with (100) part of phenolic resin. The principal application of poly (vinyl butyral) depends on their properties (4); adhesion to a wide variety of surfaces such as glass, metal, wood, ceramics and others, chemical and solvent resistance (especially when cross-linked), heat stability, film clarity. These properties, alone or in combination, make these polymers useful in adhesive formulations as principal or minor constituents. It is used with phenolic resin to form tough, strong, structural adhesives (18). The mechanism of the cross-linking between poly (vinyl butyral) and resol depends on the reactive groups in both resins (19). For a phenolic resin, its reactive group is methylol, and for poly (vinyl butyral) is a hydroxyl group. Cross-linking is a reaction between these functional groups on both polymers, which lead to the formation of ether linkage and water molecule. This cross- linking will occur at a reaction temperature within the range of (150-170) °C. The cross –linking reaction can be illustrated by the following equation (1).

It was found (20), that for poly (vinyl butyral) the final product must consist of (17-20%) of hydroxyl content and (0-2.5%) of acetate content in order to react with the phenolic resin at 160°C .

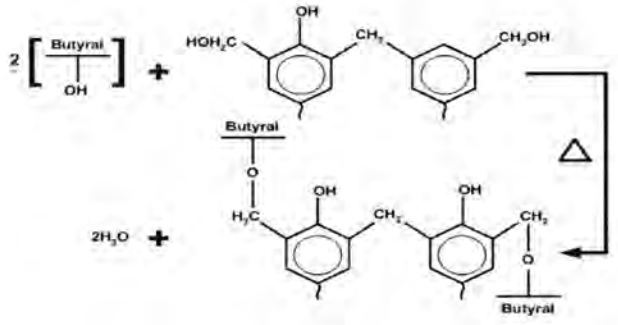

.....(1)

Where 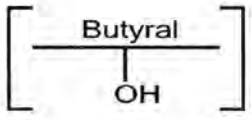 is Poly(vinyl butyral) with residual alcohol and acetate groups which can be written as follows:

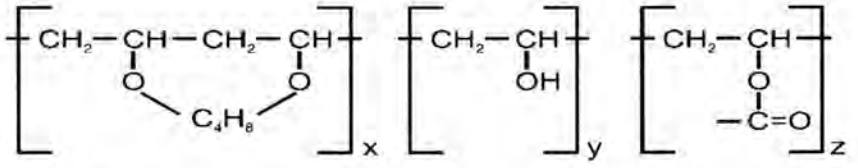

Poly (vinyl butyral) Poly (vinyl alcohol) Poly (vinyl acetate)

Thermal Characteristics of Resins

The thermal degradation of phenol formaldehyde resins, is conveniently segmented into three stages indicated by weight loss in the first stage below 200° C the polymer remains virtually intact. The quantity of carbonaceous components released during this stage consists mainly of water and unreacted monomers, phenol and formaldehyde which were entrapped during cure. Decomposition commences at approximately 300C°. From 300C° to 600C° mainly gaseous rate reaches the maximum with this range. In the second stage, water, carbon monoxide, carbon dioxide, methane, phenol cresols and xylenols are released. During this degradation stage random chain scission occurs, no depolymerization takes place. In the third stage above 600C°, CO_2, CH_4,H_2O, benzene, toluene, phenol, cresols and xylenols are liberated.(21) . The thermal stability of the prepared resins was tested by thermogravemetric technique (TGA) and (DTG). The thermograms shown in figures (2-11), were analyzed. Several thermal stability parameters were determined from TG and DTG thermograms and listed in table (1) which shows the percent weight loss at 300C°, 500 C° and half weight loss temperature, as well as the temperature of the maximum rate of decomposition and char percent at 800C°.

Considering the percent weight loss at 300, 500C°, all resins lose less than resol which loses 9.4%, 32.0% respectively. Regarding the weight loss at 300C° it is expected that the percent weight loss at this temperature for resins XIII, XIX, XXI may be due to humidity of the specimens because the thermograms showed no real decomposition at this temperature. The 50% wt loss takes place at higher temperatures (600.0, 600.0, 585.0, 570.0, 675.0C°) for resins (XII, XIII, XVI, XIX, XX) respectively, in comparison with resol at 562C°. Moreover, the temperatures of the maximum rate of decomposition T1, T2, T3 C° for all resins are higher than that for resol. The thermal stability parameters estimated from the TG and DTG curves showed that all resins are thermally stable except for resin (XIX) which diminished at 663.4 C°, due to the presence of aliphatic group. They are even more thermally stable than resol. The thermal stability of the resins according to the 50% wt loss temperature can be arranged in the following order:

XX > XIII+XII > XVI > XIX > XVII+XXI > XXII > XV > XXIII

This high thermal stability may be attributed to the linear nitrogenous backbone structure, through the presence of azomethine moieties where the nitrogen is doubly bonded to carbon. Also the ladder structure which is expected to be formed in cured resins should result in somewhat more stable than analogous linear polymers (22). A third reason for this high thermal stability is the cross-linking which improves heat resistance of a polymer primarily because more bonds must be cleaved in the same vicinity for the polymer to exhibit a weight loss. Although the wt% loss of resin (XXII) at 500C° is (32.5%) which is somewhat higher than resol (32.0%) but its temperatures of maximum rate of decomposition T1, T2, T3 (530.0, 580.2, 700.0) C° are higher than, those of resol (310.1, 479.2, 563.4) C°. Regarding resin (XVI) although the bond dissociation energy (23) of a nitrogen-nitrogen bond is relatively low (~ 160 kJ/mole or 38.2 kcal/mol) and would not be expected to be incorporated in thermally stable polymers. However, because of resonance stabilization, the N-N bond in (Resin XVI) exhibits reasonably good thermal stability.

Ablative Characteristics of the Composites

The ablative characteristics of the composite systems based on resins (XII-XXIII) were investigated and the resulting burn through time, erosion rate, charring rate and insulation indices were listed in table 2. In general the flame ablation test indicated that the erosion rate and insulation indices exhibited by the samples under study did not vary strongly. Composites based on resin (XX, XIII) perform better than others and they have higher insulation indices with low erosion and char rate. This may be due to the fact that these resins normally, exhibit much larger charring behaviors, which in turn would present an increasing porous barrier in front of the burning flame. Thus it is in fact continuously enhancing the insulating character of the thermal barrier. This is also confirmed by the values of the charring rates, which normally vary inversely with the insulating index, and they exhibited relatively low charring rates as compared with the other resins. This conclusion is confirmed by the thermogravemetric analysis results of the resins where the char % at 800°C are 15.0 and 12.0 respectively Figs.3,8. On the other hand all the other polymeric composites except the composite sample based on resin XIX Fig. 7 showed also good ablative characteristics. As expected the composite sample based on resin (XIX) showed lower ablative characteristics relative to resol composite and other composites based on methylolic Schiff base resins. This was also confirmed by the thermogravemetric analysis where resin (XIX) Fig. 7 was of the least thermal stability and completely diminished at 663.4 C° . The examined polymeric composites have the following sequence regarding their ablation indices.

XX > XIII > XII > XXIII > XV > XVI > XXI > XIV > XVII > XXII > XVIII > XIX

The good ablative characteristics of the resins under study may also be due to the fact that reinforcing fibers may act as a heat dissipater or provide a much better network for transferring heat in a random manner. This may divert the heat path away from the targeted direction much more than the uncomposited resin would do. Hence the fiber network will actually act as an additional heat barrier. At the same time it will act as a mechanical stabilizer to the charred layers, which protect this porous layer. Thus, will hinder the erosion process and in turn enhance the insulation process by maintaining the thickness of these layers.

Table-1: Thermal characteristics of resins

Fig. No.	Resin code	%wt loss at 300°C	%wt loss at 500°C	50 %wt loss Temp. °C	Temp. of max. rate of wt loss °C			Char % at 800°C
					T1	T2	T3	
2	XII	6.4	30.0	600.0	532.2	629.4	-	3.8
3	XIII	2.4	22.4	600.0	382.3	583.1	616.0	12.0
4	XV	5.0	26.4	525.0	423.8	527.9	-	1.5
5	XVI	2.4	16.0	585.0	281.0	594.2	-	7.7
6	XVII	9.23	32.0	550.0	335.4	557.5	-	5.4
7	XIX	5.0	17.6	570.0	371.4	568.3	655.5	*
8	XX	3.2	8.8	675.0	550.0	663.9	-	15.0
9	XXI	2.4	37.6	550.0	430.9	542.0	600.0	7.3
10	XXII	1.25	32.5	530.0	530.0	580.2	700.0	6.5
11	XXIII	9.4	32.0	362.5	310.1	479.2	563.4	3.5

* Final decomposition temperature is 663.4°

Table- 2: Insulating ablative parameters for the composites (60/40) % fiber glass to matrix of resins, resol, and methylolic Schiff bases

Resin code	Thickness (mm)	Burn through time (sec)	Insulation index (sec/mm)	Erosion rate (mm/sec)	Char rate (mils/sec)
	6.0	29	4.83	0.207	8.28
	6.0	32	5.33	0.188	7.50
	6.7	24	3.58	0.279	11.17
	6.5	29	4.46	0.224	8.97
	6.3	27	4.29	0.233	9.32
	6.5	23	3.54	0.283	11.30
	7	24	3.43	0.292	11.66
	6.5	20	3.08	0.325	12.99
	6.4	35	5.47	0.183	7.31
	6.8	28	4.12	0.243	9.71
	6.9	24	3.48	0.287	11.49
	7.3	35	4.79	0.209	8.35

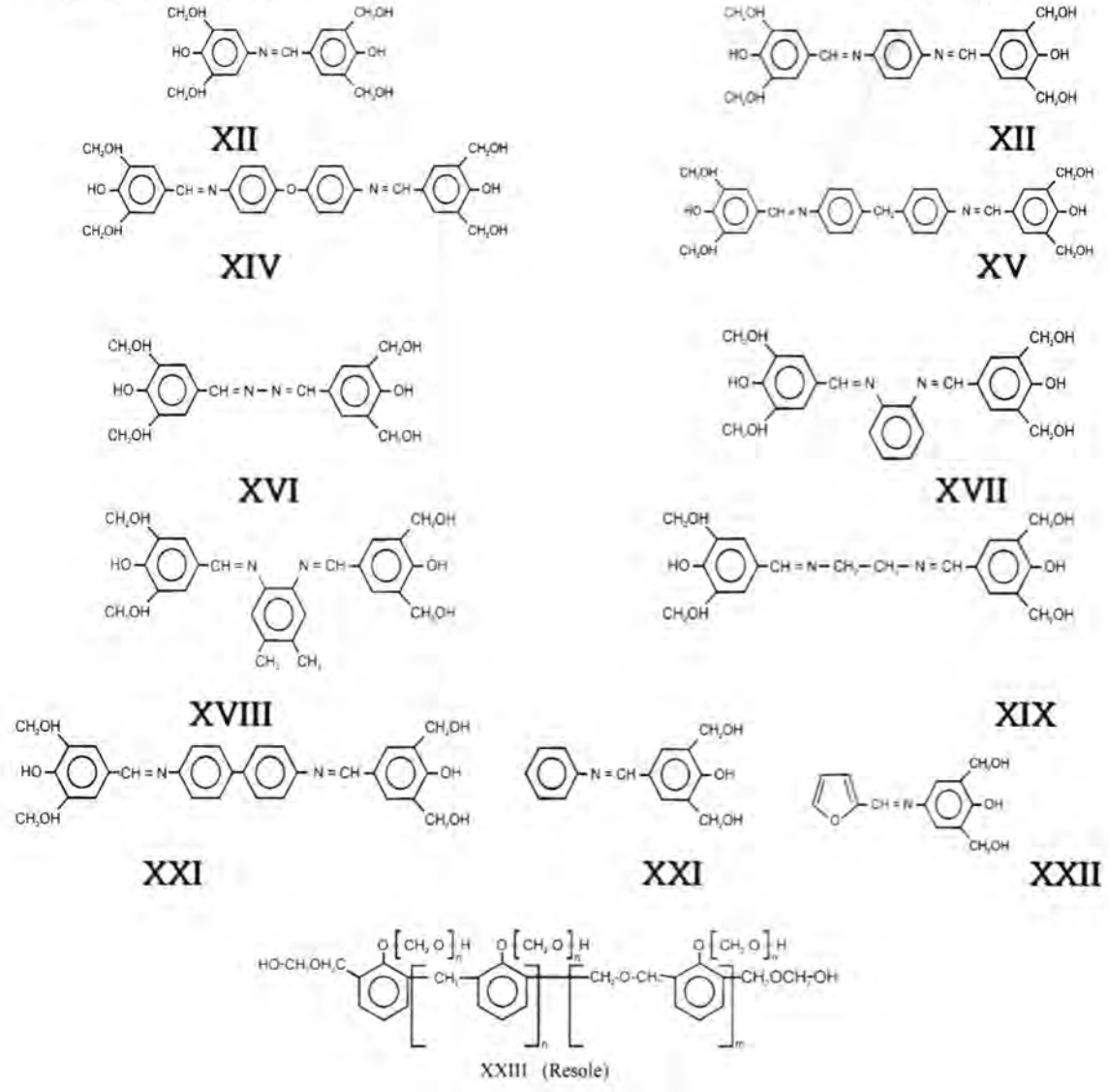

Fig. -1: Chemical structures of phenolic resin derivatives

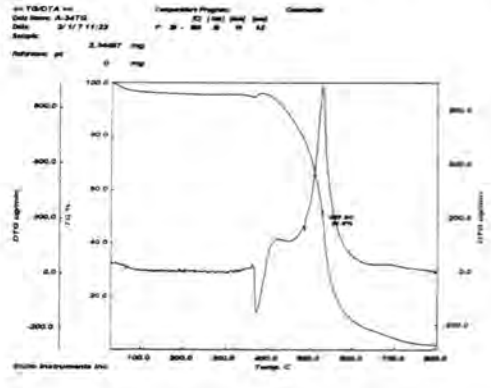

Fig. -4: TG and DTG thermogram of resin (XV)

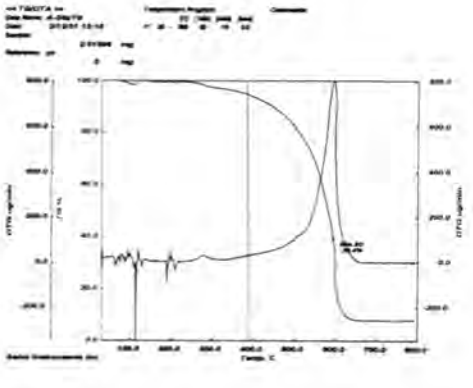

Fig. -5: TG and DTG thermogram of resin (XVI)

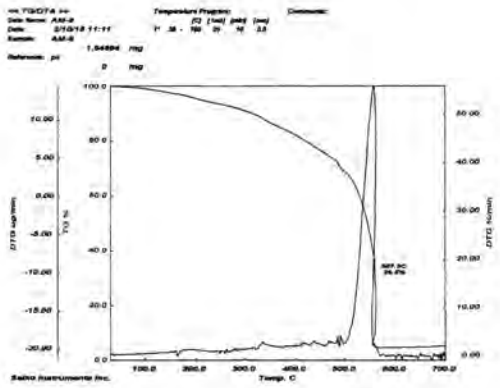

Fig. -6: TG and DTG thermogram of resin (XVII)

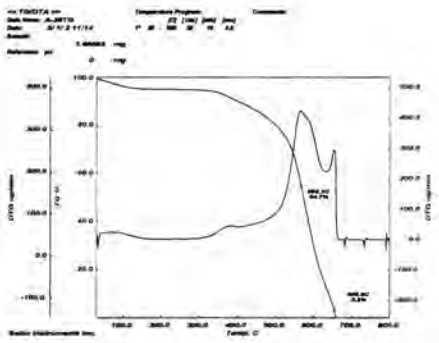

Fig. -7: TG and DTG thermogram of resin (XIX)

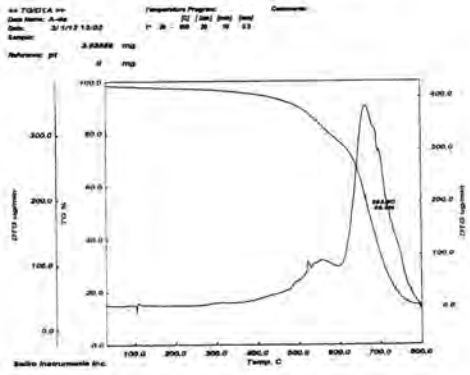

Fig.-8: TG and DTG thermogram of resin (XX)

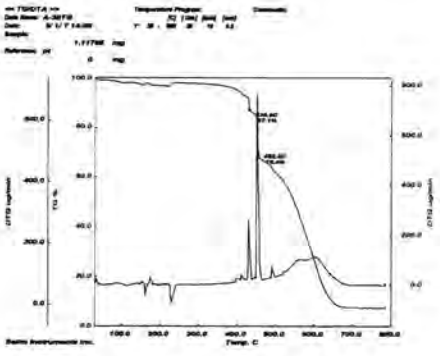

Fig. -9: TG and DTG thermogram of resin (XXI)

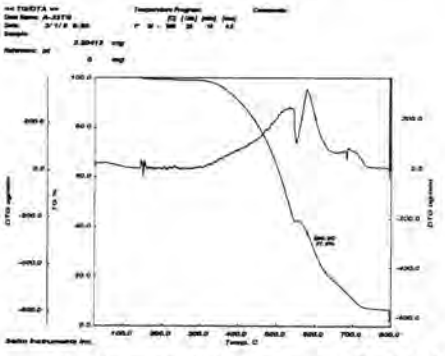

Fig.-10: TG and DTG thermogram of resin (XXII)

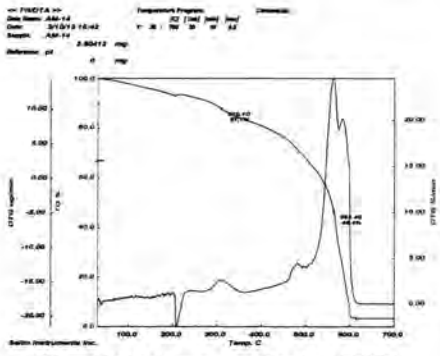

Fig. -11: TG and DTG thermogram of resin (XXIII)

REFERENCES

1.L. B. Lewis, W. F. Schleicher "The Grinding Wheel", 3rd Ed., Grinding Wheel Institute, Cleveland, Ohio, 1976.
2.Carry, R. Paul, Schneider, T. James "Updating Resin Binder Processes-Part IV". Foundry Management and Technology , 114, (5): 62-66, May (1986).
3.R.I.Eglund,E.J.Drwell, "Abrasives,Coated, Cutting Tools." Encyclopedia of Chemical Processing and Design, Marcel Dekker Inc. New York, (1976).
4.Blackwell, B. James, Marks, C. Gerald, Vereeck, Paul, Phenolic foam composites for making them, US Pat. 4, 501, 794, Feb 26, (1985).
5.H. K. Ono, A. Inove, "Adhesives and Bonded Wood Products". Forest Products Society Proceedings, (4735): 330-345, (1994).

6.Troll, Takayoshi,Sugita,Minorv,Tachkawa,Toshiyuki, Composite materials U.S.Pat. 5, 368, 934, Nov. 29, (1994).
7.G. M. Dulitskaya, E. F. Zinin, M. I. Doronina, K. S. Sidoreko, A. L. Panin, M. N. Muzafarova, Electrotekhnika, 60 (2) : 121-123, (1989).
8.J. Jang, H. Chung, M.Kim,Y.Kim, Improvement of flame retardancy in phenolic and paper-sludge/phenolic composite J.Appl. Polym.Sci. 69(10): 2043-2050, (1998).
9.Ko Th. Kuo. Ws. Chang Yh, Microstructure changes of phenolic resin during pyrolysis, J. Appl. Polym. Sci.81(5):1084-1089, (2001).
10.K.L.Forsdyke"Phonlic Resin Composites for Fire and High Temperatur. Application,Plastic and Rubber Institute Conference Reinforced Composites, Liverpool, April (1984).
11.H.R. Clements and G.T. Ward, Journal of Space Craft and Rockets, 3, (4), 483, April, (1966).
12.R. Pickering and D. Sims "Polymer in Rocket Motors" In Polymers in Defense, Plastics and Rubber Institute, International Conference Held 18-20 March, (1989) in Bristol, UK.
13.B.S.Furnass,A.T.Hannaford,V. Rogers, P.W.T. Smith And A.R. Tatchell, Vogel's Textbook of Practice Organic Chemistry"4th. Ed. Longmans, London: 792 (1986)
14.T.S.Najim, Amel M.Naji and Salah A.A. Al-Naimi, Synthesis and characterization of some phenolic Schiff base resins,Iraqi J.polymers 11(1):11-20 (2007).
15.T.S.Najim , Amel M. Naji and Mahmood M. Barbooti, Thermal and ablative properties of ipns and composite of high ortho resole resin and difurfurylidene acetone, Leonardo Electronic J. of Practices and Technologies. 13: 34-46, (2008).
16.C.H. Chiang and J.L.Koenig, Spectroscopic characterization of the matrix –silane coupling agent interface in fiber –reinforced composite, J. Polymer Sci., Polymer Phys.ed., 209110: 2135-2143 (1982).
17.Ninomiya, Hiroaki, Tomioka, Nobuyuki, Terashita, Takeshi, Nagata, Hideo, Kishi and Hajime, Phenolic resin composition for fiber –reinforced composite material,prepreg for fiber-reinforced composite material, U.S. Pat. 6, 391, 959, (2002).
18.T.P.Blomstrom,Encyclopedia of Polymer Science and Engineering, 17, 3rd. Ed. John Wiley and Sons, New York (1989).
19.E. Robert Icass Edward Levin, Chemical interactions in the poly(vinyl formal)-phenolic resin system, Ind. Eng. Chem. 50, 229, (1951).
20.K. J. Saunders "Organic Polymer Chemistry", Chapman and Hall 2nd Ed., London, (1988).
21.A. Knop, L. A., Pilato, "Phenolic Resins; Chemistry, Applications and Performance; Future Directions". Springer–Verlag – Berlin and New York, (1985).
22.J. P. Critchley, G. J. Knight and W. W. Wright "Heat-Resistant Polymers", Plenium – Press, New York, (1983).
23.P.M. Hergenrother "Heat Resistance Polymers" In Encyclopedia of Polymer Science and Engineering. 7 : 639-665,(1987).

The Prevalence of Infection with *Schistosoma Haematobium* in Balad Rouz Town, Diyala Province, Iraq

[1]Nagham Y. Al-Bayati , [2]Furhan T. Mhaisen and [3]Nada M. Al-Bashir
[1]College of Education (Al-Razi), University of Diyala,
[2]College of Education (Ibn Al-Haitham), University of Baghdad
[3]College of Medicine, University of Al-Nahrain

الخلاصة

تم جمع عينات إدرار شهريا أثناء المدة من شهر تشرين الأول 2005 وحتى كانون الأول 2006 من تلامذة المدارس والعوائل في مدينة بلد روز، محافظة ديالى. فحصت 1550 عينة إدرار فحصا مباشرا، كما تم أخذ عينات جديدة من جميع الأشخاص المصابين حيث إستخدمت لعدّ البيوض بطريقة الترشيح الدقيق. حددت شدة الإصابة على أساس طفيفة وكثيفة، كما حددت حالة التبول الدموي إلى ظاهر وغير ظاهر. كانت نسبة الإصابة لدى التلامذة تعادل 7.1% مقارنة مع 3.7% لدى العوائل في حين كانت النسبة الإجمالية للإصابة 1.2%. كانت إصابة الذكور تعادل 6.2% مقارنة مع 1% للإناث. سجلت أعلى نسبة للإصابة (8.8%) لدى الأعمار 15 – 17 سنة. سجلت شدة الإصابة الطفيفة لدى 85ر84% من الأشخاص المصابين مقارنة مع 15.15% للشدة الكثيفة. شوهد التبول الدموي الظاهر في 15.15% من العينات الموجبة مقارنة مع عدم مشاهدة أية حالة من هذا التبول لدى 1517 عينة سالبة.

ABSTRACT

Monthly urine samples were collected during the period from October 2005 to December 2006 from primary school children and households in Balad Rouz town, Diyala province. A total of 1550 urine samples were subjected to direct examination. Fresh urine samples from all infected individuals were then used for egg counts by nuclepore filtration method. The intensity of infection was determined as light and heavy, while the hematuria was classified as macrohematura and microhematura. The prevalence of infection among school children was 1.7% in comparison with 7.3% among households, while the overall infection was 2.1%. Infection among males was 2.9% in comparison with 1% among females. The highest infection (18.8%) was among 15-17 years old. Light intensity of infection was shown in 84.85% of the infected individuals in comparison with 15.15% for heavy infections. The macroscopic hematuria was noted in 15.15% of the positive samples in comparison with no cases of the 1517 negative samples.

INTRODUCTION

Schistosomiasis transmission is influenced by numerous factors including snail intermediate host distribution and human definitive host convergence in space and time with surface water(1). Climate and distribution of surface water suitable for snail and the free-swimming parasite stages are crucial in the distribution of schistosomiasis worldwide(2). The variation in the physical environment, human settlement, distribution of freshwater bodies, intensity of exposure, contamination contact by human and prevalence of pathogenic worms and host snails largely determine the prevalence of infection within endemic areas and communities(3). Schistosomiasis transmission also, depends on the active role of the human host in the transmission process through excretory contamination of snail habitats and direct contact with infective water (4). This ecological relationship makes schistosomiasis a disease closely linked to rural water resource development, population increase, inadequate sanitation and lack of effective medical treatment(5).

Urinary schistosomiasis has continued to exist for more than 6000 years in Iraq(3). Only S. haematobium is present in this country(5). In spite of this long history of occurrence and the importance of schistosomiasis, only few studies were done on its epidemiology in Iraq(5, 6, 7, 8, 9, 10, 11, 12). Among these references, only one study(12) was achieved in Balad Rouz town of Diyala province. This town was selected for the present study as it is known to be as one of the schistosomiasis foci in Iraq.

MATERIALS AND METHOD

The present study was based on screening primary school children and households in Balad Rouz town by urine examination. The study covered 1550 individuals during the period from October 2005 to December 2006. A total of 1440 pupils from five schools provided urine samples. Their ages ranged from 6-14 years. They included 915 males and 525 females. All pupils were interviewed according to a questionnaire to obtain information related to age, sex, previous history of hematuria, history of treatment of schistosomiasis, water contact behavior especially swimming and other activities. The children were asked to drink a lot of water and to run around the school building several times. Then, they were supplied with marked test tubes for urine sample which included the last urine drops. The samples were collected between 10:00-14:00 hours and were transferred in a cool-box to the laboratory of Medical Research Center, College of Medicine, University of Al-Nahrain where the direct examination was carried out. During the next day of urine collection, each pupil infected with *S. haematobium* (as indicated with the presence of ova in the urine) was asked to provide a new specimen of urine which was used for eggs count by Nuclepore filtration method(13). A total of 110 inhabitants (other than school children) were selected for the present study. Their ages ranged from 12-40 years. They were permanent residents in the area located near Al-Bazania river. All individuals, belonging to 20 families, were examined except pregnant women and those who refused to cooperate. The samples were collected between 10:00-14:00 hours. Twenty-five individuals were selected as a control group for this study. Among those 25 controls, 15 individuals, living in this endemic area, were negative for *S. haematobium* eggs in their urine (positive controls), while the other 10 individuals were living in non-endemic areas: some of them from Baghdad city and others from Al-Khalis city (negative controls). Their ages ranged from 5-40 years.

The urine was examined by a light microscope for any ova trapped in the filter. The presence of the typical terminal-spined ova indicated a positive case of infection. The individual egg count was expressed as eggs/ 10 ml urine and the intensity of infection was expressed as light infection when egg count ranged from 1-49 eggs/ 10 ml urine and heavy infection when egg counts $\geq$50 eggs/ 10 ml urine[14]. Hematuria was expressed according to the presence and/or absence of macroscopic and microscopic hematuria for all infected and non infected individuals. The macroscopic hematuria (visible hematuria) was scored as positive on urine sample with a reddish-brown color or altogether bloody(14). The

presence of one erythrocyte in urine indicated a microhematuria by microscopic examination(15).

RESULTS AND DISCUSSION

The present study was carried out on 1550 individuals from Balad Rouz town of Diyala province. Males constituted 935 (60.3%) of the studied population against 615 (39.7%) for females. A total of 1473 (95%) of this population was below 15 years of age (Table 1). Table (2) indicated that primary school children constituted 1440 (92.9%), while households constituted 110 (7.1%) of the population (Table 3). Urine examination of 1550 persons showed that 33 (2.1%) individuals were infected with *S. haematobium* (Table 1).

The present rate of prevalence of urinary schistosomiasis in Balad Rouz town (2.1%) is similar to the overall rate of 2.4% reported during 1979 in whole Iraq(5). The Iraqi rate showed slight increase in 1985 and 1986 (4.3% and 3.5%, respectively) due to increasing numbers of Egyptian and Sudanese workers who entered Iraq(9). The rate recorded in the present study is much lower than the rate of 21.5% reported from Theqar province(7), 18% in Balad Rouz town(2) and 8.7% in Albu-Hishma village of Al-Tarmia district, north of Baghdad(10). The present rate is less lower than the rate of 3.8% reported from Al-Adil district of Misan province(11). One of the main reasons for the decrease of prevalence rate recorded in the present study is the effectiveness of the control program (by using molluscicides in epidemiologically suspected canals) carried out twice a year by the Primary Health Care Center in Diyala province (personal communication with the above- named center).

The prevalence of infection among primary school children was 1.7% (Table 1) against 7.3% among households (Table 3). All infected school children were males (2.7%), while all girls were non infected. Among households, two males and six females were infected.

Urinary schistosomiasis in the present study was higher in males than in females in the first decade of life. This could be attributed to the frequent and prolonged contact with water by the males when compared with the females(16). Infection occurs while males are bathing, swimming and playing in contaminated shallow canals. Females exposure occurs through washing clothes and utensils in the river. Such female activities are much less intensive in comparison with male occurrence in water. So, females are less frequently infected(17, 18).

Among school children, the highest prevalence (4%) was among age group 12-14 years old, while the lowest prevalence (0.8%) was among age group 6-8 years (Table 2). The highest prevalence rate of infection among households (18.8%) was among age group 15-17 years (all infected individuals of this group were females). Among males, one infected individual was 13 years old and another one was 18 years old (Table 3). Previous studies in Iraq(5, 7) showed an increase in the infection during the first twenty years of life with an obvious decline afterwards. Taylor *et* al.(16) and Agi & Okafor(17) suggested that host

mechanisms, such as acquired immunity and/or changes in natural resistance with age, are responsible for age- related changes in infection level.

The light and heavy intensity of infection was 84.85% and 15.15%, respectively. The light intensity of infection was among 23 males and five females, while the heavy infection was among four males and one female. Twenty-one of the light intensity cases (75%) were found among children of 6-15 years old. All such children were males. On the other hand, only four children of 6-15 years old were heavily infected which represented 40% of the heavy infections (Table 4).

The overall intensity of *S. haematobium* infection remained low during the entire study period. Only 5/33 (15.15%) of infected individuals excreted ≥50 eggs/ 10 ml urine (Table 5). Some authors[19, 20] suggested that the intensity of *S. haematobium* depends not only on acquired resistance to re-infection but also on duration of exposure. Percentage of infected individuals with heavy infection was considerably lower than those with light infection(18, 19, 21). Schistosomiasis in endemic communities fits a negative binomial curve, with most infected persons harboring low worm burdens and only a small proportion having heavy infections. This may has multiple explanations including genetic susceptibility(22). The high intensity (Table 4) of the present study can be attributed to increased worm burden and high fecundity rate of the parasite while the opposite was encountered in adults and elderly subjects who probably have reduced schistosome worms and less eggs(17).Reduced worm burden in patients of older age may also result from the development of concomitant immunity known to occur in the infection(17, 18).

In connection with the distribution of infected individuals according to the presence of macro- and microscopic hematuria, the macroscopic hematuria was noted in 5 (15.15%) of the 33 positive samples in comparison with no cases of the 1517 negative samples. All infected individuals with positive macrohematuria were heavily infected. The microscopic examination of urine samples demonstrated that all 33 positive samples had microhematuria in comparison with 99 (6.5%) of the 1517 negative samples (Table 5). Similar high percentage of microhematuria were detected in Pemba Island, Zanzibar, Tanzania(23), in Mali(24) and in Northern Cameron(25). The present data showed that all heavy cases of intensity (≥50 eggs/ 10 ml urine) had macrohematuria in the urine. Similar high prevalence of hematuria was observed with high urinary egg count(11, 19, 21). This may be due to the severe effect caused by increasing frequency of eggs penetration(19).

The sensitivity of macrohematuria and microhematuria (as an indicator of parasitological diagnosis of schistosomiasis) was 15.15% and 100%, respectively, while the specificity was 100% and 93.5%, respectively. There was a high significant difference ($p<0.01$) between positive and negative infections for macro- and microscopic hematuria ($\chi^2 = 223.8$ and 362.4, respectively). This high sensitivity agrees with other results which indicated that hematuria is a high sensitive diagnosis tool for the presence of schistosomiasis infection in endemic

areas(23, 25). All infected individuals in the present study are responsible for environmental eggs contamination especially when took in consideration that the sewage and wastes of houses are emptied in the open canal and in Al-Bazania river which is close to these houses, in addition to urination of infected swimmers in this river.

Table-1: Distribution of urinary schistosomiasis in Balad Rouz town according to age and sex.

Age (year)	Males		Females		Total	
	No. Examined	No. Infected (%)	No. Examined	No. Infected (%)	No. Examined	No. Infected (%)
6-8	420	6 (1.4)	299	0 (0)	719	6 (0.8)
9-11	235	6 (2.6)	158	0 (0)	393	6 (1.5)
12-14	270	14 (5.2)	91	0 (0)	361	14 (3.9)
15-17	2	0 (0)	30	6 (20)	32	6 (18.8)
18-20	5	1 (20)	20	0 (0)	25	1 (4)
>20	3	0 (0)	17	0 (0)	20	0 (0)
Total	935	27 (2.9)	615	6 (1)	1550	33 (2.1)

Calculated χ^2= 54.19
P= 0.0001
Tabulated χ^2 = 9.488

Table -2: Distribution of urinary schistosomiasis among school children according to age and sex.

Age (year)	Males		Females		Total	
	No. Examined	No. Infected (%)	No. Examined	No. Infected (%)	No. Examined	No. Infected (%)
6-8	420	6 (1.4)	299	0 (0)	719	6 (0.8)
9-11	235	6 (2.6)	158	0 (0)	393	6 (1.5)
12-14	260	13 (5)	68	0 (0)	328	13 (4)
Total	915	25 (2.7)	525	0 (0)	1440	25 (1.7)

Calculated $\chi^2 = 7.75$ 13.07
P = 0.021 0.002
Tabulated $\chi^2 = 5.991$ 5.991

Table -3: Distribution of urinary schistosomiasis among household according to age.

Age (year)	Males		Females		Total	
	No. Examined	No. Infected (%)	No. Examined	No. Infected (%)	No. Examined	No. Infected (%)
12-14	10	1 (10)	23	0 (0)	33	1 (3)
15-17	2	0 (0)	30	6 (20)	32	6 (18.8)
18-20	5	1 (20)	20	0 (0)	25	1 (4)
>20	3	0 (0)	17	0 (0)	20	0 (0)
Total	20	2 (10)	90	6 (6.7)	110	8 (7.3)

Calculated $\chi^2 = 0.09$ 8.83
P = 0.761 0.012
Tabulated $\chi^2 = 3.841$ 5.991

Table -4: Intensity of infection according to age of infected individuals.

Age (year)	Intensity of Infection					
	Light (<50 eggs/ 10 ml urine)		Heavy (≥50 eggs/ ml urine)		Total	
	No.	%	No.	%	No.	%
6-10	10	35.7	1	20.0	11	33.3
11-15	11	39.3	3	60.0	14	42.4
≥ 16	7	25.0	1	20.0	8	24.3
Total	28	100	5	100	33	100.0

Calculated $\chi^2 = 3.165$
P = 0.05
Tabulated $\chi^2 = 3.841$

Table -5: Distribution of infection according to occurrence of macroscopic and microscopic hematuria.

Eggs	Hematuria					
	Macroscopic			Microscopic		
	+v	-v	Total	+v	-v	Total
+ve (%)	5 (15.15)	28 (84.85)	33	33 (100)	0 (0)	33
-ve (%)	- (0)	1517 (100)	1517	99 (6.5)	1418 (93.5)	1517
Total	5 (0.3)	1545 (99.7)	1550	132 (8.5)	1418 (91.5)	1550

Calculated $\chi^2 = 223.8$ 362.4
P = ≤ 0.01 ≤ 0.01
Tabulated $\chi^2 = 7.87$ 7.87
Sensitivity (%) = 5/33 (15.15) 33/33 (100)
Specificity (%) = 1517/1517 (100) 1418/1517 (93.5)

REFERENCES

1. Wiwanitkit, V. "Overview of clinical reports on urinary schistosomiasis in the Tropical Asia" Pak. J. Med. Sci., 21(4): 499-501, (2005).
2. W.H.O. "Epidemiology and control of schistosomiasis: Report of a WHO Expert Committee" W.H.O. Tech. Rep. Ser. 643: 88, (1980).
3. Kloos, H. & David, R. "The paleoepidemiology of schistosomiasis in ancient Egypt" Hum. Ecol. Rev., 9(1): 14-25, (2002).
4. Kloos, H.; Rodrigues, J.C.A.P.; Pereira, W.R.; Velásquez-Meléndez, G.; LoVerde, P.; Oliveira, R.C. & Gazzinelli, A. "Combined methods for the study of water contact behavior in a rural schistosomiasis- endemic area in Brazil" Acta Trop., 97(1): 31-41, (2006).
5. Baquir, H. "Bilharzia in Iraq and bilharzia project in Rijab marsh" Aab Press, Baghdad: 41, (2006).
6. Bailey, V.M. & Khamis, F. "An intestinal parasitic survey in a rural district of Baghdad" Bull. End. Dis., 2(3 &4): 148-151, (1958).
7. Bairam, A. "Epidemiological pattern and treatment of *Schistosoma haematobium* in Theqar province" Bull. End. Dis., 15(1 & 2): 31-40, (1974).
8. Tawfiq, M.A.R. "Bilharziasis: Its epidemiological pattern with stress on its features in Iraq" Dipl. Diss., Coll. Med., Univ. Baghdad, 36, (1974).
9. Abdul Amir, M.S. "Epidemiological study of imported schistosomiasis in Iraq" Dipl. Diss., Coll. Med., Univ. Baghdad, 62, (1987).
10. Mahmoud, S.N.; Jawdat, S.Z. & Aldlami, B.H. "Studies on *Bulinus truncatus* in Albu-Hishma village with notes on prevalence of urinary schistosomiasis" J. Biol. Sci. Res., 18(2): 29-42, (1987).
11. Al-Sa'ady, H.A.M. "Epidemiological, parasitological and immunological studies of Schistosoma haematobium infection in Maisan, southern Iraq" Ph. D. Thesis, Coll. Educ., Univ. Basrah: 202, (1997).
12. Al-Biaty, H.S. "Epidemiological study of *Schistosoma haematobium* in Balad-rooze sup province" M. Sc. Thesis, Coll. Vet. Med., Univ. Baghdad: 81, (In Arabic), (2000).
13. Cooppan, R.M.; Schutte, C.H.J.; Mayet, F.G.H.; Dingle, C.E.; Van Deventer, J.M.G. & Mosese, P.G. "Morbidity from urinary schistosomiasis in relation to intensity of infection in the Natal province of South Africa" Amer. J. Trop. Med. Hyg., 35(4): 765-776, (1986).
14. Kahama, A.I.; Odek, A.E.; Kihara, R.W.; Vennervald, B.J.; Kombe, Y.; Nkulila, T.; Hatz, C.F.; Ouma, J.H. & Deelder, A.M. "Urine circulating soluble egg antigen in relation to egg counts, hematuria, and urinary tract pathology before and after treatment in children infected with *Schistosoma haematobium* in Kenya" Amer. J. Trop. Med. Hyg., 61(2): 215-219, (1999).
15. Hatz, C.F.; Vennervald, B.J.; Nkulila, T.; Vounatsou, P.; Kombe, Y.; Mayombana, C.; Mshinda, H. & Tanner, M. "Evolution of *Schistosoma haematobium*-related pathology over 24 months after treatment with

prazinquantel among school children in southeastern Tanzania" Amer. J. Trop. Med. Hyg., 59(5): 775-781, (1998).

16. Taylor, M.; Jinabhai, C.C.; Naidoo, K.; Dlamini, S.B. & Sullivan, K.R. "The epidemiology of schistosomiasis among Zulu children in a rural district in South Africa: Determining appropriate community- based diagnostic tools" S. Afr. J. Epidemiol. Infect., 19(3,4): 90-95, (2004).
17. Agi, P.I. & Okafor, E.J. "The epidemiology of *Schistosoma haematobium* in Odau community in the Niger Delta area of Nigeria" J. Appl. Sci. Environ. Manag., 9(3): 37-43, (2005).
18. Abdel-Wahab, M.F.; Esmat, G.; Ramzy, I.; Narooz, S.; Medhat, E.; Ibrahim, M.; El-Boraey, Y. & Strickland, G.T. "The epidemiology of schistosomiasis in Egypt: Fayoum governorate" Amer. J. Trop. Med. Hyg., 62(2): 55-64, (2000).
19. De Clercq, D.; Vercruysse, J.; Picquet, M.; Shaw, D.J.; Diop, M.; Ly, A. & Gryseels, B. "The epidemiology of a recent focus of mixed *Schistosoma haematobium* and *Schistosoma mansoni* infections around the 'Lac de Guiers' in the Senegal river basin, Senegal" Trop. Med. Int. Heal., 4(8): 544-550, (1999).
20. Wolmarans, C.T.; de Kock, K.N.; Bornman, M. & le Roux, J. "The use of scholl- based questionnaires in the identification of factors and groups at risk of infection with *Schistosoma mansoni* in the endemic area of the Limpopo province, S. Africa" S. Afr. J. Epidemiol. Infect., 19(1): 18-22, (2004).
21. Gabr, N.S.; Hammad, T.A.; Orieby, A.; Shawky, E.; Khattab, M.A. & Strickland, G.T. "The epidemiology of schistosomiasis in Egypt: Minya governorate" Amer. J. Trop. Med. Hyg., 62(2): 65-72, (2000).
22. Uneke, C.J.; Ugwuoru, C.D.C.; Ngwu, B.A.F.; Ogbu, O. & Agala, C.U. "Public health implication of bacteriuria and antibiotic susceptibility of bacteria isolates in *Schistosoma haematobium*- infected school pupils southeast Nigeria"World Health Population:1-11.www.longwoods.com product.php? productid, (2006).
23.Savioli,L.; Hatz,C.;Dixon,H.;Kisumku,U.N. & Mott,K.E."Control of morbidity due to *Schistosoma haematobium* on Pemba Island: Egg excretion and hematuria as indicators of infection" Amer.J.Trop.Med.Hyg.,43(3):289-295. (1990).
24. Traore, M.; Traore, H.A.; Kardorff, R.; Diarra, A.; Landoure, A.; Vester, U.; Doehring, E. & Bradley, D.J. "The public health significance of urinary schistosomiasis as a cause of morbidity in two districts in Mali" Amer. J. Trop. Med. Hyg., 59(3): 407-413, (1998).
25. Takougang, I.; Meli, J.; Fotso, S.; Angwafo, F.; Kamajeu, R. & Ndumbe, P.M. "Hematuria and dysuria in the self-diagnosis of urinary schistosomiasis among school children in Northern Cameroon"Afr.J.Heal. Sci., 11(3): 121-127, (2004).

Determining Air Quality Index of pollutant particles and its Health Impacts

Hassony J . Abdulla and Zaid Sh . Naji
College of Science Biology Dept /University of Al- Mustansyria

الخلاصة

هذه الدراسة أجريت لدراسة المشاكل البيئية الناتجة من تلوثِ الهواء بالدقائق الصغيرة المعلقة في جو مدينة بغداد/ العراق.

بيانات حول الغبار وعدد المرضى الذين يعانوا من مشاكل الجهاز التنفسي والقلبي الوعائي (قلب وجهاز دوران) أخذت من مستشفات مختارة في بغداد خلال الأيام المغبرة و الغير المغبرة .

دليل نوعيةِ هواء (Air quality index) أعد من قبل الباحث وكانت قيم دليل نوعيةِ الهواء لهذه الدراسة 00 و40.00 و50.00 و50.00 و51.00 و51.00 و68.00 و 75.00 و92.00 و 98.00% للأيام 24 (يوم صافي الجو) و21 و13 و30 و 28 و 29 و 22 و 25 و 15 و 9 (يوم مغبر جدا) من الشهر الثالث 2009.

قيم دليل نوعيةِ هواء من 0 - 40 % مستويات الصحية جيدة ولا توجد بيانات تحذيرية . القيمة 90 - 100 % مستويات صحيةِ خطرة ولا بد من اتخاذ الحذر ، الأشخاص الذين يعانون بمرض الرئة أو القلبَ، وكبار السنّ، وصغار السن يَجبُ أنْ يَبْقوا في الداخل ولا يقومون بنشاطِ كبير. الآخرون أيضا يَجبُ أنْ يَتفادى أي نشاط طبيعيَ في الخارج.

العلاقة بين تركيز الغبار في الجو مقاس بمدى الرؤيا (y) وعدد المرضى الذين يعانوا من مشاكل الجهاز التنفسي والقلبي الوعائي(X) توضحه المعادلة التالية :

1- $Y = 264.7590\ X^{-0.0714}$ $r = 0.6284$
From Abn Alnafees Hospital

2 - $Y = 136.8317 + 6.2382\ X - 1.1165X\ 2$ $r = 0.8425$
From Al Kindy Hospital

3 - $Y = 298.8405 - 30.5272\ X$ $r = 0.8127$
From Medical City

عدد المرضى الذين يعانوا من مشاكل الجهاز التنفسي والقلبي الوعائي الذين يزوروا المستشفيات يزداد مع زيادة تركيز الدقائق الصغيرة المعلقة في الهواء. إن العلاقة كانت عالية المعنوية ($r = 0.8127$, $r = 0.8425$, $r = 0.6284$)

مرضى القلب قد يُطلب منهم الأطباء مستقبلا تفادي ليسَ الأطعمة الدسمة والتدخين فقط لكن تلوثَ الهواء أيضاً.

ABSTRACT

This investigation has been conducted to study the environmental problems caused by fine particulate matter air pollution in Baghdad city in Iraq . Date of observation , dust and patients suffer from respiratory and cardiovascular (heart and circulatory system) diseases as effected by particle pollution or particulate matter in the air were obtained , also air quality index combined by the author .

The air quality index values of current study were 00 , 40.00 , 50.00 , 50.00 , 51.00 , 51.00 , 68.00 , 75.00, 92.00 and 98.00 % for 21/3/2009(clearest day) , 24/3/2009 , 13/ 3 / 2009 , 30 / 3 / 2009 , 28 / 3 / 2009 , 29 / 3 / 2009 , 22/3/ 2009 , 25/3 / 2009 , 15 /3/ 2009 and 9/3/2009(most dusty day) . The value ranges 0 – 40 % Levels of Health Concern as good and cautionary Statements is none . However , The value ranges 90 – 100 % Levels of Health Concern as Hazardous and cautionary Statements , people with heart or lung disease, older adults, and children should remain indoors and keep activity levels low . Everyone else should avoid physical activity outdoors .

The relationship between the dust concentration in the atmosphere as measure of visibility(Y) and the total number of suffered patients (X) could be explained by the following regressing equation :

1- $Y = 264.7590\ X^{-0.0714}$ $r = 0.6284$
From Abn Alnafees Hospital

2 - $Y = 136.8317 + 6.2382\ X - 1.1165X\ 2$ $r = 0.8425$
From Al Kindy Hospital

3 - $Y = 298.8405 - 30.5272\ X$ $r = 0.8127$
From Medical City

The total number of the patients suffer from respiratory and cardiovascular (heart and circulatory system) diseases visited Abn Alnafees Hospital and Al Kindy Hospital in Baghdad increases with increasing dust concentration in the atmosphere , the relation was highly significant ($r = 0.6284$ Abn Alnafees $r = 0.8425$ Al Kindy and $r = 0.8127$ Medical City) .
Patients prone to heart disease may one day be told by physicians to avoid not only fatty foods and smoking but air pollution too.
Key words; air quality index , dust , visibility , Levels of Health Concern ,

INTRODUCTION

Particle pollution or particulate matter in the air is serous issue that effect human health (Latif , H .Ali , 1987) .. Those include a mixture of solids and liquid droplets. Some particles are emitted directly; others are formed in the atmosphere when other pollutants react. Particles come in a wide range of sizes. Those less than 10 micrometers in diameter are so small that they can get into the lungs, potentially causing serious health problems.Ten micrometers is smaller than the width of a single human hair .

Particles less than 2.5 micrometers in diameter are called "fine" particles;(Abdulla, H. J .and K . A . Hussien . 2008).. Sources of fine particles include all types of combustion, including motor vehicles, power plants, residential wood burning, forest fires, agricultural burning, and some industrial processes .However , **coarse dust particles** between 2.5 and 10 micrometers in diameter are referred to as "coarse." Sources of coarse particles include crushing or grinding operations, and dust stirred up by vehicles traveling on roads also dust storm (Abdulla ,H . J . and Samira M . Dawood . 2005) .

In an overview by the World Bank (World Bank report, 2000) of the 20 cities exposed to highest concentrations of particulate matter Cairo in Egypt exposed to highest concentrations of particulate matter following by two town in India, Jakarta in Indonesia and twelve big

cities in China. Particles smaller than 10 micrometers in diameter may cause or aggravate a number of health problems and may have been linked with illnesses and deaths from heart or lung diseases. These effects have been associated with both short-term exposures and long-term exposures (Quintana PJE et al,2000 and Quintana PJE et al 2001). The World Health Organisation,2002 estimated that over 800,000 people die prematurely due to air pollution. However, many more people suffer from other impacts.

In Iraq ,a lot of information are available about dust pollution (Dougrameji, J . S . and Clor , M . A . (1977), Abdulla, H. J .and K.A . Hussien . 2008 and Abdulla, H. J ., K . A . Hussien and M. Jabbar .2008) but there are a little studies on particulate matter in air and it's impacts on health need to be investigated particularly in Baghdad , so the aim of this investigation was to study the air pollution environmental problems cause by dust .

MATERIALS AND METHODS

To carry out this investigation :

Data of dust as a measure of visibility (km) were obtained from uk.weather.com/weather/today-Baghdad-IZXX0008.

The observation were taken on 9/3/2009 ,13/ 3 / 2008 ,15 /3/ 2009 , 21/3/2009 , 22/3/2009 ,24 / 3 / 2009 , 25/3 / 2009, 28 / 3 / 2009 , 29 / 3 / 2009 and 30 / 3 / 2009 . These observations were arranged as follow:(1)- 21/3/2009(clearest day) , (2)- 24/3/2009 , (3)- 13/ 3 / 2008 , (4)- 30 / 3 / 2009 ,(5)- 28 / 3 / 2009 ,(6)- 29 / 3 / 2009 ,(7)- 22/3/ 2009 , (8)- 25/3 / 2009 ,(9)- 15 /3/ 2009 and (10)- 9/3/2009 (most dusty day) .Total patients obtained from Abn Alnafees, Al Kindy and Medical City Hospitals.Patients usually suffers from respiratory and cardiovascular (heart and circulatory system) diseases

Total patients in dusty days and total patients in clear days were observed . Visibility of 10 km considered as clear day(control observation)

Computer programs (CurveExpert1.3 and SPSS Version 11) were used to analysis the data.

Air quality index combined by the author as follow:

$$\text{Air Quality Index} = \frac{\text{Control visibility} - \text{Observed visibility}}{\text{Control visibility}} \times 100$$

Control visibility = 10 km visibility

Observed visibility = variable visibility

$$\text{Example of calculation for 10 / 9 / 3 / 2009} = \frac{10 - 0.2}{10} \times 100 = 98$$

RESULTS AND DISCUSSION

Date of observation , dust and patients suffer from respiratory and cardiovascular(heart and circulatory system) diseases as effected by particle pollution or particulate matter in the air are obtained on Monday 21 / 3 / 2009 the visibility was 10 km and the corresponding total penitent suffer from respiratory and cardiovascular (heart and circulatory system) diseases visited Ben Nafase , Al Kindy and Medical City Hospitals were 89,204 and 0.0 patients . This day was the clearest day . However , on Monday 9 / 3 / 2009 was the most dusty day so the corresponding total patients suffer from respiratory and cardiovascular (heart and circulatory system) diseases were 125.00 , 309.00 and 290 pantients for the above hospitals respectively . As it can seen that there is a relationship between the dust concentration in the atmosphere as measure of visibility(Y) and the total number of suffered patients (X) table (1). The total number of the patients suffer from respiratory and cardiovascular (heart and circulatory system) diseases visited Ben Nafase ,Al Kindy and Medical City Hospitals .

increase with increasing dust concentration , the relations were highly significant (r = 0.6284 , r = 0.8425 and r = 0.8127) .

Figure (1) shows the relation between patients numbers and visibility (Particle pollution), in Al Kindy Hospital as it has been shown the following regression equation :

$Y = 136.8317 + 6.2382\ X - 1.1165X^{2}$. This equation describe the relation between patients numbers and visibility (Particle pollution).

Figure (2) shows sun behind dust storm in Baghdad city and Figure (3)shows dust storm over Baghdad city.

Table (2) date of observation , dust , air quality index values and patients suffer from respiratory and cardiovascular(heart and circulatory system) diseases from Al Kindy Hospital and Abn Alnafees Hospital as effected by particle pollution or particulate matter in the air. The days with index values of 0.0 -40.0 % considered as good .However , the days with 40 – 50 % (Unusually sensitive people should consider reducing prolonged or heavy exertion.), 50 – 70 % (People with

heart or lung disease, older adults, and children should reduce prolonged or heavy exertion), 70 – 90 (People with heart or lung disease, older adults, and children should avoid all physical activity outdoors . everyone else should avoid prolonged or heavy exertion) and 90 – 100 % (People with heart or lung disease, older adults, and children should remain indoors and keep activity levels low . Everyone else should avoid physical activity outdoors) . These considered as good , Unhealthy for Sensitive Groups , Unhealthy , Very unhealthy and Hazardous for the above index values respectively . The air quality index values of current study were 00 , 40.00 , 50.00 , 50.00 , 51.00 , 51.00 , 68.00 , 75.00 و 00..75 , and 98.00 % for 21/3/2009(clearest day) , 24/3/2009 , 13/ 3 / 2008 , 30 / 3 / 2009 , 28 / 3 / 2009 , 29 / 3 / 2009 , 22/3/ 2009 , 25/3 / 2009 , 15 /3/ 2009 and 9/3/2009(most dusty day) .

Table (3) shows air quality index values , levels of health concern , cautionary statements and examples of the investigated days. It appears that patients prone to heart disease may one day be told by physicians to avoid not only fatty foods and smoking but air pollution too.

It appears that the air quality index value ranges from 0 to 40 % Levels of health concern as good . The value ranges 90 to 100 % levels of health concern as hazardous .The total number of the patients suffer from respiratory and cardiovascular (heart and circulatory system) diseases increases with increasing dust or particle pollution in Baghdad atmosphere , the relation was highly significant

($r = 0.6284$, $r = 0.8425$ and $r = 0.8127$).

The assistance and the co-operation of Dr . Mohammad K. Al-Amery the head of Abn Alnafees Hospital and Dr . Nawras Hatif Jasam from Al Kindy Hospital are gratefully acknowledged .

Table -1: shows the equations that the relation between patients numbers and visibility (Particle pollution) . a –In Abn Alnafees Hospital , b –in Al Kindy Hospital and c – Medical City Hospital .

No.	Regression equation	Y	X	r	Hospital
1	$Y = 264.7590\ X^{-0.0714}$	patients	Visibility (Particle pollution)	0.6284	Abn Alnafees
2	$Y = 136.8317 + 6.2382\ X - 1.1165X^{2}$	patients	Visibility (Particle pollution)	0.8425	Al Kindy
3	$Y = 298.8405 - 30.5272\ X$	patients	Visibility (Particle pollution)	0.8127	Medical City

Table-2: Date of observation , dust , air quality index values and patients suffer from respiratory and cardiovascular(heart and circulatory system) diseases from Al Kindy Hospital , Abn Alnafees and Medical City Hospital as effected by particle pollution or particulate matter in the air.

NO.	Date of observation 2009	Dust (visibility,km)	air quality index values	Number of patients		
				Al Kindy Hospital	Abn Alnafees Hospital	Medical City
1	21/3	10.0	00	89.00	204.00	00
2	24/3	6.0	40.00	132.00	255.00	188
3	13/3	5.0	50.00	135.00	289.00	00
4	30/3	5.0	50.00	132.00	216.00	167
5	28/3	4.9	51.00	131.00	241.00	155
6	29/3	4.9	51.00	161.00	211.00	194
7	22/3	3.2	68.00	139.00	232.00	152
8	25/3	2.5	75.00	155.00	265.00	223
9	15/3	0.8	92.00	154.00	238.00	322
10	9/3	0.2	98.00	125.00	309.00	290
Mean ± SE		4.25± 0.89	57.50± 8..85	135.30±6.41	246.0±10.77	169.10±33.26

$$Y = 136.8317 + 6.2382\ X - 1.1165X^{2} \qquad r = 0.8425$$

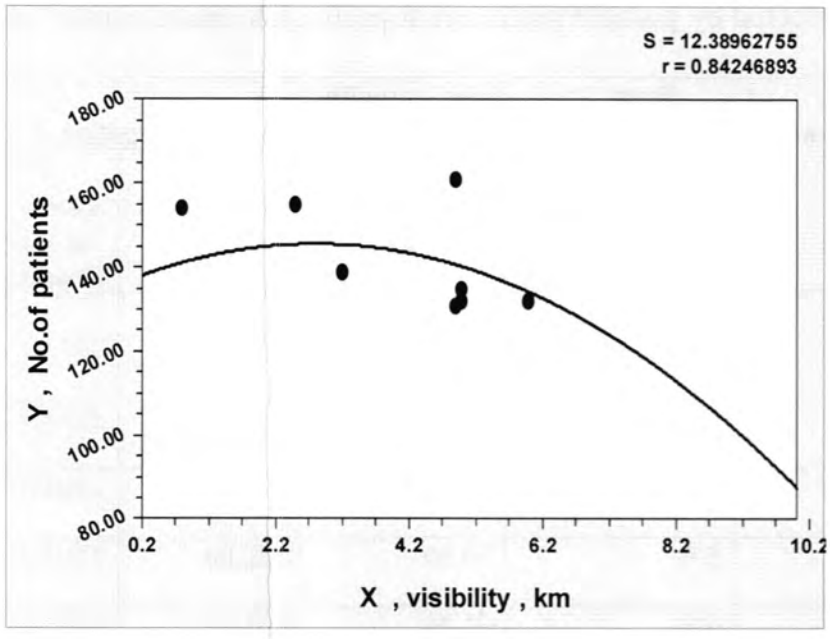

Figure -1: shows the relation between patients numbers and visibility (Particle pollution), in Al Kindy Hospital .

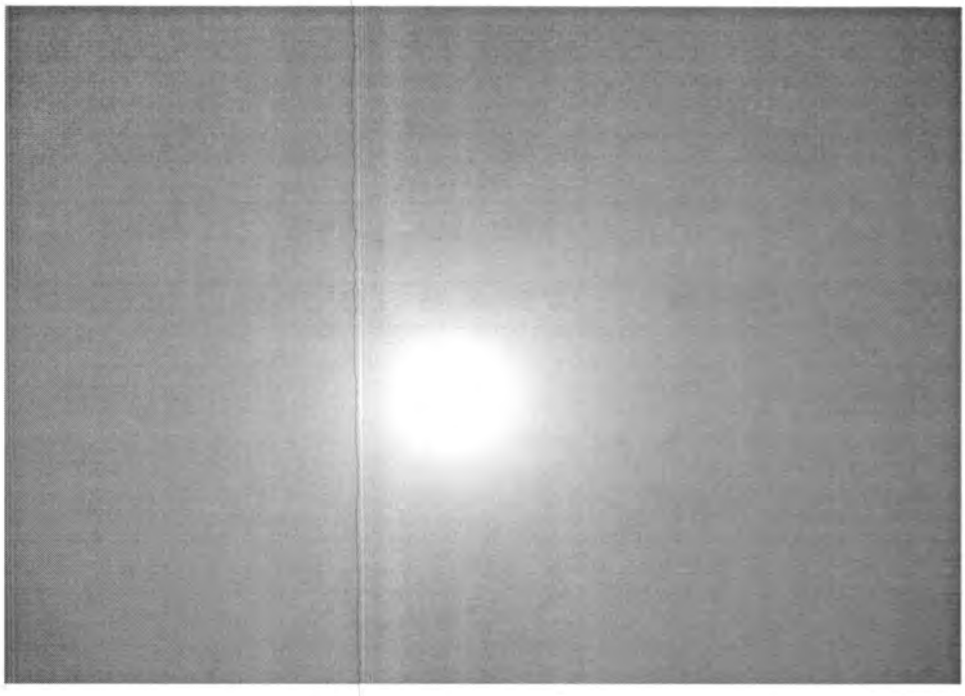

Figure -2: Sun behind dust storm in Baghdad sky

Figure -3: , 12 June 2005 dust storm over Baghdad

Table -3: shows air quality index values , levels of health concern and cautionary statements .

Index Values	Levels of Health Concern	Cautionary Statements	Examples
0.0 -40.0	good	None	21 and 24/3/2009 Clear day(control)
- 50.040.0	Unhealthy for Sensitive Groups	Unusually sensitive people should consider reducing prolonged or heavy exertion.	13 and 30/3/2009
50.0 - 70	Unhealthy	People with heart or lung disease, older adults, and children should reduce prolonged or heavy exertion	22 , 28 and 29/3/2009
70-90	Very unhealthy	People with heart or lung disease, older adults, and children should avoid all physical activity outdoors . everyone else should avoid prolonged or heavy exertion	25/3/2009
90 -100	Hazardous	People with heart or lung disease, older adults, and children should remain indoors and keep activity levels low . Everyone else should avoid physical activity outdoors .	9 and 15/3/2009 (dusty day)

REFERENCES

1. Abdulla ,H . J . and Samira M . Dawood . 2005 . Wind erosion and dust storm in relation to climate condition , in Baghdad area , Iraq . Al- Mustansiriya J . Sci.16 , (1) : 82 – 88 (2005).
2. Abdulla, H.J .and K. A . Hussien .. The Effect of Climatic Elements on Atmospheric Turbidity and Air Pollution in Baghdad City – Iraq , Jour. Eduction College Unver. Of Mustansiriyia - Baghdad–Iraq(1): 538– 545. (2008).
3. Abdulla, H. J ., K . A . Hussien and M . T . Jabbar . Pollution as a Major Cause of Desertification Phenomenon in Iraq . Medwell Journals, Envir.Research .Jour.2(4):187–188 . (2008).
4. Dougrameji, J . S . and Clor , M . A . Case study on desertification . Gearter Mussayeb Project . Iraq. United Nations Conference on Desertification. A/ CONF . , 74 / 10 , 102 (1977).
5. Latif , H .Ali , Industrial . Pollution Ministry of higher Education and Scientific Research, University of Mussel, Iraq (1987) .
6. Quintana PJE, Samimi BS, Kleinman MT, Liu S, Soto K, Buffalino C, Warner G, Valencia J, Francis D, Hovell MH, Delfino, RJ., Assessment of personal exposure to fine particulate matter in asthmatic children using a real-time sampler: sampler performance. J Expo Analysis Environ Epidemiol; 10:437-45. (2000).
7. Quintana PJE, Valenzia JR, Delfino, RJ, Liu L-J S. Monitoring of 1-minute personal particulate matter exposures in relation to voice-recorded time-activity data. Environmental Research,; 87:199-213. (2001).
8. uk.weather.com/weather/today-Baghdad-IZXX0008
9. WHO ,World Health Organisation, . (reports) (2002)
10. www.cpt.org/gallery/view photo . php
11. World Bank report: *Beyond Economic Growth*(2000)

Influence of Caffeine on Human Spermatozoal In Vitro Fertilizing Capacity of Asthenozoospermic Patients

[1]Essraa M. A. Al Essawe and [2]Saeeda A.M. Alanssari
[1]Department of Clinical Reproductive Physiology, IVF Institute for Embryo
[2]Research &Infertility Treatment – AL-Nahraine University

الخلاصه

الهدف من الدراسه الحاليه هو تحديد تأثير الكافئيين على القدره الاخصابيه للتطف البشريه الوهنه . شملت الدراسه تنشيط السائل المنوي خارج الجسم لعشرين عينه مجموعه من مرضى يعانون من وهن النطف بطريقه النبذ والسباحه للاعلى بعد اضافه 3 ملي مول كافئيين للوسط الزرعي المستخدم في التنشيط . أجري فحص القدره الأخصابيه بأستخدام بيوض الهامستر الخاليه من النطاق الشفاف لتحديد القدره الأخصابيه بوجود او عدم وجود الكافئيين في الوسط الزرعي. شملت الدراسه على عشرين عينه مجموعه من اشخاص سليمين كمجموعه سيطره ثانيه .أظهرت النتائج تحسن معنوي في القدرة الاخصابية وبدلالة احصائية معنويةعالية ($p<0.01$, $P<0.001$ تباعاً) فيما يخص نسبة البيوض المُخترقة بواسطة الحيامن اضافة الى عدد الحيامن المُخترقة للبيضة الواحدة .

اوضحت نتائج الدراسه ان اضافه مادة الكافئين وبتركيز 3 ملي مول في تنشيط النطف البشريه الوهنه خارج الجسم بطريقه النبذ والسباحه الى الأعلى قد يكون مفيدا في التلقيح الاصطناعي والاخصاب الخارجي للحصول على نسب حمل عاليه في حالة المرضى المصابين بوهن النطف .

ABSTRACT

The objective of this study was to demonstrate the effect of caffeine on human sperm fertilizing capacity of asthinozoospermic patients. The effect of *in vitro* caffeine addition to semen of 20 asthenozoospermic infertile patients was studied. .*In vitro* sperm activation by centrifugation swim up migration technique was used, 3mM caffeine concentration was supplemented to sperm preparation medium prior to sperm activation. Sperm penetration assay (SPA) using zona free hamsters oocytes was performed to determine human sperm fertilizability rate in the presence or absence of caffeine. Twenty normozoospermic semen samples involved as second control .The results showed that the *in vitro* human sperm penetration rate and penetration index were significantly increased ($p<0.001$ and $p<0.01$ respectively) in the caffeine treated group versus control groups. It was concluded that the application of 3mM caffeine to *in vitro* sperm activation by centrifugation swim up migration technique may be useful for intrauterine insemination and *in vitro* fertilization, to achieve high pregnancy rate incase of asthinozoospermia.

Key word: Caffeine, asthenospermia, invtro, SPA

INTRODUCTION

Caffeine a cyclic nucleotide phosphodiesterase inhibitor (1) acts by several mechanisms including the translocation of extracellular calcium ,inhibiting phosphodiesterase enzyme thus decrease the catabolism of cAMP and increase its cellular level (2,3).Caffeine has been reported to increase motility, life span and forward progression of poor quality spermatozoa *in vitro* (4, 5, 2). Stimulatory effect of caffeine was most obvious in patients with asthenozoospermia. (6).So caffeine may enhance sperm fertilizing potential as well as can accelerate

spermatozoal fertilizing capacity (7). Increasing the number of sperms migrating through cervical mucus with the use of chemical stimulants such as caffeine showed to increase the number of sperms reaching the site of fertilization *in vivo* and thereby increase the probability of conception (8). The best correlation with fertilizing potential is the zona free hamster oocytes penetration assay (9, 10, 11). Sperm penetration assay is an *in vitro* technique that assesses the ability of spermatozoal to successfully undergo capacitation, acrosome reaction (AR), membrane fusion with oocyte, and chromatin decondensation (12,13).This assay was initially described by Yanagimachi *et al.*in 1976(14), they demonstrated that human spermatozoa penetrate hamster oocytes that have been treated to remove the zona pellucida. These observations resulted in the use of hamster oocytes as a substitute for human ova in the assessment of the fertilizing capacity of human spermatozoa. The hamster oocyte is unique in that, in its zona free state it can be penetrated by every species sperms (15).The use of zona free hamster oocytes is a test system for evaluating the fertilizing capacity of human spermatozoa and applied to diagnose male fertility, to predict the success of assisted reproductive technique (ART) procedures and to assess certain male infertility therapy (13). This test is also used as a screening procedure before IVF (16).Yee and Cummings 1988(17) reported that SPA correlates well with male infertility *in vivo*. Since that scoring the average number of sperms penetrating per ovum (sperm penetration index) (SPI) is more suitable than the percentage of ova penetrated (18). SPI is a reflection to extent of AR in the sample, because there is no block to polyspermia in zona free hamster oocytes (19).The present study was designed to evaluate the effect of caffeine with *in vitro* sperm activation by centrifugation swim up migration technique on sperm fertilizing capacity in case of asthenozoospermic infertile patients.

MATERIALS AND METHODS

Semen samples were obtained by masturbation after 3-5 days of abstinence directly in a clean, dry and sterile disposable Petri-dish from 20 infertile patients with asthenozoospermia and 20 normozospermic semen samples, during their attendance to institute of embryo research and infertility treatment. Three-millimole concentration of caffeine was added to the sperm preparation culture medium (SPM) for an *in vitro* sperm activation (Medicult) manufactured by medicult company, Denmark. Each ejaculate was checked for seminal fluid quality after 30 minutes of liquefaction at 37Ċ . Asthenozoospermic semen samples were washed with culture medium containing 3mM caffeine and

centrifuged for 5 minutes at 2000 R.P.M. the supernatant was discarded and one ml of fresh (SPM) containing 3mM caffeine was added to the sperm pellet slowly . The pellet with culture media was incubated for 30 minutes. The seminal fluid of the control group and normozoospermic semen samples were washed and incubated with (SPM) with out caffeine supplementation. Sperm penetration assay (SPA) was done as follow: Mature females of golden hamster (age 12-16 weeks) under super ovulation program, by intra-peritoneal injection with 20 International units (IU) of Human menopausal gonadotrophin (HMG, pergonal, Serono, Italy) at any day of oestrus cycle, same dose at the same time was injected after 24 hrs. 48 hrs from the second dose 40 IU of human chorionic gonadotropin (HCG Pregnyl, Organon; Holland) was injected to induce ovulation. The animals were killed by cervical dislocation 16-17 hours from HCG injection.Oocytes were flushed out from fallopian tubes by flushing medium; medi- cult. Comp., Denmark) 1% hyluronidase was added to egg culture medium for 5-10 minutes to remove the cumulus cells then rewashed with the same medium. 0.1% Trypsin for 1 minute was added to remove zona pellucida.

The oocytes were washed twice time by the culture medium then about 8-10 hamster ova were isolated in small Petri dish and covered by liquid paraffin then incubated at 37°C, 5% Co_2 for 1-2 hrs before insemination. The oocytes were inseminated by prepared sperms using centrifugation- swim up migration technique after adjusted to $1.5X\ 10^6$ sperm/ml. Inseminated oocyte were incubated in 5% Co_2 at 37°C for 3hrs. after that eggs were rinsed to remove loosely adherent spermatozoa and placed on clean Petri dish for examination at 400 x magnification power under inverted microscope.

Sperm Penetration % is calculated by the equation:

$$\text{Sperm penetration \%} = \frac{\text{No. of penetrated oocytes}}{\text{Total no. of inseminated oocytes}} \times 100$$

While

$$\text{Sperm penetration Index} = \frac{\text{No. of sperm swollen heads per oocytes}}{\text{No. of penetrated oocytes}}$$

Statistical analysis: Paired T test in addition to the standard statistical methods to determine the mean and standard error of the mean (SEM) (16).

RESULTS AND DISCUSSION

The effect of 3mM caffeine concentration on in vitro sperm penetration percent and sperm penetration index of asthenozoospermic semen of infertile patients was demonstrated in table 1. The sperm penetration rate when 3 mM concentration of caffeine supplemented to the culture medium was significantly increased than that of first control group without caffeine (30.90% ±2.56 versus 10.30% ±2.96, $P < 0.001$ respectively) and second control group normozoospermic fertile semen sample (30.90% ±2.56 versus 24.35% ±3.04, $P < 0.05$respectively). The sperm penetration index also significantly higher ($P < 0.01$) in the 3 mM caffeine supplementation group than that of first control group (15.67 ±1.93 versus 6.52 ±1.82, respectively) and second control group (15.67 ±1.93 versus 8.57 ±1.93, respectively).

Table-1:The effect of 3mM caffeine concentration on sperm penetration assay of asthenozoospermic semen of infertile patients.

Groups	Sperm penetration % (mean ± SE)	Sperm penetration index (mean ± SE)
Control group (without caffeine) First control	10.30 ± 2.96	8.57 ± 1.93
Fertile group (with out caffeine) Second control	24.35 ± 3.04	6.52 ± 1.82
Treated group (with 3 mM caffeine)	30.90*[a] ± 2.56	15.67**ь ± 2.04

*$P < 0.001$ significantly different from the first control group.
** $P < 0.01$ significantly different from the first control group.
[a] $P < 0.05$ significantly different from the second control group.
ь $P < 0.01$ significantly different from the second control group
Number of samples per each group = 20.

The findings of the present work demonstrated that caffeine significantly increased sperm penetration percent and sperm penetration index of asthenozoospermic human semen when zona free hamster oocytes penetration assay was done after sperm activation by centrifugation swim-up migration technique. These findings are in good agreement with the results reported by Rogers in 1981(20) who indicate that caffeine can enhance the fertilizing ability of human sperm cells. Highest rates of penetrated zona-free hamster oocytes were achieved with 2mM caffeine (21), as well as caffeine

can accelerates spermatozoal fertilizing capacity (7). The use of xanthenes derivatives like methyl xanthenes, caffeine (1, 3, 7-trimethyl-2, 6-diioxopurine) has been reported to enhance spermatozoon motility as well as fertilizing ability (22, 23). While caffeine was observed to improve significantly various motility parameters in a dose-dependent manner, it did not lead to an improvement in the fertilization rates. At the highest concentration, 5 mM, it adversely affected the fertilization rate 38%, compared with 78% in controls (24). Margatioth, et.al. 1984(25) reported that caffeine significantly increases sperm motility but has no effect on sperm penetration in to zona free hamster oocyte. Moreover, spermatozoa pre-incubated with caffeine showed a significant decrease in the percentage of penetrated zona-free hamster oocytes (8). In assisted reproduction, caffeine showed an increase in sperm motility but a significant decrease in the fertilization rates and embryo development (24). The use of sperm motility stimulants such as caffeine ,estradiol , pentoxifylline to the ejaculate prior to use for intra uterine insemination **(IUI)** or *in vitro* fertilization **(IVF)** demonstrated an effective treatment for asthenozoospermic patients(26,27). This discrepancy may be due to the quality of semen, nature of semen (fresh or cryopreserved), method of sperm activation *in vitro*, type of culture medium used, incubation period and program of superovulation induction in hamster (quality of hamster oocytes) and genetic abnormality in the studied human semen. In conclusion 3mM of caffeine significantly increased sperm penetration rate and sperm penetration index of asthenospermic infertile semen when zona-free hamster oocytes penetration test was used. Caffeine as a spermatozoon motility enhancer requires further studies prior to wider clinical use in assisted pregnancy programs.

REFERENCES

1. Makler, A.; Makler, E.; Itzkovitz, J. and Brandes, J. M. Factors affecting sperm motility. IV: Incubation of human semen with caffeine, kallikrin, and other metabolically active compounds. Fertil. Steril.; 33:624-630 (1980)..
2. Chatlerjea, M. N. and Shinde, R. Diet and Nutrition. In: Text Book of Medical Biochemistry. Jaypee Brothers Medical Publishers (p) Ltd., New Delhi, India. 2nd edition: 464, 890- 892, 981(1995).
3. Goth, A. Central nervous system stimulants of the convulsant type. In: Medical Pharmacology. The C.V. Mosby Company St. Louis Toronto. 11th ed. PP: 307- 309(1984)..
4. Schoenfeld, C.; Amelar, R. D. and Dubin, L. Stimulation of ejaculated human spermatozoa by caffeine. Fertil. Steril.; 26: 158- 161(1975).

5. Amelar, D. A.; Dubin, L. and Schoenfeld, C. Sperm motility. Fertil. Steril.; 34: 197- 215(1980)..

6. Makkar G.; Ng H.Y.; Yeung S.B. and Ho P.C. Comparison of two colloidal silica-based sperm separation media with non-silica- based medium.Fertil.Steril. 72:796-802(1999)..

7. Lynn, R. F. Accelerated mouse sperm penetration *in vitro* in the presence of caffeine J. Reprod. Fertil.; 57: 377-384(1979).

8.Hammitt,D.G.;Bedi,E.;Rogers,P.R.;Syrop,G.H.;Donovan,J.F.and Williamson,R.A. Comparison of motility stimulants for cryopreserved human semen. Fertil. Steril; 52 (3): 495- 501(1989).

9.Hall, J. Relationship between semen quality and human sperm penetration of zona- free hamster ova. Fertil. Steril.; 35: 457-462(1981).

10.Karp, L. E.; Roger, A. W.; Moore, D. E.; Shy, K. K.; Plymate, S. R. and Smith, W. D. Sperm Penetration assay: useful test in evaluation of male infertility. Obstet. Gynecol.; 57: 620- 623(1981).

11. Margalioth, E. J.; Navot, D.; Laufer, N.; Mor- Yosef, S.; Rabinowitz, R.; Yarkoni, S. and Schenker, J. G. Zona- free hamster ova penetration assay as a screening procedure for *in vitro* fertilization. Fertil. Steril.; 40: 386-388(1983).

12. Urry, R.L.; Middleton, R.G. and Mayo, D. A comparison of the penetration of human sperm into bovine and artificial cervical mucus. Fertil. Steril.; 45: 135-137(1986)..

13. Dana, A. and Alan, C. M. Assessment of sperm function and clinical aspects of impaired sperm function. On- line; 09/01/96(1996).

14. Yanagimachi, R.; Yanagimachi, H. and Rogers, B. The use of zona-free animal ova as a test system for the assessment of the fertilizing capacity of human spermatozoa. Biol. Reprod.;15: 471-476(1976).

15. Rogers, B. J. The sperm penetration assay its usefulness reevaluated. Fertil. Steril.; 43: 821-840(1985).

16. Critser, J. K.; Arneson, B. W.; Aaker, D. V. and Ball, GD. Cryopreservation of hamster oocytes: effects of vitrification or freezing on human sperm penetration of zona- free hamster oocytes. Fertil. Steril.; 46: 277- 284(1986)..

17. Yee, B. and Cummings, L.M. Modification of the sperm penetration assay using human follicular fluid to minimize false negative results. Fertil. Steril.; 50: 123- 128(1988).

18. Johnson, A. Optimized sperm Penetration Assag. Hosted at infertility Resources (Johnso@rohsu. edu). Developed by Internet Health Resources(2000).

19. Siegel, M. S. and Graczykowski, J. W. Influence of porcine follicular fluid on the fertilizing capacity of human spermatozoa. Fertil. Steril.; 55: 1204-1206(1991).

20. Rogers, B. J. Factors affecting mammalian *in vitro* fertilization. In: Bioregulators of Reproduction. Jagieollo, G., and Vogel, H. J. (eds). Academic press, New York.; PP.; 459- 486(1981).
21. Aitken, R. J.; Best, F.; Richardson, D. W.; Schats, R. and Simm, G. Influence of caffeine on movement characteristics, fertilizing capacity and ability to penetrate cervical mucus of human spermatozoa. J. Reprod. Fertil.; 67: 19-27(1983).
22. Cheeck, J. H.; Zavos, P. M.; Katsoff, D. and Kiefer, D. Effects of percoll discontinuous density gradients VS sperm prep II VS saphedeax G-50 gel filtration on sperm parameters (med line) Tohoku. JExp Med; 169: 225-231(1993).
23. Ghalib, M. M. Human follicular fluid sperm hyperactivation *in vitro* and intrauterine insemination. M. Sc. Thesis. Baghdad University, PP: 124-133(1995).
24. Imoedemhe, D.A.; Sigue, A.B.; Pacpaco, E.L and Olazo, A.B. The effect of caffeine on the ability of spermatozoa to fertilize mature human oocytes. J Assist Reprod Genet; 9:155-160(1992).
25. Margalioth, E. J.; May, J. Y., Navot, D.; Laufer, N.; Ovadia, J. and Schenker, J. G. Effect of caffeine on human sperm penetration in to zona-free hamster ova. Arch. Androl.; 14: 139- 142(1984).
26. Tesarik, J. and Mendoza, C. Gamete for assisted reproduction: past, present, and future. J.androl. 24:321-328(2003).
27. Yovich, T. M.; Edirisinghe, W. R.; Cummins, J. M.and Yovich, J. L. Influence of pentoxifylline in severe male factor infertility. Fertil. Steril.; 53: 715-722(1990).

Consanguineous Marriages and Some Reproductive Health Parameters for Sample from Families in Baghdad ,Iraq.

Fadhel Mohammed Lafta
Department of Biology ,College of Science ,University of Baghdad

الخلاصة

زواج الأقارب هو ذلك التزاوج الذي يتم بين أفراد تربطهم قرابة بايولوجية.. وقد أشارت العديد من الدراسات إلى وجود ارتباط قوي بين زواجات أقارب الدرجة الأولى وظهور الاضطرابات في مؤشرات صحة التكاثر .و يهدف بحثنا إلى تحديد نمط وانتشار زواج الأقارب والعوامل المترابطة معه لعينه من العائلات في بغداد .

أجري البحث على سكان المناطق الحضرية في بغداد ، واشتملت العدد الكلي للعينة المدروسة على302 أمراه متزوجة جرى مقابلتهم في منازلهن أو أماكن عملهن .جمعت المعلومات التي تخص الصفات التكاثرية والاجتماعية والإحصائية للنساء لكل عائلة بصورة مباشرة باستخدام استبانه معدة لهذا الغرض وتم تحليل البيانات إحصائيا باستخدام برنامج SPPS .

أظهرت النتائج أن النسبة الكلية لزواج الأقارب هي 44.04 %، وقد بلغت قيمة معامل التزاوج الداخلي للعينة المدروسة 0.01851. ، وظهر بأن الزواج بين أقارب الدرجة الأولى هو النمط الأكثر شيوعاً 56.4 % بين زواج الأقارب . كما قد تبين بأن لصغر عمر المرأة عن الزواج ولانخفاض مستوى تعليمها أثرا معنوياً في زيادة زواج الأقارب (P= 0.05) . عائلات زواج الأقارب من الدرجة الأولى كانت الأكثر اختلافاً معنوية بالنسبة للإسقاط التلقائي والتشوهات الخلقية بالمقارنة مع زواج الأباعد (P=0.01) . وازدادت نسبة الخصوبة وكذلك نسبة العائلات ذات التكاثر المضطرب (52.3%) في زواج الأقارب .

وقد وجد بأن معدل انتشار زواج الأقارب وبالأخص التزاوج بين أقارب الدرجة الأولى مرتفع نسبياً في بغداد . كما إن نسبة العائلات ذات التكاثر المتأثر مرتفعة أيضاً . لذا فأن المزيد من الدراسات المستقبلية عن أسباب وآثار زواج الأقارب يجب أن تتواصل .

ABSTRACT

Consanguineous marriages are the marriages contracted between blood relatives . many studies have suggested a strong association between consanguinity and the incidence of abnormal reproductive health parameters.

The aims of this research was to determine the prevalence and type of consanguineous marriages and the associated factors for sample from families in Baghdad , Iraq.

The research was conducted in urban areas of Baghdad .A total sample of 302 married women were interviewed at their home or work places. Information on the sociodemographic and fertility characteristics of the women were gathered using a written questionnaire .Data analysis was done by SSPS program.

The overall prevalence of consanguinity was 44.04 % , with a mean of inbreeding coefficient of 0.01851 . The principal type of consanguineous marriages was first – cousins marriages , which accounted for 56.4 % of all consanguineous unions .There was a significant association) between consanguinity and sociodemographic characteristics (younger ages and lower educational level)of the participants (P = 0.005) .First cousins marriages had significantly more spontaneous abortions and congenital disorders when compared with non-consanguineous relatives (P =0.01) . Higher fertility and higher affected reproductive families (52.3 %) were associated with consanguineous marriages .

The prevalence of consanguinity and of first –cousins marriages was found to be high in Baghdad . The rate of affected reproductive health families was also very high . Further researches on the reasons for and negative outcomes of consanguineous marriages should be conducted .

INTRODUCTION

Consanguineous marriages are marriages contracted between blood relatives or union between two people who share an ancestor (1). Its widely practiced in Asia , North Africa ,Middle East and fishermen communities in Europe and America and at least 8.5% of children have consanguineous parents of these population (2).

Around the globe , consanguineous marriages have been practiced by many societies from time immemorial and it has declined remarkably in most developed countries .However ,within many populations of developing countries marriages between biological relatives remain common and favorable . this is especially true in societies where Islam prevails with consanguineous marriages accounting for 20-50% of all marriages(3). However , consanguinity is not unique to Muslim societies . Rather, it has been found that about 20-45% of unions in South India , where Hindu belief prevails, are between blood relatives . A similar trend propelled by socio-cultured customs has been documented among some sects in West and South Asia , such as Buddhist ,Christians , Jews ,Parses and Druze .Preliminary observations indicates that migrants from these areas continue to contract with close relatives when resident in North America and Western Europe (4).

The preference to consanguineous marriages has been attributed to traditions , cultural press , comply with the wish of the parents , strengthening of family ties , financial advantages relating dowry , the ease of marital agreement, closer relationship between the wife and the in-laws , grater social compatibility , marriage stability (low divorce) and durability(5).

Consanguineous marriages favored for the woman status have been associated with low socioeconomic status , illiteracy or low education and rural residence (6) . Consanguinity is also associated with increased gross fertility , due to at least in part to younger maternal age at first live birth(7).

On the other hand , consanguineous marriages could increased the risk of inheriting any one of the 4968 (autosomal recessive) genetic diseases that could effect any part of the body from the head to the foot . Due to inheritance, parents and children and brothers and sisters , commonly share 50 per cent of their genetic make-up (8). The higher risk comes as consequences of autosomal recessive conditions stemming from homozygosity by descent. In other words it is the risk of recessive mutations present in an ancestor being passed down branches of the family and coming together in the consanguineous marriages (9).

It is assumed that all of us carry at least one mutated allele that would lead to an autosomal recessive condition if present in two copies (homozygosity) . In case this mutant allele is inherited by both member of

consanguineous marriage from common ancestor , they both will be carry for this condition . Hence , they will have a one in four chance of having an effected offspring (10).

Consanguineous marriages are major responsible risk factors for bipolar disorders . This marriage system has been reported as an important factor in the appearance of autosomal recessive and polygenic or multifactorial diseases and congenital anomalies including hydrocephalus ,postaxial hand polydactyl and bilateral cleft lip cleft palate(11) , depression , epilepsy , mentally retardation (12) , reproductive disorders :sterility , spontaneous abortion , still birth , infant mortality , child morbidity , mortality (13) , also the risk of the birth defects in the offspring of first cousin mating has been increased to 5-8% compared to 2-3% in non consanguineous marriages(10).Several studies have shown that consanguinity led to death of infants before ,during or immediately after birth., and increased incidence of birth defects, and genetic diseases such as : blinding disorders, blood cancer, breathing problems, congenital hyperthyroid and increased the susceptibility to diseases(14,15,16)

Furthermoe, there are reports indicate to positive association between consanguinity and Down syndrome , ventricular – atrial septal defects , pulmonary stenosis , asthma , diabetes , multiple sclerosis , Alzheimer and Parkinson disease (17,18) .

Some scientists contradict these studies and state that other biological factors , and not consanguineous only, could accountable for the results. Recent studies suggest that having consanguineous parents seems to decrease the risk of breast cancer especially in younger women (19)and to protect against malaria (20).

Despite the advances in medical and public health , genetic diseases still accounted for an increased proportion of disease worldwide . Predictably , this burden will fall more heavily on countries and communities in which consanguinity is strongly favored . Evidence suggests that consanguinity does play negative role in human health . The social benefits of consanguinity should not outweigh the biological damages; many in the community are ignorant about these facts (21).

Among Arabs , consanguineous marriages are customary and constitute 20-50% of all marriages .First cousin marriages constitute almost one third of all marriages in many Arab countries (14). The rate of these marriages differ between countries as well as within one country . Marriages between first cousins are favored culturally and socially and considered the "usual " or "expected" pathway in life for first cousins whether they were reared in close proximity or reared far apart (22). Some studies showed decline of consanguineous marriages in Jordan ,Lebanon and Israeli Arabs (,23,24,25). However other studies reported increase in rate of consanguineous marriages in Yemen , Qatar , Kuwait , UAE (1,14,26,27) .

In Iraqi society , which is predominantly Muslim ,consanguineous marriages are quite common. The first study on consanguineous marriages in Iraq ,Baghdad was conducted by Hamamy et al. in 1986 and the prevalence was determined as 46.4% (first cousin marriages was 29.2 %) (28) .Other studies have shown the prevalence of marriages between biological related couples was about 37-43 % in Southern Iraq (29) while the prevalence of consanguinity in Northern Iraq was 25%(32)

The aim of this research is to estimate the prevalence and socio demographic predictors of consanguineous marriages and its impact on reproductive health in a sample of urban families in Baghdad ,Iraq.

MATERIALS AND METHODS

The data was collected by using questionnaire form that was arranged according to previous studies (29,30). A random sample consist of 302 families resident was investigated in urban population in Baghdad ,Iraq from the period of 14 January to 15 June 2009. The information regarding the extent of relationship was sought from each family as to whether the couple was first cousin ,second cousin , third cousin or distantly (non related). Also, information regarding education level of the women and pregnancy outcome (a detailed history about their past obstetrical record which included history of abortion , stillbirth ,neonate mortality and presence of congenital malformations in any of children) was also obtained .To assess the genetic impact of consanguineous marriages due to homozygosity of recessive lethal and detrimental allele ,the number of non-accidental mortality offspring among living children was recorded .

Standard procedure of $\chi 2$ test was employ to analysis the data using SSPS program .Coefficient of inbreeding for population was calculated by using the formula $\sum$ Pi Fi , where Pi is the proportion of certain type of consanguineous marriages and Fi is the coefficient of inbreeding of the type of consanguineous marriages (2) .

RESULTS AND DISCUSSION

The overall prevalence of consanguineous marriage in this research was 44.04 % , equivalent to a mean inbreeding coefficient of 0.01786 .The frequency of first cousin marriages was 24.83% (Table 1) . In other words , of the consanguineous marriages recorded , 56.4 %(75/133) was between first cousins and 24.06 % (32/133) between second cousins .

Table -1 : Percentages distribution of marriage types among participations

Marriage type	N	%
Non-consanguineous	169	55.96
First cousins	75	24.83
Second cousins	32	10.6
Distant related	26	8.61
Total	302	100

The incidence of consanguinity is relatively high in Baghdad , with a rate of 44.04 % .However, this percentage is less than that recorded in Baghdad in 1986 (46.4%) by Hamamy et al.(28) and by WHO in 2004(29 % ; 32),and higher than recorded by Al-Rekaby in 1997 (37 % ;30) .On the other hand, the rate of consanguinity in this search (44.04%)is higher than in Yemen (39.9% ; 1) and Lebanon (42 % ;), while lower than these in UAE (50.5 ;26) , Jordan (51 % ; 23) ,Saudi Arabia (52 % ;33) , Qatar (54 % ; 14)and Egypt(68 %;34) .The inbreeding coffecient (which is represented as an indicator to the degree of inbreeding) in the present research (0.01786) is less than that recorded in Iraq in 1998 (0.020 ;(31)) , Qatar (0.02372;(14)) and Iran (0.0185 ;(8)) .However its higher than that recorded in Turkey (0.01081 ;(2) Similar to other Arab countries , where there is a tradition of consulting with male siblings , before agreeing to the marriage of the daughter to non- relative (1), we believe the preferences are related to the deeply rooted cultural beliefs and social customs. Such marriages are considered to be more stable , due to close similarities in social and cultural values and the economic benefits of keeping wealth within families (14).

To determined the factors responsible for mating among relatives , we investigated demographic and educational characteristics of women in the present investigation . There was a significant association ($\chi 2 = 6.274$, D.F.=2, P=0.043) between consanguinity and lower educational level (illiteracy and primary school) .More consanguineously married women (36 %) were reported being illiterate and low educated than non-consanguineously married women (27.8 %). Conversely ,women with secondary and higher education were less likely to be married to cousins (61.5 % of non-consanguineously married women as compared to those in consanguineously married 47.4%) (Table 2).

Table - 2 : Distribution of marriage type by women educational level .

Women educational level	Non-consanguineous		Consanguineous	
	N	%	N	%
Illiteracy & Primary school	47	27.8	48	36.1
Intermediate	18	10.7	22	16.5
Secondary & Higher educatio	104	61.5	63	47.4
Total	169	100	133	100

$\chi 2 = 6.274$, D.F.=2 , P=0.043

This result is paralleled with literatures. For example, in Jordan , it was evident that the higher the level of education of the female partner , the lower the consanguinity rate(22).In Yemen , Jurdi and Saxena(1) confirmed the inverse association between consanguineous marriage and women education . First cousin unions were more common among women who had lower educational level and less common among those with higher educational level (2) .

On the other hand , the results showed no significant association ($\chi 2$ = 1.095 , D. F.=2 , P=0.5)between husbands educational level and consanguineous marriage (table 3)

Table -3: Distribution of marriage type by husbands educational level .

Husbands educational level	Non-consanguineous		Consanguineous	
	N	%	N	%
Illiteracy & Primary school	32	18.9	31	23.3
Intermediate	29	17.2	19	14.3
Secondary & Higher education	108	63.9	83	62.4
Total	169	100	133	100

X2 = 1.095 , D.F. = 2 , P= 0.5

However , a rather surprising finding is the lack of a negative impact of man's education on consanguinity . A plausible explanation is that since a son with higher education becomes more valuable assets , his family may put a greater pressure on him to marry a cousin as a way to maintain family property . Also in other Arab countries , the studies referred to negative relationship between husband's education and consanguineous marriage (1,23)

According to the survey , the age of the women at first marriage was statically different ($\chi 2$ = 14.66 ; D.F. =4 ; P 0.005) between the consanguineous and non-consanguineous marriages (Table 4).

Table -4: Distribution of marriage types by women age at first marriage.

Age	Non-consanguineous		Consanguineous	
	N	%	N	%
Less than 15 years	05	3	10	7.5
15-19	37	21.9	48	36.1
20-24	67	39.6	48	36.1
25-29	51	30.2	23	17.3
30-and above	9	5.3	4	3
Total	169	100	133	100

$\chi 2$ =14.664 ;D.F.= 4 ;P = 0.005

Our result supports the considerable evidence suggesting that age at marriage has been found to has direct effect in an increasing the prevalence of the consanguineous marriages(6). But these result contracted with the evidence of Yemeni study which found adverse effect of maternal age on prevalence of consanguineous marriages .This may, in turn , provide further support to the hypothesis that higher the social status of individuals , the lower the likelihood for kin marriage in a population. Therefore ,legislative measures undertaken to influence female age at marriage may have impact in lowering the prevalence of consanguinity among the population .(1)

The reproductive patterns among women in consanguineous and non-consanguineous marriages were compared and are represented in table 5 .The frequency of spontaneous abortion , stillbirth ,infant mortality and congenital malformations were significantly different between non-consanguineous and first cousins unions ($\chi 2 = 9.828$; D.F. = 3 ; P = 0.019) .These differences are represented by increased frequency of spontaneous abortion (69.3 % vs. 62.7 %) and congenital malformations (5.3 % vs. 0.6 %) as well as the decreased the frequency of stillbirth (1.3 % vs. 8.3 %) in first cousins unions group . No significant differences were recorded between second and third cousins when they were compared with non-consanguineous marriages.

Table - 5 :Percentage distribution of reproductive wastage (spontaneous abortions, stillbirths, infant death and congenital malformation) by marriage type

Marriage type	Spontaneous abortions (n=302)		Stillbirths (n=302)		Infant deaths (n=302)		Congenital disorders (n=302)	
	N	%	N	%	N	%	N	%
Non-consanguineous	106	62.7	14	8.3	16	9.5	1	0.6
First cousins *	52	69.3	01	1.3	07	9.3	4	5.3
Second cousins	22	68.8	03	9.4	03	9.4	0	0.0
Third cousins	20	76.9	02	7.8	02	7.8	0	0.0
Total	200	66.2	20	6.6	28	9.3	5	1.6

* $\chi 2 = 9.828$; D.F. = 3 ; P = 0.019

The frequency of reproductive wastages is very high in the present survey ,especially the rate of spontaneous abortion (66.2%) when compared to that recorded in Baghdad in 1997 (5.8%) by Al-Rekaby (30), in the southern region in Iraq in 2009 (29) and higher than that recorded in many neighborhood countries (2,8,23,26,33) .

The excess risk that an autosomal recessive disorders could be expressed in the progeny of consanguineous unions is inversely proportional to the frequency of disease allele in the total gene pool . For this reason , during the last decade many rare disease genes have been identified and their chromosomal locations mapped by studying highly inbred families with multiple affected members (4).The main impact of inbreeding is an increase in

the rate of homozygote for recessive disorders (6, 26) .It is believed ,although not proven , that high rates of inbreeding over multiple generation lead to elimination of deleterious recessive genes from the gene pool (14). However ,studies from South India where inbreeding has been practiced for more than 2000 years showed that there has been no appreciable elimination of recessive lethal and sublethal genes in the gene pool (35).

The results also showed that the rate of total reproductive wastages were very high (49 %), and they are also high among consanguineous families (52.3 %) .Furthermore , the total pregnancies percentage (6.1 % vs. 5.4 %) and the percentage of the number of living birth (5.3 % vs. 4.6 %)were higher in consanguineous marriages(Table 6). The percentage of affected families is very high than that reported by Al-Rekaby. (20%) in Baghdad in 1997(30)and higher than that reported in middle and south of Iraq(31-40 %) in 1999 and2009 respectively (30,31) .The high percentage of reproductive wastages-affected families may reflected the difficult conditions in Iraq during the last three decades .

Table -6 :Percentages of total reproductive wastages , total pregnancies and total living birth by marriage type.

Marriage type	Reproductive wastag Affected families		Total pregnancies		Living birth	
	N	%	N	rate per family	Total	rate per. family
Non-consanguineous (n=169)	78	46.2	913	5.4	774	4.6
Consanguineous (n = 133)	70	52.3	813	6.1	704	5.3
Total (n = 302)	148	49	1726	5.7	1478	4.9

In general , higher fertility rate(pregnancies and living birth) are reported for consanguineous marriages (4).A partial explanation for these findings is the lower parental age at marriage and the age of the first birth of couples who are close relatives (6) , subsequent birth intervals are shorter , and consanguineous couples may continue their child-bearing to comparatively later age (7). Consanguineous couples may also be less likely to use reliable methods of contraception (18) .Additionally , there is a strong possibility that greater fertility may be observed in consanguineous unions as a compensatory mechanism for infant and childhood losses (35).

Consanguineous marriages is an integral part of cultural and social life in many areas , and the attempts to discourage it at the population level are inappropriate and undesirable , even it is association with an increased birth prevalence of children with recessive disorders , Instead, an approach that

identifies the families at risk and provides them with genetic counseling is needed.

The possibility of both parents being carriers for a recessive condition is influenced by how closely they are related . This means that the offspring risk can be minimized while retaining the social and familial advantages of consanguinity , if wedding are consummated between distant relatives (third cousins rather than second cousins or second cousin rather than first cousins(10).

In conclusion , the prevalence of consanguinity and first cousins marriages was found to be high in Baghdad .However , the younger ages and lower educational level were found to may have a direct effect in increasing the prevalence of consanguinity .Furthermore , the rate of spontaneous abortions and congenital disorders were higher among first cousin marriages than non-consanguineous unions. Thus , our finding indicate the importance of conducting further researches on the prevalence , reasons for and negative outcomes of consanguineous marriages . Public education programs on the negative outcomes of consanguineous marriages need to be continued and efforts should be made to lower the associated social factors .

REFERNCES

1. Juradi,R. and Saxena, P. C. The prevalence and correlates of consanguineous marriages in Yemen : Similarities and contrasts with other Arab countries .J.BioSoc. Sci.,35(1):1-13(2003).
2. Yuksel, S. ;Kutlubay, A.; Karaoglu, L, and Yologlu, S. The prevalence of consanguineous marriages in city Malatya , Turkey .Turk. J.sci. ,39(1):133-137(2009) .
3. Bittle ,A.H. The role and significance of consanguinity as a demographic variable .Population and Development Review ,20(3) : 561-584(1994) ..
4. Bittle ,A.H. When cousin marry :a review of consanguinity in the Middle East .Perspectives in Human Biology ,1 :71-83(1995)..
5. Wahab, A. and Ahmed ,M .Consanguineous marriages in the Sikh community of Swat ,NWWP, Pakistan .J. Soc. Sci. ,10(3):153-157 (2005).
6. Bittle ,A.H. ; Mason, W.M.; Green , J. and Rao,N..Reproductive behavior and health in consanguineous marriages. Science ,252:789-794(1991) .
7. Tuncbilek ,E. and Koc, I. Consanguineous marriages in Turkey and its impact on fertility and mortality .Ann. Hum. Genet.,58 :262-267(1994).
8. Saadat ,M . and Mohabbatkar ,H. Inbreeding and its relevance to early and pre reproductive mortality rate in Iran ,an ecological study .Iranian J. Publ. Health ,32(2):9-11(2003).

9. Kanaan , Z. M. ;Mahfouz , R. and Tamim ,H. The prevalence of consanguineous marriages in an underserved area in Lebanon and its association with congenital anomalies .Genetic Testing , 12(3):367-372(2008).
10. Sathyanarayana Rao T.S : Asha, M.R; Sambamuithy ,K. and Jagannatha Roa K.S.Consanguinity : Still a challenge . Indian J. Psychiatry, 51:3-5 (2009).
11. Mehrabi Kushk ,A. and Zeyghami, B. The effect of consanguineous marriages on congenital malformation.J.Res.in Med.Sci.10(5):298-301 (2005) .
12. Mehndirattta, M.M. ;Paul, B. and Mehndriatta , P.Arranged marriage. Consanguinity and epilepsy .Neurology Asia,12(1):15-17(2007) .
13. Hashemipour , A.; Amini ,M.; Talaie ,M. ; Kelishadi, R. ;Hovespian ,S. ;Iranpour, R.; Salek, M.; Haghigh, S.; and Khatibi, K. H.Parental consanguineous marriages among parents of neonates with congenital hypothyroidism in Isfahan . Eastern Mediterranean Health Journal,13(3):1-8(2007).
14. Bener, A. and Hussain,R. Consanguineous unions and child health in the state of Qatar .Paediatr Perinat Epidemiol. ,20(5);372-378(2006) .
15. Bener, A.; Hussain, R. and Reebi, A. S.Consanguineous marriages and their effects on common adult diseases : Studies from an endogamous population. Med. Princ. Pract.,16:262-267(2007) .
16. Kumaramanickavel, G. ;Joseph, B.; Arokiasamy , T. and Shridhara Shetty . Consanguinity and ocular genetic diseases in south India , Analysis for five- years study .Community Genetics,5:182-185(2002) .
17. Modin, H. ;Masterman ,T. ;Thorlacius , T.; Stefansson, M.; Jonasdottir , A.; Stefansson ,K.; Hillert, J.and Gulcher ,J.Genome-wide linkage screen of a consanguineous multiple sclerosis kinship .Multiple Sclerosis ,9(5):128-134(2003)..
18. Bittle, A. H. Consanguinity and its relevance to clinical genetics .Clin. Genet. ,60:89-98(2001)..
19. Denic ,S. and Bener,A. Consanguinity decrease risk breast cancer – cervical cancer unaffected .Br. J. Cancer ,85(11) :1675-1679(2001) ..
20. Denic, S. and Nicholl, M. G. Genetic benefits of consanguinity through selection of genotypes protection against malaria .Hum. Biol., 79 :145-158(2007) . .
21. Bittle,A.H.Community genetics perspective on consanguineous marriages . Community Genet., 11:324-330(2008)..
22. Khoury , S.A.and Massad , D. F.Consanguinity ,fertility , reproductive wastage , infant mortality and congenital malformation .Saudi Med. J.,21(2):150-154.(2000).

23. Khoury, S.A. and Massad , M. A.Consanguineous marriages in Jordan . Am. J. Med. Genet.,43(5):769-75.(1992).
24. Khlat M. consanguineous marriage and reproduction in Beirut .Am.j med Gent ., 43; 188-196(1988).
25. Jaber, L.; Halpern, G. J. and Shahat ,T. Trends in the frequency of cousins-marriages in the Israeli Arab community .Clin. Genet.,58:106-110 .(2002).
26. AL-kandari, Y.Y.the health consequences of consanguineous marriages in Kuwait .Anthropology of Middle East, 2(2) :74-86(2007).
27. Al-Gazali , L. I , Bener , A; Abdulrazzaq, Y.M.; Micallef, R.,AL-khayat, A.I. and Gaber, T.consanguineous marriages in the united Arab Emirates. J. Biosoc . Sci, 29 (4);491-7.(1997).
28. Hamamy, H. ;Bayati, N. and Kubaisy , W. Consanguineous marriages in the Iraq urban population and the effect on pregnancy outcome and infant mortality .Iraq Med. J..34:75-79.(1986).
29. Al-Rekaby ,A.A. G. ;Mubark, H.R. and Lafta, F.M.. Reproductive health and cytogenetics parameters for workers in aluminum factories in Iraq. 3ed Scientific Conference of the Collage of Science, Univ. Baghdad :98-104(2009).
30. Al-Rekaby .A.A.G. Cytogenetics and reproductive effect of lead on workers in batteries industry in Iraq . Ph. D. thesis , Collage of Science , Al-Mustansirya University.(1997) .
31. الركابي ، عبد الامير ناصر غلوب. الاضطرابات في مؤشرات صحة التكاثر في بعض مناطق العراق الوسطى والجنوبية . مجلة ديالى ،5 : 42- 48(1998).
32. WHO .Iraqi family health survey report (IFHS).:1-65(2006).
33. Al-Abdulkareem , A.A. and Ballal, S.G .Consanguineous marriages in an urban areas of Saudi Arabia :Rates and adverse health effects on the offspring .J. of Community Health ,23(1):75-83.(1998).
34. Mokhtar , M.M. and Abdel-Fattah, M.(2001).Major birth defects among infants with Downs syndrome in Alexandria ,Egypt. East Mediterr Health, 7:441- 451(1995-2000).
35. Ahmed ,M. and Nichols ,R.A. The effects of reproductive compensation on recessive disorders within consanguineous human population. Heredity, 88: 474-479. (2002).

The Most cytotoxic Effect of Propolis Against Tumor Cells is Due to Apoptosis via Mitochondrial Pathway.

Khalid Mahdi Salih[1], Bedir Mohammed Al-Azawi[2], Nahi Yousif Yaseen[3]
[1/2] Department of Biology, College of Science, Al-Mustansiryah University
[3] Iraqi Center of Cancer Research & Medical Genetics, Al-Mustansiryah University.

الخلاصة

العكبر مادة متعددة الوضائف يستخدمها النحل لانشاء و ادامة خلاياه. و بسبب فعالياته الحياتية و الصيدلانية, فقد استخدم بشكل مكثف في الطب الشعبي. صممت الدراسة الحالية لاختيار التاثير السمي و المحرض للموت الخلوي المبرمج لمستخلص العكبر المائي تجاه بعض خطوط الخلايا الورمية (AMN-3, Hep-2) و خط الخلايا الطبيعية (Ref) باستخدام تقنية الزرع النسيجي.
أظهرت النتائج تأثيراً مضاداً للتكاثر فقط عند خطوط الخلايا الورمية و ذلك من خلال اختزال نمو الخلايا بحوالي 63% في خط AMN-3 و 66.7% في خط Hep-2 بعد 48 ساعة من التعريض للعكبر. في نفس الوقت, عدّل العكبر من المحتوى البروتيني في افرازات خطوط الخلايا ضمن الوسط الزرعي, و ذلك باختزال هذا المحتوى بحوالي 79.1% في خط AMN-3, و زيادته بحوالي 84.7% و 94.6% في كل من خطي Ref و Hep-2 على التوالي. و لغرض توضيح آلية هذا التأثير السمي للخلايا, وجد أن التعريض للعكبر بتركيز 4 ملغم/مل سبب تبدلا في جهد الغشاء المايتوكوندري و الذي حرضّ حوالي 100% من خلايا خط Hep-2 و 88.3% من خلايا AMN-3 للدخول في الموت المبرمج. هذه النتائج اشارت بوضوح على ان المستخلص المائي للعكبر يمتلك سمية قوية بواسطة الموت المبرمج ضد الخلايا الورمية من خلال المسلك المايتوكوندري.

ABSTRACT

Propolis is a multifunctional material used by bees in the construction and maintenance of their hives. Due to biological and pharmacological activities, it has been extensively used in folk medicine. The present study was designed to investigate the cytotoxic and apoptotic effect of the watery extract of propolis (WEP) on two tumor cell lines (Hep-2 & AMN-3) and one normal cell line (Ref) by using tissue culture technique.
The results showed anti-proliferative effect only against tumor cell lines by reducing cell growth about 63% in AMN-3 and 66.7% in Hep-2 after 48h exposure to WEP. At the same time, Propolis modulated the protein content in the secretions of cell lines within culture medium by reducing this content about 79.1% in AMN-3 cell line, and increasing it about 84.7% and 94.6% in both Ref and Hep-2 cell lines respectively. To explain the mechanism of this cytotoxic effect, it was found that exposure of both tumor cell lines to WEP at a concentration of 4mg/ml caused an alteration in the mitochondrial transmembrane potential that induced about 100% of Hep-2 cells and 88.3% of AMN-3 cells to undergo apoptosis. These results clearly indicated that WEP possesses a potent apoptotis-mediated cytotoxicity against tumor cells via mitochondrial pathway.

INTRODUCTION

Cancer is one of the major threats to public health in the developed world and increasingly in the developing countries (1). According to the World Health Organization, cancer accounted for 7.1 millions deaths in 2003, and it is estimated that the overall number of new cases will rise by 50% in the next 20 years (2). It has been estimated that 30-40 percent of all cancers can be prevented by life style and dietary measures alone (3). In recent years there is a growing interest in nutraceuticals which provide health benefits, disease prevention and substitution of modern medicine (4). As many as 89% of patients with cancer or other chronic conditions use nutraceuticals, some of them show potential as adjuvants with conventional oncology treatment, others may be used to eliminate the side effects of conventional treatment (5).
In Iraq, several natural products have been investigated to evaluate their anti-tumor activity against tumor cells in vitro and in vivo such as green and black tea (6), crude

extract of Miramia Salvia triloba (7), vegetable and callus parts of Melia azerach (8), Rhubarb and Thyme crude extracts (9).

Propolis is a resinous substance with varying colors and consistencies, collected by Apes mellifera bees from several sources. The word propolis comes from the Greek pro meaning in defence of and polis meaning city, i.e. defence of the hives (10). It has been revealed that propolis possesses various biological activities such as anti-bacterial, antifungal, antiviral (11, 12), anti-inflammatory (13) and anticancer (14) properties. More than 300 different compounds have been identified so far in propolis (15), flavonoids are the ones which draw greater research interest (16). Recently, it has been reported that ethanolic extract of Brazilian propolis suppresses tumor-induced angiogenesis in vivo and tube formation of endothelial cells in vitro through induction of apoptosis in endothelial cells (17, 18). Furthermore, it was found that ethanolic extract of propolis-induced apoptosis is related to the selective activation of caspase-3 and induction of BCL-2/Bax regulation (19), or via augmentation of TRAIL-mediated apoptosis in cancer cells (20).

In this study, we investigated the cytotoxic and apoptotic effects of watery extract of Iraqi propolis on two tumor cell lines (Hep-2) and (AMN-3) and one normal cell line (Ref). We also evaluated the protein content in the secretions of these cell lines in their culture medium.

MATERIALS & METHODS

Preparation of Propolis

Natural propolis, dark brown in color, multifloral origin was used for experimentation. Propolis was collected from bee hives in Khan Dhari farm, Baghdad, Iraq. Coarsely powdered propolis was extracted, five volumes of water were added to 50g of propolis and stirred for 4h at 45°c. Following removal of insoluble materials by centrifugation at 470g for 15 min, the supernatant was dried and the resultant powder was stored at -20°c until used (21), Six concentrations (4, 2, 1, 0.5, 0.25, and 0.125mg/ml) of watery extract of propolis (WER) were prepared in serum-free RPMI-1640 medium (sigma) supplemented with benzylpenicillin (100,000 IU/ml) and streptomycin (100,000µg/ml), then sterilized by filtration through 0.22µm filter.

Preparation of Cell lines

Murine mammary gland adenocarcinoma (AMN-3), epithelial cell carcinoma of human larynx (Hep-2) and normal rat embryonic fibroblasts (Ref) cell lines were obtained from Iraqi Center of Cancer Research and Medical Genetics. All cell lines were routinely kept in RPMI-1640 medium supplemented with 10% fetal calf serum at 37°c in a humidified 5% CO2 – 95% air incubator under standard conditions. Cell viability was measured by using trypan blue exclusion method to prepare a suitable concentration of cell suspension for tissue culture experiments (22).

Cytotoxicity assay

The cells were seeded in 96-well flat bottom plates at a concentration of 2×10^5 cell/well and incubated at 37°c for 24h, then the old medium was discarded and the attached cells were treated with the various concentrations pf propolis and reincubated for 48h (22).

After treatment, the old medium was aspirated from each well and transferred into eppendroff tubes to estimate its protein content later. However, the wells were stained with crystal violet solution and reincubated for 20 min, then the stain solution was discarded and the plate washed with tap water and let to dry. The absorbance (optical density OD) of each well was determined at 492nm by Elisa plate reader (23).

Determination of Protein

The eppendroff tubes obtained from previous experiment were centrifuged to eliminate any associated cells. The supernatant was referred as cell line secretion and its protein content was determined by using Bradford method (24).

Apoptosis Assay

This assay was carried out according to Mitochondria Bioassay Kit (US, Biological Company) described by Chen et al (25). The cells of Hep-2 and AMN-3 lines were plated in 8-chamber tissue culture slide (LAB-TEK, Nunc, Inc.) at concentration of 5×10^5 cells/chamber and incubated at 37°c for 24h, then the old medium was discarded from each chamber and the adherent cells were treated with the highest concentration of WEP (4mg/ml) and reincubated for 36h. After treatment, the medium was discarded and the cells were treated with the mitocapture reagent for 20 min and examined under the fluorescent microscope to count the number of apoptotic cells (green in color) and healthy cells (red in color).

Statistical Analysis

All data were expressed as Mean ∓ SE and the validity was tested by linear correlation (r) between the treatment and each parameter. However, the statistical significance of differences between treated and control groups was analyzed by Mann-Whitney at $p<0.05$ (26).

RESULTS AND DISCUSSION

The percent charge in OD of 3 cell lines after 48h exposure to various concentrations of WEP was referred as percent change in cell proliferation and illustrated in figure-1. Statistical analysis demonstrated that for concentrations of WEP (0.5, 1, 2, and 4mg/ml) caused significant reduction in cell proliferation of Hep-2 line (26.1%, 45.8%, 49% and 66.7% respectively), while three concentrations (1, 2 and 4mg/ml) caused significant reduction in AMN-3 line (27.2%, 53.7%and 63% respectively). However, all concentrations revealed no significant change in cell proliferation of Ref line.

The percent change of protein content in the secretions of treated groups were compared to those of their controls and represented in figure 2. Both Ref and Hep-2 cell lines showed significant direct correlation between WEP concentrations and protein content in their secretions ($r = 0.86$ and 0.93 respectively) with maximum increment about 84.7% in Ref line and 94.6% in Hep-2 line. However, those of AMN-3 line showed significant reverse correlation ($r = -0.95$) with maximum reduction about 79.1%.

Although several concentrations of WEP caused cytotoxic effects in tumor cell lines (Hep-2 and AMN-3), the highest concentration (4mg/ml) was chosen in apoptosis

assay. Figure 3 showed complete apoptosis induction in treated group of Hep-2 cells (100%) and severe induction in AMN-3 cells (88.3%∓3.53%) in comparison to their corresponding controls (10%∓2.89% and 18.3%∓4.41%respectively).

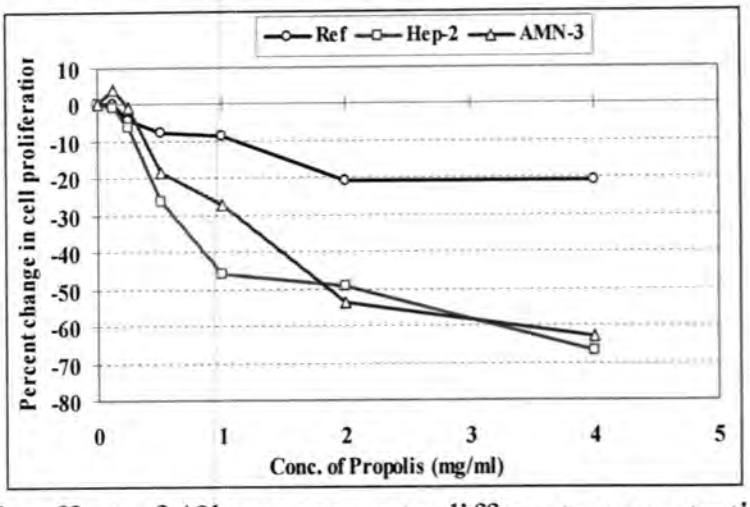

Figure -1: Cytotoxic effect of 48hr exposure to different concentrations of WEP on the proliferation of 3 cell-lines.

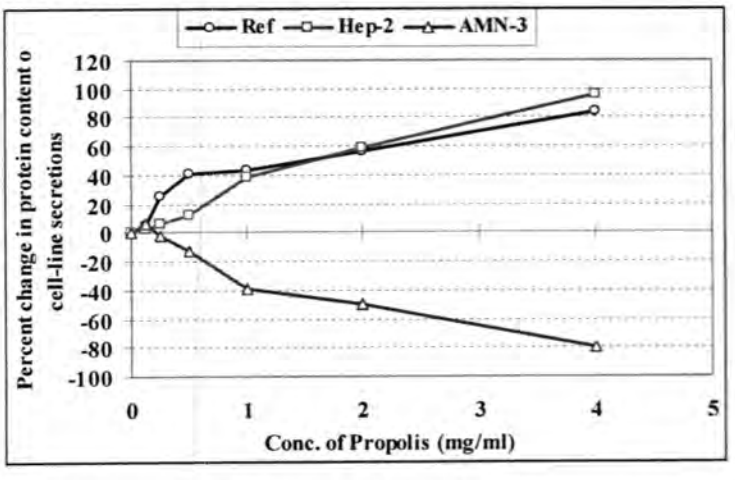

Figure- 2: modulating effect of 48hr exposure to different concentrations of WEP on the protein content in the secretions of 3 cell-lines.

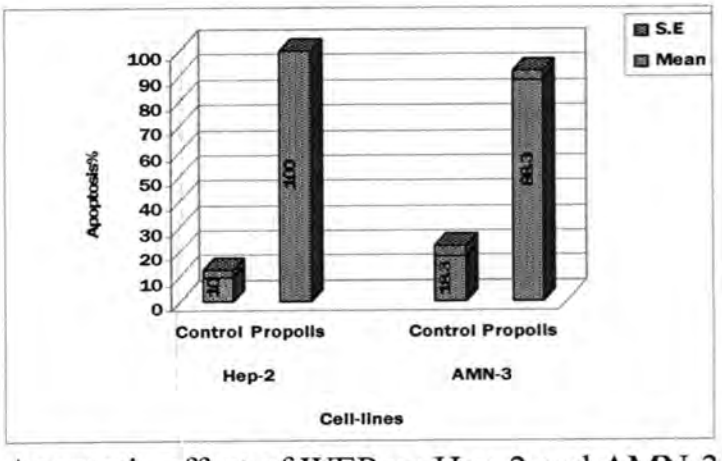

Figure -3: Apoptotic effect of WEP on Hep-2 and AMN-3 cell-lines.

In this study, we found a potent cytotxic and apoptotic activities of WEP against both tumor cell lines (figure 1,3). Understanding the mechanisms underlying the cytotoxic activity by propolis provide beneficial clue for the development of new drug and functional food candidates (21). Inducing apoptosis is one of the mechanisms for several therapeutic agents as shown in propolis by a number of studies (14, 27). It was reported that propolis can induce apoptosis in tumor cells by several pathways for instances; through activating caspases, Bid and Cytochrome-c release (28), interfering with tumor suppressor protein such as P53 and P38 MAPK (29), inhibiting telomerase expression (30), and augmentation of tumor necrosis factor related apoptosis-inducing ligand (TRAIL) which is a natural occurring anticancer agent that preferentially induces apoptosis in cancer cells and is not toxic toward normal cells (20). Because the apoptosis detection kit that was used in this study distinguishes between healthy and apoptotic cells by detecting changes in the mitochondrial transmembrane potential (25), therefore, it can be suggested that propolis induced apoptosis in tumor cells via mitochondrial-dependent pathway because disruption of the mitochondrial transmembrane potential is one of the earliest intracellular event that occur following apoptosis induction (31).

On the other hand, this study demonstrated a contrast activity of WEP on protein content in the secretions of cell lines (figure 2). The elevation of protein content in the secretions of Hep-2 culture may be due to cellular disintegration that lead to release cytosol and increase the level of protein in the culture medium (22). Similarly, protein content was significantly increase in Ref culture, although its growth was not affected. Therefore, these findings need more investigations to interpret the behavior of Ref cells. However, the result of AMN-3 is quietly questionable because at the same conditions, propolis caused significant induction of apoptosis and growth inhibition (figure 1,3). Therefore, it can be suggested that propolis might partly inhibit either the synthesis or release of certain protein molecules such as growth factors, adhesion molecules, cytokines (32, 33). Furthermore, because the apoptosis that occurred in these cells was incomplete, thus the healthy cells may engulf the apoptotic bodies of the affected cells and prevent the accumulations of their protein in the surrounding environment, which is one of the characteristic features of the final stage in apoptosis process in vitro (31).

In conclusion, this study provides evidence that the WEP possesses cytotoxic activity toward tumor cells through the induction of mitochondrial pathway leading to apoptosis, also its ability to modulate the protein content in the secretion of tumor cell lines that need further qualitative and quantitative studies.

REFERENCES

1. Peterson PE. Strengthening the prevention of oral cancer the WHO perspective. Community Dent Oral Epidemiol, 33:397-399(2005).
2. World Health Organization and International Union against Cancer (2003). Global action against cancer. Geneva, WHO.Donaldson MS. Nutrition and cancer: A review of the evidence for anticancer diet. Nutri J, 3:19-30(2004).

3. Dureja H, Kaushik D and Kumar V. Development in nutraceuticals. Ind J Pharm, 35:363-372(2003).
4. Montbriand MJ. Herbs or natural products that decreased cancer growth. Oncol Nurs Forum, 31:E75-E90(2004).
5. Sa'eed, OF. The effect of green and black tea extracts on different cell lines *in vitro*. M.Sc. Thesis, College of Pharmacy, University of Mosul, Iraq(2004).
6. Ibrahim, A.I.Effect of crude extracts of *Salvia triloba* L.f.on neoplastic,transformed and normal cell lines.Ph.D.Thesis,College of Science,University of Baghdad, Iraq(2005).
7. Taha, RH. Effect of crude extracts (vegetable and callus parts) of *Melia azerach* on cancer and normal cells *in vitro*. M.Sc. thesis, College of Science, Al-Nahrain University, Iraq(2007).
8. Karim KJ. Anti-mutagenic and anti- carcinogenic effects of Rhubarb (*Rheum ribes*) and Thyme (*Thymus syriacus*) crude extract in male albino mice (*Mus musculus*). Ph.D. Thesis, Ibin-Alhaitham, University of Baghdad, Iraq(2007).
9. Almeida EC and Menezes H. Anti-inflammatory activiy of propolis extracts: a review. J Venom Anim Toxins, 8:191-212(2002).
10. Kujumgiev A, Tsvetkova I, Sekedjeva Y, Bankova V, Christov R and Popov S. Antibacterial, antifungal and antiviral activity of propolis of different geographic origin. J Ethnopharmocol, 64:235-240(1999).
11. Salomao K, Pereira PR, Campos LC, Borba CM, Cabello PH and Marcucci MC. Brazilien propolis: correlation between chemical composition and antimicrobial activity. Evid Baseed Complem Alternat Med, 5:317-324(2008).
12. Ramos AFN and Miranda JL. Propolis: a review of its anti-inflammatory and healing actions. J Venom Anim Toxins inl Trop Dis, 13:1-7(2007).
13. Chen CN, Wing MS, Wu CL and Lin JK. Comparison of radical scavenging activity, cytotoxic effect and apoptosis induction in human melanoma cells by Taiwanese propolis from different sources. eCAM, 1:174-185(2004).
14. Marcucci MC. Propolis: chemical composition, biological properties and therapeutic activity. Apidologie, 26:83-99(1995).
15. Havsteen BH. The biochemistry and medical significance of the flavonoids. Pharmacol Therapeutics, 96:67-202(2002).
16. Ahn M-R, Kunimasa K, Ohta T, Kumazawa S, Kamihira M and Kaji K. Suppression of tumor-induced angiogenesis by Brazilian propolis: major component artepillin-C inhibits *in vitro* tube formation and endothelial cell proliferation. Cancer Letters, 252:235-243(2007).
17. Ohta T, Kunimasa K, Kobayashi T, Sakamoto M and Kaji K. Propolis suppresses tumor angiogenesis by inducing apoptosis in tube-forming endothelial cells. Biosci Biotechnol Biochem, 72:2436-2440(2008).
18. Motomura M, Kwon KM, Suh S-J, Lee Y-C, Kim Y-K, Lee I-S, Kim M-S, Kwon DY, Suzuki I&Kim C-H. Propolis induces cell cycle arrest and apoptosis in human leukemic U937 cells through Bcl-2/Bax regulation Environ Toxicol Pharmacol,26:61-67 (2008).

19. Szlizka E, Czuba ZP, Domino M, Mazur B, Zvdowiez G and Krol W. Ethanolic extract of propolis (EEP) enhances the apoptosis-inducing potential of TRAIL in cancer cells. Molecules, 14:735-754(2009).
20. Mishima S, Narita Y, Chikamatsu S, Inoh Y, Ohta S, Yoshida C, Araki Y, Akao Y, Suzuki and Nozawa Y. Effect of propolis on cell growth and gene expression in HL-60 cells. J Ethnopharm, 99:5-11(2005).
21. Freshney RI. Culture of animal cells: a manual of basic techniques. 3rd edition, Wiley-Liss Company, NewYork, :154, 201, 292(1994).
22. Mather JP and Roberts PE. Introduction to cell and tissue culture. Theory and technique. Plenum Press, NewYork,:180(1998).
23. Bradford M. A rapid and sensitive method for the quantitation of microgram quantities of protein using the principle of protein-dye binding. Anal Biochem, 72:248-256(1976).
24. Chen Y,Kramer DL,Diegelman P,Vujcic S&Proter CW.Apoptotic signaling in poly–am -ine analogue-treated SK-Mel-28 human melanoma cells.Cancer Res,61:6437-6444 (2001).
25. Hart, A. Mann-Whitney test is not just a test of medians: differences in spread can be important. BMJ, 323:391-393(2001).
26. Aso K, Kanno S, Tadano T, Satoh S and Ishikawa M. Inhibitory effect of propolis on the growth of human leukemia U937.Biol Pharm Bull,27:727-730 (2004).
27. Chen CN,Wu CL&Lin JK.Propolin C from propolis induces apoptosis through activate -ing caspases, Bid and Cytochrome-c release in human melanoma cells. Biochem Pharmac ol, 67:53-66(2004).
28. Lee YJ,Kuo HC,Chu CY,Wang CJ,Lin WC&Tseng TI.Involvement of tumor suppres - sor protein P53 and P38 MAPK in caffeic acid phenethyl ester-induced apoptosis of C6 glioma cells. Biochem Pharmacol, 66:2281-2289(2003).
29. Guduz C,Biray C,Kosova B,yilaaz B,Eroglu Z,Sahin F,Omay SB&Cogulu O. Evalua - tion of Manisa propolis effecton leukemia cell line by telomerase activity. Leukemia Res, 29:1343-1346(2005).
30. Kumara B, Abbas AK and Fausto N. Robbin's pathologic Bases of diseases. 7th ed, Elsevier Saunders, USA,:26-53(2005).
31. Harvey SR, Nayak SK, Markus G, Ouhammouch M, Hemperly JJ, Dillman RD and Doyle DJ. Cancer cells release a covalent aomplex containing disulfide-linked domains from urinary plasminogen activator, neural cell adhesion molecules and haptoglobin alpha and beta chain. Arch Biochem Biophys, 345:289-298(1997).
32. Brunetti M, Colasante A,Mascetra N,Piantelli M, Musiani P&Aiello F.IL-10 synergizes with dexamethasone in inhibitng human T-cell proliferation. J pharm Exp Therap, 285:915-919 (1998).

The Role of Some Prognostic Markers Levels in Monitoring Chronic Hepatitis B.

Amina N. Al-Thwani [1], Mohammed Abdul-Daim Saleh[2] and Ali R. Omer[3]
[1]Institute of Genetic Engineering & Biotechnology for Post Graduate
[2]Diyala University , College of Science
[3]Ministry of health

الخلاصة

جمع 50 نموذج مصلي من مرضى مصابين بالتهاب الكبد الفايروسي المزمن نوع (ب) و(50) فردا من الحاملين ألاصحاء للمستضد السطحي لفايروس التهاب الكبد نمط (ب) من المراجعين للمستشفى التعليمي لامراض الجهاز الهضمي والكبد في بغداد ومصرف الدم المركزي في بغداد للفترة من الاول من شباط 2008 ولغاية نهاية شباط 2009 ،وكانت أعمار المرضى المصابين بالتهاب الكبد الفايروسي المزمن نوع (ب) تتروح مابين20-65 سنة و أعمار الحاملين ألاصحاء للمستضد السطحي لفايروس التهاب الكبد نمط (ب) تتروح مابين 18-52 سنة وتم قياس تركيز الواسمات التالية alpha-fetoprotein, alpha-2 Macroglobulin and beta-2 micro globulin في مصل المجموعتين ، حيث أظهرت النتائج وجود زيادة معنوية في تركيز الواسمات في المرضى المصابين بالتهاب الكبد الفايروسي المزمن نوع (ب) مقارنة بالحاملين ألاصحاء للمستضد السطحي لفايروس التهاب الكبد نمط (ب) .

ABSTRACT

Fifty (50) serum samples were collected from patients with CHB who were admitted to Hepatology and Gastroenterology Teaching Hospital in Baghdad, aged 20-65 years during the period from the beginning of February / 2008 to the end of February / 2009, also serum samples were collected from Fifty (50) healthy HBs Ag carrier was discovered accidentally through attending the blood bank for donation of blood, aged from 18-52 years and served as a control group.

To determine the best marker to be used as predictive parameter in the prognosis and disease progression in some Iraqi hepatitis patients, the level of some Prognostic marker such as alpha-fetoprotein (AFP), alpha-2 Macroglobulin and beta-2 micro globulin were assessed in the sera of studied group. It was clear that a highly significant elevation was noticed in all markers with CHB patients as compared to the carrier group.

INTRODUCTION

Beta-2-microglobulin is a polypeptide containing 100 amino acid (molecular weight 11.8 KDa) together with an major histocomptability complex (MHC)-encoded heavy chain, beta 2 microglobulin forms the class I molecules human leukocyte antigen (HLA)-A, B, C that are present on the surface of most nucleated cells. It is also present in most biological fluids, at low concentration (1). Appeared as a single protein in the serum following natural cell-death and higher in tumor growth, rejection reaction after transplant and infections due to heightened activity of the immune system (1). Beta- 2 microglobulin is eliminated by kidneys where following glomerular filtration, it is reabsorbed and catabolized in the proximal tubular cells (2).

Beta-2microglobulin is associated with an activated immune response in HBs Ag infection which may be released by activated lymphocyte (T4/T8 cells), thus increasing its level might indicate increasing HBs Ag

replication- related cell death but that level may not be closely linked to viral replication rates. Nevertheless, numerous studies have confirmed an increased beta-2 microglobulin measurement as predictive marker for rates of progression to hepatitis particularly when combined with other direct immunological markers, including CD4+ T cell number (3).

Human AFP is a protein found in relatively high concentration in the serum of fetal and reappears in several pathological conditions in adults such as hepatitis ,AFP has long been considered the "gold-standard" in the field of tumor markers and it is well known as a "tumor-specific embryonic antigen" or "tumor-associated fetal protein" or "tumor-associated protein" (4).

Elevated levels of AFP in blood have been found in about 90% of patients with hepatocellular carcinoma(5), AFP is also elevated in the serum of adults with hepatitis, cirrhosis, and chronic active hepatitis, and viral hepatitis[6].It is used as a marker for both the diagnosis and monitoring of patients suffering from hepatocellular carcinoma(7). Moreover Alpha-2 macroglobulin levels are increased in some disorder such as chronic hepatitis B virus (HBV) infection ,nephrotic syndrome and also Alpha-2 macroglobulin, levels are increased in some cancer such as hepatocellular carcinoma and some type of myloma (8) .Further more, alpha-2 macroglobulin can be used as a marker for both diagnosis and monitoring of patients suffering from hepatocellular carcinoma (9). This study aimed to evaluation of the serum β 2-Microglobulin concentration, alpha-2 macroglobulin and alpha-fetoprotein , as a prognostic marker for the development of HBV infection in both groups.

MATERIALS AND METHODS

Subject groups include the following:

chronic hepatitis B patients groups

A total of (50) patients with CHB who were admitted to Hepatology and Gastroenterology Teaching Hospital in Baghdad, aged from 20-65 years with male to female ratio of 2.2:1. The patients were suffering from different clinical symptoms with previous risk factors for transmission of HBV infection.

Control groups

A total of 50 healthy HBs Ag carriers were discovered accidentally through attending blood bank for donation of blood, aged from 18-52 years.

A Cross sectional study was conducted in the period between February / 2008 and the mid of February / 2009.

Beta 2- microglobulin assay .

VIDAS beta2- microglobulin (β 2M) is an automated quantitative test for use on the VIDAS analyzer using the ELFA technique (Enzyme Linked Fluorescent Assay) .The assay principle combines a two-step enzyme immunoassay sandwich method with a final fluorescent detection (ELFA). (3)

Alpha fetoprotein (AFP) assay .

VIDAS Alpha fetoprotein (AFP) is an automated quantitative test for use on the VIDAS analyzer using the ELFA technique .The assay principle combines a two-step enzyme immunoassay sandwich method with a final fluorescent detection (ELFA). (10).

Quantitative Estimation of Serum Alpha 2 macroglobulin Using Single Radial Immunodiffusion (SRID) test:-

The concentration of alpha 2 macroglobulin were measured by a single radial immunodiffusion (SRID) method in which equal volumes of reference sera and test samples were added to wells in agarose containing monospecific antisera.

The sample diffuses radially through this gel and the substance being assayed form a precipitin ring with the monospecific antisera. Ring diameters were measured and a reference curve is constructed on graph paper. Unknown concentration was determined form the references standard curve (11).

Procedure

Before starting procedure, the plate was opened and left for 5 minutes at room temperature for evaporation of any water (if present in wells) due to storage of 4°C.

1. Five µl of each serum sample was dispensed by Hamnilton syringe in to one well of each plate (containing 16 wells) for three classes of Igs, two types of complement component and alpha 2 macroglobulin
2. The plate was left opened for (10–20) minutes, then covered and left at room temperature (20–25) °C for (3–4) days for precipitin ring to be formes.
3. The diameter at each immune precipitating using formed around each well was measured in mm by immune viewer and the concentration of alpha 2 macroglobulin level was calculated from standard curve.

RESULTS AND DISCUSSION

To realize the most excellent marker to be used as foretelling parameter in the prognosis and disease progression in Iraqi hepatitis patients. So the serum beta-2 micro globulin, alpha-fetoprotein and alpha-2 Macroglobulin are quantified in the studied group.

In the present study, the level of serum β - 2 M is higher in CHB cases than carrier group (table 1 and figure 1). This is in agreement with the results of Yegane, (14) and Elefsiniotis *etal.* (15) they have noticed that the elevated serum β - 2 M has been significantly associated with progression to chronicity of hepatitis and also they have observed that HBV–infection is strongly correlated with increased β - 2 M levels during the prognosis of disease .

Beta2-microglobulin is a subunit of the class 1 major histocompaitibility complex found on the surface of all nucleated cells, including lymphocytes. Serum levels of β 2 M are produced during cellular turnover and its increases usually reflect an indirect state of generalized lymphoid activation

(12). Although raising blood levels of β- 2 M are found in patients with cancer and other serious diseases, as well as a rising β- 2 M blood level can be used to measure the progression of hepatitis (13) .

This study confirms the opinion that beta2 microglobulin concentration is an indicator for monitoring the prognosis of chronic HBV infections at the asymptomatic hepatitis B virus carrier, thus would lead to early initiation of Interferon (IFN) treatment and to monitor the effectiveness of the therapy.

More to the point, Alpha fetoproteins are associated with liver disorder such as hepatitis and cirrhosis and it is a marker for hepatocellular and germ cell carcinoma (10).

Our data reveal that the level of AFP is higher in chronic patients than carrier group(table 1 and figure 1), this is in unison with the results of Vajro , (16) and Merican , (17) in which they have indicated that serum AFP level in CHB patients is mostly higher than upper normal limit value as compared to carrier group. This finding could be correlated to high rate of post-hepatitis cirrhosis and malignancy occurring in those patients(18) .

In the same way, the average of serum alpha-2 macroglobulin was higher in chronic patients when compared to carrier group(table and figure 1), this was in unison with results of Blacker *et al.* (8) and Kovacs, (9) they documented that serum level of alpha-2 macroglobulin was higher in chronic patients than carrier group. This finding could be linked with bad prognosis of disease and may be associated with first stage of cirrhosis leading to malignancy, therefore the alpha-2 macroglobulin can be represented as tumor marker (i.e. screening for hepatocellular carcinoma) (8).

Table -1:The mean level of some prognostic markers among chronic hepatitis B patients and carrier group.

Prognostic Marker		Number	Mean	Std. Deviation	t-test P-vale	Signaficant
Alpha -fetoprotein	healthy carrier HBV	50	7.28	3.40		
	chronic HBV	50	27.74	22.80	.000	HS
	Total	100				
Alpha 2-macroglobulin	healthy carrier HBV	50	284.12	95.54		
	chronic HBV	50	383.66	142.44	.000	HS
	Total	100				
Beta 2- microglobulin	healthy carrier HBV	50	1.610	.753		
	chronic HBV	50	2.668	.809	.000	HS
	Total	100				

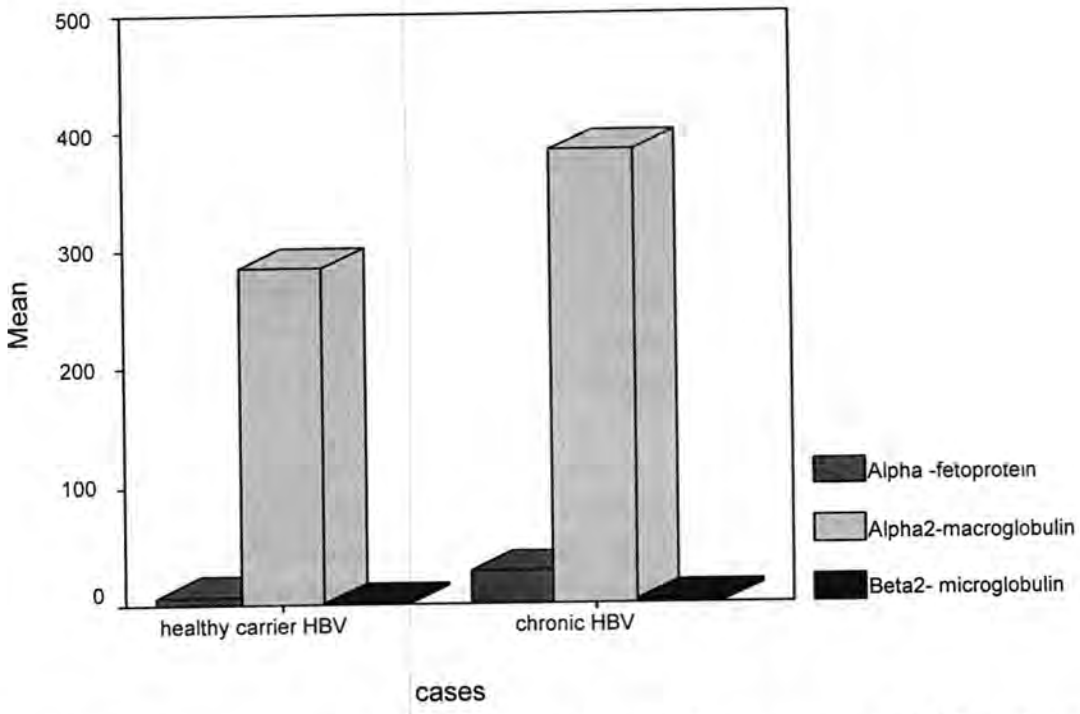

Figure -1: The mean level of some prognostic markers among CHB patients and carrier group.

REFERENCES

1. Girndt, M.; Sester, U.; Sester, M.; Deman, E. and Kohler, H. The Beta-2-microglobulin and interleukin – 10 promoter genotype determines clinical immune function in hemodialysis patients.Kidney Int.;60:2385 – 91 (2001).
2. Urbani,S.;Boni,C.;Missale,G.;Cavallo,C.and Massari,M.Virus-specific CD8+ lymphocytes share the same effector-memory phenotype but exhibit functional differences in acute hepatitis B&C.J.Virol.;76 :12423-34 (2007).
3. Bingham, F.How to monitor your blood work, in conjection with DAAIR laboratory Flow sheet and graph, Hepatitis ; 6:19 (2004).
4. Mizejewski,G.J.tumor-associated protein.Expert Rev.Anticancer Ther.;2 :709-735 (2002).
5. Dresel, S.; Kirsch, C.M.; Tatsch, K.; Zachoval, R.and Goldenberg, D.M. Tumor marker. J. Clin. Oncol.; 15: 2683-2690(1997).
6. Chen, D.S. and Sung, J.L. Tumor marker . Cancer ;40: 779-783(2001).
7. Kang,Y.;Matsuura,E.;Sakamoto,T.;Sakai,M.& Nishi,S. Monitoring of patients suffering from hepatocellular carcinoma. Tumor Biol.; 22: 254-261(2007).
8. Blacker,D.;Wilcox,M.A.;Laird,N.M.Alpha-2 macroglobulin is genetically associated with some disorder. Nat Genet.; 19 (4): 357–60 (1998).
9. Kovacs,D.M.Alpha2-macroglobulin in late-onset liver disease.Exp Gerontol.;35 (4): 473–9(2000).
10. Pollok,R.E.;Doeoshow,J.H.; Geraghty,J.G."Manual of Clinical Oncology" 7th ed.,A John Wiley and Sons Co.Inc publication; :495-496 (1994).

11. Mancini,G.;Carbonara,A.O.&Heremans,J.F.Immunochemical quantitation of antigens by single radial immuno diffusion. Immunohistochemistry; 2 :235 (1992).
12. Bardeguez, A.D.;Connor, E. ; Stephens, R.;Vanham, G. & Kestens, L. Effect of human immunodeficiency virus infection on serum Beta 2 microglobulin level in pregnant women. Obstet.& Gynecol.; 94:537-542 (1999).
13. Wells, K.R. and Odle, T.G. Effect of hepatitis on serum Beta 2 microglobulin level. World J Gastroenterol.; 94:547 -552(2004).
14. Yegane, S.; Revanli, M. & Taneli,F.The role of beta2 microglobulin levels in monitoring chronic hepatitis B. Tohoku J Exp Med.;203(1):53-7 (2004).
15. Elefsiniotis, I.S.;Moulakakis, A.;Pantazis,K.D.; Crimi,C.; Oseroff,C. & Sette,A. Relationship between serum b2-microglobulin levels&virological breakthrou -gh in HBeAg-negative chronic hepatitis B patients,under longterm treatmen t schedules including lamivudine.World J Gastroenterol.7;11(13):1922-8 (2005).
16. Vajro,P.;Fontanella,A.;De Vincenzo,A.; Lettera, P.; Lauer, G., Chung, R. &Thomas,Monitoring of serum alpha-fetoprotein levels in children with chronic hepatitis B virus infection. J Pediatr Gastroenterol Nutr.;12(1):27-32 (1991).
17. Merican,I.Screening for hepatocellular carcinoma.Med J Malaysia.Mar; 51 (1) : 12-7(1996). .
18. Devita, J.R.;Vincent, T.; Sanmel, H.; and Steven, A.R. Cancer Principle and Practice of Oncology. 5th ed. J.B. Lippincott-Raven publishers. Philadelphia. : 1562(1997).

Effect water and Soap on Some Pathogenic Bacteria That Isolation From Nipple of Breast of Suckling Mother

Buthaina Ateyah Rashid

Health and Medical Technical College

الخلاصة

يتضمن البحث اخذ مسحات لحلمة الثدي من 27 ام مرضعة قبل وبعد تنظيف منطقة حلمة الثدي بواسطة الماء والصابون فقط . وقد وجد انه قد ثبطت نمو معظم البكتريا المرضية والبكتريا المتعايشة بصورة طبيعية في تلك المنطقة ولذلك ننصح الامهات المرضعات بغسل الثدي بالماء والصابون لإزالة أي بكتريا مرضية وبالتالي حماية الاطفال الرضع من الإصابة البكتيرية .

ABSTRACT

The research contained take nipple breast swab from 27 suckling mother , after and before cleaned the area of nipple breast by water and soap only , and founded inhibition all pathogenic bacteria and normal flora therefore recommended suckling mother to washing the breast by water and soap to removed any pathogenic bacteria then protection the children from any bacterial infection .

INTRODUCTION

Epidemiological studies have been important in demonstrating that breast feeding clearly protects infants against respiratory and gastrointestinal infections, or decreases the severity of these infections. Breastfeeding can also protect against otitis media (middle ear infection), pneumonia, diarrhoea, necrotizing enterocolitis and sepsis. The primary protective factors in breast milk are the presence of specific antibody and anti-adhesion factors in human milk. However, a variety of antimicrobial factors (antiviral, antibacterial and antiparasitic) have been detected in human milk over the years (Tables 1,2,3). Most of these factors are not destroyed by pasteurization (62.5°C for 30 minutes)(1).the normal flora that isolation from skin are Staphylococcus epidermedis(2)

Microbial contaminants in human milk (Table 4) are rare, as are the associated infant infections from the milk. However, some contaminants, such as cytomegalovirus, are commonly transferred to infants from seropositive mothers, fortunately without adverse effects in infants. Human T-lymphotropic virus type 1 is transferred via human milk in endemic regions(1), while human immunodeficiency virus type 1 is also transferred through human milk - but is not the exclusive mode of transmission to infants. Pasteurisation (62.5°C for 30 minutes) has been shown to destroy all microbial contaminants in human milk (except hepatitis B, which is fortunately not transferred through milk(2)(3). With the use of new detection technology, low levels of some viruses have been found in human milk, but no epidemiological evidence suggest any transfer of these viruses from mother-to-infant via human milk. If a mother and infant have the

same virus infection, and even in some cases if that virus is detected in the mother's milk, the milk may not be the source of the virus transmission to the infant (4). Detection of virus nucleic acid does not mean enveloped viruses, in particular, are still infectious in human milk. Various bacterial contaminants present in expressed human milk have caused infections (Table 5). Infections of infants have occasionally occurred from bacterial contaminants in dried milk formula (Table 6). The effect of heat treatment and storage of human milk on some the antimicrobial factors is given in Table 1,2,3,4,5,6,.

MRIALIALS AND METHODS

Material :

1- swab
2- blood agar
3- MacConkey
4- Distal water
5- Loop
6- Oven
7- Incubator
8- Autoclave
9- Microscope
10- pHmeter
11- test tube

Methods :

take nipple breast swab from 27 suckling mother , after and before cleaned the area of nipple breast by water and soap only and cultured on blood agar and MacConkey agar then waiting for 24 hours and diagnosis by bacteriological methods .(5)

RESULTS AND DISCUSSION

E.coli * Groups Table -1:

			Groups		
			Before	After	Total
E.coli	Positive	N	20	4	24
		%	74.1%	14.8%	44.4%
	Negative	N	7	23	30
		%	25.9%	85.2%	55.6%
Total		N	27	27	54
		%	100.0%	100.0%	100.0%

	Value	df	P-value
Chi-Square	19.200	1	0.00 HS

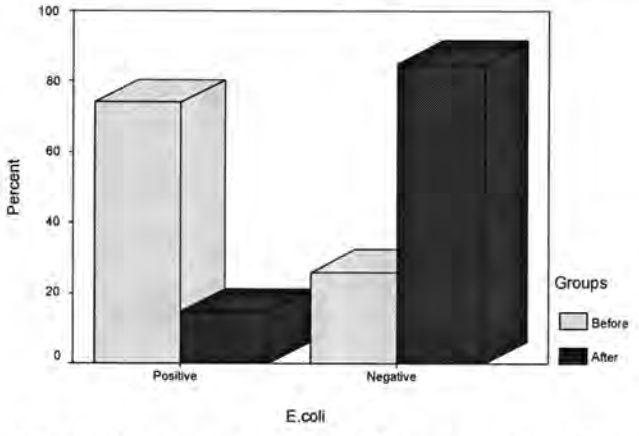

Staphylococcus aureas * Groups Table -2:

			Groups		
			Before	After	Total
Staphylococcus aureas	Positive	N	12	2	14
		%	44.4%	7.4%	25.9%
	Negative	N	15	25	40
		%	55.6%	92.6%	74.1%
Total		N	27	27	54
		%	100.0%	100.0%	100.0%

	Value	df	P-value
Chi-Square	9.643	1	0.002 HS

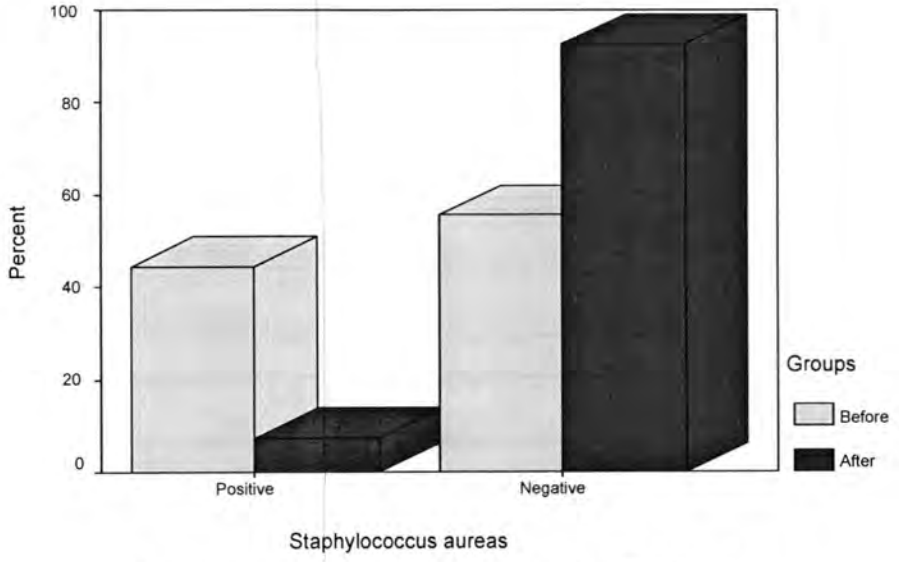

Streptococcus pyogenes * Groups Table -3:

			Groups		
			Before	After	Total
Streptococcus pyogenes	Positive	N	12		12
		%	44.4%		22.2%
	Negative	N	15	27	42
		%	55.6%	100.0%	77.8%
Total		N	27	27	54
		%	100.0%	100.0%	100.0%

	Value	df	P-value
Chi-Square	15.429	1	0.00 HS

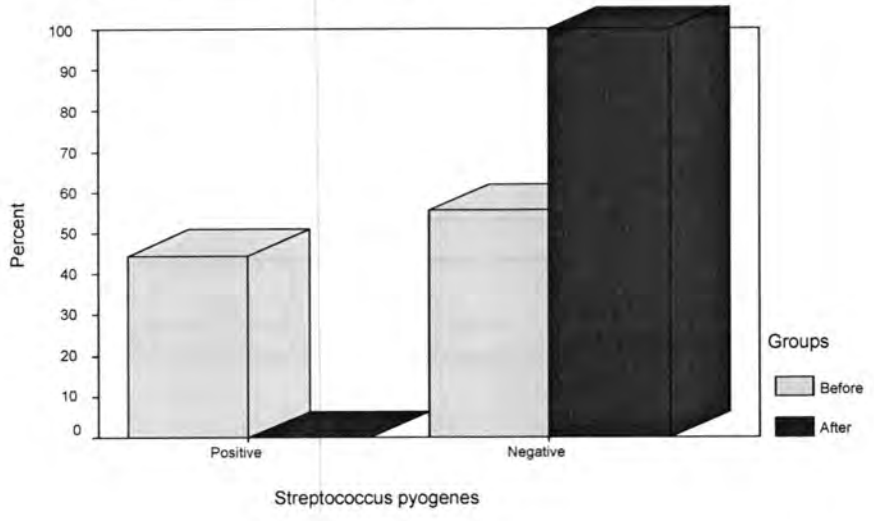

Table -4:Staph. epidermedis * Groups

			Groups		
			Before	After	Total
Streptococcus epidermedis	Positive	N	26	4	30
		%	96.3%	14.8%	55.6%
	Negative	N	1	23	24
		%	3.7%	85.2%	44.4%
Total		N	27	27	54
		%	100.0%	100.0%	100.0%

	Value	df	P-value
Chi-Square	36.300	1	0.00 HS

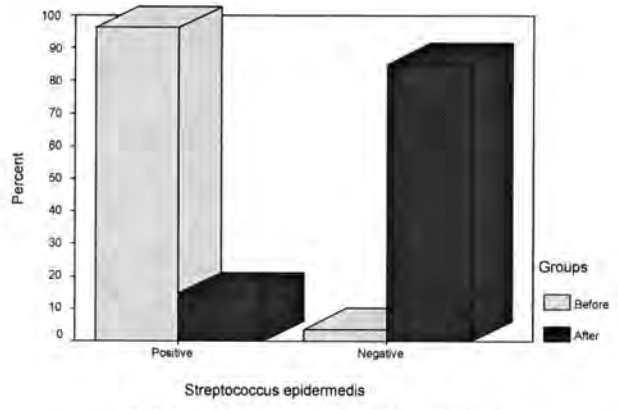

Table -5:Proteus * Groups

			Groups		
			Before	After	Total
Proteus	Positive	N	8		8
		%	29.6%		14.8%
	Negative	N	19	27	46
		%	70.4%	100.0%	85.2%
Total		N	27	27	54
		%	100.0%	100.0%	100.0%

	Value	df	P-value
Chi-Square	9.391	1	0.002 HS

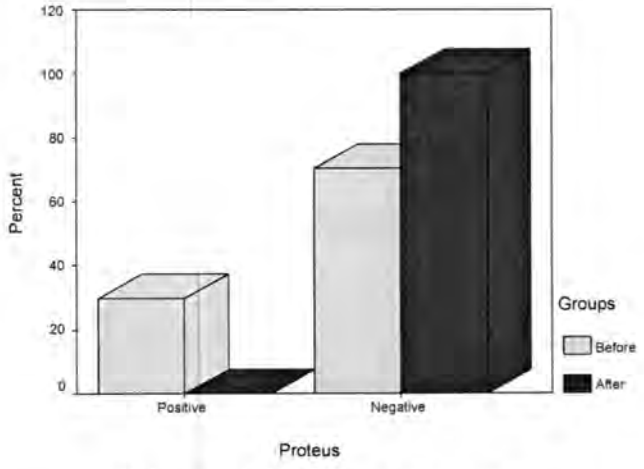

Table -6:Klebsella * Groups

			Groups		Total
			Before	After	
Klebsella	Positive	N	18		18
		%	66.7%		33.3%
	Negative	N	9	27	36
		%	33.3%	100.0%	66.7%
Total		N	27	27	54
		%	100.0%	100.0%	100.0%

	Value	df	P-value
Chi-Square	27.000	1	0.00 HS

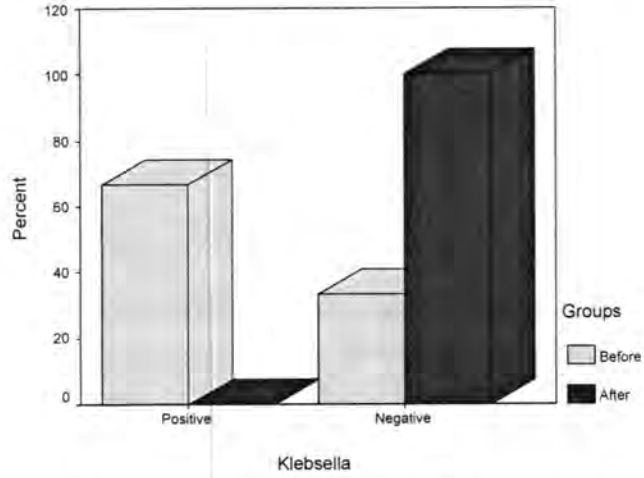

From the above tables we shall notice that *Streptococcus pyogenes* bacteria table(3) which were the most sensitive for washing by water and soap where the inhabitation rate for them was 100% due to their special nourishment needs. As for *Staphylococcus aureus* bacteria table(2) they will inhibit by water and soap but in lower degree where the inhabitation rate was 92% due to their ability to escape from the killer effect of the soap because they have for enzymes and cell wall which are able to resist this effect, while for *Proteus Sp.* Bacteria table(5), they were sensitive for soap and water effect by 100% and in table (6) we shall

see that bacteria *Klebsella Sp.* are also sensitive for water and soap effect and the inhabitation rate was 100% as for *E coil* bacteria Table(1) which sensitively for water and soap effect were relatively lower than *Klebsella Sp.*, *Streptococcus pyogenes*, *proteus Sp.*, and *Staphylococcus aureus* bacteria sensitivities, where the inhabitation rate for was 85% and that was for E coil bacteria, which still high and the picture for *Staphylococcus epidermidis* bacteria Table(1) was different in that they are considered the most resistant bacteria for water and soap for their cell wall which contain a group of proteins which lessen the effect of the soap on the fats in the cell wall and this explain *Staphylococcus epidermidis*, and sa resistance for soap. But *Staphylococcus epidermidis* contain higher ratio of fats than sa and so less effected by soap.

From this we conclude that the soap has high effect on bacteria in that it get rid of them especially for pathogenic bacteria so we recommend washing the breast nipple with soap and water in that this process is enough for killing bacteria by 95% so the breast will become safe for suckling. Where most diarrhea cases were caused by *Klebsella Sp.*,. and *E. coli* bacteria and most cases were because of *Streptococcus pyogenes* and *Staphylococcus aureus* bacteria and all of these were sensitive for the effect of soap and water by this we shall get rid of most of diseases that infect the new born babies.

REFERENCES

1. M.T. Mary. Immunochemistry. (USA.) *K. Ed.* 84: 2-6(2008).
2. J Madison B. "Application of stains in clinical microbiology". *Biotech Histochem* 76 (3): 119–25. doi:10.1080/714028138. PMID 11475314(2007).
3. J.T. May. Anti-microbial factors and microbial contaminants in human milk. *J. Ped. Child Health.* 30:470-475(1994).
4. A, Inglis, J.T. May and C. Lighton. Fact sheets on the web: A case study of the on-line dissemination of information on the anti- infective properties of breast milk. *Contemporary Nurse.* 7: 91-97(1998).
5. J.T. May. Microbial contaminants and anti-microbial properties of human milk. *Microbiol. Sciences.* 5: 42-46(1988).
6. J.T. May. Human milk - anti-microbial and microbial contaminants relevant to human milk banking. *In* Breast milk and special case nurseries: problems and opportunities. ALCA press. Melbourne. :19-24(1995).
7. J.T. May. Clinical significance and recent studies of the anti-infective properties and infectious contaminants in breast milk, *In* "Breast feeding: The natural advantage". NMAA press: Sydney. : 138-144(1997).
8. J.T. May. Breast milk and infection - a brief overview. *Breastfeeding review.* 7: 25-27(1999).
9. Extrapulmonary pathology: An Overview MARJORIE P. GOLDEN, M.D.,Yale University School of Medicine and Hospital of Saint Raphael, New Haven, Connecticut. HOLENARASIPUR R. VIKRAM, M.D., Mayo Clinic, Scottsdale, Arizona(2007).

Single Machine Scheduling To Minimize a Function of Square Completion Time and Maximum Tardiness Simultaneously

[1]Tariq Salih Abdul-Razaq And [2]Haidar younis kawi
The University of Al-[1]Mustansiriya, College of Science,Department of Mathematics
[2]The University of Al-Qadisiya ,College of Computer Science and Mathematics,Department of Mathematics

الخلاصة

في هذه الدراسة ولتصغير دالة الكلفة لمعيارين والحاصلة من جدولة n من الاعمال على ماكنة واحدة درست المسألة:

تصغير الدالة $F(\sum C_i^2 , T_{max})$ حيث ان T_{max} هي regular measure في هذه المسألة اقترحنا بعض الخوارزميات لايجاد الحل الامثل في حالة الـ (hierarchical) والحلول الكفوءة في حالة الـ (simultaneous) . وكذلك اقترحنا خوارزمية للـ (BAB) لايجاد الحل الامثل للمسألة (P4) . وقدمنا ايضا حوارزمية B لايجاد الحل الامثل للمسألة (P4) ولكن بطريقة اسرع من خوارزمية(BAB) . وقدمنا حسابات الاختبارات لخوارزميات BAB و B والتي تم تنفيذها على مجموعة كبيرة من المسائل.

ABSTRACT

In this study, to minimize a function of two cost criteria for scheduling n jobs on a single machine , the problem is discussed :

" Minimizing a function of total square completion time and maximum tardiness simultaneously".

For this problem we proposed some algorithms to find exact(optimal) solution for hierarchical case and efficient (pareto optimal) solutions for simultaneous case, Also we proposed branch and bound algorithm to find exact solution for sum of total square completion time and maximum tardiness, and present algorithm B to find exact solution in a fast way with respect to (BAB) method. We present computational experience for the (BAB) method and algorithm(B) on a large set of test problems.

INTRODUCTION

It is well known that the optimal solution of single objective models can be quite different if the objective is different (for instance, for the simplest model of one machine, without any additional constraint, the rule SPT is optimal to minimize flow time but the rule EDD is optimal to minimize the maximal tardiness T_{max}).

In fact, often each particular decision maker wants to minimize a given criterion.

Recently, research on more than one criterion scheduling has increased. Since real life scheduling problems may require the decision maker to consider a number of criteria before arriving at any decision. Nagar et al. (20) in their detailed literature survey of multiple and bi-criteria problems in scheduling point out the importance of this subject.

Because, the one-machine problem provides a useful laboratory for the development of ideas for heuristics and interactive procedure

that may prove to be useful in more general models. We consider the one-machine case in this study.

Multi-Criteria Scheduling:

In general, multiple-criteria scheduling refers to the scheduling problem in which the advantages of a particular schedule are evaluated using more than one performance criterion. The managerial relevance of considering multiple criteria for scheduling has been cited in the production and operations management literature since the 1950's. Smith (1956)(22) shows that the choice of a criterion will affect the characteristics of a "best schedule"; different optimizing criteria will result in very different schedules. Van Wassenhove and Gelders (1980)[25] and provide evidence that a schedule that performs well using a certain criterion might yield a poor result using other criteria. Hence, lack of consideration of various criteria may lead to solutions that are very difficult to implement in practice. Although the importance of multi-criteria scheduling has been recognized for many years (French, 1982(7); Nelson et al., 1986(21); George S., and Paul S. 2007(8), little attention has been given in the literature to this topic. From the problem complexity perspective, the multiple-criteria problem becomes much more complex than related single-criteria counterparts (Lenstra et al., 1975(18) Nagar et al. (1995)(20) reviews the problem in its general form whereas Lee and Vairaktarakis (1993)(16) review a special version of the problem, where one criterion is set to its best possible value and the other criterion is tried to be optimized under this restriction. Hoogeveen (2005)(11) studies a number of bi-criteria scheduling problems.Also, there are some papers about this object (Cheng et al. 2008(5), and Azizoglu et al. 2003 (1).

Approaches for Multi-Criteria Problems:

In literature there are two approaches for the bi-criteria problems: the hierarchical approach and the simultaneous approach. In the hierarchical approach, one of the two criteria is considered as the primary criterion and the other one is considered as the secondary criterion. The problem is to minimize the primary criterion while breaking ties in favor of the schedule that has the minimum secondary criterion value. The studies by Chang P. and Su L.(2001)(3) and Chen W., et al.(1997)(4) are examples of hierarchical minimization problems with earliness and tardiness costs. The computational complexity results in hierarchical minimization are reviewed in Lee and Vairaktarakis (1993)(17). In the simultaneous approach there are two types ,the first one typically generates all efficient schedules and selects the one that yields the best composite objective function value

of the two criteria .The second is to find sum of these objectives .Several scheduling problems considering the simultaneous minimization of various forms of earliness and tardiness costs have been studied in the literature (see, e.g. Hoogeveen, (1995)(12); Moslehi, et al. (2005)(19)) .

Basic definitions:

Definition(1):(14) *The term "optimize" in a multi-objective decision making problem refers to a solution around which there is no way of improving any objective without worsening at least one other objective.*

Definition(2) (14) *Suppose we have a problem P ,any schedule* $S \in \delta$ *(where* δ *is the set of all schedules) is said to be feasible if it satisfies the constraints of the problem P.*

Definition(3): (1). *A schedule S is said to be efficient if there does not exist another schedule* S' *satisfying* $f_i(S') \leq f_i(S)$, $i=1,...,k$ *with at least one of the above holding as a strict inequality. Otherwise S is said to be dominated by* S'.

Definition(4): (20) *A measure of performance is said to be regular if it is a non-decreasing function of job completion times and the scheduling objective is to minimize the performance measure. Examples of regular measures are job flowtime (*$\bar{F}$*), schedule makespan (*C_{max}*) and tardiness based performance measures.*

Definition (5): (11) *The function F(f,g) is said to be non-decreasing in both argument ,if for any pair of outcome value (x,y) of the functions f and g ,we have* $F(x,y) \leq F(x+A,y+B)$ *for each pair of non-negative value A and B.*

Theorem (1): (11) If the composite objective function F(f,g) is non-decreasing in both argument ,then there exists a pareto optimal schedule that minimize F.■

Basic Scheduling Concepts

We start with introducing some important notation where we concentrate on the performance criteria with out elaborating on the machine environment etc. We assume that there are n jobs, which we denoted by $j_1,\ldots,j_n$ these jobs are to be scheduled on a set of machines that are continuously available from time zero on words and that can handle only one job at a time .

In this paper, we only state here the notation that is used for single machine , jobs $J_i(i=1,\ldots,n)$ has:

N: set of jobs.

n: The number of jobs in a known sequence.

of the two criteria .The second is to find sum of these objectives .Several scheduling problems considering the simultaneous minimization of various forms of earliness and tardiness costs have been studied in the literature (see, e.g. Hoogeveen, (1995)(12); Moslehi, et al. (2005)(19)) .

Basic definitions:

Definition(1):(14) *The term "optimize" in a multi-objective decision making problem refers to a solution around which there is no way of improving any objective without worsening at least one other objective.*

Definition(2) (14) *Suppose we have a problem P ,any schedule* $S \in \delta$ *(where* δ *is the set of all schedules) is said to be feasible if it satisfies the constraints of the problem P.*

Definition(3): (1). *A schedule S is said to be efficient if there does not exist another schedule* S' *satisfying* $f_i(S') \leq f_i(S)$, $i=1,\ldots,k$ *with at least one of the above holding as a strict inequality. Otherwise S is said to be dominated by* S'.

Definition(4): (20) *A measure of performance is said to be regular if it is a non-decreasing function of job completion times and the scheduling objective is to minimize the performance measure. Examples of regular measures are job flowtime* ($\bar{F}$)*, schedule makespan* (C_{max}) *and tardiness based performance measures.*

Definition (5): (11) *The function F(f,g) is said to be non-decreasing in both argument ,if for any pair of outcome value (x,y) of the functions f and g ,we have* $F(x,y) \leq F(x+A,y+B)$ *for each pair of non-negative value A and B.*

Theorem (1): (11) If the composite objective function F(f,g) is non-decreasing in both argument ,then there exists a pareto optimal schedule that minimize F.■

Basic Scheduling Concepts

We start with introducing some important notation where we concentrate on the performance criteria with out elaborating on the machine environment etc. We assume that there are n jobs, which we denoted by $j_1,\ldots,j_n$ these jobs are to be scheduled on a set of machines that are continuously available from time zero on words and that can handle only one job at a time .

In this paper, we only state here the notation that is used for single machine , jobs $J_i(i=1,\ldots,n)$ has:

N: set of jobs.

n: The number of jobs in a known sequence.

$\mathbf{P_j}$: which means that it has to processed for a period of length p_j .

$\mathbf{d_j}$: a due date ,the date when the jobs should ideally be completed , the completion of job after its due date is allowed ,but a penalty is incurred . When the due date absolutely must be met , it is referred to as deadline $\bar{d}_j$, and when due date is constant for all jobs ,then called common due date.

- The completion time C_j
- The lateness $L_j=C_j - d_j$
- The tardiness $T_j=\max\{ 0, C_j-d_j\}$

For a given schedule σ we compute.

- $C_{max}(\sigma) =\max_j(C_j)$
- $L_{max}(\sigma)=\max_j(L_j)$
- $T_{max}(\sigma)=\max_j(T_j)$

Fundamental Results and Algorithms:

Theorem (2)(Smith_1956)(22). The $1/ / \Sigma C_i$ problem is minimized by sequencing the jobs according to the shortest –processing-time (SPT) rule, that is, in order of non-decreasing p_i.■

Theorem(3)(Jackson 1955)(13). The $1/ / L_{max}$ problem is minimized by sequencing the jobs according to the earliest-due- date (EDD) rule, that is, in order of non-decreasing d_i.■

Theorem(4)(Lawler 1973)(16).The $1//f_{max}$ problem, f_{max} is minimized as follows: while there are unassigned jobs, assign the job that has minimum cost when scheduled in the last unassigned position in that position.■

Hoogeveen and Van de Velde (12) provide a generalization to the case that the two criteria are $\sum C_j$ and f_{max} where f_{max} is regular cost function.

Van Wassenhove and Gelder (24)propose a pseudo-polynomial algorithm for finding all efficient schedules with respect to $\sum C_j$ and L_{max} .Their algorithm searches all possible L_{max} values .Since a given L_{max} value imposes job dead line $\bar{d}_j$,the algorithm of Smith (21) is used to solve the corresponding $1/\bar{d}_j/\sum C_j$ problem.

The Problem Classification:

In this paper, we adopt the terminology of Graham ,Lawler ,and Rinnooy Kan _(1979) [9] to classify scheduling problems.

Suppose that m machines M_i (i=1,…,m) have to process n jobs J_j $(_{j=1,\ldots,n})$. A schedule problem type can be specified using a three-field classification α/β/γ composed of the machine environment, the job characteristics, and the optimality criterion .

Minimizing Total Square Completion Time

This section deals with the Quadratic problem of scheduling jobs on a single machine such that the sum of the square of the weighted completion times of jobs is minimized(i.e. $1 //\sum_{i=1}^{n} w_i C_i^2$ problem) . Relatively little work has been done on problems involving a quadratic measure of performance for scheduling a single machine. The single machine scheduling problem with the objective of minimizing the sum of squares of the job completion times has been studied by Townsend (1978)(24), Bagga and Kalra (1980)(2), Gupta and Sen (1984)(10), and Szwarc, Posner, and Liu (1988)(23). Townsend (24) first formulated the problem and presented a branch-and-bound search method to solve it. Bagga and Kalra (2) improved the method by providing conditions for precedence among set of jobs. If $w_i = 1$ for every i , then the resulting problem $1 //\sum_{i=1}^{n} C_i^2$ is solved by the following proposition.

Proposition(1):(15)The SPT rule gives an optimal value for $1//\sum_{i=1}^{n} C_i^2$ problem.

Minimizing Total Square Completion Time and Maximum Cost

Now, we will consider the bi-criteria single machine problem concerns the simultaneous minimization of the performance measure total square completion time $\sum_{i=1}^{n} C_i^2$ and maximum cost f_{max} (i.e. $1//F(\sum_{i=1}^{n} C_i^2, f_{max})$ problem).Maximum cost is defined as $\max_{1\le i\le n}\{f_i(C_i)\}$, where each f_i denotes an arbitrary regular or irregular cost function for job i; regular means that $f_i(C_i)$ does not decrease when C_i is increased .

The $1//F(\sum_{i=1}^{n} C_i^2, f_{max})$problem is described as follows. A set of n independent jobs has to be scheduled on a single machine that is continuously available from time zero on wards and that can process at most one job at a time. Each job J_j *(j =1, ..., n)* requires an uninterrupted positive processing time p_j and has a due date d_j. Without loss of generality, we assume that the processing times and due dates are integral. A *schedule* σ specifies for each job when it is executed while observing the machine availability constraints. Hence, a schedule σ defines for each job J_j its square of completion time C_j^2 *(σ)*, which we sometimes simply write as C_j^2 .

The bi-criteria problem that we consider concerns the simultaneous minimization of the performance measures ***total square completion time*** and ***maximum cost*** f_{max}.

Hoogeveen and Van de Valde (12) proved that $1//F(\sum C_i, f_{max})$ problem is solved in polynomial time ,Van Wassenhove and Gelders(25) solved $1//F(\sum C_i, T_{max})$ problem, Emmons (6)addresses the hierarchical problem $1//Lex(f_{max}, \sum C_i)$,where f* denotes the optimal solution value of the $1//f_{max}$ problem, which is solved in $O(n^2)$ time by Lawler algorithm(16) .

Let $f_{max} = T_{max}$ in our study , since criterion T_{max} is a particular case of the function f_{max} .

Now , consider the following two problems:

$1//Lex(\sum_{i=1}^{n} C_i^2, T_{max})$ problem ,and $1//Lex(T_{max}, \sum_{i=1}^{n} C_i^2)$ problem.

The first problem $1//Lex(\sum_{i=1}^{n} C_i^2, T_{max})$

This problem can be written as:

$$\left.\begin{array}{l} \text{Min } T_{max} \\ \text{s.t} \\ \sum_{i=1}^{n} C_i^2 = C^* \quad \text{where } C^* = \sum C_i^2 \text{ (SPT)} \end{array}\right\} \ldots(P1)$$

Algorithm for problem(P1):

Setp(0): Order the jobs by SPT rule and calculate $\sum_{i=1}^{n} C_i^2$ and T_{max}.

Step(1): If there exist a tie(jobs with the same processing times) order these jobs by EDD rule to minimize T_{max} .

Note that the problem (P1) can be written as:

$$1/\ \sum_{i=1}^{n} C_i^2 = C^*\ /T_{max}.$$

Example-1: Consider the problem (P1) with the following data:

i	1	2	3	4	5
P_i	2	2	5	9	5
d_i	10	10	9	19	5

It is clear that the SPT rule is optimal for problem (P1).

i	1	2	3	5	4
P_i	2	2	5	5	9
d_i	10	10	9	5	19
C_i	2	4	9	14	23
C_i^2	4	16	81	196	529
T_i	0	0	0	9	4

Hence the SPT_1 schedule (1,2,3,5,4) with $(\sum_{i=1}^{n} C_i^2, T_{max})= (826,9)$.

But the SPT_2(break a tie of job 3 and 5) the schedule (1,2,5,3,4) with $(\sum_{i=1}^{n} C_i^2, T_{max})= (826,5)$.

The second problem 1//Lex(T_{max}, $\sum_{i=1}^{n} C_i^2$)

This problem can be written as:

$$\left.\begin{array}{l}\text{Min } \sum_{i=1}^{n} C_i^2 \\ \text{s.t.} \\ T_{max}=T^* \text{ where } T^*=T_{max}(EDD)\end{array}\right\} \ldots(P2)$$

Also the problem (P2) can be written as: $1/ T_{max}=T^* / \sum_{i=1}^{n} C_i^2$,

which is equivalent to the problem $1/\bar{d}_j/\sum_{i=1}^{n} C_i^2$ where $\bar{d}_j=d_j+T^*$.

Its clear that problem (P2) can be solved by "Smith backward" algorithm.

Algorithm(A) for problem(P2):

Step(0): Order the jobs by EDD rule and calculate $T_{max}(EDD) =T^*$.

Step(1): Find $\bar{d}_j=d_j+T^*$ $\forall j \in N$,N={1,…,n} unscheduled jobs ,and $\sigma = (\varphi)$ for schedule jobs .

Step(2): Let $t = \sum_{j=1}^{n} p_j$

Step(3): Find a job $j^* \in N$ satisfy $\bar{d}_{j^*} \geq t$ (if there exist a tie choose the job j* with largest processing time).

Step(4): Set $t= t -p_{j^*}$, $N =N-\{j^*\}$, $\sigma =(\sigma(j^*) ,\sigma)$, if $N= \varphi$ go to step (5), else go to step (3).

Step(5): Calculate $\sum_{i=1}^{n} C_{i\,(\sigma)}^2$ and $T_{max}(\sigma)$.

It is clear from the algorithm (A) ,we are interested in the minimization of $1//Lex(T_{max}, \sum_{i=1}^{n} C_i^2)$ problem. Since the SPT schedule minimizes $\sum_{i=1}^{n} C_i$ and $\sum_{i=1}^{n} C_i^2$ for the single machine problem [see proposition(1)] .Hence $1//Lex(T_{max}, \sum_{i=1}^{n} C_i^2)$ problem is equivalent to $1//Lex(T_{max}, \sum_{i=1}^{n} C_i)$ problem . The later problem is a particular case of

the 1//F(T_{max} , $\sum_{i=1}^{n} C_i$) problem which is solved by Van Wassenhove and Gelders [25].This means that we can solve 1//Lex(T_{max}, $\sum_{i=1}^{n} C_i^2$) problem and this can be done by algorithm (A).

Example-2: Consider the problem (P2) with the following data:

i	1	2	3	4	5
P_i	5	8	8	10	9
d_i	11	8	14	10	10

EDD rule gives the schedule (2,4,5,1,3) with T_{max}(EDD)=26=T*

i	2	4	5	1	3
P_i	8	10	9	5	8
d_i	8	10	10	11	14
C_i	8	18	27	32	40
T_i	0	8	17	21	26

Since $\bar{d}_j$ =d_i +T* ,hence by using algorithm(A),

$\bar{d}_1$ =37 , $\bar{d}_2$ = 34 , $\bar{d}_3$ = 40 , $\bar{d}_4$ = 36 , $\bar{d}_5$ = 36

j	t	j*
1	40	3
2	32	4
3	22	5
4	13	2
5	5	1

Hence the schedule (1,2,5,4,3) with (T_{max}, $\sum_{i=1}^{n} C_i^2$) =(26, 3302).

In the following section we consider the general problem F(($\sum_{i=1}^{n} C_i^2$,T_{max}).

Total Square Completion Time and Maximum Tardiness

In this section we will try to find an efficient (pareto optimal) solutions for 1/ /F($\sum_{i=1}^{n} C_i^2$,T_{max}) problem.

The 1/ /F($\sum_{i=1}^{n} C_i^2$,T_{max}) problem can be written as:

$$\left.\begin{array}{l} \text{Min } \sum_{i=1}^{n} C_i^2 \\ \text{s.t.} \\ T_{max} \le T \quad \text{where } T \in [\, T_{max}(EDD),\, T_{max}(SPT)] \end{array}\right\} \ldots(P3)$$

Theorem (5)[11]: Consider the composite objective function F with $F(\pi) = F(f_1(\pi),\ldots,f_k(\pi))$,where F is non- decreasing in all performance criteria f_k . There is a pareto optimal schedule with respect to $f_1,\ldots,f_k$ that minimizes the function F.■

Note that in the following proposition $H = \sum_{i=1}^{n} C_i^2$ and $T = T_{max.}$.

Proposition(2):(15) *There exists an efficient sequence for problem (P3) that satisfy the SPT-rule.*

Note that an analogous proposition for the EDD rule does not hold in general as shown by the following example :

i	1	2	3	4
P_i	2	3	1	2
d_i	3	4	5	6

SPT* sequence (3,1,4,2), H(SPT*) = 99, T(SPT*) = 4
EDD sequence(1,2,3,4), H(EDD) = 129, T(EDD) = 2
SPT* is efficient by Proposition (2.1).
EDD is not efficient since it is dominated by sequence (3,1,2,4) with H = 110 and T = 2.

It is clear that the $1//F(\sum_{i=1}^{n} C_i^2, T_{max})$ problem originates from $1//\sum_{i=1}^{n} C_i^2$ problem and $1//T_{max}$ problem. Both problems are solvable in O(n log n) time.
In order to find the set of pareto optimal points , we solve the problem of minimizing $\sum_{i=1}^{n} C_i^2$ subject to $T_{max} \le T^{**}$, where T^{**} corresponds to the T_{max} value of a pareto optimal point.

The next algorithm solve problem $1//F(\sum_{i=1}^{n} C_i, T_{max})$.

Algorithm(B) for (P3):
Step(0): Compute T_{max}(EDD) ,and T_{max} (SPT) ;let k=1 , T_{max} (SPT)=T**.
Step(1): Solve $1/ T_{max} \le T^{**} / \sum_{i=1}^{n} C_i^2$ by algorithm(A) for (P2) ; this produces the k pareto optimal schedule $\sigma^{(k)}$, and the k pareto optimal point $(\sum_{i=1}^{n} C_i^2(\sigma^{(k)}), T_{max}(\sigma^{(k)}))$.
Step(2): T**=T** -1, k=k+1.
Step(3): If T**< T_{max}(EDD) stop, else ,go to step (1).

Example-3: Consider the problem (P3) with the following data:

i	1	2	3	4	5
P_i	3	1	7	7	10
d_i	4	12	14	8	10

$T_{max}(EDD)=14$, $T_{max}(SPT)=18=T^{**}$.

Now, by proposition (2.1) ,SPT rule gives efficient schedule(2,1,3,4,5) then the first point is (1246,18).

$T^{**}=18-1=17$

Now we will solve 1/ $T_{max}\leq 17$ /$\sum_{i=1}^{n} C_i^2$ by algorithm(A) for (P2) .Hence

$\bar{d}_1=21$, $\bar{d}_2=29$, $\bar{d}_3=31$, $\bar{d}_4=25$, $\bar{d}_5=27$.

j	t	j*
1	28	3
2	21	5
3	11	4
4	4	1
5	1	2

Hence the second efficient schedule (2,1,4,5,3), and the second point is (1363,14).

$T^{**}=14-1=13< T_{max}(EDD)$. Stop.

It is clear that from the example that the EDD schedule (1,4,5,2,3) with (1734,14) is not efficient.

The $1//\sum_{i=1}^{n} C_i^2 + T_{max}$ problem:

In this section we decompose the $1//\sum_{i=1}^{n} C_i^2 + T_{max}$ problem into two subproblems with a simpler structure , and state some results which help us in solving it.

This problem can be written as:

$$M_1=\min_{\sigma\in S}\{\sum_{i=1}^{n} C_i^2 + T_{max}(\sigma)\}$$

s.t.

$$C_{\sigma(1)} \geq p_{\sigma(1)}$$

$$C_{\sigma(i)} = C_{\sigma(i-1)}+P_{\sigma(i)}$$

$$T_{\sigma(i)} \geq C_{\sigma(i)} - d_{\sigma(i)}$$

$$T_{\sigma(i)} \geq 0$$

...(P4)

This problem can be decomposed into two subproblems (SP1) and (SP2) .

$$V_1=\min_{\sigma\in s}\sum_{i=1}^{n}C_{\sigma(i)}^2$$

s.t.

$$c_{\sigma(i)}\geq p_{\sigma(i)} \quad i=1,\ldots,n$$

$$c_{\sigma(i)}=C_{\sigma(i-1)}+P_{\sigma(i)} \quad i=2,\ldots,n$$

...(SP1)

$$V2=\min_{\sigma\in s}\{\max\{T_{\sigma(i)}\}\}$$

s.t.

$$T_{\sigma(i)}\geq C_{\sigma(i)}-d_{\sigma(i)} \quad i=1,\ldots,n$$

$$T_{\sigma(i)}\geq 0 \quad i=1,\ldots,n$$

...(SP2)

Theorem(6)(20) :

V1+V2≤ M1 where V1 ,V2 ,and M1 are the minimum objective function values of (SP1),(SP2), and (P4) respectively .■

Some Special Cases for the Problem (P4).

Case(1): If for every schedule $C_i \leq d_i \ \forall i\in N$ then SPT rule gives an optimal value for (P4).

Proof: Since $C_i \leq d_i$ then $T_i=0 \ \forall i\in N$ $T_{max}=0$.

Hence the problem (P4) reduce to $1//\sum_{i=1}^{n}C_i^2$ problem .Then by proposition(1) SPT rule gives optimal value .■

Case(2): If $p_i=p \ \forall i\in N$ then EDD rule gives an optimal value for (P4).

Proof: If $p_i=p \ \forall i\in N$ then $\sum_{i=1}^{n}C_i^2$ is constant for every sequence ,since EDD rule gives minimum value for T_{max} , then EDD rule gives optimal value for (P4).■

Case(3): If $d_i=d \ \forall i\in N$ then SPT rule gives an optimal value for (P4).

Proof: If $d_i=d \ \forall i\in N$ then T_{max} is constant for every sequence ,since SPT rule gives minimum value for $\sum_{i=1}^{n}C_i^2$, then SPT rule gives optimal value for (P4).■

Case(4): If the due date is agreeable (i.e.$p_1\leq\ldots\leq p_n$ and $d_1\leq\ldots\leq d_n$) then the SPT and EDD rule give an optimal schedule .

Proof: Since $p_1\leq\ldots\leq p_n$ then $\sum_{i=1}^{n}C_i^2$ is minimum value , and at the same time $d_1\leq\ldots\leq d_n$ then T_{max} is minimum value ,then $\sum_{i=1}^{n}C_i^2+T_{max}$ is the minimum value .■

Heuristic to calculate upper bound (UB) for the problem (P4).

To calculate upper bound (UB_T)order the jobs by SPT rule and then calculate $\sum_{i=1}^{n} C_i^2$ and T_{max}.

Derivation of lower bound (LB)

To calculate a lower bound (LB) apply theorem (6).

Example-4 : Consider the problem (P4) with the following data:

i	1	2	3	4
P_i	3	4	8	7
d_i	12	4	10	7

The SPT rule gives the schedule (1,2,4,3) where $\sum_{i=1}^{n} C_i^2$=738,

The EDD rule gives the schedule (2,4,3,1) where T_{max}=10

Hence the LB=738+10=748.

Note that the exact solution for problem (P4) obtained by (BAB) method. The optimal schedule is (1,2,4,3) with $\sum_{i=1}^{n} C_i^2 + T_{max}$=750.

The lower bound of each node in the solution search tree are written against the nodes of the tree. To find the optimal solution for (P4), we applied the methods for lower and upper bounds that will be used in BAB algorithm. Where (BAB) Branch and bound method can be used for solving many combinatorial optimization problems. These procedures can be conveniently represented as a search (scheduling, branching) tree whose nodes correspond to subsets of a feasible solution. To minimize an objective function of a particular scheduling problem, first an upper bound UB of the minimum of this objective function is needed. A branching rule is used to partition feasible solutions at a node into subsets and a bounding rule calculates a lower bound LB on the value of each solution in a subset.

Computational experience

An intensive work of numerical experimentations has been performed. We first present how instances (tests problem) can be randomly generated .

There exists in the literature a classical way to randomly generate tests problem of scheduling problems.

- The processing time P_i are uniformly distributed in the interval [1,10].
- The due dates d_i are uniformly distributed in the interval [p(1- TF-RDD/2), p(1+ TF+ RDD/2)] ; where $p=\sum_{i=1}^{n} p_i$, depending on the relative range of due date (RDD) and on the average tardiness factor (TF).

For both parameters, the values 0.2,0.4,0.6,0.8and 1.0, are considered . For each selected value of n, one problem was generated for each of five values of parameters producing five problems for each value of n . The BAB and B algorithms were tested by coding them in matlab7 and running on Pentium IV at 2800MHz with Ram 512MB computer. The BAB algorithm is tested on problems with size (10,20,30) .

For problems that are not solved to optimally because the execution time exceed 30 minutes, the optimal solution for these unsolved problems found by our algorithm B .

Table(1) shows the results for problem (P4) obtained by BAB algorithm. The first column "n" refers to the number of jobs, the second column "EX" refers to the number of example for each instance n, the third column "optimal" refers to the optimal value obtained by BAB algorithm for problem (P4), the fourth column "UB" refers to the upper bound , the fifth column "ILB" refers to the initial lower bound , the sixth column "nodes" refers to the number of nodes , the seventh column "time" refers to the time cost 'by seconds' to solve the problem, the last column "status" refers to the problem solved '0' or not '1'. The symbol "*" refers to the optimal=UB, we stopped when the sum of status' column ≥ 3.

Table(2) , show the results for problem (P4) obtained by algorithm (B). The first two columns as the same columns in table(1), the third column "value" refers to the minimum value that we get by algorithms B, and the last column "time" refers to the time cost 'by seconds' to solve the problem .

Table (3)compare between *BAB and algorithm (B) to solve a problem(P4)(time by seconds).* It is clear from table (3) that the BAB method can not solved problems with $n \geq 30$.

Table -1:*The performance of initial lower bound,upper bound and computational time of BAB algorithm for (P4).*

n	EX	optimal	UB	ILB	nodes	time	status
10	1	5868	5868*	5863	222	0.083753	0
	2	14653	14653*	14644	668	0.05233	0
	3	9629	9629*	9614	241	0.022428	0
	4	9798	9803	9792	71	0.008206	0
	5	5518	5518*	5499	266	0.025065	0
20	1	74030	74030*	74010	17887	1.331111	0
	2	52867	52877	52810	417071	29.22711	0
	3	78694	78694*	78661	1043412	81.99179	0
	4	71171	71182	71096	240860	16.87217	0
	5	46104	46114	46037	1097334	78.07866	0
30	1	210893	210893*	210891	23445581	1800	1
	2	157867	157867*	157847	22422037	1800.001	1
	3	157309	157318	157293	21096053	1800.001	1
	4	215258	215268	215137	21573266	1800.001	1
	5	232131	232131*	232053	21280420	1800	1

Table -3:*BAB Vs algorithm (B) to solve a problem(P4) (time by seconds).*

n	BAB	B
10	0.02	0.01
20	40	0.09
30	1800	0.1
100	1800	0.1
200	1800	75
300	1800	200
400	1800	510
500	1800	1550

Table - 2:*Results of algorithm B for (P4).*

n	ex	value	time
10	1	5868	0.09719246
	2	14653	0.00887009
	3	9629	0.01406612
	4	9798	0.01021048
	5	5518	0.0208633
20	1	74030	0.08547378
	2	52867	0.13290581
	3	78694	0.06773622
	4	71171	0.16499083
	5	46104	0.15121613
30	1	210893	0.06058998
	2	157867	0.08748179
	3	157309	0.09807895
	4	215258	0.46199023
	5	232131	0.26577637
100	1	5868	0.05231801
	2	14653	0.010738
	3	9629	0.01390555
	4	9798	0.01086037
	5	5518	0.02007836
200	1	46373355	71.2329712
	2	55521683	74.9988027
	3	52408900	114.055689
	4	43625257	47.1273153
	5	45305234	78.6391166
300	1	180481870	28.6847228
	2	189083219	252.168852
	3	183437469	127.6062
	4	157888207	223.006137
	5	164142954	352.721073
400	1	421801412	308.649517
	2	423348248	848.978298
	3	430915881	921.210297
	4	394605521	355.380809
	5	413688655	531.261101
500	1	712946851	1496.9584
	2	763797269	1551.28829
	3	755495302	1676.87384
	4	782832453	1768.17998
	5	750245041	1633.0393

REFERENCES

1. Azizoglu M.,Kondakci S., and Kokslan M.," Single machine scheduling with maximum earliness and number tardy", Computers & Industrial Engineering ,45 : 257–268 (2003).
2. Bagga P.C., Kalra K.R.," A node elimination procedure for Townsend's algorithm for solving the single machine quadratic penalty function scheduling problem", Management Science, 26, :633–636(1980).
3. Chang P., Su L.," Scheduling n jobs on one machine to minimize the maximum lateness with a minimum number of tardy jobs", computer& industrial engineering, 40 : 49-60(2001).
4. Chen T., Qi X., and Tu F., "Single machine scheduling to minimize weighted earliness subject to maximum tardiness", computer of operation research, 24:147-152(1997).
5. Cheng ,et al.," A survey of scheduling problems with setup times or costs", European Journal of Operational Research 187: 985–1032 (2008).
6. Emmons H., "A note on a scheduling problem with dual criteria", Naval Res. Logis. Quarterly, 22: 615-516 (1975).
7. French S.," Sequencing and Scheduling: An Introduction to the Mathematics of the Job-Shop", John Wiley & Sons, New York(1982).
8. 8)George S., Paul S., " Pareto optima for total weighted completion time and maximum lateness on a single machine", Discrete Applied Mathematics 155: 2341 – 2354(2007).
9. 9)Graham R.L., Lawler E.L., Lenstra J.K., and Rinnooy K.A.," Optimization and approximation in deterministic
10. sequencing and scheduling: A survey", Annals of Discrete Mathematics 5: 287–326(1979).
11. 10) Gupta S. K., Sen T.," On the single machine scheduling problem with quadratic penalty function of completion times: an improved branching procedure", Management Science, 30: 644–647(1984).
12. 11) Hoogeveen J.A, " Invited Review Multi-criteria scheduling ", European Journal of Operational Research 167 : 592–623(2005).
13. 12) Hoogeveen, J.A., van de Velde, S.L., " Minimizing total completion time and maximum cost simultaneously is solvable in polynomial time", Operations Research Letters 17: 205–208(1995).
14. 13) Jackson J.R.," Scheduling a production line to minimize maximum tardiness", Research Report 43, Management Sciences Research Project, UCLA(1955).
15. 14) Jouni L., "Multi-objective Nonlinear Pareto-Optimization ", Lappeenranta University of Technology(2000).

16.15) Kawi Haidar Y. ,"Single machine scheduling for multi-objective functions", M.Sc. thesis , Dept. of mathematics, college of science, University of AL-Mustansiriya,(2009).

17.16) Lawler E.L.,"Optimal sequencing of a single machine subject to precedence constraints"Management Science 19/5:544-546 (1973).

18.17) Lee C.Y., Vairaktarakis G.L.," Complexity of single machine hierarchical scheduling: A survey", Complexity in Numerical Optimization, 19: 269–298(1993).

19.18) Lenstra J.K.,Rinnooy Kan, and Brucker P.,"Complexity of machine scheduling problems", Annals of Discrete Mathematics 1, :343-362(1979).

20.19) Moslehi G., Moghaddam R., Vasei M., and Azaron A., "A branch-and-bound algorithm for a single machine sequencing to minimize the sum of maximum earliness and tardiness with idle insert ",Applied Mathematics and Computation 174 : 388–408(2006)

21.Nagar A., Jorge H., and Sunderesh H., " Multiple and bi-criteria scheduling: A literature survey", European Journal of Operational Research North-Holland,81:8-104 (1995).

22.Nelson R.T., Sarin R.K., and Daniels R.L., "Scheduling with multiple performance measures: The one-machine case", Management Science 32: 464-479(1986).

23.Smith W.E. , "Various optimizers for single stage production", Naval Research Logistics Quarterly 3/1: 59-66(1956).

24.Szwarc W., Posner M. E., and Liu J.," The single machine problem with quadratic cost function of completion times", Management Science, 34: 1480–1488(1988).

25.Townsend W. ," The single machine problem with quadratic penalty function of completion times: a branch and bound solution", Management Science, 24: 530–534(1978).

26.Van Wassenhove L.N., and Gelders F., "Solving a bicriterion scheduling problem", European Journal of Operational Research 4/1: 42-48(1980).

Some Forms of bi-continuous Multifunctions

Umilkeram Q. Al-Ramadhan
Department of Mathematics ,College of Science, Al-Mustanisiryah University

الخلاصة

في هذا البحث قمنا بتقديم مفهوم المجموعة المفتوحة $\theta-\tau_1\tau_2$ وبالاعتماد على هذا المفهوم قمنا بتعريف مفاهيم أخرى . كذلك قمنا بتقديم مفاهيم خاصة بالدوال المتعددة القيم ثنائية الاستمرارية مع بعض مكافآت وخواص لهذه الدوال ودرسنا العلاقة فيما بينهم .

ABSTRACT

In this paper we introduce a new concept $\theta-\tau_1\tau_2$ open set and some concepts are defined on it . Also we introduce a new concepts of bi-continuous multifunctions and obtain some characterizations and some properties of multifunctions and study the relationships among them.

INTRODUCTION

The concept of bitopological space was introduced in 1963 by killy J.C. in his work "Bitopological space" and the concept of multifunctions can be found in (1) . The concept of θ-open set was introduced in 1968 by Velicko N.V. in his work " H-closed topological spaces ". This concept has been studied intensively by many authors and they found that the collection of all θ-open sets in a topological space (X,Γ) forms a topology Γ_θ on X which is weaker than Γ. In this paper we join among those concepts and introduce the concept of $\theta-\tau_1\tau_2$ open set .If X is a non-empty set ,then a bitopological space (X,τ_1,τ_2) satisfies the property (say γ) : the intersection of a finite number of $\tau_1\tau_2$ open sets is $\tau_1\tau_2$ open ,then the collection of all $\theta-\tau_1\tau_2$ open sets forms a topology on X and is denoted by $\Gamma_{\theta_{\tau_1\tau_2}}$, and as definitions of θ-derived ,θ-border ,θ-frontier and θ-exterior of a set in (2) .We introduce and study topological properties of $\theta-\tau_1\tau_2$ derived ,$\theta-\tau_1\tau_2$ border ,$\theta-\tau_1\tau_2$ frontier and $\theta-\tau_1\tau_2$ exterior of a set using the concept of $\theta-\tau_1\tau_2$ open sets . Finally we introduce some concepts of bi-continuous multifunction and we obtain some characterizations and some properties of multifunctions .We define the concepts weakly , weakly* ,Strong ,almost and almost*-bi-continuous multifunction and we study the relationships among them .

PRELIMINARIES

Throughout the present paper ,(X,τ_1,τ_2) and (Y,σ_1,σ_2) (or simply X and Y) denote bitopological spaces.

Definition(1.1)[3]: A subset A of a bitopological space (X,τ_1,τ_2) is called $\tau_1\tau_2$ open if $A\in\tau_1\cup\tau_2$ and the complement of $\tau_1\tau_2$ open set is $\tau_1\tau_2$ closed .

Example(1.2): Let $X=\{a,b,c\},\tau_1=\{\phi,X,\{a\}\}$ and $\tau_2=\{\phi,X,\{b\}\}$.The sets in $\{\phi,X,\{a\},\{b\}\}$ are
called $\tau_1\tau_2$ open and the sets in $\{\phi,X,\{b,c\},\{a,c\}\}$ are called $\tau_1\tau_2$ closed .

Definition(1.3)[3]: Let A be a subset of X .
(1) The $\tau_1\tau_2$ closure of A ,denoted by $\tau_1\tau_2 cl(A)$,is defined by $\cap\{F: A\subset F$ and F is $\tau_1\tau_2$ closed$\}$.
(2) The $\tau_1\tau_2$ interior of A ,denoted by $\tau_1\tau_2 int(A)$,is defined by $\cup\{U: U\subset A$ and U is $\tau_1\tau_2$ open$\}$.

Lemma(1.4): Let A be a subset of a bitopological space (X,τ_1,τ_2).Then $x\in\tau_1\tau_2 cl(A)$ if and only if $U\cap A\neq\phi$ for every $\tau_1\tau_2$ open set U containing x .

Proof: Suppose that there exists $\tau_1\tau_2$ open set U containing x such that $U\cap A=\phi$.Then $A\subset X\setminus U$ and $X\setminus U$ is $\tau_1\tau_2$ closed, implies that $\tau_1\tau_2 cl(A)\subset X\setminus U$. Since $x\in U$, we have $x\notin\tau_1\tau_2 cl(A)$,this is a contradiction .
Conversely: Suppose that $x\notin\tau_1\tau_2 cl(A)$. Then there exists $\tau_1\tau_2$ closed subset F of X such that $A\subset F$ and $x\notin F$. Thus there exists $\tau_1\tau_2$ open subset $X\setminus F$ containing x such that $(X\setminus F)\cap A=\phi$, this is a contradiction.

Lemma(1.5): Let A be a subset of a bitopological space (X,τ_1,τ_2),then the following hold:
(i) If A is $\tau_1\tau_2$ open set ,then $A=\tau_1\tau_2 int(A)$.
(ii) If A is $\tau_1\tau_2$ closed set ,then $A=\tau_1\tau_2 cl(A)$.

Proof: (i) It is obvious from definition (1.3) .
(ii) Since A is $\tau_1\tau_2$ closed ,then $X\setminus A$ is $\tau_1\tau_2$ open and by (i) we have $X\setminus A=\tau_1\tau_2 int(X\setminus A)$.
It implies and by definition (1.3) ,that $X\setminus A=X\setminus\tau_1\tau_2 cl(A)$,then $A=\tau_1\tau_2 cl(A)$.

Remark(1.6): The following example shows that the converse of lemma (1.5),(i) and (ii),is not true.

Example(1.7): Refer example (1.2).Let A={a,b},then $A = \tau_1\tau_2\,\mathrm{int}(A)$ and clearly A is not $\tau_1\tau_2$ open set .
Now, if A={c} ,then it is clear that $A = \tau_1\tau_2 cl(A)$, but is not $\tau_1\tau_2$ closed set .

θ-$\tau_1\tau_2$ OPEN SETS

In this section we introduce the concept of θ-$\tau_1\tau_2$ open set and study some properties .

Definition(2.1): Let (X,τ_1,τ_2) be a bitopological space and A be a subset of X .The θ-$\tau_1\tau_2$ interior of A is defined by: θ-$\tau_1\tau_2\,\mathrm{int}(A) = \bigcup\{U : \tau_1\tau_2 cl(U) \subseteq A, U \text{ is } \tau_1\tau_2 \text{ open }\}$. A is called θ-$\tau_1\tau_2$ open iff $A = \theta$-$\tau_1\tau_2\,\mathrm{int}(A)$ and the complement of A is called θ-$\tau_1\tau_2$ closed .
Definition(2.2): Let (X,τ_1,τ_2) be a bitopological space and A be a subset of X . A point x of X is said to be θ-$\tau_1\tau_2$ cluster of A iff $\tau_1\tau_2 cl(U) \cap A \neq \phi$ for every $\tau_1\tau_2$ open set U containing x .The set of all θ-$\tau_1\tau_2$ cluster points of A is said to be θ-$\tau_1\tau_2$ closure of A and is denoted by θ-$\tau_1\tau_2 cl(A)$.

Remark(2.3): Note that the concept of θ-$\tau_1\tau_2$ open sets and $\tau_1\tau_2$ open sets are ,in general , independent as seen from the following two examples :

Example(2.4): Let X={a,b,c}, τ_1={ϕ,X,{a},{b,c}},and τ_2={ϕ ,X,{b}, {a,c}}. So the sets in {ϕ,X,{a},{b,c},{b},{a,c}}are $\tau_1\tau_2$ open and the sets in{ϕ,X,{b,c},{a},{a,c},{b}}are $\tau_1\tau_2$ closed.
Clearly{a,b}is not $\tau_1\tau_2$ open but it is θ-$\tau_1\tau_2$ open since {a,b}=θ-$\tau_1\tau_2\,\mathrm{int}(\{a,b\})$.

Example(2.5): Let X={a,b,c}, τ_1={ϕ,X,{a}}, and τ_2={ϕ,X}.So the sets in{ϕ,X,{a}}are $\tau_1\tau_2$ open and the sets in{ϕ,X,{b,c}}are $\tau_1\tau_2$ closed. Clearly {a}is $\tau_1\tau_2$ open but it is not θ-$\tau_1\tau_2$ open since {a}$\neq\theta$-$\tau_1\tau_2\,\mathrm{int}(\{a\})=\phi$.

Remark(2.6): If X is a non-empty set ,then
(1) A bitopological space (X,τ_1,τ_2) is said to have the property (β) if the union of any family of
$\tau_1\tau_2$ open sets is $\tau_1\tau_2$ open .

(2) A bitopological space (X,τ_1,τ_2) satisfy (β) have the following : Every $\theta-\tau_1\tau_2$ open is $\tau_1\tau_2$ open .

Remark(2.7): It is clear that $\theta-\tau_1\tau_2\,\mathrm{int}(\phi)=\phi$, $\theta-\tau_1\tau_2\mathrm{cl}(\phi)=\phi$, $\theta-\tau_1\tau_2\,\mathrm{int}(X)=X$,
$\theta-\tau_1\tau_2\mathrm{cl}(X)=X$.

Theorem(2.8): Let (X,τ_1,τ_2) be a bitopological space and A,B are subsets of X, then the following hold:

(i) $\theta-\tau_1\tau_2\mathrm{cl}(X\setminus A)=X\setminus\theta-\tau_1\tau_2\,\mathrm{int}(A)$ and $\theta-\tau_1\tau_2\,\mathrm{int}(X\setminus A)=X\setminus\theta-\tau_1\tau_2\mathrm{cl}(A)$.

(ii) $A\subseteq\tau_1\tau_2\mathrm{cl}(A)\subseteq\theta-\tau_1\tau_2\mathrm{cl}(A)$ and $\theta-\tau_1\tau_2\,\mathrm{int}(A)\subseteq\tau_1\tau_2\,\mathrm{int}(A)\subseteq A$.

(iii) If $A\subseteq B$, then $\theta-\tau_1\tau_2\,\mathrm{int}(A)\subseteq\theta-\tau_1\tau_2\,\mathrm{int}(B)$ and $\theta-\tau_1\tau_2\mathrm{cl}(A)\subseteq\theta-\tau_1\tau_2\mathrm{cl}(B)$.

(iv) A is $\theta-\tau_1\tau_2$ closed iff $A=\theta-\tau_1\tau_2\mathrm{cl}(A)$.

Proof:

(i) Let $x\in\theta-\tau_1\tau_2\mathrm{cl}(X\setminus A)\Leftrightarrow\forall\ \tau_1\tau_2$ open set U containing x $,\tau_1\tau_2\mathrm{cl}(U)\cap(X\setminus A)\neq\phi$

$\Leftrightarrow\forall\ \tau_1\tau_2$ open set U containing x $,\tau_1\tau_2\mathrm{cl}(U)\not\subset A\Leftrightarrow x\notin\theta-\tau_1\tau_2\,\mathrm{int}(A)$ $\Leftrightarrow$

$x\in X\setminus\theta-\tau_1\tau_2\,\mathrm{int}(A)$.

Now, let $x\in\theta-\tau_1\tau_2\,\mathrm{int}(X\setminus A)\Leftrightarrow\exists\ \tau_1\tau_2$ open set U containing x such that $\tau_1\tau_2\mathrm{cl}(U)\subset X\setminus A$

$\Leftrightarrow\exists\ \tau_1\tau_2$ open set U containing x such that $\tau_1\tau_2\mathrm{cl}(U)\cap A=\phi\Leftrightarrow x\notin\theta-\tau_1\tau_2\mathrm{cl}(A)\Leftrightarrow$

$x\in X\setminus\theta-\tau_1\tau_2\mathrm{cl}(A)$.

(ii) From definition (1.3), $A\subseteq\tau_1\tau_2\mathrm{cl}(A)$. Now, to prove $\tau_1\tau_2\mathrm{cl}(A)\subseteq\theta-\tau_1\tau_2\mathrm{cl}(A)$.

Let $x\in\tau_1\tau_2\mathrm{cl}(A)$,then by lemma (1.4) $U\cap A\neq\phi$, $\forall\ \tau_1\tau_2$ open set U containing x .

Since $U\subseteq\tau_1\tau_2\mathrm{cl}(U)$,then $\tau_1\tau_2\mathrm{cl}(U)\cap A\neq\phi,\forall\ \tau_1\tau_2$ open set U containing x .

Hence $x\in\theta-\tau_1\tau_2\mathrm{cl}(A)$.

Now, from definition (1.3), $\tau_1\tau_2\,\mathrm{int}(A)\subseteq A$. To prove $\theta-\tau_1\tau_2\,\mathrm{int}(A)\subseteq\tau_1\tau_2\,\mathrm{int}(A)$.

Let $x\in\theta-\tau_1\tau_2\,\mathrm{int}(A)$,then $\exists\ \tau_1\tau_2$ open set U containing x such that $\tau_1\tau_2\mathrm{cl}(U)\subset A$.

Since $U \subseteq \tau_1\tau_2 cl(U)$,then $\exists\ \tau_1\tau_2$ open set U containing x such that $U \subset A$.

Hence $x \in \tau_1\tau_2\ int(A)$.

(iii) By definitions (2.1) and (2.2).

(iv) A is θ-$\tau_1\tau_2$ closed $\Leftrightarrow X \setminus A$ is θ-$\tau_1\tau_2$ open $\Leftrightarrow$ $X \setminus A = \theta$-$\tau_1\tau_2\ int(X \setminus A) \Leftrightarrow$

$X \setminus A = X \setminus \theta$-$\tau_1\tau_2 cl(A) \Leftrightarrow A = \theta$-$\tau_1\tau_2 cl(A)$.

Theorem(2.9): Let (X, τ_1, τ_2) be a bitopological space and A,B are subsets of X, then the following hold:

(i) θ-$\tau_1\tau_2 cl(A \cup B) = \theta$-$\tau_1\tau_2 cl(A) \cup \theta$-$\tau_1\tau_2 cl(B)$.

(ii) θ-$\tau_1\tau_2 cl(A \cap B) \subseteq \theta$-$\tau_1\tau_2 cl(A) \cap \theta$-$\tau_1\tau_2 cl(B)$.

(iii) θ-$\tau_1\tau_2\ int(A \cup B) \supseteq \theta$-$\tau_1\tau_2\ int(A) \cup \theta$-$\tau_1\tau_2\ int(B)$.

(iv) θ-$\tau_1\tau_2\ int(A \cap B) \subseteq \theta$-$\tau_1\tau_2\ int(A) \cap \theta$-$\tau_1\tau_2\ int(B)$.

Proof:

(i) Since $A \subset A \cup B$ and $B \subset A \cup B$, then by theorem (2.8)(iii), we get θ-$\tau_1\tau_2 cl(A \cup B) \supseteq \theta$-$\tau_1\tau_2 cl(A) \cup \theta$-$\tau_1\tau_2 cl(B)$.

Now, let $x \in \theta$-$\tau_1\tau_2 cl(A \cup B)$,then $\forall\ \tau_1\tau_2$ open set U containing x , $\tau_1\tau_2 cl(U) \cap (A \cup B) \neq \phi$.

It implies $\tau_1\tau_2 cl(U) \cap A \neq \phi$ or $\tau_1\tau_2 cl(U) \cap B \neq \phi$, therefore $x \in \theta$-$\tau_1\tau_2 cl(A) \cup \theta$-$\tau_1\tau_2 cl(B)$.

(ii) Since $A \cap B \subset A$ and $A \cap B \subset B$, then by theorem (2.8)(iii), we get θ-$\tau_1\tau_2 cl(A \cap B) \subseteq \theta$-$\tau_1\tau_2 cl(A) \cap \theta$-$\tau_1\tau_2 cl(B)$.

(iii) Let $x \in \theta$-$\tau_1\tau_2\ int(A) \cup \theta$-$\tau_1\tau_2\ int(B)$, then $x \in \theta$-$\tau_1\tau_2\ int(A)$ or $x \in \theta$-$\tau_1\tau_2\ int(B)$.

If $x \in \theta$-$\tau_1\tau_2\ int(A)$,then $\exists\ \tau_1\tau_2$ open set U containing x such that $\tau_1\tau_2 cl(U) \subseteq A \subseteq A \cup B$.

Hence $x \in \theta$-$\tau_1\tau_2\ int(A \cup B)$ and the same if $x \in \theta$-$\tau_1\tau_2\ int(B)$.

(iv) Since $A \cap B \subset A$ and $A \cap B \subset B$, then by theorem (2.8)(iii), we have θ-$\tau_1\tau_2\ int(A \cap B) \subseteq \theta$-$\tau_1\tau_2\ int(A) \cap \theta$-$\tau_1\tau_2\ int(B)$.

Remark(2.10): The equality of (ii) , (iii) and (iv) in above theorem is not true , in general , as seen from the following examples .

Example(2.11):

(1) Let $X=\{a,b,c,d\}, \tau_1=\{\phi,X,\{b\},\{b,c\}\}$and $\tau_2=\{\phi,X,\{a\}\}$. So the sets in$\{\phi,X,\{b\},\{b,c\},\{a\}\}$

are $\tau_1\tau_2$ open and the sets in$\{\phi,X,\{a,c,d\},\{a,d\},\{b,c,d\}\}$are $\tau_1\tau_2$ closed .

Let $A=\{a,b\}$,$B=\{a,c\}$,then $\theta-\tau_1\tau_2 cl(A)=X$ and $\theta-\tau_1\tau_2 cl(B)=X$, but $A\cap B=\{a\}$ and

$\theta-\tau_1\tau_2 cl(A\cap B)=\{a,d\}$. Hence $\theta-\tau_1\tau_2 cl(A\cap B)\neq\theta-\tau_1\tau_2 cl(A)\cap\theta-\tau_1\tau_2 cl(B)$.

(2) Now, let $A=\{a,b\}$, $B=\{c,d\}$,then $\theta-\tau_1\tau_2 int(A)=\phi$ and $\theta-\tau_1\tau_2 int(B)=\phi$, but $A\cup B=X$ and

$\theta-\tau_1\tau_2 int(A\cup B)=X$. Therefore $\theta-\tau_1\tau_2 int(A\cup B)\neq\theta-\tau_1\tau_2 int(A)\cup\theta-\tau_1\tau_2 int(B)$.

(3) Let $X=\{a,b,c,d\}, \tau_1=\{\phi,X,\{b\},\{b,c\}\}$and $\tau_2=\{\phi,X,\{a\},\{a,c\},\{a,d\}$ $,\{a,c,d\}\}$. So the sets in

$\{\phi,X,\{b\},\{b,c\},\{a\},\{a,c\},\{a,d\},\{a,c,d\}\}$are $\tau_1\tau_2$ open and the sets in$\{\phi,X,\{a,c,d\},\{a,d\},$

$\{b,c,d\},\{b,d\},\{b,c\},\{b\}\}$are $\tau_1\tau_2$ closed. Let $A=\{b,c\}$ $,B=\{a,c,d\}$,then $\theta-\tau_1\tau_2 int(A)=\{b,c\}$

and $\theta-\tau_1\tau_2 int(B)=\{a,c,d\}$, but $A\cap B=\{c\}$and $\theta-\tau_1\tau_2 int(A\cap B)=\phi$.

Therefore $\theta-\tau_1\tau_2 int(A\cap B)\neq\theta-\tau_1\tau_2 int(A)\cap\theta-\tau_1\tau_2 int(B)$.

Remark(2.12): Let A be any non-empty subset of (X,τ_1,τ_2) ,then the following example shows that

$\theta-\tau_1\tau_2 cl(\theta-\tau_1\tau_2 cl(A))\neq\theta-\tau_1\tau_2 cl(A)$ and $\theta-\tau_1\tau_2 int(\theta-\tau_1\tau_2 int(A))\neq\theta-\tau_1\tau_2 int(A)$.

Example(2.13): Refer example (2.11)(1),let $A=\{a\}$,then $\theta-\tau_1\tau_2 cl(A)=\{a,d\}$and $\theta-\tau_1\tau_2 cl(\theta-\tau_1\tau_2 cl(A))=X$.Hence $\theta-\tau_1\tau_2 cl(\theta-\tau_1\tau_2 cl(A))\neq\theta-\tau_1\tau_2 cl(A)$.

Now , if $A=\{a,b,d\}$,then $\theta-\tau_1\tau_2 int(A)=\{a\}$ and $\theta-\tau_1\tau_2 int(\theta-\tau_1\tau_2 int(A))=\phi$. Hence $\theta-\tau_1\tau_2 int(\theta-\tau_1\tau_2 int(A))\neq\theta-\tau_1\tau_2 int(A)$.

Remark(2.14):

(1) The collection of all $\theta-\tau_1\tau_2$ open sets is denoted by $\theta_{\tau_1\tau_2}$.

(2) If X is a non-empty set ,then a bitopological space (X,τ_1,τ_2) is said to have property (γ) if the

intersection of any finite number of $\tau_1\tau_2$ open sets is $\tau_1\tau_2$ open .

(3) A bitopological space (X,τ_1,τ_2) satisfy (γ) have the following theorem gives a topology $\Gamma_{\theta_{\tau_1\tau_2}}$

(consist of the collection of all θ-$\tau_1\tau_2$ open sets) induced by $\tau_1\tau_2$ open sets .

Theorem(2.15): Let (X,τ_1,τ_2) be a bitopological space satisfy (γ) , then the following hold:

(1) X,ϕ are θ-$\tau_1\tau_2$ open .

(2) The intersection of finite θ-$\tau_1\tau_2$ open sets is θ-$\tau_1\tau_2$ open .

(3) The union of any family of θ-$\tau_1\tau_2$ open sets is θ-$\tau_1\tau_2$ open .

Proof:

(1) It is obvious from remark (2.7) .

(2) Let A_1, A_2 be θ-$\tau_1\tau_2$ open sets of X, to prove $A_1 \cap A_2$ is θ-$\tau_1\tau_2$ open set

i.e. θ-$\tau_1\tau_2\,\text{int}(A_1 \cap A_2) = A_1 \cap A_2$.

It is clear by theorem (2.8)(ii) ,that θ-$\tau_1\tau_2\,\text{int}(A_1 \cap A_2) \subset A_1 \cap A_2$.

Now, let $x \in A_1 \cap A_2$ implies $x \in A_1$ and $x \in A_2$,then $x \in \theta$-$\tau_1\tau_2\,\text{int}(A_1)$ and

$x \in \theta$-$\tau_1\tau_2\,\text{int}(A_2)$. Hence $\exists\ \tau_1\tau_2$ open set U containing x such that $\tau_1\tau_2\text{cl}(U) \subseteq A_1$ and

$\exists\ \tau_1\tau_2$ open set V containing x such that $\tau_1\tau_2\text{cl}(V) \subseteq A_2$. Then by lemma (1.4)

$\tau_1\tau_2\text{cl}(U \cap V) \subseteq \tau_1\tau_2\text{cl}(U) \cap \tau_1\tau_2\text{cl}(V) \subseteq A_1 \cap A_2$ .Since X satisfy (γ) ,then $U \cap V$ is $\tau_1\tau_2$ open

and $x \in U \cap V$ implies that $x \in \theta$-$\tau_1\tau_2\,\text{int}(A_1 \cap A_2)$. Hence θ-$\tau_1\tau_2\,\text{int}(A_1 \cap A_2) = A_1 \cap A_2$.

(3) Let $A_i \in \theta_{\tau_1\tau_2}$, $\forall\ i \in I$. To prove $\bigcup_{i\in I} A_i \in \theta_{\tau_1\tau_2}$ (i.e. θ-$\tau_1\tau_2\,\text{int}(\bigcup_{i\in I} A_i) = \bigcup_{i\in I} A_i$) .Let $x \in \bigcup_{i\in I} A_i$

implies that $x \in A_i$ for some i ,then $x \in \theta$-$\tau_1\tau_2\,\text{int}(A_i)$. Hence $\exists\ \tau_1\tau_2$ open set U containing x

such that $\tau_1\tau_2\text{cl}(U) \subseteq A_i \subseteq \bigcup_{i\in I} A_i$. Therefore $x \in \theta$-$\tau_1\tau_2\,\text{int}(\bigcup_{i\in I} A_i)$. Then by theorem (2.8)(ii) ,

we get θ-$\tau_1\tau_2\,\text{int}(\bigcup_{i\in I} A_i) = \bigcup_{i\in I} A_i$.

Remark(2.16): If (X,τ_1,τ_2) does not satisfy (γ) ,then the intersection of finite $\theta-\tau_1\tau_2$ open sets is not always $\theta-\tau_1\tau_2$ open we can show that by example (2.11)(3) , it is clear that if A={b,c}, B={a,c,d},then $\theta-\tau_1\tau_2$ int(A) = A , $\theta-\tau_1\tau_2$ int(B) = B (i.e. $A,B\in\theta_{\tau_1\tau_2}$) but $A\cap B\notin\theta_{\tau_1\tau_2}$.

Remark(2.17): Let (X,τ_1,τ_2) be a bitopological space and $A\subseteq X$,then we can prove :

(1) Let U be $\tau_1\tau_2$ open set and $A\subseteq X$, if $U\cap A=\phi$, then $U\cap\tau_1\tau_2$cl(A) = ϕ.

(2) If U is $\tau_1\tau_2$ open set ,then $\tau_1\tau_2$cl(U)=$\theta-\tau_1\tau_2$cl(U).

(3) If U is $\tau_1\tau_2$ open set and $\tau_1\tau_2$ closed set ,then U is $\theta-\tau_1\tau_2$ closed .

(4) If (X,τ_1,τ_2) satisfy (β) and U is $\tau_1\tau_2$ open set ,then U is $\tau_1\tau_2$ closed iff U is $\theta-\tau_1\tau_2$ closed .

(5) If A is $\tau_1\tau_2$ closed ,then $\tau_1\tau_2$ int(A) = $\theta-\tau_1\tau_2$ int(A).

Remark(2.18): The converse of (3) in the remark (2.17) is not true, in general, as the following example shows .

Example(2.19): Let X={a,b,c}, τ_1={ϕ,X,{a},{c},{a,c}}and τ_2={ϕ,X,{b}}. So the sets in {ϕ,X,{a},{c},{a,c},{b}}are $\tau_1\tau_2$ open and the sets in{ϕ,X,{b,c},{a,b},{b},{a,c}}are $\tau_1\tau_2$ closed . Let U={c},then U is $\tau_1\tau_2$ open and U is $\theta-\tau_1\tau_2$ closed since U = $\theta-\tau_1\tau_2$cl(U),but clearly U is not $\tau_1\tau_2$ closed .

SOME PROPERTIES OF $\theta-\tau_1\tau_2$ OPEN SETS

The following definitions and results are the $\theta-\tau_1\tau_2$ version of those definitions and results in (2).

Definition(3.1): Let (X,τ_1,τ_2) be a bitopological space and $A\subseteq X$. A point $x\in X$ is said to be $\theta-\tau_1\tau_2$ limit point of A if for each $U\in\theta_{\tau_1\tau_2}$ such that $x\in U$,then $U\cap(A\setminus\{x\})\neq\phi$. The set of all $\theta-\tau_1\tau_2$ limit points of A is called $\theta-\tau_1\tau_2$ derived set of A and is denoted by $\theta-\tau_1\tau_2$ d(A).

Theorem(3.2): Let (X,τ_1,τ_2) be a bitopological space and A,B are subsets of X, then the following hold:

(1) If $A\subseteq B$,then $\theta-\tau_1\tau_2$ d(A)$\subseteq$ $\theta-\tau_1\tau_2$ d(B).

(2) $\theta-\tau_1\tau_2$ d(A$\cap$B)$\subseteq$ $\theta-\tau_1\tau_2$ d(A)$\cap$ $\theta-\tau_1\tau_2$ d(B).

(3) $\theta\text{-}\tau_1\tau_2\, d(A) \cup \theta\text{-}\tau_1\tau_2\, d(B) = \theta\text{-}\tau_1\tau_2\, d(A \cup B)$.
(4) $\theta\text{-}\tau_1\tau_2\, d(\theta\text{-}\tau_1\tau_2\, d(A)) \setminus A \subseteq \theta\text{-}\tau_1\tau_2\, d(A)$.
(5) $\theta\text{-}\tau_1\tau_2\, d(A \cup \theta\text{-}\tau_1\tau_2\, d(A)) \subseteq A \cup \theta\text{-}\tau_1\tau_2\, d(A)$.

Proof:(1) It is obvious from definition .**(2)** and **(3)** are proved from (1) and definition .

(4) Let $x \in \theta\text{-}\tau_1\tau_2\, d(\theta\text{-}\tau_1\tau_2\, d(A)) \setminus A \Rightarrow \forall\, U \in \theta_{\tau_1\tau_2}$ such that $x \in U$, $U \cap (\theta\text{-}\tau_1\tau_2\, d(A) \setminus \{x\}) \neq \phi$.

Then, let $y \in U \cap (\theta\text{-}\tau_1\tau_2\, d(A) \setminus \{x\}) \Rightarrow y \in U$ and $y \in \theta\text{-}\tau_1\tau_2\, d(A)$,then $U \cap (A \setminus \{y\}) \neq \phi$.

Then let $z \in U \cap (A \setminus \{y\}) \Rightarrow z \in U$ and $z \in A \setminus \{y\}$,since $x \notin A \Rightarrow z \neq x$, hence

$z \in U \cap (A \setminus \{x\})$ and $U \cap (A \setminus \{x\}) \neq \phi$. So $x \in \theta\text{-}\tau_1\tau_2\, d(A)$.

(5) Let $x \in \theta\text{-}\tau_1\tau_2\, d(A \cup \theta\text{-}\tau_1\tau_2\, d(A))$. If $x \in A$,then $x \in A \cup \theta\text{-}\tau_1\tau_2\, d(A)$ and if $x \notin A$,then

$x \in \theta\text{-}\tau_1\tau_2\, d(A \cup \theta\text{-}\tau_1\tau_2\, d(A)) \setminus A$. Hence $\forall\, U \in \theta_{\tau_1\tau_2}$ such that $x \in U$ and

$U \cap (A \cup \theta\text{-}\tau_1\tau_2\, d(A)) \setminus \{x\} \neq \phi$,then $U \cap (A \setminus \{x\}) \neq \phi$ or $U \cap (\theta\text{-}\tau_1\tau_2\, d(A) \setminus \{x\}) \neq \phi$.

Since $x \notin A$, then by (4) $x \in \theta\text{-}\tau_1\tau_2\, d(A)$.

Definition (3.3): Let (X, τ_1, τ_2) be a bitopological space and $A \subseteq X$. The set $\theta\text{-}\tau_1\tau_2\, b(A) =$
$A \setminus \theta\text{-}\tau_1\tau_2\, \text{int}(A)$ is said to be $\theta\text{-}\tau_1\tau_2$ border of A.

Theorem(3.4): Let (X, τ_1, τ_2) be a bitopological space and $A \subseteq X$, then the following hold:

(1) $A = \theta\text{-}\tau_1\tau_2\, \text{int}(A) \cup \theta\text{-}\tau_1\tau_2\, b(A)$.
(2) $\theta\text{-}\tau_1\tau_2\, \text{int}(A) \cap \theta\text{-}\tau_1\tau_2\, b(A) = \phi$.
(3) A is $\theta\text{-}\tau_1\tau_2$ open iff $\theta\text{-}\tau_1\tau_2\, b(A) = \phi$.
(4) $\theta\text{-}\tau_1\tau_2\, \text{int}(\theta\text{-}\tau_1\tau_2\, b(A)) = \phi$.
(5) $\theta\text{-}\tau_1\tau_2\, b(A) = A \cap \theta\text{-}\tau_1\tau_2\, \text{cl}(X \setminus A)$.

Proof: (1) ,(2) and **(3)** are trivial .
(4) Assume that $\theta\text{-}\tau_1\tau_2\, \text{int}(\theta\text{-}\tau_1\tau_2\, b(A)) \neq \phi$,then there is $x \in \theta\text{-}\tau_1\tau_2\, \text{int}(\theta\text{-}\tau_1\tau_2\, b(A)) \subseteq \theta\text{-}\tau_1\tau_2\, b(A)$.

Now since $\theta\text{-}\tau_1\tau_2\,\mathrm{int}(\theta\text{-}\tau_1\tau_2\,\mathrm{b}(A)) \subseteq \theta\text{-}\tau_1\tau_2\,\mathrm{int}(A)$,then $x \in \theta\text{-}\tau_1\tau_2\,\mathrm{b}(A) \cap \theta\text{-}\tau_1\tau_2\,\mathrm{int}(A)$, this is a

Contradiction. Therefore $\theta\text{-}\tau_1\tau_2\,\mathrm{int}(\theta\text{-}\tau_1\tau_2\,\mathrm{b}(A)) = \phi$.

(5) $\theta\text{-}\tau_1\tau_2\,\mathrm{b}(A) = A \setminus \theta\text{-}\tau_1\tau_2\,\mathrm{int}(A) = A \setminus (X \setminus \theta\text{-}\tau_1\tau_2\mathrm{cl}(X \setminus A)) = A \cap \theta\text{-}\tau_1\tau_2\mathrm{cl}(X \setminus A)$.

Definition (3.5): Let (X, τ_1, τ_2) be a bitopological space and $A \subseteq X$. The set $\theta\text{-}\tau_1\tau_2\,\mathrm{fr}(A) =$
$\theta\text{-}\tau_1\tau_2\,\mathrm{cl}(A) \setminus \theta\text{-}\tau_1\tau_2\,\mathrm{int}(A)$ is said to be $\theta\text{-}\tau_1\tau_2$ frontier of A.

Theorem(3.6): Let (X, τ_1, τ_2) be a bitopological space and $A \subseteq X$, then the following hold:

(1) $\theta\text{-}\tau_1\tau_2\,\mathrm{cl}(A) = \theta\text{-}\tau_1\tau_2\,\mathrm{fr}(A) \cup \theta\text{-}\tau_1\tau_2\,\mathrm{int}(A)$.
(2) $\theta\text{-}\tau_1\tau_2\,\mathrm{fr}(A) \cap \theta\text{-}\tau_1\tau_2\,\mathrm{int}(A) = \phi$.
(3) $\theta\text{-}\tau_1\tau_2\,\mathrm{b}(A) \subseteq \theta\text{-}\tau_1\tau_2\,\mathrm{fr}(A)$.
(4) $\theta\text{-}\tau_1\tau_2\,\mathrm{fr}(A) = \theta\text{-}\tau_1\tau_2\,\mathrm{cl}(A) \cap \theta\text{-}\tau_1\tau_2\mathrm{cl}(X \setminus A)$.
(5) $\theta\text{-}\tau_1\tau_2\,\mathrm{fr}(A) = \theta\text{-}\tau_1\tau_2\,\mathrm{fr}(X \setminus A)$.
(6) $\theta\text{-}\tau_1\tau_2\,\mathrm{int}(A) = A \setminus \theta\text{-}\tau_1\tau_2\,\mathrm{fr}(A)$.

Proof:(1) ,(2) and **(3)** are obvious from definition.

(4) $\theta\text{-}\tau_1\tau_2\,\mathrm{cl}(A) \cap \theta\text{-}\tau_1\tau_2\mathrm{cl}(X \setminus A) = \theta\text{-}\tau_1\tau_2\,\mathrm{cl}(A) \cap (X \setminus \theta\text{-}\tau_1\tau_2\,\mathrm{int}(A)) = \theta\text{-}\tau_1\tau_2\,\mathrm{cl}(A) \setminus \theta\text{-}\tau_1\tau_2\,\mathrm{int}(A)$
$= \theta\text{-}\tau_1\tau_2\,\mathrm{fr}(A)$.

(5) $\theta\text{-}\tau_1\tau_2\,\mathrm{fr}(X \setminus A) = \theta\text{-}\tau_1\tau_2\mathrm{cl}(X \setminus A) \setminus \theta\text{-}\tau_1\tau_2\,\mathrm{int}(X \setminus A) = (X \setminus \theta\text{-}\tau_1\tau_2\,\mathrm{int}(A)) \setminus (X \setminus \theta\text{-}\tau_1\tau_2\,\mathrm{cl}(A)) =$
$\theta\text{-}\tau_1\tau_2\,\mathrm{cl}(A) \setminus \theta\text{-}\tau_1\tau_2\,\mathrm{int}(A) = \theta\text{-}\tau_1\tau_2\,\mathrm{fr}(A)$.

(6) It is clear by definition.

Definition (3.7): Let (X, τ_1, τ_2) be a bitopological space and $A \subseteq X$. The set $\theta\text{-}\tau_1\tau_2\,\mathrm{ext}(A) =$
$\theta\text{-}\tau_1\tau_2\,\mathrm{int}(X \setminus A)$ is said to be $\theta\text{-}\tau_1\tau_2$ exterior of A.

Theorem(3.8): Let (X, τ_1, τ_2) be a bitopological space and A,B are subsets of X, then the following hold:

(1) $\theta\text{-}\tau_1\tau_2\,\text{ext}(\theta\text{-}\tau_1\tau_2\,\text{ext}(A)) = \theta\text{-}\tau_1\tau_2\,\text{int}(\theta\text{-}\tau_1\tau_2\,\text{cl}(A))$.
(2) If $A \subseteq B$,then $\theta\text{-}\tau_1\tau_2\,\text{ext}(B) \subseteq \theta\text{-}\tau_1\tau_2\,\text{ext}(A)$.
(3) $\theta\text{-}\tau_1\tau_2\,\text{ext}(A \cup B) \subseteq \theta\text{-}\tau_1\tau_2\,\text{ext}(A) \cup \theta\text{-}\tau_1\tau_2\,\text{ext}(B)$.
(4) $\theta\text{-}\tau_1\tau_2\,\text{ext}(A) \cap \theta\text{-}\tau_1\tau_2\,\text{ext}(B) \subseteq \theta\text{-}\tau_1\tau_2\,\text{ext}(A \cap B)$.
(5) $\theta\text{-}\tau_1\tau_2\,\text{ext}(X \setminus \theta\text{-}\tau_1\tau_2\,\text{ext}(A)) \subseteq \theta\text{-}\tau_1\tau_2\,\text{ext}(A)$.
(6) $\theta\text{-}\tau_1\tau_2\,\text{int}(A) \subseteq \theta\text{-}\tau_1\tau_2\,\text{ext}(\theta\text{-}\tau_1\tau_2\,\text{ext}(A))$.
(7) $X = \theta\text{-}\tau_1\tau_2\,\text{int}(A) \cup \theta\text{-}\tau_1\tau_2\,\text{ext}(A) \cup \theta\text{-}\tau_1\tau_2\,\text{fr}(A)$.

Proof:

(1) $\theta\text{-}\tau_1\tau_2\,\text{ext}(\theta\text{-}\tau_1\tau_2\,\text{ext}(A)) = \theta\text{-}\tau_1\tau_2\,\text{int}(X \setminus \theta\text{-}\tau_1\tau_2\,\text{ext}(A)) = \theta\text{-}\tau_1\tau_2\,\text{int}(X \setminus \theta\text{-}\tau_1\tau_2\,\text{int}(X \setminus A))$
$= \theta\text{-}\tau_1\tau_2\,\text{int}(\theta\text{-}\tau_1\tau_2\,\text{cl}(A))$.

(2) It is obvious from definition .**(3)** and **(4)** are proved by (2).

(5) $\theta\text{-}\tau_1\tau_2\,\text{ext}(X \setminus \theta\text{-}\tau_1\tau_2\,\text{ext}(A)) = \theta\text{-}\tau_1\tau_2\,\text{ext}(X \setminus \theta\text{-}\tau_1\tau_2\,\text{int}(X \setminus A))$
$= \theta\text{-}\tau_1\tau_2\,\text{int}(X \setminus X \setminus \theta\text{-}\tau_1\tau_2\,\text{int}(X \setminus A)) = \theta\text{-}\tau_1\tau_2\,\text{int}(\theta\text{-}\tau_1\tau_2\,\text{int}(X \setminus A)) \subseteq \theta\text{-}\tau_1\tau_2\,\text{int}(X \setminus A)$
$= \theta\text{-}\tau_1\tau_2\,\text{ext}(A)$.

(6) $\theta\text{-}\tau_1\tau_2\,\text{int}(A) \subseteq \theta\text{-}\tau_1\tau_2\,\text{int}(\theta\text{-}\tau_1\tau_2\,\text{cl}(A)) = \theta\text{-}\tau_1\tau_2\,\text{int}(X \setminus \theta\text{-}\tau_1\tau_2\,\text{int}(X \setminus A))$
$= \theta\text{-}\tau_1\tau_2\,\text{int}(X \setminus \theta\text{-}\tau_1\tau_2\,\text{ext}(A)) = \theta\text{-}\tau_1\tau_2\,\text{ext}(\theta\text{-}\tau_1\tau_2\,\text{ext}(A))$.

(7) $\theta\text{-}\tau_1\tau_2\,\text{int}(A) \cup \theta\text{-}\tau_1\tau_2\,\text{ext}(A) \cup \theta\text{-}\tau_1\tau_2\,\text{fr}(A)$
$= \theta\text{-}\tau_1\tau_2\,\text{int}(A) \cup \theta\text{-}\tau_1\tau_2\,\text{int}(X \setminus A) \cup \theta\text{-}\tau_1\tau_2\,\text{cl}(A) \setminus \theta\text{-}\tau_1\tau_2\,\text{int}(A)$
$= \theta\text{-}\tau_1\tau_2\,\text{int}(X \setminus A) \cup \theta\text{-}\tau_1\tau_2\,\text{cl}(A) = X \setminus \theta\text{-}\tau_1\tau_2\,\text{cl}(A) \cup \theta\text{-}\tau_1\tau_2\,\text{cl}(A) = X$.

Remark(3.9): Note that $\theta\text{-}\tau_1\tau_2\,\text{fr}(A)$ is not necessarily $\theta\text{-}\tau_1\tau_2$ closed ,also $\theta\text{-}\tau_1\tau_2\,\text{ext}(A)$ is not necessarily $\theta\text{-}\tau_1\tau_2$ open as seen from the following example.

Example (3.10): Refer example (2.11)(1) , let $A=\{a\}$,then $\theta\text{-}\tau_1\tau_2\,\text{cl}(A) = \{a,d\}$ and
$\theta\text{-}\tau_1\tau_2\,\text{int}(A) = \phi$, hence $\theta\text{-}\tau_1\tau_2\,\text{fr}(A) = \{a,d\}$ but $\{a,d\}$is not $\theta\text{-}\tau_1\tau_2$ closed since
$\{a,d\} \neq \theta\text{-}\tau_1\tau_2\,\text{cl}(\{a,d\}) = X$.

Now, let A = {c}, then $X \setminus A = \{a,b,d\}$ and $\theta\text{-}\tau_1\tau_2 \text{ext}(A) = \theta\text{-}\tau_1\tau_2 \text{int}(X \setminus A) = \{a\}$ but $\{a\}$ is not $\theta\text{-}\tau_1\tau_2$ open since $\{a\} \neq \theta\text{-}\tau_1\tau_2 \text{int}(\{a\}) = \phi$.

SOME FORMS OF BI-CONTINUOUS MULTIFUNCTIONS

We recall the definition of multifunction. A multifunction $F: X \to Y$ from a topological space (X, τ) into a topological space (Y, σ) is a point to set correspondence such that $F(x) \neq \phi$ for all $x \in X$.

Definition(4.1): Let $F: (X, \tau) \to (Y, \sigma)$ be a multifunction from a topological space (X, τ) into a topological space (Y, σ).

1- The upper and lower inverse of a set B of the space Y are denoted by $F^+(B)$ and $F^-(B)$,

respectively and defined as $F^+(B) = \{x \in X : F(x) \subseteq B\}$, $F^-(B) = \{x \in X : F(x) \cap B \neq \phi\}$. (1)

2- Let p(Y) be the collection of all non-empty subset of Y, we define $V^+ = \{B \in p(Y) : B \subseteq V\}$ and

$V^- = \{B \in p(Y) : B \cap V \neq \phi\}$. (4)

3- $X \setminus F^+(K) = F^-(Y \setminus K)$, $X \setminus F^-(K) = F^+(Y \setminus K)$ for every subset K of Y.(1)

Definition(4.2): Let $F: (X, \tau_1, \tau_2) \to (Y, \sigma_1, \sigma_2)$ be a multifunction from a bitopological space (X, τ_1, τ_2) into a bitopological space (Y, σ_1, σ_2). F is said to be weakly-bi-continuous (briefly w-bi-continuous)(resp. bi-continuous) on X iff for each point $x \in X$ and for each $\sigma_1\sigma_2$ open sets V_1, V_2 of Y such that $F(x) \in V_1^+ \cap V_2^-$,there exists $\tau_1\tau_2$ open set U containing x such that $F(u) \in (\sigma_1\sigma_2 \text{cl}(V_1))^+ \cap (\sigma_1\sigma_2 \text{cl}(V_2))^-$ (resp. $F(u) \in V_1^+ \cap V_2^-$) for all $u \in U$.

Definition(4.3): A multifunction $F: (X, \tau_1, \tau_2) \to (Y, \sigma_1, \sigma_2)$ where X is non-empty set with a bitopological space (X, τ_1, τ_2) into a bitopological space (Y, σ_1, σ_2) is said to be weakly*-bi-continuous (briefly w*-bi-continuous) (resp.strong-bi-continuous, briefly s-bi-continuous) on X iff for each point $x \in X$ and for each $\sigma_1\sigma_2$ open sets V_1, V_2 of Y such that $F(x) \in V_1^+ \cap V_2^-$,there exists $\tau_1\tau_2$ open set U containing x such that $F(u) \in (\sigma_1\sigma_2 \text{cl}(V_1))^+ \cap (\sigma_1\sigma_2 \text{cl}(V_2))^-$ (resp. $F(u) \in V_1^+ \cap V_2^-$) for all $u \in \tau_1\tau_2 \text{cl}(U)$.

Remark(4.4): Every w*-bi-continuous multifunction is w-bi-continuous but the converse,in general, is not true and every s-bi-continuous is bi-continuous but the converse, in general, is not true. To show that see the following example.

Example(4.5): Let $F:(X,\tau_1,\tau_2)\to(Y,\sigma_1,\sigma_2)$ be a multifunction from a bitopological space (X,τ_1,τ_2) into a bitopological space (Y,σ_1,σ_2) such that $X=\{a,b,c\},\tau_1=\{\phi,X,\{a\},\{a,c\}\}$, $\tau_2=\{\phi,X,\{b\}\}$ and $Y=\{1,2,3\},\sigma_1=\{\phi,Y,\{1\},\{2\},\{1,2\}\},\sigma_2=\{\phi,Y,\{3\},\{1,3\},\{2,3\}\}$.
Let F(a)={1}, F(b)={2}and F(c) =Y. Then the sets in$\{\phi,X,\{a\},\{a,c\},\{b\}\}$are $\tau_1\tau_2$ open and the sets in$\{\phi,Y,\{1\},\{2\},\{1,2\},\{3\},\{1,3\},\{2,3\}\}$are $\sigma_1\sigma_2$ open . Hence F is w-bi-continuous but not w*-bi-continuous and F is bi-continuous but not s-bi-continuous .

Remark(4.6): It is clear that every s-bi-continuous is w*-bi-continuous and every bi-continuous is w-bi-continuous but ,in general, the converse is not true as illustrated in the following example.

Example(4.7): Let $X=\{a,b,c\},\tau_1=\{\phi,X,\{a\}\},\tau_2=\{\phi,X,\{c\},\{b,c\}\}$and $Y=\{1,2,3\},\sigma_1=\{\phi,Y,\{1\}\}$, $\sigma_2=\{\phi,Y,\{1,2\}\}$.Let $F:X\to Y$ be a multifunction such that F(a) ={1}, F(b) ={1,2}and F(c) ={3}.
Then the sets in$\{\phi,X,\{a\},\{c\},\{b,c\}\}$are $\tau_1\tau_2$ open and the sets in$\{\phi,Y,\{1\},\{1,2\}\}$are $\sigma_1\sigma_2$ open. Hence F is w*-bi-continuous but not s-bi-continuous and F is w-bi-continuous but not bi-continuous

Theorem(4.8): For a multifunction $F:(X,\tau_1,\tau_2)\to(Y,\sigma_1,\sigma_2)$ the following are equivalent:-
(1) F is w*-bi-continuous.
(2) $F^+(G_1)\cap F^-(G_2)\subseteq\theta-\tau_1\tau_2\ \mathrm{int}(F^+(\sigma_1\sigma_2\mathrm{cl}(G_1))\cap F^-(\sigma_1\sigma_2\mathrm{cl}(G_2)))$ for every $\sigma_1\sigma_2$ open sets G_1,G_2 of Y.
(3) $\theta-\tau_1\tau_2\mathrm{cl}(F^+(\sigma_1\sigma_2\ \mathrm{int}(K_1))\cup F^-(\sigma_1\sigma_2\ \mathrm{int}(K_2)))\subseteq F^+(K_1)\cap F^-(K_2)$ for every $\sigma_1\sigma_2$ closed sets K_1,K_2 of Y.
(4) $\theta-\tau_1\tau_2\mathrm{cl}(F^+(\sigma_1\sigma_2\ \mathrm{int}(\sigma_1\sigma_2\mathrm{cl}(K_1)))\cup F^-(\sigma_1\sigma_2\ \mathrm{int}(\sigma_1\sigma_2\mathrm{cl}(K_2))))$

$\subseteq F^+(\sigma_1\sigma_2 cl(K_1)) \cup F^-(\sigma_1\sigma_2 cl(K_2))$ for every $\sigma_1\sigma_2$ closed sets K_1, K_2 of Y.

Proof: (1) $\Rightarrow$ (2). Let G_1, G_2 be any $\sigma_1\sigma_2$ open sets of Y and let $x \in F^+(G_1) \cap F^-(G_2)$.
Then $F(x) \in G_1^+ \cap G_2^-$ and hence there exists $\tau_1\tau_2$ open set U, $x \in U$ such that
$F(u) \in (\sigma_1\sigma_2 cl(G_1))^+ \cap (\sigma_1\sigma_2 cl(G_2))^-$ for all $u \in \sigma_1\sigma_2 cl(U)$.
Then $u \in F^+(\sigma_1\sigma_2 cl(G_1)) \cap F^-(\sigma_1\sigma_2 cl(G_2))$ for all $u \in \sigma_1\sigma_2 cl(U)$.
That is $\tau_1\tau_2 cl(U) \subseteq F^+(\sigma_1\sigma_2 cl(G_1)) \cap F^-(\sigma_1\sigma_2 cl(G_2))$.
Hence $x \in \theta - \tau_1\tau_2 \text{ int}(F^+(\sigma_1\sigma_2 cl(G_1)) \cap F^-(\sigma_1\sigma_2 cl(G_2)))$.

(2) $\Rightarrow$ (3). Let K_1, K_2 be any $\sigma_1\sigma_2$ closed sets of Y ,then $Y \setminus K_1, Y \setminus K_2$ are $\sigma_1\sigma_2$ open sets in Y .
Then by (2) ,
$X \setminus (F^+(K_1) \cup F^-(K_2)) = (X \setminus F^+(K_1)) \cap (X \setminus F^-(K_2)) = F^-(Y \setminus K_1) \cap F^+(Y \setminus K_2)$
$\subseteq \theta - \tau_1\tau_2 \text{ int}(F^-(\sigma_1\sigma_2 cl(Y \setminus K_1)) \cap F^+(\sigma_1\sigma_2 cl(Y \setminus K_2)))$.
$= \theta - \tau_1\tau_2 \text{ int}(X \setminus F^+(\sigma_1\sigma_2 \text{ int}(K_1)) \cap X \setminus F^-(\sigma_1\sigma_2 \text{ int}(K_2)))$.
$= \theta - \tau_1\tau_2 \text{ int}(X \setminus (F^+(\sigma_1\sigma_2 \text{ int}(K_1)) \cup F^-(\sigma_1\sigma_2 \text{ int}(K_2))))$.
$= X \setminus \theta - \tau_1\tau_2 cl(F^+(\sigma_1\sigma_2 \text{ int}(K_1)) \cup F^-(\sigma_1\sigma_2 \text{ int}(K_2)))$.
Hence $\theta - \tau_1\tau_2 cl(F^+(\sigma_1\sigma_2 \text{ int}(K_1)) \cup F^-(\sigma_1\sigma_2 \text{ int}(K_2))) \subseteq F^+(K_1) \cap F^-(K_2)$.

(3) $\Rightarrow$ (4). Let K_1, K_2 be any $\sigma_1\sigma_2$ closed sets in Y ,then $\sigma_1\sigma_2 cl(K_1), \sigma_1\sigma_2 cl(K_2)$ are $\sigma_1\sigma_2$ closed sets in Y and by (3) ,we get :
$\theta - \tau_1\tau_2 cl(F^+(\sigma_1\sigma_2 \text{ int}(\sigma_1\sigma_2 cl(K_1))) \cup F^-(\sigma_1\sigma_2 \text{ int}(\sigma_1\sigma_2 cl(K_2))))$
$\subseteq F^+(\sigma_1\sigma_2 cl(K_1)) \cup F^-(\sigma_1\sigma_2 cl(K_2))$.

(4) $\Rightarrow$ (2). Let G_1, G_2 be any $\sigma_1\sigma_2$ open sets in Y ,then $Y \setminus G_1$, $Y \setminus G_2$ are $\sigma_1\sigma_2$ closed sets in Y and by (4), we get :
$F^+(G_1) \cap F^-(G_2) = F^+(\sigma_1\sigma_2 \text{ int}(G_1)) \cap F^-(\sigma_1\sigma_2 \text{ int}(G_2))$.
$= (X \setminus F^-(Y \setminus \sigma_1\sigma_2 \text{ int}(G_1))) \cap (X \setminus F^+(Y \setminus \sigma_1\sigma_2 \text{ int}(G_2)))$.
$= X \setminus (F^-(Y \setminus \sigma_1\sigma_2 \text{ int}(G_1)) \cup F^+(Y \setminus \sigma_1\sigma_2 \text{ int}(G_2)))$.
$= X \setminus (F^-(\sigma_1\sigma_2 cl(Y \setminus G_1)) \cup F^+(\sigma_1\sigma_2 cl(Y \setminus G_2)))$.
$\subseteq X \setminus \theta - \tau_1\tau_2 cl(F^-(\sigma_1\sigma_2 \text{ int}(\sigma_1\sigma_2 cl(Y \setminus G_1))) \cup F^+(\sigma_1\sigma_2 \text{ int}(\sigma_1\sigma_2 cl(Y \setminus G_2))))$.
$= X \setminus \theta - \tau_1\tau_2 cl(X \setminus F^+(\sigma_1\sigma_2 cl(\sigma_1\sigma_2 \text{ int}(G_1))) \cup X \setminus F^-(\sigma_1\sigma_2 cl(\sigma_1\sigma_2 \text{ int}(G_2))))$.
$= X \setminus \theta - \tau_1\tau_2 cl(X \setminus (F^+(\sigma_1\sigma_2 cl(\sigma_1\sigma_2 \text{ int}(G_1))) \cap F^-(\sigma_1\sigma_2 cl(\sigma_1\sigma_2 \text{ int}(G_2)))))$.
$= \theta - \tau_1\tau_2 \text{ int}(F^+(\sigma_1\sigma_2 cl(\sigma_1\sigma_2 \text{ int}(G_1))) \cap F^-(\sigma_1\sigma_2 cl(\sigma_1\sigma_2 \text{ int}(G_2))))$.
Hence $F^+(G_1) \cap F^-(G_2) \subseteq \theta - \tau_1\tau_2 \text{ int}(F^+(\sigma_1\sigma_2 cl(G_1)) \cap F^-(\sigma_1\sigma_2 cl(G_2)))$.

$(2) \Rightarrow (1)$. Let G_1, G_2 be any $\sigma_1\sigma_2$ open sets of Y such that $F(x) \in G_1^+ \cap G_2^-$

$\Rightarrow x \in F^+(G_1) \cap F^-(G_2) \subseteq \theta - \tau_1\tau_2 \text{ int}(F^+(\sigma_1\sigma_2 cl(G_1)) \cap F^-(\sigma_1\sigma_2 cl(G_2)))$.

Then there exists $\sigma_1\sigma_2$ open set U, $x \in U$ and $\sigma_1\sigma_2 cl(U) \subseteq F^+(\sigma_1\sigma_2 cl(G_1)) \cap F^-(\sigma_1\sigma_2 cl(G_2))$.

Hence $u \in F^+(\sigma_1\sigma_2 cl(G_1)) \cap F^-(\sigma_1\sigma_2 cl(G_2))$ for all $u \in \tau_1\tau_2 cl(U)$.

Then $F(u) \in (\sigma_1\sigma_2 cl(G_1))^+ \cap (\sigma_1\sigma_2 cl(G_2))^-$ for all $u \in \tau_1\tau_2 cl(U)$. So F is w*-bi-continuous.

Theorem(4.9): For a multifunction $F:(X,\tau_1,\tau_2) \to (Y,\sigma_1,\sigma_2)$ the following are equivalent:-

1) F is s-bi-continuous.

(2) $F^+(G_1) \cap F^-(G_2) = \theta - \tau_1\tau_2 \text{ int}(F^+(G_1) \cap F^-(G_2))$ for every $\sigma_1\sigma_2$ open sets G_1, G_2 of Y.

(3) $F^+(K_1) \cup F^-(K_2) = \theta - \tau_1\tau_2 cl(F^+(K_1) \cup F^-(K_2))$ for every $\sigma_1\sigma_2$ closed sets K_1, K_2 of Y.

(4) $\theta - \tau_1\tau_2 cl(F^+(K_1) \cup F^-(K_2)) = F^+(\sigma_1\sigma_2 cl(K_1) \cup F^-(\sigma_1\sigma_2 cl(K_2))$ for every $\sigma_1\sigma_2$ closed sets K_1, K_2 of Y.

(5) $\theta - \tau_1\tau_2 \text{ int}(F^+(G_1) \cap F^-(G_2)) = F^+(\sigma_1\sigma_2 \text{ int}(G_1)) \cap F^-(\sigma_1\sigma_2 \text{ int}(G_2))$ for every $\sigma_1\sigma_2$ open sets G_1, G_2 of Y.

Proof: $(1) \Rightarrow (2)$. Let G_1, G_2 be any two $\sigma_1\sigma_2$ open subsets of Y and let $x \in F^+(G_1) \cap F^-(G_2)$,

then there exists $\tau_1\tau_2$ open set U containing x such that $F(u) \in G_1^+ \cap G_2^-$ for all $u \in \sigma_1\sigma_2 cl(U)$.

This implies that $u \in F^+(G_1) \cap F^-(G_2)$ for all $u \in \sigma_1\sigma_2 cl(U)$.

Hence $\sigma_1\sigma_2 cl(U) \subseteq F^+(G_1) \cap F^-(G_2)$, then $x \in \theta - \tau_1\tau_2 \text{ int}(F^+(G_1) \cap F^-(G_2))$.

$(2) \Rightarrow (3)$. Let K_1, K_2 be any two $\sigma_1\sigma_2$ closed sets of Y . Since $Y \setminus K_1, Y \setminus K_2$ are $\sigma_1\sigma_2$ open sets in Y ,then by (2) , we get $F^+(K_1) \cup F^-(K_2) = (X \setminus F^-(Y \setminus K_1)) \cup (X \setminus F^+(Y \setminus K_2))$.

$= X \setminus (F^-(Y \setminus K_1) \cap F^+(Y \setminus K_2))$

$= X \setminus \theta - \tau_1\tau_2 \text{ int}(F^-(Y \setminus K_1) \cap F^+(Y \setminus K_2))$.

$= X \setminus \theta - \tau_1\tau_2 \text{ int}((X \setminus F^+(K_1)) \cap (X \setminus F^-(K_2)))$.

$= X \setminus \theta - \tau_1\tau_2 \text{ int}(X \setminus (F^+(K_1)) \cup F^-(K_2)))$.

$= \theta - \tau_1\tau_2 \text{cl}(F^+(K_1) \cup F^-(K_2))$.

(3) $\Rightarrow$ (4). Let K_1, K_2 be any two $\sigma_1\sigma_2$ closed sets of Y ,then by (3) , we get

$\theta - \tau_1\tau_2 \text{cl}(F^+(K_1) \cup F^-(K_2)) = F^+(K_1) \cup F^-(K_2)$
$= F^+(\sigma_1\sigma_2 \text{cl}(K_1)) \cup F^-(\sigma_1\sigma_2 \text{cl}(K_2))$.

(4) $\Rightarrow$ (5). Let G_1, G_2 be any two $\sigma_1\sigma_2$ open sets of Y ,then $Y \setminus G_1$, $Y \setminus G_2$ are $\sigma_1\sigma_2$ closed sets
in Y and by (4), we get :
$F^+(\sigma_1\sigma_2 \text{ int}(G_1)) \cap F^-(\sigma_1\sigma_2 \text{ int}(G_2))$
$= X \setminus F^-(Y \setminus \sigma_1\sigma_2 \text{ int}(G_1)) \cap X \setminus F^+(Y \setminus \sigma_1\sigma_2 \text{ int}(G_2))$.

$= X \setminus (F^-(Y \setminus \sigma_1\sigma_2 \text{ int}(G_1)) \cup F^+(Y \setminus \sigma_1\sigma_2 \text{ int}(G_2)))$.

$= X \setminus (F^-(\sigma_1\sigma_2 \text{cl}(Y \setminus G_1)) \cup F^+(\sigma_1\sigma_2 \text{cl}(Y \setminus G_2)))$.

$= X \setminus \theta - \tau_1\tau_2 \text{cl}(F^-(Y \setminus G_1) \cup F^+(Y \setminus G_2))$.

$= X \setminus \theta - \tau_1\tau_2 \text{cl}((X \setminus F^+(G_1) \cup (X \setminus F^-(G_2)))$.

$= X \setminus \theta - \tau_1\tau_2 \text{cl}(X \setminus (F^+(G_1) \cap F^-(G_2)))$.
$= \theta - \tau_1\tau_2 \text{ int}(F^+(G_1) \cap F^-(G_2))$.

(5) $\Rightarrow$ (1) Let G_1, G_2 be $\sigma_1\sigma_2$ open sets in Y such that $F(x) \in G_1^+ \cap G_2^-$.
Then $x \in F^+(G_1) \cap F^-(G_2) = F^+(\sigma_1\sigma_2 \text{ int}(G_1)) \cap F^-(\sigma_1\sigma_2 \text{ int}(G_2))$ and by (5), we get
$x \in \theta - \tau_1\tau_2(F^+(G_1) \cap F^-(G_2))$.Then there exists $\tau_1\tau_2$ open set U, $x \in U$ such that
$\sigma_1\sigma_2 \text{cl}(U) \subseteq F^+(G_1) \cap F^-(G_2)$,that is $u \in F^+(G_1) \cap F^-(G_2)$ for all $u \in \tau_1\tau_2 \text{cl}(U)$.
Then $F(u) \in G_1^+ \cap G_2^-$ for all $u \in \tau_1\tau_2 \text{cl}(U)$. So F is s-bi-continuous.

Remark(4.10): From theorem (4.9), we have the following:
(1) F is s-bi-continuous.

(2) $F^+(G_1)\cap F^-(G_2)$ is $\theta-\tau_1\tau_2$ open subset of X ,for every $\sigma_1\sigma_2$ open sets G_1, G_2 of Y .

(3) $F^+(K_1)\cap F^-(K_2)$ is $\theta-\tau_1\tau_2$ closed subset of X ,for every $\sigma_1\sigma_2$ closed sets K_1, K_2 of Y .

Theorem(4.11): For a multifunction $F:(X,\tau_1,\tau_2)\to(Y,\sigma_1,\sigma_2)$ the following are equivalent:-

(1) F is w-bi-continuous.

(2) $F^+(G_1)\cap F^-(G_2)\subset\tau_1\tau_2\,\mathrm{int}(F^+(\sigma_1\sigma_2\mathrm{cl}(G_1))\cap F^-(\sigma_1\sigma_2\mathrm{cl}(G_2)))$ for every $\sigma_1\sigma_2$ open sets G_1, G_2 of Y.

(3) $\tau_1\tau_2\mathrm{cl}(F^+(\sigma_1\sigma_2\,\mathrm{int}(K_1))\cup F^-(\sigma_1\sigma_2\,\mathrm{int}(K_2)))\subset F^+(K_1)\cap F^-(K_2)$ for every $\sigma_1\sigma_2$ closed sets K_1, K_2 of Y.

(4) $\tau_1\tau_2\mathrm{cl}(F^+(\sigma_1\sigma_2\,\mathrm{int}(\sigma_1\sigma_2\mathrm{cl}(K_1)))\cup F^-(\sigma_1\sigma_2\,\mathrm{int}(\sigma_1\sigma_2\mathrm{cl}(K_2))))$
$\subset F^+(\sigma_1\sigma_2\mathrm{cl}(K_1))\cup F^-(\sigma_1\sigma_2\mathrm{cl}(K_2))$ for every $\sigma_1\sigma_2$ closed sets K_1, K_2 of Y.

Proof: (1) $\Rightarrow$ (2) Let G_1, G_2 be any $\sigma_1\sigma_2$ open sets in Y such that $x\in F^+(G_1)\cap F^-(G_2)$,then $F(x)\in G_1^+\cap G_2^-$ and hence there exists $\tau_1\tau_2$ open set U such that $x\in U\subset F^+(\sigma_1\sigma_2\mathrm{cl}(G_1))\cap F^-(\sigma_1\sigma_2\mathrm{cl}(G_2))$.
Then we have $x\in\tau_1\tau_2\,\mathrm{int}(F^+(\sigma_1\sigma_2\mathrm{cl}(G_1))\cap F^-(\sigma_1\sigma_2\mathrm{cl}(G_2)))$.

The proofs of $(2)\Rightarrow(3)$, $(3)\Rightarrow(4)$ and $(4)\Rightarrow(2)$ are similar to that of theorem (4.8).

$(2)\Rightarrow(1)$ Let G_1, G_2 be any $\sigma_1\sigma_2$ open sets in Y such that $F(x)\in G_1^+\cap G_2^-$.
Then $x\in F^+(G_1)\cap F^-(G_2)\subset\tau_1\tau_2\,\mathrm{int}(F^+(\sigma_1\sigma_2\mathrm{cl}(G_1))\cap F^-(\sigma_1\sigma_2\mathrm{cl}(G_2)))$.
Then there exists $\tau_1\tau_2$ open set U such that $x\in U\subset F^+(\sigma_1\sigma_2\mathrm{cl}(G_1))\cap F^-(\sigma_1\sigma_2\mathrm{cl}(G_2))$.
Hence $F(u)\subset\sigma_1\sigma_2\mathrm{cl}(G_1)$ and $F(u)\cap\sigma_1\sigma_2\mathrm{cl}(G_2)\neq\phi$ for every $u\in U$. So F is w-bi-continuous.

Definition(4.12): Let $F:(X,\tau_1,\tau_2)\to(Y,\sigma_1,\sigma_2)$ be a multifunction from a bitopological space (X,τ_1,τ_2) into a bitopological space (Y,σ_1,σ_2). F is said to be almost-bi-continuous (briefly a-bi-continuous) on X iff for each point $x\in X$ and for each $\sigma_1\sigma_2$ open sets V_1, V_2 of Y such that $F(x)\in V_1^+\cap V_2^-$,there

exists $\tau_1\tau_2$ open set U containing x such that $F(u) \in (\sigma_1\sigma_2\ \mathrm{int}(\sigma_1\sigma_2\mathrm{cl}(V_1)))^+ \cap (\sigma_1\sigma_2\ \mathrm{int}(\sigma_1\sigma_2\mathrm{cl}(V_2)))^-$ for all $u \in U$.

Definition(4.13): Let $F:(X,\tau_1,\tau_2) \to (Y,\sigma_1,\sigma_2)$ be a multifunction from a bitopological space (X,τ_1,τ_2) into a bitopological space (Y,σ_1,σ_2). F is said to be almost*-bi-continuous (briefly a*-bi-continuous) on X iff for each point $x \in X$ and for each $\sigma_1\sigma_2$ open sets V_1, V_2 of Y such that $F(x) \in V_1^+ \cap V_2^-$,there exists $\tau_1\tau_2$ open set U containing x such that $F(u) \in (\sigma_1\sigma_2\ \mathrm{int}(\sigma_1\sigma_2\mathrm{cl}(V_1)))^+ \cap (\sigma_1\sigma_2\ \mathrm{int}(\sigma_1\sigma_2\mathrm{cl}(V_2)))^-$ for all $u \in \tau_1\tau_2\mathrm{cl}(U)$.

Remark(4.14): Every a*-bi-continuous multifunction is a-bi-continuous but the converse,in general, is not true .To show that , F in example (4.5) satisfies that .

Theorem(4.15): If $F:X \to Y$ is w*-bi-continuous and F(x) is $\sigma_1\sigma_2$ open subset in Y for each $x \in X$,then F is a*-bi-continuous.

Proof: Let $x \in X$ and G_1, G_2 be $\sigma_1\sigma_2$ open sets in Y such that $F(x) \in G_1^+ \cap G_2^-$.
Since F is w*-bi-continuous , then there exists $\tau_1\tau_2$ open set U containing x such that $F(u) \in (\sigma_1\sigma_2\mathrm{cl}(G_1))^+ \cap (\sigma_1\sigma_2\mathrm{cl}(G_2))^-$ for all $u \in \tau_1\tau_2\mathrm{cl}(U)$. Since F(u) is $\sigma_1\sigma_2$ open set in Y, then
$F(u) = \sigma_1\sigma_2\ \mathrm{int}(F(u)) \subseteq \sigma_1\sigma_2\ \mathrm{int}(\sigma_1\sigma_2\mathrm{cl}(G_1))$ and $F(u) \cap \sigma_1\sigma_2\mathrm{cl}(G_2) \neq \phi$ implies $F(u) \cap \sigma_1\sigma_2\ \mathrm{int}(\sigma_1\sigma_2\mathrm{cl}(G_2) \neq \phi$ for all $u \in \tau_1\tau_2\mathrm{cl}(U)$.Hence $F(u) \in (\sigma_1\sigma_2\ \mathrm{int}(\sigma_1\sigma_2\mathrm{cl}(G_1)))^+ \cap (\sigma_1\sigma_2\ \mathrm{int}(\sigma_1\sigma_2\mathrm{cl}(G_2)))^-$ and so F is a*-bi-continuous.

Definition(4.16): A subset A of a bitopological space (X,τ_1,τ_2) is said to be (1,2)* regular open iff $\tau_1\tau_2\ \mathrm{int}(\tau_1\tau_2\mathrm{cl}(A)) = A$.

Theorem(4.17): If a multifunction $F:(X,\tau_1,\tau_2) \to (Y,\sigma_1,\sigma_2)$ is a*-bi-continuous then $F^+(G_1) \cap F^-(G_2)$ is $\theta - \tau_1\tau_2$ open for every (1,2)* regular open sets G_1, G_2 of Y .

Proof: Let G_1, G_2 be (1,2)* regular open sets in Y and $x \in F^+(G_1) \cap F^-(G_2)$,then there exists $\tau_1\tau_2$ open set U containing x such that
$F(u) \in (\sigma_1\sigma_2\ \mathrm{int}(\sigma_1\sigma_2\mathrm{cl}(G_1)))^+ \cap (\sigma_1\sigma_2\ \mathrm{int}(\sigma_1\sigma_2\mathrm{cl}(G_2)))^-$ for all $u \in \tau_1\tau_2\mathrm{cl}(U)$.

That is $F(u) \in G_1^+ \cap G_2^-$ for all $u \in \tau_1\tau_2 cl(U)$,then $u \in F^+(G_1) \cap F^-(G_2)$ for all $u \in \tau_1\tau_2 cl(U)$.
Hence $\tau_1\tau_2 cl(U) \subseteq F^+(G_1) \cap F^-(G_2)$,then $x \in \theta - \tau_1\tau_2\, int(F^+(G_1) \cap F^-(G_2))$.
So $F^+(G_1) \cap F^-(G_2)$ is $\theta - \tau_1\tau_2$ open .

Remark(4.18): Every s-bi-continuous multifunction is a*-bi-continuous and every a*-bi-continuous multifunction is w*-bi-continuous but,in general,the converse is not true.To show that ,F in example (4.7) satisfies that F is a*-bi-continuous but not s-bi-continuous . Also the following example show that F is w*-bi-continuous but not a*-bi-continuous .

Example (4.19): Let
$X=\{a,b,c\}, \tau_1=\{\phi,X,\{a\}\}, \tau_2=\{\phi,X,\{b\},\{b,c\}\}$ and $Y=\{1,2,3\}, \sigma_1=\{\phi,Y,\{1\}\}$, $\sigma_2=\{\phi,Y,\{2\},\{1,2\}\}$. Let $F:X \to Y$ be a multifunction such that F(a)={1,3}, F(b)={1}and
F(c) ={3}. Then the sets in$\{\phi,X,\{a\},\{b\},\{b,c\}\}$are $\tau_1\tau_2$ open and the sets in $\{\phi,Y,\{1\},\{2\},\{1,2\}\}$
are $\sigma_1\sigma_2$ open . Hence F is w*-bi-continuous but not a*-bi-continuous .

Remark(4.20): Every bi-continuous multifunction is a-bi-continuous and every a-bi-continuous multifunction is w-bi-continuous but,in general,the converse is not true.To show that ,F in example (4.7) satisfies that F is a-bi-continuous but not bi-continuous . Also the following example show that F is w-bi-continuous but not a-bi-continuous .

Example (4.21): Let $X=\{a,b,c\}, \tau_1=\{\phi,X,\{a\}\}, \tau_2=\{\phi,X,\{b,c\}\}$ and $Y=\{1,2,3\}, \sigma_1=\{\phi,Y,\{1\}\}$, $\sigma_2=\{\phi,Y,\{2\},\{1,2\}\}$. Let $F:X \to Y$ be a multifunction such that F(a)={1,3}, F(b)={1}and
F(c) ={3}. Then the sets in$\{\phi,X,\{a\},\{b,c\}\}$are $\tau_1\tau_2$ open and the sets in$\{\phi,Y,\{1\},\{2\},\{1,2\}\}$are
$\sigma_1\sigma_2$ open . So F is w-bi-continuous but not a-bi-continuous .

Remark(4.22): The following diagram explains the relation among the forms of bi-continuous :

s-bi-continuous ⇒ a*-bi-continuous ⇒ w*-bi-continuous

↓ ↓ ↓

bi-continuous ⇒ a-bi-continuous ⇒ w-bi-continuous

REFERENCES

1. Noiri,T.and Popa,V.,On upper and lower M-continuous multifunction, Filomat 14 :73-86 (2000) .
2. Caldas,M.,Jafari,S.and Kovar,M.M.,Some properties of θ-open sets , Divulgaciones, matematicas , .12 ,(2):161-169(2004) .
3. Ravi,O.and Thivagar,M.L.,A Bitopological (1,2)* Semi-generalized Continuous Maps,Bull. Mallays. Math. Soc.(2)29 (1) :79-88 (2006).
4. Przemski,M.,Some generalizations of continuity and quasicontin - uity of multivalued maps, Demonstratio Math. 26 :381-400 (1993).

Modules Whose Direct Summands Are Stable

Mehdi Sadik Abbas and Saad Abdulkadhim ALSaadi
Department of Mathematics , College of Science , Al-Mustansiriya University

الخلاصة

في هذا البحث، تم تقديم و دراسة مفهوم المقاسات من النمط SS كتعميم فعلي لمقاسات تامة الاستقرارية. نقول عن مقاس بأنه من النمط SS اذا كان كل مركبة مجموع مباشر من M يكون مستقر.

تم اعطاء العديد من التشخيصات و الخواص لمقاسات من النمط SS. على سبيل المثال، مقاس M يكون من النمط SS أذا وفقط أذا كل مركبة مجموع مباشر من M يكون تام الثبات.

العديد من النتائج المعروفة في المقاسات تامة الاستقرارية عممت لمقاسات من النمط SS. على سبيل مثال، اذا كان مقاس M منتظم ومن النمط SS فأن حلقة التشاكلات التقابلية للمقاس M يكون تام الاستقرار.

تمّ دراسة العلاقة بين المقاسات من النمط SS وأصناف من مقاسات معروفة. في الحقيقة، تم الحصول على المؤديات الفعلية الأتية:

مقاسات الجدائية $\Leftarrow$ مقاسات من النمط SS $\Leftarrow$ خاصية تقاطع مركبة المجموع المباشر

أكثر من ذلك، من خلال الأمثلة ، أكدنا بأن هذه المؤديات غيرقابلة للعكس.

ABSTRACT

In this paper, we introduce and study SS-module as a proper generalization of fully stable modules. A module M is called SS-module if every direct summand of M is stable.

Many characterizations and properties of SS-modules are given. For example, an R-module M is SS-module if and only if each direct summand of M fully invariant.

Various known results about fully stable modules are generalized to SS-modules. For example, If M is regular SS-module, then $End_R(M)$ is fully stable.

Known modules related to SS-modules are considered. In fact, we investigate the next implications: Multiplication modules $\Rightarrow$ SS-modules $\Rightarrow$ The summand intersection property. Moreover, through examples, it can be asserted that these implications are not reversible.

INTRODUCTION

Recall that a submodule N of an R-module M is fully invariant if $f(N) \subseteq N$ for each R-endomorphism f of M [1, p.40]. An R-module M is called duo if, every submodule of M is fully invariant [2]. As stronger than that of duo modules M.S.Abbas [3] introduced the concept of fully stable modules. A submodule N of an R-module M is called stable,if $f(N) \subseteq N$ for each R-homomorphism $f: N \longrightarrow M$ .An R-module M is fully stable if, every submodule of M is stable. Clearly, every fully stable module is duo, but the converse is not true in general [3]. In this paper we introduce and study a proper generalization of fully stable modules as follows:

Definition (1): An R-module M is called SS-module if, every direct summand of M is stable. A ring R is right (left) SS-ring if, R is SS-module as right (left) R-module.

Remarks and Examples (2):

(1) Every fully stable module is SS-module, while the converse is not true in general (for example see (2) , (3) and Remark (22)).

(2) Every uniform module is SS-module since the only direct summands of a uniform R-module M are *(0)* and M, so they are stable of M. In particular, Q as Z-module is SS-module, but, Q_Z is not fully stable [3].

(3) The Z-module Z is uniform and so (by (2)) it is SS-module, while the Z-module Z is not fully stable .In fact, if $h:5Z \longrightarrow Z$ is defined by $h(5x)=3x$ for each $x \in Z$. Obviously, h is a Z-homomorphism. But $h(5Z) \not\subset 5Z$ .Then $5Z$ is not stable submodule of Z.

(4) The converse of (2) is not true in general. For example, the Z-module Z_6 is SS-module but it is not uniform.

(5) Let $R=\begin{pmatrix} Z_4 & Z_4 \\ 0 & Z_4 \end{pmatrix}$ and consider the ideal $I_R=\begin{pmatrix} 0 & Z_4 \\ 0 & 2Z_4 \end{pmatrix}$ of R. It is shown that in [4], if $g \in Hom(I_R, I_R) \cong \begin{pmatrix} Z_4 & Z_4 \\ 2Z_4 & Z_4 \end{pmatrix}$ then $g(\alpha)=\begin{pmatrix} a & c \\ 2b & d \end{pmatrix}\alpha$, for any $\alpha \in I$ and for some $a,b,c,d \in Z_4$. It is easy to verify that $K=\begin{pmatrix} 0 & Z_4 \\ 0 & 0 \end{pmatrix}$ is a right direct summand of I_R. But $g\begin{pmatrix} 0 & Z_4 \\ 0 & 0 \end{pmatrix}= \left\{\begin{pmatrix} 0 & ax \\ 0 & 2bx \end{pmatrix} \middle| x \in Z_4\right\} \not\subset \begin{pmatrix} 0 & Z_4 \\ 0 & 0 \end{pmatrix}$ for $b=1 \in Z_4$. Thus, K is not fully invariant of I_R and hence it is not stable. Therefore, I_R is not SS-module.

(6) If M is a semi-simple R-module (recall that an R-module M is semi-simple if, every submodule of M is direct summand), then the following assertions are equivalent:

(a) M is fully stable.
(b) M is SS-module.

(8) As an R-module M is extending (or CS-module) if every closed submodule of M is a direct summand (5). Thus, if M is an extending module, then the following conditions are equivalent:
(a) M is SS-module;
(b) Every closed submodule of M is fully invariant;
(c) Every closed submodule of M is stable. □

M.S.Abbas in (3) proved that, a complement of a direct summand of an R-module M is unique if and only if it is a stable submodule of M. This result motivates us to get a characterization of SS-modules as follows:

Proposition (3): An R-module M is SS-module if and only if for each direct summand K of M, there exists unique complement H of K in M such that $M=K \oplus H$.

Proof: ($\Rightarrow$). By using [3, proposition (4.5)].
($\Leftarrow$). Let D be a direct summand of M, then there is a submodule C such that $M=D\oplus C$, and consider π_D and π_C the projection mappings of M onto D and C respectively. Assume that D is not stable submodule of M, then there exists an R-homomorphism f: $D \longrightarrow M$ with $f(D) \not\subset D$. Moreover, we may extend f to M by putting $f(x)=0$ for each $x \in C$. Then $f\circ \pi_D=f$ and $f\circ \pi_C=0$. Consider the two R-homomorphisms $(\pi_C+ \pi_C\circ f)$ and $(\pi_D - \pi_C\circ f)$, it is easy to check that these two R-homomorphisms are sum-1 orthogonal idempotents. By [3,lemma ( )], M is direct sum of the submodules $(\pi_C+ \pi_C\circ f)(M)$, and $(\pi_D - \pi_C\circ f)(M)$ of M, but $(\pi_C+ \pi_C\circ f)(M)$=C and $(\pi_D - \pi_C\circ f)(M) \not\subset D$. Thus, $M=C\oplus D'$ (where $D' = (\pi_D - \pi_C\circ f)(M)$) where $D\neq D'$ which is contradicts the assumption. Then, D is a stable submodule of M and therefore M is SS-module.

In the following result we give another characterization of SS-module which helps us to get more characterizations and properties of SS-modules.

Lemma (4): An R-module M is SS-module if and only if every direct summand of M is fully invariant.

Proof: ($\Rightarrow$). It is clear since every stable submodule is fully invariant(3).
($\Leftarrow$). Let N be a direct summand of an R-module M . By hypothesis, N is fully invariant.To prove that N is a stable submodule of M. Let f: $N \longrightarrow M$ be any R-homomorphism. Since N is a direct summand of M thus there is the projection mapping π: $M \longrightarrow N$. Hence $(f\circ\pi)$: $M \longrightarrow M$ and since N is a fully invariant of M , then we have $(f\circ\pi)(N)\subseteq N$ and so $f(N)=f(\pi(N)= (f\circ\pi)(N)\subseteq N$. Thus, N is a stable submodule of M and so M is SS-module.□

Remark (5): Directly by lemma (4), we can conclude that every duo module is SS-module and hence have the following implications:

fully stable modules $\Rightarrow$ duo modules $\Rightarrow$ SS-modules

Also, note that Q as Z-module is SS-module which is not duo since Z is not fully invariant of Q_Z.

Corollary (6): Every duo semi-simple module is fully stable.

The following lemma which appeared in (6) helps us to get another characterization of SS-modules. We give its proof for the sake of completeness.

Lemma (7): Let $M=H\oplus K$. Then H is fully invariant in M if and only if $Hom_R(H,K)=0$.

Proof: ($\Leftarrow$). Let π be the projection of $M=H\oplus K$ onto K with kernel H and let $\varphi \in End_R(M)$. If $Hom_R(H,K)=0$, then the restriction of $\pi\varphi$ to H

must be trivial. But this means that $\varphi(H) \subseteq H$. Thus H is fully invariant of M.

($\Rightarrow$). Let $\varphi' \in Hom_R(H, K)$. Then φ' extends a map $\varphi \in End_R(M)$ by $\varphi(h+k) = \varphi'(h)$. If H is fully invariant of M, then for all $h \in H$, $\varphi'(h) = \varphi(h) \in H$. But $\varphi'(h) \in K$ and $H \cap K = 0$. Thus $Hom_R(H, K) = 0$.

We provide a useful characterization of SS-modules based on lemma (7).

Proposition (8): An R-module M is SS-module if and only if for every decomposition $M = H \oplus K$, $Hom_R(H, K) = 0$.

Proof: ($\Rightarrow$).It is clear by Remarks and Examples (2)(5), and Lemma(7).

($\Leftarrow$).Let H be a direct summand of M, thus there is a direct summand K of M such that $M = H \oplus K$. By hypothesis, $Hom_R(H, K) = 0$ and by Lemma (7), H is fully invariant of M. Therefore, by Remarks and Examples (2) (5), M is SS-module.

Recall that, an R-module M is said to have the summand intersection property (SIP) if the intersection of any two direct summands of M is a direct summand (7). Equivalently, an R-module M has the (SIP) property if and only if for every decomposition $M = H \oplus K$ and every homomorphism $f: H \longrightarrow K$, the kernel of f is a direct summand of M (8).

Motivated by proposition (8), the next result asserts that the class of SS-modules is contained in the class of modules that has the SIP property.

Proposition (9): Every SS-module has the SIP property.

Proof: Assume that M is an SS-module and let $M = A \oplus B$ be a decomposition. By proposition (8), we have $Hom_R(A,B) = 0$ (i.e.) every homomorphism $\alpha: A \longrightarrow B$ is trivial, and so the kernel of α is A, hence is a direct summand of M. Therefore, by above motivation M has the SIP property.

Corollary (10): Every duo (and hence fully stable) module has the SIP property.

Remarks and Examples (11):

(1) The converse of proposition (9) is not true in general. For example, the vector space $V = F^{(2)}$ over the field F is semi-simple F-module and clearly it has the SIP property, but $V = F^{(2)}$ is not SS-module. In fact, let $S = \{(\alpha, 0) \mid \alpha \in F\}$ and $S' = \{(0,\beta) \mid \beta \in F\}$, then S and S' are subspaces of V. Then, they are spanned by the vectors $(1, 0)$, $(0, 1)$ respectively. Thus each of them is of dimension one. $S \cap S' = (0)$, this yields that $S + S' = S \oplus S'$, then $dim(S \oplus S') = dim(S) + dim(S') = 1 + 1 = 2$, hence $V = S \oplus S'$. But S' is not stable submodule of V. In fact, if $f: S' \longrightarrow V$ such

that $f((0, x) = (x, 0)$ for all $x \in F$, thus $f(S') \not\subset S'$. Thus V is not SS-module.

(2) As an application of proposition (8), we have the following example: Consider $M=Z_p^{\infty} \oplus Z_p^{\infty}$ as Z-module. Thus, M is not SS-module since we can define a Z-homomorphism f: $Z_p^{\infty} \longrightarrow Z_p^{\infty}$ as follows $f(\frac{n}{p^t}+Z) = \frac{n}{p^{t-1}}+Z \quad \forall n \in Z, t \in N$. It is clear that $f \neq 0$.

(3) Consider Z_4 and Z_2 as Z-modules. Now, define f: $Z_4 \longrightarrow Z_2$ as follows $f(x) = 2x \quad \forall x \in Z_4$. It is clear that f is non-trivial Z-homomorphism. Thus, by proposition (8), $Z_4 \oplus Z_2$ does not have SS-module property.

We noticed that every fully stable module is SS-module and the converse is not true in general (Examples and Remarks (2),(1)). In the following proposition, we obtain a condition under which the converse is true. Firstly, recall that R-module M is regular if given any element m in M, there exists $f \in Hom_R(M,R)$ such that $m=f(m)m$ (9). Equivalently, every cyclic submodule of M is a direct summand.

Proposition (12): Every regular SS-module is fully stable.

Proof: Let N be a cyclic submodule of SS-module regular R-module M. By regularity of M, N is direct summand of M. So since M is SS-module, thus N is a stable submodule of M. Therefore by [3, Corollary (1.5)], M is fully stable.

Corollary (13): If M is regular R-module then, M is fully stable if and only if M is SS-module.

Remark (14): The condition of regularity of the module in corollary (13) is necessary because the Z-module Q of rational numbers is not regular and Q_Z is SS-module but it is not fully stable (3).

The following corollary generalizes the result due to M.S.Abbas [3,Theorem (2.4)] to SS-module.

Corollary (15): If M is regular SS-module, then $End_R(M)$ is fully stable.

Whereas, if $End_R(M)$ is fully stable ring then this is not sufficient to make M fully stable R-module [3], the following proposition ensures that this condition is sufficient to make M is SS-module.

Proposition (16): If $End_R(M)$ is a right fully stable ring, then M is SS-module.

Proof: Let N be a direct summand of M and let $\alpha : N \longrightarrow M$ be any R-homomorphism. Consider $I = Hom_R(M,N)$, I is a right ideal of $End_R(M)$. Define $\theta : I \longrightarrow End_R(M)$ by $\theta(f) = \alpha \circ f$ for each $f \in I$. Clearly, $\theta(f) \in End_R(M)$. Also, θ is an $End_R(M)$-homomorphism. Since $End_R(M)$ is a right fully stable ring, then $\theta(I) \subseteq I$, that is for

each $f \in I$, $\alpha \circ f \in I$ so $\alpha \circ f : M \longrightarrow N$. But N is a direct summand of M, then the natural projection π_N of M onto N is in I, hence $\alpha \circ \pi_N \in I$, that $\alpha \circ \pi_N : M \longrightarrow M$ and because π_N is onto , then $\alpha : N \longrightarrow N$ (i.e.) $\alpha(N) \subseteq N$. So M is SS-module.

It is known that, if M is a fully stable module over a commutative ring R, then $End_R(M)$ is commutative (1) but the converse is not true in general. The following result asserts that if $End_R(M)$ is commutative is sufficient to make M is SS-module (i.e.) we have the implications:

M is fully stable $\Rightarrow$ $End_R(M)$ is commutative $\Rightarrow$ M is SS-module

Proposition (17): If $End_R(M)$ is commutative , then M is SS-module.

Proof: Let N be a direct summand of M and $f : N \longrightarrow M$ be any R-homomorphism. There exists a submodule K of M such that $M = N \oplus K$. f can be extended to an R-homomorphism $g : M \longrightarrow M$ by putting $g(k) = 0$ for each $k \in K$. Define $h : M \longrightarrow M$ by $h(x, y) = x$ for each $x \in N$ and $y \in K$. Let $f(x) = y + z$ for some $y \in N$ and $z \in K$. Now $(h \circ g)(w) = (h \circ g)(x + y) = h(f(x)) = h(y + z) = y$ and on other hand, $(g \circ h)(w) = (g \circ h)(x + y) = g(x) = f(x) = y + z$. Since $End_R(M)$ is commutative, then $h \circ g = g \circ h$, and so $z=0$. Then $f(x) \in N$, therefore $f(N) \subseteq N$, hence M is SS-module.

By using proposition (17), corollary (15), proposition (16) and proposition (12) we have the following corollary.

Corollary (18): Let M be a regular R-module then the following statements are equivalent:

(1) $End_R(M)$ is commutative;
(2) $End_R(M)$ is fully stable;
(3) M is fully stable;
(4) M is SS-module.

Recall that a ring R is right (left) SS-ring if, every right (left) ideal of R which is direct summand of R is stable. Equivalently from lemma (4), a ring R is right (left) SS-ring if and only if every right (left) ideal which is direct summand of R is ideal.

It is known that the endomorphism ring of a fully stable module need not be fully stable (3), the following proposition shows it is SS-ring.

Proposition (19): If M is a fully stable R-module, then $End_R(M)$ is SS-ring.

Poof: From the above mentioned motivation.

Recall that an R-module M is multiplication if, each submodule of M is of the form IM for some ideal I of R (10). M.S.Abbas observed that in (1) the concepts of fully stable modules and multiplication modules are different. In the following proposition we prove that the class of multiplication modules is contained in the class of SS-modules.

Proposition (20): Every multiplication module is SS-module.

Proof: Let N be a direct summand of a multiplication R-module M and $f: N \longrightarrow M$ be any R-homomorphism. Since M is multiplication, then $N = IM$ for some ideal I of R. But N is a direct summand of M, thus f can be extended to an R-homomorphism $g: M \longrightarrow M$. Now, $f(N) = g(N) = g(IM) = Ig(M) \subseteq IM = N$. Thus, N is a stable of M. Therefore, M is SS-module.

Remark (21): The converse of proposition (20) is not true in general. For example, the module Q of rational numbers over the ring of integers Z is SS-module (since Q_Z is uniform) , but it is not multiplication.

Corollary (22): Every cyclic module over commutative ring is SS-module.

Corollary (23): Every commutative ring is SS-ring.

Remark (24): The corollary (23) gives us a good source of examples which they are SS-modules but not fully stable modules. For instance, [3, Examples(1.13)(b)] , let $R=Z_2[x,y]/\langle x^2,y^2\rangle$ be the polynomial ring in two indeterminates x , y modulo the ideal $\langle x^2,y^2\rangle$. Let $\overline{R}=R/\langle \overline{xy}\rangle$, then $\langle \overline{0}\rangle$, $\langle \overline{x}\rangle$,$\langle \overline{y}\rangle$,$\langle \overline{x}, \overline{y}\rangle$ and $\overline{R}$ are the only ideals of $\overline{R}$. Since $\mathrm{ann}_{\overline{R}}(\mathrm{ann}_{\overline{R}}(\langle \overline{x}\rangle) = \mathrm{ann}_{\overline{R}}(\mathrm{ann}_{\overline{R}}(\langle \overline{x}, \overline{y}\rangle) = \mathrm{ann}_{\overline{R}}(\langle \overline{x}, \overline{y}\rangle) = \langle \overline{x}, \overline{y}\rangle \neq \langle \overline{x}\rangle$ where $\overline{x}$ is an element in $(Z_2[x,y]/\langle x^2,y^2\rangle)/\langle \overline{xy}\rangle$. Thus $\overline{R}$ is not fully stable ring. But $\overline{R}$ is commutative ring, thus by corollary (23) $\overline{R}$ is SS-ring.

As an application of proposition (12), we get the next result due to M.S.Abbas [3, Example and Remark (1.6) (a)].

Corollary (25): Every commutative regular ring is fully stable.

A natural question about any algebraic structure is whether the property is inherited by direct sum or direct summands. The following result shows that direct summands of an SS-module inherit the property.

Proposition (26): Every direct summand of SS-module is SS-module.

Proof: Let M be a SS-module and N be direct summand of M. Let K be a direct summand of N and let $f: K \longrightarrow N$ be any homomorphism. Now, since N is a direct summand of M, then K is direct summand of M [5, p.77]. By SS-module of M, we have K is a stable submodule of M.

Thus $(i \circ f): K \longrightarrow M$ where $i: N \longrightarrow M$ is the inclusion mapping and so $(i \circ f)(K) \subseteq K$ (i.e.) $f(K) \subseteq K$. Thus K is stable submodule of N. Hence N is SS-module.

Remarks (27):

(1) The direct sum of SS-modules need not be SS-module. For example, consider Z and Z_p as Z-modules (where p is a prim number) . Since Z and Z_p are uniform Z-modules, then they are SS-modules. But $M = Z \oplus Z_p$ as Z-module is not SS-module. In fact, by uniformity of Z and Z_p the only direct summands of M are $0 \oplus \bar{0}$, $Z \oplus \bar{0}$, $0 \oplus Z_p$ and M .But $Z \oplus \bar{0}$ is not stable submodule of M. For define $\psi: Z \oplus \bar{0} \longrightarrow M$ by $\psi((x,\bar{0})) = (0,\bar{x})$ for each $(x,\bar{0}) \in Z \oplus \bar{0}$ .Clearly, ψ is a Z-homomorphism. But $\psi(Z \oplus \bar{0}) \not\subset Z \oplus \bar{0}$

(2) It is known that, every fully stable domain is a field. Here we see that it is not true every SS-domain is a field. For example, the ring of integers numbers Z is SS-ring and domain but it is not field.

(3) Recall that, an idempotent endomorphism of an R-module M is central if it commutes with all endomorphisms of M (1). We can assert that, modules in which all idempotent endomorphisms are central are SS-modules. In fact, if N is a direct summand of an R-module M such that all idempotent endomorphisms of M are central. By [1, lemma (8.3)], there exists an idempotent endomorphism f of M such that $N=fM$. Now, let $g \in End_R(M)$ hence $g(N)=g(fM)=f(g(M) \subseteq fM=N$. Thus, N is fully invariant and moreover, by (Remark and Example (2) (5)), M is SS-module.

Recall that, an element x of a ring R is (left) stable if every R-homomorphism of $({}_R\langle x\rangle)$ $\langle x\rangle$ into R is a multiplication by an element of R (11). Also, a ring R is fully stable if and only if every element of R is stable (3). On the other hand, it is known that every left ideal which is direct summand of a ring R is generated by idempotent element of R [1, lemma (2.3)]. These motivations lead us to get a characterization of SS-rings as follows:

Proposition (28): A ring R is left SS-ring if and only if every idempotent element x of R is left stable.

Proof: ($\Rightarrow$). Assume that a ring R is left SS-ring. Let x be an idempotent element in R, then a left ideal $A={}_R\langle x\rangle$ generated by x is a direct summand of R and since R is a left SS-ring, then $A={}_R\langle x\rangle$ is stable of R. So we have x is left stable.

($\Leftarrow$). Conversely, let A be a left ideal of R which is direct summand. By, [1, lemma (2.3)], A is generated by an idempotent element x of R (i.e.) $A={}_R\langle x\rangle$. By hypothesis, we have x is left stable element in R, thus A is a left stable ideal of R. Therefore, R is a left SS-ring.

Recall that, a commutative ring R is fully stable if and only if $ann_R(ann_R(\langle x\rangle)=\langle x\rangle$ for each element x in R (3). The next result gives us another characterization of SS-ring.

Proposition (29): A ring R is left SS-ring if and only if $ann_R^r(ann_R^\ell\langle x\rangle)={}_R\langle x\rangle$ for each idempotent element x in R.

Proof: ($\Rightarrow$). Assume that R is a left SS-ring. Let x be an idempotent element in R and let $s\in ann_R^r(ann_R^\ell\langle x\rangle)$. Since x is an idempotent element in R, then ${}_R\langle x\rangle$ is direct summand of R. Now, Since R is left SS-ring, then ${}_R\langle x\rangle$ is stable of R. Define f: ${}_R\langle x\rangle \longrightarrow R$ by $f(rx)=rs$ for each $r\in R$, if $rx=r'x$, then $r-r'\in ann_R^\ell\langle x\rangle$, then $(r-r')s=0$ or $rs=r's$. Thus f is well-defined and it is clear that f is R-homomorphism. Now, since ${}_R\langle x\rangle$ is stable of M, then we have $s=f(x)\in {}_R\langle x\rangle$. This implies that $ann_R^r(ann_R^\ell\langle x\rangle)\subseteq {}_R\langle x\rangle$, hence $ann_R^r(ann_R^\ell\langle x\rangle)={}_R\langle x\rangle$.

($\Leftarrow$). Assume that $ann_R^r(ann_R^\ell\langle x\rangle)={}_R\langle x\rangle$ for each idempotent element x in R. Let A be a left ideal of R which is direct summand, then $A={}_R\langle e\rangle$. Let f: $A={}_R\langle e\rangle \longrightarrow R$ be any R-homomorphism. Now, let $s\in ann_R^\ell\langle e\rangle$, thus we have $sf(e)=f(se)=f(0)=0$, so $f(e)\in ann_R^r(ann_R^\ell\langle e\rangle)={}_R\langle e\rangle$. Thus, $f(A={}_R\langle e\rangle)\subseteq A={}_R\langle e\rangle$, (i.e.) A is stable of R. Therefore, R is left SS-ring.

Recall that an R-module M is fully stable if and only if every cyclic submodule of M is stable (3). In fact, we do not know in general whether SS-modules have analogous result. We have the following result:

Proposition (30): A ring R is left SS-ring if and only if every left ideal of R generated by idempotent element is stable.

Proof: The proof stand on the fact, every left (right) ideal generated by idempotent element is direct summand and conversely every left (right) ideal which is direct summand is generated by idempotent [1, lemma (2.3)]. □

REFERENCES

1. Wisbauer R.: Foundations of Modules and Rings theory, reading: Gordon and Breach, (1991).
2. Lam T.Y. : Lectures on Modules and rings, Springer-Verlag,Berlin, Heidelberg, New York, (1998).
3. Abbas M. S. : On fully stable modules, Ph.D. Thesis, Univ. of Baghdad, (1991).
4. Birkenmeier G.F. ; Park J. K. and Rizvi S. T. : Modules in which every invariant submodule is essential in a fully invariant direct summand, Comm. Alg. , 30(4): 1833-1852(2002).
5. Dung N. V.; Huynh D. V.; Smith P. F. and Wisbauer R.: Extending modules, Pitman Research Notes in Mathematics Series, 313(1994).
6. Lady E. L.: Direct sums Decompositions, E-book (Internet), 1998.
7. G. V. Wilson: Modules with the summand intersection property, Comm. Algebra 14, 21-38(1986).
8. Hausen J.:Modules with the summand intersection property,17,:135-148 (1989).
9. Zelmanowitz J. : Regular modules, Trans. Amer. Math. Soc., 163: 341-355(1972).
10. Barnard A.: Multiplication modules,J.Algebra,71:174-178 (1981).
11. Alamelu S.: On commutativity of endomorphism rings of ideals II, proc. Amer. Math. Soc. 55: 271- 274(1976).

The Box Counting Dimension of The Condensation Set

[1]Adil Mahmood Ahmed,[2]Abdul Sammee AL–Janabi, [1]Arkan Jassim Mohammed

[1]University of Taiz-College Of Science- Yemen

[2]Al-Mustansiriah University - College of Science- Department of Mathematics

الخلاصة

الهدف من بحثنا هو ايجـاد بعـد حـساب الـصندوق (Box Counting Dimension) لـبعض الكسوريات والتي تسمى المجموعة المركزة (Condensation Set) C_∞ المتكونة بواسطة منظومة الدوال التكرارية في $\mathcal{H}(X)$ الى المجموعة الكسورية $A_0 \in \mathcal{H}(X)$ وقد برهنا وجود ووحدانية المجموعة المركزة C_∞ في فضاء الكسوريات $\mathcal{H}(X)$. ووجدنا أن بعد المجموعة المركـزة C_∞ مـساوي لبعـد المجموعـة الكسورية A_0.

ABSTRACT

In this paper We will find the dimension of some fractals that are called the condensation sets constructed by the iterated function system on $\mathcal{H}(X)$, and we will prove that the condensation set exists and it is unique in the space of fractalss $\mathcal{H}(X)$. Also, in this paper we will prove that the dimension of the condensation set which is called C_∞ of the fractal set A_0 has the same dimension of A_0.

INTRODUCTION

Before introducing the Condensation set, the following definitions and basic concepts are introduced:

Definition 1: Let (X, d) be a complete metric space. Then $\mathcal{H}(X)$ denotes the set whose points are the non empty compact subsets of X.(1).

Definition 2: Let $A \in \mathcal{H}(R^m)$ and let $\mathcal{N}(A, \varepsilon)$ be the smallest number of m-dimensional boxes of side length ε, required to cover A. Then the box-counting dimension of A is defined to be $D(A) = \lim_{\varepsilon \to 0} \left\{ \frac{\ln(\mathcal{N}(A, \varepsilon))}{\ln(1/\varepsilon)} \right\}$.

We will use the notation D = D (A) and we will say "A has box dimension D. (1)

Theorem 1: (Box Counting Theorem): Let $A \in \mathcal{H}(R^m)$, where the Euclidean metric is used. Cover R^m by closed square boxes of side length $(1/2^n)$. Let $\mathcal{N}_n(A)$ denote the number of boxes of side length $(1/2^n)$ which intersect the attractor.

If $D(A) = \lim_{n \to \infty} \left\{ \frac{\ln(\mathcal{N}_n(A))}{\ln(2^n)} \right\}$, then A has box dimension D. (2).

Theorem 2 :(Contraction Mapping Theorem on the Space of Fractals)

Let{X; ω_n, n = 1, 2,..., N} be an iterated function system(IFS) with contractivity factor r. Then the transformation W : $\mathcal{H}(X) \longrightarrow \mathcal{H}(X)$ defined by: $W(B) = \bigcup_{n=1}^{N} \omega_n(B)$, for all B $\in \mathcal{H}(X)$, is a contraction mapping on the complete metric space ($\mathcal{H}(X)$, h(d)) with contractivity factor r. That is h(W(B), W(C)) $\leq$ r h(B, C), for all B, C $\in \mathcal{H}(X)$.Its unique fixed point, A $\in \mathcal{H}(X)$, satisfies: $A = W(A) = \bigcup_{n=1}^{N} \omega_n(A)$,and is given by:

$$A = \lim_{n\to\infty} W^{[n]}(B), \text{ for any } B \in \mathcal{H}(X). \quad (3)$$

Definition 3: The fixed point A $\in \mathcal{H}(X)$ described in the theorem 2 is called the attractor of the IFS. This attractor set A is what we call a fractal. The fractal itself is the limit as the number of iterations approaches infinity. (3)

Lemma 1: Let (X, d) be a metric space. Let {ω_n: n = 1, 2, ..., N} be contraction mappings on ($\mathcal{H}$(x),h). Let the contractivity factor for ω_n be denoted by r_n for each n.

Define W: $\mathcal{H}(X) \longrightarrow \mathcal{H}(X)$, by:

$$W(B) = \omega_1(B) \cup \omega_2(B) \cup ... \cup \omega_N(B) = \bigcup_{n=1}^{N} \omega_n(B), \text{for each } B \in \mathcal{H}(X).$$

Then W is a contraction mapping with contractivity factor r = max{r_n : n = 1, 2, ..., N}.(4)

Now, we will define a fractal set constructed by iterated function system which is called the condensation set.

Definition 4: Let (X, d) be a complete metric space and let {X; ω_1, ω_2, ..., ω_N} be IFS with contractivity factor $0 \leq r < 1$ and $A_0 \in \mathcal{H}(X)$.

Let W:$\mathcal{H}(X) \longrightarrow \mathcal{H}(X)$,be a transformation define by: $W(A_0) = \bigcup_{i=1}^{N} \omega_i(A_0)$, for all $A_0 \in \mathcal{H}(X)$,

and $A_1 = \bigcup_{i=1}^{N} \omega_i(A_0) = W(A_0)$,$A_2 = \bigcup_{i=1}^{N} \omega_i(A_1) = W(A_1) = W^{[2]}(A_0)$,

$A_3 = \bigcup_{i=1}^{N} \omega_i(A_2) = W(A_2) = W^{[3]}(A_0)$, ...,$A_n = \bigcup_{i=1}^{N} \omega_i(A_{n-1}) = W(A_{n-1}) = W^{[n]}(A_0)$.

Consider $C_0 = A_0$, and

$C_1 = A_0 \cup A_1 = A_0 \cup (W(A_0))$, $C_2 = A_0 \cup A_1 \cup A_2 = A_0 \cup (W(A_0)) \cup (W^{[2]}(A_0))$,

$C_3 = A_0 \cup A_1 \cup A_2 \cup A_3 = A_0 \cup (W(A_0)) \cup (W^{[2]}(A_0)) \cup (W^{[3]}(A_0)),\ldots,$

$C_n = A_0 \cup A_1 \cup \ldots \cup A_n = A_0 \cup (W(A_0)) \cup (W^{[2]}(A_0)) \cup \ldots \cup (W^{[n]}(A_0))$.

By taking $\lim_{n\to\infty} C_n = C_\infty$, then C_∞ is called the condensation set of A_0 with respect to the IFS $\{X; \omega_1, \omega_2, \ldots, \omega_N\}$.[1]

Definition 5: Let (X, d) be a complete metric space and let $A_0 \in \mathcal{H}(X)$. Define a transformation $\omega_0 : \mathcal{H}(X) \longrightarrow \mathcal{H}(X)$, by:$\omega_0(B) = A_0$, for all $B \in \mathcal{H}(X)$.

Then ω_0 is called a condensation transformation and A_0 is called the associated condensation set. (1)

Definition 6: Let $\{X; \omega_1, \omega_2, \ldots, \omega_N\}$ be an IFS with contractivity factor $0 \le r < 1$.

Let $\omega_0 : \mathcal{H}(X) \longrightarrow \mathcal{H}(X)$ be a condensation transformation. Then $\{X; \omega_0, \omega_1, \ldots, \omega_N\}$ is called IFS with condensation, with contractivity factor r. (1)

THE EXISTENCE AND THE UNIQUENESS OF THE CONDENSATION SET C_∞.

Our aim in this section is to prove that the condensation set C_∞ exists and is unique in the space of fractals, that is, $C_\infty \in \mathcal{H}(X)$.

Theorem 3: Let $\{X; \omega_0, \omega_1, \ldots, \omega_N\}$ be an iterated function system with condensation, with contractivity factor r. Then the transformation $W_0 : \mathcal{H}(X) \longrightarrow \mathcal{H}(X)$, defined by:

$W_0(B) = \bigcup_{i=0}^{N} \omega_i(B)$, for all $B \in \mathcal{H}(X)$, is a contraction mapping on the complete metric space $\mathcal{H}(X)$,with contractivity factor r. It's unique fixed point, $C_\infty \in \mathcal{H}(X)$, satisfying

$C_\infty = W_0(C_\infty) = \bigcup_{i=0}^{N} \omega_i(C_\infty)$ .And is given by: $C_\infty = \lim_{n\to\infty} W_0^{[n]}(B)$, for any $B \in \mathcal{H}(X)$.

Proof: Let $\{X; \omega_1, \omega_2, \ldots, \omega_N\}$ be an IFS with contractivity factor $0 \le r < 1$, and define

$W : \mathcal{H}(X) \longrightarrow \mathcal{H}(X)$, by :$W(B) = \bigcup_{i=1}^{N} \omega_i(B)$, for all $B \in \mathcal{H}(X)$.

Let $A_0 \in \mathcal{H}(X)$ and $\{X; \omega_0, \omega_1, \ldots, \omega_N\}$ be an iterated function system with Condensation contractivity factor r and condensation transformation $\omega_0 : \mathcal{H}(X) \longrightarrow \mathcal{H}(X)$, such that $\omega_0(B) = A_0$, for all $B \in \mathcal{H}(X)$, Since $W_0 : \mathcal{H}(X) \longrightarrow \mathcal{H}(X)$, is defined by:

$W_0(B) = \bigcup_{i=0}^{N} \omega_i(B)$, for all $B \in \mathcal{H}(X)$.

Then $W_0(B) = \omega_0(B) \cup (\bigcup_{i=1}^{N} \omega_i(B)) = \omega_0(B) \cup W(B) = A_0 \cup W(B)$.

Let $B = A_0 = C_0$.

$C_1 = W_0(C_0) = A_0 \cup W(C_0) = A_0 \cup W(A_0)$.

$C_2 = W_0^{[2]}(C_0) = W_0(C_1)$.

$= A_0 \cup W(C_1) = A_0 \cup W(A_0 \cup W(A_0)) = A_0 \cup W(A_0) \cup W^{[2]}(A_0)$.

$C_3 = W_0^{[3]}(C_0) = W_0^{[2]}(C_1) = W_0(C_2)$

$= A_0 \cup W(C_2) = A_0 \cup W(A_0 \cup W(A_0) \cup W^{[2]}(A_0))$.

$= A_0 \cup W(A_0) \cup W^{[2]}(A_0) \cup W^{[3]}(A_0)$.

$\vdots$

$C_n = W_0^{[n]}(C_0) = A_0 \cup W(A_0) \cup W^{[2]}(A_0) \cup \ldots \cup W^{[n]}(A_0)$.

To find the fixed set K, such that $W_0(K) = K$.

By lemma (1), we have:$(A_0 \cup W(A_0) \cup W^{[2]}(A_0) \cup \ldots \cup W^{[n]}(A_0)) \in \mathcal{H}(X)$,

and $\lim_{n\to\infty} C_n = \lim_{n\to\infty} (A_0 \cup W(A_0) \cup W^{[2]}(A_0) \cup \ldots \cup W^{[n]}(A_0))$

$= \lim_{n\to\infty} W_0^{[n]}(C_0) = K \in \mathcal{H}(X)$.

By theorem 2, the transformation$W_0 : \mathcal{H}(X) \longrightarrow \mathcal{H}(X)$, has a unique fixed point $K \in \mathcal{H}(X)$, which satisfies $K = W_0(K) = \bigcup_{i=0}^{N} \omega_i(K)$, and is given by :$K = \lim_{n\to\infty} W_0^{[n]}(B)$, for any

$B \in \mathcal{H}(X)$. Hence, $C_\infty = K$ exists and belong to $\mathcal{H}(X)$. This tell us that $\{C_n\}$ is a cauchy sequence in $\mathcal{H}(X)$ that converges to the attractor of IFS, $K = C_\infty$. We observe that

$C_n = A_0 \cup W(A_0) \cup W^{[2]}(A_0) \cup \ldots \cup W_0^{[n]}(A_0)$, provides an increasing sequence of compact set. It follows immediately that the limit set C_∞ satisfies $W_0(C_\infty) = C_\infty$. ■

Example 1: Let (X, d) be a complete metric space and $A_0 \in \mathcal{H}(X)$, and let $\{X; \omega_1, \omega_2, \omega_3\}$ be an IFS with contractivity factor $0 < r < 1$.We want to find the condensation set C_∞ of A_0 with respect to the IFS $\{X; \omega_1, \omega_2, \omega_3\}$. Let $W: \mathcal{H}(X) \longrightarrow \mathcal{H}(X)$, be defined as :$W(A_0) = \bigcup_{i=1}^{3} \omega_i(A_0)$, for all $A_0 \in \mathcal{H}(X)$.First, we consider $C_0 = A_0$ and by definition (4), we have:

$A_1 = \bigcup_{i=1}^{3} \omega_i(A_0) = \omega_1(A_0) \cup \omega_2(A_0) \cup \omega_3(A_0) = W(A_0)$.So, $C_1 = A_0 \cup A_1 = A_0 \cup (W(A_0))$.

$A_2 = \bigcup_{i=1}^{3} \omega_i(A_0) = \omega_1(A_1) \cup \omega_2(A_1) \cup \omega_3(A_1)$

$= \omega_1(\omega_1(A_0) \cup \omega_2(A_0) \cup \omega_3(A_0)) \cup \omega_2(\omega_1(A_0) \cup \omega_2(A_0) \cup \omega_3(A_0)) \cup \omega_3(\omega_1(A_0) \cup \omega_2(A_0) \cup \omega_3(A_0))$.

$= (\omega_1^{[2]}(A_0) \cup \omega_1\omega_2(A_0) \cup \omega_1\omega_3(A_0)) \cup (\omega_2\omega_1(A_0) \cup \omega_2^{[2]}(A_0) \cup \omega_2\omega_3(A_0)) \cup (\omega_3\omega_1(A_0) \cup \omega_3\omega_2(A_0) \cup \omega_3^{[2]}(A_0))$

$= W(A_1) = W^{[2]}(A_0)$.So, $C_2 = A_0 \cup A_1 \cup A_2 = A_0 \cup (W(A_0)) \cup (W^{[2]}(A_0))$

$A_3 = \bigcup_{i=1}^{3} \omega_i(A_2) = \omega_1(A_2) \cup \omega_2(A_2) \cup \omega_3(A_2)$

$= \omega_1((\omega_1^{[2]}(A_0) \cup \omega_1\omega_2(A_0) \cup \omega_1\omega_3(A_0)) \cup (\omega_2\omega_1(A_0) \cup \omega_2^{[2]}(A_0) \cup \omega_2\omega_3(A_0)) \cup (\omega_3\omega_1(A_0) \cup \omega_3\omega_2(A_0) \cup \omega_3^{[2]}(A_0))) \cup \omega_2((\omega_1^{[2]}(A_0) \cup \omega_1\omega_2(A_0) \cup \omega_1\omega_3(A_0)) \cup (\omega_2\omega_1(A_0) \cup \omega_2^{[2]}(A_0) \cup \omega_2\omega_3(A_0)) \cup (\omega_3\omega_1(A_0) \cup \omega_3\omega_2(A_0) \cup \omega_3^{[2]}(A_0))) \cup \omega_3((\omega_1^{[2]}(A_0) \cup \omega_1\omega_2(A_0) \cup \omega_1\omega_3(A_0)) \cup (\omega_2\omega_1(A_0) \cup \omega_2^{[2]}(A_0) \cup \omega_2\omega_3(A_0)) \cup (\omega_3\omega_1(A0) \cup \omega_3\omega_2(A_0) \cup \omega_3^{[2]}(A_0)))$.

$= [(\omega_1^{[3]}(A_0) \cup \omega_1^{[2]}\omega_2(A_0) \cup \omega_1^{[2]}\omega_3(A_0)) \cup (\omega_1\omega_2\omega_1(A_0) \cup \omega_1\omega_2^{[2]}(A_0) \cup \omega_1\omega_2\omega_3(A_0)) \cup (\omega_1\omega_3\omega_1(A_0) \cup \omega_1\omega_3\omega_2(A_0) \cup \omega_1\omega_3^{[2]}(A_0))] \cup [(\omega_2\omega_1^{[2]}(A_0) \cup \omega_2\omega_1\omega_2(A_0) \cup \omega_2\omega_1\omega_3(A_0)) \cup (\omega_2^{[2]}\omega_1(A_0) \cup \omega_2^{[3]}(A_0) \cup \omega_2^{[2]}\omega_3(A_0)) \cup (\omega_2\omega_3\omega_1(A_0) \cup \omega_2\omega_3\omega_2(A_0) \cup \omega_2\omega_3^{[2]}(A_0))] \cup [\omega_3\omega_1^{[2]}(A_0) \cup \omega_3\omega_1\omega_2(A_0) \cup \omega_3\omega_1\omega_3(A_0)) \cup (\omega_3\omega_2\omega_1(A_0) \cup \omega_3\omega_2^{[2]}(A_0) \cup \omega_3\omega_2\omega_3(A_0)) \cup (\omega_3^{[2]}\omega_1(A_0) \cup \omega_3^{[2]}\omega_2(A_0) \cup \omega_3^{[3]}(A_0))]$.

$= W(A_2) = W^{[3]}(A_0)$. So:$C_3 = A_0 \cup A_1 \cup A_2 \cup A_3$.

$\vdots$

$A_n = \bigcup_{i=1}^{3} \omega_i(A_{n-1}) = W(A_{n-1}) = A^{[n]}(A_0)$.So,

$C_n = A_0 \cup A_1 \cup \ldots \cup A_n$

$= A_0 \cup (W(A_0)) \cup (W^{[2]}(A_0)) \cup \ldots \cup (W^{[n]}(A_0))$.

Letting $n \longrightarrow \infty$, then $C_n \longrightarrow C_\infty$ is the condensation set of A_0 with respect to IFS $\{X; \omega_1, \omega_2, \omega_3\}$, see figure -1:

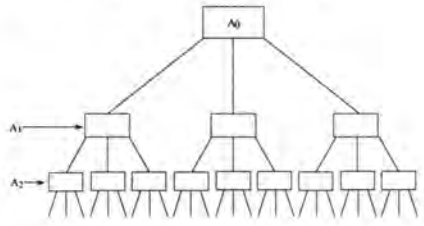

Figure -1:C_∞ is the condensation set of A_0 with respect to IFS $\{X; \omega_1, \omega_2, \omega_3\}$

THE BOX COUNTING DIMENSION OF THE CONDENSATION SETS

In this section, we will find by using box-counting theorem the dimension of the condensation set C_∞ of the set $A_0 \in \mathcal{H}(X)$ with respect to the IFS $\{X; \omega_1\}$ and also we will find the relation between the dimension of C_∞ and the dimension of A_0.

Example 2: Let $\{R^2, \omega_1\}$ be an IFS, where $\omega_1 : \mathcal{H}(R^2) \longrightarrow \mathcal{H}(R^2)$, be the transformation defined by: $\omega_1\begin{pmatrix} x \\ y \end{pmatrix} = \frac{1}{2}\begin{pmatrix} 1 & 0 \\ 0 & 1 \end{pmatrix}\begin{pmatrix} x \\ y \end{pmatrix}$,with contractivity factor $r = \frac{1}{2}$, and let $A_0 \in \mathcal{H}(R^2)$, where A_0 is defined by: $A_0 = \{(x, y) \in R^2$, such that $x = 1$ and $0 \le y \le 1\}$.

By definition (4), we have .Let $C_0 = A_0$.

$A_1 = \omega_1(A_0) = \{(x, y) \in R^2 : x = 1/2, 0 \le y \le 1/2\}$.

$C_1 = A_0 \cup A_1 = A_0 \cup \omega_1(A_0)$.

$A_2 = \omega_1(A_1) = \omega_1^{[2]}(A_0) = \{(x, y) \in R^2 : x = 1/4, 0 \le y \le 1/4\}$.

$C_2 = A_0 \cup A_1 \cup A_2 = A_0 \cup \omega_1(A_0) \cup \omega_1^{[2]}(A_0)$.

$A_3 = \omega_1(A_2) = \omega_1^{[2]}(A_1) = \omega_1^{[2]}(A_0) = \{(x, y) \in R^2 : x = 1/8, 0 \le y \le 1/8\}$.

$C_3 = A_0 \cup A_1 \cup A_2 \cup A_3 = A_0 \cup \omega_1(A_0) \cup \omega_1^{[2]}(A_0) \cup \omega_1^{[3]}(A_0)$.

$\vdots$

$A_n = \omega_1(A_{n-1}) = \ldots = \omega_1^{[n]}(A_0)$

$= \{(x, y) \in R^2: x = 1/(2)^n, 0 \le y \le 1/(2)^n, n = 0, 1, \ldots\}$. So that:

$C_n = A_0 \cup A_1 \cup \ldots \cup A_n = A_0 \cup \omega_1(A_0) \cup \omega_1^{[2]}(A_0) \cup \ldots \cup \omega_1^{[n]}(A_0)$

$$= C_0 \cup \omega_1(C_0) \cup \omega_1^{[2]}(C_0) \cup \ldots \cup \omega_1^{[n]}(C_0).$$

Taking $n \longrightarrow \infty$, then $C_n \longrightarrow C_\infty$ which is the condensation set of A_0 with respect to the IFS $\{ R^2; \omega_1\}$, see figure -2:

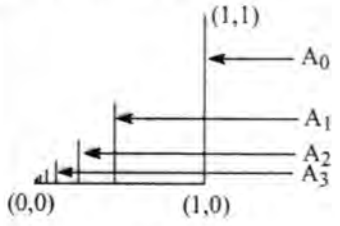

Figure -2:The sketch of the condensation set C_∞ of A_0, the attractor of IFS with condensation.

Now, we find the dimension of A_0 by using the box-counting theorem.

Let $\varepsilon_n = (1/2)^n$, n = 0, 1, ...; then we have:

Table to calculate $\mathcal{N}_n(A_0)$.

n	ε_n	$\mathcal{N}_n(A_0)$
0	1	1
1	1/2	2
2	$(1/2)^2 = 1/4$	4
3	$(1/2)^3 = 1/8$	8
4	$(1/2)^4 = 1/16$	16
5	$(1/2)^5 = 1/32$	32
⋮	⋮	⋮
n	$(1/2)^n$	2^n

$$D_B(A_0) = \lim_{n\to\infty} \frac{\ln(\mathcal{N}_n(A_0))}{\ln(2^n)} = \lim_{n\to\infty} \frac{\ln(2^n)}{\ln(2^n)} = 1.$$

Now, we find the dimension of the condensation set C_∞ of A_0 by using the box-counting theorem, as follows

Table to calculate $\mathcal{N}_n(C_\infty)$.

n	ε_n	$\mathcal{N}_n(C_\infty)$
0	1	1
1	1/2	3
2	1/4	7
3	1/8	15
4	1/16	31
5	1/32	63
⋮	⋮	⋮
n	$(1/2)^n$	$1 + 2 + 2^2 + \ldots + 2^n = \sum_{i=0}^{n} 2^i$

$\mathcal{N}_n(C_\infty) = 1 + 2 + 2^2 + \ldots + 2^n$ .....(1)

$2\mathcal{N}_n(C_\infty) = 2 + 2^2 + \ldots + 2^{n+1}$ .....(2)

and upon subtracting equation (1) from equation (2) to get: $\mathcal{N}_n(C_\infty) = 2^{n+1} - 1$.

So $\mathcal{N}_n(C_\infty) = \sum_{i=0}^{n} 2^i = 2^{n+1} - 1$.

Hence $D_B(C_\infty) = \lim_{n\to\infty} \frac{\ln(\mathcal{N}_n(C_\infty))}{\ln(2^n)} = \lim_{n\to\infty} \frac{\ln(2^{n+1}-1)}{n\ln(2)} = 1$. Therefore, $D_B(A_0) = D_B(C_\infty)$.

Example 3: Let $\{ R^2; \omega_1\}$ be an IFS, where $\omega_1 : \mathcal{H}(R^2) \longrightarrow \mathcal{H}(R^2)$, be a transformation defined by: $\omega_1\begin{pmatrix} x \\ y \end{pmatrix} = \frac{1}{2}\begin{pmatrix} 1 & 0 \\ 0 & 1 \end{pmatrix}\begin{pmatrix} x \\ y \end{pmatrix}$, with contractivity factor r = 1/2.

Let $A_0 \in \mathcal{H}(R^2)$, defined by $A_0 = \{(x, y) \in R^2 : 1/2 < x \le 1, 0 \le y \le 1\}$

Let $C_0 = A_0$.

$A_1 = \omega_1(A_0) = \{(x, y) \in R^2 : 1/4 < x \le 1/2, 0 \le y \le 1/2\}$.

$C_1 = A_0 \cup A_1 = A_0 \cup \omega_1(A_0)$.

$A_2 = \omega_1(A_1) = \omega_1^{[2]}(A_0) = \{(x, y) \in R^2 : 1/8 < x \le 1/4, 0 \le y \le 1/4\}$.

$$C_2 = A_0 \cup A_1 \cup A_2 = A_0 \cup \omega_1(A_0) \cup \omega_1^{[2]}(A_0).$$

$$A_3 = \omega_1(A_2) = \omega_1^{[2]}(A_1) = \omega_1^{[3]}(A_0)$$
$$= \{(x, y) \in R^2 : 1/16 < x \le 1/8, 0 \le y \le 1/8\}.$$

$$C_3 = A_0 \cup A_1 \cup A_2 \cup A_3 = A_0 \cup \omega_1(A_0) \cup \omega_1^{[2]}(A_0) \cup \omega_1^{[3]}(A_0).$$

$$\vdots$$

$$A_n = \omega_1(A_{n-1}) = \ldots = \omega_1^{[n]}(A_0)$$
$$= \{(x, y) \in R^2 : 1/2^{n+1} < x \le 1/2^n, 0 \le y \le 1/2^n\}.$$

$$C_n = A_0 \cup A_1 \cup A_2 \cup A_3 \cup \ldots \cup A_n$$
$$= C_0 \cup \omega_1(C_0) \cup \omega_1^{[2]}(C_0) \cup \ldots \cup \omega_1^{[n]}(C_0).$$

and by definition (4), we obtain that $\lim_{n\to\infty} C_n = C_\infty \in \mathcal{H}(R^2)$.Therefore, C_∞ is the condensation set of A_0 with respect to the IFS $\{ R^2; \omega_1\}$, see figure -3:

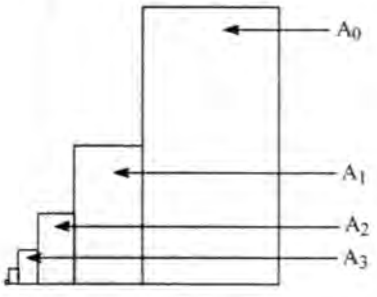

Figure -3:The condensation set C_∞ of A_0 with respect to the IFS $\{R^2, \omega_1\}$, the attractor of the IFS with condensation.

Take $\varepsilon = (1/2)^n$, n = 1, 2, … .

Table to calculate $\mathcal{N}_n(A_0)$.

n	ε_n	$\mathcal{N}_n(A_0)$
1	1/2	$2 = 1\times2 = 2^0\times2$
2	1/4	$8 = 2\times4 = 2\times2^2$
3	1/8	$32 = 4\times8 = 2^2\times2^3$
4	1/16	$128 = 8\times16 = 2^3\times2^4$
5	1/32	$512 = 16\times32 = 2^4\times2^5$
⋮	⋮	⋮
n	$(1/2)^n$	$2^{n-1}\times2^n$

Hence $D_B(A_0) = \lim_{n\to\infty} \frac{\ln(\mathcal{N}_n(A_0))}{\ln(2^n)} = \lim_{n\to\infty} \frac{\ln(2^{n-1}\times 2^n)}{\ln(2^n)} = \lim_{n\to\infty} \frac{\ln(2^{2n-1})}{\ln(2^n)} = 2.$

By the box-counting theorem, we count

Table to calculate $\mathcal{N}_n(C_\infty)$.

n	ε_n	$\mathcal{N}_n(C_\infty)$
1	1/2	$3 = 1 + 1\times2$
2	1/4	$11 = 1 + 1\times2 + 2\times4$
3	1/8	$43 = 1 + 1\times2 + 2\times4 + 4\times8$
4	1/16	$171 = 1 + 1\times2 + 2\times4 + 4\times8 + 8\times16$
5	1/32	$512 = 1 + 1\times2 + 2\times4 + 4\times8 + 8\times16 + 16\times32$
⋮	⋮	⋮
N	$(1/2)^n$	$1 + 1\times2 + 2\times2^2 + 2^2\times2^3 + 2^3\times2^4 + 2^4\times2^5 + \ldots + 2^{n-1}\times2^n$

$$\mathcal{N}_n(C_\infty) = 1 + 2 + 2^3 + 2^5 + \ldots + 2^{2n-1} \quad \ldots\ldots(3)$$

$$2^2\mathcal{N}_n(C_\infty) = 2^2 + 2^3 + \ldots + 2^{2n+1} \quad \ldots\ldots(4)$$

and upon subtracting equation (3) from equation (4) to get: $3\mathcal{N}_n(C_\infty) = 1 + 2^{n+1}$. Hence $\mathcal{N}(C_\infty) = \frac{1+2^{n+1}}{3}$. So $D_B(C_\infty) = \lim_{n\to\infty} \frac{\ln(\mathcal{N}_n(C_\infty))}{\ln(2^n)} = \lim_{n\to\infty} \frac{\ln\left(\frac{2^{n+1}+1}{3}\right)}{n\ln(2)} = 2.$

Hence the dimension of the condensation set C_∞ of A_0 with respect to the IFS $\{R^2; \omega_1\}$ is 2 , and since $D_B(A_0) = 2$, it follows that, $D_B(C_\infty) = D_B(A_0)$.

Example 4: Let $\{ R^2; \omega_1\}$ be an IFS, where $\omega_1 : \mathcal{H}(R^2) \longrightarrow \mathcal{H}(R^2)$, be a transformation defined by:$\omega_1\begin{pmatrix} x \\ y \end{pmatrix} = \frac{1}{2}\begin{pmatrix} 1 & 0 \\ 0 & 1 \end{pmatrix}\begin{pmatrix} x \\ y \end{pmatrix}$, with contractivity factor $r = 1/2$.Let $A_0 \in \mathcal{H}(R^2)$, where A_0 is the Sierpinski triangle with vertices at (1/2, 0), (1, 0) and (0, 1/2).

From (1) we have $D_B(A_0) = \frac{\ln 3}{\ln 2} \cong 1.58$

Now, we want to find the dimension of the condensation set C_∞ of A_0 with respect to the IFS $\{ R^2; \omega_1\}$.Let $C_0 = A_0$ and by definition 4, we have:

$A_1 = \omega_1(A_0).C_1 = A_0 \cup A_1 = A_0 \cup \omega_1(A_0).$

$A_2 = \omega_1(A_1) = \omega_1^{[2]}(A_0).C_2 = A_0 \cup A_1 \cup A_2 = A_0 \cup \omega_1(A_0) \cup \omega_1^{[2]}(A_0).$

$\vdots$

$A_n = \omega_1(A_{n-1}) = \ldots = \omega_1^{[n]}(A_0).C_n = A_0 \cup A_1 \cup A_2 \cup A_3 \cup \ldots \cup A_n$

$= A_0 \cup \omega_1(A_0) \cup \omega_1^{[2]}(A_0) \cup \omega_1^{[3]}(A_0) \cup \ldots \cup \omega_1^{[n]}(A_0).$

Taking $n \longrightarrow \infty$, so we have $C_n \longrightarrow C_\infty \in \mathcal{H}(R^2)$and therefore C_∞ is the condensation set of the Sierpinski triangle A_0 with respect to the IFS $\{ R^2, \omega_1\}$.

Let $\varepsilon_n = (1/2)^n$, n = 1, 2, … .

Table to calculate $\mathcal{N}_n(C_\infty)$.

n	ε_n	$\mathcal{N}_n(C_\infty)$
1	1/2	$1 + 1 = 2$
2	1/4	$1 + 1 + 3 = 5$
3	1/8	$1 + 1 + 3 + 9 = 1 + 1 + 3 + 3^2 = 14$
4	1/16	$1 + 1 + 3 + 9 + 27 = 1 + 1 + 3 + 3^2 + 3^3 = 41$
5	1/32	$1 + 1 + 3 + 9 + 27 + 81 = 1 + 1 + 3 + 3^2 + 3^3 + 3^4 = 122$
⋮	⋮	⋮
N	$(1/2)^n$	$= 1 + 1 + 3 + 3^2 + 3^3 + \ldots + 3^n$

$$\mathcal{N}_n(C_\infty) = 1 + 1 + 3 + 3^2 + \ldots + 3^n \quad \ldots\ldots(5)$$

$$3\mathcal{N}_n(C_\infty) = 3 + 3 + 3^2 + 3^3 + \ldots + 3^{n+1} \quad \ldots\ldots(6)$$

and upon subtracting equation (5) from equation (6) to get: $2\mathcal{N}_n(C_\infty) = 1 + 3^{n+1}$. Hence $\mathcal{N}_n(C_\infty) = \frac{1+3^{n+1}}{2}$.Therefore, $D_B(C_\infty) = \lim_{n\to\infty} \frac{\ln(\mathcal{N}_n(C_\infty))}{\ln(2^n)} = \lim_{n\to\infty} \frac{\ln\left(\frac{3^{n+1}+1}{2}\right)}{n\ln(2)} \cong 1.58.$

Hence the dimension of the condensation set C_∞ of A_0 with respect to the IFS

$\{ R^2; \omega_1\}$ is 1.58, so, $D_B(C_\infty) = D_B(A_0)$.

Example 5: Let $\{ R^2; \omega_1\}$ be an IFS, where $\omega_1 : R^2 \longrightarrow R^2$, be a transformation defined by:$\omega_1\begin{pmatrix} x \\ y \end{pmatrix} = \frac{1}{2}\begin{pmatrix} 1 & 0 \\ 0 & 1 \end{pmatrix}\begin{pmatrix} x \\ y \end{pmatrix}$, with contractivity factor r = 1/2.

Let $A_0 \in \mathcal{H}(R^2)$, where $A_0 = B_1 \cup B_2$, and $B_1 = \{(x, y) \in R^2 : x = 1, 0 \leq y \leq 1\}$.$B_2 = \{(x, y) \in R^2 : x = \sigma, 0 < y < \sigma\}$.By definition (4), we have

$C_0 = A_0 = B_1 \cup B_2$.

$A_1 = \omega_1(A_0) = \omega(B_1 \cup B_2) = \omega_1(B_1) \cup \omega_1(B_2)$.

Where

$\omega_1(B_1) = \{(x, y) \in R^2 : x = 1/2, 0 \leq y \leq 1/2\}$.$\omega_1(B_2) = \{(x, y) \in R^2 : x = \sigma/2, 0 < y , \sigma/2\}$.

$C_1 = A_0 \cup A_1 = A_0 \cup \omega_1(A_0)$.

$A_2 = \omega_1(A_1) = \omega_1^{[2]}(A_0) = \omega_1(\omega_1(B_1) \cup \omega_1(B_2)) = \omega_1^{[2]}(B_1) \cup \omega_1^{[2]}(B_2)$.

Where $\omega_1^{[2]}(B_1) = \{(x, y) \in R^2 : x = 1/4, 0 \leq y \leq 1/4\}$.

$\omega_1^{[2]}(B_2) = \{(x, y) \in R^2 : x = \sigma/4, 0 < y < \sigma/4\}$.

$C_2 = A_0 \cup A_1 \cup A_2 = A_0 \cup \omega_1(A_0) \cup \omega_1^{[2]}(A_0)$.

$\vdots$

$A_n = \omega_1(A_{n-1}) = \ldots = \omega_1^{[n]}(A_0)$

$= \omega_1^{[n]}(B_1 \cup B_2) = \omega_1^{[n]}(B_1) \cup \omega_1^{[n]}(B_2)$.Where $\omega_1^{[n]}(B_1) = \{(x, y) \in R^2 : x = 1/2^n, 0 \leq y \leq 1/2^n\}$.

$\omega_1^{[n]}(B_2) = \{(x, y) \in R^2 : x = \sigma/2^n, 0 < y < \sigma/2^n\}$.

$C_n = A_0 \cup A_1 \cup A_2 \cup A_3 \cup \ldots \cup A_n$

$= A_0 \cup \omega_1(A_0) \cup \omega_1^{[2]}(A_0) \cup \omega_1^{[3]}(A_0) \cup \ldots \cup \omega_1^{[n]}(A_0)$.

By theorem 3 we have $\lim_{n\to\infty} C_n = C_\infty \in \mathcal{H}(R^2)$, and C_∞ is the condensation set of A_0 with respect to IFS $\{ R^2; \omega_1\}$, see figure -4.(we take for example $\sigma = 3/4$)

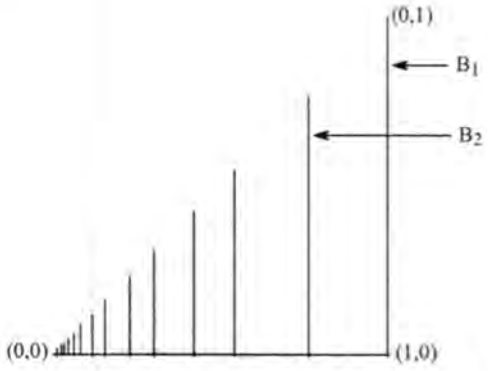

Figure -4:The condensation set C_∞ of $A_0 = B_1 \cup B_2$ with respect to the IFS $\{ R^2, \omega_1\}$.

By using the box counting theorem. From we have $D_B(B_1) = 1$. Now, to find $D_B(B_2)$. Let:$\sigma = \frac{\sigma_1}{2} + \frac{\sigma_2}{(2)^2} + \frac{\sigma_3}{(2)^3} + \frac{\sigma_4}{(2)^4} + \dots$.

where $\sigma_i \in \{0, 1\}$, for all i = 1, 2, ...; and we suppose that $\sigma = (\sigma_1\sigma_2\sigma_3\sigma_4\dots)_2$, for example 3/4 = (11000...).

Table to calculate $\mathcal{N}_n(B_2)$.

n	$\varepsilon_n = (1/2)^n$	$\mathcal{N}_n(B_2)$
1	1/2	2
2	1/4	$2 + 1 + \sigma_2 = 2\times2 - 1 + \sigma_2$
3	1/8	$2[2^2 - 1 + \sigma_2] - 1 + \sigma_3 = 2^2 + 1 + 2\sigma_2 + \sigma_3$
4	1/16	$2[2^2 + 1 + 2\sigma_2 + \sigma_3] - 1 + \sigma_4 = 2^3 + 1 + 2^2\sigma_2 + 2\sigma_3 + \sigma_4$
5	1/32	$2[2^3 + 1 + 2^2\sigma_2 + 2\sigma_3 + \sigma_4] - 1 + \sigma_5 =$ $2^4 + 1 + 2^3\sigma_2 + 2^2\sigma_3 + 2\sigma_4 - 1 + \sigma_5$
⋮	⋮	⋮
n	$(1/2)^n$	$2^{n-1} + 1 + 2^{n-2}\sigma_2 + 2^{n-3}\sigma_3 + 2^{n-4}\sigma_4 + \dots + \sigma_n$

So, we have :$D_B(B_2) = \lim_{n\to\infty} \frac{\ln(\mathcal{N}_n(B_2))}{\ln(2^n)}$

$$= \lim_{n\to\infty} \frac{\ln(2^{n-1} + 1 + 2^{n-2}\sigma_2 + 2^{n-3}\sigma_3 + \dots + \sigma_n)}{n\ln(2)}$$

Suppose $I_n(\sigma) = 2^{n-2}\sigma_2 + 2^{n-3}\sigma_3 + 2^{n-4}\sigma_4 + \dots + \sigma_n$.If all $\sigma_i = 0$, i = 2, ..., n; then $I_n(\sigma) = 0$, and therefore, we have:

$$D_B(B_2) = \lim_{n\to\infty}\frac{\ln\left(2^{n-1}+1\right)}{n\ln(2)} \cong \lim_{n\to\infty}\frac{\ln\left(2^{n-1}\right)}{n\ln(2)} = 1.$$

If all $\sigma_i = 1$, i = 2, …, n; then

$$I_n(\sigma) = 2^{n-2} + 2^{n-3} + 2^{n-4} + \ldots + 1 \quad \ldots\ldots(7)$$

$$2\,I_n(\sigma) = 2^{n-1} + 2^{n-2} + 2^{n-3} + 2^{n-4} + \ldots + 2 \quad \ldots\ldots(8)$$

Now, upon subtracting (7) from (8), gives $I_n(\sigma) = 2^{n-1} - 1$. So

$D_B(B_2) = \lim_{n\to\infty}\frac{\ln(2^{n-1}+1+2^{n-1}-1)}{n\ln(2)} = 1$.Hence $D_B(B_2) = 1$, for all cases.

Now, since $A_0 = B_1 \cup B_2$, then $\mathcal{N}_n(A_0) = \mathcal{N}_n(B_1) + \mathcal{N}_n(B_2)$

$$= 2^n + 2^{n-1} + 1 + 2^{n-2}\sigma_2 + 2^{n-3}\sigma_3 + \ldots + \sigma_n$$

from the following table:

Table to calculate $\mathcal{N}_n(A_0) = \mathcal{N}_n(B_1 \cup B_2)$.

n	$\varepsilon_n = (1/2)^n$	$\mathcal{N}_n(A_0) = \mathcal{N}_n(B_1 \cup B_2)$
1	1/2	$2 + 1 + 1$
2	1/4	$2^2 + 2 + 1 + \sigma_2$
3	1/8	$2^3 + 2^2 + 1 + 2\sigma_2 + \sigma_3$
4	1/16	$2^4 + 2^3 + 1 + 2^2\sigma_2 + 2\sigma_3 + \sigma_4$
5	1/32	$2^5 + 2^4 + 1 + 2^3\sigma_2 + 2^2\sigma_3 + 2\sigma_4 + \sigma_5$
⋮	⋮	⋮
N	$(1/2)^n$	$2^n + 2^{n-1} + 1 + 2^{n-2}\sigma_2 + 2^{n-3}\sigma_3 + 2^{n-4}\sigma_4 + \ldots + \sigma_n$

$$D_B(A_0) = \lim_{n\to\infty}\frac{\ln(\mathcal{N}_n(A_0))}{\ln(2^n)} = \lim_{n\to\infty}\frac{\ln(2^n + 2^{n-1} + 1 + 2^{n-2}\sigma_2 + 2^{n-3}\sigma_3 + \ldots + \sigma_n)}{n\ln(2)}$$

Let $I_n(\sigma) = 2^{n-2}\sigma_2 + 2^{n-3}\sigma_3 + \ldots + \sigma_n$.

If all $\sigma_i = 0$, i = 2, 3, …, n; then, $D_B(A_0) = \lim_{n\to\infty}\frac{\ln(2^n + 2^{n-1} + 1)}{n\ln(2)} = 1$,

and if for all $\sigma_i = 1$, i = 2, 3, …, n; then, $I_n(\sigma) = 2^{n-2} + 2^{n-3} + \ldots + 2 + 1$; so $I_n(\sigma) = 2^{n-1} - 1$

$$D_B(A_0) = \lim_{n\to\infty}\frac{\ln(2^n + 2^{n-1} + 1 + 2^{n-1} - 1)}{n\ln(2)} = 1.$$

Hence $D_B(A_0) = 1$, for all cases

$$\mathcal{N}_n(C_\infty) = \sum_{i=1}^{n} 2^i + \sum_{i=1}^{n} 2^{i-1} + \sum_{i=1}^{n} 1 + \sigma_2 \sum_{i=2}^{n} 2^{i-2} + + \ldots + \sigma_n$$

$$= 2^{n+2} - 2 + 2^n - 1 + n + \sigma_n(2^{n-1} - 1) + \sigma_3(2^{n-2} - 1) + \ldots + \sigma_2(2 - 1)$$

$$= 2^{n+1} + 2^n - 3 + n + \sigma_2(2^{n-1} - 1) + \sigma_3(2^{n-2} - 1) + \ldots + \sigma_n(2 - 1)$$

Let $I_n(\sigma) = \sigma_2(2^{n-1} - 1) + \sigma_3(2^{n-2} - 1) + \ldots + \sigma_n(2 - 1)$.

If all $\sigma_i = 0$, $i = 2, 3, \ldots, n$; we obtain $\mathcal{N}_n(C_\infty) = 2^{n+1} + 2^n - 3 + n$

$$D_B(C_\infty) = \lim_{n\to\infty} \frac{\ln(\mathcal{N}_n(C_\infty))}{\ln(2^n)} = \lim_{n\to\infty} \frac{\ln(2^{n+1} + 2^n - 3 + n)}{n \ln(2)} = 1$$

If all $\sigma_i = 1$, then $I_n(\sigma) = (2^{n-1} - 1) + (2^{n-2} - 1) + \ldots + 1$

$$= 2^{n-1} + 2^{n-2} + \ldots - n + 1 \quad \ldots\ldots(9)$$

$$2\, I_n(\sigma) = 2^n + 2^{n-1} + \ldots - 2n + 2 \quad \ldots\ldots(10)$$

Now, upon subtracting (9) from (10), yields $I_n(\sigma) = 2^n - n + 1$

So $D_B(C_\infty) = \lim_{n\to\infty} \frac{\ln(\mathcal{N}_n(C_\infty))}{\ln(2^n)} = \lim_{n\to\infty} \frac{\ln(2^{n+2} - 2)}{n \ln(2)} = 1$

Hence $D_B(C_\infty) = 1$, for all cases. Therefore, the dimension of the condensation set C_∞ of A_0 with respect to $\{ R^2; \omega_1\}$ is 1.Thus, $D_B(A_0) = D_B(C_\infty) = 1$.

Theorem 4: The dimension of the condensation set C_∞ of $A_0 \in \mathcal{H}(X)$ with respect to the IFS $\{X; \omega_1\}$ is equal to the dimension of A_0.

Proof: Let $A_0 \in \mathcal{H}(X)$ and has the dimension $D_B(A_0) = \lim_{n\to\infty} \frac{\ln(\mathcal{N}_n(A_0))}{\ln(2^n)}$,

and consider C_∞ to be the condensation set of A_0, with respect to the IFS $\{X; \omega\}$. Let the dimension of C_∞ is :$D_B(C_\infty) = \lim_{n\to\infty} \frac{\ln(\mathcal{N}_n(C_\infty))}{\ln(2^n)}$ Since A_0 is a subset of C_∞, $D_B(A_0) \le D_B(C_\infty)$.

Now, to count the dimension of C_∞ by using the box-counting theorem, we take

$\varepsilon = (1/2)^n$, $n = 0, 1, \ldots$

N	ε	$\mathcal{N}_n(A_0)$	$\mathcal{N}_n(C_\infty)$
N	$(1/2)^n$	$\mathcal{N}_n$	$\sum_{i=0}^{n} \mathcal{N}_i(A_0)$

$$S_n = \mathcal{N}_0A_0) + \mathcal{N}_1A_0) + \ldots + \mathcal{N}_n(A_0)$$

$$\leq (n+1)\,\mathcal{N}_n(A_0), \text{where:} \mathcal{N}_0(A_0) < \mathcal{N}_1(A_0) < \ldots < \mathcal{N}_n(A_0),$$

so that: $D_B(C_\infty) = \lim_{n\to\infty} \frac{\ln(\mathcal{N}_n(C_\infty))}{\ln(2^n)}$

$$= \lim_{n\to\infty} \frac{\ln(\sum_{i=0}^{n} \mathcal{N}_i(A_0))}{\ln(2^n)} \leq \lim_{n\to\infty} \frac{\ln((n+1)\mathcal{N}_n(A_0))}{n\ln(2)} +$$

$\lim_{n\to\infty} \frac{\ln(\mathcal{N}_n(A_0))}{n\ln(2)} = D_B(A_0).$

Hence $D_B(C_\infty) \leq D_B(A_0)$. Therefore we have :$D_B(C_\infty) = D_B(A_0)$. ■

REFERENCES

1)Barnsley,M.F."Fractals Every Where"Academic Press,Inc.,New York (1993).

2)Gulick,D.,"Encounters with Chaos",(1992) McGraw-Hill, Inc.

3)Salamat,S.and Taylor J.H.,"Chaos in Nonlinear Dynamical Systems", University of New Brunswiek, Fredericton; N. B., Canada, E3B 5A3, (2001).

4)Sarraille,"Developing Algorithms for Measuring Fractal Dimension" , Notes by J. J. Sarraille, June 14/02-1/10,(2002).

Supercyclic And Cyclic Sequences Of Operators

Arwa Nazar Mustafa
AL-Mustansiriya University , College of Science ,Department of Mathematic

الخلاصة

لقد قمنا في هذا البحث بتعريف المتتابعة الدورية الفائقة والمتتابعة الدورية وبرهان بعض النظريات عليها .

ABSTRACT

In this paper we define a supercyclic sequence of operators and cyclic sequence of operators and we prove some theorems about them .

INTRODUCTION

Let X be a Banach space and Let $\{T_n\}_{n\in N}$ be a sequence of operators (bounded linear transformation) on X.

A vector x $\in$ X is called hypercyclic for $\{T_n\}_{n\in N}$ if the set $\{T_n x\}_{n\in N}$ is dense in X. The sequence $\{T_n\}_{n\in N}$ is called hypercyclic if there is at least one vector hypercyclic for $\{T_n\}_{n\in N}$ (1) . We say that an operator T : X $\longrightarrow$ X is hypercyclic if the sequence of its iterates $\{T^n\}_{n\in N}$ is hypercyclic, (2).

Similarly, an operator T is said to be supercyclic if there exists a vector x $\in$ X such that the set $\{\lambda T^n x : \lambda \in C, n \in N\}$ is dense in X, (3). An operator T is said to be cyclic if there exists a vector x $\in$ X such that the linear span of $\{T^n x : n \in N\}$ is dense in X, or equivalently $\{\rho(T)x : \rho \text{ is a polynomial}\}$ is dense in X, (4) . It is clear that T is a hypercyclic operator if and only if $\{T^n\}_{n\in N}$ is hypercyclic . Also T is supercyclic if and only if $\{\lambda_{n_k} T^{n_k}\}$ is hypercyclic where $\{n_k\}_{k\in N} \subset N$ and $\{\lambda_{n_k}\}_{k\in N} \subset C$.

Saavedra and Muller in (5) proved that if $\{T_n\}_{n\in N}$ be a hypercyclic, then the set of all hypercyclic vectors for $\{T_n\}_{n\in N}$ is a $G_\delta - set$, where $G_\delta - set$ is a countable intersection of open sets,(4) . Mustafa , A . N in (6) proved that $\{T_n\}_{n\in N}$ has a dense $G_\delta - set$ of hypercyclic vectors if and only if for all non- empty open subsets U, V of X there is $n \in N$ such that $T_n(U) \cap V \neq \phi$ if and only if $\forall x, y \in X$ there is a sequence $\{x_k\}_{k\in N}$ in X, $\{n_k\}_{k\in N}$ *in* N such that $x_k \to x, T_{n_k} x_k \to y$ if and only if $\forall x, y \in X, \in > 0$ there is $n \in N$ and there is $z \in X$ such that $\|z - x\| < \in$ and $\|T_n z - y\| < \in$.

Remark: We denote by $B(x, \in)$ the neighborhood of x of radius $\in$

1- SUPERCYCLIC SEQUENCES OF OPERATORS

Definition : Let X be a Banach space and Let $\{T_n\}_{n\in N}$ be a sequence of operators on X. Then $\{T_n\}_{n\in N}$ is said to be supercyclic if there exists x $\in$ X such that $\{\alpha T_n x : n\in N, \alpha \in C\}$ is norm dense in X, and such a vector x is called a supercyclic vector for $\{T_n\}_{n\in N}$.

Remark: T is supercyclic if and only if $\{T^n\}$ is supercyclic, since T is supercyclic if and only if there is $x\in X$ such that $\{\alpha T^n x : n\in N, \alpha\in C\}$ is norm dense in X if and only if $\{T^n\}_{n\in N}$ is supercyclic.

Proposition 1: Let $\{T_n\}_{n\in N}$ be a supercyclic sequence of operators on the Banach space X. Then the set of all supercyclic vectors for $\{T_n\}$ is a $G_\delta - set$.

Proof : Let $\{U_i\}_{i\in N}$ be a countable base for the topology on X .The vector x is supercyclic for $\{T_n\}_{n\in N}$ if and only if $\{\alpha T_n x : n\in N, \alpha\in C\}$ is norm dense in X if and only if for all i ≥ 1 there is $n\in N, \alpha\in C$ such that $\alpha T_n x \in U_i$ if and only if for all i ≥ 1 $x\in T_n^{-1}(\frac{1}{\alpha}U_i)$ if and only if for all i ≥ 1 $x\in \bigcup_n T_n^{-1}(\frac{1}{\alpha}U_i)$ if and only if for all i ≥ 1, $x\in \bigcup_{\substack{\alpha\in c\\ \alpha\neq 0}}\bigcup_n T_n^{-1}(\frac{1}{\alpha}U_i)$ if and only if for all i $\geq$ 1, $x\in \bigcap_i(\bigcup_{\substack{\alpha\in C\\ \alpha\neq 0}}\bigcup_{n\geq 1} T_n^{-1}(\frac{1}{\alpha}U_i))$, therefore the set of all supercyclic vectors for $\{T_n\}_{n\in N}$ is $\bigcap_i(\bigcup_\beta\bigcup_n T_n^{-1}(\beta U_i))$.

Now, since T_n is a continuous function for each $n\in N$ and $U_i, i\geq 1$ is open in X, then $T_n^{-1}(\beta U_i)$ is open in X, therefore $\bigcap_i(\bigcup_\beta\bigcup_n T_n^{-1}(\beta U_i))$ is the intersection of a countable union of open sets, then it is $a\ G_\delta - set$.

The following theorem gives a characterization of the density of the set of supercyclic vectors for a sequence of operators $\{T_n\}_{n\in N}$.

Proposition 2 : Let $\{T_n\}_{n\in N}$ be a sequence of operators on the Banach space X . Then the following statements are equivalent:

1- $\{T_n\}_{n\in N}$ has a dense $G_\delta - set$ of supercyclic vectors.

2- For every non-empty open sets U,V in X, there are $n\geq 0$ and a non- zero $\alpha\in C$ such that $T_n(\alpha U)\cap V\neq\phi$.

3- For each $x,y\in X$, there exist sequences $\{x_k\}$ in X, $\{n_k\}$ in N, $\{\alpha_k\}$ in $C, \alpha_k\neq 0$ for all k such that $x_k\to x$ and $T_{n_k}(\alpha_k x_k)\to y$.

4- For each $x,y\in X, \in>0$, there is $n\in N$ and $z\in X$, a non- zero $\alpha\in C$ such that $\|z-x\|<\in$ and $\|T_n(\alpha z)-y\|<\in$.

Proof : (1) $\to$ (2)

Let U,V be a non–empty open subsets of X. By (1) there is a supercyclic vector x for $\{T_n\}_{n\in N}$ such that $x\in U$, and since x is supercyclic vector for $\{T_n\}_{n\in N}$, then *thereis* $n\in N,\alpha\in C$ such that $T_n x\in V$, then $T_n(\alpha x)\in V$, thus $T_n(\alpha U)\cap V\neq\phi$.

(2) → (3)

Let $x,y\in X$, Let $B_1=B(x,1),B_1'=B(y,1)$, by (2) there is $n_1\in N,\alpha_1\in C$ such that $T_{n_1}(\alpha_1 B_1)\cap B_1'\neq\phi$, then there is $x_1\in B_1$. Such that $T_{n_1}(\alpha_1 x_1)\in B_1'$ Now , Let $B_2=B(x_1,\frac{1}{2})$, $B_2=B(y,\frac{1}{2})$, by (2) there is $n_2\in N,\alpha_2\in C$ *such that* $T_{n_2}(\alpha_2 B_2)\cap B_2'\neq\phi$ then there is $x_2\in B_2$ such that $T_{n_2}(\alpha_2 x_2)\in B_2'$ ..... and so on. Therefore we get sequences $\{x_k\}$ in X *such that* $x_k\in B_k$ $\forall k\geq 1$, and $\{n_k\}$ in N, $\{\alpha_k\}$ in C *suchthat* $T_{n_k}(\alpha_k x_k)\in B_k'$ *forall* $k\geq 1$.

Hence $\|x_k-x\|<\frac{1}{k}$ and $\|T_{n_k}(\alpha_k x_k)-y\|<\frac{1}{k}$ .Then we get $x_k\to x$ and $T_{n_k}(\alpha_k x_k)\to y$ as $k\to\infty$.

(3) → (1)

Let $\{U_n\}_{n\in N}$ be a basis for the topology on X. For a fixed n in N and α in C , Let $y\in X$ and $x_n\in U_n$, then for all n ∈ N there is a sequence $\{x_n\}$ in X, $\{n_k\}$ in N, $\{\alpha_k\}$ in C such that $x_k\to y$ and $T_{n_k}(\alpha_k x_k)\to x_n$, therefore for all large k, $T_{n_k}(\alpha_k x_k)\in U_n$,*hence* $x_k\in T_{n_k}^{-1}(\frac{1}{\alpha_k}U_n)$ then $x_k\in\bigcup_{n_k}T_{n_k}^{-1}(\frac{1}{\alpha_k}U_n)$ for all large k , and for all $n\in N$.

Therefore there is a subsequence $\{x_k'\}$ of $\{x_k\}$ such that $x_k'\in\bigcup_k T_{n_k}^{-1}(\beta_k U_n)$ and $x_k'\to y$. Then $\bigcup_k T_{n_k}^{-1}(\beta_k U_n)$ is dense in X, and since T is continuous ,then $T_{n_k}^{-1}(\beta_k U_k)$ is open, , $\bigcup_k T_{n_k}^{-1}(\beta_k U_n)$ is open and by Bair's Category theorem[5], $\bigcap_n(\bigcup_k T_{n_k}^{-1}(\beta_k U_n))$ is dense in X, then from proposition (1) the set of all supercyclic vectors for T is dense in X, then it is a dense $G_\delta-set$.

(2) → (4)

Let $x,y\in X$, and Let $B(x,\in)=U,B(y,\in)=V$, then U,V are non- empty open subsets of X. Thus by (2) there is $n\in N,\alpha\in C\ni T_n(\alpha U)\cap V\neq\phi$, then there is $z\in U$ such that $T_n(\alpha z)\in V$ and hence $\|z-x\|<\in$, $\|T_n(\alpha z)-y\|<\in$.

(4) → (2)

Let U,V be non- empty open subsets of X, then there is $x\in U,y\in V$ .Let $\in>0$ by (4) there is $n\in N,z\in X$, such that $\|z-x\|<\in,and\|T_n(\alpha z)-y\|<\in$ then $z\in U,T_n(\alpha z)\in V$ and hence $T_n(\alpha U)\cap V\neq\phi$.

2-CYCLIC SEQUENCES OF OPERATORS

Definition : Let $\{T_n\}_{n\in N}$ be a sequence of operators on Banach space X, then $\{T_n\}$ is said to be cyclic if there is $x\in X$ such that the linear span of $\{T_1x,T_2x,T_3x.....\}$ is dense in X, and such a vector x is called a cyclic vector for $\{T_n\}_{n\in N}$.

Remark : The operator T is cyclic if and only if there is $x\in X$ such that the linear span of $\{x,Tx,T^2x,.....\}$ is dense in X if and only if $\{T^n\}$ is cyclic sequence.

Notice that every hypercyclic sequence of operators is supercyclic sequence and then it is cyclic sequences.

Proposition 1: The set of all cyclic vectors for $\{T_n\}$ is a $G_\delta - set$.

Proof : Let $\{U_i\}_{i\in N}$ be a countable base for a topological on X. The vector x is cyclic for $\{T_n\}$ if and only if the (linear span of$\{T_1x,T_2x,T_3x,...\}$ $)=S$ is dense in X if and only if there is an element $sx\ in\ S$ such that $sx\ in\ U_i$ for all i if and only if $x\in s^{-1}(U_i)$ if and only if $x\in\bigcup_s s^{-1}(U_i)$ if and only if $x\in\bigcap_i\bigcup_s s^{-1}(U_i)$

Since $U_i\ open$ for all i and s continuous $,s^{-1}(U_i)\ open\ ,\bigcup_s s^{-1}(U_i)$ open then $\bigcap_i(\bigcup_s s^{-1}(U_i))$ is a countable intersection of open set then it is a $G_\delta - set$.

Remark : In the fowloing proposition Let the (linear span of (T_1 , T_2 , ...)) = S

Proposition 2: Let $\{T_n\}$ be a sequence of operators on the Banach space X, then the following are equivalent :

1) $\{T_n\}$ has a dense set of cyclic vectors.

2) For any pair of non- empty open sets W ,V there exists an $s\in S$ such that $s(W)\cap V\neq\phi$

3) For each $x,y\in X$, there exist sequences $\{x_k\}_{k\in N}$ in X and $\{s_k\}$ in S such that $x_k\to x\ \ and\ s_kx_k\to y$.

4) For each $x,y\in X$ and each neighborhood W for zero in X, there is $z\in X$ such that $z-x\in W and\ sz-y\in W$ were s $\in$ S

Proof: (1) $\to$ (2)

Let W ,V be non-empty open subsets of X then $\bigcap_i(\bigcup_s s^{-1}(U_i))$ is the set of all cyclic vectors for $\{T_n\}_{n\in N}$ (see proposition (1)) , then $\bigcap_i(\bigcup_s s^{-1}(U_i))$ is dense in X (by (1)),thus $\bigcup_s s^{-1}(U_i)$ is dense in X for all $n\in N$

Now assume that for each $s\in S\ ,s(W)\cap V=\phi,then\ W\cap s^{-1}(V)=\phi$, but $V=\bigcup U_m\in\{U_i\}_{i\in N}$

Therefore $W\bigcap s^{-1}(U_m)=\phi,W\bigcap[\cup s^{-1}(U_m)\ ]=\phi$ which is a contradiction with the density of $\bigcup_s s^{-1}(U_i)$.

(2) → (3)

Let $x, y \in X$, Let $B_1 = B(x,1)$ and $B_1' = B(y,1)$, by (2) *there is* $s_1 \in S$ *such that* $s_1(B_1) \cap B_1' \neq \phi$, then there is $x_1 \in B_1$ .such that $s_1 x_1 \in B_1'$.

Now , Let $B_2 = B(x,1/2)$, $B_2' = B(y,1/2)$, by (2)there is $s_2 \in S$ such that $s_2(B_2) \cap B_2' \neq \phi$,then there is $x_2 \in B_2$ such that $s_2 x_2 \in B'$ … and so on.

Therefore we get sequences $\{x_k\}$ in X, $x_k \in B_k$ for all k ≥ 1 and $\{s_k\}$ in S such that $s_k x_k \in B_k'$ for all k ≥ 1 Then $\|x_k - x\| < 1/k$ and $\|s_k x_k - y\| < 1/k$, then we get $x_k \to x$ *and* $s_k x_k \to y$ as $k \to \infty$.

(3) → (1)

Let $\{U_i\}_{i \in N}$ be a basis for the topology on X.

We want to prove that $\bigcap_i [\bigcup_S s^{-1}(U_i)]$ is dense in X.

For a fixed i, Let $y \in X$ and $x_i \in U_i$, by (3) there is sequences $\{x_k\}$ in X and $\{s_k\}$ in S *such that* $x_k \to y$ *and* $s_k x_k \to x_i$ therefore for all large K, $s_k(x_k) \in U_i, x_k \in s_k^{-1}(U_i)$ then $x_k \in \bigcup_{s_k \in S} s_k^{-1}(U_i)$ for all large ℓ, therefore there is a subsequence $\{x_k'\}$ of $\{x_k\}$*such that* $x_k' \in \bigcup_{s_k \in S} s_k^{-1}(U_i)$ and $x_k' \to y$ Then $\bigcup_{s_k \in S} s_k^{-1}(U_i)$ is dense in X, and since s_k is continuous thus $s_k^{-1}(U_i)$ is open, then $\bigcap_i [\bigcup_{s \in S} s^{-1}(U_i)]$ is dense in X (from Baire Category theorem).

Then the set of all cyclic vectors for $\{T_n\}_{n \in N}$ dense in X (from proposition (1))

(3) → (4)

Let $x, y \in X$ and W be a neighborhood of zero in X, by (3) there is sequences $\{x_\ell\}$ in X, $\{s_\ell\}$ in S such that $x_\ell \to x$ *and* $s_\ell x_\ell \to y$ .Let $\epsilon > 0$ then there is k > 0 such that $\|x_k - x\| \leq \epsilon$ and $\|s_k x_k - y\| < \epsilon$ *for all* $k > \ell$,thus, since W is a neighborhood of zero, there is $\ell \in N$ such that $x_\ell - x \in W$ and $s_\ell x_\ell - y \in W$. Hence we get $z - x \in W$ and $s_\ell z - y \in W$ by taking $z = x_\ell$

(4) → (3)

Let $x, y \in X$, $B_1 = B(0,1)$, by (4) there is $x_1 \in X, s_1 \in S$ such that $x_1 - x \in B_1$ and $s_1 x_1 - y \in B_1$ Let $B_2 = B(0,1/2)$ by (4) there is $x_2 \in X, s_2 \in S$ such that $x_2 - x \in B_2$ and $s_2 x_2 - y \in B_2$ …. and so on. Then we get sequences $\{x_k\}$ in X, $\{s_k\}$ in S such that $x_k - x \in B_k$ and $s_k x_k - y \in B_k$ for all k Then, $\|x_k - x\| < 1/k$, and $\|s_k x_k - y\| < 1/k$, and

Hence $x_k \to x$ *and* $s_k x_k \to y$ *as* $k \to \infty$.

REFERENCES

1. BermuDez, T., Bonilla, A. and Peris, A. ,"On hypercyclicity and supercyclicity criteria", Bull. Aust. Math. Soc.70: 45-54,(2004)
2. Beauzamy, B.," Introduction to operator theory and invariant subspaces" Elsevier science publishers B.V. (1988).
3. Hilden, H. M. and Wallen, L. J.,"Some cyclic and non-cyclic vectors of certain operators", Indiana University Mathematics J.23(7): 557-565, (1974).
4. Halmos,P.R.," A Hilbert space broplem book"springe- verlag. New York Heidelberg Berlin .
5. Mukherjea , A. , and pothorem ,K.," Real and functional analysis"Pleum press . new York and London (1978) .
6. Mustafa , A.N. ," chaotic polynomials on Banach spaces"Ph. D. thesis , University of AL-Mustansyiriah (2006).

Fixed Piont Theorem For k- Set Contractive Mapping

Eman Mohmmed Nemah
Department of Mathematics/College of Eduction (Ibn Al-Haitham)/University of Baghdad.

الخلاصة

الهدف من هذا البحث هو دراسة قياس المجموعات غير المرصوصه والدوال الأنكماشيه من نمط المجموعة- k والمعرفة على فضاء بناخ. وتحديد مبرهنات النقطة الصامدة للدوال الأنكماشيه من نمط المجموعة- k
تتائجنا جديدة وتمثل اثبات ذو معنى للنتائج المعروفة سابقا. بعض الحالات الخاصة تمت مناقشتها.

ABSTRACT

The objective of this paper to study the measure of noncompactness and obtain a fixed point theorem for k-set contractive mapping of Banach space. Our results are new and reprsents a signitfiant improvement of previously known results. Some special cases are discussed.

INTRODUTION AND PRELIMINARY DEFINITIONS

Fixed point theorem have been a major theoretical toll in the fields of differential equations, topology, economics, game theory, dynamics, optical control and functional analysis. Moreover the usefulness of the concept for applications for computing fixed point.

Historically, Darbo (1), was the first to show the special case of k-set contractive mapping $0 \le k < 1$, defined on a nonempty closed bounded convex subset of a Banach space has a fixed point. As well as, Sadovskii (2), was prove that every condensing mapping defined on a nonempty closed bounded convex subset of a Banach space has a fixed point. And Jimene (3), was show a fixed point theorem for condensing mapping under a new condition. Later, Neela (4), was show a fixed point theorem for a condensing mapping defined on a closed convex subset of a Banach space under various boundary conditions.

Throughout this paper X will be a Banach space, C is a nonempty closed bounded convex subset of X and T:C→C is k- set contractive mapping. We begin with following known:

In section two of this paper we prove a fixed point theorem for a k-set contractive mapping ($k > 0$) which defined on a closed bounded convex subset of a Banach space and then we prove another one for the sum of two mappings, where the first one is compact mapping and the second is k- set contractive mapping. Also, section three, includes a theorem for k-set contractive mapping defined on a closed convex subset of a Banach space under various boundary conditions. The following theorem is given in (4),

Let X be a Banach space, C convex subset of X, U an open subset of C and $p \in U$. Suppose that $T : \overline{U} \to C$ is a continuous compact map. Then

i. T has a fixed point in $\overline{U}$ or

ii. there is $u \in \partial U$ (boundary of U in C) and $\lambda \in (0,1)$ with $u = \lambda T(u) + (1-\lambda)p$.

In this section also we prove the above theorem in which U need not be boundary and T is k-set contractive mapping. We also replace the above boundary condition by other equivalent condition to prove the same result. In section four

of this paper we exam the behavior of k-set contractive mapping defined on $\overline{B_s}$ (the close ball of radius s and center 0) with values in real Hilbert space X. In particular we prove Leray- Schauder(5, p.245), type for k-set contractive mapping.

Now, we introduce our notations and definitions:

Definition 1.1. (6) Let C be a bounded subset of a metric space X Define the measure of non compactness $\alpha[C]$ of C by

$\alpha[C]$=inf $\{\varepsilon > 0$: C can be covered by finitely many sets of diameter $\leq \varepsilon\}$

Proposition 1.1. (6) Let X be a Banach space. Then for all bounded subsets A, $A_1, \ldots, A_n$ and B of X we have the following results.

i- $\alpha[A] = 0$ if and only if $\overline{A}$ is compact where $\overline{A}$ is closure of A

ii- $\alpha[A] \leq \alpha[B]$ whenever $A \subseteq B$

iii- $\alpha[A+B] \leq \alpha[A] + \alpha[B]$

iv- $\alpha[A] = \alpha[\overline{A}]$

v- $\alpha\left[\bigcup_{i=1}^{n} A_i\right] = \max\{\alpha[A_1], \ldots, \alpha[A_n]\}$

vi- $\alpha[A] = \alpha[co(A)] = \alpha[\overline{co}(A)]$ where $co(A)$ is closed convex hall of A

Definition 1.2. (3) Let $T: X \to X$ be a continuous mapping of a Banach space X. For all $A \subset X$ with A bounded set

i. If $\alpha[T(A)] \leq k\alpha[A]$, $0 < k < 1$, then T is a k-set contraction mapping.

ii. If $\alpha[T(A)] < \alpha[A]$, for all $\alpha[A] > 0$, then T is condensing mapping.

iii. If $\alpha[T(A)] < k\alpha[A]$, $k > 0$, $\alpha[A] > 0$ then T is a k-set contractive mapping

(i.e., $\alpha[T(A)] < k\alpha[A]$, for all k>o, $\alpha[A] > 0$ and $\alpha[T(A)] = \alpha[A]$, if $\alpha[A] = 0$).

Obviously, every k-set contraction with o<k<1 is k-set contractive and thus, every condensing is k-set contractive.

Definition 1.3.(5, p.756) A subset C of a topological space X is called a relatively compact if $\overline{C}$ is compact.

Definition 1.4.(3) Let X and Y be Banach spaces. A mapping $T: X \to Y$ is called compact if and only if T is continuous and T maps of bounded set into relatively compact set.

Definition 1.5. (6) Let (X, d) be a metric space with C$\subseteq$X. A mapping $T: C \to X$ is nonexpansive if T satisfies

d(T(x), T(y))$\leq$ d(x, y) for all $x, y \in C$

We remark that a nonexpansive map is also a 1- set contractive.

MAIN RESULT

Theorem 2.1. Let C be a nonempty closed bounded convex subset of a Banach space X, $T: C \to C$ is a k-set contractive mapping ($k > 0$). Then T has a fixed point in C.

Proof: The proof is based on the following simple idea construct a subset B of C which is mapping into itself by T in such a way that the Schauder's fixed point

theorem can be applied to restriction $T:B\to B$. The resulting fixed point a trivially a fixed point of the original mapping $T:C\to C$.

Choose a point $m\in C$ and let $\sum$ denoted the system of all closed convex subset K of C for which $m\in K$ and T(K)$\subseteq$K. Also set

$$B=\bigcap_{K\in\sum} K,\quad S=\overline{co}\{T(B)\bigcup\{m\}\}.$$

$\sum\neq\varnothing$ since $C\in\sum$ (C subset of C with $m\in C$ and T(C)$\subseteq$C). And B$\neq\varnothing$ since $m\in K$ for all $K\in\sum$, $m\in\bigcap_{K\in\sum} K$, i.e., $m\in B$. As well as T(B)$\subseteq$B because: let

$y\in T(B)\to\exists x\in B$ s.t. $y=T(x)$

$$\Rightarrow x\in\bigcap\nolimits_{K\in\sum} k$$
$$\Rightarrow x\in K \quad \text{for all } K\in\sum$$
$$\Rightarrow y=T(x)\in T(K)\subseteq K$$
$$\Rightarrow y\in K \quad \text{for all } K\in\sum$$
$$\Rightarrow y\in\bigcap\nolimits_{K\in\sum} k=B$$

Since $m\in B$ and T(B)$\subseteq$B, implies $\{T(B)\bigcup\{m\}\}\subseteq B$, then

$$S=\overline{co}\{T(B)\bigcup\{m\}\}\subseteq B.$$

so that, S$\subseteq$B.This implies that $T(S)\subseteq T(B)\subseteq S$, so that $S\in\sum$, and hence $B\subseteq S$. Then $T(B)\subseteq S$, implies that $T(B)\subseteq B$. By (i), (v) and (vi) in proposition(1.1) implies that $\alpha[B]=\alpha[S]=\alpha[T(S)]$. Since T is k-set contractive, it follows that $\alpha[B]=0, implies\ \alpha[T(B)]=0, i.e., \overline{T(B)}$ compact, T(B) is relatively compact. Obviously B is also convex. Thus the Schauder s fixed point for the mapping $T:B\to B$. Δ

Corollary 2.1.[1. Dorbo Th.] Let C be a nonempty closed bounded convex subset of a Banach space X and $T:C\to C$ is k-set contraction mapping $(0<k<1)$. Then T has a fixed point.

Corollary 2.2.[2. Sadovskii Th.] Let C be a nonempty closed bounded convex subset of a Banach space X and $T:C\to C$ is condensing mapping. Then T has a fixed point.

Propsition 2.1. Let X be a Banach space, C be a nonempty subset of X and $T:C\to C$ be a compact mapping. Then T is k- set contractive mapping ($k>0$).

Proof: Let A be a bounded subset of C. Since T compact mapping. We have $\alpha[T(A)]=0$. Therefore we get $\alpha[T(A)]=0\le k\alpha[A], k>0$ for all bounded set A$\subset$C. Thus, T is k- set contractive mapping. Δ

Corollary 2.3.[5. Schauder s Th., p.56] Let C be a nonempty closed bounded convex subset of a Banach space X and $T:C\to C$ is a compact mapping. Then T has a fixed point.

Theorem 2.2. Let C be a nonempty closed bounded convex subset of a Banach space X and $T:C\to X$ is given by $T=T_1+T_2$ and have the property $T(C)\subseteq C$. If T_1

is k- set contractive mapping (k>0) and T_2 is compact mapping, then T has a fixed point in C.

Proof: Let A bounded subset of C, then

$$\begin{aligned}\alpha[T(A)] &= \alpha[(T_1+T_2)A] \\ &= \alpha[T_1(A)+T_2(A)] \\ &\le \alpha[T_1(A)]+\alpha[T_2(A)]\end{aligned}$$

Since T_2 is compact (maps bounded sets to a relatively compact set).We have $\alpha[T(A)]=0$. Therefore we get,

$\alpha[T(A)] \le \alpha[T_1(A)] < k\alpha[A], k>0$. which implies that T is k- set contractive mapping. Hence by Theorem (2.1), we have T has a fixed point in C. Δ

Corollary 2.4. (5. Theorem 11.B, p.501) Let C be a nonempty closed bounded convex subset of a Banach space X and $T,S:C\to X$ have the property $T(C)\subseteq C$. If T k- set contraction mapping $(0<k<1)$ and S is compact mapping, then T+S has a fixed point in C.

3.FIXED POINT RESULTS FOR K-SET CONTRACTIVE MAPPING

Theorem 3.1. Let X be a Banach space, C a nonempty closed convex subset of X, U an open subset of C and $p\in U$. Suppose $T:\overline{U}\to C$ is k-set contractive mapping $(k>0)$ with $T(\overline{U})$ is bounded set in C and $T|_{\partial U}=p$. Then T has a fixed point in $\overline{U}$.

Proof: Define a map N:C$\to$C by

$$N(x)=\begin{cases}T(x), & if\ x\in\overline{U}\\ p, & if\ x\in C\setminus\overline{U}\end{cases}$$

Now N:C$\to$C is bounded in C as $T(\overline{U})$ is bounded in C. To show N is k- set contractive map, let A be a bounded subset of C with

$$N(A)\subset T(\overline{U}\bigcap A)\bigcup\{p\}$$

We have that

$$\begin{aligned}\alpha[N(A)] &\le \alpha[T(\overline{U}\bigcap A)] \\ &\le \alpha[T(A)] \\ &< k\,\alpha[A]\ ,\ k>0\end{aligned}$$

Therefore N:C$\to$C is k- set contractive mapping. Hence by Theorem (2.1), there exists an x$\in$C with x=N(x). In fact x$\in$U since p$\in$U and therefore x=N(x)=T(x), i.e., T has a fixed point in C. Δ

Corollary 3.1.(4. Theorem 2.1) Let X be a Banach space, C a closed convex subset of X, U an open subset of C and $p\in U$. Suppose $T:\overline{U}\to C$ is condensing mapping with $T(\overline{U})$ is bounded set in C and $T|_{\partial U}=p$. Then T has a fixed point in $\overline{U}$.

Theorem 3.2. Let X be a Banach space, C a nonempty closed convex subset of X, U an open subset of C and $p\in U$. Suppose $T:\overline{U}\to C$ is k- set contractive mapping (k>0) with $T(\overline{U})$ is bounded set in C. Then either:

i. T has a fixed point in $\overline{U}$ or

ii.there is a $u \in \partial U$ and $\lambda \in (0,1)$ with $u = \lambda T(u) + (1-\lambda)p$.

Proof: Suppose (i) does not hold and T has no fixed pint on ∂U (otherwise we are finished). Then $u \neq \lambda T(u) + (1-\lambda)p$ for $u \in \partial U$ and $\lambda \in (0,1)$.

Consider

$B = \{ x \in \overline{U} : x = tT(x) + (1-t)p \text{ for some } t \in [0,1] \}$.

Since $p \in U$, $B \neq \varnothing$. Also the continuity of T implies that B is closed. And $B \bigcap \partial U = \varnothing$, hence by Urusohn's lemma, there exists a continuous map $\mu : \overline{U} \to [0,1]$ with $\mu(B) = 1$ and $\mu(\partial U) = 0$.

Let

$$N(x) = \begin{cases} \mu(x)T(x) + (1-\mu(x))p, & \text{if } x \in \overline{U} \\ p, & \text{if } x \in C \setminus \overline{U} \end{cases}$$

Now it is clear that N:C→C is continuous mapping and N(C) is bounded in C as $T(\overline{U})$ is

bounded in C. To show N is k- set contractive mapping, let A be a bounded subset of C with

$N(A) \subseteq \overline{co}(T(\overline{U} \bigcap A) \bigcup \{p\})$

We have that

$$\begin{aligned} \alpha[N(A)] &\leq \alpha[T(\overline{U} \bigcap A)] \\ &\leq \alpha[T(A)] \\ &< k\,\alpha[A], \; k > 0 \end{aligned}$$

Therefore N:C→C is k- set contractive mapping. Hence by Theorem (2.1), there exists an $y \in C$ with y=N(y). But N(y)=p, if $y \in C \setminus \overline{U}$ and so $y \in \overline{U}$. Thus

$$y = N(y) = \mu(y)T(y) + (1-\mu(y))p.$$

It follows that $y \in B$. Since $\mu(B) = 1$, we get $\mu(y) = 1$. This implies that y=T(y). i.e., T has a fixed point in C. Δ

Corollary 3.2.(7. Theorem 5.1, p.48) Let X be a Banach space, C a nonempty closed convex subset of X, U an open subset of C and $p \in U$. Suppose $T : \overline{U} \to C$ is compact.Then either:

i. T has a fixed point in $\overline{U}$ or

ii.there is a $u \in \partial U$ and $\lambda \in (0,1)$ with $u = \lambda T(u) + (1-\lambda)p$.

4.THE BEHAVIOR OF K-SET CONTRACTIVE IN $\overline{B_s}$

We now examine the behavior of k- set contractive mapping defined on $\overline{B_s}$ (the close ball of radius s and center 0) with values in Banach space X. In particular we prove nonlinear alternatives of Leray- Schauder[5, p.245], type for k- set contractive mappings.

Theorem 4.1. Let X be a Banach space and $\overline{B_s} = \{x \in X : \|x\| \leq s\}$ with s>0. Then each k- set contractive mapping (k>0) $T : \overline{B_s} \to X$ has at least one of the following two properties:

i. The set of fixed point of T in $\overline{B_s}$ is nonempty,

ii.there is a $B \subseteq \partial \overline{B_s}$ and $\lambda \in (0,1)$ with $B = \lambda T(B)$.holds.

Proof: Define a retraction mapping r: $X \to \overline{B_s}$ by:

For any subset A of X

$$r(A)=\begin{cases} A & if\ \alpha[A]\le s \\ s\dfrac{A}{\alpha[A]} & if\ \alpha[A]>s \end{cases}$$

r is k- set contractive, because for any bounded subset A of $\overline{B_s}$,

$$\alpha[r(A)]=\begin{cases} \alpha[A]<k\alpha[A], & if\ \alpha[A]\le s \\ \alpha[s\dfrac{A}{\alpha[A]}]\le\alpha[A]<k\alpha[A], & if\ \dfrac{s}{\alpha[A]}<1, \end{cases}$$

As result $r\circ T:\overline{B_s}\to\overline{B_s}$ is k- set contractive because, for any bounded subset A of $\overline{B_s}$,

$$\alpha[(r\circ T)A]=\alpha[r(T(A))]$$
$$<k\alpha[r(A)]<k^2\alpha[A],\quad k^2>0 \text{ and } k^2 \text{ constant.}$$

Therefore $r\circ T$ is k- set contractive mapping on a nonempty closed convex bounded subset $\overline{B_s}$ of Banach space X. By theorem (2.1), the set of fixed point of T in $\overline{B_s}$ is nonempty, i.e., there exists set of fixed point of T in $\overline{B_s}$ say B with $r\circ T$ (B)=B, then $r(T(B))=B$. If $T(B)\subseteq\overline{B_s}$, so that $B=r(T(B))=T(B)$ and T has a fixed point, that is (i) occurs.

If does not belong to $\overline{B_s}$ then B=$r(T(B))=s\dfrac{T(B)}{\alpha[T(B)]}=\lambda T(B)$ with $\lambda=\dfrac{s}{\alpha[T(B)]}<1$, i.e., B=$\lambda T(B)$. That is, (ii) occurs, since $B\subseteq\partial\overline{B_s}$. Δ

It is easy to put condition on T to guarantee that the second possibility (ii) in the previous theorem does not occur:

Theorem 4.2. Let X be a Banach space and $T:\overline{B_s}\to X$ be k- set contractive mapping (k>0). Suppose for all bounded subset A of $\overline{B_s}$ one of the following condition hold:

i. $\alpha[T(A)]\le\alpha[A]$

ii. $\alpha[T(A)]\le\alpha[A-T(A)]$

iii. $(\alpha[T(A)])^2\le(\alpha[A])^2-(\alpha[A-T(A)])^2$.

Then the set of fixed point of T in $\overline{B_s}$ is nonempty.

Proof: If T has no a fixed point, then by theorem (4.1), there exists a $A\subseteq\partial\overline{B_s}$ and $\lambda\in(0,1)$ with $A=\lambda T(A)$.(In particular T(A)$\neq\varnothing$) and

i. $\alpha[T(A)]\le\alpha[A]=\alpha[\lambda T(A)]=|\lambda|\alpha[T(A)]$,

Since $\lambda<1$. Then this is a contradiction.

ii. $\alpha[T(A)]\le\alpha[A-T(A)]$

$$=\alpha[\lambda T(A)-T(A)]$$
$$=\alpha[(\lambda-1)T(A)]$$
$$=|1-\lambda|\alpha[T(A)],$$

Since $\lambda-1<1$. Then this is a contradiction.

iii. $(\alpha[A])^2-(\alpha[A-T(A)])^2=(\alpha[\lambda T(A)])^2-(\alpha[\lambda T(A)-T(A)])^2$

$=(\alpha[\lambda T(A)])^2-(\alpha[(\lambda-1)T(A)])^2$

$=\lambda^2(\alpha[T(A)])^2-(\lambda-1)^2(\alpha[T(A)])^2$

$=(\lambda^2-\lambda^2+2\lambda-1)(\alpha[T(A)])^2$

$=(2\lambda-1)(\alpha[T(A)])^2$

Since $(\alpha[T(A)])^2\le(\alpha[A])^2-(\alpha[A-T(A)])^2$, then $(\alpha[T(A)])^2\le|2\lambda-1|(\alpha[T(A)])^2$. Therefore $|2\lambda-1|\ge 1$. Then this is a contradiction. Δ

REFERENCES

1. Darbo G., "Punti Unitti in transformation a condominio non compatto", Rend. Sem. Univ. Paduo, 24, : 84-92, (1955).
2. Sadovskii, "On a Fixed Point Principle", Analizi Prilozen, 1, :74-76, (1967).
3. Jimenes- Melado A. and Claudio H.M., "Fixed point theorems under the Interior Condition", Proc. Amer. Soc., 8, : 501-597, (2005).
4. Neela S., "Some Fixed Point Theorems for Non Self Maps", Int. Journal of Math. Analysis, 1, (28):1389-1395 (2007).
5. Zeilder F., "Nonlinear Functional Analysis and Applications (Fixed Point Theorem)", Springer Verlag New York Ine., (1986).
6. Kim E.S. and Kirk W.A., "A not on Picard Iterates of Nonexpansive Mapping", Annaless Polonicl Mathematical LXXXV,3, : 189-196,(2001).
7. Agarwal R.P., Maria Meehan and Regan D.O., "Fixed point theory and applications", Cambridge University Press, (2001).

A note on Baer and Quasi-Baer modules

Mehdi S. Abbas, Ali H. AL-Saedi
Department of Mathematics; College of Science; Mustansiriya University

الخلاصة

أعطينا تمييزيات جديدة لمقاسات بير و شبه – بير . درسنا مركبات الجمع لمقاسات (شبه -) بير و أعطينا الشرط الكافي الذي يجعل مركبات الجمع لمقاسات (شبه -) بير تمتلك خاصية (شبه -) بير. كذلك عممنا بعض النتائج من نظرية الحلقات إلى نظرية المقاسات. درسنا حلقة التشاكلات لمقاسات بير و شبه – بير وبينا : إذا كان المقاس شبه – انغماري فأن المقاس يكون بير إذا و فقط اذا كانت حلقته التشاكلية هي حلقة فان نيومان المنتظمة. كذالك بينا إذا كانت الحلقة التشاكلية للمقاس هي حلقة موسعة فأن المقاس بير إذا و فقط إذا كانت حلقته التشاكلية غير شاذة. بالإضافة الى ذلك بينا إذا كانت الحلقة التشاكلية للمقاس ليس لها مجموعه غير منتهية من العناصر المحايدة غير الصفرية فأن المقاس يكون بير إذا و فقط إذا كانت حلقته التشاكلية هي حلقة ريكارت.

ABSTRACT

We give new characterizations of Baer and quasi-Baer modules. We study the direct sums of (quasi-)Baer modules and we give a sufficient condition under which the direct sums of (quasi-)Baer modules has the (quasi-)Baer property. Also we extended some results from the rings theory to the modules theory. We study the endomorphism ring of Baer and quasi-Baer modules and we show that : If M is a quasi-injective R-module . Then M is Baer iff $S = End_R(M)$ is Von Neumann regular ring. Also we show that if M is an R-module whose endomorphism ring $S = End_R(M)$ is extending, then M is Baer iff S is right nonsingular ring. As another we show that if M is an R-module such that $S = End_R(M)$ has no infinite set of non-zero orthogonal idempotents. Then M is Baer iff S is right Rickart ring.

Keywords : Baer and quasi-Baer modules and rings.

INTRODUCTION AND SOME DEFINITIONS

Throughout this paper, R will denote an associative ring with identity, The modules are unital right modules and denoted by M and its endomorphism ring by $S = End_R(M)$. In (1) Kaplansky introduced Baer rings (i.e., rings in which the right annihilator of every nonempty subset is generated (as a right ideal) by an idempotent) to abstract various properties of rings of operators on Hilbert spaces. In (2), Clark introduced quasi-Baer rings (i.e., rings in which the right annihilator of every right ideal is generated (as a right ideal) by an idempotent. which are generalizations of Baer rings and used them to characterize a finite dimensional twisted matrix units semigroup algebra over an algebraically closed field. The study of Baer and quasi-Baer rings has its roots in functional analysis. In (3), Those two definitions generalize to the module theoretical setting by C. S. Roman as following : A right R-module M is called a (quasi-)Baer module if for each left (two sided) ideal I of $S = End_R(M)$, $r_M(I) = eM$ for $e^2 = e \in S$. Equivalently, for each submodule (fully invariant submodule) N of M, $l_S(N) = Se$ for $e^2 = e \in S$. A module is said to have the summand intersection property (SIP) if the intersection of any two direct summands of M is a direct summand. A module is said to have the strong summand intersection property (SSIP) if the intersection of any family of direct summands of M is a direct summand(4). A module M is called monoform, if for each non-zero submodule N of M and nonzero R-homomorphism $\alpha : N \to M$, α is monomorphism. Equivalently, for each non-zero submodule N of M is rational,(i.e. $\forall\ x,y \in M, x \neq 0$, there is $(0 \neq) r \in R$ such that $xr \neq 0$ and $yr \in N$) (5). A module M is called fully stable, if for

each submodule N of M and R-homomorphism $\alpha : N \to M$, $\alpha(N) \subseteq N$ (6). A module M is called abelian if all idempotent endomorphisms are central (i.e., commute with any endomorphism) (3). A module M is called a cogenerator, if for any R-module A, $\mathbf{0} = \bigcap_{\varphi \in Hom_R(A,M)} Ker\varphi$ (7). A module M is called quasi-injective if every submodule N of M and homomorphism $f : N \to M$ there exists a homomorphism $g : M \to M$ such that $g_{|N} = f$, i.e., $g(n) = f(n)$ $\forall n \in N$ (8). A submodule N of a module M is called closed in M if it has no proper essential extension in M (8). A module M is called extending if every submodule of M is essential in a direct summand (or, equivalently, each closed submodule of M is a direct summand) (8). A module M is Quasi Dedekind if for each nonzero R-endomorphism of M is a monomorphism (9). An idempotent $e \in R$ is called left (respectively, right) semicentral if $xe = exe$ (respectively, $ex = exe$), for all $x \in R$. The set of all left (respectively, right) semicentral of R dented by $S_l(R)$ (respectively, $S_r(R)$)(10). A ring R is called right (respectively left) semihereditary if every finitely generated right (respectively left) ideal of R is projective (8). A ring R is called right (respectively left) Rickart if every cyclic right (respectively left) ideal of R is projective . Equivalently, the right(respectively left) annihilator of any element of R is a generated as a right (respectively left) ideal by an idempotent of R (8). An element $m \in M$ is called a singular element of M if the right ideal $r_R(m)$ is essential in R_R. The set of all singular element of M denoted by $Z(M)$. M_R is called a nonsingular (resp. singular) module if $Z(M) = \mathbf{0}$ (resp. $Z(M) = M$). In particular, R is called right nonsingular if $Z(R_R) = \mathbf{0}$. Left nonsingular ring are defined similarly, and "nonsingular ring" shall mean a ring that is both right and left nonsingular (8) . Finally, $N \leq M$ means N is a submodule of M ; $N \leq^{e} M$ means N is essential in M; $N \leq^{c} M$ means N is closed in M; $N \leq^{\oplus} M$ means N is direct summand of M; N (M means N is fully invariant submodule of M (i.e. $\forall$ $\alpha \in End_R(M)$, $\alpha(N) \subseteq N$); N ($^{\#}$ M, where # stands, respectively, for e, c and $\oplus$ means N is fully invariant and essential, closed and respectively direct summand of M.

1. BAER MODULES

Firstly, we start with the following result.

Theorem (1.1) : *An R-module M is Baer iff for each family $\{\alpha_\lambda\}_{\lambda \in \Lambda}$ of endomorphisms of M, where Λ be an index set, $\cap_{\lambda \in \Lambda} Ker(\alpha_\lambda) \leq^{\oplus} M$.*

Proof. Given M is Baer and let $\{\alpha_\lambda\}_{\lambda \in \Lambda}$ be a family of endomorphisms of M, where Λ be an index set . Let I be the left ideal of $S = End_R(M)$ generated by the family $\{\alpha_\lambda\}_{\lambda \in \Lambda}$, since M is Baer then $r_M(I) \leq^{\oplus} M$. Since each $\alpha_\lambda \in I$, then $r_M(I) \leq r_M(\alpha_\lambda) = Ker(\alpha_\lambda)$, thus $r_M(I) \subseteq \cap_{\lambda \in \Lambda} Ker(\alpha_\lambda)$, Now if $m \in \cap_{\lambda \in \Lambda} Ker(\alpha_\lambda)$ then $\alpha_\lambda(m) = 0$ for each $\lambda \in \Lambda$, if $\theta \in I$ implies $\theta = \sum_{i=1}^{n} s_i \alpha_i$ where $s_i \in S$ and $\alpha_i \in \{\alpha_\lambda\}_{\lambda \in \Lambda}$ for each $i = 1, \ldots, n$, then $\theta(m) = \sum_{i=1}^{n} s_i \alpha_i(m) = \sum_{i=1}^{n} s_i(0) = 0$ implies $m \in r_M(I)$, Then we have $r_M(I) = \cap_{\lambda \in \Lambda} Ker(\alpha_\lambda) \leq^{\oplus} M$. Conversely : Let I be a left ideal of S, then $r_M(I) = \cap_{\alpha \in I} Ker(\alpha)$. By hypothesis, $r_M(I) \leq^{\oplus} M$.

The following theorem which appears in (3), it Is a useful characterization of Baer modules based on SSIP.

Theorem (1.2)(3),Proposition 2.1.4, P.10] : *A module M is Baer if and only if M has the strong summand intersection property and $Ker(\varphi) \leq^{\oplus} M$, $\forall \varphi \in S$.*

It's well known that if an R-module M has a direct summand say A then for each R-homomorphism from A to M can be extended to an R-endomorphism of M by putting the image of the complement of A is zero and by using this fact we can generalization Theorem(1.1) and Theorem(1.2) to the following Proposition :

Proposition (1.3) : *An R-module M is Baer iff for each family $\{\alpha_\lambda\}_{\lambda\in\Lambda}$ of endomorphisms of M, where Λ be an index set, and for each R-homomorphism f: $\cap_{\lambda\in\Lambda} Ker(\alpha_\lambda) \to M$, $Kerf \leq^{\oplus} M$. In other word we can say that M_R is Baer iff for each family $\{A_\lambda\}_{\lambda\in\Lambda}$ of direct summands of M, where Λ be an index set, and for each R-homomorphism $f: \cap_{\lambda\in\Lambda} A_\lambda \to M$, $Kerf \leq^{\oplus} M$ and $Ker(\varphi) \leq^{\oplus} M$, $\forall \varphi \in S$.*

Proof. Since M is Baer, then by Theorem(1.1), $\cap_{\lambda\in\Lambda} Ker(\alpha_\lambda) \leq^{\oplus} M$, then there is a submodule B of M such that $M = \cap_{\lambda\in\Lambda} Ker(\alpha_\lambda) \oplus B$. Since f can be extended f' : $M \to M$ by putting $f'(B) = \mathbf{0}$, again M is Baer then $Kerf' \leq^{\oplus} M$. It's easy to show that $Kerf' = Kerf \oplus B$.Then we have $Kerf \leq^{\oplus} Kerf' \leq^{\oplus} M$, implies that $Kerf \leq^{\oplus} M$. Conversely, let $\{\alpha_\lambda\}_{\lambda\in\Lambda}$ be a family of endomorphisms of M, where Λ be an index set, define $f : \cap_{\lambda\in\Lambda} Ker(\alpha_\lambda) \to M$ define by $f(x) = 0 \ \forall \ x \in \cap_{\lambda\in\Lambda} Ker(\alpha_\lambda)$, by hypothesis $Kerf = \cap_{\lambda\in\Lambda} Ker(\alpha_\lambda) \leq^{\oplus} M$, then by Theorem(1.1), M is Baer.

We define the following relative property of Baer modules.

Definition (1.4) : Let M be an R-module and let N be a submodule of M, M is called N-Baer or M is Baer module relative to N, if for each subset I of $Hom_R(M,N)$, $r_N(I) \leq^{\oplus} M$.

Proposition (1.5) : *For any R-module M, the following statements are equivalent:*

1) *M is Baer .*
2) *Any two direct summands A and B with $B \leq A$, then A is B-Baer.*
3) *M is Baer module relative to any direct summand of itself .*

Proof. (1)⇒(2) Let I be a subset of $Hom_R(A,B)$, since A and B are direct summands of M then there are a submodules C and D of M such that $M = A \oplus C = B \oplus D$, now consider π_C and π_D are the projection maps onto C and D respectively, since for each $\alpha \in I$, α can be extended to $\acute{\alpha}$ by putting $\acute{\alpha}(C) = \mathbf{0}$, since M is Baer then by Theorem(1.1) we have $Ker\pi_C \cap Ker\pi_D \cap (\cap_{\alpha\in I} Ker\acute{\alpha}) = A \cap B \cap (\cap_{\alpha\in I} Ker\acute{\alpha}) \leq^{\oplus} M$ where $Ker\pi_C = A$ and $Ker\pi_D = B$. Since $Ker\acute{\alpha} = C \oplus Ker\alpha$. By the help of modular law we have $A \cap Ker\acute{\alpha} = A \cap C + A \cap Ker\alpha = Ker\alpha$, then $B \cap (\cap_{\alpha\in I} Ker\alpha) = B \cap A \cap (\cap_{\alpha\in I} Ker\acute{\alpha}) \leq^{\oplus} M$. But $r_B(I) = B \cap (\cap_{\alpha\in I} Ker\alpha)$. Thus $r_B(I) \leq^{\oplus} M$.

(2) ⇒ (3) ⇒ (1) It's clear .

Proposition (1.6) : *An R-module M is Baer iff for any two direct summands A and B of M and for each subset I of $Hom_R(A,B)$, $r_A(I) \leq^{\oplus} M$.*

Proof. Since A is direct summand of M, then there is a submodule C of M such that $M = A \oplus C$, since for each $\alpha \in I$, α can be extended to $\acute{\alpha}$ by putting $\acute{\alpha}(C) = \mathbf{0}$, now consider π_C be the projection map onto C, since M is Baer then by

Theorem(1.1) and by the similar way of the proof of Proposition(1.5) we have $r_A(I) = \cap_{\alpha \in I} Ker\alpha = A \cap (\cap_{\alpha \in I} Ker\acute{\alpha}) = Ker\pi_C \cap (\cap_{\alpha \in I} Ker\acute{\alpha}) \leq^{\oplus} M$.
Conversely, put $A = B = M$.

Corollary (1.7) : *Let M be a Baer R-module . Any decomposition* $M = \oplus_{i \in I} A$ *and any subset I of* $Hom_R(A_i, A_j)$, $r_{Ai}(I) \leq^{\oplus} A_i$.

Corollary (1.8) : *Let M be a Baer R-module . Any decomposition* $M = \oplus_{i \in I} A$ *and any R-homomorphism* $\alpha : A_i \longrightarrow A_j$, $Ker\alpha \leq^{\oplus} A_i$.

Proposition (1.9) : *Let M be a fully stable R-module. The following statements are equivalent :*

1) *M is monoform.*
2) *Each non zero submodule of M is indecomposable Baer.*
3) *Each non zero submodule of M is Quasi Dedekind.*

Proof. (1)⇒(2) Consider a non-zero R-homomorphism $\alpha : N \to N$, where $\mathbf{0} \neq N \leq M$, since M is monoform then α is monomorphism, by (3) ,Theorem 2.3.5], N is indecomposable Baer.
(2)⇒ (1) Let $\alpha : N \to M$ be a non-zero R-homomorphism, since M is fully stable, then $\alpha(N) \subseteq N$, thus $\alpha : N \to N$. But M is Baer then $Ker\alpha \leq^{\oplus} N$, while N is indecomposable and $\alpha \neq 0$, thus $Ker\alpha = \mathbf{0}$.
(2)⇔ (3) By (3) ,Theorem 2.3.5].

Proposition (1.10) : *Let M be an abelian R-module, then M is Baer iff for each* $N \leq M$, *there is* $e^2 = e \in S = End_R(M)$ *such that* $N \subseteq (1\text{-}e)M$ *and* $l_S(N) \cap S(1\text{-}e) = \mathbf{0}$.

Proof. Since M is Baer there is $e^2 = e \in S$ such that $l_S(N) = Se$, thus $N \subseteq r_M(l_S(N)) = (1\text{-}e)M$ and $l_S(N) \cap S(1\text{-}e) = Se \cap S(1\text{-}e) = Se(1\text{-}e) = \mathbf{0}$.
Conversely, let $N \leq M$, by hypothesis there is $e^2 = e \in S$ such that $N \subseteq (1\text{-}e)M$ and $l_S(N) \cap S(1\text{-}e) = \mathbf{0}$, since $eN \subseteq e(1\text{-}e)M = \mathbf{0}$, thus $Se \subseteq l_S(N)$, now let $\alpha \in l_S(N)$, since $(1\text{-}e)$ is central then $(1\text{-}e)\alpha = \alpha(1\text{-}e) \in l_S(N) \cap S(1\text{-}e) = \mathbf{0}$, implies $\alpha = \alpha e \in Se$, thus $l_S(N) = Se$ and hence M is Baer .

Proposition (1.11) : *Let M be an abelian and neotherian R-module, then M is Baer iff for each* $m \in M$, $l_S(m) = Se$ *for some* $e^2 = e \in S$.

Proof. Let $N \leq M$, since M is neotherian then there are $m_1, m_2, \ldots, m_n \in N$ such that $N = \sum_{i=1}^{n} m_i R$, by hypothesis there are $e_i^2 = e_i \in S$ such that $l_S(m_i) = Se_i$ for each $i = 1, \ldots, n$, then we have $ls(N) = l_S(\sum_{i=1}^{n} m_i R) = \bigcap_{i=1}^{n} l_S(m_i R) = \bigcap_{i=1}^{n} l_S(m_i) = \bigcap_{i=1}^{n} Se_i$. Now M is abelian then each e_i is central, so $e = e_1 e_2 \ldots e_n$ is idempotent and $l_S(N) = \bigcap_{i=1}^{n} Se_i = Se$, thus M is Baer. The other direction is trivial.

The following lemma which appears as an exercise in (7), we give its proof.

Lemma (1.12) : *If M is a cogenerator R-module and* $S = End_R(M)$, *then for each* $A \leq M$, $A = r_M(l_S(A))$.

Proof. It is clear that $A \subseteq r_M(l_S(A))$, now let $m \notin A$, since M is a cogenerator then $A = \bigcap_{\alpha \in Hom_R(M/A, M)} Ker\alpha$, then there is $\alpha_o : M/A \to M$ such that $\alpha_o(m + A) \neq 0$, now let $\pi : M \to M/A$ be the natural epimorphism then $\alpha_o \pi(A) = 0$, thus $\alpha_o \pi \in$

$l_S(A)$, but $\alpha_o \pi(m) = \alpha_o\ (m + A) \neq 0$, then $m \notin r_M(l_S(A))$, then $r_M(l_S(A)) \subseteq A$. Therefore $A = r_M(l_S(A))$.

Proposition (1.13) : *If M is a cogenerator R-module, then M is Baer iff M is semisimple.*

Proof. Let $A \leq M$ then $l_S(A)$ is left ideal of $S = End_R(M)$, since M is Baer then $r_M(l_S(A) \leq^{\oplus} M$, since M is a cogenerator then by Lemma(1.12) we have that $A = r_M(l_S(A)) \leq^{\oplus} M$. Thus M is semisimple. The other direction is trivial.

In the following proposition we give a characterization of semisimple modules in terms of Baer modules.

Proposition (1.14) : *Let M be an R-module and $S = End_R(M)$, then M is semisimple iff M is Baer and $A = r_M(l_S(A))\ \forall A \leq M$.*

Proof. Let M be a semisimple module, it is enough to show that $A = r_M(l_S(A))$ $\forall A \leq M$. Since M is semisimple then A is a direct summand of M, there is an idempotent $e \in S=End_R(M)$such that $A=eM$,so$r_M(l_S(A))=r_M(l_S(eM))=r_M(S(1-e))=eM=A$.The complete of the proof is similar to proof of Proposition(1.13).

2. DIRECT SUMMANDS AND DIRECT SUMS OF BAER MODULES

A natural question about any algebraic structure is whether inherited by direct sums or direct summands. The following first result was proved in [3] and shows that direct summands of a Baer module inherit the property.

Theorem (2.1)(3), Theorem 3.3.1, P. 17] : *Let M be a Baer module. Then every direct summand N of M is also a Baer module.*

Corollary (2.2)(3),Corollary 2.3.2, Page 17] : *Let R be a Baer ring, and let $e^2 = e \in R$ be any idempotent of R. Then $M = eR$ is an R-module which is Baer.*

Corollary(2.2) provides rich source of examples of Baer modules. As an application of the above results, C. S. Roman proved a characterization of all Baer modules in the class of finitely generated **Z**-modules as following : *A finitely generated* **Z***-module M is Baer if and only if M is semisimple or torsion-free* (3), Proposition (2.3.3), Page 17]. And by using (3), Remark (2.3.4)], we can generalize this proposition to the next result.

Proposition (2.3) : *Let R be a PID and M be a finitely generated R-module then M is Baer iff M is semisimple or torsion-free.*

Proof. Assume that M is finitely generated Baer module which is not semisimple to show that M is torsion-free. Now by (5),Corollary (8.3), page 125], we can always decompose $M = t(M) \oplus f(M)$ where $t(M)$ is the torsion submodule of M and $f(M)$ is the torsion-free submodule of M. Assume $t(M) \neq \mathbf{0}$ and $f(M) \neq \mathbf{0}$, and by (5),Theorem (8.14), page 134] we have $t(M) = \oplus_{p \in P} Mp^{n(p)}$, where $P \subseteq R$ is a finite collection of primes (irreducibles) and $Mp^{n(p)}$ is a non-trivial cyclic modules of prime power order $p^{n(p)}$ where $n(p) \in \square$. Also by (5), Lemma (8.17), page 136] we have the only submodules of $Mp^{n(p)}$ are : $\mathbf{0} = p^{n(p)}\ Mp^{n(p)} \leq p^{n(p)-1}\ Mp^{n(p)} \leq \ldots \leq p\, Mp^{n(p)} \leq Mp^{n(p)}$. Let p_0 be a prime so that $n(p_0) \neq 0$ (such a prim must exist) and let $\varphi : R \to Mp_0^{n(p_0)}$ be the morphism defined by $\varphi\ (x) = \bar{x}$, for $x \in R$, then $\mathbf{0} \neq Ker(\varphi) = p_0^{n(p_0)} R$ is essential in R_R because R is PID, but M is Baer and by Corollary(1.8) then $Ker(\varphi)$ is direct summand of R, a contradiction. Then $t(M)$

$= \mathbf{0}$ or $f(M) = \mathbf{0}$. Assume $f(M) = \mathbf{0}$. Then $M = t(M)$; it is a direct sum of modules of the form $Mp^{n(p)}$ which is describe as above, where p is prim number and $n(p) \in \square$. Therefore by Theorem(2.1) $Mp^{n(p)}$ must be Baer. Since M is not semisimple, then M can not decomposition as a direct sum of simple modules, then there is a prime number p such that $n_0(p) > 1$. Let $\theta : Mp^{n_0(p)} \to Mp^{n_0(p)}$ define by $\theta(\bar{x}) = p\bar{x}$, thus $\theta \neq 0$ because $\theta(Mp^{n_0(p)}) = p\,Mp^{n_0(p)} \neq 0$, since $Mp^{n_0(p)}$ is Baer, then $Ker(\theta) = p^{n_0(p)-1} Mp^{n_0(p)} \leq^{\oplus} Mp^{n_0(p)}$ which is contradiction. Then we have $t(M) = \mathbf{0}$, thus $M = f(M)$.

Conversely, if M is semisimple then M is obviously Baer. If M is finitely generated and torsion-free then $M \cong R^n$ for some $n \in \square$, and hence we have M is Baer.

Theorem (2.4) : *Let M_1 and M_2 be Baer R-modules. If we have the following conditions:*

1) $\forall\ N \leq M_1 \oplus M_2$ *implies that* $N = N_1 \oplus N_2$, *where,* $N_i \leq M_i$, $i = 1,2$.
2) $\bigcap_{\alpha \in Hom_R(M_i, M_j)} Ker(\alpha) = \mathbf{0}$ $(i \neq j,\ i, j = 1,2)$.

Then $M_1 \oplus M_2$ is Baer.

Proof. Let $S = End_R(M_1 \oplus M_2)$, and let I be a left ideal of S. Then by (1), $r_M(I) = N_1 \oplus N_2$ where, $N_i \leq M_i\ \forall\ i = 1,2$. Since S can be written in the following matrix form

$$S = \begin{pmatrix} S_1 & Hom_R(M_2, M_1) \\ Hom_R(M_1, M_2) & S_2 \end{pmatrix}$$

Now consider the following sets :

$I_{11} = \{\varphi \in S_1 |\ \varphi = \xi_{11}$ with $(\xi_{ij})_{i,j=1,2} \in I\} \leq_{S_1} S_1$,

$I_{22} = \{\varphi \in S_2 |\ \varphi = \xi_{22}$ with $(\xi_{ij})_{i,j=1,2} \in I\} \leq_{S_2} S_2$,

$I_{12} = \{\psi \in Hom_R(M_1, M_2) |\ \psi = \xi_{21}$ with $(\xi_{ij})_{i,j=1,2} \in I\}$, and

$I_{21} = \{\psi \in Hom_R(M_2, M_1) |\ \psi = \xi_{12}$ with $(\xi_{ij})_{i,j=1,2} \in I\}$.

Let $N_1' = r_{M_1}(I_{11})$, It's easy to cheek that $N_1 = N_1' \cap (\cap_{\psi \in I_{12}} Ker\psi)$. Now we claim that $\psi(N_1') = \mathbf{0}\ \ \forall\ \psi \in I_{12}$, i.e., $N_1' \subseteq \cap_{\psi \in I_{12}} Ker\psi$, let $f \in Hom_R(M_2, M_1)$, thus $\begin{pmatrix} 0 & f \\ 0 & 0 \end{pmatrix} \in S$ and hence $\begin{pmatrix} 0 & f \\ 0 & 0 \end{pmatrix}\begin{pmatrix} \alpha_{11} & \alpha_{12} \\ \alpha_{21} = \psi & \alpha_{22} \end{pmatrix} = \begin{pmatrix} f\psi & f\alpha_{22} \\ 0 & 0 \end{pmatrix} \in I$, thus $f\psi \in I_{11}\ \forall\ \psi \in I_{12}$, now if $n \in N_1'$ then $n \in r_{M_1}(I_{11})$ and hence $f\psi(n) = 0$, by condition(2) we get $\psi(n) = 0$, but n is an arbitrary element in N_1', thus $\psi(N_1') = \mathbf{0}$ and hence $N_1' \subseteq Ker\psi\ \ \forall\ \psi \in I_{12}$, then we have that $N_1' \subseteq \cap_{\psi \in I_{12}} Ker\psi$. Since M_1 is Baer therefore $N_1 = N_1' \leq^{\oplus} M_1$. By similar way $N_2 = N_2' \cap (\cap_{\psi \in I_{21}} Ker\psi) = N_2' = r_{M_2}(I_{22}) \leq^{\oplus} M_2$. Then we have $r_{M_1 \oplus M_2}(I) = N_1 \oplus N_2 \leq^{\oplus} M_1 \oplus M_2$.

Corollary (2.5) : *Let M_1 and M_2 be Baer R-modules. If we have the following conditions:*

1) $r_R(M_1) + r_R(M_2) = R$
2) $\bigcap_{\alpha \in Hom_R(M_i, M_j)} Ker(\alpha) = \mathbf{0}$ $(i \neq j,\ i, j = 1,2)$.

Then $M_1 \oplus M_2$ is Baer.

Proof. Since $r_R(M_1) + r_R(M_2) = R$ by (1), Prop.(4.2)], $\forall N \leq M_1 \oplus M_2$ implies that $N = N_1 \oplus N_2$, where, $N_i \leq M_i$, i =1,2. Thus by Theorem(2.4), $M_1 \oplus M_2$ is Baer.

Theorem (2.6) : *Let M_1 and M_2 be Baer R-modules. If we have the following conditions :*

1) $\forall\ N \leq M_1 \oplus M_2$ *implies that* $N = N_1 \oplus N_2$, *where,* $N_i \leq M_i$, i=1,2.
2) $\forall\ \psi \in Hom(M_i, M_j)$, $Ker\ \psi \leq^{\oplus} M_i$, *where* $i \neq j$, i,j = 1,2.

Then $M_1 \oplus M_2$ is Baer.

Proof. By the similar fashion of the proof of last Theorem, we have that $N_1 = N_1' \cap (\cap_{\psi \in I_{12}} Ker\psi)$, where $N_1' = r_{M_1}(I_{11}) \leq M_1$ because M_1 is Baer. Now by condition (2), $Ker\psi \leq^{\oplus} M_1\ \forall \psi \in I_{12}$, by Theorem(1.2), M_1 has SSIP, thus $N_1 = N_1' \cap (\cap_{\psi \in I_{12}} Ker\psi) \leq^{\oplus} M_1$ Also by same way $N_2 = N_2' \cap (\cap_{\psi \in I_{21}} Ker\psi) \leq^{\oplus} M_2$, where $N_2' = r_{M_2}(I_{22})$ then we have $r_{M_1 \oplus M_2}(I) = N_1 \oplus N_2 \leq^{\oplus} M_1 \oplus M_2$. Then we have $M_1 \oplus M_2$ is Baer.

Corollary (2.7) : *Let M_1 and M_2 be a Baer R-modules. If we have the following conditions:*

1) $r_R(M_1) + r_R(M_2) = R$
2) $\forall\ \psi \in Hom(M_i, M_j)$, $Ker\psi \leq^{\oplus} M_i$, *where* $i \neq j$, i,j = 1,2.

Then $M_1 \oplus M_2$ is Baer.

3. QUASI-BAER MODULES

C.S. Roman introduced the concept of quasi-Baer modules without giving a description of characterizations. The following next theorems give characterizations of quasi-Baer modules

Theorem (3.1) : *An R-module M is quasi-Baer iff for each family $\{\alpha_\lambda\}_{\lambda \in \Lambda}$ of endomorphisms of M with $Ker\alpha_\lambda$ ($M\ \forall\ \lambda \in \Lambda$, implies $\cap_{\lambda \in \Lambda} Ker\alpha_\lambda$ ($^{\oplus} M$.*

Proof. Let I ($S = End_R(M)$, then $I = \sum_{\alpha \in I} S\alpha S$, then $r_M(I) = r_M(\sum_{\alpha \in I} S\alpha S) = \cap_{\alpha \in I} r_M(S\alpha S)$. But $r_M(S\alpha S) = Ker(\alpha)$ (M, then by hypothesis $r_M(I) = \cap_{\alpha \in I} Ker\alpha_\lambda$($^{\oplus} M$, thus M is quasi-Baer.

Conversely, let $\{\alpha_\lambda\}_{\lambda \in \Lambda}$ be a family of endomorphisms of M with $Ker\alpha_\lambda$ ($M\ \forall\ \lambda \in \Lambda$.. Set $I = \sum_{\lambda \in \Lambda} S\alpha_\lambda S$ (S, since M is quasi-Baer then $r_M(I)$ ($^{\oplus} M$, but $Ker\alpha_\lambda$ ($M\ \forall\ \lambda \in \Lambda$, thus $r_M(S\alpha S) = Ker(\alpha)$ (M implies $r_M(I) = \cap_{\lambda \in \Lambda} r_M(S\alpha S) = \cap_{\lambda \in \Lambda} Ker\alpha_\lambda$($^{\oplus} M$.

Theorem (3.2) *An R-module M is quasi-Baer iff the intersection of any family of fully invariant direct summands of M is direct summand and for all $\varphi \in S = End_R(M)$, $r_M(S\alpha S)$ ($^{\oplus} M$.*

Proof. The second assertion of the necessary condition is obviously true, as the set of principal two sided ideals is a subset of the set of all two sided ideals, i.e., $r_M(S\varphi S)$ ($^{\oplus} M$, $\forall \varphi \in S$. Let $\{ A_\alpha \}_{\alpha \in \Lambda}$ be a family of fully invariant direct summands of M. Now Consider $\pi_\alpha : M \to M$ be the projection map onto $A_\alpha\ \forall\ \alpha \in \Lambda$, it's clear that $l_S(A_\alpha) = l_S(\pi_\alpha M) = S(1- \pi_\alpha)\ \forall\ \alpha \in \Lambda$. Since A_α (M, then

$l_S(A_\alpha) = S(1-\pi_\alpha)$ (S. Set $I = \sum_{\alpha\in\Lambda} S(1-\pi_\alpha)$, thus I (S, since M is quasi-Baer then $r_M(I)$($^{\oplus}M$,but$\cap_{\alpha\in\Lambda} A_\alpha=\cap_{\alpha\in\Lambda}Ker(1-\pi_\alpha) = r_M(\sum_{\alpha\in\Lambda} S(1-\pi_\alpha)) = r_M(I)$ ($^{\oplus}M$. Conversely, let I (S, then $I = \sum_{\alpha\in I} S\alpha S$. Since $r_M(I) = r_M(\sum_{\alpha\in I} S\alpha S) = \cap_{\varphi\in I} r_M(S\alpha S)$, but by hypothesis $r_M(S\alpha S)$ ($^{\oplus}M$ and the intersection of any family of fully invariant direct summands is direct summand, then $r_M(I)$ ($^{\oplus}M$.

Theorem (3.3) : *An R-module M is quasi-Baer iff all N* (*M,* $\exists$ $e \in S_l(S)$, *where* $S = End_R(M)$, *such that* $N \subseteq eM$ *and* $eS \cap l_S(N) = eS(1-e)$.

Proof. Assume M is quasi-Baer and N (M, then there is $\alpha(=\alpha^2)\in S$ such that $l_S(N) = S\alpha$, since N (M, then by(3), Lemma 1.2.9, P.7], $l_S(N)$(S (i.e. $l_S(N)$ is two sided ideal of S), then by (10), Lemma(1.1), P.40], $\alpha \in S_r(S)$(the set of right semicentral idempotents) and it's clear that $N \subseteq r_M(l_S(N)) = r_M(S\alpha) = (1-\alpha)M$. Now let $e = 1-\alpha$ also by (10), Lemma(1.1), P.40], $e \in S_l(S)$ (the set of left semicentral idempotents) and $N \subseteq eM$. Now to show that $l_S(N) \cap eS = eS(1-e)$, its clear that $eS(1-e) \subseteq S(1-e) \cap eS = l_S(N) \cap eS$.*Let* $\varphi \in S(1-e) \cap eS$ implies $\varphi = es_1=s_2(1-e)$ for some $s_1,s_2 \in S$, thus $es_1 = s_2-s_2e = s_2-es_2e$ because $e \in S_l(S)$ implies that $es_1+es_2e = s_2 \Rightarrow \varphi = s_2(1-e) = es_1(1-e) + es_2e(1-e) = es_1(1-e) \in eS(1-e)$, then $eS \cap l_S(N) = S(1-e) \cap eS = eS(1-e)$.

Conversely, let N (M and assume there exist $e \in S_l(S)$ such that $N \subseteq eM$ and $eS \cap l_S(N) = eS(1-e)$. It's clear that $S(1-e) \subseteq l_S(eM) \subseteq l_S(N)$, let $\psi \in l_S(N)$, then $\psi = \psi e + \psi(1-e)$, so $e\psi = e\psi e + e\psi(1-e)$, *but* $e\psi \in eS \cap l_S(N) = eS(1-e)$, then there is $s \in S$ such that $e\psi = es(1-e)$, *thus* $e\psi e = es(1-e)e = 0$. But $e \in S_l(S)$ then $0 = e\psi e = \psi e$.*Thus* $\psi=\psi(1-e) \in S(1-e)$implies that$l_S(N)=S(1-e)$ and hence M is quasi-Baer.

Corollary (3.4)(10), Proposition 1.2, page 41] : *A ring R is quasi-Baer iff whenever I is a two sided ideal of R there exist* $e \in S_l(R)$ *such that* $I \subseteq eR$ *and* $l_R(I) \cap eR = eR(1-e)$.

Corollary (3.5)[[10], Corollary 1.3, page 42,] : *If R is quasi-Baer ring and I is two sided ideal of R then there exist* $e \in S_l(R)$ *such that* $I \subseteq eR$ *and* $I + eR(1-e)$ *is right essential in eR and eR(1-e) is a two sided ideal of R . In particular, if I contains the prime radical of R (for example, R is semiprime) or e is central, then I is right essential in eR .Moreover if I is not essential in eR, then there exist a closed rigt ideal* $\mathbf{0} \neq X = eX(1-e)$ *such that* $I \cap X = \mathbf{0}$ *and* $I \oplus X$ *is right essential in eR .*

4. DIRECT SUMMANDS AND DIRECT SUMS OF QUASI-BAER MODULES

From the definition of quasi-Baer module, we see that the tools that using in this definition are difficult more than the tools that using of the definition of Baer modules, for example a direct summand of Baer module is always Baer as it is easily proved, but the following theorem which appears in [3], showed that a direct summands of quasi-Baer modules are, in fact, inheriting the property as it is difficultly.

Theorem (4.1)(3), Theorem 3.3.1, P. 35] : *Let M be a quasi-Baer R-module. Then any direct summand N of M is also a quasi-Baer module.*

Theorem (4.2) : *Let M_1 and M_2 be quasi-Baer R-modules. If we have the property :* $\forall\ \psi \in Hom_R(M_i,M_j)$ *implies* $Ker\psi$ ($\overset{\oplus}{} M_i$ ($i \neq j$, $i,j = 1,2$) *then* $M_1 \oplus M_2$ *is quasi-Baer.*

Proof. Let $S = End_R(M_1 \oplus M_2)$, and let I (S. As mention

$$S = \begin{pmatrix} S_1 & Hom_R(M_2, M_1) \\ Hom_R(M_1, M_2) & S_2 \end{pmatrix}$$

Now consider the following properties :

$I_{11} = \{\varphi \in S_1 |\ \varphi = \xi_{11}$ with $(\xi_{ij})_{i,j=1,2} \in I\}$ (S_1.

$I_{22} = \{\varphi \in S_2 |\ \varphi = \xi_{22}$ with $(\xi_{ij})_{i,j=1,2} \in I\}$ (S_2.

We also define

$I_{12} = \{\psi \in Hom_R(M_1, M_2) |\ \psi = \xi_{21}$ with $(\xi_{ij})_{i,j=1,2} \in I\}$, and

$I_{21} = \{\psi \in Hom_R(M_2, M_1) |\ \psi = \xi_{12}$ with $(\xi_{ij})_{i,j=1,2} \in I\}$.

By the similar way of proof of Theorem(2.4), we have that $N_1 = N_1' \cap (\cap_{\psi \in I_{12}} Ker\psi)$ where $N_1' = r_{M_1}(I_{11})$ ($\overset{\oplus}{} M_1$ because M_1 is quasi-Baer. Now by condition (2), $Ker\psi$ ($\overset{\oplus}{} M_1$ $\forall \psi \in I_{12}$, by Theorem(3.2), the intersection of any family of fully invariant direct summands is fully invariant direct summand of M_1, then N_1 ($\overset{\oplus}{} M_1$. Also $N_2 = N_2' \cap (\cap_{\psi \in I_{21}} Ker\psi)$ ($\overset{\oplus}{} M_2$ where $N_2' = r_{M_2}(I_{22})$. Thus $r_{M_1 \oplus M_2}(I) = N_1 \oplus N_2$ ($\overset{\oplus}{} M_1 \oplus M_2$. Then $M_1 \oplus M_2$ is quasi-Baer.

5. ENDOMORPHISM RING

An interesting connection between (quasi-)Baer modules and their endomorphism rings. A good result makes the definitions of Baer and quasi-Baer modules the more valuable, as they can provide a source of Baer and quasi-Baer rings, by considering their endomorphism rings.

Theorem (5.1)(3), Theorem 4.4.1, P. 42]: *Let M be a Baer (respectively, quasi-Baer) R-module. Then S = End(M) is a Baer (respectively, quasi-Baer) ring.*

On the other hand, the fact that the endomorphism ring of a module is Baer (resp.,quasi-Baer) does not imply that the module itself is Baer (resp.,quasi-Baer).

Example (5.2)(3), Example 4.1.2] : Let $M = \mathbf{Z}p\infty$, considered as a $\mathbf{Z}$-module. Then it is well-known that $End_{\mathbf{Z}}(M)$ is the ring of p-adic integers [[11], Example 3, page 216]. Since the ring of p-adic integers is a commutative domain, it is a (quasi-) Baer ring. However $M = \mathbf{Z}p\infty$ is not a (quasi-) Baer module.

Proposition (5.3) : *Let M be a quasi-injective R-module . Then M is Baer iff* $S = End_R(M)$ *is Von Neumann regular ring .*

Proof. Since M is quasi-injective then by (8), Theorem (13.1)-(1),(2) page 359]], the Jacobson radical of S, $J(S) = \{f \in S \mid Kerf \leq^{e} M\}$ and $S/J(S)$ is von Neumann regular ring. But M is Baer then each $f \in S$ implies $Kerf \leq^{\oplus} M$, if $f \in J(S)$, then we have $f = 0$, thus $J(S) = \mathbf{0}$. But $S/J(S) = S/0 \cong S$ and hence S is regular ring .

Conversely, Since M is quasi-injective then M is extending, but S is regular ring then by (3), Proposition 4.3.3, P. 51], we obtain M is Baer .

Corollary (5.4) : *Let R be a right(or left) self-injective ring. Then R is Von Neumann regular iff R is Baer ring.*

Proposition (5.5) : *Let M be a quasi-injective R-module only with countable many direct summands . Then M is Baer iff $S = End_R(M)$ is semisimple artinian .*

Proof. Since M is quasi-injective and Baer then by Proposition(5.3), S is regular and by Theorem(5.1), S is Baer ring, thus S is regular Baer ring. But M has countably many direct summands then also is for S (and conversely), now by (12), Theorem1] : A regular Baer ring with countable many idempotents is semisimple Artinian. Then S is semisimple artinian .

Conversely, since S is semisimple artinian then S is regular ring, so by Proposition(5.3) we obtain M is Baer .

Proposition (5.6) : *Let M be an R-module whose endomorphism ring $S = End_R(M)$ is right extending, then M is Baer iff S is right nonsingular ring.*

Proof. Given M is Baer and let $\alpha \in S$, with $r_S(\alpha) \leq^{e} S$, since M is Baer then by Theorem(5.1) we have S is Baer ring, thus $r_S(\alpha) \leq^{\oplus} S$ implies that $r_S(\alpha) = S$, then $\alpha = 0$ and hence S is right nonsingular ring .

Conversely, let $N \leq M$, then by (3), Lemma 1.2.12, P. 9], we obtain $r_S(l_S(N))$ is closed, But S is right extending then $r_S(l_S(N)) = eS$ for some $e^2 = e \in S$. Now by (3), Lemma 1.2.9, P.7], we obtain $l_S(N) = l_S(r_S(l_S(N))) = S(1\text{-}e)$, thus M is Baer.

We recall the following chart of basic implication. It is not hard to verify that all implication are irreversible (8).

$$\begin{array}{ccccccc} & & \text{(Baer ring)} & & & & \\ & & \Downarrow & & & & \\ \begin{pmatrix}\text{von Neumann}\\ \text{regular ring}\end{pmatrix} & \Rightarrow & \begin{pmatrix}\text{right}\\ \text{semihereditary}\end{pmatrix} & \Rightarrow & \begin{pmatrix}\text{right}\\ \text{Rickart}\end{pmatrix} & \Rightarrow & \begin{pmatrix}\text{right}\\ \text{nonsingular}\end{pmatrix} \end{array}$$

In (13) , B. L. Osofsky has shown that the endomorphism ring of a quasi-injective module is right self injective and hence its right extending. Then we obtain the following theorem which it is a consequence of Proposition(5.3) and Proposition(5.6).

Theorem (5.7) : *Let M be a quasi-injective R-module and $S = End_R(M)$. Then the following statements are equivalent :*

1) *M is Baer.*
2) *S is von Neumann regular.*
3) *S is right semihereditary.*
4) *S is right Rickart.*
5) *S is right nonsingular*

Proof. (1)$\Leftrightarrow$(2) By Proposition (5.3).

(2)$\Rightarrow$(3) $\Rightarrow$(4) $\Rightarrow$(5) It is clear.

(1)$\Leftrightarrow$(5) By Proposition(5.6). Since M is quasi-injective, then by (13) S is right self-injective and hence S is right extending.

Corollary (5.8) (8), Theorem(7.52)(1) , P.262] : *Let R be any right self-injective ring. Then the following statements are equivalent :*

1) *R is Baer.*
2) *R is von Neumann regular.*

3) *R is right semihereditary.*
4) *R is right Rickart.*
5) *R is right nonsingular.*

In one of main theorems in this section which extend that Smell's result to the general setting of modules and provide an analogous characterization for Baer modules. Firstly, we need to extend the following lemma which appears in (8).

Lemma (5.9)(8), Lemma 7.56, P. 64] : *Let R be a right Rickart ring. Then any non-zero left annihilator of R contains a non-zero idempotents.*

Lemma (5.10) : *Let M be an R-module such that $S = End_R(M)$ is right Rickart ring. Then any nonzero left annihilator $l_S(N)$, where N be any submodule of M, contains a nonzero idempotents.*

Proof. Let $N \leq M$ with $l_S(N) \neq \mathbf{0}$, then there is $0 \neq \alpha \in l_S(N)$. Since S is right Rickart then $r_S(\alpha) = eS$ for some $e = e^2 \neq 1$ in S. But $r_S(l_S(N)) \subseteq r_S(\alpha)$. Taking left annihilator, we have $S(1-e) = l_S(r_S(\alpha)) \subseteq l_S(r_S(l_S(N))) = l_S(N)$, thus $0 \neq 1-e \in l_S(N)$.

Theorem (5.11) : *Let M be an R-module such that $S = End_R(M)$ has no infinite set of non-zero orthogonal idempotents. Then the following are equivalent :*

1) *M is Baer.*
2) *S is right Rickart ring.*

Proof. (1)$\Rightarrow$(2). Since M is Baer then by Theorem(5.1),S is Baer, thus S is Rickart. (2)$\Rightarrow$(1). Assume S is right Rickart ring. Let N be a submodule of M, if $l_S(N) = \mathbf{0}$ then the proof is complete . Now suppose that $l_S(N) \neq \mathbf{0}$, by Lemma(5.10) there is $0 \neq e^2 = e \in S$ such that $e \in l_S(N)$. By hypothesis, S has no infinite set of non-zero orthogonal idempotents. According to [[8], Prop.6.59, P. 231] the direct summands of ${}_SS$ satisfies the DCC. Among all non-zero idempotents in $l_S(N)$(which exist by Lemma(5.10)), choose e with $S(1-e) = l_S(eM)$ minimal, i.e., the set $\{ S(1-e) : e \in l_S(N)\}$ has minimal element say $S(1-e)$. We claim $l_S(N) \cap S(1-e) = \mathbf{0}$. Indeed if $\mathbf{0} \neq l_S(N) \cap S(1-e) = l_S(N) \cap l_S(eM) = l_S(N + eM)$, also by Lemma(5.10) there is a non-zero idempotent $f \in l_S(N + eM)$. Since $fe = 0$, let $e' = e + (1-e)f$, it is clear that $e' \in l_S(N)$. To check that $e'^2 = e'$

$$\begin{aligned} e'^2 &= (e + (1-e)f)(e + (1-e)f) \\ &= e^2 + e(1-e)f + (1-e)fe + (1-e)f(1-e)f \\ &= e + 0 + 0 + (1-e)f^2 - (1-e)fef \\ &= e + (1-e)f = e' \end{aligned}$$

Also $e'e = e^2 + (1-e)fe = e$ implies that $e' \neq 0$ and if $\alpha \in l_S(e'M)$, then $\alpha e = \alpha e'e = 0$, thus $l_S(e'M) = S(1-e') \subseteq l_S(eM) = S(1-e)$. This inclusion is proper, since $fe = 0$ but

$$fe' = fe + f(1-e)f = f \neq 0.$$

This contradicts the choice of e, so we have proved our claim. But $S = Se \oplus S(1-e)$, since $Se \subseteq l_S(N)$ then by the help of modular law $l_S(N) = l_S(N) \cap S = l_S(N) \cap Se \oplus l_S(N) \cap S(1-e) = Se$, so M is Baer.

Corollary (5.12)(8), Theorem 7.55, P. 263] : *Let R be any ring that has no infinite set of non-zero orthogonal idempotents . Then the following are equivalent:*

1) *R is Baer.*
2) *R is right Rickart.*

REFERENCES

1. I. Kaplansky, "Rings of operators", W. A. Benjamin. 1968.
2. W.E.Clark,"Twisted matrix units semigroup algebras", Duke Math J.,34 : 417–424 (1967).
3. C.S. Roman, "Baer and quasi-Baer modules", Ph.D. Thesis, The Ohio State University, (2004).
4. G. V. Wilson, "Modules with the summand intersection property", Comm. Alg.,14(1) : 21–38.(1986)
5. B. Hartely and T. O. Haekes, "Rings, Modules and Linear Algebra", London (1970).
6. M. S. Abbas, "On fully stable modules", Ph.D. Thesis, University of Baghdad, (1991).
7. F. Kasch, "Modules and Rings", Acad. Press, London(1982).
8. T.Y. Lam, "Lectures On Modules And Rings", Springer Verlag(1999).
9. A. S. Mijbass, "Quasi-Dedekind Modules", Ph.D. Thesis, University of Baghdad, (1997).
10. G.F. Birkenmeier; J. Y. Kim and J. K. Park, "Quasi-Baer ring extensions and biregular rings ", Bull. Austral. Math., 61(2000): 39-52.
11. L. Fuchs, "Infinite Abelian Groups", I. Academic Press(1970).
12. K. M. Rangaswamy, "Regular and Baer rings", Proc. Amer. Math. Soc,. 42(2) :354-358(1974).
13. B. L. Osofsky, "Endomorphism rings of quasi-injective modules", Canad. J. Math. 20, 895-903, (1968).
14. J.M. Zelmanowitz, "Representation of rings with faithful polyform modules", Comm. Alg., 14(6),1141–1169 (1986).

An Identity on θ-Centralizers of Lie Ideals in Prime Rings

Abdulrahman H. Majeed And Mushreq I. Meften
Department of Mathematics/College of Science/Baghdad University

الخلاصة

الهدف من البحث هو برهان النتيجة الآتية : لتكن R حلقة أولية طليقة الالتواء من الدرجة الثانية وU مثالي لي مغلق تربيعيا في R و $\theta,T: R\to R$ دالتان جمعيتان وT تحقق $\theta(x)T(y)\theta(x) = T(xyx)$ لكل x,y في U. اذا كان θ دالة تشاكلية شاملة على U و T(u) ∈ U لكل u ∈ U فان $T(xy)= T(x)\theta(y) = \theta(x)T(y)$ لكل x,y في U .

ABSTRACT

The main result: Let R be a 2-tortion free prime ring, U a square closed Lie ideal of R, and let $T,\theta: R\to R$ are additive mappings. Suppose that $T(xyx) = \theta(x)T(y)\theta(x)$ holds for all pairs $x,y \in U$. In this case $T(xy) = T(x)\theta(y) = \theta(x)T(y)$ for all $x,y \in U$, where θ is a surjective endomorphism of U, and $T(u) \in U$, for all $u \in U$.

Keywords

prime ring, semiprime ring, derivation, Jordan derivation, Jordan triple derivation, left (right) centralizer, left (right) Jordan centralizer, centralizer , left (right) θ-centralizer, left (right) Jordan θ-centralizer, θ-centralizer

INTRODUCTION

This research has been motivated by the work of BreŠar (1), Zalar (2) and (3)(4)(5)(6)(7).

Throughout, R will represent an associative ring with center Z(R). A ring R is n-torsion free, where n is an integer, in case nx = 0, $x \in R$ implies x = 0. As usual the commutator xy - yx will be denoted by [x, y]. We shall use basic commutator identities [xy, z] = [x, z]y + x[y, z] and [x, yz] = [x, y]z + y[x, z]. Recall that R is prime if aRb = (0) implies a = 0 or b = 0, and is semiprime if aRa = (0) implies a = 0. A subgroup U of R is called a square closed Lie ideal if $u^2 \in U$ and $[u,x] \in U$ for all $u \in U, x \in R$. An additive mapping $D : R \to R$ is called a derivation if D(xy) = D(x)y + xD(y) holds for all pairs $x, y \in R$ and is called a Jordan derivation in case $D(x^2) = D(x)x + xD(x)$ is fulfilled for all $x \in R$. A derivation D is inner in case there exists $a \in R$ such that D(x) = [a, x] holds for all $x \in R$. Every derivation is a Jordan derivation. The converse is in general not true. A classical result of Herstein (8) asserts that any Jordan derivation on a 2-torsion free prime ring is a derivation. A brief proof of Herstein's result can be found in (9). Cusack (10) has generalized Herstein's result to 2-torsion free semiprime rings (see also (11) for an alternative proof). An additive mapping $T: R\to R$ is called a left (right) centralizer in case T(xy) = T(x)y (T(xy) = xT(y)) holds for all $x, y \in R$. T is called centralizer in case T is both a left and right centralizer. In case R has an identity element $T: R\to R$ is a left (right) centralizer iff T is of the form T(x) = ax (T(x) = xa) for some fixed element $a \in R$. An additive mapping $T: R\to R$ is called a left (right) Jordan centralizer in case $T(x^2) = T(x)x$ ($T(x^2) = xT(x)$) holds for $x \in R$. Following ideas from (11), Zalar (2) has proved that any left (right) Jordan centralizer on a 2-torsion free semiprime ring is a left (right) centralizer. In (12) J.Vukman proved that in case we have an

additive mapping T: R→R, where R is a 2-torsion free semiprime ring, satisfying the relation $2T(x^2) = T(x)x + xT(x)$ for all $x \in R$, then T is a centralizer.

An additive mapping T: R→R is called a left (right) θ-centralizer in case $T(xy) = T(x)\theta(y)$ ($T(xy) = \theta(x)T(y)$) holds for all $x, y \in R$. T is called θ-centralizer in case T is both a left and right θ-centralizer. In case R has an identity element T: R→R is a left (right) θ-centralizer iff T is of the form $T(x) = a\theta(x)$ ($T(x) = \theta(x)a$) for some fixed element $a \in R$. An additive mapping T: R→R is called a left (right) Jordan θ-centralizer in case $T(x^2) = T(x)\theta(x)$ ($T(x^2) = \theta(x)T(x)$) holds for $x \in R$. Following ideas from (11), we (3) proved that any left (right) Jordan θ-centralizer on a 2-torsion free ring is a left (right) θ-centralizer under some condition. In (5) we generalized this result on lie ideal . In (4) we proved that in case we have an additive mapping T: R→R, where R is a 2-torsion free ring, satisfying the relation $2T(x^2) = T(x)\theta(x) + \theta(x)T(x)$ for all $x \in R$, then T is a θ-centralizer, under some condition . In (6) we generalized this result on lie ideal .

An additive mapping D: R→R, where R is an arbitrary ring, is a Jordan triple derivation in case $D(xyx) = D(x)yx + xD(y)x + xyD(x)$ holds for all pairs $x, y \in R$.One can easily prove that any Jordan derivation is a Jordan triple derivation (see 9). BreŠar (1) has proved that any Jordan triple derivation on 2-torsion free semiprime ring is a derivation. If T: R→R is a centralizer, where R is an arbitrary ring, then T satisfies the relation

$$T(xyx) = xT(y)x \qquad x, y \in R$$

In(13)J.Vukman proved the converse when R is 2- torsion free semiprime ring . In (7) we generalize this result to θ-centralizer .In this paper we generalize this result on lie ideal .

Theorem 1

Let R be a 2-tortion free prime ring, U a square closed Lie ideal of R, and let T,θ: R→R are additive mappings. Suppose that $T(xyx) = \theta(x)T(y)\theta(x)$ holds for all pairs $x,y \in U$. In this case $T(xy) = T(x)\theta(y) = \theta(x)T(y)$ for all $x,y \in U$, where θ is a surjective endomorphism of U, and $T(u) \in U$, for all $u \in U$.

For the proof of the result above we shall need the lemmas below

Lemma 1.[14]

If $U \not\subset Z$ is Lie ideal of a 2-tortion free prime ring R and $a , b \in R$ such that $aUb = \{0\}$, then a=0 or b=0 .

Lemma 2.[6]

Let R be a 2-tortion free prime ring , U be a square closed Lie ideal of R. Suppose that the relation $axb + bxc = 0$ holds for all $x \in U$ and some $a , b , c \in U$. In this case $(a + c)xb = 0$ is satisfied for all $x \in U$.

Proof of Theorem 1:

$$T(xyx) = \theta(x)T(y)\theta(x) \qquad \text{for all } x, y \in U \qquad (1)$$

We intend to prove the relation

$$[T(x) , \theta(x)] = 0, \qquad \text{for all } x \in U \qquad (2)$$

If U is a commutative , we obtain (2)

If U is a non commutative

For the proof of the relation(2) we shall need the weaker relation below

$$[[T(x), \theta(x)], \theta(x)] = 0, \quad \text{for all } x \in U \tag{3}$$

Putting $x + z$ for x in relation (1) (linearization), we obtain

$$T(xyz + zyx) = \theta(x)T(y)\theta(z) + \theta(z)T(y)\theta(x), \quad \text{for all } x, y, z \in U \tag{4}$$

Putting $y = x$ and $z = y$ in (4) one obtains

$$T(x^2y + yx^2) = \theta(x)T(x)\theta(y) + \theta(y)T(x)\,\theta(x), \quad \text{for all } x, y \in U \tag{5}$$

Putting 4xyx for y in (5), we obtain

$$T(xyx^3 + x^3yx) = \theta(x)T(x)\theta(xyx) + \theta(xyx)T(x)\,\theta(x) \text{ for all } x, y \in U \tag{6}$$

The substitution $x^2y + yx^2$ for y in relation (1) gives

$$T(xyx^3 + x^3yx) = \theta(x)T\,(x^2y + yx^2)\theta(x), \quad \text{for all } x, y \in U \tag{7}$$

which gives because of (5)

$$T(x^3yx + xyx^3) = \theta(x^2)T(x)\,\theta(yx) + \theta(xy)T(x)\,\theta(x^2), \quad \text{for all } x, y \in U \tag{8}$$

Combining (6) with (8), we arrive at

$$\theta(x)[T(x), \theta(x)]\,\theta(yx) - \theta(xy)[T(x), \theta(x)]\,\theta(x) = 0 \text{ for all } x, y \in U \tag{9}$$

From the above relation and Lemma 2 it follows that

$$[[T(x), \theta(x)], \theta(x)]\,\theta(yx) = 0, \quad \text{for all } x, y \in U \tag{10}$$

Let $\theta(y)$ be $2\theta(y)[T(x), \theta(x)]$ in (10). We have

$$[[T(x), \theta(x)], \theta(x)]\,\theta(y)\,[T(x), \theta(x)]\,\theta(x) = 0, \quad \text{for all } x, y \in U \tag{11}$$

Right multiplication of (10) by $[T(x), \theta(x)]$ gives

$$[[T(x), \theta(x)], \theta(x)]\,\theta(yx)\,[T(x), \theta(x)] = 0, \quad \text{for all } x, y \in U \tag{12}$$

Subtracting (12) from (11) one obtains $[[T(x), \theta(x)], \theta(x)]\,\theta(y)\,[[T(x), \theta(x)], \theta(x)] = 0$, for all $x,y \in U$, and (3) follows by Lemma 1. The next step is the relation

$$\theta(x)[T(x), \theta(x)]\,\theta(x) = 0, \quad \text{for all } x \in U \tag{13}$$

The linearization of (3) gives

$$[[T(x),\theta(x)],\theta(y)] + [[T(x),\theta(y)],\theta(x)] + [[T(y),\theta(x)],\theta(x)] + [[T(y), \theta(y)],\theta(x)] + [[T(y),\theta(x)], \theta(y)] + [[T(x), \theta(y)], \theta(y)] = 0, \text{ for all } x, y \in U$$

Putting -x for x in the above relation and comparing the relation so obtained with the above relation, we arrive at

$$[[T(x),\theta(x)],\theta(y)]+[[T(x),\theta(y)],\theta(x)]+[[T(y),\theta(x)],\theta(x)]=0, \text{ for all } x,y\in U \tag{14}$$

Putting 4xyx for y in (14) and using (1), (3) and (14), we obtain

$$0 = [[T(x),\theta(x)],\theta(xyx)] + [[T(x),\theta(xyx)],\theta(x)] + [[\theta(x)T(y)\theta(x),\theta(x)], \theta(x)] = \theta(x)[[T(x),\theta(x)],\theta(y)]\theta(x) + [[T(x),\theta(x)]\theta(yx) + \theta(x)[T(x),\theta(y)]\,\theta(x) + \theta(xy)[T(x),\theta(x)],\theta(x)] + [\theta(x)[T(y),\theta(x)]\theta(x),\theta(x)] = \theta(x)\,[[T(x), \theta(x)],\theta(y)]\theta(x) + [T(x),\theta(x)][\theta(y),\theta(x)]\theta(x) + \theta(x)[[T(x),\theta(y)],\theta(x)]\theta(x) + \theta(x)[\theta(y),\theta(x)][T(x),\theta(x)] + \theta(x)[[T(y),\theta(x)],\theta(x)]\theta(x) = [T(x),\theta(x)]\,[\theta(y),\theta(x)]\theta(x) + \theta(x)[\theta(y),\theta(x)][T(x),\theta(x)] = [T(x),\theta(x)]\theta(yx^2) - \theta(x^2y)\,[T(x),\theta(x)] + \theta(xyx)[T(x),\theta(x)] - [T(x),\theta(x)]\theta(xyx)$$

We have therefore $[T(x),\theta(x)]\theta(yx^2) - \theta(x^2y)[T(x),\theta(x)] + \theta(xyx)\,[T(x), \theta(x)] - [T(x), \theta(x)]\,\theta(xyx) = 0$, for all $x, y \in U$, which reduces because of (3) and (9) to

$$[T(x), \theta(x)]\,\theta(yx^2) - \theta(x^2y)\,[T(x), \theta(x)] = 0, \text{ for all } x,y \in U$$

Left multiplication of the above relation by $\theta(x)$ gives

$$\theta(x)[T(x), \theta(x)]\,\theta(yx^2) - \theta(x^3y)[T(x), \theta(x)] = 0, \quad \text{for all } x, y \in U$$

One can replace in the above relation, according to (9), $\theta(x)[T(x),\theta(x)]\theta(yx)$ by $\theta(xy)[T(x),\theta(x)]\theta(x)$, which gives

$$\theta(xy)[T(x),\theta(x)]\theta(x^2) - \theta(x^3y)[T(x),\theta(x)] = 0, \quad \text{for all } x,y \in U \qquad (15)$$

Left multiplication of the above relation by $T(x)$ gives

$$T(x)\theta(xy)[T(x),\theta(x)]\theta(x^2) - T(x)\theta(x^3y)[T(x),\theta(x)]=0, \text{ for all } x,y \in U \qquad (16)$$

The substitution $2T(x)\theta(y)$ for $\theta(y)$ in (15) leads to

$$\theta(x)T(x)\theta(y)[T(x),\theta(x)]\theta(x^2)-\theta(x^3)T(x)\theta(y)[T(x),\theta(x)]=0, \text{ for all } x,y\in U \qquad (17)$$

Subtracting (17) from (16), we obtain

$$[T(x),\theta(x)]\theta(y)[T(x),\theta(x)]\theta(x^2) - [T(x),\theta(x^3)]\theta(y)[T(x),\theta(x)] = 0, \quad \text{for all } x,y \in U$$

From the above relation and Lemma 2 it follows that

$$([T(x),\theta(x^3)] - [T(x),\theta(x)]\theta(x^2))\,\theta(y)\,[T(x), \theta(x)] = 0, \quad \text{for all } x,y \in U$$

which reduces to

$$(\theta(x)[T(x),\theta(x)]\theta(x)+\theta(x^2)[T(x),\theta(x)])\theta(y)[T(x),\theta(x)]= 0, \quad \text{for all } x,y \in U$$

Relation (3) makes it possible to write $[T(x)\,,\,\theta(x)]\,\theta(x)$ instead of $\theta(x)\,[T(x)\,,\,\theta(x)]$, which means that $\theta(x^2)\,[T(x)\,,\,\theta(x)]$ can be replaced by $\theta(x)\,[T(x)\,,\,\theta(x)]\,\theta(x)$ in the above relation. Thus we have

$$\theta(x)\,[T(x)\,,\,\theta(x)]\,\theta(xy)\,[T(x)\,,\,\theta(x)] = 0, \quad \text{for all } x,y \in U$$

Right multiplication of the above relation by $\theta(x)$ and substitution $2\theta(yx)$ for $\theta(y)$ gives finally

$$\theta(x)\,[T(x)\,,\,\theta(x)]\,\theta(xyx)\,[T(x)\,,\,\theta(x)]\,\theta(x) = 0, \quad \text{for all } x,y \in U$$

By the surjectivity of θ and Lemma 1, we get relation (13). Next we prove the relation

$$\theta(x)\,[T(x)\,,\,\theta(x)] = 0, \quad \text{for all } x \in U \qquad (18)$$

The substitution $2yx$ for y in (9) gives because of (13)

$$\theta(x)\,[T(x)\,,\,\theta(x)]\,\theta(yx^2) = 0, \quad \text{for all } x,y \in U \qquad (19)$$

Putting $2\theta(y)T(x)$ for $\theta(y)$ in the above relation, we obtain

$$\theta(x)\,[T(x)\,,\,\theta(x)]\,\theta(y)\,T\,(x)\,\theta(x^2) = 0\,, \quad \text{for all } x,y \in U \qquad (20)$$

Right multiplication of (19) by $T(x)$ gives

$$\theta(x)\,[T(x)\,,\,\theta(x)]\,\theta(y)\,\theta(x^2)\,T(x) = 0\,, \quad \text{for all } x,y \in U \qquad (21)$$

Subtracting (21) from (20), we obtain $\theta(x)\,[T(x)\,,\,\theta(x)]\,\theta(y)\,[T(x)\,,\,\theta(x^2)] = 0$, for all $x,y \in U$ which can be written in the form

$$\theta(x)[T(x),\,\theta(x)]\,\theta(y)\,([T(x)\,,\,\theta(x)]\,\theta(x) + \theta(x)\,[T(x)\,,\,\theta(x)]) = 0, \quad \text{for all } x,y \in U$$

According to (3) one can replace $[T(x),\theta(x)]\theta(x)$ in the relation above by $\theta(x)[T(x),\,\theta(x)]$,which gives $\theta(x)[T(x),\theta(x)]\theta(yx)[T(x),\theta(x)] = 0$, for all $x,y\in U$, By the surjectivity of θ and Lemma 1, we get relation (18). From (3) and (18) it follows that

$$[T(x)\,,\,\theta(x)]\,\theta(x) = 0, \quad \text{for all } x \in U$$

From the above relation one obtains (see how relation (14)was obtained from (3))

$$[T(x),\theta(x)]\theta(y) + [T(x),\,\theta(y)]\,\theta(x) + [T(y),\,\theta(x)]\,\theta(x) = 0, \quad \text{for all } x,y \in U$$

Right multiplication of the above relation by $[T(x)\,,\,\theta(x)]$ gives because of (18)

$[T(x), \theta(x)]\,\theta(y)\,[T(x), \theta(x)] = 0$, for all $x,y \in U$
which implies (2).
Our next task is to prove the relation

$$T(xy + yx) = T(y)\,\theta(x) + \theta(x)T(y), \quad \text{for all } x,y \in U \tag{22}$$

In order to prove the above relation we need the relations below

$$\theta(x)A(x,y)\theta(x) = 0 \quad \text{for all } x,y \in U \tag{23}$$

$$[A(x,y), \theta(x)] = 0, \quad \text{for all } x,y \in U \tag{24}$$

where $A(x,y)$ stands for $T(xy+yx)-T(y)\theta(x)-\theta(x)T(y)$. Let us first prove relation (23). The substitution $xy + yx$ for y in (1) gives

$$T(x^2yx + xyx^2) = \theta(x)\,T(xy+yx)\,\theta(x), \quad \text{for all } x,y \in U \tag{25}$$

On the other hand we obtain by putting $z = x^2$ in (4)

$$T(x^2yx + xyx^2) = \theta(x)T(y)\theta(x^2) + \theta(x^2)T(y)\theta(x), \quad \text{for all } x,y \in U \tag{26}$$

By comparing (25) and (26), we arrive at (23).
If $U \subset Z(R)$
From (23) one obtains (see how (14) was obtained from (3))
$\theta(x)A(x,y)\theta(z) + \theta(x)A(z,y)\theta(x) + \theta(z)A(x,y)\theta(x) = 0$, for all $x,y,z \in U$
Right multiplication of the above relation by $A(x,y)\theta(x)$ gives because of (23)

$$\theta(x)A(x,y)\,\theta(z)\,A(x,y)\,\theta(x) = 0, \quad \text{for all } x,y,z \in U \tag{27}$$

Right multiplication of the above relation by r, where $r \in R$, we have

$$(\theta(x)\,A(x,y))^2\ r\ \theta(z) = 0, \quad \text{for all } x,y,z \in U, r \in R$$

By primness of R, we obtain

$$\theta(x)\,A(x,y) = 0, \quad \text{for all } x, y \in U \tag{28}$$

Replacing x by $x + z$, we obtain

$$\theta(x)\,A(z,y) + \theta(z)\,A(x,y) = 0, \quad \text{for all } x, y, z \in U$$

Left multiplication of the above relation by $A(x,y)$ gives because of (28)

$$\theta(z)\,A(x,y)^2 = 0, \quad \text{for all } x, y, z \in U$$

By primness of R, and θ is onto, we obtain

$$A(x,y) = 0, \quad \text{for all } x, y \in U$$

If $U \not\subset Z(R)$
Let us prove relation (24). The linearization of (2) gives

$$[T(x), \theta(y)] + [T(y), \theta(x)] = 0, \quad \text{for all } x,y \in U \tag{29}$$

Putting $xy+yx$ for y in the above relation and using (2), we obtain $0 = [T(x),\theta(xy+yx)] + [T(xy+yx),\theta(x)] = \theta(x)[T(x),\theta(y)] + [T(x),\theta(y)]\theta(x) + [T(xy+yx),\theta(x)]$. Thus we have

$$[T(xy+yx),\theta(x)] + \theta(x)[T(x),\theta(y)] + [T(x), \theta(y)]\,\theta(x) = 0, \text{ for all } x,y \in U$$

According to (29) one can replace $[T(x),\theta(y)]$ by $-[T(y),\theta(x)]$ in the above relation. We have; therefore $[T(xy+yx),\theta(x)] - \theta(x)[T(y),\theta(x)] - [T(y),\theta(x)]\theta(x) = 0$, which can be written in the form $[T(xy+yx)-T(y)\theta(x)-\theta(x)T(y), \theta(x)] = 0$. The proof of relation (24) is therefore complete. Relation (24) makes it possible to replace in (27) $\theta(x)A(x,y)$ by $A(x,y)\theta(x)$. Thus, we have

$$A(x,y)\theta(x)\,\theta(z)\,A(x,y)\theta(x) = 0, \quad \text{for all } x,y,z \in U \tag{30}$$

By the surjectivity of θ and Lemma 1, we get

$$A(x,y)\,\theta(x) = 0, \quad \text{for all } x,y \in U \tag{31}$$

Of course, we have also

$$\theta(x)\,A(x,y) = 0, \quad \text{for all } x,y \in U \tag{32}$$

The linearization of (31) with respect to x gives

$A(x,y)\,\theta(z) + A(z,y)\,\theta(x) = 0$, for all $x,y,z \in U$

Right multiplication of the above relation by A(x,y) gives because of (32)

$A(x,y)\,\theta(z)\,A(x,y) = 0$, for all $x,y,z \in U$

which gives $A(x,y) = 0$, for all $x,y \in U$, by the surjectivity of θ and Lemma 1 .

The proof of relation (22) is therefore complete.

In particular for y = x relation (24) reduces to

$2T(x^2) = T(x)\,\theta(x) + \theta(x)\,T(x)$, for all $x \in U$

Combining the above relation with (2), we arrive at

$T(x^2) = T(x)\,\theta(x)$, for all $x \in U$

and

$T(x^2) = \theta(x)\,T(x)$, for all $x \in U$

By Theorem 1.3 in [5] it follows that $T(xy) = T(x)\theta(y) = \theta(x)T(y)$ for all $x,y \in U$, which completes the proof of the theorem. □

Corollary 1

Let R be a 2-tortion free prime ring , U a square closed Lie ideal of R, and let T: U→U be an additive mapping. Suppose that T(xyx) =xT(y)x holds for all pairs $x,y \in U$. In this case T is a centralizer .

Putting y = x in relation (1) we obtain

$$T(x^3) = \theta(x)\,T(x)\,\theta(x), \quad x \in U \tag{33}$$

The question arises whether in a 2-torsion free semiprime ring the above relation implies that $T(xy) = T(x)\theta(y) = \theta(x)T(y)$ for all $x,y \in U$. Unfortunately, we were unable to answer this question in general. However, we succeeded in proving that the answer is affirmative in case R has an identity element.

Theorem 2.

Let R be a 2-torsion free prime ring with an identity element , U a square closed Lie ideal of R with an identity element, and let T,θ: R→R are additive mappings. Suppose that $T(x^3) = \theta(x)T(x)\theta(x)$ holds for all $x \in U$. In this case, $T(xy) = T(x)\theta(y) = \theta(x)T(y)$ for all $x,y \in U$, where θ is a surjective endomorphism of R .

Proof:

Putting x+1 for x in relation (33), where 1 denotes the identity element, one obtains after some calculations

$3T(x^2)+2T(x)=T(x)\theta(x)+\theta(x)T(x)+\theta(x)a\theta(x)+ a\theta(x) + \theta(x)a$, for all $x \in U$

where a stands for T(1). Putting -x for x in the relation above and comparing the relation so obtained with the above relation, we obtain

$$6T(x^2) = 2T(x)\theta(x) + 2\theta(x)T(x) + 2\theta(x)a\theta(x), \text{ for all } x \in U \tag{34}$$

and

$$2T(x) = a\theta(x) + \theta(x)a , \quad \text{for all } x \in U \tag{35}$$

We intend to prove that $a \in Z(R)$. According to (35) one can replace $2T(x)$ on the right side of (34) by $a\theta(x)+\theta(x)a$ and $6T(x^2)$ on the left side by $3a\theta(x^2)+3\theta(x^2)a$, which gives after some calculation

$a\theta(x^2) + \theta(x^2)a - 2\theta(x)a\theta(x) = 0 , \quad \text{for all } x \in U$

The above relation can be written in the form

$$[[a , \theta(x)] , \theta(x)] = 0 , \quad \text{for all } x \in U \tag{36}$$

The linearization of the above relation gives

$$[[a , \theta(x)] , \theta(y)] + [[a , \theta(y)] , \theta(x)] = 0 , \text{ for all } x,y \in U \tag{37}$$

Putting $2xy$ for y in (37), we obtain because of (36) and (37)

$0=[[a,\theta(x)],\theta(xy)]+[[a,\theta(xy)],\theta(x)]=\theta(x)[[a,\theta(x)],\theta(y)]+[\theta(x)[a,\theta(y)],\theta(x)]+[[a,\theta(x)]\theta(y),\theta(x)]$

Thus, we have

$$[a , \theta(x)][\theta(y) , \theta(x)] = 0 , \quad \text{for all } x,y \in U$$

The substitution $2\theta(y)a$ for $\theta(y)$ in the above relation gives

$$[a , \theta(x)] \theta(y) [a , \theta(x)] = 0 , \text{ for all } x,y \in U \tag{38}$$

whence it follows $a \in Z(R)$ by the surjectivity of θ and Lemma 1, if $U \not\subset Z(R)$, which reduces(35) to the form $T(x)=a\theta(x)$, for all $x \in U$

If $U \subset Z(R)$

Right multiplication of the relation(38) by r, where $r \in R$, and By primness of R, and θ is onto, we obtain $a \in Z(R)$, which also reduces(35) to the form $T(x)=a\theta(x)$, for all $x \in U$

The proof of the theorem is complete. □

Corollary 2

Let R be a 2-torsion free prime ring with an identity element , U a square closed Lie ideal of R with an identity element, and let $T: R \to R$ an additive mapping. Suppose that $T(x^3) = xT(x)x$ holds for all $x \in U$. In this case, $T(xy) = T(x)y = xT(y)$ for all $x,y \in U$.

Theorem 3

Let R be a 2-torsion free semiprime ring with an identity element and let $T:R \to R$ be an additive mapping. Suppose that $T(xyx) = \theta(x)\, T(y)\, \theta(x)$ holds for all $x,y \in R$. In this case T is a θ-centralizer , where θ is a surjective endomorphism of R and $\theta(Z(R)) = Z(R)$.

Proof :

By Theorem 1[7] we get T is Jordan left and right θ-centralizer on R

By Theorem 1[15], it follows that T is left and right θ-centralizer on R, , which completes the proof. □

REFERENCES

1. BreŠar M.Jordan mappings of semiprime rings,J.Algebra,127:218-228, (1989)
2. Zalar B. On centralizers of semiprime rings, Comment. Math. Univ. Carolinae, 32: 609-614, (1991)
3. Majeed A.H. Meften M.I. Jordan θ-Centralizers of Prime and Semiprime Rings, Baghdad Science Journal,??, ???-???, (2010).
4. Majeed A.H. Meften M.I. On θ-Centralizers of Prime and Semiprime Rings, AL-Qadisiya J. for Comp. Sci. and Math.,1 (1):58-66, (2009).
5. Majeed A.H. Meften M.I. Lie Ideals and Jordan θ-Centralizers Of Prime Rings, JNUS, 1,14, ???-??? , (2011).
6. Majeed A.H. Meften M.I. Lie Ideals and θ-Centralizers of Prime Rings. (submitted to conference of the College of Education, University of AL-Mustansiriyah 2010).
7. Majeed A.H. Meften M.I. An Identity on θ-Centralizers of Prime and Semiprime Rings. Proceeding of 3rd scientific conference of the College of Science, University of Baghdad : 523-528(24 to 26 March 2009).
8. Herstein I.N. Jordan derivations of prime rings, Proc. Amer. Math. Soc., 8 :1104-1110, (1957)
9. BreŠar M. Vukman J. Jordan derivations on prime rings, Bull. Austral. Math. Soc., 37:321-322, (1988)
10. Cusack,J.Jordan derivations on rings,Proc.Amer.Math.Soc.53:321-324(1975)
11. BreŠar M. Jordan derivations on semiprime rings,Proc.Amer.Math.Soc., 104 :1003-1006, (1988)
12. Vukman J. An identity related to centralizers in semiprime rings, Comment. Math. Univ. Carolinae 40: 447-456(1999).
13. Vukman J.Centralizers on semiprime rings, Comment. Math. Univ. Carolinae, 42:237-245, (2001)
14. Bergen J. Herstein I.N. and Ker J.W. Lie ideals and derivation of prime rings , J. Algebra 71:259-267, (1981)
15. Albas E.,On τ-Centralizers of semiprime rings,Siberian Math.J.48,2:191-196, (2007)

On the resolution of Wely module in the Case of Two-Rowed Skew-Shape (p+t,q)/(t,0)

Haytham R. Hassan
Department of Mathematics, College of Science, University of Al-Mustansiriyah

الخلاصة

في هذا البحث نوقش تحلل مقاس وايل في حالة شبه شكل صفين (p+t,q)/(t,0) ,عندما F , D_rF مقاس حرو والجبر ذو القوة المقسمة ذو الدرجة r على التوالي .
كذلك اعطيت وطبقت نظريا مثالين على تحلل مقاس وايل المرتبطه بالشكل شبه الصفي عندما يكون بروز الصف الثاني الى يسار الصف الاول بمقدار 1،2على التوالي.

ABSTRACT

In this paper, the resolution of Weyl module in the case of the skew-partition (p+t,q)/(t,0), where F and D_rF are free module and divided power algebra of degree r, respectively, have been discussed.

Two examples of the resolution of Weyl module which associate to the two-rowed skew-shape when the protuberance of the second row to the left of the first is 1, 2 respectively, have also been demonstrated.

INTRODUCTION

Let F be a free module over a commutative ring R and D_r be divided power of degree r underlying the free module F, there is an important general problem which is the representation theorem of $GL_n(R)$ .To study this problem, in 1998 David Buchsbam (1) had started with new techniques by using letter place algebra and differential bar complex.

We reconstruct the resolution for the two-rowed Weyl module as it is described in (2), we do this for two reasons; to illustrate the use of classical bar-complex (3) in our context, and to make explicit the fact that, using letter place techniques.

Recall that the Weyl module associated to the skew-shape

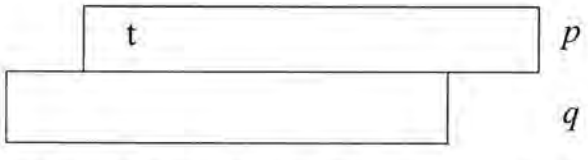

is the image of $D_p \otimes D_q$ under the Weyl map. The 'box map' refered to earlier in this paper was described in [4] as the map

$$\sum_{k>t} D_{p+k} \otimes D_{q-k} \longrightarrow D_p \otimes D_q$$

which sends an element $x \otimes y$ of $D_{p+k} \otimes D_{q-k}$ to $\sum x_p \otimes x'_k y$, where $\sum x_p \otimes x'_k$ is the component of the diagonal of x in $D_p \otimes D_k$. To put this all in letter place perspective, we see that if we take a double standard tableau say $\begin{pmatrix} w \\ w' \end{pmatrix}, \begin{vmatrix} 1^{(p)}2^{(k)} \\ 2^{(q-k)} \end{vmatrix}$ in $D_p \otimes D_q$, the Wely map can defined as the composition of place polarizations (1).

As in (2) let Z_{12} stand for the generator of divided power algebra in one free generator, we see that $Z_{12}^{(k)}$ acts on $D_{p+k} \otimes D_{q-k}$ and carries it to $D_p \otimes D_q$.

In this paper we shall omit the letter F when we write the divided powers, and other functors applied to F.

Section 2. The two rowed case

In this section we look at the general two-rowed skew shape

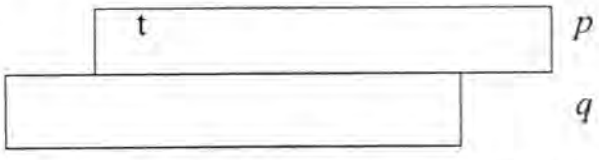

where the top row has p boxes, the second row has q boxes and the protuberance of the second row to the left of the first is t. Expressed in terms of skew partitions this is simply (p + t,q)/(t,0).(2)

The weyl module associated to this shape has the resolution

$$0 \longrightarrow M_{q-t} \xrightarrow{d_{q-t}} M_{q-t-1} \xrightarrow{d_{q-t-1}} \ldots \xrightarrow{d_3} M_2 \xrightarrow{d_2} M_1 \xrightarrow{d_1} M_0$$

Where

$$M_0 = D_p \otimes D_q$$

$$M_1 = \sum_{\ell>t} Z_{21}^{(\ell)} x D_{p+\ell} \otimes D_{q-\ell}$$

$$\vdots$$

$$M_k = \sum_{\ell_1>t} Z_{21}^{(\ell_1)} x Z_{21}^{(\ell_2)} x \ldots x Z_{21}^{(\ell_k)} x D_{p+|\ell|} \otimes D_{q-|\ell|}$$

$$\vdots$$

$$M_{q-t} = Z_{21}^{(t+1)} x Z_{21}^{(1)} x \ldots x Z_{21}^{(1)} x D_{p+q} \otimes D_0$$

By D_r we mean the divided power of degree r of the underlying free module F. The symbol $Z_{21}^{(\ell)}$ stands for the divided power of degree ℓ of the free generator Z_{21} and the action of $Z_{21}^{(\ell)}$ on any term $D_u \otimes D_v$ is as place polarization of degree ℓ from place one to place two. By $|\ell|$ we mean the sum $\ell_1 + \ell_2 + ... + \ell_k$ and the symbol x stands for separator variable (in the sense 0f [B-R2] (3). All the indices ℓ_i are assumed to be positive. The boundery maps are those of the Bar complex as described in the same article. For example, using letter place notation for the basis elements of $D_u \otimes D_v$, with our complex given above, Buchsbaum in (1) defined the homotopy as follows :

$$s_0 : D_p \otimes D_q \longrightarrow \sum_{k>0} Z_{21}^{(t+k)} x D_{p+t+k} \otimes D_{q-t-k}$$

is defined by sending the double standard tableau $\begin{pmatrix} w \\ w \end{pmatrix}, \begin{vmatrix} 1^{(p)} 2^{(k)} \\ 2^{(q-k)} \end{pmatrix}$ to zero if $k \le t$ and to $Z_{21}^{k} x \begin{pmatrix} w \\ w \end{pmatrix}, \begin{vmatrix} 1^{(p+k)} \\ 2^{(q-k)} \end{pmatrix}$ if $k > t$. For higher dimensions,

$$s_\ell : \sum_{k_i>0} Z_{21}^{(t+k_1)} x Z_{21}^{(k_2)} x ... x Z_{21}^{(k_\ell)} x D_{p+t+|k|} \otimes D_{q-t-|k|} \longrightarrow$$

$$\sum_{k_i>0} Z_{21}^{(t+k_1)} x Z_{21}^{(k_2)} x ... x Z_{21}^{(k_{\ell+1})} x D_{p+t+|k|} \otimes D_{q-t-|k|}, \ \ell > 0$$

is defined by sending $Z_{21}^{(t+k_1)} x Z_{21}^{(k_2)} x ... x Z_{21}^{(k_\ell)} x \begin{pmatrix} w \\ w \end{pmatrix}, \begin{vmatrix} 1^{(p+t+|k|)} 2^{(m)} \\ 2^{(q-t-m)} \end{pmatrix}$ to zero if $m = 0$, and to $Z_{21}^{(t+k_1)} x Z_{21}^{(k_2)} x ... x Z_{21}^{(k_\ell)} x Z_{21}^{(m)} x \begin{pmatrix} w \\ w \end{pmatrix}, \begin{vmatrix} 1^{(p+t+|k|+m)} \\ 2^{(q-t-m)} \end{pmatrix}$ if $m > 0$.

Section 3. The case of the skew-shape

In this section we stady the resolution of Weyl module in the case of the skew-shape **(5,4)/(1,0)** and the protuberance of the second row to the left of the first is one.

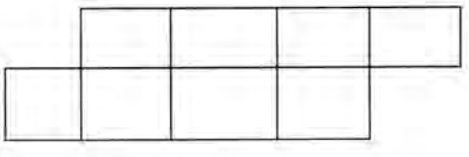

The resolution of Weyl module associated to this shape has the following terms.

$$M_0 = D_4 \otimes D_4$$

$$M_1 = Z_{21}^{(2)} x D_6 \otimes D_2 \oplus Z_{21}^{(3)} x D_7 \otimes D_1 \oplus Z_{21}^{(4)} x D_8 \otimes D_0$$

$$M_2 = Z_{21}^{(2)} x Z_{21} x D_7 \otimes D_1 \oplus Z_{21}^{(3)} x Z_{21} x D_8 \otimes D_0 \oplus Z_{21}^{(2)} x Z_{21}^{(2)} x D_8 \otimes D_0$$

$$M_3 = Z_{21}^{(3)} x Z_{21} x Z_{21} x D_8 \otimes D_0 .$$

$$\begin{array}{ccccccc} M_3 & \xrightarrow{\partial x} & M_2 & \xrightarrow{\partial x} & M_1 & \xrightarrow{\partial x} & M_0 \\ id \uparrow & \swarrow s_2 & \downarrow id & \swarrow s_1 & \downarrow id & \swarrow s_0 & \downarrow id \\ M_3 & \xrightarrow{\partial x} & M_2 & \xrightarrow{\partial x} & M_1 & \xrightarrow{\partial x} & M_0 \end{array}$$

As for homotopics we have

$s_0 : M_0 \longrightarrow M_1$ where

$$s_0\left(\begin{matrix} w \\ w' \end{matrix} \middle| \begin{matrix} 1^{(4)} 2^{(k)} \\ 2^{(4-k)} \end{matrix}\right) = \begin{cases} Z_{21}^{(k)} x \left(\begin{matrix} w \\ w' \end{matrix} \middle| \begin{matrix} 1^{(4+k)} \\ 2^{(4-k)} \end{matrix}\right) & k = 2,3,4 \\ 0 & if\ k \le 1 \end{cases}$$

and $s_1 : M_1 \longrightarrow M_2$ where

$$s_1\left(Z_{21}^{(k+1)} x \left(\begin{matrix} w \\ w' \end{matrix} \middle| \begin{matrix} 1^{(5+k)} 2^{(m)} \\ 2^{(3-k-m)} \end{matrix}\right)\right) = \begin{cases} Z_{21}^{(k+1)} x Z_{21}^{(m)} x \left(\begin{matrix} w \\ w' \end{matrix} \middle| \begin{matrix} 1^{(5+k+m)} \\ 2^{(3-k-m)} \end{matrix}\right) & if \quad m = 1,2 \\ 0 & if \quad m = 0 \end{cases}$$

and $s_2 : M_2 \longrightarrow M_3$ where

$$s_2\left(Z_{21}^{(k+1)} x Z_{21}^{(k_2)} x \left(\begin{matrix} w \\ w' \end{matrix} \middle| \begin{matrix} 1^{(5+k_1+k_2)} 2^{(m)} \\ 2^{(3-k_1-k_1-m)} \end{matrix}\right)\right)$$

$$= \begin{cases} Z_{21}^{(k_1+1)} x Z_{21}^{(k_2)} x Z_{21}^{(m)} x \left(\begin{matrix} w \\ w' \end{matrix} \middle| \begin{matrix} 1^{(5+k_1+k_2+m)} \\ 2^{(3-k_1-k_2-m)} \end{matrix}\right) & if \quad m = 1 \\ 0 & if \quad m = 0 \end{cases}$$

Now

$$s_0 \partial x \left(Z_{21}^{(k+1)} x \left(\begin{matrix} w \\ w' \end{matrix} \middle| \begin{matrix} 1^{(5+k)} 2^{(m)} \\ 2^{(3-k-m)} \end{matrix}\right)\right) = s_0 \partial_{21}^{(k+1)} \left(\begin{matrix} w \\ w' \end{matrix} \middle| \begin{matrix} 1^{(5+k)} 2^{m} \\ 2^{(3-k-m)} \end{matrix}\right)$$

$$= \binom{k+1+m}{m} s_0 \left(\begin{matrix} w \\ w' \end{matrix} \middle| \begin{matrix} 1^{(4)} 2^{(k+1+m)} \\ 2^{(3-k-m)} \end{matrix}\right) = Z_{21}^{(k+1+m)} \left(\begin{matrix} w \\ w' \end{matrix} \middle| \begin{matrix} 1^{(5+k+m)} \\ 2^{(3-k-m)} \end{matrix}\right)$$

and

$$\partial x s_1(Z_{21}^{(k+1)} x \begin{pmatrix} w \\ w' \end{vmatrix} \begin{matrix} 1^{(5+k)} 2^{(m)} \\ 2^{(3-k-m)} \end{matrix} \end{pmatrix} = \partial x (Z_{21}^{(k+1)} x Z_{21}^{(m)} x) \begin{pmatrix} w \\ w' \end{vmatrix} \begin{matrix} 1^{(5+k+m)} \\ 2^{(3-k-m)} \end{matrix} \end{pmatrix}$$

$$= -\binom{k+1+m}{m} Z_{21}^{(k+1+m)} x \begin{pmatrix} w \\ w' \end{vmatrix} \begin{matrix} 1^{(5+k+m)} \\ 2^{(3-k-m)} \end{matrix} \end{pmatrix} + Z_{21}^{(k+1)} x \begin{pmatrix} w \\ w' \end{vmatrix} \begin{matrix} 1^{(5+k)} 2^{(m)} \\ 2^{(3-k-m)} \end{matrix} \end{pmatrix}$$

It is clear that $s_0 \partial x + \partial x s_1 = id$

Now

$$s_1 \partial x (Z_{21}^{(k+1)} x Z_{21}^{(k_2)} x) \begin{pmatrix} w \\ w' \end{vmatrix} \begin{matrix} 1^{(5+k_1+k_2)} 2^{(m)} \\ 2^{(3-k_1-k_2-m)} \end{matrix} \end{pmatrix}$$

$$= s_1(-\binom{k_1+k_2+1}{k_2} Z_{21}^{(k_1+1+k_2)} x \begin{pmatrix} w \\ w' \end{vmatrix} \begin{matrix} 1^{(5+k_1+k_2)} 2^{(m)} \\ 2^{(3-k_1-k_2-m)} \end{matrix} \end{pmatrix}$$

$$+ Z_{21}^{(k_1+1)} x \begin{pmatrix} w \\ w' \end{vmatrix} \begin{matrix} 1^{(5+k_1)} 2^{(k_2)} 2^{(m)} \\ 2^{(3-k_1-k_2-m)} \end{matrix} \end{pmatrix}$$

$$= s_1(-\binom{k_1+k_2+1}{k_2} Z_{21}^{(k_1+k_2+1)} x \begin{pmatrix} w \\ w' \end{vmatrix} \begin{matrix} 1^{(5+k_1+k_2)} 2^{(m)} \\ 2^{(3-k_1-k_2-m)} \end{matrix} \end{pmatrix}$$

$$+ \binom{k_1+m}{m} Z_{21}^{(k_1+1)} x \begin{pmatrix} w \\ w' \end{vmatrix} \begin{matrix} 1^{(5+k_1)} 2^{(k_2+m)} \\ 2^{(3-k_1-k_2-m)} \end{matrix} \end{pmatrix}$$

$$= -\binom{k_1+k_2+1}{k_2} Z_{21}^{(k_1+k_2+1)} x Z_{21}^{(m)} x \begin{pmatrix} w \\ w' \end{vmatrix} \begin{matrix} 1^{(5+k_1+k_2+m)} \\ 2^{(3-k_1-k_2-m)} \end{matrix} \end{pmatrix}$$

$$+ \binom{k_2+m}{m} Z_{21}^{(k_1+1)} x Z_{21}^{(k_2+m)} x \begin{pmatrix} w \\ w' \end{vmatrix} \begin{matrix} 1^{(5+k_1+k_2+m)} \\ 2^{(3-k_1-k_2-m)} \end{matrix} \end{pmatrix}$$

and

$$\partial x s_2(Z_{21}^{(k+1)} x Z_{21}^{(k_2)} x) \begin{pmatrix} w \\ w' \end{vmatrix} \begin{matrix} 1^{(5+k_1+k_2)} 2^{(m)} \\ 2^{(3-k_1-k_2-m)} \end{matrix} \end{pmatrix}$$

$$= \partial x (Z_{21}^{(k_1+1)} x Z_{21}^{(k_2)} x Z_{21}^{(m)} x \begin{pmatrix} w \\ w' \end{vmatrix} \begin{matrix} 1^{(5+k_1+k_2+m)} \\ 2^{(3-k_1-k_2-m)} \end{matrix} \end{pmatrix}$$

$$= \partial x (Z_{21}^{(k_1+1)} x Z_{21}^{(k_2)} x Z_{21}^{(m)} x \begin{pmatrix} w \\ w' \end{vmatrix} \begin{matrix} 1^{(5+k_1+k_2+m)} \\ 2^{(3-k_1-k_2-m)} \end{matrix} \end{pmatrix}$$

$$+ \binom{k_1+k_2+1}{k_2} Z_{21}^{(k_1+k_2+1)} x Z_{21}^{(m)} x \begin{pmatrix} w \\ w' \end{vmatrix} \begin{matrix} 1^{(5+k_1+k_2+m)} \\ 2^{(3-k_1-k_2-m)} \end{matrix} \end{pmatrix}$$

$$- \binom{k_2+m}{m} Z_{21}^{(k_1+1)} x Z_{21}^{(k_2+m)} x \begin{pmatrix} w \\ w' \end{vmatrix} \begin{matrix} 1^{(5+k_1+k_2+m)} \\ 2^{(3-k_1-k_2-m)} \end{matrix} \end{pmatrix}$$

$$+ Z_{21}^{(k_1+1)} x Z_{21}^{(k_2)} x \begin{pmatrix} w \\ w' \end{vmatrix} \begin{matrix} 1^{(5+k_1+k_2)} 2^{(m)} \\ 2^{(3-k_1-k_2-m)} \end{matrix} \end{pmatrix}$$

So we get $s_1\partial x + \partial x s_2 = id$, hence $\{s_0, s_1, s_2\}$ is a contracting homotopy, which implies the complex

$$0 \longrightarrow M_3 \longrightarrow M_2 \longrightarrow M_1 \longrightarrow M_0$$

is exact.

Section 4. The case of the skew-shape (6,6)/(2,0)

In order to look at the resolution of Weyl module which associate to the two rowed skew-shape when the protuberance of the second row to the left of first is two, in this section we study the resolution of Weyl module in the case of the skew-shape **(6,6)/(2,0)** when t=2.

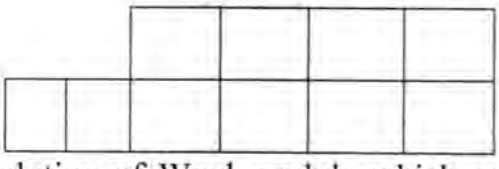

The resolution of Weyl module which associated to this skew-shape has the following termes

$$M_0 = D_4 \otimes D_6$$

$$M_1 = Z_{21}^{(3)} x D_7 \otimes D_3 \oplus Z_{21}^{(4)} x D_8 \otimes D_2 \oplus Z_{21}^{(5)} x D_9 \otimes D_1 \oplus Z_{21}^{(6)} x D_{10} \otimes D_0$$

$$M_2 = Z_{21}^{(3)} x Z_{21} x D_8 \otimes D_2 \oplus Z_{21}^{(4)} x Z_{21} x D_9 \otimes D_1 \oplus Z_{21}^{(3)} x Z_{21}^{(2)} x D_9 \otimes D_1$$
$$\oplus Z_{21}^{(5)} x Z_{21} x D_{10} \otimes D_0 \oplus Z_{21}^{(4)} x Z_{21}^{(2)} x D_{10} \otimes D_0 \oplus Z_{21}^{(3)} x Z_{21}^{(3)} x D_{10} \otimes D_0$$

$$M_3 = Z_{21}^{(3)} x Z_{21} x Z_{21} x D_9 \otimes D_1 \oplus Z_{21}^{(4)} x Z_{21} x Z_{21} x D_{10} \otimes D_0$$
$$\oplus Z_{21}^{(3)} x Z_{21}^{(2)} x Z_{21} x D_{10} \otimes D_0 \oplus Z_{21}^{(3)} x Z_{21} x Z_{21}^{(2)} x D_{10} \otimes D_0$$

$$M_4 = Z_{21}^{(3)} x Z_{21} x Z_{21} x Z_{21} x D_{10} \otimes D_0$$

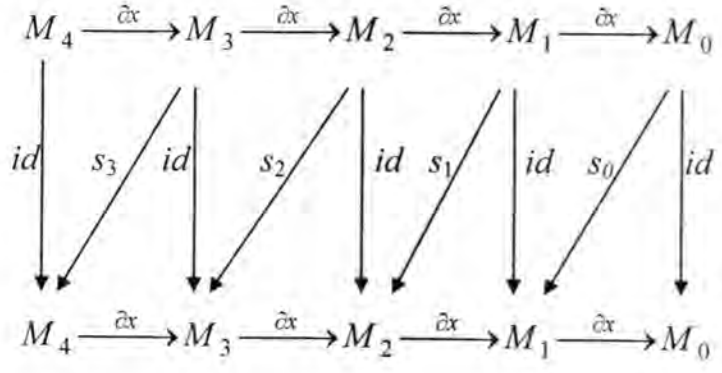

As for homotopies we have

$s_0 : M_0 \longrightarrow M_1$ where

$$s_0\left(\begin{pmatrix} w \\ w' \end{pmatrix} \middle| \begin{matrix} 1^{(4)}2^{(k)} \\ 2^{(6-k)} \end{matrix}\right) = \begin{cases} Z_{21}^{(k)} x \begin{pmatrix} w \\ w' \end{pmatrix} \middle| \begin{matrix} 1^{(4+k)} \\ 2^{(6-k)} \end{matrix} & if \ k = 3,4,5 \\ 0 & if \ k = 2 \end{cases}$$

and $s_1 : M_1 \longrightarrow M_2$ where

$$s_1(Z_{21}^{(k+2)} x \begin{pmatrix} w \\ w' \end{pmatrix} \middle| \begin{matrix} 1^{(6+k)}2^{(m)} \\ 2^{(4-k-m)} \end{matrix}) = \begin{cases} Z_{21}^{(k+2)} x Z_{21}^{(m)} x \begin{pmatrix} w \\ w' \end{pmatrix} \middle| \begin{matrix} 1^{(6+k+m)} \\ 2^{(4-k-m)} \end{matrix} & if \ m = 1,2,3 \\ 0 & if \ m = 0 \end{cases}$$

and $s_2 : M_2 \longrightarrow M_3$ where

$$s_2(Z_{21}^{(k_1+2)} x Z_{21}^{(k_2)} x \begin{pmatrix} w \\ w' \end{pmatrix} \middle| \begin{matrix} 1^{(6+k_1+k_2)}2^{(m)} \\ 2^{(4-k_1-k_i-m)} \end{matrix})$$

$$= \begin{cases} Z_{21}^{(k_1+2)} Z_{21}^{(k_2)} x Z_{21}^{(m)} x \begin{pmatrix} w \\ w' \end{pmatrix} \middle| \begin{matrix} 1^{(6+k_1+k_2+m)} \\ 2^{(4-k_1-k_2-m)} \end{matrix} & if \ m = 1,2 \\ 0 & if \ m = 0 \end{cases}$$

and $s_3 : M_3 \longrightarrow M_4$ where

$$s_3(Z_{21}^{(k_1+2)} x Z_{21}^{(k_2)} x Z_{21}^{(k_3)} x \begin{pmatrix} w \\ w' \end{pmatrix} \middle| \begin{matrix} 1^{(6+k_1+k_2+k_3)}2^{(m)} \\ 2^{(4-k_1-k_2-k_3-m)} \end{matrix})$$

$$= \begin{cases} Z_{21}^{(k_1+2)} x Z_{21}^{(k_2)} x Z_{21}^{(k_3)} x Z_{21}^{(m)} x \begin{pmatrix} w \\ w' \end{pmatrix} \middle| \begin{matrix} 1^{(6+k_1+k_2+k_3+m)} \\ 2^{(4-k_1-k_2-k_3-m)} \end{matrix} & if \ m = 1 \\ 0 & if \ m = 0 \end{cases}$$

Now

$$s_0 \partial x (Z_{21}^{(k+2)} x \begin{pmatrix} w \\ w' \end{pmatrix} \middle| \begin{matrix} 1^{(6+k)}2^{(m)} \\ 2^{(4-k-m)} \end{matrix}) = s_0(\partial_{21}^{(k+2)} \begin{pmatrix} w \\ w' \end{pmatrix} \middle| \begin{matrix} 1^{(6+k)}2^{(m)} \\ 2^{(4-k-m)} \end{matrix})$$

$$= \binom{k+2+m}{m} s_0 \left(\begin{pmatrix} w \\ w' \end{pmatrix} \middle| \begin{matrix} 1^{(4)}2^{(k+2+m)} \\ 2^{(4-k-m)} \end{matrix} \right)$$

$$= \binom{k+2+m}{m} Z_{21}^{(k+2+m)} x \left(\begin{pmatrix} w \\ w' \end{pmatrix} \middle| \begin{matrix} 1^{(6+k+m)} \\ 2^{(4-k-m)} \end{matrix} \right)$$

and

$$\partial x s_1 \left(Z_{21}^{(k+2)} x \begin{pmatrix} w \\ w' \end{pmatrix} \middle| \begin{matrix} 1^{(6+k)}2^{(m)} \\ 2^{(4-k-m)} \end{matrix} \right) = \partial x \left(Z_{21}^{(k+2)} x Z_{21}^{(m)} x \begin{pmatrix} w \\ w' \end{pmatrix} \middle| \begin{matrix} 1^{(6+k+m)} \\ 2^{(4-k-m)} \end{matrix} \right)$$

$$=-\binom{k+2+m}{m} Z_{21}^{(k+2+m)} x \begin{pmatrix} w \\ w' \end{pmatrix} \begin{vmatrix} 1^{(6+k+m)} \\ 2^{(4-k-m)} \end{vmatrix} + Z_{21}^{(k+2)} x \begin{pmatrix} w \\ w' \end{pmatrix} \begin{vmatrix} 1^{(6+k)} 2^{(m)} \\ 2^{(4-k-m)} \end{vmatrix}$$

It is clear that $s_0 \partial x + \partial x s_1 = id$

Now

$$s_1 \partial x \left(Z_{21}^{(k_1+2)} x Z_{21}^{(k_2)} x \begin{pmatrix} w \\ w' \end{pmatrix} \begin{vmatrix} 1^{(6+k_1+k_2)} 2^{(m)} \\ 2^{(4-k_1-k_2-m)} \end{vmatrix} \right)$$

$$= s_1 (-\binom{k_1+k_2+2}{k_2} Z_{21}^{(k_1+k_2+2)} x \begin{pmatrix} w \\ w' \end{pmatrix} \begin{vmatrix} 1^{(6+k_1+k_2)} 2^{(m)} \\ 2^{(4-k_1-k_2-m)} \end{vmatrix}$$

$$+\binom{k_2+m}{k_2} Z_{21}^{(k_1+2)} x \begin{pmatrix} w \\ w' \end{pmatrix} \begin{vmatrix} 1^{(6+k_1)} 2^{(k_2+m)} \\ 2^{(4-k_1-k_2-m)} \end{vmatrix}$$

$$=-\binom{k_1+k_2+2}{k_2} Z_{21}^{(k_1+k_2+2)} x Z_{21}^{(m)} x \begin{pmatrix} w \\ w' \end{pmatrix} \begin{vmatrix} 1^{(6+k_1+k_2+m)} \\ 2^{(4-k_1-k_2-m)} \end{vmatrix} +$$

$$+\binom{k_2+m}{k_2} Z_{21}^{(k_1+2)} x Z_{21}^{(k_2+m)} x \begin{pmatrix} w \\ w' \end{pmatrix} \begin{vmatrix} 1^{(6+k_1+k_2+m)} \\ 2^{(4-k_1-k_2-m)} \end{vmatrix}$$

and

$$\partial x s_2 \left(Z_{21}^{(k_1+2)} x Z_{21}^{(k_2)} x \begin{pmatrix} w \\ w' \end{pmatrix} \begin{vmatrix} 1^{(6+k_1+k_2)} 2^{(m)} \\ 2^{(4-k_1-k_2-m)} \end{vmatrix} \right)$$

$$= \partial x \, (Z_{21}^{(k_1+2)} x Z_{21}^{(k_2)} x Z_{21}^{(m)} x \begin{pmatrix} w \\ w' \end{pmatrix} \begin{vmatrix} 1^{(6+k_1+k_2+m)} \\ 2^{(4-k_1-k_2-m)} \end{vmatrix}$$

$$=\binom{k_1+k_2+2}{k_2} Z_{21}^{(k_1+k_2+2)} x Z_{21}^{(m)} x \begin{pmatrix} w \\ w' \end{pmatrix} \begin{vmatrix} 1^{(6+k_1+k_2+m)} \\ 2^{(4-k_1-k_2-m)} \end{vmatrix} -$$

$$\binom{k_2+m}{m} Z_{21}^{(k_1+2)} x Z_{21}^{(k_2+m)} x \begin{pmatrix} w \\ w' \end{pmatrix} \begin{vmatrix} 1^{(6+k_1+k_2+m)} \\ 2^{(4-k_1-k_2-m)} \end{vmatrix} +$$

$$Z_{21}^{(k_1+2)} x Z_{21}^{(k_2)} x \begin{pmatrix} w \\ w' \end{pmatrix} \begin{vmatrix} 1^{(6+k_1+k_2)} 2^{(m)} \\ 2^{(4-k_1-k_2-m)} \end{vmatrix}$$

It is clear that $s_1 \partial x + \partial x s_2 = id$

Now

$$s_2 \partial x \left(Z_{21}^{(k_1+2)} x Z_{21}^{(k_2)} x Z_{21}^{(k_3)} x \begin{pmatrix} w \\ w' \end{pmatrix} \begin{vmatrix} 1^{(6+k_1+k_2+k_3)} 2^{(m)} \\ 2^{(4-k_1-k_2-k_3-m)} \end{vmatrix} \right)$$

$$= s_2 (+\binom{k_1+k_2+2}{k_2} Z_{21}^{(k_1+k_2+2)} x Z_{21}^{(k_3)} x \begin{pmatrix} w \\ w' \end{pmatrix} \begin{vmatrix} 1^{(6+k_1+k_2+k_3)} 2^{(m)} \\ 2^{(4-k_1-k_2-k_3-m)} \end{vmatrix} -$$

$$\binom{k_2+k_3}{k_3} Z_{21}^{(k_1+2)} x Z_{21}^{(k_2+k_3)} x \begin{pmatrix} w \\ w' \end{pmatrix} \begin{vmatrix} 1^{(6+k_1+k_2+k_3)} 2^{(m)} \\ 2^{(4-k_1-k_2-k_3-m)} \end{vmatrix} +$$

$$+\binom{k_3+m}{m} Z_{21}^{(k_1+2)} x Z_{21}^{(k_2)} x \begin{pmatrix} w \\ w' \end{pmatrix} \begin{vmatrix} 1^{(6+k_1+k_2)} 2^{(k_3+m)} \\ 2^{(4-k_1-k_2-k_3-m)} \end{vmatrix} =$$

$$\binom{k_1+k_2+2}{k_2} Z_{21}^{(k_1+k_2+2)} x Z_{21}^{(k_3)} x Z_{21}^{(m)} x \begin{pmatrix} w \\ w' \end{pmatrix} \begin{vmatrix} 1^{(6+k_1+k_2+k_3+m)} \\ 2^{(4-k_1-k_2-k_3-m)} \end{vmatrix} -$$

$$\binom{k_2+k_3}{k_3} Z_{21}^{(k_1+2)} x Z_{21}^{(k_2+k_3)} x Z_{21}^{(m)} x \begin{pmatrix} w \\ w' \end{pmatrix} \begin{vmatrix} 1^{(6+k_1+k_2+k_3+m)} \\ 2^{(4-k_1-k_2-k_3-m)} \end{vmatrix} +$$

$$\binom{k_3+m}{m} Z_{21}^{(k_1+2)} x Z_{21}^{(k_2)} x Z_{21}^{(k_3+m)} x \begin{pmatrix} w \\ w' \end{pmatrix} \begin{vmatrix} 1^{(6+k_1+k_2+k_3+m)} \\ 2^{(4-k_1-k_2-k_3-m)} \end{vmatrix}$$

and

$$\partial x s_3 \left(Z_{21}^{(k_1+2)} x Z_{21}^{(k_2)} x Z_{21}^{(k_3)} x \begin{pmatrix} w \\ w' \end{pmatrix} \begin{vmatrix} 1^{(6+k_1+k_2+k_3)} 2^{(m)} \\ 2^{(4-k_1-k_2-k_3-m)} \end{vmatrix} \right)$$

$$= \partial x \left(Z_{21}^{(k_1+2)} x Z_{21}^{(k_2)} x Z_{21}^{(k_3)} x Z_{21}^{(m)} x \begin{pmatrix} w \\ w' \end{pmatrix} \begin{vmatrix} 1^{(6+k_1+k_2+k_3+m)} \\ 2^{(4-k_1-k_2-k_3-m)} \end{vmatrix} \right) =$$

$$-\binom{k_1+k_2+2}{k_2} Z_{21}^{(k_1+k_2+2)} x Z_{21}^{(k_3)} x Z_{21}^{(m)} x \begin{pmatrix} w \\ w' \end{pmatrix} \begin{vmatrix} 1^{(6+k_1+k_2+k_3+m)} \\ 2^{(4-k_1-k_2-k_3-m)} \end{vmatrix} +$$

$$\binom{k_2+k_3}{k_3} Z_{21}^{(k_1+2)} x Z_{21}^{(k_2+k_3)} x Z_{21}^{(m)} x \begin{pmatrix} w \\ w' \end{pmatrix} \begin{vmatrix} 1^{(6+k_1+k_2+k_3+m)} \\ 2^{(4-k_1-k_2-k_3-m)} \end{vmatrix} -$$

$$\binom{k_3+m}{m} Z_{21}^{(k_1+2)} x Z_{21}^{(k_2)} x Z_{21}^{(k_3+m)} x \begin{pmatrix} w \\ w' \end{pmatrix} \begin{vmatrix} 1^{(6+k_1+k_2+k_3+m)} \\ 2^{(4-k_1-k_2-k_3-m)} \end{vmatrix} +$$

$$Z_{21}^{(k_1+2)} x Z_{21}^{(k_2)} x Z_{21}^{(k_3)} x \begin{pmatrix} w \\ w' \end{pmatrix} \begin{vmatrix} 1^{(6+k_1+k_2+k_3)} 2^{(m)} \\ 2^{(4-k_1-k_2-k_3-m)} \end{vmatrix}$$

It is clear that $s_2 \partial x + \partial x s_3 = id$

Which mean that $\{s_0, s_1, s_2, s_3\}$ is a contracting homotopy for the complex $M_4 \longrightarrow M_3 \longrightarrow M_2 \longrightarrow M_1 \longrightarrow M_0$ which implies that the complex is exact.

REFERENCES

1. D.A.Buchsbaum,Letter-place Methods and Homtopy,Birkhauser :41-62 (1998).
2. D.A.Buchsbaum and G.C.Rota,Approaches to resolution of Weyl module, Adv in Applied Math. 27: 82-191 (2001).
3. D.A.Buchsbaum and G.C.Rota,A new Construction in Homological Algebra, Nati Acad. Sci. USA 91: 4115-4119 (1994).
4. K.Akin & D.A.Buchsbaum,Schur Functors and Schur Complexes , Adkances in Mathematics (44) : 207-278 (1982).
5. L.R.Vermani,An elementary approach to homological algebra, Chapman and Hall / XRC, Monographs and Surveys in pure and applied mathematics (2000).

Dailey Rainfall Persistence of Selected Stations in Iraq

Amani Ibraheem Al-Temimi
Department of Atmospheric Science / College of Science/Al-Mustansiriyah University

الخلاصة

يتطرق هذا البحث الى استخدام احد طرق التنبؤ وهي دوامية(استمرارية) العناصرالجوية ذات الطبيعة غير المستمرة مثل تساقط الامطارحيث يعد التغاير في دوامية تساقط الامطار من الحقائق المهمة بالنسبة الى الزراعة , تم حساب معامل الدوامية بدلالة بيسون(R_B) ومعامل الدوامية الشبيه بمعامل الارتباط (r_B) لتساقط الإمطار لأربعة محطات تمثل شمال وجنوب وشرق وغرب العراق وهي المحطات (موصل , رطبة ,بغداد والبصرة)حيث تم حساب المتوسط اليومي الشهري للإمطار الساقطة خلال الفترة الزمنية من سنة(1971-2000)ولقد أظهرت النتائج بوجود دوامية تساقط الإمطارجيدة في محطات الدراسة لكل من قيم (R_B, r_B) حيث كانت القيم تقترب من الواحد. أعلى دوامية تساقط أمطار في محطة الرطبة و بقيمة(R_B=0.98) وقيمة(r_B=0.75) وفيما يخص محطة بغداد بلغت قيمة دوامية تساقط الأمطار (R_B =0.92) و (r_B= 0.73),و تأتي محطة البصرة في المرتبة الثالثة حيث بلغت قيمة دوامية تساقط الأمطار R_B (=0.89) و(r_B=0.72) اما اقل دوامية فهو في محطة الموصل على الرغم من أن متوسط تساقط الإمطار اليومي عالي نسبياحيث إن (R_B =0.81, r_B =0.69).

ABSTRACT

This research deals with one of predication methods that are persistence (continuity) of the meteorological elements which have discontinuous nature such as rainfall.Avariation in rainfall persistence is one of the important facts which effects on agriculture. Besson's coefficient of persistence (R_B) and a coefficient comparable to a correlation coefficient (r_B) for rainfall persistence have been calculated for four stations (Mosul , Rutba, Baghdad , Basra) representing the north, south, east and west of Iraq. We have used the mean daily monthply rainfall during the period of the year (1971 - 2000) and the results have shown for each of the values of (R_B, r_B) a good persistence in rainfall where were all the values close to one. The highest persistence rainfall in Rutba station where(R_B = 0.98) (r_B = 0.75) ,while Baghdad is the second station of a persistence rainfall (R_B = 0.92) (r_B = 0.73), then Basra is the third station in persistence rainfall (R_B = 0.89) (r_B = 0.72) and the lowest value of Besson's coefficient of persistence(R_B) and the coefficient comparable to a correlation coefficient(r_B) for the rainfall in Mosul station (R_B=0.81),(r_B=0.69) although the highest total number of rainy days was in this station, but it 's the lowest persistence of rainfall among the selected station during the time period.

INTRODUCTION

A meteorological observation is not usually independent of preceding conditions though the dependence decreases with the length of the time interval between successive observation .For example, the amount of rainfall in a year bears practically no relation to the amount in the preceding year, but the amount of rainfall in a month is influenced to a small but definite extent by the amount in the preceding month. This is due to the fact that rainfall tends to "persist" from day to day (1). The persistence method works well when weather patterns change very little and features on the weather maps move very slowly. It also works well in places like southern California, where summertime weather conditions vary little from day to day. However, if weather conditions change significantly from day to day, the persistence method usually breaks down and is not the best forecasting method to use. It may also appear that the persistence method would

work only for shorter-term forecasts (e.g. a forecast for a day or two), but actually one of the most useful roles of the persistence forecast is predicting long range weather conditions or making climate forecasts. For example, it is often the case that one hot and dry month will be followed by another hot and dry month. So, making persistence forecasts for monthly and seasonal weather conditions can have some skill. Some of the other forecasting methods, such as numerical weather prediction, lose all their skill for forecasts longer than 10 days. This makes persistence a "hard to beat" method for forecasting longer time periods (2). The quality of "persistence" is of major importance in meteorological statistics .The method used to measure the persistence is the Besson's coefficient. There's many studies about persistence of rainfall such as Monthly Rainfall Climatology for Puerto Rico by (Matt Carter and J.B. Elsner,1997) (3), (Jim Goodride, 1998) gave research about persistence in California weather patterns(4) .(Ian Simmonds, Pandora Hope,2007) calculated Persistence Characteristics of Australian Rainfall Anomalies(5) .In Iraq, the great variability in time and space is an outstanding phenomena where recognized the precipitation, however no attempt was made to evaluated the persistence of rainfall. The objective of this research is to give a simplified picture of the persistence (continuity) of rainfall for four selected stations in Iraq.

MATERIALS AND METHODS

The simplest kind of discrete variety is one which can assume only one of two values, 0 and 1, corresponding to non-occurrence and occurrence of an event. If (P) is the general probability of an event (*i.e.* the total number of occurrences in a given period divided by the number of possible occurrences) and (P_1) is the probability that the event will occur after an occurrence on the occasion next preceding, then persistence as defined by Besson is(3):

$$R_B = \frac{1 - P}{1 - P_1} - 1 \quad \text{..... (1)}$$

Where

$$P_1 = \frac{P+1}{P+2} \quad \text{..... (2)}$$

Where R_B is Besson' s coefficient of persistence .This expression is zero when there is no persistence ,*i.e.* if $P_1=P$, and would become infinite if occurrence of the event were always followed by another occurrence ,*i.e.* if $P_1=1$. A coefficient comparable to a correlation coefficient can be derived from Besson's formula by putting-

$$r_B = 1 - \frac{1}{(R_B + 1)^2} \quad \text{..... (3)}$$

$$r_B = 1 - \left(\frac{1-P_1}{1-P}\right)^2 \quad \text{..... (4)} \qquad \textit{i.e.}$$

This coefficient varies from 0(when $P_1=P$) to 1(when $P_1=1$).If P_1 were

less than P ,r_B would be negative and would represent a tendency for occurrences and non- occurrences to oscillate(6).

RESULTS AND DISCUSSION

Calculation of the total rainfall during the period 1971-2000 was carried out for stations (Mosul, Rrutba, Baghdad, Basrah) data were obtained from the Iraqi Meteorological Organization (7). Table (1) shows the mean of daily monthly rainfall for stations.

Table -1: The mean of dailv monthlv rainfall for stations (MOSUL. RUTBA BAGHDAD. BASRAH)

Years	MOSUL The mean of daily monthly rainfall (mm)	RUTBA The mean of daily monthly rainfall(mm)	BAGHDAD The mean of daily monthly rainfall (mm)	BASRAH The mean of daily monthly rainfall (mm)
1971	0.80	0.68	0.50	0.32
1972	1.20	0.68	0.46	0.46
1973	1.20	0.09	0.26	0.14
1974	0.63	0.54	0.79	0.45
1975	1.36	0.35	0.47	0.49
1976	1.02	0.39	0.31	0.41
1977	1.05	0.26	0.38	0.40
1978	0.92	0.16	0.28	-
1979	0.73	0.21	0.34	0.41
1980	0.92	0.62	0.41	0.47
1981	1.34	0.18	0.31	0.24
1982	1.18	0.85	0.32	0.33
1983	1.18	0.25	0.16	0.20
1984	0.68	0.23	0.32	0.54
1985	0.83	0.36	0.32	0.38
1986	1.03	0.26	0.45	0.82
1987	0.63	0.24	0.13	0.14
1988	-	-	-	-
1989	1.44	0.37	0.82	0.31
1990	0.71	0.25	0.25	0.13
1991	1.10	0.21	0.19	0.68
1992	1.58	0.31	0.24	0.45
1993	1.73	0.29	0.22	0.30
1994	1.20	0.49	0.41	0.39
1995	0.82	0.66	0.27	0.36
1996	1.40	0.36	0.26	0.59
1997	0.99	0.61	0.31	0.60
1998	0.61	0.24	0.33	0.20
1999	0.46	0.20	0.13	0.67
2000	0.74	0.23	0.12	0.35

The mean annual and the standard deviation annual of rainfall for each station were calculated by using statistical program software (STATISTICA) as shown in table (2)

Table -2:The mean annual and the standard deviation annual of rainfall for each station

Station Name	Mean Annual of rainfall(mm)	Mean Annual Standard Deviation(*S.D*)
Mosul	4.3	17.8
Rutba	3.69	17.9
Baghdad	3.66	17.9
Basrah	7.04	25.3

The probability(P)for each station were calculated by calculated the rainy days through the period 1971-2000 , as shown in table (3)

Table-3:The total number of rainy days for each station during the time period 1971-2000

Station Name	The total number of ainy days during the time period 1971-2000	he total number of days during the time period 1971-2000
Mosul	1657	10291
Rutba	861	10231
Baghdad	740	10114
Basrah	870	9882

And we calculated the probability that the event will occur after an occurrence on the occasion next preceding (P_1) from the equation (2), as shown in table (4)

Table -4: The value of P, P_1 for each station

Station Name	P	P_1
Mosul	0.16	0.537
Rutba	0.08	0.520
Baghdad	0.07	0.518
Basrah	0.09	0.521

From equation (1) and (4) Besson's coefficient of persistence (R_B) and the coefficient comparable to a correlation coefficient (r_B) were calculated for each station, as shown in table (5)

Table -5: Shows the value of (R_B, r_B) for each

Station Name	R_B	r_B
Mosul	0.81	0.69
Rutba	0.98	0.75
Baghdad	0.92	0.73
Basrah	0.89	0.72

The above results indicate the presence of rainfall persistence, which they relatively large values because all the values of (R_B , r_B) are close to one and this fit with the relatively large values of the annual mean of the rainfall in most stations, Where found that the highest value of Besson' s coefficient of persistence (R_B) and the coefficient comparable to a correlation coefficient (r_B) for the rainfall in Rutbe station (R_B=0.98) , (r_B=0.75) and the annual mean of the rainfall was (3.69mm)and this is due to the hilly physiographic nature of this region, and also it fit with the high value of standard deviation for the annual mean of the rainfall(*S.D.*=17.9). The next value is Baghdad station where , (R_B=0.81),(r_B=0.69) and the annual mean of the rainfall was (3.66mm) and this fit with the high value of standard deviation for the annual mean of the rainfall(*S.D*=17.9),Basrah station it 's come in the third order where,(R_B=0.89) , (r_B=0.72) and the annual mean of the rainfall was (7.04 mm)and the standard deviation (*S.D.*=25.3).The lowest value of Besson' s coefficient of persistence(R_B) and the coefficient comparable to a correlation coefficient(r_B) for the rainfall in Mosul station (R_B=0.81),(r_B=0.69) although the highest total number of rainy days was in this station, but it 's the lowest persistence of rainfall among the selected station during the time period and the value of annual mean of the rainfall was (4.3 mm) and this fit with the high value of standard deviation for the annual mean of the rainfall(*S.D.*=17.8).

REFERENCES

1. C.E.P. Brooks, D.Sc and N.Carruther, B.Sc" Handbook of Statistical Methods in Meteorology., http//:www.itl. nist. gov/div898/handbook" : 309-329 (1953).
2. Persistence Method: today equals tomorrow, the University of Illinois at Urbana-Champaign http//:www. WW(2010).
3. Matt Carter, J.B. Elsner CITM, Shawn Bennet SOO, WSFO San Juan and Puerto Ricot" Monthly Rainfall Climatology for Puerto Rico", Florida State University (1997)
4. Ian Simmonds & Pandora Hope "Persistence Characteristics of Australian Rainfall Anomalies"International Journal of Climatology,17(I.6):597– 613., (1998)
5. Jim Goodride," Persistence in California Weather Patterns"state climatologist (Retired), (2007)
6. Besson,L"On the Probability of Rain in Mon.Weath.Rev"D.C.,52:308,Paris (1924)
7. Iraqi Meteorological Organization, Baghdad. Data unpublished.

Security Proposal Method to Protect Domain Name System

Samer Saeed Essa and Rana M. Al_Salman
AL_Mustansiriya University ,College of Science ,Computer Science Department

الخلاصة

إنّ نظام اسم الملكية (DNS) هو نظام هرمي معقد مِنْ قاعدةِ البيانات المُوَزَّعةِ الذي معتمد على بعضهم البعض مِنْ مستعملي الشبكةِ. في هذا البحثِ، نُوضّحُ مفهومَ نظام اسم الملكيةِ الذي يَتضمّنُ التركيبَ، المكوّنات، الأمنَ وأنواع سجل المصادرَ. أيضاً نُقدّمُ إقتراحَ أمن نظام اسم الملكية الذي يَستعملُ مفتاحَ عامَّ معقدَ لزيَادَة أمن الحمايةِ الذي سَيَستعملُ بنائه بشكل كفوء و بثقة مِنْ جذر نظام اسم الملكيةِ إلى الخادم الموثوق. يرْبطُ هذا المفتاح العامَّ المعقدِ المُقتَرَح بمفتاح سري وهو مضمون بالإستعمال السري في تقنيات التشفيّر.

ABSTRACT

The Domain Name System (DNS) is a complex hierarchical system of distributed database which are dependent upon each other of network users. In this paper, we explain the concept of DNS that including the structure, the components, the security and the resource records types. Also we present the DNS security proposal using complex public key to increase the security of protection that will be used to efficiently build a trust from a DNS root to the authoritative server. A proposed complex public key binds to a secret key and it is garneted by using secret key cryptographic techniques.

INTRODUCTION

The Internet is a seemingly limitless source of information. It provides the power of collective knowledge and information to a vast array of users who access innumerable resources for countless reasons. These resources are typically accessed by using a human readable name designed to be easily remembered, thus increasing the usability of the resource. These human readable names, as the very term implies, are for the sake of the human users. Network devices, however, find each other by using a number, referred to as IP (Internet Protocol) addresses. The Domain Name System is the service that maps the human readable names to device specific IP addresses creating the user friendly nature of networked systems. The Internet and millions of other networks are dependent upon the functionality of the Domain Name System. **(1)**

The Domain Name System (DNS) is a hierarchically distributed database that provides information fundamental to Internet operations, such as translating between human readable host names and Internet Protocol (IP) addresses. Due to the importance of the information served by DNS, there is a strong demand for securing communication within the DNS system. The current (insecure) DNS does not prevent attackers from modifying or injecting DNS messages. Users accessing hosts on the Internet rely on the correct translation of host names to IP addresses by the DNS system. A typical attack, referred to as DNS

spoofing, allows an attacker to manipulate DNS answers on their way to the users. If an attacker makes changes in the DNS tables of a single server, those changes will propagate across the Internet. (2)

Domain Name System Security (DNSSEC) is a specification of an extension to the DNS through the definition of additional DNS Resource Records that can be used by DNS clients to validate the authenticity of a DNS response, the data integrity of the DNS response, and where the response indicates no such domain or resource type exists, this negative information can also be authenticated. In other words, if an attacker attempts to create a DNS response that has been altered from the original authentic response in some fashion, and the attacker then attempts to pass the response off as an authentic response, then a DNSSEC-aware DNS client should be able to detect the fact that the response has been altered and that the response does not correspond to the authoritative DNS information for that zone. In other words, DNSSEC is intended to protect DNS clients from forged DNS data. This protection does not eliminate the potential to inject false data into a DNS resolution transaction, but it adds additional information to DNS responses to allow a client to check that the response is authentic and complete. (3)

Recently, the RSA Security web page was hijacked by spoofing the DNS tables. In short, the attacker created a fake web page and then redirected to it all the legitimate traffic to the RSA Security's original page.

Increasingly, DNS is also being used to perform load distribution among replicated servers. For instance, companies have used DNS to provide Web content distribution. Moreover, there is consensus that, since DNS is a global and available database, it can be employed as a Public Key Infrastructure (PKI) which would help with enabling e-commerce applications by making public keys globally accessible. (2)

Domain Name System (DNS)

The Domain Name System provides a mechanism of con-version with a double functionality: it translates both symbolic host names to IP addresses and IP addresses to host names.**(4)**

The host file was a single growing text document that had to be centrally maintained. DNS is a distributed database. DNS data is distributed across literally thousands of DNS servers where zone data maintenance, the job of updating, adding and deleting resolution information, is distributed as well. A DNS server is a computer running a program referred to generically as a name server. The name server is responsible for the name resolution process. The administrator is responsible for maintaining the DNS data on that name server.

A host file was a single document requiring uniqueness on the part of every host name in the file. It was a flat data structure much like MAC addressing for those familiar with Message Authentication Code (MAC) versus IP addressing comparisons. The Internet population explosion made it even more important to have a naming resolution system that scaled well and obviously a flat text file does not scale well. DNS provides this scalability by implementing levels in the naming scheme referred to as domains**. (1, 5)**

Domain Name System Structure

To understand the concept of domains, remember that DNS is a distributed database. It is a single, monstrous, data set that has been chopped into pieces and these pieces have been placed on thousands of different name servers. Each domain can potentially have dozens of child domains. Figures 1 and 2 give graphical depictions of parts of the DNS structure. **(1)**

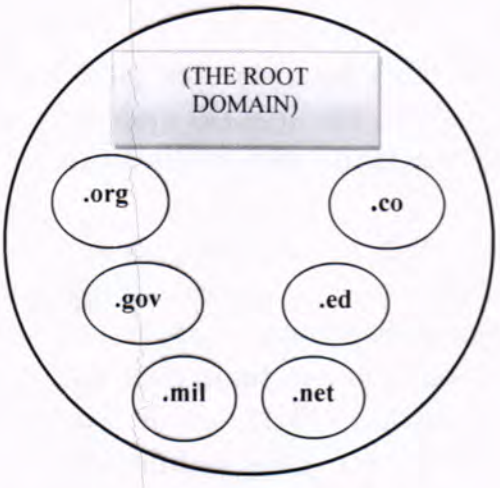

Figure -1: Top Level Domain

In the Figure (1) refers to the root domain and some of the top-level domains or TLDs. The root domain as in a file system is the starting point, or root of the DNS database. Information about the root domain is maintained by root DNS servers. Circles are used here to help the reader understand that what is represented by a domain is not a computer but a group of computers or other devices, or in the case of the root domain, other sub-groups. The DNS database is much like a file system. File systems are made up of directors (folders) and files. Folders allow us to organize files. In the same way, domains are like directories in that they allow us to create and organize sub-domains (like sub-directories) and hosts names (like files). And, like in a file

system, only the names in a domain have to be unique. So I can have a host named 'mail' in the ubuntu.com domain as well as one named 'mail' in the redhat.com domain.

In the Figure (2) depicts this principle as well as that of a top-level domain having second-level domains beneath it.**(1, 5)**

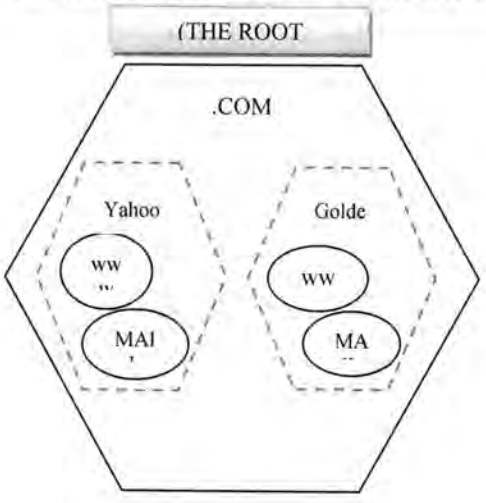

Figure -2: Second Level Domain

In the Figure (3) shows a common web address that a user might enter and labels each section. This is called a full qualified domain name or FQDN. A fully qualified name contains at least a top-level domain, second-level domain and host name. So there could be a web address of ftp.Yahoo.com where Yahoo is a sub-domain of 'com' and finally 'com' is a sub-domain of the root domain typically noted as simply a '.' that most normal web users would never need to reference. It is theoretically possible to have up to 127 domain levels in a name.**(1, 6)**

Figure -3: Full Qualified Domain Name

Each domain represents a piece of the database and each piece, or domain has its own name server which is responsible for maintaining correct entries that resolve the names to IP addresses. These entries are called resource records, which will be shown later. Each name server is also responsible for answering queries regarding names in the domain

or domains it is responsible for maintaining. One name server may maintain information for more than one domain. **(1)**

Domain Name System Component

The DNS has three major components; the ***first*** one is **Domain Name Space** and **Resource Records**, which are specifications for a tree structured name space and the data associated with these names. The ***second*** component is **Name Servers** are server programs which maintain the information about the DNS tree structure and can set information. A name server may cache information about any part of the domain tree, but in general it has complete in-formation about a specific part of the DNS. This means the name server has authority for that sub-domain of the name space therefore it will be called authoritative and the ***third*** one is **Re-solvers** component are programs that extract the information from name servers in response to client requests. It is assumed that the reader is familiar with the basic notions about DNS. **(4, 7)**

Domain Name System Security

Domain Name System Security (DNSSEC) defines a number of new DNS resource records (RRs), namely the DNS Public Key (DNSKEY), Resource Record Signature (RRSIG), Next Secure (NSEC), and Delegation Signer (DS) RRs, and two new message header bits: checking Disabled (CD) and Authenticated Data (AD), and it relies on functions provided by Extended DNS mechanisms (EDNSO). With DNSSEC a zone administrator "digitally signs" a Resource Record Set (RRSet), and publishes this digital signature, along with the zone administrator's public key, in the DNS. In checking a DNS response, a DNSSEC client can retrieve the related RRset digital signature and then check this signature using the public key against the locally calculated hash value of the RRset, and then validate the zone administrator's public key against a hierarchical signature path that leads to a point of trust. If all these checks succeed than the client has some confidence that the DNS response was complete and authentic.

DNSSEC implies different actions for different roles. For a DNS zone administrator, DNSSEC is essentially the process of signing RRSets with a private key, publishing these signatures for each RRset in the zone file, and publishing the zone public key in the zone file. In addition the zone administrator has to get the zone's public key signed by the parent zone administrator. For a DNS client DNSSEC is the ability to perform a number of additional checks on a DNS response

that can result in greater trust in the authenticity and accuracy of the DNS response. And for the DNS itself DNSSEC essentially represents a number of additional Resource Records that hold digital signatures of DNS information, as well as key information. (3, 7, 8)

Domain Name System Resource Records Types

The Domain Name System Security (DNSSEC) extensions introduce four new DNS resource record types, these resource records are: DNS Public Key (DNSKEY), Resource Record Signature (RRSIG), Next Secure (NSEC), and Delegation Signer (DS).

DNSKEY: Every DNSSEC secured DNS zone has an associated private and public key pair, as generated by the zone's administrator. The private key remains the (closely guarded) secret of the zone administrator. The associated public key for the zone is published in the zone file in the form of a DNSKEY resource record.

RRSIG: A "Resource Record set" (RRset) is a collection of RRs in a DNS ZONE that share a common name, class and type. In DNSSEC RRsets are digitally signed by the zone administrator. This signature is generated by generating a hash of the RRset, then encrypting the hash using the zone administrator's private key. For a zone that contains SOA, NS, A, MX, DNSKEY resource records there are, minimally 5 distinct RRsets, and each RRSET would have its own RRSIG Resource Record. This implies that the granularity of DNSSEC signing is not that of an entire zone, but is aligned to a unit of a DNS query response.

NSEC: The DNSKEY and RRSIG records can be used to check the authenticity of a DNS response, where there is a DNS response, but where there is no authoritative data to return then authentication requires additional information.

DS: The issue of validation of the zone public key remains unaddressed with the first three Resource Record types. An attacker would simply need to supply the DNSKEY and RRSIG data to match the bogus RRset data in order to make the response look 'authentic'. So we are back to the same public key validation question - how can a client validate the DNSKEY record?

The approach adopted by DNSSEC is to use a chain of trust within the hierarchical delegation structure of the DNS itself. Apart from the root zone, every DNS zone has a parent zone. The Delegation Signer (DS) RR contains the hash of the public key of the child zone.

This record is signed by the parent zone's private key with a matching RRSIG RR. To validate a zone's DNSKEY, the associated DS, RRSIG(DS) and DNSKEY of the parent zone is retrieved. The DS record is validated by using the DNSKEY to encrypt the RRSIG(DS) record, and then checking that the result matches the DS record. This is the zone public key, according to the zone's parent. This can be compared to the DNSKEY record of the zone in question. This relies on the parent zone key, and the question is how can this key be validated? The same process can be applied here. The process stops when the DNSSEC client encounters a "trusted" key. The ideal "trust key" would be the DNSKEY of the root zone, but in the absence of such a trust anchor each DNSSEC client has to configure their trust validation system with known trust points where there is no parent validation.**(3, 8, 9).**

Domain Name System Authentication

When requested by the client, DNSSEC adds additional data to the DNS protocol responses that provide additional information to allow the DNS client to authenticate the RRset data response. From the perspective of the protocol transaction between a query agent and an authoritative name server, the change is the addition of a RRSIG part to the data response where there is a response that can be generated, and the use of an NSEC RR response, plus its accompanying RRSIG record if there is no authoritative data to respond to the query. In addition to an RRSIG response covering the RRset records in the answer section of the DNS response there is also an RRSIG response covering the records in the authority section and one or more RRSIG responses relating to records in the additional response section.

The client can take the RRset response and use the algorithm referenced in the RRSIG record to generate the hash of the data. The RRSIG value can be encrypted using the DNSKEY public key which will, in effect, decrypt the hash in the RRSIG record. To do this the client must also have at hand the DNSKEY record for the zone. This operation allows the client to check that the hash of the RRset data matches the decrypted RRSIG hash.

The DNSKEY would normally be provided as part of the additional section of a DNSSEC response. If the client has not validated the DNSKEY within some locally defined period, then the client should also validate the DNSKEY value. This entails verifying the RRSIG record on the DNSKEY value, using the same procedure as for the RRset validation. However domain zone key validation also entails the

construction of a trust chain back to a trust anchor point. If this domain key is not already a trust anchor then the client needs to query the parent zone for the DS record of the child zone, which returns both a public key value and an RRSIG value, and a DNSKEY RR. This public key needs to be validated using the DNSKEY of the parent zone. This parent zone public key, in turn, must be validated. This iterative process constructs a trust chain that, hopefully, leads back to a trust anchor. At that point the DNS response can be considered to be validated. **(3)**

Public Key Cryptography

In 1976, Diffie and Hellman (11) proposed a new type of cryptography that distinguished between encipherment and decipherment keys. One of the keys would be publicly known; the other would be kept private by its owner. Classical cryptography requires the sender and recipient to share a common key. Public key cryptography does not. If the encipherment key is public, to send secret messages simply encipher the message with the recipient's public key. Then send it. The recipient can decipher it using his private key. Because one key is public, and its complementary key must remain secret, a public key cryptosystem must meet the following three conditions. (10)

1. It must be computationally easy to encipher or decipher a message given the appropriate key.
2. It must be computationally infeasible to derive the private key from the public key.
3. It must be computationally infeasible to determine the private key from a chosen plaintext attack.

We can reduce the problem of key proliferation by using a public key approach. In a public key or **asymmetric encryption system**, each user has two keys: a public key and a private key. The user may publish the public key freely because each key does only half of the encryption and decryption process. The keys operate as inverses, meaning that one key undoes the encryption provided by the other key.

To see how, let k_{PRIV} be a user's private key, and let k_{PUB} be the corresponding public key. Then, encrypted plaintext using the public key is decrypted by application of the private key; we write the relationship as

$$P = D(k_{PRIV}, E(k_{PUB}, P)) \quad \ldots\ldots\ldots (1)$$

That is, a user can decode with a private key what someone else has encrypted with the corresponding public key. Furthermore, with

some public key encryption algorithms, including RSA, we have this relationship:

$P = D(k_{PUB}, E(k_{PRIV}, P))$ ..... (2)

In other words, a user can encrypt a message with a private key, and the message can be revealed only with the corresponding public key. These two properties tell us that public and private keys can be applied in either order. In particular, the decryption function D can be applied to any argument so that we can decrypt before we encrypt. With conventional encryption, we seldom think of decrypting before encrypting. But the concept makes sense with public keys, where it simply means applying the private transformation first and then the public one.

We have noted that a major problem with symmetric encryption is the sheer number of keys a single user has to store and track. With public keys, only two keys are needed per user: one public and one private. Let us see what difference this makes in the number of keys needed. Suppose we have three users, B, C, and D, who must pass protected messages to user A as well as to each other. Since each distinct pair of users needs a key, each user would need three different keys; for instance, A would need a key for B, a key for C, and a key for D. But using public key encryption, each of B, C, and D can encrypt messages for A by using A's public key. If B has encrypted a message using A's public key, C cannot decrypt it, even if C knew it was encrypted with A's public key. Applying A's public key twice, for example, would not decrypt the message. (We assume, of course, that A's private key remains secret.) Thus, the number of keys needed in the public key system is relatively small. (12)

Proposal Security Method

In this section we describe our proposal security that works in secure communication based on proposed Complex Public Key (CPK) algorithm via Message Authentication Code (MAC) function.

1. Using Message Authentication Code (MAC)

A practical construction for MAC functions is described in details by two references (13, 14). To achieve private and authenticated channels, we can combine complex public key (CPK) encryption techniques with message authentication code (MAC) functions.

In our system, we would encrypt a message m as follows:

E_{CPK} [m, MAC (m)] = E_{CPK} [MAC (m) + m]

Where the symbol + denotes the concatenation operation and E_{CPK} is a complex public key (CPK) encryption algorithm.

We assume that the complex public key (CPK) encryption algorithm, E_{CPK}, is secure against chosen-plaintext attacks. Furthermore, we assume that the message authentication code is secure against chosen-message attacks.

In particular, encrypting first the message and then computing the MAC function over the cipher-text is usually preferable since the encryption function and invalid cipher-texts can be discarded without the overhead of decryption. However, direct authentication of the plaintext is a desirable property, and also notices that we employ the MAC to authenticate messages that are not necessarily private and that can be predictable or induced.

2. Using Proposed Complex Public Key (CPK)

This section covers a proposed of complex public-key (CPK) algorithm, the main idea in this system uses two complex problems to create the public key and the private key, these two problems are Integer factorization Problem and Discrete logarithm Problem, these two problems make the messages be very difficult to decrypt by any attacker because he faces breaking, the message, Integer factorization Problem and Discrete logarithm Problem. In this system the finite field F_q and the "base element" $g \in F_q$ (preferably, but not necessarily a generator of the group of elements on F_q) are public information.

Proposed Complex Public-Key (CPK) algorithm:

Initial State:

State 1: A and B publicly choose a finite field F_q.

State 2: They publicly choose a random base element $g \in F_q$ such that g generates a large subgroup of F_q.

State 3: B chooses two large prime numbers p_1 and p_2.

Key Generation State:

State 1: B chooses a secret random integer b.

State 2: B Computes Fast-Exponential $Q= g^b$.

State 3: B compute the multiplication $n=p_1 * p_2$.

State 4: Choose $1 > e >(p_1 - 1)*(p_2 -1)$, with gcd $(e, (p_1 -1)*(p_2 - 1))=1$.

State 5: Compute e^{-1} .

State 6: Compute $d= e^{-1} \bmod (p_1-1)*(p_2-1)$.

State 7: Make (Q, n, and e) public and keep b and d secret.

Encryption State:

State 1: A sends the message M to B.

State 2: Represent the message M as an element in F_q.

State 3: Select random integer **a** in interval [2,q].

State 4: Compute Fast-Exponential g^a.
State 5: Compute $a_c = g^a \bmod q \in F_q$.
State 6: Compute Fast-Exponential Q^a.
State 7: Compute $CPK = Q^a \bmod q$.
State 8: Compute the multiplication M* CPK.
State 9: Compute $H = (M * CPK) \bmod q$.
State 10: Compute Fast-Exponential H^e.
State 11: Compute cipher-text $C = H^e \bmod n$.
State 12: Transmit the pair points (C, a_c).

Decryption State:

State 1: B retrieves the message
State 1.1: Compute Fast-Exponential a_c^b.
State 1.2: Compute $CPK = a_c^b \bmod q$.
State 1.3: Compute Inverse CPK^{-1}.
State 1.4: Compute $CPK^{-1} \bmod q$.
State 2: Compute Fast-Exponential C^d.
State 3: Compute $H = C^d \bmod n$.
State 4: compute the multiplication $M = H * CPK^{-1}$.

2.1 Proof of Proposed Complex Public-Key (CPK) algorithm

this section, present the proof of our proposed Complex Public-Key (CPK) algorithm of leading the ciphertext to the plaintext by encryption and decryption process as follows.

We have: $\text{Ciphertext} = H^e \bmod n$

$= (M * CPK)^e \bmod n.$

$= (M * Q^a \bmod q)^e \bmod n$

$= (M * g^{ba} \bmod q)^e \bmod n$

And $M = H * CPK^{-1} \bmod q$

$H = C^d \bmod n = ((M * CPK)^e)^d \bmod n$

$= M * CPK$

And $CPK = a_c^b \bmod q = g^{ab}.$

Compute $CPK^{-1} \bmod q$

Then $M = (M * CPK) * CPK^{-1} \bmod q$

$= M *(g^{ab}) * (g^{ab})^{-1} \bmod q$

$= M$

3. Using Secure Communication (SC)

Secure communication based on public-key cryptography has several positive aspects and in particular. The uses the entire DNS tree of domains as an on-line certification authority that, for each request of host mapping information, returns the public key of the authoritative server responsible for that host.

When Given the DNS tree of domains, it is assumed that each node shares a key with its parent:

CPK_{AB}: Public and secret keys (CPKAB1, CPK_{AB2}) these keys are shared by A and B sides.

Where:

CPK_{AB1}: Public and secret keys shared used for encryption and decryption state.

And:

CPK_{AB2}: Public and secret keys shared used for message authentication code (MAC) function.

In the beginning, we supposed the root domain (Top Level) .com with a sub-domain (Second Level) saeed.com and finally the host name domain **yahoo.iq.com**.

Then for instance, the node saeed.com (sub-domain) shares a key with **.com** (root domain) that is referred to as the public and secret key (CPK_{AB1}) of **iq.com.** The root domain has an a to as the public and secret key (CPK_{AB2}) as well as it's own the other keys that is not shared with any other node.

The root's key is used to start the process of building the chain of trust from root to the authoritative servers.

Where:

CPK_R: root's (R) key pair (CPKR1, CPK_{R2}).

And:

PE_R: Public key encryption under root public key.

As example: suppose that a local name server (acting as a re-solver) U queries the root domain server for the IP address of ali.ahmed.com. The root (ahmed.com) is not authoritative for this query and thus will refer the re-solver to the DNS saeed.com.

Note:-

We assumed that U has an authentic copy of the root's public key.

Where:

P_{RU}: U⟶ R: PE_R (CPK_{R1}, CPK_{R2})

Then:

U⟶ R: P_{RU} (CPK_R, MAC (CPK_{R1}, CPK_{R2})).

The root server generates a secret key Ka which is sent (encrypted) to U along with a symmetric certificate for .com. The key Ka will be shared by U and the server .com. The symmetric certificate is

an encryption under the key of .com of the key Ka and information about U. The name server U queries .com by sending the original DNS request along with the symmetric certificate generated by the root server. The .com server will retrieve the key Ka from the certificate and use it to encrypt a freshly generated key Kb. To safely communicate such a key to .ahmed.com, the server .com inserts the key Kb into another symmetric certificate created for .ahmed.com. The key Kb will be shared by U and the server .ahmed.com. Finally, the server .ahmed.com will send the IP address of ali.ahmed.com to U symmetrically signed with Kb.

- The DNS face the problem of trusting the information that came from a non-authentication authority, the name base authentication process and the problem of accepting additional information that was not requested and that may be incorrect.
- The DNS security proposed is presented and explained from both theoretical and partial point of view that explained in existing security features of implementation.
- The DNS security proposed present some of the defensive that can be helped to present some of the defensive that can be helped to protect against some of these common threats.
- The proposed complex public key that is used in the DNS security proposal, it combine the factorizations problem computing and discrete algorithm problem complexity therefore the degree of security become more complex.

REFERENCES

1. Jeff S. Drake, "DNS Security and Threat Mitigation: An Overview of Domain Name System Threats and Strategies for Securing a BIND Name Server", (2007).
2. Giuseppe Ateniese and Stefan Mangard, "A New Approach to DNS Security (DNSSEC)", (2002).
3. Geoff Huston, "A Fundamental Look at DNSSEC, Deployment, and DNS Security Extensions", (2006).
4. Antonio Lioy, Fabio Maino, Marius Marian, and Daniele Mazzocchi, "DNS Security" Torino (Italy) , Terena Networking Conference, May, (2000).
5. Liu, C., & Albitz, "DNS and BIND, Sebastopol", (2006).
6. Brain, M., "How Domain Name Servers Work", (2006).
7. David Wager, "DNS Security", October (2007).
8. Olaf Kolkman, "DNSSEC HOWTO, a tutorial in disguise", March, (2007).
9. Arends, et al., "DNSSEC Resource Records", March (2005).

10. Matt Bishop, "Introduction to Computer Security", Publisher: Prentice Hall PTR, (2005).
11. W. Diffie and M. Hellman , "New Directions in Cryptography," IEEE Transactions on Information Theory 22 (6) :644-654 (Nov. 1976).
12. Charles P. Pfleeger, "Security in Computing", Fourth Edition, Publisher: Prentice Hall, (2007).
13. M. Bellare, R. Canetti, and H. Krawczyk, "Keying hash functions for message authentication". In Advances in Cryptology - Crypto 1996 Proceedings, LNCS . 1109, N. Koblitz ed, Springer-Verlag, (1996).
14. H. Krawczyk, M. Bellare, R. Canetti, "HMAC: Keyed-Hashing for Message Authentication", RFC 2104, February (1997).

Colored Image Compression Using Discrete Transformations for Sine and Cosine Functions

Mohammed M. Siddeq, Amal S. Toma and Hassan K. Abdul-Rahman
S.W Engineering Dept. S.W Engineering Dept. Computer systems Dept.
Technical College/Kirkuk Technical College/Kirkuk Technical Institute/ Kirkuk

الخلاصة

يعد ضغط الصور واحد من اهم المواضيع في حقل معالجة الصور.في هذا البحث يتم مناقشة فكرة جديدة لضغط الصور تتضمن الخطوات التالية :
1- تطبيق 1D-DCT على كل صف من الصورة الملونة المدخلة.
2- تطبيق دالة 1D-DST على كل عمود من الصورة الناتجة من الخطوة الاولى.
3- ثم استخدام عملية (Quantization) لزيادة عدد الاصفار في المصفوفة التي ستتحول الى مصفوفة ذات بعد واحد بواسطة تتبعها عمود بعد الاخر,
4- ثم تطبيق خوارزمية (RLE) لتقليل عدد المعاملات.
5- اخيرا تطبيق خوارزمية الترميز الرياضي لضغط المصفوفة النهائية.
خوارزمية فتح الضغط على الصورة سوف تعكس خطوات الضغط المستخدمة اعلاه. واخيرا اجراء مقارنة بين الصورة المستحصلة من تطبيق الخوارزمية المستخدمة في هذا البحث والخوارزميات التقليدية مثل JPEG بواسطة استخدام Mean-Square-Error and compression ratio.

ABSTRACT

Image compression is one of the important aspects in image processing field. This paper discusses an idea for image compression, consists of the following steps:
1- Applying 1D-DCT on each row of an input colored image.
2- Applying 1D-DST on each column of matrix obtained from the first step.
3- Quantization process is applied to increase number of zeros; this matrix is converted into one-dimensional array by scanning the matrix column by column.
4- Using Run Length Encoding, to minimize the number of coefficients.
5- Using Arithmetic coding procedure, to compress the minimized array.

The decompression algorithm will reverse the compression steps used above. The decompressed image is compared with JPEG by Mean-Square-Error (MSE) and compression ratio as a measurement for the comparison between the conventional methods and our algorithm.
Keywords: DCT, DST, Quantization, RLE, Arithmetic coding.

INTRODUCTION

Image compression has been pushed to the front of image processing field. The rapid growth in computer power and the advances in video technology are creating a demand for new, better, and faster image compression algorithms.

Image compression involves reducing the size of image data files, while retaining necessary information. An image of a resolution 512*512 occupies 786,432 bytes, and at a resolution of 1024*1024 it gets as four times as big, requiring 3,145,728 bytes. This is why image compression is so important.

An image, when it is compressed, it is okay to lose some image features for which human eye is not sensitive. This is the main idea for image compression algorithms used in the computer world.

The most widely used image compression transformations are Discrete Cosine Transform (DCT) and Discrete Wavelet Transform (DWT). The DCT is usually applied to small, regular blocks of image samples (e.g. 8 x 8 squares) and the DWT

is usually applied to larger image sections ('tiles') or to complete images. Many alternatives have been proposed, for example 3-D transforms (dealing with spatial and temporal correlation), variable block size transforms, and fractal transforms, Gabor analysis. The DCT has proved particularly durable and is at the core of most of the current generation of image and video coding standards, including JPEG, H.261, H.263, H.263+, MPEG-l, MPEG-2 and MPEG-4(2).

Discrete Cosine Transform (DCT)

One-dimensional DCT is used to transform each row from spatial domain to frequency domain, to obtained Transformed Image called "TI". One-dimensional DCT is given by the following equation[8] :

$$TI(i) = \frac{\sqrt{2}}{n} C(i) \sum_{t=0}^{n-1} I(t) \cos\left[\frac{(2t+1)i\pi}{2n}\right] \qquad (1)$$

where : $C(i)$ $\begin{cases} = 2^{-1/2}, \text{if } i = 0 \\ = 1 \ , \text{if } i > 0 \end{cases}$ $i = 0,1,2,3,\ldots,n\text{-}1$

The input is a set of n image values "$\boldsymbol{I}$" , and the output is a set of n DCT transformed coefficients "$\boldsymbol{TI}$".

The first coefficient is called the DC coefficient, and the rest are referred to as the AC coefficients. Notice that the coefficients are real numbers, and rounded to be integer coefficients. The important feature of the DCT, it so useful in data compression, is that it takes correlated input data and concentrates its energy in just the first few transform coefficients(9).

If input data consists of correlated quantities, then most of the n transformed coefficients produced by the DCT are zeros or small numbers, and only a few are large (normally the first values). The early coefficients contain the important (low-frequency) image information and the later coefficients contain the less-important (high-frequency) image information. This feature gives a good compression performance (13).

The following experiment illustrates the power of the DCT in one dimension. Applying the DCT on a set of eight correlated data items I ={12, 10, 8, 10, 12, 10, 8, 11}, and get the eight coefficients X={28.6375, 0.571202, 0.46194, 1.757, 3.18198, −1.72956, 0.191342, −0.308709}, after rounding getting: X={29, 1, 0, 2, 3, -2, 0, 0}. As shown in Figure-1. To return image data, using the DCT coefficients in sets of "n" and uses the inverse DCT (IDCT) to reconstruct the original image values then rounding them; $\hat{I}$ ={ 12, 10, 8, 10, 13, 10, 8, 11}. The one-dimensional IDCT is given by (14):

$$I(t) = \frac{\sqrt{2}}{n}\sum_{j=0}^{n-1} C(j)TI(j)\cos\left[\frac{(2t+1)j\pi}{2n}\right] \quad (2)$$

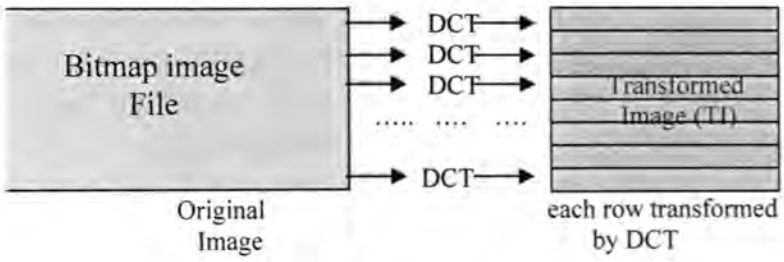

Figure – 1: Apply DCT on grayscale image

Discrete Sine Transform (DST)

DST is used for image compression. Its equation is represented in the following formula (11) :

$$FT(k) = \sum_{n=1}^{N} TI(n)\, Sin(\pi \frac{k*n}{N+1}) \quad (3)$$

$k=1,2,...N$

$$TI(n) = \frac{2}{N+1}\sum_{k=1}^{N} FT(k)\, Sin(\pi \frac{k*n}{N+1}) \quad (4)$$

Equation (3) is used to transform "n" values from TI matrix into "n" coefficients contains low-frequency coefficients which represent image information, and contains high-frequency coefficients less important information. In our algorithm one-dimensional DST applied on each column from TI matrix called *Final Transformed* "FT" as shown in Figure-2. The DST is equivalent to the imaginary part in Discrete Fourier Transformation (DFT) and the result of the DST is just real numbers like DCT (See previous section) [12]. The main advantage for using the DST to keep for the quality of the IT coefficients and increase the number of zeros, it is playing main role in our algorithm.

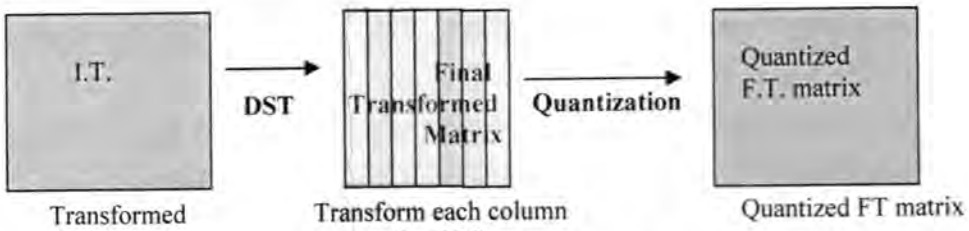

Figure -2: using DST to generate FT

Quantization

After using DST we obtained FT matrix. In this section quantization is applied on FT matrix. The quantization means lost information from an image (except for some unavoidable loss because of finite precision calculations in other steps). Each

coefficient in the FT matrix is divided by the corresponding number from the particular "*Quantization table*" used, and the result is rounded to the nearest integer. By the following equation, quantization table is obtained (7):

$$Q(i,j)=(i+j) * V \quad (5)$$

Where V >0

In equation (5), V is a real number greater than zero. This value is effects on the image quality, where the (V <1) means best image quality, or if (V >= 1) decreasing the quality of an image. For example assume you have a matrix 8x8, the Quantized Table size is the same image size as show in Figure-3.

Table -1: Quantized Table

	1	2	3	4	5	6	7	8
1	4	6	8	10	12	14	16	18
2	6	8	10	12	14	16	18	20
3	8	10	12	14	16	18	20	22
4	10	12	14	16	18	20	22	24
5	12	14	16	18	20	22	24	26
6	14	16	18	20	22	24	26	28
7	16	18	20	22	24	26	28	30
8	18	20	22	24	26	28	30	32

5. Coding Algorithm

In this part we discuss two important algorithms used for *data compression*; Run-Length-Encoding (RLE) and Arithmetic coding. At first we apply the RLE on the FT matrix. Because this matrix contains more redundant zeros and more less important information in high-frequency domain, also the RLE convert the FT matrix in to one-dimensional array called "$Array_{(RLE)}$ ". Finally apply the arithmetic coding to convert the array into bits.

Run length encoding (RLE) is a simple technique to compress digital data by representing successive runs of the same value in the data as the value followed by the count, rather than the original run of values. The goal is to reduce the amount of data needed to be stored or transmitted.

Example of RLE:

Original

1	1	1	0	0	1	1	1

RLE Representation

1	3	0	2	1	3

As we can see from the above simple example, RLE works the best when applied to data where there are successive runs of the same values. the real world application of RLE is in image processing. During image compression, higher spatial frequencies are filtered out. This is done by applying a 2-D DFT (Discrete Fourier Transform) or DCT (Discrete Cosine Transform), then multiplying the result with a quantization matrix to reduce the amount of precision stored in the higher spatial frequencies (i.e. the higher spatial frequency components will be 0 or

very close to 0). The resulting image is often stored as a vector of values and they are read in from the 2-D matrix using a zig-zag technique that maximizes the number of consecutive 0's so that RLE would be most efficient.

Then the stream of data (i.e. compressed data from RLE) is taken and converted to single floating point value. This output value in range less than 1 and greater than 0, when decoded this single value getting exact stream of data (5). The arithmetic coding need to compute the probability of all data and assign range for each data, the value is ranged from low to high value. The arithmetic coding algorithm is shown in the following procedure (8):-

```
Begin
Set Low =0.0;
Set High = 1.0;
While (not reached end of data)
  data = read_data_from_vector ();
  Range = High – Low;
  High = Low + Range * High_Range(data);
  Low = Low + Range * Low_Range(data);
End;
End.
```

Assume the following compressed data from RLE, compress it again with arithmetic coding:-

Data = **[74, 19, 70, 70, 32, 75, 238, 69, 37, 65]**

First compute the probability for above data and assign low and high values for each data as shown in the Table 2:-

Table -2: assign *Low* and *High* values.

Data	Probability	Low	High
32	1/10	0	0.1
238	1/10	0.1	0.2
74	1/10	0.2	0.3
37	1/10	0.3	0.4
75	1/10	0.4	0.5
19	1/10	0.5	0.6
70	2/10	0.6	0.8
65	1/10	0.8	0.9
69	1/10	0.9	1.0

As stream of data to compress it by arithmetic coding algorithm, the Table 3 shows arithmetic operation:-

Table- 3: Arithmetic Compression

Data	Low	High
74	0.0	1.0
19	0.2	0.3
70	0.25	0.26
70	0.256	0.258
32	0.2572	0.2576
75	0.25720	0.2574
238	0.257216	0.257220
69	0.2572164	0.2572168
37	0.25721676	0.2572169
65	0.2572167752	0.257216776

The final value "***low* = 0.2572167752**" this value converted to binary code (28-bits). This means the arithmetic coding compress 10-byte to 28-bits. Arithmetic decompression, return the original data from *Low* value as shown in table 4, the decompression algorithm can be illustrates in the following procedure(8):-

```
While (Low >=0 )
  For I = 0 to 10
    IF ( Low >= Low_Range(I) AND Low < High_Range (I) ) THEN
          Range = High_Range(I) – Low_Range(I);
          Low = Low – Low_Range(I);
          Low = Low / Range;
    End // if
  End // for
End // while
```

Table- 4: Arithmetic decompression

Low Value	Data	Low	High
0.2572167752	74	0.2	0.3
0.572167752	19	0.5	0.6
0.72167752	70	0.6	0.8
0.6083876	70	0.6	0.8
0.041938	32	0.0	0.1
0.41938	75	0.4	0.5
0.938	238	0.2	0.3
0.38	69	0.9	1.0
0.8	37	0.3	0.4
0.0	65	0.8	0.9

Decompression Algorithm

The decompression algorithm in reverse the compression algorithm can be illustrated in the following steps:

1- Decode the compressed data by using arithmetic coding.

2- Generate FT matrix by using RLE. This step it is meaning read the one-dimensional array to build columns for the FT matrix.
3- Multiply element by element between the quantize table and FT matrix.
4- Apply inverse Discrete Sine transform (See equation 4) on each column to generate Transformed matrix IT.
5- Finally apply Inverse Discrete Cosine Transform (See equation 2) on each row of IT to obtain approximately original image.

Computer Results

Our algorithm tested on two different color images, applied on the MATLAB language using CPU –AMD 2.2GHz with RAM 2Gbyte. The color images consist of three layers R,G,B; these layers are converted into another three layers YC_bC_r as shown in Figure-4 (10).

$$\begin{bmatrix} R \\ G \\ B \end{bmatrix}\begin{bmatrix} 0.3 & 0.6 & 0.1 \\ -0.15 & -0.3 & 0.45 \\ 0.438 & -0.375 & -0.063 \end{bmatrix}=\begin{bmatrix} Y \\ C_b \\ C_r \end{bmatrix} \quad \text{(a)}$$

$$\begin{bmatrix} Y \\ C_b \\ C_r \end{bmatrix}\begin{bmatrix} 1 & 0.0016 & 1.5987 \\ 1 & -0.3341 & -0.7994 \\ 1 & 2 & 0 \end{bmatrix}=\begin{bmatrix} R \\ G \\ B \end{bmatrix} \quad \text{(b)}$$

Figure – 4(a): Transform matrix from RGB to YC_bC_r,
(b) Transform matrix from YC_bC_r to RGB

The idea from using this type of transformation is to increase compression ratio for the algorithm and also for comparison with JPEG technique, because JPEG technique used color transformation. After applied the color transformation we need to the algorithm to compress each layer independently. The Figure-3 shows original image used by algorithm.

(a) Original **Lena** image with dimension 500 x 500

(b) Original Animal image with dimension 960 x 720

Figure -3: Original images tested by the algorithm

The first test for algorithm on **Lena** image size "**732 Kbyte**", this image transformed to YC_bC_r , then each layer compressed by algorithm. The quantized table is used in the algorithm contain the parameter (V) (See equation 5). Table 5 shows different parameters used by the compression algorithm.

Table -5: Lena image results

Parameter "V"	Compressed image size	Compressed image size with Header file	Compression Ratio
V=0.5	98 KByte	126.48 kByte	5.78
V=1.0	53 KByte	68.3 kByate	10.71
V=2.0	28.81 KByte	37 kByte	19.78

Table 5 shows the compression ratio for the algorithm used which is computed by equation (6). The compression ratio shows how many times the compressed image size is smaller than original size.

$$Compression\ Ratio = \frac{Original\ image\ size}{Compressed\ image\ size} \qquad (6)$$

Lena image compressed three times according to V used in the Quantized Table (See equation 5), the figure 4 shows three decompressed **Lena** image

(a) V=0.5 (b) V=1

(c) V=2

Figure-4 (a-c) decompressed **Lena** image

Second test: **Animal** image of size 1.9Mbyte, also this image transformed by using YC_bC_r. Table 6 shows the compressed size for **Animal** image by using same parameter "V" in Quantized table. Figure 5 shows the decompressed Animal image.

Table- 6: Animal image results

Parameter "V"	Compressed image size	Compressed image size with Header file	Compression Ratio
V=0.5	187.35 KByte	241.44 kByte	8.05
V=1.0	101.43 KByte	130.5 kByate	14.9
V=2.0	54.39 KByte	69.75 kByte	27.89

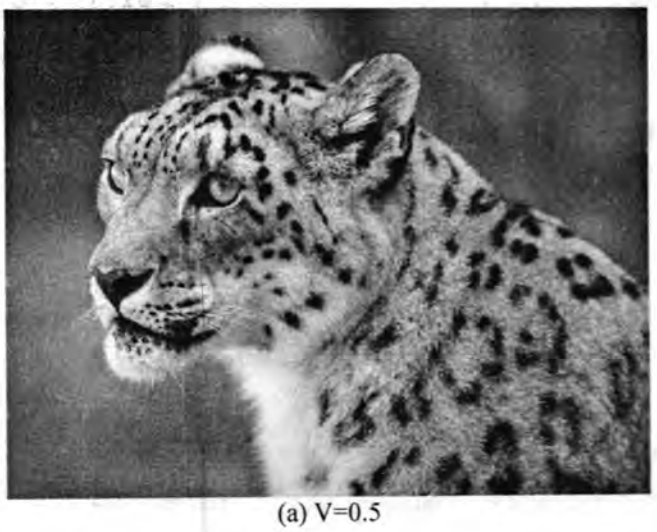

(a) V=0.5

(b) V=1

(c) V=2

Figure -5: Decompressed Animal image

JPEG technique is very important in image compression. In this research we use it to compress the same images for comparison with our algorithm. The JPEG algorithm start by convert the original image into 8x8 squares , then each square compressed by 2D-DCT. The quantization process is approximately same used in this research, then using zigzag scan to convert the transformed square into one-dimensional array. Finally apply the RLE and Huffman coding to get compressed image, the Figure-6 shows the JPEG algorithm.

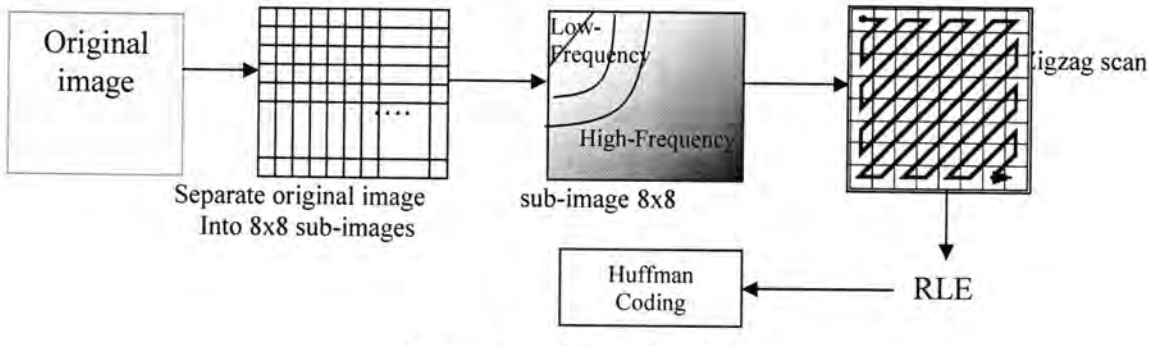

Figure -6: JPEG algorithm

Before the comparison between our research and JPEG, we need to compute Mean-Square-Error (MSE) between the original images and decompressed images to compare image quality, between our algorithm and JPEG. Table 7, Table 8 shows the comparison between JPEG and our algorithm for **Lena** image and **Animal** image respectively.

Table- 7: Comparison with our algorithm using **Lena** image

Technique	Parameters Used by the Technique	Compressed image size with Header file	Compression Ratio	MSE
JPEG	Quality =100%	245 Kbytes	2.98	10.88
	Quality=85%	77 Kbytes	9.5	24.62

	Quality=50%	34.9 Kbytes	20.9	39.6
Our Algorithm	V=0.5	126.48 Kbytes	5.78	26.82
	V=1.0	68.3 Kbytes	10.71	46.51
	V=2.0	37 Kbytes	19.78	71.81

Table- 8: Comparison with our algorithm using **Animal** image

Technique	Parameters Used by the Technique	Compressed image size with Header file	Compression Ratio	MSE
JPEG	Quality =100%	586 Kbytes	3.32	1.2
	Quality=85%	197 Kbytes	9.87	6.85
	Quality=5`0%	91.8 Kbytes	21.19	26.1
Our Algorithm	V=0.5	241.44 Kbytes	8.05	50.28
	V=1.0	130.5 Kbytes	14.9	78.14
	V=2.0	69.75 Kbytes	27.89	108.55

This paper presented a new idea for image compression using DCT and DST functions together, which has some advantages illustrated in the following steps:

1- Using one-dimensional DCT and DST functions. which means increasing the number of high-frequency domains, and most regions of images contain high frequency domain.

2- The main reason for using DST is to keep image quality. Because the DST increases high frequency domains and all coefficients are reconstructable by inverse DST.

3- RLE algorithm used in this paper minimizes the number of coefficients and generates header data contains bits, that indicates to compress, or not compress.

4- Arithmetic coding is used for compress the data after RLE is used. This algorithm converts data into floating point values. Arithmetic Coding is better than huffman coding that used in JPEG technique.

5- The value V used in quantization has important roll to increase number of zeros in matrix, this value increases compression ratio for algorithm used.

Also this paper has some disadvantages:

1- The value V used in quantization effects on image quantity, this make a small degradation on an image, this make JPEG has better quality more than our algorithm.

2- Header data and head for arithmetic coding effects on file size, for the image used in this paper, header size reached to more than 20 kbytes.

REFERNCES

1. Umbaugh S. E., Computer vision and image processing, Prentice Hall PTR, (2001).
2. Sayood K., Digital image compression, Morgan Kaufmann Publishers, Inc., San Francisco, CA, 2nd edition, (2000).
3. Tsai, M. and Hung H., DCT and DWT based Image Watermarking Using Sub-sampling, in Proc. Of the 2005 IEEE Fourth Int. Conf. on Machine Learning and Cybernetics,: 5308-5313,China, (2005).
4. Castelli. V., Robinson j., and Turek j.j., Multiresolution lossless/lossy compression and storage of data for efficient processing, U.S. Patent,6,141,445. Octobar, (2000).
5. Dembo A. and Kontoyainnis I., Source coding large deviations and approximate pattern matching, Invited paper in IEEE Trans. Theory special issue on Shannon theory, dedicated to Aaron D. Wyner, 48. : 1590 - 1615, June, (2002).
6. Pennebaker W.B. and Mitchell J.L., JPEG still image data compression standard. Van Nostrandm Reinhold, (1993).
7. Rao K. R. and Yip P., Discrete Cosine Transform, Academic Press, (1990).
8. Pradhan S. S., Ramchandran K., Enhancing analog image transmission systems using digital side information: A new wavelet-based image coding paradigm, in:Proc. IEEE Data Compression Conf. (DCC), Snowbird,UT, : 63–72(2001).
9. Gonzalez R. C., Richard E. W., Digital Image Processing, Addison Wesley publishing company – (2001).
10. Jain, A. K., Fundamentals of Digital Image Processing, Englewood Cliffs, NJ, Prentice Hall : 150-153(1989).
11. Martucci S. A., Symmetric convolution and the discrete sine and cosine transforms, IEEE Trans. Sig. Processing SP-42: 1038-1051 (1994).

Vol. 21
No. 5
2010

مجلة علوم المستنصرية

تصدر عن كلية العلوم الجامعة المستنصرية

عدد خاص
بحوث المؤتمر العلمي السادس
لكلية العلوم - الجامعة المستنصرية
للفترة 9-10 شباط لسنة 2010

Mobile: 07706289924
e-mail: mustjsci@yahoo.com

بسم الله الرحمن الرحيم

تعليمات النشر لمجلة علوم المستنصرية

1. تقوم المجلة بنشر البحوث الرصينة التي لم يسبق نشرها في مكان آخر بعد إخضاعها للتقويم العلمي من قبل مختصين وبأي من اللغتين العربية او الانكليزية .
2. يقدم الباحث طلبا تحريريا لنشر البحث في المجلة على أن يكون مرفقا بأربع نسخ من البحث مطبوعة على الحاسوب ومسحوب بطابعة ليزرية وعلى ورق ابيض قياس (A4) مع قرص مرن (Disk) محمل بأصل البحث ويكون عدد صفحات البحث 10 صفحات وبضمنها الاشكال والجداول على ان لايكون الحرف اصغر من قياس 12 .
3. يطبع عنوان البحث واسماء الباحثين (كاملة) وعناوينهم باللغتين العربية والانكليزية على ورقة منفصلة شرط ان لاتكتب اسماء الباحثين وعناوينهم في أي مكان اخر من البحث ، وتعاد كتابة عنوان البحث فقط على الصفحة الاولى من البحث .
4. تكتب اسماء الباحثين كاملة بحروف كبيرة وفي حالة استخدام اللغة الانكليزية وكذلك الحروف الاولى فقط من الكلمات (عدا حروف الجر والاضافة) المكونة لعنوان البحث ، وتكتب عناوين الباحثين بحروف اعتيادية صغيرة .
5. تقدم خلاصتان وافيتان لكل بحث ، احداهما بالعربية والاخرى بالانكليزية وتطبع على ورقتين منفصلتين بما لايزيد على (250) كلمة لكل خلاصة.
6. تقدم الرسوم التوضيحية منفصلة عن مسودة البحث ، وترسم على ورق شفاف (Tracing Paper) بالحبر الصيني الاسود ، وترفق ثلاث صور لكل رسم وتكتب المعلومات تحته على ورقة منفصلة.
7. يشار الى المصدر برقم يوضع بين قوسين بمستوى السطر نفسه بعد الجملة مباشرة وتطبع المصادر على ورقة منفصلة ، ويستخدم الاسلوب الدولي المتعارف عليه عند ذكر مختصرات اسماء المجلات.
8. يفضل قدر الامكان تسلسل البحث ليتضمن العناوين الرئيسة الاتية : المقدمة ، طرائق العمل ،النتائج والمناقشة ، الاستنتاجات ، المصادر ،

وتوضع هذه العناوين دون ترقيم في وسط الصفحة ولا يوضع تحتها خط وتكتب بحروف كبيرة عندما تكون بالانكليزية .

9. يتبع الاسلوب الاتي عند كتابة المصادر على الصفحة الخاصة بالمصادر: ترقيم المصادر حسب تسلسل ورودها في البحث ، يكتب الاسم الاخير (اللقب) للباحث او الباحثين ثم مختصر الاسمين الاولين فعنوان البحث ، مختصر اسم المجلة ، المجلد او الحجم ، العدد ، الصفحات ، (السنة) . وفي حالة كون المصدر كتابا يكتب بعد اسم المؤلف او المؤلفين عنوان الكتاب ، الطبعة ، الصفحات ، (السنة) الشركة الناشرة ، مكان الطبع .

10. بخصوص اجور النشر يتم دفع مبلغ (20000) عشرون الف دينار عند تقديم البحث للنشر وهي غير قابلة للرد ومن ثم يدفع الباحث (20000) عشرون الف دينار اخرى عند قبول البحث للنشر وبهذا يصبح المبلغ الكلي للنشر (40000) اربعون الف دينار .

٢٢٢٢٢٢٢٢٢

المحتويات

دراسة قابلية تحسس الويب كاميرا enet للتصوير تحت شروط اضاءة مختلفة لمصباح الفلورسنت

زينب ارحيم حسين الأسدي وعلي عبد داود الزكي و رغد عبد العالي عزيز الشمخي
قسم الفيزياء ./ كلية العلوم /الجامعة المستنصرية

ABSTRACT

The color photography process is studied with using test paper in the box which was possible to control with its light by fluorescent lamp and a group of different images at different intensities of light are captured (at different voltages) and calculate the power of the light system , Analysis these images and calculate the standard deviation and the mean for the intensities values for RGB bands and L the brightness component and estimate the quantity effect of the sensors of the enet web camera by changing the intensity of light of the fluorescent lamp . The relation between standard deviation although the mean for the color bands RGB and L the brightness component for the captured images with the power of illumination system .We observed rigidity and stability in distribution of the intensity of light for all color bands from (0-60) volt which the sensors of the web camera an able to sense through this range of the light voltages and observed with increasing the supplied power of the system increasing the mean value and this increase take parabola form and rigidity and stability occurred in the mean value for all color bands with continuity of increasing . Also, observed stability in the standard deviation value at low different light less than (80) volt which there wasn't noise in this range of voltages and the noise increase at high intensities of light for the fluorescent lamp until it reach level of stability again and for all color bands RGB and L component .

الخلاصة

تم دراسة عملية التصوير الملون بأستخدام الورقة الاختبارية (Test Paper) في الصندوق الذي يمكن التحكم بأضاءته بمصباح الفلورسنت وتم التقاط مجموعة من الصور المختلفة عند شدات الاضاءة المختلفة (عند الفولتيات المختلفة) و حساب القدرة لمنظومة الأضاءة . تم دراسة تجانس توزيع الأضاءة على هذه الورقة من خلال دراسة الصور وتحليلها وحساب الانحراف المعياري و المعدل لقيم الشدات للحزم RGB والمركبة L وتخمين مقدار تأثرمتحسسات الويب كاميرا بتغير شدة أضاءة مصباح الفلورسنت . حيث تم دراسة العلاقة بين الانحراف المعياري STD وكذلك المعدل Mean للحزم اللونية RGB والمركبة L للصور الملتقطة مع قدرة منظومة الاضاءة (Power) عند شدات اضاءة مختلفة و يلاحظ ثبات واستقرار في توزيع شدات الاضاءة لجميع الحزم اللونية من (0-60) فولت أي ان متحسسات الكاميرا ليس لها القابلية على التحسس ضمن هذا المدى من فولتيات الاضاءة ويلاحظ عند زيادة القدرة المجهزة للمنظومة زيادة في قيمة المعدل وتأخذ الزيادة شكل القطع المكافيء و يحصل ثبات واستقرارية في قيمة المعدل لجميع الحزم اللونية بالاستمرار بالزيادة . كما ويلاحظ استقرارية في قيمة الانحراف المعياري عند الاضاءات المنخفضة الاقل من (80) فولت أي لاتوجد ضوضاء عند هذا المدى من الفولتيات وتزداد الضوضاء عند شدات اضاءة عالية لمصباح الفلورسنت الى ان تصل مرحلة من الاستقرارية مرة اخرى ولجميع الحزم اللونية RGB ومركبة الشدة L .

المقدمــة

تعتبر الإضاءة عنصر شديد الأهمية في المعالجة اللونية حيث يكون الضوء الداخل للعين هو نتيجة لكثافة الإضاءة ومعامل انعكاس السطح لاي طول موجي كان (1) . يتأثر الإحساس اللوني في العين اذا حصلت تغيرات في لون السطح نتيجة تغير في الإضاءة ، يقوم الجهاز العصبي البصري البشري بالتعويض التلقائي لهذه التغيرات عند الانتقال من غرفة مضاءة

بضوء صناعي الى ضوء الشمس ونحن لا ندرك عادة تأثير الإضاءة على لون السطح بخلاف ذلك لا تقوم آلة التصوير الكاميرا بمثل هذا التعويض ويكون للتغيرات الحاصلة في الإضاءة تأثير شديد على قيم اللونية لعنصر الصورة للحزم اللونية RGB في الصورة الملونة ولذلك فمن المهم توفير إضاءة ثابتة سواء في التركيب الطيفي ام في الكثافة (2,3) .

الاضائية تشير الى الاضاءة العالية Lightness او العتمة Darkness في كل الصورة ، يمتلك اللون الاسود كثافة واطئة و المصطلح الصحيح يسمى النصوع Luminance ويمتلك اللون الابيض كثافة عالية او نصوع عالي الشكل (1) يبين طريقة تمثيل الحافة بشكل تخطيطي يلاحظ من الشكل ان الجانب الايسر واطئ النصوع ثم يتصاعد ليكون عالي النصوع من الجانب الأيمن.

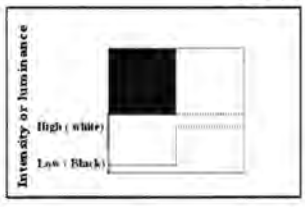

شكـــــل -1 : طريقة تمثيل الحافة[3]

ان الاضائية هي الكثافة المحسوسة لجسم عاكس وتشير الى سلسلة من التدرجات اللونية ابتداء من اللون الابيض الى الاسود من خلال تدرج رمادي والمدى في اغلب الاحيان يشير الى المستوى الرمادي وهناك تعبير مماثل للاضائية هو السطوع Brightness حيث يشير الى مقدار الكثافة المحسوسة من جسم مضاء ذاتياً مثل انبوبة الاشعة الكاثودية CRT ان العلاقة بين السطوع والكمية المحسوسة والكثافة المضيئة هي كمية خاضعة للموديل أللوغاريتمي للقياس . ان الإضاءة ترتبط بملاحظات حسية لشدة اللون وتتراوح قيمتها بين الصفر والواحد اما اللمعان فيرتبط مع الإضاءة ويمكن تعريفه بانه مقدار الاستجابة الحاصلة في العين والناجمة عن الإضاءة (4,5) .

أما اللون فهو الصفة المرئية لكل الأشكال والهيئات وهو من الناحية العلمية الفيزيائية يعتبر صفة للضوء وهو واحد من أشكال الطاقه الأشعاعية ويأخذ أسمهُ من الأحساس الناتج عن أثارة العين بطاقه أشعاعية معينه أوبضوء ذي طول موجي معين وتستطيع عين الأنسان أن ترى مزيجاً لعدد من الأطوال الموجية للضوء المرئي التي تبدأ بأطولها وهو الأحمر وتنتهي بأقصرها وهوالبنفسجي وهذه الأطوال الموجية تحمل معلوماتها الى النظام المرئي للأنسان حيث تغزو الألوان الى الأشياء التي تظهرها وبأقترانها مع أنواع أخرى من المعلومات كالهيئة والحجم وغيرها ينتج الأحساس الذي يفسرهُ العقل باللون (6) .

وعلى هذا الأساس فاللون ليس صفة متأصله في السطح ، وأنما بنية لون الضوء الذي يسقط على السطح هو المسؤول عن الألوان التي تراها العين الصحيحة لمادة ذلك السطح ولذلك فأن أدراك اللون يعتمد على عدة عوامل منها (7):-

1- بنية لون الضوء (أنواعه طبيعي أم صناعي ، مباشر أم غير مباشر) .
2 - مادة السطح (نوعها) .
3- صحة عين الأنسان وعمره.

وتشير البحوث الى أن أستجابة الأنسان هي أستجابة موضوعية وذاتية فالعين تتكيف عندما تستقبل موجات الضوء الأحمر والتي تركز خلف الشبكية ولذلك فان عدسة العين تتحدب بشكل كبير للتركيز على اللون الأحمر وتسقط موجاتها الى الأمام وهذا يخلق نوعاً من الخداع البصري للسطوح الحمراء حيث تبدو أقرب وأكبر مماهي علية في الحقيقة . أما اللون الأزرق فتأثيره عكس تأثير اللون الاحمر تماماً فهو يسبب تاثير بايولوجي في تحسس العين ويؤدي الى شد العضلات المتصلة بالعدسة مما يسبب تسطيح العدسة ويؤدي الى تقليل في البعد البؤري وتكوين صورة أصغر حجماً من الصورة المتكونة باستخدام اللون الاحمر . بينما الضوء

الأخضر تتركز أمواجهُ مباشرة على الشبكية ولهذا السبب فان الأخضر هو الأكثرراحة للبصر(8).

التصوير في نطاق الطيف المرئي

يعتبر نطاق الطيف المرئي اكثر النطاقات المستخدمة في التصوير لان الادراك البشري للصـــــورة ينحصر في تلك الصور التي تقع في النطاق المرئي من الطيف الكهرومغناطسي (9,10) . ان التطور الهائل في التقنية الحاسوبية ، والتقدم الكبير في مجال التسجيل الرقمي للصور ، ساعد على ظهور الأجهزة التي تسمح بالحصول على الصورة بدون معالجة كيميائية . أن أهم المزايا التي يوفرها التصوير الرقمي هي ثبات جودة الصورة بغض النظر عن طول فترة التخزين وإمكانية المعالجة بالحاسوب. عند استعمال الكاميرات العادية (غير الرقمية) فان الصورة في هذه الحالة ناتجة من تحسس الإشارة الضوئية بواسطة متحسسات كيميائية (الفيلم) . يتكون الفيلم من بلورات هاليدات الفضة ، ولإظهار الصورة يتم بوضع الفيلم في محاليل كيميائية تعمل على أظهار وتثبيت الصورة ، بينما الكاميرات الرقمية تحتوي بدلا من الفيلم على متحسسات ضوئية ، حيث تتركز الصورة على بلورة شبه موصلة حساسة للضوء تسمى جهاز الشحن المزدوج Charge Coupled Device ويرمز لها اختصارا CCD والكاميرا الرقمية تتكـون من الأجزاء التالية (11,12) :

1. وحدة الكاميرا التي تحتوي على شريحة CCD ، والنظام البصري المكون من العدسات المستخدمة للتقريب والتبعيد والتبئير والتحكم بفتحة العدسة .
2. شاشة العرض (Liquid Crystal Display) واختصارا يرمز لها LCD .
3. الوحـــدة التـــــي تحـــول الإشارة التماثليـــــة الى إشارة رقميـــة Analog to Digital Signal Converter (ADC)

الخصائص الاحصائية للصورة الرقمية

ان اهم خصائص الصورة الرقمية والتي تمثل احصائياً وهي المعدل والانحراف المعياري وهما كما يلي :

1- المعدل : Mean

معدل الإضاءة في الصورة يعرف بأنه معدل قيم الشدة لعناصر هذه الصورة ويحسب المعدل μ من العلاقة (13,14) :

$$\mu = \frac{1}{MN}\sum_{x=1}^{M}\sum_{y=1}^{N} f(x,y) \qquad \ldots\ldots\ldots (1)$$

M,N طول وعرض الصورة على التوالي وحاصل ضربهما يساوي عدد عناصر

2- الانحراف المعياري : Standard Deviation

أبرز مقاييس التشتت هو الانحراف المعياري ، و ينضوي تحت لوائه مجموعة من المقاييس الرياضية التي تعتمد كمراحل (خطوات) لاستيعاب الانحراف المعياري و الوصول اليه . وهو يعتمد في الكثير من الطرائق الإحصائية المختلفة ، و يشكل محورا جوهريا في العديد منها . لذا فقد تعددت و تنوعت طرائق حسابه ، وهي جميعا تستند على المنطق نفسه . إن استيعاب الانحراف المعياري كمقياس يصف توزيع القيم يساعد كثيرا في إدراك المنطق الرياضي للعديد من التحليلات الإحصائية المتقدمة . ولهذا المقياس استعمالات متنوعة جدا في الدراسات العلمية عامة و يعرف بأنه مقدار انحراف القيم للإشارة عن المعدل ويحسب الانحراف المعياري σ من العلاقة الآتية (13,14):

$$\sigma = \sqrt{\frac{1}{MN}\sum_{x=1}^{M}\sum_{y=1}^{N}\left(f(x,y)-\mu\right)^2} \qquad \ldots\ldots\ldots (2)$$

مكونات منظومة التصوير

1- الكاميرا نوع ENET :

هي جهاز التقاط الصور حيث تتمكن الكاميرا من التقاط منظر ثلاثي الأبعاد وتحويله الى صور ثنائية الأبعاد والكاميرا المستخدمة ذات متحسس نوع (CMOS) وتتصف بالمواصفات التالية :

1- صور فديوية (Video Capture) : 480x640 بيكسل .
2- صور ثابتة (Still Image Capture) : 640x480 بيكسل .

2- مصباح الفلورسنت :

يتكون مصباح الفلورسنت من أنبوب زجاجي مجوف يحتوي على غاز بخار الزئبق تحت ضغط منخفض جدا « وهذا يساعد على إبقائه على هيئة غاز» ، يحتوي الوجه الداخلي للإنبوب على مادة فوسفورية تقوم بامتصاص الأشعة الفوق البنفسجية التي تطلق لدى مرور تيار في غاز بخار الزئبق ، وتطلق موجات ضوئية بجميع الأطوال الموجية مما ينشئ لون أبيض . يوجد في طرفية مصباح الفلورسنت فتيلتي تنكستين عاديتين كل واحدة يستخدم منها طرفين كما في الشكل (2) . يمر التيار من المصدر الرئيسي إلى دائرة الملف في المصباح والتي تحكم التيار وتمنع مرور تيار مرتفع ثم يمر إلى أحد طرفي المصباح ويوصل الطرف الآخر مباشرة بمصدر التيار، بسبب كون الغاز بارد فإن الإلكترونات ستلاقي مقاومة للمرور عبر الغاز، لهذا ستمر عبر الفتيلتين ثم عبر المكثف ومصباح النيون، وضع المكثف ليمنع كل التيار من الوصول إلى مصباح النيون، بمرور التيار عبر الفتيلتين سيسخنان بشكل كبير « تلك اللحظة التي يحمر فيها طرفي المصباح » ، ومعروف أن الإلكترونات تكون سريعة في المواد الساخنة، سيجعل ذلك عملية قذف الإلكترونات أسهل ليمر عبر الغاز فتمر أول دفعة «تسخن الغاز قليلا» ثم تقل درجة حرارة الفتيلتين فينتقل مرة أخرى إلى المكثف ، لتسخن الفتيلتين من جديد وينتقل الدفعة الثانية من الإلكترونات عبر الغاز . تتكرر هذه العملية عدة مرات حتى يسخن الغاز بشكل كاف ليكون مرور اللإلكترونات عبره أسهل من مرورها عبر المكثف لهذا يومض المصباح عدة مرات قبل أن يعمل (15) .

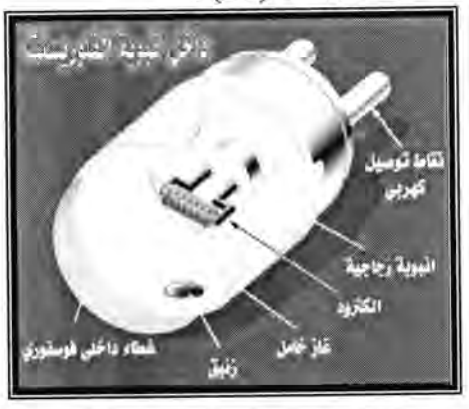

شكل -2 : التركيب الداخلي لمصباح الفلورسنت [20] .

مميزات مصابيح الفلورسنت :

1– القدرة W(18)
2– الفولتية volt (220 – 80) .
3– يبعث الاطوال الموجية للطيف المرئي (بنسب تختلف عن ضوء الشمس) .

3- مقياس الفولتية والتيار :

يتم استخدام جهاز الاميتر لقياس التيار المار بالمصابيح وجهاز الفولتميتر لقياس الفولتية المسلطة على المصابيح وذلك لغرض ايجاد القدرة الكهربائية عند كل شدة اضاءة مستخدمة في التصوير .

4- منظم الفولتية :

يستخدم منظم الفولتية لكي يتم التحكم بالتيار المار في منظومة التصوير وبالتالي يمكن التحكم بشدة ضوء المصباح في منظومة التصوير .

5- الصورة الاختبارية : (Test Image)

وهي صورة ذات نمطين متناوبين هما (الابيض ذو الشدة العالية والاسود ذو الشدة الواطئة) ، وهذه الصور ممثلة بـ (24 bits) حيث الغرض من أستخدام الصورة الاختبارية ذات النمطين الأبيض والأسود لتحديد أفضل صورة وذلك بتطبيق تقنيات التباين المختلفة من خلال تحديد أفضل أضائية معتمدة في التصوير في حالة منظومة الأضاءة بمصدر الفلورسنت كما في الشكل (3) .

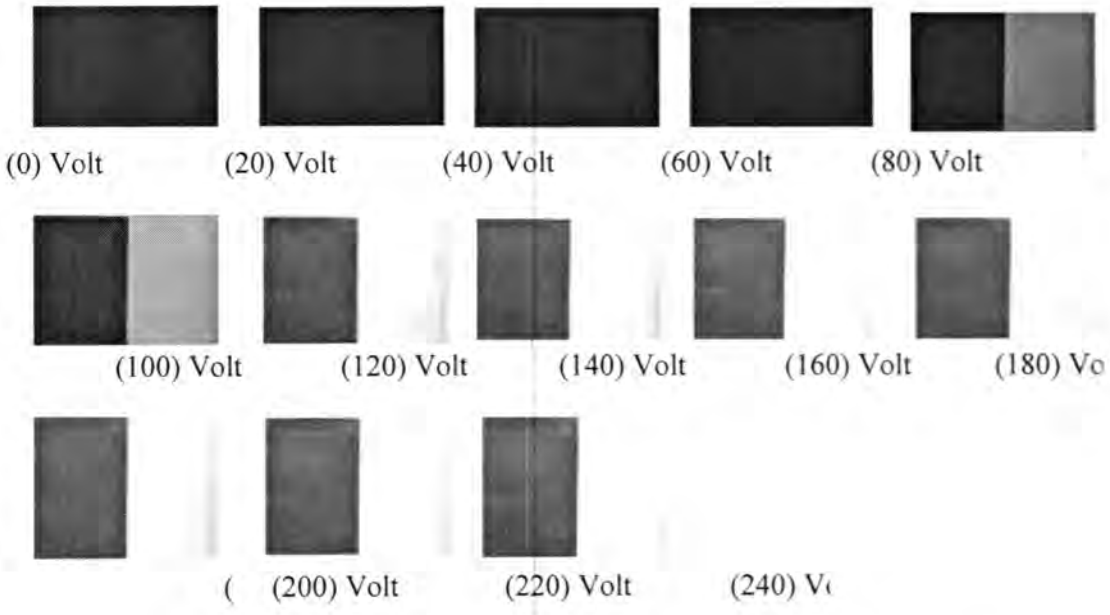

شكل-3 : الصورالأختبارية الناتجة للشدات المختلفة بالأضاءة بأستخدام مصباح الفلورسنت

النتائج والمناقشة

ان الصورة وخصائصها تعتمد على شدة الإضاءة وطبيعة الضوء المستخدم وان شدة الإضاءة تعتمد على القدرة الكهربائية حيث تم استخدام مصباح الفلورسنت ذو شدات إضاءة مختلفة اعتمادا على الفولتية المسلطة , تم في هذه الدراسة تحليل نتائج تصوير صورة اختبارية (Test Image) نصفها ابيض والنصف الاخر اسود بواسطة الويب كاميرا نوع ENET Web Camera , حيث تم تصوير الورقة الاختبارية في الصندوق الذي يمكن التحكم بأضاءته بمصباح الفلورسنت وتم التقاط مجموعة من الصور المختلفة عند شدات الاضاءة المختلفة (عند الفولتيات المختلفة) , حيث تم التحكم بشدة الأضاءة بأستخدام الدائرة الكهربائية الموضحة بالشكل (4-a) وتم تسجيل التيار والفولتية لدائرة منظومة الأضاءة ومن ثم حساب القدرة لمنظومة الأضاءة وتم ألتقاط صورة للورقة الاختبارية لكل تغير في شدة الأضاءة . تتم عملية التصوير على شكل إلتقاط صور عن طريق الحاسبة بربط الكاميرا بواسطة كيبل بالحاسبة وكما يظهر في الشكل (4-b) و بعد عملية حفظ الصور الملتقطة في الحاسبة وترتيبها

وفقا إلى قيمة الفولتية المسلطة على منظومة التصوير وخزنها كصور منفصلة وبصيغة Bit map تم دراسة تجانس توزيع الأضاءة على هذه الورقة من خلال دراسة الصور وتحليلها وحساب الانحراف المعياري و المعدل لقيم الشدات للحزم RGB ومركبة الاضاءة L وتخمين مقدار تأثرمتحسسات الويب كاميرا بتغير شدة أضاءة مصباح الفلورسنت .

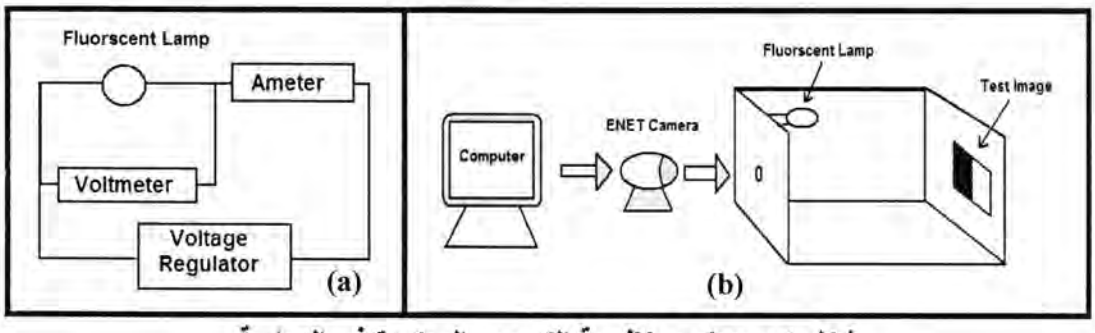

شكل-4 : يوضح منظومة التصوير المعتمدة في الدراسة

حيث تم دراسة الخصائص الإحصائية لكل من الحزم اللونية الثلاثة RGB ومركبة الإضاءة L , ودرسنا توزيع الاضاءة في مستوي الصورة برسم المخطط التكراري لكل صورة وهذه الرسوم موضحة بالشكل (5) , يلاحظ ظهور قمتين عند الفولتية (80) القمة ذات الشدة العالية تعود الى المنطقة البيضاء اما القمة ذات الشدة الواطئة فتمثل المنطقة السوداء من الورقة الاختبارية ويلاحظ بأن شدة الحزمة الزرقاء أقل مقارنة بباقي الحزمتين RG وكذلك مركبة الشدة L وبزيادة الفولتية الى (100) يلاحظ تساوي القمتين تقريباً لجميع الحزم RGB ومركبة الشدة L وبالاستمرار بزيادة قيمة الفولتية يلاحظ انخفاض في شدة القمة اليسرى يقابلها زيادة في قمة الشدة اليمنى أي من (120) ولغاية (240) فولت ويلاحظ عند الفولتية (240) انخفاض شديد في ارتفاع القمة اليسرى . كما ويلاحظ عند زيادة القدرة المجهزة لمنظومة الاضاءة زيادة في قيمة المعدل يظهر ذلك في الشكل (6) وتأخذ الزيادة شكل القطع المكافيء ويلاحظ عند زيادة الفولتية من (100-240) فولت ثبات واستقرارية في قيمة المعدل لجميع الحزم اللونية . اما بالنسبة للانحراف المعياري فقد لوحظ استقرارية في قيمتة عند الاضاءات المنخفضة الاقل من (80) فولت كما في الشكل (7) أي لاتوجد ضوضاء عند هذا المدى من الفولتيات وتزداد الضوضاء عند شدات اضاءة عالية لمصباح الفلورسنت . ويلاحظ كلما كانت المسافة قريبة بين الجسم والمصدر كان توزيع الأضاءة أكثر أنتظاماً . وان مستويات شدة الإضاءة لمركبة الإضاءة L والحزم اللونية RGB تكون متقاربة عند استخدام مصباح الفلورسنت وهذا ناتج عن طبيعة الضوء لمصباح الفلورسنت الذي يكون لونه ابيض فتكون مشاركة الحزم اللونية والإضاءة متساوية تقريباً .

(0-60) volt

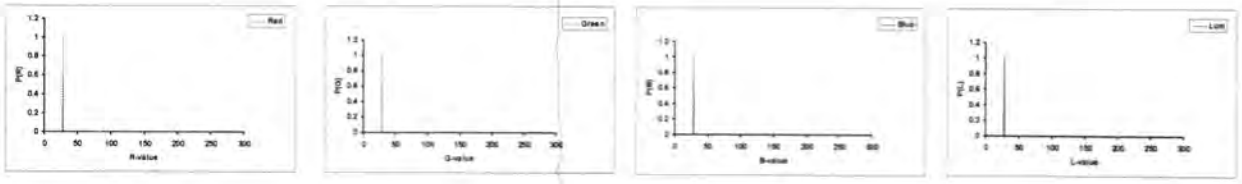

(80) volt

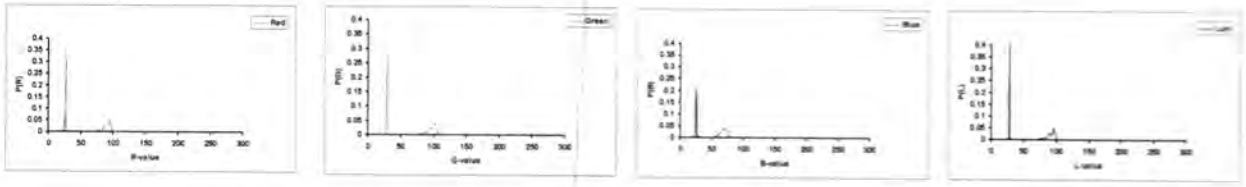

(100) volt

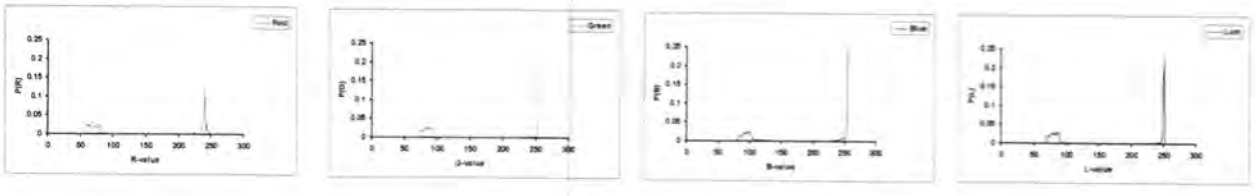

(120) volt

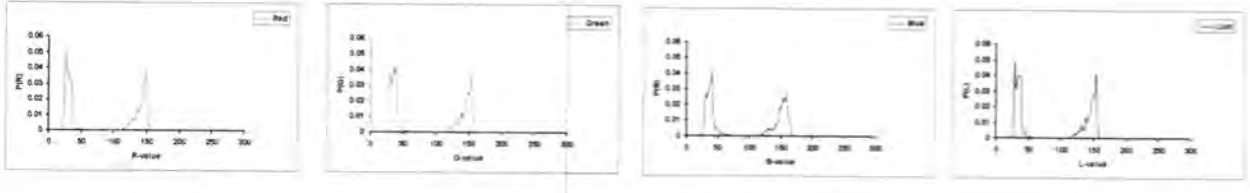

(140) volt

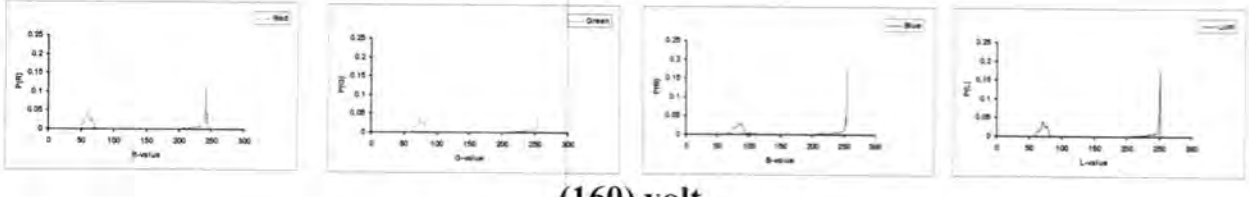

(160) volt

شكل-5 : يوضح المخطط التكراري للحزم اللونية RGB ومركبة الاضاءة L لشدات الاضاءة المختلفة (فولتيات مختلفة)

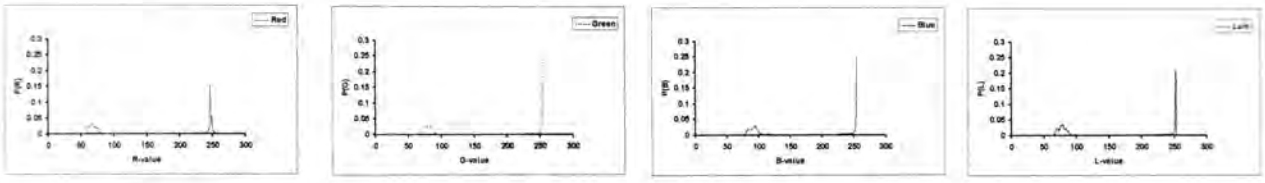

(180) volt

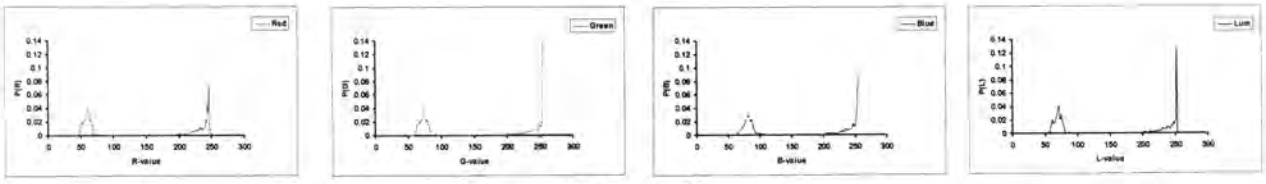

(200) volt

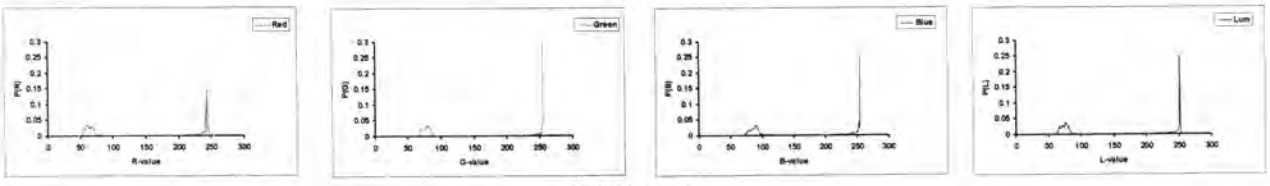

(220) volt

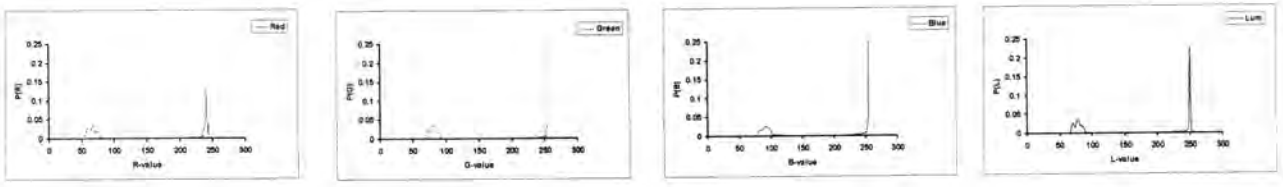

(240) volt

تابع الى الشكل (5)

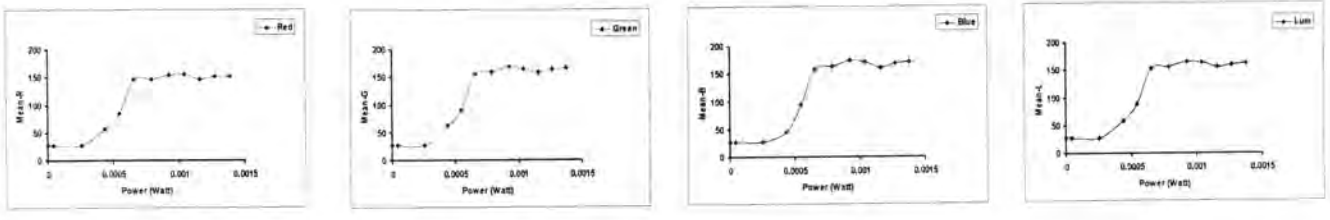

شكل–6: يوضح علاقة المعدلMean مع القدرة Power

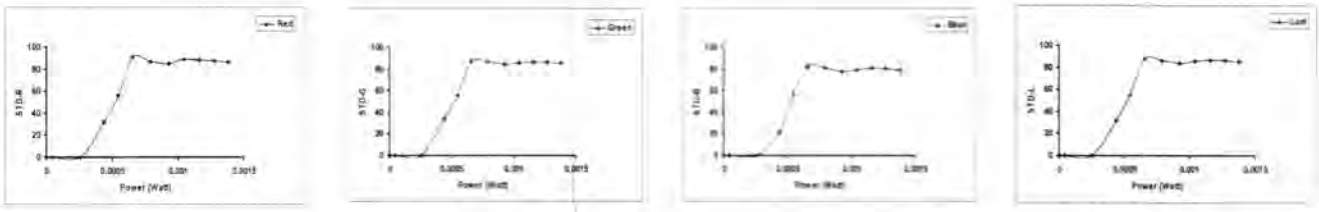

شكل-7: يوضح علاقة الانحراف المعياريSTD مع القدرة Power

1- يبدأ تحسس الويب كاميرا ENET عند (80) فولت أي عندما يبدأ مصباح الفلورسنت بالتوهج لان مصباح الفلورسنت لايعمل في الفولتيات الواطئة وذلك لأن أساس عمله يحتاج الى فولتيات عالية أعلى من (60v) لكي تسبب التأينات اللازمة لأنبعاث الضوء . لذا يلاحظ ثبات واستقرار في توزيع شدات الاضاءة لجميع الحزم اللونية من (0-60) فولت أي ان متحسسات الكاميرا ليس لها القابلية على التحسس ضمن هذا المدى من فولتيات الاضاءة .

2- ظهور قمتين عند الفولتية (80) ويلاحظ بأن شدة الحزمة الزرقاء أقل مقارنة بباقي الحزمتين RG وكذلك مركبة الشدة L وبزيادة الفولتية الى (100) يلاحظ تساوي القمتين تقريباً لجميع الحزم RGB ومركبة الشدة L وبالاستمرار بزيادة قيمة الفولتية يلاحظ انخفاض في شدة القمة اليسرى يقابلها زيادة في قمة الشدة اليمنى أي من (120) ولغاية (240) فولت ويلاحظ عند الفولتية (240) انخفاض شديد في ارتفاع القمة اليسرى .

3- عند زيادة القدرة المجهزة لمنظومة الاضاءة يلاحظ زيادة في قيمة المعدل وتأخذ الزيادة شكل القطع المكافيء ويلاحظ عند زيادة الفولتية من (100-240) فولت ثبات واستقرارية في قيمة المعدل لجميع الحزم اللونية .

4- استقرارية في قيمة الانحراف المعياري عند الاضاءات المنخفضة الاقل من (80) فولت أي لاتوجد ضوضاء عند هذا المدى من الفولتيات وتزداد الضوضاء عند شدات اضاءة عالية لمصباح الفلورسنت الى ان تصل مرحلة من الاستقرارية مرة اخرى وخصوصاً عند (100) فولت ولغاية (240) فولت ولجميع الحزم اللونية RGB ومركبة الشدة L .

المصادر

1. Nezamzbad M. and Berns R.S . , *" The Effect of Image Size on the Color appearance of Image reproduction using Calorimetrically Calibrated LCD and DLP displays"* , J. Soc .Inf .DISP.14(9) :773, (2006) .
2. Holst G.C. , *" CCD Arrays Cameras and Displays "* , 2nd ed , (1998) .
3. Wandell B.A and Farrell J.E. , Water in to Wine , " Convert in Scanner RGB to Tristimulus XYZ " , Proceeding .SPIE (1993).
4. Cernasov A." *New high – dynamic range Camera architecture* " , Proceeding SPIE 6246, 12 May , (2006) .
5. Scharff L.F.V. and Ahumada A.J., *" Contrast Measure For Predicting text readability "* , (2003) .

6. شبر ، ندى ماجد ،"*التصميم الداخلي في الحركات المعمارية الحديثة* " ، رسالة ماجستير ، كلية الهندسة ، جامعة بغداد ، (1988) .

7. Steffy , Gray , " *Architectural Lighting Design* " , Second edition ,John Wiley & Sons ,Inc , NewYork , (2002).
8. Michel , Lou , " *Light, The Shape of Space ,Desinning With Space and Light* " , John Willey and Sons , Inc , (1996).
9. Gonzalez R. C. , Wood R. E. , " *Digital Image Processing* " , (1992) .
10. Umbaugh S.E , " *Computer Vision and Image Processing* " , prentice .Hall , (1998) .
11. Smith S.W. , " *The Scientist and Engineers Guide to Digital Signal Processing* " , California Publishing ISBNO – 966176 – 33 , (1997) .
12. Russ J. C. , " *The Image Processing Hand Book* " , 3rd edition , Materials Science and engineering , Department North Carolina State University , ISBN : 0849325323 , (1998) .
13. BP103 datasheet pdf datenblatt – Siemens Semiconductor Group – NPN – Silizium , http : //www. Alldatasheet .com / datasheet – pdf / pdf / 44647/ SIEMENS/BP103.html , (2003 – 2008).
14. Kai – Yu and Liang Ji, " *How to Optimize Optical Coherent Tomography OCT Image* " , Department of Automation , Tsinghua University , (2001) .
15. Byrne A. and Hilbelt D. R., *"Colure realism & colure science"* , Behavioral and Brain Sciences , 26:3-21, (2003) .

دراسة تاثير لون النص على وضوحيته للاضاءة الجيدة المنتظمة

أحلام مجيد كاظم
الجامعة المستنصرية / كلية العلوم / قسم الفيزياء

ABSTRACT

Color imaging effective field for since research it is continue development as a result to fast development that happened in computer world. The studies text image is a part of this development .In this research we are imaging three types of text which are writing in arabic language on wight background by digital camera and the picturing happen in complete lumence to the room , by using Soble operator to determine the edges for the different text images then we are study the contrast mean for the image edges as afunction of the distance between the black bored and camera.

الخلاصة

ان التصوير الملون باستخدام الكاميرا الرقمية مجال فعال في البحث العلمي وهو في تطور مستمر نظرا للتطور السريع الحاصل في عالم الحاسوب ودراسة الصور النصية هي جزء من هذا التطور. تم في هذا البحث تصوير ثلاث نصوص مكتوبة بثلاث الوان مختلفة وباللغة العربية على خلفية بيضاء بواسطة كاميرا رقمية وتم التصوير بانارة كاملة داخل القاعة التي اجريت فيها الدراسة ستخدام مؤثر الصوبل تم الحصول على صورة الحافات لكل صورة نصية ولخمس عتبات لمؤثر الصوبل وتم دراسة معدل التباين لصور الحافات كدالة للمسافة بين لوحة الكتابة وكاميرا التصوير ومدى تاثير ذلك على وضوحية الصورة .

المقدمة

ان الضوء هو شكل الطاقة المرئية التي تكون صادرة من مصدر أو منعكسة من جسم مثل الشمس أو اللهب أو الشمعة اوالمصباح الكهربائي ، والضوء ضمن المفهوم الفيزيائي هو نوع خاص من الطاقة يعرف بالطاقة الكهرومغناطيسية وبالنسبة للإنسان فإنه يمثل الإدراك الحسي البصري وتمثل هذه الطاقة الإشعاعية الكهرومغناطيسية بحزم من الأطوال الموجية المرئية للعين ومداها المرئي يقع ما بين (300 – 700)nm ، أما ما ندعوه بالضوء الأبيض هو في الحقيقة مزيج من الطاقة الإشعاعية لأطوال موجية معينة وأي موجة تنفصل من المزيج تشير إلى كونها لوناً وبهذا فإن كل من الضوء واللون متلازمين(1) .إن الضوء الذي تتحسسه العين ينشأ أما من الإضاءة الذاتية للجسم المرئي أو من الضوء المنعكس من الجسم نتيجة سقوط الضوء من مصدر ضوئي معين فاذا كانت $E(\lambda)$ تمثل توزيع الطاقة للضوء المنبعث من مصدر ضوئي معين $r(\lambda)$, $t(\lambda)$ تمثل الانعكاسية والنفاذية لجسم معين فان توزيع الطاقة الضوئية للجسم النفاذ تعطى بالمعادلة التالية:

$$C(\lambda) = t(\lambda)E(\lambda) \qquad (1)$$

وتوزيع الطاقة الضوئية للجسم العاكس تعطى بالمعادلة: (2)

$$C(\lambda) = r(\lambda)E(\lambda) \qquad (2)$$

تعتبر الإضاءة عنصراً شديد الأهمية في المعالجات اللونية آذ تحتوي العديد من منظومات التصوير (الكاميرات الرقمية)على وحدات للضوء داخلها وإن إضاءة هذه الوحدات ليست قوية وإنما مفيدة حين يكون الضوء منخفضاً ، فعند ظروف الإضاءة المختلفة في الشدة لا تبقى كفاءة إضاءة الصورة جيدة قد تصبح الصورة داكنة أو معرضة قليلاً للضوء وبذلك تصبح تفاصيل المعلومات أقل في الصورة حيث لا يمكننا تعديل التباين والإضاءة للتعويض عن النقص دون فقدان التفاصيل المضيئة والمظلمة وهنالك العديد من الدراسات السابقة التي اهتمت

بتحسين الصور الملونة من خلال تحسين الاضائية ودراسة تأثير الإضاءة على جودة الصورة وفيما يلي إيجاز أهم هذه الدراسات

- عام **1990** اقترح **Jonhson** استخدام طريقة التباين للكشف عن الحافات الموجودة في الصورة ذات الإضاءة غير المتساوية أو الضعيفة حيث أن هذه الطريقة لا تعتمد على القيمة المطلقة للإضاءة Absolute Brightness كما أستخدم الباحث نوافذ حيزيه 5×5 ذات عوامل التدرج للكشف عن الحافات إذ تعد طريقة التباين مناسبة للصور المرئية والصور بالأشعة تحت الحمراء حيث يمكن اعتماد هذه الطريقة في تطبيقات الإنسان الآلي التي لا يمكن فيها السيطرة على الإضاءة (3)
- عام **1996** اجري الباحث **Peli Eli** دراسة حول تأثير الإضاءة والتردد المكاني على تحسس التباين ما فوق العتبة واستعمال أنماط اختباريه مختلفة الإضاءة والتردد المكاني لغرض مقارنة التباين ، ففي حالة العتبة كان انخفاض الإضاءة اقل ما يمكن من التأثير على تحسس التباين فوق العتبة عند الترددات الواطئة.
ان نتائج هذه الدراسة مهمة للنماذج البصرية المستخدمة في تحليل جودة الصورة (4).
- عام **1997** قدم **Curlandar** بحثاً يهدف إلى تحسين الجودة العالية للصورة الرقمية من خلال استخدام المرشحات المحسنة لاسترجاع الحافات وتحسين معالم الصورة حيث قام الباحث ببناء برنامج حاسوبي لزيادة حدة الحافات sharpening edges عن طريق حساب القيمة العليا المثلى فوق الإضاءة العالية over shoot كدالة للسطوع والتباين إذ توصل إلى أن القيمة العليا المثلى فوق الإضاءة العالية تزداد مع زيادة كلاً من السطوع والتباين (5) .

الصور الملونة (Color Images)

الصورة الملونة تمثل بنموذج يتكون من ثلاث حزم لبيانات أحادية اللون وكل حزمه من هذه البيانات تعود إلى اللمعان في كل لون من الألوان الأساسية الأحمروالأخضروالأزرق وباستخدام 8) bits) لكل عنصر في كل حزمه لونية فإن عنصر الصورة الملونة يمثل بـ (24bits) كما في الشكل (1) الذي يوضح عملية تمثيل الصورة الملونة وعملية إظهار الصورة الملونة بثلاث حزم. وأن العدد الكلي للألوان الحقيقية في الصورة بحدود (16) مليون أي ما يكافئ [6,7] $(2^8)^3$

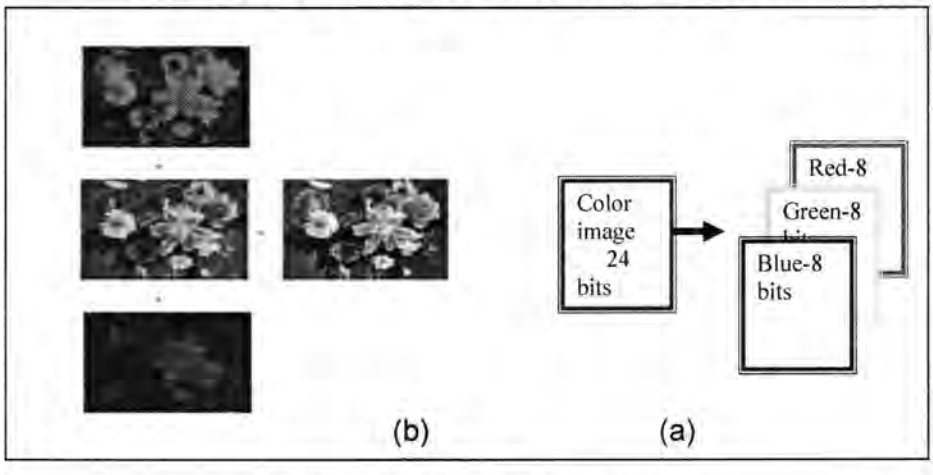

الشكل -1: a– كيفية تمثيل الصورة الملونة

b– عملية أظهار الصورة الملونة المركبة من ثلاث حزم [8].

الفضاء اللوني الأساسي Basic Color Space

يستخدم الفضاء اللوني الأساسي RGB كثيراً في طرق المعالجة المختلفة لأن الكاميرات الملونة والماسح الضوئي وأغلب أجهزة الإظهار تستخدم هذا الفضاء في عملها بصورة أساسية

كإشارات إدخال أو أخراج . يبين الشكل (2) هذا الفضاء كمكعب لوني (Color Cubic) يعين اللون فيه كنقطة في فضاء ثلاثي الأبعاد بدلالة الأحمر R (Red) والأخضر (Green) G والأزرق B (Blue) . في هذا الفضاء تعين المستويات الرمادية في قطر المكعب المحصور بين النقطة (0,0,0) التي تعين اللون الأسود والنقطة (N,N,N) تعين الضوء الأبيض وتمثل N أعظم قيمة لأي من المركبات الثلاثة R أو G أو B وهي تساوي (1) في حالة المعايرة (Normalization) وبخلاف ذلك تكون قيمتها (255) ، أما زوايا المكعب الأخرى فتحدد الألوان (الأحمر، الأصفر(Yellow) ، الأخضر ، الأزرق الداكن (Cyan) ، الأزرق ، الأرجواني (Magenta)) كما موضح في الشكل (2) . إن هذا الفضاء يعمل بصورة جمعية ويستخدم أساساً للتحويل إلى أنظمة أخرى بسب المساوئ التي يتصف بها هذا الفضاء ومنها (9,10,11) :

- ❖ الارتباط العالي بين مركباته يجعل هذا الفضاء غير ملائم لكثير من التطبيقات في مجال معالجة الصور الملونة.
- ❖ لا يتناسب مع طبيعة الإدراك الحسي لعين الإنسان.
- ❖ غير منتظم أي لايمكن تحديد الإختلاف بين الألوان عند الإحساس بها على أساس الإختلاف في خطوات القياس على طول محاور الإحداثيات عند تمثيل الألوان بهذا الفضاء

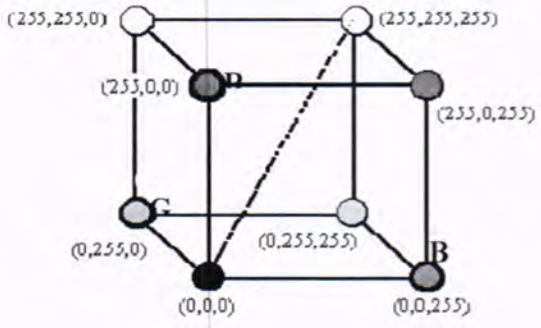

الشكل-2: يمثل الفضاء اللوني الأساسي(12).

التقنيات المستخدمة

- ❖ **حساب تباين القيمة الصغرى والكبرى مع العنصر الوسطي**

ومخطط نافذة العمل لهذه التقنية موضح بالشكل (3) تعتمد هذة التقنية على عناصر الحافات لحساب التباين حيث تؤخذ نافذة ثلاثية حول عنصر الصورة الذي يمثل نقطة حافة ثم ايجاد اصغر قيمة من العناصر المجاورة للعنصر الوسطي اما اكبر قيمة فهي تمثل العنصر الوسطي I_{max} وان معادلة التباين في هذه التقنية تكون باصيغة التالية (13) .

$$C_{\min} = \frac{I_{\max} - I_{\min}}{I_{\max} + I_{\min}} \qquad (3)$$

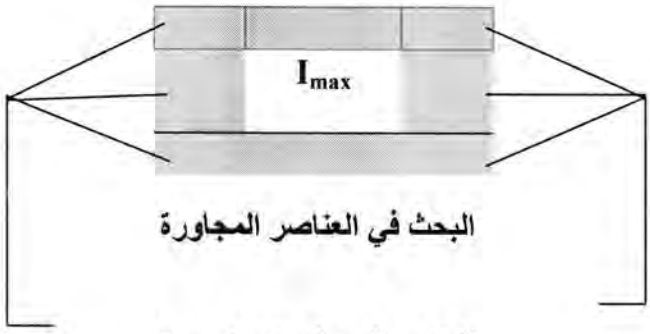

الشكل -3: نافذة العمل حول العنصر الوسطي الأكبر

- **تقنية حساب التباين المباشر**
- وتعتمد هذه التقنية على استخدام المعادلة (3) وتطبيقها على نقاط الصورة مناطق الحافات فقط ويتم ذلك باخذ نافذة ثلاثية حول نقطة الحافات في الصورة والبحث على اوطا واعلى قيمة في الشدة لعناصر الصورة التابعة للحافات .

المواد وطرائق العمل

تم كتابة نص بالغة العربية على لوحة كتابة (سبورة) بيضاء اللون معلقة في قاعة دراسية تحتوي على شباك من الجانب الأيمن وباب من الجانب الأيسر مع أجهزة إنارة سقفية والشكل (4) يوضح التكوين الهندسي لقاعة المحاضرات .
تم كتابة نص مكون من ثلاث كلمات (**الطمع رق مؤبد**) كتب النص مرة باللون الأسود ومرة باللون الأخضر ومرة ثالثة باللون الأزرق والشكل (5) يوضح صورة النص بالألوان الثلاثة وللمسافات الثلاثة , وتم التصوير بواسطة كاميرا رقمية ولمسافات مختلفة بين لوحة الكتابة والكاميرا الرقمية (100cm ,200cm 300cm) وفي كل مسافة تم تصوير مشهد فديوي لمدة دقيقتين ولكل واحد من النصوص الملونة الثلاثة وتم قطع صورة واحدة من كل مشهد فديوي باستخدام برنامج Ulead للتقطيع .

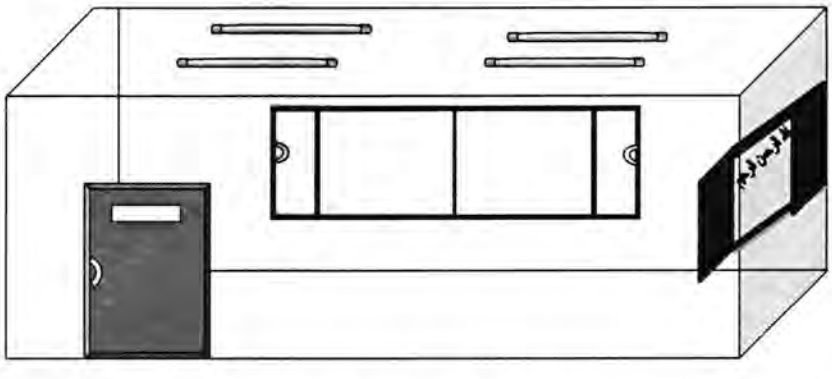

الشكل - 4: المخطط الهندسي للقاعة

باستخدام مؤثر الصوبل تم الحصول على صورة الحافات لكل نص من النصوص الثلاثة حيث تم استخدام خمس عتبات في العمل (20,40,60,80,100) لغرض كشف الحافات وقد حصلنا على صورة الحافات لكل عتبة ولكل صورة نصية وتم تحليل كل صورة نصية الى مركباتها اللونية الاربعة(L-R-G-B) وتم حساب التباين (contrast) لكل مركبة لونية .

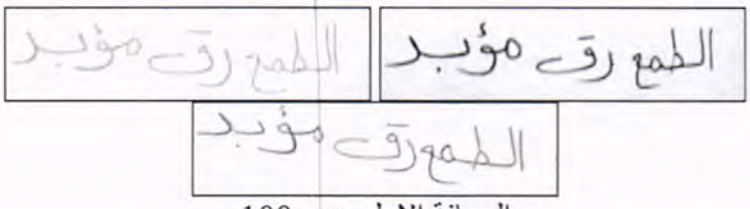

المسافة الاولى 100 cm

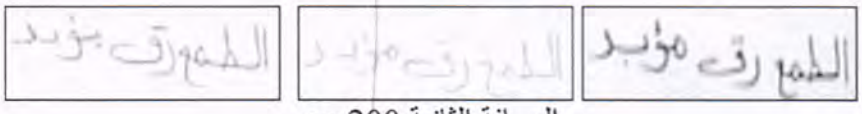

المسافة الثانية cm200

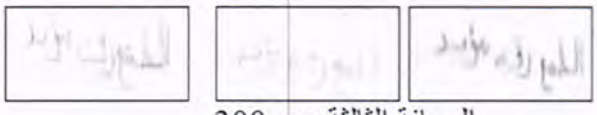

المسافة الثالثة 300 cm

الشكل -5: الصور النصية لثلاث مسافات

النتائج والمناقشة

تم رسم العلاقة البيانية بين المسافات الثلاثة المعتمدة في التصوير (Distance (cm مع معدل التباين $\mu_{contrast}$ لكل مركبة لونية من المركبات الأربعة (L-R-G-B) حيث يلاحظ أن التباين لصورة النصوص الثلاثة (الأسود والأخضر والأزرق) يقل مع ازدياد المسافة بين لوحة الكتابة والكاميرا الرقمية وعند مقارنة نتائج صورة النص الاسود مع صور النصين الاخضر والازرق يلاحظ ما يلي:

- يقل معدل التباين مع زيادة المسافة الفاصلة بين لوحة الكتابة والكاميرا الرقمية وهذا ما يلاحظ من الاشكال(11-10-9-8-7-6) ولكافة العتبات المستخدمة في العمل وللصور النصية الثلاثة ولكلا التقنيتين المستخدمتين لحساب التباين.
- للمركبات اللونية الأربعة للصور النصية الثلاثة وهذا ما يلاحظ من الشكل(-10-9-8-7-6 11) حيث انه كلما زادت العتبة المعتمدة لكشف حافات الصورة يزداد معها معدل التباين ونحصل على اعلى تباين للمنحني الذي يمثل العتبة 100واقل تباين هو للمنحني الذي يمثل العتبة 20 وهذا واضح للصور النصية الثلاثة ولكلا التقنيتين (التباين المباشر والتباين الاصغر والاكبر) .
- ان معدل التباين لصورة النص الاسودهي اعلى من معدل التباين لصورة النصين الاخضر والازرق حيث ان اقل قيمة لمعدل التباين $\mu_{contrast}$ للنص الاسود هي للمنحني الذي يمثل العتبة 20 هي تقريبا 0.18 وهي قيمة اعلى من اكبر قيمة للتباين للنص الاخضر الذي يصل اعلى تباين له تقريبا 0.16 اما اعلى تباين للنص الازرق هي تقريبا 0.17 والكلام السابق صحيح للصورالنصية الثلاثة و لكل المركبات اللونية (L-R-G-B) والكلام السابق يصح لكلا التقنيتين المستخدمتين لحساب التباين .
- ان منحنيات (تمثل العتبات المستخدمة) معدل التباين لصورة النص الاسود تتقارب فيما بينها ويزداد هذا التقارب بزيادة المسافة الفاصلة بين لوح الكتابة والكاميرا الرقمية وهذا ما يمكن ملاحظته من الشكلين (6,9), وعند مقارنة الشكلين (7,10) يظهر ان التقارب بين منحنيات معدل التباين للنص الازرق وللمركبات اللونية (L-R-G-B) يظهر بشكل واضح جدا ولكل

المسافات الفاصلة بين لوح الكتابة والكاميرا الرقمية على حد سواء اما الشكلين (11, 8) فيبدو من ملاحظته ان التباعد بين منحنيات العتبات للنص الاخضر اكثر مما هو ظاهر لصور النصين الاسود والازرق والكلام السابق يصح لكلا التقنيتين المستخدمتين لحساب التباين .

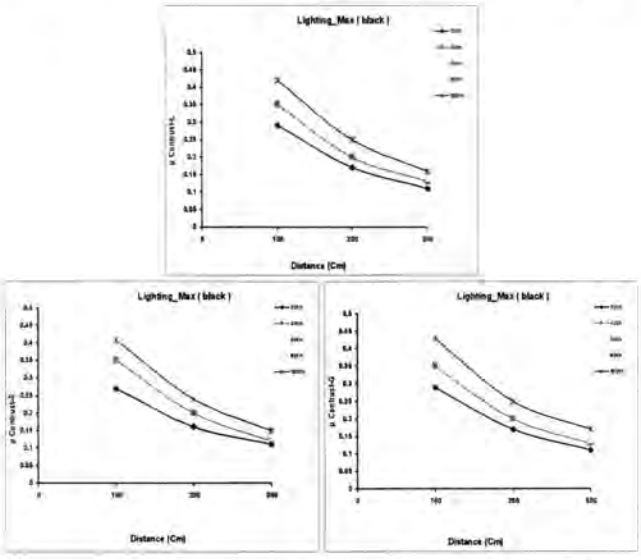

شكل - 6 : العلاقة بين التباين المباشر كدالة لبعد الكاميرا والسبورة للنص الاسود (إضاءة منتظمة) للحزم اللونية RGB

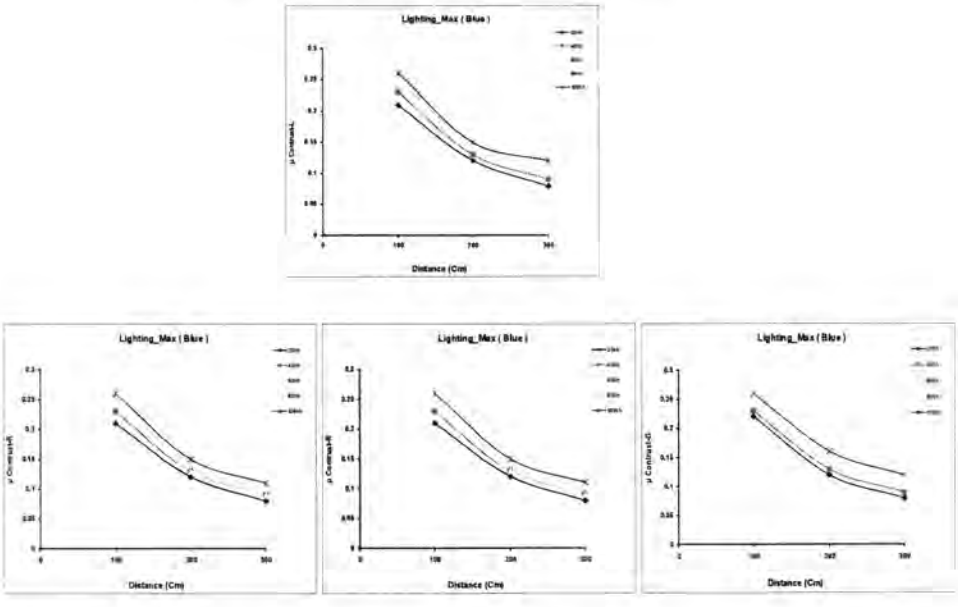

شكل - 7 : العلاقة بين التباين المباشر كدالة لبعد الكاميرا والسبورة للنص الازرق (إضاءة منتظمة) للحزم اللونية RGB

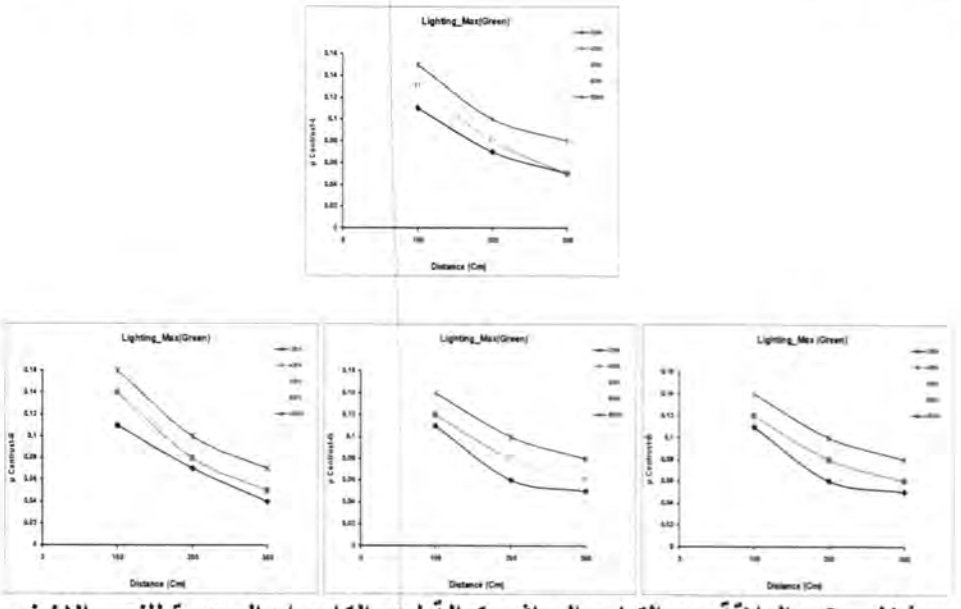

شكل - 8 : العلاقة بين التباين المباشر كدالة لبعد الكاميرا والسبورة للنص الاخضر (إضاءة منتظمة) للحزم اللونية RGB

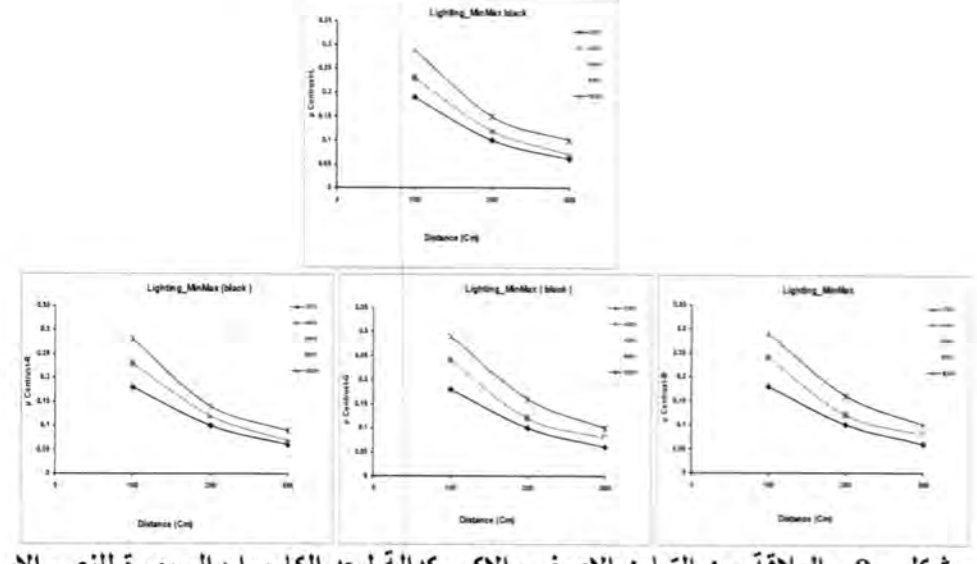

شكل - 9 : العلاقة بين التباين الاصغر والاكبر كدالة لبعد الكاميرا والسبورة للنص الاسود (إضاءة منتظمة) للحزم اللونية RGB

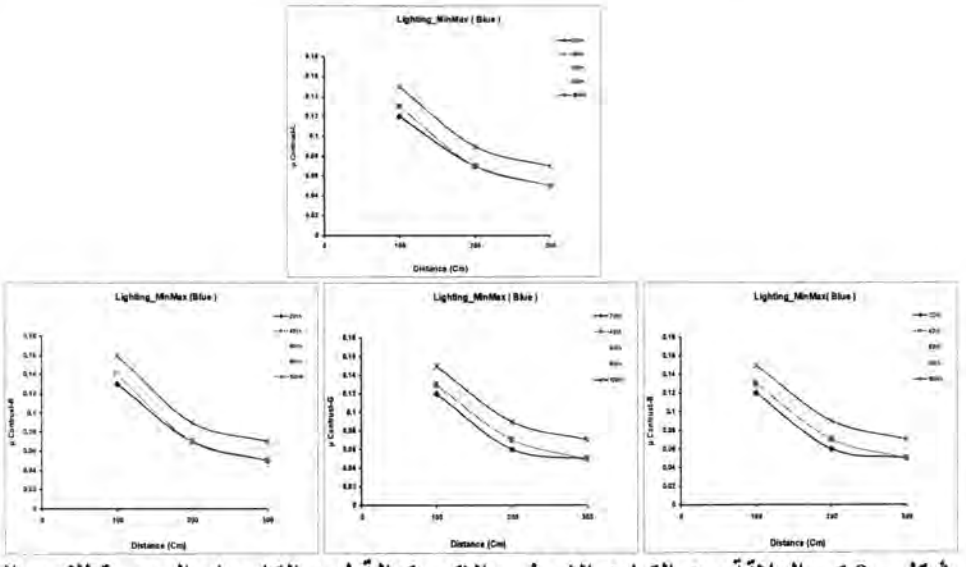

شكل - 10 : العلاقة بين التباين الاصغر والاكبر كدالة لبعد الكاميرا والسبورة للنص الازرق (إضاءة منتظمة) للحزم اللونية RGB

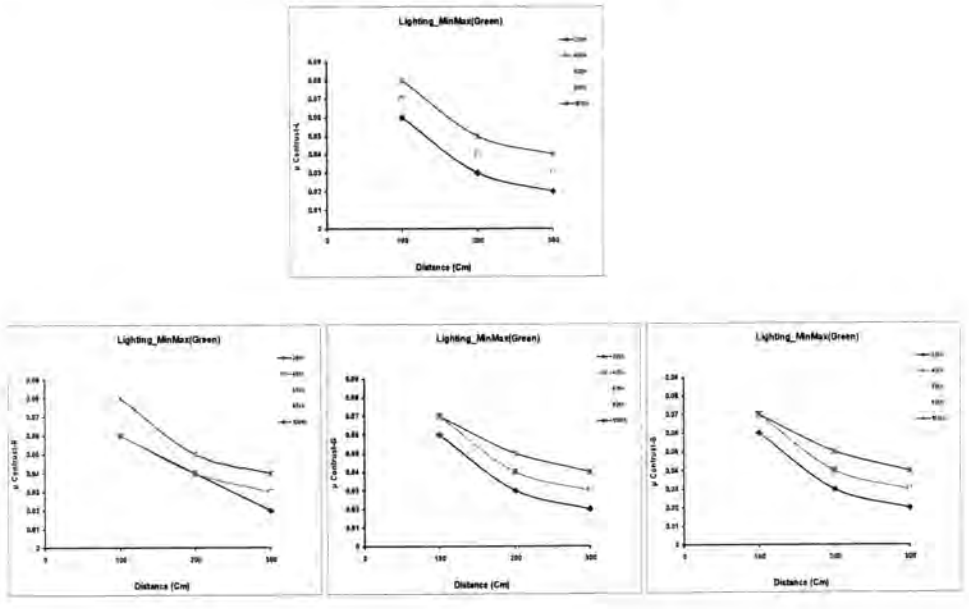

شكل -11 : العلاقة بين التباين الاصغر والاكبر كدالة لبعد الكاميرا والسبورة للنص الاخضر (إضاءة منتظمة) للحزم اللونية RGB

يزداد معدل التباين لصورة النصوص الثلاثة كلما قلت المسافة بين الكاميرا الرقمية ولوح الكتابة ويزداد معدل التباين $\mu_{contrast}$ كلما زادت العتبة المستخدمة لكشف حافات الصورة وان صورة النص الاسود ولكل المسافات الفاصلة بين لوح الكتابة والكاميرا الرقمية هي الأعلى في معدل التباين من صورة النصين الاخضر والازرق ويلاحظ تقارب ملحوظ في المنحنيات الممثلة لعتبات مؤثر الصوبل لصورة النص الاخضر اكثر مما هو موجود لصور النصين الاسود والازرق .

REFERENCES

1. Zugas,Didie and Lattuati Vicen "Anew approach of color image segmentation basic on fusing and edge segmentation output", Pattern Recognition,31,2,:105-113, (1998).
2. Digital Image Processing: PIKS Inside, Third Edition. William K. Pratt Copyright © 2001 John Wiley & Sons, Inc.
3. Jonhson R .P ., " *Contrast Based on Edge Detection* " , pattern Recongition , 23 , 3/2 , (1990)
4. Eli Peli , Lawrence Arend , Angrla T.Labiance , " Contrast Perception a Cross Change in Luminance and spatial frequency " , Optical Society America ,(1996)
5. Curlander , R .J., " *Image Enhancement Using Digital Adaptive Filtering*_" , M.Sc – Thesis , Department Electrical Engineering , University of Colorado , (1997).
6. R. Marshall, "Computer graphic in application", Prentice Hall, (1987).
7. Weinman,"Color display primer"(2003)http://www.ifo.med.yale.edj/Caim.
8. حازم كاطع دواي الخزاعي، "ازالة الضوضاء الجمعية من الصور الملونة باستخدام طريقة المربعات الصغرى لتقريب المنحنيات" رسالة ماجستير, جامعة بغداد/ كلية التربية/ ابن الهيثم (2004).
9. Sangwine S.J. and R. E.N.orne"The color image processing Handbook", Chapman & Hall (1998).
10. Haim Levkowitz, "Color theory and modeling for computer graphics, visualization, and multimedia applications ", Kluwer Academic Publishers, (1997).
11. Kurtich ,John and Eakin , Garrel ., " *Interior Architecture* ", Van Nostrand Reinhold , New York ,(1993).
12. Ziad M. Abood Al-Bayati, "Digital Image Processing Techniques for Breast Cancer Cells Detection" Ph.D. Thesis, Al- Mustansiriya University , College of Education. (2005).
13. www.Practical .home theater . Guide .com . extensive coverage of practical contrast ratio .

تأثير طول الليف على قياس الانكسار الثنائي النمطي داخل الليف البصري أحادي النمط

سيامي عبد اللطيف محمد
قسم الفيزياء – كلية العلوم- الجامعة المستنصرية

ABSTRACT

In this research the intrinsic modal birefringence has been measured for single-mode optical fiber without any extrinsic effect .It was taken a single- mode optical fiber ,the diameter of core material was (5μm) and the total diameter was (210μm) for different lengths of this fiber. Show the result has been obtained from research which the magnitude of model birefringence of this fiber ($B=5.74\times10^{-7}$ deg.m^{-1}), beat length ($L_b=1.09$m) and the value of the difference in the propagation constants between the two axis the fast and the slow ($\Delta\beta=328$ deg.m^{-1}).

الخلاصة

في هذا البحث تم قياس الانكسار الثنائي النمطي الذاتي لليف البصري أحادي النمط وبدون أي تأثير خارجي، إذا تم اخذ ليف بصري أحادي النمط ذو قطر لمادة اللب (5μm) وقطر كلي (210μm) ولعدة أطوال مختلفة من هذا الليف. بينت نتائج الدراسة التي حصلنا عليها من البحث بان مقدار الانكسار الثنائي النمطي لهذا الليف هو ($B=5.74\times10^{-7}$) وطول الضربة له ($L_b=1.09$m) والفرق بين ثابتي الانتشار للمحور السريع والبطئ هو ($\Delta\beta=328$ deg.m^{-1}).

المقدمة

عند تقدم الضوء داخل الليف البصري أحادي النمط بتناظر دائري غير تام ، فان النمط الأساسي HE_{11} سوف ينحل إلى مركبتين منفصلتين هما HE_{11x} وHE_{11y} باستقطابات متعامدة وعدم التماثل لمقطع الليف يسبب اختلافا كبيراً في معاملات الانكسار وسرع الطور لهذين النمطين الذين يمتلكان أستقطابين متعامدين (1) حيث المحور السريع (Fast axis) الذي يمتلك أكبر سرعة طور (أي أقل معامل انكسار) والمحور البطئ (Slow axis) الذي يمتلك أقل سرعة طور(أكبر معامل انكسار) ونتيجة لاختلاف الطور بين هذين النمطين يؤدي إلى اختلاف كبير في ثوابت الانتشار β_x و β_y لهذين النمطين لذا يسلك الليف سلوك وسط ذو انكسار ثنائي يسمى بالانكسار الثنائي النمطي (Modal Birefringence)(3,2)

الدراسات السابقة Review of Literature

في عام (1978) قام كل من (Ramasway V) و(French W.G.) و(Standley R.D.) بدراسة تأثير التناظر اللادائري للب الليف البصري على خصائص الاستقطاب فيه حيث استخدموا ليف بصري ذو مقطع عرضي قريب للشكل البيضوي(4) وفي العام نفسه قامت هذه المجموعة أيضا بدراسة تأثير الاستقطاب في أطوال قصيرة من الليف البصري أحادي النمط (5). وفي عام (1982) قام (Rashleigh S.C.) بدراسة العلاقة بين الانكسار الثنائي النمطي والطول الموجي في الألياف ذات الانكسار النمطي العالي (6) .
وفي العام نفسه قام كل من (Payne D.N.) و(Barlow A.J) و(Hansen.J.J.R.) بدراسة الانكسار الثنائي العالي والواطئ في الألياف البصرية (7) . وفي عام (1985) قام كل من (Ren.Z.B.) و(Robert.Ph.) و(Paratte.P.A.) بقياس الانكسار الثنائي الخطي في الليف البصري احادي النمط للضوء المستقطب دائريا (8) . أما في عام (1998) قام كل من (Huttner B.) و(Reecht J.) و(Gisin N.) و(Passy R.) و(Vonderweid J.P) بقياس الانكسار الثنائي في الألياف البصرية للتردد المتشاكه بمقياس

دومان (9) . وفي عام (1999) قام كل من (Escamilla BI.) و(Ku Zin E) و(Ayala JmE.) و(Laguna RR.) بطريقة جديدة لقياس الانكسار الثنائي الواطئ في الليف البصري (10) . أما في عام (2000) قام كل من (Galtarossa A.) و(Palmieri L.) و(Schiano M.) و(Tambosso T.) لقياس طول الضربة وطول الاضطراب في الالياف البصرية أحادية النمط القصيرة (11) . وفي العام نفسه قام كل من (Marshalla W.K.) و(Eyal A.) و(Li y.). بحساب الطول المعتمد على نمط الاستقطاب للرتبة العالية . وفي عام (2001) قام كل من (Galtarossa A.) و(Palmieri L.) و (TambossoT.) بقياس طول الارتباط للانكسار الثنائي في ألياف أحادية النمط القصيرة (12) . أما في عام (2002) قام محمد خضير بدراسة تأثير الانكسار الثنائي على انتقال الضوء المتشاكه خلال الليف البصري أحادي النمط (13).

الجزء النظري Theoretical Part

1- الانكسار الثنائي النمطي Modal Birefringence

أن الضوء المستقطب خطياً إذا دخل وسط ذو انكسار ثنائي فأنه سوف يخرج مستقطباً بيضوياً . ويعتمد هذا على اتجاه مستوى الاستقطاب الداخل إلى الوسط نسبة إلى المحور السريع أو المحور البطئ وكذلك على مقدار الانكسار الثنائي لهذا الوسط حيث إن قيمة الانكسار الثنائي هي كالآتي[14،15]:

$$B = \frac{(\beta_x - \beta_y)\lambda}{2\pi} \quad \text{.....(1)}$$

أن الفرق في سرعة الطور تؤدي بالليف إلى أن يظهر إعاقة خطية (Linear retardation) (Z) Φ والتي تعتمد على طول الليف البصري وتعطى بالعلاقة الآتية:

$$\Phi(Z) = (\beta_x - \beta_y) \cdot L \quad \text{.....(2)}$$

أن الضوء الداخل لليف البصري يصنع فيه مستوي الاستقطاب زاوية (45) مع احد المحورين الأساسين وليكن (x) فأن الضوء المستقطب خطيا سوف يتحول فيه الاستقطاب من خطي إلى استقطاب دائري ($\phi = \pi/2$) . وبعدها سوف يتحول إلى استقطاب خطي عندما ($\phi = \pi$)لكن بمستوى استقطاب متعامد مع المستوى الأصلي لاستقطاب الضوء الداخل . وهكذا تستمر الدورة إلى إن يعود مستوى الاستقطاب خطياً كما كان في البداية ($\phi = 2\pi$).وان طول الليف البصري الذي تحصل فيه هذه الدورة الكاملة يدعى بطول الضربة (beat length) L_b كما مبين في الشكل (1).

$$L_b = \lambda / B \quad \text{..... (3)}$$

وبالتعويض عن قيمة B في المعادلة (1) نحصل على :

$$L_b = \frac{2\pi}{(\beta_x - \beta_y)} \quad \text{.....(4)}$$

وبتعويض المعادلة (4) في المعادلة (2) نحصل على Φ كدالة لطول الضربة (L_b) .

$$\Phi(L_b) = (\beta_x - \beta_y)L_b = 2\pi \quad \text{.....(5)}$$

أن طول الضربة يعرف بأنه طول الليف البصري الذي يحصل فيه تأخير في المحور البطئ عن المحور السريع بمقدار طول موجي واحد(14،15)

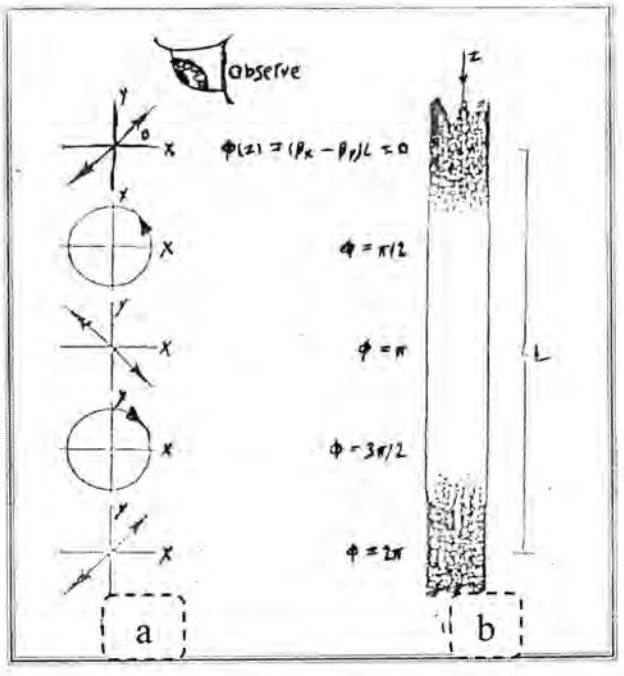

شكل -1: يبين طول الضربة لليف البصري احادي النمط (14).
(a) يمثل مستوى الاستقطاب بالنسبة للزاوية ϕ
(b) يمثل توزيع الشدة لطول ضربة واحدة في ليف بصري.

2- العوامل الذاتية المسببة للانكسار الثنائي داخل الليف البصري هي:

أ- تأثير الشكل (Shape effect)

أن تأثير الشكل على الانكسار الثنائي هو أن يكون المقطع العرضي للب بيضوياً أكثر مما هو دائري , حيث كلما زاد الشكل البيضوي كلما زاد الانكسار داخل الليف البصري وجعل الانكسار الثنائي النمطي بسبب تأثير المحور السريع والمحور البطئ ، حيث ان الشكل البيضوي لمقطع الليف يمتلك محورين أ حدهما يدعى المحور الكبير (Major axis) والأخر يدعى المحور الصغير (Minor axis) ، لذا فأن المحور الصغير سيكون ثابت التقدم (β) له يختلف عن ثابت التقدم للمحور الكبير وهذا سوف يؤدي الى ظهور تأثير الانكسار الثنائي النمطي (16،17).

ب- تأثير الشوائب (Dopant effect)

أن المواد المستخدمة في صناعة الليف البصري تمتلك معاملات تمدد حراري مختلفة لذا فان إي تغير في درجة الحرارة سوف يولد أجهاداً داخليا وهذا بدوره سوف يؤثر على الانكسار الثنائي النمطي (18).

المواد وطرائق العمل

تم استخدام المنظومة المبينة في الشكل (2) لدراسة الانكسار الثنائي النمطي الذاتي والتي تتكون من عدة أجهزة:

شكل-2: يمثل منظومة قياس الانكسار الثنائي النمطي الذاتي بدون إي تأثير خارجي (19)

- **المصدر الضوئي Light source**

في هذه الدراسة تم استخدام ليزر هليوم نيون (He – Ne Laser) يعمل بموجة مستمرة (CW) وبطول موجي مقداره (632.8 nm) وله قدرة ضوئية خارجة (ImW) ويعمل بالنمط الأساسي (TEM_{oo}) حيث أن الطول ألموجي لليزر المستخدم ضمن تردد القطع لليف البصري المستخدم في دراسة الانكسار الثنائي النمطي لكي يحقق شرط القطع (Cut off condition) لليف البصري أحادي النمط (20) .

- **الليف البصري Optical Fiber**

أستخدم في هذا البحث ليف بصري أحادي النمط يمتاز بمرونة عالية وخصائصه مبينة في جدول(1) .

جدول رقم -1: يبين المعلمات الرئيسية لليف البصري المستخدم (20).

المعلمة parameters	الليف البصري المستخدم
الفتحة العددية N.A.	0.098
قطر اللب(μm)	5
طول موجة القطع(nm)λc	630
قطر الليف(μm)	210

- **المستقطب والمحلل ولوح ربع الموجة**
Polarizer and Analyzer and quartered Wave plate

ثم استخدام مستقطب للتحكم باتجاه مستوى الاستقطاب عند دخول الضوء إلى الليف البصري وعند خروج الضوء من الليف البصري استخدم لوح ربع الموجة وذلك لتحويل الاستقطاب من بيضوي إلى خطي وثم وضع محلل خلف لوح ربع الموجة وذلك لتعيين اتجاه الاستقطاب ومنه يمكن معرفة قيمة الانكسار الثنائي النمطي(21)

- عدسات مجهريه (Microscope Objective) وبفتحة عددية أقل من الفتحة العددية لليف البصري .
- حاملات دقيقة لليف البصري لتسهيل عملية الترصيف (Micropositioner)
- مسطرة بصرية (Optical bench)

- حاجز Screen

في هذه المنظومة تم أستخدام الليف البصري بأطوال مختلفة وضعه بشكل مستقيم ومن ثم تم تغير مستوى الاستقطاب للضوء الداخل إلى الليف البصري بواسطة المستقطب وتدوير المحلل إلى أن نحصل على اختفاء تام للضوء ثم نسجل زاوية المحلل (θ_A) وزاوية المستقطب (θ_p) حيث تمثل زاوية المستقطب لأحد المحورين الأساسيين اللذين إذا دخل الضوء المستقطب بموازاة احدهما فأنه سوف يخرج بمستوى الاستقطاب نفسه وبعدها نضيف زاوية (45°) على زاوية المستقطب (θ_p) فيكون الضوء الخارج مستقطب بيضوياً لذا نضع لوح ربع موجه الذي يحول الاستقطاب من بيضوي إلى خطي ثم ندور المحلل إلى إن نحصل على اختفاء تام فنرمز لهذه الزاوية ب (θ'_A) ثم نقوم بعدها بحساب الزاوية (α) والتي تمثل الفرق بين (θ'_A) و (θ_A) كما مبين في العلاقة الآتية :

$$\alpha = \theta'_A - \theta_A \quad \ldots\ldots\ldots\ldots (6)$$

علماً أن الزاوية (α) تمثل نصف زاوية الإعاقة الخطية (Linear retardation) ϕ

وكما مبين في العلاقة الآتية :

$$\phi = 2\alpha \quad \ldots\ldots\ldots\ldots (7)$$

جدول -2: تأثير طول الليف على قياس الانكسار الثنائي النمطي الذاتي من دون أي تأثير خارجي عند الطول ألموجي (λ=632.8nm)

L (m)	θ_p	θ_A	θ'_p	θ'_A	α	$<\alpha>$	ϕ deg	$\Delta\beta=\frac{\phi}{L}$ (deg/m)	$L_b=\frac{360}{\Delta\beta}$ (m)	$B=\left(\frac{\Delta\beta\cdot\lambda}{360}\right)$ $\times 10^{-7}$
1.3	40 140 235 335	70 155 240 340	95 185 280 380	129 205 285 25	50 45 45 45	46.25	92.5 4360= 452.5	348	1.03	6.11
1.1	35 130 210 305	65 152 240 335	80 175 255 350	70 155 245 340	185 183 185 185	184.5	369	335	1.07	5.89
0.92	25 118 205 295	60 150 239 333	70 163 250 340	30 120 211 305	150 150 152 152	151	302	328	1.09	5.77
0.77	15 105 190 285	72 152 235 315	60 150 235 330	195 275 360 80	123 123 125 125	124	248	322	1.11	5.66
0.62	10 100 205 295	81 175 262 353	55 145 250 340	180 273 360 90	99 98 98 97	98	196	316	1.13	5.55
0.45	5 95 178 310	109 164 249 328	45 140 223 355	175 230 315 50	66 66 66 82	70	140	311	1.15	5.46

حيث إن:

L : طول الليف

θ_p° : زاوية المستقطب الموازية لأحد المحورين الأساسيين لليف البصري

θ_A° : زاوية المحلل

$\theta_p^{\circ\prime}$: زاوية المستقطب مضاف إليها 45 $\left[\theta_p^{\circ\prime} = \theta_p^\circ + 45\right]$

α : نصف زاوية الإعاقة الخطية

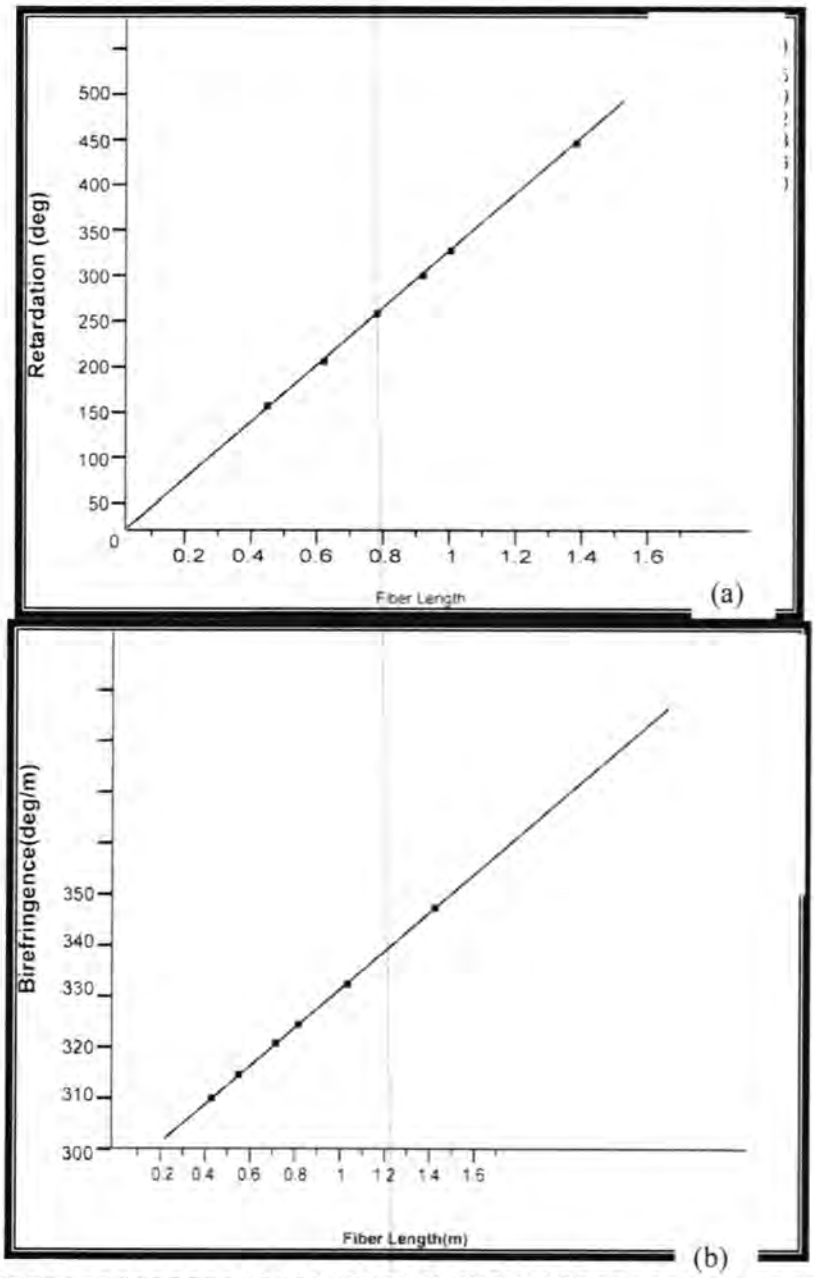

مع الانكسار الثنائي النمطي عند الطول (b) مع الإعاقة 3(a):يبين تغير طول الليف -شكل
بدون إي تأثير خارجي ($\lambda = 632.8nm$) ألموجي

النتائج والمناقشة

تم وضع الليف بشكل مستقيم ولعدة أطوال مختلفة في الليف البصري وقمنا بدراسة العلاقة بين طول الليف والإعاقة وكذلك بين طول الليف والانكسار الثنائي النمطي الذاتي عند الطول ألموجي (λ = 632 . 8nm) .

فكانت العلاقة خطية وهذا ما يبينه الشكل ((a, b)3)، إذ كلما كان طول الليف اكبر كلما كان مقدار الإعاقة اكبر وبالتالي مقدار الانكسار الثنائي النمطي اكبر وهذا ما حصلنا عليه من النتائج المدونة في الجدول (2) وظهر لنا من خلال الحسابات أن مقدار الانكسار الثنائي النمطي لليف البصري الذي استخدمناه في هذه الدراسة وكمعدل يبلغ ($B=5.74\times10^{-7}$) وطول الضربة له (L_b= 1 . 0 9m).

وهذا يبين لنا بأن الليف البصري المستخدم في هذه الدراسة يمتلك انكسار ثنائي نمطي ذاتي ويعزى هذا الانكسار الثنائي النمطي إلى عوامل ذاتية داخلية خلال تصنيع الليف أما بتأثير الشكل (Shape effect) الذي يكون فيه شكل اللب غير دائري (بيضوي أو أهليجي) لبعض مناطق الليف البصري وهو الذي يسبب الانكسار الثنائي النمطي . أو بتأثير الإجهاد الداخلي الناتج عن اختلاف معاملات التمدد الحراري ما بين منطقة اللب والإحاطة الذي يـــكون سببه تأثير الشوائب(Dopant effect) التي تدخل في صناعة الليف البصري وهذا بدوره سيولد انكسار ثنائي نمطي (6 ,22 ,23) .

1-أن الليف البصري يمتلك انكسار نمطي ذاتي يعزى ذلك إلى تأثير الشكل أو الإجهاد الداخلي على لب الليف البصري

2- أن العلاقة بين طول الليف والانكسار الثنائي النمطي هي علاقة خطية ، فكلما زاد طول الليف تزداد الإعاقة بالليف وبالتالي يؤدي إلى زيادة الانكسار الثنائي النمطي والعكس صحيح

3- أن الليف البصري بانكسار ثنائي نمطي واطئ يتطلب تقليل كل من الاهليجية للمقطع العرضي للب الليف البصري وكذلك تقليل الإجهاد على لب الليف إذ أن اختلال التوازن بين مركبات الإجهاد والمستعرض على طول محوري اللب الاهليجي أو الإحاطة يضعف ويقلل من مستوى إجهاد اللب ككل، فيقلل من الإعاقة بالليف ومن ثم يقلل من مقدار الانكسار الثنائي النمطي .

المصادر

1.Senior J. M."Optical Fiber Communications Principles and Practice" , Prentice -Hall International Inc. London. (1992)

2.Kang Liu M. M. "Principles and Application of Optical Communication " , John Wiley and Sons, New York(1998).

3. الأستاذ الدكتور محمد عبد الرحمن الحيدر " اتصالات الألياف البصرية"مكتبة العبيكان ، فهرست مكتبة الملك فهد الوطنية' السعودية(1995) .

4. Ramaswamy V. ,FrenchW.G. and Standley R.D " Polarization Characteristics of Noncircular Core Single-Mode Fibers", Appl.Opt. 17 (18) :3014-3017 (1978).

5. Ramaswamy V.,French W.G., Standlay R.D. and Szeand D " Polarization Effects in Short Length Single – Mode Fibers", B.S.T.J.,57(3):635-651(1978).

6. Rashleigh S.C. " Wavelength Dependence of Birefringence in High Birefringence Fiber ", Opt. lett,.7(6) :249-296(1982) .

7.Payne D.N.,Barlow A.j.and Hansen J.J.R." Development of Low andHigh Birefringence Optical Fibers",IEEE.J.Quant.Elect.18,(4): 477-487 .(1972).

8. Ren Z. B., Robert ph .and paratte P.A. " Linear Birefringence Measurement in Single-Mode Optical Fiber With Circularly Polarized Input Light ",J .phys .E . 18,(1):859-862(1985).
9.Huttner B. ,Reecht J. ,Gisin N. ,pass R. and Vonderweid J.P. " Local BirefringenceMeasurements in Single Mode Fiber With Coherent Optical Frequency Domain Reflectometrly", Photon . Techno .lett ., 10,(10):1458-1460(1998) .
10.Escamilla BI .,Kuzin E .,Ayala Jme. and Lagunarr R. " Anew Method for Measurement o Low Birefringence in Optical Fibers ", Rev .Mex .fis. ,45 (2):144-149(1999).
11.Galtarossa A .,Palmieri L. ,Schiano M. and Tambossa T.," Measurement of beat length and perturbation Length in long sigle – mode fiber", opt.Lett., 25(6):384-386 (2000).
12.GaltarossoA.,palmieri L.,schiano M.and Tambosso T.," Measurement of Birefringence Correlation Length in Long Single- Mode Fibers",Opt.lett.26(13):962-964(2001).
13. محمد خضير حمادي " تأثير الانكسار الثنائي على الانتقال الضوئي المتشاكه خلال الليف البصري أحادي النمط " أطروحة ماجستير مقدمة إلى كلية العلوم / الجامعة المستنصرية (2002).
14.KamiowI.P." Polarization in Optical Fiber", IEEEI. Quant.Elect, 17 (1):15-22 (1998).
15.Rashleigh S.C.," Origins and Control of Polarization Effect in Single-Mode Fibers",Light Ware Tech.,LT-1,(2):312-331 ,New York.(1993).
16-Eickhof W .,yen y., and UIrich R. " Wavelength Dependence of Birefringence in Single-Mode Fiber",Appl.Opt.,20,(19):3428-3435 .(1981).
17.Hasegawa A."Theory of Information Transfer in Optical Fibers" Optical Fiber Tech.,10,(10):150-170(2004).
18.Eickhoff W. "Stress-Induced Single-Mode Fiber" Opt.lett. 7(12): 629-631 (1982).
19.Smith A.M. " Automated Birefringence Measurement System ",J. phys. E12,12:927-930(1979).
20.Agrawal G.P. " Fiber-Optic Communication Systems ",John Wiley and Sons ,Inc. Rochester.(2002).
21.Hetch E. and Zajac A.," Optics" ,Addison-Wesley Publishing Co .Inc .,Canada(1987).
22.UIrich R.,Rashleigh S.C.&Eickhoff W."Bending-Induced Birefrin - gence in Single-Mode Fiber"Opt.lett.5,(6) :273-275) (1980) .
23.Huang W. "Fiber Birefringence Modeling for Polarization Mode Dispersion", Thesis of Doctor of Philosophy in Physics, University of Waterloo, Canada(2007).

دراسة تأثير المسافة على التباين لنص مكتوب باللوان متعددة مع اللون الاسود على لوحة بيضاء في قاعة دراسة مضاءة

[1]اسراء فاخر خلف و [2]سليمة سلطان سلمان و[1]محمد يوسف كامل
[1]الجامعة المستنصرية / كلية العلوم/قسم الفيزياء
[2]كلية الصيدلة/ جامعة بغداد

ABSTRACT

The importance of the study the contrast lies in two things: first is to know the visibility of the written text to compare the visibility text with other text written on the same plate, and the study of visibility for same text differ by differ the using color and by text background. i.e. by depend on contrast between the text and background.

In this research we study two types of contrast (statistical contrast and direct contrast) on text which written on a whiteboard by multi-colors (red, green, blue and black) in light classrooms and study the effect the change of the distance of scenes (camera) on the range of visibility of this text.

Shown us that distances of near to be the contrast was high (the text more clearly), also found that the statistical contrast to show the details the written text is the best from direct contrast, and different colors on the plate found that the blue color compare with red and green color is more visibility if it written on whiteboard in the same lighting conditions of the classroom, which was filmed in which texts.

الخلاصة

ان اهمية دراسة التباين تكمن في امرين الأول هو لمعرفة وضوحية تفاصيل النص المكتوب لمقارنة وضوحية نص مع نص آخر مكتوبان على نفس اللوحة ، وان دراسة وضوحية نص معين تختلف عن دراسته بأختلاف اللون المستخدم وتختلف باختلاف خلفية النص أي بالاعتماد على التباين بين النص والخلفية.

تم في هذا البحث دراسة نوعين من انواع التباين (التباين الاحصائي والتباين المباشر) على نص مكتوب على لوحة بيضاء باللوان متعددة وهي الاحمر والاخضر والازرق والاسود في قاعة دراسية مضاءة اضاءة منتظمة ، ودراسة تأثير تغير مسافة المشاهد (الكاميرا) على مدى وضوحية ذلك النص.

وقد تبين لنا انه بالمسافات القريبة يكون التباين عاليا اي ان النص اكثر وضوحا ، كما وجد ان التباين الاحصائي في اظهار تفاصيل النص المكتوب هو افضل من التباين المباشر ، وباختلاف الالوان على اللوحة وجدنا ان اللون الازرق من بين الاحمر والاخضر هو اكثر وضوحا اذا كتب على لوحة بيضاء في نفس شروط الاضاءة للقاعة التي تم تصوير النصوص فيها.

المقدمة

ان قابلية رؤية الاجسام تعتمد على حجم الجسم ، الإضاءة ، التباين ، موقع الجسم من المحور البصري ، مقدار الضوضاء في المشهد . يمكن تصور العين البشرية كنظام موجب ثنائي العدسة يُسقط صورة حقيقية على سطح حساس للضوء يمر الضوء الداخل إلى العين من خلال القزحية (iris) وهي عبارة عن بقعة في فتحة العين . حيث ان بؤبؤ العين يتغير ما بين mm (7 – 2) متكيفا مع مستوى ضوء المحيط ، ثم يمر خلال العدسة التي يتغير بعدها البؤري بواسطة العضلات المرتبطة بها (1).

استخدم العديد من مؤثرات كشف الحافات لتطبيقها على الصور المختلفة لغرض تحليلها وهي عبارة عن مؤثرات تستخدم نوافذ ذات أبعاد مختلفة مثل (3x3) , (5x5) ومن ثم تحسب قيمة مجموع العمليات في النافذة والتي قد تكون ناتجة من عمليات الانحدار او الالتفاف الرياضي باستنتاج قيمة موضعية يتم مقارنتها مع عتبة محدده لتحديد الحافات [(2). عملية كشف الحافات تعتمد أساسا على عدم الاستمرارية في دالة التجانس لصفات مناطق الصورة

ومن اهم هذه المؤثرات مؤثر سوبل Soble Operator، ومؤثر برويت Prewit Operator وهذا المؤثر يشابه مؤثر سوبل ولكن الاختلاف يكون في قيم معاملات النوافذ ، ومؤثر روبرت Robert Operator هذا المؤثر يمتاز بسرعة الأداء لان إبعاد نافذة روبرت (2x2) لكنه حساس جدا للضوضاء ويكون ذا استجابة عالية للحافات الحادة جدا (3) .
يعتبر مؤثر سوبل من أهم مؤثرات كشف الحافات باستخدام المشتقة لدالة الصورة الثنائية حيث يمثل مشتقة من الدرجة الأولى ، ويعتمد أساس عمل هذا المؤثر على اختيار نافذة من الصورة ذات أبعاد (3x3) والنقطة المركزية لها (f(x,y ثم حساب مركبتي الانحدار باتجاه المحورين العمودي والأفقي على التوالي عند تلك النقطة. حيث تستخدم هذه النوافذ الموضحة في الشكل (1) (4) :

-1	-2	-1
0	0	0
1	2	1

نافذة المسح الأفقي(G_y)

-1	0	1
-2	0	2
-1	0	1

نافذة المسح العمودي(G_x)

شكل -1 : نافذتي سوبل

ان مؤثر سوبل يكشف الحافات الأفقية والعمودية للصورة ولكن بغض النظر عن موقع النقطة بالنسبة للحافات أي يكشف الحافات ذات التغيير من الأبيض الى الأسود والحافات ذات التغيير من الأسود الى الأبيض . ان لب الالتفات لمؤثر سوبل يعطي للصورة الداخلة تنعيم فيكون اقل حساسية للضوضاء (5) .

الضوء ووضوحية الصورة:

تعرف جودة الصورة بانها مقدار الحدة او التباين في الصورة .ان جودة الصورة في أي منظومة بصرية تعتمد على نسبة التباين ، السطوعية ، الوضوحية ، دالة التضمين للانتقال البصري ولذلك يستعمل مستخدموا المعالجة الصورية التباين Contrast ، السطوع Brightness ، ومساواة المخطط التكراري Histogram equalization لغرض تحسين جودة الصورة(6) .
يعتبر التباين خاصية إدراكية أساسية وثابتة ، ان حساسية العين البشرية للتباين المتغير مكانيا تناقش دراستها في مستويين مستوى العتبة (threshold) وفوق العتبة (super threshold (حيث تختص حساسية تباين مستوى العتبة بدراسة أدنى تباين يتطلبه الكشف البصري للإشكال بينما تختص حساسية تباين فوق العتبة بدراسة التباين المحسوس عندما يكون فوق أدنى مستوى للعتبة (7) ، تبين هذه الدراسات بأنه يمكن تحديد مقدار حساسية تمييز التباين بواسطة متغير واحد وبالذات في مستويات ما فوق العتبة وبعبارة أخرى أن عتبة كشف التباين للحساسية تساوي (معكوس حد العتبة) وقد تبين انها تتفاوت الى حد كبير مع التغيرات الحاصلة في ظروف المراقبة ويكون التباين الظاهر لمحفز ما فوق العتبة قليلة التأثر بمثل هذه المتغيرات (8) .
ان التباين خاصية من خواص الصور الثنائية ويعرف التباين بانه النسبة بين المنطقة الاكثر لمعانا Brightest والمنطقة المعتمة darkest في الصورة ، عجز هذا التعريف عن توضيح كيفية تغيير نسبة التباين مع التردد المكاني . ان خصائص التباين ضمن مدى التردد المكاني تتوضح من خلال دالة نقل التضمين (MTF) Modulation Transfer Functionوان بعض حالات الزيغ الصغيرة في ادوات التصوير والعناصر البصرية تؤدي

الى تقليـــل MTF مع ازدياد التردد المكاني كما موضح في الشكل (2) بينما تتعامل دالة نقل التضمين MTF مع تقييدات التباين في منظومة التصوير ، هناك ايضا تقييدات له علاقة بالرؤية البشرية حيث تتفاوت قدرتنا على معرفة اشكال التباين المنخفض مـــع حجـــم الشكـــل او تـــردده المكانـــي ان دالة عتبة التباين (Contrast Threshold Function CTF) هي مقياس لأدنى حد من التباين المطلوب للصور لكي تصبح قابلة للتمييز ، تكون هنالك حاجة الى مقادير عالية من الحد الادنى للتباين عند المستويين الواطى جدا والعالي جدا من الترددات المكانية . تجتمع كل من دالة نقل التضمين لمنظومة التصوير ودالة عتبة التباين للرؤية البشرية لتحديد أعلى وضوحية قابلة للتحسس كما موضـــــح في الشكل (2) ونلاحظ من الشكل ان التباين للمنظومـــة البصـــرية سيهبط الى اقل من الحد الأدنى المطلوب لتمييز شكل ما عند تردد مكاني معين . تحـدد هذه النقطة المنتقلة أعلى وضوحية محسوسة (9).

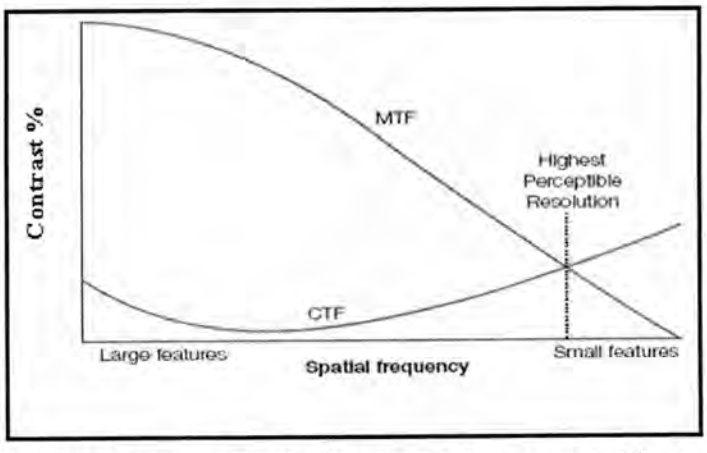

الشكل -2: العلاقة بين التردد المكاني ودالة نقل التضمين (MTF)[10]

يكون التباين نوعين ، التباين الموقعي Local Contrast وهو تباين كل جزء صغير small للصورة والتباين العام Global Contrast هو معدل التباين الموقعي للأجزاء الصغيرة من الصورة ، ان الصورة ذات التباين العام العالي يعني ان الصورة تحتوي على تفاصيل عالية وغنية بالتغايرات في مقابل ذلك نجد ان الصورة ذات التباين العام القليل تحتوي على تفاصيل اقل ولها تغايرات متدرجة من الصعب كشفها بصريا (11) .
الأجسام التي ترى عادة بسهولة مثل الكتابة السوداء على لوحة إعلانات بيضاء سيصعب رؤيتها ان أصبحت لون كل من الكتابة السوداء والخلفية البيضاء رماديا ، ان التباين يشير الى الفرق بين الاضائية للعناصر المتجاورة في مناطق الصورة المختلفة ينتج بسبب الاختلاف في الإضاءة أي ان اصغر فرق في الشدة الضوئية ممكن تحسسه بين جسمين متجاورين في الصورة يدعى وضوحية التباين Contrast Resolution لذا يمكن قياس هذا التباين بأخذ الفرق في الشدة لعناصر الصورة المتجاورة .

تصوير النصوص في قاعة الدرس:

اعتمدنا في هذه الدراسة التقاط صور لنصوص مكتوبة على السبوره باستخدام اقلام سبوره مختلفة نوع Dry – Erase ولمسافات مختلفة cm (100 , 200 , 300) واضاءات مختلفة الاتجاهات لقاعة الدرس حيث تم التقاط صور النص المكتوب على اللوحة بواسطة الكاميرا الرقمية Sony – Digital Camera والشكلين (3) و (4) يوضحان الصور الناتجة من منظومة العمل باختلاف المسافة والإضاءة والكاميرا الرقمية المستخدمة في العمل على التوالي.

الشكل -3: الصور باللون الاسود الناتجة من عملية التصوير

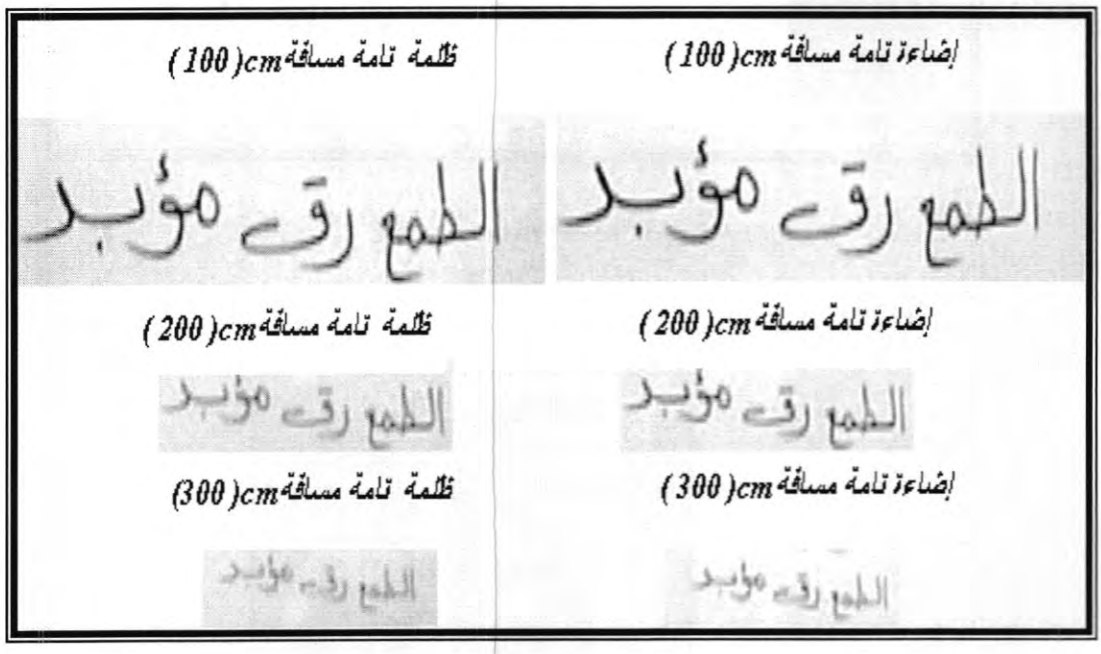

الشكل -4: الكاميرا الرقمية المستخدمة في عملية التصوير

تمت عملية التصوير في قاعة دراسية مخططها موضح في الشكل (5) في الساعة العاشرة صباحا من يوم 14/ 4/ 2009 حيث استخدم جهاز قياس شدة الإضاءة الموضح في الشكل (6) لقياس شدة الإضاءة في مختلف الاتجاهات للقاعة الدراسية.

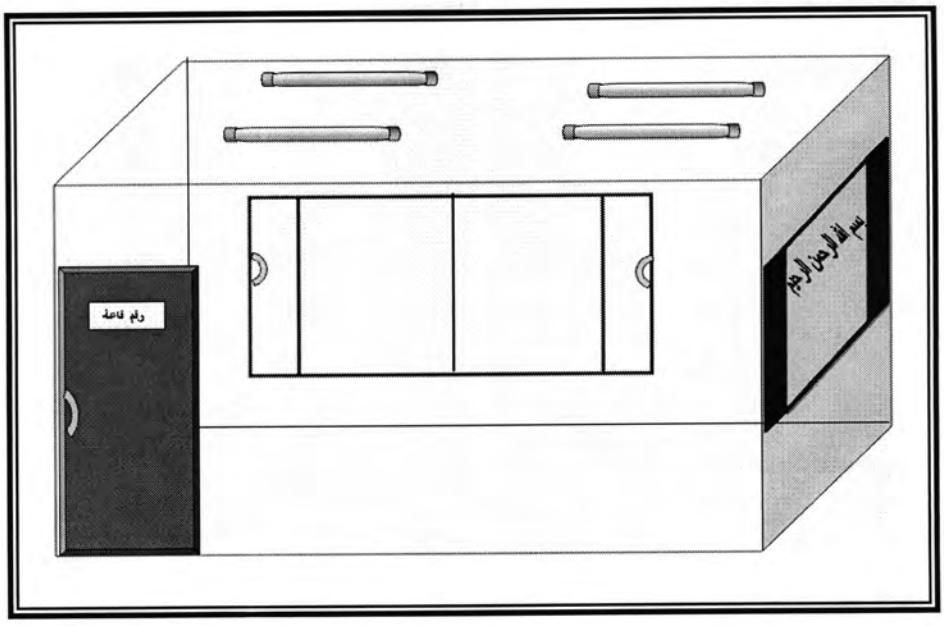

شكل - 5 : قاعة الدرس المستخدمة في التصوير

شكل -6: جهاز قياس شدة الإضاءة

تم جدولة قراءات جهاز قياس شدة الإضاءة في الجدول رقم (1) عندما تكون الاضاءة منتظمة.

جدول- 1: قيم شدة الإضاءة والتباين
في حالة اضاءة قاعة الدرس باضاءة تامة منتظمة

مباشرة(Direct)

Lux (1)	Lux(2)	Lux(3)	Lux(4)	Lux(average)
443	348	334	305	72.33
C1	C2	C3	C4	
0.005	0.045	0.06	0.02	

شباك (Window)

Lux (1)	Lux(2)	Lux(3)	Lux(4)	Lux(average)
181	192	170	162	176.25
C1	C2	C3	C4	
0.029	0.024	0.055	0.06	

باب (Door)

Lux (1)	Lux(2)	Lux(3)	Lux(4)	Lux(average)
371	336	309	292	327
C1	C2	C3	C4	
0.049	0.028	0.11	0.041	

الاعلى (Upper)

Lux (1)	Lux(2)	Lux(3)	Lux(4)	Lux(average)
391	395	383	364	383.25
C1	C2	C3	C4	
0.005	0.025	0.035	0.015	

الاسفل (Down)

Lux (1)	Lux(2)	Lux(3)	Lux(4)	Lux(average)
118	117	105	92	108
C1	C2	C3	C4	
0.004	0.065	0.12	0.054	

وقد تم استخدام تقنية التباين المباشر لحساب التباين من العلاقة الآتية

$$C = \frac{I_{\max} - I_{\min}}{I_{\max} + I_{\min}} \quad \ldots\ldots\ldots\ldots\ldots\ldots (1)$$

بالاعتماد على اكبر وأصغر شدة من نقاط الحافات للحزم اللونية ومركبة الإضاءةL حيث أستخدم مؤثر سوبل في الكشف الحافي لعتبات مختلفة (20,40,60,80,100) ولمسافات مختلفة.

واستخدمت ايضا تقنية التباين الاحصائي حيث تعتمد هذه التقنية على قيمة المعدل للانحراف المعياري لعناصر الحافات.

المناقشة والنتائج

يبين الشكل (7) نتائج تقنية التباين الاحصائي للنص المكتوب باللوان RGB ومركبة الاضاءة (L) لقاعة ذات (اضاءة منتظمة) للحزم اللونية RGB والمكتوبة على اللوحة البيضاء ، والعلاقة كما موضحة بين عتبة تحديد الحافات للنص (threshold) لمؤثر سوبل على المحور (x-axis) والتباين (contract) الناتج عند كل حالة على المحور (y-axis) ضمن مسافات محددة بين (100,200,300 cm) يتضح ان اللون الازرق يمتلك اعلى نسبة تباين بينما نجد ان اللون الاحمر له اقل نسبة تباين مقارنة مع اللون الازرق عند نفس قيم العتبة لكلا اللونين ، في حين ان التغير في التباين للون الاخضر يكون طفيفا كما واضح من الشكل (7) ان العلاقة ما بين العتبة والتباين هي علاقة طردية شبه خطية .

الشكل (8) يبين تقنية التباين الاحصائي للنص المكتوب باللون الاسود لقاعة الدراسة ذات اضاءة تامة للحزم اللونية RGB ومركبة الاضاءة (L) ومن الواضح بالشكل (8) ان العلاقة تربط ما بين عتبة تحديد الحافات للنص المكتوب باللون الاسود باستخدام مؤثر سوبل وما بين التباين الاحصائي للنص المكتوب وقد لوحظ من خلال الشكل والنتائج التي حصلنا عليها ان الحزمة الزرقاء سجلت اعلى قيم تباين ويأتي بعدها الحزمة الحمراء بينما الحزمة الخضراء سجلت قيم تباين قليلة عند القيم ذاتها من العتبة .

وقد تبين من خلال الشكلين (7 و8) انه بالمسافة القريبة يكون التباين عالي وكما هو معلوم ان الغاية الاساسية من حساب تباين النص هو تحديد افضل صورة من بين مجموعة من الصور الملتقطة .

الشكل (9) يوضح العلاقة ما بين عتبة تحديد الحافات للنص المكتوب باللوان RGB ومركبة الاضاءة (L) لقاعة ذات اضاءة تامة والتباين الذي يحصل في كل حالة ضمن المسافات المبينة في الشكل . نلاحظ انه مع زيادة قيمة العتبة يزداد مقدار التباين للحزم اللونية ككل الأ ان اللون الازرق عند نفس قيم العتبة لكل من الازرق والاحمر يحتل المرتبة الاولى من ناحية الزيادة في قيمة التباين ، بينما يمتلك اللون الاخضر اقل قيمة للتباين ويتوسط اللون الاحمر في معدل الزيادة الطردية الخطية الحاصلة ما بين العتبة والتباين .

الشكل (10) يبين تقنية التباين المباشر للنص المكتوب باللون الاسود لقاعة الدراسة ذات اضاءة تامة للحزم اللونية RGB ومركبة الاضاءة (L) فقد لوحظ ان العلاقة البيانية ما بين العتبة والتباين تكون شبه خطية عند القيم المنخفضة للتباين وبزيادة قيم التباين عند نفس قيم العتبة المؤخوذة نحصل على شبه منحني غير منتظم تبدأ قيم التباين فيه بالتقارب من بعضها البعض عند زيادة قيم العتبة .

من الشكلين (7) و (8) بالنسبة للتباين الاحصائي والشكلين (9) و (10) بالنسبة للتباين المباشر نستنتج ان التباين الاحصائي المعتمد في حساب تقنية التباين هو افضل تقنية في اظهار التفاصيل للنص المكتوب من تقنية التباين المباشر لنفس قيم العتبة المأخوذة ضمن المسافات المختلفة عند الاضاءة المنتظمة لقاعة الدراسة يسجل التباين اعلى قيم لتقنية التباين الاحصائي مقارنة بما نحصل عليه من قيم في تقنية التباين المباشر .

ويستنتج من ذلك:

1. تعتبر تقنية التباين الاحصائي في اظهار تفاصيل نص مكتوب على لوحة بيضاء بألوان احمرواخضر وازرق واسود هي افضل من تقنية التباين المباشر .
2. تزداد وضوحية النص المكتوب بالوان احمرواخضر وازرق واسود على اللوحة البيضاء كلما كانت المسافة اقرب وهذا يؤدي الى الزيادة في قيم التباين الذي نحصل عليه .
3. يعتبر اللون الازرق هو اللون الذي يمتلك اعلى قيم للتباين عند كتابته على لوحة بيضاء في قاعة درس ذات اضاءة منتظمة مقارنة مع اللون الاحمر والاخضر.

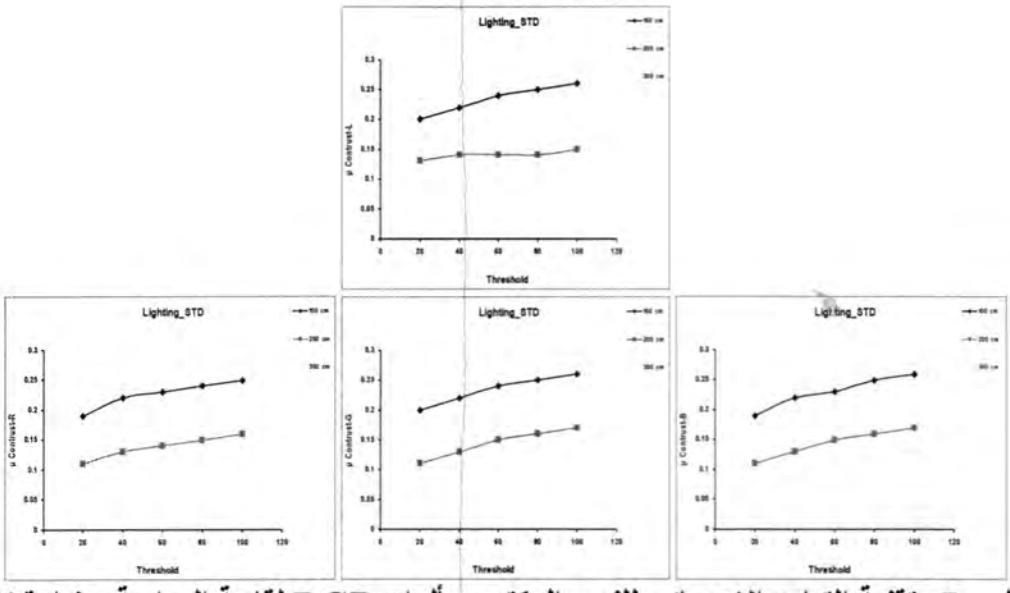

شكل – 7: تقنية التباين الإحصائي للنص المكتوب بألوان RGB لقاعة الدراسة مضاءة تامة (إضاءة منتظمة) للحزم اللونية RGB

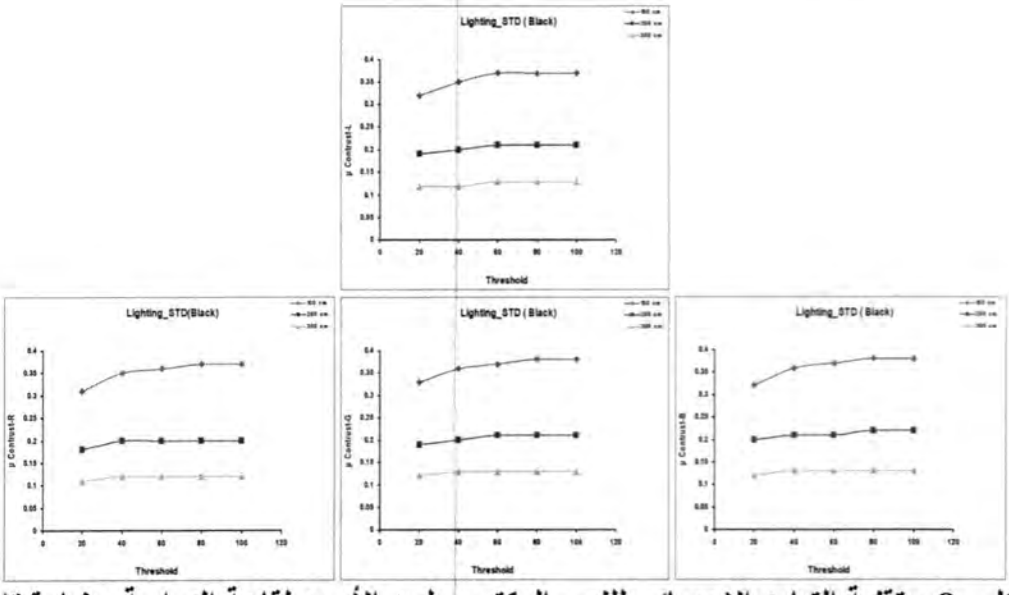

شكل - 8 : تقنية التباين الإحصائي للنص المكتوب بلون الأسود لقاعة الدراسة مضاءة تامة (إضاءة منتظمة) للحزم اللونية RGB

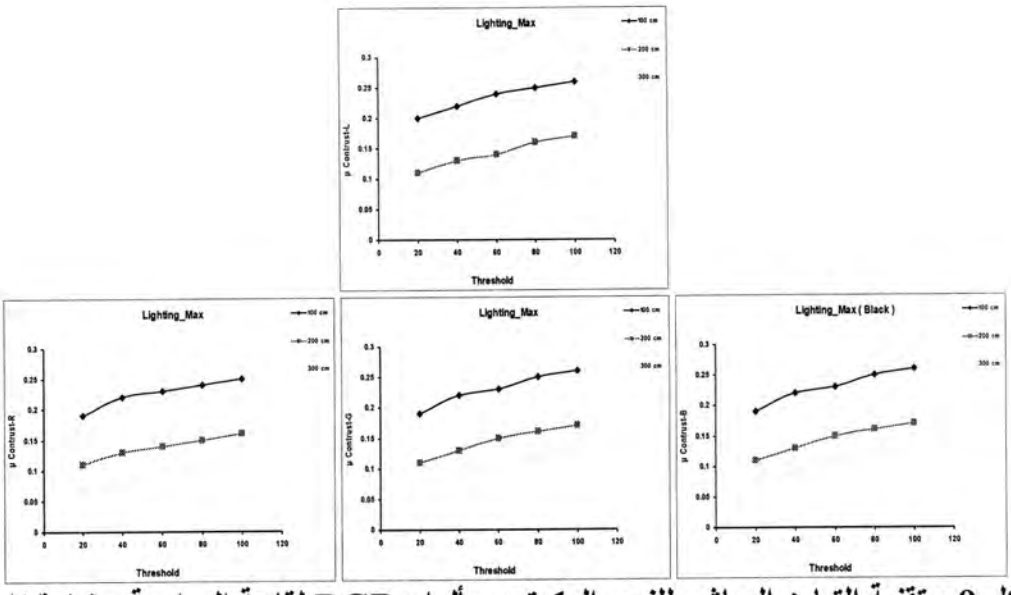

شكل-9 : تقنية التباين المباشر للنص المكـتوب بألوان RGB لقاعة الدراسـة مضاءة تامـة (إضاءة منتظمة) للحزم اللونية RGB

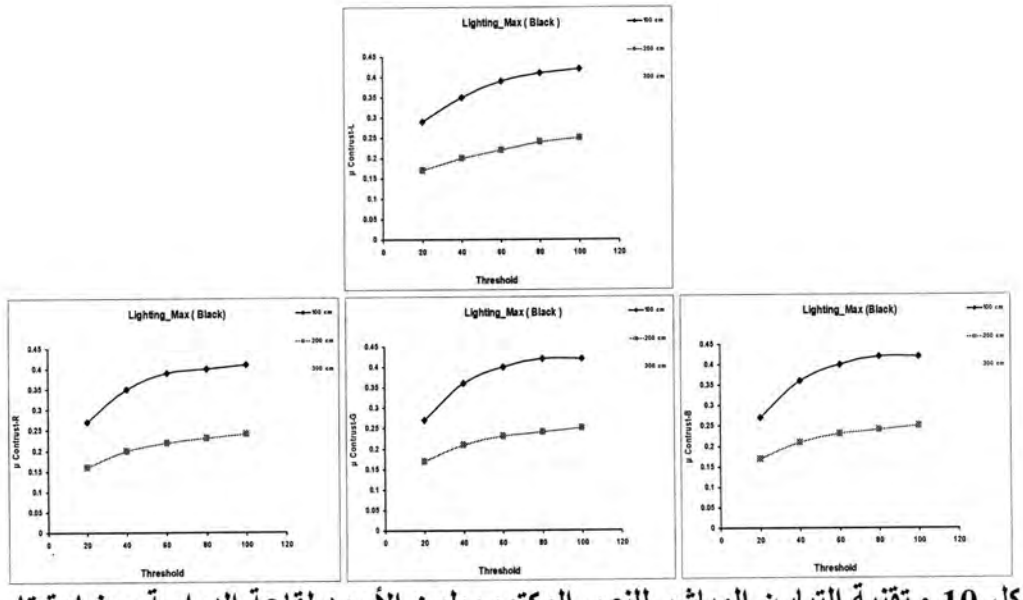

شكل-10 : تقنية التبايـن المباشر للنص المكتوب بلون الأسود لقاعة الدراسة مـضاءة تامـة (إضاءة منتظمة) للحزم اللونية RGB

المصادر

1. Robertr S. , " The Art and Science of Optical Design", Cambridge University , (1997) .
2. Kai Y. and Liang J., " How to Optimize Optical Coherent Tomography OCT Image", optic Express24, v–9, n-1, (2001)
3. Tinku A. and Ajoyk R. , " Image Processing Principle and application " , Dep. of Electrical Engineering , University Arizona State , (1997) .
4. Zhou , W ., " Edge Detection " , department of electrical and Computer Engineering , University of New Maxico , 2005 .
5. Ramamurthy , V., N. Naren dran , J . P. Freyssinier and Boyce , " Determining Contrast Sensitivity function for Monochromatic light emitted By high – Brightness " Third international Conference on solid state , 2004 .
6. Neumann L. , sbert M. , Gooch B. , " Global Contrast factor – Anew approach to image contrast " , Computational Aesthetics in Graphics , Visualization and Imaging , (2005) .
7. Lamming D., " Contrast Sensitivity " , chapter (5) , in Cronly Dillon , Vision and Visual Dysfunction , vo.15 , London , (1997) .
8. Nezamzbad M. and Berns R. , " The Effect of Image Size on the Color appearance of Image reproduction using Colorimetrically Calibrated LCD and DLP displays" , J. Soc .Inf . DISP.14(9) ,:773, (2006) .
9. Smith G. and Atchison D. , " The Eye and Visual Optical Instrument " , New York , Cambridge University , (1997) .
10. Lamming D., " spatial Frequency Channels " , chapter (8) , incronly – Dillon j., vision and visual Dysfunction , 15,London Macmillan , 1991.
11. Cline D. , Hosfstetter H. , Griffinj R . , " Dictionary of Visual Science " , 4th ed Butter worth Heinemann Boston , (1997) .

مقارنة وضوحية نص مكتوب بالالوان الرئيسية مع اللون الاسود في قاعة دراسية مظلمة

[1]علي عبد داود الزكي و [1]اسراء فاخر خلف و [2]سليمة سلطان سلمان و[3] رغد عبد العال الشمخي
[1]قسم الفيزياء/ كلية العلوم/ الجامعة المستنصرية
[2]كلية الصيدلة/ جامعة بغداد
[3]كلية البنات/ جامعة بغداد

ABSTRACT

To determine the accuracy of the details for the text written on a whiteboard is determined through the visibility of this text and contrast between the text and board is written and the separation distance between the vision and written text as well as light and his kind, and the contrast of the major role to determine the details of the written text of what determines the degree of clarity or deceiving the text, and the high contrast between text and the written painting we found more apparent.

In this research, we have to write text on a white plant on (red, green, blue, and black) in dark classrooms (without lighting) and studied the contrast of written text, we concluded that the written text in black color on a white board in the dark classrooms is more clear than we written in the other colors in the same conditions, and the distance a role in determine the details of the text if it is found that the more the distance the text is far less clear and there was difficulty in determining the details of the discrepancy because the contrast is this case is little.

الخلاصة

ان تحديد دقة التفاصيل لنص مكتوب على لوحة بيضاء يتحدد من خلال وضوحية ذلك النص والتباين الحاصل ما بين النص واللوحة المكتوب عليها والمسافة الفاصلة ما بين الرؤيا والنص المكتوب اضافة الى الاضاءة ونوعها ، وان للتباين دور كبير في اظهار تفاصيل النص المكتوب لما يتحدد من خلاله درجة وضوح او غشاوة ذلك النص وكلما كان التباين عاليا ما بين النص واللوحة المكتوب عليها كان اكثر وضوحا .

وفي هذا البحث قمنا بكتابة نص على لوحة بيضاء بالالوان (الاحمر ، الاخضر ، الازرق ، الاسود) في قاعة دراسية مظلمة (بدون اضاءة) ودرسنا التباين للنص المكتوب وقد استنتجنا ان النص المكتوب باللون الاسود على لوحة بيضاء في قاعة دراسية مظلمة يكون اكثر وضوحية فيما لوكتب بالالوان الاخرى تحت نفس الشروط ، وان للمسافة دورا في تحديد تفاصيل النص اذ تبين انه كلما كانت المسافة بعيدة كان النص اقل وضوحا وكانت هناك صعوبة في تحديد تفاصيله لان التباين عند هذه الحالة يكون قليلا .

المقدمة

أن تحسس الإنسان للألوان يعتمد على طبيعة الضوء المنعكس عن الجسم . فالجسم الذي يعكس كل الأطوال الموجية في النطاق المرئي بنفس الدرجة نراه بوضوح بينما الجزء الذي يمتص معظم تلك الأطوال ويعكس الأطوال الخاصة باللون الأخضر مثلاً يظهر باللون الأخضر ،أما الضوء الخالي من الألوان فيدعى بالضوء الأحادي اللون Monochromatic or Achromatic وتعد الشدة هي الخاصية الوحيدة لهذا الضوء ، حيث يستخدم مصطلح المستوى الرمادي Gray Level لوصف شدة الضوء أحادي اللون وذلك لأنه يمتد من الأسود الى الأبيض مروراً بالتدرجات الرمادية بخلاف الضوء المتعدد الألوان الذي يعتمد على ثلاث كميات أساسية لوصف جودة هذا الضوء وهي الإشعاعية Radiance والسطوع Brightnessوالنصوع Luminance .

حيث تمثل الإشعاعية كمية الطاقة التي تنبعث من مصدر الضوء وتقاس عادة بالواط (watt). بينما السطوع يمثل شدة الإضاءة المستقبلة من قبل متحسس الصورة وهي وصف ذاتي لتحسس الضوء الذي يستحيل قياسه عملياً وهذا يوضح فكرة اللالونية للشدة التي تعتبر من

العوامل الأساسية في وصف الإحساس باللون ،أما النصوع فيعتبر مقياس لكمية الطاقة التي يتحسسها الناظر من المصدر الضوئي وتقاس بوحدة اللومين Lum (1).

الجانب النظري:

تعتمد قابلية المشاهد على رؤية أي جسم على حجم الجسم ، التباين ، الإضاءة ، موقع الجسم من المحور البصري ، مقدار الضوضاء في المشهد . يمكن تصور العين البشرية كنظام موجب ثنائي العدسة يُسقط صورة حقيقية على سطح حساس للضوء يمر الضوء الداخل إلى العين من خلال القزحية وهي عبارة عن بقعة في فتحة العين . يتغير بؤبؤ العين ما بين 7 mm (2 –) متكيفا مع مستوى ضوء المحيط ، ثم يمر خلال العدسة التي يتغير بعدها البؤري بواسطة العضلات المرتبطة بها (2).

يمكن تعريف جودة الصورة بانها مقدار الحدة او التباين في الصورة . ان جودة الصورة في أي منظومة بصرية تعتمد على نسبة التباين ، السطوعية ، الوضوحية ، لذلك تستعمل في المعالجة الصورية التباين Contrast ، السطوع Brightness ، مساواة المخطط التكراري Histogram equalization لغرض تحسين جودة الصورة (3) .

التباين هو النسبة بين إضاءة الجسم object وإضاءة الخلفية Back ground التي تحيط بالجسم. ان تحسس التباين يعتمد على التوزيع الحيزي للمناطق المضيئة والمعتمة في الصورة ويمكن تحسين الصور باستخدام هذه الخاصية ، حيث يمكن استخدام مرشح لغرض تحسين نسبة التباين في الصورة وذلك عن طريق طرح نسبة معينة من قيمة كل وحدة لونية في الصورة وذلك لزيادة التباين بين نقاط الصورة الشكل (1) يوضح دالة التحسس للتباين لدى الإنسان Contrast Sensitivity Function ومختصرها CSF التي تعتمد على الإضاءة Luminance والتوزيع الحيزي للألوان في الصورة فكلما زاد التردد ، قلت قدرة العين على تمييز الألوان (4) .

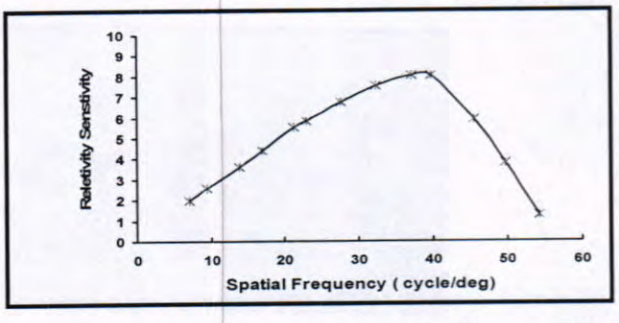

شكل -1 : علاقة حساسية التباين مع التردد الحيزي (5)

يمكن الاستفادة من خاصية التباين بعملية ضغط الصور وتشفيرها عن طريق اختيار البيانات الاكثر ترددا وتخصيصها للمناطق الأكثر حساسية للتردد الحيزي .

ان التباين يشير الى الفرق بين الاضائية للعناصر المتجاورة في مناطق الصورة المختلفة ينتج بسبب الاختلاف في الإضاءة أي ان اصغر فرق في الشدة الضوئية ممكن تحسسه بين جسمين متجاورين في الصورة يدعى وضوحية التباين Contrast Resolution لذا يمكن قياس هذا التباين بأخذ الفرق في الشدة لعناصر الصورة المتجاورة . فالصورة ذات التباين العالي تكون لها من الناحية النموذجية تغايرات في الشدة او اللون كبيرة بين الاجسام المختلفة في الصورة . من ثَمّ يكون من السهل من الناحية البصرية تحديد حدود الجسم والصفات المميزة في الأجسام . الصورة ذات التباين الواطى تكون ذات اختلافات تدريجية من الصعب اكتشافها من الناحية البصرية ان طرق تحسين التباين تقوم بتكبير التغايرات في الشدة الموقعية او اللونية في الصورة وهذا ما يزيد من قابلية رؤية التفاصيل (6) .

هناك عدة طرق لتحسين التباين منها التحسين باستخدام مساواة المخطط التكراري و تحسين التباين باستخدام النافذة و التحسين باستخدام نوافذ اللاحدة و تحسين التباين بالتغاير الثابت [7].

المواد وطرائق العمل

اعتمدنا في هذه الدراسة على كتابة نص باستخدام الوان قلم بورد مختلفة نوع Dry – Erase ولمسافات مختلفة cm (300 , 200 , 100) واضاءات مختلفة الاتجاهات لقاعة الدرس حيث تم التقاط صور النص المكتوب على اللوحة بواسطة الكاميرا الرقمية Sony – Digital Camera والشكل (2) و (3) يوضح الصور الناتجة من منظومة العمل باختلاف المسافة والإضاءة والكاميرا الرقمية المستخدمة في العمل على التوالي .

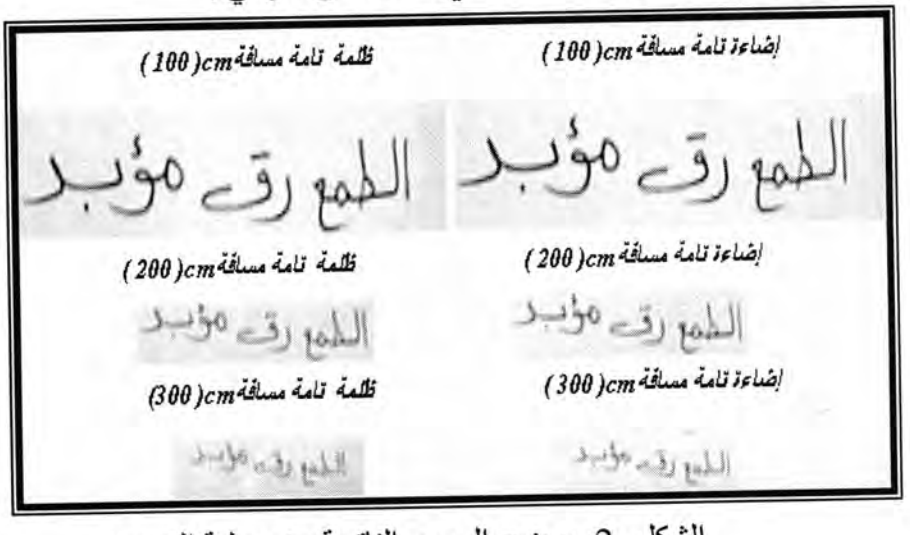

الشكل -2: يوضح الصور الناتجة من عملية التصوير

الشكل -3: يوضح الكاميرا الرقمية المستخدمة في عملية التصوير

تمت عملية التصوير في قاعة دراسية كما موضحة في الشكل (4) في صباح الساعة العاشرة من يوم 14/ 4/ 2009 حيث استخدم جهاز قياس شدة الإضاءة الموضح في الشكل (5) لقياس شدة الإضاءة في مختلف الاتجاهات للقاعة الدراسية .

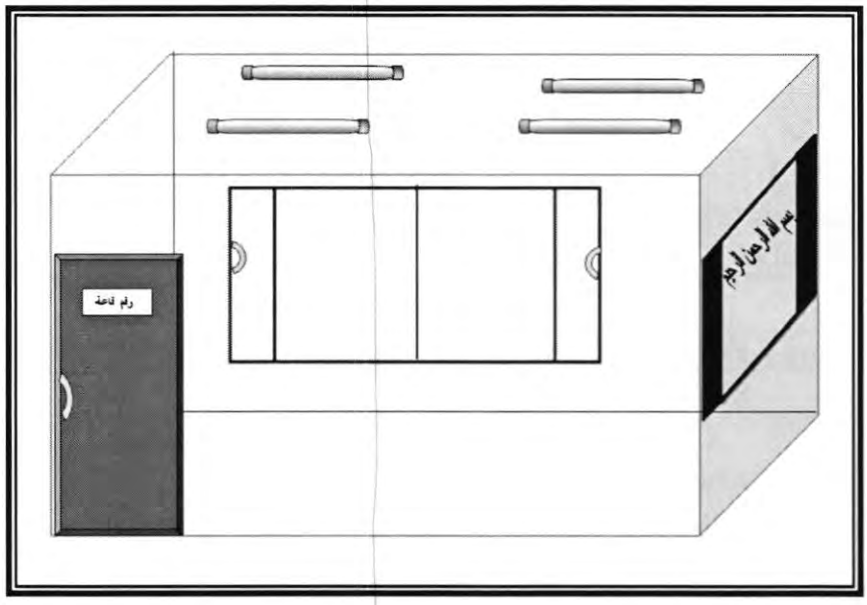

شكل - 4 : قاعة الدرس المستخدمة في التصوير

شكل -5: جهاز قياس شدة الإضاءة

وكانت قراءات جهاز قياس شدة الإضاءة الموضحة في الجدول (1) لغرفة مظلمة (اضاءة منتظمة) .

جدول-1: قيم شدة الإضاءة والتباين في حالة مظلمة (إضاءة منتظمة)

مباشرة (Direct)

Lux (1)	Lux(2)	Lux(3)	Lux(4)	Lux(average)
128	129	127	129	128.25
C1 (Horizontal)	**C2(Horizontal)**	**C3(Vertical)**	**C4(Vertical)**	
0.0038	0.0078	0.0038	0.0078	

يمين (Window)

Lux (1)	Lux(2)	Lux(3)	Lux(4)	Lux(average)
82	87	76	77	.580
C1 (Horizontal)	**C2(Horizontal)**	**C3(Vertical)**	**C4(Vertical)**	
290.0	50.006	670.0	0.0065	

يسار (Door)

Lux (1)	Lux(2)	Lux(3)	Lux(4)	Lux(average)
133	124	123	124	126
C1 (Horizontal)	**C2(Horizontal)**	**C3(Vertical)**	**C4(Vertical)**	
0.035	0.004	0.035	0.004	

للأعلى (Upper)

Lux (1)	Lux(2)	Lux(3)	Lux(4)	Lux(average)
101	96	93	95	96.25
C1 (Horizontal)	**C2(Horizontal)**	**C3(Vertical)**	**C4(Vertical)**	
250.0	.00530	0.03	0.015	

للأسفل (Down)

Lux (1)	Lux(2)	Lux(3)	Lux(4)	Lux(average)
43	44	42	41	42.5
C1 (Horizontal)	**C2(Horizontal)**	**C3(Vertical)**	**C4(Vertical)**	
0.011	0.012	0.011	0.023	

وقد تم استخدام تقنية التباين المباشر لحساب التباين من العلاقة الآتية

$$C = \frac{I_{\max} - I_{\min}}{I_{\max} + I_{\min}}$$

بالاعتماد على اكبر أصغر شدة من نقاط الحافات للحزم اللونية ومركبة الإضاءة L ، حيث أستخدم مؤثر سوبل في الكشف الحافي لعتبات مختلفة (100, 80, 60, 40, 20) ولمسافات مختلفة.

واستخدمت ايضا تقنية التباين الاحصائي حيث تعتمد هذه التقنية على قيمة المعدل للانحراف المعياري لعناصر الحافات.

المناقشة والنتائج

يمثل الشكل رقم (6) تقنية التباين الاحصائي للنص المكتوب باللوان RGB ومركبة الاضاءة (L) لقاعة درس مظلمة (اضاءة منتظمة) للحزم اللونية RGB ويقصد بعبارة اضاءة منتظمة ان نسبة توزيع الاضاءة في انحاء القاعة تكون متساوية . وكما هو واضح من الشكل ان العلاقة المرسومة بين عتبة تحديد النص المكتوب التي تبدأ من (20) الى (100) بزيادة قدرها (20) لكل قراءة والتباين الحاصل لكل قيمة من قيم العتبة للحزم اللونية RGB ، اذ نلاحظ ان معدل الزيادة في التباين بصورة عامة هو قليل يقترب في بعض الاحيان الى الخط المستقيم ومن الملاحظ ايضا ان التباين الحاصل للون الازرق هو اكثر قيمة من اللون الاحمر والاخضر لنفس قيم العتبة وعند المسافات (100,200,300 cm) .

اما في الشكل رقم (7) فيمثل التباين الاحصائي للنص المكتوب باللون الاسود لقاعة الدراسة المظلمة للحزم اللونية RGB ومركبة الاضاءة (L) ، نستدل من الرسم البياني ان علاقة العتبة باستخدام مؤثر سوبل والتباين هي علاقة طردية لكن الزيادة غير منتظمة لكل الالوان فهي تقترب احيانا من الخط المستقيم اذ بمقارنة قيمة التباين لأول قيمة عتبة وهي (20) مع آخر قيمة عتبة مستخدمة وهي (100) نلاحظ من المقارنة ان الفرق بين القيمة الاولى والأخيره قليل جدا خاصة للون الاحمر والاخضر بينما يزداد الفرق في قيمة التباين للون الازرق ، وعند المسافة (300 cm) نلاحظ ان الحزم RGB تسجل اقل قيم للتباين .

ومن الشكل (6) و (7) نستنتج ان النص المكتوب باللون الاسود في قاعة دراسة مظلمة يسجل اعلى قيم تباين من الالوان RGB اذ يصل اعلى قيمة تباين لنص مكتوب باللون الاسود في غرفة مظلمة عند المسافة (300 cm) الى قيمة (0.33) كما هو واضح في الشكل رقم (7) ، بينما يسجلالنص المكتوب باللوان RGB في قاعة دراسة مظلمة اعلى قيمة تباين عند مسافة (300 cm) وقدرها (0.21) كما واضح في الشكل رقم (6) .

يوضح الشكل رقم (8) العلاقة البيانية ما بين عتبة تحديد النص المكتوب باللوان RGB ومركبة الاضاءة (L) والتباين الحاصل لكل لون لقاعة الدراسة المظلمة باستخدام تقنية التباين المباشر ، اذ تم حساب التباين بعتبات مختلفه باستخدام مؤثر سوبل وهي (20,40,60,80,100) ، وان الغاية لاستخدامنا لاكثر من تقنية هي تحديد اعلى قيمة للتباين الحاصل من كل صورة من صور النص كما ان الغاية من حساب التباين هي ايجاد افضل صورة للنص المكتوب عندما تكون القاعة الدراسية مظلمة .

يتبين لنا من خلال الشكل رقم (8) ان علاقة التباين مع العتبة هي علاقة طردية شبه خطية وتقترب من العلاقة الخطية كلما قلت المسافة في حسن يظهر من خلال الشكل انه عند السافة (300 cm) لقيم عتبة (20,40) تكون خطية ويبدأ الفرق بالزيادة بالنقصان تدريجيا عند العتبات (60,80,100) للمسافة المذكورة آنفا .

اما في الشكل رقم (9) الذي يبين لنا تقنية التباين المباشر للنص المكتوب باللون الاسود لقاعة الدراسة المظلمة (اضاءة منتظمة) للحزم اللونية RGB ومركبة الاضاءة (L) فقد تم تسجيل اعلى قيمة تباين في هذه الحالة وكان (0.37) للحزمة الزرقاء تليها الحزمة الخضراء التي سجلت اعلى قيمة تباين قدرها (0.36) بينما سجلت الحزمة الحمراء تباينا قدره (0.35) ضمن نفس المسافة التي تساوي (100 cm) ، وقد لوحظ ان مقدار التزايد في قيم التباين للحزم اللونية RGB ومركبة الاضاءة (L) يقل مع زيادة قيم العتبة ضمن المسافات (200,300 cm) .

نستنتج مما سبق انه كلما كانت المسافة قريبة كان التباين عاليا كما اننا نجد ان تقنية التباين المباشر هي افضل من تقنية التباين الاحصائي في اظهار تفاصيل النص المكتوب على اللوحة البيضاء لقاعة دراسية مظلمة .

1. من خلال ماحصلنا من نتائج في هذا البحث نستنتج ان التباين بنوعيه (الاحصائي والمباشر) يزداد مع زيادة قيم العتبة لنص مكتوب على لوحة بيضاء بالوان (الاحمروالاخضر والازرق) ولمركبة الاضاءة (L) في قاعة دراسية مظلمة .
2. تعتبر كتابة اللون الاسود على لوحة بيضاء في قاعة دراسية مضلمة ضمن مسافات محددة هو اكثر وضوحا فيما لو كتب النص بألوان (الاحمر والحضر والازرق) .
3. للمسافة دور كبير في زيادة قيم التباين للنص المكتوب على اللوحة البيضاء وبالتالي فهي تؤثر على وضوحية ذلك النص فيكون النص لكثر وضوحا في المسافات القريبة والعكس صحيح .

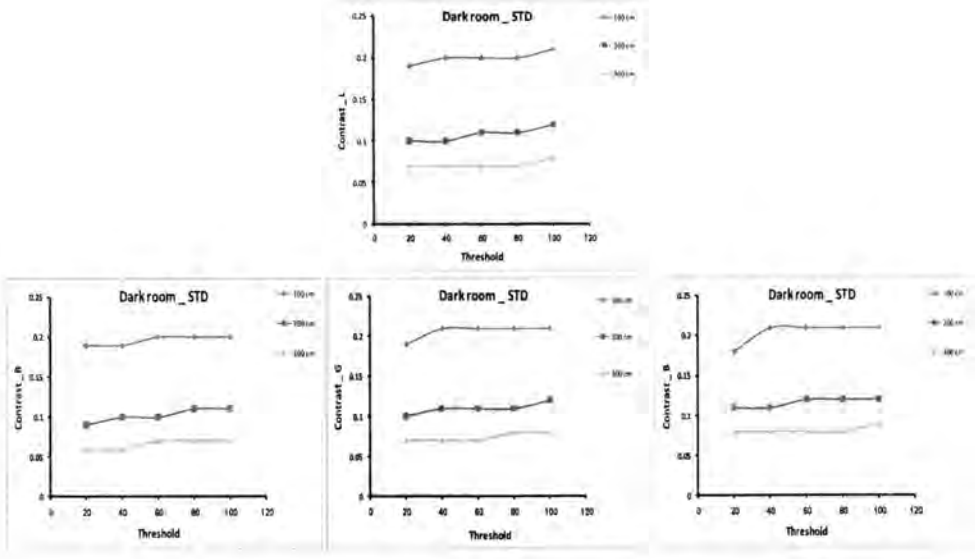

شكل -6: تقنية التباين الإحصائي للنص المكتوب بألوان RGB لقاعة الدراسة ظلمة (إضاءة منتظمة) للحزم اللونية RGB

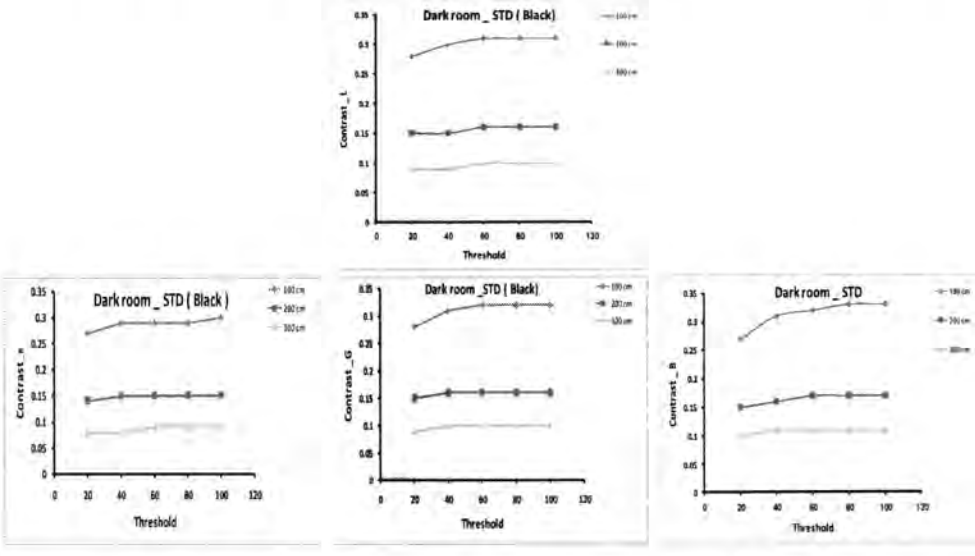

شكل- 7 : تقنية التباين الإحصائي للنص المكتوب بلون الأسود لقاعة الدراسة ظلمة (إضاءة منتظمة) للحزم اللونية RGB

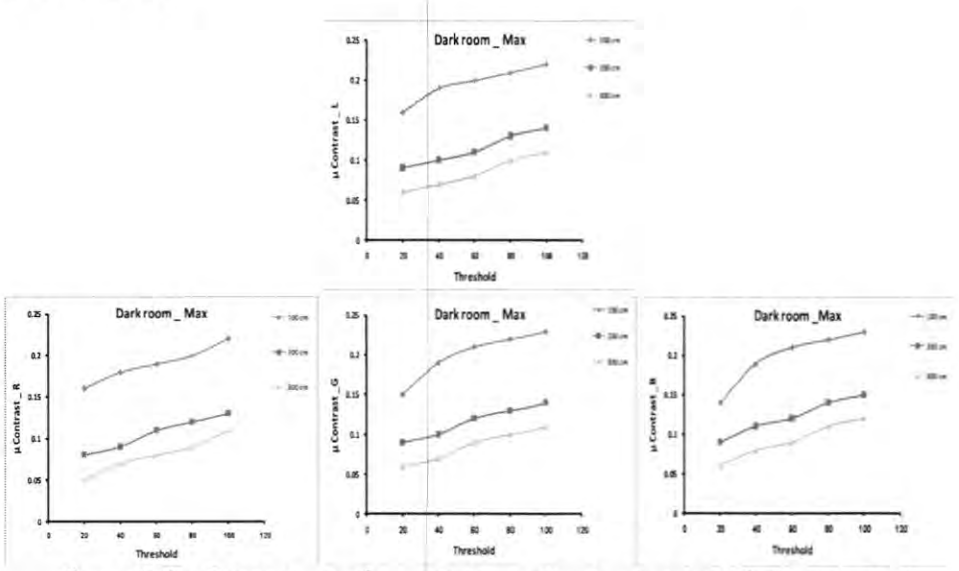

شكل -8 : تقنية التباين المباشر للنص المكتوب بألوان RGB لقاعة الدراسة ظلمة (إضاءة منتظمة) للحزم اللونية RGB

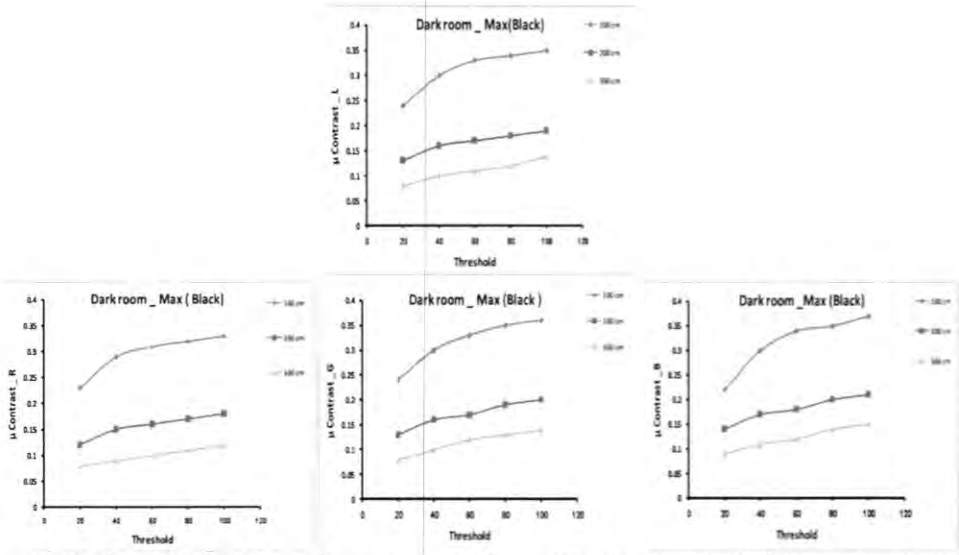

شكل - 9 : تقنية التباين المباشر للنص المكتوب بلون الأسود لقاعة الدراسة ظلمة (إضاءة منتظمة) للحزم اللونية RGB

المصادر

1. Ian.T. , Jonj G. , Lucas J. , " Fundamentals of Image Processing " , (1995) .
2. S.W. Smith , " The Scientist and Engineers Guide to Digital Signal Processing " , California Publishing ISBNO – 966176 – 33 (1997) .
3. NeumannL., Matkovick, Purgathafer W., " The Global Contrast Factor " , in proceeding of the first seminar on Computer Graphics and Visualization , : 108 – 119 (2002) .

4. Campbell , Fw and Robson , " Application of Fourier Analysis to Visibility of grating " , J. Physio , JG, (1968) .
5. Rafal C.Gonzalez , Richared E.wood , " Digital Image Processing using Matlab " , Parson Prentice – Hall , (2004) .
6. Naglaa Yehya Hasssan , Norio Aakamatsu , " Contrast Enhancement Technique of dark Blurred Image " , University of Tokushima , Graduate School of Engineering , Tokushima , Japan , (2006) .
7. Sangwine S. and Novne R. , " The Colour Image Processing Hand Book , Chapman and Hall " ,(1998) .

الخصائص الكهربائية لـ بولي مثيل ميثاكريلات المشوَّب بملح التيتانيوم $TiCl_3$

فاضل تركي معن و زينب عبد السلام الرمضان
كلية التربية / الجامعة المستنصرية

ABSTRACT

In this research, samples were prepared as films of PMMA with different thicknesses (100, 120, 140, 160) μm, undoped and doped by Titanium salt with a wight ratios vary from 1% to 5% to study the electrical properties with different temperatures rang from 40°C to 100°C.

The results showed increase in electrical conductivity from $10^{-15}(\Omega.cm)^{-1}$ to $10^{-10}(\Omega.cm)^{-1}$ with the increasing of doping ratio and a decrease in the electrical conductivity with the increase of thickness. The activation energy was decrease with the doping ratio increase, and it increase with the thickness increase.

الخلاصة

تم في هذا البحث تحضير عينات على شكل أغشية من PMMA وبأسماك مختلفة (100, 120, 140, 160) μm نقية ومشوبة بملح التيتانيوم $TiCl_3$ وبنسب وزنية تتراوح من 1% إلى 5% لدراسة الخصائص الكهربائية وبدرجات حرارة مختلفة من مدى 40 °C إلى 100°C.

أظهرت النتائج الكهربائية زيادة التوصيلية الكهربائة من $10^{-15}(\Omega.cm)^{-1}$ إلى $10^{-10}(\Omega.cm)^{-1}$ مع زيادة نسبة التشويب لكنها تقل مع زيادة سمك العينة. أما طاقة التنشيط فإنها تقل مع زيادة نسبة التشويب وتزداد مع زيادة سمك العينة.

المقدمة

دخلت البوليمرات مجال المواد الموصلة وشبه الموصلة حيث يتم تحول البوليمرات العازلة الى موصلات بالتطعيم بالشوائب لتسمى احيانا المعادن البلاستيكية[1] ففي عام 1977 تم اكتشاف البوليمرات الموصلة الذاتية intrinsic conducting polymers(2) والتي أحدثت طفره كبيرة في إنتاج الصناعات الالكترونية مثل الترانستورات والبطارية القابلة للشحن والخلايا الشمسية(3). استخدمت البوليمرات في البصريات (Optics) لصنع العدسات التي استخدمت في أحدث الأجهزة البصرية لخفة وزنها، حيث ان وزن البوليمرات يعادل نصف وزن الزجاج وقابلية التحمل الكبيرة ضد الكسر، كما استعملت لتقليل تأثير أشعة الشمس في أجهزة الطائرات وعيون الطيارين ولتقليل عملية الانعكاس المتضاعف داخل المادة (Multiple Reflection)(4،5) وكذلك في تغطية الصفائح المعدنية للتوهين في تكنلوجيا التخفي ومنع التآكل والتأكسد (6) وفي صنع النوافذ الانيقة التي تتحكم بكمية الضوء المار خلالها(7)

من العوامل المؤثرة في الصفات الكهربائية وجود الشوائب في نظام متجانس من (البوليمر + مواد مضافة) إذ تسهم هذه الإضافات في التأثير على البناء البلوري كما لهذه الإضافات من تأثير على الأواصر الكيميائية إذ تسهم هذه الإضافات في زيادة ناقلات الشحنة عن طريق توفير الالكترونات أو الايونات لعملية التوصيل(8،9،10). فكان الهدف من البحث دراسة تأثير السمك ونسب التراكيز لملح التيتانيوم المضاف لـPMMA على الخصائص الكهربائية (التوصيلية الكهربائية المستمرة σ_{dc} وطاقة التنشيط) ومجال استخدامها في التطبيقات العملية والتكنولوجية من خلال تحسين خصائصها الكهربائية لتتحول من مواد عازلة الى مواد شبه موصلة .

الجزء النظري

يقصد بالتوصيلية الكهربائية المستمرة بإنها الخاصية الكهربائية الناشئة عن وجود مادة تحت تأثير مجال كهربائي ثابت القيمة والاتجاه ذي تيار مستمر DC نتيجة لانجراف الشحنات الحرة عبر المادة باتجاه الأقطاب (11)، يمكن حساب المقاومة النوعية الحجمية ρ_v لجسم منتظم ذي مقطع عرضي ثابت مساحته A على امتداد الطول L ويمتلك مقاومة حجميه R_v من خلال العلاقة الرياضية

$$R_V = \rho_v \frac{L}{A} (\Omega) \quad \text{.....(1)}$$

إي إن

$$\rho_v = \frac{R_V A}{L} (\Omega . m) \quad \text{.....(2)}$$

حيث ان :

R_v المقاومة الحجمية

ρ_v المقاومة النوعية الحجمية والتي تكون صفة مميزة للمواد إذ تختلف باختلاف المادة وترتبط بعلاقة عكسية مع التوصيلة σ_v إذ تساوي مقلوب التوصيلية الحجمية أي إن التوصيلية الحجمية

$$\sigma_V = \frac{1}{\rho_V} = \frac{L}{R_V A} (\Omega . m)^{-1} \quad \text{.....(3)}$$

L معدل سمك العينة

A مساحة الاقطاب الفعالة

المواد وطرائق العمل

تم اضافة $TiCl_3$ (Titeinium (111) Chloride) الى Soluation hydro cloricacid 15% وهو من منتجات شركة (Riedel-de-Haen Germeny analysis) وزنه الجزيئي 154.25 g/mol الى PMMA إذ تم تحضير العينات على شكل افلام مكونه من خليط من البوليمر وأحد تراكيز $TiCl_3$ عن طريق إذابة PMMA للأوزان (0.40,0.35,0.30,0.25)gm في الكلورفورم ثم أضافة $TiCl_3$ بنسب مختلفة وهي 5%,4%,3%,2%,1% لكل وزن الآنف الذكر.

ولكون $TiCl_3$ محلول مائي ولايمكنه التجانس مع المذيب الكلورفورم والذي هو مذيب عضوي لذا تم تحويل $TiCl_3$ من حالته السائلة الى مركب صلب وذلك عن طريق تجفيفه في فرن (Vacuum oven) نوع (Gallenhamp-Germeny) يرتبط معه محرك ذو مضخة ماصة للابخرة الناتجة من التسخين تستمر العملية من 5-6 ساعات وحسب الكمية المراد تجفيفها ينتج لدينا مركب صلب ذو لون بنفسجي قاتم مائل للزرقة يترك الى أن يبرد ثم يطحن على هيئة مسحوق وينقى بحجم مقداره $75(\mu m)^3$ عن طريق استخدام (Test sieve) مجهز من شركة (Retsch Gmbh company Germeny) لتضاف الى محلول البوليمر حسب النسب المستخدمة ويرج جيداً لغرض ضمان التوزيع المتجانس للاضافات داخل المحلول البوليمري ثم يصب الخليط في احواض تم عملها من الزجاج ابعاد الحوض (5×5)cm يوضع على سطح منضدة مستوية مع استخدام ميزان التسوية للتاكد من استوائية الاحواض ولضمان الحصول على افلام متجانسة بالاسماك (100,120,140,160) µm تم قياس سمك الافلام بجهاز مايكروميتر (Micrometer) بعد جفافها بعملية التبخير البطئ للكلوروفورم.

تم استخدام طريقة الخلية ثلاثية الاقطاب (طريقة الاقطاب الدائرية المعزولة بواسطة التفلون وفقا لتوصيات ASTM (D257-66)[12] لدراسة تأثير الاضافات ودرجة الحرارة

على التوصيلية الحجمية للانظمة البوليمرية ويمكن ايجاد التوصيلية الحجمية من خلال العلاقة (3) وفي هذا التصميم تم استخدام اقطاب دائرية ذات مساحة $A = \frac{\pi D^2}{4}$ إذ ان D تمثل قطر القطب الفعال المستخدم ويساوي 2.5cm. تجهز الدائرة الكهربائية بفولتية مستمرة من مجهز قدره مستمر من صنع شركة (PHYWE) فولتيته الخارجة بحدود (0-3KV) وفي هذا البحث تم استخدام فولتية قدرها 1KV والتيار الخارج يقاس بواسطة جهاز Keithly (616) digital solid state electrometer. توضع العينة (الفيلم) بين القطبين النحاسيين ثم نطابقهما بالشد على بعضهما بواسطة البراغي الاربعة ثم توضع المنظومة (اقطاب+عينة) داخل الفرن L7C(MANFREDI) صنع في ايطاليا تسجل قراءات التيار في كل مرة يتم زيادة الفولتية من مدى KV (0.1 – 1.0) تكرر هذه العملية لدرجات حرارة مختلفة من مدى (40 – 100) ^{o}C.

النتائج والمناقشة

يمثل الشكل (1) علاقة التوصيلة الكهربائية المستمرة σ_{dc} مع درجات الحرارة للأسماك (100, 120, 140, 160) µm إذ يلاحظ ارتفاع التوصيلية الكهربائية (σ_{dc}) بارتفاع درجة الحرارة (T) لـ بولي مثيل ميثاكريلات (PMMA) النقي. ويعزى سبب ذلك الى التغيرات التي تحصل في الشبيكة البوليمرية والناتجة عن الازدواج القوي بين الفونون والالكترونات في جزيئة البوليمر عن طريق الزيادة الحاصلة في الطاقة الحركية للسلاسل البوليمرية مما يضيف مرونة أكبر على هذه السلاسل وزيادة في ابعاد الحركة الموضعية للجزيئات الداخلية للبوليمر(8، 13). كما يمثل الشكل (2) علاقة التوصيلية الكهربائية المستمرة σ_{dc} مع السمك لدرجات حرارة مختلفة لـPMMA نقي إذ يلاحظ انخفاض التوصيلية الكهربائية المستمرة مع زيادة سمك العينة ويعود السبب ان الشحنة المتولدة بين قطبي المنظومة التي يفصلها عازل (مادة PMMA) تعتمد على عدة عوامل(13،14) ومن ضمنها سمك العازل حيث يؤدي الى إضعاف المجال الكهربائي المسلط والجدول (1) يبين قيم التوصيلية الكهربائية المستمرة σ_{dc} المقابلة لدرجات حرارة مختلفة وأسماك مختلفة لـ PMMA نقي.

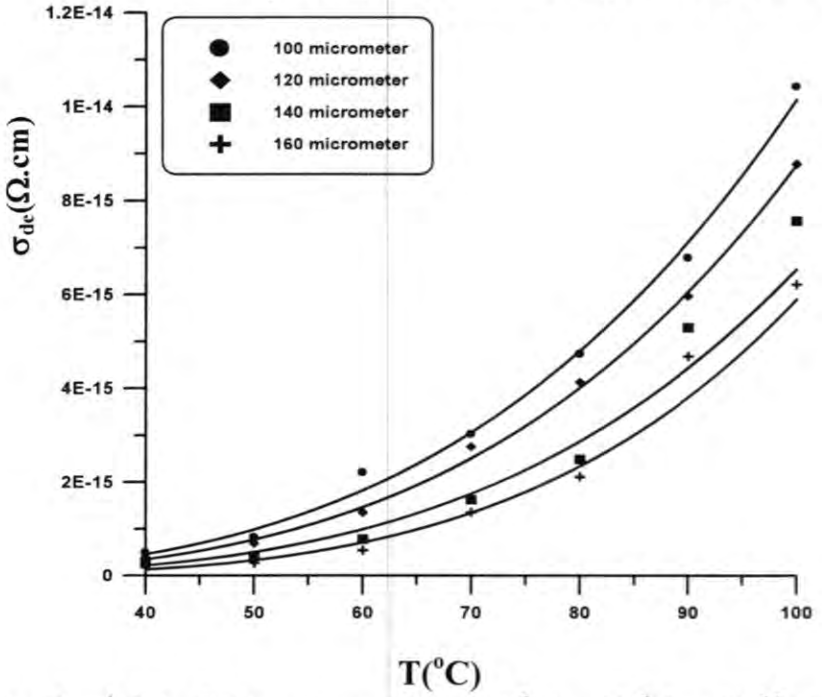

شكل -1: علاقة التوصيلية الكهربائية المستمرة σ_{dc} مع درجات الحرارة لأسماك مختلفة.

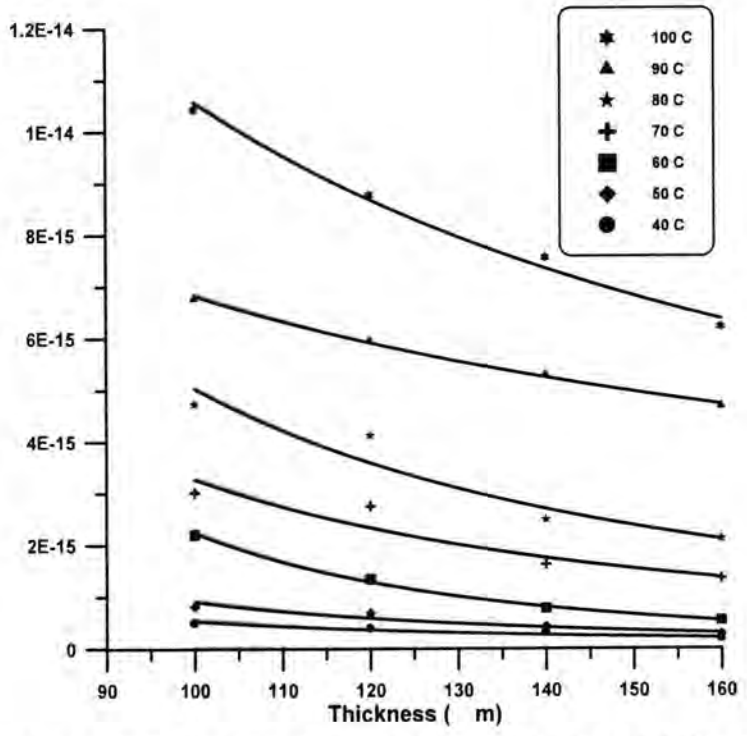

شكل -2: علاقة التوصيلية الكهربائية المستمرة σ_{dc} مع السمك لدرجات حرارة مختلفة لـ نقي (PMMA).

جدول -1: قيم التوصيلية الكهربائية المستمرة σ_{dc} المقابلة لدرجات حرارة مختلفة ولأسماك مختلفة PMMA نقي

سمك	قيم التوصيلية الكهربائية $\sigma_{dc}\times10^{-15}(\Omega.cm)^{-1}$						
	T=40°c	T=50°c	T=60°c	T=70°c	T=80°c	T=90°c	T=100°c
100μm	0.491	0.816	2.200	3.016	4.726	6.778	10.425
120μm	0.387	0.685	1.346	2.753	4.125	5.958	8.773
140μm	0.301	0.426	0.780	1.627	2.488	5.293	7.566
160μm	0.177	0.274	0.542	1.356	2.114	4.677	6.213

يمثل الشكل (3) علاقة $\ln\sigma_{dc}$ بمقلوب درجات الحرارة K^{-1} (1000/T) ولاسماك مختلفة إذ يلاحظ انخفاض قيم $Ln\delta_{dc}$ مع ارتفاع قيم K^{-1} (1000/T) ومن الشكل البياني نحصل على خط مستقيم ومن ميل هذا الخط نحصل على طاقة التنشيط.

أما تأثير السمك على طاقة التنشيط E_{act} لـPMMA نقي فأنه من الشكل (3) تم الحصول على قيم طاقات التنشيط بيانياً للأسماك μm (100,120,140,160) إذ يلاحظ ان قيم طاقات التنشيط تزداد بزيادة سمك العينة وكما موضح بالشكل (4) ويعزى سبب ذلك(14,13) أنه في أشباه المواصلات والعوازل يتراوح عرض طاقة الفجوة ما بين 10-0.1 الكترون فولت وهذا ما يتفق مع النتائج المستحصلة لدينا بخصوص التوصيلية وطاقة التنشيط ويتفق ايضا مع النتائج التي توصل اليها الباحث(15) . ولوحظ ايضا ان سلوك PMMA مشابه لسلوك بولي ستارين التي تم دراسته من قبل الباحث(16) . ومن خلال التجربة وعند اجراء القياسات

الكهربائية لافلام ذو سمك 80 µm فما دون ويعود السبب الى ان توصيلية العازل الكهربائي تزداد مع زيادة شدة المجال الكهربائي وبع تجاوز فرق جهد معين بين الاقطاب في تجربتنا 0.5kv سيؤدي الى زيادة حادة في التيار المار مما يسبب الى انهيار العزل الكهربائي حيث يفقد العازل صفاته المميزة ويتحول الى موصل(14) .

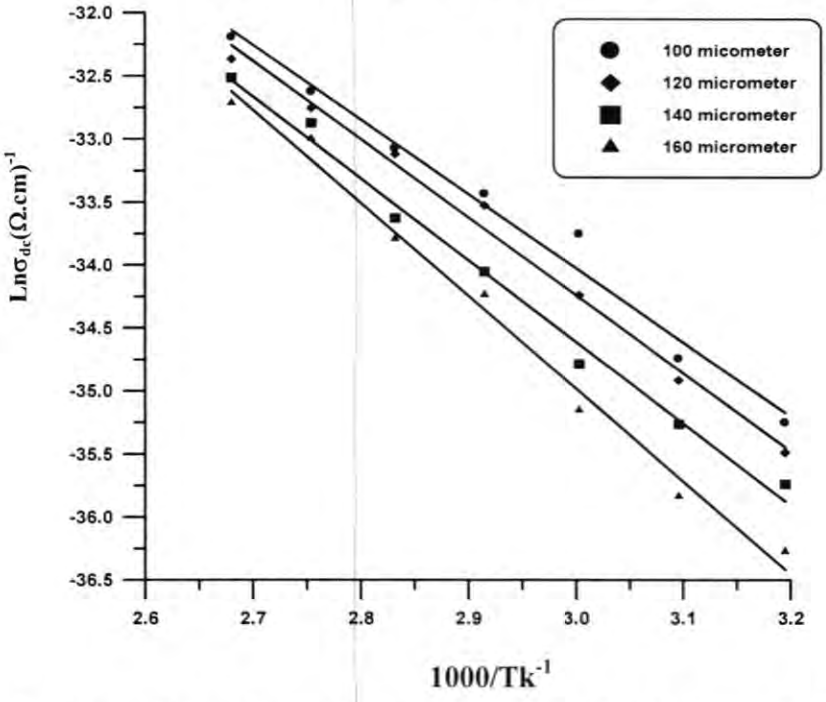

شكل -3: علاقة التوصيلية الكهربائية المستمرة $\ln\sigma_{de}$ مع مقلوب درجات الحرارة $(1000/T)K^{-1}$ لـPMMA نقي

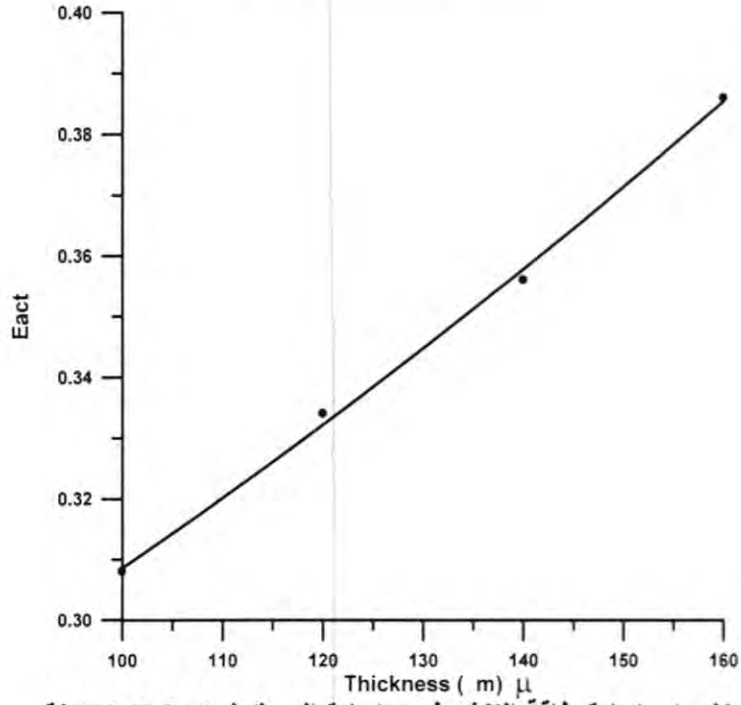

شكل -4: زيادة طاقة التنشيط مع زيادة السمك لـ (PMMA) نقي

يمثل الشكل (5) E,D,C,B,A علاقة التوصيلية الكهربائية المستمرة σ_{dc} مع السمك لـPMMA مشوب ولدرجات حرارة مختلفة ومنه نلاحظ:

أولا: تزداد التوصيلية الكهربائية المستمرة بزيادة درجة الحرارة ويعود السبب الى:

1. زيادة عدد الفراغات في نقاط الشبيكة البوليمرية إذ إن زيادة درجة الحرارة تزيد من احتمالية زيادة هذه الفراغات.
2. زيادة درجة الحرارة تؤدي الى اكتساب الايون طاقة إضافية تعمل على زيادة حركته وبالتالي يمكنه القفز عبر الفراغات المتجاورة (17)

ثانيا: تقل التوصيلية الكهربائية المستمرة بزيادة سمك العينة لـPMMA مشوب ويعود السبب هو إن زيادة سمك العينة لـPMMA مشوب يؤدي الى أضعاف المجال الكهربائي المسلط وبالتالي تقل الشحنة.

اما الشكل (6) D,C,B,A يمثل علاقة التوصيلية الكهربائية المستمرة مع نسبة الشائبة لدرجات حرارة مختلفة بثبوت السمك μm (100,120,140,160) على التوالي ومنه نلاحظ ما يلي:

أولا: في الشكل (6) A تزداد التوصيلية الكهربائية المستمرة σ_{dc} عند إضافة ملح التيتانيوم كشائبة بنسبة 1% الى PMMA حيث ترتفع هذه التوصيلية بمقدار $10^3(\Omega.cm)^{-1}$ مقارنة مع PMMA النقي.

ثانيا: تزداد هذه التوصيلية كلما زادت نسبة الشائبة ولعدة مراتب عشرية. وكما في الشكل (6) D,C,B وتعليل ذلك أن هذه الاضافات لها تأثير على البناء البلوري والأواصر الكيميائية إذ تزداد ناقلات الشحنة عن طريق توفير الالكترونات أو الايونات لعملية التوصيل (9،10،18) إذ تتحرك الايونات باتجاه القطب المعاكس تحت تأثير المجال الكهربائي المسلط نتيجة تأين الملح المضاف وتزداد هذه التوصيلة بزيادة تركيز الملح المضاف بسبب زيادة ناقلات الشحنة الموجودة في النظام حيث تقوم بعض جزيئات البوليمر عمل المذيب الصلب للمادة الشائبة حيث تمتلك هذه الجزيئات القدرة على ترتيب ايونات الملح من خلال تأثير جزيئات البوليمر نفسها على ايونات الملح (19).

الجدول (2) يمثل قيم التوصيلية الكهربائية المستمرة σ_{dc} المقابلة لدرجات الحرارة ونسب التراكيزمن $TiCl_3$ وللأسماك μm (100,120,140,160).

الشكل (7) والجدول (3) يوضحان العلاقة بين قيم طاقات التنشيط والسمك وتفسير ذلك هو ان زيادة سمك العينة يؤدي الى أضعاف ألمجال الكهربائي المسلط كما أن طاقة التنشيط تعتمد مباشرة على التوصيلة الكهربائية وهذه الأخيرة تتناسب عكسيا مع السمك لذا فأنه بزيادة السمك تزداد طاقة التنشيط على الرغم من وجود الكترونات حرة نتيجة الإضافة (9,20). ونلاحظ من الشكل (8) والجدول (3) العلاقة بين قيم طاقات التنشيط ونسبة التراكيز. وتفسير ذلك هو عند اضافة الشائبة فأنها تؤثر على البناء البلوري وعلى الأواصر الكيميائية حيث تزداد ناقلات الشحنة عن طريق توفير الالكترونات أو الايونات لعملية التوصيل إذ تتولد حالة عدم توازن في مستويات الطاقة تؤدي الى انتقال حاملات الشحنة من موضع الى آخر داخل البوليمر وكلما زاد تركيز الإضافة زادت حاملات الشحنة حيث تمتلك بعض جزيئات البوليمر القدرة على ترتيب ايونات الملح المضاف وفصلها وتحركيها باتجاه الأقطاب الكهربائية المعاكسة المتولدة من تأثير المجال الكهربائي الخارجي التي تؤدي الى حدوث التوصيل الايوني (6، 7، 8).

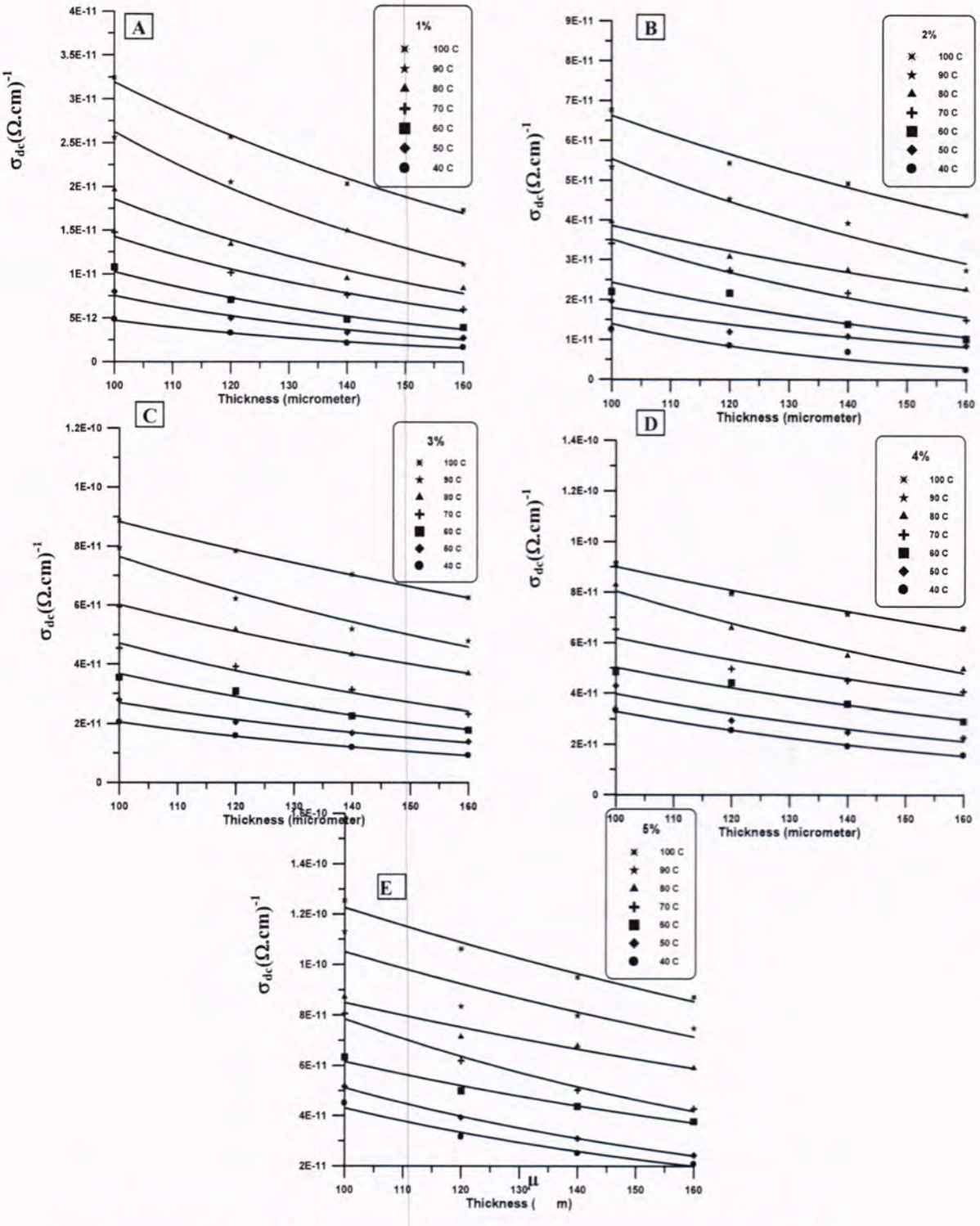

شكل -5: علاقة التوصيلية الكهربائية المستمرة σ_{dc} مع السمك لدرجات حرارة مختلفة ولنسب التراكيز 5%,4%,3%,2%,1%

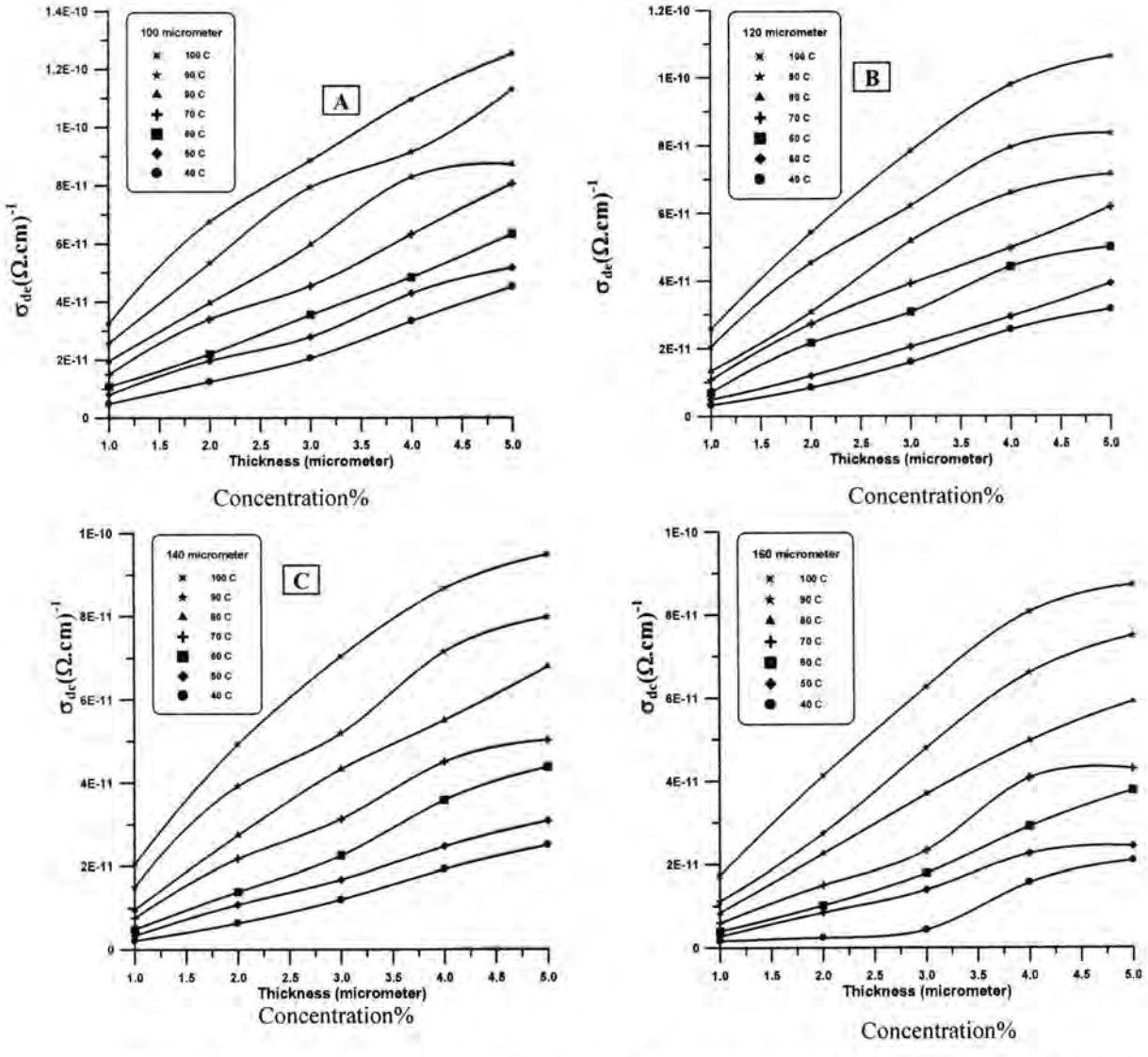

شكل -6: علاقة التوصيلية الكهربائية المستمرة σ_{dc} مع نسبة الشائبة لدرجات حرارة مختلفة للأسماك (160,140,120,100)µm

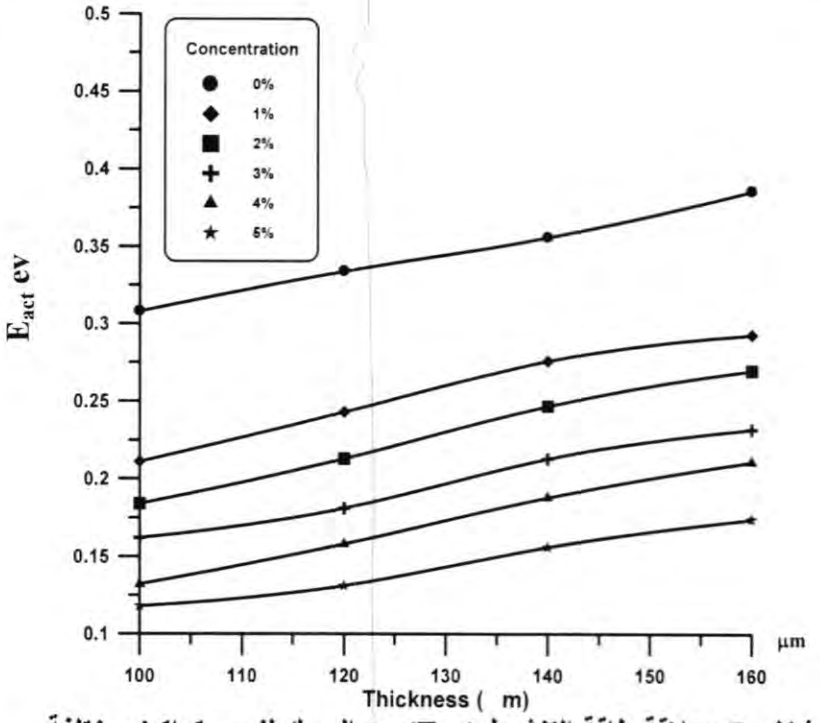

شكل -7: علاقة طاقة التنشيط (E_{act}) مع السمك لنسب تراكيز مختلفة

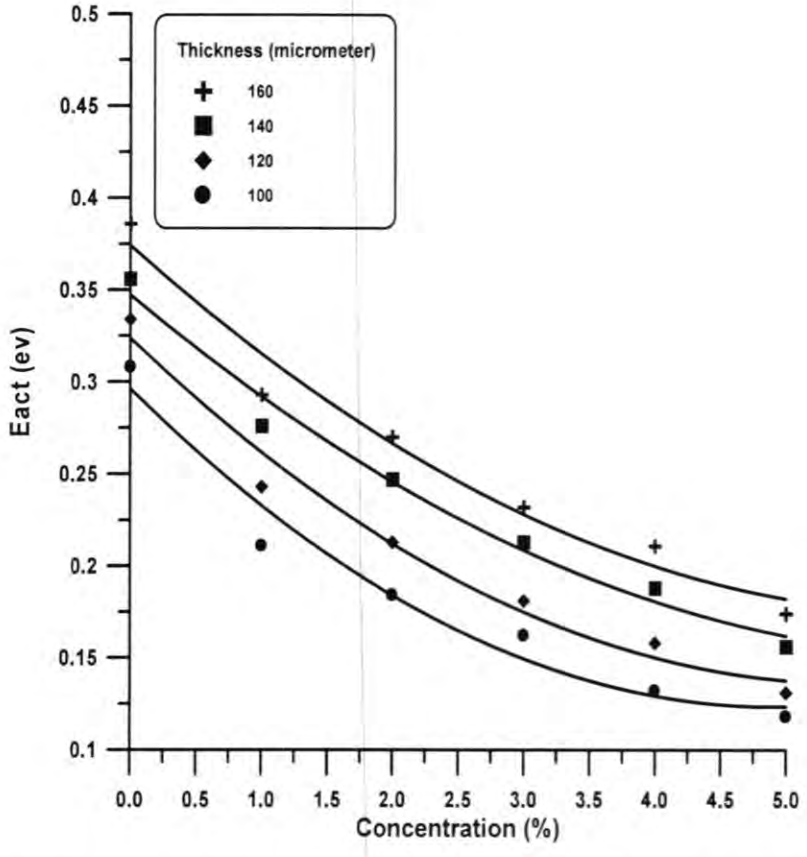

شكل -8: علاقة طاقة التنشيط (E_{act}) مع نسبة التراكيز ولأسماك مختلفة

المصادر

1. Blythe, A.R *'' Electrical Properties of polymers''* Cambridge university press (1979)
2. De Young. H.G. High Technology/JAN.*''conductive polymers Imitate Metals''* (1983)
3. S. Bhattacharya, V.K. Sachdev, R.P.Tandon 2nd National conference Mathematical Techniques Emerging Paradigms for Electronic & IT Industries, :100-101, (2008)
4. مالكوم ب ستيفن *"كيمياء البلمرة"* ترجمة الدكتور قيس عبد الكريم كاظم غياض اللامي جامعة البصرة (1984)
5. LU. J., N.*J Pinto*, and Mac Diarmid A.G; ***J. Appl. Phys***, 10 :(6033) ,(2002)
6. Richard W.H *"physics of thin films"* , 8, Academic press, Interscience, New York (1975)
7. M. Hamzah, ESaion, A. Kassim, E.Mahmud, M.Yousf & I. Shahrim, Journal for the advancement of science & arts, 1, (1), (2009)
8. Leite N. F., Fran A. H., Torres Filho A.and Miranda L. M., J. "***Apply. Polymer Sci.***, 39, : 1361 (1990)
9. Hans F Hespe, J*" Appl poly"* 44(N): 2029 (1992)
10. Sekhon. S.S J "***Bull Moter***" sci, 26, (3):321.328 April (2003)
11. Mark H.F. and Gaylord N.G" ***Encyclpedia of polymer science and engineering"*** 2nd ed, 5, 531 (1971)
12. Annual Book of ASTM standards V.O.8.01 platics (1): c177.D1600 U.S.A (1983)
13. مؤيد جبرائيل يوسف *"فيزياء الحالة الصلبة"* ج 2 وزارة التعليم العالي والبحث العلمي. جامعة بغداد (1980)
14. د. صبحي سعيد الراوي د. شاكر جابر، د. يوسف مولود*"فيزياء الحالة الصلبة"* /جامعة الموصل (1988)
15. Sreejith V. (India) Jornal of ***"Pure and Appliied Physice"*** (2004)
16. زينب عبد السلام *"تحوير الخصائص الكهربائية والبصرية للبوليمرات المرنة حراريا بواسطة الايون المزدوج لمعقد الفناديوم (o) العضوي الفلزي"* أطروحة دكتوراه.كلية العلوم.الجامعة المستنصرية (2003)
17. Kaiser A.B "***Electronic propertic of conjugated polymers***" P, 2.6 (1989)
18. Somayajulu D.R.S J. "***Bull Mater. Sci***,24.(4) (2001)
19. .MG Cowi J and sadaghiani zadah K *"polymer"* 30, 509 (1989)
20. ف.بوش *"أساسيات الفيزياء"* الدار الدولية للتوزيع والنشر طبعة تاسعة (1998)

بعض الخصائص التركيبية لأغشية (SnO_2 وSnO_2:Sb) المحضرة بطريقة الترسيب الكيميائي الحراري

رشيد هاشم جبار وهشام مطر فاضل وحسن علوان عطارو رياض أحمد حنون و محمد خماس خلف
وزارة العلوم والتكنولوجيا/دائرة علوم وبحوث الفيزياء

ABSTRACT

In the present work, structural properties investigated of pure(SnO_2) thin films and doped by Antimony (1,2,3,4,5 wt.%) which prepared by chemical spray pyrolysis were deposited on (550°C) glass substrates with a thickness of (250 nm).

X-ray diffraction (XRD) analysis showed that films are polycrystalline in nature, the deposited films exhibit excellent crystalline structure with (110),(101) preferential orientation.

doping with Antimony caused increase the grain size, decrease of dislocation density, micro strain, and interplaner spacing in general.

الخلاصة

في هذا البحث تمت دراسة أغشية ثاني أوكسيد القصدير(SnO_2) النقي والمشوب بالأنتيمون بالنسب الوزنية (1,2,3,4,5)% المحضرة بطريقة الترسيب الكيميائي الحراري على قواعد زجاجية بدرجة حرارة (550°C) وبسمك (250nm).

أظهرت نتائج حيود الأشعة السينية أن جميع الأغشية هي ذات تركيب متعدد التبلور مع ظهور الاتجاهين التفضيليين (101) و(110).

التشويب بالأنتيمون أدى إلى زيادة الحجم البلوري، وتناقص كل من: كثافة الانخلاع، المطاوعة الميكروية والمسافة بين السطوح الذرية بشكل عام.

المقدمة

مادة(SnO_2) من المواد شبه موصلة التي تنتمي إلى مجموعة الأكاسيد الموصلة الشفافة (Transparent Conducting Oxides(TCO)) التي تمتاز بنفاذية عالية في المنطقة المرئية وامتصاصية في المنطقة فوق البنفسجية وتوصيلية جيدة من النوع السالب (n-type) (1,2)، وتمتلك الأغشية الرقيقة المحضرة من مركب(SnO_2) فجوة طاقة عالية تقريبا(3.5-4 eV) وتصلح أن تستعمل كنافذة للخلايا الشمسية(3).

يهدف هذا البحث إلى تحضير أغشية رقيقة من مادة ثاني أوكسيد القصدير(SnO_2) النقي والمشوب بالأنتيمون(SnO_2:Sb) بالنسب الوزنية %(1,2,3,4,5) ، ودراسة خصائصها التركيبية وتأثير نسب التشويب فيها بواسطة حيود الأشعة السينية (XRD).

المواد وطرائق العمل

تم تحضير أغشية(SnO_2) باستخدام مادة كلوريدات القصدير المائية ($SnCl_4.5H_2O$) وزنها الجزيئي (350.58gm) وهي عبارة عن مسحوق أبيض سريع الذوبان بالماء، وتم تحضير الأغشية المشوبة بالانتمون من($SbCl_3$) وزنها الجزيئي(228.11) بنسب تشويب وزنية %(1,2,3,4,5)، باعتماد مولارية للمحاليل مقدارها (0.1)، بطريقة الترسيب الكيميائي الحراري على قواعد زجاجية مصنوعة من زجاج بأبعاد(1x76x26mm) باستخدام منظومة الترسيب الكيميائي الحراري.

لقد اعتمدت الظروف التالية في تحضير الأغشية(درجة حرارة القاعدة (550) درجة مئوية، معدل رش المحلول ($10cm^3/min$)، المسافة العمودية بين فتحة خروج المحلول والقاعدة الزجاجية ($28\pm1cm$)، ضغط الهواء الداخل إلى الغرفة الهوائية الزجاجية ($10^5N/m^2$)، فترة الرش(5) ثوان ثم التوقف لمدة (55) ثانية).

تم استخدام تقنية حيود الأشعة السينية لمعرفة وتشخيص التركيب البلوري للأغشية المشوبة بالفضة وغير المشوبة.

لقد وجد إن مقدار الاتساع الناتج عن الجهاز(β_i) Instrumental broadening) ينشأ عن المكونات البصرية غير المثالية المستخدمة في الجهاز مثل عرض الشق (فتحة خروج أشعة أكس Slit) (width) وعرض الطول الموجي (Wavelength widths)، التي يجب تصحيحها للحصول على الحجم البلوري الصحيح(4). أما في البلورة المثالية(الخالية من العيوب) كما هو الحال في بلورة السليكون القياسية(Standard defect free Si sample) إذ لا يوجد اتساع في منحنى الحيود لهذه البلورة، فيظهر الاتساع الناتج عن جهاز حيود الأشعة السينية فقط (5)، ومقدار الاتساع الناتج عن جهاز حيود الأشعة السينية المستخدم في هذه الحسابات يساوي($\beta i \approx 0.11$ (deg.)).

النتائج والمناقشة

تم التعرف على التركيب البلوري للأغشية المحضرة بواسطة جهاز حيود الأشعة السينية(XRD) كما في الشكل(2) وفقا لبطاقة(ASTM)، إذ تبين إن جميع الأغشية المحضرة هي ذات تركيب متعدد التبلور(Polycrystalline)، وأظهرت نتائج (XRD) إن الاتجاهين (110) و(101) أكثر شدة من باقي الاتجاهات وإن الإنماء البلوري (crystal growth)استمر بهذين الاتجاهين في نسب التشويب كما مبين في الجدول(1).

الجدول-1: قيم زاوية الحيود و(FWHM) التي تم الحصول عليها من جهاز حيود الأشعة السينية(XRD)

Sample	Doping(%)	(110)		(101)	
		2θ (deg.)	FWHM (deg.)	2θ (deg.)	FWHM (deg.)
1	0	26.5359	1.825	33.814	01.45
2	1	26.4984	001.9	33.680	1.316
3	2	26.5982	01.85	33.889	01.05
4	3	26.6294	1.762	33.726	1.975
5	4	26.6357	1.775	34.138	1.100
6	5	26.6132	02.17	33.739	001.8
ASTM		26.611		33.893	

استخدمت معادلة العالم (Scherrer) في حساب معدل الحجم الحبيبي وهي[6]:-

$$D = 0.94\,\lambda / [\,\beta \cos(\theta)\,] \qquad \ldots\ldots\ldots\ldots\ldots (1)$$

إذ إن: λ: طول موجة الأشعة السينية الساقطة.

β: عرض المنحنى (بالزاوية النصف قطرية radian) عند منتصف الشدة العظمى (Full Width at Half Maximum) (FWHM).

θ: زاوية براك(بالدرجات Degree).

لإيجاد معدل الحجم البلوري الصحيح يجب إضافة عامل تصحيح للمعادلة الأساسية (1) للأخذ بنظر الاعتبار اتساع منحنى حيود الأشعة السينية(XRD) الناتج عن الجهاز(β_i)، وقد افتُرضت عدة طرق لهذا الغرض منها:-

طريقة (وورين- شرر) والتي تعتبر منحنى حيود الأشعة السينية مشابها لدالة (Cauchy) وتمثلها العلاقة التالية:

$$\beta_{cs} = \beta_m - \beta_i \quad \ldots\ldots\ldots (2)$$

إذ إن:

β_m : عرض منحنى حيود الأشعة السينية عند منتصف الشدة العظمى المقاس عملياً.

β_i : عرض منحنى حيود الأشعة السينية عند منتصف الشدة العظمى الناتج عن الجهاز المستخدم.

β_{cs} : عرض منحنى حيود الأشعة السينية عند منتصف الشدة العظمى الناتج عن البلورة.

بتعويض(2) في العلاقة(1) نحصل على:-

$$\mathbf{D = 0.94\ \lambda / [(\beta_m - \beta_i)\cos(\theta)]} \quad \ldots\ldots\ldots \mathbf{(3)}$$

أما في حال اعتبار منحنى حيود الأشعة السينية مشابهاً لدالة (Gauss) فإن الدقة تكون أعلى بسبب التشابه الكبير بين هذه الدالة ومنحنيات الحيود، فقد اقترح (Warren) التصحيح بالشكل(7):-

$$\beta_{cs}^2 = \beta_m^2 - \beta_i^2 \quad \ldots\ldots\ldots (4)$$

يسمى هذا التصحيح بـ (Warren's Correction)

بتعويض(4) في العلاقة(1) نحصل على:-

$$\mathbf{D = 0.94\ \lambda / [(\beta_m^2 - \beta_i^2)^{1/2}\cos(\theta)]} \quad \ldots\ldots\ldots \mathbf{(5)}$$

إضافة إلى ذلك فقد اقترح(Warren) علاقة تأخذ بنظر الإعتبار المعنى الهندسي وهي(8):-

$$\beta_{cs} = [(\beta_m - \beta_i)(\beta_m^2 - \beta_i^2)^{1/2}]^{1/2} \quad \ldots\ldots\ldots (6)$$

بتعويض(6) في العلاقة(1) نحصل على:-

$$\mathbf{D = 0.94\ \lambda / [[(\beta_m - \beta_i)(\beta_m^2 - \beta_i^2)^{1/2}]^{1/4}\cos(\theta)]} \quad \ldots\ldots\ldots \mathbf{(7)}$$

عند حساب معدل الحجم الحبيبي(D) بتعويض القيم التي تم الحصول عليها من جهاز الحيود والمبينة في الجدول(1) في معادلة (Scherrer) قبل التصحيح (المعادلة(1)) ومعادلة (Scherrer) بعد التصحيح (المعادلة (3)) ومعادلة التصحيح لـ (Warren)(5) ومعادلة(Warren) الثانية(7) التي تأخذ المعنى الهندسي بنظر الإعتبار سنحصل على القيم المبينة في الجدول (2 و 3) للمستويين(110) و (101) على التوالي، إذ يتضح إن قيم معدل الحجم الحبيبي الذي تم حسابه من معادلة (Scherrer) قبل التصحيح هي أقل من القيم الأخرى لأن اتساع الجهاز يضاف إلى اتساع منحنى(XRD) فيكون عرض منحنى الحيود عند منتصف الشدة العظمى (FWHM) أكثر من الاتساع الناتج عن الحبيبات لأنه يمثل مجموع الاتساع الناتج عن الجهاز والاتساع الناتج عن الحبيبات.

نلاحظ كذلك إن الضرب في مقدار الفرق $(\beta_m-\beta_i)$ يبين المقصود بالمعنى الهندسي الذي اقترحه العالم (Warren) إذ تبين النتائج التي تم الحصول عليها من المعادلة (7) إن قيمها أقل من قيم المعادلة (3) وأكبر من قيم المعادلة (5) كما يوضح ذلك الشكل (3 و 4)، عند تشويب (SnO_2) بالأنتيمون(Sb) تستبدل ذرات (Sn) بذرات(Sb) في مواقع الذرات الخارجية والداخلية كما يبين ذلك الشكل(1)(9) .

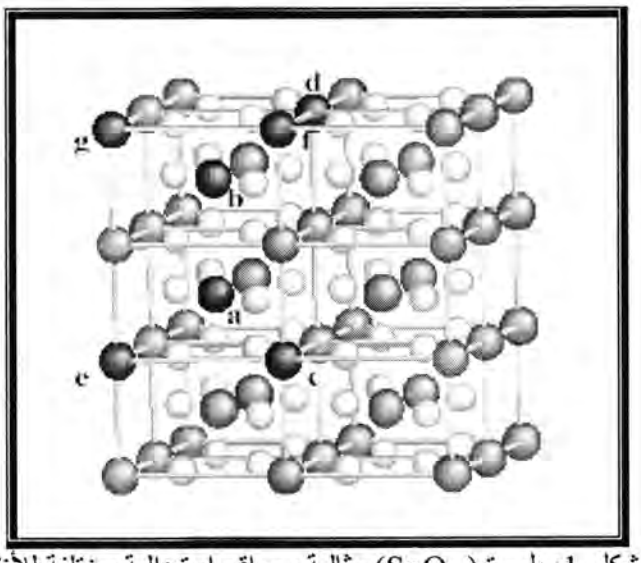

الشكل-1: بلورة (SnO_2) مثالية ومواقع استبدالية مختلفة للأنتيمون فيها، إذ إن (a,b) مواقع داخلية و(c, d, e, f, g) خارجية(9)

كذلك تسهم ذرات الشائبة في ملء الفراغات في الغشاء مما يؤدي إلى تحسين التركيب البلوري وبالتالي زيادة معدل الحجم البلوري إلى أن يصل إلى أعلى قيمة ثم يقل تأثير التشويب بعدها إذ تكون زيادة نسبة الشوائب بمثابة عيوب تتسبب بتناقص الحجم الحبيبي، كما مبين في الشكل(3 و4).

جدول-2: معدل الحجم الحبيبي عند المستوى(110) باستخدام معادلات التصحيح لكل من (Scherrer) و(Warren) ومقارنتها مع معادلة (Scherrer) قبل التصحيح

Doping(%)	D(nm) معادلة (1) (Scherrer)	D (nm) معادلة (3) Scherrer) correction)	D (nm) معادلة (5) (Warren correction)	D (nm) معادلة (7) (Warren geometrical correction)
0	4.67	4.97	4.68	4.82
1	4.48	4.76	4.49	4.62
2	4.61	4.90	4.61	4.75
3	4.84	5.16	4.84	5.00
4	4.80	5.12	4.81	4.96
5	3.93	4.14	3.93	4.03

جدول-3: معدل الحجم الحبيبي عند المستوى(101) باستخدام معادلات التصحيح لكل من (Scherrer) و(Warren) ومقارنتها مع معادلة (Scherrer) قبل التصحيح

Doping(%)	D(nm) معادلة (1) (Scherrer)	D (nm) معادلة (3) (Scherrer correction)	D (nm) معادلة (5) (Warren correction)	D (nm) معادلة (7) (Warren geometrical correction)
0	5.98	6.47	6.00	6.23
1	6.58	7.18	6.61	6.89
2	8.26	9.23	8.31	8.75
3	4.39	4.65	4.39	4.52
4	7.894	8.771	7.934	8.342
5	4.81	5.13	4.82	4.97

تم حساب مقدار كثافة الانخلاعات الناتجة عن الحجم الحبيبي من المعادلة التالية[10]:-

$$\rho = 1/D^2 \qquad .....(8)$$

وذلك باعتماد قيم معدل الحجم الحبيبي في المعادلة (7) على اعتبار أنها تمثل متوسط القيم، ويبين الجدول(4) قيم كثافة الانخلاعات عند المستويين(110) و (101)، والشكل (5) يبين تغيرها كدالة لنسب التشويب، إن زيادة معدل الحجم الحبيبي تعني نقصان كثافة الانخلاعات وذلك لتناقص العيوب البلورية كما توضح ذلك العلاقة الرياضية بينهما في المعادلة (8) إذ تتناسب كثافة الإنخلاع عكسيا مع مربع معدل الحجم الحبيبي.

الجدول -4: قيم كثافة الانخلاع

Doping(%)	D (nm) المعادلة (7)	Dislocation density (10^{12} lines/cm^2)	
		(110)	(101)
0	4.82	4.29	2.57
1	4.62	4.66	2.10
2	4.75	4.41	1.30
3	5.00	3.99	4.88
4	4.96	4.05	1.43
5	4.03	6.13	4.03

قيم المسافة بين السطوح الذرية(d) (Interplaner spacing) التي تم الحصول عليها من جهاز حيود الأشعة السينية والمبينة في الجدول(5) تم اعتمادها لحساب ثوابت الشبيكة (a,c) من العلاقة التالية (11):-

$$(1/d^2) = (h^2 + k^2 / a^2) + (\ell^2 / c^2) \quad .....(12)$$

إذ إن : (hkℓ): معاملات ميلر.

(a,b,c) : تمثل أبعاد الشبيكة، إذ إن (a=b≠c).

علما إن النسبة بين (a,c) تعطى في بطاقة (ASTM) بالعلاقة التالية:-

$$(c/a) = 0.6726 \quad .....(13)$$

الجدول -5: ثوابت الشبيكة لجميع نسب التشويب مقارنة مع القيم القياسية (ASTM)

Sample	Doping (%)	d(nm)		a (nm)		c (nm)	
		(110)	(101)	(110)	(101)	(110)	(101)
1	0	0.33563	0.26487	0.47465	0.47457	0.31925	0.31919
2	1	0.33610	0.26589	0.47531	0.47639	0.31969	0.32042
3	2	0.33486	0.26430	0.47356	0.47355	0.31852	0.31851
4	3	0.33447	0.26553	0.47302	0.47576	0.31815	0.32000
5	4	0.33440	0.26242	0.47291	0.47019	0.31808	0.31625
6	5	0.33467	0.26544	0.47330	0.47559	0.31834	0.31988
ASTM		**335020.**	**0.26445**	**473820.**		**0.31871**	

وهذه القيم متطابقة بشكل جيد مع قيم البحث(12).

تغير المسافة بين السطوح الذرية(d) يعني وجود تشوه في البلورة(Crystal distortion) ويسمى(المطاوعة الميكروية) (Micro strain) مما يعني إن (d) لا تكون متساوية في كل نقطة من نقاط البلورة، ويمكن حساب المطاوعة الميكروية(δ) من المعادلة التالية[13]:-

$$\delta = [\,|\,C_{ASTM} - C_{XRD}\,|\,/\,C_{ASTM}\,] * 100\% \quad ..... \quad (14)$$

إذ إن :-

C_{ASTM}: مقدار ثابت الشبيكة(c) القياسي.

C_{XRD} : مقدار ثابت الشبيكة (c) المقاس عن طريق جهاز الحيود(XRD).

الجدول(6) يبين قيم المطاوعة الميكروية عند المستويين(110) و (101)، والشكل(6) يبين تغيرها مع نسب التشويب، إذ نلاحظ إن تغيرها متشابه في كلا المستويين مما يعني أن التأثيرات التي تتسبب في تشوه السطوح الذرية الناتج عن تغير(d) متشابهة.

وفي كلا المستويين(110) و (101) نلاحظ إن زيادة(d) عن قيمتها القياسية في بطاقة (ASTM) المبينة في الجدول(5) تؤدي إلى تناقص زاوية الحيود(2θ)، ففي الشكل(8) نلاحظ إن زيادة(2θ) للمستوى(110) تعني تناقص(d) كما في الشكل(10)، ونفس الشيء يقال للمستوى(101)، لأن التناسب بينهما عكسي كما مبين في معادلة براك[11] (Bragg):-

$$n\lambda = 2d \sin(\theta) \quad .....(15)$$

(n): تمثل مرتبة الحيود، وغالباً تؤخذ مرتبة الحيود الأولى (n =1).
(λ): الطول الموجي للأشعة السينية الساقطة ويساوي(0.15406 nm) .
(θ) : زاوية براك (Bragg's angle).

الجدول-6: قيم المطاوعة الميكروية

Doping(%)	Micro strain (10^{-3}) (110)	Micro strain (10^{-3}) (101)
0	1.835	1.599
1	3.226	5.445
2	0.468	0.552
3	1.617	4.117
4	1.850	7.638
5	1.020	3.754

1- أدى التشويب بالأنتيمون إلى زيادة الحجم البلوري بشكل عام، وتناقص كثافة الانخلاع، والمسافة بين السطوح الذرية.
2- أدى التشويب إلى تناقص المطاوعة الميكروية للنموذج المحضر بهذه الطريقة لكلا المستويين(110) و (101) بشكل متشابه مما يعني إن التأثيرات التي تتسبب في تشوه السطوح الذرية الناتج عن تغير(d) متشابهة.
3- أدى التشويب إلى زيادة حجم الشبيكة للنموذج المحضر بهذه الطريقة بشكل عام لكلا المستويين(110) و (101).

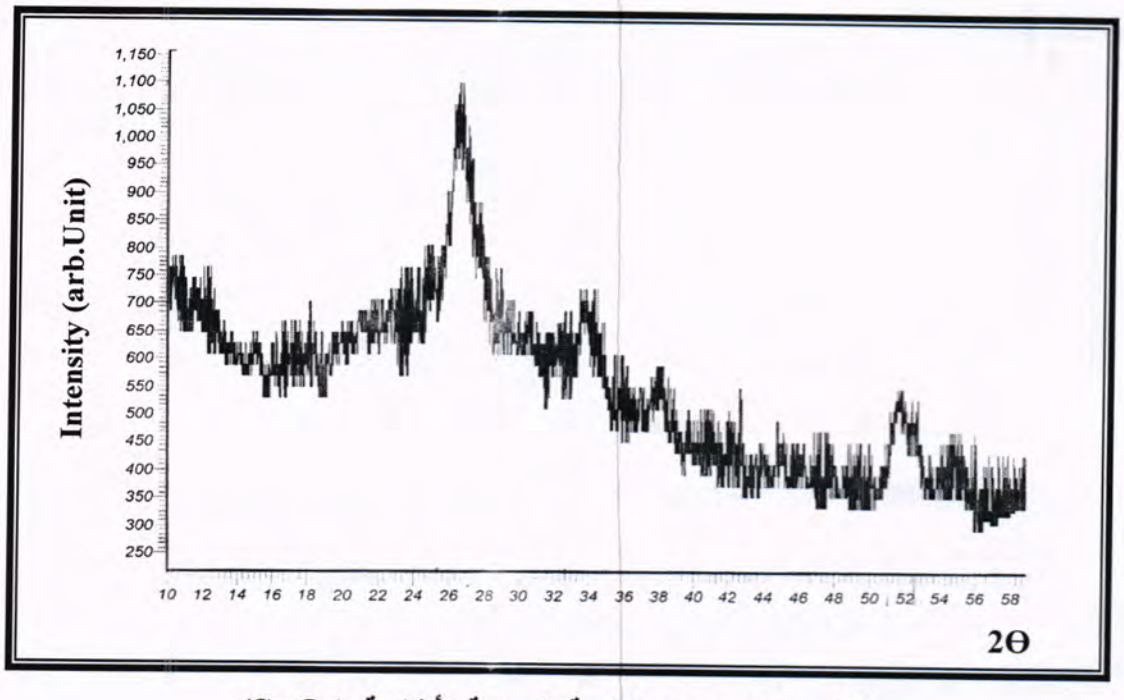

شكل- 2 : حيود الاشعة السينية لأغشية (SnO_2)

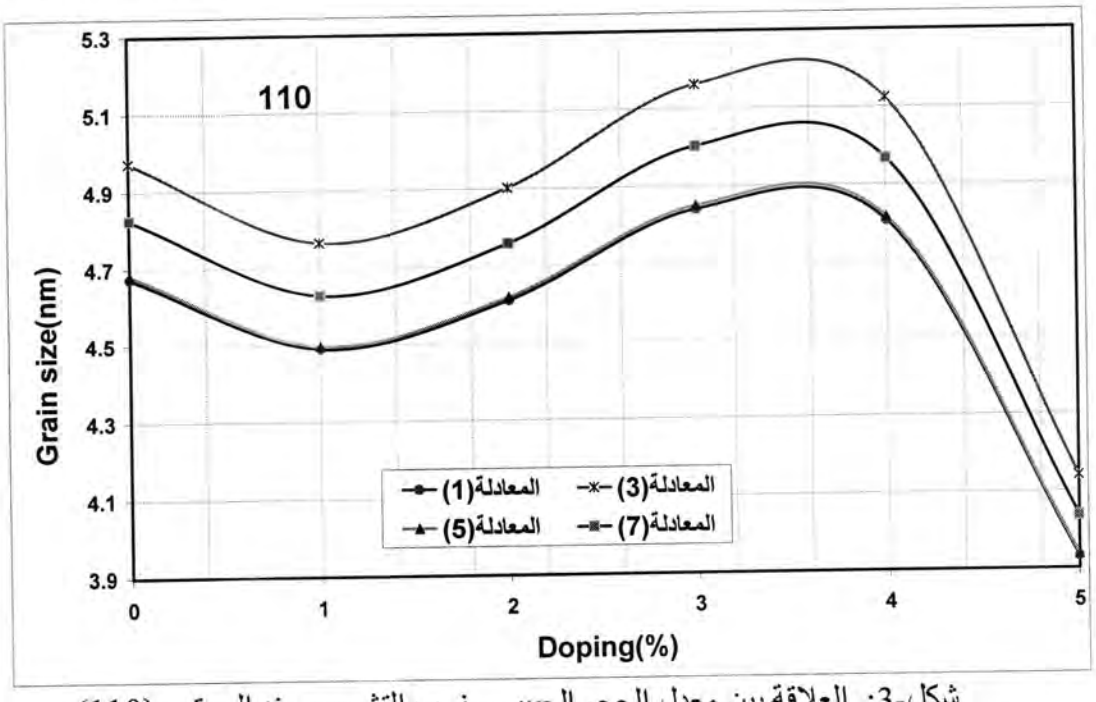

شكل-3: العلاقة بين معدل الحجم الحبيبي ونسب التشويب عند المستوى(110)

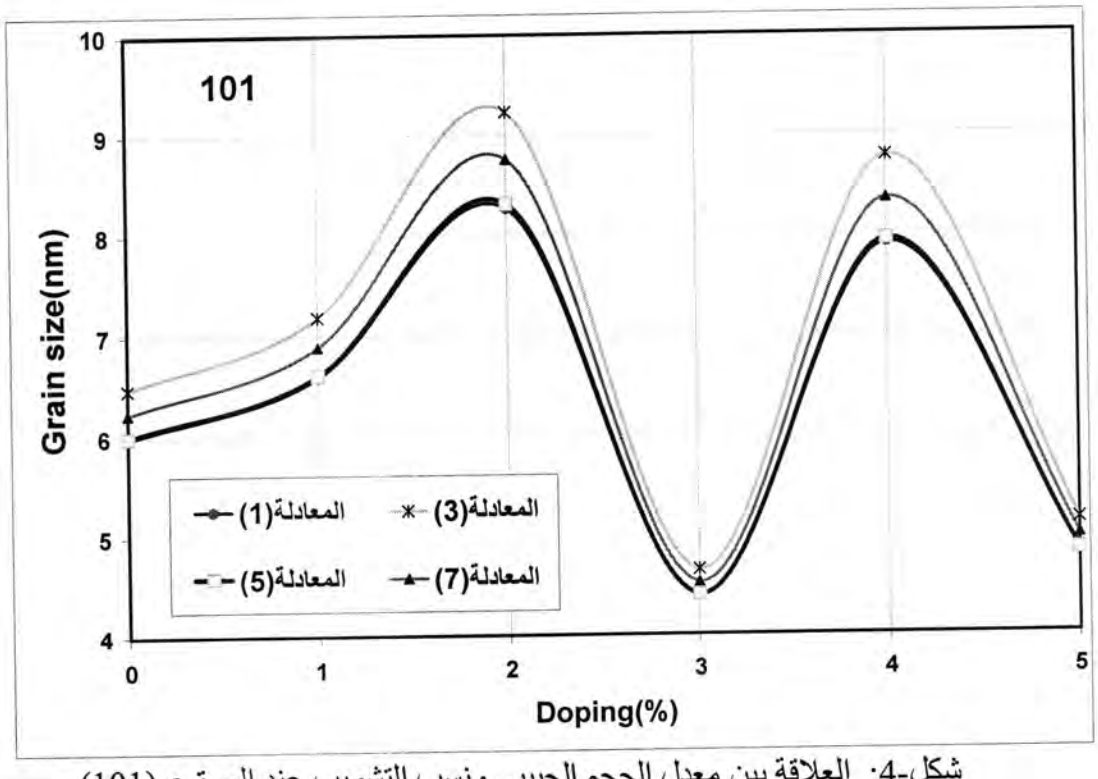

شكل-4: العلاقة بين معدل الحجم الحبيبي ونسب التشويب عند المستوى(101)

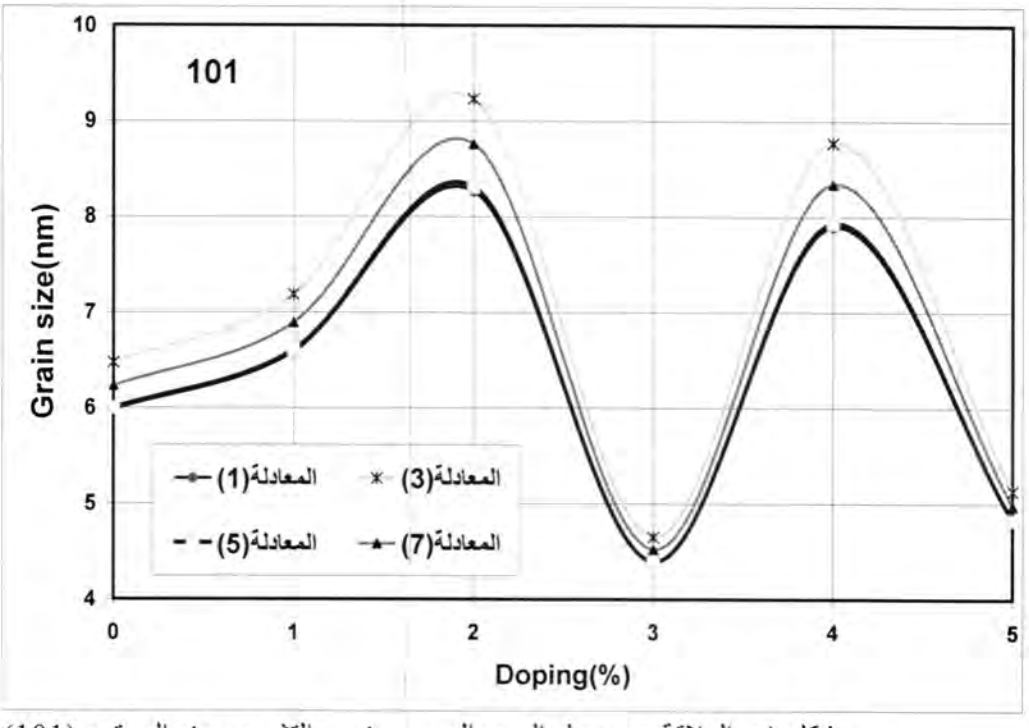

شكل-4: العلاقة بين معدل الحجم الحبيبي ونسب التشويب عند المستوى(101)

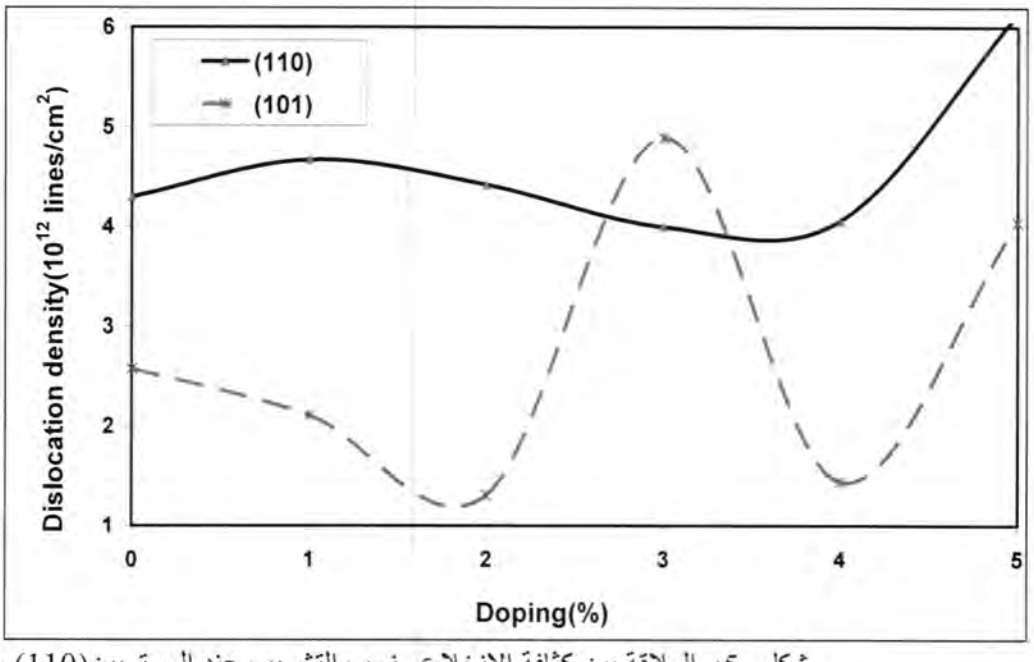

شكل -5: العلاقة بين كثافة الانخلاع ونسب التشويب عند المستويين(110) و(101)

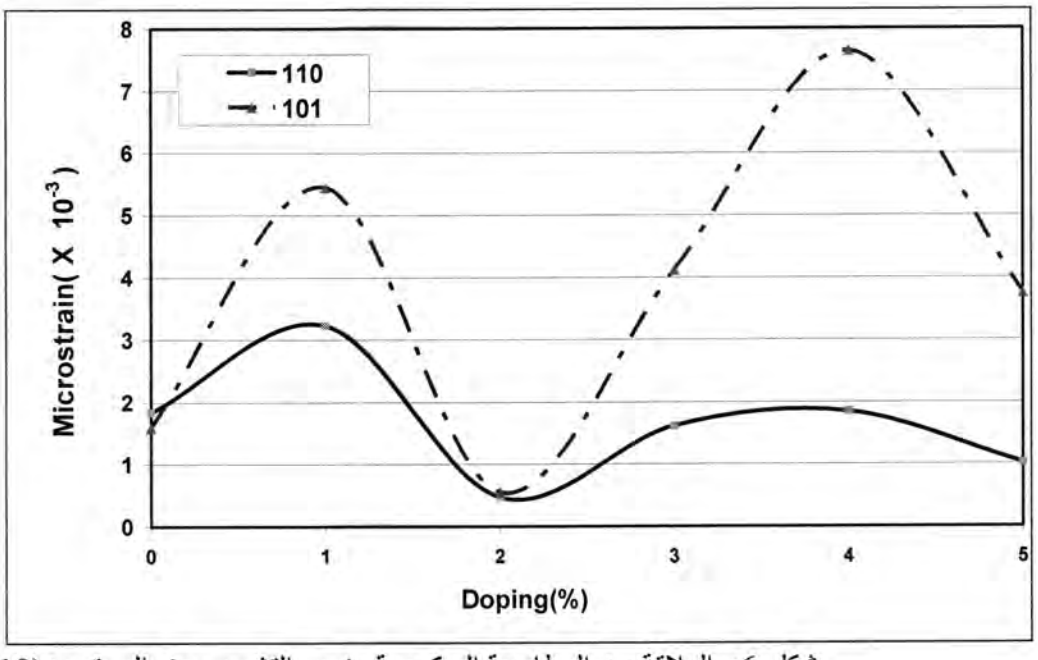

شكل-6: العلاقة بين المطاوعة الميكروية ونسب التشويب عند المستويين(110 و 101)

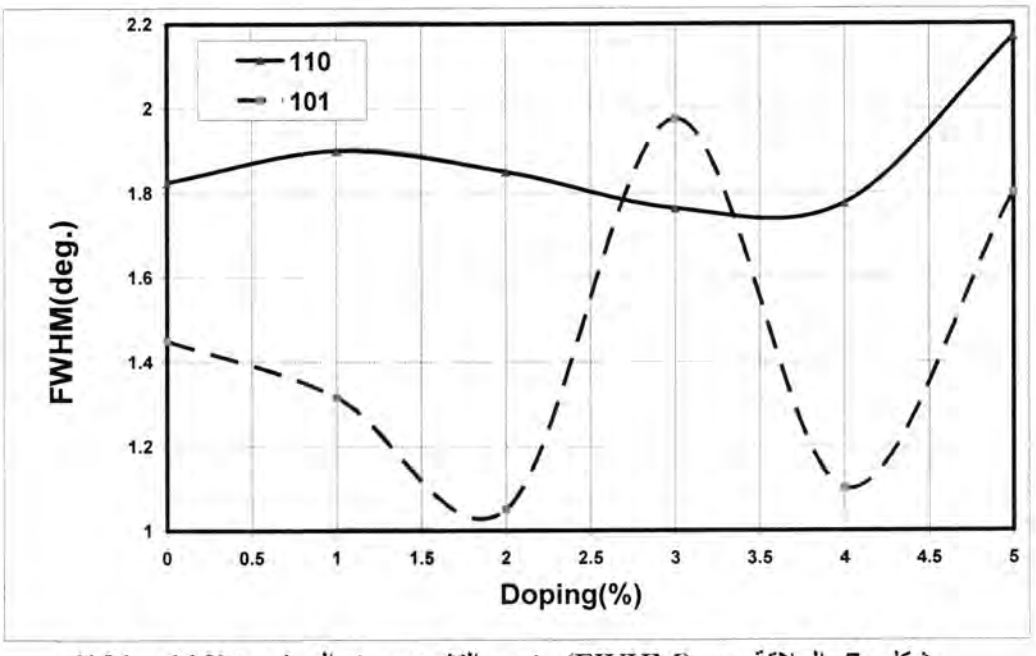

شكل -7: العلاقة بين (FWHM) ونسب التشويب عند المستويين(110 و 101)

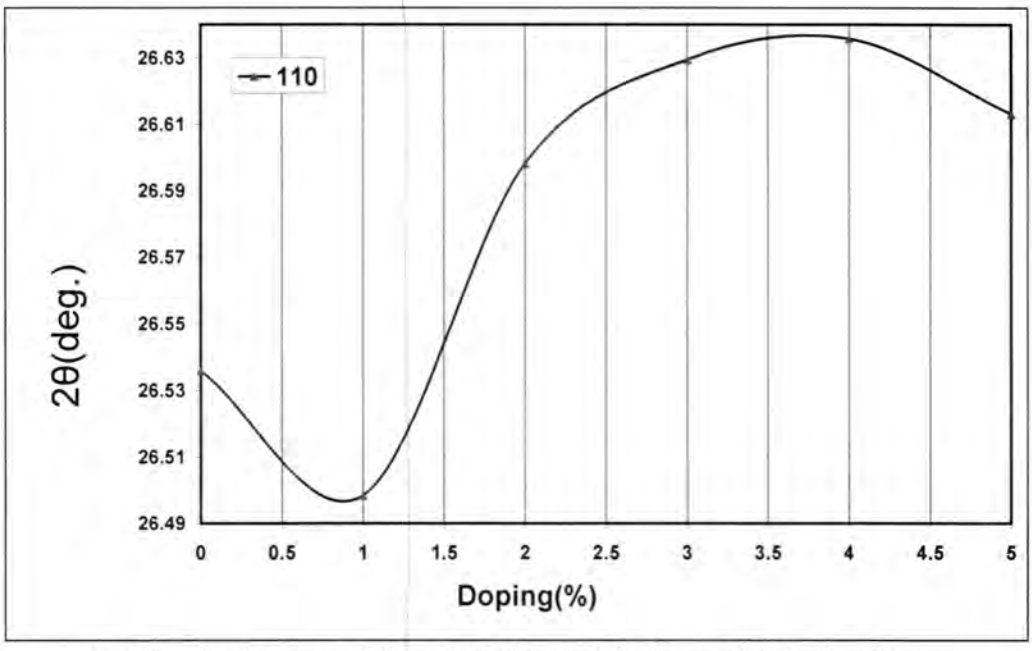

شكل -8: العلاقة بين زاوية الحيود(2θ) ونسب التشويب عند المستوى(110)

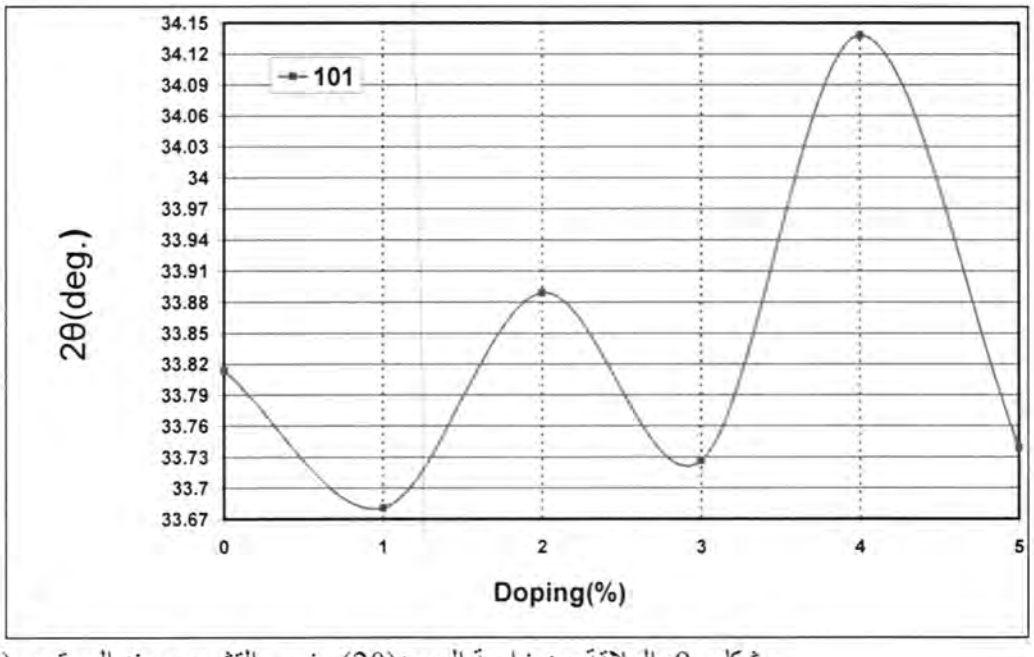

شكل -9: العلاقة بين زاوية الحيود(2θ) ونسب التشويب عند المستوى (101)

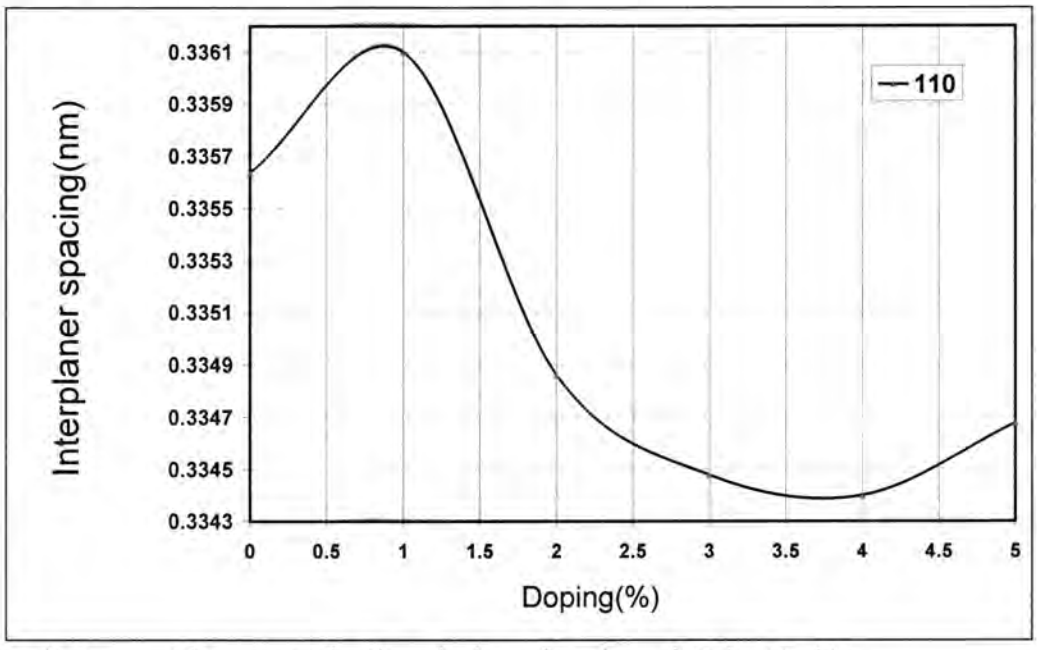

شكل-10: العلاقة بين المسافة بين السطوح الذرية(d) ونسب التشويب عند المستوى(110)

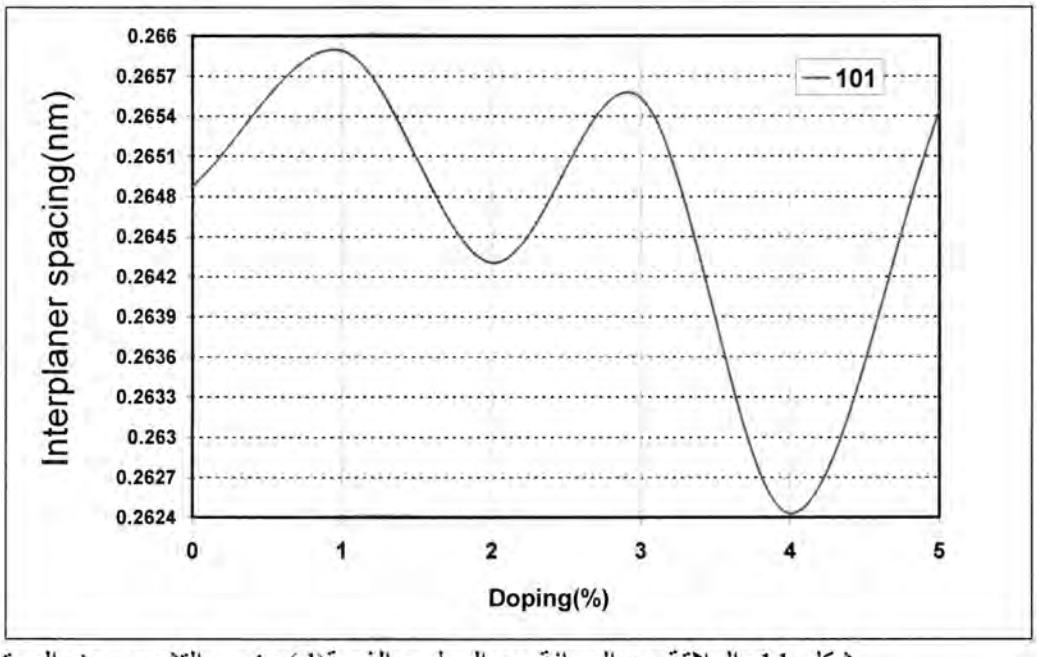

شكل-11: العلاقة بين المسافة بين السطوح الذرية(d) ونسب التشويب عند المستوى(101)

المصادر

1. Shawqi. Khalaf. Mohammad ," Studies on optical properties of Tin oxide (SnO_2) thin film doped by Silver oxide (Ag_2O) prepared by the chemical spray pyrolysis"(2005) .

2. Mohammad .Odda. Dawood,"Improvement the efficiency of the Silicon Solar cell by using some oxides TCOs to layer antireflection," M.sc.thesis .Science college ,AL-Mustansiriya university (2006) .
3. S. C Ray, M. K. Karanjai, D. Dasgupta, Surface & Coatings Technol. 102, 73 (1998).
4. Sattar Aboud Abass AL-Agudee," Determination of Crystallite Size and Strain in MgO prepared by Thermal Decomposition",University Of Saddam,Ph D. thesis, 15-18 , (1997).
5. P.Mukherjee, A. Sarkar, P.Barat, Baldev Raj and U.Kamachi Mudali," Microstructural studies on lattice imperfections in irradiated Titanium and Ti-5%T a-2%Nb by X-Ray Diffraction Line Profile Analysis",Kalpakkam-603 102.
6. A. I. Gusev and S. V. Rempel," X-ray Diffraction Study of the Nanostructure Resulting from Decomposition of (ZrC) 1 – x (NbC)x Solid Solutions",Inorganic Materials, 39(1) :43–46,(2003).
7. L.V. Azarooff, " Elementary of X-Ray Crystallography " Mc Graw-Hill Book Company: 552-556(1968).
8. Th.H.DE.Keijser, et al., J. Appl. Cryst., 15:308-314(1982) .
9. V. Geraldo, L. V. Scalvi, C. V. Santilli, V. Briois," X-ray absorption study of Sb-doped SnO_2 thin films preparedby sol-gel dip-coating method",(2007).
10. A. Moses Ezhil Raj, L. C. Nehru, M. Jayachandran, and C. Sanjeeviraja," Spray pyrolysis deposition and characterization of highly (100) oriented magnesium oxide thin films", Cryst. Res. Technol. 42,(9:) 867 – 875 / DOI 10.1002/crat.200710918(2007).
11. مؤيد جبرائيل يوسف، " فيزياء الحالة الصلبة " , ((1987)
12. Shigetoshi MURANAKAY, oshichika B ANDO a nd Toshio TAKADA," Preparation and Properties of Sb-doped Sn02 Films by Reactive Evaporation" Bull. Inst. Chem. Res., Kyoto Univ., 64, (4) (1986).
13. T. Obata , K. Komeda , T. Nakao , H. Ueba , and C. Tasygama , J. Appl. Phys. , 81, 199, (1997).

دراسة وضوح الكتابة بالالوان المختلفة على لوحة بيضاء في حالة الاضاءة الضعيفة

علي عبد داود الزكي واحلام مجيد كاظم وبشرى خماس
الجامعة المستنصرية / كلية العلوم / قسم الفيزياء

ABSTRACT

The good lightness inside class room is important for resolution of written lesson on the board it's one of the condition to connect the lesson and to protect the student safety, we write three texts (black, green, blue) on a board inside class room without use florescent, we only indirect sun light that come from window. The text on different distances from the board mean contrast picturing using digital camera has been study as a function of distance between board and digital camera. The image edge estimated using soble operator for three texts to introduce which color that give best resolution in the case absent lighting inside class room. It is found that using black color in writing given god result in resolution of written text picture on the board.

الخلاصة

ان الاضاءة الجيدة داخل غرفة الصف لها دور مهم جدا في وضوحية الدرس المكتوب على السبورة وهو من الشروط التي يجب مراعاتها لتوصيل المادة العلمية وللمحافظة على سلامة الطلاب من نواحي عديدة , تم كتابة ثلاث نصوص (اسود,اخضر,ازرق) على سبورة في صف دراسي وبدون تشغيل لمصابيح الصف وتم الاعتماد على ضوء الشمس الداخل من الشباك وصورت النصوص بواسطة كاميرا رقمية وعلى عدة مسافات من السبورة وتم دراسة معدل التباين كدالة للمسافة الفاصلة بين السبورة والكاميرا الرقمية لصورة الحافات الناتجة من استخدام مؤثر سوبل للنصوص الثلاثة لمعرفة أي لون هو الاكثر وضوحية في حالة عدم وجود انارة داخل الصف الدراسي. واظهرت النتائج ان استخدام اللون الاسود في الكتابة يعطي نتائج جيدة في وضوحية صورة النص المكتوب على السبورة.

المقدمة

الإنسان الذي يشاهد أي من مصادر الضوء سيدرك المصادر بشكل مختلف . فضوء الشمس يبدو كضوء ساطع جدا بلون ابيض يميل إلى الصفرة ، وضوء المصباح الزئبقي يكون ساطع جدا بلون ابيض مزرق ، أما ضوء الليزر فيولد شعاعا متلألئاً . الشكل (1) يبين توزيع شدة الضوء لمصادر الضوء المختلفة .

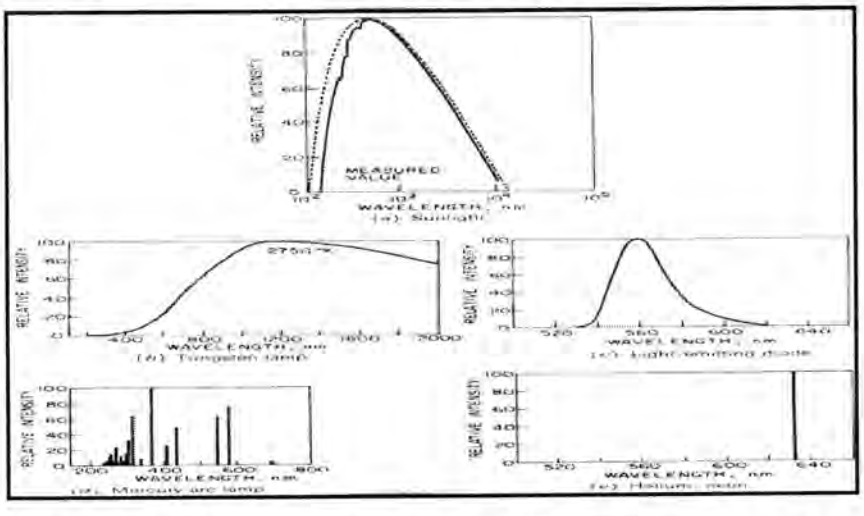

شكل - 1 : توزيع شدة الضوء لعدة مصادر شائعة للضوء (ضوء الشمس ، مصباح التنكســـتن ، الثنائي المشع للضوء ، مصباح الزئبقي ، ليزر الهليوم - النيون) (1)

تعتمد قابلية المشاهد على رؤية أي جسم على حجم الجسم ، التباين ، الإضاءة ، موقع الجسم من المحور البصري مقدار الضوضاء في المشهد . يمكن تصور العين البشرية كنظام موجب ثنائي العدسة يُسقط

صورة حقيقية على سطح حساس للضوء يمر الضوء الداخل إلى العين من خلال القزحية iris وهي عبارة عن بقعة في فتحة العين . يتغير بؤبؤ العين ما بين mm (2 – 7) متكيفا مع مستوى ضوء المحيط ، ثم يمر خلال العدسة التي يتغير بعدها البؤري بواسطة العضلات المرتبطة بها (2).

الأشعة التي تصل الى العين , سواء كانت قادمة من الشمس او من مصادر ضوئية أخرى , تتجاوز عادة مدى الضوء المرئي . والحقيقة ان الشبكية تتأثر الى حد بعيد بالأشعة الضوئية الواقعة في المنطقة فوق البنفسجية . ان قرنية العين تمتص معظم طاقة الأشعة التي يكون طولها الموجي اقل من 3×10^{-7} متر ، اما تلك الاشعة الضوئية الواقعة في المنطقة تحت الحمراء والتي يبلغ طولها الموجي أكثر من 12×10^{-7} متر فيتم امتصاص معظم طاقتها من جزئيات الماء الموجودة في القرنية (3). وعلى اية حال فان الإصباغ العينية لا تستجيب مطلقا للضوء الذي يبلغ طوله الموجي أكثر من 8×10^{-7} متر كما انها لا تكون حساسة جدا للضوء الذي يبلغ طوله الموجي أكثر من 7×10^{-7} متر ، والعين لا تستجيب بنفس الدرجة لجميع الألوان في المنطقة المحصورة بين طول موجي قدره $10^{-7} \times 7 - 10^{-7} \times 3.8$ متر. ان استجابة العين في النور الساطع مختلفة عن استجابتها في النور الخافت ، فإذا كان الشخص في محيط ساطع الإنارة قيل عنه انه متكيف للضوء الساطع وانه يستعمل الأبصار في النور، أما أذا كان الشخص في محيط معتم قيل عنه انه متكيف للعتمة وانه يستعمل الأبصار في العتمة . وفي أي من هذين المحيطين يمكن ان يطلب من شخص الجلوس مقابل شاشة يمكن إنارة قسم منها بومضات من الضوء المكون من لون واحد ولفترات ذات أمد قصير بحيث يمكن تغير شدة الضوء عندئذ تعرف عتبة ذلك اللون بأنها شدة الضوء اللازمة لكي يستطيع الشخص الجالس رؤية 50% من الومضات . وأن معكوس هذه الكمية يدعى بالتألق والشكل(2) يبين منحنيات التألق لعين نموذجية . المنحني الصلد يمثل نتائج الإبصار في العتمة ، اما المنحني المنقط فيمثل نتائج الإبصار في النور . وبالرغم مما يبدو من ان ارتفاع ذروة المنحنين في الشكل متساويان ، الا ان الإبصار في النور يتطلب شدة ضوء أعلى مما يتطلبه الإبصار في العتمة ان هذه النتيجة بطبيعة الحال مألوفة عند الجميع فالعين المكيفة للنور الساطع لا تستطيع رؤية أي شيء في الغرفة المعتمة عند إطفاء النور فيها بعد فترة وجيزة تتكيف العين للعتمة وعندها يكون كل شيء مرئيا في الغرفة (4)

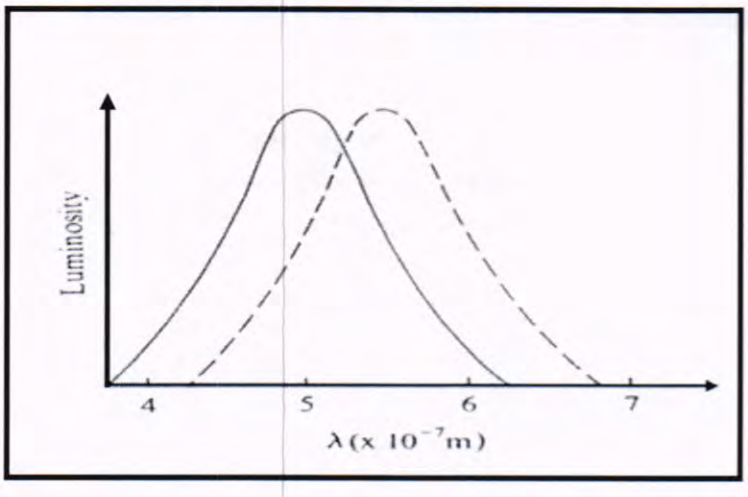

شكل- 2: منحنيات التألق لعين الإنسان (4)

هنالك العديد من الدراسات السابقة التي أهتمت بتحسين الصور الملونة من خلال تحسين التباين والاضائية لها وفيما يلي أيجاز أهم هذه الدراسات

- في عام2003 اقترح الباحث وليام ثومسون خوارزمية معالجة لتحسين الصور للمناظر الليلية، حيث تمكنت هذه الخوارزمية من جعل الصور المأخوذة في ضوء النهار وكإنها مأخوذة ليلاً حيث تقوم بتقليل التباين وتقليل اضائية الصورة. وجعل الصور بازاحة زرقاء، وشملت دراستهم المناظر الحقيقية المشاهدة ليلاً والضوضاء المرافقة لها ومقدار التشوه الحاصل فيها(5).

- في عام2005 اقترح الباحثان Aditi Majumder و Sandy Irani تقنية لتحسين تباين الصورة باستخدام حساسية التباين البشري حيث يتم تحسين التباين الصورة الموقعي بوساطة التحكم بميل الصورة الموقعي اعتمادا على الدراسة التي اثبت ان حساسية تباين العين البشرية في تمييز التباين تخضع لقانون ويبر (Weber) لمستويات ما فوق العتبة وان هذه الطريقة تقوم بتحسين التباين دون تقسيم الصورة سواء في المجال المكاني او المجال الترددي(6) .
- في عام 2005 درست الباحثة Ayten Noori Husian Al-Biaty جودة الصورة الاختباريه بتحديد الحافات بالأعتماد على حساب التباين Contrast لمناطق الحافات في الصورة اضافه الى الخصائص الأحصائيه (المعدل Mean والأنحراف المعياري STD) لتلك المناطق (7)

الكاميرا الرقمية

ان التطور الهائل في التقنية الحاسوبية ، والتقدم الكبير في مجال التسجيل الرقمي للصور ، ساعد على ظهور الأجهزة التي تسمح بالحصول على الصورة بدون معالجة كيميائية . أن أهم المزايا التي يوفرها التصوير الرقمي هي ثبات جودة الصورة بغض النظر عن طول فترة التخزين وإمكانية المعالجة بالحاسوب . عند استعمال الكاميرات العادية (غير الرقمية) فان الصورة في هذه الحالة ناتجة من تحسس الإشارة الضوئية بوساطة متحسسات كيميائية (الفيلم) . يتكون الفيلم من بلورات هاليدات الفضة ، ولإظهار الصورة يتم بوضع الفيلم في محاليل كيميائية تعمل على أظهار وتثبيت الصورة ، بينما الكاميرات الرقمية تحتوي بدلا من الفيلم على متحسسات ضوئية ، حيث تتركز الصورة على بلورة شبه موصلة حساسة للضوء تسمى جهاز الشحن المزدوج Charge Coupled Device ويرمز لها اختصارا CCD والكاميرا الرقمية تتكون من الأجزاء الآتية (8)

1. وحدة الكاميرا التي تحتوي على شريحة CCD ، والنظام البصري المكون من العدسات المستخدمة للتقريب والتبعيد والتبئير والتحكم بفتحة العدسة .
2. شاشة العرض (Liquid Crystal Display) واختصارا يرمز لها LCD .
3. الوحدة التي تحول الإشارة التماثلية الى إشارة رقمية Analog to Digital Signal Converter(ADC)

المواد وطرائق العمل

باستخدام كاميرا رقمية تم التقاط ثلاث صور رقمية لثلاث نصوص مكتوبة بثلاث الوان مختلفة (الاسود ,الاخضر , الازرق) على السبورة والشكل (3) يوضح صور النصوص الثلاثة المستخدمة في البحث ولثلاث مسافات مختلفة.

المسافة الاولى 100 cm

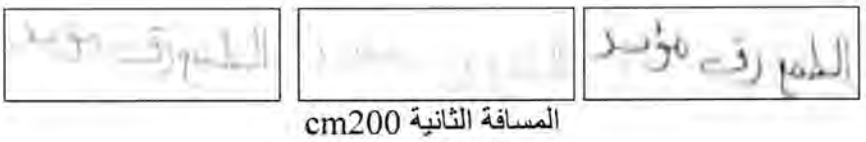

المسافة الثانية cm200

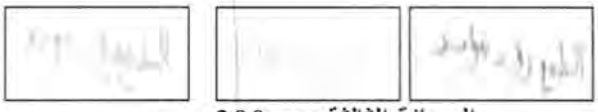

المسافة الثالثة 300 cm

شكل -3: الصور النصية لثلاث مسافات

كتبت النصوص باللغة العربية على سبورة بيضاء اللون معلقة على احد جدران صف دراسي مع عدم تشغيل أي مصدر ضوئي داخل القاعة وبالاعتماد على ضوء الشمس غير المباشر الداخل الى الصف من الشباك والشكل(4) يبين الشكل الهندسي للصف الدراسي.

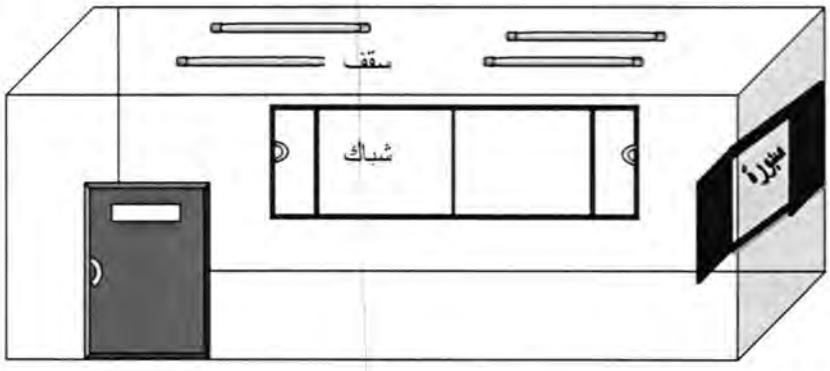

شكل -4 : الشكل الهندسي الصف الدراسي المستخدم في التصوير

إن نوع الكاميرا الفيديويه المستخدمة في الدراسة هي Sony Video Lens كما مبين بالشكل (5) وأهم مواصفاتها هي:

- البعدالبؤري Focal Length للعدسات المستخدمة في الكاميرا (50 – 2.5) ملمتر.
- الوضوحية (Resolution) لعدد عناصر الصورة تكون 10240000 Byte × 8= 8MP.

شكل-5: يوضح الكاميرا الرقمية المستخدمة في عملية التصوير

- التكبير البصري للكاميرا هو X 20 .
- التكبير والتصغير الرقمي هو X 990 .

إن الكاميرا الرقمية المستخدمة في منظومة العمل تستخدم حزمة الضوء المرئي(VIS) في التصوير.

التقنيات المستخدمة في البحث

باستخدام مرشح السوبل Soble filter تم الحصول على صورة الحافات لصور النصوص الثلاثة حيث تظهر النقاط التي تمثل حافة باللون الابيض وباقي نقاط الصورة تظهر باللون الاسود كما يوضحها الشكل (6) حيث تم اعتماد خمس عتبات (80,100, 60, 40, 20) لمؤثر السوبل لكل صورة من صور النصوص الثلاثة ولكل مسافة فاصلة بين السبورة والكاميرا الرقمية وتم استخراج معدل التباين $\mu_{contrast}$ لكل صورة حافات (بعتباتها المختلفة) ورسمت العلاقة البيانية لمعدل التباين كدالة للمسافة الفاصلة بهدف دراسة وضوحية الصورة بدون استخدام انارة للصف والاعتماد على ضوء النهار فقط في الرؤية .

شكل -6 : صورة الحافات الناتجة من استخدام مؤثر سوبل

نتائج استخدام تقنية التباين المباشر

تعتمد هذه التقنية على استخدام معادلة التباين وتطبيقها على نقاط الصورة في مناطق الحافات فقط ويتم ذلك بأخذ نافذة ثلاثية حول نقطة الحافات في الصورة والبحث عن اقل I_{min} واعلى قيمة I_{max} في الشدة لعناصر الصورة التابعة للحافات ثم يحسب التباين من العلاقة :

$$CT = \frac{I_{max} - I_{min}}{I_{max} + I_{min}} \qquad (1)$$

يلاحظ من الشكل (7) ان معدل التباين للنص الاسود عند المسافة 100 cm تكون قيمة متباعدة لحافات سوبل المختلفة وتتقارب القيم للمسافتين الثانية والثالثة (200 cm , 300 cm) وللمركبات اللونية الثلاث (R ,G ,B) ومركبة الاضاءة (L) ويقل معدل التباين مع زيادة المسافة الفاصلة بين السبورة والكاميرا الرقمية وللمركبات الاربعة(R-G-B-L) ,اما نتائج المخططات البيانية للنص باللون الازرق فيظهر من الشكل (8) ان معدل التباين يهبط بشكل سريع عند المسافة الثانية وان منحنيات معدل التباين لعتبات السوبل المختلفة تتقارب بشكل ملحوظ اكثر مما هو موجود للنصين الاخضر والاسود وللمركبات الاربعة(R-G-B-L), بالنسبة للنتائج التي حصلنا عليها للنص الاخضر فمن ملاحظة الشكل (9) يظهر ان قيم معدل التباين وللمركبات الاربعة(R-G-B-L) تتباعد لحافات سوبل المختلفة عند المسافة الثالثة اكثر مما هو موجود للمسافتين الثانية والاولى

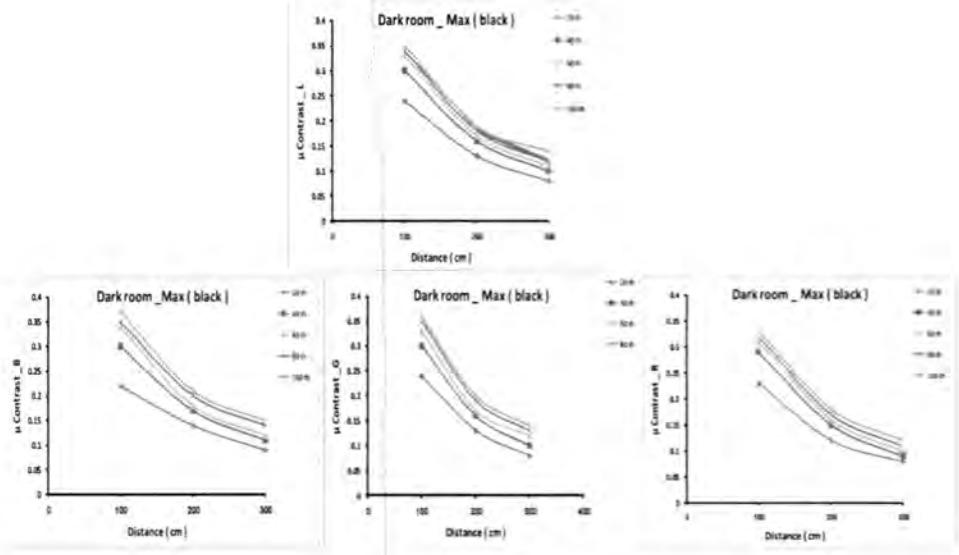

شكل - 7 :العلاقة بين التباين كدالة للبعد بين كاميرا التصوير والسبورة و للحزم اللونية RGB للنص الاسود

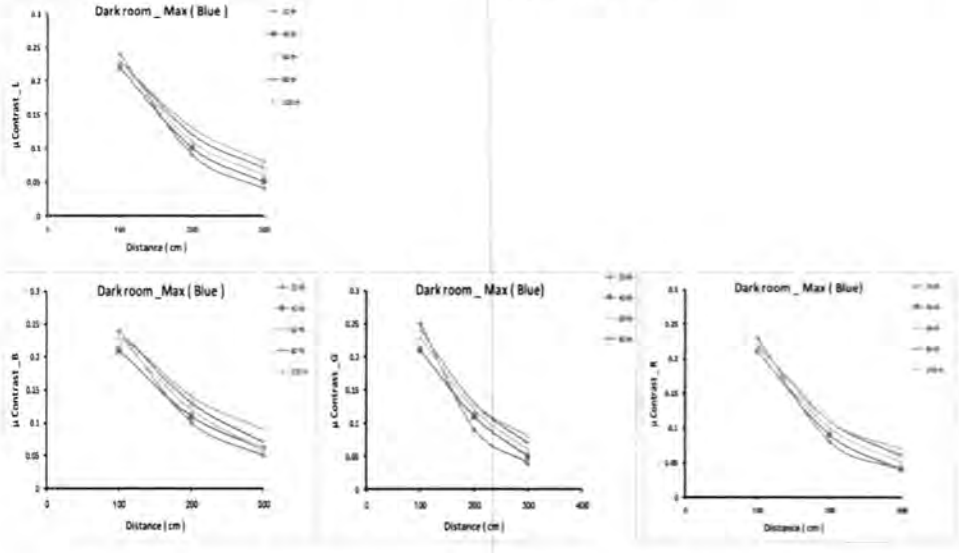

شكل - 8 :العلاقة بين التباين كدالة للبعد بين كاميرا التصوير والسبورة و للحزم اللونية RGB للنص الازرق

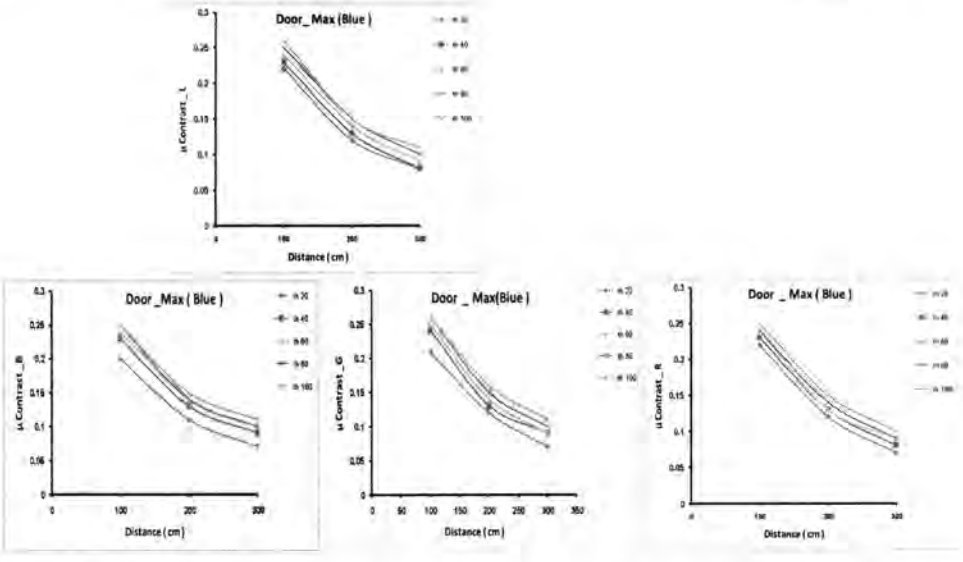

شكل - 9 :العلاقة بين التباين كدالة للبعد بين كاميرا التصوير والسبورة و للحزم اللونية RGB للنص الاخضر

نتائج تقنية التباين الأصغر والأكبر

أن هذه الطريقة تعتمد على عنصر الحافات لحساب التباين حيث يؤخذ نافذة ثلاثية حول العنصر الوسط الذي سيعتبر العنصر الأصغر وأيجاد أكبر عنصر من العناصر المجاورة للعنصر الوسطي بحسب النافذة الثلاثية ويمكن تمثيل هذه الطريقة كما في الشكل (10) :

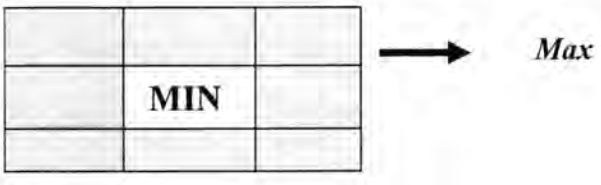

شكل - 10:النافذة الثلاثية حول العنصر الوسطي الأصغر

ثم يحسب التباين من المعادلة (1) ومن ملاحظة الشكل (11) تظهر الزيادة في معدل التباين مع زيادة عتبة المرشح سوبل واضحة بالنسبة للنص الاسود بشكل واضح ويلاحظ هبوط سريع في قيمة معدل التباين للمسافة الثانية ثم تظهر استقرارية نسبية في قيمة معدل التباين وللمركبات الاربعة (R-G-B-L) , اما النص الاخضر فيلاحظ من الشكل (12) ان التقارب بين المنحنيات التي تمثل عتبات السوبل يكون اكبر منه للنصين الاسود والازرق , اما النص الازرق فيظهر ان التباعد للمنحنيات التي تمثل عتبات السوبل يبدو واضحا جدا من خلال الشكل ( ) اكثر مما هو موجود للنصين الاسود والاخضر كما هو واضح من الشكل (13) .

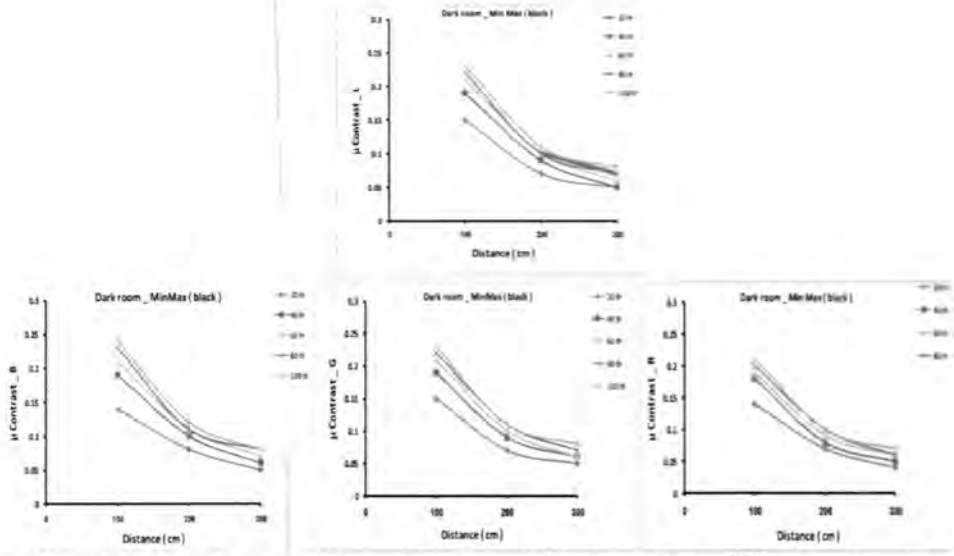

شكل - 11 :العلاقة بين التباين كدالة للبعد بين كاميرا التصوير والسبورة للنص الاسود و للحزم اللونية RGBL

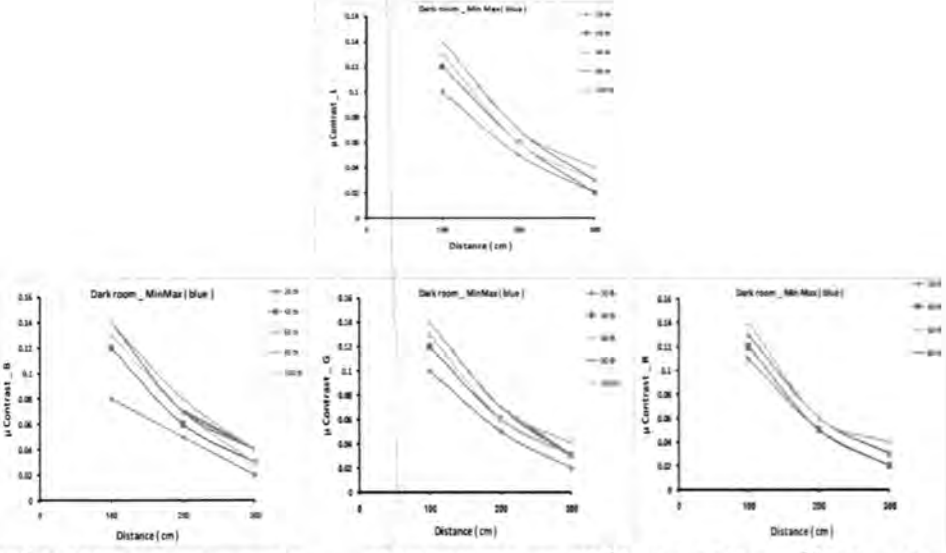

شكل - 12 :العلاقة بين التباين كدالة للبعد بين كاميرا التصوير والسبورة و للحزم اللونية RGB للنص الازرق

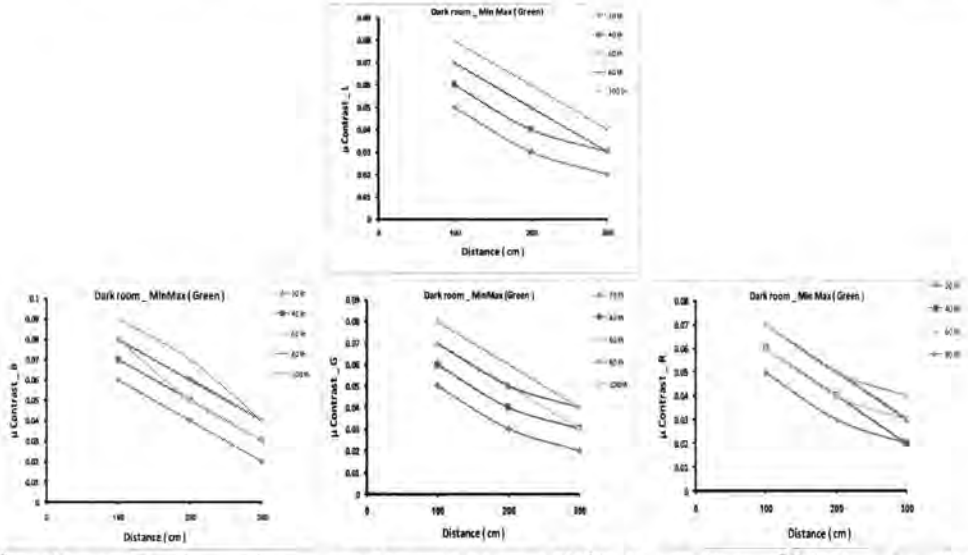

شكل - 13 :العلاقة بين التباين كدالة للبعد بين كاميرا التصوير والسبورة و للحزم اللونية RGBللنص الاخضر

ان النص يكون اوضح كلما قلت المسافة بين السبورة والكاميرا الرقمية وهذا بديهي وتم محاكاتة حاسوبيا وحسابة بشكل كمي والنص الاسود هو الاعلى في معدل التباين من النصين الاخضر والازرق كما يلاحظ هبوط معدل التباين عند المسافة الثانية ثم يلاحظ استقرارية نسبية في معدل التباين مع زيادة المسافة الفاصلة بين السبورة والكاميرا الرقمية ,تتداخل المنحنيات التي تمثل عتبات سوبل بالنسبة للنص المكتوب باللون الاخضر وقد يعود السبب الى ان اللون الاخضر افتح من اللونين الاسود والازرق.

المصادر

1. William K. , " Digital Image Processing " , 3rd ,John Wiley & Sons, Inc. ,ISBNS: 0– 471–37407–5(Hard back),0–471–22132–5 (electronic) ,(2001).
2. Robertr S. , " The Art and Science of Optical Design " , Cambridge University , (1997) .
3. Lioyd J. , " Thermal Imaging System " , Plenum press , New York , (1975) .
4. Desmon D. , Simon G. , " Physics for Biology and per Medical Students " , 2nd edition , University of Dundee , (1975)
5. William.B .Thompson , peter. Shirly , and J.A. Ferwerdo , " A spatial Post Processing Alogrithum for Images of Night Scences " , Auther Address : Unive of Utah and Cornellh Unive. , (2003).
6. Aditi Majumder , Sandy Irani , "contrast Enhancement of Image Using Human Contrast Sensitivity " , Computer Science Department , University of California , Irvine (2005).
7. أيتن نوري البياتي، " تقنيات محسنة لتخمين الحدة في الصورة بالاعتماد على كشف الحافات" ، ، كلية العلوم قسم الفيزياء ، الجامعه المستنصريه ، (2005).
8. Smith S. , " The Scientist and Engineers Guide to Digital Signal Processing " , California Publishing ISBNO–966176–33, (1997) .

دراسة معدل التغير في الاشارة المسجلة بواسطة الويب كاميرا Enet لشدات اضاءة تنكستن مختلفة

شيماء حسين عبد مسلم[1] و هبة خضير عباس[2] و علي عبد داود الزكي[1]
[1]الجامعة المستنصرية –كلية العلوم- قسم الفيزياء
[2] جامعة بغداد -كلية العلوم للبنات-قسم الفيزياء

ABSTRACT

We Study the effect of light intensity on the efficiency of the enet web camera to imaging the White Image (Test Image) A4 we can control to the luminous intensity by change the Voltage on the luminous System ; since we get the 13 different images . In the low voltage range the distribution of luminous intensity will be regular **for three color composites RGB and lighting composites L, and in the higher voltage rang the tungsten lamp given afare from each other, and when study the relation between power and mean we saw the mean value was stable in the low voltage for three color composites RGB and lighting composites L , and in the higher range of power than 0.00234 Watt we get the mean values increased with the power , after that it's begin stable , and the curve of Green band similar to the lighting composites L because it's given a ratio sharing about %60.**

الخلاصة

تم دراسة تأثير تغيير شدة الاضاءة على كفاءة الويب كاميرا ENET لتصوير ورقة اختبارية بيضاء حجم A4 وقد تم التحكم بشدة الاضاءة بتغيير الفولتية المسلطة على منظومة الاضاءة حيث حصلنا على 13 صورة مختلفة . ولاحظنا انه في مدى الفولتيات الواطئة يكون توزيع شدة الاضاءة منتظما للحزم اللونية الثلاث RGB ولمركبة الاضاءة L ،وفي مدى الفولتيات العالية فأن مصباح التنكستن يعطي شدات متباعدة ،وعند دراسة العلاقة بين القدرة والمعدل نلاحظ انه في مدى الفولتيات الواطئة استقرار في قيم المعدل للحزم اللونية الثلاث RGB ولمركبة الاضاءة L ،وفي مدى القدرات الاعلى من Watt 0.00234 تزداد قيم المعدل خطيا مع القدرة ثم تبدأ بالاستقرار ويكون منحني الحزمة الخضراء مشابه الى حد كبير منحني المركبةL وذلك لأنها تعطي مشاركة نسبتها بحدود 60 % في تكوين الشدة L في الصورة.

المقدمة

أن المعالجة الصورية تعد واحدة من أهم مقومات الثورة المعلوماتية التي سهلت أستلام وأرسال المعلومات الرقمية عبر الأقمار الصناعية ومحطات الأرسال لمختلف أرجاء الكرة الأرضية حيث تتركز وظائف المعالجة الصورية حاسوبياً بجانبين :-

الجانب الأول :- يهدف الى معالجة بيانات الصورة الرقمية لغرض تسهيل عملية تحليلها حاسوبياً وتوضيح ملامحها بالنسبة للأنسان .

الجانب الثاني :- يهدف الى معالجة الصورة الرقمية لغرض أستفادة الحاسوب منها في عمليات أخرى وتعرف بالرؤيا الحاسوبيه Computer Vision (1).

يهدف هذا البحث إلى أيجاد معايير كفوءة لتقييم جودة الصور الاختبارية الملتقطة باضائيات المصدر الضوئي المختلفة ودراسة تأثير الإضاءة في تحديد وضوحية الصور الاختبارية التي تستخدم لتحديد كفاءة أجهزة العرض وأجهزة التصوير وأيضا دراسة الحزم اللونية RGB ومركبة الإضاءة L وكيفية تأثرها بالإضاءة المختلفة في الصورة.

الضوء هو شكل من اشكال الطاقة والتي تكون صادرة من مصدر أو منعكس من جسم مثل الشمس أو اللهب أو الشمعة والمصباح الكهربائي ، والضوء بالنسبة للفيزياوي هو نوع خاص من الطاقة يعرف بالطاقة الكهرومغناطيسية وبالنسبة للأنسان فأنه يمثل الأدراك الحسي البصري (2). و تمثل هذه الطاقة الأشعاعية

الكهرومغناطيسية بحزم من الأطوال الموجية المرئيه للعين ومداها المرئي يقع ما بين nm(350 – 700) (3 ، 4) ، أما ما ندعوه بالضوء الأبيض هو في الحقيقة مزيج من الطاقة الأشعاعية لأطوال موجية مختلفة وبنسب مختلفة كما يظهر توزيعها في ضوء الشمس وأي موجة تنفصل من المزيج تشير الى كونها لوناً وبهذا فأن كل من الضوء و اللون متلازمين(5).ويعتمد قياس الضوء على قياس ثلاث كميات اساسية وهي(6):

a.قوة الاضاءة:تقاس قوة الاضاءة عادة بالشمعة وذلك لأن الشمعة كانت بالاصل مصدرا للانارة وحيث ان قوة اضاءة أي مصدر تختلف باختلاف الاتجاه الذي تقاس منه قوة الاضاءة فأن من الضروري أخذ جميع الاتجاهات وحساب معدل قوة الاضاءة على مقياس كروي.

b.السيل او الفيض الضوئي : ان المعدل الزمني لتدفق الاشعة المرئية يسمى بالسيل او الدفق الضوئي أي ان السيل الضوئي هو ذلك الجزء من الطاقة الضوئية الكلية التي يشعها مصدر مضيء خلال وحدة الزمن ويولد الاحساس بالرؤية والابصار . اما وحدة السيل الضوئي فهي لومن (Lumen).

c.الاستضاءة: ان زيادة قوة اضاءة المصدر تسبب زيادة في السيل الضوئي الواصل الى كل وحدة من مساحة السطح وبالتالي زيادة السيل الساقط على وحدة المساحة تلك الزيادة التي تسبب زيادة في شدة استضاءته . وما نعنيه بشدة الاستضاءة هو كثافة السيل على سطح من السطوح .فأذا أضيء سطح اضاءة متجانسة منتظمة في كل ناحيه منه فأن شدة استضاءته عندئذ نسبة بين السيل الساقط على السطح ومساحة ذلك السطح(6).

ان الفكرة الأساسية لعمل المتحسس هو تحويل الطاقة التي يتحسسها الى أشارة كهربائية وذلك بوضع متحسس يتأثر سطحه بدرجة الاضاءة ويحولها الى اشارة كهربائية يمكن تضخيمها وتسجيلها ويمكن بعد ذلك تحويل الإشارة التماثلية إلى أشارة رقمية (7) .

الكاميرا الرقمية

ان التطور الهائل في التقنية الحاسوبية ، والتقدم الكبير في مجال التسجيل الرقمي للصور ، ساعد على ظهور الأجهزة التي تسمح بالحصول على الصورة بدون معالجة كيميائية . أن أهم المزايا التي يوفرها التصوير الرقمي هي ثبات جودة الصورة بغض النظر عن طول فترة التخزين وإمكانية المعالجة بالحاسوب . أن الفرق الوحيد بين الكاميرا الرقمية والكاميرات الأعتيادية (التقليدية) هو وجود أوغياب الفيلم حيث تستعيض الكاميرا الرقمية عن الفيلم بمصفوفة من المتحسسات وتعرف هذه المنظومة او مصفوفة المتحسسات بأسم محول الضوء الى كهرباء أو جهاز الشحنة المزدوجة Charge Couple Device للأختصار تكتب CCD . أن كاميرا CCD تعمل على تحويل الضوء الى شحنات كهربائية وأن قوة هذه الشحنات تتغير تبعاً لقوة الضوء الذي يسقط على عناصرها ولذا فهي تشبه الى حد معين الفيلم وذلك بأستبدال العناصر بنقاط من الطبقات الحساسة للضوء على قطعة من الفيلم حيث نعود الى البداية كأننا نستعمل فيلماً عادياً . فعندما نضغط على مفتاح الكاميرا الرقمية تقوم المتحسسات بتمرير المعلومات التي يتم تحسسها الى محول رقمي ويرسلها الى الذاكرة Ram في الحافظه حيث تخزن وتكون جاهزه للأستعمال (8).

إحصائيات الصورة الرقمية

أن أحصائيات الصورة الرقمية Digital Image Statistics تكون أساسية في أغلب عمليات معالجة الصورة الرقمية. تعتبر في كثير من الأحيان هذه الأحصائيات واصفة لطبيعة الصور وكيفية توزيع المعلومات فيها .والأحصائيات تكون مرتبطة بمبدأ أحتمالية توزيع المعلومات للصورة حيث يمكن أن تعرف دالة أحتمالية توزيع الأضائيةBrightness Probability Density Function بأنها دالة كثافة الأحتمالية للأضاءة وهذه الخواص للصورة g(x ,y) هي(10) :

a) المعدل (μ)

معدل الشدات في الصورة ويعرف بأنه معدل الشدة في الصورة ويحسب المعدل μ من العلاقة الأتية (10).

$$\mu = \frac{1}{MN}\sum_{X=1}^{M}\sum_{Y=1}^{N} I(x,y) \qquad (1)$$

حيث أن I(x,y) يمثل عنصر الصورة في الموقع (x,y).

M طول الصورة ، N عرض الصورة وحاصل ضربها يمثل عددعناصر الصوره .

b) الأنحراف المعياري (σ)

يعرف الأنحراف المعياري بأنهُ مقدار أنحراف قيم الشدة للاشارة للحزم اللونية الثلاث RGB و مركبة الشدة Lعن المعدل ويحسب الأنحراف المعياري (σ) من العلاقة [10] :

$$\sigma = \sqrt{\frac{1}{MN}\sum_{x=1}^{M}\sum_{y=1}^{N}\left(I(x,y)-\mu\right)^2} \qquad (2)$$

ويعتبر هذا المقياس من المعايير المهمة في تحديد مقدار التفاصيل في الصورة ومقدار التذبذب في قيم الاشارة في المناطق المتجانسة من الصورة لذا يمكن من خلاله تخمين الضوضاء كما ونوعا وتوزيعا .

c) معدل مربع الخطأ (MSE)

يعتبر من المعايير التي يتم من خلالها معرفة جودة الصورة ويحسب حسب العلاقة الأتية (10):

$$(MNS) = \frac{1}{MN}\sum_{i=1}^{M}\sum_{j=1}^{N}\left(I(x,y)-I'(x,y)\right)^2 \qquad (3)$$

حيث أن

$I(x,y)$: تمثل بيانات الصورة الأصلية .

$I'(x,y)$: تمثل بيانات الصورة المعالجة أو المشوهه.

d) نسبة الأشارة الى الضوضاء (SNR)

الفرق بين اشارة الصورة الداخلة واشارة الصورة الخارجة هو مقدار للتشوه اوالضوضاء بحيث ان كل إشارة عنصر في الصورة الخارجة تتألف من إشارة عنصر الصورة الداخلة إضافة الى ضوضاء . والإشارة تمثل بصيغ مختلفة حيث يمكن ان تقع بين قيمتين محدودتين كما في العلاقة الآتية(11) :

$$I_{min} < I < I_{max} \qquad (4)$$

لذا فان نسبة الإشارة الى الضوضاء تعطى كما يأتي (11):

$$SNR = 20\log\frac{(I_{max} - I_{min})}{\sigma_n} \qquad (5)$$

حيث ان σ_n يمثل مقدار الانحراف المعياري للضوضاء ، أما إذا كانت الإشارة غير محددة وإنما لها توزيع إحصائي فان نسبة الإشارة الى الضوضاء تعطى وفقا العلاقتين الآتيتين(11) :

$$SNR = 20\log\frac{\mu}{\sigma_n} \qquad (6) \qquad \text{dB}$$

حيث ان μ معدل الإشارة و σ_n الانحراف المعياري للضوضاء .

كما توجد صيغة اخرى لهذا المعيار يعبر عنها بالمعادلة التالية :-

$$SNR = 20\log\frac{\sigma_1}{\sigma_n} \qquad (7)$$

حيث ان σ_I الانحراف المعياري للإشارة و σ_n الانحراف المعياري للضوضاء.
ان حساب نسبة الإشارة الى الضوضاء للصورة الكاملة لا يكون معيار دقيق لوصف جودة الصورة وذلك يرجع الى الاختلافات في سطوع الصورة . لذا يفضل حساب نسبة الإشارة الى الضوضاء موقعيا في المناطق المختلفة المتجانسة المختلفة في الصورة بالاعتماد على معادلة (6)(11) .

المواد وطرائق العمل

منظومة التصوير المعتمدة في الدراسة

ان تصميم آلات التصوير الرقمي يعتمد على المبادئ الصحيحة لقياس الشدة اللونية وتشكل التدابير الوقائية المختلفة امراً ضروريا لضمان أفضل دقة لونية لالتقاط الصورة . ومن هذه التدابير الوقائية هي توفير إضـــاءة ثابتة وكافية لعملية التصوير لهذا يتم صنع صندوق الإضاءة Lighting enclosure يوضع في داخله مصدر ضوئي ، المهم هنا هو ضمان ضبط مصدر الضوء للمشهد المراد تصويره وكذلك تفادي الاختلافات الموجودة في الطبيعة حيث ان موقع الشمس في السماء والظروف الجوية يؤثران في كثافة الضوء الساقط . يساعد صندوق الإضاءة على تفادي ظلال تنقل الأشخاص المراقبين ، وانعكاس الضوء المتغير الصادر من ملابسهم . . ان تنظيم شدة الإضاءة لجسم متحرك يراد تصويره يعد عملا صعبا ، حيث ان الجهاز البصري البشري يقوم بالتعويض عن الحركة بشكل يتناسب مع الإضاءة لكن الكاميرا لا تستطيع التعويض ولذلك يظهر تغير واضح في قيم عناصر الصورة ، ولتحقيق تنظيم إضاءة مقبول يجب ان يكون مصدر الضوء كبير مقارنة بالجسم الخاضع للدراسة.
لقد تم بناء منظومة العمل الموضحة بالشكل (1) حيث تتألف منظومة العمل من صندوق مظلم ذا أبـعاد cm^3 (120×74× 61) عندما تكون المسافة بين الجسم ومصدر الإضاءة 120 cm ، يحتوي الصندوق في أحد الجوانب على مصدر الإضاءة (مصباح التنكستن) وفي نفس الجانب يحتوي على فتحة للتصوير توضع عليها الكاميرا وفي الجانب المقابل توضع الصور والأجسام المراد تصويرها تحت شروط أضاءة مختلفة حيث يتم التحكم بشدة الإضاءة باستخدام الدائرة الالكترونية الموضحة في الشكل (2)

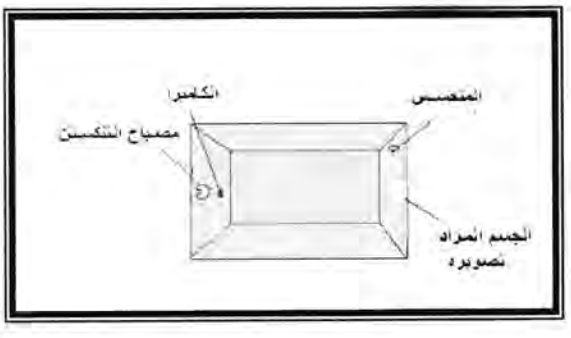

شكل -1: منظومـــــة التصوير المقترحة.

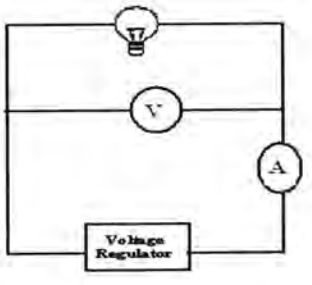

شكل -2: الدائرة الالكترونية لمنظومة التصوير.

وفيما يلي شرح لمكونات منظومة التصوير المقترحة حيث تتكون هذه المنظومة :

1.الويب كاميرا المستخدمة في الدراسة

أن نوع الكاميراالرقمية المستخدمة في الدراسة هيenet web Camera , ذات متحسس من النوع SMOSوأهم مواصفاتها هي :

1-تلتقط صور فيديوية (Video Capture): بوضوحية حيزية 480x640 بيكسل.
2- تلتقط صورثابتة (Still Image Capture): بوضوحية حيزية 480x640 بيكسل.
3-نسبة عدد اللقطات (Fram Rate): اكثرمن 48 لقطة لكل ثانية.

2.الترانزستور الضوئي الكاشف

هذا المتحسس هو عبارة عن شريحة تحتوي عدد كبير من الخلايا المتحسسة للضوء والتي تستطيع أن تلتقط الضوء الساقط عليها حيث يستعمل لقياس شدة الضوء .أن المتحسس المستخدم في منظومة العمل هو الترانستور الكاشف الضوئيPhoto Transistor Detector وهو عبارة عن شريحة من مادة شبة موصلة من السيلكون نوع NPN (bp 103) أن أهم خصائصهُ:-

1. يفيد في كشف الضوء الذي تتراوح أطواله الموجية ما بينnm (420 - 1130) أي يتحسس المنطقة المرئية وفي المنطقة تحت الحمراءIR.
2.يمتاز هذا الكاشف بالعلاقة الخطية العالية بين شدة الضوء والقدرة التي يتحسسها الكاشف .
3.يستخدم هذا المتحسس في الحاسوب في وحدات السيطرة وكذلك يستخدم في الدوائر الألكترونية المتكاملة.

3.مصباح خويط التنكستن المضبب

يطلق عليه اسم المصباح المتوهج وهو شائع الاستعمال كمصدر ضوئي حراري ، ويتركب في ابسط صورة من انتفاخ زجاجي مفرغ يحتوي على خويط من مادة جيدة التوصيل للكهرباء (تنكستن) وترفع درجة حرارة الخويط الى حوالي 2000°C بإمرار تيار كهربائي مناسب الشدة فيتحول جزء صغير 2% من الطاقة الكهربائية في تسخين الخويط الى طاقة ضوئية . أي ان المصباح الكهربائي الذي قدرته 100 W يعطي طاقة ضوئية بمعدل 2Watt. ان الضوء المنبعث من مصباح خويط التنكستن ضوء مائل الى الصفرة ويشابه ضوء الشمس لكن بنسب طيفية مختلفة ان خصائص المصباح المستخدم هي :
القدرة W(100) .الفولتية volt (250 – 0) .يبعث الاطوال الموجية للطيف المرئي (ليس بنفس النسب لضوء الشمس) .

4.جهاز الفولتميتر والاميتر

تم استخدام جهاز الفولتميتر لقياس الفولتية المسلطة على المصابيح وجهاز الاميتر لقياس التيار المار بالمصابيح وذلك لغرض أيجاد القدرة الكهربائية المصروفة عند كل شدة إضاءة مستخدمة .

5.منظـــــم الفولتية

يستخدم منظم الفولتية لكي يتم التحكم بالتيار المار في المنظومة وبالتالي يمكن التحكم بشدة ضوء المصابيح او مصباح الإضاءة داخل الصندوق .

النتائج والمناقشة

تم دراسة تأثير شدة الاضاءة على كفاءة الويب كاميرا لتصويرورقة بيضاء اختبارية A4 وضعت هذه الورقة داخل صندوق مظلم يمكن التحكم بأضائيته ومخططه موضح بالشكل (1)
.وتم التحكم بشدة الاضاءة بتغيير الفولتية المسلطة على منظومة الاضاءة داخل الصندوق ومن ثم تصوير الورقة البيضاء A4 وتسجيل القدرة لمنظومة الاضاءة وتسجيل شدة الضوء الساقط على الورقة بأستخدام الترانزستور الكاشف الضوئي حيث تم الحصول على مقطع فديوي للصور التي تم الحصول عليها بشروط الاضاءة المختلفة (أي بفولتية مسلطة على منظومة الاضاءةمختلفة) ثم تم تقطيع هذا الملف الفديوي للحصول على 13 صورة مختلفة كل صورة سجلت لفولتية مختلفة وهذه الصور موضحة بالشكل (3) نلاحظ في الاضاءات الواطئة الصورة سوداء ثم تبدأ الصورة تكون اكثر نصوعا وبشكل تدريجي مع

زيادة الاضاءة (أي زيادة فولتية منظومة الاضاءة).كما تم قياس التيار المار بالمصابيح وذلك لغرض أيجاد القدرة الكهربائية المصروفة عند كل شدة إضاءة مستخدمة .

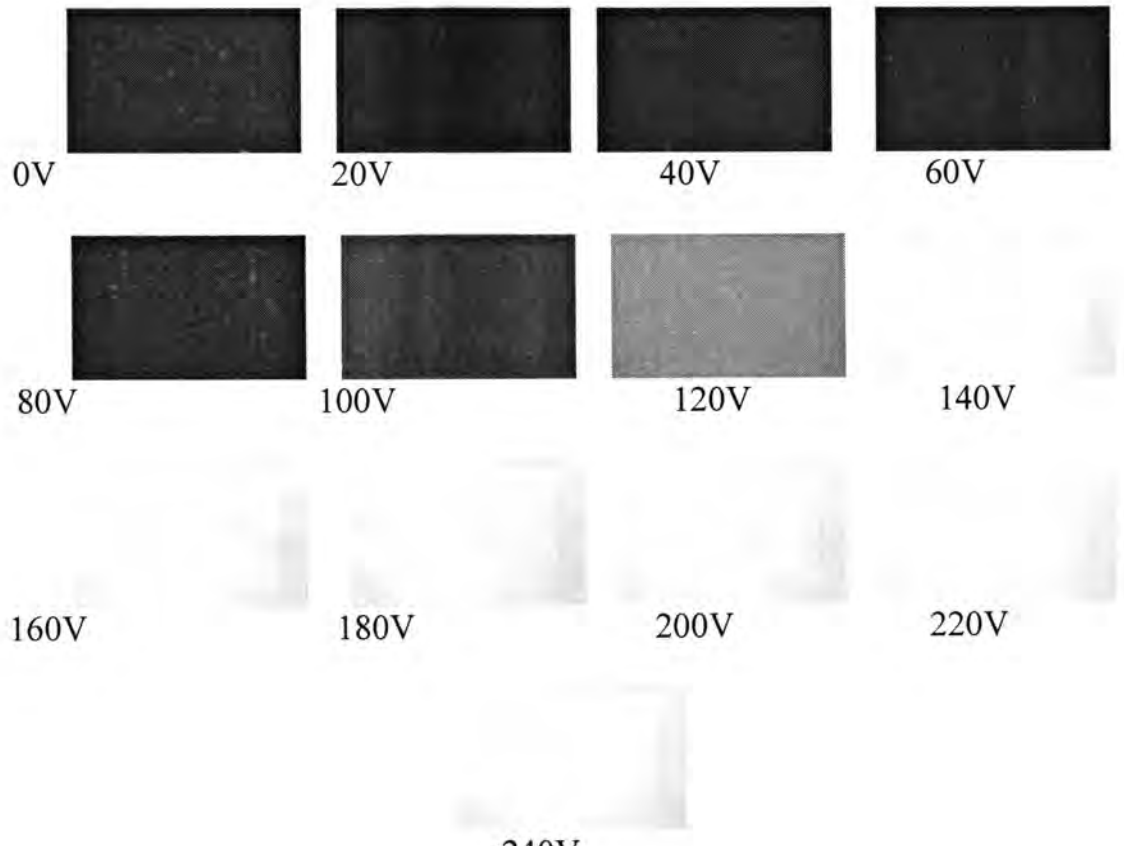

شكل -3: يمثل الصور الملتقطة بواسطة الويب كاميرا لشدات اضاءة تنكستن مختلفة.

تم دراسة تجانس الإضاءة لمنظومة التصوير وذلك بتصوير الصورة الاختبارية A4 باضائيات التنكستن المختلفة و المسافة ***120 cm*** بين الصورة الاختبارية المراد تصويرها ومصدر الإضاءة وكما موضح في الشكل (4)حيث يمكن ملاحظة أن توزيع شدة الإضاءة عندما تكون الفولتية في المدى 60– 0) volt(تكون منتظمة وقيم شدة الإضاءة تكون قليلة ومنحنيات الحزم اللونية RGB ومركبة الإضاءة L متساوية تقريبا . اما في مدى الفولتيات الاعلى فنلاحظ ارتفاع في قيم المعدل والانحراف المعياري ونلاحظ ان قيم الانحراف المعياري للحزمة الزرقاء اعلى من الحزمتينRG والمركبة L وذلك لمساهمتها العالية في الضوضاء. أن زيادة المعدل والانحراف المعياري تدل على زيادة الوضوحية داخل الصورة التي تعتمد على الإضاءة حيث زيادة كلا القيمتين تدل على زيادة الوضوحية.

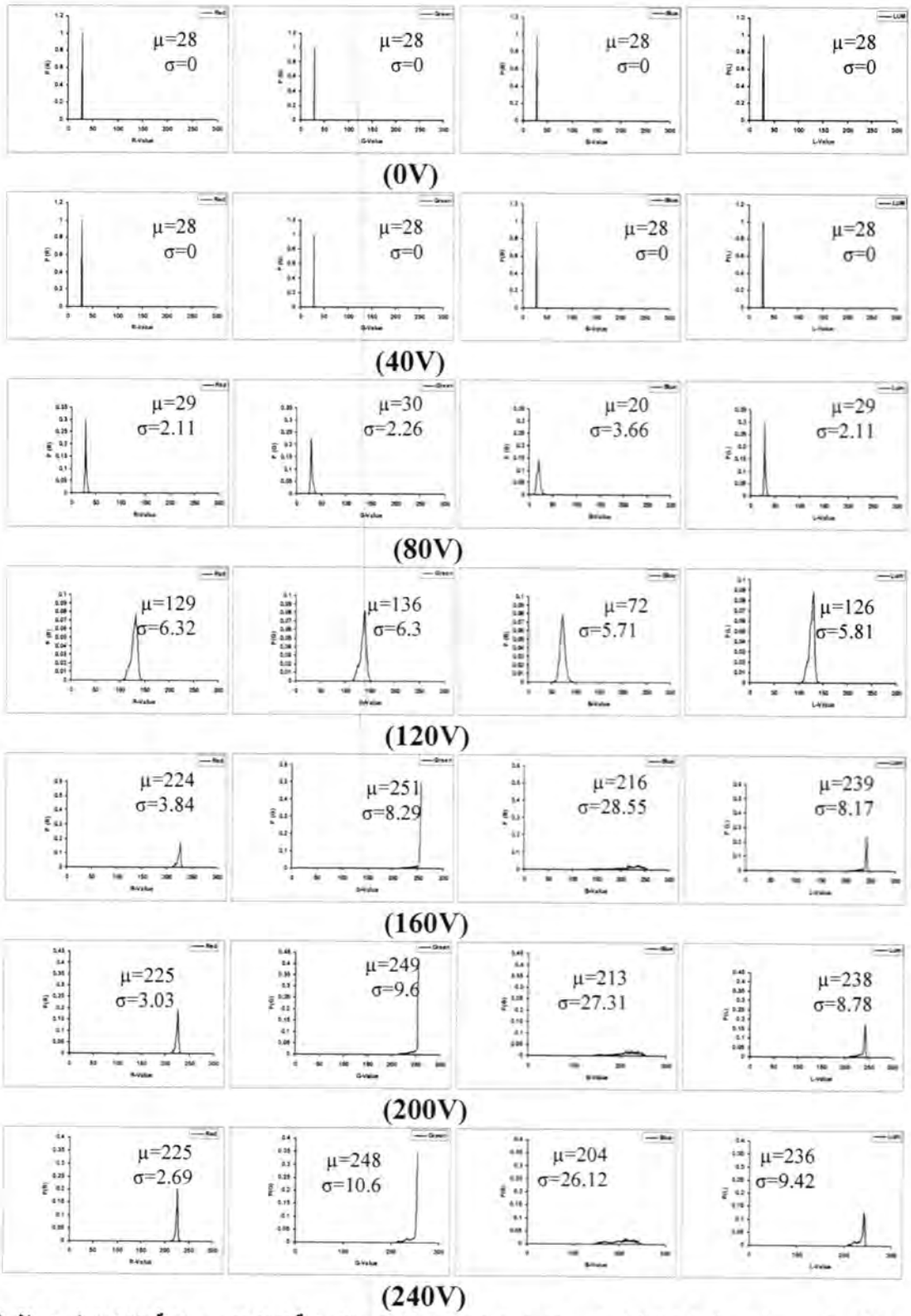

شكل -4 : يوضح المخطط التكراري لتوزيع الشدات للحزم اللونيةRGB ومركبة الإضاءة L لفولتيات الاضاءة المختلفة.

نتائج دراسة العلاقة بين القدرة والمعدل

نلاحظ من الشكل (5)استقرار لقيم المعدل للحزم اللونية RGB ولمركبة الاضاءة L عندما تكون القدرة في مدى watt (0-0.001492) اما في مدى القدرة -0.00234) watt(0.004266نلاحظ ان قيم المعدل تزداد خطيا مع القدرة وفي مدى القدرة الاعلى (شدة الاضاءة الاعلى) ان قيم المعدل تكون ثابتة نسبيا عدا بعض الشذوذ بالنسبة للحزمة الزرقاء وهذه يدل على أن توزيع الأضاءة لمصباح التنكستن يكون بشكل مستقر ومنتظم حيث شكل منحني المركبه L يعطي تقارب كبير مع منحني الحزمة الخضراء وذلك ناتج عن كون الحزمة الخضراء تعطي مشاركة نسبتها بحدود 60 % في تكوين الشدة L في الصورة .

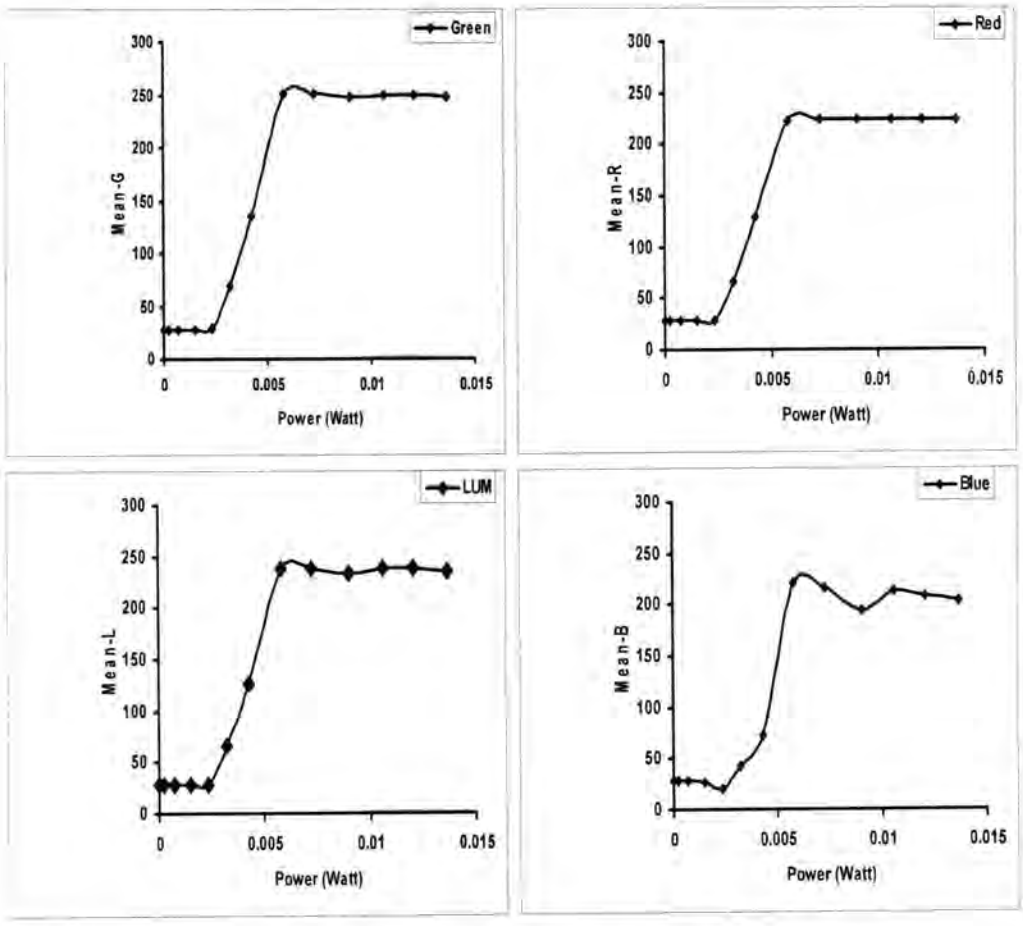

شكل -5: يوضح العلاقة بين القدرة والمعدل .

ويستنتج من ذلك ما يلي:

1. نلاحظ انه في مدى الفولتيات Volt (60 – 0) ان توزيع شدة الاضاءة يكون منتظما وقيم منحنيات المركبات اللونية RGB ومركبة الاضاءة L متساوية تقريبا.
2. اما في مدى الفولتيات الاعلى نلاحظ ان قيم توزيع شدة الاضاءة تكون متباعدة بعضها عن بعض للحزم اللونية الثلاثة ولمركبة الاضاءة L وهذا يدل على ان الضوء الذي لا يحصل فيه تطابق يعني ذلك ان الضوء لا يقترب من ضوء الشمس الابيض.
3. في مدى الفولتيات (60-0)نلاحظ ان قيم المعدل تكون ثابتة تقريبا للحزم اللونية الثلاثة RGBولمركبة الاضاءة Lاما في مدى الفولتيات (120-80)نلاحظ ان قيم المعدل تزداد خطيا مع القدرة وفي مدى الفولتيات الاعلى تكون قيم المعدل مستقرة تقريبا للحزم اللونية ومركبة الاضاءة عدا بعض الشذوذ بالنسبة للحزمة الزرقاء.

المصادر

1. Umbaugh S.E. ," Computer Vision And Image Processing ", prentice –Hall , New Jersey ,(1998).
2. Ball, Victoria Kloss, "The Art of Interior Design ",John Wiely Sons, New York,(1982).
3. Barker Geoffrey H. Le Corbusier ," An Analysis of from.Van Nostrand Reinhold", New York ,(1989) .
4. Turner ,Jaret. ," An Introduction To Light, Lighting and Light Use ", B.T Bats Ford Ltd London, (1994).
5. Kurtich ,John and Eakin , Garrel ., " Interior Architecture "Van Nostrand Reinhold , New York,1993.
6. ناجي عبد الصاحب ،د.نور الدين الربيعي "البصريات والكهربائية" مطبعة الحكومة،–بغداد،1969.
7. Roorda A . and Williams D.R , " The Arrangement of three Cone Classes in the Living Human Eye " , Nature 11: 520 – 522 , (1999).
8. كارلا روز" تعلم فن التصوير الرقمي والكاميرات الرقمية خلال 14 يوم " ترجمة مركز التعريب والبرمجة ، الدار العربية للعلوم ،(1996).
9. Jiang , M ., " Digital Image Processing" , Department of Information Science ,School of Mathematics, peking University , Iowo,(2003).
10. Young. I. T ,Gerbrands.J. and Van Vliet L. J., " Fundammental of Image Processing ", Printed in Netherlands at Delf Univ. of Technology , ISBN 90 -75691 -10 -7 , NUGI 841, (1998).
11. Kai – Yu and Liang Ji, " How to Optimize Optical Coherent Tomography OCT Image ", Department of Automation , Tsinghua University, (2001) .

طاقة جهد السطح للنوى شديدة التشوه ذات التناظر الديناميكي SU(3)

ايمان طارق العلوي وعطاء علي حسن
قسم الفيزياء/ كلية العلوم /الجامعة المستنصرية

ABSTRACT

In this work, the nuclear structure has been studied for strongly deformed nuclei with mass number (A=170,174,182) for even-even $(^{170}_{68}Er_{102}, ^{174}_{72}Hf_{102}, ^{182}_{74}W_{108})$ nuclei respectively using the Interacting Boson Model (IBM-1). The dynamical symmetry SU(3) has been predicated for each nuclei . The potential energy surface parameters have been derived and calculated in terms of the Hamiltonian operator parameters. The potential energy surface for each nucleus has been studies and calculated in terms of these parameters using (PES.for) program, also contour lines, axially symmetries and mesh grid has been drown.
The results have been compared with typical scheme and band structure, and the results of comparisons have given a good agreement.

الخلاصة

تم خلال البحث دراسة التركيب النووي للنوى شديدة التشوه ذات الأعداد الكتلية (A=170,174,182) لكل من الانوية الزوجية-زوجية $(^{170}_{68}Er_{102}, ^{174}_{72}Hf_{102}, ^{182}_{74}W_{108})$ على التوالي ذات التناظر الديناميكي SU(3) لكل نواة باستخدام نموذج البوزونات المتفاعلة الأول (IBM-1).لقد تم اشتقاق و حساب اعلومات طاقة جهد السطح بدلالة اعلومات دالة مؤثر هاملتون حيث تم حساب طاقة جهد السطح لهذه الانوية باستخدام برنامج (PES.for) ورسم الخطوط الكنتورية والتناظرات المحورية لها والخطوط الشبكية المتعامدة والتي أعطت توافقا جيدا مع المخططات المثالية و تركيب الحزم.

المقدمة

ان الحركة الدورانية التجميعية النووية (Nuclear Collective Rotation Motion) تحدث عندما يكون شكل النواة في حالة تشوه شديد (Strong Deformation) ويكون عزم القصور الذاتي (Moment of Inertia) للنواة قريب من حالة الجسم الصلد (Rigid Body) هذه الظاهرة تسمى بالتشوه الشديد ويكون لها عزم رباعي القطب الكهربائي (Electric Quadrupole Moment) الناتج من توزيع الشحنات للنوى غير الكروية (Non Spherical) وان التشوهات (Deformations) تنشأ بسبب ان الطريقة التي تترتب بها النيوكليونات تكون في قشر غير مملوءة(1,2).

ان معظم النوى المشوهة (Deformed Nuclei) هي مثال جيد لخصائص التناظر الديناميكي SU(3). في البحث الحالي قمنا بتعزيز هذه الخصائص بالتأكيد على النوى المختارة قيد الدراسة $(^{170}_{68}Er_{102}, ^{174}_{72}Hf_{102}, ^{182}_{74}W_{108})$ كأفضل مثال على للنوى شديدة التشوه (Strong Deformation). هنالك عدة حقائق مقنعة لتوافق النتائج العملية مع الحسابات النظرية للنوى المشوهة (Deformed Nuclei) و كالاتي :(2,3)

1. النوى التي تمتلك عدد البروتونات والنيوترونات بين الاعداد السحرية (Magic Numbers) تكون نوى مشوهة في مستوياتها الارضية (Ground States).
2. ان التشوه (Deformation) يحدث بسبب ان النيوكليونات التكافؤية (Valence Nucleons) ترتب نفسها باغلفة غير مملوءة، اي ان التشوه يظهر اذا كانت اغلفة البروتونات والنيوترونات (Protons and Neutrons Shells) مملوءة جزيئاً، ويكون شكل النواة اهليليجياً (Ellipsoidal) حيث يكون اثنان من ثلاث محاور اساسية متساوية. فأذا كان المحور الثالث اكبر من المحورين الاخرين المتساويين يكون شكل النواة اهليليجياً متطاولاً (Prolate) اما اذا كان المحور الثالث اصغر من المحورين الاخرين المتساويين يكون شكل النواة اهليليجياً مفلطحاً (Oblate).

3. ان النوى المشوهة (Deformed Nuclei) نجدها في الجدول الدوري (Periodic Table) عند الاعداد الكتلية $150\leq A\leq 190$ وكذلك عند الاعداد الكتلية $A\geq 220$. في المجموعة الاولى البروتونات والنيوترونات تملئ الاغلفة التي هي فوق $Z=50$ و $N=82$، اما في المجموعة الثانية فان البروتونات والنيوترونات التي هي فوق $Z=82$ و $N=126$. ان الانوية الزوجية – زوجية (Even-Even Nuclei) في هذه المناطق يكون المستوي المتهيج الاول 2_1^+ ذو طاقة واطئة جداً (Very Low Lying). فعلى سبيل المثال تكون الطاقات الواطئة للمستوي المتهيج الاول 2_1^+ في الانوية ($^{170}_{68}Er_{102}, ^{174}_{72}Hf_{102}, ^{182}_{74}W_{108}$) المختارة في العمل الحالي هي(0.0786,0.0910,0.1001MeV) على الترتيب.
4. تمتلك النوى المشوهة عزوماً كهربائية رباعية القطب (Electric Quadrupole Moments) لتوزيع الشحنات.

وان طاقة الجهد (Potential Energy) تتغير بتغيرتشوه النيوكليونات ويكون الحد الادنى (Minimum) للجهد عند التشوهات المطابقة للمستوى الارضي (Ground-State) اي يحدث تغير في شكل تشوه المستوي الارضي للنواة ويؤدي الى زيادة في طاقة الجهد وعندما يصل التشوه الى قيمة التشوه الشديد (Strongly Deformation) ينتج عنه استقرار اضافي يؤدي الى رفع الحد الادنى للجهد مرة ثانية. ان هذا التاثير يعرف باستقرارية القشرة (Stabilization Shell).

واذا كانت حركة النيوكليونات دورانية وتاثير القوة المركزية (Central Force) على التركيب الداخلي للنيوكليونات المساندة في زيادة التشوهات ففي هذه الحالة تصنع النيوكليونات دوران بسرعة كافية لتكون مشابهة للزيادة في طاقة المستوي وان هذا هو اساس الحزمة الدورانية في شكل التشوه الشديد (Strongly Deformed Shape) .

اقترح كل من (Bohr and Mottelson) عام (1975) (1) نظام هندسي خاص بالنواة يفترض هذا النظام ان النواة لها سطح محدد ولها شكلاً تذبذبياً (Oscillation Shape) وان التشوهات الناتجة عن عزم رباعي القطب هي الاكثر شمولية في الحركة الجماعية (Collective Motion) ولوصف الحركة الدورانية للنواة افترض هذا النظام الشكل الاهليليجي (Ellipsoid) لوصف تشوه النوى، وافترض وجود متغيران هما (β,γ) ليمثلان اعلومتي التشوه اذ تمثل (β) مقياساً للتشوه وتقترب قيمتها من الصفر في النوى الكروية (Spherical Nuclei) بينما قيمتها لاتساوي صفر في النوى المشوهة (Deformed Nuclei) واذ قيم $(\beta=0\rightarrow 2.4)$ (4,5).

اما قيمة γ فانها تساوي صفر $(\gamma=0^o)$ في النوى المشوهة (Deformed Nuclei) من النوع الاهليليجي المتطاول (Prolate)، في حين ان قيمتها تساوي $(\gamma=60^o)$ في النوى المشوهة (Deformed Nuclei) من النوع الاهليليجي المفلطح (Oblate) (4,5).

في عام (1999) قام (Chiang) وجماعته(6) بدراسة وحساب التشوه بأستخدام نموذج البوزونات المتفاعلة(IBM) للمنطقة (A=150) وقد وجدوا ان الحركة الجماعية للنوى شديدة التشوه ويمكن ان توصف بتعدد بوزونات s,d وطاقة البوزون المتكافئة الواطئة حول اللب وقد نجحوا ايضاً في وصف مستويات الطاقة للنوى المشوهة للمنطقة (A=190). و قام (Bender) وجماعته(7) في عام (2003) بوضع صورة منهجية منظمة لدراسة طاقة جهد السطح (Potential Energy Surface) ولاحظوا ان دالة الموجة للمستوي المتهيج تكون قمتها مشوهة بشدة (Strongly Deformation) وتكون متطاولة (Prolate) او مفلطحة (Oblate) ولاحظوا ان قيم احتمالية الانتقال الكهربائي رباعي القطب B(E2) صغيرة جداً بين الحزم. وفي عام (2006) وضع (Van Iscaker) وجماعته (8) دراسة للتناظرات الديناميكية (Dynamical Symmetries) في النوى الزوجية-زوجية (Even-Even) ضمن اطار نموذج (IBM) (Interacting Boson Model) لجبر لي وان هذا النموذج تعامل مع ازواج s و d كبوزونات من نوع s (s-boson) وبوزونات من نوع d (d-boson). وفي عام (2007) قام (Hellemans) وجماعته (9) بدراسة طاقة جهد السطح (PES) (Potential Energy Surface) والذي يعتمد على اعلومتان هما β و γ، حيث ان (β) تعطي تشوهات رباعي القطب المحوري (Deformation Axial Quadrupole) و (γ) تعطي تشوهات رباعي القطب غير

المحوري (Deformation Non-Axial Quadrupole) وبينوا ان مساهمة نموذج البوزونات المتفاعلة (Interacting Boson Model) (IBM) والنموذج الجبري (Algebraic Model) لتقريب الازواج المزدوجة لـ 0^+ و 2^+ كبوزونات s,d اعطت الخصائص الجيدة لهذا النموذج المعتمدة على المعلومات الحقيقة للحركة الجماعية النووية (Nuclear Collective Motion).

الاسس النظرية

لغرض وصف الطاقات لنظام نووي معين نحتاج الى مؤثر دالة هاملتون لذلك النظام، ان المؤثر الهاملتوني (Hamiltonian Operator) لنموذج البوزونات المتفاعلة الاول (IBM-1) يتضمن نوعين من جسيمات البوزونات احدهما بوزون -s بزخم زاوي مداري j=0 والاخر بوزون -d بزخم زاوي مداري j=2 وبالتالي يمكن كتابة مؤثر دالة هاملتون $\hat{H}$ متضمناً حدان لتفاعلات الجسيمات المنفردة (One Body Interactions) وسبعة حدود اخرى لتفاعلات الجسيم والجسيمين (One Body and Two Body Interactions) بالشكل التالي (4,5,10):

$$\hat{H}=\varepsilon_s(\hat{s}^\dagger.\tilde{\hat{s}})+\varepsilon_d\sum_m(\hat{d}^\dagger_m.\tilde{\hat{d}}_m)+\hat{W} \qquad \ldots(1)$$

$$\hat{H}=\varepsilon_s(\hat{s}^\dagger.\tilde{\hat{s}})+\varepsilon_d\sum_m[\hat{d}^\dagger_m.\tilde{\hat{d}}_m]$$
$$+\sum_{L=0,2,4}\frac{1}{2}\sqrt{2L+1}\;c_L[[\hat{d}^\dagger\times\hat{d}^\dagger]^{(L)}\times[\tilde{\hat{d}}\times\tilde{\hat{d}}]^{(L)}]_0^{(0)}$$
$$+\frac{1}{2}v_o[[\hat{d}^\dagger\times\hat{d}^\dagger]^{(0)}\times[\tilde{\hat{s}}\times\tilde{\hat{s}}]^{(0)}+[\hat{s}^\dagger\times\hat{s}^\dagger]^{(0)}\times[\tilde{\hat{d}}\times\tilde{\hat{d}}]^{(0)}]_0^{(0)}$$
$$+\frac{1}{\sqrt{2}}v_2[[\hat{d}^\dagger\times\hat{d}^\dagger]^{(2)}\times[\tilde{\hat{d}}\times\tilde{\hat{s}}]^{(2)}+[\hat{d}^\dagger\times\hat{s}^\dagger]^{(2)}\times[\tilde{\hat{d}}\times\tilde{\hat{d}}]^{(2)}]_0^{(0)}$$
$$+\frac{1}{2}u_o[[\hat{s}^\dagger\times\hat{s}^\dagger]^{(0)}\times[\tilde{\hat{s}}\times\tilde{\hat{s}}]^{(0)}]_0^{(0)}+u_2[[\hat{d}^\dagger\times\hat{s}^\dagger]^{(2)}\times[\tilde{\hat{d}}\times\tilde{\hat{s}}]^{(2)}]_0^{(0)} \qquad \ldots(2)$$

حيث ان: $\varepsilon_d,\varepsilon_s$ تمثل طاقة (s-boson) و (d-boson) على التوالي

m: تأخذ القيم m=0,±1,±2، اما $\hat{W}$: يمثل مؤثر تفاعل البوزون- بوزون Boson-Boson (Interaction، حيث تمثل u_L (L=0,2) و v_L(L=0,2) و c_L(L=0,2,4) اعلومات تفاعل البوزونات (Bosons Interaction). ان الرموز مابين الاقواس تمثل ازدواج الزخم الزاوي (Angular Momentum Coupling).

ويمثل الحدين الاول والثاني طاقات تفاعل بوزون- بوزون للجسيم الواحد اما الحدود السبعة الاخرى فتمثل طاقات تفاعل بوزون- بوزون للجسيم الواحد والجسيمين.

ان درجات الحرية (Degrees of Freedom) تكتب بالشكل التالي (2,5,10):

$$\tilde{\hat{s}},\tilde{\hat{d}}_m,\hat{s}^\dagger,\hat{d}^\dagger_m\ (m=0,\pm1,\pm2) \qquad \ldots(3)$$

حيث ان:

$\hat{s}^\dagger,\hat{d}^\dagger_m$ مؤثرات الخلق (Creation Operators):

$\tilde{\hat{s}},\tilde{\hat{d}}_m$ مؤثرات الهدم (الفناء) (Annihilation Operators):

وان هذه المؤثرات تحقق العلاقات التبادلية (Commutation Relations) التالية (4,5,10):

$$\left.\begin{aligned}&[\hat{\tilde{s}},\hat{s}^{\dagger}]=1;[\hat{\tilde{s}},\hat{\tilde{s}}]=[\hat{s}^{\dagger},\hat{s}^{\dagger}]=0\\&[\hat{\tilde{d}}_m,\hat{d}_m^{\dagger}]=\delta_{mm};[\hat{\tilde{d}}_m,\hat{\tilde{d}}_m]=[\hat{d}_m^{\dagger},\hat{d}_m^{\dagger}]=0\\&[\hat{\tilde{s}},\hat{d}_m^{\dagger}]=[\hat{s}^{\dagger},\hat{\tilde{d}}_m]=0\end{aligned}\right\} \quad ...(4)$$

ان المؤثرات $\hat{\tilde{d}},\hat{\tilde{s}}$ يعطيان بالعلاقة التالية (4,5):

$$\hat{\tilde{s}}=\hat{s};\hat{\tilde{d}}_m=(-1)^m\hat{d}_m \quad ...(5)$$

وبالامكان ايجاد القيم الذاتية (Eigen Values) بصورة تحليلية (Analytically) وتأخذ الحالات الذاتية (Eigen States) الصيغة التالية (5,10,11):

$$\left.\begin{vmatrix}U(6)\supset SU(3)\supset O(3)\supset O(2)\\ \downarrow \quad \downarrow \quad \downarrow \quad \downarrow\\ [N] \quad (\lambda,\mu)\tilde{\chi} \quad L \quad M_L\end{vmatrix}\right\rangle \quad ...(6)$$

حيث ان:

N: العدد الكلي للبوزونات (Total Number of Bosons) = $(N_\pi+N_\upsilon)$.

N_π: عدد بوزونات البروتونات (Proton Bosons Number).

N_υ: عدد بوزونات النيوترونات (Neutron Bosons Number).

ان N تشير الى التمثيل غير القابل للاختزال المتناظر كليا للزمرة الوحدوية U(6) (Totally Symmetric Irreducible Representation of U(6)).

المتناظر تعني ان البوزونات تتميز بدوال موجية متناظرة (Symmetrical wave functions) اما (λ,μ) فهي عبارة عن تمثيلات غير قابلة للاختزال للزمرة SU(3) (Irreducible Representation of SU(3)). وان L و M_L تمثلان الزخم الزاوي ومسقطه على المحور z على التوالي، وان $\tilde{\chi}$ هو عدد كمي اضافي لـ Vergados (2,5) له علاقة بمسقط الزخم الزاوي.

يمكن الحصول على طاقة جهد السطح من مؤثر دالة هاملتون على اعتبار ان الطاقة هي دالة لكل من العدد الكلي للبوزونات (N) واعلومات التشوه (β,γ) كما في المعادلة التالية (4,5):

$$V(N,\beta,\gamma)=\frac{<N,\beta,\gamma|\hat{H}|N,\beta,\gamma>}{<N,\beta,\gamma|N,\beta,\gamma>} \quad ...(7)$$

وباشتقاق معادلة طاقة جهد السطح $V(N,\beta,\gamma)$ بالنسبة لـ (β,γ) ومساواة الاشتقاق الى الصفر (Minimizing) نحصل على التالي (4,5):

$$\frac{\partial V}{\partial\beta}=0,\frac{\partial V}{\partial\gamma}=0 \quad ...(8)$$

ونحصل على معادلة طاقة جهد السطح التي صيغتها العامة هي كما يأتي (4,5):

$$V(N,\beta,\gamma)=\frac{N}{1+\beta^2}(\varepsilon_s+\varepsilon_d\beta^2)+\frac{N(N-1)}{(1+\beta^2)}(f_1\beta^4+f_2\beta^3\cos3\gamma+f_3\beta^2+f_4) \quad ...(9)$$

حيث ان:

N: تمثل عدد البوزونات الكلي (Total Number of Bosons).
β: تمثل مقدار تشوه النواة (Magnitude of Nuclear Deformation) وتأخذ القيم (0-2.4).
γ: تمثل زاوية عدم التناظر (Asymmetry Angle) وتتراوح قيمتها (0^o-60^o).
f_1,f_2,f_3,f_4 : اعلومات ترتبط مع اعلومات مؤثر دالة هاملتون (c_L,v_L,u_L) المذكورة في المعادلة (2) وكما يلي [4,5]:

$$f_1 = \frac{c_o}{10} + \frac{c_2}{7} + \frac{9}{35}c_4 \qquad \ldots(10)$$

$$f_2 = -\sqrt{\frac{8}{35}}.v_2 \qquad \ldots(11)$$

$$f_3 = \frac{(v_o + u_2)}{\sqrt{5}} \qquad \ldots(13)$$

$$f_4 = u_o \qquad \ldots(14)$$

الشكل (1) يمثل المخطط المثالي للخطوط الكنتورية (Contour lines) للتناظرات الديناميكية الاهتزازية SU(5) والدورانية SU(3) وكاما غير المستقرة O(6) (12). اما الشكل (2) فيمثل المخطط المثالي للخطوط الكنتورية والتناظرات المحورية للتناظر الديناميكي SU(3)(13).

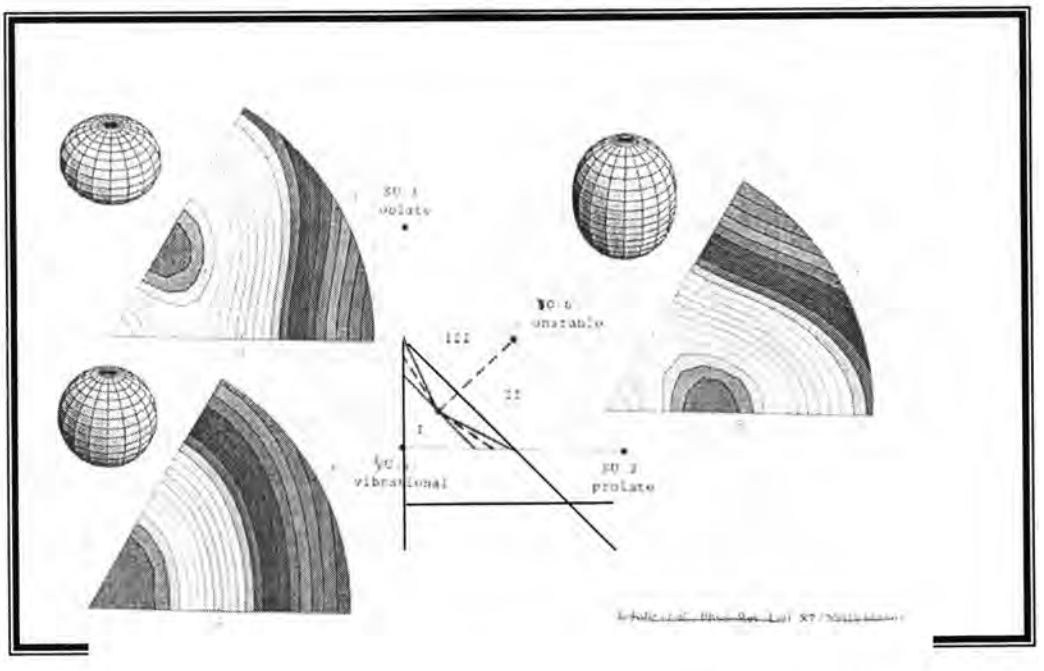

شكل-1: المخطط المثالي للخطوط الكنتورية (Contour lines) للتناظرات الديناميكية الاهتزازية SU(5) والدورانية SU(3) وكاما غير المستقرة O(6)(12).

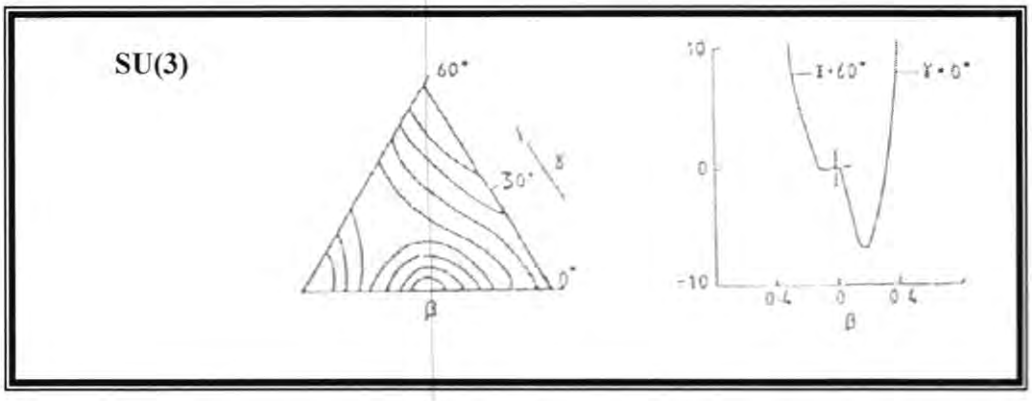

شكل -2: المخطط المثالي للخطوط الكنتورية والتناظر المحوري للتناظر الديناميكي SU(3) (13).

النتائج والمناقشة

لقد تم حساب اعلومات طاقة جهد السطح $(\varepsilon_s,\varepsilon_d,f_1,f_2,f_3,f_4)$ بشكل مباشر من خلال برمجة العلاقات الرياضية في برنامج (IBS1.for) والتي تم صياغتها للمعادلات (10←13) بدلالة اعلومات دالة هاملتون في معادلة (2).

ومن تعريف الاعلومات f_1,f_2,f_3,f_4 بدلالة c_L,v_L,u_L الوارد في المعادلات (10←13) تمكننا من اعادة كتابتها على مبدأ Van Iscacher and Chen (14) بدلالة مؤثرات الخلق والفناء (Creation and Annihilation) $\hat{\tilde{s}},\hat{s}^\dagger,\hat{\tilde{d}},\hat{d}^\dagger$ والتي تم استخدامها في البرنامج (IBM-1) لحساب هذه الاعلومات والتي تضمنها البرنامج الفرعي (PES.for) لحساب طاقة جهد السطح وكما يلي:

$$f_1=\frac{1}{20}[(\hat{d}^\dagger\times\hat{d}^\dagger)^{(0)}\times(\hat{\tilde{d}}\times\hat{\tilde{d}})^{(0)}]_0^{(0)}+\frac{\sqrt{5}}{14}[(\hat{d}^\dagger\times\hat{d}^\dagger)^{(2)}\times(\hat{\tilde{d}}\times\hat{\tilde{d}})^{(2)}]_0^{(0)}+$$
$$\frac{27}{70}[(\hat{d}^\dagger\times\hat{d}^\dagger)^{(4)}\times(\hat{\tilde{d}}\times\hat{\tilde{d}})^{(4)}]_0^{(0)} \quad ...(14)$$

$$f_2=-\sqrt{\frac{8}{35}}[(\hat{d}^\dagger\times\hat{d}^\dagger)^{(2)}\times(\hat{\tilde{s}}\times\hat{\tilde{s}})^{(2)}]_0^{(0)}+(\hat{d}^\dagger\times\hat{s}^\dagger)^{(2)}\times(\hat{\tilde{d}}\times\hat{\tilde{d}})^{(2)}]_0^{(0)} \quad ...(15)$$

$$f_3=\frac{1}{2\sqrt{5}}[(\hat{d}^\dagger\times\hat{d}^\dagger)^{(0)}\times(\hat{\tilde{s}}\times\hat{\tilde{s}})^{(0)}+(\hat{s}^\dagger\times\hat{s}^\dagger)^{(0)}\times(\hat{\tilde{d}}\times\hat{\tilde{d}})^{(0)}]_0^{(0)}$$
$$+\frac{1}{\sqrt{5}}[(\hat{d}^\dagger\times\hat{s}^\dagger)^{(2)}\times(\hat{\tilde{d}}\times\hat{\tilde{s}})^{(2)}]_0^{(0)} \quad ...(16)$$

$$f_4=[(\hat{\tilde{s}}\times\hat{\tilde{s}})^{(0)}+(\hat{s}^\dagger\times\hat{s}^\dagger)^{(0)}]_0^{(0)} \quad ...(17)$$

ان برنامج (PES.for) كتب بلغة (Fortran 90) وتم تنفيذه باستخدام البرنامج التشغيلي (Compaq Visual Fortran V6.6) قد صمم لحساب طاقة جهد السطح بوصفه دالة لكل من (β,γ) ولعدد البوزونات الكلي N.

ان هذه الاعلومات تستخدم لتغذية برنامج (PES.for) كمدخلات لحساب جهد السطح $V(N,\beta,\gamma)$ في المعادلة (9)، لغرض رسم الخطوط الكنتورية (Contour Lines) والتناظرات المحورية لتحديد تصرف كل نواة من الانوية قيد الدراسة والتحقق من ان هذه الانوية شديدة التشوه ذات التناظر الديناميكي الدوراني SU(3).

ان احد الطرق الهندسية لمعرفة تشوه التركيب النووي هو دراسة حساب طاقة جهد السطح للنواة. اضافة لذلك فان الوصف الهندسي للحركة الجماعية للنواة يساعد على وصف المستويات المتهيجة للنوى

المشوهة (Deformed Nuclei) ليبين مدى مقدرتها في ايجاد طاقة جهد السطح V(N,β,γ) باستخدام نموذج (IBM-1).

ان طاقة جهد السطح قد تم حسابها بعد تحديد المعلومات (parameters) مؤثر دالة هاملتون لكل نواة يبين الجدول (1) الاعلومات المستخدمة في برنامج (PES.for) لحساب طاقة جهد السطح V(N,β,γ).

جدول -1: الاعلومات المستخدمة في حساب طاقة جهد السطح V(N,β,γ).

Nuclei	N	ε_s (MeV)	ε_d (MeV)	f_1 (MeV)	f_2 (MeV)	f_3 (MeV)	f_4 (MeV)
$^{170}_{68}Er_{102}$	17	-0.055	0.240	0.046	-0.031	-0.044	0.000
$^{174}_{72}Hf_{102}$	15	-0.050	0.237	0.041	-0.028	-0.040	0.000
$^{182}_{74}W_{108}$	13	-0.086	0.232	0.043	-0.049	-0.069	0.000

الاشكال (3) و (4) و (5) تبين الخطوط الكنتورية (Contour Lines) لزوايا عدم التناظر المحوري (Asymmetric Angle) ($\gamma=0^o,\gamma=30^o,\gamma=60^o$) لطاقة جهد السطح المحسوبة. حيث اظهرت الخطوط الكنتورية لنواة $^{170}_{68}Er_{102}$ في الشكل (3) منخفضاً واضحاً عند (β=0.4-1.0) بلغت قيمته 0.5MeV وانخفضت الى 0.3MeV في حين انحدرت قيم جهد السطح من 8.5MeV عند β=2.4 الى 1.3MeV عند β=1.0 لما يقابلها من تغيير في الزوايا المحورية لعدم التناظر ($\gamma=0^o,60^o$) ونلاحظ انحدار اخر في الجهد من 1.6MeV عند β=0.2 الى 3MeV عند β=0.3.

اما الخطوط الكنتورية لنواة $^{174}_{72}Hf_{102}$ والمبينة في الشكل (4) اظهرت منخفضاً مماثلاً لنواة $^{170}_{68}Er_{102}$ ولكن عند قيم جهد 0.3MeV انخفضت الى 0.2MeV عند (β=0.5-1.0) الى انحداراً في طاقة جهد السطح من 6.5MeV عند β=2.4 الى 0.9MeV عند β=1.1 وانحداراً من 0.25MeV عند β=0.4 الى 0.75 عند β=0.3.

والشكل (5) يوضح الخطوط الكنتورية لنواة $^{182}_{74}W_{108}$ ذات منخفض لطاقة جهد السطح عند (β=0.6-1.2) بلغت قيمته 0.5MeV وانخفضت الى0.2MeV. في حين اظهر انحدارا في طاقة جهد السطح من 5.5MeV عند β=2.4 الى 1.0MeV عند β=1.4 وانحداراً اخر من 1.9MeV عند β=0.4 الى 1.5MeV عند β=0.2. ومن الجدير بالذكر بان الخطوط الكنتورية في الاشكال (3) و (4) و (5) للانوية ($^{170}_{68}Er_{102}$, $^{174}_{72}Hf_{102}$, $^{182}_{74}W_{108}$) كانت ذات تصرف متماثل من حيث موقع المنخفضات والانحدارات في طاقة جهد السطح وكانت متطابقة مع الشكل المثالي للتناظر الديناميكي SU(3)، الشكل (1) و (2)، مما يؤكد صحة الحسابات والنتائج لهذه النوى. كما تبين الاشكال (3) و (4) و (5) التناظرات المحورية للنوى قيد الدراسة حيث تم رسم طاقة جهد السطح كدالة لاعلومة التشوه(β= 0 → 2.4) حيث تبين ان اقل قيمة لطاقة جهد السطح لنواة $^{170}_{68}Er_{102}$ تحدث عند 1.605MeV- عندما يكون شكل النواة اهليليجياً متطاولاً عند β=0.6 و $\gamma=0^o$ بينما اقل قيمة لطاقة جهد السطح لنواة $^{174}_{72}Hf_{102}$ تحدث عند 0.976MeV- عندما يكون شكل النواة اهليليجياً متطاولاً عند β=0.6 و $\gamma=0^o$ واما اقل قيمة لطاقة جهد السطح لنواة $^{182}_{74}W_{108}$ تحدث عند - 2.254MeV عندما يكون شكل النواة اهليليجياً متطاولاً عند β=0.8 و $\gamma=0^o$.

وعندما اخذ شكل النواة الشكل الاهليليجي المفلطح فان اقل قيمة لطاقة جهد السطح لنواة $^{170}_{68}Er_{102}$ تحدث عند 1.366MeV- عندما β=0.2 و $\gamma=60^o$ وفي النواة $^{174}_{72}Hf_{102}$ فتأخذ الشكل الاهليليجي المفلطح فان اقل قيمة لطاقة جهد السطح تحدث عند 0.015MeV- عندما β=1.0 و $\gamma=60^o$، اما في نواة $^{182}_{74}W_{108}$ تاخذ الشكل الاهليليجي المفلطح عند اقل قيمة لطاقة جهد السطح 0.372MeV- عند β=0.2 و $\gamma=60^o$.

وقد تم عمل معيارية (Normalization) لهذه القيم الواطئة لطاقة جهد السطح لقيمة الصفر للنوى قيد البحث، وقد كانت طاقة جهد الصفر (Energy of zero point motion EZPM) للانوية $(^{170}_{68}Er_{102}, ^{174}_{72}Hf_{102}, ^{182}_{74}W_{108})$ هي (1.605MeV, 0.976MeV,2.254MeV) على الترتيب. و الجداول (2) و (3) و (4) تبين نتائج حسابات القيم المعايرة لطاقة جهد السطح للانوية قيد البحث على الترتيب.

وقد قمنا برسم طاقة جهد السطح باستخدام الخطوط الشبكية المتعامدة (Grid Mesh) للمحاور الثلاثة (β=0→2.4) و (γ=0°→60°) وقيم طاقة جهد السطح V(N,β,γ) والمتمثلة بالمحاور (x,y,z) على الترتيب والمبينة في الاشكال (3) و (4) و (5) للانوية $(^{170}_{68}Er_{102}, ^{174}_{72}Hf_{102}, ^{182}_{74}W_{108})$ على الترتيب ايضاً.

يبين الشكل (3) انحدار الخطوط الشبكية المتعامدة لطاقة جهد السطح لنواة $^{170}_{68}Er_{102}$ من القيمة 14.411MeV الى 1.605MeV عند γ=60° ومن القيمة 9.309MeV الى 1.605MeV عند γ=0° مروراً بطاقة جهد نقطة الصفر عندما تتغير (β=0→2.4).

اما الشكل (4) فيبين انحدار الخطوط الشبكية المتعامدة لطاقة جهد السطح لنواة $^{174}_{72}Hf_{102}$. ونلاحظ انحدار قيمة طاقة جهد السطح من القيمة 10.337MeV عند γ=60° ومن القيمة 6.779MeV الى 0.976MeV مروراً بطاقة جهد نقطة الصفر عندما تتغير (β=0→2.4). وهذا الانحدار متماثل مع انحدارات الخطوط الكنتورية لطاقة جهد السطح.

في حين الشكل (5) يؤكد مرة اخرى تماثل انحدار الخطوط الشبكية المتعامدة لطاقة جهد السطح لنواة $^{182}_{74}W_{108}$. حيث اظهرت انحداراً من المقدار 9.697MeV عند γ=60° ومن المقدار 5.022MeV الى 2.254MeV مروراً بطاقة جهد نقطة الصفر عندما تتغير (β=0→2.4).

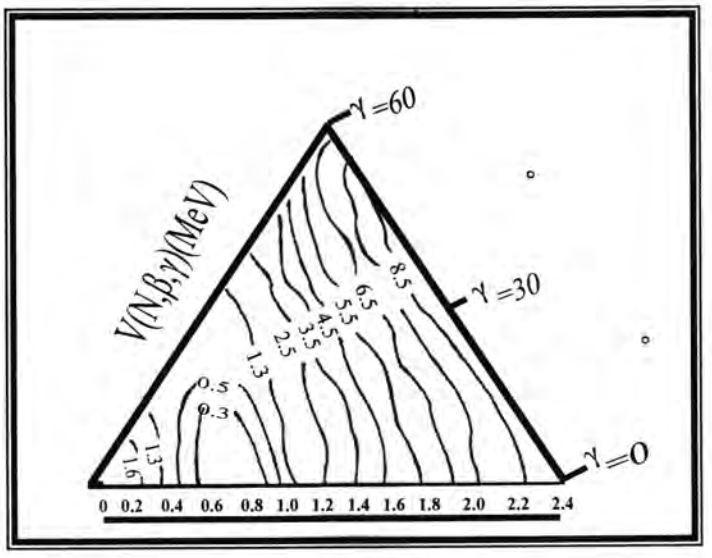

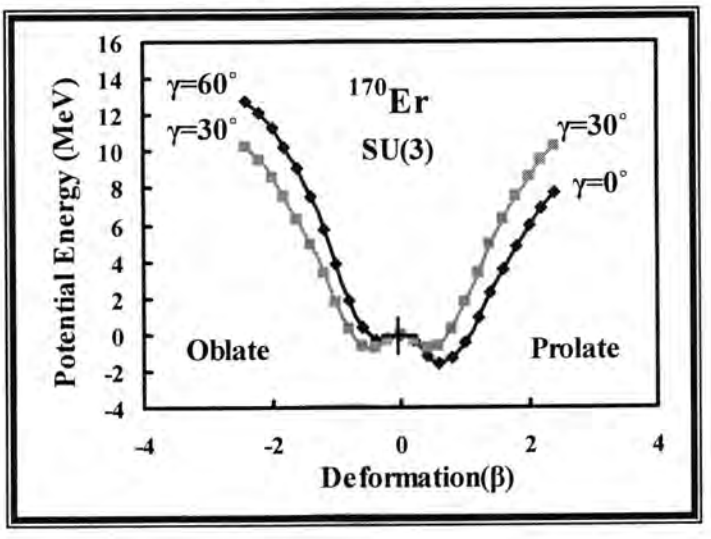

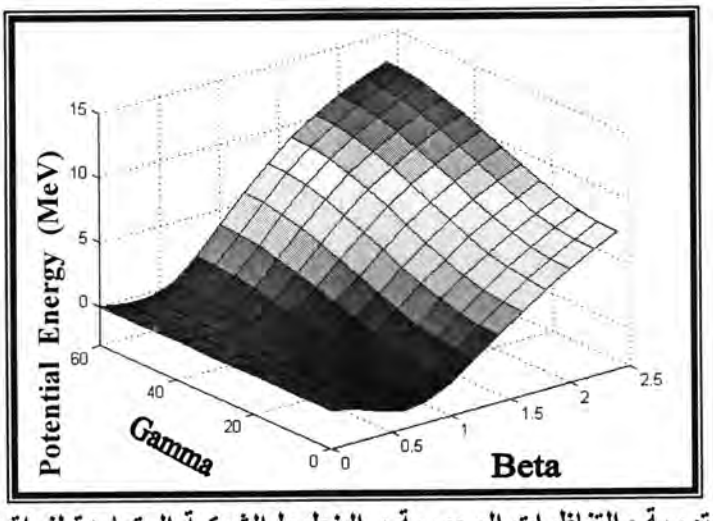

شكل -3 : الخطوط الكنتورية والتناظرات المحورية و الخطوط الشبكية المتعامدة لنواة Er(A=170).

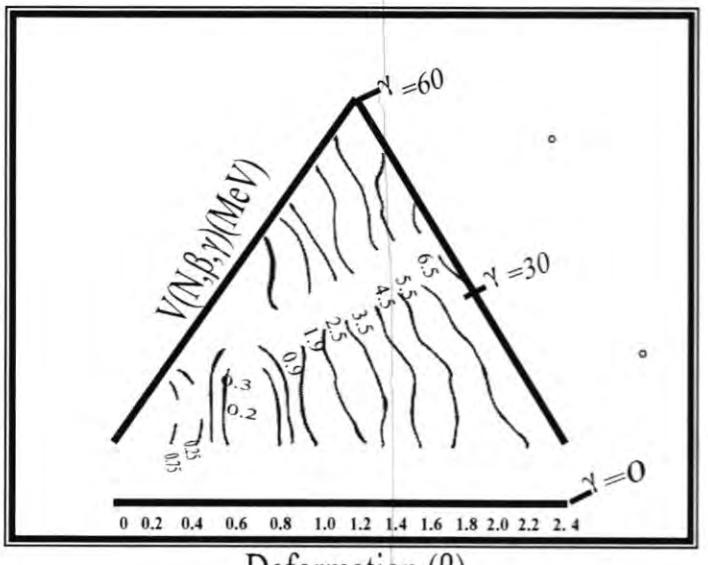

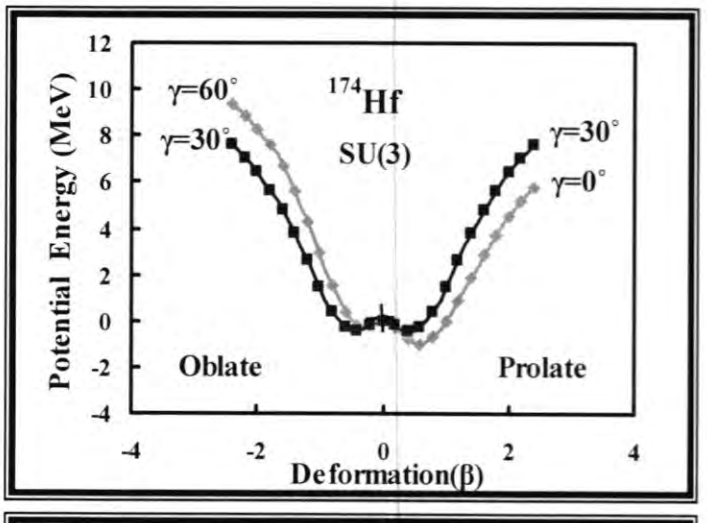

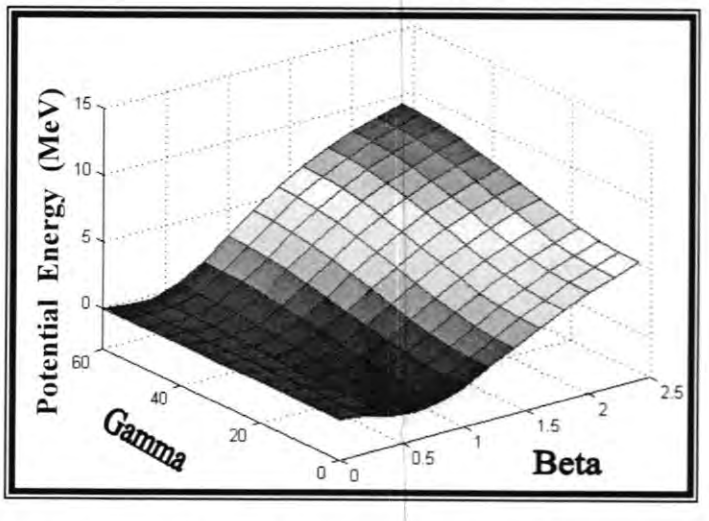

شكل -4 : الخطوط الكنتورية و التناظرات المحورية و الخطوط الشبكية المتعامدة لنواة Hf(A=174).

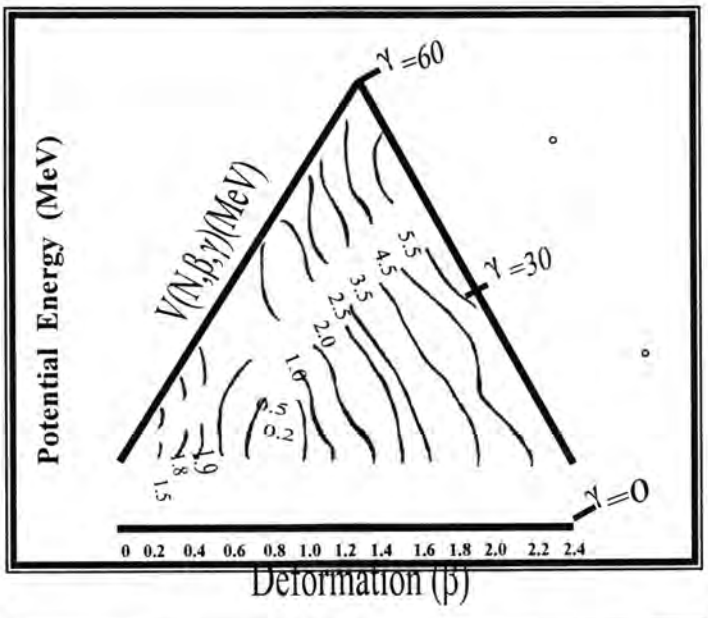

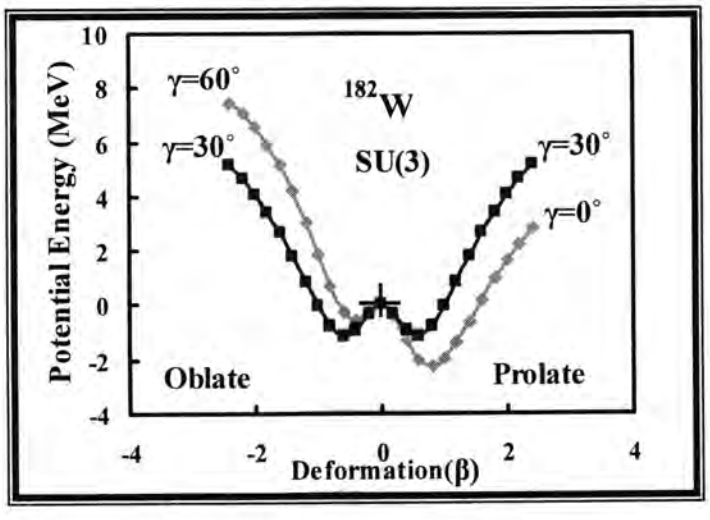

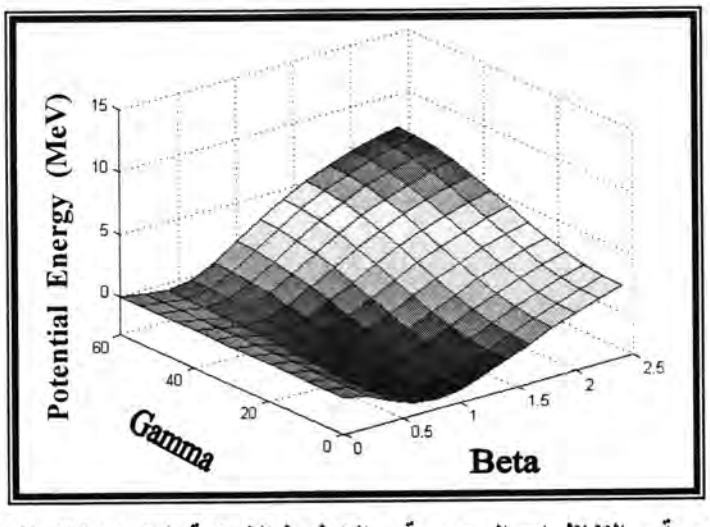

شكل -5 : الخطوط الكنتورية و التناظرات المحورية و الخطوط الشبكية المتعامدة لنواة W(A=182).

جدول -2: قيم طاقة جهد السطح V(N,β,γ) لنواة Er(A=170).

Beta	γ=0°	γ=5°	γ=10°	γ=15°	γ=20°	γ=25°	γ=30°	γ=35°	γ=40°	γ=45°	γ=50°	γ=55°	γ=60°
0.0	0.000	0.000	0.000	0..000	0.000	0.000	0.000	0.000	0.000	0.000	0.000	0.000	0.000
0.2	-0.366	-0.363	-0.357	-0.347	-0.334	-0.319	-0.303	-0.287	-0.272	-0.259	-0.249	-0.243	-0.241
0.4	-1.152	-1.139	-1.099	-1.035	-0.952	-0.855	-0.751	-0.647	-0.551	-0.468	-0.404	-0.364	-0.350
0.6	-1.605	-1.571	-1.473	-1.316	-1.113	-0.875	-0.620	-0.365	-0.128	0.076	0.233	0.331	0.365
0.8	-1.320	-1.266	-1.105	-0.850	-0.518	-0.130	0.285	0.700	1.088	1.42	1.675	1.835	1.890
1.0	-0.399	-0.328	-0.117	0.218	0.655	1.163	1.709	2.254	2.763	3.199	3.534	3.745	3.816
1.2	0.872	0.955	1.200	1.589	2.096	2.686	3.319	3.953	4.543	5.050	5.439	5.683	5.767
1.4	2.250	2.340	2.604	3.024	3.571	4.208	4.891	5.575	6.212	6.759	7.178	7.442	7.532
1.6	3.589	3.682	3.954	4.387	4.952	5.609	6.314	7.019	7.677	8.241	8.674	8.946	9.039
1.8	4.817	4.910	5.184	5.618	6.185	6.44	7.552	8.260	8.920	9.487	9.921	10.195	10.288
2.0	5.911	6.003	6.272	6.701	7.910	7.910	8.609	9.307	9.958	10.517	10.946	11.215	11.307
2.2	6.869	6.959	7.222	7.641	8.821	8.821	9.502	10.183	10.818	11.364	11.782	12.045	12.135
2.4	7.705	7.791	8.046	8.452	9.595	9.595	10.255	10.915	11.531	12.059	12.464	12.719	12.806

جدول -3: قيم طاقة جهد السطح V(N,β,γ) لنواة Hf(A=174).

Beta	γ=0°	γ=5°	γ=10°	γ=15°	γ=20°	γ=25°	γ=30°	γ=35°	γ=40°	γ=45°	γ=50°	γ=55°	γ=60°
0.0	0.000	0.000	0.000	0..000	0.000	0.000	0.000	0.000	0.000	0.000	0.000	0.000	0.000
0.2	-0.234	-0.232	-0.228	-0.221	-0.212	-0.201	-0.190	-0.179	-0.168	-0.159	-0.152	-0.148	-0.147
0.4	-0.728	-0.718	-0.690	-0.646	-0.588	-0.520	-0.448	-0.376	-0.308	-0.250	-0.206	-0.178	-0.168
0.6	-0.976	-0.952	-0.884	-0.775	-0.632	-0.467	-0.289	-0.111	0.054	0.196	0.306	0.374	0.398
0.8	-0.712	-0.674	-0.562	-0.384	-0.153	0.117	0.407	0.697	0.967	1.199	1.376	1.488	1.526
1.0	-0.015	0.035	0.182	0.416	0.720	1.075	1.455	1.835	2.190	2.494	2.728	2.875	2.925
1.2	0.916	0.974	1.145	1.416	1.769	2.181	2.623	3.064	3.476	3.829	4.101	4.271	4.329
1.4	1.912	1.975	2.159	2.451	2.833	3.277	3.753	4.230	4.674	5.056	5.348	5.532	5.595
1.6	2.872	2.937	3.127	3.429	3.822	4.281	4.773	5.264	5.723	6.116	6.418	6.608	6.673
1.8	3.750	3.815	4.005	4.308	4.703	5.163	5.657	6.151	6.611	7.006	7.309	7.500	7.565
2.0	4.529	4.593	4.781	5.080	5.470	5.923	6.410	6.897	7.351	7.741	8.040	8.228	8.292
2.2	5.211	5.273	5.457	5.748	6.129	6.571	7.046	7.522	7.964	8.345	8.636	8.820	8.882
2.4	5.804	5.864	6.042	6.325	6.693	7.122	7.582	8.043	8.472	8.840	9.123	9.301	9.361

جدول -4 : قيم طاقة جهد السطح V(N,β,γ) لنواة W(A=182).

Beta	γ=0°	γ=5°	γ=10°	γ=15°	γ=20°	γ=25°	γ=30°	γ=35°	γ=40°	γ=45°	γ=50°	γ=55°	γ=60°
0.0	0.000	0.000	0.000	0..000	0.000	0.000	0.000	0.000	0.000	0.000	0.000	0.000	0.000
0.2	-0.372	-0.370	-0.364	-0.355	-0.343	-0.330	-0.315	-0.301	-0.287	-0.275	-0.266	-0.261	-0.259
0.4	-1.254	-1.242	-1.205	-1.148	-1.072	-0.985	-0.890	-0.796	-0.709	-0.633	-0.576	-0.39	-0.527
0.6	-2.015	-1.985	-1.896	-1.754	-1.569	-1.354	-1.123	-0.892	-0.676	-0.491	-0.350	-0.260	-0.230
0.8	-2.254	-2.205	-2.059	-1.828	-1.527	-1.176	-0.799	-0.422	-0.072	0.230	0.461	0.606	0.656
1.0	-1.976	-1.911	-1.720	-1.416	-1.020	-0.560	-0.065	0.430	0.891	1.286	1.590	1.781	1.846
1.2	-1.366	-1.290	-1.068	-0.716	-0.256	0.279	0.853	1.427	1.962	2.422	2.774	2.996	3.072
1.4	-0.604	-0.522	-0.283	0.097	0.593	1.170	1.790	2.410	2.987	3.483	3.863	4.102	4.184
1.6	0.189	0.273	0.520	0.912	1.424	2.020	2.659	3.294	3.895	4.406	4.799	5.046	5.130
1.8	0.948	1.032	1.280	1.674	2.188	2.786	3.427	4.069	4.667	5.181	5.575	5.823	5.907
2.0	1.643	1.727	1.971	2.360	2.866	3.456	4.089	4.722	5.312	5.819	6.208	6.452	6.535
2.2	2.266	2.348	2.586	2.965	3.460	4.035	4.653	5.271	5.846	6.340	6.720	6.958	7.039
2.4	2.818	2.897	3.128	3.496	3.974	4.532	5.131	5.729	6.287	6.766	7.133	7.364	7.443

المصادر

1. Bohr A., and Mottelson B.R, "Symmetry and Shape of Nuclear Equilibrium Deformation", Mat. Fys. Medd. Dan.Vid. Selsk, Vol.27, P.16 (1953).
2. Casten R.F and Warner D.D., "The Interacting Boson Approximation", Rev.Mod.Phys., 60 : 389 (1988).
3. Lilley J.S. "Nuclear Physics Principle and Application ", John Wiley and Sons,Ltd., New York, :53-63(2002).
4. Arima A. and Iachello F., "The Interacting Boson Model", The Syndicate Press of the University of Cambridge, England, :3-127(1987).
5. Bonatsos D. "Interacting Boson Model of Nuclear Structure" Oxford University Press, New York, : 1- 271 (1988).
6. Chiang H.C.,Hsien S.T.,Jiang C.W.,Sun H.Z. and Han Q.Z., "Calculation of Superdeformed Interacting Boson Model for the A=190 Region",Chain Journal of Physics, 37, :25 (1999).
7. Bender M.,Bonche P.,Duguet T. and Heenen P.H., "Spectroscopy of Heavy Nuclei by Configuration Mixing of Symmetry Restored Mean-Field States : Shape Coexistence in Neutron-Deficient Pb Isotopes", arXiv:Nucl-Theo.1, :0302057(1) (2003).
8. Van Iscaker P.,Ganil A., and France I., "Symmetries of the Interacting Boson Model", Workshop on Subatomic Physics, Tunis, P.1(2006)..
9. Hellemans V., Van Iscaker P., Baerdemacker D. and Heydek I.,"Phase Transitions in the Configuration Mixed Interacting Boson Model SU(3) ",Acta Physica Polonica B, 38, :1599 (2007).

10. Talmi I., "Simple Models of Complex Nuclei, The Shell Model and Interacting Boson Model ", Harwood Academic Publishers, :187-198(1993).
11. Pfiefer W. "An Introduction to the Interacting Boson Model of the Atomic Nucleus", Part.II, :13-28(1998).
12. Jolie J.,Casten R.F.,Brentano V.P. and Werner V., "Quantum Phase Transition for γ-Soft Nuclei", Phys.Rev.Lett.,87: 1625(1) (2001).
13. Lo Iudice A. and La Revistal Del Nuovo C., "Deformation Energy Surfaces of Nucleus ", 23, :9 (2000).
14. Van Iscaker P. and Chen J.Q, "The Investigation Potential of Even-Even Nuclei Under the Frame Work of (IBM-1) ", Phys.Rev.C, 24:684 (1981).

دراسة امتزاز ترايبروليدين وميتوكلوبرأمايد هيدروكلورايد من محاليلها المائيةعلى سطوح البنتونايت والكاؤولين

يوسف كاظم عبد الامير ومدير مبارك مرزا
الجامعه المستنصرية / كلية العلوم / قسم الكيمياء

ABSTRACT

The objective of this work is to search for a selective naturally active surfaces (Bentonite and Kaolin) for adsorption of Triprolidine and Metoclopramide drugs that causes poisoning when taken orally at doses.
The results of this study showed full applicably of Frendlich model of his adsorption of two drugs and S-shape according to Gilles classification.
The study was extended to cover the effect of temperature and determined the thermodynamic function such as ΔH, ΔG and ΔS.
The effect of the ionic strength showed that the quantity of adsorption decreased with increasing the concentration of salt, and also the adsorption was affected by the pH of the solution.
The adsorption of the two drugs was decreased with the particle size of the clays.

الخلاصة

تمت دراسة امتزازالمادتين الدوائيتين Triprolidine and Metoclopramide على سطوح البنتونايت والكاؤولين المتوافرة محلياً في العراق ، وذلك بهدف التوصل الى معرفة فعالية هذه السطوح وإمكانية إستخدامها كترياقات فيزيائية لمعالجة حالات التسمم بهاتين المادتين الدوائيتين إذا تمّ تعاطيها بجرعات تفوق جرعاتها الاعتيادية . يكون شكل الايزوثيرم للمادتين من نوع فريندلش وينتمي الى الصنف (S) حسب تصنيف جيليس. وأظهر البنتونايت قابلية أعلى من الكاؤولين في امتزاز المادتين الدوائيتين. كما درس تأثير درجة الحرارة وبينت الدراسة إن العملية باعثة للحرارة ,وكذلك تم حساب الدوال الثرموديناميكية (ΔH, ΔG,ΔS). كما درس تأثير الشدة الآيونية على الامتزاز فوجد ان كمية الامتزاز تقل بزيادة تركيز الملح. وبينت النتائج ان المادتين الدوائيتين تتأثر بتغير الدالة الحامضية , وان الامتزاز يقل بزيادة حجم دقائق الطين.وتبين النتائج التي حصلنا عليها إمكانية أستخدام هذه السطوح كمواد مازة لازالة المواد السامة والمركبات العضوية من محاليلها بكفاءة عالية.

المقدمة

تعد المعادن الطينية من أكثر المعادن شيوعاً , وقد تتكون المعادن الطينية من معدن واحد، أو قد تحتوي على كميات متفاوتة من المعادن الطينية مثل: الكوارتز أو الكالسايت , كما إن الكثير من المواد الطينية تحتوي على مواد عضوية وأملاح قابلة للذوبان في الماء,ومن خصائص البنتونايت انه حينما يمتص الماء في الوسط المحيط به فأن حجمه يمكن ان يكبر الى ستة اضعاف حجمه الاصلي(1). ويمتاز مسحوق البنتونايت بإمتلاكه مساحة سطحية كبيرة، وقدرته العالية على التبادل الايوني(2). وكل صفيحة تتكون من ثلاث طبقات ، طبقة من أوكسيد الالمنيوم ثمانية السطوح الواقعة بين طبقتين من أوكسيد سليكات رباعية السطوح ، أي بنسبة (1:2).

أما عن أهميته في المجال الطبي فهو يدخل في صناعة المراهم، وكذلك في تحضير المحلول الطبي كالامين (Calamine lotion) (3). ويستعمل ايضاً كمادة مازة (4) .

أما سطح الكاؤولين فيتكون من طبقتين هما: السيليكات (SiO_2) رباعي السطوح، والألمنيوم [$Al_2(OH)_4$] ثماني السطوح أي بنسبة (1:1) ، ووجد أن الكاؤولين لايحتوي على جزيئات مائية داخل الطبقات مقارنة بالبنتونايت، وليس له القابلية على التبادل الأيوني(5)،

وله أهمية طبية حيث يدخل في تركيب بعض المستحضرات الطبية مثل البكتوكاؤولين (Pectokaolin)(3).

ومن الدراسات السابقة نُشرت دراسة تتضمن امتزاز كل من (Chlordiazepoxide.Hcl , Amitriptyline.Hcl , chlorpromazine.Hcl) على سطح البنتونايت عند ظروف مختلفة من درجة الحرارة والشدة الايونية لمحلول الامتزاز ، ولقد بَينَ ان امتزاز المركبات الدوائية المذكورة عند درجة حرارة جسم الانسان الاعتيادية تكون وفق الترتيب الاتي(6) :

Chlordiazepoxide.Hcl > chlorpromazine.Hcl> Amitriptyline.Hcl

وفي دراسة أخرى قام **(Chukwuenweniwe)** وجماعته بدراسة امتزاز (Flouroquinolones) على بعض المواد الصيدلانية المازة (الفحم المنشط والكاؤولين والبنتونايت) فوجدوا ان الفحم المنشط يرتبط بسرعة مع (Flouroquinolones) وذات سعة امتزاز عالية , ثم يليها البنتونايت ، بينما الكاؤولين فكان له أقل سعة امتزاز من كليهما(7) .

كمااجرى **(Camazano)** دراسة لأمتزاز (Chlorpheniramine maleate) على سطح المونتموريلونايت في محاليل مختلفة الدالة الحامضية، ووجدوا إنه بزيادة الدالة الحامضية للمحلول تزداد كمية الدواء الممتزة على السطح , وأيضاً فسرت هذه الدراسة ان عملية الامتزاز تتم عن طريق تبادل الايونات الموجبة بين الدواء والسطح(8) .

كما استخدم **(Cooney)** وزملاؤه أربعة أنواع من الفحم المنشط المتوافرة محلياً في عملية الامتزاز، ودرسوا قابلية هذه الانواع الاربعة على امتزاز الادوية الآتية: (Chlorpheniramine maleate , Phenobarbital , Theophylline) . وفسروا الاختلاف في سعة الامتزاز من حيث المساحة السطحية ، فكلما كانت المساحة السطحية كبيرة كلما زادت سعة الامتزاز(9). وسيجري في هذا البحث دراسة امتزاز المادتين الدوائيتين ترايبروليدين وميتوكلوبرأمايد على السطوح البنتونايت والكاؤولين،

وايضاً دراسة تأثير كل من درجة الحرارة والدالة الحامضية والشدة الايونية وحجم الحبيبات على عملية الامتزاز.

المواد وطرائق العمل

تم استخدام المواد الكيميائية الاتية Sodium (Ka-GaraniteSwitzerland 99.5% Chloride وكذلك Hydrogen Chloride(BDH England) 37w/w ،وتم استخدام جهاز(UV/VIS Conc.VARIAN,USA100في المدى900-200)وحمام مائي مزود بجهاز رج ومسيطر على درجة حرارته،و جهاز قياس الدالة الحامضية، جهاز الطرد المركزي، مناخل ذات قياسات mesh(80 , 100 , 200).

أجرينا دراسة تحديد البيانات الامتزازية للمادتين الدوائيتين هما ترايبروليدين وميتوكلوبرأميد أثناء امتزازهما على سطوح البنتونايت والكاؤولين من محاليلهماالمائية، وذلك بتعيين تراكيز المحاليل التوازنية بعد الامتزاز باستخدام الطريقة الطيفية .

وقد تم العمل وفقاً للخطوات الآتية :

- تعيين الطول الموجي المناسب لانشاء منحني المعايرة القياسي (امتصاص- تركيز) للمادتين الدوائيتين بتركيز(1×10^{-4} mole/L) باستخدام الجهازUV/VIS فكانت (276 nm) لمادة ترايبروليدين و(272 nm) لمادة ميتوكلوبرأمايد .
- تعيين منحني المعايرة من خلال تحضير عدة محاليل ($10^{-5}\times(10 - 1)$ mole/L)وقياس الامتصاص لها .

تم غسل الاطيان المستخدمة بالماء المقطروتجفيفها عند الدرجة (160 °C)لمدة ثلاث ساعات. لغرض إيجاد آيزوثيرم الامتزاز لكل مادة دوائية مع كل سطح ، تم تحضير سبعة محاليل مختلفة التركيز لكل مادة دوائية في المدى (1×10^{-4} - 30 $\times10^{-4}$ mole/L) ، وأضيف لكل

حجم (12.5 ml) من هذه التراكيز (0.25 gm) من كل طين من الاطيان المستخدمة في هذه الدراسة ذات الحجم الحبيبي أقل من (75 µm)، في قناني حجمية سعة (50 ml) مجهزة بسدادات محكمة، ثم وضعت القناني في حمام مائي مزود بهزاز وبسرعة (120 rpm) عند درجة حرارة (37.5 °C) ولزمن الاتزان المحدد ساعتين للمادة ترايبروليدين وساعتين ونصف للمادة ميتوكلوبرأمايد, وبعدالترشيح والفصل تم قياس الامتصاص وتعيين تركيز الاتزان بعد الرجوع الى منحني المعايرة.

وبنفس الخطوات تمت دراسة العوامل المؤثرة في الأمتزاز (الدالة الحامضية ، درجة الحرارة ، الشدة الآيونية ، مزج السطحين ، حجم الجسيمات) .

النتائج والمناقشة

لغرض تعيين آيزوثيرمات الامتزازتم حساب كمية المادة الممتزة (mg/g) من العلاقة الاتية(10):

$$Q_e = \frac{V_{sol}\ (C_o - C_e)}{m} \quad \text{..... ....(1)}$$

إذ ان : (V_{sol}) = حجم المحلول المأخوذ (L) .

(C_o) = التركيز الأبتدائي لكل محلول (mg/L).

(C_e) = تركيز المحلول عند الاتزان(mg/L).

(m) = وزن الطين (gm).

وبرسم العلاقة البيانية بين كمية المادة الممتزة (Q_e) مقابل تركيز الاتزان (C_e)،تم ايجاد نوع الايزوثيرم كما مبين في الشكل (1) .

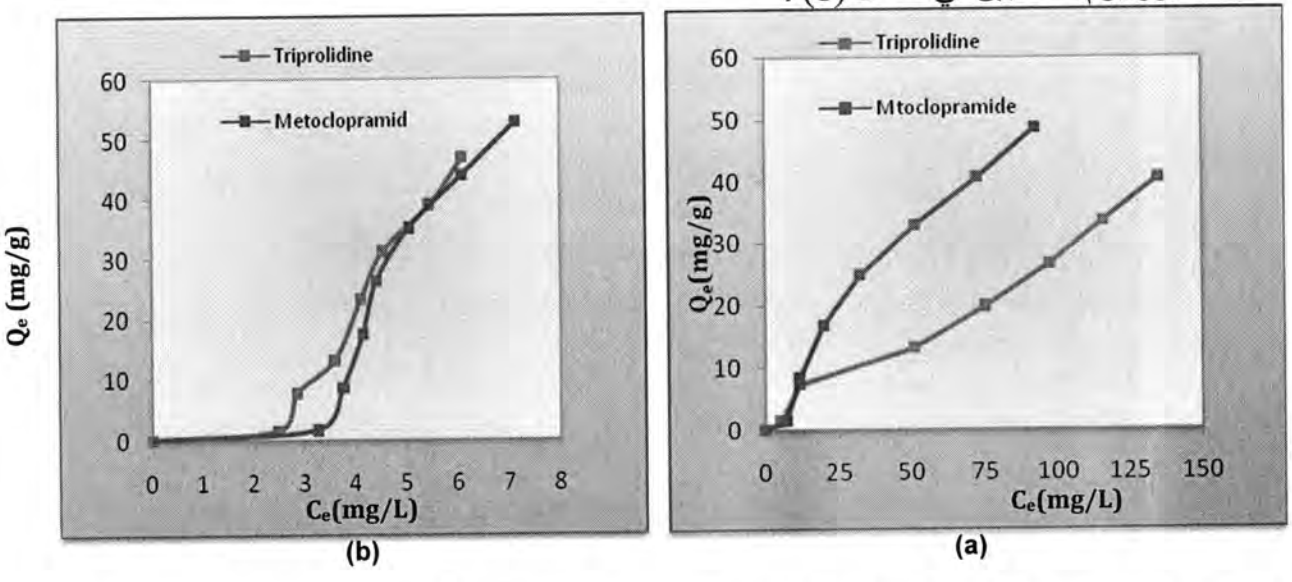

الشكل -1: آيزوثيرمات الأمتزاز Triprolidine.HCl و Metocloprmid.HCl على سطحي a) البنتونايت b) الكاؤولين عند درجة حرارة 310.5 K و pH ≈ 7 .

النوع (S) المستند الى أساسيات فريندلش للأمتزاز يتحقق على السطوح غير المتجانسة (11). وباستخدام معادلة فريندلش

$$\log Q_e = \log K_f + \frac{1}{n} \log C_e \quad \text{..... ... .(2)}$$

نحصل على العلاقات الخطيةالاتية:

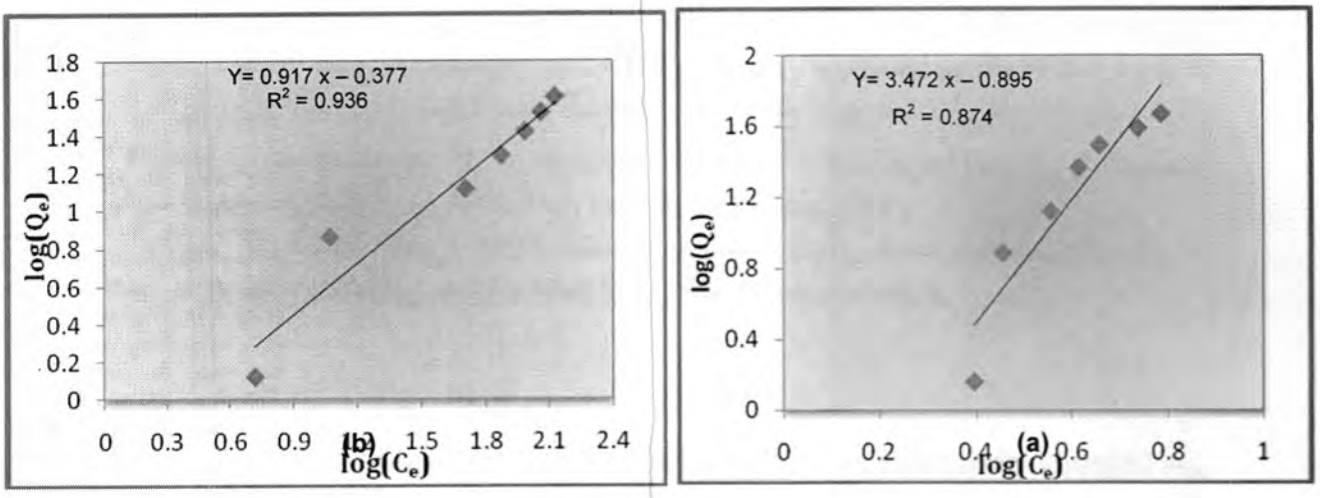

الشكل- 2: مستقيمات Freundlich لمادة Triprolidine.HCl الممتزة على سطحي : a) البنتونايت b) الكاؤولين .

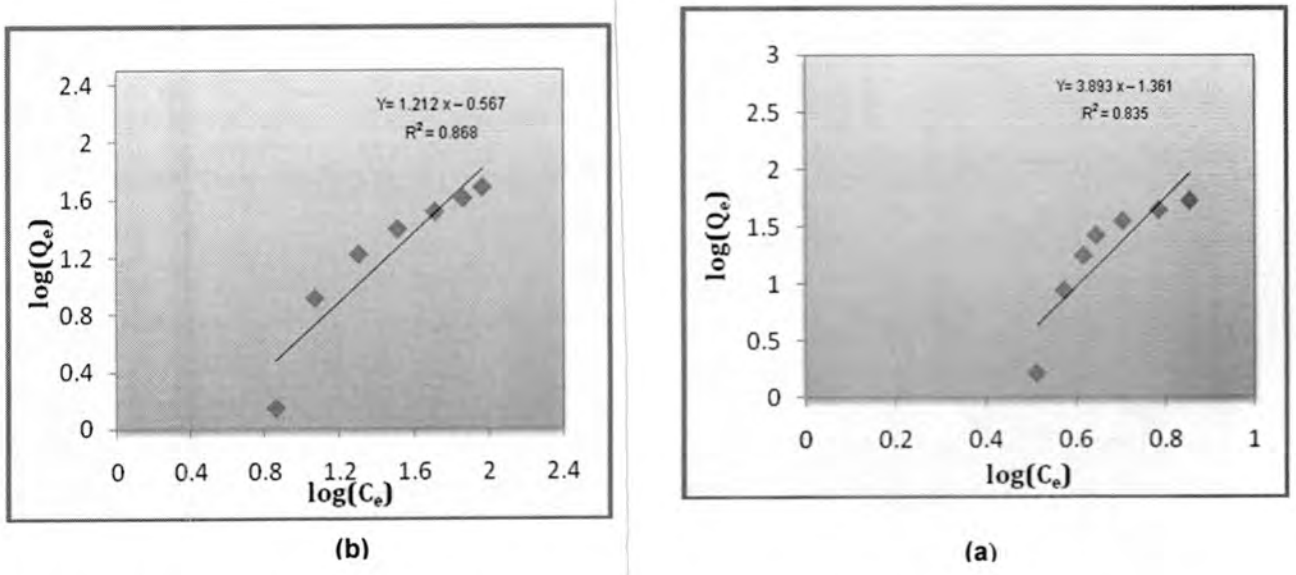

الشكل–3: مستقيمات Freundlich لمادة Metocloprmide.HCl الممتزة على سطحي : a) البنتونايت b) الكاؤولين

الجدول -1: يوضح قيم معاملات الأرتباط وثوابت Freundich التجريبية لكل من *Triprolidine .HCl* و Metaclopramide .HCl الممتزة على سطحي الكاؤولين والبنتونايت عند درجة حرارة 37.5 °C ودالة حامضية7≈ pH.

Clays	Triprolidine.Hcl			Metoclopramide.Hcl		
	n	k_f (mg/g)	R	n	k_f (mg/g)	R
Bentonite	0.2880	0.1273	0.874	0.2568	0.0435	0.835
Kaolin	1.0905	0.4197	0.936	0.8250	0.2710	0.868

إذ إن قيمة (K_f) تمثل سعة الامتزاز ، و(n) تمثل شدة الامتزاز أو درجة أعتمادية الامتزاز على التركيز(12) .

القيمة الواطئة لـ (n) تشيرالى إن هذه السطوح تكون فعّالة عند التراكيز الواطئة للمادة الدوائية (13) ، وكذلك حصول آلية امتزاز مناسبة وتكوين أوآصر قوية نسبياً بين المادة المازة والمادة الممتزة ، وان قيمة (n) العالية نسبياً للكاؤولين مقارنة مع البنتونايت تدل على أن عدد المواقع المناسبة في هذا السطح هو أقل من البنتونايت .أما قيم (K_f) المستخرجة تشيرالى إن السطحين لهما القابلية على امتزاز وإزالة المادتين الدوائيتين من المحلول(14) .

وبعض الدراسات الأخيرة (15) أثبتت إن ثوابت فريندلش ليست لها معنى فيزيائي أو كيميائي واضح بخصوص عمليات الامتزاز في أنظمة (صلب – سائل).

تأثير درجة الحرارة في الامتزاز:

لدراسة تأثير درجة الحرارة في امتزاز (Triprolidine) و (Metaclopramide) على سطحي البنتونايت والكاؤولين في محاليلها المائية أجريت تجارب لأمتزاز المادتين في درجات حرارية مختلفة (283 , 298 , 310.5 , 318 K) . كما موضح في الاشكال (4) و (5) .

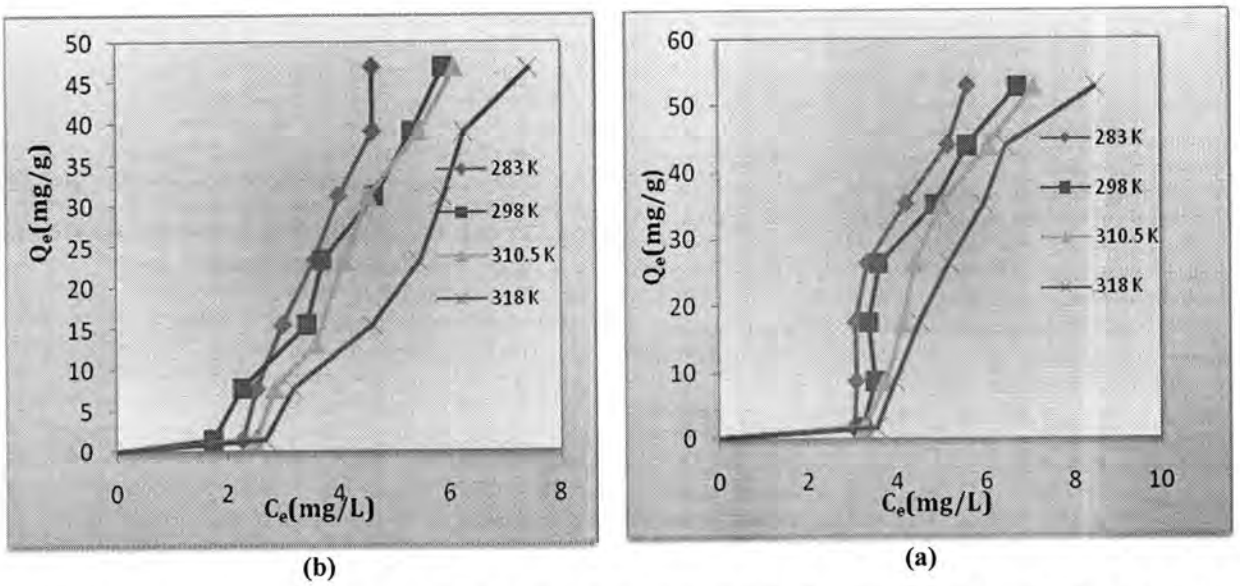

الشكل –4: ايزوثيرمات الامتزاز للمادتين الدوائيتين a) Triprolidine.HCl و b) Metoclopramide.HCl على سطح البنتونايت عند درجات حرارة مختلفة و pH ≈ 7.

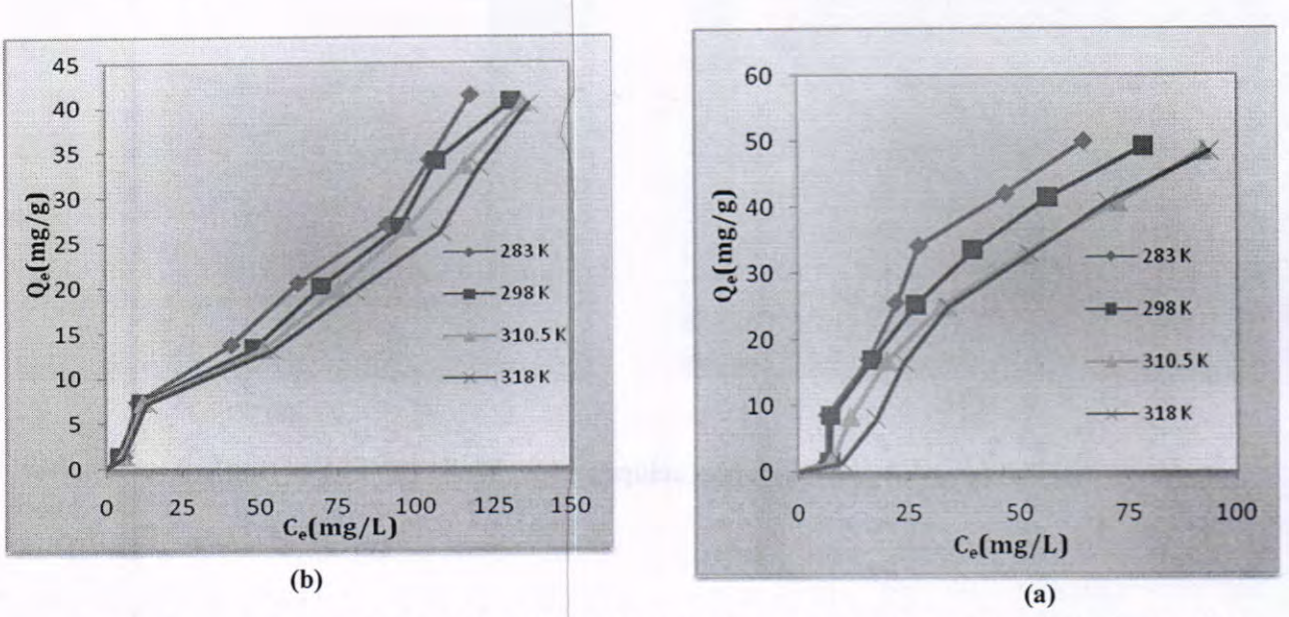

الشكل -5: ايزوثيرمات الامتزاز للمادتين الدوائيتين (a Triprolidine.HCl وb) Metoclopramide.HCl على سطح الكاؤولين عند درجات حرارة مختلفة و7 pH.

يلحظ من الشكلين (4)و(5) أن كمية المادة الممتزة للمادتين الدوائيتين على سطح البنتونايت والكاؤولين تقل بزيادة درجة الحرارة ، أي أن عملية الامتزاز هي باعثة للحرارة (Exothermic) ، وهذا يتفق مع الخواص الثرموديناميكية للأمتزاز لكون العملية باعثة للحرارة ، ويمكن تفسير ذلك نتيجة لضعف قوى التجاذب بين جزيئات الدواء والسطح المازكلما أرتفعت درجة الحرارة . بالاضافة الى ذلك فأن زيادة درجة الحرارة قد تزيد من ذوبانية المذاب في المذيب وبذلك تقل الألفة الأمتزازية نحو السطح (16) .

حساب قيم الدوال الثرموديناميكية:

إستناداً الى المعادلة (3) (Van't Hoff –Arrehenius equation) تم حساب كمية الحرارة المصاحبة لأمتزاز(ΔH) للمادتين الدوائيتين على السطحين، وذلك برسم قيم لوغارتيم أعظم كمية ممتزة (log Xm) عند قيمة معينة لتركيز الأتزان مقابل مقلوب درجة الحرارة (1/T) وكما موضح في الشكلين (6)و(7) .

$$\log X_m = \frac{-\Delta H}{2.303\,RT} + \frac{\Delta s}{R} \quad \text{..... ....(3)}$$

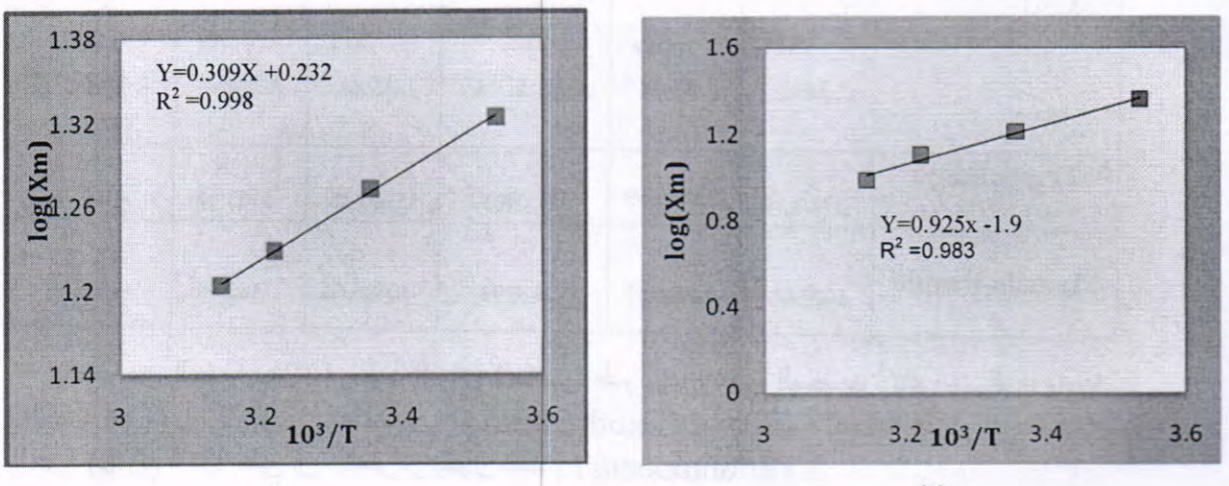

الشكل -6: قيم ($\log X_m$) مقابل($10^3/T$) للمادة Triprolidine.HCl الممتزة على سطحي a) البنتونايت b)

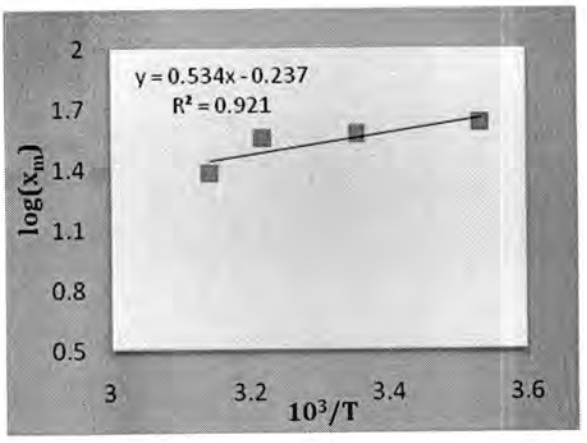

(a)

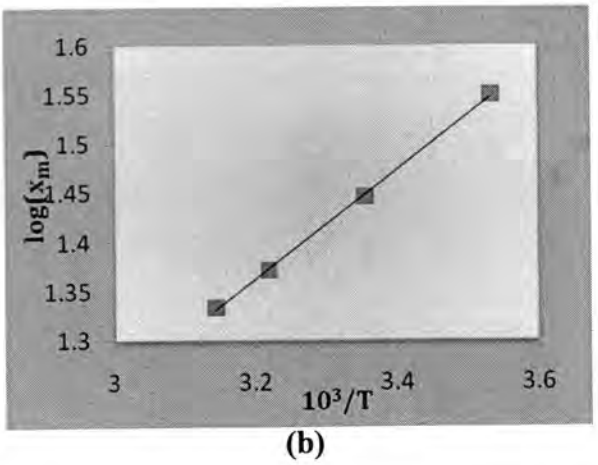

(b)

الشكل -7: قيم ($\log X_m$) مقابل($10^3/T$) للمادة Metoclopramide الممتزة على سطحي a) البنتونايت b) الكاؤولين

كما ويمكن حساب قيم (ΔG)

من المعادلة الاتية :

$\Delta G^\circ = -RT \ln K$ .....(4)

إذ ان : K = ثابت التوازن

وتم حسابه من المعادلة الآتية :

$$K = \frac{Q_e \, m_{(g)}}{C_e \, V_{(L)}} \quad \text{.....(5)}$$

ومن خلال إستعمال المعادلة (6) :

$$\Delta S = \frac{\Delta H}{T} \quad \text{.....(6).}$$

تم الحصول على قيمة (ΔS) ودونت النتائج في الجدول (2) .

الجدول -2: يوضح قيم($\Delta H\ \Delta S\ \Delta G$) لكل من Triprolidine و Metoclopramide الممتزة على سطحي البنتونايت الكاؤولين عند درجة حرارة 310.5 K .

Drugs	Bentonite			Kaolin		
	ΔH $J.Mole.^{-1}$	ΔG $J.Mole.^{-1}$	ΔS $J.Mole.^{-1}K^{-1}$	ΔH $J.Mole.^{-1}$	ΔG $J.Mole.^{-1}$	ΔS $J.Mole.^{-1}K^{-1}$
Triprolidine	-17711.10	-11070.69	-57.0405	-5916.46	-4263.61	-19.0546
Metoclopramide	-10224.57	-12795.57	-32.9293	-10626.66	-7102.94	-34.2243

يلحظ من الجدول (2) إن قيم (ΔH) للمادتين الدوائيتين على السطحين تكون سالبة، وهذا يتناسب مع كون الامتزاز باعثاً للحرارة (Exothermic) ، أما القيمة السالبة للتغير في الطاقة الحرة (ΔG) فتدل على أن الامتزاز يكون تلقائياً (Spontaneous) .

من ناحية أخرى وجد أن قيم (ΔS) للمادتين الدوائيتين على سطح الكاؤولين والبنتونايت تكون سالبة، وهذا يدل على أن الجزيئات الممتزة تنتظم على السطح نتيجة إرتباطها بالسطح الماز ، أي إن الجزيئات الممتزة تكوّن أنتظاماً خلال وجودها في المحلول (16) .

تأثير الشدة الآيونية:

أجريت دراسة تأثير الشدة الايونية في امتزاز المادتين الدوائيتين (Triprolidine , Metaclopramide) على سطحي البنتونايت والكاؤولين عند درجة حرارة جسم الانسان (310.5K) في محاليلها المائية ، وذلك بأستخدام ثلاثة تراكيز مختلفة من ملح كلوريد الصوديوم (NaCl) وهي (0.4 F , 0.2 , 0.154) وتمت مقارنتها مع نتائج الامتزاز في المحلول الخالي من ملح كلوريد الصوديوم وكما مبين في الشكل (8) و(9).

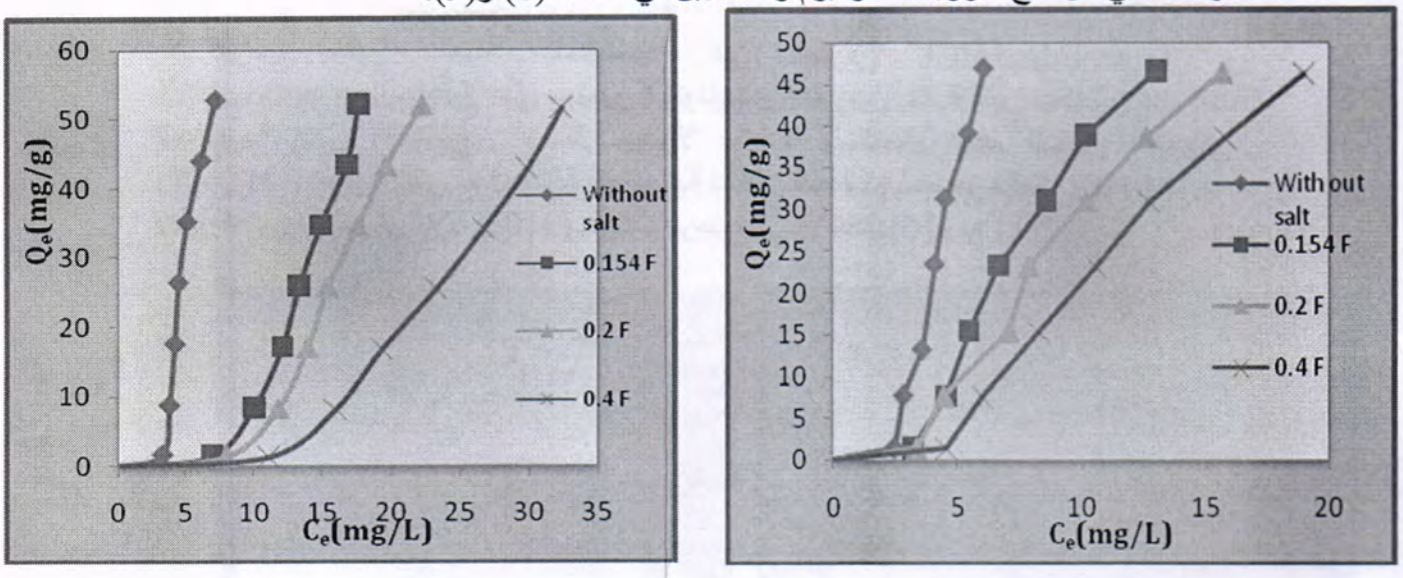

الشكل-8: ايزوثيرمات الامتزاز للمادتين الدوائيتين a) Triprolidine.HCl وb) Metoclopramide.HCl على سطح البنتونايت بتراكيز مختلفة من (NaCl) عند درجة 310.5K و pH ≈ 7 .

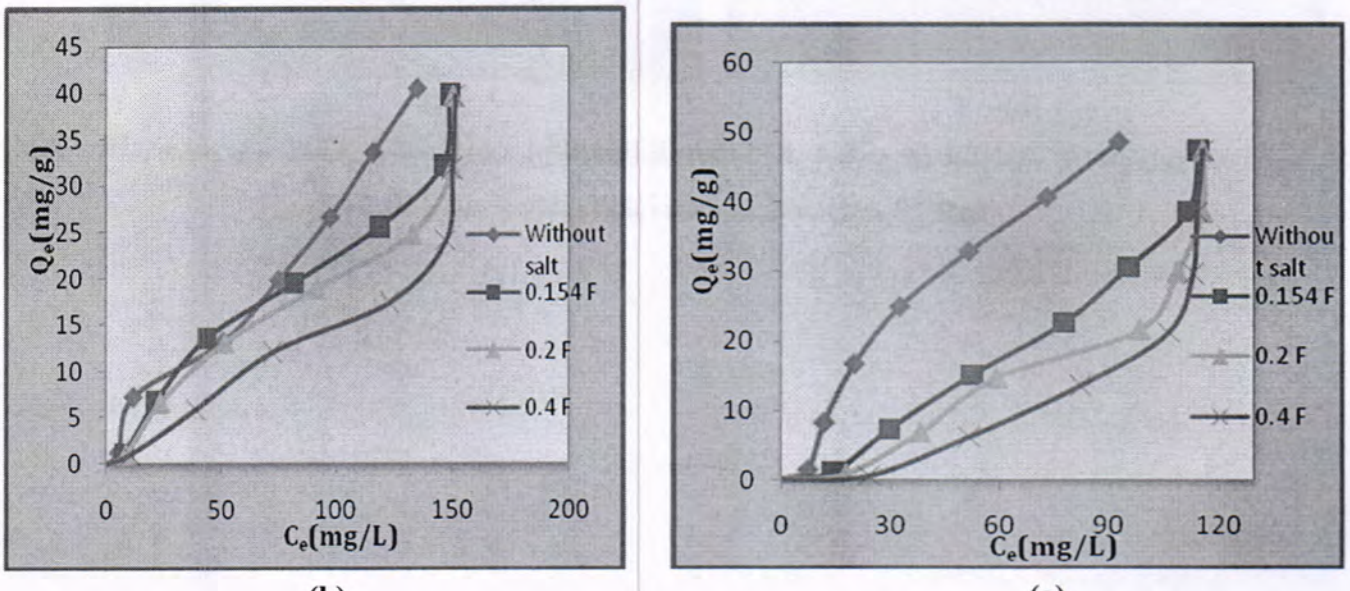

(b) (a)

الشكل -9: ايزوثيرمات الامتزاز للمادتين الدوائيتين a) Triprolidine.HCl وMetocloramide.HCl على سطح الكاؤولين بتراكيز مختلفة من (NaCl) عند 310.5K و pH ≈ 7

وعند مقارنة آيزوثيرمات الإمتزاز التي تم الحصول عليها بعد إضافة تراكيز مختلفة من ملح كلوريد الصوديوم
مع آيزوثيرمات الأمتزاز للمحلول الخالي من الملح تحت الظروف نفسها، وجد ان كمية المادة الممتزة للدوائين على السطحين تقل بزيادة تركيز محلول كلوريد الصوديوم ، أي ان بزيادة الشدة الآيونية تقل كمية المادة الممتزة.

ويمكن تفسير التأثير المثبط للألكتروليت المضاف (NaCl) على الأمتزاز بأن أيونات (Na^+) و(Cl^-) سوف تنافس جزيئات الدواء على المواقع الفعالة للسطح ، ويبدو ان التجاذب بين الايونات والسطح يكون أكبر من التجاذب بين جزيئات الدواء والسطح، لذلك سوف يقل التجاذب الألكتروستاتيكي بين السطح الماز والمادة الممتزة، وينتج عن ذلك نقصان في سعة الامتزاز .

تأثير الدالة الحامضية:

دُرس تأثير الدالة الحامضية في أمتزاز Triprolidine.HCl و Metoclopramide.HCl على سطحي البنتونايت والكاؤولين عند قيمتين مختلفتين من الدالة الحامضية وهي (pH≈7) وتمثل محلولاً متعادلاً بأستعمال الماء المقطر اللاآيوني، والآخر (pH=1.2) التي تمثل الدالة الحامضية لسائل المعدة تم تحضيرها من 0.1M HCl ، وبثبوت درجة الحرارة (310.5 K) ، وكما موضح في الأشكال(10) و(11).

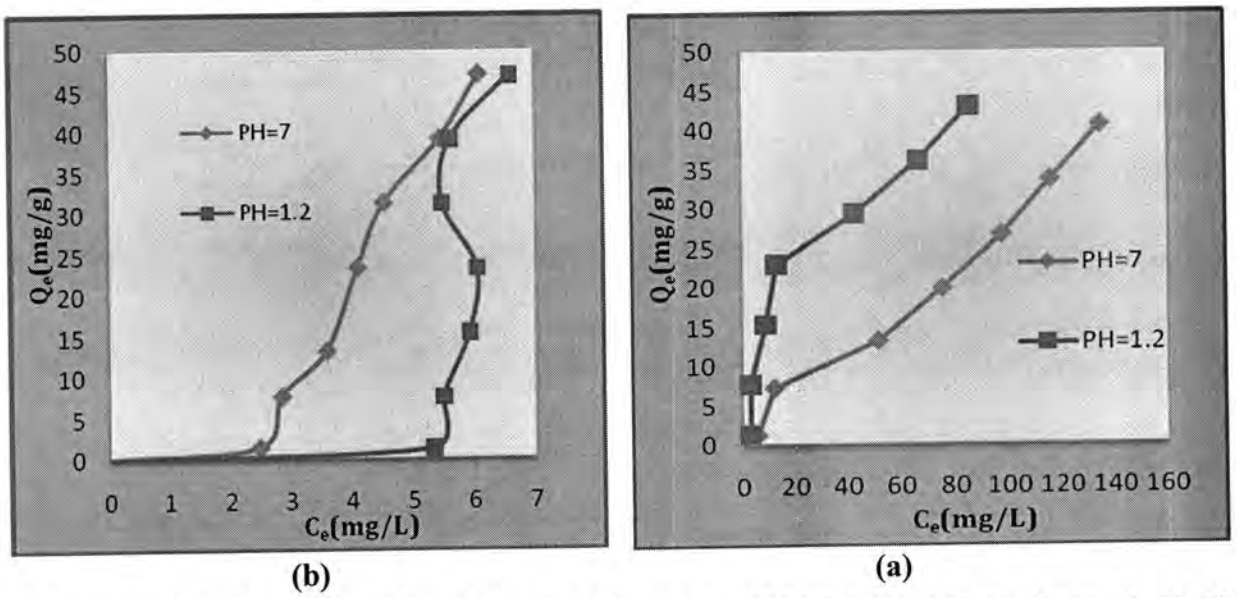

الشكل -10: ايزوثيرمات الامتزاز للمادة الدوائية Triprolidine.HCl على سطحي a) البنتونايت b) الكاؤولين عند درجة (310.5K) من محاليلها المائية و عند (pH = 1.2 ، pH ≈ 7)

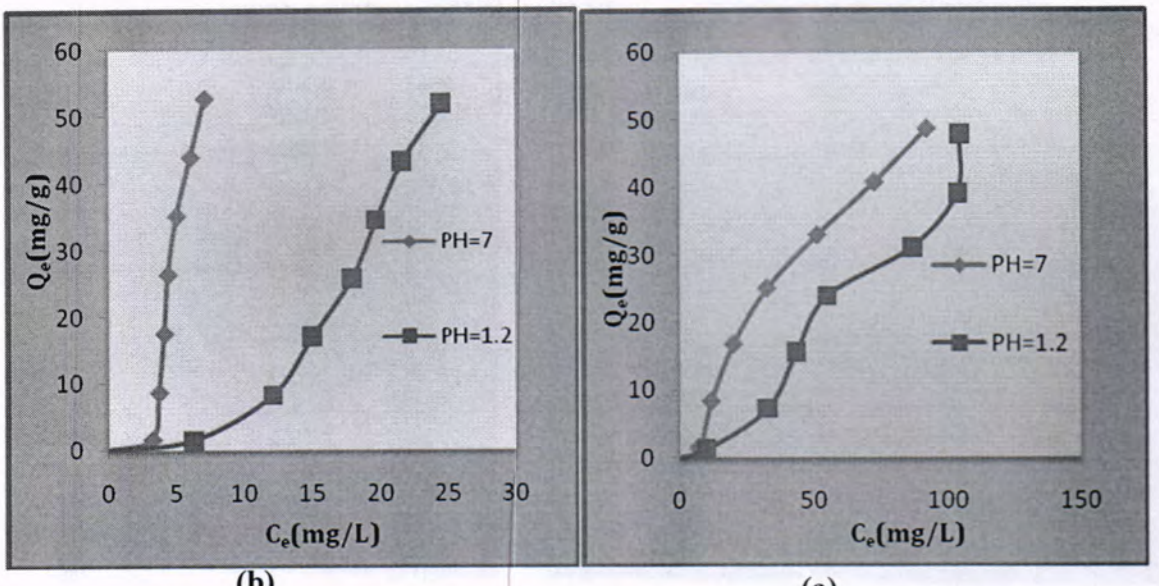

الشكل -11: ايزوثيرمات الامتزاز للمادة الدوائية Metoclopramide.HCl على سطحي a) البنتونايت b) الكاؤولين عند درجة (310.5K) من محاليلها المائية وعند($pH^{\approx}7$و$pH=1.2$)

حامضية (محلول حامضي)، مقارنة بسعة الامتزاز عندما يكون المحلول متعادلاً (pH≈7) ، ويمكن تفسير ذلك على أساس المنافسة التي تبديها آيونات الهيدروجين الموجبة (H^+) على المواقع الفعالة للسطح الماز، عندما (pH=1.2) أي عندما المحلول حامضي(17) .

أما تأثيرالدالة الحامضية في سطح الكاؤولين فنلحظ إن سعة امتزاز (Triprolidine.HCl) في المحلول الحامضي (pH=1.2) تزداد مقارنة مع سعة الامتزاز عند إستخدام الماء المقطر اللاأيوني كمذيب (pH≈7) ، ويمكن ان يعزى ذلك الى إمكانية التغير في صفات سطح الطين عند أقل دالة حامضية بسبب تأثير البروتون للحامض على المجاميع القطبية للسطح، والتي يحصل عندها تداخل بين السطح الماز وجزيئات المادة الدوائية التي تؤثر بدورها على عملية الامتزاز(18).

تأثير حجم دقائق الطين في الامتزاز:

أجريت دراسة تأثير حجم الدقائق لأطيان البنتونايت والكاؤولين في امتزاز Triprolidineو Metoclopramide وذلك بإستخدام تركيز ثابت من كل مادة دوائية وثلاث عينات من دقائق السطحين ذوات أوزان متساوية وبحجوم مختلفة (75,150,250 µm) عند درجة حرارة (310.5K) في محاليها المائية (pH≈7) ، وكما في الشكل (12).

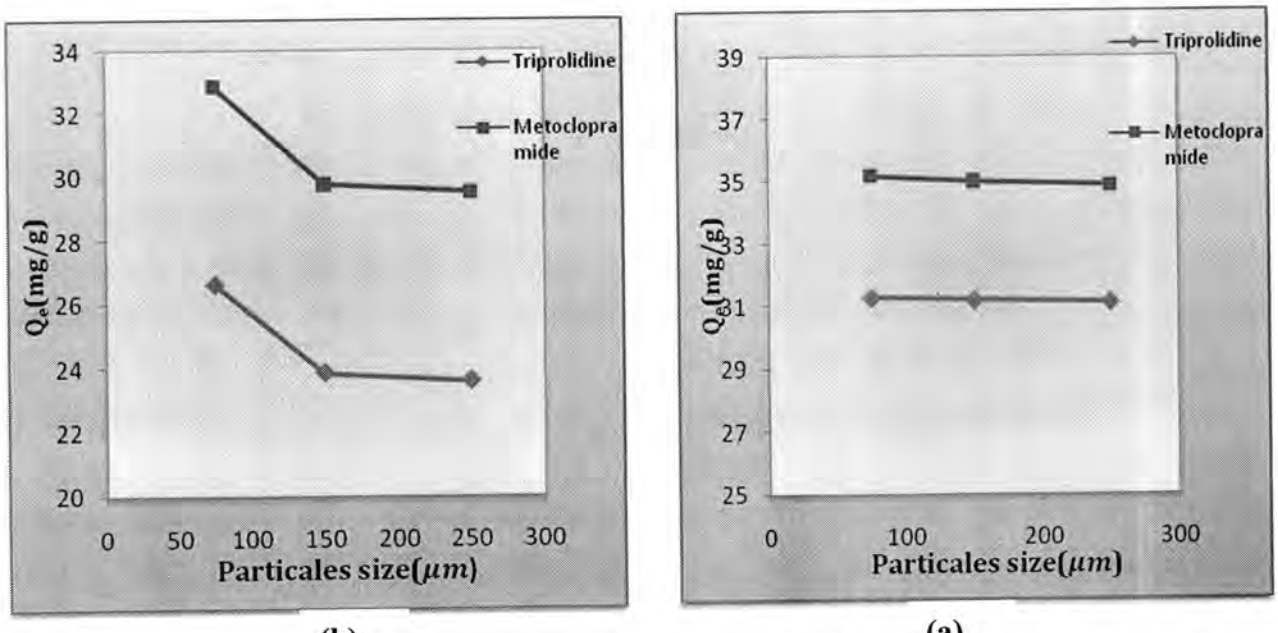

الشكل -12: تاثير حجم دقائق الطين على كمية امتزاز كل من Triprolidine.HCl و Metoclopramide.HCl على سطحي a) البنتونايت b) الكاؤولين عند درجة حرارة (310.5K) و pH ≈ 7

النتائج المبينة في الشكل (12) يوضح أن كمية الامتزاز للمادتين الدوائيتين تزداد على سطحي البنتونايت والكاولين بنقصان حجم دقائق الطين، أي بزيادة المساحة السطحية للمادة المازة ، وهذا أمر متوقع لأن المساحة السطحية تزداد مع نقصان حجم الحبيبات لوزن معين من الأطيان، وبالتالي يزداد الامتزاز كلما زادت المساحة السطحية بسبب توافر المواقع الفعالة للسطح الماز.

من النتائج التي تم الحصول عليها من الدراسة يمكن ان نستنتج مايأتي :

1- إن آيزوثيرمات الامتزاز للمادتين الدوائيتين (Triprolidine.Hcl) و (Metoclopramide.Hcl) على سطحي البنتونايت والكاؤولين تتبع معادلة فريندلش والشكل (S) حسب تصنيف (Giles) .

2- بالرغم من فعالية السطحين لأمتزاز المادتين الدوائيتين لكن البنتونايت كان ذا سعة امتزازية أعلى من الكاؤولين ، وهذا الترتيب يبقى ثابتاً مع تغير درجة الحرارة والقوة الآيونية والأس الهيدروجيني للمحلول .

3- كمية المادة الدوائية (Metoclopramide) على السطحين أكثر من كمية المادة الدوائية (Triprolidine) على السطوح نفسها .

4- أظهرت الدراسة إن امتزاز المادتين الدوائيتين (Triprolidine) و (Metoclopramide) على السطحين هو امتزاز باعث للحرارة (Exothermic)، ويكون متوافقاً مع طبيعة الامتزاز الفيزيائي من المحاليل على السطوح الصلبة، الذي يكون عادةً باعثاً للحرارة .

5- وجد ان سعة الامتزاز لكل من (Triprolidine) و(Metoclopramide) تقل بزيادة درجة الحرارة ، وان قيمة (ΔH) لهما سالبة على السطحين ، وايضاً (ΔG) سالبة تدل على ان الامتزاز تلقائي ،

اما قيم (ΔS) للمادتين على السطحين وجد انها سالبة فأنها تشير الى ان إنتظام الجزيئات الممتزة على السطحين .

6- تقل سعة الامتزاز للمادتين الدوائيتين على السطحين بزيادة الشدة الآيونية للمحلول عند إضافة كميات مختلفة من كلوريد الصوديوم ، وان سطح البنتونايت كان قليل التأثر بالشدة الآيونية، مما يشير الى إمكانية وجود ترابط عالٍ نسبياً بينه وبين المادة الدوائية.
7- تزداد سعة الامتزاز للمادة (Metoclopramide) على سطحي البنتونايت والكاؤولين بزيادة الدالة الحامضية. اما كمية الامتزاز للمادة (Triprolidine) فتزداد على سطح البنتونايت، وتقل على سطح الكاؤولين بزيادة الدالة الحامضية .
8- بنقصان حجم دقائق الطين تزداد كمية الامتزاز للمادتين الدوائيتين على سطحي البنتونايت والكاؤولين.

المصادر

1. K.M.Banat, "Principle of Clay Mineralogy", Baghdad University press, Baghdad, : 138 (1980).
2. العلعالي "*جبال البنتونايت في الاردن* " ، عمان ص (1-36)(1999).
3. *"Martindale: theExtra Pharmacopoeia "*, 32nd edition, Pharma. Press, USA, : 405, 409, 1178, 1195, 1471 (1999).
4. *"Martindale: the Extra Pharmacopoeia "*, 31st edition, London, : 827, 830, 937, 1205: 1222, 1536 (1996).
5. M. Trckova, L. Matlova, L. Dvorska,"*Kaolin, Bentonite and Zeolites as feed supplements for animals: health Advantages and risks "*, Vet. Med. – Czech, 49(10) : 389 -399 (2004).
6. Saadoon A. Isa. ,Sameer .M. J. and Hussein K.A.H. ," *Inverstigation of Bentonite clay Surface as a Physical Antidote in Adsorption of some drugs from solution* " J. Iraqi Sci. (2001) :8-2 (2002) .
7. Chukwvenweniwe J. Eboka, and Aderemi B. Afola,*"In – Vitro Adsorption of Fluoroquinolones on some Pharmaceutical Adsorbents "*, Tropical Journal of Pharmaceutical Research, 5 (1): 533-538, June (2006).
8. Camazano M.S., Sanchez M.J., Vicent M.T. and Dominguez-Gil A. *"Adsorption of chlorpheniramine maleate by montmorillonite"* Int. J. Pharm. 6:243-251 (1980).
9. Cooney-Do *"In vitro Desorption of Phenobarbital, Chlorphenir-imine Maleate, and Theophylline by four commercially available activated charcoal suspensions"*,J.Toxicol.Clin.Toxical.33(3):213-217 (1995).
10. Raheb , I. ,"*Influence of acidic treatment on the propertie of Syrian Zeolite"*, Tishreen Unv. J. for studies Sci. res. Basic Sci.26, (3), (2004).
11. Willian D. Burgos , Nipon Pisutpaisal , Micheal Co., Mazzarese , and Chorover ,*"Adsorption of Quinoline to Kaolinite and Montmorillonite "*, Environ , 19 (2) Mary Ann Liebert ,Inc. , (2002)

12.Nasiruddin M. , *"Adsorptive Removal of Non-Ionic Surfactants from Water Using Granite Sand"*, J. Iranian. Chem. Soc., 1 (2), :152-158, (2004).

13.Tella A. C. and S. O. Owalude ,*"Some Langmuir and Freundlich parameters of Adsorption studies of chlorpheniramine maleate "*, Research J. of Applied Sci. , 2 (8) :875 -878 (2007) .

14.Nagernaik , P. B. , A. G. Bhole and G. C. Natarajan , *"Arsenate (I I I) removal by Adsorption of rice husks carbon "*, Int. J. Environ. Studies , 5: 1097 -1164 (2002) .

15.Beate R., Stefan D., and Claus B., *"Temperature Effects on Iodine Adsorption on Organo-Clay Minerals"*, Appl. Clay. Sci., l(16):1-13, (2000).

16.Kippling J.J. , *"Adsorption from Solution of Non-Electrolytes"* Academic Press, London, New York : 257-259, (1965).

17.Al-Gohary O.,Lyall J.&Murry J.B.,"Adsorption of antihypertensives by suspensions", Part II:*" The adsorption of acebutolol, metoprolo., nadolol oxprenolol and timolol by attapulgite, charcoal, kaolin and magnesium trisilicate"*, Pharm. Acta. Helv. 63 (1): 13-18, (1988).

18.Al-Gohary O.M.N.*"In-Vitro Adsorption of Mebeverine HCl onto Kaolin and Its Relationship to Pharmacological Effect of the Drug in Vivo", Pharm. Acta. Helve.* 72 : 11-21 (1997).

تأثير التدخين على تركيز (MDA) و فيتامين (A) و عنصري السيلينيوم والحديد

جعفر هاشم محسن[1] وجميل موسى[2] و حنان فاضل عباس[1] وحليمة جابر محمد[1]
[1]وزاره العلوم والتكنولوجيا
[2] الجامعه المستنصريه / كلية العلوم / قسم الكيمياء

ABSTRACT

In this study we attempted to shed alight on the possible relation ships between lipids per oxidation marker, serum malondialdehyde (MDA) with the effect of smoker Using serum samples obtained from (60) smoker due to their occupation. These smokers were divided in to two groups according to their occupational period. The third group consists of healthy volunteers that were No smokers in the control group.

Our results showed that

The level of (MDA) was elevated in the smoker and the highest level was found to be (48.00) n mol/dL for smoker with longest period compared to the control group (9.6) n mol\dL.

Some serum antioxidants such as vitamin (A) were evaluated and were found to be lower in all smokers compared to the control group. Serum, Fe, levels were also evaluated and were found higher in smoker than that in the control group. , Se, found to be lower in all smokers compared to the control group.

الخلاصة

اهتمت هذه الدراسة بإلقاء الضوء على العلاقات المحتملة بين الدليل الكيميائي الحياتي لعملية الأكسدة الفوقية للدهون (المالون ثنائي الالدهايد MDA) ، فيتامين (A) والعناصر الأساسية(Fe, Se) وتأثير التدخين في مصل دم (60) من المدخنين ، وقد قسمت مجاميع المدخنين إلى مجموعتين حسب فترات التدخين.

أما المجموعة الثالث فقد كانت من المتطوعين الأصحاء غيرالمدخنين. تم قياس معدل الأكسدة الفوقية للدهون بمقدار ما يتكون من المالون ثنائي الالدهايد ولوحظ ارتفاع في مستوى الـ (MDA) حيث بلغت (48) نانومول/100 مل، لمجاميع المدخنين مقارنة مع مجموعة السيطرة التي بلغ فيها مستوى الـ (MDA) (9.6) نانومول/100 مل، وأيضاً تم قياس تركيز فيتامين (A) وأظهرت الدراسة إن هنالك نقصاً واضحاً في فيتامين (A) لدى المدخنين مقارنة مع مجموعة السيطرة. كما تم قياس مستويات بعض العناصر الأساسية(Fe, Se) وقد وجد إن هناك زيادة حاصلة في تركيز الحديد وقلة السيلينيوم لمجاميع المدخنين مقارنة بمجموعة السيطرة.

أثبتت نتائج الدراسة دور الأكسدة الفوقية للدهون والجذور الحرة في التلف الحاصل في خلايا الأعضاء التي تتأثر بالتدخين وهذا يقترن بالقلة في مستويات الأنظمة الدفاعية من مضادات الأكسدة لدى المدخنين.

المقدمة

يعد التدخين من المشاكل الاقتصاديه والصحية للإنسان، و خاصة أمراض سرطان الرئة (1) و أمراض القلب وامراض الكبد وتشير منظمة الصحة العالمية بموت شخص كل ست ثوان ونصف بسبب التدخين،(2).

وجد أن التدخين يتسبب فى زيادة السمية لكثير من الأدوية بسبب تحفيزه لبعض الانزيمات التى تتعامل مع هذه الأدوية بالكبد و يتسبب أيضا التدخين فى اضعاف قدرة الكبد على التخلص من الماده الضارة التى تدخل الجسم ومن الممكن أن تؤثر أيضا فى مستوى الأدوية التى يتناولها المريض لعلاج مرض الكبد. وكذلك وجد ارتباط بين التدخين و سرطان الكبد.

ويزيد التدخين أيضا من شدة التهاب الكبد الناتج عن الفيروسات كما فى مرضى الالتهاب الفيروسى المزمن نتيجة لفيروس "سى" و ينعكس ذلك على مستوى انزيمات الكبد فنجدها أعلى لدى المرضى المدخنين مقارنة بغيرهم من غير المدخنين. وقد وجد أن درجة الالتهاب و مرحلة التليف الناتج عن الفيروس الكبد ى "سى" أشد فى المدخنين عن غيرهم . ومن المعروف أن المدخنين لا يعانون من نقص الهيموكلوبين و ذلك لاستمرار انتاجه فى النخاع بسبب احساس الأنسجة بنقص فى الاوكسجين, المعادن الثقيلة تُسبّبُ ضرر بالغ بشكل ملحوظ على الصحةِ الإنسانيةِفي الحقيقة، وضّحتْ بَعْض الإستطلاعاتِ بأنّ محتويات بَعْض المعادن الثقيلةِ السامّةِ، (2,3) ويدخل الحديد فى تركيب الهيموكلوبين لذا فان مستوى الحديد بالدم يكون مرتفعا لدى المدخنين. ومن المعروف أيضا أن الحديد سام للكبد اذا ارتفعت مستوياته فى الأنسجة. ومرضى الفيروس "سى" المدخنين يستجيبون أقل للعلاج بمضادات الفيروس.
لذا على مريض الكبد إن يتوقف عن التدخين ويعتبر من الخطوات العلاجية الهامة التى لا تكلف وربما تقلل من الحاجة الى بعض الأدوية الأخرى وأيضا فان التوقف عن التدخين يزيد من نسب نجاح العلاج بمضادات الفيروس مثل الانترفيرون يحتوي دخان السكائر خليطا Mixture كيميائيا معقدا للغاية وخطيرا على صحة الإنسان وعلى كافة عناصر البيئة ، فهو يحتوي على أكثر من 3800 مادة كيميائية سامة ، ومن أهمها نذكر أول أكسيد الكربون CO وكبريتيد الهيدروجين H_2S والأمونيا NH_3 والفورمالدهايد HCHO والأسيتالدهايد CH_3CHO وسيانيد الهيدروجين HCN (4)، بالإضافة إلى طائفة كبيرة من الأحماض المختلفة ، من أهمها حامض الكربونيك H_2CO_3 وحامض النيتريك HNO_3 وحامض الخليك CH_3COOH وحامض الفورميك HCOOH (5).

المواد وطرائق العمل

1- طريقة تقدير مستوى الأكسدة في مصل الدم بمقدار ما يتكون من الـMDA

إن المالون داي الديهايد هو من النواتج الثانوية للأكسدة الفوقية للدهون لذا فان قياس هذه المادة تعطي انطباعاً عن مستوى الأكسدة والطريقة المستخدمة هي طريقة لونيه تعتمد على التفاعل بين مركب حامض الثايوباريتورك والمالون داي الديهايد ليعطي مركباً لونياً أعلى امتصاص له في (532) نانومتر وقد استخدمت طريقة (Fong) لهذا الغرض (6)

2-قياس فيتامين (A) في مصل الدم بتقنية ال HPLC

تستعمل في هذه الطريقة أعمدة صغيرة ذات أقطار بنحو (1-3) ملم تحتوي على ساند مؤلف من دقائق إحجامها بنحو (30) مايكرومتر يضغط محلول الاسترداد (Eluent) خلال العمود بمعدل جريان عالٍ (1-5) مل/دقيقة وعمليات الفصل بهذه الطريقة أسرع (100) مرة من طريقة كروموتغرافيا عمود السائل الاعتيادي. لذا وجد لـ (HPLC) تطبيقات واسعة في تشخيص المركبات العضوية وفصلها على نطاق واسع حيث تم استخدام الطور المتحرك(% 99)ميثانول (1%) ماء مقطر بطول موجيnm 330 نوع العمود (ODS) C-18 (7).

3-تقدير العناصر(سيلينيوم، حديد) في مصل الدم بطريقة الامتصاص الذري:-

يعرف التحليل بالامتصاص الذري بأنه طريقة لحساب أو تقدير عنصر (أو مجموعة عناصر) وذلك بقياس مقدار الامتصاص لشعاع رنين ذلك العنصر بعد مروره عبر بخاره الذري. وبدأت أهمية طيف الامتصاص الذري (AA أو AAs) في منتصف الستينات وان المبدأ الأساس لهذه التقنية هو قياس امتصاص أحادى الموجة بوساطة غيمة من ذرات المادة المحللة (Analyses).

تم عمل نماذج من تراكيز مختلفة الحديد في الماء المقطر الخالي من الأيونات وتؤخذ هذه النماذج لسحبها بأنبوب الرذاذ الخاص بجهاز الامتصاص الذري الذي من خلاله يمكن إيجاد الامتصاص (A) لكمية الحديد الموجودة في كل تركيز من هذه النماذج وبعدها يمكن قراءة الامتصاصية لكمية الحديد الموجودة في المصل. وقد استخدم مصباحا بطول موجي (248.3) نانومتر خاص بعنصر الحديد. يحدد منحنى قياسي بين الامتصاصية وتركيز أيونات الحديد.كما حضرت محاليل قياسية مختلفة للعنصر Se لغرض عمل منحني قياسي للعنصر وذلك بسبب كميات مختلفة من العنصر في قناني حجميه وإكمالها للعلامة بالماء اللايوني وقد استخدم مصباحا بطول موجي (196) نانومتر خاص بعنصر السيلينيوم

النتائج والمناقشة

يبين لنا الجدول رقم (1) إن هنالك زيادة في معدل مستويات الأكسدة الفوقية للدهون لمجاميع المدخنين مقارنة بمجموعة السيطرة. إذ استطاع الباحثون (8) تفسير ميكانيكية الزيادة في معدل الأكسدة الفوقية للدهون بسبب ارتفاع في مستويات الـ (ROS) وهي مولدات للجذور الحرة وسوف يحصل زيادة في التلف الحاصل في الخلايا ويسرع من عملية انتقال الإلكترونات والأكسدة الفوقية للدهون في الأنسجة البيولوجية داخل الخلية الحية. وإن هذه النتائج تتفق مع بحوث حديثة (9،10) وكذلك فان نتائجنا لا تتفق مع الباحثين (11).
وعند زيادة هذه الأكسدة فان الجذور الحرة المتولدة والمتزايدة تؤدي إلى التلف الكثير للأغشية الخلوية والنهايات العصبية في الدماغ(12).

جدول رقم -1: يحدد معدل الانحراف القياسي والمعدل ومستوى الدلالة (MDA) عند مجموعة السيطرة ومجاميع المدخنين.

T	Mean	±S.D معدل (MDA) (n mol/dL)	العدد	المجاميع
---	10.5	0.92	30	Control C
P<0.05	16.12	1.20	60	A
P<0.001	33.87	2.73	60	B

A = مجموعة المدخنين (من سنة إلى 10 سنوات).
B = مجموعة المدخنين (من 11 سنة فما فوق).
C = مجموعة السيطرة.

يبين لنا الجدول رقم (2) انخفاض في مستوى تركيز فيتامين (A) بالنسبة إلى العاملين مقارنة مع قيم السيطرة ونجد انخفاضا في مستوى فيتامين (A) مع طول مدة التعرض.
يعد فيتامين A من مركبات الكاروتينات التي لها فعالية كمضادة للأكسدة (13,14) وان فعاليته الكيميائية تأتي من السلسلة الطويلة الحاوية على أواصر مزدوجة متعاقبة التي تكون معوضة بمختلف المجاميع أن أل Ros التي يمكن أن يكتسبها فيتامين A هي O_2 وجذر البيروكسي (peroxy radical) (15)
ولفيتامين A عدة وظائف منها المشاركة في عملية الإبصار بالتفاعل مع بروتين (obsin) مكونا الأرجوان البصري كما يعد ضروريا في تكوين الكاربوهيدرات المخاطية المكونة لمادة

مخاطية لإفراز الطبقة الطلائية التي توفر الحماية للقنوات الجسمية مثل القنوات التنفسية والبولية والتناسلية وكذلك ملتحمة العين والقرنية واللثة.
كذلك للفيتامين دور في تكوين عدد من الهرمونات مثل الكورتزون(cortisone) والذي تفرزه غدة الأدرنالين والتي لها دور في تمثيل الدهون الكاربوهيدرات و(vit .a) أهمية في تقليل مستوى الأكسدة ويعد من الفيتامينات المضادة للأكسدة وكما هو معلوم فان بيتا- كاروتين (B-carotene) يعتبر المولد للفيتامين (A) وهو ايضا من المواد المضادة للأكسدة ويوجد بيتا –كاروتين في (LDLC) مع فيتامين (E) وبذلك يمنع أكسدة (LDLC) .
كما يوصي بتناول فيتامين(A) لما له أهمية في الحفظ على شبكة العين وملتحمة العين والقرنية من الإضرار التي تلحق بالعين وكذلك لفيتامين (A)دور في رفع مستوى(-apo A)ومن ثم رفع (HDLC) في الدم (16).

جدول رقم -2: يحدد معدل الانحراف القياسي والمعدل ومستوى الدلالة لفيتامين A عند مجموعة السيطرة ومجاميع المدخنين.

T	Mean	±S.D معدل (Vit-A) (mg/dL)	العدد	المجاميع
---	69.8	10.2	30	Control C
P<0.05	44.6	14.2	60	A
P<0.001	35.05	16.7	60	B

A,B,Cكما في جدول رقم (1)

يبين لنا الجدول رقم (3) إن مستوى الحديد الحر في المصل يزداد في مجاميع المدخنين مقارنة بمجموعة السيطرة.

ويمكن تفسير ذلك بان الحديد محفزاً للأكسدة الفوقية للدهون من خلال تفاعل (فنتون).
إن أيونات الحديد تعمل على اختزال (H_2O_2) من خلال تفاعل فنتون وهي بذلك تولد نوعاً من أنواع الـ (ROS) التي تكون اخطر من (H_2O_2) نفسه مثل جذر ($O^{\bullet}H$) داخل الجسم (In vivo) حيث إن تفاعل فنتون يتبع المعادلة التالية: -

$$M^{+n} + H_2O_2 \rightarrow M^{+(n+1)} + \dot{O}H + OH^-$$

وإن (M^{+n}) حديد أو نحاس.(17)
إن التفاعل الذي يقوم به الحديد معروف ويمكن تمثيله بالمعادلة والميكانيكيات المقترحة

$$Fe^{+2} + H_2O_2 \rightarrow Fe^{+3} + O^{\bullet}H + OH^-$$

إن الناتج الأولي لتفاعل فنتون قد يكون معقد حديد أوكسجين (Oxo-iron complex) باحتمال تكون الفيريل (Ferryl) والذي يتحلل ليعطي جذر الهايدروكسيل وفق المعادلة التالية.

$$Fe^{+2} + H_2O_2 \rightarrow [FeOH]^{+3} \text{or} [FeO]^{+2} \rightarrow \dot{O}H + Fe^{+3} + \bar{O}H$$

إن تكون جذر الفيريل الذي فيه يكون العد التاكسدي للحديد (4+) قد اقترح من قبل العالم (Walling, C) (18) كما إن جذر الفيريل (Ferryl radical) يكون جذراً فعالاً في بعض أنزيمات البيروكسيديز(19).

أما التفاعل بين جذر ($^{\bullet}O_2^-$) والـ (H_2O_2) بوجود أيونات الحديديك (Fe^{+3}) قد اطلق عليه تفاعل هابر- ويبس المحفز بالحديد (Iron-Catalyzed Haber Weiss reactions)

الذي يطلق عليه في بعض الاحيان السوبر اوكسايد المؤدي الى تفاعل فنتون

(Super Oxide driven Fenton Reaction)

$$^{\bullet}O_2^- + H_2O_2 \xrightarrow{Fe^{+3}} \dot{O}H + O\bar{H} + O_2$$

إن هذا التفاعل يؤدي إلى جزء من التلف الحاصل في الخلايا الحية وذلك عن طريق تولد الـ (ROS). إن الشد التاكسدي (Oxidative Stress) يعمل على تحرير الأيونات من البروتينات المرتبطة بها وبهذا تجهز هذه الأيونات لتفاعلات الجذور الحرة ممثلاً (O_2) يمكن أن يحرر الحديد من الفرتين (Ferrittin) لذا سوف يرتفع مستوى الحديد في المصل(20)

جدول رقم -3: يحدد معدل الانحراف القياسي والمعدل ومستوى الدلالة للحديد عند مجموعة السيطرة ومجاميع المدخنين.

T	Mean	±S.D معدل الـ Fe (µg/dL)	العدد	المجاميع
---	193.9	14.25	30	Control C
P<0.01	283.3	42.51	60	A
P<0.001	371.5	52.12	60	B

A,B,Cكما غي جدول رقم واحد

يبين لنا الجدول رقم (4) انخفاض مستوى السيلينيوم لدى مجاميع المدخنين مقارنة بمجموعة السيطرة.
ويعلل دوراهما زيادة استهلاك السيلينيوم الذي يلعب دورا مهما وكمادة أساس في عمل أنزيم الكلوتاثايون بيروكسيديز حيث يعتبر أنزيم الكلوتاثايون بيروكسيديز من الأنزيمات المضادة للأكسدة ويتواجد في معظم أعضاء الجسم (21).

جدول رقم -4: يحدد معدل الانحراف القياسي والمعدل ومستوى الدلالة للسلينيوم عند مجاميع المدخنين ومجموعة السيطرة.

T	Mean	±S.D معدل الـ Se (µg/dL)	العدد	المجاميع
--	0.93	0.14	30	Control
P<0.001	0.85	0.98	60	A
P<0.001	0.79	0.83	60	B

A,B,Cكما في جدول رقم واحد

المصادر

1. Doll, Rich; and Hilly, A. Bradford January. "Smoking and carcinoma of the lung. Preliminary report". *British Medical Journal* 2 (4682): 739–48 NIH Publication No. 99-9492-(1999).
2. mussalo-rauhamaa H., Salmela S.S "Some trace and heavy metals and pesticides in man" , Arch. Environ . Health 41,49-55,(1986).
3. El-Agha O., and Gokmen I.G,"smoking habits and cadmium intake in. turkey", boil. Trace Elem.,Res., 88 (1), 31-43.,(2002).
4. Okubo,M.;Kuroki, T.;Kametaka, H.;Yamamoto,T. Industry Applications, IEEE Transactions onVolume 37, Issue 5, Sep/Oct :1447 – 1455, (2001).
5. von Hanns K. Frank Technology & Engineering – 290 Seiten– (1992)
6. Fong. K. L. McCay, P.B. & Poyer, J.L. *J. Bio. Chem.* 248:7792-7 (1973).
7. Parke, D.V. & Sapota, A., *INT. J Occp. Med. Environ. Health.*, 9:33 1 (1996).
8. Badger, A.M., Hanldler, J. A., Genell. C.A., Herzyk, D., gore, E., polsky, R., Webb, L. & bugelski, P.J., *INT. J. Immuno. Pharmacol.*, 21:161(1999)
9. Taraza, C., Mohra, M., Vargolici, B., Dinu, V., *Rom. J., Intern. Med.*, 35:89. (1997).
10. Ernst. P., *Am. So. Nutr. Sci.*, 147:9625 (1999).
11. Strubelt-O., Kremer- J, Tilse-A., Keogh- J, Pentz-R., Younes- M *J. Toxicol – Environ-Health.* Feb.23: 47(3): 267-83. (1996)
12. Dabrwska-Bouta, B., Struzynska, L. & Rafalowska, U., *Mol. Chem. Neuropathol.*, 29:127 (1996).
13. 13-Parknay,M,.EdThe use of recovery factors in trace analysis ,Royal Society of Chemistry, (1996).
14. Strubelet,O.;Kremer,J.;Tilse,A.;Keogh,J. & Younes,M.J.Toxical Environ , 1-Iealth .,Feb:47(3):267-283 (1 996).
15. Taraza,C.; Mohra, M.; Vargolici,B.; Dinu,V. Rom.J.Intern.Med ., 35 :890 (1997).
16. Richard S. Brunoa, Maret G. TraberbVolume 13, Issue 3: 143-149 (August 2006).
17. Halliwell, B. & Gutteridge,J.M. C., *Methods Enzymol.*, 136:1 (1990).
18. Wallings, C., "*Oxidases Related Redox System*," Oxford. :85-97 (1982).
19. Dunford, H. B., *Adv. Lonorg. Bio chem.*, 4:41-68 (1982).
20. H. Karamifar,1 M. Shahriari1 and N. Sadjadian1 9, (1/2) ,January (2003).
21. Halliwell, B. & Auoroma, O. I., , *J. Clin. Chem.* 281:9 (1991).

تحضير بعض المشتقات الجديدة للكومارين

مازن جليل حبيب و حنان غضبان شعبان
الجامعة المستنصرية /كلية العلوم/ قسم الكيمياء

ABSTRACT

The coumarin derivatives are very important compound that are used in medical and industrial fileds, This study include preparation many of new amino coumarin derivatives.
This study is chivied by the following steps:-
Synthesis of starting material (4-methyl-7-hydroxy coumarin) [H_1] from reaction of resorcinol with Ethyl aceto acetate in the presence of Conc. H_2SO_4 at (10 C°).Then Nitration of [H_1] by the reaction with mixture of Conc. (HNO_3+H_2SO_4) at temperature (0 -5 C°) to get [H_2]. Reduction of compound [H_2] by its reaction with Iron powder and Conc. HCL in absolute ethanol as a solvent gave the compound 6-amino-4-methyl-7-hydroxy coumarin [H_3] .
Also new Schiff's bases 7-hydroxy-4-methyl-6-[Substituted amino]-2H-chromen-2-one [H_4-H_8] were synthisised through the reaction of amino coumarin derivatives with different aromatic aldehydes and ketones. After that a new derivatives containing heterocyclic moieties of coumarin were prepare by the reaction of Schiff's bases with α- mercapto acetic acid to obtain the derivative 3-(7-hydroxy-4-methyl-2-oxo-2H-chromen-6-yl)-1, 3-Thiazolidin-4-one-2-substituted [H_9-H_{13}] .The work also includes synthesis of new amino derivatives of coumarin compounds [H_{15}-H_{19}].The last step includes Synthesis of Maunich bases derived from coumarin 4-methyl-6-nitro-7-(substituted)-2h-chromen-2-one [H_{21}-H_{25}] .
The prepared compounds were characterized by spectroscopic means namely infrared (IR) and Ultraviolet (UV) and studying Their physical properties.

الخلاصة

تعد مشتقات الكيومارين من المركبات المهمة بسبب أستخدامها في المجالات الطبية و الصناعية ، فقد تم في هذا البحث تحضير وتشخيص عدد من المشتقات الامينية الجديدة للكيومارين ويمكن اجمال ما جاء في البحث بما يلي:
تحضير المركب الاساس [H_1] 4-مثيل-7-هيدروكسي كيومارين عن طريق تفاعل الريسورسينول مع أثيل اسيتواسيتات بوجود حامض H_2SO_4 المركز عند درجة حرارة (10C°), ثم اجراء نيترة عليه باستخدام (حامض النتريك والكبريتيك المركزين) عند درجة حرارة (0 – 5C°) للحصول على المركب [H_2],يليه اختزال المركب [H_2] باستخدام مسحوق الحديد وحامض الكبريتيك المركز في مذيب الايثانول لتحضير المركب 6-امينو-4-مثيل-7-هيدروكسي كيومارين[H_3] .تبع ذلك تحضير مشتقات جديدة من قواعد شيف [H_4-H_8] من خلال تفاعل المشتقات الامينية للكيومارين مع الديهايدات او كيتونات مختلفة.كما تم تحضير مشتقات حلقية غير متجانسة للكيومارين، فقد حضرت بعض مشتقات الثايازوليدين الجديدة للكيومارين [H_9-H_{13}] من خلال تفاعل قواعد شيف المحضرة مع حامض الفا مركبتوالخليك .اضافة لذلك تم تحضير مشتقات أمينية جديدة للكيومارين [4-methyl-2-oxo-2H-chromen-7-yl]sustituted acetate .[H_{15}-H_{19}] واخيرا تم تحضير بعض قواعد مانخ الجديدة للكيومارين 4-methyl-6-nitro-7-(substituted)-2h-chromen-2-one [H_{21}-H_{25}] من خلال تحضير المشتق الاستيليني للكيومارين 4-methyl-2-oxo-2H-chromen-7-yl(di propyl amino)acetate [H_2O].
تم تشخيص جميع المركبات وبدراسة الخواص الفيزياوية لها وبأستخدام الطرائق الطيفية مثل مطياف الاشعة تحت الحمراء (IR) و مطياف الاشعة فوق البنفسجية (UV) .

المقدمة

لقد تم عزل وتشخيص عدد كبير من مشتقات الكيومارين في النباتات التي لديها فعالية بايولوجية عالية لعلاج العديد من الامراض وزيادة مناعةالانسان ضد الامراض ، إذ تعمل بعض مشتقات الكيومارينات كمواد مضادة للاكسدة وتثبط تكسر الصفيحات الدموية وكعوامل مضادة للالتهابات والاورم(1). عزل العالم Kofinas وجماعته سبعة مركبات من مشتقات الكيومارين من الاجزاء العليا لنبات Tordylium a pulum وقد تم التعرف على تراكيبها بالطرائق الطيفية، واختبرت الفعالية البايولوجية لهذه المركبات كمضادات لبعض انواع الامراض(2).

كما تم عزل المركب 7- Methoxy Coumarin (Herniain) [1] من نبات الـ Matricaria الذي ينموفي شمال العراق والمادة الفعالة تستعمل كخافض للحرارة (3) ، وفي حالات الروماتيزم والقرحة ومضادات لالتهاب الفم والاسنان(4).

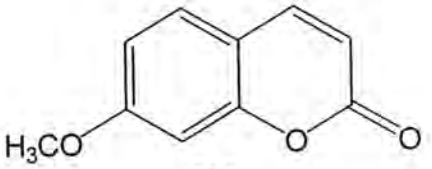

[1]

وتمتلك الكيومارينات فعاليات بايولوجية مختلفة ، إذ تستخدم كمواد دوائية للامراض الجلدية من خلال التحسس الضوئي والحساسية الضوئية وكموسع للاوعية الدموية ومضاد للبكتريا ومضاد للديدان ومخدراً وتم حديثاً" تقييم مشتقات الكيومارين في معالجة نقص المناعة المكتسب (HIV) Human Immunodeficiency Virus إذ تعمل هذه المشتقات لتثبيط فايروسات (HIV) وانزيماتها (5,6,7).

هناك العديد من التقارير التي تشير الى أن معظم مركبات الكيومارين من نوع 7-Hydroxy Coumarin [2] تثبط العديد من الخلايا المولدة لانواع مختلفة من السرطان (8,,9) مثل سرطان البروستات والعوامل المسببة للورم القيتاميني وسرطان الخلايا الكلوي(10,11).

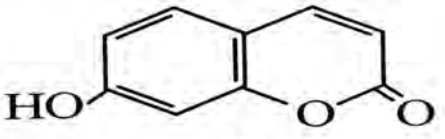

[2]

كما ان للكومارين فعالية كمادة منومة ومسكن للالم و خافض للحرارة(12,13).وهناك تقاريرعن فعالية الكيومارينات النقية ضد بكتريا كرام (+)و (-) وكذلك مضاد للفطريات(14) ، والعديد من الدراسات الحديثة قد أوضحت الفعالية المضادة للجراثيم لمركبات الكيومارين المحضرة صناعياً التي من الممكن أن تتكون في الطبيعة أيضاً(14,,15).

المواد وطرائق العمل

عام

تم قياس درجات الانصهار للمركبات المحضرة باستعمال انابيب شعرية وبأستخدام جهاز(Gallen (Kamp MFB-600-Melting point apparatus علماً" أن درجات الانصهار غير مصححة.

تم قياس الاشعة أطياف تحت الحمراء (FTIR- 8400S) بأستخدام جهاز Fourier Transform Infrared Spectro Photo meter من نوع Shimadzu ضمن المدى (400- 4000 cm^{-1}) بأستخدام قرص (KBr). تم قياس الاشعة فوق البنفسجية والمرئية بأستخدام جهاز (U.V 200) Hitachi Spectro photometer.

تحضير المركب *4-methyl-7-hydroxy Coumarin[H_1]* (16)

في دورق دائري يضاف 250 ml من حامض H_2SO_4 المركز في حمام ثلجي ويضاف له محلول مكون من (0.227 مول) من الريسورسينول في (0.257 مول) من أثيل اسيتو اسيتات (المقطر حديثاً") بشكل قطرات مع التحريك.

بعد أنتهاء الاضافة يترك المزيج مع التحريك لمدة ساعة ونصف بدرجة 10م ، بعدها يترك المزيج في درجة حرارة الغرفة لمدة 18 ساعة تقريباً" .ثم يضاف المحلول الناتج الى(500غم) .

يرشح الراسب الناتج ويغسل ثلاث مرات متعاقبة بـ(15 مل) من الماء البارد ، ويذاب بعدها في (350مل) من محلول NaOH 5% ، ويرشح ثم يضاف حامض H_2SO4 المركز 10% بمقدار(135مل) الى الراشح مع التحريك الشديد ، الى أن يصبح المحلول حامضي .

يجمع الراسب الناتج وتعاد البلورة بأستخدام الايثانول وهو عديم اللون ودرجة أنصهاره 188م° - 190م° ، كمية الناتج (35 غم) 80% .

تحضير المركب [H_2] (17)6-Nitro-7-hydroxy-4-methyl Coumarin

تم تحريك مزيج من (0.02 مول) من المركب [H_1] في (10مل) من حامض H_2SO_4 المركز في درجة 0 م° لمدة 15 دقيقة، بعد ذلك تتم أضافة مزيج من (0.092مول) من حامض HNO_3 المركز(0.092مول) من حامض H_2SO4 المركز على شكل قطرات على درجة حرارة (5-0) م° ، يترك بعد ها المزيج لمدة ساعة واحدة مع التحريك في درجة حرارة 5 م° . بعد ذلك يضاف الناتج الى جريش الثلج والماء البارد ، ويرشح بعدها الراسب المتكون وينقى بأستخدام كروموتغرافيا العمود بأستخدام السيليكا جل بواسطة مزيج من مذيب الايثر والبنزين بنسبة (1:1) ، الجدول-1- يوضح الصفات الفيزياوية للمركب[H_2]

جدول-1: يوضح الصفات الفيزياوية للمركب[H_2]

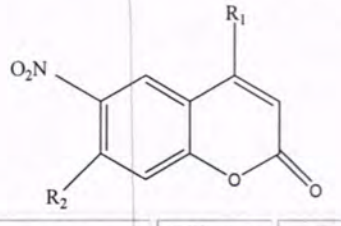

Comp. no.	R_1	R_2	m.p C°	Yield %	Purification Solvent	Molecular Formula
H_2	$-CH_3$	-OH	175	79	Ether-Benzene 1 : 1	$C_{10}H_7NO_5$

تحضير المركب [H_3] 6-Amino-4-methyl -7-hydroxy Coumarin

يذاب (0.01 مول) من [H_2] في مزيج متكون من (15مل) من HCL المركز و(15مل) من الايثانول، يضاف الى هذا المزيج بحذر(4غم) من مسحوق الحديد ، ويصعد لمدة ست ساعات ثم يبرد المحلول ويرشح ويغسل الراسب بالماء عدة مرات يجفف الراسب ويعاد بلورته بالايثانول ، والجدول-2- يوضح الخواص الفيزياوية للمركب [H_3].

جدول-2: يوضح الصفات الفيزياوية للمركبين [H_3]

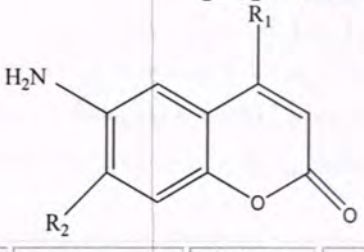

Comp. no .	R_1	R_2	m.p C°	Yield %	Purification solvent	Molecular Formula
H_3	$-CH_3$	-OH	198-200	80.3	Ethanol	$C_{10}H_9NO_3$

تحضير قواعد شيف [H_4-H_8]

يذاب (0.01 مول) من المركب [H_3] في (30مل) من الايثانول المطلق ، ويضاف لهذا المزيج (0.01 مول) من الالديهايد أو الكيتون الاروماتي المناسب ويصعد المزيج لمدة ست ساعات ، ويبرد المزيج ويرشح الناتج ويعاد بلورته بالمذيب المناسب ، الجدول-3- يوضح الصفات الفيزياوية للمركبات [H_4-H_8]

جدول – 3: يوضح الصفات الفيزياوية للمركبات [H_4 -H_8]

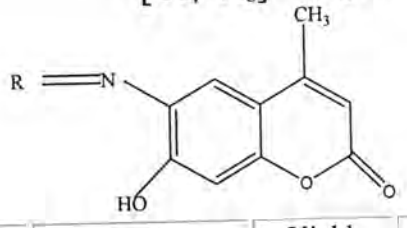

Comp. n o.	R	m.p C°	Yield %	Purification Solvent	Molecular Formula
H_4	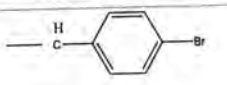	281-283	42.6	Ethanol	$C_{17}H_{12}NO_3Br$
H_5	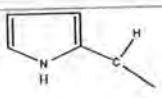	oily	49.2	Ethanol	$C_{17}H_{12}N_2O_5$
H_6	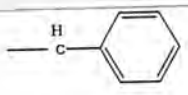	285-286	54.8	Ethanol	$C_{17}H_{13}NO_3$
H_7	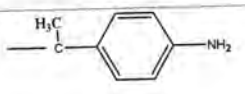	119-120	40	Ethanol	$C_{18}H_{16}N_2O_3$
H_8	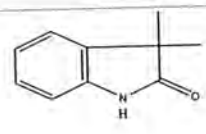	139-140	33	Ethanol	$C_{20}H_{12}N_2O_4$

تحضير مشتقات الثايازوليدين [H_9 – H_{13}] (طريقة عامة)

3-(7-hydroxy-4-methyl-2-oxo-2H-chromen-6-yl)-1, 3-Thiazolidin -4-one derivative

يضاف مزيج من(0،01 مول) من مركبتو حامض الخليك مذاب في (15مل) من البنزين الجاف بصورة بطيئة مع التحريك الى مزيج من (0.01مول) من قواعد شيف [H_4-H_8] مذابة في (15مل) من البنزين الجاف مع تصعيد لمدة عشر ساعات ، يحفظ بعدها في درجة حرارة الغرفة لمدة 24 ساعة.

بعدها يتم تركيز المزيج ومعادلته بيكاربونات الصوديوم (10%) ،يرشح الراسب ويعاد بلورته بالمذيب المناسب . الجدول-4- يوضح الصفات الفيزياوية لمركبات الثايازوليدين الناتجة.

جدول-4: يوضح الصفات الفيزياوية لمركبات الثايازوليدين [$H_9 - H_{13}$]

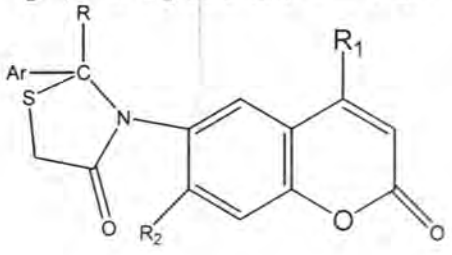

Comp. no.	Ar	R	R_1	R_2	m.p C°	yeild %	Purification Solvent	Molecular Formula
H_9	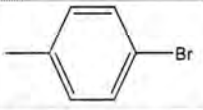	H	$-CH_3$	-OH	220-222	51.7	Ethanol: water 1 : 2	$C_{19}H_{14}NO_4BrS$
H_{10}	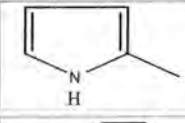	H	$-CH_3$	-OH	212-210	50	Ethanol: water 1 : 2	$C_{17}H_{14}N_2O_4S$
H_{11}	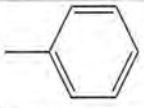	- H	$-CH_3$	-OH	232-234	65	Ethanol: water 1 : 2	$C_{19}H_{15}NO_4S$
H_{12}	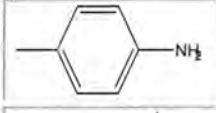	$-CH_3$	$-CH_3$	-OH	269-270	68.4	Ethanol: water 1 : 2	$C_{20}H_{18}N_2O_4S$
H_{13}	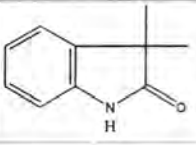	$-CH_3$	$-CH_3$	-OH	202-204	80	Ethanol: water 1 : 2	$C_{20}H_{14}N_2O_5S$

تحضير المركب [H_{14}] (طريقة عامة) 4-methyl-2oxo-2H-chromen-7-yl chloro acetate.

يذاب (0.01مول) من المركب [H_1] في مزيج يتكون من (30مل) بنزين و(3مل) ثلاثي مثيل أمين، يضاف (0.01مول) من 98 % كلوروأستايل كلورايد على شكل قطرات و يصعد المزيج لمدة ست ساعات . بعد اكمال التفاعل يتم تبخيرالكمية المتبقية من البنزين تحت الضغط المخلخل و الراسب المتكون يغسل ببيكاربونات الصوديوم(2%)ثم بالماء المقطر و يعاد بلورته بالايثانول، النسبة المئوية للناتج(60 %) ودرجة انصهاره M.P (158-160) م° .

تحضير المركبات[H_{15}- H_{19}] (طريقة عامة) 4-methyl-2-oxo-2H-chromen-7-yl acetate derivatives.

يذاب (0.01مول) من المركب [H_{14}] في (20مل) من الايثانول بعدها يضاف الى المزيج أعلاه (0.03مول) من أمين ثانوي مناسب ويصعد التفاعل لمدة ست ساعات ، يتم تبخير الزائد من الايثانول تحت ضغط مخلخل بعد أكمال التفاعل ، الراسب المتكون يغسل بـ(2 %) من بيكاربونات الصوديوم ثم بالماء المقطر و يعاد بلورة الناتج بالمذيب المناسب. الجدول -5- يبين الخواص الفيزياوية للمركبات [H_{15}- H_{19}]

جدول -5: يوضح الصفات الفيزياوية للمركبات [H_{15}- H_{19}].

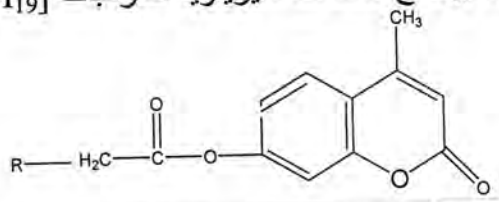

Comp. No.	R	m.p C°	Yield %	Purification Solvent	Molecular Formula
H_{15}	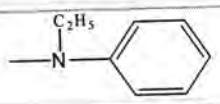	162-163	50	Ethanol:water 2 : 1	$C_{20}H_{19}NO_4$
H_{16}	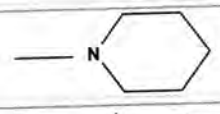	Oily	52	Ethanol: water 2 : 1	$C_{17}H_{19}NO_4$
H_{17}	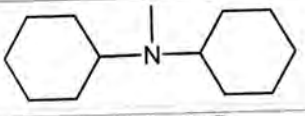	172-173	66	Ethanol: water 2 :1	$C_{24}H_{40}NO_4$
H_{18}	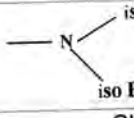	149-150	32.3	Ethanol: water 2: 1	$C_{20}H_{27}NO_4$
H_{19}	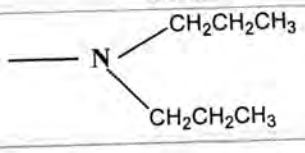	150-152	41.4	Ethanol: water 2: 1	$C_{18}H_{23}NO_4$

تحضير المركب [H_{20}] 4-methyl-6-nitro-7-(prop-2-ynyloxy)-2H-chromen-2-one.

يذاب(1،0مول) من المركب [H_2] في (20مل) من الايثانول المطلق ويضاف اليه (1.1مل) من ثلاثي اثيل أمين ويحرك لمدة 10 دقائق ، يضاف الى المزيج أعلاه وعلى شكل قطرات (0.01مول) من كلوريد البربرجيل خلال 15 دقيقة ، ويصعد المزيج لمدة ست ساعات ، بعدها يضاف ناتج التصعيد الى (20 مل) من الماء المثلج ، يرشح الراسب المتكون ويعاد بلورته بمزيج من ماء- أيثانول (2:1) ، درجة أنصهار الراسب (m.p = 129 -130) والنسبة المئوية للناتج (84.9%).

تحضير قواعد مانخ [H_{21}- H_{25}] (طريقة عامة)

Preparation of Mannich bases

مزيج من (0.005مول) من المركب [H_{20}] مع (0.005مول) من الفورمالديهايد في (10مل) من دايوكسان مع (0.1 غم) من كلوريد النحاس (CuCl) يسخن في دورق دائري الى درجة 70 م° .

عند نفس درجة الحرارة يضاف (0.005 مول) من أمين ثانوي مناسب على شكل قطرات بعدها يصعد المزيج لمدة ثلاث ساعات ، ثم يبرد الناتج ويضاف الى (20مل) من ماء مثلج و يرشح الراسب الناتج و يعاد بلورته بالمذيب المناسب .

الجدول -6- يبين الخواص الفيزياوية لقواعد مانخ .

جدول -6: يبين الخواص الفيزياوية لقواعد مانخ

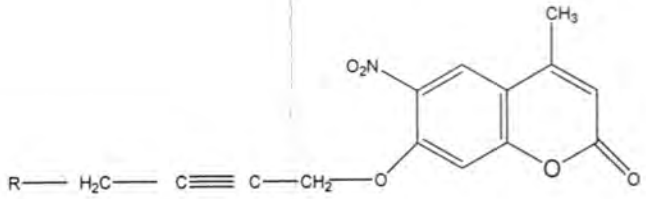

Comp. No.	R	m.p C°	Yield %	Purification Solvent	Molecular Formula
H_{21}	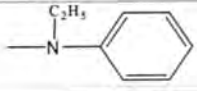	-170 169	38	Ethanol: water 2 : 1	$C_{21}H_{18}N_2O_5$
H_{22}	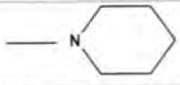	Oily	60	Ethanol: water 2 : 1	$C_{18}H_{18}N_2O_5$
H_{23}	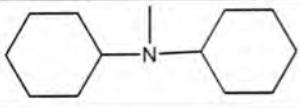	-150 149	37.3	Ethanol: water 2 :1	$C_{25}H_{30}N_2O_5$

المناقشة

المخططات 1و2 تمثل سلسلة التفاعلات المتضمنة في البحث:

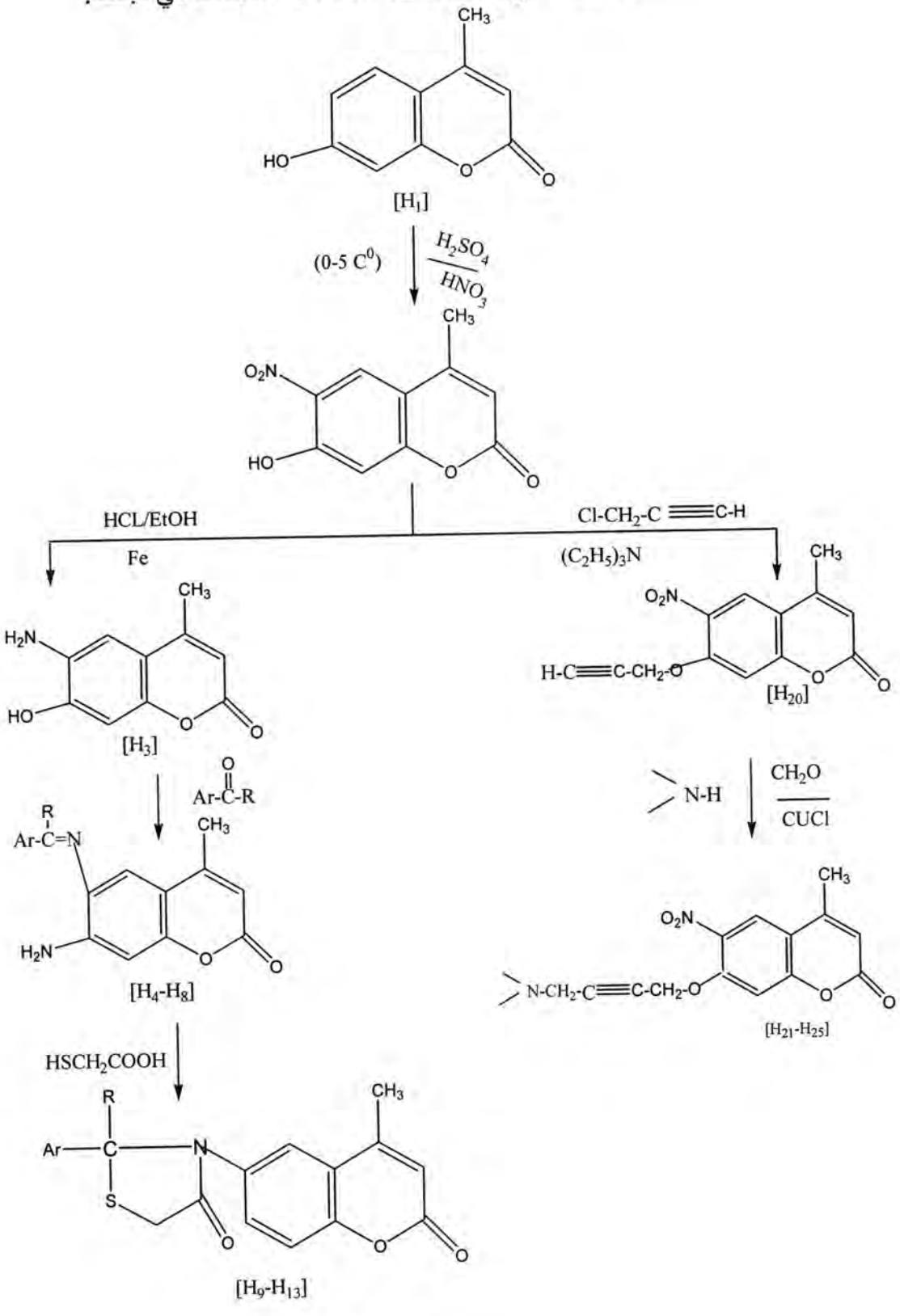

مخطط -1-

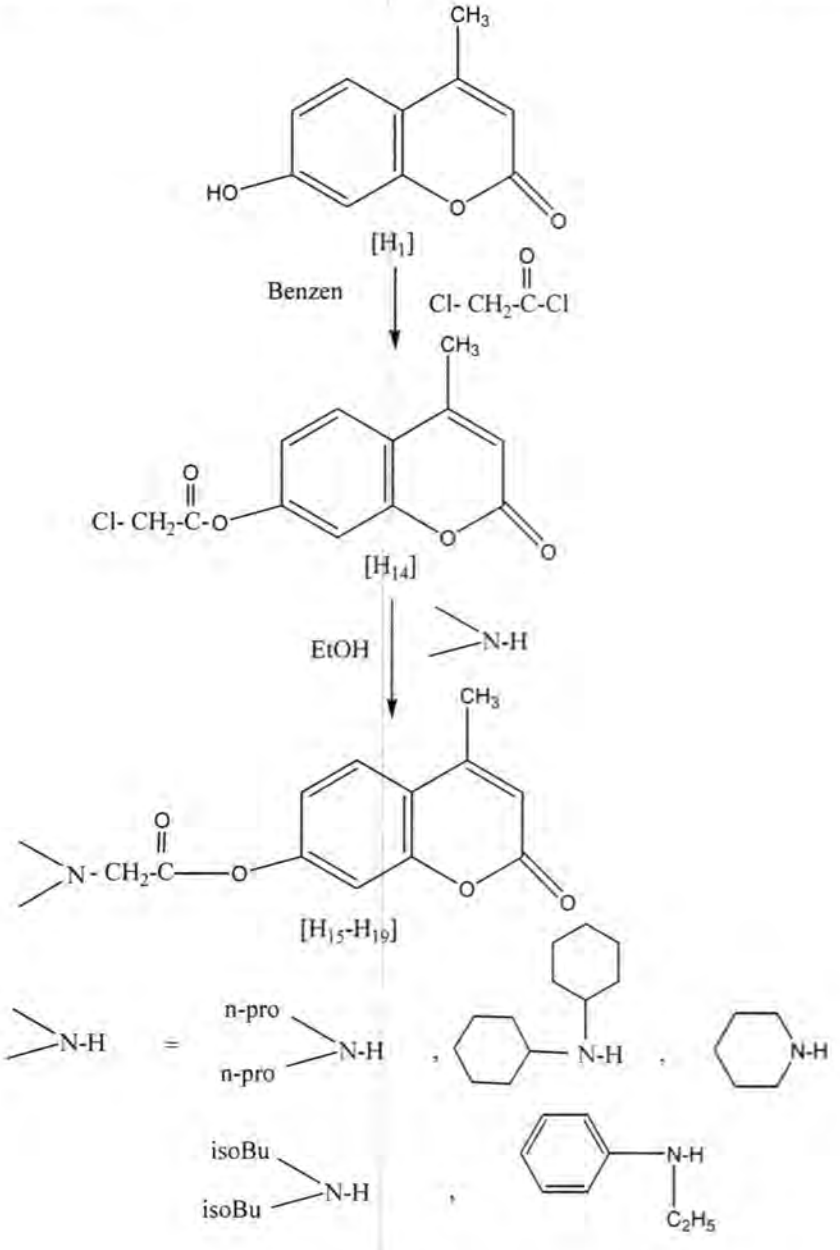

مخطط-2-

تحضير وتشخيص المركب 4-methyl-7-hydroxy Coumarin[H_1]

إن تحضير المركب [H_1] يتم من خلال تفاعل Pechman لـethyl aceto acetate مع نسب مولية من الـResorcinol بوجود حامض H_2SO_4 المركز كما في المعادلة الاتية :

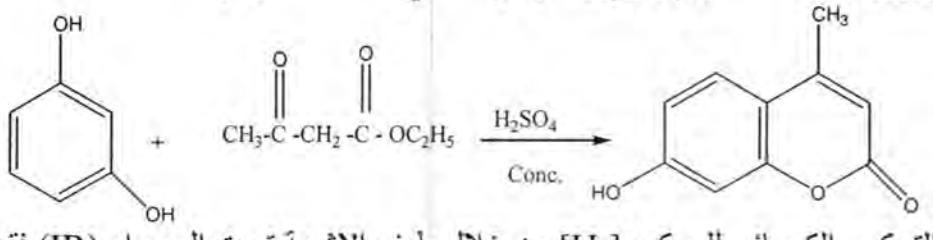

تم أثبات التركيب الكيميائي للمركب [H_1] من خلال طيف الاشعة تحت الحمراء (IR) فقد لوحظ ظهور حزمة عند ($1680cm^{-1}$) تعود الى أهتزازات مط الاصرة الكربونيل الاسترية أما أهتزازات مط الاصرة (C-O) الاسترية فقد ظهرت لها حزمة عند ($1271cm^{-1}$) وحزمة أمتصاص عند ($3267cm^{-1}$) تعود لاهتزازات المط لمجموعة (OH-). وتم تشخيص المركب ايضاً من خلال أطياف الاشعة فوق البنفسجية

(UV) في مذيب الايثانول ، فقد ظهر للمركب قمة أمتصاص عند (323 nm) تعود للانتقالات الالكترونية ($n \rightarrow \pi^*$) للالكترونات اللاتأصرية وقمتا أمتصاص عند (217 nm) و(204 nm) تعود الى الانتقالات الالكترونية($\pi \rightarrow \pi^*$) للالكترونات التأصرية للمركب.

تحضير وتشخيص المركبات [H_2]

تم تحضير المركب [H_2] بنيترة المركب [H_1] بأستخدام مزيج من H_2SO_4 المركز و HNO_3 المركز عند درجة حرارة (0 – 5 C°) كما في المعادلة :

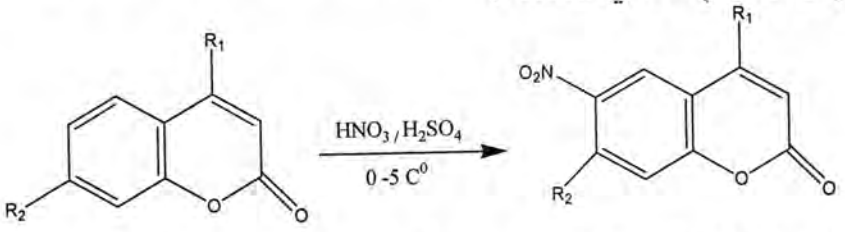

إن دخول الالكتروفيل (NO_2^+) في الموقع (6) يعود الى أن هذا الموقع هو الاكثر كثافة الكترونية نسبة الى ذرات الكاربون الاخرى في الكيومارين(18).

تم تشخيص المركب [H_2] من خلال أطياف الاشعة تحت الحمراء (IR) الجدول (7)

جدول- 7: يوضح قمم الامتصاصات الطيفية للمركبات [H_2].

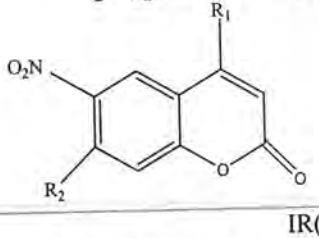

Comp No.	R_1	R_2	UV λmax nm	IR(cm^{-1}) KBr						
				υ (OH) cm^{-1}	υ (C=O) cm^{-1}	υ (C-O) cm^{-1}	υ (CH_3) cm^{-1}	υ (C=C) arom cm^{-1}	υ (C-H) arom cm^{-1}	υ (NO_2) cm^{-1}
H_2	CH_3	OH	205 414 259 348	3444	1768	1251 1303	1369	1590	3050	1549 1369

تحضير المركب 6-Amino-7-hydroxy-4-methyl Coumarin[H_3]

حضر هذا المركب من أختزال المركب [H_2] بأستخدام مسحوق الحديد في مزيج من الايثانول وHCL المركز

من ملاحظة أطياف الاشعة تحت الحمراء (IR) ظهر وبوضوح حزمتا أمتصاص أحدهما عند ($3350cm^{-1}$) والاخرى ($3400cm^{-1}$) وهما تعودان الى أهتزاز مط للاصرة (NH_2) للمركب [H_3] بالاضافة الى أمتصاصات أخرى قد تم توضيحها في الجدول (8).

الجدول -8: يوضح قمم الامتصاصات الطيفية للمركب [H_3].

Comp No.	R_1	R_2	UV λmax nm	IR(cm^{-1}) KBr						
				υ (OH) cm^{-1}	υ (C=O) cm^{-1}	υ (C-O) cm^{-1}	υ (CH_3) cm^{-1}	υ (C=C) arom cm^{-1}	υ (C-H) arom cm^{-1}	υ (NH_2) cm^{-1}
H_3	CH_3	OH	220	3200	1680	1186 1217	2900	1496 1500	3100	3350 3400

تحضير وتشخيص قواعد شيف[H_4-H_8]

تم تشخيص قواعد شيف المحضرة من خلال أطياف الاشعة تحت الحمراء(IR) والاشعة الفوق بنفسجية الجدول (9) يوضح قمم الامتصاص الطيفية للمركبات [H_4-H_8]

جدول -9: يوضح قمم الامتصاص الطيفية للمركبات[H_4-H_8]

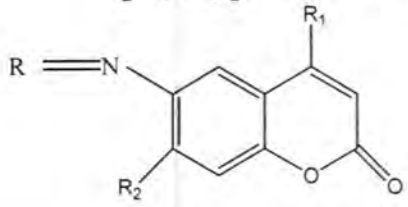

Comp No.	R_1	R_2	R	UV λmax nm	IR(cm^{-1}) KBr						
					υ (OH) cm^{-1}	υ (C=O) cm^{-1}	υ (C-O) cm^{-1}	υ (CH_3) cm^{-1}	υ (C-H) aliph cm^{-1}	υ (C=N) cm^{-1}	υ (others) cm^{-1}
H_4	CH_3	OH	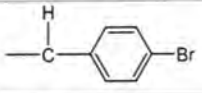	203 240	3338	1683	1319 1278	1423	2960	1612	(C-Br) 750
H_5	CH_3	OH	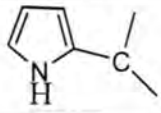	205 236 289	3400	1689	1203 1298	1480	2926	1595	(N-H) Pyrrol 3150
H_6	CH_3	OH	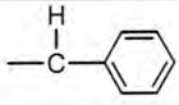	204 227	3379	1680	1178 1292	1325	2677	1562	–
H_7	CH_3	OH	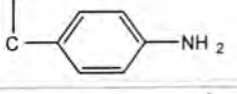	203 230 317	3400	1695	1117 1276	1359	2896	1593	(NH_2) 3380 3410
H_8	CH_3	OH	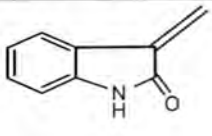	210 242 294	3500	1719	1332	1462	2890	1618	(C=O) Indole 1700 (NH) Lactum 3212

تحضير وتشخيص مشتقات الثايازوليدين[H_9-H_{13}]

حُضرت هذه المركبات من تفاعل قواعد شيف المحضرة [H_4-H_8] مع α -mercapto acetic acid حيث تتم الاضافة النكليوفيلية من خلال مهاجمة الزوج الالكتروني في ذرة الكبريت لمجموعة (C=N) مكونا" مركبا" وسطيا" باتحاد ذرة النتروجين الواقعة في الطرف الثاني من الاصرة مع ذرة كاربون مجموعة الكاربونيل مع لفظ جزيئة ماء حسب الميكانيكية الاتية(19):

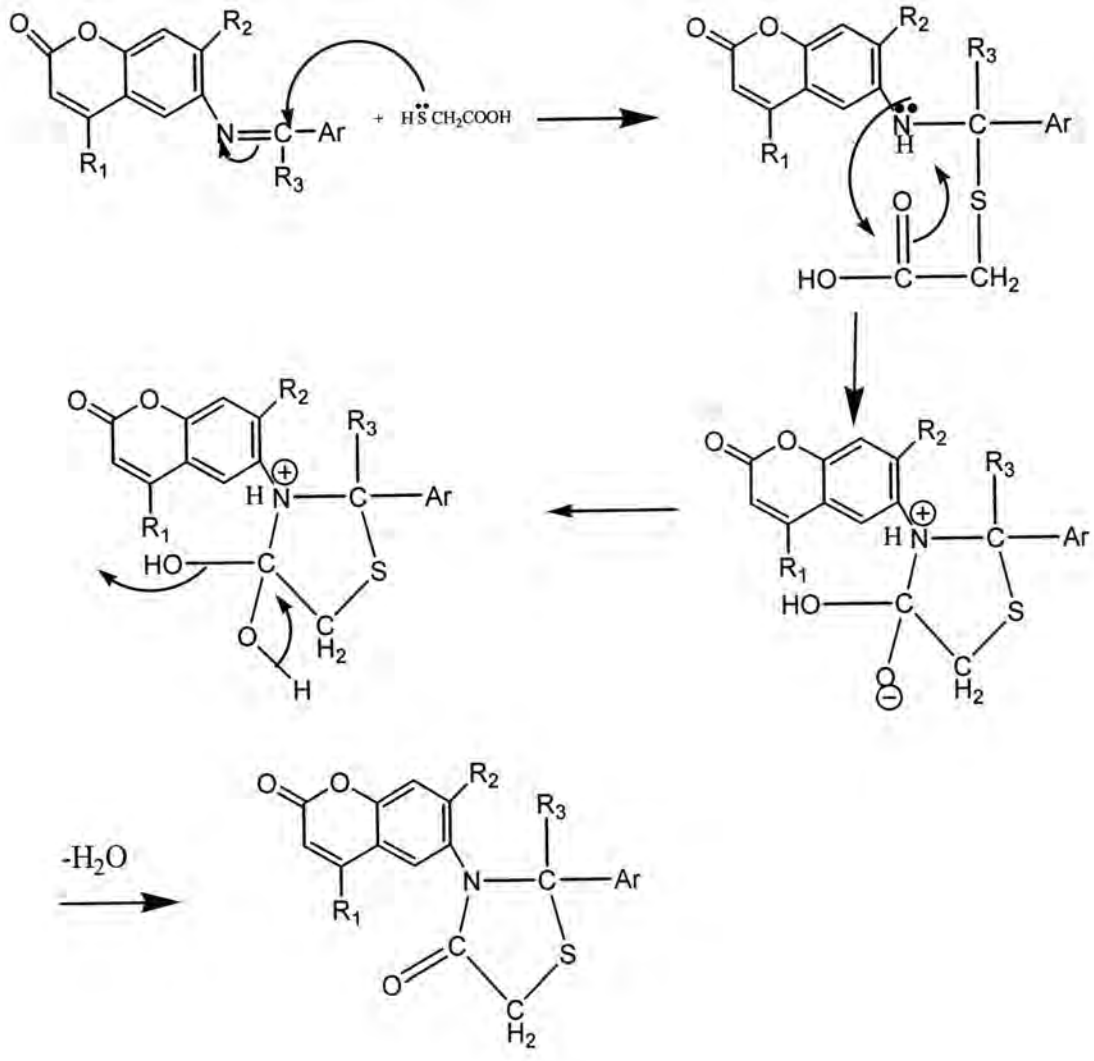

$[H_9 - H_{13}]$: $R_1 = CH_3$, $R_2 = OH$
$[H_{34} - H_{38}]$: $R_1 = H$, $R_2 = H$
$R_3 = CH_3$, H

AR = 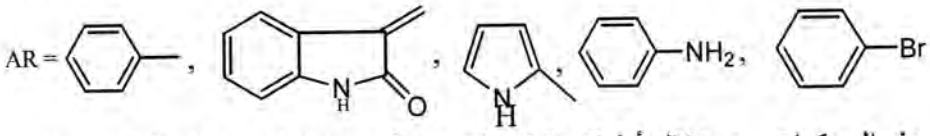

وتم تشخيص هذه المركبات من خلال أطياف الاشعة تحت الحمراء(IR) والاشعة الفوق بنفسجية الجدول (10)

جدول -10: يوضح قيم الامتصاص للمركبات [H_9-H_{13}] .

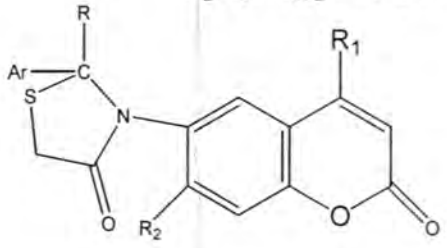

Comp. no	R_1	R_2	Ar	UV λmax nm	IR (cm^{-1}) KBr							
					υ (OH) cm^{-1}	υ (C=O) cm^{-1} Amide	υ (C-O) cm^{-1}	υ (C-H) aliph cm^{-1}	υ (C-S) cm^{-1}	υ (CH_3) cm^{-1}	υ (C-N) cm^{-1}	υ (others) cm^{-1}
H_9	CH_3	OH	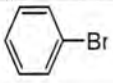	213	3348	1683	1269 1157	2924	700	1388	1217	(C-Br) 750
H_{10}	CH_3	OH	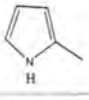	210	3516	1720	1300	2825	700	1398	1320	(N-H) Pyrrole 3112
H_{11}	CH_3	OH		201	3443	1705	1211 1136	2920	705	1413	1249	-
H_{12}	CH_3	OH	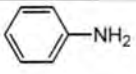	196 292	3358	1695	1143 1209	2920	677	1483	1273	($-NH_2$) 3300 3400
H_{13}	CH_3	OH	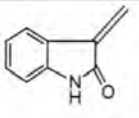	202	3500	1729	1250	2925	700	1475	1330	(C=O) Indol689 (NH) Lactum 3220

تحضير وتشخيص مركبات أمينية للكيومارين [H_{15} – H_{19}]

تم تشخيص المركب [H_{14}] من خلال أطياف الاشعة تحت الحمراء(IR) وقد لوحظ أختفاء حزمة (OH) عند ($3500cm^{-1}$) و ظهور حزمة أمتصاص عند ($600cm^{-1}$) تعود الى أمتصاص مط الاصرة –C) (CL وعدد من الحزم الاخرى.

أما بالنسبة للمركبات [H_{15} – H_{19}] فقد تم تشخيصها من خلال أطياف الاشعة تحت الحمراء(IR) إذ يمتاز طيف المركب [H_{18}] بظهور حزمة أمتصاص عند ($1242cm^{-1}$) تعود الى أهتزاز مط الاصرة – C) (N بالاضافة الى الحزم الاخرى الموضحة في الجدول(11).

جدول -11: يوضح قمم الامتصاص الطيفية للمركبات [H_{15}-H_{19}] .

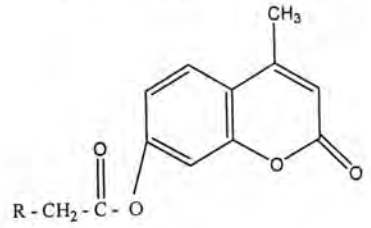

Comp. no	R	λmax nm	IR (cm^{-1}) KBr					
			υ (C=O) Ester cm^{-1}	υ (C-O) Ester cm^{-1}	υ (C-N) aliph cm^{-1}	υ (C-H) aliph cm^{-1}	υ (CH_3) cm^{-1}	υ (C=C) Arom cm^{-1}
H_{15}	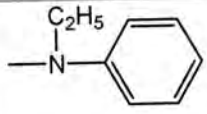		1672	1145	1250	2937	1450	1600
H_{16}	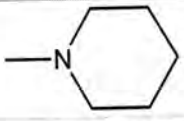	202 232	1714	1269	1325	2933	1383	
H_{17}	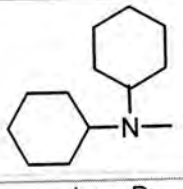	210 325	1714	1145	1255	3000	1450	1614
H_{18}	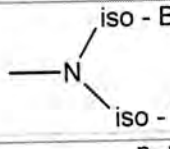	204 323	1735	1155	1242	2896	1458	1612
H_{19}	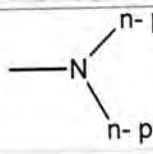	216 323	1720	1141	1088	2996	1367	1560

تحضير وتشخيص المشتق الاستليني للكيومارين [H_{20}]

يُعد هذا المركب هو المفتاح لتحضير العديد من قواعد مانخ أذ يتم تحضيره من تفاعل مولات متساوية من المركب [H_2] مع كلوريد البروبرجيل بوجود ثلاثي أثيل امين .

تم التشخيص للمركب [H_{20}] من خلال أطياف الاشعة تحت الحمراء(IR) حيث لوحظ ظهور حزمة أمتصاص عند ($2733cm^{-1}$) تعود الى أهتزاز مط الاصرة (C=C) وأختفاء حزمة (OH) عند ($3200cm^{-1}$).

كما شُخص المركب من خلال أطياف الاشعة فوق البنفسجية (UV) في مذيب الايثانول والماء حيث وجد قمة أمتصاص عند (255nm) تعود للانتقالات الالكترونية ($\pi \rightarrow \pi^*$) للالكترونات التاصرية في المركب وقمتا أمتصاص عند (290nm) و(400nm) تعود للانتقالات الالكترونية ($n \rightarrow \pi^*$) للالكترونات اللاتاصرية في المركب.

تحضير وتشخيص قواعد مانخ [$H_{21} - H_{25}$]

وتم تشخيص قواعد مانخ من خلال أطياف الاشعة تحت الحمراء(IR) فقد أظهر المركب [H_{21}] حزمة أمتصاص ($1348cm^{-1}$) وعند ($1518cm^{-1}$) وهما تعودان لاهتزاز مط اصرة(NO_2) وحزمة أمتصاص عند ($1253cm^{-1}$) تعود لاهتزاز مط الاصرة (C–N) مع أختفاء حزمة مط الاصرة لـ (C --C– H) عند ($2733cm^{-1}$) وحزم أخرى موضحة في الجدول (12).

و تم التعرف على تركيب المركبات من خلال أطياف الاشعة فوق البنفسجية (UV) في مذيب الايثانول والماء فقد اعطى المركب [H_{22}] قمة أمتصاص عند (395nm) تعود للانتقالات الالكترونية للالكترونات اللاتاصرية في المركب وقمة أمتصاص عند (250nm) و(215nm) تعود للانتقالات الالكترونية للالكترونات التاصرية في المركب.

جدول -12: يوضح قمم الامتصاص الطيفية للمركبات [H_{21}-H_{19}] .

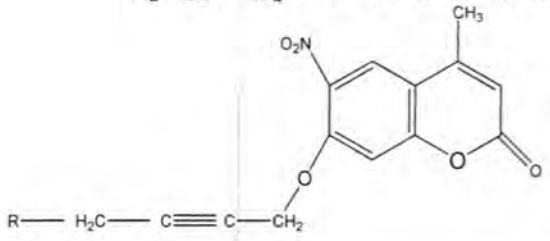

Comp no	R	UV maxλ (nm)	IR (cm^{-1}) KBr							
			υ (C=O) cm^{-1}	ν (C-O) cm^{-1}	υ (CH_3) cm^{-1}	υ (NO_2) cm^{-1}	υ (C-N) cm^{-1}	υ (C=C) arom. cm^{-1}	υ (C-H) aliph cm^{-1}	υ (C-H) arom cm^{-1}
H_{21}	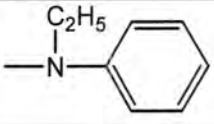	203 247	1666	1118	1460	1348 1518	1253	1612	2968	3125
H_{22}	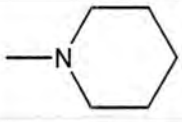	215 250 395	1680	1120	1452	1367 1527	1120	1527	2943	3078
H_{23}	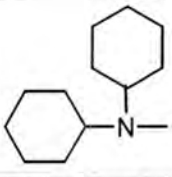	206 230 411	1688	1116	1452	1375 1509	1261	1504	2931	3248
H_{24}	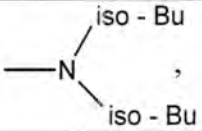	206 260 406	1680	1219 1278	1495	1384 1527	1219	1527	2958	3010
H_{25}	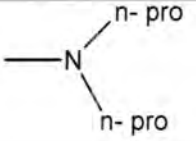	144 266 410	1680	1118	1467	1355 1551	1265	1521	2964	3150

المصادر

1. Irena K."Synthesis and natural coumarin as cytoxic agent"Curr.Med.Chem.5(1) :37, (2005).
2. Kofinas C.,chinou I.,L.A.,Harvala C.,Roussakis C.,Maillard M., Hostettman K.,"Potential effects of warrning and drying on peatl and plant community composition" Planta Med, 64, 174, (1998).
3. Hasnaa A.,H.Al-Zanki"Synthesis, characterization & Bioassay of Some Coumarin derivaties"M.Sc.Thesis,Chem. Dept.Baghdad Univ.Baghdad,Iraq, (1998).
4. Sethna S. & phadke R.,"Synthesis of coumarins by condensation of phenols with B-keto esters in the presence of lewis acid catalyst" Chem.Reviews, 36,10,(1945).
5. Kirkiacharian S.,Thuy D.T.Sicsic S.,Bakhchinian R.,Kurkjian R. and Tonnair T.,"The natural coumarins chichester", IL Fomaco, 57, (9):703-708, (2002).
6. Yu D.Suzuki M.,xie L., Morris-Natschke S.L., and Lee K. H.,"Naturally occuring coumarins"Medcinal Res.Reviews,23, (3) :322-345, (2003).
7. Tummino P.J.,Ferguson D.,Hupe D.,"A traditional Chinese medicine plant-compound database and its application for searching" Biochem. Biophys. Res. Commun 201, 290, (1994).
8. Marshall M.E.,Kervin K. , Benefield C. et al.,"Antitumer compounds " **J**.of Cancer Res.And clinical Oncology, vol.120, Suplement 1, pp.S_3-S_{10} (1994).
9. Lake B.G.,"Coumarin metabolism",Toxicity & Carcinogenicity: relevance for human risk assessment" food and chemical Toxicology, 37(4) :423-453, (1999).
10. Thornes R.D,Daly L.,Lynch G.,Bteslin B.,Browne H.,Browne H. Y.,Corrigan T.,Daly P.,Edwards G.,Gaffiney E.J.,"Pharmacology and application of Chinese material medica" Cancer Res. Cinical Oncology, 12, S32, (1994)
11. Mohler J.L.,Gomella L.G.,Crawford E.D.,Glode L.M.,Zippe C.D.,Fair W.R.,Marshal M.E.,"Bioorganic & medicinal chemistry coumarin-based prodrugs" Prostate, 20, 123, (1992).
12. C.Caspian,"Baku-Ashgabat thaw could have energy impact"Baku,: 57-80, (2003).
13. Kennedy R.,Thornes Rd (eds),"Coumarins-Biology, Applications and Mode of Action", John wiley & Sones Ltd., Chichester, (1997).
14. Borges F.,Roleira F.,Mithazes N.,Santaua L.,Urite E.,Curr. "Design and synthesis of coumarin substituted oxathiadiazole derivatives having anti-inflammatory activity possibly through p3 MAP kinase inhibition"Med.Chem., 12, 887, (2005).
15. Devinne K.F.,Gon Calves R. M.,Gomes Coetho R.Vilegas W.,Photomedicine 12, 378, (2005).
16. Arthur I.Vogel,"a Text Book of Practical Organic Chemistry",Longman,2^{ed}, :855 , London, (1972).
17. Nofel Z.M., ALZahar M.L. and Abdel karim S.S.,Molecules,5 :99-113, (2000).
18. Meyer H."Chemistry and pharmacology of natural coumarins" Acta Chem.. Scand., ser. B, 29, 133, (1975).
19. Fahmay H., Kassem E. M. M., Abdon W. A. M. and Mahmoud S.A.,"Kinetics and mechanism of the replacement reaction of 1,10-phenathroline with trisoxato cobatate (111) complex in DMF-water" Egypt J. Pharm., 38 (3), 13, (1997).

التعيين الجهدي لايون اللوتيشيوم باستخدام القطب الانتقائي المعتمد على معقدات بعض الايثرات التاجية في غشاء كلوريد متعدد الفنيل

نضال حميد كريم و نبيل شوكت نصوري و عدي احمد عبد الستار
مركز بحوث الكيمياء/وزارة العلوم والتكنولوجيا

الخلاصة

تضمن هذا البحث تحضير اقطاب سائلة تعتمد على اغشية انتقائية لايون اللوتيشيوم لغرض تعيين اللوتيشيوم في نماذج مختلفة، صنعت مجموعة اغشية من معقد بكرات اللوتيشيوم مع الايثر التاجي-18-crown-6الذائب بتجانس تام في الغشاء المتكون من كلوريد بولي فنيل مع DOPP الذي يعتبر مادة ملدنة جيدة المواصفات.

درست استجابات هذا القطب في محاليل قياسية تحتوي على كلوريد اللوتيشيوم مدى تركيزه يتراوح بين $1x10^{-1}M$ الى $1x10^{-6}M$ حيث وجد ان الاستجابة كانت خطية في المدى $1x10^{-1}M$ الى $1x10^{-4}M$ وكانت قيم الميل النرنستي 15mV/decade وجد التحسس مقدارة $7x10^{-5}M$ في حالة احتواء القطب محلول مالئ داخلي تركيزة $1x10^{-1}M$ في حين كان الميل النرنستي مساويا الى 16mV/decade وحد التحسس $7x10^{-5}M$ عندما يكون تركيز المحلول المالئ الداخلي $1x10^{-2}M$ كما وان مدى الPH الذي تعطي فيه الاقطاب استجابة ثابتة تراوحت بين 3 الى 7.

تم تعيين تركيز اللوتيشيوم في محاليل قياسية محضرة من اللوتيشيوم بواسطة الاقطاب المحضرة مختبريا وباستخدام طريقة التسحيح الجهدي وطريقة الاضافات القياسية المتعددة (طريقة كران).

ABSTRACT

In this work liquid membrane electrodes selective for lutetium ions were prepared and used for determination of lutetium in different samples.Membrane for lutetium was prepared from lutetium picrate complex with crown ether 18-crown-6 , it was incorporated in PVC membrane .

The properties of this electrode were evaluated practically by using standard procedures. For this membrane Nernestian slope , linear working range , detection limit, measurement stability , response time and electrode life time were studied .

The electrode showed that have linear working ranges were 10^{-4}- 10^{-1}M with Nernestian slope value in the range of 16mv/decade.

The stable pH ranges were between 3-7, and concentration of standard solutions of Lu were determined by using Gran' s plot standard addition method .

Key words: lutetium, Ion selective electrode, Crown ether

المقدمـــــة

اصبحت تقنية الاقطاب الانتقائية الايونية من الطرق البسيطة والسريعة والفعالة لتعيين ايونات العناصر في نماذج مختلفة كانت بداية تحضير الاقطاب السائلة من قبل (Ross) حيث تم تصنيع اقطاب الكالسيوم المعتمد على استرات حامض الفسفوريك ، بعدها تطورت طرق تصنيع الاقطاب السائلة والتي تحتوي على المركبات التاجية منها قطب البوتاسيوم والصوديوم والليثيوم المستخدمة للاغراض الطبية لقياس هذه الايونات في مصل الدم (1,2).

كما تم تحضير اقطاب سائلة حاوية على المركبات التاجية لاستخدامها في قياس الملوثات منها اقطاب الرصاص (3) باستخدام المادة الفعالة الايثر الحلقي الثنائي (bis crown ether) من قبل (kum-chul) (3)وجماعته.

حضر kogi ومجموعة قطب الصوديوم الانتقائي باستخدام 15- crown-5 (7) واستخدام Cairo وجماعته مشتقات الايثر التاجي 18- crown-6لتصنيع قطب السيزيوم الانتقائي (8) اما Mastshi فقد صنع قطب الفضة من Mono thio crown ether (9) في حين ان Ming- Tian قد استخدم Dithio crown ether (10) في تصنيع اقطاب انتقائية

لايون الزئبق $Hg\prod$ والفضة (10) . لقد استخدمت الايثرات الحلقية Podands في تصنيع اقطاب لايونات الفضة من قبل Shim وجماعته (11) .

في هذا البحث تم تصنيع قطب اللوتيشيوم وهو نوع من انواع اقطاب السائلة المعتمد على غشاء يحتوي على المادة الفعالة 18-crown-6 والمادة الملدنة ثنائي اوكتيل فنيل فوسفونيت DOPP حيث اعطت استجابة نرنستية جيدة 16mv/decade وحد تحسس $7x10^{-5}M$ (12-13) .

استخدمت طريقة التسحيح الجهدي (4) وطريقة الاضافات القياسية (5) في تعيين تراكيز اللوتيشيوم في المحاليلها المائية المختلفة.

المواد وطرائق العمل

الاجهزة المستخدمة

- **جهاز قياس الجهد نوع :** Microprocessor Ion analysis, Orion research, model (901) (USA)
- **جهاز الدالة الحامضية للمحاليل :** Expandable Ion analysis, Orion research, model EA940
- **قطب الكالوميل القياسي المرجعي نوع :** Calomel refrence Electrode , gallenkamp(England)

المواد الكيمياوية

- المركب التاجي 18-Crown-6من شركة Merck بنقاوة 99% .
- الملدنة DOPP مزود من شركة Fluka بنقاوة 99.9% .
- اوكسيد اللوتيشيوم مزود من شركة BDH بنقاوة 99.9% .
- tetrahydrofuran (THF)- مزود من شركة Merck .
- املاح اخرى مستخدمة في العمل ذات نقاوة عالية من مناشئ مختلفة اذيبت جميعها بالماء المقطر اللايوني

- تحضير ملح بكرات اللويتشيوم.

تم تحضير ملح بكرات اللوتيشيوم $Lu(pic)_3$ من حامض البكريك واوكسيد اللوتشيوم وذلك بتسخينها في حمام مائي لحين الحصول على محلول رائق ، ثم يتم تبخير المحلول بتعريضة الى الجو للحصول على بلورات صفراء من بكرات اللوتيشيوم.

- تحضير معقد الايثر التاجي 18-crown-6 .

تمت اذابة ملح بكرات اللوتيشيوم والايثر التاجي 18-crown-6 في(ايثانول- ثنائي كلورو ايثان) وتسخين المزيج لحين الحصول على محلول رائق ثم يبخر ببطيء للحصول على بلورات المعقد.

- تحضير وصب الغشاء.

حضر الغشاء القطب بطريقة (Gragg) (6) وجماعتة باستخدام 0.04gm من معقد اللوتيشيوم والايثر التاجي 18-crown-6 مع 0.36 gm من المادة الملدنة و 0.17 gm من مسحوق PVC النقي المذاب في 6-7 ml من THF لحين الحصول على محلول رائق. ثم يصب في القالب الزجاجي الاسطواني ويترك ليتبخر المذيب ببطيء للحصول على الغشاء السائلmembrane liquid بسمك (0.1-0.5 mm) يتم لصق جزء منه في انبوبة من ال PVC التي تربط بدورها على انبوبة القطب الزجاجي ويربط الطرف الاخر لانبوبة القطب بسلك من Ag/AgCl المغمور في المحلول المالئ الداخلي ويوصل السلك الى الدائرة الكهربائية .

النتائج والمناقشة

تم تعيين مواصفات قطب اللوتيشيوم والمعتمدة على اغشية حاوية على 18-crown-6 كمادة فعالة والمادة الملدنة DOPP .

جدول-1: مواصفات قطب اللوتيشيوم باستخدام المادة الفعالة 6 - 18-crown والمادة الملدنة DOPP

عمر القطب	زمن الاستجابة sec	مدى التركيز M	حد التحسس M	الانحدار mV/decade	المادة الملدنة	المادة الفعالة
اسبوعين	120 sec	10^{-1}-10^{-4}	$7x10^{-5}$	16	DOPP	18-crown-6

كما تمت دراسة تاثير المحلول المالئ الداخلي للقطب (IFS) . Internal Filling Solution باستخدام ثلاثة تراكيز مختلفة من محاليل قياسية للوتيشيوم وهي على التوالي : $1x10^{-1}$M -$1x10^{-2}$M -$1x10^{-3}$M وكانت متشابهة الى حد كبير وكانت جميعها مطابقة للمواصفات حيث ان الانحدار تراوح 14-16 mV/decade وتراوح مدى التركيز $1x10^{-1}$ M – $1x10^{-4}$ M وكان حد التحسس لجميع هذه الاقطاب مساوية الى قيمة $7x10^{-5}$ M

كما تبين من التجارب المختبرية ان القطب الذي يحتوي على المحلول المالئ الداخلي الذي تركيزه Lu $1x10^{-2}$ M اكثرهم استقرارا واسرعهم استجابة ولهذا السبب تم اعتماد هذا التركيز في تعيين منحني المعايرة واستخراج ثوابتة وخصائصه .

جدول -2: مواصفات قطب اللوتيشيوم باستخدام محاليل مالئه داخلية مختلفة 0.1,0.01,0.001M

IFS M	زمن الاستجابة Sec,	مدى التركيز M	حد التحسس M	الانحدار mV/decade
0.1	100-120	10^{-1}-10^{-4}	$7x10^{-5}$	15
0.01	60-100	10^{-1}-10^{-4}	$7x10^{-5}$	16
0.001	120-140	10^{-1}-10^{-4}	$7x10^{-5}$	14

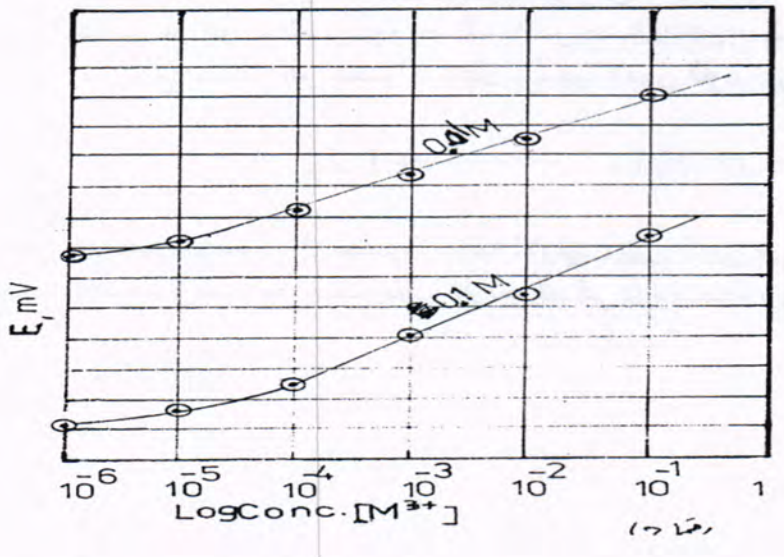

الشكل -1: منحني المعايرة لتركيزين10^{-1}M, 10^{-2}M لايون اللوتيشيوم

تمت دراسة تاثير ال pH المحلول على استجابة القطب المحضر مختبريا كما في الشكل (2) والذي يبين قيم لمدى محدد من ال pH والذي ثبت فيه قيم الجهدالكهربائي للقطب عند الدالة الحامضية 3-7 .

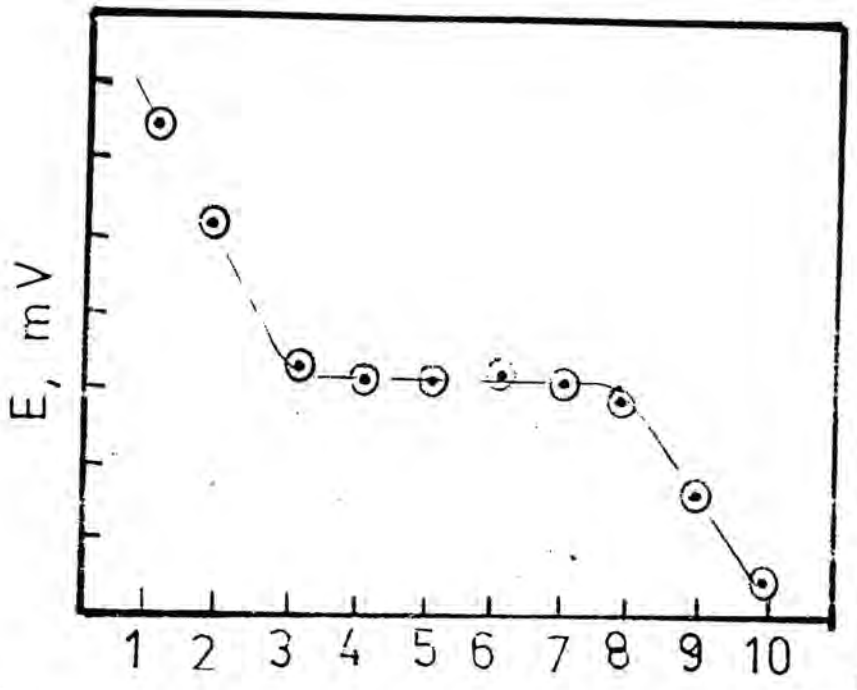

الشكل -2: مدى تاثير ال pH الذي يعمل به قطب اللوتيشيوم بثبات الجهد الكهربائي للقطب

في هذا الشكل نلاحظ عند قيم ال pH الواطئة حدوث تاثير لايون الهيدروجين على المعقد داخل الغشاء وربما يؤدي الى تفكك المعقد وكذلك في الوسط القاعدي كان تاثير ايون (OH) واضح على جهد الخلية نتيجة لتداخل ايونات الهيدروكسيل ذات التاثير السلبي حيث تستجيب الايونات الموجبة من المحلول مكونة رواسب من هيدروكسيدات الايونات .
كما استخدمت طريقة الاضافات القياسية وطريقة التسحيح الجهدي التي تعتمد على استخدام مسحح titrent هو محلول قياسي من فلوريد الصوديوم يضاف بالتدريج gradually الى خلية التسحيح titration cell . ان الذي يحصل هو حصول تفاعل ترسيب لايون اللوتيشيوم على شكل فلوريد غير ذائب .

$$Lu^{+3} + 3F^{-}(NaF) \longrightarrow LuF_3$$

ولزيادة الدقة يرسم منحني التسحيح التفاضلي (او منحني المشتقة الاولى) يبين التغير في الجهد لكل وحدة تغير في حجم الكاشف او المسحح حيث يعطي الرسم البياني ذروة حادة هي نقطة النهاية .

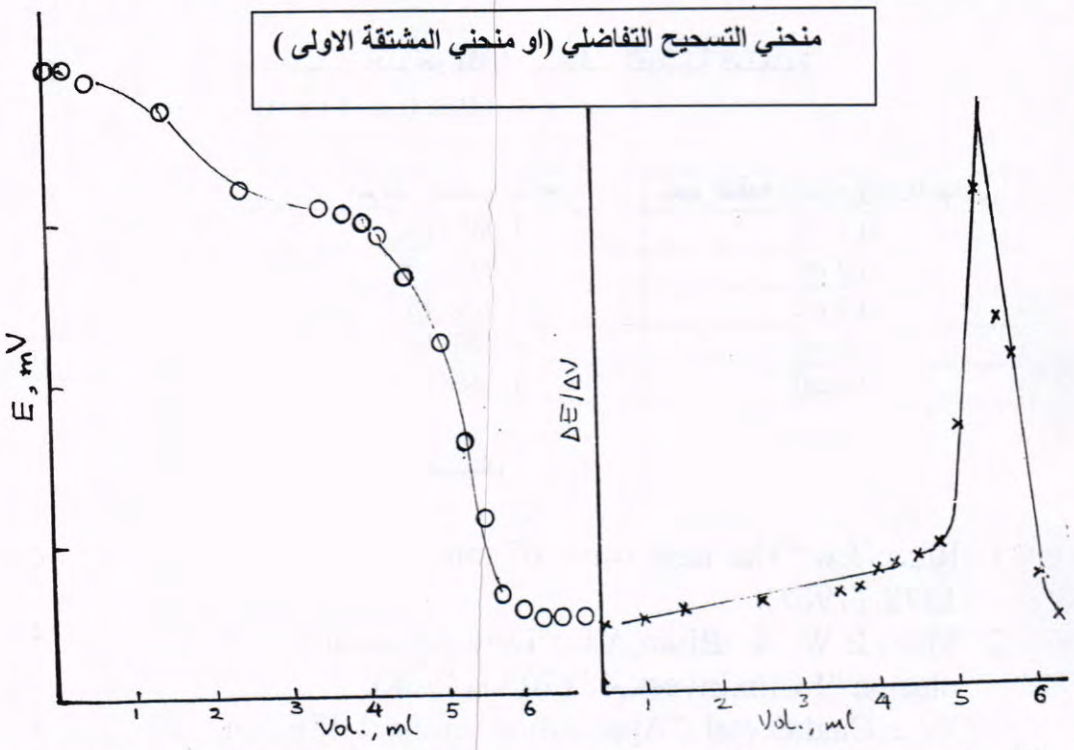

الشكل -3: منحني التسحيح الاعتيادي والتسحيح التفاضلي (المشتقة الاولى) لايون اللوتيشيوم

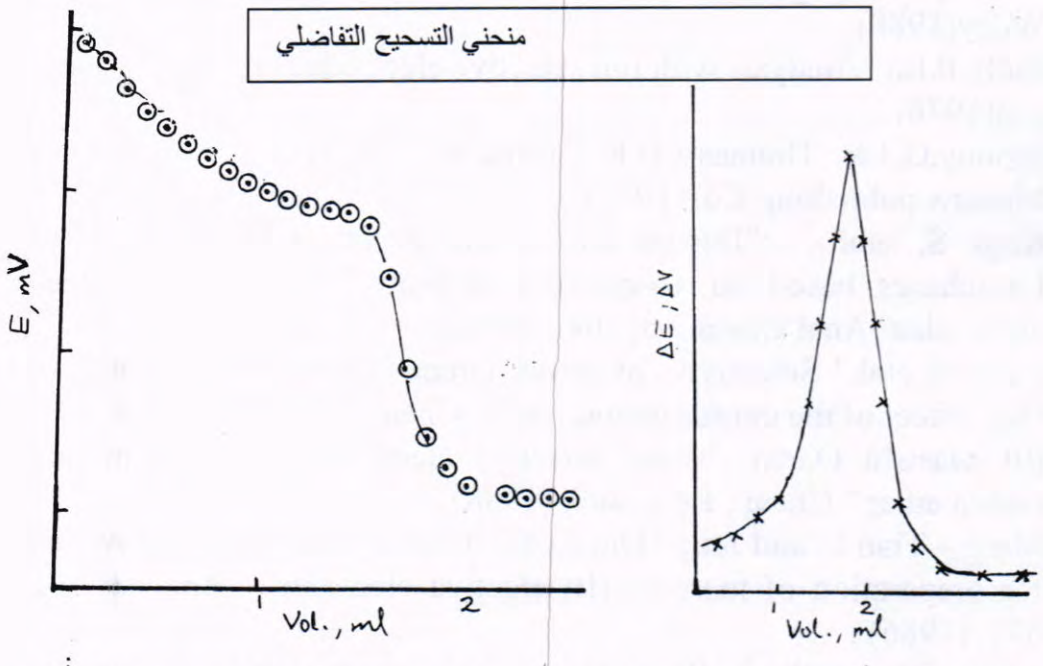

الشكل -4: منحني التسحيح الاعتيادي والتسحيح التفاضلي (المشتقة الاولى) لايون اللوتيشيوم

وكانت النتائج متقاربة مع القيم المحسوبة نظريا وبنسبة خطأ(5%) .
أما الطريقة الثانية لتعيين التركيز لايون اللوتيشيوم هي طريقة الاضافات القياسية حيث تمت مقارنتها مع نتائج التسحيح الجهدي والتي تعتمد على اضافة حجم معين من الكاشف الى النموذج ثم يقاس التغيير الحاصل في جهد الخلية وتكون هذه الكواشف عبارة عن محاليل قياسية عالية التركيز ولزيادة الدقة تستخدم طريقة الاضافات القياسية المتعددة .

جدول -3: تعيين تركيز اللوتيشيوم باستخدام طريقة الاضافات القياسية المتعددة
المعدل الرياضي يساوي $M\ x10^{-3}$ (1.039± 0.051)

حجم الدفعة تركيزه 0.1M قياسي	التركيز المحسوب M	التركيز المحضر
0.1 ml	$1.080x10^{-3}$	$1x10^{-3}$ M
0.2 ml	$1.007x10^{-3}$	
0.3 ml	$1.016x10^{-3}$	
0.4 ml	$1.070x10^{-3}$	
0.5 ml	$1.056x10^{-3}$	

المصـــادر

1. Ross. J.w."The new wave of Ion-Selective electrodes", science,156, 1378, (1967).
2. Moor.E.W & Blum,A.L.;"Determenation of Na,K &La in blood plasma "J.Clin.Invest.,47 (70A),(1968).
3. Kum.Chal,O.etal.;"Application of lead ISE for analysis of lead in environmental samples" Bull.Korean Chem. Soc.20, 556,(1999).
4. Cotton,A.&willkinson,G.; "Advanced inorganic chemistry".John Wiley(1988).
5. Baily P.L.; "Analysis with Ion selective electrodes",Hyden &
6. sun(1976).
7. Moody,G.J.& Thomas,J.D.R." selective ion sensitive electrodes " Merrow publishing Co. (1971).
8. Kogi S. etal , .;"Design and synthesis of sodium ion-selective Ionophores based on 16-crown-5 derivatives for an ion-selective electrodes" Anal Chem. 68, 208, (1996) .
9. Cairo B etal." Selectivity of calix[4]arene-crown-6 for cesium ion in ISE: effect of the conformation" Anal. Chem . 67 , 4234, (1995).
10. [9] Mastshi O,etal ,"silver selective electrode based on monothio crown ether " Chem , Lett , 409, (1988) .
11. Ming – Tian L. and Jeng . Dheug S. ,"Utilization of dithio crown ether for preperation of mercary (II)selective electrode " Analyst , 111 , 891, (1986) .
12. Shim S.L. etal, " Podands a polymer immobilised ionophore membrane for determenation of silver ions" Chem.Comm. 965,(1997).
13. Catrral , R.w. , Chemical Sensors , Oxford,(1997).
14. N.S.Nassory and N.H.karim, " Uranyl ion selective electrode based on crown ether in PVC matrix membrane"Tr.J.Chemisty, 18, 120,(1994).

تأثير مستخلصات نبات الكبار *Capparis spinosa* L. على نمو بعض الاحياء المجهرية المرضية

[1]سراء نصيف مسلم و[1]نزار أدور ناصر و[2]رضا أبراهيم حسين
[1] قسم علوم الحياة - كلية العلوم – الجامعة المستنصرية
[2] قسم علوم الكيمياء – كلية العلوم – الجامعة المستنصرية

ABSTRACT

This study dealt with the effect of watery and alcoholic extracts of root , leaves and fruits of *Capparis spinosa* on the growth *Escherichia coli* , *Staphylococcus aureus*, *Klebsiella* spp., *Pseudo-monas aeruginosa* and *Candida albicans* isolated from patients suffering from skin infection .

Agar-well diffusion method was used for this purpose. chemical analysis were done on the plant for identification of active compounds; Alkaloids, Glycosides, Tanins, Saponins, Phenoles and Flavones from the watery extracts, beside the Rasins compound being isolated from the alcoholic extracts .

The activity of extracts from roots, leaves and fruits, had been tested, separately regarding their inhibitory effects on the growth of the pathogenic isolates used in this study . The synergistic isolates used in this study . The synergistic effect of these extracts had been also studed .

The variation in the results of the inhibitory activity found to be related to the type of the extracts, their preparation method and the strain of the microorganism .

The study showed Gram +ve bacteria being more sensitive to the effect of the mentioned extracts .While the isolate of *Klebsiella* spp.(Gram –ve)was more resistant for the effect of these extracts .

الخـلاصـــة

اجريت هذه الدراسة لمعرفة تأثير المستخلصات المائية والكحولية لثمار واوراق وجذور نبات الكبار *Capparis spinosa* في نمو عزلات من*Escherichia coli* و *Staphylococcus aureus* و *Klebsiella* sp.و *Pseudomonas aeruginosa* و *Candida albicans* العزولة من الاصابات الجلدية، وذلك باستخدام طريقة الحفربالاكار .

تم استخلاص كل من المركبات كلايكوسيدات و قلويدات و صابونيات و تانينات و الفلافونات والفينولات من المستخلص المائي، اضافة الى المركبات الراتينجية من المستخلص الكحولي. تم اختبار فعالية هذه المستخلصات لكل من الثمار والاوراق و الجذور كل على حدة في امكانية تثبيطها لنمو العزلات المرضية المستخدمة في الاختبار، فضلا عن اختبار التأثير التآزري لها لنفس الغرض . وقد اختلفت نتائج دراسة الفعالية التثبيطية للمستخلصات باختلاف نوع المستخلص وطريقة تحضيره فضلا عن نوع الكائن المجهري.

اظهرت الدراسة ان عزلات البكتريا الموجبة لصبغة كرام كانت أكثرحساسية لتأثير المستخلصات المذكورة في حين كان لبكتريا *Klebsiella* sp. السالبة لصبغة كرام أكثر مقاومة لتأثير هذه المستخلصات .

المقدمة

نتيجة ظهور سلالات طافرة من الاحياء المجهرية المرضية بسبب كثرة استخدامات العقاقير المصنعة خلال اواخر القرن الماضي (1), الى جانب المضاعفات الجانبية الناتجة عن استخدام هذه العقاقير مثل الحساسية من بعض الادوية وهي من الاعراض التي لم تكن معروفة سابقا, فقد عاد الانسان يبحث عن مصادر علاجية طبيعية للتقليل من المضاعفات الجانبية , فقد اشارت منظمة الصحة الدولية (2) الى ان اكثر من 80% من البشر يعتمدون على مستخلصات او بعض مكونات النباتات الطبية المختلفة في علاج الحالات المرضية التي يعانون منها.

علما بأن المستخلصات النباتية تحتوي الى جانب المركبات العضوية الفعالة، العديد من العناصر والفيتامينات والمركبات الكيميائية الثانوية والتي لها علاقة في نمو الجسم، (3).
وقد أثارت المستخلصات النباتية الاهتمام مؤخرا وخاصة في معالجة الاصابات الجلدية المختلفة (4)، ولاعتبارها مصدرا للمنتجات الطبيعية ، فهي تمتلك مواصفات وقاية وحماية ضد الاصابة بالامراض كبدائل علاجية للاصابات (5) .
لذلك فقد هدف البحث الى امكانية استخدام المستخلصات المائية و الكحولية لنبات الكبار (جذرو ورقة و ثمرة) في تثبيط نمو بعض الاحياء المجهرية المرضية و المعزولة من اصابات جلدية مختلفة .

المواد وطرائق العمل

- الاوساط الزرعية تم استخدام عدد من الاوساط الزرعية المختبرية لأغراض تنمية عزلات الاحياء المجهرية قيد الدراسة والاختبارات التأكيدية لها وهي :

الوسط الزرعي	الشركة المجهزة
وسط آكار الماكونكي	DIFCO , USA
وسط آكار الدم الاساس	DIFCO , USA
وسط آكار المانيتول الملحي	DIFCO , USA
وسط مرق خلاصة المخ و القلب	DIFCO , USA
وسط آكار خلاصة المخ و القلب	DIFCO , USA
وسط آكار مولر – هنتن	DIFCO , USA
وسط المرق المغذي	BDH , England
وسط آكار المغذي	BDH , England
وسط آكار السابروید دیکستروز	Oxoid , England

- اقراص المضادات الحياتية

استخدمت مجموعة من اقراص المضادات الحياتية شائعة الاستخدام ضد عزلات البكتريا المشمولة في هذه الدراسة , وذلك لاغراض المقارنة مع معدلات تأثير مستخلصات النبات على نمو الكائنات المجهرية حسب طريقة (6) , وهي:
Aztreonam وAmoxicillin وCarbenicillin وCefoxin وCephalthin و Ciprofloxacin وErythromycin وGentamicin وImipenean وVancomycin .

- العزلات المرضية

تم الحصول على عزلات بكتيرية نقية من مختبرات الدراسات العليا في قسم علوم الحياة , كلية العلوم في الجامعة المستنصرية, وشملت:
Pseudomonas aeruginosa و*Klebsiella* sp. و *Escherichiacoli* و *Staphylococcus aureus* كما تم الحصول على عزلة خميرة نقية *Candida albicans* من مختبر الصحة المركزي في بغداد .
وقد اجريت الفحوصات المظهرية والبايوكيميائية للعزلات المذكورة للتأكد من تشخيصها استنادا الى (7) و (8) .

- جمع وتحضير العينات النباتية

تم جمع عينات نبات الكبارمن محافظة ديالى (حيث موطنه الطبيعي) خلال شهرحزيران عام 2007 ، وقد عزلت عينات الجذور والاوراق والثمار كل على حدة، ثم نظفت من الشوائب وتركت في الظل لمدة ثلاثة ايام لتجف، ثم طحنت بطاحونة

كهربائية، ثم اجريت عملية الكشف عن مكوناتها. علما بأنه تم تشخيص النبات من قبل الاستاذ الدكتور علي الموسوي في كلية العلوم في جامعة بغداد، وقد ثبت الاسم العلمي للنبات *Capparis spinosa* والذي ينتمي الى عائلة Capparidaceae.

حضرت اربعة انواع من المستخلصات النباتية من مساحيق العينات النباتية، وهي المستخلص المائي الحار والبارد والمستخلص الكحولي الحار والبارد، وحسب طريقة (9) بعدها تم الكشف عن المجاميع والمركبات الكيميائية الفعالة الموجودة في الاجزاء المختلفة للنبات قيد الدراسة و بالشكل الاتي :

الكشف عن الراتنجات(10) والكشف عن التانينات(11) والكشف عن الكومارين (12) والكشف عن الفلافونات (13) والكشف عن الصابونيات (11) والكشف عن القلويدات (14) والكشف عن الفينولات (15) والكشف عن الكلايكوسيدات (16)، وقد حضرت تراكيز مختلفة ومتدرجة لكل من المستخلصات الاربعة المذكورة اعلاه باضافة (5) غرام من كل مسحوق على حدة الى (10) ملليتر من الماء المقطر, فنحصل على محاليل تركيز كل منها (500) ملغم / مل . رشحت المحاليل لاغراض التعقيم بمرشحات (0,22) مايكرون بعد ذلك حضرت التراكيز المتدرجة للمحاليل (250 و 125 و 62,5 و 31,25) ملغم/ مل, باستخدام الماء المقطر بموجب طريقة (17) لاغراض التخفيف وعينات السيطرة .

النتائج و المناقشة

الكشف عن المركبات الكيميائية الفعالة بينت نتائج الكشوفات الكيميائية عن المركبات الفعالة الموجودة في المستخلصات الخام لكل من الجذور والاوراق و الثمار لنبات الكبار, وهي عبارة عن نواتج ايضية ثانوية للنبات , وجود كل من التانينات والكلايكوسيدات والصابونيات والفلافونات والراتنجات والكومارين والقلويدات والفينولات, وكما موضحة في الجدول / 1 , حيث تم التأكد من وجود مركبات كيميائية فعالة في مستخلصات جذور واوراق وثمار نبات الكبار، مثل التانينات والكلايكوسيدات والفينولات الموجودة في جميع المستخلصات، في حين وجدت القلويدات والفلافونات و الصابونيات والراتنجات بمعدلات أقل , بينما مادة الكومارين وجدت في مستخلص الورقة الكحولي البارد فقط , في أس هيدروجيني تراوح مابين 5,0 و 6,2، ان سبب التباين في درجة ذوبان المواد اعلاه هوالعامل الحراري فضلا في درجة ذوبان المواد اعلاه هو العامل الحراري فضلا عن نوعية المذيب العضوي , (18) .

جدول -1 : الكشف عن المركبات الكيميائية الفعالة في المستخلصات النباتية لنبات الكبار

المركبات الكيميائية الفعالة	مستخلص الجذر				مستخلص الورقة				مستخلص الثمرة			
	مائي		كحولي		مائي		كحولي		مائي		كحولي	
	حار	بارد	حار	بارد	حار	بارد	حار	بارد	حار	بارد	حار	بارد
التانينات	+	+	+	+	+	+	+	+	+	+	+	+
الكلايكوسيدات	+	+	+	+	+	+	+	+	+	+	+	+
الصابونيات	+	+	+	-	+	+	-	-	+	+	-	-
الفلافونات	+	+	+	-	+	+	+	-	+	+	+	-
الراتنجات	-	-	+	-	-	-	+	-	-	+	+	-
الكومارين	-	-	-	-	-	-	-	+	-	-	-	-
القلويدات	+	+	+	+	+	+	+	-	+	+	+	+
الفينولات	+	+	+	+	+	+	+	+	+	+	+	+
pH	5,4	5,0	5,6	6,1	5,0	6,2	5,5	5,3	6,0	6,0	5,7	5,3

حساسية البكتريا للمضادات الحياتية تم اختبار حساسية العزلات البكترية المستخدمة في هذه الدراسة تجاه عشرة انواع من المضادات الحياتية شائعة الاستعمال ,

حيث تم تحديد المقاومة للمضادات الحياتية اعتمادا على قياس قطر منطقة تثبيط النمو البكتيري وذلك وفقا للقياسات العالمية (19), الجدول / 2 يوضح ذلك :

جدول- 2 : مقاومة عزلات البكتريا قيد الدراسة للمضادات الحياتية

Escherichia coli	*Klebsilla sp.*	*Staphylococuus aureus*	*Pseudomonas aeruginosa*	اسم المضاد الحيوي
R	R	R	R	Amoxicillin
R	R	R	R	Carbenicillin
R	R	R	R	Gentamicin
R	S	R	R	Cephalthin
R	R	R	S	Erythromycin
R	R	S	R	Vancomycin
R	S	R	S	Cefoxin
R	S	S	S	Aztreonam
R	S	S	S	Ciprofloxacin
S	S	S	S	Imipenean
% 10	% 50	% 40	% 50	نسبة الحساسية
% 90	% 50	% 60	% 50	نسبة المقاومة

عزلة بكتيرية مقاومة للمضاد الحياتي : R , عزلة بكتيرية حساسة للمضاد الحياتي : S

تأثير المستخلصات النباتية في نمو البكتريا و الخمائر قيد الدراسة :

تم اختبار تأثير تراكيز متدرجة من المستخلصات النباتية التي تم الحصول عليها في هذه الدراسة على نمو عزلات بكتيرية والخميرة . وقد بينت النتائج وجود تأثير متباين لكل من المستخلصات الحارة والباردة للجذور والاوراق والثما ر لنبات الكبارفي نموالبكتريا والخميرة.

أظهرت النتائج أن المستخلصات المائية و الكحولية الباردة لجميع اجزاء النبات وضمن التراكيز (500 و250 و125 و62,5 و31,25) ملغرام /مل لايوجد لها تأثير لفعالية مؤثرة مضادة للعزلات قيد الدراسة, وهذه النتيجة تتفق مع ماذكره (20 و 21) بكفاءة المستخلصات الحارة الكحولية بكفاءة المستخلصات الحارة الكحولية مقارنة مع المستخلصات الباردة منها , كذلك تتفق مع ماذكره (22) بكفاءة المستخلص المائي الحار مقارنة بتأثير المستخلص المائي البارد . الجداول / 3 و 4 و 5 و 6 و 7 توضح تأثير المستخلصات الحارة لاجزاء النبات على نمو عزلات الكائنات المجهرية قيد الدراسة .

المستخلص المائي الحار للجذر , سجلت له فعالية تثبيطية واضحة على نمو العزلات قيد الدراسة مقارنة مع تأثير المستخلص الكحولي الحار للجذر , عدا في تأثيرهما على نمو الخميرة فقد كانت النتيجة متغايرة .

مستخلصات المائية الحارة للورقة كان لها تأثير مماثل كما في حالة الجذر ذات فعالية تثبيطية اكبر (عدا تأثيرها على الخميرة فقد كانت النتيجة متعاكسة) , مما هي للمستخلص الكحولي الحار للورقة والتي كانت تساوي صفرا في حالة بكتريا *Escherichia coli* و *Klebsiella* sp. بينما كانت جيدة ضد بكتريا *Staphylococuus aureus* وبكتريا *Pseudomonas aeruginosa* وضعيفة تجاه الخميرة .اما المستخلص المائي الحار للثمرة فقد كان عديم التأثيرعلى نمو العزلات قيد

الدراسة, بينما تأثير المستخلص الكحولي الحار للثمرة كان يتصف بالكفاءة في جميع الاختبارات وبدرجة أقل قليلا في حالة تأثيره على نمو الخميرة .

جدول - 3 : تأثير التراكيز المتدرجة لمستخلصات المائية والكحولية الحارة لاجزاء النبات على بكتريا *Staphylococuus aureus*

نوع المستخلص	تراكيز المستخلصات (ميلغرام / مل)				
	500	250	125	62,5	31,25
المستخلص المائي للجذر	*38	*31,5	*24,5	*16	-
المستخلص الكحولي للجذر	21	-	-	-	-
المستخلص المائي للورقة	39	31	24	16	-
المستخلص الكحولي للورقة	39	31	25,5	14	-
المستخلص المائي للثمرة	-	-	-	-	-
المستخلص الكحولي للثمرة	39,5	32	24	14	-

* قطر منطقة تثبيط نمو العزلات البكتيرية قيد الدراسة (ملم) .

جدول- 4 : تأثير التراكيز المتدرجة لمستخلصات المائية والكحولية الحارة لاجزاء النبات على بكتريا *Escherichia coli*

نوع المستخلص	تراكيز المستخلصات ميلغرام / مل				
	500	250	125	62,5	31,25
المستخلص المائي للجذر	* 29,5	* 21,5	* 14,5	-	-
المستخلص الكحولي للجذر	19	15	-	-	-
المستخلص المائي للورقة	22,5	18	14	-	-
المستخلص الكحولي للورقة	-	-	-	-	-
المستخلص المائي للثمرة	-	-	-	-	-
المستخلص الكحولي للثمرة	22,5	17,5	11,5	-	-

* قطر منطقة تثبيط نمو العزلات البكتيرية قيد الدراسة (ملم).

جدول - 5 : تأثيرالتراكيز المتدرجة لمستخلصات المائية والكحولية الحارة لاجزاء النبات على بكتريا

Klebsiella sp.

نوع المستخلص	تراكيز المستخلصات ميلغرام/مل				
	500	250	125	62,5	31,25
المستخلص المائي للجذر	* 26	* 19	* 15	-	-
المستخلص الكحولي للجذر	16	-	-	-	-
المستخلص المائي للورقة	25,5	20,5	16,5	-	-
المستخلص الكحولي للورقة	-	-	-	-	-
المستخلص المائي للثمرة	-	-	-	-	-
المستخلص الكحولي للثمرة	37	29,5	25	16,5	11

* قطر منطقة تثبيط نمو العزلات البكتيرية قيد الدراسة (ملم) .

جدول- 6 : تأثير التراكيز المتدرجة لمستخلصات المائية والكحولية الحارة لاجزاء النبات على بكتريا *Pseudomonas aeruginosa*

نوع المستخلص	تراكيز المستخلصات ميلغرام/مل				
	500	250	125	62,5	31,25
المستخلص المائي للجذر	* 39,5	* 29,5	* 24,5	* 13	-
المستخلص الكحولي للجذر	23	16,5	12,5	-	-
المستخلص المائي للورقة	36	30,5	26	16	-
المستخلص الكحولي للورقة	17,5	14	10,5	-	-
المستخلص المائي للثمرة	-	-	-	-	-
المستخلص الكحولي للثمرة	38	32,5	23	16,5	-

* قطر منطقة تثبيط نمو العزلات البكتيرية قيد الدراسة (ملم) .

جدول -7 : تأثير التراكيز المتدرجة لمستخلصات المائية والكحولية الحارة لاجزاء النبات على الخميرة *Candida albicans*

نوع المستخلص	تراكيز المستخلصات ميلغرام/مل				
	500	250	125	62,5	31,25
المستخلص المائي للجذر	* 33,5	* 21,5	-	-	-
المستخلص الكحولي للجذر	30,5	21	15,5	-	-
المستخلص المائي للورقة	15,5	12	-	-	-
المستخلص الكحولي للورقة	16	-	-	-	-
المستخلص المائي للثمرة	-	-	-	-	-
المستخلص الكحولي للثمرة	21	11,5	-	-	-

* قطر منطقة تثبيط نمو العزلات البكتيرية قيد الدراسة (ملم) .

من مقارنة تأثير المستخلصات المختلفة لجذر واوراق وثمار نبات الكبار , يتضح أن أفضل مستخلص هو المائي الحار للجذر , لما له من تأثير واسع تجاه العزلات البكتيرية قيد الدراسة , فقد أثر على جميع العزلات البكتيرية والتي كان لبعضها مقاومة ملحوظة لبعض المضادات الحياتية . وهذا دليل على امتلاك المستخلص فعالية حيوية تجاه العوامل المرضية من خلال تثبيط نموها, وتعزى هذه الفعالية الى وجود المركبات الكيميائية الفعالة التي يحتويها.
يليه في كفاءة الفعالية التثبيطية ,مستخلص الاوراق الذي لايقل اهمية عن مستخلص الجذر لامتلاكه الكثير من المركبات الفعالة ذات التأثير الواسع تجاه الكائنات المجهرية والذي تقارب نتائجه مع ما وجد من نتائج مستخلص الجذر , و المستخلص المائي الحار للثمرة لم يأثر على جميع العزلات قيد الدراسة في حين المستخلص الكحولي الحار للثمرة كان مؤثرا بشكل جيد جدا (تراوحت اقطار مناطق تثبيط النمو ما بين 21,0 - 39,5 ملم) . علما بأن لهذه المركبات الفعالة تأثير ايجابي عند استخدامها للسيطرة على الامراض البكتيرية والفطرية التي تصيب كل من الانسان والحيوان , (18 و 23 و 24) .
كما أن تأثير التانينات يكون في تثبيط عمل الانزيمات الناقلة الموجودة في غشاء الخلية (25) والفينولات لها القدرة على تكوين معقدات مع Sulphhydryl groups فتسبب بذلك خللا في وظيفة جدار الخلية (26), اما القلويدات فتمتاز بالقدرة على اختراق الخلية البكتيرية والتداخل مع الحامض النووي DNA (25) في حين تأثير الصابونيات يكون في تخفيض تركيز السكر داخل الخلية البكتيرية فتؤدي الى

موتها , كما هو الحال مع تأثير الكلايكوسيدات, لكن تأثير الاخيرة يكون أقل مما هو للصابونيات (27) .

التأثير التآزري للمستخلصات قيد الدراسة على نمو العزلات البكتيرية والخميرة :

أن التأثير التآزري لمستخلصات المائية الحارة من الجذر والثمرة (اجزاء نباتية هوائية و ترابية) كانت عديمة التأثير في جميع حالات الاختبار, بينما المستخلصات الكحولية الحارة من نفس المصادر كان لها تأثير متباين ما بين عديم التأثير الى تأثير ضعيف أو تأثير جيد كما في حالة بكتريا *Pseudomonas aeruginosa* .

اما التأثير التآزري للمستخلصات المائية الحارة للجذر مع الورقة (اجزاء نباتية هوائية وترابية) فقد كانت كفاؤتها أفضل من الحالات السابقة , و كانت ما بين ضعيفة الى جيدة جدا تجاه بكتريا *Pseudomonas aeruginosa* وخميرة *Candida albicans* , في حين التأثير التآزري للمستخلص الكحولي الحار من الجذر و الورقة قد تميز بحالة أفضل في تأثيرها على نمو العزلات قيد الدراسة , وقد تراوح تأثيرها ما بين ضعيف تجاه الخميرة وجيد جدا تجاه العزلات البكتيرية (جدول / 8) .

أن سبب التباين في التأثير على نمو العزلات المدروسة يعود الى اختلاف المركبات الكيميائية الفعالة في قابليتها على الذوبان في المذيبات المستخدمة وتأثير العامل الحراري في ذلك .

جدول-8: تأثيرالتآزري لمستخلصي الجذر والثمرة , والجذر والورقة على نمو العزلات قيد الدراسة:

الكائن المجهري	اجزاء النبات	نوع المستخلص	تراكيز المستخلصات ميلغرام/مل (قياس اقطار مناطق تثبيط النمو بالميلليتر) 500	250	125	62,5	31,25
Staphylococcus aureus	جذر+ثمرة	مائي	-	-	-	-	-
		كحولي	16	-	-	-	-
	جذر+ورقة	مائي	19,5	-	-	-	-
		كحولي	17,5	13	-	-	-
Escherichia coli	جذر+ثمرة	مائي	-	-	-	-	-
		كحولي	-	-	-	-	-
	جذر+ورقة	مائي	21	16	-	-	-
		كحولي	17	14,5	-	-	-
Klebsiella sp.	جذر+ثمرة	مائي	-	-	-	-	-
		كحولي	13,5	-	-	-	-
	جذر+ورقة	مائي	18	14	11	-	-
		كحولي	20,5	15,5	-	-	-
Pseudomonas aeruginosa	جذر+ثمرة	مائي	-	-	-	-	-
		كحولي	19,5	15	-	-	-
	جذر+ورقة	مائي	20	16,5	13	-	-
		كحولي	19,5	14,5	-	-	-
Candida albicans	جذر+ثمرة	مائي	-	-	-	-	-
		كحولي	-	-	-	-	-
	جذر+ورقة	مائي	23,5	16,5	-	-	-
		كحولي	16,5	-	-	-	-

المصادر

1. Nascimento,G.G.F.;Locatelli,J.;Freitas,P.C.;.and Silva,G.L.: Antiba - cterial activity of plant extracts and phytochemical antibiotic resistant bacteria. Brazilian j. of microbial,31:247–56,(2000).
2. WHO(Word Health Organization):Summary of WHO Guideness for Assessment of herbal medicines WHO tech.Ser.Genera.Annex,11:178–184 ,(1993) .
3. Ahmad, I.; Mehmood,Z. and Mohammad, F.: Screning of some Indian Medicinal plant for their antimicrobial properties,J. Ethnopharma - cology , 62:183 – 93 , (1998) .
4. درويش , غزوان خالد حاتم : دراسة كيميائية مقارنة لبعض المركبات الكيميائية المستخلصة والعناصر الغذائية بين نباتي جنسي الاشنان التابعة للعائلة الرمرامية . رسالة ماجستير , كلية العلوم , الجامعة المستنصرية , (2005) .
5. عجينة, صبا جعفر محسن: الفعالية التثبيطية لمستخلصات بعض النباتات في نمو بعض الاحياء المجهرية و كمضادات أكسدة في الانظمة الحيوية و تطبيقه في النظم الغذائية . اطروحة دكتوراه , كلية الزراعة, جامعة بغداد , (2006) .
6. Baur, A.M. and Kirby,W.M.:Antibiotics susceptibility testing by astandarised Single disc method,Am.J.Clin. Pthol.,45:493–96,(1966).
7. Holt,J.G.;Krieg,N.R.& Sneath,P.A.:Bergès Manual of Determinati - ve Bacteriology,9th ed.Edited by Williams & Wilkins,Library of Congress Cataloging, Baltimore,(1994) .
8. Ellis, D.H.: Clinical mycology:The Human Opportunistic Mycosis : Ptizere, NewYork, : 166. (1994) .
9. EL – Fallal, A. A. and EL – Kattan, M. H. : Effect of plant extract on mycelial Growth of some cultivated Mushrooms,Egypt J.microbial.32 (1):41– 48 (1997).
10. الشامي , سامي آغا : دراسة بعض صفات الدوائية و السمية لازهار القيصوم , رسالة ماجستير , كلية الطب البيطري , جامعة بغداد , (1982) .
11. Shihata, I. M. : Pharmacological study of *Anagallis arvensis* , M. D. Vet. Thesis,Cairo university, (1951) .
12. Geisman,T.A.:Chemistry of Flavonoids compounds,Macmillan Co. New York,(1962).
13. Jaffer,H.J.;Mahmod,M.J.;Jawad,A.M.;Naji,A.&Al-Naib,A.:Phytoche mical and biological screening Iraqi plants,Fitoferapis,LLX,299(1983)
14. Fahmy,I.R.:Constituents of plant crude drugs,1st ed. Poul Barbey, Cairo , (1933) .
15. Harborne, J.B: Phytochemical method,Champman & Hall.,London, New york (1973) .
16. الشيخلي, محمد عبد الستار , فريال حسين عبد الجليل و العزاوي, حسين فياض: الكيمياء الحياتية / الجزء العملي كلية العلوم , الجامعة المستنصرية , (1993) .
17. صالح, نجاة صالح : المبادئ الاساسية في الكيمياء التحليلية . وزارة التعليم العالي و البحث العلمي , الجامعة المستنصرية , (1991) .

18.الثويني , آمنة نعمة , العاملي , زينة و السماك , ميثم : دراسة تأثير بعض المستخلصات النباتية في علاج الاصابات الجلدية بخمائر *C.albicans* المعزولة من الحيوانات و الاشخاص العاملين على تربيتها في الزجاج و الحيوانات المختبرية . مجلد 2 عدد 2 , (2005) .

19.NCCLS , (National Commit for Laboratory Standards) , : Methods for dilution antimicrobial susceptibility tests for bacteria that grow acrobically Aroved standard M 7–A5,5th ed. NCCLS, Pansylvania, (2000).

20.Sebastian,P.;Fernandez,Cristina Wasowski,; Leonardo,M.; Losealzo, Renee,E.;Granger;Graham,A.R.; Johnston , Alejandro, C.Paladini and Mariel Marder:Central nervous system depressant action of flavonoid glycosides, European J. of harmacol. , 539,Issue3:168–176,(2006).

21.Suker , D. K. ; AL-Mallak , M.K. and AL-Toma , M.L. : The effect of two therapeutic doses of saponin on organs , Basrah , J. Sci. 18 (2) :51-56 (2000).

22.22 – الربيعي، زيد شاكر ناجي : تأثير المستخلصات المائية و الكحولية لنباتي الحنظل *Citrullus colocynthis* وعنب الذيب *Solanum nigrum* في نمو بعض البكتريا المعزولة من اخماج الحروق , رسالة ماجستير , كلية العلوم،الجامعة المستنصرية، (2008) .

23.Jawad,A.I.; Dhahier,A.B.J. and Hussain,A.M. :Lactones extracted from Iraqi composite. J. Basrah Sci. Res.16 (1) :5 –18 (1985) .

24.Tyler,V.E.;Brady,L.R. & Robberts,J.E.:"Pharmacoghnosy"9th ed. Lea and Febiger, Philadelphia. (1988) .

25.Phillipson,J.D.& Oneill,M.J.:New loads to the treatment of protozoal infections based on natural products molecules , Acta. Pharm. Nord; 1: 131–44(1987)

26.Rhauha,J.P.:The search for biological activity in finish plant extracts containing phenolic compounds. Academic dissertation, Faculty ofScience,Helsinki university,(2001).

27.Hussein, F.T.K.:Medicinal plant in Libya, AL-Fath university arab Encyclopedia Hous, Libya, 1st ed., Libya, (1985).

وتراكيز المستخلص المنتخبة وذلك يعود الى الفعل التثبيطي لعقار MMC لانقسام الخلايا الجسمية لتداخله مع الـ DNA (32) وقد تعزى زيادة الوزن للحيوانات المعاملة بالمستخلص لوجود المواد الفعالة (الفلافونات و الكومارينات و التانينات) والتي سببت زيادة انقسام الخلايا وخاصة الخلايا اللمفاوية الموجودة في الطحال وتكاثرها, أو قد يعود احتواء المستخلص على الأحماض الأمينية التي تساهم في صناعة البروتينات ,وكذلك زيادة الشهية و زيادة عدد كريات الدم الحمراء نتيجة لفعالية خلايا نقي العظم (6).

جدول- 3: تأثير مستخلص السذب على معدلات أوزان الفئران المعاملة به

التركيز ملغم / كغم	الوزن(غم) في اليوم 1 المعدل ± الخطأ القياسي	الوزن(غم) في اليوم 12 المعدل ± الخطأ القياسي
السيطرة السالبة **	AB 0.816 ± 20.92	AB 0.88 ± 22.270
السيطرة الموجبة ***	A 1.27 ± 19.690	A 1.04 ± 20.91
* 58	AB 1.23 ± 20.225	AB 1.13 ± 21.56
* 88	B 1.17 ± 23.87	B 1.32 ± 25.212
* 176	AB 0.79 ± 22.420	AB 0.16 ± 23.93

A و B تدل على المقارنة الإحصائية عمودياً

- الأحرف المتشابهة تدل على عدم وجود فروق معنوية .
- الأحرف المختلفة تدل على وجود فروق معنوية عند مستوى احتمالية < 0.05 .

* حقنت بالمستخلص (0.1) مل لمدة 12 يوماً .

** حقنت بـ PBS (0.1) مل لمدة 12 يوماً.

*** حقنت بـ MMC (0.1) مل في اليوم الأول و حقنت بـ PBS (0.1) مل لمدة 11 يوماً.

-منعت الفئران جميعها في اليومين(4 و 8)قبل نهاية التمنيع بـ (0.2) مل من كريات الدم الحمراء للخروف SRBCs بتركيز 10% في التجويف الصفاقي.

- شرحت المجاميع بعد مرور 12 يوماً .

2- فرط الحساسية العاجل (تفاعل آرثس) وفرط الحساسية الآجل (DTH)

يشير الجدول (4) الى ارتفاع غير معنوي (P> 0.05) في قيم تفاعل آرثس في الفئران الممنعة بمستخلص اوراق نبات السذب عند مقارنتها مع مجاميع السيطرة السالبة والموجبة ماعدا التركيز الثالث (176)ملغم/كغم إذ أظهر فرق معنوي(P< 0.05) عند مقارنته مع السيطرة الموجبة , بينما المعاملة بعقار MMC (السيطرة الموجبة)سبب انخفاض في معامل آرثس مقارنة مع السيطرة السالبة , جدول (3) , وذلك يدل على فعل العقار المثبط للاستجابة المناعية الخلطية وتكوين الاضداد(33).

يعتمد تفاعل آرثس على انتاج الاضداد ,وتكوين الوذمة (Odema) نتيجة لتجمع خلايا الدم المتعددة أشكال النوى PMN ,وذلك بعد مرور 4 ساعات من الحقن(34).

إن الدعم المناعي لنبات السذب أعطى صورة ايجابية لقابليته على تعزيز المناعة النوعية التي قد تعزى إلى المركبات الفعالة التي يحتويها النبات منها الفلافونات, والتانينات، والكومارينات.

جدول – 4 : تأثير مستخلص السذب على معدل فرط الحساسية العاجل في الفئران البيض (بعد 4 ساعات)

التركيز ملغم / كغم	فرط الحساسية العاجل بعد مرور 4 ساعات المعدل ± الخطأ القياسي
السيطرة السالبة	AB 0.016 ± 0.087
السيطرة الموجبة	A 0.143 ± 0.064
58	AB 0.015 ± 0.080
88	AB 0.003 ± 0.102
176	B 0.005 ± 0.114

A و B تدل على المقارنة الإحصائية عمودياً.
- الأحرف المتشابهة تدل على عدم وجود فروق معنوية .
- الأحرف المختلفة تدل على وجود فروق معنوية عند مستوى احتمالية < 0.05 .
- منعت الفئران جميعها في اليومين(4 و 8)قبل نهاية التمنيع بـ (0.2) مل من كريات الدم الحمراء للخروف SRBCs بتركيز 10% في التجويف الصفاقي.
- حقنت الفئران جميعها بـ (0.05) مل من كريات الدم الحمراء للخروف SRBCs بتركيز 10% في راحة قدم الخلفية اليمنى و (0.05) مل من محلول PBS في راحة القدم الخلفية اليسرى. أما بالنسبة لمعدلات قيم فرط الحساسية الآجل DTH (جدول 5) أي بعد مرور (24) ساعة من التحفيز بـ SRBCs , فقد وجد هنالك ارتفاع في قيم DTH بزيادة تركيز المستخلص ,وبدون فروق معنوية ($P > 0.05$) بينها وبين حيوانات السيطرة السالبة, وبفروقٍ معنوية($P < 0.05$) عند المقارنة مع السيطرة الموجبة وخاصة للتركيزين (88 و 176)ملغم /كغم.

إن الانخفاض في قيمة DTH الناتج عن المعاملة بالعقار MMC يؤكد على إن هذا العقار مثبط للمناعة الخلوية, وهو يثبط انقسام الخلايا اللمفاوية التائية نتيجة لتثبيطهُ IL-2 ومنع تكوينهُ (35) , يعد اختبار DTH هو دليل لمعرفة دور مستخلص السذب في تعزيز الاستجابة ضد مستضدات كريات الدم الحمراء للخروف , وبينت النتائج قدرة المستخلص الكحولي لهذا النبات على زيادة DTH المتوافقة مع قيم Arthus ,إذ إن هذا النوع من الاستجابة يعتمد أساسا على الاستجابة المناعية الخلوية التي تعد مهمة في حماية الجسم من الإصابة السرطانية والفيروسية ,إذ تلعب الخلايا اللمفاوية التائية الدور الرئيسي والتي لها القابلية على انتاج الحركيات الخلوية(IFN, ILS), إذ تنظم هذه العوامل فعالية الخلايا الأخرى (36,37), وقد تعود قدرة مستخلص السذب في رفع قيم DTH إلى المواد الفعالة التي يحويها النبات وخاصة الكومارينات ومنها, (bergapten وpsoraline و xanthotoxin) التي لها القدرة على تحفيز انتاج الحركيات الخلوية مثل (IFN-γ) , أو قد يعود لاحتوائه على بعض الفيتامينات(38) .

جدول-5: تأثير مستخلص السذب على معدل فرط الحساسية الآجل في الفئران البيض(بعد24 ساعة)

التركيز ملغم / كغم	فرط الحساسية الآجل بعد مرور 24 ساعة المعدل ± الخطأ القياسي
السيطرة السالبة	AB 0.011 ± 0.080
السيطرة الموجبة	A 0.015 ± 0.068
58	AB 0.02 ± 0.077
88	B 0.006 ± 0.114
176	B 0.008 ± 0.118

A و B تدل على المقارنة الإحصائية عمودياً.
- الأحرف المتشابهة تدل على عدم وجود فروق معنوية.
- الأحرف المختلفة تدل على وجود فروق معنوية عند مستوى احتمالية < 0.05 .
- منعت الفئران جميعها في اليومين (4 و 8)قبل نهاية التمنيع بـ (0.2) مل من كريات الدم الحمراء للخروف SRBCs بتركيز 10% في التجويف الصفاقي للفئران البيض.
- حقنت الفئران جميعها بـ (0.05) مل من كريات الدم الحمراء للخروف SRBCs بتركيز 10% في راحة قدم الخلفية اليمنى و (0.05) مل من محلول PBS في راحة القدم الخلفية اليسرى .

3- تأثير المستخلص الكحولي لأوراق نبات السذب في تفعيل الخلايا البلعمية الصفاقية

ارتفاع معنوي (P <0.05) للنسبة المئوية للخلايا البلعمية المفعلة بالتراكيز الثلاث للمستخلص مقارنة مع السيطرة الموجبة , أما المقارنة مع السيطرة السالبة فكانت الزيادة معنوية (P <0.05) فقط للحيوانات المعاملة بالتركيز (176) ملغم/كغم كما هو موضح في الجدول (6).

إن زيادة فاعلية البلاعم تتناسب مع حجم البلاعم وأشكالها (39) وهذا مايؤكد صحة اعتماد التغاير الشكلي معياراً للتفعيل, وبالتالي قدرة المستخلص على تفعيل الخلايا البلعمية وتحولها من خلايا راقدة إلى خلايا تمتلك القدرة لإبادة الجراثيم (microbecidal)(40). تبين النتائج الموضحة في الجدول (6) قابلية المستخلص الكحولي لنبات السذب على تفعيل الخلايا البلعمية الصفاقية من خلال قابليتها على الالتصاق بالزجاج (41) ,وكبر حجمها والتغاير في شكلها(19), كما ان نقصان نسبة الخلايا المفعلة للحيوانات المعاملة بعقار MMC فأنها متوقعة لأن العقار هو مثبط مناعي وسام للخلايا.

جدول -6: تأثير مستخلص السذب في النسبة المئوية لتفعيل الخلايا البلعمية الصفاقية

التركيز ملغم / كغم	النسبة المئوية للتفعيل المعدل ± الخطأ القياسي
السيطرة السالبة	A 1.66 ± 59.72
السيطرة الموجبة	B 1.04 ± 31.00
58	A 1.14 ± 62.75
88	A 1.60 ± 62.13
176	C 1.39 ± 73.76

A و B و C تدل على المقارنة الإحصائية عمودياً.
- الأحرف المتشابهة تدل على عدم وجود فروق معنوية.

- الأحرف المختلفة تدل على وجود فروق معنوية عند مستوى احتمالية < 0.05

4- تأثير المستخلص الكحولي لأوراق نبات السذب في معامل البلعمة لبلعمة خلايا الخميرة المقتولة بالتسخين

أظهرت النتائج زيادة معنوية ($P < 0.05$) في قيمة معامل البلعمة لمجاميع الفئران المعاملة بالمستخلص الكحولي للسذب مقارنة مع السيطرتين السالبة والموجبة وسجل التركيز (176) ملغم / كغم أعلى نسبة وبفرق معنوي عن التركيزين الآخرين ($P < 0.05$) , أيضا ظهر انخفاض معنوي ($P > 0.05$) في معامل البلعمة للفئران المعاملة بالعقار MMC مقارنة مع السيطرة السالبة , جدول (7) .

تعد عملية البلعمة من الوسائل الدفاعية الأولية واللانوعية للجسم (42) وتتصف الخلايا البلعمية المفعلة بقدرتها على التعرف والارتباط بالخلايا الغريبة وقد وصف Adams و Marino (43) هذا الارتباط بكونه يتم بصورة انتخابية (Selectively) ويكون من الناحية الكمية أكبر مقارنة بالخلايا البلعمية غير المفعلة المعرضة للهدف نفسه , كذلك تتميز الخلايا البلعمية بفاعليتها العالية في عمليات البلعمة. إن الزيادة في قيم معامل البلعمة للفئران المعاملة بالمستخلص الكحولي للسذب يمكن ان يعزى الى زيادة افراز الحركيات الخلوية Cytokines ومنها IL-1 و TNF وذلك بسبب زيادة تحفيز التعبير الجيني المسؤول عن افراز هذه الحركيات من الخلايا البلعمية (44) وقد جاءت هذه النتائج لتؤيد نتائج اختبار تفعيل الخلايا البلعمة .

جدول -7: تأثيرالتمنيع بمستخلص أوراق نبات السذب في بلعمة خلايا الخميرة المقتولة بالتسخين.

التركيز ملغم / كغم	النسبة المئوية لمعامل البلعمة المعدل ± الخطأ القياسي
السيطرة السالبة	A 1.57 ± 44.33
السيطرة الموجبة	B 0.82 ± 24.53
58	C 2.09 ± 52.54
88	C 1.29 ± 55.42
176	D 1.28 ± 66.46

- A و B وCو D تدل على المقارنة الإحصائية عمودياً
- الأحرف المتشابهة تدل على عدم وجود فروق معنوية .
- الأحرف المختلفة تدل على وجود فروق معنوية عند مستوى احتمالية < 0.05 .

5- تأثير التمنيع بالمستخلص الكحولي لأوراق نبات السذب في معدل عيارية الأضداد

يبين الجدول (8) معدلات عيارية الاجسام المضادة في مصول الفئران المعاملة بمستخلص اوراق نبات السذب والممنعة في اليوم 4 و8 من برنامج التمنيع بخلايا الدم الحمراء للخروف , إذ إرتفعت معدلات عيارية الاجسام المضادة في مصول الفئران المعاملة بالمستخلص مقارنة مع السيطرة وبدون فروق معنوية ($P > 0.05$) وكان أعلى معدل لعيارية الاجسام المضادة بتركيز (176) ملغم / كغم وهذا دلالة على حصول استجابة مناعية خلطية معتمدة على الخلايا اللمفاوية البائية التي ازدادت عند هذا التركيز, وبالتالي زيادة تفعيل هذه الخلايا وانقسامها وتمايزها إلى خلايا بلازما منتجة للأجسام المضادة (45)وإن معظم الاختبارات المصلية تكشف عن تكوين أجسام مضادة عند (12-14) يوماً من التمنيع (17,46) , لذا اعتمدت فترة 12 يوماً في الدراسة الحالية .

جدول -8: تأثير مستخلص السذب في معدل عيارية الأضداد

التركيز ملغم / كغم	فحص تثبيت المتمم * المعدل ± الخطأ القياسي
السيطرة السالبة	A 304.10 ± 554.7
السيطرة الموجبة	A 228.9 ± 1024.0
58	A 262.34 ± 896.0
88	A 133.90 ± 405.3
176	A 339.7 ± 1322.7

A و B تدل على المقارنة الإحصائية عمودياً
- الأحرف المتشابهة تدل على عدم وجود فروق معنوية
- الأحرف المختلفة تدل على وجود فروق معنوية عند مستوى احتمالية < 0.05 .
* تم القياس بملاحظة (50 %) تحلل دموي .
- منعت الفئران جميعها بـ (0.2) مل من عالق كريات الدم الحمر للخروف (SRBCs) في التجويف الصفاقي في اليومين (4 و 8) قبل نهاية التمنيع .

6- علاقة الاختبارات المناعية فيما بينها:

أظهرت النتائج الموضحة في الجدول (9) ان علاقة فحص الحساسية العاجل مع فحص الحساسية الآجل والتفعيل والبلعمة هي علاقات طردية قوية (0.954 و 0.874 و 0.914) على التوالي, فيما علاقته بـ C.F.T فكانت عكسية ضعيفة (0.002-)وأيضا علاقة DTH مع والتفعيل والبلعمة علاقة طردية قوية بمعامل ارتباط (0.721 و 0.826) على التوالي بينما علاقته معC.F.T فهي طردية ضعيفة (0.034) اما علاقة التفعيل بـ البلعمة فهي (0.972) وهي علاقة طردية قوية أما علاقته بـ المتمم فهي (0.026) طردية ضعيفة وأخيرا علاقة البلعمة بـ المتمم (0.116) وهي علاقة طردية ضعيفة.

جدول -9: معامل الارتباط (r) بين التحريات المختبرية المناعية قيد الدراسة

الأختبارات	فرط الحساسية الآجل	التفعيل	البلعمة	فحص تثبيت المتمم
فرط الحساسية العاجل	*** 0.954	*** 0.874	*** 0.914	* -0.002
فرط الحساسية الأجل		*** 0.721	*** 0.826	* 0.034
التفعيل			*** 0.972	* 0.026
البلعمة				* 0.116

(-) يعني علاقة عكسية .
(+) يعني علاقة طردية .
* 0.0 – 0.3 يعني علاقة ضعيفة .
** 0.4 – 0.6 يعني علاقة متوسطة .
*** 0.7 –0.9 يعني علاقة قوية.
**** 1 يعني علاقة تامة .

مما سبق فإن زيادة معايير الاستجابة المناعية في الدراسة الحالية يعني زيادة قدرة الخلايا المناعية على اداء وظيفتها, وقد يفسر هذا ماتوصل اليه الباحثون في إن مستخلصات نبات السذب تمتلك فعالية مضادة للبكتريا والفطريات(48,47,28).وان المستخلص قام بتحفيز المناعة النوعية وانتاج الاضداد من خلال فحص الحساسية العاجل و المتمم ,كذلك الاستجابة المناعية المتواسطة بالخلايا متمثلة بفحص DTH وأيضا رفع قيم كل من التفعيل والبلعمة للخلايا الصفاقية مما يعني تحفيزالمناعة اللانوعية للجسم , لذلك من الممكن استخدامه كمقومناعي (Immunopotentiating agent)لتنشيط القدرة المناعية في الجسم بعد اجراء دراسات أخرى وبإستخدام تقنيات متقدمة .

المصادر

1. قطب،فوزي طه. النباتات الطبية زراعتها مكوناتها، الدار العربية للكتاب- ليبيا. (1979).
2. الشحات ، نصر أبوزيد. الزيوت الطيارة. الدار العربية للنشر والتوزيع.القاهرة، مصر.(2000).
3. Wagner , H . Leading structures of plant origin for drug development . J. Ethnopharmacol. 38:105-112 . (1993).
4. Wong, C. K.;Lcung, K. N.; Fung, K. P. and Choy,Y.M. Immunomod - ulatory and anti-tumor polysaccharides from medicinal plants. Int .J. Med. Res. 22: 299-312. (1994).
5. Jeffrey, W. H. and Deborah, H. Rue Medicina Antiqua. (1995).
6. AL-Sagiar,O. Expermentaly Challenged Reactivity of the pituitary-adrenal-Hematological Axis After *Ruta chalepensis* Administration J. Applied Res. 4(4):606-609 .(2004)
7. Rethy, B.; Zupko, I.; Minorics, R.; Hohmann, J.; Ocsovszki,I. and Falkay , G. Investigation of cytotoxic activity on human cancer cell lines of arborinine and furano-acridones isolated from *Ruta graveolens*. Planta J.Med.73(1): 41-48. (2007).
8. Pathak,S.;Multani,A.S.;Banerji,P.and Banerji, P. Ruta 6 selectively induces cell death in brain cancer cell but proliferation in normal peripheral blood lymphocytes:Anovel treatment for human brain cancer. International Onco.23(4) :975- 982. (2003).
9. Preethi,K.C.;Kuttan,G.and Kuttan,R. Anti Tumor Activity of *Ruta graveolens* Extract. Asian Specific J.Cancer Prevention.7:439-443. (2006).
10. Harborne,J.B. Phytochemical methods.Science Paper backs,Chapman and Hall. London ,UK. (1973).
11. Cannell,B. How to approach the isolation of natural products,1st ed Human press.inc. (1998).
12. Evans,J.Cytological methods for detecting chemical mutagens. In : Hollaender,A.1st ed.Chemical Mutagens principles & Methods for Their detection Volume Four,Plenum press,New york & London,:5-6. (1976).
13. Harborne,J.B. Phytochemical methods.2nd ed.Chapman and Hall:288. (1984).
14. Geisman,T.A. Chemistry of flavonoids compounds. Macmillan Co. NewYork(1962).

15. Dixon,W.J.Efficient analysis of experimental observation. Ann. Res. Pharmacol-Toxicol.,20:441-462. (1980).
16. Xian-guo, H. and Uersella,M. Anti Fungal Compounds from *Solanum nigrescens*.J. Ethnopharm. 43: 173-177. (1994).
17. AL-Joofy , I. K. Studies on immunogenic properties of *Rhizobium* polysaccharide in Balb/c Mice. M.Sc.thesis .Sci. College of AL-Mustansiriyah Uni. (1996).
18. Triolo, A.J. Osterholm,J. L. and Krathy ,M. T. Enhancement of the Arthus reaction and suppression of Delayed-type hypersensitivity (DTH) by pluronic F68, edetergent frequently used to prepare perfluoro -carbon emulsions .Int. J . (1989) .
19. Crowle,A.J.and May, M. Ahanging drop macrophage function test. J. Reticuloendothelial Soci. 24(2) :169 -185. (1978).
20. Weber,B.;Nickol,M.M.;Jagger,K.S.and Saelinger, C.B. Interaction of Pseudomonas exoproduct with phagocytosis cells. Can.J. Microbiol. 28:679-685. (1982).
21. Adams,D.C.; Edeloson, P.J. and Koren,H. Methods for studying Mononuclear Phagocytosis. Academic Press. New York. (1981).
22. Fox,W. Advances in tuberculosis research.Serology of tuberculosis and BCG Vaccination. Karger company(1984).
23. Al-Mohammed,N.T.;Al-Rawi,K.M.; Younis, M. A. and Al-Morani, W. K. Principle of statistics. Al-Mousl Uni. (1986).
24. الذهيبة،عمار حقي سلمان. دراسة دوائية وسمية لنباتي السذب والسدر وفعلهما المضاد للاسكريديا كالي *Ascaridia galli* في الزجاج .رسالة ماجستير-كلية الطب البيطري-جامعة بغداد. (1997).
25. أحمد،سمراء عبدالهادي.دراسة تأثير مستخلص نبات السذب *Ruta chalepensis* على الانقسام الخلوي،رسالة ماجستير، كلية العلوم/الجامعة المستنصرية. (2008).
26. قطب،فوزي طه. النباتات الطبية وزراعتها ومكوناتها.دار المريخ للنشر, الرياض(1981).
27. هيكل، محمد السيد وعبدالله عبدالرزاق عمر. النباتات الطبية والعطرية، كيمياؤها، انتاجها، فوائدها. الطبعةالثانية .منشأة المعارف الاسكندرية(1993).
28. Ratheesh, M. and Helen, A. Anti-inflammatory activity of *Ruta graveolens* Linn on carrageenan induced paw edema in wistar male rats.African. J. Biotech. 6(10): 1209-1211. (2007).
29. الشحات،نصر أبوزيد. النباتات والأعشاب الطبية. دار البحار-بيروت(1986).
30. Pronczuk,J. Rutaceae.WWW.IPCS. org. (1989).
31. Francis,G.;Kerem,Z.; Makkar, H. P. S. and Backer, K. The biological action of saponins in animal system. Areview British. J. Nutration. 88: 587-605. (2002).
32. Perticone,P.;Cozzi,R.and Gustarino,B. Sister chromatid exchange induced by DNA demthylating agent persist through several cell cycle in mammalian cells.Carcinogenesis.8(8):1059-1063. (1987).
33. Cuppes,T.R.;Edgar,L.C.;Thomas,C.A&Fauci,A.S.Multiple Mechanisms of B-cell immunoregulation in man after administration of *In vivo* corticosteroids. J . immunol. 132(1) :170-175. (1984).

34.Roitt, I.M. Essential Immunology. Black well Scientific publication . Oxford. London. Edinburgh Boston Paloalto Melbourne(1984) .

35.Kelso,A.and Munk,A. Glucocorticoid inhibition of lymphokine secretion by alloreactive T-lymphocyte clonse.J.Immunol.133(2):784-791. (1980).

36.Schleimer,R.P.;Jacoues,A.;Shin,H.S.;Lichtenstein,L.M. and Plaut, M. Inhibition of T cell-mediated cytotoxicity by antiinflamatory steroids. J. Immunol. 132(1) : 266-271. (1984).

37.Stites,D.P.;Terr,A.I.and Parslow,T.G.Medical Immunology.9th ed.Prentic -Hull International Inc.London.PP:190- 191. (1997).

38.Raghav,S.K.;Gupta,B.;Shrivastava,A.;Das,H.R.Inhibition of lipopolysa -ccharide -inducible nitric oxide synthase and IL-1β Through Suppression of NF-Kβ activation by3 (1-1-dimethyl-allyl)- 6-hydroxy-7-methoxy- Coumarin isolated from Ruta graveolens L. European J. Pharmacol. 560: 69 - 80. (2007).

39.Bernaudin,J.F.;Hamauchi,K.;Wewers,M.D.;Tocci,M.J.;Ferrans,V.J.& Crystal , R.G. Regulation of cell volum and amount of mRNA IL-1 synthesis in LPS activated macrophage,J.Immunol.140:3822-3829 (1988).

40.Green,S.T.;Meltzer,M.S.;Hibbs,J.J.B. and Nacy,C.A. Macrophages activated by interferon -γ destroy intracellular Leishmania major amastigotes by an larginine dependent killing mechanism. J. Immunoph -armacol. 9(3): 157. (1989).

41.Krahenbuhi,J. and Remington.J. The role of activated macrophages in specific and non specific cytostasis of tumor cells. J. Immunol. 113: 507-516. (1974).

42.Claman,H. N. Glucocorticosteroids: Anti-inflamatory mechanisms. Hosp pract. 18: 123-134. (1983).

43.Adams,D. O. and Marino , Ph. A . Evidence for amultistep mechanism of cytolysis by BCG- activated macrophages: The interrelationship between the capacity for cytolysis , target binding and secretion of cytolytic factor . Immunol. 126 (3) : 981- 987. (1981) .

44. Freudenberg,M.A.;Keppler,D.and Galanos,C. Requirement for lipopolysaccharide responsive macrophages in galactosaine induced sensitivity to endotoxin .Infect. Immuno. 51:891. (1986).

45.Barrett,T.Text Book of Immunology.5th ed. The C.V.Mosby Co(1988).

46.Pier,G.B.and Bennett,S.E. Structural analysis and immuongenicity of *Pseudomonas aeruginosa* immunotype 2 high molecular weight polysaccharide.J. Clin.Invest. 77: 491- 495. (1986).

47.Ojala,T.Biological Screening of Plant Coumarins.2nd ed.:18-21. (2001).

48. Oliva,A.;Meepagala,K.M.;Wedge,D.E.;Harries,D.; Hale,A.L.;Aliotta, G. and duke, S. O. Natural fungicides from *Ruta graveolens L* Leaves including anew quinolone alkaloids.Agric. Food. Chem. 51 (4): 890-896. (2003).

دراسة تأثير بعض المستخلصات النباتات الطبيعة على التغيرات الانزيمية في الحيوانات المختبرية

أقبال فاضل علوان [1]و عصام فاضل الجميلى[2] و عمار مولى حمود و حسين علي محمد[1]و حليمة جابر
[1]وزارة العلوم و التكنولوجيا / دائرة بحوث الكيمياء – الجادرية- بغداد – العراق . ص. ب. 785.
[2]فرع التقنية الاحيائية – معهد الهندسة الوراثية و التقنية الاحيائية للدراسات العليا – جامعة بغداد .

ABSTRACT

Plants contain natural compounds used antioxidants to protect cells from damage , or merger, which echidna during oxidative processes .

The compound of flovonaid Arcata antioxidant compounds have been studies in this research within the installed operating avadavat of oxidative stress and cancer are the seeds of grapes and green tea and pomegranate and the horse tail .

Containing components of the extraction 40mg of acid Ellagic , 100mg of alcoholic to extract the seeds of grapes,100 mg of green tea extract and 10 mg of plant extract to the bottom of the alcohol horses.

Study the impact of three different concentration of the extraction is (0.75, 3.75, 18.75, mg / 0.1 ml) to the effectiveness of liver enzymes (GST, ALP ,GPT, GOT) through the dosage by mouth to laboratory mouse during the period of three weeks .

Results signal that there is no moral difference level ($p< 0.05$) for the concentration of alcohol .Extracts of plants , on the effectiveness of specific liver enzymes it was free of any toxic effects dose used compared to control animals.

الخلاصة

تحتوي النباتات الطبيعية على مركبات مضادة للاكسدة تستخدم لوقاية الخلايا من التلف الذي يصيبها اثناء عمليات الاكسدة .ويعد مركب البولي فينول من المركبات المضادة للأكسدة التي تم دراستها في هذا البحث ضمن المستخلصات الكحولية التي تعمل كمضادات للسرطان و الاكسدة في بذور العنب و الشاي الأخضر و شحم الرمان و ذيل الحصان .

تحتوي مكونات هذه التركيبة على 40 ملغم من المستخلص الكحولي لحامض اللاجيك ، 100 ملغم من مستخلص الكحولي لبذور العنب ، 100 ملغم من مستخلص الكحولي للشاي الأخضر و 10 ملغم من المستخلص الكحولي لنبات ذيل الحصان .

تم دراسة تاثير ثلاثة تراكيز مختلفه من هذه التركيبة و هي (3.75,18.75, 0.75 ملغم /0.1 مليليتر) على فعاليه انزيمات الكبد (**GST,ALP,GPT,GOT**) من خلال التجريع عن طريق الفم للفئران المختبرية خلال فترة 3أسابيع . أشارت النتائج بأنه لا توجد فروقات معنوية بمستوي ($p<0.05$) لتراكيز المستخلصات الكحولية للنباتات على الفعالية النوعية لانزيمات الكبد و تشير على انها خالية من اي تأثيرات سمية بالجرع المستخدمة مقارنة بحيوانات السيطرة .

المقدمة

لقد أزداد اهتمام خبراء الصحة بالوقت الحاضر باستعمال طب الأعشاب بصوره ملحوظة ، وذلك بسبب كونها المصدر الطبى العلاجى الوحيد المتوفر في البلدان النامية أو لأنها أصبحت العلاج الطبى البديل الشائع عن العقاقير المصنعه فى البلدان النامية . و نظرا لأهميه هذه النباتات من الناحيه الطبيه فقد انتشرت زراعتها فى جميع بقاع العالم و تنوع استخدامها (1) .

أجريت العديد من الدراسات لمعرفة التأثيرات السمية للنباتات الطبية المستخدمة في علاج الامراض السرطانية و المركبات الكيميائية و بالجرع التي يتناولها الانسان ، لغرض الكشف عن التأثيرات الجانبية من خلال دراسة تأثيرات المركبات على زيادة او نقصان فعالية إنزيمات الكبد وألآعضاء الرئيسية التي تتم فيها عملية تأيض المركبات الكيميائية (2 ، 3) .

ومن جانب آخر لاحظ Singh و جماعته (4) أن المواد المضادة للآكسدة تؤدي الى استحثاث الزيادة في نشاط انزيم Glutathione-S-Transfers (GST) إذ يعد هذا الانزيم من الانزيمات متعددة الوظائف من خلال أزالة المتأيضات السمية لبعض المسرطنات و المطفرات .

أن الزيادة في فعالية الانزيم يمكن ان تحدث نتيجة لزيادة عمليات التصنيع في الخلية أو كأستجابة لعمليات النمو الحاصلة في الخلية . توجد ثلاث أنزيمات مختلفة و Glutamate pyruvic Transaminase (GPT), Glutamate oxaloacetate Transaminase (GOT), Alkaline phosphates (ALP) تستخدم لقياس او تحديد مدى الضرر الذي يحصل في الخلايا الكبدية و خصوصاً الانزيمين (GPT),(ALP) . اذ يتركز كل من هذين الانزيمين في الخلايا الكبديه(5).

تحتوي النباتات التي تتكون منها المستخلصات الكحولية للنباتات الطبية على مركبات البولي فينول و التي تستخدم لعلاج الأمراض السرطانية و هي مستخلص Oligameric (OPC) Pronthocyanidine لبذور العنب و مستخلص الشاى ألأخضر (Green tea catechins (GTC) و كذلك حامض الاجيك(acid Ellagic) من شحم الرمان بأنها تعطي قدره ضده عملية الأكسدة (2) . وهذه المستخلصات تستخدم لعلاج امراض السرطان أو منع بعض الالتهابات و كذلك امراض الكبد .

الهدف من هذه الدراسة هو معرفة فعالية وقوة المستخلصات الكحولية ضد عملية الأكسدة ودمج خلايا الكبد وذلك من خلال عمل الانزيمات(GOT, GPT, ALP) في الاعضاء الحيوان المختبري بعد تجريع الحيوانات المختبرية بتراكيز مختلفة خلال فترة زمنية و هي ثلاثة أسابيع و كذلك إنزيم GST .

المواد وطرائق العمل

المحاليل المستخدمة

المحلول دارئ الفوسفات الفسلجي – Phosphate Buffer Saline (PBC) , P^H=7.4

إدارة الحيوانات المختبرية :-

استخدم (16) فأر ذكر من نوع Balb بعمر (5- 8) أسابيع بوزن تقريبي (20-25) غم و وزعت عشوائيا الى اربعة مجاميع متساوية منفصلة ووضعت في اقفاص بلاستيكية . تم تغذيتها بالاضافة الى العلف المركز و الماء على تراكيز مختلفة من التوليفة لمستخلصات الكحولية النباتية وهي (0.75 ، 3.75 ، 1.875 ملغم / 0.1 مليليتر) يومياً و لمدة3أسابيع بعدها تم قتل الحيوانات وأخذ الكبد والدم وحفظ لحين اجراء الاختبارات عليه .

الاختبارات الانزيمية : Enzymatic Assays

تحديد مستوى وفعالية انزيمي (GOT, GPT)

تمت دراسة مستوى وفعالية هذين الانزيمين بأخذ كبد الفأر و تقطيعه الى قطع صغيره وهرسه وزنه 3 غم مع حجم معلوم من دارئ الفوسفات الفسيولوجي(3 مل) (PBS) إلى الراسب و يعمل له طرد مركزي (6) و بعد هذه الحالة تم الحصول على المستخلص (راشح الكبد المهروس) و الذي من خلاله تم تحديد فعالية هذين الانزيمين حسب طريقة (Reitman) و جماعته (7) وكما يلي :

تم استخدام انبوبتي اختبار لكل نموذج ، تمثل الاولى العينه الضابطه Reagent blank و الثانية عينة النموذج Sample ويمكن تحضير هذه النماذج كما في الجدول المرفق و يمكن معرفة فعالية هذين الانزيمين في المصل الاستخلاص عن طريق جدول خاص لكل انزيم من هذين الانزيمين وفق الطريقة المذكورة من قبل الشركة المجهزة Rand ox, U.K. .

تحديد مستوى و فعالية انزيم (ALP) :

ان العينه المستخدمة في هذا الاختبار هي المصل (Serum) و الذي تم الحصول عليه بنفس الطريقه عند القيام بتحديد فعالية انزيمي (GPT ، GOT) و لتحديد فعالية انزيم (Alkaline

(ALP) (phosphates، تم اتباع طريقة (Kind& King, 1945) (8) حيث تم استخدام اربعة انابيب اختبار لكل نموذج تمثل الأولى عينة النموذج Sample و الثانية ضابطة النموذج أو المحلول الصوري Sample blank و الثالثة تمثل العينة القياسية Standard واخيراً تمثل الرابعة العينه الضابطه Reagent blank ويمكن تحضير هذه النماذج كما في الجدول المرفق مع العدة ، مزجت جيدا ووضعت الانابيب في مكان مظلم لمدة دقائق ، بعدها يتم قياس الكثافة الضوئية للمحاليل على طول موجي (510nm) باستخدام جهاز المطياف الضوئي .
و تقاس فعالية أنزيم ALP بواسطة المعادلة التالية :

$$\text{الفعالية الإنزيمية (وحدة/ لتر)} = \frac{\text{الامتصاص للعينية النموذج} - \text{الامتصاص المحلول الصوري}}{\text{الامتصاص للعينة القياسية}} \times 142$$

تحضير محلول الدم :
تقتل الحيوانات عن طريق الازاحة العنقية و يأخذ الدم من قلب الفأره و يوضع في أنبوبة أختبار يحتوي على (EDTA) كمادة مانعه التخثر و يمزج الدم مع محلول ملح الطعام (0.9%) و يعمل له عملية فصل بواسطة جهاز الطرد المركزي بسرعة 2000rpm لمدة 10 دقيقة . يترك الراشح ويضاف 1مل من الماء المقطر ثم يمزج جيداً و يحفظ بدرجة -20^{0}م إلى حين استخدامه لقياس أنزيم GST وكذلك لقياس انزيم ALP .

تحديد مستوى و فعالية أنزيم GST:
النموذج المستعمل هو نفس النموذج المحضر والذي أستخدم لقياس كفاءة أنزيم glutathione – S- transfers ، وفق طريقة Francoise et al. (9) .
أن كفاءة انزيم GST تقاس ووفق المعادلة التالية:-

$$\text{GST activity in RBC (u.g}^{-1}\text{ Hb)} = \frac{31.25 \times \Delta A}{\text{Hb (g /d/)}}$$

ΔA : الفرق في الامتصاص

اخضعت نتائج مستويات الانزيمات(ALP, GOT, GPT) الكبد ومصل الدم GST الى تحليل التباين باستخدام برنامج الاحصائي الجاهز SPSS(2001) لمعرفة اصغر فرق معنوي بين معدلات المجاميع تم استخدام تحليل Least Significant difference / LSD عند مستوى احتمالية ($p<0.05$)لمعرفة الفروق المعنوية بين مستويات المعاملات المختلفة .

النتائج و المناقشة

مستوى فعالية أنزيم ALP
يوضح جدول رقم (1) نتائج دراسة أنزيم ALP في محلول مستخلص الكبد لمعرفة تأثيره على الحيوان المختبري باستخدام تراكيز مختلفة من مستخلصات النباتات الطبية خلال مدة التجريع مقارنة مع نماذج السيطرة فوجد بأنه ليس هناك فروقات معنوية ($p<0.08$) لها تأثير على نشاط وفعالية إنزيم ALP عند التراكيز العالية للمستخلصات الكحولية في مستخلص الكبد مما يدل على إنه لا يوجد تأثير سمي للنباتات الطبية الدوائية على الانسان عند استخدامها لعلاج الامراض السرطانية وذلك بان هذه المستخلصات للنباتات تحتوي على مواد فينولية والعديد من الفيتامينات(A,E,C) وكل هذه المواد تظهر فعالية مضاده للتطفير . تتغير فعالية الانزيم بتغاير درجة الحرارة وقيمة الرقم الهدروجيني p^H، وكذلك تركيز المادة الاساس مع وجود المواد المنشطة أو المثبطة في وسط التفاعل(13) ومن الإنزيمات المستخدمة في هذه الدراسة ALP،GOT،GPT أن أنزيم ALP واسع الانتشار في مناطق مختلفة من الجسم مثل الامعاء و نخاع العظم والكبد و الكلية ولكن بتراكيز مختلفة و قليله مقارنة بالانزيمات الاخرى (10).

جدول – 1:تأثير المستخلص الكحولي للنباتات الطبية على فعالية أنزيم ALP في الحيوانات المختبرية لمدة 3 أسابيع .

	الفعالية النوعية (وحدة /لتر)	الفعالية النوعية (وحدة / لتر)	الفعالية النوعية (وحدة /لتر)
تراكيز المعاملة ملغم0.1/مليليتر	/ ALPالكبد	/ALPالكلية	**/ALPالدم**
السيطرة ماء مقطر0.1 / مليليتر	63.62 ± 0.11[a]	168.2 ± 0.08[b]	44.2 ± 0.03[a]
0.75ملغم0.1/مليليتر	63.63 ± 0.08[a]	168.28 ± 0.05[b]	44.1 ± 0.09[a]
3.75ملغم0.1/مليليتر	63.69 ± 0.05[a]	168.32 ± 0.04[b]	44.3 ± 0.09[a]
/18.75ملغم0.1/ مليليتر	63.67 ± 0.09[a]	168.43 ± 0.05[b]	44.39 ± 0.05[a]

الحروف المتشابه تعني عدم وجود مستوي معنوي

مستوى فعالية أنزيم GOT, GPT

ان انزيم GPT يتواجد بنسب عالية في الكبد أكثر من بقية الانزيمات و يعتبر كمقياس لمعرفة مدى تضرر الخلايا الكبدية . اما أنزيم GOT يتضح بان نسبته تتذبذب بين الارتفاع و الانخفاض علماً بان هناك بعض الامراض المؤدية الى رفع او خفض نسبة انزيمات الكبد عن القيمة الطبيعية لها و علاقة دور هذه النباتات في خفض نسبة الانزيمات عند ارتفاعها أو رفع نسبتها عند انخفاضها و ذلك للاحتوائها على مركبات بولي فينول .

يلاحظ في الجدول (2) بان فعالية الإنزيمات GOT,GPT لم تسجل اية فروقات معنوية ($P<0.05$) بالمقارنة مع السيطرة الموجبة خلال فترة تجريع المستخلص الكحولي للنباتات الدوائية بالتراكيز المختلفة و خلال فترة الدراسة . لذا يمكن الاستنتاج بان النباتات الدوائية ليس لها تأثير على انزيمات الكبد قيد الدراسة . وهذه النتائج جاءت مطابقة لما ورد في كل من (11, 12).

جدول-2 : تأثير التراكيزالمختلفة لمستخلصات الكحولية للنباتات الطبية على فعالية الانزيمي GOT, GPT في حيوانات المختبرية لمدة 3 أسابيع .

	الفعالية النوعية (وحدة / لتر)	الفعالية النوعية (وحدة / لتر)	الفعالية النوعية (وحدة / لتر)	الفعالية النوعية (وحدة / لتر)
تراكيز المعاملة ملغم0.1/مليليتر	GPT الكبد/	GPTالدم /	GOT الكبد /	GOT الدم /
السيطرة الماء المقطر	152.4 ± 0.11^{a}	84.8 ± 0.05^{a}	70.15 ± 0.04^{a}	57.15 ± 0.05^{b}
0.75ملغم0.1/ مليليتر	152.61 ± 0.08^{a}	84.82 ± 0.05^{a}	70.59 ± 0.04^{a}	57.17 ± 0.00^{b}
3.75ملغم0.1/مليليتر	152.60 ± 0.08^{a}	84.82 ± 0.04^{a}	70.46 ± 0.06^{a}	57.18 ± 0.13^{b}
18.75ملغم0.1/مليليتر	152.6 ± 0.04^{a}	84.82 ± 0.06^{a}	70.34 ± 0.05^{a}	57.17 ± 0.12^{b}

الحروف المتشابه تعني عدم وجود مستوي معنوي

اما الجدول (3) فيبين تقدير فعالية إنزيم GST في مصل دم الحيوانات المختبرية ويتضح من النتائج بانه لا توجد فروقات معنوية للانزيم GST في مصل دم الحيوانات التي تم معاملتها مع تراكيز مختلفة من المستخلص الكحولي للنباتات الدوائية مقارنة مع السيطرة الموجبة ($p<0.01$) ، يتضح من النتائج اعلاه بان المستخلصات الكحولية للنباتات الطبية لها القابلية على تعزيز قوة المادة المزيلة للأكسدة تقلل أو تحول عدم حدوث سرطان بواسطة تحفيز مختلف فعالية الإشكال المتساوية من أنزيم كليتوثايونين -S- الانتقالي في جميع حالات سرطان الكبد . هناك العديد من البحوث و التقارير تحتوي على تأثير أنواع مختلفة من أمراض السرطان منها سرطان المريء و العصارات المعوية أي سرطان المعدة و تأثير على (1) فعالية أنزيم GST و(2) يحافظ على توازن معدل وجود أنزيم GST و(3) لمحافظة على محتويات أو مكونات أنزيم GST .

جدول -3 : تأثير معاملة مستخلص الكحولي للنباتات الطبية على أنزيم GST في الحيوانات المختبرية لمدة 3 أسابيع .

معاملة / الانزيم	السيطرة ماء مقطر	0.1مليليتر/0.75ملغم	0.1مليليتر/3.75ملغم	0.1مليليتر/ 18.75ملغم
لتر / وحدة GST	0.97 ± 0.005^{a}	0.971 ± 0.003^{a}	0.972 ± 0.009^{a}	0.972 ± 0.01^{a}

الحروف المتشابه تعني عدم وجود مستوي معنوي

يتضح من نتائج الدراسه بانه لا توجد فروقات معنوية لتراكيز المستخلصات الكحولية للنباتات الدوائية مما يدل بأنها خالية من التأثيرات السميه بالجرع المستخدمه و هذا ما أستنبط من نتائج لمعاملة كل من أنزيم ALP وكذلك إنزيمي GOT, GPT في مستخلص الكبد ، و أنزيم GST في مصل دم الحيوان.

المصادر

1. Tyler, V.E., Bradley, L. R. and Robbers, J.E. pharmacognsoy, 192d. Lea and Feigner: 4-5 (1998).
2. Gentler E. The role of antioxidants in the prevention of tumors. Brazils leek lusty ; 96 : 199- 209. (1999).
3. Kavaratskhella, M.,Winkles, C., Naldrett, M.T., et al.,; A Novel high activity cationic ascorbate peroxides from tea (camellia sine sis) – a Class 111 peroxides with unusual substrate specificity J of plant physiology ; 154: 273-282 (2004) .
4. Singh, S.v.; Creadon , G. ; Das, M.; Mukhtar, H. and Awasthi, Y.C. (1987)Glutathione- S-transferases of mouse lung selective binding of benzo (a) pyrene metabolites by the subunit which are preferentially by t-butylated hydroxyanisole . Biochem. J., 243, 351-358(1987), .
5. Boyd, J.W.Serum enzyme in the diagnosis of disease in man and animals , J. Comp. path. 98 : 381-400(1988) .
6. Morton , K. ; The purification of alkaline phosphates of animal tissues, J. Bio .chem., 57: 595- 603 (1954) .
7. Reitaman,S. & Franker,S.,:A colorimetric method for the determination of serum glutamic oxaloacetatic and glutamic pyruvic transaminases Amer. J. Clin. Path.18: 6b(1975) .
8. Kind,R.R. and King,E.G.; A colorimetric method for the determination of serum alkaline phosphates, J.Clin. path. 7; 322-326(1954).
9. Francoise, C., Pierre, M. Jacqueline, R. and Henri,J., chemical clinical, Acta ; 209-217(1989).
10. Tenneco,K.H.,Arundathits,S.J.,Asovriya,P.K. and Karunamayake,E.H . Possible hepatoxicity of Nigella sativa seedsand Dredeavolubleleave,J. Ethno, 31: 283-289(2003).
11. Khan,B.A.,Abraham,A. & Leclanma,S.Hematological & histological studies after curry leaf (Murray a Koenig I) & mustered (Brasses jounce) feeding in rats , Indian, J. Med. Res., 102: 184-186 (2003) .
12. Paula, D.C.F. and Andreas, K., Combined used of serum enzyme levels as tumor marker in cervical carcinoma patients Tumor Biol. 15, 9, 1773-78(2005).
13. Berg Meyer, H.U.;methods of enzymatic analysis,V- 111,3rd Edit, Verlag Chemises, Weinhein. Cited by Boyd, JW(1988).

تأثير المستخلصات الخام لثمار تمر الزهدي في تثبيط نمو بعض خطوط الخلايا السرطانية في الزجاج وفي علاج سرطان الغدة اللبنية المغروس في الفئران البيض

ياسر الجريصي[1] و ناهي يوسف ياسين [2] وبدري العاني[3]
1 - في قسم علوم الحياة/ كلية العلوم/ الجامعة المستنصرية
2- مدير عام المركز العراقي لبحوث السرطان والوراثة الطبية
3- قسم علوم الحياة/ كلية العلوم / جامعة بغداد

ABSTRACT

The present investigation represents a preliminary study of the effect of crude extracts of date palm fruits (*Phoenix dactylifera* L. cv. Zahdi) on two malignant cell lines (human laryngeal carcinoma-Hep2 and murine mammary adenocarcinoma-AMN3) and one normal cell line (rat embryo fibroblast-REF). The study also includes evaluation of the effect of these extracts on several cytogenetic parameters such as mitotic index (MI%), blast index (BI%) and chromosomal aberrations (CA) after *in vitro* culture of peripheral blood lymphocytes. This work also includes a study of the therapeutic potential of one of these extracts in the treatment of transplanted murine mammary adenocarcinoma in mice.

The *in vitro* cell growth assay showed that there was time- and concentration-dependent cytotoxic effects of crude extracts of date palm fruits on Hep2 and AMN3 cell lines. The highest significant effect of these extracts was achieved after 72 hrs of exposure with the highest concentration (10000 µg/ml). Aqueous extract of fruits (AF) caused growth inhibition percentage 76.3% , 84.1% for Hep2 and AMN3 respectively. However, 72 hrs exposure to AF at concentration of 10000 µg/ml caused slight inhibitory effect on REF cell line, reaching 21.1%.

On the other hand, the crude extracts of fruits caused significant reduction in the mitotic index and blast index of peripheral human lymphocytes, but without any structural or numerical chromosomal aberrations. Also these extracts neither replaced phytohemagglutinin (PHA) as mitogenic agent, nor colcemide as mitotic arresting agent at metaphase.

The therapeutic doses of AF were determined according to LD50 in mice. The results indicated high effectiveness of this extract in a dose- and time-dependent manner. The highest therapeutic doses of AF (1.2 gm/kg B.wt.) showed the best therapeutic effect by reducing the tumor volume in mice to about 73.9%.

The comparison of relative tumor volumes of different groups revealed highly significant differences among all treated groups and those of untreated (control) group.

الخلاصة

يمثل هذا البحث دراسة أولية لتقييم تأثير المستخلصات الخام لثمار نخيل التمر صنف الزهدي *Phoenix dactylifera* L. cv. Zahdi في اثنين من الخطوط الخلوية السرطانية ، هما خط خلايا سرطان الحنجرة البشري (Hep-2) وخط خلايا سرطان الغدة اللبنية الفأري (AMN3) ، وفي الخط الخلوي الطبيعي لجنين الجرذ (REF)، وتقييم تأثير هذه المستخلصات في مزارع خلايا الدم المحيطي البشري في الزجاج (*in vitro*) بوساطة حساب معامل التحول الأرومي Blast index (BI%) ومعامل الانقسام الخيطي Mitotic index (MI%) ، ودراسة حالات الزيغ الكروموسومي Chromosomal aberration (CA) . وتضمنت دراسة الفعالية العلاجية لأحد هذه المستخلصات في الفئران المختبرية الحاملة لسرطان الغدة اللبنية Mammary adenocarcinoma .

كان التأثير السمّي للمستخلصات الخام في كلا خطي الخلايا السرطانية Hep-2 و AMN3 في الزجاج (*in vitro*) معتمداً على التركيز المستخدم منها ومدة التعرض لها ، وكان التأثير المعنوي الأعلى لتلك المستخلصات بعد 72 ساعة من تعريضها على الخلايا بالتركيز 10000 مايكروغرام/مل ، فقد بلغت نسبة التثبيط الأعلى للمستخلص المائي 76.3% و 84.1 % في خلايا Hep-2 و خلايا AMN3 على الترتيب . وقد أبدت المستخلصات جميعها تأثيرات تثبيطية طفيفة في خط الخلايا الطبيعية (REF) ، فقد وصلت أعلى نسبة تثبيط في هذه الخلايا 21.1% عند التركيز 10000 مايكروغرام/مل للمستخلص المائي.

بيّنت دراسة تأثير المستخلصات الخام لثمار في إنقسام الخلايا اللمفاوية للدم المحيطي البشري إنخفاضاً معنوياً في معدلات معامل التحول الأرومي (BI%) ومعامل الإنقسام الخيطي (MI%) بشكل يعتمد على التركيز المستخدم من تلك المستخلصات ، ولم تُحدث هذه المستخلصات أي تغيرات تركيبية أو عددية في كروموسومات تلك الخلايا . إن التراكيز المستعملة جميعها من هذه المستخلصات لم تعمل كعوامل موقفة لإنقسام الخلايا اللمفاوية في الطور الإستوائي Metaphase عندما إستعملت بديلاً عن الكولسمايد Colcemid ، فضلاً عن إنها لم تنجح بالعمل كعوامل مشطرة بديلاً عن المادة المشطرة Phytohemagglutinin (PHA).

تم تحديد الجرع العلاجية من المستخلص المائي للثمار إعتماداً على قيمة الجرعة المميتة النصفية (LD50) . وأثبتت التجارب العلاجية فعالية عالية لهذا المستخلص في إختزال حجم الورم بشكل يعتمد على الجرعة المستخدمة منه ومدة التجريع . وكانت الجرعة العلاجية الأعلى له (1.2 غم/كغم من وزن الفأرة) هي الأفضل تأثيراً من خلال إختزالها لحجم الورم في الفئران بنسبة 73.9%.

تشير نتائج هذه الدراسة إلى الفعالية السمية العالية للمستخلص المائي للثمار في الخطوط الخلوية السرطانية Hep-2 و AMN3 بشكل متخصص Specifically دون إحداث تأثير سمي في الخلايا الطبيعية المتمثلة بخلايا REF ، والمدى الواسع لسلامة استخدام هذا المستخلص في الفئران ، والفعالية العالية ضد الورمية له عند استعماله في علاج سرطان الغدد اللبنية في الفئران.

المقدمة

يُعدّ السرطان واحداً من المخاطر الأساس التي تهدد حياة الإنسان في مختلف بلدان العالم ، لكون هذا المرض لا يقف عند عضو معين فهو ينتشر إلى كثير من أعضاء الجسم الأخرى ليفتك بها ، وهو أحد الأسباب الرئيسة للوفاة في العالم ، إذ يأتي بالمرتبة الثانية بعد أمراض القلب والشرايين (1،2)، وفي العراق بشكل خاص يعدّ السرطان مشكلة متنامية تجلب الموت للآلاف من الأشخاص خلال العام الواحد (3).

إن العلاجات التقليدية لهذا المرض مبنية على أساس العلاج الجراحي ، والعلاج الإشعاعي والعلاج الكيميائي أو الجميع معاً ، وبشكل عام فإن العلاجين الجراحي والإشعاعي يُستعملان في حالات الأورام الموضعية ، أما العلاج الكيميائي فيُستعمل عند إنتشار الخلايا السرطانية في الجسم (4،5). على الرغم من فوائد هذه العلاجات إلا أنها تمتلك تأثيرات جانبية تعود سلباً على صحة المريض لاسيما العلاجات الكيميائية والإشعاعية التي تتسبب بسُميّتها للأنسجة الطبيعية في الجسم أو بإحداث الطفرات الوراثية لخلاياه أو إضعاف الجهاز المناعي فيه (6،7).

لقد لجأ مرضى السرطان فضلاً عن كثير من الأطباء إلى المنتجات الطبيعية في علاج الأمراض التي تواجههم لكونها تُبعد أعراض المرض وتُحسّن من صحة الإنسان ، فضلاً عن أنها قليلة الكلفة (8). إن إستعمال المنتجات الطبيعية لا سيما النباتية منها لم يكن بالشئ الجديد فقد إستعملها الإنسان منذ القدم وكان الإستطباب بالأعشاب من الأمور المعروفة جيداً لدى العرب والإغريق والصينيين في العالم القديم ، وعند الهنود الحمر في العالم الحديث (9).

يوجد في الطبيعة ما لا يقل عن 250000 نوع نباتي ، شُخص منها أكثر من ألف نبات بإمتلاكه خواصاً فعّالة مضادة للسرطان (10). وقد استُعملت النباتات لعهود طويلة في علاج السرطان ، وكان هناك الكثير من المواد الفعالة المستخرجة من النباتات استُعملت في الوقاية من مرض السرطان وفي علاج مراحل متقدمة من الأورام الخبيثة (11).

أما في العراق فقد دأب المركز العراقي لبحوث السرطان و الوراثة الطبية وضمن خطة بحثية شاملة ومنذ سنوات عديدة على دراسة تأثير مستخلصات أنواع مختلفة من النباتات المتوافرة في البيئة العراقية في الخلايا السرطانية خارج الجسم الحي وداخله وشملت مستخلصات نبات سم الفراخ ، واليقطين والزنجبيل والحرمل ، والشاي الأخضر والأسود ، والسِعِد ، والهيل ، والشيح ، والتين ، والميرامية ، ونبات عين البزون، والعليق الصيني ونباتي الراوند والزعتر البري ونباتات أخرى (12)، إذ توصلت هذه الدراسات إلى أن لمستخلصات تلك النباتات تأثيرات سمّية في مختلف أنواع خطوط الخلايا السرطانية ، وما زالت البحوث جارية لإختبار فعالية مستخلصات نباتات أخرى ، سعياً ومحاولة لإيجاد العلاج المناسب للسرطان.

يعدّ نخيل التمر أكثر أشجار الفاكهة أهمية في البلدان العربية بشكل عام ، ودول الخليج بشكل خاص (13) ، فقد أستعملت ثمار التمر كغذاء منذ 6000 عام ، لما وُجد فيها من قيمة غذائية عالية مفيدة للإنسان ، فهو مُقوي Tonic ومُثير للجنس Aphrodisiac (14)، ويُستعمل في تحضير بعض المشروبات كالدبس والخل (15).

لقد وجد Vayalil (16) أن المستخلص المائي لثمار التمر يمتلك فعالية مُضادة للأكسدة Antioxidant activity ويثبط الفعالية المؤكسدة للجذور الحرة (Superoxide & hydroxyl radicals) ، كما أنه يمتلك فعالية مُضادة للتطفير Antimutagenic activity فقد ثبط الفعالية التطفيرية لمركب Benzo(a)pyrene في سلالتين من بكتريا السالمونيلا . وتمكنَ Mansouri وجماعته (17) من عزل مواد فينولية من ثمار التمر ذات فعالية مضادة للأكسدة أيضاً ، وبيّن Ishurd & Kennedy (18) الفعالية المضادة للسرطان للكلوكان Glucan الذي هو عديد السكريد Polysaccharide معزول من ثمار التمر .

إن دور ثمار التمر في الخلايا السرطانية سواء في المختبر أو داخل أجسام الحيوانات فإنه لم يُدرس حتى الآن ، وبما أن العراق هو من أكبر مصادر التمر في العالم ولما يُشكل التمر من مصدر غذائي مهم (19)، لذا تم اقتراح هذه الدراسة لمعرفة التأثير التثبيطي لثمار ونوى التمر في خطوط الخلايا السرطانية في المختبر و داخل أجسام الفئران.

المواد وطرائق العمل

تحضير المستخلصات الخام لثمار التمر

حُضر المستخلص المائي حسب الطريقة المتّبعة من قبل Harborne وجماعته (20) ، حيث وُضعت ثمار التمر المقطعة مع الماء المقطر بنسبة 5:1 في دورق محكم الغلق ، ثم وضع الدورق على جهاز المحرك الدوار Magnetic stirrer ليُخلط جيداً لمدة 72 ساعة بدرجة حرارة الغرفة. ورُشح المزيج بورق الترشيح. وتم تركيز المستخلص المُحضر باستخدام جهاز المبخر الدوار Rotary evaporator لحين الحصول على مسحوق جاف منه. حينها تم وزنه وحساب النسبة المئوية للإستخلاص. وتم تحضير المستخلص الإيثانولي بنفس طريقة تحضير المستخلص المائي لكن باستعمال الكحول الأثيلي بتركيز 70 % بدلاً من الماء المقطر .

تهيئة الوسط الزرعي وخطوط الخلايا

تمت تهيئة الوسط الزرعي تبعاً لـ Freshney (21) ، ثم عُقم الوسط الزرعي باستعمال مرشح دقيق ، ووُزّع في قنان زجاجية حفظت بدرجة حرارة (-20)°م لحين الاستعمال ، وتم الحصول على الخطوط الخلوية السرطانية (AMN3, Hep-2) والخط الخلوي لجنين الجرذ (REF) من المركز العراقي لبحوث السرطان والوراثة الطبية (ICCMGR) . وتم إجراء الخطوات الخاصة بالزرع النسيجي كما جاء في Freshney (22) التي تتضمن توزيع الخلايا في قناني زرع جديدة وحضنها بدرجة حرارة 37 °م حتى تكوّن طبقة أحادية متكاملة من الخلايا ، وتسمى هذه العملية بالزرع الثانوي Subculturing process . أختبار سُمية المستخلصين في نمو الخطوط الخلوية

حُضرت المستخلصات تبعاً لـ Mahony وآخرون (23) ، و Abdul-Majeed (24) بإذابة مسحوق المستخلص الخام في محلول دارئ الفوسفات ، وحضرت منه ثمانية تراكيز باستعمال الوسط الخالي من المصل تحت ظروف معقمة . واستخدمت جميع التراكيز المحضرة مباشرة بعد إكمال عملية التحضير.

جُهز عالق الخلايا ووُضع في حفر طبق معايرة الزرع النسيجي ذي القعر المسطح وحُضنت لحين التصاق الخلايا في الحفرة ، بعدها عوملت بالتراكيز المحضرة ، وبعد مرور مدة التعريض المحددة للحضن ، صُبغت الأطباق بصبغة البنفسج البلوري Crystal violet stain ، ثم قُرئت النتائج باستخدام جهاز الإليزا عند طول موجي 492 نانومتر . تم حساب النسبة المئوية لتثبيط نمو الخلايا لكل تركيز من تراكيز المستخلصات النباتية بحسب ما جاء في Betancur-Galvis وآخرون (25) عن طريق المعادلة الآتية:

نسبة التثبيط % = [(قراءة السيطرة – قراءة المعاملة لكل تركيز) / قراءة السيطرة] X100%

دراسة تأثير المستخلصين في الخلايا اللمفاوية البشرية

دراسة تأثير المستخلصين في إنقسام الخلايا اللمفاوية البشرية: جُهزت المحاليل وأجريت طرائق العمل تبعاً لطريقة Yaseen وآخرون (26) و Yaseen (27) ، إذ تتضمن العملية زرع الدم المحيطي في أنابيب الزرع الحاوية على الوسط الزرعي RPMI-1640 الخالي من المصل ، ثم تُضاف إليها التراكيز المستخدمة للمستخلصات قيد الدراسة ، وتُحضن لحين بدء مرحلة الحصاد التي حينها تُعامل بالكولسيمايد لمدة نصف ساعة ، ثم تُعامل بعدها بمحلول KCl المُدفأ في حمام المائي بدرجة 37 °م ، ثم يُعزل الراسب ويُضاف له المثبت البارد (المحضر آنياً من الميثانول االمطلق وحامض الخليك الثلجي وبنسبة مزج 3 : 1) تدريجياً مع الرج المستمر ، ثم توضع الأنابيب في الثلاجة مدة 30 دقيقة ، تُكرر عملية إضافة المثبت البارد ثلاث أو أربع مرات حتى الحصول على عالق خلايا ضبابي أبيض اللون ، لتُقطر هذه الخلايا على شرائح زجاجية باردة ، ثم تُصبغ بصبغة كمزا Giemsa stain وتُفحص تحت المجهر الضوئي بقوة تكبير (100 X) ليتم حساب معامل التحول الأرومي ومعامل الانقسام الخلوي وفق طريقة Stites (28) و Shubber & Al-Allak (29) تبعاً للمعادلات الآتية:

معامل التحول الأرومي = (عدد الخلايا الأرومية / العدد الكلي للخلايا) X100%

معامل الانقسام الخيطي = (عدد الخلايا المنقسمة / عدد الخلايا المنقسمة وغير المنقسمة) X100%

ولغرض الحصول على الكروموسومات بشكل G-Banding ، جُففت الشرائح المقطرة ووضعت في فرن كهربائي (65 °م) لساعة واحدة . عوملت بعدها بالتربسين المُدفأ لمدة 10 ثوان، ثم غُسلت وصُبغت بصبغة كمزا ، فُحصت الشرائح بالمجهر الضوئي لتقييم خلايا الطور الاستوائي وتحديد التغيرات الكروموسومية غير الطبيعية فيها حسب ISCN (30).

دراسة استعمال المستخلصين بديلاً عن الكولسيمايد في إيقاف انقسام الخلايا اللمفاوية: تعاد خطوات الدراسة السابقة ذاتها (دراسة تأثير المستخلصين في إنقسام الخلايا اللمفاوية) غير أن إضافة المستخلصين بتراكيزهما المختلفة تتم في مرحلة الحصاد وبالتحديد عند الساعة 71.5 من مدة الحضن بدلاً من الكولسيمايد ، تم حساب معامل الانقسام الخيطي تبعاً للمعادلة المذكورة أعلاه .

دراسة إستعمال المستخلصين بوصفهما مواد مشطرة للخلايا اللمفاوية: أتبعت الخطوات ذاتها المذكورة في دراسة تأثير المستخلصين في إنقسام الخلايا اللمفاوية لكن دون إضافة المادة المشطرة (PHA) ويضاف بدلها المستخلصين بتراكيزهما المختلفة ، وحُسب معامل الإنقسام الخيطي تبعاً للمعادلة المذكورة أعلاه .

تحديد الجرعة المميتة النصفية LD50 للمستخلص المائي في الفئران

إعتمدت طريقة الصعود والنزول Up & down method التي ذكرها Dixon (31) لتحديد الجرعة المميتة النصفية للفئران البيضاء، في هذه الطريقة تُجرع الفأرة عن طريق الفم بالمستخلص النباتي وتؤخذ النتيجة النهائية لهذه المعاملة (وهي إما هلاك الفأرة أو بقاؤها على قيد الحياة) خلال 24 ساعة من التجريع ، فإذا بقيت الفأرة على قيد الحياة تؤخذ فأرة أخرى وتُجرّع بتركيز أعلى ، أما إذا هلكت الفأرة فيجب أخذ فأرة أخرى وتجريعها بتركيز أقل ، ثم تتابع حالة الفأرة الثانية وهكذا تستمر العملية صعوداً أو نزولاً بالتركيز المستعمل عند كل فأرة إعتماداً على النتيجة النهائية للتجريع ، وحسب عدد الفأرات المستعمل في هذه التجربة يتم تثبيت آخر جرعة إستعملت ، لتُطبق المعادلة الآتية :

$$LD50 = xf + kd$$

xf : آخر جرعة إستعملت

d : مقدار الزيادة والنقصان الثابت في الجرعة المعطاة

k : القيمة الجدولية ، حيث أن : (O) هو رمز لبقاء الحيوان حياً خلال 24 ساعة من التجريع

(X) هو رمز لهلاك الحيوان خلال 24 ساعة من التجريع

دراسة التأثير العلاجي للمستخلص المائي في سرطان الغدة اللبنية في الفئران المختبرية

تم البدء بالتجارب العلاجية حال وصول حجم الورم إلى ما لايقل عن 100 ملم3 في الأناث المغروسة بالورم (32)، تم التجريع عن طريق الفم Orally administration ، وأستُعملت ثلاثة تراكيز من المستخلص إعتماداً على نتائج تجربة الجرعة المميتة النصفية LD50 ، وذلك بإختيار 0.1 ، 0.05 ، 0.025 من الجرعة المميتة النصفية لكل مستخلص ، فكانت التراكيز هي (0.3 ، 0.6 ، 1.2) غم/كغم . إستمر تجريع الفئران يومياً ولمدة 25 يوماً متتالية ، مع تسجيل حجم الورم في فئران المعاملة والسيطرة في الأيام (صفر ، 5 ، 10 ، 15 ، 20 ، 25) من بداية المعاملة .

تم قياس حجم الورم بإستعمال آلة قياس Vernia calipers وأخذت قياسات الطول والعرض مع تطبيق المعادلة الآتية (33) :

$$\text{Tumor volume} = (a)(b)^2 / 2$$

حيث أن : a = الطول b = العرض

وتم حساب النسبة المئوية لتثبيط نمو الورم من خلال المعادلة الآتية (34):

النسبة المئوية لتثبيط نمو الورم = [(حجم الورم في مجموعة السيطرة – حجم الورم في المجموعة المعالجة) / حجم الورم في مجموعة السيطرة] X 100%

وتم حساب حجم الورم النسبي من خلال المعادلة الآتية (35):

حجم الورم النسبي (لليوم س) = [حجم الورم (باليوم س) / حجم الورم (باليوم صفر)] X 100%

التحليل الإحصائي: أخضعت نتائج الدراسة إلى التحليل الإحصائي وفق تحليل التباين أحادي الاتجاه (ANOVA) ، وعدت الفروق مهمة إحصائياً وعالية المعنوية على مستوى ($P\leq0.001$) لإحتمال الخطأ ، وأجريت الاختبارات باستعمال برنامج SPSS version/10 الإحصائي من شركة Microsoft .

النتائج والمناقشة

الأستخلاص: أعطى الاستخلاص المائي لثمار التمر مستخلصاً لزجاً بلون بني فاتح ، بنسبة 24.33% . أما الاستخلاص الايثانولي للثمار فأعطى مستخلصاً أقل لزوجة وبلون أصفر مع احتوائه على بقع بنية بنسبة 14.2% .

سُمية المستخلصين في نمو الخطوط الخلوية

أظهر المستخلصان الخام لثمار التمر بشكل عام تأثيرات تثبيطية في خلايا Hep-2 وخلايا AMN3 ، وهذا التأثير التثبيطي كان يعتمد على التركيز المستعمل منها وعلى مدة التعريض Dose- and time-dependent effect ، إذ يلاحظ جلياً في الجدولين (1) و (2) إرتفاع الفعالية التثبيطية لهذين المستخلصين مع زيادة التركيز المستعمل ومدة التعريض ، على الرغم من أن التركيز الأوطئ (78.125 مايكروغرام/مل) من المستخلص المائي قد أظهر فعالية تثبيطية أعلى من التراكيز الأعلى منه بقليل.

قد ترجع الفعالية التثبيطية لهذين المستخلصين إلى احتوائهما على مركبات تؤثر في الحالة الفسلجية لهذه الخلايا ومن ثم تسبب هلاكها ، أو احتوائهما على مركبات تعمل على إيقاف دورة الخلايا السرطانية Arrest cell cycle عند طور معين وتمنعها من التكاثر، أو احتوائهما على مركبات تحفز الخلايا السرطانية على الموت المبرمج Apoptosis.

لقد إستعملت خلايا REF في هذه الدراسة لغرض تقييم التأثير السمّي للمستخلصين في الخلايا الطبيعية ، وقد عُرِّضت هذه الخلايا لأطول مدة تعريض استعملت في الخلايا السرطانية (72 ساعة) ، وذلك للتأكد من تأثير هذان المستخلصان في الخلايا الطبيعية لمدة التعريض الطويلة ، أما مدد التعريض الأقل (24 ، 48) ساعة فهي غير مجدية في هذا الغرض .لقد أظهر هذان المستخلصان فعالية تثبيطية واطئة جداً في حيوية هذه الخلايا بعد ثلاثة أيام من تعريضها مقارنة بما أظهره هذان المستخلصان في الخلايا السرطانية (Hep-2 و AMN3) ، وكما يظهر في الجدول (3) ، وهذا ما يشير إلى أن هذين المستخلصين غير مؤذيين للخلايا الطبيعية ، وأن فعاليتهما التثبيطية كانت إنتخابية على الخلايا السرطانية Selectively affecting . قد يكون السبب في ذلك أن آلية تأثير المستخلص النباتي لها علاقة بالمستقبلات Receptors الموجودة على أسطح الخلايا، ومن المعلوم أن للخلايا السرطانية مستقبلات تختلف عن تلك التي تمتلكها الخلايا الطبيعية.

جدول -1: النسبة المئوية لتثبيط حيوية خلايا Hep-2 بالمستخلصين المائي والإيثانولي لثمار التمر بعد مدد التعريض الثلاث

التراكيز المستعملة (مايكروغرام/مل)	النسبة المئوية للتثبيط (%) بعد 24 ساعة		بعد 48 ساعة		بعد 72 ساعة	
	المائي	الإيثانولي	المائي	الإيثانولي	المائي	الإيثانولي
78.125	29.1 *	0.5	37.5 *	3.8	42.3 *	3.2
156.25	10.2 *	1	4.5	3.7	13.0 *	4.7
312.5	8.9 *	2.7	1.7	5.2	10.2 *	3.8
625	18.5 *	3.1	3.4	8.1	36.2 *	16.7 *
1250	22 *	4.5	28.7 *	5.4	45.4 *	23.6 *
2500	24.5 *	9.3 *	31.2 *	9.2 *	62.0 *	24.1 *
5000	44.3 *	8.8 *	53.0 *	24.0 *	71.5 *	31.4 *
10000	48.6 *	26.4 *	64.5 *	26.2 *	76.3 *	33.0 *

علامة (*) تعني أن الفرق معنوي مقارنة بعينة السيطرة عند مستوى إحتمالية ($P \leq 0.001$)

جدول -2: النسبة المئوية لتثبيط حيوية خلايا AMN3 بالمستخلصين المائي والإيثانولي لثمار التمر بعد مدد التعريض الثلاث

التراكيز المستعملة (مايكروغرام/مل)	النسبة المئوية للتثبيط (%) بعد 24 ساعة		بعد 48 ساعة		بعد 72 ساعة	
	المائي	الإيثانولي	المائي	الإيثانولي	المائي	الإيثانولي
78.125	3.0	0.8	2.4	0.7	14.2 *	2.3
156.25	6.2	0.7	8.9	2.1	21.5 *	4.9
312.5	11.1 *	1.8	15.6 *	3.8	36.2 *	7.2
625	21.4 *	2.2	22.4 *	10.5	37.6 *	12.2 *
1250	26.7 *	3.5	24.0 *	16.7 *	42.1 *	27.6 *
2500	40.3 *	10.2	36.7 *	22.0 *	52.3 *	31.5 *
5000	39.7 *	18.3 *	44.1 *	22.4 *	68.7 *	37.0 *
10000	42.5 *	14.7 *	58.7 *	37.4 *	84.1 *	47.0 *

جدول -3: النسبة المئوية لتثبيط حيوية خلايا REF بالمستخلصين المائي والإيثانولي لثمار التمر بعد مرور 72 ساعة من التعريض

التراكيز المستعملة (مايكروغرام/مل)	النسبة المئوية للتثبيط (%)	
	المائي	الإيثانولي
78.125	-	-
156.25	0.3	-
312.5	2.5	0.4
625	2.7	0.8
1250	5.2	1.2
2500	9.7	4.1
5000	12.6 *	7.6
10000	21.1 *	9.8

علامة (-) تشير إلى عدم وجود تثبيط ، علامة (*) تعني أن الفرق معنوي عند مستوى إحتمالية ($P \leq 0.001$).

دراسة تأثير المستخلصان في إنقسام الخلايا اللمفاوية البشرية

تم إجراء بعض التجارب الخاصة بالسمية الخلوية للمستخلصين في مزارع الخلايا اللمفاوية ، وتمت دراسة أكثر الإختبارات حساسية لتقييم التأثير المحتمل للعوامل المطفرة Mutagenic أو المسرطنة Carcinogenic و هي المقاييس الوراثية الخلوية Cytogenetic parameters كحساب معامل التحول الأرومي (BI %) ، ومعامل الانقسام الخيطي (MI %) ودراسة الزيغ الكروموسومي Chromosomal aberration (36).

بينت النتائج أن المستخلصين خفّضا بشكل معنوي عدد الخلايا في الطور الأرومي، كما خفّضا عدد الخلايا في الطور الخيطي (لاحظ جدول 4)، كما تبيّن أن معاملة الخلايا اللمفاوية بمختلف التراكيز المستعملة من المستخلصين المدروسين لم تُحدث أي تغيرات مظهرية أو عددية في كروموسومات تلك الخلايا.

جدول -4: معدل قيم معامل التحول الارومي (BI%) ومعامل الانقسام الخيطي (MI%) للخلايا اللمفاوية البشرية الطبيعية بعد معاملتها بالمستخلصين الخام لثمار التمر

التراكيز المستعملة (مايكروغرام/مل)	معامل التحول الارومي (%) المائي	معامل التحول الارومي (%) الإيثانولي	معامل الانقسام الخيطي (%) المائي	معامل الانقسام الخيطي (%) الإيثانولي
0	38.91	45.31	3.73	4.14
78.125	36.52	45.41	3.66	4.06
156.25	32.26	44.93	3.64	4.21
312.5	27.61	40.32	3.57	3.67
625	22.97 *	36.67	3.42	3.54
1250	21.54 *	34.59	2.81	2.94
2500	19.60 *	34.33 *	2.46 *	1.97 *
5000	18.77 *	32.20 *	1.78 *	1.92 *
10000	16.30 *	30.19 *	1.64 *	1.82 *

علامة (*) تعني أن الفرق معنوي مقارنة بالتركيز صفر (عينة السيطرة) عند مستوى إحتمالية ($P \leq 0.001$)

إن انخفاض أعداد الخلايا في الطورين الأرومي والخيطي بفعل المستخلصان قد يرجع إلى أنهما قد أحدثا تداخلاً في العلاقة بين الخلايا اللمفاوية والمادة المشطرة (PHA) التي تحثها على الإنقسام .
استعمال المستخلصان بديلاً عن الكولسيمايد في إيقاف انقسام الخلايا اللمفاوية
إن المستخلصين بجميع التراكيز المستعملة منهما لم توقف انقسام الخلايا في الطور الاستوائي ، حيث لم تشاهد أي خلية تمر في هذا الطور في شرائح المعاملة ، وهذا ما يؤكد أن هذين المستخلصين لا يمتلكان الفعالية التي يمتلكها الكولسمايد تجاه الخلايا .
إستعمال المستخلصان بوصفهما مواد مُشطِرة للخلايا اللمفاوية
لم يعمل المستخلصان بتراكيزهما المختلفة عمل المادة المشطرة Phytohemagglutinin (PHA) في تحفيز خلايا الدم المحيطي على الانقسام ، وقد يكون السبب في ذلك هو إختلاف الطبيعة الكيميائية للمواد الفعالة الموجودة في هذين المستخلصين عن تلك التي تمتلكها المادة المشطرة المستخدمة بشكل روتيني في الدراسات الوراثية. إن المادة المشطرة المستخدمة في الدراسات الوراثية هي عبارة عن مادة مستخلصة من نبات الفاصوليا *Phaseolus vulgaris* ، تعمل على تحفيز انقسام خلايا مزارع الدم المحيطي لتجعل الدراسة الكروموسومية في تلك المزارع أمراً مُيسراً وسريعاً (37).
تحديد الجرعة المميتة النصفية LD50 للمستخلص المائي لثمار التمر والإيثانولي للنوى
إن القيمة العالية للجرعة المميتة النصفية (LD50) للمستخلص المائي لثمار التمر التي بلغت 12.186 غم/كغم من وزن الحيوان (لاحظ جدول 5)، تعكس حقيقة أن هذا المستخلص هو أمين وغير سامّ للأجهزة الحيوية عند استعماله داخل جسم الكائن الحي (*in vivo*) .

جدول -5: تحديد الجرعة المميتة النصفية LD50 للمستخلص المائي للثمار في الفئران المختبرية بطريقة الصعود والنزول

مقدار الزيادة أوالنقصان في الجرعة (d)	موت الحيوان او بقاؤه حياً بعد 24 ساعة	قيمة K الجدولية	آخر جرعة إستعملت (xf)	الجرعة المميتة النصفية (LD50)
0.5 غم/كغم	OOXXOO	0.372	12.0 غم/كغم	12.186غم/كغم

علامة (O) تعني بقاء الحيوان على قيد الحياة خلال 24 ساعة من المعاملة بالمستخلص
علامة (X) تعني موت الحيوان خلال 24 ساعة بعد المعاملة بالمستخلص

دراسة التأثير العلاجي للمستخلص المائي للثمار في سرطان الغدة اللبنية في الفئران المختبرية
تم تجريع الفئران المختبرية بالمستخلص المائي عن طريق الفم ، وذلك لأن هذا الجزء من نخيل التمر يعدّ مصدراً غذائياً للإنسان والحيوان ، لذا فإن إستعماله عن طريق الفم في الدراسات التجريبية يحاكي طبيعة تناوله .
تم إستعمال إثنين من المقاييس لتقييم التغير بحجم الورم في مجاميع الفئران المجرّعة بالمستخلص والمجموعة المجرعة بدارئ الفوسفات (مجموعة السيطرة) ، وهما معدل تثبيط النمو Growth inhibition(GI %) وحجم الورم النسبي Relative tumor volume(RTV) ، وهذان المقياسان كانا جيدين لمتابعة تقدم حجم الورم مع استمرار مدة التجريع بالمستخلص . ثم أجريت المقارنة أولاً بين الفئران غير المعاملة (السيطرة) والمجاميع المعاملة بالمستخلص عند كل وقت من أوقات تسجيل حجم الورم (5 ،

10 ، 15 ، 20 ، 25) يوم ، ومقارنة أخرى أجريت لتحديد حجم الورم النسبي لكل يوم من أيام التسجيل مقارنة باليوم (صفر) لكل مجموعة ، بيّنت النتائج التأثير التثبيطي الواضح للمستخلص في حجم الورم بشكل يعتمد على الجرعة المستخدمة ومدة التجريع Dose- and time-dependent manner . لقد أعطا المستخلص المائي للثمار نسبة تثبيط عالية تجاه نمو الورم بجميع الجرع المستخدمة منه، وكانت الجرعة العلاجية الأفضل له هي 1.2 غم/كغم ، أما الجرع الأخرى فكانت أقل تأثيراً (لاحظ الشكلين1 و 2)

تعد ثمار التمر مصدراً جيداً لمركبات Anthocyanins (38). وتمتلك مركبات Anthocyanins فعالية مضادة للأكسدة Antioxidant effect وقد يكون لها دوراً هاماً في تثبيط عمليات الأكسدة المرتبطة بعملية تكوّن الورم Tumorigenesis (39). كما تعود الخواص المضادة لتكوّن الأوعية الدموية الصغيرة في الورم Antiangiogenic properties التي تُظهرها بعض المستخلصات النباتية إلى احتوائها على هذه المركبات (40)، إذ أن المستخلصات النباتية الغنية بها تثبط إستحثاث عامل النمو Vascular endothelial growth factor بواسطة بيروكسيد الهيدروجين Hydrogen peroxide والعامل Tumor necrosis factor (TNF-α) وبالنتيجة التسبب بخفض حجم الورم (41).

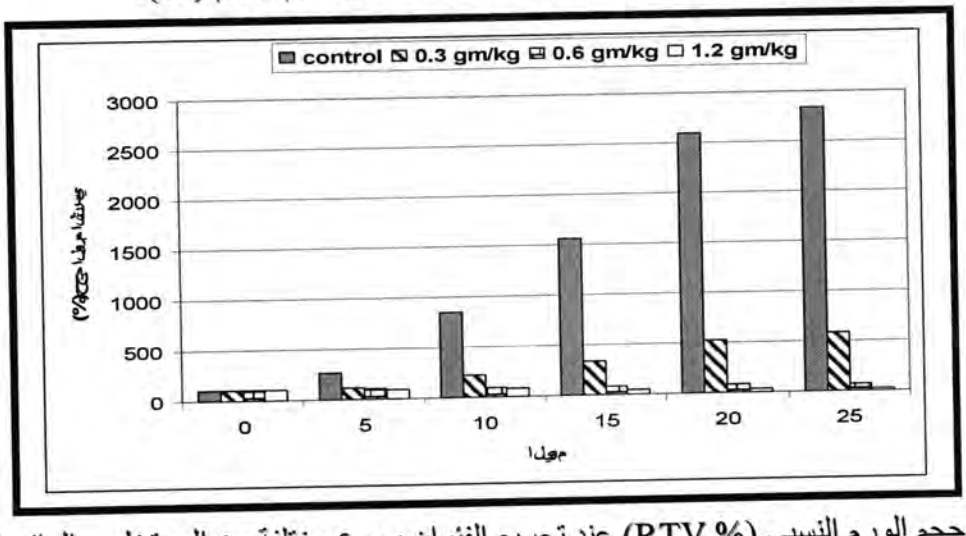

شكل -1: حجم الورم النسبي (RTV %) عند تجريع الفئران بجرع مختلفة من المستخلص المائي للثمار

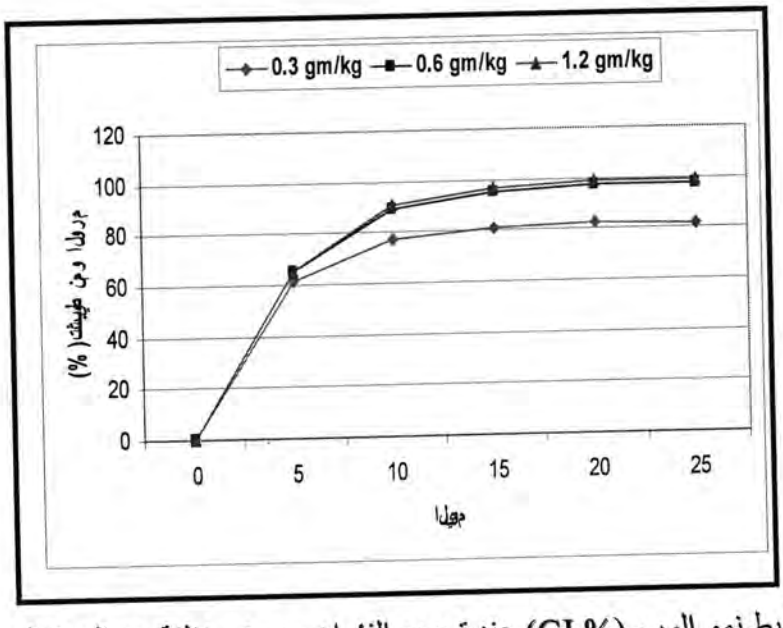

شكل -2: معامل تثبيط نمو الورم (GI %) عند تجريع الفئران بجرع مختلفة من المستخلص المائي للثمار

المصادر

1. Greenlee, R.T. ; Hill-Hamon, M.B. ; Murray, T. and Thun, M.. Cancer statistics 2001. *CA. Cancer J. Clin.*, 51:15-36(2001).
2. Jemal, A. ; Siegel, R. ; Ward, E. ; Murray, T. ; Xu, J. and Thun, M.J.. Cancer Statistics, 2007. *CA Cancer J. Clin.*, 57:43-66(2007).
3. Ministry of Health. Results of Iraqi Cancer Registry 1999-2001, Iraqi Cancer Board, Baghdad, Iraq (2003).
4. Hellman, S.. Principles of cancer management: Radiation therapy . In: V.T. DeVita ; S. Hellman and S.A. Rosenberg (Eds.), Cancer: principles and practice of oncology,(5th ed),Lippincott-Raven Publishers,Philadelphia,:307-332(1997).
5. Lopez-Lazaro, M.. Flavonoids as anticancer agents: structure-activity relationship study. *Curr. Med. Chem.-Anti-Cancer Agents*, 2:691714(2002).
6. DeVita, V.T.. Principles of cancer management : chemotherapy. In:V.T. DeVita ; S. Hellman ; S.A. Rosenberg and L.H. Raven (ed.). Cancer principles and practice of oncology (5th ed.),Lippincott-Raven Publishers,Philadelphia,:333-348 (1997) .
7. Kirn, D.H.. Replication-selective microbiological agents : Fighting cancer with targeted germ warfare. *J. Clinc. Invest.*, 105:837-839(2000) .
8. Katz, A.E.. Flavonoid and botanical approaches to prostate health. *The Journal of Alternative and Complementary Medicine*, 8:813-821(2002) .
9. Azaizeh, H. ; Saad, B. ; Khalil, K. and Said, O.. The state of the art of traditional arab herbal medicine in the eastern region of the mediterranean: A review. *eCAM*, 3:229-235(2006).
10. Mukherjee, A.K. ; Basu, S. ; Sarkar, N. and Ghosha, A.C.. Advances in cancer therapy with plant based natural products. *Current Medicinal Chemistry*, 8:1467-1486(2001).
11. Jiménez-Medina, E. ; Garcia-Lora, A. ; Paco, L. ; Algarra, I. ; Collado, A. and Garrido, F.. A new extract of the plant *Calendula officinalis* produces a dual *in vitro* effect: cytotoxic anti-tumor activity and lymphocyte activation. *BMC Cancer*, 6:119-132(2006).
12. Yaseen, N.Y.; Hussein, S.M.; Saleh, F.S. and Mohammad, M.H.. Plant and biological extracts in cancer therapy. Iraqi Center for Cancer and Medical Genetics Research(ICCMGR), Baghdad, Iraq(2008).
13. 13-Ahmed,I.A.;Ahmed,A.W.K.and Robinson,R.K.Chemical composition of date varieties as influenced by the stage of ripening.*Food Chemistry*,54:305-309 (1995).
14. Al-Qarawi, A.A. ; Ali, B.H. ; Al-Mougy, S.A. and Mousa, H.M.. Gastrointestinal transit in mice treated with various extracts of date (*Phoenix dactylifera* L.). *Food and Chemistry Technology*, 41: 37-39(2003) .
15. Barreveld, W.H.. Date palm products. FAO Agricultural Services Bulletin No. 101. Food and Agriculture Organization of the United Nations, Rome, Italy(1993).
16. Vayalil, P.K.. Antioxidant and antimutagenic properties of aqueous extract of date fruit (*Phoenix dactylifera* L. Aracaceae). *J. Agric. Food Chem.*, 50:610-617(2002).
17. Mansouri, A. ; Embarek, G. ; Kokkalou, E. and Kefalas, P.. Phenolic profile and antioxidant activity of the Algerian ripe date palm fruit (*Phoenix dactylifera*). *Food Chemistry*, 89: 411-420 (2005).
18. Ishurd, O. and Kennedy, J.F.. The anti-cancer activity of polysaccharide prepared from Libyan dates (*Phoenix dactylifera* L.). *Carbohydrate Polymers*, 59:531-535(2005) .

19. Erskine,W;Moustafa,A.T.;Osman,A.E.;Lashine,Z.;Nejatian,A.;Tamer Badawi ,T.and Ragy,S.M.Date Palm in the GCC countries of the Arabian Peninsula. Available at: {**http://www.icarda.org/aprp/Datepalm/introduction/intro-body .htm**}.
20. Harborne, J.B. ; Marbay, T.J. and Mabray, H.. Physiology and function of flavonoids. Academic Press, New York, pp.970(1975).
21. Freshney, R.I.. Culture of animal cells: A manual for basic technique (4th ed.). Wiley-liss, A John Wiley & Sons Inc. publication, New York (2000).
22. Freshney, R.I.. Culture of animal cells: A manual for basic technique (3th ed.). Wiley-liss, A John Wiley & Sons Inc. publication, New York (1994).
23. Mahony, D.E. ; Gilliat, T. ; Dawson, S. ; Stockdale, E. and Lee, S.H.. Vero cell assay for rapid detection of *Clostridium perfringens* enterotoxins. *Applied and Environmental Microbiology*. Pp:2141-2143(1989).
24. Abdul-Majeed, M.R.. Induction and characterization of SU.99 plasmacytoma cell line and its effect on mice immune response. Ph.D. Thesis, Nahrain University, Baghdad (2000).
25. Betancur-Galvis, L.A. ; Saez, J. ; Granades, H. ; Salazer, A. and Ossa, J.E.. Antitumor and antiviral activity of Colombian medicinal plant extracts. *Mem. Inst. Oswaldo Cruz*, 94: 531-535(1999).
26. Yaseen, N.Y. ; Tawfiq, M.S. ; Hamadi, A.A. and Estivan, A.G.. Cytogenetic studies on patient with chronic mylocytic leukemia. *Med. J. Tikrit University*, 4:5-9 (1998).
27. Yaseen, N.Y.. Cytogenetic study on human colorectal cancer cell. Ph.D. Thesis, University of Sheffield (1990).
28. Stites, D.. Laboratory methods of detection cellular immune function. In: Fundberg, H.H. ; Stites, D. and Coldwell, J. (ed). Basic and clinical immunuology, LAGE, Medical Publication, California, pp. 318-322 (1979).
29. Shubber, E.K. and Al-Allak, B.M.. Spontaneous chromosomal aberration and SCE in human lymphocytes : Effects of culture conditions. *Nucleus*, 22: 92-98 (1986).
30. ISCN. An international system for human cytogenetic nomenclature (1995). Mitelman, F.(ed.), S. Karger Publishers, Inc., Basel, Switzerland (1995).
31. Dixon, W.J.. Efficient analysis of experimental observations. *Ann. Rev. Pharmacol. Toxicol.*, 20: 441-462 (1980).
32. Shibata, T. ; Giaccia, A.J. and Brown, M.. Hypoxia-inducible regulation of a prodrug-activating enzyme for tumor-specific gene therapy. *Neoplasia*, 4:40-8(2002).
33. Grote, D. ; Russell, S.J. ; Cornu, T.I. ; Cattaneo, R. ; Vile, R. ; Poland, G.A. and Fielding, A.K.. Live attenuated measles virus induces regression of human lymphoma xenografts in immunodeficient mice. Blood, 97(12):3746-3754 (2001).
34. Blumenthal, R.M. ; Sharkey, R.M. ; Natale, A.M. ; Kashi, R. ; Wong, G. and Goldenberg, D.M.. Comparison of equitoxic radio-immunotherapy and chemotherapy in treatment of human colonic cancer xenografts. *Cancer Res.*, 54: 142-151 (1994).
35. Phuangsab, A. ; Lorence, R.M. ; Reichard, K.W. Peeples, M.E. and Walter, R.J.. Newcastle disease virus therapy of human tumor xenografts : antitumor effects of local or systemic administration. *Cancer Letters*, 172: 27-36 (2001).
36. Shubber, E.K. ; Amin, N.S. and El-Adhami, B.H.. Cytogenetic effects of copper-containing intrauterine contraceptive device (IUCD) on blood lymphocytes. *Mutat. Res.*, 417: 57-63 (1998).
37. Miller, O.J. and Therman, E.. Human chromosome, (4th ed.), Springer-Verlag Inc., New York, pp.4 (2001).
38. Al-Farsi, M. ; Alasalvar, C. ; Morris, A. ; Baron, M. and Shahidi, F.. Comparison of antioxidant activity, anthocyanins, carotenoids, and phenolics

of three native fresh and sun-dried date (*Phoenix dactylifera* L.) varieties grown in Oman. *J. agric. food chem.*, 53: 7592-7599 (2005).
39. Neto, C.C.. Cranberry and its phytochemicals: A review of *in vitro* anticancer studies. *J. Nutr.*, 137: 186S-193S (2007).
40. Bagchi, D. ; Sen, C.K. ; Bagchi, M. and Atalay, M.. Anti-angiogenic, antioxidant and anticarcinogenic properties of a novel anthocyanin-rich berry extract formula. *Biochemistry (Mosc)*, 69: 75-80 (2004).
41. Atalay, M. ; Gordillo, G. ; Roy, S. ; Rovin, B. ; Bagchi, D. ; Bagchi, M. and Sen, C.K.. Anti-angiogenic property of edible berry in a model of hemangioma. *FEBS Lett.*, 544: 252-257 (2003).

دراسة تأثير بعض العوامل في الفعالية التثبيطية لبكتريا حامض اللاكتيك ضد بعض البكتريا المرضية والتالفة للأغذية

[1]نبراس نزار محمود و [1]سمير فتح الله سمعان و [2]عبد الواحد باقر الشيباني
[1]قسم علوم الحياة- كلية العلوم- الجامعة المستنصرية
[2] قسم التقانة الاحيائية- كلية العلوم جامعة النهرين

ABSTRACT

Fifty isolates of lactic acid bacteria were obtained from raw milk, Yoghurt and fermented vegetables. Two of them were selected (*Lb. fermentum* and *Lc. raffinolactis* due to their inhibitory activity against test bacteria (*Staphylococcus aureus Ps. fluorescence, Salmonella typhi, Escherichia coli, Bacillus cereus, S. typhimurium*).

The two isolates were; then, grown in different liquid media (MRS, MRS fortified by vitamins and Tomato juice enriched with some materials) at different temperatures and periods to evaluate their inhibitory activity .

No observable inhibitory activity was detected for the unconcentrate filtrates of LAB grow in MRS broth against the test bacteria. Adversely, one-fold concentrated filtrate gave position results, especially after 24hr. against *Ps. fluorescence* deteriorating meat and milk. Best inhibitory activity was obtained by *Lb. fermentum* when grow in MRS broth fortified by Thiamine & Biotin, and for *Lc. raffionlactis* when grown in MRS broth contained Thiamine only. But most efficient inhibitory activity for the lactic filtrates was obtained after grown in Tomato juice medium fortified with glucose, Pepton, NaCl, Tween 80.

الخلاصة

جمعت(50) عزلة من بكتريا حامض اللاكتيك (LAB) من الحليب الخام واللبن الرائب والخضروات المتخمرة، وانتخبت أفضل عزلتين(*Lactococcus raffinolactis, Lactobacillus fermentum*) لأعطائهما فعالية تثبيطية عالية ضد بكتريا الأختبار (*Staphylococcus aureus, Pseudomonase fluorescens, Salmonella typhi, Escherichia coli, Bacillus cereus, Salmonella typhpimurium*)
بعدها نميت عزلتي الـ (LAB) في أوساط زرعية سائلة (MRS,MRS المدعم بالفيتامينات ووسط عصير الطماطا المدعم بمواد مختلفة) بدرجات حرارية ومدد زمنية مختلفة لتقييم كفاءتها التثبيطية، وكفاءة رواشحهما المركزة وغير المركزة.

لم تظهر فعالية تثبيطية ملموسة تجاه بكتريا الاختبار لدى إستخدام الرواشح غير المركزة للعزلتين المنماة في وسط (MRS)، في حين أعطت رواشحهما المركزة نتائج ايجابية ملحوظة لاسيما بعد (24) ساعة من تنميتهما تجاه بكتريا *Ps. fluorescens* المسببة لفساد اللحم والحليب. كما وأعطت العزلة *Lb. fermentum* أفضل فعالية تثبيطية عند تنميتها في وسط MRS المدعم بفيتاميني الثايمين والبايوتين. فيما كانت العزلة *Lc. raffinolactis* الأكفأ في وسط MRS المدعم بالثايمين فقط. لكن أعلى فعالية تثبيطية سجلت لرواشح العزلتين لدى تنميتهما في وسط عصير الطماطا الحاوي على الكلوكوزوالبيتون وكلوريد الصوديوم و80 Tween.

Studying the Effect of some Factors on the Inhibitory Activity of Lactic Acid Bacteria Against some Food Spoiling and Pathogenic Bacteria

المقدمة

يؤدي التأثير التضادي لبعض الاحياء المجهرية دوراً مهماً في السيطرة الاحيائية (Biological control) مما جعله يحظى بأهتمام كبير من الباحثين الذين حاولوا ومازالوا الإفادة من هذا التأثير على حياة الإنسان. ومن المجاميع البكتيرية التي نالت قسطاً كبيراً من الاهتمام بكتريا حامض اللاكتيك حيث استخدمت منذ آلاف السنين في كثير من منتجات الأغذية ولأغراض مختلفة (2,1).

ازداد الاهتمام في السنوات الاخيرة الماضية بالاستعانة بالأنظمة الحيوية لعلاج الأمراض أذ لوحظ ان الأستعانةبالمضادات الحيوية في العلاج يمكن ان يؤدي الى ظهور تأثيرات صحية جانبية فضلاً عن كلفتها العالية، ومن بين هذه الأنظمة ايضاً استخدام بكتريا حامض اللاكتيك في حفظ الأغذية (3) لاسيما في الدول والمناطق التي لا تتوافر فيها الطرائق الحديثة والمكلفة لحفظ الأغذية (4).

توجد *Lactococcus* في حليب الأبقار ومنتجات الألبان ويمكن عزلها أيضاً من النباتات كالبطاطا والخيار واللهانة والعشب (5). فقد أكد Ruyter (6) الدور المهم لهذه البكتريا في صناعة الاجبان الصلبة لقدرتها على إنتاج الإنزيمات المحللة للبروتين، أما بالنسبة لبكتريا *Lactobacillus* فتتواجد في مختلف أنواع الأغذية كالحليب
ومنتجاته والفواكه والخضروات والمخللات والعصائر(7). تمتلك بكتريا حامض اللاكتيك كثيراً من الآليات التي تظهر من خلال تأثيراتها المفيدة (8)، فهي تنتج أنواع مختلفة من المواد المضادة للأحياء المجهرية مثل البكتريوسينات وبيروكسيد الهيدروجين والداي استيل والحوامض العضوية (9). وتعتمد مستويات انتاج هذه المواد على السلالة والعوامل البيئية النامية فيها وطبيعة الوسط (10)، وأكد Maydani وHa (11) ان الفعالية التثبيطية ضد الكائنات المجهرية الأخرى المسببة للأمراض تعود أساساً الى نوعين من المواد التي تنتجها البكتريا هي البكتريوسينات والحوامض العضوية(11).
تنتج البكتريوسينات من بعض سلالات بكتريا حامض اللاكتيك التي تظهر فعالية ضد الأحياء المجهرية المسببة لأنواع الفساد في الاغذية والممرضات المحمولة بالغذاء ومن ضمنها بكتريا *Staph. aureus*(12). أشار Vignolo وجماعته أن لراشح المزارع السائلة تأثير فعال ضد البكتريا الموجبة لصبغة غرام مثل *S.aureus, Bacillus subtilis* (13) وضد البكتريا السالبة لصبغة غرام مثل *Ps .fluorescense, Salmonella typhimurium, E.coli* (14).
جاءت هذه الدراسة لتهدف الى عزل وتشخيص بكتريا حامض اللاكتيك من مصادر غذائية مختلفةودراسة العوامل الرئيسية مثل المدة الزمنية ودرجة الحرارة المؤثرة في الفعالية التثبيطية لبكتريا حامض اللاكتيك ضد بعض البكتريا المسببة لتلف وتسمم الأغذية ،و تنميةعزلات بكتريا حامض اللاكتيك في أوساط اخرى ومحاولة دراسة فعاليتها التثبيطية في تلك الأوساط.

المواد وطرائق العمل

- **جمع عينات اللبن الرائب والحليب الخام**

جمعت (26) عينة من اللبن الرائب الريفي و (13) عينة من الحليب الخام في حاويات معقمة بمدينة بغداد في حاويات معقمة ونقلت الى المختبر تحت ظروف معقمة مبردة وذلك من الأسواق المحلية بمدينة بغداد.

- **جمع عينات الخضروات المتخمرة:-**

خمرّت (11) عينة من الزيتون والخيار وذلك بغسلها بالماء غسلاً خفيفاً ووضعها في حاوية، ثم أضيف لها محلول (3%) كلوريد الصوديوم وتركت مغطاة في الحاضنة لمدة (3) أيام كي تتخمر (15).

- **عزل بكتريا حامض اللاكتيك:-**

لقحت أنابيب حاوية على وسط (MRS) السائل المعقم بنسبة 1% من العينات المذكورة أعلاه وحضنت بحرارة (37)^{o}م ولمدة (24) ساعة تحت ظروف لا هوائية وحسب ما ورد في (15).

- **تقدير الفعالية التثبيطية لبكتريا حامض اللاكتيك.**

* **تقدير الفعالية التثبيطية لبكتريا حامض اللاكتيك في الوسط الصلب.**

زرعت كلاً من عزلتي بكتريا LAB (*Lb.ferementum Lc.raffinolactis*) المنماة مسبقاً في وسط MRS السائل بطريقة التخطيط المتعامد على وسط MRS الصلب وحضنت بظروف لاهوائية لمدة (24-48) ساعة (16)، وتم فحص قدرتها على إنتاج مواد مثبطة وذلك بتكوّن مناطق تثبيط وحسب ما ورد في (17).

* **تقدير الفعالية التثبيطية لبكتريا حامض اللاكتيك في الوسط السائل**

استخدمت الطريقة الواردة في (13) وذلك بتنمية عزلتي بكتريا LAB لمدد زمنية مختلفة (36, 30, 24, 18,12) ساعة وتحت ظروف لاهوائية وتم تركيز رواشح بكتريا حامض اللاكتيك لمرة واحدة ولمرتين باستخدام طريقة التجفيد(Freeze drayer) وقدرت الفعالية حسب الطريقة الواردة (18).

* **تقدير الفعالية التثبيطية لبكتريا حامض اللاكتيك باستخدام وسط MRS المدعم بالفيتامينات**

استخدمت الأوساط MRS السائلة المدعمة بفيتاميني الثايمين والبايوتين (كلاً على حدة) وكذلك الاثنين معاً وحسب ما ورد في الفقرة السابقة.

* **تقدير الفعالية التثبيطية لبكتريا حامض اللاكتيك باستخدام وسط عصير الطماطا**

حضر الوسط حسب ما جاء في (19) وعقم بالموصدة لمدة (10) دقائق بعد ان أضيف (20) غم كلوكوز و (15) غم ببتون و (5)غم كلوريد الصوديوم و(1) مل Tween80 للتر الواحد من عصير الطماطا وقورنت الفعالية مع وسط MRS السائل.

* **التحليل الإحصائي:-**

تم توزيع المتوسط ± الانحراف المعياري لكل معالجة ضمن كل عزلة من عزلات بكتريا حامض اللاكتيك تجاه بكتريا الاختبار المستخدمة، ثم المقارنة بين المعالجات جميعاً.ولاختبار معنوية الفروق فيما بينها تم تطبيق تحليل التباين الاحادي [One way Analysis of Variance/ANOVA](26).

النتائج والمناقشة

كانت جميع عزلات البكتريا سالبة لفحوصات الجيلاتينيز والاوكسديز والكاتاليز، وموجبة لفحص اللتموس عندما أنتجت خثرة وحموضة في وسط حليب اللتموس مؤدية الى خفض رقم الاس الهيدروجيني للوسط من (6.5) الى (4.5) وأحيانا لغاية (4) بأنتهاء فترة الحضن (جدول 1).

جدول-1: الفحوصات الكيموحيوية لعزلات بكتريا حامض اللاكتيك والمصادر الغذائية التي عزلت منها.

نوع الفحص / رمز العزلة	الجيلاتينيز	الاوكسيديز	الكاتاليز	النمو في وسط حليب اللتموس	انتاج الامونيا من الارجنين	النمو في(45)م	النمو بوجود 0.1% ازرق المثيلين	النمو في (10)م	النمو في 4% كلوريد الصوديوم	مصدر العزل
Lb1	-	-	-	+	-	-	*	*	*	لبن رائب
Lb2	-	-	-	+	-	-	*	*	*	لبن رائب
Lb3	-	-	-	+	-	-	*	*	*	لبن رائب
Lb4	-	-	-	+	-	-	*	*	*	خضروات متخمرة
Lb7	-	-	-	+	-	-	*	*	*	لبن رائب
Lb8	-	-	-	+	+	+	*	*	*	لبن رائب
Lb9	-	-	-	+	+	+	*	*	*	لبن رائب
Lb10	-	-	-	+	+	+	*	*	*	خضروات متخمرة
Lb11	-	-	-	+	+	+	*	*	*	خضروات متخمرة
Lb12	-	-	-	+	+	+	*	*	*	خضروات متخمرة
Lb17	-	-	-	+	-	-	*	*	*	حليب خام
Lb18	-	-	-	+	+	+	*	*	*	لبن رائب
Lb19	-	-	-	+	-	-	*	*	*	لبن رائب
Lb20	-	-	-	+	+	+	*	*	*	لبن رائب
Lb21	-	-	-	+	-	-	*	*	*	لبن رائب
Lb26	-	-	-	+	-	-	*	*	*	لبن رائب
Lb27	-	-	-	+	-	-	*	*	*	خضروات متخمرة
Lb29	-	-	-	+	+	+	*	*	*	لبن رائب
Lb30	-	-	-	+	+	+	*	*	*	لبن رائب
Lb33	-	-	-	+	-	-	*	*	*	خضروات

نوع الفحص / رمز العزلة	الجيلاتينيز	الاوكسيديز	الكاتاليز	النمو في وسط حليب اللتموس	انتاج الامونيا من الارجنين	النمو في(45)م	النمو بوجود 0.1% ازرق المثيلين	النمو في (10)م	النمو في 4% كلوريد الصوديوم	مصدر العزل
										متخمرة
Lb34	-	-	-	+	-	-	*	*	*	لبن رائب
Lb36	-	-	-	+	+	+	*	*	*	لبن رائب
Lb37	-	-	-	+	+	+	*	*	*	خضروات متخمرة
Lb38	-	-	-	+	-	-	*	*	*	لبن رائب
Lb39	-	-	-	+	-	-	*	*	*	حليب خام
Lb40	-	-	-	+	-	-	*	*	*	لبن رائب
Lb41	-	-	-	+	-	-	*	*	*	لبن رائب
Lb42	-	-	-	+	-	-	*	*	*	خضروات متخمرة
Lb44	-	-	-	+	-	-	*	*	*	خضروات متخمرة
Lb45	-		-	+	-	-	*	*	*	لبن رائب
Lb46	-	-	-	+	-	-	*	*	*	حليب خام
Lb47	-	-	-	+	-	-	*	*	*	لبن رائب
Lb48	-	-	-	+	-	-	*	*	*	خضروات متخمرة
Lb49	-	-	-	+	-	-	*	*	*	حليب خام
Lb50	-	-	-	+	-	-	*	*	*	خضروات متخمرة
Lc5	-	-	-	+	+	-	+	+	+	لبن رائب
Lc6	-	-	-	+	+	-	+	+	+	لبن رائب
Lc13	-	-	-	+	+	-	+	+	+	حليب خام
Lc14	-	-	-	+	+	-	+	+	+	لبن رائب
Lc15	-	-	-	+	+	-	+	+	+	لبن رائب
Lc16	-	-	-	+	+	-	+	+	+	لبن رائب
Lc22	-	-	-	+	+	-	+	+	+	حليب خام
Lc23	-	-	-	+	+	-	+	+	+	حليب خام
Lc24	-	-	-	+	+	-	+	+	+	لبن رائب
Lc25	-	-	-	+	-	-	-	+	-	حليب خام
Lc28	-	-	-	+	-	-	-	+	-	حليب خام
Lc31	-	-	-	+	-	-	-	+	-	حليب خام
Lc32	-	-	-	+	-	-	-	+	-	حليب خام
Lc35	-	-	-	+	-	-	-	+	-	حليب خام
Lc43	-	-	-	+	-	-	-	+	-	حليب خام

+ **(نتيجة موجبة)** ، - **(نتيجة سالبة)** ، * **(لم يجرى الفحص)** ، *Lb= Lactobacillus* ، *Lc= lactococcus*

أظهرت النتائج ان اعلى فعالية تثبيطية للعزلتين *Lb. fermentum, Lc. Raffinolactis* كانت لدى تنميتهما لمدة (18،24)ساعة بدرجة 37°م،اذتراوحت مناطق التثبيط (11.33 و18.33)ملم وكمامبين في الشكلين (1و2)

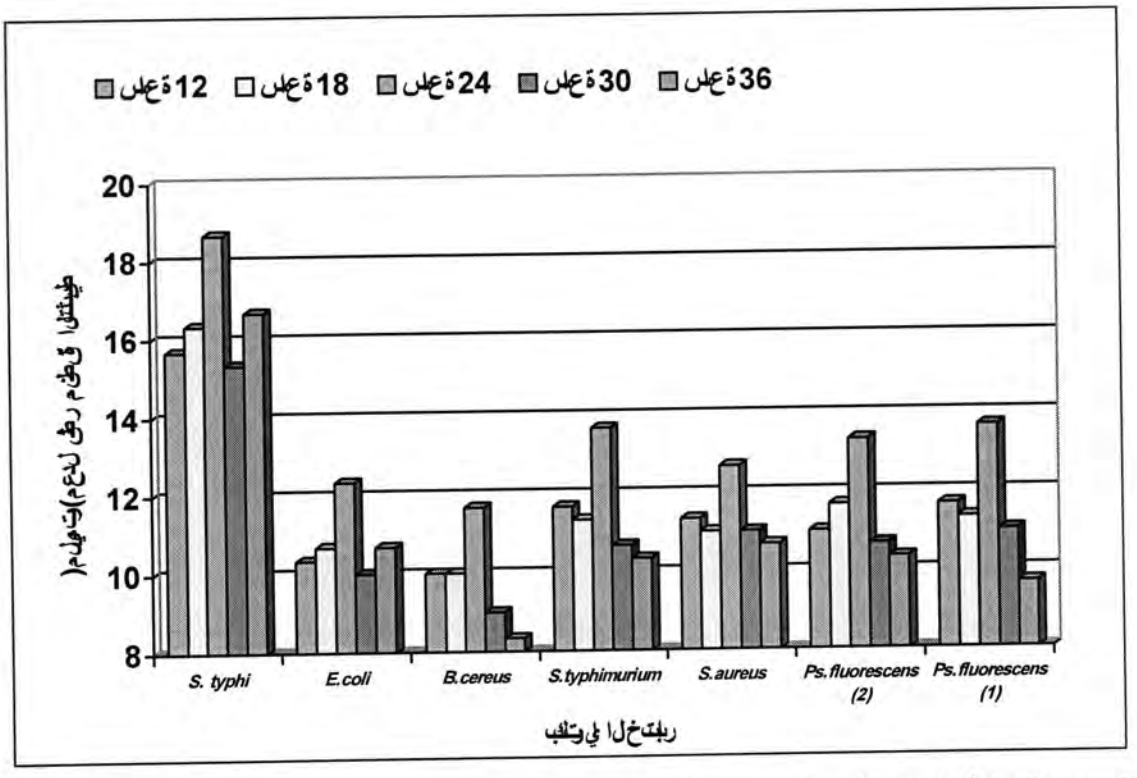

شكل -1: الفعالية التثبيطية لراشح العزلة *Lc. raffinolactis* المركز لمرة واحدة بعد التنمية لمدد حضن مختلفة تجاه بكتريا الاختبار
(1): البكتريا المسببة لتلف الحليب؛ (2): البكتريا المسببة لتلف اللحم

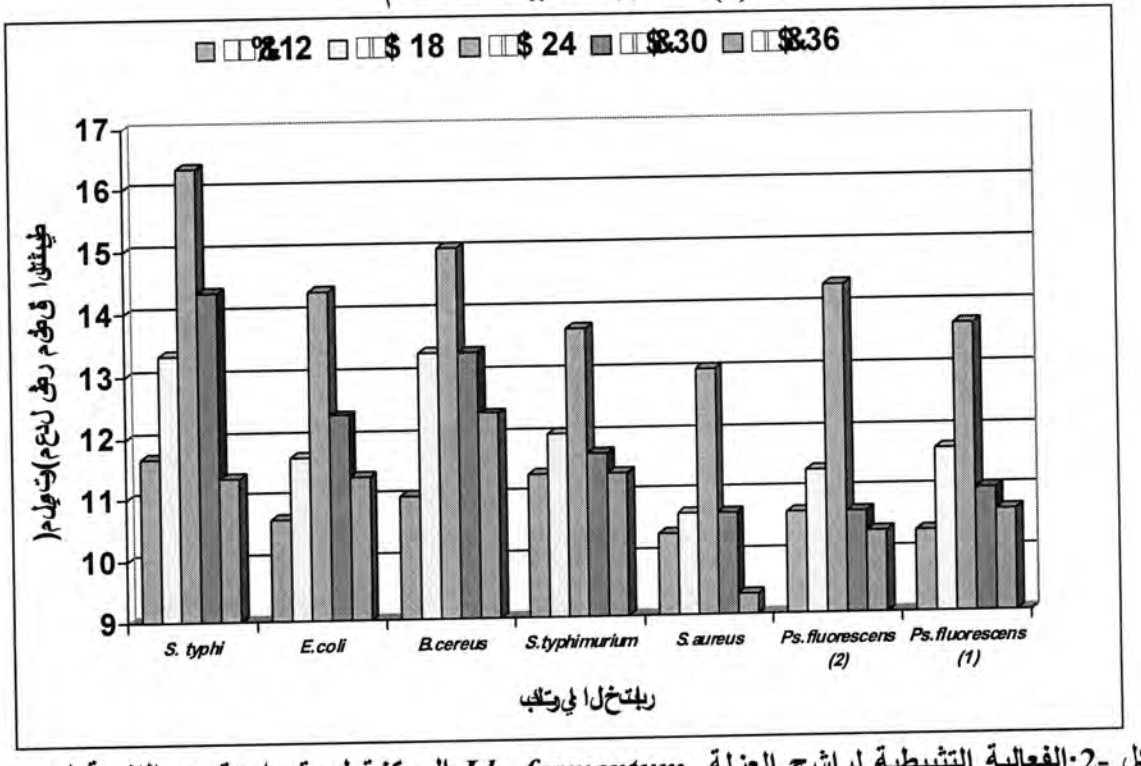

شكل -2:الفعالية التثبيطية لراشح العزلة *Lb. fermentum* المركزة لمرة واحدة بعد التنمية لمدد حضن مختلفة تجاه بكتريا الاختبار
(1): البكتريا المسببة لتلف الحليب؛ (2): البكتريا المسببة لتلف اللحم

ويؤكد ذلك ما ذكره Tagg وجماعته (20) من ان أعلى إنتاجية للبكتروسين أمكن الحصول عليها في المزرعة السائلة فيما أشار Vignolo وجماعته (13) الى إن إنتاج البكتريوسين يكون بصورة مستمرة خلال أطوار النمو. ولدى تركيز رواشح عزلتي بكتريا حامض اللاكتيك أمكن الحصول على تحسين ملحوظ في الفعالية التثبيطية وبفروق معنوية عند مستوى ($p<0.05$) لجميع مدد الحضانة، وذلك من خلال زيادة أقطار مناطق التثبيط من (9) الى(2.15) ملم وكما في الشكلين (3 و4).

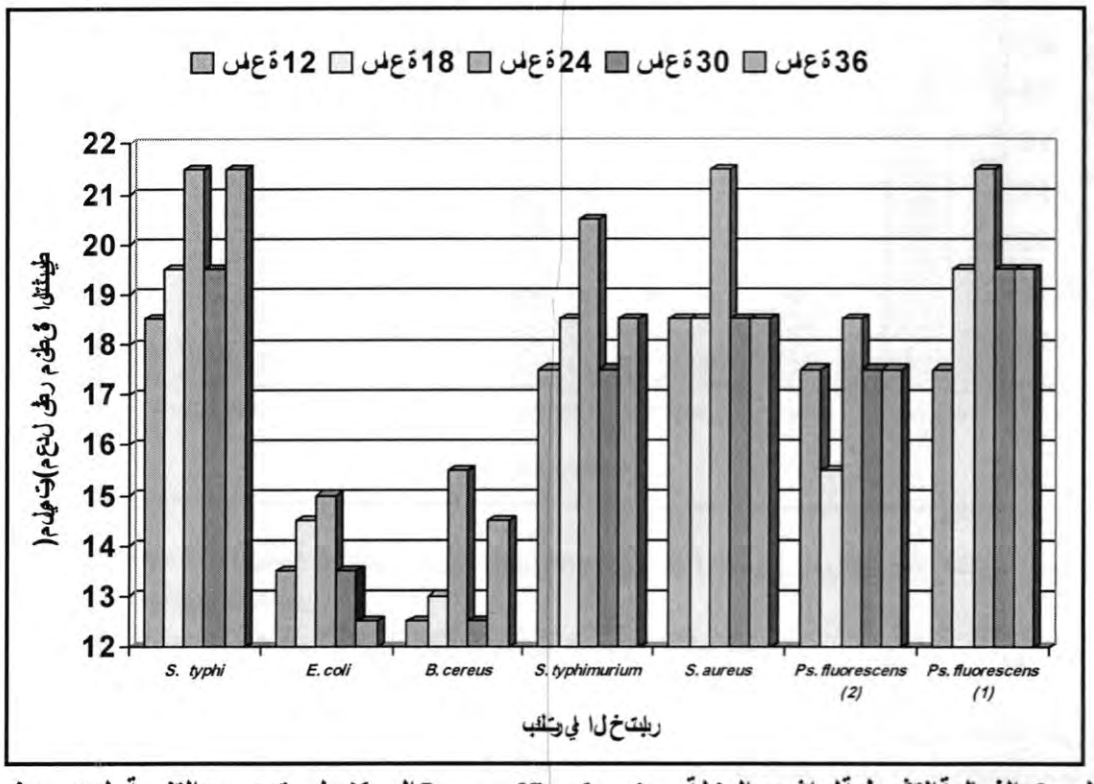

شكل -3:الفعاليةالتثبيطيةلراشح العزلة *Lc. raffinolactis* المركز لمرتين بعدالتنمية لمدد حضن مختلفة تجاه بكتريا الاختبار
(1): البكتريا المسببة لتلف الحليب؛ (2): البكتريا المسببة لتلف اللحم

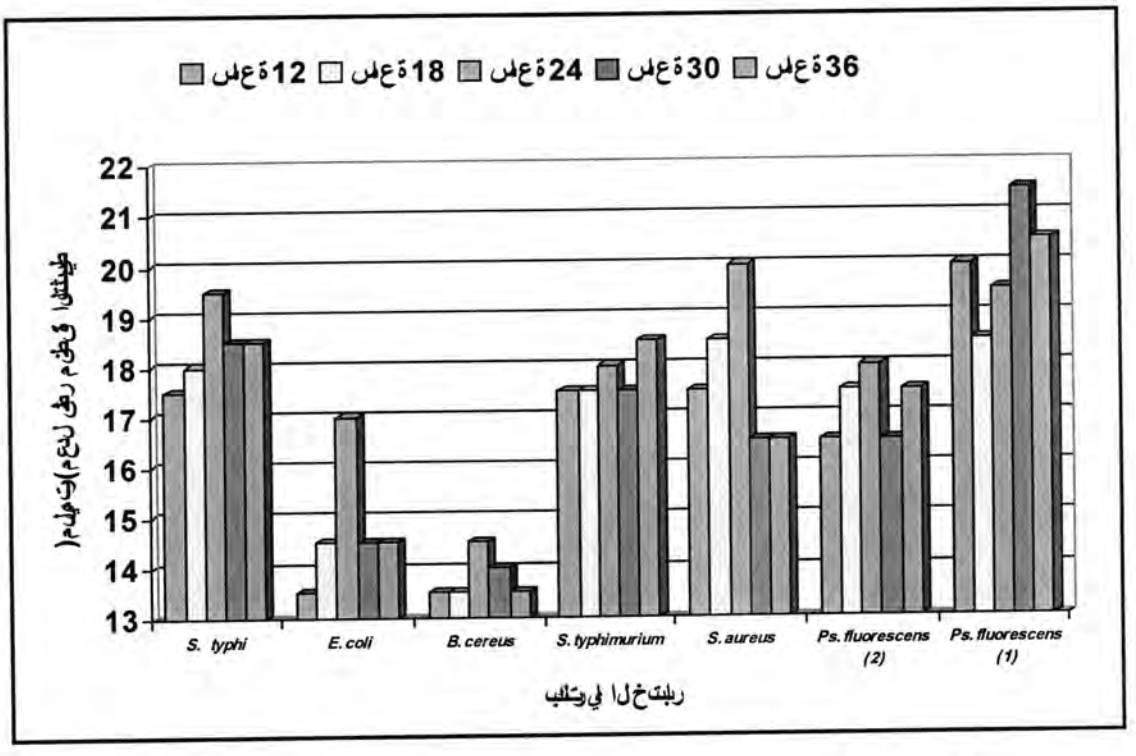

شكل -4:الفعالية التثبيطية لراشح العزلة *Lb. fermentum* المركز لمرتين بعد التنمية لمدد حضن مختلفة تجاه بكتريا الاختبار
(1): البكتريا المسببة لتلف الحليب؛ (2): البكتريا المسببة لتلف اللحم

أما بالنسبة للفاعلية التثبيطية لبكتريا LAB في الوسط المدعم بالفيتامينات فقد اشارت النتائج الى وجود فروق معنوية بمستوى معنوية ($p<0.05$) لصالح الوسط المدعم بفيتاميني البايوتين والثايمين معاً عندما بلغ معدل أقطار مناطق التثبيط (22.5) ملم للعزلة *Lb. fermentum* تجاه بكتريا الاختبار *Ps. fluorescense* المسببة لفساد الحليب وكما مبين في الشكل (5). اما العزلة *Lc. raffinolactis* فقد ظهرت فروق معنوية بمستوى معنوية ($p<0.05$) ولصالح التنمية في وسط MRS المدعم بالثايمين فقط وكما في الشكل(6)، فقد سجلت أعلى معدلات تثبيط عند تنميتها في الوسط المذكور تجاه جميع بكتريا الاختبار السبعة المستخدمة بأقطار مناطق تثبيط بلغت معدلاتها (12.5) ملم تجاه بكتريا *E. coli* (16.5) ملم تجاه بكتريا *Ps. fluorescencse* المسببة لفساد الحليب.

يتضح من ذلك أن نمو بكتريا حامض اللاكتيك يحتاج الى احتواء وسط التنمية على الفيتامينات، وهذا ما ظهر لدى تركيز رواشح العزلتين *Lb. fermentum, Lc. raffinolactis* الناميتين في وسط MRS المدعم بالفيتامينات. حيث سجلت بكتريا *Lc. Raffinolactis* النامية في وسط MRS المدعم بالثايمين فقط أعلى معدل لأقطار مناطق التثبيط بلغ (30.5) ملم تجاه كل في بكتريا الاختبار *Salmonella typhimurium* و *Ps. fluorescense* المسببة لفساد اللحم.

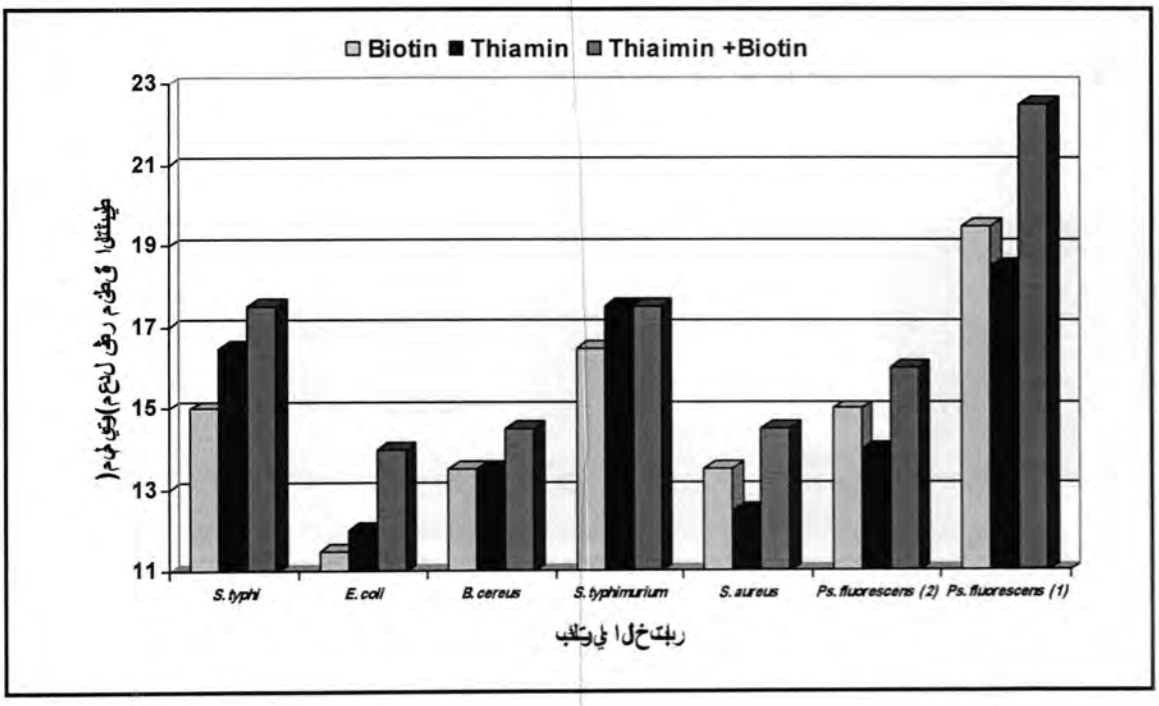

شكل -5:الفعالية التثبيطية لراشح العزلة *Lb. fermentum* المركز لمرة واحدة بعد التنمية في وسط MRS السائل المدعم بالفيتامينات (Biotin ,Thiamine ,Biotin مع Thiamine) تجاه بكتريا الاختبار

(1): البكتريا المسببة لتلف الحليب؛ (2): البكتريا المسببة لتلف اللحم

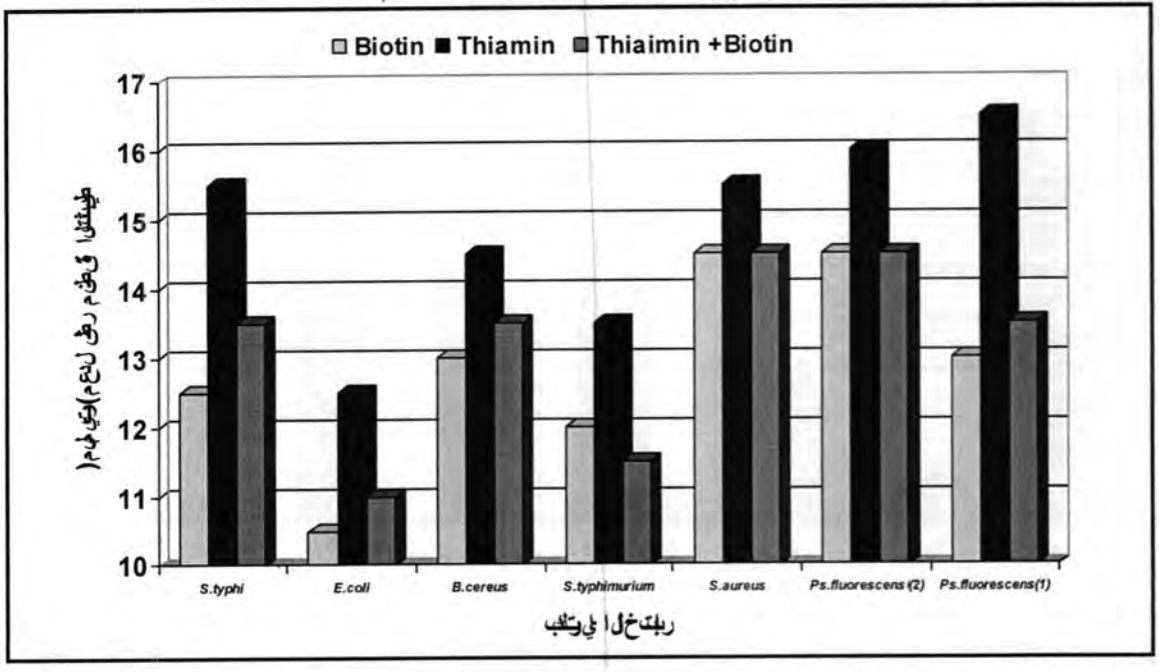

شكل -6:الفعالية التثبيطية لراشح العزلة *Lc.raffinolactis* المركز لمرة واحدة بعد التنمية في وسط MRS السائل المدعم بالفيتامينات(Biotin ,Thiamine ,Biotin معThiamine) تجاه بكتريا الاختبار

(1): البكتريا المسببة لتلف الحليب؛ (2): البكتريا المسببة لتلف اللحم

في حين لم تظهر فروق معنوية تجاه بكتريا الاختبار *B. cereus* وكما في الشكل (7).أما العزلة *Lb. fermentum* فقد لوحظ وجود فروق معنوية لدى تنميتها في وسط MRS المدعم بالبايوتين والثايمين معاً وكما في الشكل (8).

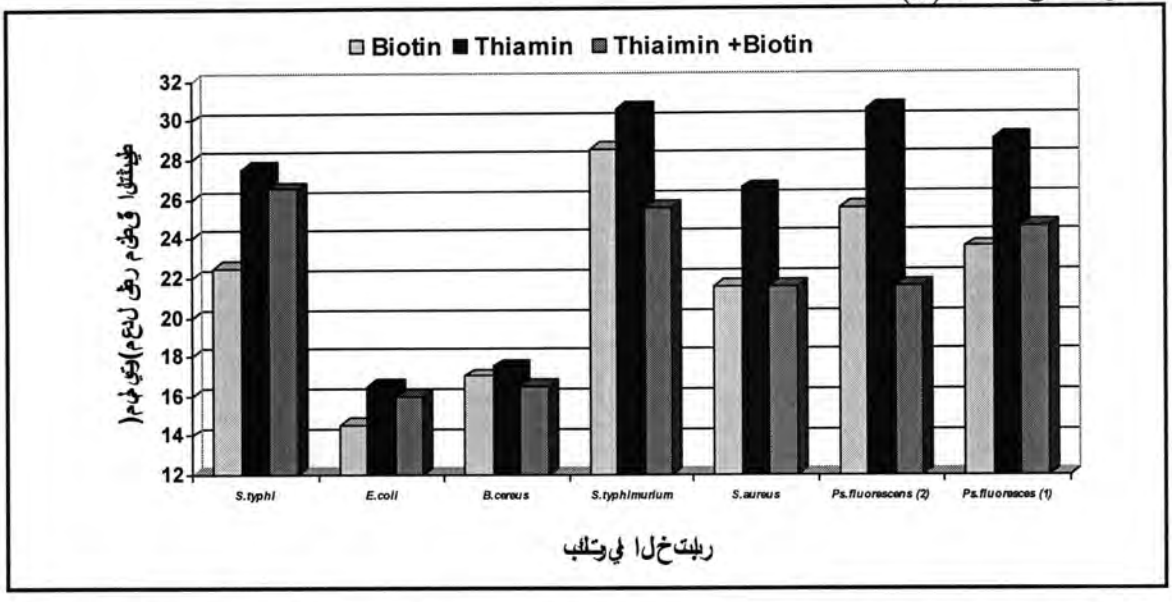

شكل -7:الفعالية التثبيطية لراشح العزلة *Lc.raffinolactis* المركز لمرتين بعد التنمية في وسط MRS السائل المدعم بالفيتأمينات(Biotin ,Thiamine ,Biotin مع Thiamine) تجاه بكتريا الاختبار

(1): البكتريا المسببة لتلف الحليب؛ (2): البكتريا المسببة لتلف اللحم

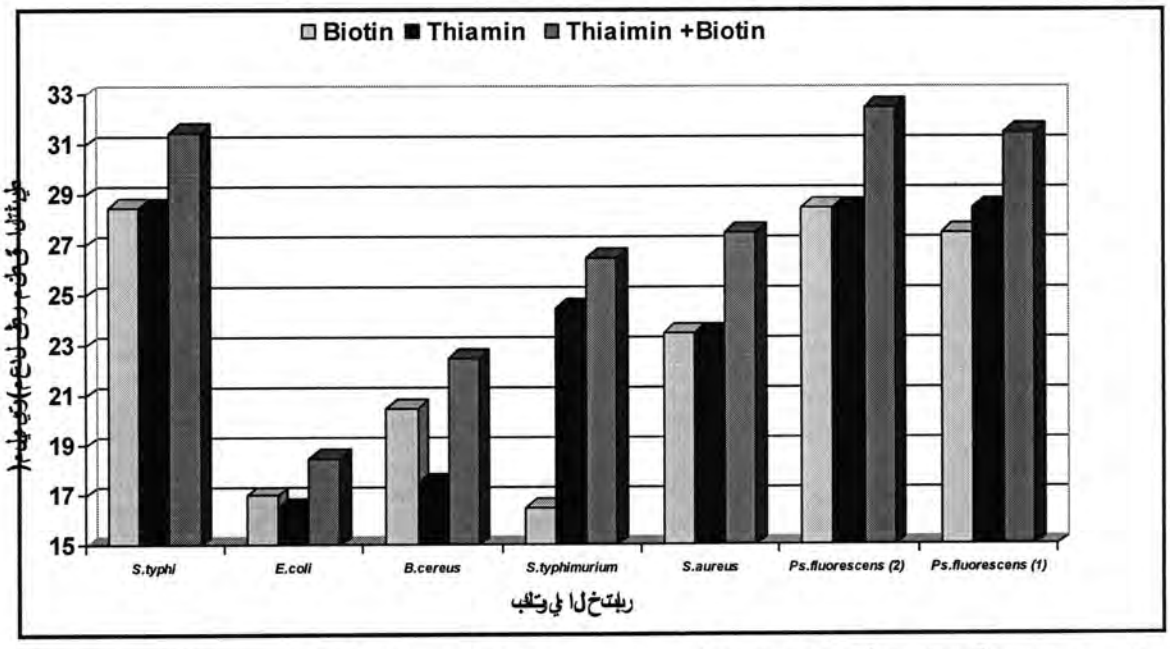

شكل -8: الفعالية التثبيطية لراشح العزلة *Lb. fermentum* المركز لمرتين بعد التنمية في وسط MRS السائل المدعم بالفيتأمينات(Biotin ,Thiamine ,Biotin معThiamine)تجاه بكتريا الاختبار

بعد تنمية عزلتي بكتريا حامض اللاكتيك في وسط عصير الطماطا لوحظ أن العزلة *Lc.raffinolactis* أعطت فعالية تثبيطية عند نموها في وسط MRS السائل مقارنة بوسط عصير الطماطا وذلك عندما بلغت معدلات أقطار مناطق التثبيط (16.33, 13.67, 15.33, 18.33) ملم مقارنة بتنميتها في وسط عصير الطماطا(10.67,10, 11.33) (13.33, ملم تجاه بكتريا الاختبار *Ps.fluorescence, E.coli, S.typhi* المسببة لفساد اللحم والمسببة لفساد الحليب. وعلى العكس من ذلك لم تسجل فروق معنوية بين الوسطين عند تنمية العزلة نفسها تجاه كل من بكتريا الاختبار *Staph. aureus, S. typhimurinm, B.cereus* وكما في الشكل(9).

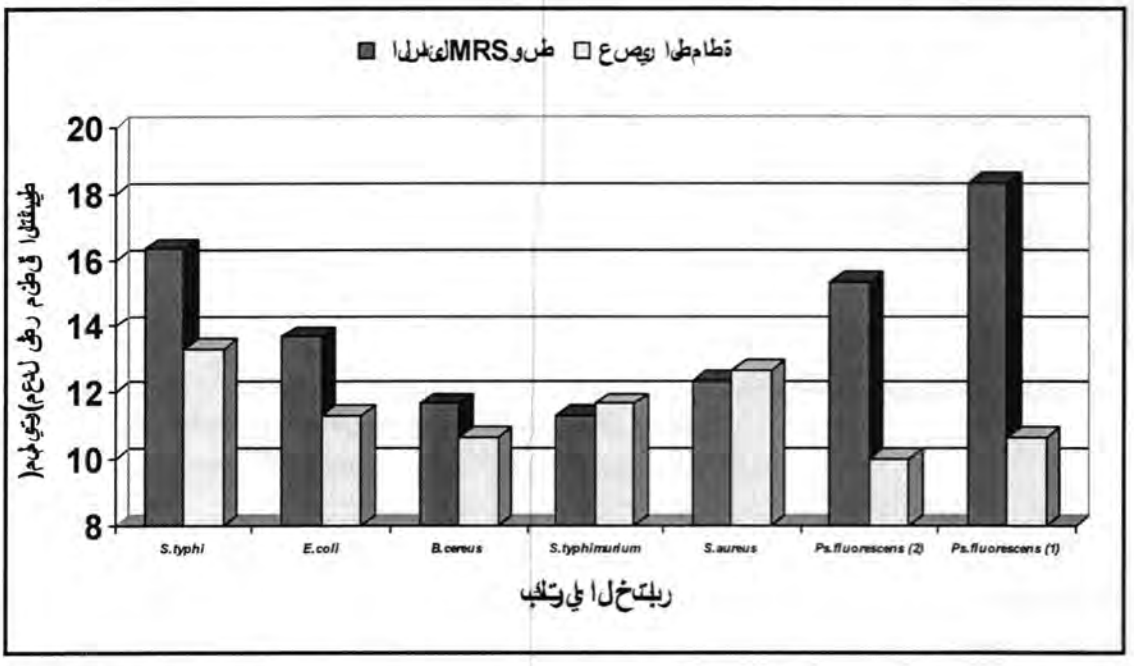

شكل -9:مقارنة الفعالية التثبيطية لراشح العزلة *Lc.raffinolactis* بعد التنمية في وسط MRS السائل ووسط عصير الطماطا والمعامل بعدة معاملات تجاه بكتريا الاختبار
(1): البكتريا المسببة لتلف الحليب؛ (2): البكتريا المسببة لتلف اللحم

أعطت العزلة *Lb. fermentum* معدلات أقطار مناطق تثبيط عند تنميتها في وسط MRS السائل أعلى من تلك التي أعطتها عند تنميتها في وسط عصير الطماطا وكما في الشكل (10).

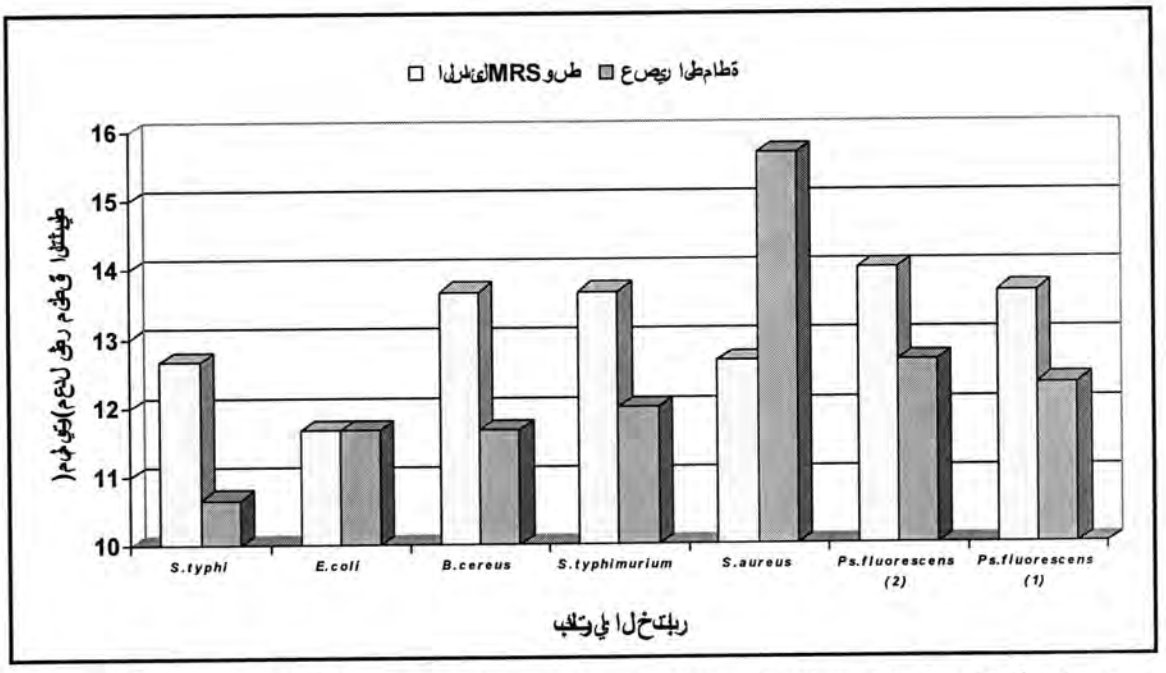

شكل -10:مقارنة الفعالية التثبيطية لراشح العزلة *Lb. fermentum* بعد التنمية في وسط MRS السائل ووسط عصير الطماطا والمعامل بعدة معاملات تجاه بكتريا الاختبار
(1): البكتريا المسببة لتلف الحليب؛ (2): البكتريا المسببة لتلف اللحم

يظهر من النتائج أعلاه ان وسط MRS السائل أفضل من وسط عصير الطماطا في الحصول على فعالية تثبيطية جيدة تجاه بكتريا الاختبار وذلك لتميز وسط MRS بتحفيز نمو عصيات ومكورات بكتريا حامض اللاكتيك على حد سواء.

وهذا ما أشار اليه De Man وجماعته (21) من ان وجود النترات والخلات فضلاً عن Tween 80 في وسط MRS جعله وسطاً ملائماً لنمو هذه البكتريا، كما ان الاملاح الموجودة في الوسط مثل كبريتات المغنيسيوم وكبريتات المنغنيز تجهز البكتريا بالكبريت اللازم لنموها، فيما توفر خلاصة كل من اللحم والخميرة والببتون مصدراً مهماً للنتروجين (22). أشار كل من Leroy وDe Vuyst (23) و Verluyten وجماعته (24) الى ان نمو الخلية وفعالية البكتريوسين يتأثران بتغير المواد المغذية الموجودة في وسط التنمية أذ يحصل أعلى إنتاج للبكتريوسين في وسط MRS.

من هنا يتضح أن مدة الحضانة ودرجات الحرارة والأس الهيدروجيني ومكونات الوسط لها تأثير ملموس على انتاج البكتريوسين من قبل بكتريا حامض اللاكتيك وهذا ما أكده Carolissen-Mackay وجماعته(25).

المصادر

1. Lindgren, S.E. and Dobrogosz, W.J Antagonistic activities of latic acid bacteria in food and feed fermentation. FEMS Microbiology Revi., 87:149-164. (1990)
2. Hernandez, P.E.; Rodriguez, J.M.; Cintas, L.M.; Moreira, W.L.; Sobrino, O.J.; Fernandez, M.F. and Sanz, B. Utilization of lactic bacteria in the control of pathogenic microorganisms in food. Microbiologia, 9:37-48(1993) (Abst).
3. Settanni, L. and Corsetti, A. Application of bacteriocins in Vegetable food biopreservation. Int.J.Food Microbiol. 121(2): 123-138.(2008).
4. Nigatiu, A. and Gashe, B. A. Survival and growth of selected pathogens in fermented: kocho (ensete ventri consum).East African medical J.71(1):514-518 (1994)
5. Sandine, W.E.; Muralidhara, K.S.; Elliker, P.R.and England, D.C. Lactic acid bacteria in food and health; A review with special reference to enteropathogenic *Escherichia coli* as well as certain enteric disease and their treatment with antibiotics and lactobacilli. J.Milk food Technol. 35(12): 691-702 (1972).
6. Ruyter, P: Development molecular characterization and exploitation of the nisin controlled expression system in *Lactococcus lactis* WAU Dissertation (2494).(1998)
7. Hammes, W.P.and Vogel, R.F. The genus *Lactobacillus* in : The Genera of Lactic acid Bacteria ed. Wood, B.J.B, and Holzapfed, W.H., Blackie A .(1995).
8. Heyman, M. Effect of lactic acid bacteria on Diarrheal diseases. J.Am. C.Nutr. 19 (2): 1378-1468 (2000).
9. Sreekumar, O. and Hosono, A. Immediate effect of *Lactobacillus acidophilus* on the intestinal flora and fecal enzymes of rates and the in vitro inhibition of *Escherichia coli* in coculture, J.Dairy Sci., 83 (5): 931-939 (1999).
10. Delgado, A.; Brito, D.; Fevereiro, P.;Peres, C. and Marques, J.F., AntiMicrobiol activity of *Lb. plantarum*, isolated from a traditional lactic acid fermentation of table olives INRA. EDP. Science. Lait., 81:203-215(2001)
11. Maydani, S.N.and Ha,W. Immunologic effects of Yoghurt. Am.J.Clin. Nutr. 71:861-872(2000).
12. Galves A., Lopez R.L., Abrionel, H., Valdivia, E. and Omar, N.B. Application of Baceriucins in the control of food borne pathogenic and spoilage bacteria. Crit.Rev. Biotechnol.28 (2): 125-152(2008) (Med line).
13. Vignolo, G.M.; Suriani, F.;Holgado, A.P.R. and Oliver, GAntibacterial activity of Lactobacillus strains isolated from dry fermented sausages.J.Appl. Bacteriol., 75:344-349(1993).
14. Trias, R., Baneras, L., Badosa E. And Montesinos, E. Bioprotection of Golden Delicious apples and lceberg lettuce against food borne bacterial pathogens by lactic acid bacteria. Int.J.Food Microbiol. 123(1-2): 50-60.(Medline) (2008)
15. Harrigan, W.F. and Mac Cance, M.E. Laboratory methods in food & dairy Microbbiology .Academic press. London. (1976).

16. Silva, M.; Jacobus, N.V,; Deneke. C. and Gorbach, SL. Antimicrobial substance from a human Lactobacillus strain. Antimicrob. Agents Chemother., 31(8):1231-1233(1987).

17. القصاب، عبد الجبار عمر والخفاجي، زهرة محمود. تأثير الظروف المختلفة على الفعالية التثبيطية للعصيات اللبنية المعوية تجاه البكتريا المعوية المسببة للإسهال. مجلة العلوم الزراعية العراقية، المجلد(3). العدد (1) : 18-26. (1992)

18. Yang, Z. AntiMicrobiol compounds and extracelluar polysaccharides produced by lactic acid bacteria: structures and properties. Department of Food Technology, University of Helsinki. (2000).

19. Cox, G.P. and Briggs, M. Experiments on growth media for lactobacilli. J. Appl. Bacteriol.17 :18-26(1954).

20. Tagg, J.R., Dajain, A.S.and Wannamaker, L.W. Bacteriocins of gram positive bacteria. Bacteriol. Rev., 40(3):722-756(1976)

21. De Man, J.C.; Rogosa, M. and Sharpe, M.E. A medium for the cultivation of lactobacilli.J. Appl. Bacteriol., 23(1):130-135(1960)

22. El- Shafei, H.A.; Abd-El- Sabour, H.; Ibrahim, N. and Mostafa, Y.A. Isoltion, screening and characterization of bacteriocin –producing lactic acid bacteria isolated from traditional fermented food. Microbiol. Res., 154(4):321-331. (2000) (Abstract).

23. Leroy, F and De Vyst, L. Growth of the bacteriocin producing *Lactobacillus sakei* strain CTC 494 in MRS broth is strongly reduced due to nutrient exhaustion: a Nutrient depletion model for the growth of lactic acid bacteria. Appl. Environ. Microbiol. 67 (10): 4407-4413(2001)

24. Verluyten, J.; Leroy, F. and De Vuyst, L. Influence of complex nutrient source on growth and curvacian a production by sausage Isolate *Lactobacillus curvatus* LTH 1174. Appl. Environ. Microbiol.70 (9): 5081-5088 (2004).

25. Carolissen-Mackay,V.;Arendse, G.and Hastings;J.W.Purification of bacteriocins of lactic acid bacteria: problems and pointers. Int. J.Food. Microbiol., 34:1-16. (1997).

26. المشهداني، محمود حسن والمشهداني، كمال علوان خلف. تصميم وتحليل التجارب. جامعة بغداد. (1987)

استخلاص وتشخيص قلويدي (Atropine) و(Scopolametel) في مختلف اعضاء نبات (Datura metel)

ساجدة عباس[1] حسين وزينب طالب عبد زيد[2] ومنى محمود [1] وعصام شاكر[1] وايمان محمد[1] وسهام مزهر[1] ومنى عبد جعفر حسين[1] وعلية حسين عليوي[1]

[1]وزارة و العلوم والتكنولجيا

[2]الجامعة المستنصرية / كلية الهندسة / قسم الهندسة البيئية

ABSTRACT

For the reason that a lot off people suffers from poisoning due to organophosphate compounds, which has been recorded every year by the national health organization. This could be cured by using atropine Alkalies, so a lot off quantities of it are needed and then consumed. The aim of the research is to find materials to be used instead of atropine Alkalies. Atropine and Scopolamine Alkalies were extracted with sulfuric acid (3%) from different organs of Datura metel plant, the extracted material were passed on external (Merck) columns, and HPLC technique was used for determination of the extraction. The results showed that extraction from Datura metel seeds contains the highest possible percentage of Atropine (36%), which scopolamine alkaloid was predominated in other different organs of *Datura metel* . Using the weighting method, the extraction from leaves showed the highest alkaloid contents (82%). The Datura metel plant was taken from Al. Tajji – city in baghdaded.

Key words: Datura metel, Alkaloids, Extraction, Identification, Scopolamine, Atropine, World Health Organization (WHO)

الخلاصة

نظرا" للإعداد الكبيرة لضحايا التسمم بالمبيدات الفسفورية العضوية التي تسجلها منظمة الصحة العالمية سنويا والتي يتم معالجتها باستخدام قلويد Atropine مما ينتج عنه استهلاك كميات كبيرة منه يهدف: البحث إلى إيجاد بدائل لمواد الترياق Antidote من خلال البحث عن أعلى مستوى لقلويد Atropine و Scopolamine في أجزاء مختلفة من نبات *Datura metel* البري (ورق، بذور، جذر، ساق) الطريقة: تم استخلاص قلويد Atropine و Scopolamine باستخدام حامض الكبريتيك (3%) ثم تم امرار المستخلص على عمود التنقية والفصل Extrelu (Merck) Columns واستخدمت تقنية HPLC لغرض التشخيص.النتائج: أظهرت نتائج الدراسة الحالية أن مستخلص بذور نبات Datura metel سجل أعلى نسبة مئوية من قلويد Atropine بلغت 36% ,في حين ساد قلويد Scopolamine على قلويد Atropine في كل من ورق، ساق النبات، وباستخدام الطريقة الوزنية تبين بأن مستخلص الورق يمتلك أعلى محتوى من القلويدات (0.82%).

المقدمة

يعود نبات *Datura metel* إلى العائلة الباذنجانية *Solanaceae* والتي بدورها تحتوي على عدة أنواع, يوجد في العراق ثلاثة أنواع هي *D. innoxia* , *D. stromonium* فضلا عن *Datura metel* تتوزع على شمال ووسط وجنوب العراق والاسم الشائع له انجيل الشيطان (1)، ونظرا لما تحتويه هذه النبتة وبكل أنواعها من قلويدات ذات أهمية طبية جرت العديد من الدراسات من اجل تقييم المحتوى القلويدي لها وبشكل خاص بذور هذه النبتة إلا إن البحوث الحديثة تحاول وبشكل جاد تقييم المحتوى القلويدي لمختلف أجزاء النبتة من أوراق وجذور وسيقان ولمختلف مراحلها التطورية وباستخدام تقنيات أكثر تطورا مثل HPLC/MS ، GC/MS (2,3).

تعد قلويدات Tropane من أهم أنواع القلويدات المشتقة من عدد كبير من النباتات أمثال العائلة الباذنجانية وتحتوي هذه القلويدات على جزئيين هما: الحامض العضوي والكحول وبشكل خاص

atropine- 3d-ol ويمثل قلويد Atropine واحد من أهم أنواع قلويدات Tropane والذي تم عزله من قبل mein عام 1833 (4).

يتأثر المحتوى القلويدي لجنس نبات *Datura* وسيادة القلويد بعوامل عديدة مثل نوع النبات والبيئة وعوامل المناخ فضلا عن عضو النبات الخاضع للفحص والمرحلة التطورية له، فقد بينت دراسة (5) بأن السيادة واضحة لقلويدي *Scopolamine, Hyoscyamine* في ورق وعلب نبات*stramonium Datura* , أما دراسة(6) أشارت إلى أن المحتوى القلويد يتركز في ورق وساق نفس النوع من النبتة في حين أوضحت نتائج دراسات كل من الباحثين (7,8,9) والتي أجريت على نبات *Datura metel* وباستخدام تقنيات حديثة بان التركيز االأعلى هو لقلويد *Scopolamine* وأشارت دراسة (7), بان المحتوى القلويدي يزداد في الفصول الحارة عنه في الفصول الممطرة وأضافت دراسة (8) بأن تراكم قلويد *Scopolamine* يكون اكبر نسبيا" في الأجزاء الهوائية للنبات، وعلى الرغم من أن دراسة (9) كانت قد أكدت ما جاءت به كل من نتائج دراسة الباحثين (7,8) بان قلويد *Scopolamine* هو السائد في نبات *Datura metel* ألا أن نتائجهما أكدت على أن تراكم القلويد يكون في بذور، أوراق و إزهار النبتة عنه في أجزاءها الأخرى.

وقد استخدمت العديد من الدراسات التحليلية لتقدير القلويدات في نبات جنس *Datura* وبشكل خاص قلويد *Atropine* (4) ومع تطور تقنيات الكروموتوغرافيا الحديثة وبشكل مذهل وسريع لفصل وتشخيص القلويدات مثل تقنية HPLC للتقدير الآني لقلويد *Atropine* وبعض القلويدات الأخرى الموجودة في جذور بعض نباتات العائلة الباذنجانية باستخدام عمود الطور العكوس (10) وكانت النتائج لأبأس بها على النطاق التجاري عند استخدام نوعين من المكاشف الضوئي والتفلوري (11), وازدادت كفاءة الفصل ودقة التقدير عندما قام الباحث(2) بتهجين تقنية الكروموتوغرافيا مع تقنيات أخرى حيث شخص 36 قلويد في نيات *D. Ceratocaula* وذلك بالاعتماد على المواد القياسية وامتصاص الكتلة لقلويدات غير مشخصة مسبقا" باستخدام تقنية GC/MS.

الأهمية الطبية لكل من *Scopolamine* و*Atropine* : أن من أهم الاستخدامات الطبية المعروفة لقلويد *Atropine*هي استخدامه في السيطرة على الأعراض المصاحبة لاضطرا بات القناة المعوية *gastrointestinal Tract* حيث يعمل على خفض حركة دوران المعدة والأمعاء المصحوبة بغثيان وخفض افرازات المعدة الحامضية، ويستخدم في معالجة تشنجات المثانة *bladder Spasms* والقرحة *Ulcer Peptic* والتهاب الزائدة الدودية *diverticulitis* ومغص القولون *Colic* والتهاب المثانة *Cystitis* والبنكرياس *Pancreatitis* ويستخدم أيضا"لزيادة معدل ضربات القلب ويقلل من إنتاج اللعاب *saliva* (12) أما فيما يخص استخدامات قلويد *Scopolamine* الطبية فانه يستخدم لمعالجة حالات الغثيان *Nausea* وتشنجات الأمعاء *Intestinal Cramping* ولإغراض معالجة العين *Ophthalmic* وعموما يستخدم كمخدر ومسكن للألم.

حديثا يعتقد بان بالامكان تجربة مدى كفاءة كل من قلويد *Atropine* و *Scopolamine* في معالجة حالات التسمم بالمبيدات الفسفورية العضوية وذلك لامتلاكهم خصائص مضادة لإنزيم *Acetylcholine* حيث تعمل كمنافسات مقاومة للإنزيم (5).

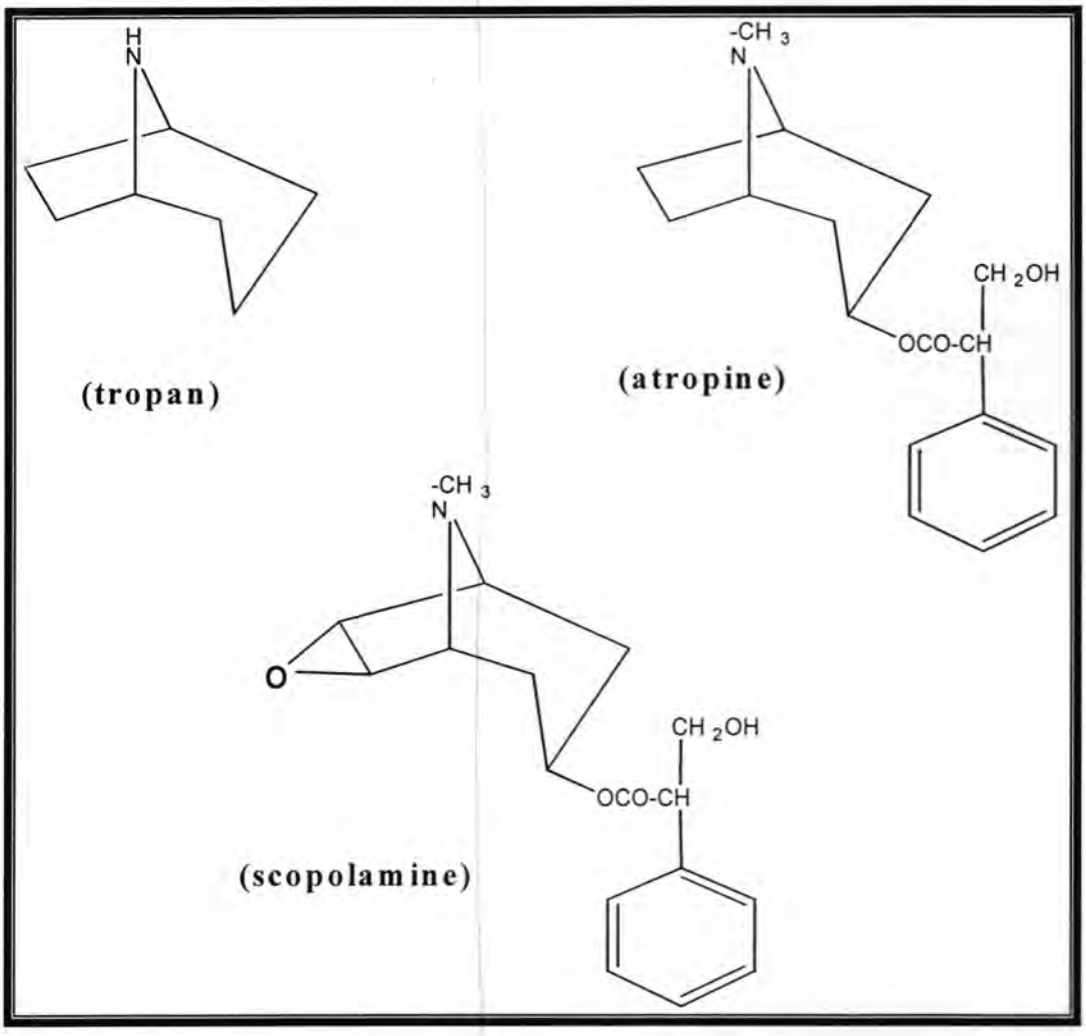

المواد وطرائق العمل

الاستخلاص

تم جلب عينة نبات *Datura metel* البري من منطقة التاجي وتم الاستعانة بالاستاذ الدكتور علي الموسوي / كلية العلوم – جامعة بغداد لتصنيف النبات, حيث تم اخذ اربع نماذج من النبات (اوراق, ساق, جذور, بذور), ووزن كل نموذج هو 100غرام ومن ثم تم عمل الخطوات الاتية علية:

1- طحن 100غم من نبات *Datura metel* (بذور،أوراق،ساق وجذور) وذلك بعد تجفيفه بدرجة حرارة 50م لمدة ساعتين.

2- نقع النموذج بمحلول حامض الكبريتيك (200ml) تركيز3% لمدة ساعتين بدرجة حرارة الغرفة ورشح النموذج باستخدام ورق ترشيح مناسب.

ملاحظة: تم استخدام محلول ماير في هذه المرحلة للكشف عن وجود القلويدات في المستخلص.

3-رفع الأس الهيدروجيني باستخدام محلول الامونيا إلى 10-9 = PH.

استخلاص الطور الصلب

1-تم امرار1ml من النموذج المستخلص خلال عمود Extrelut وترك لمدة 10-5 دقائق.

2-أضيف الى العمود 6ml من المثلين كلورايد وتم جمع المحلول النازل من العمود وترك ليجف بدرجة حرارة الغرفة.

3- تم إذابة الراسب بكمية 0.5m من الميثانول لغرض تهيئة النموذج للفحص(2).

الكشف النوعي
تم استخدام كاشف ماير للكشف النوعي عن القلويدات ويدل تكون راسب ابيض أو مضبب على وجود القلويدات وللتأكيد تم استخدام كرموتوكرافيا الطبقة الرقيقة Thin layer Chromatography(TLC) حيث تم خلط أكثر من مذيب عضوي لكل قلويد.

التقدير الكمي لكل من *Atropine* و *Scopolamine*
تم استخدام جهاز HPLC لتقدير كل من قلويد *Atropine* و *Scopolamine* في مستلخص نبات *Datura metel* وذلك بمقارنة نتائج التحليل مع نتائج المادة القياسية الموضحة في كل من الشكل رقم (2,1) على التوالي، إذا تم امرار محلول المستخلص على عمود نوع ODSc18 (25cm 4.6mm) مع استعمال الطور المتحرك المكون من ميثانول وبفرالفوسفات (0.1m) وبنسبة (30:70) ومعدل جريان 0.5ml/mint وبمكشاف طيفي عند الطول الموجي 228nm.

النتائج والمناقشة

يبين الجدول رقم (1) بان أعلى نسبة استخلاص للقلويدات بلغت 0.82% وكانت لمستخلص ورق نبات *Datura metel* ، يليه مستخلص البذور 0.36 ثم الساق والجذور 0.13,0.15 على التوالي , إلا أن نوع القلويد وسيادة القلويد تختلف من عضو نباتي لأخر وهذا يعتمد على موقع تصنيع وتوزيع القلويدات, حيث كانت السيادة واضحة في مستخلص الأوراق لقلويد *Scopolamine* ويوضح الجدول أيضا إلى أن مستخلص البذور يحتوي على أعلى نسبة مئوية لقلويد *Atropine* 36.00 و أدناه في مستخلص الجذور11.40.

جدول - 1: يبين النسبة المئوية لمستخلص القلويدات لأجزاء النبات المختلفة مع النسب المئوية لكل من قلويد *Atropine* و *Scopolamine* في مستخلص القلويدات

ت	العضو النباتي	Alkaloids% من الوزن الكلي للنبات	Atropine% من الوزن الكلي للمستخلص	Scopolamine% من الوزن الكلي للمستخلص
1	أوراق	0.82	13.00	36.00
2	بذور	o.36	36.00	18.00
3	ساق	o.15	15.88	34.00
4	جذر	0.13	11.40	26.00

يمثل الشكل رقم (2,1) مخططات فحص HPLC لكل من قلويد *Atropine* و *Scopolamine* القياسيتين متمثلة بزمن الاحتجاز Retention time (Rt) أما الاشكال 6,5,4,3 تمثل مخططات فحص HPLC لمستخلص ورق , بذور، ساق وجذر نبات *Datura metel* على التوالي, وبالاعتماد على معدل زمن الاحتجاز (Rt) لكل قلويد ولان طريقة الاستخلاص المستخدمة لا تستخلص إلا القلويدات وبالاعتماد على نتائج كل البحوث المنشورة والتي تم الإشارة لها في مقدمة البحث والتي أكدت على أن النبات قيد الدراسة لا يحتوي إلا على القلويدات تم تحديد أكثر من 12 قلويد متوزعة على مختلف أجزاء النبات وعلى الرغم من اختلاف نسب وجود كل من قلويد *Atropine* و *Scopolamine* إلا أن كل أعضاء النبات تحتوي على كلا القلويدين وان السيادة كانت واضحة لقلويد *Scopolamine* وفي جميع الأعضاء باستثناء مستخلص البذور وهذا مماثل لنتائج كل الدراسات التي تم الاشاره لها في مقدمة الدراسة الا إنها مخالفة لنتائج الدراسات المحلية والتي غالبا ما تعتمد على المذيبات العضوية وبشكل خاص الكلورفورم كمذيب عضوي نهائي قد لا يكون له القدرة على إذابة قلويد *Scopolamine* مما يؤدي إلى ظهور قلويد *Atropine* على

انه القلويد السائد في مستخلص ورق نبات *Datura metel* وهذا ما سيتم إيضاحه وإثباته في دراسة لاحقة أن شاء الله. وعموما يشكل كل من قلويد *Atropine* و *Scopolamine* في هذه الدراسة ما مقداره 50% من وزن المستخلص القلويدي الكلي.

إن إعادة تقييم المحتوى القلويدي وتحديد سيادة القلويد ولمختلف أعضاء النبات وباستخدام تقنيات أكثر تطورا مثل HPLC اظهر وجود أعداد من القلويدات لم يتم تسجيلها مسبقا وهذا مماثل لنتائج دراسة(2) حيث اظهر وجود 36 قلويد متوزعة على مختلف أعضاء نبات *Datura ceratocaula* وذلك باستخدام تقنية GC/MS وبالاعتماد على الوزن الجزيئي لكل قلويد وزمن الاحتجاز (Rt).

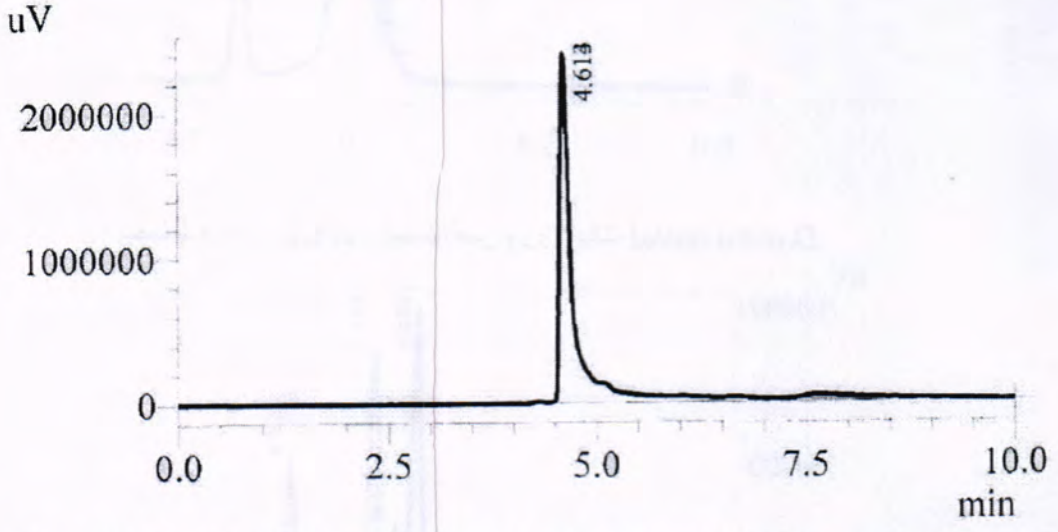

شكل -1: مخطط فحص HPLC للمادة القياسية *atropine* متمثل بزمن الاحتجاز Rt = 4.618

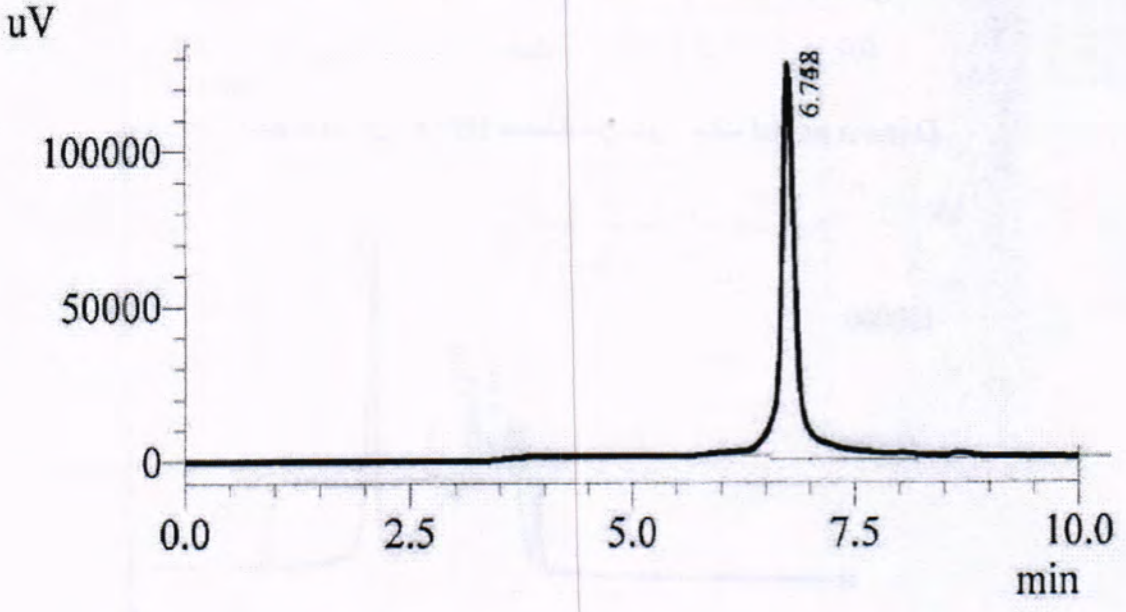

شكل -2: مخطط فحص HPLC للمادة القياسية *Scopolanine* متمثل بزمن الاحتجاز Rt = 6.748

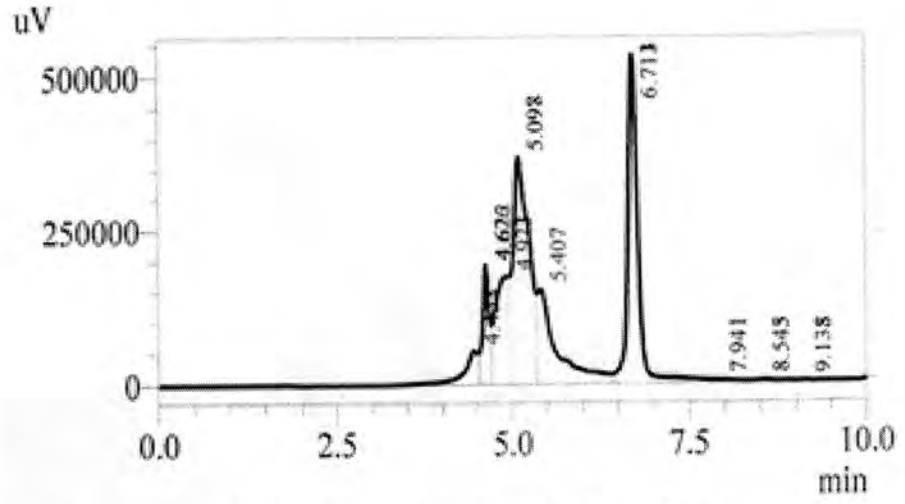

شكل -3: مخطط فحص HPLC للمستخلص ورق نبات *Datura metel*

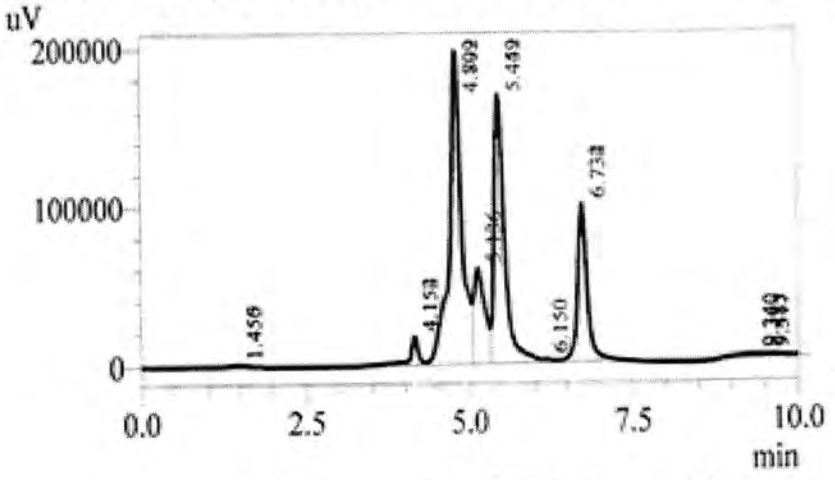

شكل -4: مخطط فحص HPLC للمستخلص بذور نبات *Datura metel*

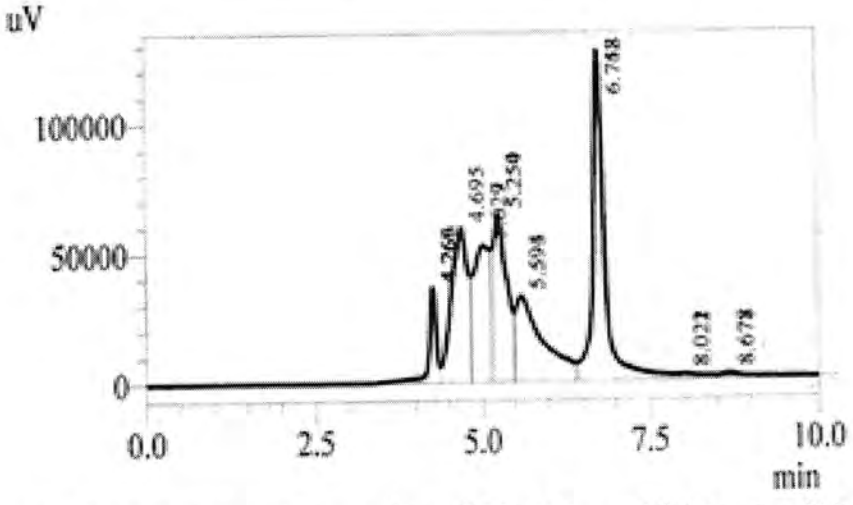

شكل -5: مخطط فحص HPLC للمستخلص ساق نبات *Datura metel*

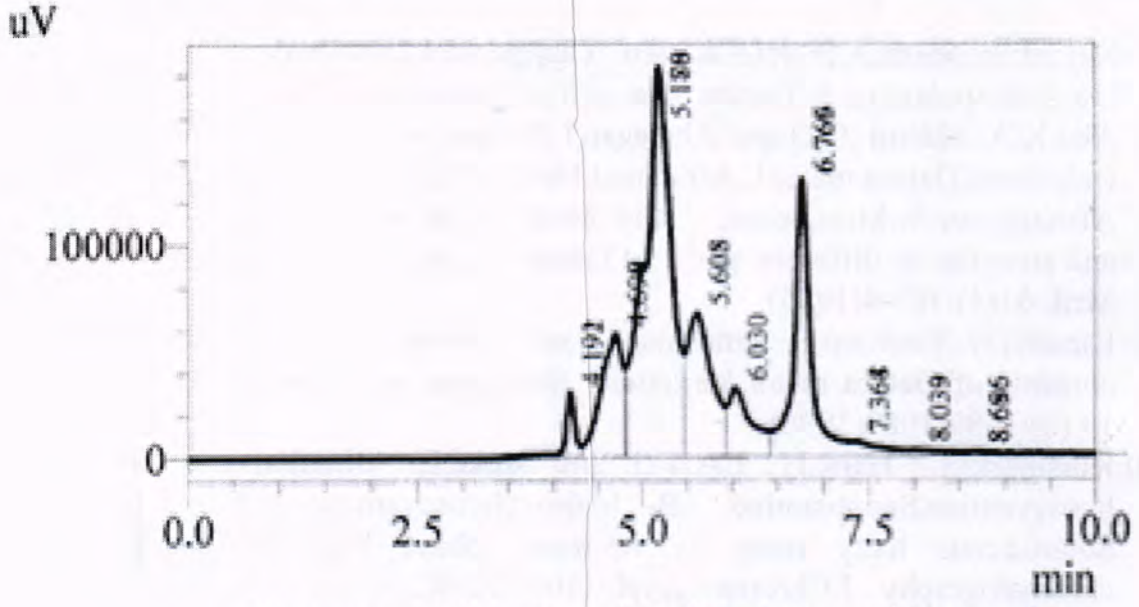

شكل -6: مخطط فحص HPLC للمستخلص جذور نبات *Datura metel*

1- تم تحديد أعلى نسبة مئوية لقلويد *Atropine* في مستخلص بذور نبات *Datura* metel حيث بلغت (36%) من الوزن الكلي للمستخلص.
2- سيادة واضحة لقلويد *Scopolamine* في مستخلص جميع أعضاء نبات *Datura metel* باستثناء مستخلص البذور وبنسب تتراوح (18%-36) من الوزن الكلي للمستخلص.
3- تحديد أعلى نسبة مئوية للقلويدات في مستخلص ورق نبات *Datura metel* حيث بلغت نسبتها حوالي (0.82%) من الوزن الكلي للنبات.
1- أجراء تجارب مختبرية وباستخدام الحيوانات التجريبية لمعرفة مدى كفاءة مستخلص بذور واوراق نبات *Datura metel* الحاوي على نسبة عالية من قلويد *Atropine* و *Scopolamine* في معالجة حالات التسمم بالمبيدات الفسفورية العضوية.
4- أعادة تقييم المحتوى القلويدي لبعض النباتات الطبية منها على وجه الخصوص وباستخدام تقنيات أكثر تطورا مثل HPLC/MS, GC/MS لإعادة تصنيفها لاسيما التي تم تصنيفها بالاعتماد على محتواها من القلويدات وسيادة القلويد.

المصادر

1. السامرائي ،خ.و.ع.(1983). توزيع القلويدات واهميتها التصنيفية في بعض الانواع البرية من العائلة الباذنجانية Solanaceae في العراق. رسالة ماجستير (كلية العلوم / جامعة بغداد).
2. Berkov,SAlkaloids of Datura Ceratocaula.Z.Naturforsch.58c:455-8. (2003).
3. Goren,A.C.;Bilsel,G.bilsel,M.andyenisoy-Karakas,S.Simple high-performance Liquid chromatographic method for determination of atropine and obidox - ime in aparenteral injection device .J. chromatography A.1057:237 .9 (2004).
4. Snell,F.D. and Hilton,C.L.Encyclopedia of Industrial Chemical Analysis. 4:594(1967).
5. Iranbkhsh,A.;Oshaghi,M.A.and Majd,A.Distribution of atropine and Scopola - mine indifferent organs on stages of development in D.Stramonum L. (Solanaceae). Structure and Ultrastructure. of Biosynthesizing cells .ACTA Biologica Cracoviens Series Botanion 48,1:13-8(2004).

6. Miraldi,E.;Masti,A.;Ferri,S.&Barni Comparini,I,Distribution of hyoscyam - ine & Scopolamine in Datura Stramonium.Fitoterapia.72(6):644-8 (2001).
7. Abo,K.A.;Salami ,O.O.and Abelegan,I.O.varation of total hyoscine content of Cultivated Datura metel L.Afr.J.med.Med.Sci.22(1):45-7 (1993).
8. Afsharypuor,S.;Mostajeran, A.and Mokhtary,R.Variation of Scopolamine and arropine in different parts of Datura metel during development . Plant. Med. 61(4):383-4(1995).
9. Hiraoka,N.;Tashimo,K.:Kinoshita,C. and Hirooka,M.Genotypes and alkaloid contents of Datura metel Varicties. Biological and Pharmaceutical bulletin. 19 (8):1086-1089(1996).
10. Kursinszki,L.; Hank,H.; Laszlo,I. and Szoke,E. Simultaneous Analysis of hyoscyamine,Scopolamine, 6B- hydroxyhyoscyamine and apoatropine in Solanaceous hairy roots by reversed- phase high-Performance Liquid chromatography . J.Chromatography.1091:32-9(2005).
11. Cieri,U.R.Determination of Altropine (Hyoscyamine) Su.Commercial Prod - ucts by Lijuid chromatography with UV Absorbance and Fluorescence Deteet multilaboratory stuody.J.AOAC INTERN-ATONAL.86:1128-1134 (2003).
12. Inter net Medmaster Patient Drug Information American Society of Health System Parmacists Hyoscyamine(2008).

تحديد بعض مستويات العناصر والانزيمات للمريضات المصابات بداء المقوسات Toxoplasmosis

[1]سالم رشيد العبيدي و [2]بدر محمد العزاوي و[2]آمال خضير عباس و[2]شذى خضير عباس
[1] جامعة بغداد / كلية الطب
[2] الجامعة المستنصرية / كلية العلوم / قسم علوم الحياة

ABSTRACT

Our study includes biochemical changes accompanied the pregnancies women twenty five infection with Toxoplasmosis. In comparison with the results of 10 normally delivered pregnancies. The results of present study summarized as follows:

- Significant increase in trace and essential elements levels (Mg, Mn, Cu, Ca) in blood serum of patient groups while no significant increase in Se (18 mmmol/L) (0.265 ppm) and (0.93 µmmol/L) (22.8 mmol/L) respectively, in compared with control groups (10.4 mmol/L, 0.043 mmol/L, 0.49 µmmol/L, 9.7 mmol/L) while Se 0.043 ppm in compared with control groups 0.033 ppm.
- The result of lipid peroxidation (MDA) showed significant increase for all patient groups (0.0107 mmol/L) in compared with control groups (0.0065 mmol/L) and we can consider the level of MDA as marker for evaluating the disease.
- Analysis activity of all other antioxidants (Cat, GSH and SoD) showed significant decrease 73.4 u/g, 0.143 mmol/L, 17.67 u/L for all patient groups in compared with normal was 158.9 u/g, 0.84 mmol/L, 20.9 u/g. The correlation factor was (0.170) between MDA and GSH.

الخلاصة

اجريت هذه الدراسة لمعرفة بعض المتغيرات الكيمائية الحياتية المرافقة لحالات الاصابة بداء المقوسات اثناء الحمل حيث تم اختيار (25) نساء حامل مصابة بداء المقوسات اجريت المقارنة مع (10)نساء ذات حمل طبيعي انتهى حملهن بولادة طبيعية . بينت نتائج الدراسة المعطيات الاتية:-

* ان نواتج الاكسدة الفوقية للدهون(MDA) في بلازما الدم اظهرت ارتفاعا معنويا البالغ (0.01017) في المريضات مقارنة بالسيطرة (0.0065) ومن الممكن اعتبار مستوى ال(MDA) في البلازما علاقة جيدة لتقديم المرض.
* أظهرت النتائج انخفاضا في (GSH,SOD,CAT) البالغ (73.6 U/g,17.6 U/L, 0.143mmol/L) مقارنة بنساء السيطرة (0.845mm0L/L,620.96U/L,150.97U/g,) .

لوحظ وجود علاقة سالبة بين (GSH,MDA) وكان عامل الارتباط المصحح (r) وقيمته (0.170).

* ارتفعت بشكل معنوي مستويات العناصر النزرة الاساسية (Ca,Cu, Mn, Mg)وغير معنويSe في المريضات (18mmoL/L±0.87) و(0.265ppm±0.0087) و(0.93mmol/l±0.07) و(22.8mmol/l±4.5) على التوالي مقارنة بنساء السيطره (10.4mmol/l±1.18) (0.043ppmt0..0008) (0.49mm0l/l±0.083) و(9.7mmol/l±0.56)؛ اما السلينوم فبلغ مستواه(0.043ppm±0.005) عند مقارنتها بالسيطرة (0.33ppm±0.037).

المقدمة

يحدث داء المقوسات Toxoplasmosis في الإنسان نتيجة الإصابة بالطفيلي Oocyst الموجود في براز القطط أو أكل اللحوم غير المطهية بصورة جيدة (1). كما يمكن أن ينتقل الطفيلي عموديا من الأم إلى الجنين خصوصا خلال الأشهر الثلاثة الأولى من الحمل مؤدياً إلى حالات نقص ولادي شديدة يمكن أن تطول بصورة أساسية الجهاز العصبي المركزي للجنين و هذا ما يؤدي إلى التخلف العقلي أو الموت الذي ينتهي بإجهاض المرأة الحامل لذلك الجنين (2).

توجد في الجسم بعض العناصر بكميات قليلة لدرجة انه سميت بالعناصر النزرة. ان كمية هذه المواد في الأطعمة ضئيلة أيضا، غير أنها على قلتها تعد ذات أهمية كبيرة في حياة الكائن الحي كأهمية العناصر الأساسية في الجسم (3 ,4).

أشار الباحثون (5)، أن حصول تذبذب في مستويات تلك العناصر في مصل دم الحامل نتيجة قلة تناول أو الزيادة في محتوى المواد الغذائية ينتج عنها مشاكل صحية خطيرة لكل من الأم و جنينها لذلك تشير دراسات عديدة إلى الدور الواضح لعناصر النحاس copper (Cu) و المغنيسويم magnesium (Mg) و المنغنيز manganese (Mn) و السلينيوم selenium (Se) و الكالسيوم calcium (Ca) أثناء فترة الحمل (6, 7, 8).

على الرغم من تكون الجذور الحرة بشكل مستمر وكبير داخل الخلايا الحية هنالك مجموعة من الانظمة الدفاعية لمضادات التأكسد التي اما ان تمنع تكون الجذور الحرة او تعادل تاثيرها الضار بعد تكوينها ويمكن تعريف مضادات التاكسد بانها (اي مادة عند توفرها بتراكيز واطئة مع المادة القابلة او المعرضة للتأكسد تؤخر او تمنع عملية التاكسد) ويمكن لهذه المركبات او الانظمة ان تعمل على مستويات وبائية مختلفة منها (9).

متلازمة فرط الاكسدة نتيجة لتزامن معظم الحالات المعروفة التي تم دراستها بعمق مع تكوين كميات كبيرة من الجذور الحرة والتي بدورها تكون مسؤولة عن احداث العديد من التغييرات الكيمياوية الحياتية داخل الخلايا ظهرت تسمية متلازمة فرط الاكسدة التي يتم الاخذ بها كتفسير منطقي لالية حدوث المرض وموت الخلايا وتعد حالة اقفار العضلة القلبية من الحالات التي تحدث فيها متلازمة فرط الاكسدة القلبية بوضوح عام. وهنالك عوامل عديدة يمكن ان تؤدي الى حدوث متلازمة فرط الاكسدة واهمها (الصدمة, الحرارة, الاشعاعات الايونية) والخناق (Hypoxia) السموم والتمارين العنيفة (9).

يعرف المالون الديهايد على انه جزئية تتكون من ثلاث ذرات كربون مع مجموعتي الدهايد تعملان على زيادة فعالية مالون الديهايد (MDA) مع الجزيئات الاخرى (10).

يعد الـ(MDA) واحد من اهم الدلائل التي تستعمل للبحث عن وجود فرط الاكسدة ويشكل (20%) من النواتج النهائية المشتقة من الدهون، وهنالك مركبات مثل (الالدهايدات طويلة السلسلة) والالدهايدات قصيرة السلسلة, الكينونات عند تفاعلها مع (MDA) تكون اصنافا عالية الفعالية وتكون ما يسمى فرط الكاربونايل (Carbonyl stress) والذي يعد مظهر شائع للمرض.

يكون التأثير السمي لمركبات الالدهايدات ناشئ من قابليتها على التفاعل مع الجزيئات الخلوية الحية مكونة مركبات تسبب فقدان الخلية لوظيفتها الفسلجية (11, 12) .

السوبر اوكساید دسميوتيز هو احد الانزيمات المضاد للاكسدة Metaleprotein وله اهمية بايولوجية حيث يوجد في جميع الخلايا التي تؤيض الاوكسجين طبيعيا خلال الفسفرة التأكسدية (الفسفرة الهوائية)(Oxidative –phosphorlation) حيث يقوم بتخليصها من الجذور الحرة لأيون الاوكسيجين الفائق Anions superoxidate (O_2^-) وان اول من اكتشفه (Fidovich) وكان يعرف سابقا باسم Indophenol oxidase (14). اشار الباحث (13) الى انه في خلايا حقيقية النواة هنالك ثلاثة انواع من انزيم السوبر اوكساید دسيموتيز (SOD) من بينهم Cuizn-SOD ويقع في العصارة الخلوية Cytosol للخلايا الحيوانية و mn-SOD يقع في المايتوكوندريا، اما EC-SOD فيتواجد في البكتريا والطحالب والنباتات الراقية.

الهدف من الدراسة : معرفة تأثير مضادات الاكسدة الغير الانزيمية مثل الكلوتاثيون (GSH) والانزيمية مثل كاتلايز(Cat و SOD) وبعض العناصر النزرة على المصابات بداء المقوسات .

المواد وطرق العمل

عينات الدراسة

تم اختيار 35 عينة، 25 عينة مصابة بداء المقوسات Toxoplasma gondii و 10 عينات سيطرة غير مصابات بداء المقوسات. استخدم في هذا الفحص عدة جاهزة (Toxoplasmosis Kit) . وتم تعيين ثنائي مالون الالديهايد MDA (Malondialdehyde). تم تعيين MDA في البلازما وفق طريقة (15). وتعيين مستوى الكلوتاثيون Glutathion (GSH) في البلازما وفقا لطريقة (16). وتعيين مستوى إنزيم الكاتاليز Catalase (CAT) . في كريات الدم الحمراء باستخدام طريقة (17).

قياس فعالية انزيم السوبر اوكساید دسميوتيز الكلية Determination of Superoxide Dismutase Activity

اتبعت طريقة باير و فريدوفج (18) لقياس فعالية الإنزيم الكلية.

قياس تركيز بعض العناصر النزرة والأساسية للنحاس والمغنسيوم و المنغنيز و السلينوم والكالسيوم في مصل الدم

استخدام تقنية الامتصاص الذري اللالهيبي Flameles atomic absorption spectrophotometer(FAAS)

لقياس تركيز عناصر (النحاسCU و المغنسيوم Mg والمنغنيز Mn والسلينومSe) , استخدمت طريقة الامتصاص الذري اللالهيبي FAAS والتي هي الطريقة الأكثر حساسية وأجريت طريقة العمل بإتباع تعليمات الشركة المصنعة, التي يعتمد مبدا العمل فيها على ذرات العنصر في حالتها المستقرة تمتص ضوء الطول الموجي نفسه كما هو ينبعث في حين تهيجها, هذا وقد تمت معايرة الجهاز باستخدام محاليل Cu^{+2} و Mg^{+2} و Mn^{+2} و Se^{+2} القياسية. وان مستويات العناصر (Cu^{+2} و Mg^{+2} و Mn^{+2} و Se^{+2}) تم تحديدها على طول موجي قدره 196nm,200nm,285nm,324nm, على التوالي وعبر عن تراكيزها بـ ppm لكل من عنصري المنغنيز والسلينوم, وبـ mmol/L لعنصر المغنسيوم وبـ µmmol/L لعنصر النحاس .(19)

النتائج والمناقشة

يتبين من النتائج زيادة في مستوى (MDA) (0.202 mmol/L) مقارنة بالسيطرة 0.033 mmol/L و السبب حصول زيادة في تكوين اصناف جذور الاوكسجين الحرة (Ros) ادى الى زيادة كبيرة في اكسدة الدهون كما هو واضح من الزيادة الكبيرة في مستويات (MDA) و هذا يتفق مع ما توصل اليه الباحثون (21, 22, 23). و لقد لاحظ الباحثين (24) وجود خلل واضح في عمل الانظمة المضادة للتاكسد في خلايا الدم عند المرضى الذين يعانون من امراض الذبحة غير المستقرة و احتشاء العضلة القلبية مما يؤدي الى ارتفاع مستويات (MDA) في البلازما و هو دليل واضح على الدور المهم الذي تلعبه عملية تكوين الجذور الحرة و التي تؤدي الى تلف الانسجة.

كما لوحظ انخفاض كبير في مضاد الاكسدة الطبيعي (GSH) في المريضات كان 0.143 mmol/L مقارنة بالسيطرة 0.845 mmol/L. ان هذا الانخفاض في مستوى (GSH) يمكن ان يعزى الى زيادة حالة فرط الاكسدة و تكوين الجذور الحرة التي تستهلك بسرعة هذه العامل المضاد للتاكسد و الذي يعد خط الدفاع الاول (25) كما ان مستوى الكلوتاثيون (GSH) يمكن ان يتاثر بعوامل اخرى (العمر – درجة النمو – الحالة الغذائية – ا لتوازن الغذائي – و مستوى تصنيع (GSH) داخل الخلايا (26).

تبين النتائج أن هناك انخفاضا معنويا في مستوى انزيم Catalase في المريضات 73.6 u/L مقارنة بالسيطرة 158.9 u/L و يمكن أن نعزي انخفاض مستوى الكاتاليز إلى الأسباب الاتية:

- ينخفض مستوى (catalase) بازدياد مستوى الـ(H2O2) الذي له القابلية على تحفيز عملية بيروكسيد الدهون في المصل بمعدل عدة أضعاف عما هو عليه في الحالة الطبيعية (27).
- ينخفض مستوى (catalase) من جراء الضرر الحاصل في تلف الأنسجة نتيجة الانخفاض في الوظيفة الدفاعية لكل من (SoD, GSH, CAT) الذي يؤدي إلى زيادة نفوذية الغشاء الخلوي مما يؤدي إلى فقدان الإنزيمات الموجودة داخل الخلية (28).
- يعد الكاتاليز احد المزيلات و الطاردات للجذور الحرة إذ يقوم بإزالة تأثير الـ(H2O2) السمي في الخلية(29).
- ينخفض مستوى الـ(CAT) نتيجة إنتاج كريات الدم البيضاء الملتهمة بيروكسيد الهيدروجين بكميات محسوسة و عندما تحفز كريات الدم البيضاء نتيجة الايض الخلوي فان فعالية الإنزيمات الموجودة في السايتوبلازم تنخفض بسرعة بسبب تثبيط البيروكسيدات (30).
- إن حالة تكون الجذور الحرة و زيادة فرط الأكسدة تساعد على استهلاك هذا الإنزيم الدفاعي الموجود داخل الخلية بسرعة (28)، أما إنزيم (SOD) فقد كان انخفاض معنويا في المريضات إذ بلغ مستواه

17.67 u/L مقارنة بالسيطرة 20.96 u/L و هو من مضادات الأكسدة الانزيمية و التي لها دور في المحافظة على الفسلجة الخلوية الطبيعية و مقاومة الأمراض بالإضافة إلى إزاحة (Ros) الجذور الاوكسجينية الفعالة الحرة فهي إحدى الميكانيكيات التي ترجع المناعة و الأذى النسيجي يعتمد على التوازن بين مستويات المؤكسدات oxidants و مضادات الأكسدة antioxidants (31).

إن الانخفاض في مستوى SOD ربما حدث من جراء الضرر الحاصل نتيجة الانخفاض في الوظيفة الدفاعية (GSH, CAT) و الذي يؤدي إلى زيادة نفوذية الغشاء الخلوي مما يؤدي إلى فقدان الإنزيمات الموجودة داخل الخلية (28). إن إنتاج كريات الدم البيضاء الملتهمة لـ H_2O_2 بكميات محسوسة و عندما تحفز هذه الخلايا نتيجة الايض الخلوي فان فعالية الإنزيمات الموجودة في السايتوبلازم تنخفض بسبب تثبيط البيروكسيدات (30). كذلك زيادة تكون الجذور الحرة و زيادة فرط الأكسدة تساعد على استهلاك هذا الإنزيم الموجود داخل الخلية بسرعة (28).

و يمكن أن يفسر الارتفاع في عنصر النحاس إلى اختزال في عملية انتقال هذا العنصر من الأم إلى جنينها بسبب حدوث خلل في وظيفة و كفاءة المشيمة و بالأخص النسيج الظهاري لها المتمثل بخلايا الأرومة الغاذية أدى إلى قلة امتصاصه و انتقاله إلى الجنين (32).

أما المغنيسوم كان في المريضات 0.87 ± 18 mmol/L و السيطرة 1.18 ± 0.45 mmol/L و هذا ما يتفق مع الباحثون (33) الذين أشاروا الى ارتفاع تركيز عنصر المغنيسوم خلال مراحل الحمل المختلفة، أما الباحثان (34) فقد لاحظا انخفاضا في مستويات تركيز هذه العناصر لدى النساء الحوامل الأصحاء، و قد يعزى ارتفاع المغنسيوم في أمصال النساء المريضات إلى حصول تلف في الخلايا مما يؤدي إلى زيادة تركيزه خارج الخلايا و بالتالي زيادة تركيزه في مصل الدم، إذ أن تركيز هذه العنصر داخل الخلايا يكون اكبر منه في السوائل خارج الخلايا في الحالة الطبيعية (35).

أما نسبة عنصر المنغنيز في النساء الحوامل المصابات 0.008 ± 0.265 ppm مقارنة بنساء السيطرة 0.0008 ± 0.043 ppm. و هذه النتائج متفقة مع نتائج الباحثين (7) الذين أشاروا إلى ارتفاع تركيز عنصر المنغنيز في النساء المصابات بداء المقوسات و قد اوعزوا السبب في ذلك إلى اختزال انتقال هذه العنصر من الأم إلى جنينها مما يؤدي إلى ارتفاع تركيزه لديهن، أما انخفاض تركيزه في نساء الحمل الطبيعي فقد أوضح الباحث (36) أن مثل هذه الانخفاض في الحوامل الأصحاء يعود إلى استهلاك هذه العنصر من قبل الأجنة أثناء مراحل الحمل .

أما عنصر السلنيوم كان في المريضات (0.0058 ± 0.045 ppm) مقارنة بنساء السيطرة كان (0.0087 ± 0.033 ppm) و لكن هذا الارتفاع غير معنويا و يمكن تعليل هذا الارتفاع إلى احتمال حدوث خلل في عملية النقل المشيمي لعنصر السلنيوم أو عدم نمو المشيمة بشكل جيد و بالتالي قلة انتقاله عبرها إلى الجنين غير إن هذه النتائج لم تتفق مع ما توصل إليه الباحثون (37) الذين أشاروا إلى تساوي تركيز هذه العنصر في أمصال النساء المريضات و النساء ذوات الحمل الطبيعي.

وعنصر الكالسيوم كان في المريضات (4.56 ± 22.8 mmol/L) مقارنة بنساء السيطرة (9.7 ± 0.56 mmol/L) و كان الارتفاع معنويا و يمكن تعليل هذه الارتفاع إلى حاجة الجنين للكالسيوم خلال مراحل الحمل و هذا يتفق مع الباحثين (32, 38) الذين أشاروا إلى ارتفاع تركيز هذا العنصر خلال مراحل الحمل المختلفة و كذلك متفقة مع ما اشار به الباحث (39) إلى زيادة كمية الكالسيوم الممتص خلال المرحلة الثانية من الحمل أكثر من المرحلة الأولى و هذا ما تم ملاحظته في نتائج الدراسة الحالية و قد يعزى ذلك إلى زيادة حاجة الجنين لكميات إضافية من عنصر الكالسيوم التي يأخذها من مجرى دم الأم و التي يستخدمها في بناء و نمو هيكله العظمي (38).

جدول -1 : مستوى MDA و GSH في مجاميع المرضى و السيطرة

Groups	n	MDA, mmol/L	n	GSH, mmol/L
Control	10	0.0338±0.00650 a	10	0.8450±0.01939 a
Patient	25	0.2024±0.01017 b	25	0.1436±0.00529 b

الحروف المتشابهة تعنى عدم وجود فروق معنوية و الحروف المختلفة تعني وجود فروق معنوية عند مستوى احتمالي < 0.05.

جدول 2 : مستوى (CAT) و (SoD) كدليل لمضادات الأكسدة في مجاميع المرضى و السيطرة

Groups	n	CAT activity , u/g Hb	n	SOD, u/L
Control	10	158.97±0.406 a	10	20.96±0.563 a
Patient	25	73.66±1.645 b	25	17.670±0.5730 b

الحروف المتشابهة تعنى عدم وجود فروق معنوية و الحروف المختلفة تعني وجود فروق معنوية عند مستوى احتمالي < 0.05.

جدول -3 : معدل تركيز عنصر النحاس في مصل الدم لمجموعة نساء السيطرة و مجموعة النساء المصابات بداء المقوسات

تركيز النحاس µmmol/L في مصل الدم					
المجموعة	العدد	المعدل	الخطأ القياسي	اقل قيمة	أعلى قيمة
السيطرة	10	0.490 a	0.083	0.2	0.8
المرضى	25	0.93 b	0.07	0.4	1.5

الحروف المتشابهة تعنى عدم وجود فروق معنوية و الحروف المختلفة تعني وجود فروق معنوية عند مستوى احتمالي < 0.05.

جدول -4 : يبين معدل تركيز عنصر المغنسيوم في مصل الدم لدى مجموعة نساء السيطرة و مجموعة النساء المصابات بداء المقوسات

تركيز المغنسيوم mmol/L في مصل الدم					
المجموعة	العدد	المعدل	الخطأ القياسي	اقل قيمة	أعلى قيمة
السيطرة	10	10.45 a	1.18	5	16.5
المرضى	25	18.04 b	0.87	11.5	27

الحروف المتشابهة تعنى عدم وجود فروق معنوية و الحروف المختلفة تعني وجود فروق معنوية عند مستوى احتمالي < 0.05.

جدول -5 : بين معدل عنصر المنغنيز في مصل الدم لمجموعة نساء السيطرة و مجموعة النساء المصابات بداء المقوسات

تركيز المغنيز ppm في مصل الدم					
المجموعة	العدد	المعدل	الخطأ القياسي	اقل قيمة	أعلى قيمة
السيطرة	10	0.043 a	0.0008	0.002	0.01
المرضى	25	0.265 b	0.0087	0.003	0.13

الحروف المتشابهة تعنى عدم وجود فروق معنوية و الحروف المختلفة تعني وجود فروق معنوية عند مستوى احتمالي < 0.05.

جدول -6 : معدل تركيز عنصر السلنيوم في مصل الدم لمجموعة نساء السيطرة و مجموعة النساء المصابات بداء المقوسات

في مصل الدمppmتركيز السلنيوم					
المجموعة	العدد	المعدل	الخطأ القياسي	اقل قيمة	أعلى قيمة
السيطرة	10	0.033 a	0.0087	0.01	0.08
المرضى	25	0.045 a	0.0058	0.02	0.08

الحروف المتشابهة تعنى عدم وجود فروق معنوية و الحروف المختلفة تعني وجود فروق معنوية عند مستوى احتمالي < 0.05.

جدول -7 : معدل تركيز عنصر الكالسيوم في مصل الدم لدى مجموعة السيطرة و مجموعة النساء المصابات بداء المقوسات

في مصل الدم mmol/L تركيز الكالسيوم					
المجموعة	العدد	المعدل	الخطأ القياسي	اقل قيمة	أعلى قيمة
السيطرة	10	9.7 a	0.56	5.2	11.5
المرضى	25	22.8 b	4.56	20	95.5

الحروف المتشابهة تعنى عدم وجود فروق معنوية و الحروف المختلفة تعني وجود فروق معنوية عند مستوى احتمالي < 0.05.

REFERNCES

1. Frenkel, J.K. & Reyer. Specific and protective Immunity to Toxoplasma gondii Infect Immune, 51: 856-863. (1987)
2. Dubey, J. P.. Toxoplasma gondii Med micro chapter 84 : 35. (1995)
3. Arese, N.K.; Erear, R.; Zhang. W. & Schatt, A. Trace elements in wheat flour, and bread and their relation in Trace elements in man and animals. Fisher. P.W.F., Abbe M.R; Cockell; A.C. Coibsor, R.S. 9th Ed NRC Research press Craws. (1997)
4. Tietz,W.N. Fundamental of Clinical Chemistry 3rd Ed., Sanders, W.B. Co., Philadephia, London, Toronto. (1987).
5. Reis.F.; Abdulla, M.; Parr, R.M. (1994). Trace elements contents in food determined by neutron activation analysis and other techniques, Biol, Trace Elem-Res. 43-45, 481-487. Richie, J.R.; Skowronsk, L.; Abrahan, P.; and Lentzinger, Y. Clinical chemistry 42 (1): 64-70. (1996).
6. Kolasa,F. Krajewski, J. Dee, W. Serum copper levels in healthy pregnant women at term and in prolonged pregnancy. Clinekol. Pol; 52(10): 903-905. (1981).
7. Borella, p. Szilagy; A; Than, G; Maternal plasma concentration of magnesium, calcium, zinc and copper in normal and pathological pregnancies Sci. Environ, 99:67-76. (1990).
8. Graham, T.W.; Thurmond, M.C.; Cershwiny, N.E.; Serum Zinc and Copper Concentration in relation to spontaneous abortion in cows: Implicatious for human fetal loss. J. Rep. Fer. 102: 253-262(1994).

9. Hallwell, B. The Lancet,344:721-724(1994).
10. Hundelman, G.J. Evaluation of oxidant in dialysis patients Blood purify, 18: 343-349(2000).
11. Esterbaues, H.; Schaur, R.J.; Zollner, H. Chemistry and biochemistry of 4-hydroxynonenal, malondiaaldehyde and related aldehydes-free radic, Biol. Med, 11:81-128(1991).
12. Miyata,I.;Sanito,A.;Kurokawa,K.Advanced glycation and lipoxidation enproducts; reactive carbonyl compounds-related uremic toxicity, Nephrol Dial Transplant, 16: 8-1(2001).
13. Sun, W. Manganese superoxide Dismutase free radical & Radiation Biology program medical carborator B-180. The University of Lowa. (2001).
14. Misra, H.P Fridovich, I. the role of superoxide anion in the auto oxidation of epinephrine and simple assay for superoxide dismutase, the J. bio chem., 247(10), : 3170-3175 (1972).
15. Aust, S.D. & Buege, J.A. Method Enzymol, 1st Ed; 52:302. (1978).
16. Eillman, G.L. free radicals and anti oxidants. Arch, Biochem Biophys, 2(82): 70-77(1959).
17. Aebi, H. Methods in Enzymatic Analysis. Bergmeryer, H. ed. verlay Chem. Wrinbeim 673. (1974).
18. Beyer, W. F. & Fridovich, I. Assaying for superoxide dismutase activity some large consequences for minor changes in conditions Annaly-Biochem-161:559-560. (1987).
19. Luft, B. Remington, J.S. Toxoplasma encephalitis in patients with the acquired immunodeficiency syndrome medicines, 71: 224-239. (1992).
20. Al-Zamely, A.M. Toward understanding the ischemic heart disease via oxidative hypothesis. Ph.D.Thesis. College of science. Al-Mustansirya University. (2001).
21. Ktawna, O.J. Analysis of biological devlopmen. Ph.D. thesis , college of science of Baghdad univ. (1999).
22. Zhao, X.; Fu. W.; Yuan, W.; Wn, Zig & Yang, Z.; free radicals in biology and medicine , Chin. Med. J-Engl, 109(2): 926-929. (1996).
23. Muzakova,V.;Kandar,R.;Vojtisek,P.Physio, Res, 50(4): 389-396. (2001).
24. Davies,M.J.Pathology of coronary atherosclerosis"In Alexandary R.W.; Schalant,R.C. and Fuster V. Eds Hurts The Heart Arteries and Veins 9th Ed., I: 1161-1173,New York MC. Craw-Hill. (1998).
25. Bridges,A.B.;Scott,N.A.;&Pringleg,T.H.Cloincord; 15:169-194. (1993).
26. Meister,A.Selective modification of Glutathione metabolism,Science, 220 : 472-470. (1983).
27. Baland,L.S.;Review,J.;Nutr.Envir,Med,rell of three radicals and cataly - tic metal ions in human disease , 5:255-280. (1995).
28. Biswas,T.;Pel,I.k.;Naskar, K. et al. Mol-cell Biochem, The free radicals and anti oxidant, 146(2) 99-105(1995).
29. Bagchi, M.; Mukher Jec,S.;&Basu,MK;Indian,J.Bochen-Biophys, oxida

-tive stress and anti oxidant metabolites in patients with thyroid disease , 30(5): 277-281(1993).

30. Beauchamp,and Fridovich, L-Biochem Biophys-Acta, clinical chemistry in diagnoses; 3(7): 50-54. (1973).
31. Schnackenberg,C.G.,Physiological and pathophysiological roles of oxygen radicals in the renal microw as culature. Am.J. Physiol. Reg W. Intergr. Comp. Physiol, 282(2): 335-342(2002).
32. Abdulla, M.T. Zinc & Copper Status in Abortion. MD. Ch.B. Thesis. Coll-Med Univ. Baghdad. (1996).
33. Pikin, R.M.;Reynddus,W.A.;Williams C.A.&Aragis,G.K.Calcium metab -olism in normal pregnancy along Alongitudinal study.Am.J.Obstet & Gynecol, 133(7): 781-790(1979).
34. Prithchard,J.A.& Macdonald,P.C.Williams Obstetrics 6th Ed.,Appleton. Centry. Crofts, New York. (1980).
35. Zilva,J.Fpannall,L.Clinical chemistry in diagnosis and treatment 4th Ed. Lloyd-Luke-LTD, London. (1984).
36. Puls,R.Mineral levels in animal health diagnostic datasherpa internatio - nal, Glearbook, B.C Canada. (1988).
37. Zachra,B.A.;Dobrzgnski,W.;Trafikowska,U.;&Szymanski,W.Blood selenium and glutathione peroxidases in miscarriage 13JOG;108(3):244-247. (2001).
38. Hambidge, K.M. & Droegemuller, W. Changes in plasma and hair concentration of Zink, Copper, Chromium & Maganese during pregnancy Obstet & Gynecol, 44(5): 666-671(1974).
39. Shenolikar, I.S. Absorption of dietary calcium in pregnancy, Am.J. Clin Nutr. 23(1): 63-67(1970).

القيمة الغذائية لبقايا أوراق الشاي غير المستعملة

ثريا عبد الحسين عباس
الجامعة المستنصرية / كلية العلوم / قسم علوم الحياة

ABSTRACT

The study aimed at estimating the nutritional value of tea leaves refuse and the possibility of making use of such refuse as livestock fodder.

The study included the estimation of dry material, proteins, oils, carbohydrates, fibres, and ashes in tea leaves refuse.

Moreover, the study included the estimation of essential and non-essential amino acids in addition to estimating macro elements like Ca and P and micro elements like Fe and Mn. Energy had also been calculated.

The outcome of the study also revealed the possibility of using tea leaves refuse as ruminants fodder, rather than poultry.

الخلاصة

هدفت الدراسة الى تقدير القيمة الغذائية لبقايا اوراق الشاي وامكانية استخدام هذه البقايا كعلف حيواني. وتضمنت الدراسة تقدير المادة الجافة، البروتينات، الدهون، الكاربوهيدرات، الألياف والرماد في بقايا اوراق الشاي. كما وتضمنت الدراسة تقدير الاحماض الامينية الاساسية وغير الاساسية فضلا عن تقدير الطاقة والعناصر المعدنية الكبرى مثل الكالسيوم والفوسفور والعناصر الصغرى مثل الحديد والمنغنيز بينت نتائج الدراسة امكانية استخدام هذه البقايا في تغذية المجترات وليس الدواجن.

المقدمة

يعد الشاي *Camellia sinensis* ثاني مشروب في العالم بعد الماء الذي يمثل المرتبة الاولى وتعد قارة اسيا الموطن الاصلي للشاي وخصوصاً الصين والهند ان الصين والهند من اكثر الدول المنتجة للشاي في العالم في حين ان العرب من اكثر الدول استهلاكاً للشاي كما تعد العراق مستهلكاً كبيراً للشاي والجدول -1- يبين حجم مايستورده العراق من الشاي ومقارنته بالدول الاخرى والجدول -2- يبين المكونات المهمة للشاي. (1،2،3،4).

ونظراً لاهمية الاعلاف في تغذية الحيوانات ولكون معظم الاعلاف مستوردة وتكلف الدولة الكثير من العملة الصعبة ارتأت الضرورة ايجاد بدائل رخيصة الثمن وغير مكلفة. علماً بان هنالك الكثير من البحوث التي اجريت وتجرى لغرض الاستفادة من النباتات وبقاياها في تغذية الحيوانات منها الذرة، الحنطة، الشعير، الرز، كسبه السمسم، جوز الهند، بذور المطاط وبقايا الشاي وغيرها الكثير (5،6،7) إن الدراسة التي قام بها (1) تبين القيمة الغذائية لـ23 مادة علفية من ضمنها بقايا أوراق الشاي وأهميتها في تغذية الحيوانات. كما وتبين بان هنالك كميات كبيرة من بقايا أوراق الشاي ترمى كفضلات في العراق.

من اهداف هذه الدراسة هو تقدير القيمة الغذائية لبقايا اوراق الشاي وامكانية استخدام هذه البقايا في تغذية الحيوانات.

جدول -1: استيراد العراق من الشاي ومقارنته بالدول الاخرى مقدرة بالطن المتري

الدول المستوردة للشاي	1984	1985	1986
العراق	56494	38000	43000
المملكة العربية السعودية	20609	21045	17713
مصر	39499	40678	45000
المغرب	22586	21580	20400
الباكستان	95870	84256	83099

جدول -2: التركيب الكيميائي للشاي

المكونات		% على اساس الوزن الجاف
البروتينات	Proteins	ـــــ
الكاربوهيدرات	Carbohydrates	ـــــ
الاحماض الامينية	Amino acids	15 - 13
المعادن	Minerals	10
الكاروتين	Carotene	29 - 13
الكافئين	Caffeine	4 - 2
الكلايكوسيدات	Glycosides	0.6
متعدد الفينولات	Polyphenols	25 - 10
فلافونول	Flavonol	0.7 - 0.6
الزنك	Zinc	جزء من مليون 30 - 75
المغنيسيوم	Magnesium	جزء من مليون 200 - 400
الفلورايد	Floride	جزء من مليون 90 - 350

المواد وطرق العمل

تم تقدير المادة الجافة، البروتين، الدهن، الآلياف، الرماد والكاربوهيدرات حسب الطرق القياسية المذكورة في AOAC (9). اما العناصر المعدنية الكبرى فتم تقديرها بواسطة جهازي Flame photometer و Spectrophotometer .

اما العناصر الصغرى فتم تقديرها بواسطة جهاز Atomic absorption.

الاحماض الامينية الاساسية وغير الاساسية فقد تم تقديرها بواسطة جهاز تقدير الاحماض الامينية الاوتوماتيكيLKB 4151 automatic amino acid analyzer

قدرت الطاقة حسب الطريقة المذكورة في (13)

النتائج والمناقشة

يظهر من الجدول -3- التركيب الكيميائي لبقايا اوراق الشاي ومقارنته مع بعض البذور والمواد العلفية.

يظهر من نتائج التحليل ان نسبة المادة الجافة قد قاربت بعض البذور وتفوقت على البعض الآخر.

اما فيما يخص المواد البروتينية فنلاحظ ان بقايا اوراق الشاي قد فاقت الشعير والحنطة والذرة الصفراء والبازليا والحمص والعدس وبذور القطن والكتان لذا فانها تصلح ان تكون مصدر بروتيني تستخدام في صناعة الاعلاف كما هو مشار اليه في(8،10،11،12)اما نسبة الدهن فقد تفوقت على الحنطة والشعير والبازليا والعدس. كما لوحظ ان الألياف الموجودة في بقايا اوراق الشاي قد فاقت معظم نباتات المقارنة عدا بذور القطن.ولوحظ أيضاً من النتائج ان الرماد قد ارتفع على معظم نباتات المقارنة عدا فول الصويا وكسبة القطن والسمسم.وكانت نسبة الكاربوهيدرات في اوراق الشاي مقاربة بعض الشيء لبعض المواد ومرتفعه على البعض الآخر(2).

اما الجدول رقم (4) فلوحظ ان نسبه الكالسيوم في بقايا اوراق الشاي قد تفوقت على عناصر المقارنة ماعدا الباقلاء وكسبة السمسم. وان نسبة الفوسفور في بقايا اوراق الشاي كانت قليلة جداً مقارنة مع جميع عناصر المقارنة اما العناصر الصغرى مثل الحديد والمنغنيز فكانت اعلى من جميع نباتات المقارنة.

الجدول -5- يبين الاحماض الامينية الاساسية وغير الاساسية ومقارنتها مع نبات الحنطة. يلاحظ من الجدول بان الاحماض الامينية الاساسية مثل Thr, Lys, Leu, Ile في بقايا اوراق الشاي هي اعلى ماهي عليه في الحنطة اما الاحماض الامينية غير الاساسية في بقايا اوراق الشاي كانت نسبها اعلى ماهي عليه في الحنطة مثل.Asp الاسبارتك، .Ser السيرين، .Gly الكلايسين .Ala الآنين، .His الهستدين، .Arg والأرجنين.

جدول -3: التركيب الكيميائي لمجموعة من المواد العلفية ومقارنتها مع بقايا اوراق الشاي

المواد	المادة الجافة %	البروتين%	الدهن%	الآلياف%	الرماد%	الكاربوهيدرات%
الشاي	91.7	23.6	3.1	12	5	60
الشعير	92.50	10.72	1.42	1.50	3.82	72.39
الحنطة	92.50	16.50	1.72	3.15	2.10	19.5
الذرة الصفراء	89.24	9.03	4.34	2.10	2.33	71.49
البازلاء	90.30	22.45	1.11	7.42	3.60	55.72
العدس	90.43	23.3	0.71	3.72	4.40	58.28
فول الصويا	93.46	34.40	20.13	5.73	6.27	25.12
بذور القطن	91.70	16.40	16.10	30.20	2.10	23.10
الكتان	95.75	22.30	33.60	10.50	4.10	24.95

جدول -4: العناصر المعدنية في أوراق الشاي ومقارنتها مع مواد علفية أخرى

المواد العلفية	العناصر المعدنية الكبرى%		العناصر المعدنية الصغرى mg/kgm	
	الكالسيوم Ca	الفوسفور P	الحديد Fe	المنغنيز Mn
بقايا أوراق الشاي	0.88	0.085	478	497
الشعير	0.24	0.20	260	28
الحنطة	0.10	0.33	52	44
الذرة الصفراء	0.04	0.26	37	8
الباقلاء	1.35	0.49	61	6
الحمص	0.28	0.30	44	19
كسبة بذور القطن	0.31	0.75	148	20
كسبة السمسم	3.22	1.33	190	45
كسبة فول الصويا	0.23	0.76	280	45

جدول -5: مقارنة الاحماض الامينية الموجودة في بقايا اوراق الشاي مع حبوب الحنطة (غم/كغم)

الأحماض الامينية الأساسية Essential a. a	الشاي Tea	الحنطة Wheat
Ile.	5.08	3.2
Leu.	7.21	6.5
Lys.	4.85	2.5
Me + Cys	0.37	3.9
Ph + Tyr	6.5	7.5
Thr.	3.96	1.7
Val.	3.40	4.0
الأحماض الامينية غير الأساسية Non essential a.a	**الشاي Tea**	**الحنطة Wheat**
Asp.	8.63	6.1
Ser.	5.2	4.8
Glu.	8.11	32.0
Pro.	3.62	10.2
Gly.	4.93	4.1
Ala.	4.67	3.4
His.	3.21	2.2
Arg.	4.52	4.4

اما الجدول -6- فيبين فيه الطاقة الحرارية التي يحصل عليها من بقايا اوراق الشاي مقارنة بالمواد الاخرى وكانت كميتها عالية مقارنة بالشعير والحنطة والذرة والباقلاء والعدس وبذور القطن مما يؤكد امكانية استخدام هذه البقايا في تزويد الحيوانات بالطاقة الحرارية. من النتائج التي تم الحصول عليها تبين انه يمكن اعتبار بقايا اوراق الشاي مصدر للبروتين والاحماض الامينية الاساسية وغير الاساسية. فضلاً عن العناصر الكبرى والصغرى والطاقة بالنسبة للمجتبرات وليس الدواجن. لان بقايا اوراق الشاي تحتوي على نسبة عالية من المواد متعددة الفينولات وهذا يعد غير مناسب في تغذية الدواجن كما ذكر(1)

جدول -6: الطاقة كمية لنباتات مختلفة ومقارنتها ببقايا باوراق الشاي

المواد	(Kcal/100gm) energy value
بقايا أوراق الشاي	362.3
الشعير	337.22
الحنطة	357.5
الذرة الصفراء	361.14
الباقلاء	322.67
الحمص	356.57
العدس	332.71
بذور فول الصويا	416.25
بذور القطن	329.9
بذور الكتان	494.1

المصادر

1. Sundara, B. R. and V. Rarindran. Metabolisable energy values for growing chicks of some feedstuffs from srilanka.J.Sci. Food. Agric. 1057 – 1064 (1985).
2. الغذاء والتغذية. نشرة صحية علمية تعنى بمواضيع الغذاء والتغذية. العدد 43 . 4-2 (2007)
3. موسى، طارق ناصر. دراسة مقارنة كيميائية بين شاي كجرات والشاي، مجلة ابن الهيثم للعلوم الصرفة والتطبيقية، العدد 267/5 (1993).
4. Saeed, O.F. The effect of green tea and black tea extract on different cell lines in vitro. M. SC. Thesis, collage of pharmacy. University of Mosul, Iraq (2004).
5. Hubell. C. H. Feedstuffs analysis table. Feed stuffs (USA) 52 (3):42-47(1980).
6. NRC. Nutrient requirements of Domestic Animals.(I)Requirements of Poultry. The National Research Council. Washington (1977).
7. Oluyemi. J. A.; fetuga. B. L.; Endeley. H.N.L. The metabolisable energy value of some feed ingredients for young chicks. Poult. Sci. 55, 611-618 (1967).
8. العاني،رغد نايف عبد الهادي دراسة التأثير التأزري لمستخلص الشاي الاخضر والبابونك مع بعض المضادات الفطرية تجاه خميرة *candida albicas* رسالة ماجستير كلية التربية ابن الهيثم. جامعة بغداد (2005).
9. AOAC., Association of official Analytical chemists.Official methods of Analysis, 13th ed. Washington, D.C. USA (1980).
10. القيسي، مهدي صمد. الصفات الكيمياوية والفيزياوية لزيت بذور الحبة السوداء المحلية *Nigella sativa L.* مجلة علوم المستنصرية،14،(1) (2003).

11.البدري، معد عبد الكريم محمود: تأثير استخدام كسبة العصفر (القرطم) كبديل جزئي وكلي عن بروتينات كسبة فول الصويا في الاداء الانتاجي للدجاج البياض. أطروحة دكتوراه كلية الزراعة. جامعة بغداد (2005).
12.العبيدي، شهاب احمد: تأثير إضافة مستويات مختلفة من مسحوق الحبة السوداء وتفلها الى العليقة في بعض الصفات الانتاجية والمناعية لفروج اللحم. رسالة ماجستير كلية الزراعة – جامعة بغداد (2005).
13.Pearson, D. The chemical analysis of food. Chemical publishing Co. Inc. New yourk (1976).

متابعة استحثاث فعالية انزيم Glutathione S-transferase في الخلايا الورمية والطبيعية المعاملة بعقاري Doxorubicin و Mytomycin-C

محفوظة عباس عمران
جامعة بغداد . كلية العلوم . قسم التقنيات الاحيائية

ABSTRACT

Specific activity of Glutathione S. transferase (GSTs) were studied in cytoplasmic and nuclear fraction of three tumor cell lines (Hep.2, AMN.3 and brain tumor) and normal cells (REF) by tissue culture techniques.

The results revealed that specific activity of GST in cytoplasmic and nuclear fractions of brain tumor cells was increased gradually and significantly from 8.2-17.5 U/mg protein and 4.28-10.27 U/mg protein, respectively with passages progression.

A clear effects of induction GST production in both fractions of tumor and normal cells were revealed after cells were treated with two concentrations of Doxorubicin (DOX) and Mytomycin-C (MMC) only dependent on dose concentrations, in comparison with enzyme levels in negative control cells. And there were low induction of GST in cytoplasmic fractions of tumor cells – except AMN-3 - and normal cells pretreated with catechins then followed by Dox treatment, while the specific activity of GST was increased significantly in cytoplasmic fractions of Hep-2 and REF cells pretreated with catechins then followed by MMC treatment, in comparison with enzyme levels in there cells treated by drugs only . In contrast of , there were significant decreasing of GST production in nuclear fractions of tumor and normal cells pretreated with catechins then followed by DOX and MMC compared in enzyme activity in same fractions of cells treated with drugs (DOX and MMC) only, and unsignificant difference between their activities (pretreated with catechins and drugs) in nuclear fractions of tumor cells except (AMN-3) and normal cells in comparison with enzyme level in negative control cells.

الخلاصة

استخلصت انزيمات Glutathione S-transferase (GST) من سايتوبلازم وانوية اربع خطوط خلوية ، ثلاثة منها ورمية متمثلة بخط خلايا سرطان الحنجرة البشري (Hep-2) ، وخط خلايا سرطان الغدة اللبنية (AMN-3) ، وخط خلايا سرطان الدماغ البشري ، والرابع خط الخلايا الطبيعية لجنين الجرذ (REF).

سجلت نتائج متابعة الفعالية النوعية لانزيمات GST المستخلصة من سايتوبلازم وانوية تمريرات متباينة لخط خلايا سرطان الدماغ البشري ارتفاعاً معنوياً في الفعالية النوعية للانزيم مصاحباً لتقدم تمريرات الخط الخلوي ما بين 22-65 ، تراوحت بين 8.2 – 17.5 وحدة / ملغم بروتين في السايتوبلازم و 4.28 – 10.27 وحدة / ملغم بروتين في الانوية .

اظهرت نتائج معاملة الخطوط الخلوية الورمية (AMN-3 و Hep-2 وخط خلايا سرطان الدماغ) والطبيعية (REF) بعقاري Doxorubicin (DOX) و Mytomycin-C (MMC) بمفردهما قدرة معنوية على حث فعالية انزيم GST في سايتوبلازم وانوية الخلايا معتمداً على تراكيز الجرعة قياساً بمستوى فعالية الانزيم في خلايا السيطرة السالبة ، واستحثاث اقل لفعالية الانزيم في الجزء السايتوبلازمي للخلايا الورمية (باستثناء AMN-3) و الطبيعية المعاملة بالكاتيكينات التي تسبق المعاملة بعقار DOX . بينما ارتفعت الفعالية النوعية معنوياً في الجزء السايتوبلازمي لخلايا Hep-2 و Ref المعاملة بالكاتيكينات التي تسبق المعاملة MMC قياساً بمستوى الانزيم في الخلايا المعاملة بمفردي العقارين .

في حين سجل انخفاض معنوي في فعالية انزيم GST بالجزء النووي للخلايا الورمية و الطبيعية المعاملة بالكاتكينات التي تسبق المعاملة بـ DOX و MMC قياساً مع الفعالية النوعية للانزيم في الاجزاء النووية للخلايا بالعقارين بمفردهما ، و فروق غير معنوية في تلك الفعاليات (للمعاملات المتداخلة) في الاجزاء النوية للخلايا الورمية (باستثناء AMN-3) و الطبيعية قياساً بفعالية الانزيم في الاجزاء النووية لخلايا السيطرة السالبة.

المقدمة

يُعبر عن انزيمات Glutathione S-transferase (Ec 2.5.1.18) بشكل رئيس في سايتوبلازم الخلايا ، اذ تعد من الانزيمات المحثة المتعددة الوظائف ذات الاهمية في تأيض العديد من المركبات غير الاحيائية ، والمتضمنة المسرطانات البيئية وانواع Reactive oxygen species

(ROS)(1) والعوامل العلاجية الكيميائيه(2) فضلاً عن الحماية ضد الجهد التأكسدي للدهون والاحماض النووية (3) .

يزداد مستوى تعبير بعض متناظرات GST بشكل متباين في الانسجة الورمية البشرية او الانسجة الورمية الابتدائية ، فقد سجل ازدياد مستوى GSTπ في انواع مختلفة من الانسجة الورمية للانسان ، كما انه يعد مؤشراً وراثياً لهذه الامراض ، كما سجلت زيادة في فعالية الانزيم في الخلايا السرطانية المقاومة لعقار DOX (Doxorubicin hydrochloride) (4). و cis diamminedichloride) CDDP (platinum) (5) . وقد بينت العديد من الدراسات ارتفاع مستوى الكلوتايثون المختزل Reduced Glutathione (GSH) داخل الخلايا السرطانيه المقاومةDOX و CDDP (6) ، وان لمعاملة الخلايا السرطانية بمثبط للـ γ-glutamyl cysteine synthetase احد الانزيمات الاساسية لتصنيع(GSH) يقلل من مستوى GSH ويزيد من حساسية الخلايا للعقارات المضادة للسرطان خارج الجسم الحي (7) ، اذ يعتقد ان مستوى GSH يرتبط بنظام تدفق DOX و CDDP من خلال النواقل المتعاقبة (ABCs) التي تنشأ بسبب المقاومة للعقار .

يستعمل DOX بوصفه عقاراً ضد السرطان حاو على حلقات متعددة من الانتراسايكلين الفطري (Fungal anthracycline) وله تأثيرات متعددة على الدنا (DNA) ، اذ يتأثر العقار مع معقد الدنا Topolsomorase II مؤدياً الى تكوين كسور في السلسلة المزدوجة للدنا ، او بوساطة التكليب (Intercalating) مباشرة مع الدنا وبالتالي يثبط تضاعف واستنساخ m-RNA ، كما يعرف بكونة عقاراً متخصصاً بطور S-phase من بناء الدنا في دورة الخلية (8) . ويستعمل المايتوماسين _سي (مضاد حيوي مستخلص من *Streptomces capspitosus*) بوصفه عقاراً مطفراً ومضاد للسرطان ، اذ يعمل على تمزيق تضاعف الدنا عن طريق ارتباطه وتكوين ترابطات عرضية مع السلسلة المزدوجة للدنا مؤدياً الى تغير تركيب الدنا وبالتالي يثبط فعالية استنساخ m-RNA ، كما انه يعمل على تكوين كسور في الكروموسوم ، لذا لا تتمكن الخلايا المعاملة به من ادامة نفسها (9) . وقد ثبت ان الخلايا الورمية تكون اكثر حساسية للمايتومايسين _سي في مرحلة متأخرة من طور G1 لدورة الخلية وخلال المراحل المبكرة من تصنيع الدنا (10) .

لذا اقترحت هذه الدراسة لتقييم مستوى انزيمات GST في سايتوبلازم وانوية الخلايا الورمية والطبيعية ومتابعة تأثير معاملتها بعقار DOX و MMC في استحثاث الفعالية الانزيمية GST داخل مزارع الخلايا ، وتأثير استعمال الكاتيكنيات المستخلصة من الشاي الأخضر مع العقار في استنفاذ GSH داخل الخلايا وزيادة حساسية الخلايا الورمية للعلاجات الكيميائية .

المواد وطرائق العمل

تمريرات خط خلايا سرطان الدماغ

جهزت تمريرات مختلفة من خط خلايا سرطان الدماغ المجمدة والمحفوظة في انابيب Cryopresservation داخل النتروجين السائل بدرجة 196- م والمتمثلة بالتمريرات 22 و 37 و 38 ، فضلا عن التمريرتين 58 و 65 للخلايا ذاتها والمنماة في اوعية الزرع النسيجي الحاوي على الوسط المغذي RPMI-1640 والمدعم بـ 5% من مصل العجل الجنيني (FCS) .

تفكيك الخلايا وترسيبها

اذيبت تمريرات مزارع الخلايا المجمدة بوضعها في حمام مائي بدرجة 37 م° ثم نقلت الى انابيب صغيرة (Eppendorff tube) . في حين تم تفكيك تمريرات مزارع الخلايا المنماة في اوعية الزرع النسيجي 25سم^3 (متمثلة بالتمريرتين 58 و 65) باضافة 2 مللتر من محلول التربسين-فرسين الدافئ (المحضر بمزج 20مللتر من محلول التربسين 1% ، و10 مللتر من محلول الفرسين 1% ، و370 مللتر من المحلول الملحي PBS ذو رقم هيدروجيني 7.2) والمعقم من خلال فلتر 0.22 مايكروميتر بغسل الخلايا بالمحلول أولاً ثم تحضينها لمدة 5 دقائق بدرجة 37 م مع 2 مليلتر من محلول الفرسين ، بعدها فككت الخلايا باضافة 3 مللتر من الوسط الزرعي المغذي الكامل والمزج جيدا وتوزيع عالق الخلايا في انابيب صغيرة .

نبذت عوالق الخلايا الموضوعة في الانابيب بسرعة 2000 دورة/دقيقة لمدة 10 دقائق وبدرجة 4 م ، واهمل الرائق ثم غسلت الخلايا المترسبة بـ 1 مللتر من محلول PBS الدافئ واعيد نبذ الخلايا بالظروف ذاتها للتخلص من بقايا الوسط واهمال الرائق ثانية.

استخلاص بروتينات السايتوبلازم والنواة من تمريرات خلايا سرطان الدماغ

استخلصت بروتينات السايتوبلازم وانوية الخلايا الورمية والطبيعية اعتمادا على الطريقة الموصوفة في (11) بالخطوات الاتية:

* اضيف 1-1.5 مللتر من محلول الاستخلاص السايتوبلازمي (Hypotonic solution) المتكون : من 0.5 mM PMSF، 1 mM DTT، 0.1 mM EDTA ، 10 mM KCL، 10 mM HEPES الى راسب الخلايا وتفكيكها ومزجها باستخدام المازج (vortex) وبمرات متناوبة من المزج والتبريد ، ثم المزج لحين تفكيك الخلايا في الانابيب والاحتفاظ بها لمدة 2 ساعة في الثلاجة . نبذت الخلايا بسرعة 1800 دورة/دقيقة ولمدة 2 دقيقة وبدرجة 4 م.

سحب الرائق الذي عدَّ المستخلص السايتوبلازمي (cytoplasmic fraction) واحتفظ به في انابيب صغيرة نظيفة لتقدير فعالية انزيم GST و تركيز البروتين . ثم غسلت الخلايا المترسبة 0.5 مللتر من محلول الاستخلاص السايتوبلازمي مرة ثانية وازيل الرائق المذكور.

* اضيف 0.8 مللتر من محلول الاستخلاص النووي المتكون من: 0.5 mM PMSF ، 1 mM DTT، 0.1 mM EDTA، 420 mM KCL، 50 mM HEPES، 5 mM $MgCl_2$ الى الخلايا المترسبة لاستخلاص البروتينات النووية باستخدام المازج لتفكيك الخلايا وبمرات متناوبة من المزج والتبريد والتجميد اعقبها التذويب ثم المزج ثانية بالظروف ذاتها وبمحلول الاستخلاص نفسه لمرتين بشكل متعاقب لمدة تزيد عن 6 ساعات ثم التجميد لليوم الثاني.

ذوبت الخلايا واعيد النبذ بسرعة 1800 دورة/دقيقة ولمدة 30 دقيقة بدرجة 4 م.

سحب الرائق والذي يمثل مستخلص الجزء النووي (nuclear fraction) لتقدير الفعالية الانزيمية GST وتركيز البروتين.

تقدير فعالية انزيم GST

قدرت فعالية انزيم GST في المستخلصات السايتوبلازمية والنووية والمستحصل عليها من الخطوات المذكورة في اعلاه بالطريقة المعتمدة في (12) باستخدام المطياف الضوئي عن طريق قياس امتصاص المركب المتكون من تفاعل الكلوتاثيون (GSH) والمادة الاساس 1-chloro 2,4-dinitrobenzene (CDNB) على طول موجي 340 نانوميتر بأوقات متعاقبة كل 30 ثانية لمدة 5 دقائق .

حسبت الفعالية الانزيمية (وحدة/مللتر) بالاعتماد على معامل امتصاص المركب 2,4-Dinitrophenylglutathione المساوي الى $\varepsilon = 9.6\ mM^{-1}.cm^{-1}$ (12) استناداً إلى المعادلة الاتية:

$$\text{Enzyme activity(U/ml)} = \frac{\text{Vol assay}}{\varepsilon \times b \times \text{Vol enzyme}} \times \Delta A / \Delta t$$

تعريف وحدة الفعالية

تعرف وحدة الفعالية بانها كمية الانزيم التي تحفز تكوين 1 مايكرومول من 2,4-dinitrophenyl glutathione بالدقيقة وبدرجة 30 م وبتركيز 1 ملي مولار من GSH و CDNB . (12)

حسبت الفعالية النوعية للانزيم تبعا للمعادلة الاتية :

$$\text{الفعالية النوعية (وحدة / ملغم بروتين)} = \frac{\text{الفعالية الأنزيمية (وحدة / مل)}}{\text{تركيز البروتين (ملغم / مل)}}$$

تقدير تركيز البروتين

قدر تركيز البروتين في المستخلصات (السايتوبلازمية والنووية) استنادا الى الطريقة المعتمدة في (13).

تعيين فعالية انزيم GST في مزارع خطوط الخلايا المعاملة بـ DOX أو MMC و الكاتيكينات :

خطوط الخلايا الورمية والطبيعية

جهزت خطوط الخلايا الورمية المتمثلة بـ Hep-2 و AMN-3 ، وخط خلايا سرطان الدماغ ، والطبيعية (REF-3) المنماة في اوعية الزرع النسيجي حجم 25 سم^3 الحاوي على الوسط الزرعي RPMI-1640 المدعم 10% FCS وبالتمريرات ما بين (221-225) و (138-144) و (60-64) و (65-71) على التوالي ، وبواقع 5 أوعية لكل خط من الخطوط الخلوية وفي مرحلة نمو يسبق اكتمال تكون الطبقة الاحادية الكاملة بحيث تغطي الخلايا النامية مايقارب 50% من سطح الوعاء لغرض اعطاء الفرصة للخلايا بالنمو والتكاثر بوجود العقار أو الكاتيكينات والعقار وحسب التقسيمات الاتية :

* عد الوعاء الاول سيطرة سالبة
* اضيف الى الوعاء الثاني الدواء المضاد للسرطان DOX بتركيز 10 مايكروغرام/مللتر لكل الخطوط الخلوية السرطانية والطبيعية قيد الدراسة مع تغير الوسط الزرعي المغذي بآخر جديد.
* اضيف الى الوعاء الثالث الحاوي على خط خلايا Hep-2 و خط خلايا سرطان الدماغ العقار (DOX) بتركيز 15 مايكروغرام/مللتر ، وتركيز 20 مايكروغرام/مللتر الى الوعاء الحاوي على خط خلايا AMN-3 ، REF-3.
* اضيف الى الوعاء الرابع الحاوي على خلايا Hep-2 ، AMN-3 ، خط خلايا سرطان الدماغ على التوالي الكاتيكينات بتركيز 31.5 و 62.5 و 125 مايكروغرام/مللتر ، و بالتركيز الاخير من الكاتيكينات لخلايا REF-3 وبوجود الوسط الزرعي المغذي الجديد ، اعقبها حضن الاوعية بدرجة 37 م ولمدة 6 ساعات ، ثم اضيف DOX بتركيز 10 مايكروغرام/مللتر الى كل الاوعية الحاوية على الخطوط الخلوية الورمية والطبيعية .
* اضيف الى الوعاء الخامس الحاوي على خلايا Hep-2 ، AMN-3 خط خلايا سرطان الدماغ على التوالي الكاتيكينات بتراكيز 31.5 و 62.5 و 125 مايكروغرام/مللتر ، فضلا عن خلايا REF-3 بالتركيز الاخير من الكاتيكينات وبوجود الوسط الزرعي المغذي الجديد . حضنت الاوعية جميعاً بدرجة 37 م ولمدة 24 ساعة.

كما استخدمت 5 اوعية زرع نسيجي اخرى لكل خط من الخطوط الخلايا الورمية والطبيعية لمعاملتها بالكاتيكينات وعقار Mytomycin-C حسب التقسيمات الاتية:

* عد الوعاء الاول كسيطرة سالبة.
* اضيف الى الوعاء الثاني المايتومايسين للحصول على تركيز نهائي 5 مايكروغرام/مللتر لكل الخطوط الخلوية (الورمية والطبيعية) مع تغيير الوسط الزرعي المغذي باخر جديد.
* اضيف الى الوعاء الثالث المايتومايسين للحصول على تركيز نهائي 10 مايكروغرام/مللتر لكل الخطوط الخلوية مع تغيير الوسط الزرعي المغذي باخر جديد.
* اضيف الى الوعاء الرابع الحاوي على خلايا Hep-2 ، و AMN-3 ، و سرطان الدماغ ، الكاتيكينات للحصول على تركيز نهائي 125 مايكروغرام/مللتر، والتركيز 62.5 مايكروغرام/مللتر الى خلايا REF-3 بوجود الوسط الزرعي المغذي ، تلاها حضن الاوعية لمدة 6 ساعات بدرجة 37 م ، ثم اضيف المايتومايسين بتركيز 5 مايكروغرام/مللتر لخطي خلايا Hep-2 ، و REF-3 ، والتركيز 10 مايكروغرام/مللتر لخطي الخلايا AMN-3 ، و سرطان الدماغ .
* اضيف الى الوعاء الخامس الحاوي على الخلايا Hep-2 ، AMN-3 ، وخط خلايا سرطان الدماغ الكاتيكينات للحصول على تركيز نهائي 125 مايكروغرام/مللتر في الوسط الزرعي المغذي المضاف لخطوط ، والتركيز 62.5 مايكروغرام/مللتر الى خلايا REF-3.

حضنت الاوعية جميعا بدرجة حرارة 37 م ولمدة 24-48 ساعة. ومتابعة نمو الخلايا في اوعية الزرع النسيجي .

تمثل التراكيز المعتمدة في الدراسة من DOX و MMC التراكيز المثلى لتثبيط نمو الخلايا الورمية ، كما تمثل التراكيز المتداخلة من العقارين مع الكاتيكينات التوليفة المثلى لتثبيط نمو الخلايا الورمية (بحث مرسل للنشر) .

حصاد الخلايا

سكب الوسط الزرعي الحاوي على عقار DOX اوMMC والكاتيكينات من الاوعية بعد انتهاء مدة التحضين ، غسلت الخلايا الملتصقة بسطوح الاوعية 2-3 مللتر من محلول PBS المعقم والدافيء ، اعقبها تفكيك الخلايا بمحلول التربسين – فرسين ثم اضيف 2 مللتر من الوسط الزرعي المغذي المدعم 5% FCS الى الاوعية لمجانسة عالق الخلايا الذي نقل الى انابيب صغيرة ، واجراء عملية النبذ بسرعة 1000 دورة/دقيقة لمدة 5 دقائق بدرجة 4 م للتخلص من الوسط الزرعي ومحلول التربسين – فرسين (الذي أجري اختبار فعالية أنزيم GST في راشح المزرعة) .

استخلصت بروتينات السايتوبلازم والانوية من الخلايا الورمية والطبيعية المترسبة بعد حصادها بالظروف ذاتها التي تم فيها استخلاص بروتينات سايتوبلازم وانوية خلايا سرطان الدماغ سابقة الذكر في بداية طرائق العمل استناداً الى (11).

استخدم الجزئين (السايتوبلازمي او النووي) لتقدير فعالية انزيم GST وتركيز البروتين لحساب الفعالية النوعية لانزيم GST في الاوعية الخمسة لكل نوع من أنواع الخطوط الخلوية المعاملة بعقاري DOX و MMC والكاتيكينات .

التحليل الاحصائي

اجري التحليل الاحصائي باستخدام نظام احصائي جاهز (Statistical SPSS Version 6 Pakage for Social Scienes) . حللت متغايرات هذه الدراسة والمعتمدة على الفعالية النوعية لانزيم GST. فقد استعمل تحليل التباين (ANOVA) واختبار دنكن لتقويم الفروق المعنوية بين المعاملات ، اذ عدت قيم P المساوية او التي تقل عن 0.05 ذات معنوية احصائيا.

النتائج والمناقشة

متابعة فعالية انزيم GST في خط خلايا سرطان الدماغ البشري خلال تمريرات مختلفة

تبين النتائج الموضحة في الشكل (1) التغاير في الفعالية النوعية لانزيمات GSTs المستخلصة من سايتوبلازم وانوية خط خلايا سرطان الدماغ للتمريرات 22 و 37 و38 و 58 و 65 ، اذ لوحظ وجود ارتفاع تدريجي ومعنوي ($P<0.05$) في الفعالية النوعية لانزيمات GST المستخلصة من سايتوبلازم الخلايا تراوحت بين 8.2-17.51 وحدة/ملغم بروتين مصاحباً لتقدم تمريرات الخط الخلوي السرطاني ، فضلا عن الارتفاع المعنوي ($P<0.05$) في الفعالية النوعية لانزيمات GST المستخلصة من انوية الخلايا تراوحت بين 4.28-10.27 وحدة/ملغم بروتين بتقدم تلك التمريرات .

يعبر عن انزيمات GSTs بشكل رئيس في السايتوبلازم ، اذ تعد من الانزيمات المتعددة الوظائف التي تشارك في التحول الحيوي للمركبات غير الاحيائية وتايض العقارداخل الخلايا ، كما اشارت الدراسات الصيدلانية بمشاركة تلك الانزيمات في ازالة السمية لعدد من الكيميائيات العالية الضرر فضلا عن الدور الحيوي لانزيمات GST لتحفيز اضافة GSH الى المركبات غير الاحيائية الجاذبة للالكترونات (14) ، وللتعبير المفرط لانزيمات GST المتكون في سايتوبلازم الخلايا بتقدم التمريرات دوراً في ازالة أنواع ROS التي تزداد بصورة ايجابية مع انقسامات الخلايا نتيجة الانحرافات الوراثية التي تحدث بتقدم التمريرات ودوراً في اضعاف او اقلال الحساسية الخلوية للعقارات المضادة للسرطان (15).

سجل وجود المتناظر GST_{π} كواحدا من عائلة انزيمات GSTs في الانسجة الورمية او الانسجة التي تسبق التسرطن في الانسان ، لذا فقد استخدم مؤشراً ورمياً للبحث عن السرطان في بعض الأنسجة ، فقد

وجد الباحث Goto (16) فعالية مناعية لـ GST في سايتوبلازم الخلايا السرطانية ، اذ كانت تلك الفعالية عالية نسبيا في الخطوط الخلوية السرطانية المتمثلة بـ T98G و PC-6 و A549 بالقياس مع الخطوط الخلوية THP-1 ، A2780 ، HCT8 ، فضلاً عن ملاحظة الفعالية النوعية لـ GST_{π} في انوية الخلايا T98G و PC-6 وA549 ، في حين لم يكشف عن مثل هذه الفعالية في انوية الخلايا THP-1وA2840 . كما اثبتت تلك الدراسة احتواءه بعض انوية الخطوط السرطانية على المتناظر الانزيمي GSTπ وانه لم ينقل لها بفعل التلوث المحتمل من بروتينات السايتوبلازم لعدم الكشف عن بروتينات أخرى مثل Cu – Zn SOD في النواة التي كشف عنها في السايتوبلازم عن طريق الترحيل الكهربائي للبروتينات السايتوبلازمية والنووية في هلام SDS-PAGE (17) . كما يعتقد بأن بيروكسيد الهيدروجين المتولد من تضاعف الخلايا السرطانية وبقية الـ ROS في النقل النووي للمتناظر الانزيمي (GSTπ) والمقاومة للعقار(18) ، إذ يمكن ان يستنتج من الزيادة المتدرجة في فعالية GST في السايتوبلازم او النواة والمصاحبة لتقدم تمريرات خلايا سرطان الدماغ علاقة بزيادة مقاومة الخلايا السرطانية للعلاج بالعقارات الكيميائية .

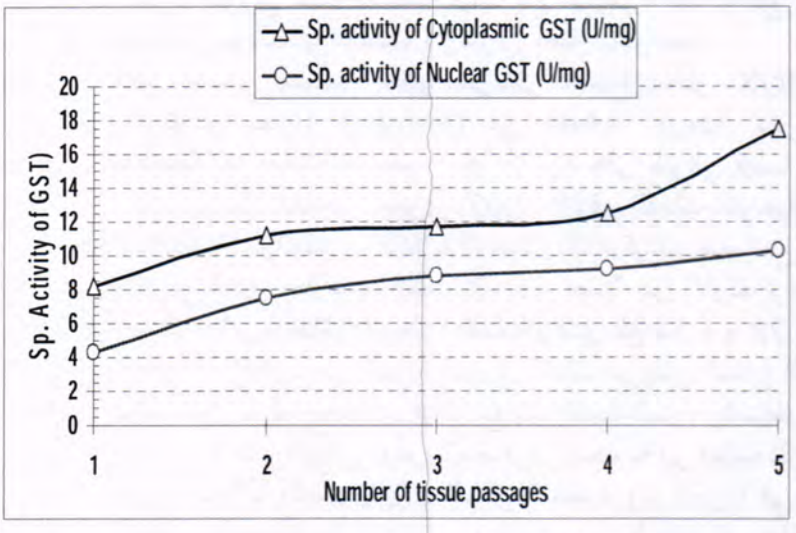

أرقام التمريرات

1: 22
2: 37
3: 38
4: 58
5: 65

شكل -1 : تطور الفعالية النوعية لأنزيم GST في السايتوبلازم والانوية لخلايا الخط السرطاني للدماغ البشري خلال تمريرات مختلفة.

تعيين فعالية انزيم GST في خطوط الخلايا السرطانية المعاملة بـ DOX

اظهرت النتائج الموضحة في الشكل (2-a) تأثير معاملة خلايا Hep-2 بتركيزين من عقار DOX (10 و 15) مايكروغرام/مللتر ارتفاعاً معنوياً ($P<0.05$) في الفعالية النوعية للانزيم في الجزء السايتوبلازمي لتلك الخلايا قياساً مع السيطرة السالبة التي بلغ الارتفاع معها 1.27 و 1.48 مرة على التوالي. ولم تسجل فروق معنوية في الفعالية النوعية للانزيم في الخلايا ذات المعاملة المتداخلة الكاتيكينات مع العقار بتركيز 10 مايكروغرام/مللتر مع الخلايا المعاملة بتركيز 10 مايكروغرام/مللتر والخلايا المعاملة بالكاتيكينات فقط ، بينما سجلت الفعالية لتلك المعاملة المتداخلة إرتفاعاً معنوياً قياساً بالسيطرة السالبة و مع الخلايا المعاملة بالعقار ، كما سجلت فروقاً معنوية في فعالية الانزيم للخلايا المعاملة بالكاتيكينات فقط قياساً مع السيطرة السالبة والمعاملة بتركيزي العقار.

وقد تميزت الفعالية النوعية للانزيم في الجزء النووي لخلايا Hep-2 المعاملة بالعقار بتركيز 10 و 15 مايكروغرام/مللتر بارتفاع معنوي ($P<0.05$) قياساً مع المعاملات الاخرى ، والسيطرة السالبة التي بلغ معها مقدار الارتفاع 1.70 و 2.12 مرة على التوالي . كما ظهر انخفاض معنوي في الفعالية النوعية للانزيم في الجزء النووي للخلايا ذات المعاملة المتداخلة بالكاتيكينات والعقار معا قياساً مع فعالية الانزيم

للخلايا المعاملة بتركيزي العقار بمفردهما ، في حين لم تكن الفروق معنوية قياساً مع السيطرة السالبة والخلايا المعاملة بالكاتيكينات.

اظهر التأثير السمي لعقار DOX بتركيز 10 و 20 مايكروغرام/مللتر بمفردهما لخلايا AMN-3 ارتفاعا معنويا ($P<0.05$) في الفعالية النوعية لانزيم GST في الجزء السايتوبلازمي قياساً مع السيطرة السالبة التي بلغ معها الارتفاع الى 1.61 و 2.03 مرة على التوالي (الشكل 2 -b) . ولم تسجل فروق معنوية في الفعالية النوعية للانزيم في الخلايا المعاملة بالعقار بتركيز 10 مايكروغرام/مللتر قياساً مع فعالية الأنزيم في الخلايا المعاملة بالكاتيكينات، فضلاً عن عدم ظهور فروق معنوية في فعالية الانزيم بين الخلايا المعاملة بتركيز 20 مايكروغرام/مللتر من العقار بمفرده والخلايا ذات المعاملة المتداخلة للعقار والكاتيكينات .

وتميزت قيم الفعالية النوعية للانزيم في الجزء النووي لخلايا AMN3 المعاملة بتركيز 10 و 20 مايكروغرام/مللتر بارتفاع معنوي ($P<0.05$) قياساً مع بقية المعاملات ، والسيطرة السالبة التي بلغ معها الارتفاع 1.99 و 2.18 مرة على التوالي (الشكل 2-b). كما وتسبب عن معاملة الخلايا بالكاتيكينات بتركيز 62.5 مايكروغرام/مللتر مع العقار بتركيز 10 مايكروغرام/مللتر ارتفاعا معنوي في فعالية الانزيم للجزء النووي لتلك المعاملة قياساً مع السيطرة السالبة بلغ 1.47 مرة ، وانخفاضا معنويا قياساً مع فعالية الانزيم للخلايا المعاملة بتركيزي العقار بمفردهما.

ولوحظ إن للتأثير السمي لمعاملة خلايا سرطان الدماغ بعقار DOX بتركيز 10 و 15 مايكروغرام/مللتر ارتفاعا معنويا ($P<0.05$) في الفعالية النوعية لانزيم GST في الجزء السايتوبلازمي لكلتا المعاملتين بلغت الضعف و 2.38 مرة على التوالي قياساً الفعالية لخلايا السيطرة السالبة (الشكل 2- c) ، وسجل انخفاض معنوي ($P<0.05$) في الفعالية النوعية للانزيم في الخلايا ذات المعاملة المتداخلة بالكاتيكينات والعقار، والخلايا المعاملة بالكاتيكينات قياساً مع الفعالية النوعية للانزيم للخلايا المعاملة بتركيزي العقار بمفردهما (شكل 2- c)، فضلا عن الارتفاع المعنوي لكلتا المعاملتين الأخريتين قياساً مع فعالية الانزيم لخلايا السيطرة السالبة والذي بلغ 1.54 و 1.28 مرة على التوالي.

وتميزت الفعالية النوعية للانزيم في الجزء النووي لخلايا سرطان الدماغ المعاملة DOX بتركيز 10 و 15 مايكروغرام/مللتر بارتفاع معنوي قياساً مع بقية المعاملات ، والسيطرة السالبة الذي بلغ معها الارتفاع 1.41 و 1.63 مرة على التوالي، ولم يلاحظ فروق معنوية في فعالية الانزيم معتمدة على تركيز العقار في الجزء النووي للخلايا (شكل 2-c) . كما لم تلاحظ فروق معنوية في الفعالية النوعية للانزيم في الجزء النووي للخلايا المعاملة بالكاتيكينات مع العقار ، و الخلايا المعاملة بالكاتيكينات قياساً مع للسيطرة السالبة .

واظهرت البيانات الموضحة في الشكل (2-d) الخاصة بمعاملة خلايا REF-3 ارتفاع معنوي ($P<0.05$) في الفعالية النوعية للانزيم في سايتوبلازم الخلايا المعاملة بتركيزين من العقار 10 و20 مايكروغرام/مللتر قياساً مع الخلايا المعاملة بالكاتيكينات ، والسيطرة السالبة والذي بلغ الإرتفاع معها 1.26 و 1.64 مرة على التوالي ، ولم تسجل فروق معنوية في تلك الفعالية النوعية للانزيم في الخلايا ذات المعاملة المتداخلة (الكاتيكينات مع العقار) قياساً مع الفعالية النوعية للأنزيم في الخلايا المعاملة بالتركيز ذاته من العقار بغياب الكاتيكينات. كما لوحظ عدم وجود فروق معنوية في الفعالية النوعية للأنزيم في الخلايا المعاملة بالكاتيكينات ، قياساً مع السيطرة السالبة.

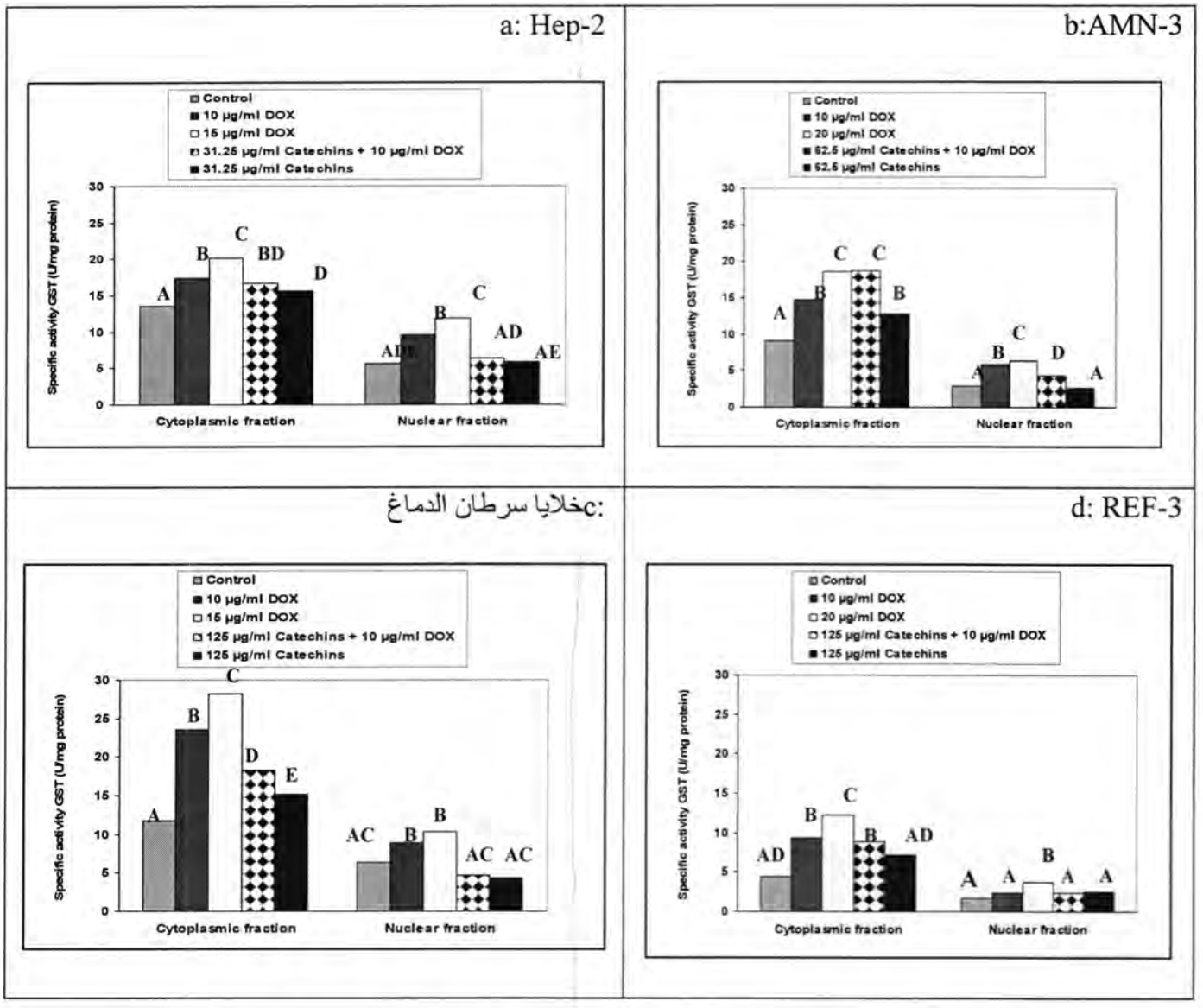

الشكل - 2 : تأثر الفعالية النوعية لأنزيم GST في الجزء السايتوبلازمي و النووي في الخطوط الخلوية السرطانية و الطبيعية لمعاملة بـ DOX و الكاتيكينات .

وسجلت النتائج الموضحة في الشكل (2-d) ارتفاعا معنويا في الفعالية النوعية للانزيم في الجزء النووي للخلايا المعاملة بالعقار بتركيز 10 مايكروغرام/مللتر ، والمعاملة بالتركيز ذاته من العقار بوجود الكاتيكينات و الخلايا المعاملة بالكاتيكينات ، قياساً مع فعالية الانزيم لخلايا السيطرة السالبة ، وتميزت الفعالية النوعية للانزيم في الجزء النووي لخلايا REF-3 المعاملة بالعقار بتركيز 20 مايكروغرام/مللتر بارتفاع معنوي قياساً مع فعالية الانزيم لبقية المعاملات والسيطرة السالبة التي بلغ معها الارتفاع الى 2.23 مرة .

تبين من معاملة الخلايا الورمية بعقار DOX ارتفاع الفعالية النوعية لانزيم GST مصاحبة لازدياد تراكيز العقار نتيجة حث الخلايا على انتاج المزيد من هذا البروتين بفعل العقار مؤدية الى زيادة فعاليته ابتداءاً في السايتوبلازم ، كونه من الأنزيمات المحثة والمزيلة للسمية Phase II ذات الأهمية في تأيض العوامل العلاجية ، وربما لزيادة مستواه هذا دوراً تسبب بطريقة ما للنقل النووي لهذا البروتين ومن ثم

تراكمه في النواة. وان زيادة الفعالية النوعية للانزيم المعتمدة على تركيز الجرعة من العقار ربما تدعم هذه النتائج والاقتراح بوجود نظام نقل خاص افضل من الانتشار البسيط (Simple diffusion) للنقل النووي لاحد متناظرات انزيم GST ، وان وجود مثل هذا المتناظر الانزيمي في النواة يترجم الدور المضاد للموت المبرمج للخلايا الحاوية له ، في حين تكون الخلايا السرطانية التي تخلو انويتها من هذا المتناظر حساسة لعقار DOX وللموت المبرمج (16) .

كما اشارت الدراسات الصيدلانية بمشاركة المتناظر الانزيمي GST في تايض العقارات المضادة للاكسدة مثل DOX و CPT ومن ثم يكون للتعبير المفرط لانزيم GST دور في اقلال او اضعاف الحساسية الخلوية للعقار(19) ، فضلا عن مقاومة الخلايا السرطانية للعقار بفعل التعبير المفرط للنواقل التي يتم بوساطتها نقل DOX خارج الخلية مثل P-glycoprotein , MRP-1 مؤديا الى خفض كمية DOX داخل الخلية (19).

كما يرجح أن GST دورا في تكوين المحور الاساس DOX-GST ، وان لتكون هذا المحور اهمية في تدفق وضخ العقار خارج الخلية (20) ، وقد أشار Awasthiوجماعته(21) ان معاملة الخلايا السرطانية بحامض Ethacrylic acid (مادة اساس لانزيم GST) يزيد من سمية DOX نتيجة تثبيط تكوين DOX-GST .

اما الانخفاض المستحصل في الفعالية النوعية لانزيم GST في الجزء السايتوبلازمي والنووي بفعل المعاملة المسبقة للخلايا بالكاتيكينات التي يعقبها المعاملة بالعقار DOX فانه ربما يعود الى دورالكاتيكينات ونفاذيتها من خلال غشاء البلازما التي قد تثبط النقل النووي للبروتينات بالية يمكن ان تكون مشابهه لفعل لاكتين الحنطةWGA(wheat grem agglutinin) اوربما بآلية مماثلة لما سجله الباحث Yu وجماعته (22) والاشادة بكفاءة دخول ABL(*Agricus bisporus* lectin) الى السايتوبلازم و تثبيط تضاعف مزارع الخلايا ، إذ يتموقع حول النواة ويتأثر ببروتينات النقل النووي بغلق فتحات الغشاء النووي و المعتمدة على تتابعات NLS(Nuclear length signals) معينة تسمح من خلالها نفاذية تلك المركبات للنواة.

تعيين فعالية انزيم GST في خطوط الخلايا السرطانية المعاملة بـ MMC

درس التأثير السمي لتركيزين من العقار MMC في خطوط الخلايا السرطانية بغياب الكاتيكينات وبوجودها في الفعالية النوعية لانزيم GST في جزئي السايتوبلازم والنواة لتلك الخلايا. وقد اظهرت النتائج الموضحة في الشكل (3-a) معاملة خلايا Hep-2 بعقار MMC بتركيز 5 و 10 مايكروغرام/مللتر ، والمعاملة بتركيز 5 مايكروغرام/مللتر بوجود الكاتيكينات ارتفاعا معنويا في الفعالية النوعية لانزيم GST في الجزء السايتوبلازمي بلغ 1.53 و 1.71 و 1.9 مرة على التوالي قياساً مع الفعالية النوعية للانزيم في السيطرة السالبة ، في حين لم تسجل فروق معنوية في فعالية الأنزيم في سايتوبلازم الخلايا المعاملة بالكاتيكينات قياسا بالسيطرة السالبة .

كما سجل ارتفاع معنوي في الفعالية النوعية للأنزيم في الجزء النووي للخلايا المعاملة بالمايتومايسين بتركيز 5 و 10 مايكروغرام/مللتر ، تجاوز الضعف ليصل إلى 2.04 و 2.66 مرة قياساً مع السيطرة السالبة (شكل 3-a). في حين لم تظهر فروق معنوية في الفعالية النوعية للانزيم في الجزء النووي للخلايا المعاملة بالكاتيكينات و الخلايا ذات المعاملة المتداخلة (الكاتيكينات و العقار) ، قياساً مع السيطرة السالبة. فضلاً عن الانخفاض المعنوي والعالي للفعالية في الخلايا ذات المعاملة المتداخلة قياساً مع فعالية الانزيم في الخلايا المعاملة بتركيزي العقار،

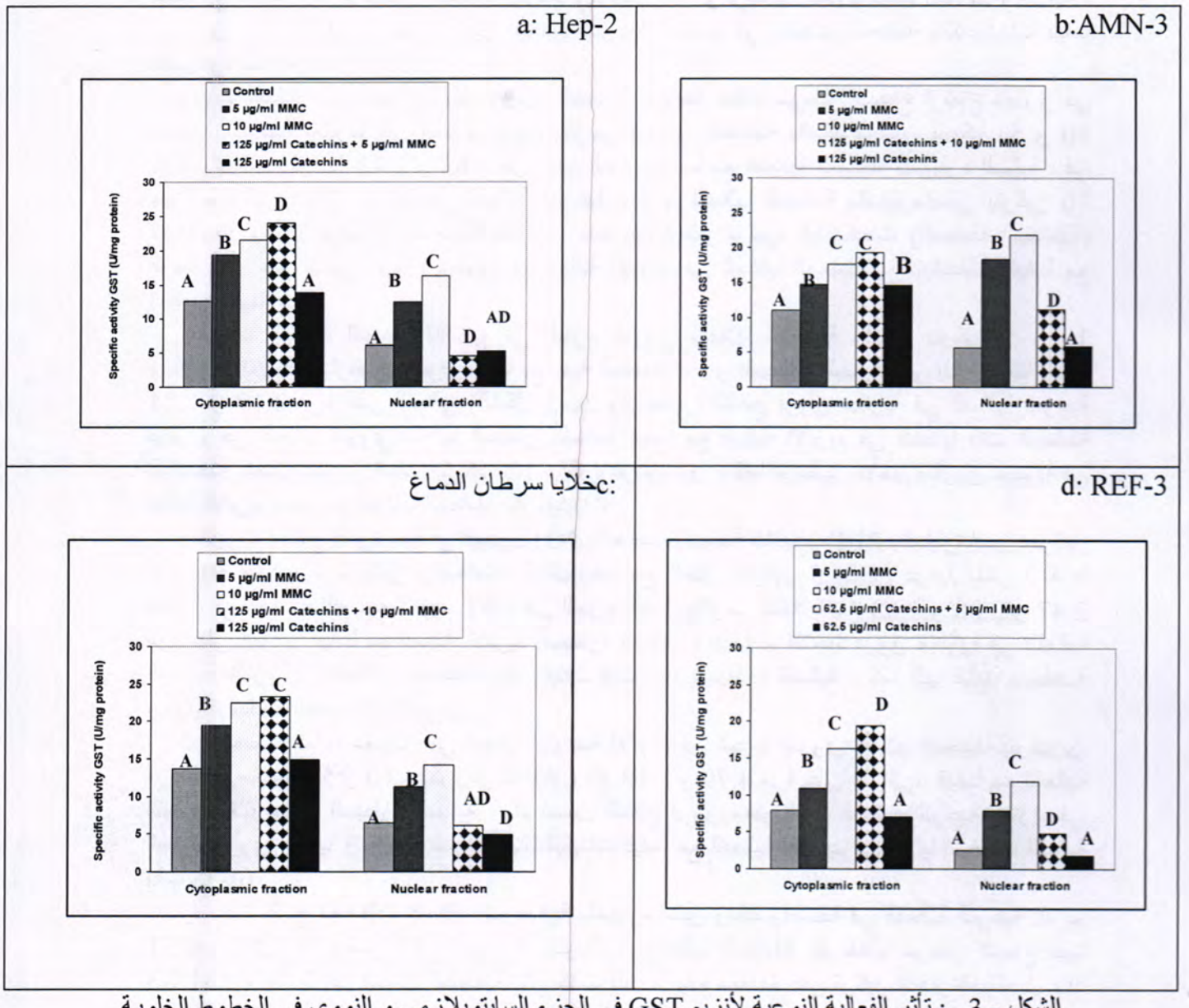

الشكل - 3 : تأثر الفعالية النوعية لأنزيم GST في الجزء السايتوبلازمي و النووي في الخطوط الخلوية السرطانية و الطبيعية المعاملة بـ MMC و الكاتيكينات .

واظهر التأثير السمي للمايتومايسين بتركيز 5 و 10 مايكروغرام/مللتر ارتفاعا معنويا في الفعالية النوعية للانزيم في الجزء السايتوبلازمي لخلايا AMN-3 بلغ 1.33 و 1.59 مرة على التوالي قياساً مع الفعالية النوعية في السيطرة السالبة (الشكل 3-b). ولم تظهر فروق معنوية في الفعالية النوعية للانزيم في الجزء السايتوبلازمي للخلايا ذات المعاملة المتداخلة (الكاتيكينات مع 10 مايكروغرام / مليلتر MMC) وفعالية الأنزيم في الخلايا المعاملة بالتركيز ذاته من العقار بغياب الكاتيكينات .كما لم تسجل فروق معنوية في فعالية الأنزيم في الخلايا المعاملة بالعقار بتركيز 5 مايكروغرام/مللتر وفعالية الأنزيم بالخلايا المعاملة بالكاتيكينات ، الخلايا المعاملة بالمايتومايسين بتركيز 10 مايكروغرام/مللتر بوجود الكاتيكينات والمعاملة بالتركيز ذاته من العقار بغياب الكاتيكينات.

وتبين ان هناك ارتفاع معنوي في الفعالية النوعية للانزيم في الجزء النووي للخلايا المعاملة بالعقار بتركيزي 5 و 10 مايكروغرام/مللتر بلغ 3.27 و 3.90 مرة على التوالي قياساً مع السيطرة السالبة ، كما تميزت فعالية الأنزيم في أنوية الخلايا ذات المعاملة المتداخلة بالكاتيكينات والعقار بانخفاض معنوي

قياساً مع فعالية الانزيم للخلايا المعاملة بتركيزي العقار معاً و ارتفاعاً معنويا قياساً بالسيطرة السالبة ، في حين لم تكن الفروق معنوية بين الفعالية النوعية للانزيم في الخلايا لمعاملة بالكاتيكينات قياساً بالسيطرة السالبة .

وبينت النتائج الموضحة بالشكل (c-3) الخاصة بمعاملة خلايا سرطان الدماغ ارتفاع معنوي في الفعالية النوعية للانزيم في الجزء السايتوبلازمي للخلايا المعاملة بالمايتومايسين بتركيز 5 و 10 مايكروغرام/مللتر بلغ 1.42 و 1.63 مرة على التوالي قياساً مع الفعالية المسجلة للسيطرة السالبة ، في حين لم تظهر فروق معنوية في الفعالية النوعية للانزيم للخلايا المعاملة بالمايتومايسين بتركيز 10 مايكروغرام/مللتر والخلايا المعاملة بالتركيز ذاته من العقار بوجود الكاتيكينات (المعاملة المتداخلة) فضلا عن عدم ظهور فروق معنوية في فعالية الانزيم في الخلايا المعاملة بالكاتيكينات قياساً مع السيطرة السالبة.

وتميزت الفعالية النوعية للانزيم في الجزء النووي للخلايا المعاملة بالعقار بتركيز 5 و 10 مايكروغرام/مللتر بارتفاع معنوي قياساً مع بقية المعاملات ، و السيطرة السالبة التي بلغ الارتفاع فيها 1.74 و 2.19 مرة على التوالي (الشكل c-3). ولم تظهر النتائج فروق معنوية في الفعالية النوعية للانزيم في الجزء النووي لخلايا السيطرة السالبة قياساً مع فعالية الانزيم في الخلايا ذات المعاملة المتداخلة بالكاتيكينات و العقار بتركيز 10 مايكروغرام/مللتر ، كما لم تظهر الاخيرة فروق معنوية في فعالية الانزيم قياساً مع الخلايا المعاملة بالكاتيكينات .

واظهرت النتائج الموضحة في الجدول (d-3) الخاصة بمعاملة خلايا REF-3 بالمايتومايسين بتركيز 5 و 10 مايكروغرام/مللتر والمعاملة بالكاتيكينات مع العقار بتركيز 5 مايكروغرام/ مللتر ارتفاعا معنويا في الفعالية النوعية لانزيم GST في الجزء السايتوبلازمي للخلايا بلغ 1.38 و 2.08 و 2.47 مرة على التوالي قياساً مع فعالية الانزيم للسيطرة السالبة ، بينما لم تلاحظ فروق معنوية في الفعالية النوعية للانزيم في الخلايا المعاملة بالكاتيكينات قياساً مع السيطرة السالبة ، كما انها كانت منخفضة معنويا قياساً مع المعاملات الاخرى.

كما وجـد ارتفاعا معنويا في الفعالية النوعية للانزيم في الجزء النووي للخلايا المعاملة بتركيزين من المايتومايسين (5 و 10 مايكروغرام/مللتر) بلغ 3.18 و 4.79 مرة على التوالي، قياساً مع الفعالية النوعية للأنزيم في السيطرة السالبة. و لم تسجل النتائج فروق معنوية في الفعالية النوعية للانزيم في الجزء النووي لخلايا REF-3 المعاملة بالكاتيكينات قياساً مع الفعالية للانزيم في خلايا السيطرة السالبة (شكل d-3) .

أوضحت نتائج معاملات الخلايا السرطانية بالمايتومايسين زيادة واضحة في الفعالية النوعية لانزيم GST وبشكل اكثر وضوحاً في الجزء السايتوبلازمي لخلايا Hep-2 ثم خلايا سرطان الدماغ تليها AMN-3 ، فضلاً عن الخلايا الطبيعية التي كانت تلك الزيادة معتمدة على تركيز العقار المستعمل ، اذ ظهر إن انزيمات GST تلعب دورا مهما واساسيا في عملية ابطال السمية الخلوية (cellular detoxification) بفعل العقار عن طريق تسريع ارتباطها بالمركبات المختلفة وبذلك توقف النشاط السرطاني او دخول الخلية الموت المبرمج (23) . كما يرتبط التنشيط الحيوي للمايتومايسين بفعالية انزيمات DTD (DT diaphorase) في الظروف الطبيعية للاوكسجين ، في حين يكون مرتبطا بانزيمات السايتوكروم P450 في الظروف التي ينقص فيها الاوكسجين(24) ، فقد تبين ان المايتومايسين يكون مادة اساس لانزيم DTD في الظروف الحامضية ، بينما يكون تحت الظروف الفيسيولوجية الطبيعية ليس فقط مادة اساس ضعيفة بل مثبط لفعالية الانزيم (25) . اذ ان الية عمل المايتومايسين والمركبات ذات العلاقة بتركيب Indolquinone (EOq) معقدة جدا ويصعب التوصل الى تنبأت دقيقة حول اسناد تلك المسؤولية الى انزيم مفرد . وقد سجلت علاقة جيدة بين الاستجابة للعقار ومعدل اختزال EOq في متجانسات انسجة ورمية بفعل تايض العقار والاختزال الحيوي في عدد محدود من الاورام (26).

كما لوحظت زيادة في الفعالية النوعية لانزيم GST في الجزء النووي لخطوط الخلايا السرطانية مصاحبة لارتفاع تراكيز العقار ، اذ تميزت خلايا AMN-3 بارتفاع كبير في تلك الفعالية تليها Hep-2 ثم خلايا سرطان الدماغ فضلاً عن إرتفاع الفعالية للجزء النووي لخلايا REF-3. وقد يبين ارتفاع النتائج

المستحصلة في الفعالية النوعية للانزيم في الجزء النووي للخلايا المعاملة قياساً مع الجزء ذاته من الخلايا السيطرة السالبة انتقال هذا البروتين (الانزيم) من السايتوبلازم الى النواة بآلية معينة نتيجة الحث لزيادة تعبير هذه الانزيمات بفعل العقارات المضادة للسرطان (19) . التي تؤدي الى اضطرابا ت في التعبير الجيني لعائلة الجينات gst_s ينتج عنها تضخيم الجين ناشى عن زيادة الانحرافات الكروموسومية حسب استعمال العقار ولما لهذا التعبير المفرط من تأثيرات مستقبلية لاحقة في تأيض العقارات (15).

كما تبين ان معاملة الخلايا السرطانية بالكاتيكينات قد خفض من الفعالية النوعية لانزيمات GST بشكل اكثر وضوحا في الجزء النووي للخلايا المعاملة بها قياساً مع الجزء السايتوبلازمي ، وربما تكون للكاتيكينات دور في تخفيض النقل النووي لبروتينات السايتوبلازم ومنها الـ GST التي تعمل على حماية الدنا من التلف والدمار بفعل العقارات ، وتلعب الكاتيكينات دوراً في إختزال ROS المتكونة ومن ضمنها بيروكسيد الهيدروجين التي تلعب دوراً مهماً في النقل النووي للمتناظر الانزيمي GSTπ الى النواة . كما يمكن ان يكون للكاتيكينات تأثيرا مشابها lectin *Agaricus bisporus* (ABL) في تثبيط النقل النووي لبعض البروتينات السايتوبلازمية ، في حين لم يكن لها تأثيرا تثبيطيا للنقل النووي لبروتين P53 المعروف بموقعه في السايتوبلازم والنواة لامتلاكه اشارة نووية NLS(Nuclear Length Signal) تسمح له بالنفاذ من خلال الغشاء النووي ودفع الخلية نحو الموت المبرمج ، فضلاً عن دور الكاتيكينات كونها من الفلافونيدات الطبيعية التي تستهدف الاخلال بتنظيم تقدم دورة الخلية وانها واحدة من الاصناف الرئيسة الطبيعية التي تظهر كونها عوامل مضادة للسرطان عن طريق تسكين دورة الخلية بوصفها الية رئيسة في خلايا سرطانية مختلفة (27).

المصادر

1. Hayes, J.D. and Pulford, D.J. The glutathione S-transferase supergene family : regulation GST and the contribution of the isoenzyme to cancer chemoprotection and drug resistance. Crit. Rev. Biochem. Mol. Biol., 30:445-600(1995).
2. Engel. L.S.; Taioli, E.; Pfeiffer, R.; Garcia-Closas, M.; Marcus, P.; Lan, Q.; Boffetta, P.; Vineis, P.; Autrup, H.; Bell, D.A. and et al., Pooled analysis and metaanalysis of glutathione S-transferase M1 and bladder cancer. Am. J. Epidemiology, 162(2) : 95-109, (2002).
3. Meyer,D.J.;Belae,D.;Tan,K.H.;Coles,B. and Kettever,B. Glutathione transferase in primary rat hepatomas : the isolation of the a form GSH peroxidase activity. FEBS. Lett.,184:139 – 143., (1985).
4. Hirata,S.; Odajima,T.; Kohama,G.; Ishigaki,S. and Niitsu,Y. Significance of glutathione s- transferase-π as a tumor marker in patients with oral cancer. Cancer,70:2381 – 2387. (1992).
5. Bai, F.; Nakanishi, Y.; Kawasaki, M.; Takayama, K.; Yatsunumi,J.; Pei, X.H.; Tsuruta, N.; Wakamatsu, K. and Hara, Immunohistochemical expression of glutathione S-transferase II can predict chemotherapy of response in patients with normal cell lung carcinoma. Cancer, 78:416-421, (1996).
6. Meijer,C.;Mulder,N.H.;Hospers,G.A.;Uges,D.R. and Devries,E.G. The role of glutathione in resistance to Cisplatin in human small lung cancer cell line. Br. J. Cancer, 62:72 – 77. (1990).
7. Godwin, A.K.; Meister,A.; O'Dwyer, P.J.; Huang, C.S.; Hamilton,T.C. and Anderson , M.E). High resistance to Cisplantin in human ovarian cancer

cell lines is associated with marked increase of glutathione synthesis. Proc. Natl. Acad. Sci. USA, 89:3070 – 3074, .(1992)

8. D'Arpa,P. and Liu,L. Topoisomerase – targeting antitumor drugs. Biochem. Biophys. Acta., 989:163 – 177. .(1989).
9. Costes,V.P.;Mostter,M. and Wilson,R.P.Effects to typical mytomycin C and combined procedures. Br. J. Opthalmol.,77:693 – 697. .(1993).
10. Undeger,U.;Ayden,S.;Bassaran,A. and Bassaran,N. The modulation of effects of quercetin and rutin on mytomycin C induced DNA damage. Toxic Lett.,151:143 – 149. .(2004).
11. Dignam,J.D.;Lebouitz,R.M. and Roeder R.G.Accurate transcription intiation by RNA Polymerase II in a Soluble extract from isolated mammalin nucli. Nucleic Acid Res. 11,1475 – 1489. .(1983).
12. Habig,W.H. and Jakoby,W.B.Glutathione– S – transferase (Rat and Human). In: Detoxicafication and drug metabolism conjugated and related system (S.P. Colowick and N.O. Kaplan eds.). Methods in Enzymology, Vol.:77,218 – 231. Academic Press , NewYork. .(1981).
13. Bradford,M.MA. Rapid and sensitive method for the quantitation of microgram quantities of protein utilizing the principle of protein dye binding. Anal. Biochem.,72:248 – 254. .(1976).
14. Garrett, R.H. and Grisham, C.M . Biochemistry 3rd edition. Thomson Brooks / Cole U.S.A. . (2005).
15. علي ، امال محمد . دراسة وراثية خلوية ومناعية لخط خلايا سرطان الحنجرة Hep-2 . رسالة ماجستير. كلية العلوم جامعة بغداد(2004) العراق / بغداد-
16. Goto,S.;Ihara,Y.;Izumi,S.;Abe,K.;Koji,T. and Kondo,T. Doxorubicin – induced DNA intercalation and scavenging by nuclear glutathione S-transferase π. FASEB J.,15:2702 – 2714. .(2001).
17. Ali-Osman,F.;Brunner,J.M.;Kutluk,T.M. & Hess,K. Prognostic significance of glutathione S-transferase π expression and subcellular localization in human gliomas. Clin. Cancer Res.,3:2253 – 2261. .(1997).
18. Sinha,B.K. and Mimnaugh,E.G. Free radical and anticancer drug resistance : Oxygen free radical in the mechanisms of drug cytotoxicity and resistance by certain tumors. Free Radic. Biol. Med.,8:567 – 581. .(1990).
19. Goto,S.;Iida,T.;Cho,S.;Oka,M.;Kohno,S. and Kondo,T. Overexpression of glutathione S – transferase π enhances the adduct formation of cisplatin with glutathione in human cancer cells. Free Radic. Res.,31:549 – 558. .(1999).
20. Serafino,A.;Sinibaldi–Vallebona,P.; Gaudiano,G.; Koch,T.H.; Rasi,G.; Garaci,E.and Ravagnan, G. Cytoplasmic localization of anthracyclin antitumor drugs conjugated with reduced glutathione: a possible correlation with multidrug resistance mechanisms.Anticancer Res.,:18:1159 – 1166. .(1998).
21. Awasthi,S.; Singhal,S.S.; He,N.; Chaubey,M. Zimniak,P.; Sivasta,S.K.; Singh,S.V.and Awasthi, Y.C. Modulation of doxorubicin cytotoxicity by ethacrynic acid. Int. J. Cancer,68:333 – 339. .(1996).

22. Yu,L.G.; Fernig,D.G.; White,M.R.H.;Spiller,D.G.;Appleton,P.;Evans,R.C. ;
Grierson,I.;Smith,J.A.;Davies,H.,Gerasimenko,O.V.;Petersen,O.H.;Milton, J. D.and Rhodes,J.M.Edible mushroom *Agricus bisporus* lactin,which reversibly inhibits epithelial cell proliferation, blocks nuclear localization sequence – dependent nuclear protein import. J. Biol. Chem.,274:4890 – 4899. (1999).
23. Shoieb, A.M; Elgayyar, M.; Dudrick, P.; Bell, E. and Titnof, P.K. Inhibition of growth and induction of apoptosis in cancer cell lines by Thimoquinol. *Int. Oncology,* 22:107-113. .(2003).
24. Belcourt,M.F.; Hodnick,W.F.; Rockwell,S. and Sartorelli,A.C. Differntial toxicity of mytomycin C and Profirmycin to aerobic and hypoxic Chinese hamster overy cells overexpression human NADPH:cytochrome p450 reductase. Proc. Natl. Acad. Sci. USA,93:456 – 460. .(1996).
25. Siegel,D.;Beall,H.D.;Kasai,M.;Arai,H.;Gibson,N.W. and Ross,D. PH dependent in activation of DT – diaphorase by mitomycin C and profiromycin. Mol. Pharmacol.,44:1128 – 1134. (1993).
26. Prasher,J.M.;Lalai,A.S.;Antonissen,C.H.;Ploemacher,R.E. and Nidernhofer, L.J. Reduced hematopoietic reseves in DNA interstrand cross link repair – deficient *Ercc* / mice. EMBO. J.,24:861 – 871. (2005).
27. Singh,R.P. and Agarwal,R. Natural flavonoids targeting deregulated cell cycle progression in cancer cells.Purchase Curr. Drug Targets,7:345 – 354. .(2006).

دراسة كيميائية حياتية ومناعية لطفيلي المشعرات المهبلية *Trichomonas* *Vaginalis* في مدينة بغداد

شذى خضير عباس
الجامعة المستنصرية / كلية العلوم/ قسم علوم الحياة

ABSTRACT

Within the period from December, 2006 to July, 2007 a study epidemic, immunology and chemical about spread of the **Trichomonas vaginalis** of patient women in Ibn Al-Baladi hospital for women and children and Al-Habibia hospital for delivery, who suffer from viginal secretion only automatic microscope diagnosis was mad to examine 326 sample which collected under the physician observation.

The results of the study show that the infection of the **Trichomonas vaginalis** differs according to the months of the year, also, it shows the infection was high in the women who their ages between 17-19 year. It was 30% of the number of infections samples.

In additional, it was noticed that the percentage of infection among educated women was less than it level of the uneducated women.

The levels of (1L-6) were increased in serum of patient groups (106-54pg/ml) compared with control groups (70pg/ml) while 1L-1a levels were decreased in patient groups (9.47 pg/ml) compared with control groups (19.53 pg/ml), and the levels of immunoglobulin IgG, IgM and IgA were increased in the serum of the patients groups of women being 174.58 mg/dl, 996.0555mg/dl and 409.79 mg/dl in comparison with control groups women 99.860 mg/dl, 149.640 mg/dl and 731.4333 mg/dl consequently.

Lymphocytes phenotyping: the result of this study concerned with Lymphosite Phenotyping shows that the mean percentage of T-lymphocytes CD8+cells was significantly increased in the patients groups (22.76%) in compared with control groups women (21.73%).

This deviation was much more clear in CD4+cells (48.4%) compared with control groups women (19.3%).

The B-lymphocytes CD20 was also significantly decreased in the patients groups (15.12%) compared with control groups women (17.03%).

The levels of complements C3 & C4 was significantly increased ($P<0.005$) in the serum of infected women 143.97mg/dl, 28.100mg/dl in comparison with control groups women 21.1200 mg/dl, 107.990 mg/dl.

The result of lipid peroxidation (MDA)showed no significant increase for all patient groups (0.61 mmol/l) in comparison with control groups (0.035 mmol/l) which can consider the level of MDA as maker for evaluating the disease.

The result which of antioxidants (GSH) showed no significant decrease for all patient groups (o.146 mmol/l) comparison with normal was (0.90532 mmol/l).

الخلاصة

تم خلال الفترة المحصورة ما بين كانون الأول 2006 ولغاية تموز 2007 دراسة مسحية ومناعية وكيميائية حياتية حول انتشار الطفيلي المهبلي Trichomonas vaginalis لدى النساء المراجعات لمستشفى ابن البلدي للأطفال والنسائية ومستشفى الحبيبية للولادة ممن يشكون من إفرازات مهبلية، وتم استخدام الفحص المجهري فقط كعمل روتيني لتشخيص طفيليات المشعرات المهبلية إذ تم جمع 326 مسحة، أظهرت نتائج الدراسة أن الإصابة بالمشعرات المهبلية تختلف بحسب أشهر السنة كذلك إن الإصابة كانت عالية للفئة العمرية (17 – 19) سنة إذ بلغت 30% من مجموع الإصابة الكلية إضافة إلى أن نسبة الإصابة كانت واطئة لدى النساء المتعلمات مقارنة بغير المتعلمات. تبين أن هناك فروقات معنوية بنسب الإصابة بأشهر السنة وكذلك الفئات العمرية والمستويات التعليمية.

أوضحت النتائج إرتفاعاً في نسبة(1L-6) حيث بلغ مستواه في لدى المصابات (106.54 pg/ml) مقارنة بالسيطرة (70 pg/ml) وانخفضت نسبة (1L-1a) لدى المصابات (9.4700 pg/ml) مقارنة بالسيطرة (19.53 pg/ml)، وارتفعت

مستويات الكلوبينات المناعية IgG و IgM و IgA إذ بلغت 174.580 mg/dl و 996.0555mg/dl و 409.79 mg/dl مقارنة بالسيطرة 149.640 mg/dl و 731.4333 mg/dl و 99.8600 mg/dl على التوالي. وكانت النسبة المئوية للخلايا اللمفاوية التائية الحاملة للواسم CD8 (22.76%) في المصابات مقارنة بنساء السيطرة (21.73%) وكان هذا الإرتفاع أكثر وضوحاً في الخلايا التائية الحاملة للواسم CD4 (48.4%) مقارنة بنساء السيطرة (19.3%). أما الخلايا اللمفاوية الحاملة للواسم CD20 فقد إنخفضت نسبته في المصابات إلى 15.2100% مقارنة بنساء السيطرة (17.03%) هذا وقد إرتفعت مستويات جزء المتمم C4, C3 في أمصال النساء المصابات 143.97mg/dl و 28.100mg/dl مقارنة بنساء السيطرة 107.990 mg/dl و 21.1200 mg/dl.

وأظهرت نواتج الأكسدة الفوقية للدهون (MDA) في بلازما الدم إرتفاعاً غير معنوي 0.61005 m mol/l مقارنة بالسيطرة 0.0344 mmol/l.

أما الـ GSH فقد أظهر إنخفاضاً واضحاً حيث كانت نسبته (0.146422 mmol/L) مقارنة بالسيطرة 0.90532 mmol/L.

المقدمة

تم تشخيص الطفيلي Trichomonas vaginalis لأول مرة من قبل العالم Donne سنة (1836) وعده من مسببات الإلتهابات المهبلية Vaginitis بعد رؤية الإفرازات المهبلية (1).

شخص المرض الناجم عن هذا الطفيلي Trichomonas Vaginalis بكونه من الأمراض التي تنتقل عن طريق الإتصال الجنسي (2) وأشار (1) إلى أن نسبة الإصابة بالمشعرات المهبلية في النساء السود في ولاية جورجيا الأمريكية كانت 52% وهي أكثر من نسبة الإصابة بين النساء البيض 20% وتم إجراء العديد من الدراسات حول انتشار طفيلي المشعرات المهبلية في العراق منذ سنة 1979 ولغاية 2002 حيث وجدت في العراق نسب متفاوتة بالإصابة بهذا الطفيلي في مناطق مختلفة من القطر بلغت النسبة ما بين (1.36 - 19.55%) (3), (4) , (5) وبعدها جاءت بحوث عديدة حول انتشار طفيلي المشعرات في العراق فقد أجرى (6) دراسة لمعرفة انتشار المشعرات المهبلية والأحياء المجهرية الأخرى في الإنسان خلال خمسة سنين في مختبر الصحة المركزي في بغداد وكانت نسبة الإصابة بالطفيلي 3%.

ونظراً إلى الأعراض المرضية التي يحدثها هذا الطفيلي للنساء المصابات فقد إقتضى القيام بالبحث في مناطق بغداد المزدحمة بالسكان لمعرفة دور العوامل الوبائية في إنتشار الإصابة إذ لوحظ وجود علاقة بين الإصابة بالمشعرات المهبلية والمستوى التعليمي، أن أعلى نسبة إصابة كانت بين النساء غير المتعلمات مقارنة بأوطأ نسبة إصابة لدى ذوات التعليم العالي وهذا يتفق مع (4) و (6) و (7) و (8).

تعد الكلوبيولنيات المناعية المحصلة النهائية للإستجابة المناعية الخلطية والمناعة المكتسبة تحدد هذه الكلوبيولينات في خمسة أصناف أساسية (Classes) هي IgM, IgG, IgD, IgE, IgA. يعتمد هذا التصنيف بصورةٍ أساسية على صنف السلسلة الثقيلة التي تدخل في بناء جزيئة الكلوبين المناعي ولقد اقتصرت الدراسة الحالية على ثلاثة أصناف من هذه الكلوبنيات (IgG, IgM, IgA).

تعد المتممات من الأنظمة الفعالة في الإستجابة المناعية المتأصلة حيث تظهر بروتيناته فعالية عالية في تحلل الكثير من البكتريا نبه الباحثون (9) إلى وجود أجزاء مناعية لبروتين نظام المتمم C3, C4 أثناء تشخيصهم لبعض الأمراض في نسيج الرحم مثل التهابات بطانة الرحم Endometriosis وأمراض التهابات الحوضي (Pelvic Inflammatory).

تشكل الخلايا اللمفاوية حوالي 20% - 25% من المجموع الكلي لخلايا الدم البيض في الدم المحيطي ولها دور هام في الاستجابة المناعية المكتسبة ومن خلال نوعين من الخلايا وهي الخلايا اللمفاوية التائية T-Lymphocytes التي تتوسط الاستجابة المناعية الخلوية والخلايا اللمفاوية البائية B-Lymphocytes والتي تتوسط المناعة الخلطية Humoral Immunity. تتميز هذه الخلايا عن بعضها البعض مظهرياً بوساطة واسمات على سطحها تدعى CD-Marker. (15)

ويمكن تقسيم الخلايا اللمفاوية التائية وفي ضوء واسماتها إلى نوعين مميزين وظيفياً وهي خلايا (CD8, CD4) تسمى الأولى بالخلايا المساعدة (T-Helper) وتسمى النوع الثاني بالخلايا السمية الخلوية T-Suppresser Cytotoxic أما الخلايا البائية فإن سطحها مميز بواسمات سطحية مثل (CD21, CD20, CD19, CD2). **السايتوكنين (Cytokines)** هي مواد بروتينية ذات أوزان

جزيئية واطئة تشبه الهرمون تتواصل مع الخلايا المناعية وتلعب دور في بدء وتتابع تنظيم الإستجابة المناعية (11). تقوم Monocyte خلايا وحيدة الخلية المولدة للألياف Fibroblast على إنتاج (1L) ذلك الساتيوكين الكبير وهذا الساتيوكين هو المسؤول عن النضج النهائي للـ B-Cell وإنتاج الكلوبيولنيات المناعية (12).

على الرغم من تكون الجذور الحرة بشكل مستمر وكبير داخل الخلايا الحية هنالك مجموعة من الأنظمة الدفاعية لمضادات التأكسد التي أما أن تمنع الجذور الحرة أو تعادل تأثيرها الضار بعد تكوينها ويمكن تعريف مضادات التأكسد بأنها أي مادة عند توفرها بتراكيز واطئة مع المادة القابلة أو المعرضة للتأكسد تؤخر أو تمنع عملية التأكسد (13) ويمكن تقسيمها مضادات الأكسدة غير الأنزيمية التي تكون صغيرة الحجم ذائبة في الوسط المائي أو الشحمي للخلايا مثل Glutathione (GSH) (14) ومضادات الأكسدة الأنزيمية مثل Peroxide Dismutas, Catalase (SOD) هذا ويعرف المالون الديهايد على أنه جزيئة تتكون من ثلاث ذرات كربون مع مجموعتي الدهايد طرفية تعملان على زيادة فعالية (MDA) مع الجزيئات الأخرى (15). ويعد (MDA) واحد من أهم الدلائل التي تستعمل للبحث عن وجود فرط الأكسدة ويشكل (20%) من النواتج النهائية لأكسدة الدهون وهنالك مركبات عن تفاعلها مع (MDA) تكون أصناف عالية الفعالية وتكون ما يسمى فرط الكاربونايل (Carbonyl Stress) والذي يعد مظهر شائع للمرض.

المواد وطرق العمل

تم إجراء مسح لمعرفة نسب الإصابة بالمشعرات المهبلية لمستشفيين هما مستشفى ابن البلدي للأطفال والنسائية ومستشفى الولادة في الحبيبية وكانت جميع المريضات يشكين من إفرازات مهبلية. تم إجراء المسح أثناء المدة المحصورة ما بين كانون الأول 2006 ولغاية تموز 2007. أخذت معلومات من كل مريضة كالاسم والعمر وعدد أفراد العائلة ومنطقة السكن والتحصيل العلمي، كما وتم سؤال كل مريضة عن الأعراض والإفرازات ولونها ورائحتها وحصول أو عدم حصول حكة أو حرقة أو ألم أسفل البطن وتاريخ تناول العقار.

تم جمع العينات عن طريق أخذ مسحة مهبلية Vaginal Swab باستخدام الناظور وبمساعدة الطبيبة النسائية بواسطة مسحة قطنية حضرت مسبقاً بطريقة يدوية ونقلت جميع العينات إلى المختبر التابع للمستشفى خلال 50 دقيقة بعد ذلك تم إضافة 2 مللتر من المحلول الفسلجي Normal Saline للمسحة مع رجها جيدامن أجل فحص المسحة الرطبة مجهريا وتشخيص المشعرات المهبلية تم عمل شريحتين وضعت عليها قطرة أو قطرتين من العالق وتغطيتها بغطاء الشريحة Cover Slip وفحصها تحت المجهر الضوئي إذ تم ملاحظة وجود الخلايا القيحية Pus Cell أما العينة الثانية وضعت عليها قطرة أو قطرتين من العالق وتركت تجف في الهواء ثم مررت على لهب لتثبيت العينة (16).

تم تعيين MDA في البلازما وفقاً لطريقة (17) تم الكلوتاثيون GSH في البلازما وفقا لطريقة (18) تم تقدير مستويات كل من القلوبينات المناعية IgM, IgA, IgG، فضلاً عن مكوني بروتين نظام المتمم C4, C3 بطريقة الانتشار المناعي الإشعاعي المتردد Signal Radia Immunodiffusion (RID) وفقاً لطريقة (19)

جمع عينات الدم Blood Sample Collection:

تم سحب 10 ml من الدم الوريدي لكل من المرضى وأفراد السيطرة وقسم حسب ما يلي :

1- وضع (4 مل) من الدم في أنبوبة إختبار حاوية على الهيبارين (مانع تخثر) لغرض دراسة توصيف الخلايا اللمفاوية Lymphocytes Phenotyping عن طريق واسماتها السطحية (CD Markers).

2- وضع (6 مل) دم في أنبوبة إختبار خالية من الهيبارين لحين تكون الخثرة ثم فصلت بجهاز النبذ المركزي Centrifuge بسرعة (3000 rpm) ابندروف Appendrof tube ثم خزنت في المجمدة بدرجة (-20°C) لحين إجراء الفحوص اللاحقة واستخدام المصل لتقدير مستويات الكلوبينات المناعية وبروتينات المتمم (C4, C3) إضافة إلى (1L-6) و (L-1a1) والمالون الديها والكلوتاثيون.

طريقة توصيف الخلايا Phenotyping Method :

تم مزج 10 مايكرولتر من عالق الخلايا اللمفاوية (1-10 ^{6})خلية/ملم3 مع 10 مايكرولتر من الضد النوعي الخاص بالواسم والمعلم بالفلورسين في أنبوبة إختبار Eppendroff Tube مغلفة بغلاف معتم Aluminum Foil وتركت في الحاضنة بدرجة حرارة ($37^{o}C$) لمدة ساعة ثم غسلت الخلايا بداريء الفوسفات الفسيولوجي المعقم، ونبذت بسرعة 2000 دورة بالدقيقة ولمدة 5 دقائق ولعدة مرات، بعد ذلك علقت الخلايا في 20 مايكرولتر من الداريء نفسه ووضعت على شريحة زجاجية وغطيت بغطاء الشريحة وفحصت باستخدام المجهر المتألق Fluorescent Microscope لغرض حساب النسبة المئوية للخلايا اللمفاوية المعلمة بالفلورسين.

$$\text{النسبة المئوية} = \frac{\text{عدد الخلايا اللمفاوية المعلمة بالفلورسين (u. v. light)}}{\text{العدد الكلي للخلايا اللمفاوية (الضوء العادي)}} * 100 \ (20)$$

تعيين كمية 1L-6 بوساطة E1A :

تم تعيين (1L-6) حسب العدة المجهزة من الشركة وباستخدام طريقة IA Immunotech – Company – France

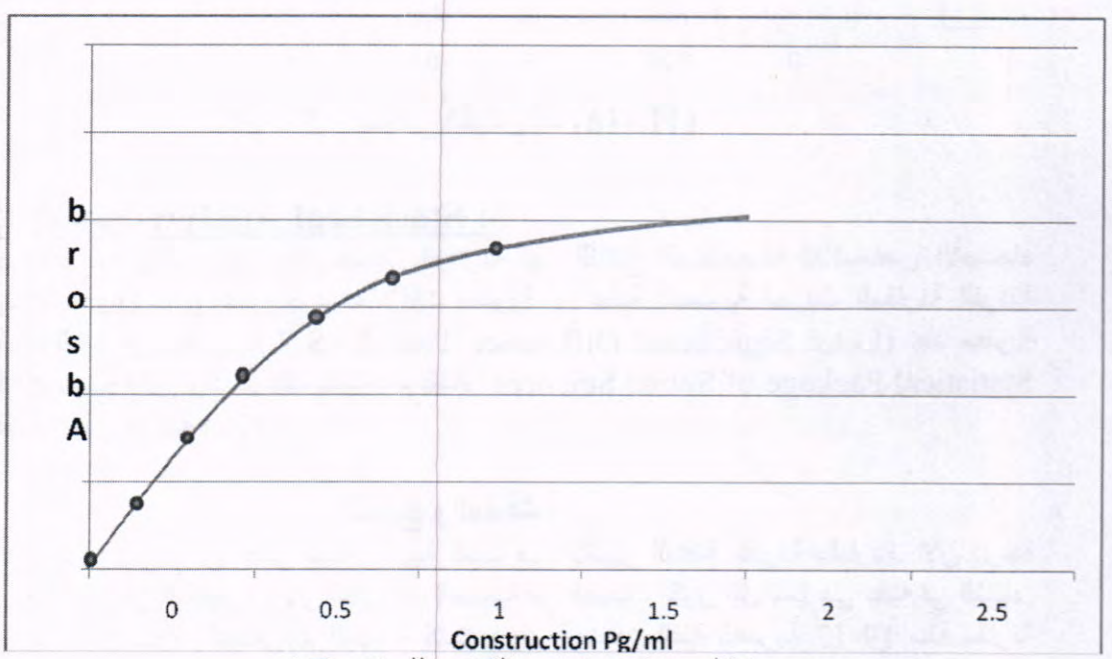

شكل – 1 : منحنى القياس للـ (1L-6)

طريقة قياس 1L-1a :

تم تعيين (L-1a1) حسب العدة المجهزة من الشركة وباستخدام طريقة EIA Immunotech – Company - France

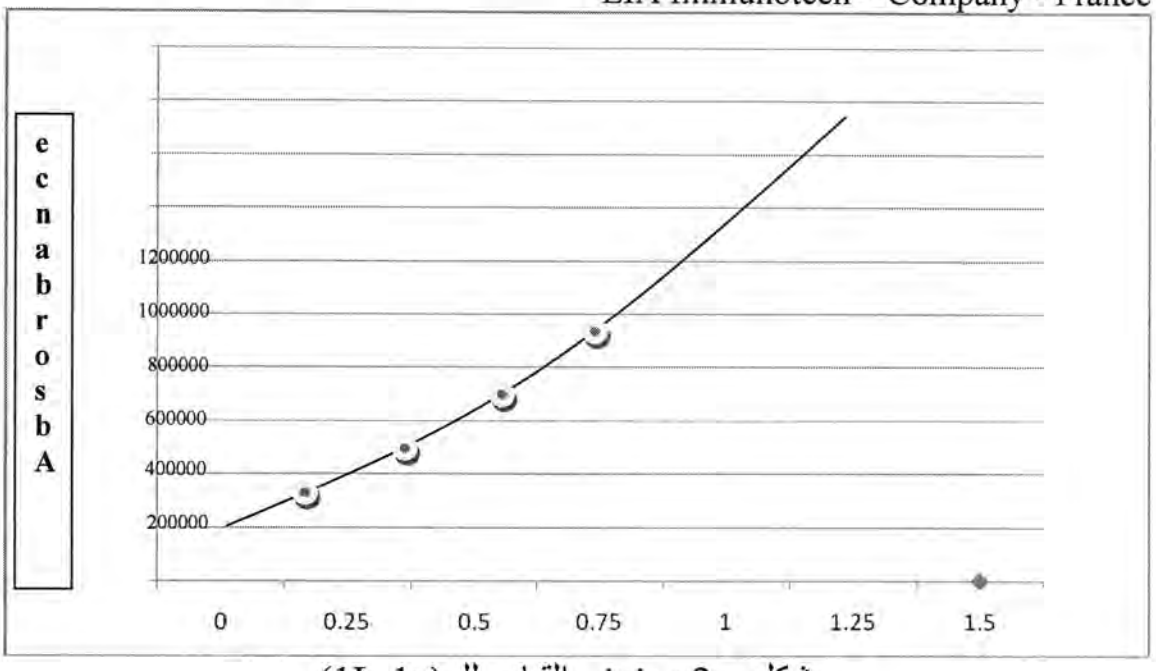

شكل – 2 : منحنى القياس للـ (1L-1a)

التحليلات الأحصائية Statistical Analysis :

تم التعبير عن النتائج بشكل M±SE وقسمت المقارنة بين النتائج المستحصلة للأشخاص الأصحاء والمرضى بإجراء T-Test وعند وجود اختلافات معنوية أو عالية المعنوية أجريت المقارنة الفردية بوساطة مقياس أقل فرق معنوي (Least Significant Difference Test (L. S T)) عند معنوية P<0.05 وكذلك مربع كأي. وقد تم ذلك باستخدام نظام Statistical Package of Social Sciences (BPSS) اعتمادا على طريقة (21).

النتائج والمناقشة

تبين النتائج في الجدول (1) أن أعلى نسبة إصابة كانت في الأشهر الدافئة مقارنة بالباردة، لأن درجة الحرارة تكون ملائمة لنمو الطفيلي، ولأن الظروف الصحية في الصيف تكون أقل مما هي عليه في الشتاء. كما لوحظ أن نسبة الإصابة بالمشعرات المهبلية كانت مرتفعة ضمن الفئة العمرية 17-19 سنة مقارنة بالفئات العمرية الأخرى وخاصة لدى النساء في سن اليأس 50-59 وكما هو موضح في الجدول (2) وهذه النسب تتفق مع ما سجله كل من (22) و (23) و (24) وهذا يفسر أن أعلى نشاط جنسي يحصل بين تلك الفئات العمرية على عكس نساء سن اليأس.أما)25(فقد أوضح إن أعلى نسبة إصابة كانت في سن 17-20 عندما أجرى تجارب على نساء حوامل في غزة في فلسطين.

أما النتائج في الجدول (3) توضح أن نسبة الإصابة بين النساء غير المتعلمات مرتفعة مقارنة بالمستويات التعليمية الأخرى، إذ بلغت نسبة الإصابة للنساء غير المتعلمات (59.3%) تلتها البقية التي تمتلك التعليم الابتدائي والثانوي إذ بلغت (23.3% - 11.6%).

تبين النتائج في الجدول (4) حصول انخفاض معنوي في مستوى (1L-1a) في المصابات بداء المشعرات المهبلية (9.4700pg/ml ± 0.36149) مقارنة بنساء السيطرة (19.5300pg/ml ± 0.27891) وارتفاعاً معنوياً في مستوى (1L-6) في المصابات (106.5400pg/ml ± 0.93953)مقارنة بنساء السيطرة (70 pg/ml ± 0.1989 pg/ml) وهذه النتائج لا تتفق مع)26(عندما أجرو تجارب على خلايا

Astrocytes في الإنسان بثلاثة أنواع من السايتوكينات (1L-1a) و (1L-6) و 1FN-alpha وكانت الخلايا المصابة بـ Toxoplasma Gondil وبعد (1 – 3 – 6 – 24) ساعة لم توجد أي فروق معنوية في مستوى 1L-6 و 1L-1a.

إن الارتفاع في مستوى 1L-6 متفق مع)27(عند إعطائه لخلايا مصابة بالالتهاب في الدماغ من جراء الإصابة بـ Toxoplasma Gondil مما أدى إلى قلة الالتهاب الحاد في الدماغ الناتج عن تأثير Tachyzoites وحاجة الخلايا إلى (1L-6) وهذا يوضح الارتباط في مستوى (1L-6) وتراكيز الضد الحالية في المصل لدى النساء المصابات وكذلك التغير في الحالة الفسيولوجية ربما تغير الجهاز المناعي والخلايا المناعية.

وتعتبر العقاقير من المثبطات التي تمنع إنتاج (1L-1a) وربما العقاقير المتناولة لعلاج داء المشعرات خفض المستوى (1L-1a) (26). وكذلك زيادة (1L-1a) في الجسم تؤدي إلى زيادة البروتينات الخاصة بالأعراض المرضية الحادة كالحمى والتعرق وزيادة أعداد الخلايا العدلة في الجسم (28) جدول (4).

لقد كانت النتائج في جدول (5) تبين أن نسبة IgG في المصابات (996.0555±0.61669) مقارنة بنساء السيطرة (731.4333±0.50305) ارتفاعا معنوياً، وهذه النتائج متفقة مع ما توصل إليه الباحثان (29) اللذان أشارا إلى ارتفاع مستوى القلوبين المناعي IgG في مصل النساء نتيجة لموت الأجنة في الرحم أو حدوث أي التهاب نتيجة لحدوث خلل في الاستجابة المناعية لجسم الأم. أما IgM فكانت (409.7900±0.19969)في المصابات مقارنة بنساء السيطرة (99.8600±0.16680) ويمكن أن يفسر إرتفاع هذا القلوبين المناعي بهدف إزالة الطفيلي نتيجة لحدوث استجابة مناعية من قبل المصابة (30).

أما IgA فكانت (174.5800±0.48644) في المصابات مقارنة بالسيطرة (149.6400±0.47004) وهذه متفقة مع نتائج الباحثين (29) و (30) و (31) و (32) ويعزى هذا الارتفاع إلى حدوث الالتهابات أو الخمج داخل الرحم ويعد IgA أحد المكونات الرئيسية ضمن إفرازات الرحم إذ أنه يوجد بكميات كبيرة ضمن بطانة الرحم لا سيما في منطقة الساقط، وأنه يكون نظام مناعي يكون على تماس مع المحيط الخارجي ويتعرف إلى العديد من الجسام الغريبة (33).

وعند ملاحظة جدول (6) أظهرت الخلايا للواسمة CD8 زيادة معنوية واضحة في الدم المحيطي للمصابات بداء المشعرات المهبلية (22.76%) عند مقارنتها بنساء السيطرة (21.73%) وهذا يشير بوضوح إلى أن الإصابة بداء المشعرات المهبلية تنشط هذه الخلايا وتجبر الطفيلي أن يبقى داخل الخلايا بهيئة إصابة مزمنة بحيث لا يستطيع أن يشكل إصابة حادة. وما يؤيد ذلك ما توصل إليه الباحثون من دور الخلية التائية في السيطرة على الإصابة بداء المقوسات (34).

وقد أظهرت الخلايا المساعدة (CD4+Cell) زيادة معنوية واضحة في الدم المحيطي لمصابات داء المشعرات (48.43%) مقارنة مع عينات السيطرة (19.30%) بحيث كانت الزيادة موازية لتلك الحاصلة في الخلايا اللمفاوية التائية CD8 وهذا ما يؤشر أهمية تلك الخلايا في إبقاء الإصابة في المرحلة المزمنة ومنع انتشار الإصابة في الجسم أو حدوث إصابة ثانية، وهذا ما أوضحه تجريبياً (35) في الفئران حيث لاحظ بأن عدد خلايا CD4 يزداد وبعد سبعة أيام من إصابة الفئران بطفيلي داء المقوسات.

وعند استعراض نتائج الخلايا البائية ذات الواسم (CD20) يلاحظ انخفاض معنوي في المصابات (15.21%) مقارنة بنساء السيطرة (17.03%) وهذا لا يتفق مع ما جاء به الباحثان (36) اللذان بينا أن الخلايا البائية تنشط بفعل الإصابة وذلك عن طريق الحركيات الخلوية المنتجة من قبل الخلية المساعدة الأولى، حيث يؤثران 1L-2, 1FN-Y في وظيفة الخلايا اللمفاوية البائية حيث أن 1FN-Y يؤثر في عملية إختيار الكلوبين المناعي (Ig Class Selection) في حين يعد 1L-2 عامل مؤثر في تمايز الخلايا اللمفاوية البائية. تبين نتائج جدول (7) أن معدلات C3 , C4 في المصابات (143.970mg/dl±0.55016) و (28.1000mg/dl±0.34577) مقارنة بنساء السيطرة (107.99 mg/dl ± 0.7419) و (21.1200 mg/dl ± 0.43838)، حيث كان الإرتفاع معنويا وهذا يتفق مع نتائج العالم (37) الذي أشار إلى ارتفاع C4, C3 لدى النساء المصابات بداء المقوسات وإن الارتفاع معنوياً دليل على أن المصابات بداء المشعرات المهبلية كانت غير مزمنة أي أن الطفيلي متوفر حر (خارج الخلايا) لكي يصبح هدفا للأضداد النوعية والتي باتحادها مع مستضدات الطفيلي تكون معقدات مناعية على

سطح الطفيلي لها القابلية على تنشيط المسلك التقليدي Calssical Pathway لنظام المتمم، وهذا ما يعزز قتل الطفيلي (10)، حيث أن العاملين C4, C3 من المكونات المهمة التي تتوسط هذا المسلك في التثبيط.
في الجدول (8) نلاحظ ارتفاعاً معنوياً في MDA (0.6100mmol/L) مقارنة بنساء السيطرة 0.034400 mmol/L والسبب حصول زيادة في تكوين أصناف جذور الأوكسجين الحرة أدى إلى زيادة كبيرة في أكسدة الدهون، وهذا يتفق مع ما توصل إليه الباحثون (32) و (39) و (40).
كما لوحظ انخفاض كبير في مضاد الأكسدة الطبيعي GSH في المصابات كان 0.146422 mmol/L مقارنة بنساء السيطرة 0.905329 mmol/L ويمكن أن يعزى هذا الانخفاض إلى زيادة فرط الأكسدة وتكوين الجذور الحرة التي تستهلك بسرعة هذا العامل المضاد للتأكسد (41)، كما أن مستوى GSH الكلوتاثيون يمكن أن يتأثر بعوامل العمر و درجة النمو و الحالة الغذائية والتوازن الغذائي (42).

جدول - 1 : التغيرات الشهرية في نسب الإصابة بالمشعرات المهبلية في النساء المراجعات لمستشفى الحبيبية وابن البلدي

Month	No. of Sample Examination	No. of Sample Patient (+ve)	State Percentage %
December	40	5	12.5%
January	40	6	15.0%
February	36	7	19.4%
March	40	14	35.0%
April	35	5	14.3%
May	45	9	20.0%
June	40	8	20%
July	50	7	14%
Total	326	51	18.7%

X^2 0.05 المحسوبة = 9.640
X^2 0.05 الجدولية = 14.07

جدول -2 : العلاقة بين عمر المراجعات في مستشفى الحبيبية وابن البلدي

Age	No. of Sample Examination	No. of Sample Patient	Percentage
15-17	30	2	6.7%
17-19	30	9	30%
20-29	90	20	22.2%
30-39	100	25	25%
40-49	38	2	5.2%
50-59	38	3	7.8%
Total	326	61	18.7

جدول - 3 : العلاقة بين المستوى التعليمي للنساء المراجعات لمستشفى الحبيبية وابن البلدي وإصابتهن بالمشعرات المهبلية

Education	No. of Sample Examination	No. of Sample Patient	Percentage
Nothing	107	51	59.3%
Primary	90	10	11.6%
Secondary	95	20	23.3%
High	34	2	5.8%
Total	326	83	26.7%

جدول - 4 : مستوى 1L-6 pg/ml و L-1a pg/ml1 بين مجموعة نساء السيطرة والمصابات

المجموعة	العدد	1L-6 بين مستوى pg/ml المجموعتين Mean ± SE	مستوى L-1a pg/ml1 Mean ± SE
السيطرة	10	70±0.81989 A	19.5300±0.2789 A
الإصابة	10	106.5400±0.93953 B	9.4700±0.36149 B

جدول – 5 : مستوى mg/dl IgA, IgG, IgM في مصل الدم لمجموعة النساء المصابات ونساء السيطرة

المجموعة	العدد	مستوى mg/dl IgG Mean±SE	مستوى mg/dl IgM Mean±SE	مستوى mg/dl IgA Mean±SE
السيطرة	10	731.4333±0.50305 A	99.8600±0.16680 A	149.6400±0.47004 A
الإصابة	10	996.0555±0.61669 B	409.7900±0.19969 B	174.5800±0.48644 B

الحروف المتشابهة تعني عدم وجود فروق معنوية والحروف المختلفة تعني وجود فروق معنوية عند مستوى احتمالي < 0.05

جدول - 6 : النسبة المئوية للخلايا اللمفاوية الحاملة للواسمات CD20 و CD4 و CD8 لدى المصابات وعينات السيطرة

المجموعة	العدد	CD8 Mean±SE	CD4 Mean±SE	CD20 Mean±SE
السيطرة	10	21.7300±0.12472 A	19.3000±0.26541 A	17.0300±0.16869 A
الإصابة	10	22.7600±0.21919 B	48.4300±0.31765 B	15.2100±0.18163 B

الحروف المتشابهة تعني عدم وجود فروق معنوية والحروف المختلفة تدل على وجود فروق معنوية عند مستوى احتمالي < 0.05

جدول - 7 : معدل مستوى الكلوبين المناعي C3 و C4 في مصل الدم لمجموعة نساء السيطرة ومجموعة النساء المصابات

المجموعة	العدد	معدل مستوى C4 mg/dlفي مصل الدم Mean±St	معدل مستوى C3 mg/dlفي مصل الدم Mean±St
السيطرة	10	21.1200±0.43838 A	107.9900±0.24196 A
الإصابة	10	28.1000±0.34577 B	143.9700±0.55016 B

الحروف المتشابهة تعني عدم وجود فروق معنوية والحروف المختلفة تدل على وجود فروق معنوية عند مستوى احتمالي < 0.05

جدول - 8 : مستوى MDA و GSH لمجموعة نساء السيطرة ومجموعة النساء المصابات

Group	No.	MDA , mmol/L	No.	GSH mmol/L
Control	5	0.034400±0.01242025 A	9	0.905329±0.580818
Patient	5	0.6100500±0.24494693 B	9	0.146422±0.0014853

المصادر

1. Fouts, A. C. and Krans,J.J. Trichomonas Vaginalis Revolution of its Clinical Presentation and Laboratory Diagnosis infect. Dis, U. 141(2) 137-143. (1980)
2. United Kingdom National Guideline,U.K.N.G.;.The management of **Tricho -monas vaginalis** (2007)
3. Al-Mallah,O.A.R.Studies on Trichomonas Vaginalis Infection in Mousl S.Sc. Thesis Coll. Med. Univ. Mousil, :68. (1981)
4. Al-Shabender,N.Histopathological Study Vaginal Trichomoniasis Msc. Thesis, Coll. Med. Univ. Baghdad (Cited by Al-Mallah, 1981). (1979).
5. Al-Delaim, F. S. Sexually Transmitted Discoses in Baghdad City. Dipl thesis Coll. Med. Univ. Baghdad :33. (1988).
6. Al-Rawi, M. A. M. Epidemiological Study of Trichomonasis and other Microorganis among Iraq Women Complaining of Vaginal Discharges. Dipl. Diss. Saddam Coll. Med. Saddam Univ. :63. (1993).
7. Al-Murayaty, A. Y. Aclinico-Epidemiological Study of Bacterial Women from Baghdad City Fellowship Iraqi Comm. Med. Spec. Thesis :72. (1996).
8. Al-Mudhaaffar,Z.M.J.Trichomonas Vaginalis Infection Clinical, Immunnolo- gical and Biochemical Studies among Iraqi Women Com Planning of Vaginal Discharge. Msc. Thesis Saddam Coll. Med, Saddam, Univ. :91. (1995).
9. Bartosi,K.D.;Dam Janov,L.V.;Viscarell,R.R.and Reiley,J. A. Immunoproeins in the Endomethium; Clinical Correlates of the Presence of Complement Fractions C3 and C4 Am.J.Obstet&Gynecol 156(1):11-5. (1987).
10. Mcleod,R.D. & Dowel, M. C. Basic Immunology in the Fetus and Newborn Ambriosoe-Thomosp, Peterson. Ed. 15:136-142. (2000).
11. Firesteia,G.S.Role of Cytokines in the immune System.J.Immunol 157:3850-3858. (1996).
12. Kishimoto, Tand Hirano, T. Molecular Regulation of Lymphocytes Response Ann. Rev. Immunol 61:485-484. (1988).
13. Hallwell, B. The Lancet. 344:721-724. (1994).
14. Hallwell,B.; Gutterade, J.M.C. & Cross, C.E.Lab.Clin.Med.119(6):598-615 (1992).
15. Hundelman, G. J. Evaluation of Oxidant in Dialysis Patients Blood Purify. 18:343-349. (2000).
16. Gupto, S. The Short Text Book of Medical Microbiology 3rd Ed, Jayee Bros; New Delhi :464. (1989).
17. Aust, S. D. and Bueye, J. A. (1978). Method Enzymol, 1st Ed; 52:302.
18. Eillman, G. L. Arch Biochem Biophys 2(82):70-77. (1959).
19. Macin,G.;Carbonara,A.D.& Heremans, G. F. Immunochemical Quantation of Antigens by Single Radial Immunodiffion Immunochemistry, 2:230. (1965).
20. Suzuki, Y and Kang H; Requirement of Non-T-Cells that Produce Gamma

Interferon for Prevention of Reactivation of Toxoplasma Gondii Infection in the Brain Infect Immunol, 155:2920-2927. (2001).

21. Steel. R.; G. and Torier, G.; H. Principle and Procedure of Statistics 2nd Ed. Mccrow Hill Book Company, New York :122-130. (1980).
22. Ali, N. M. H.; Dakheel, S. H. and Abdul Kareem, F. A. The Incidence of Trichomonas Vaginalis in Baghdad Amony Random Sample of the Population with Special Reference to Males infection Tech. Res. J. 2: 276-287. (1989).
23. Al-Kaisi, A. A. R. The Incidence Trichomonas Vaginalis among Females with Vaginal Discharge. Msc. Thesis Coll. Med. Univ. Baghdad. pp:85. (1998).
24. Al-Kubaisy,A.H.M., Al-Aoudi, H. A. and Al-Saad, A. A. Epidemiological Study Trichomonas Vaginalis in Karbala J. of Kibala (In press). (2002).
25. Al-Hindi,A.;&Lubbad;A.M Trichomonas vaginalis infection among Palestinian women:,Prevalence&trends during 2000-2006,Jurk J.Med Sci(6).371-375(2006).
26. Pelloux. H.; Pernod, G.; Polack, B.; Coursange, E. R.; Card, J.; Verna, J. M.; Ambroise. Thomas. P. Influence of Cytokines Toxoplasma. Gondi Growth in Human Astrocytoma Dorived Cell Parasitol, Res; 82(7):598-603. (2005).
27. Suzuki, Y; Yang, L.; Conley, F.; K.; Abrams J.; S. and Remington, J.; S.; Antihody Against Interleukin-6 Reduces Inflammation and Numbers of Cysts in Brains of Mice with Toxoplasma Encephalitis, 62(7):2772-2778. (2004).
28. Cont. P.; Kempura J. D.; Gtachino, M.; Boucher, W.; Kader, K. B. a. R. C; Realmy Felaco, M. Frogdas S. and Thochorides, T. C. Edieoria. Interleukin-6 and Mast Coll Allergy. 23(5)5. (2002).
29. Bensted,B.&Wood,E.J.Immunoglobulins Levels in Normal Pregnancy and Pregnancy Complicated by Hypertension.J.Obstet&Gynecol.Brit Comm,77:518-525. (1970).
30. Gusdon, S. P. Fetal and Maternal Immunoglobulin Levels During Pregnancy. Am. J. Obstet & Gynecol 103:895-900. (1969).
31. Cochrah. T. E. Fetal Maternal Immunoglobulin Concentrations and Delivery and Postpartum. J. Obstet & Gynecol. Brit. Comm, 99-238. (1972).
32. Mundoi, V., Kucknoor, As.,; Chang, T. H and Alderete, J. F; Anovel Surface protein of Trichomonas vaginalis is regulated independently by low iron and contact with vaginal epithelial cells. Biomed central 6(6) (1-12). (2006).
33. Hurlimann, J.; Thorbeck, C. and H.ockwald, G. The Liveas the Site of CRP Formation. J. Exp. Med; 123:365. (1966).
34. Mordne, D. G.; Monorgorgy, F.; Laregina, M.; Dirnarello, C. A. and Sibley, L. D. A Cute Toxoplasmosis Leads to Lethal Over Production of the Cytokine J. J, Immunol, 167:4575-4584. (2001).
35. Prigion, L.; Facehetet, P.; Chiotto, F.; Tasso, P. and Pistola, V. Toxoplasma Gondi. Specific CD4 + T Cell Clones From Healthy Latently Infected Humans Displasy Aprofile of Cytokine Scration Enr. J. Immunol; 25:1298-1305. (1995).

36. Peakman, M and Vergan, D. Basic and Clincal Immunology Pearson Professional Ltd. U. K. : 554-559. (1997).
37. Petri, M.; Globus, M. and Anerson, R. ANA. LA and ACA in Women with Idiopathic Habitual Abortion Arthritis & Rheumafish 30(6):601-606. (1987).
38. Al-Zamely, A. M. Toward understanding the Ischemic Heart Disease Via Oxidative Hypothesis Ph.D Thesis College of Science, Al-Mustansirya Univ. (2001).
39. Katwna, O. J. Analysis of Biological Development. PhD Thesis College of Science of Baghdad Univ. (1999).
40. Zhao,X,Fu;W;Yunan,W;Wn;Zig and Yang, Z;Chin. Med.J;Engl,109(2):926-929. (1996).
41. Bridges,A.B.;Scott,N.A.and Pringleg T.H.Cloincord. The Enzymes 15:169-194. (1993).
42. Meister. A. Selective Modification of Glutathione Metabolism, Science, 220:472-470. (1983).

خفض الملوثات العضوية من مياه المخلفات باستخدام الفطريات المائية *Achlya proliferoids, Saprolegnia parasitica*

خالد فالح حسن و انعام نوري علي و شيماء فخري جاسم و سفيان محمد شرتوح و أمل حمزة حمود
وزارة العلوم والتكنولوجيا / دائرة تكنولوجيا معالجة المياه / قسم البحوث والدراسات

ABSETRACT

Achlya proliferoids and *Saprolegnia parasitica* aquatic fungi were used to reduce the dissolved organic matter from the final discharge of wastewater treatment plant in Baghdad (Al-Rustumya) by measuring BOD_5, COD , TOC and fungi dry weight in laboratorial conditions (pH 4.5-4.8 and temperature 20 °c in a Batch culture system and a treatment period of 3-7 days). *Achlya proliferoids* showed the reduced percent for TOC 66.26% at higher propaply $p<0.01$ in all treatment period as compared with the sample before treatment, and BOD_5 by 63% and COD 43.36% at higher propaply $p<0.01$, while *Saprolegnia parasitica* showed ability to reduce COD about 50.45% at higher propaply $p<0.01$ in all treatment period and TOC by 62%, BOD_5 45.52% at higher propaply $p<0.01$ in all treatment period.

Key words: Wastewater, BOD_5, COD, TOC, Pollution, aquatic fungi.

الخلاصة

استخدمت عزلتان نقيتان من الفطريات المائية *Saprolegnia parasitica* , *Achlya proliferoids* لخفض المواد العضوية الذائبة في عينات من مياه التصريف النهائي لمحطة معالجة مياه الصرف الصحي في بغداد (الرستمية). قيست كفاءة الفطريات في خفض الملوثات العضوية من خلال فحص عوامل المتطلب الحيوي للاوكسجين BOD_5 و المتطلب الكيميائي للاوكسجين COD و الكاربون العضوي الكلي TOC وقياس الوزن الجاف للعزلات الفطرية في المختبر تحت ظروف اس هيدروجيني 4.5 – 4.8 وحرارة 20 °م وباستخدام النظام الزرعي المستقر Batch culture system ولفترة معاملة 3 – 7 ايام. سجل الفطر *Achlya proliferoids* نسبة اكبر على خفض تركيز TOC بنسبة 66.26 % وبمعنوية عالية $p<0.01$ لجميع فترات المعاملة في حين كانت نسبة خفض BOD_5 وCOD (63 % و 43.36 %) بمعنوية عالية $p<0.01$ ولجميع فترات المعاملة, بينما اظهر الفطر *Saprolegnia parasitica* قدرة اكبر على خفض COD بنسبة 50.45% و لباقي العوامل 62 % TOC و 45.52 % BOD_5 و بمعنوية عالية لكل فترات المعاملة.

الكلمات الدالة: مياه صرف صحي , BOD , COD , TOC , تلوث , فطريات مائية.

المقدمة

تعتبر مياه المخلفات الصناعية والزراعية والسكانية من المصادر الاساسية لتلوث المسطحات المائية بعد قذفها الى الانهار بدون معالجة مناسبة او معالجة جزئية حيث تحوي هذه المخلفات على الكثير من المواد العضوية والمسببات المرضية التي تؤدي الى تدني حالة المياه الطبيعية والاخلال بالتوازن للبيئة المائية وحدوث التلوث (1,2). نا صفات وتركيب و قابلية التحلل البايولوجي لملوث ما يتأثر بنوع الصناعة الناتج منها و تواجد ملوثات اخرى و الظروف البيئية كدرجة الحرارة والرطوبة ودرجة تركيز الملوث اذ تشكل مياه الصرف الصحي مركب معقد يحتوي على الالاف من الملوثات العضوية وغير العضوية, ان معالجة الفضلات السائلة بوجود الاحياء المجهرية ذات اهمية كبيرة بالنظر الى قابلية استهلاك هذه الاحياء للمركبات النتروجينية و الفسفورية اضافة الى الكاربون ومركبات الميثان (4).

للفطريات المائية دور مهم في توازن البيئة المائية ولاسيما المياه العذبة حيث تقوم بتحليل الكثير من الملوثات العضوية بواسطة انزيماتها التي تفرزها مثل انزيم cellulase , estrase و اعادتها الى مكوناتها الاصلية (3).

هدفت الدراسة الحالية الى اختبار كفاءة الفطريات المائية *Achlya proliferoids* و *Saprolegnia parasitica* وهي ضمن صنف الفطريات البيضية Oomycetes على خفض تراكيز الملوثات العضوية من مياه التصريف النهائي لمحطة الرستمية لمعالجة مخلفات الصرف الصحي بدلالة عوامل المتطلب الحيوي للاوكسجين BOD_5 و المتطلب الكيميائي للاوكسجين COD و الكاربون العضوي الكلي TOC و باستخدام النظام الزرعي المستقر Batch culture system وفي ظروف المختبر.

المواد وطرائق العمل

1- جمع و تهيئة العينات :

جمعت اربعة نماذج من مياه نهر دجلة قرب منطقة الجادرية لغرض عزل وتشخيص وتنمية الفطريات المائية باستخدام قناني زجاجية معتمة ومعقمة سعة 250 مليلتر, وتم جلب عينة من مياه المخلفات من التصريف النهائي لمحطة الرستمية لمعالجة مياه الصرف الصحي باستخدام قناني بلاستيكية polyethylene سعة 5 لتر ونقلت الى المختبر لاجراء التجارب بعد ترشيحها بجهاز Vacuum وباستخدام ورق ترشيح بحجم ثقوب 0.45 مايكرون,عقمت بجهاز الموصدة Autoclave بدرجة حرارة 121 م° وضغط 1.5 بار ولمدة 20 دقيقة.

2- عزل وتنقية وتشخيص الفطريات المائية:

عزلت الفطريات المائية بطريقة الطعوم baiting method (10) باستخدام بذور السمسم sesame indium سكبت عينات الماء في اطباق زجاجية معقمة سعه 9 سم وبواقع 20-25 مليلتر للطبق الواحد واضيف اليها الطعوم اعلاه لتشجيع السبورات السابحة للفطريات المائية على الانبات و النمو , تم اضافة المضاد الحيوي chloramphenicol المحضر باذابة 250 ملغم من المضاد الحيوي في 250 مليلتر من الماء المقطر بواقع 1مليلتر لكل طبق لغرض التخلص من التلوث البكتيري , حضنت الاطباق في 20 م° وفحصت بعد 48 ساعة بواسطة مجهر ضوئي لمراقبة نمو الخيوط الفطرية غير المقسمة , نقلت البذور التي ظهر عليها النمو بعد غسلها بالماء المقطر المعقم الى اطباق زجاجية معقمة حاوية على ماء مقطر وبذرة سمسم جديدة و 1 مليلتر من المضاد الحيوي وتركت لمده 72 ساعة حتى تستطيل الخيوط الفطرية ليمكن فصلها.تم عمل المزارع النقية من هذه الأطباق بقطع خيط واحد أو مجموعة خيوط بواسطة إبرتين زجاجيتين معقمتين ووضعت في طبق حاوي على ماء مقطر معقم لغسلها ونقلت إلى أطباق حاوية على وسط Mineral Salt Agar , المضاف له المضاد الحيوي (15) حضنت الأطباق في الحاضنة لمده 48 ساعة ولوحظ تكون مستعمرة نقية , تم اخذ قرص بقطر 7 ملم من حافة المستعمرة باستخدام ثاقبة فلين معقمة ووضع في طبق زجاجي معقم حاوي على ماء مقطر معقم و 1 مليلتر من المضاد الحيوي وبذرة سمسم وبعدها حضنت الأطباق في الحاضنة (18-20) م° وتركت لتنمو ومراقبة التكاثر اللاجنسي والجنسي لغرض التشخيص بالاعتماد على المصادر العلمية (6 و 12 و 13) و باستخدام المجهر الضوئي , وقد تم عزل نوعين من الفطريات السابرولكنية للدراسة وهما: *Achlya proliferoids* و *Saprolegnia parasitica* .

3- قياس الوزن الجاف :

استخدمت دوارق حجمية حاوية على 100 مليلتر من عينة التصريف النهائي لمحطة الرستمية لمعالجة مياه الصرف الصحي بعد تعقيمها وبواقع 3 مكررات للعينة وتم اضافة قرص مأخوذ من حافة المستعمرة الفطرية النامية على وسط Mineral Salt Agar وبعمر 4 ايام للفطر *Saprolegnia* و6 ايام للفطر *Achlya* ووضعت في الحاضنة بحرارة 18 – 20 م° وبعد 3- 7 ايام تم حصاد الخيوط الفطرية وقياس الوزن الجاف من خلال ترشيح العينة باستخدام اوراق ترشيح بحجم ثقوب 0.45 مايكرون وقياس وزن الورقة بعد ترشيح العينة, جففت الاوراق في الفرن الكهربائي بدرجة حرارة 80 م° ووزنت اوراق الترشيح بعد 24 ساعة وحسب الوزن الجاف (7):

الوزن الجاف = وزن الورقة مع الخيوط الفطرية قبل التجفيف – وزن الورقة بعد التجفيف.

4- الفحوصات الكيميائية ألمختبرية :

قيست العوامل BOD_5 و COD و TOC لعينة مياه التصريف النهائي لمحطة الرستمية قبل وبعد المعاملة بالفطريات المنتخبة واعتمدت طرق التحليل القياسية رقم 5210-B BOD و 5220-B COD و TOC (1).

نسبة الخفض = التركيز الاولي – التركيز النهائي/ التركيز الاولي × 100%

5- التحليل الاحصائي :

تم تحليل النتائج احصائيا باستعمال اختبار Analysis of Variation (ANOVA) لتحليل التباين وباستخدام البرنامج الاحصائي SPSS (16).

النتائج والمناقشة :

1- **قياس العوامل BOD_5, COD, TOC** : يوضح الجدول (1) كفاءة الفطر *Achlya proliferoids* في خفض تراكيز المواد العضوية لعينة مياه التصريف النهائي لمحطة الرستمية, من الجدول يلاحظ حدوث انخفاض عالي المعنوية ($p<0.01$) في قيم BOD_5 ,COD ,TOC مع زيادة فترة المعاملة ولوحظ ان اعلى خفض لتراكيز العوامل اعلاه بعد 7 ايام من المعاملة وبنسبة خفض 63% و 43.36% و 66.26% على التوالي بعد 7 أيام من المعاملة بالفطر بقيمة أس هيدروجيني تراوح بين 4.5-4.8 أذ كانت قيم العوامل BOD_5 ,COD ,TOC هي 60.4, 110 و340 جزء بالمليون قبل المعاملة و بعد معاملة العينة بالفطر *Achlya proliferoids* ولفترة معالجة 3 أيام انخفض تركيز العوامل إلى 49.2, 96.4, 256 جزء بالمليون و بمعنوية عالية بلغت $p<0.01$ مقارنة بالعينة قبل المعاملة, وبعد 5 أيام من المعالجة أصبح تركيز هذه العوامل 31.89 , 70.8 , 197.6 جزء بالمليون و بمعنوية عالية $p<0.01$, وبعد استمرار التجربة لليوم السابع للمعاملة أصبح التركيز للعوامل الثلاثة 22.3, 62.3, 114.7 جزء بالمليون وعلى التوالي.

يوضح الجدول (2) نسبة خفض العوامل BOD_5 ,COD ,TOC لعينة مياه المخلفات عند معاملتها بالفطر *Saprolegnia parasitica* أذ وجد من خلال التحليل الاحصائي وجود فروقات عالية المعنوية $p<0.01$ في قيم العوامل BOD_5 ,COD ,TOC بعد مرور 3, 5 و 7 ايام من المعاملة مقارنة بقيم العوامل قبل المعاملة و بنسبة خفض لتراكيز العوامل 45.52% و 50.45% و 62% على التوالي ولمدة 7 أيام من المعاملة بأس هيدروجيني 4.8. انخفضت تراكيزالعوامل BOD_5 ,COD ,TOC بعد 3 أيام من المعاملة الى 59.3 , 98.4 , 310 جزء بالمليون وبمعنوية عالية بلغت $p<0.01$ و بعد استمرار التجربة 5 أيام أصبح تركيز هذه العوامل 42.2, 71.6, 252 جزء بالمليون وبمعنوية عالية $p<0.01$ وفي اليوم السابع لمعاملة العينة بالفطر أصبحت تراكيز العوامل على التوالي 32.9, 54.5, 128 جزء بالمليون.

اظهر الفطر *Achlya* قدرة اكبر على خفض تركيز BOD_5 بنسبة 63% مقارنة بالفطر *Saprolegnia* 45.52% خلال 7 ايام من المعاملة وهذا يعود الى كفاءة انزيماته الخارج خلوية التي يفرزها على المواد العضوية لغرض تكسير الاواصر التي تربط السلاسل الكاربونية واستغلال الكاربون لادامة حياته (11), اضافة الى ان التماس المباشر للخيوط الفطرية مع العينة له دور كبير في زيادة كفاءة الفطر في خفض تركيز TOC بنسبة 66% مقارنة بالفطر *Saprolegnia* بنسبة 62% اذ توافقت الدراسة مع (8) حول تجاربهم على فطر *Fusarium flocciferum* اذ اثبت هذا الفطر قدرته على خفض تراكيز المواد العضوية المختلفة من عينة تصريف المياه الصناعية.

اظهر الفطر *Saprolegnia* كفاءة اكثرفي خفض تركيز COD بنسبة 50.45% مقارنة بالفطر *Achlya* 43.36% خلال 7 ايام من المعاملة وهذا يدل على ملائمة الظروف لمعيشة هذا الفطر وتحمله للظروف البيئية لمياه مخلفات مياه الصرف الصحي اذ وجد (9) في دراستهم تجمعات من الفطر *Saprolegnia sp.* في مياه المجاري المعروفة بكثرة المواد العضوية وهذا دليل على مقدرة هذا الفطر على العيش والتكيف في هذه البيئة واستغلال المواد العضوية وامتلاكه مجموعة كفوءة من الانزيمات تمكنه من استهلاك وتحليل مجموعة كبيرة من المواد العضوية المختلفة لديمومة حياته, كذلك توافقت الدراسة الحالية مع (5) حول دراستهم على الفطر المائي *Clavariopsis acuatica* وقدرته على خفض تركيز الملوث nonylphenol من مياه المجاري وتحويله الى مركبات ابسط واقل سمية بفعل إنزيم laccase.

2- **قياس الوزن الجاف** : يوضح الشكل (1) و (2) العلاقة بين الوزن الجاف للفطريات المنتخبة و نسبة خفض تراكيز BOD_5 ,COD ,TOC , اذ حصلت زيادة في الوزن الجاف للفطر *Achlya proliferoids* وخلال ايام المعالجة و عند استمرار التجربة حصل تثبيط للنمو وانكماش للمستعمرة الفطرية وهذا يعود الى انخفاض تراكيز الاوكسجين وعدم قدرة هذا الفطر على تحمل هذه الظروف مقارنة بالفطر *Saprolegnia parasitica* اذ سجل زيادة في الوزن الجاف ولفترة اطول و يعزى هذا الى قدرة هذا الفطر على المعيشة

في ظروف قلة الاوكسجين وزيادة تراكيز المواد العضوية. ان الزيادة في وزن المستعمرة خلال فترة المعالجة يدل على قابلية هذه الانواع الفطرية على المعيشة والنمو في التراكيز العالية للمواد العضوية واعتمادها على هذه المواد لديمومة حياتها بعد تحليلها وتكسير الاواصر التي تربط بين السلاسل الكاربونية لهذه المواد وهذا ما اثبته (2) حول دراسته على فطر *Phanerochaete chrysosporium* وهو من الفطريات البازيدية وقدرته على تحطيم وتحليل الكثير من المواد كالاصباغ والمبيدات ومخلفات المستحضرات الطبية والمشتقات النفطية.

جدول -1: نسبة خض العوامل BOD_5, COD, TOC للفطر *Achlya proliferoids* لعينة مياه التصريف النهائي لمحطة الرستمية لفترة معالجة 3, 5 و 7 أيام

ت	العوامل	قبل المعاملة جزء بالمليون	بعد المعاملة جزء بالمليون			نسبة الخفض % بعد 7 ايام
			3 أيام	5 أيام	7 أيام	
1	BOD_5	0.31 ±60.4	** 49.2 0.46 ±	+** 31.89 0.57 ±	■♦** 22.3 0.30 ±	% 63
2	COD	0.58 ±110	** 96.4 0.44 ±	+** 70.8 0.12 ±	■♦** 62.3 0.23 ±	% 43.36
3	TOC	0.58 ±340	** 256 0.58 ±	+** 197.6 0.46 ±	■♦** 114.7 0.43 ±	% 66.26

** عالية المعنوية $p<0.01$ مقارنة بقبل المعاملة
♦ عالية المعنوية $p<0.01$ مقارنة مع 3 ايام معاملة
■ عالية المعنوية $p<0.01$ مقارنة مع 5 ايام معاملة
+ عالية المعنوية $p<0.01$ مقارنة مع 3 ايام معاملة

جدول -2: نسبة خفض العوامل BOD_5, COD, TOC للفطر *Saprolegnia parasitica* لعينة مياه التصريف النهائي لمحطة الرستمية لفترة معالجة 3, 5 و 7 أيام.

ت	العوامل	قبل المعاملة جزء بالمليون	بعد المعاملة جزء بالمليون			نسبة الخفض % بعد 7 ايام
			3 أيام	5 أيام	7 أيام	
1	BOD_5	0.31 ±60.4	59.3 0.35 ±	+** 42.2 0.53 ±	■♦** 32.9 0.21 ±	% 45.52
2	COD	0.58 ±110	** 98.4 0.31 ±	+** 71.6 0.19 ±	■♦** 54.5 0.32 ±	% 50.45
3	TOC	0.58 ±340	** 310 0.58 ±	+** 252 0.58 ±	■♦** 128 0.58 ±	% 62

** عالية المعنوية $p<0.01$ مقارنة بقبل المعاملة
♦ عالية المعنوية $p<0.01$ مقارنة مع 3 ايام معاملة
■ عالية المعنوية $p<0.01$ مقارنة مع 5 ايام معاملة
+ عالية المعنوية $p<0.01$ مقارنة مع 3 ايام معاملة

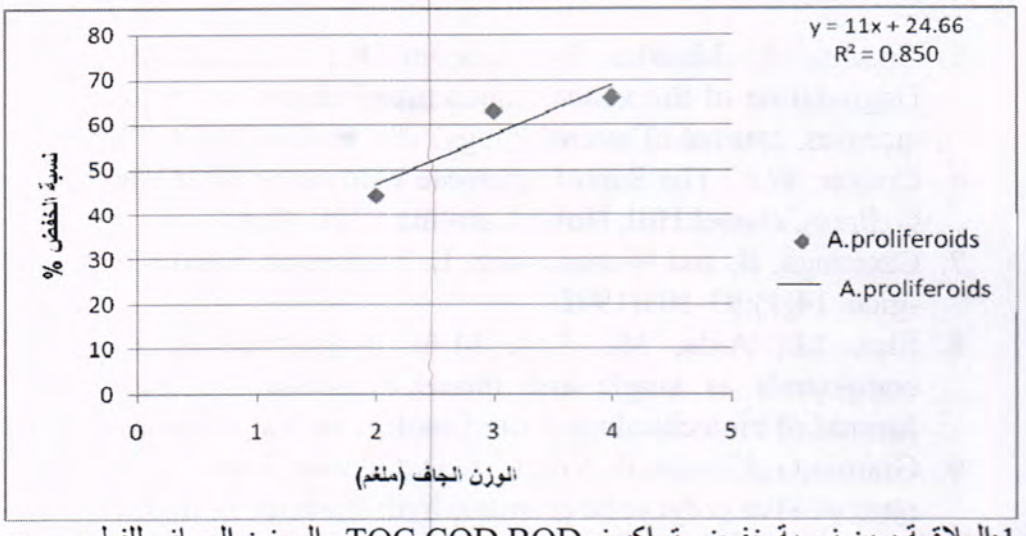

شكل-1:العلاقة بين نسبة خفض تراكيز TOC,COD,BOD_5 والوزن الجاف للفطر *Achlya proliferoids*

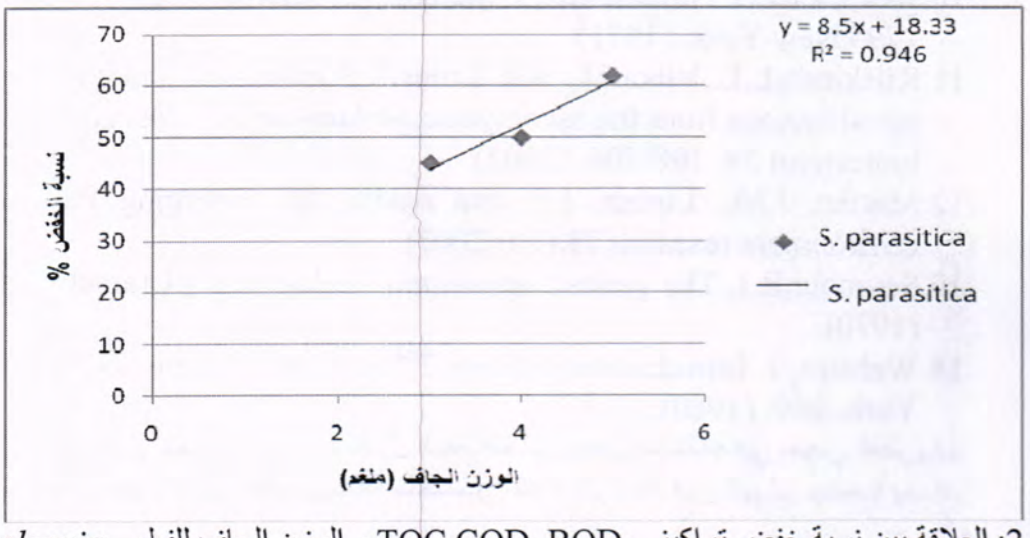

شكل -2: العلاقة بين نسبة خفض تراكيز TOC,COD ,BOD_5 و الوزن الجاف للفطر *Saprolegnia parasitica*

المصادر

1. APHA. Standard method for the examination of water and wastewater, 16th ed. American public Health Association, American water works Association and water pollution control federal, Washington, D.C.(1985).
2. Bennet, J.W.; Wunch, K.G. and Faison, B.D. Use of fungi biodegradation. Manual of environmental microbiology, second edition. ASM press Washington, D.C.(2002).
3. Bermingham, S.; Maltby, L. and Cooke, R.C. Effect of acoal mine effluent on aquatic hyphomycetes.Field study.J.Appl.Ecol.33:1311-1321 (1996).
4. Bayramoglu, G.; Celik, G.; Yalsin, E. Modification of surface properties of *Lentinus sajor-caju* mycelia by physical and chemical methods. Journal of Hazardous materials,119. (3), : 219-229. (2005).

5. Charles, J.; Monika, M.; Gurden, K.; Claudia, M. and Dietmar, S. Degradation of the xenoestrogen nonyl phenol by Aquatic fungi and their laccases. Journal of microbiology, 151: 45-57(2005).
6. Cocker, W.C. The Saprolegniaceae with notes other water molds. Univ. N. C. Press, chapel Hill, North Carolina.: 201. (1965).
7. Czeczuga, B. and Woronowicz, L. Studies on aquatic fungi.Acta– Mycolo -gica. 14(1):93-103(1992).
8. Elsa, M.; Aida, M.; Ana, M.A. Biodegradation of natural phenolic compounds as single and mixed substrates by *Fusarium flocciferum.* Journal of biotechnology.Univ.Catolica de Valparaiso,Chile.7(1) (2004).
9. Gramss,G.;Kirsche,B.;Volgt, K.D.;Gunther,T.and Fritsche,W.Conversion rates of Five polycyclic aromatic hydrocarbons in liquid culture of 58 fungi and the concomitant production of oxidative enzymes. Mycol. Res. 103:1009-1018.(2004).
10. Jones, E.B.G. Aquatic fungi. Methods in Microbiology.4, Academic press. : 795 New York. (1971).
11. Kiiskinen,L.L.;Viikari,L. and Kruus,K.Purification and characterization of noval laccase from the ascomycete *Melanocarpus albomyces* .Appl microb biotechnol 59: 198-204. (2002).
12. Martha, J.M.; Lorien, J.F. and Audra, M. Emerging Pollutants. Water environment research,79.(10)(2007).
13. Seymour,R.L.The genus *Saprolegnia*.Verlag Von j.Cramer,Germany, 124. (1970).
14. Webster, J. Introduction to fungi.2nd ed. Cambridge University Press, New York.:669. (1980).
15. الطائي, شذى علي شفيق. تاثير واستغلال النفط الخام وبعض مشتقاته في بعض الفطريات المائية المعزولة من نهر دجلة. رسالة ماجستير, كلية التربية- ابن الهيثم. جامعة بغداد. (1999).
16. العقيلي, صالح رشيد و الشايب, محمد سامر. استخدام البرنامج الاحصائي spss. مطبوعات جامعة بغداد. دار الشرق للطباعة: 358.(1998).

إختبار الفعالية التثبيطية لبعض المستخلصات النباتية ضد فايروس موزائيك الطماطة *Tomato Mosaic Virus*

ياسرحسين الجريصي و.إحسان شفيق دميرداغ
قسم علوم الحياة/ كلية العلوم/ الجامعة المستنصرية

الخلاصة

إن من الأسباب الرئيسة المسببة لفقدان نسبة كبيرة من إنتاج الطماطة في العالم هو إصابتها بفايروس موزائيك الطماطة وفايروسات أخرى ، ونظراً لعدم توفر مبيد أو مادة فعالة أخرى ضد الأمراض الفايروسية التي تصيب النبات يمكن استعمالها في مقاومة المرض والحد من انتشاره ، لذا تم القيام بهذه الدراسة وذلك بانتخاب سبعة أنواع نباتية متوفرة في البيئة العراقية وعلى أساس الاستخدامات العلاجية لهذه النباتات وورود بعضها في المراجع العلمية من الناحية الكيميائية ، على أمل العثور على بعض المواد الداخلة في تركيب هذه المستخلصات التي يمكن إن يكون لها دور فعال على مرض موزائيك الطماطة وهذه النباتات هي:

Amaranthus caudatus , *Chenopodium amaranticolor*, *C. murale* , *Convolvulus arvensis* , *Datura innoxia* , *D. stramonium* and *Portulaca oleracea*

وتم تحضير مستخلصات أوراق هذه النباتات بسحق أوراقها في هاون خزفي مع الماء المقطر ، ثم رُشحت العصارة الناتجة خلال أربع طبقات من الشاش الطبي ، ثم عُرض الراشح للانتباذ ليهمل الراسب ويُركز الطافي ليستعمل في الاختبارات اللاحقة ، حيث دُرست الفعالية التثبيطية لهذه المستخلصات بخلطها بتراكيز مختلفة مع اللقاح الفايروسي ولقحت بها أوراق تبغ *Nicotiana glutinosa* بطريقة تلقيح نصف الورقة Half-leaf inoculation ، وإحتُسب عدد البقع الموضعية الدالة على حيوية الفايروس .

وقد أظهر مستخلصا أوراق نبات *Chenopodium amaranticolor* و *C. murale* فعالية تثبيطية عالية بلغت 100% لجميع التراكيز المستخدمة ، أما مستخلصات أوراق النباتات المستعملة الأخرى فكانت ذات فعالية تثبيطية اقل .

ABSTRACT

The search for novel antiviral phytoproducts continues. Plant extracts that can eliminate the virus reproduction may have agricultural advantage for the elimination of epidemic plant viruses. This work includes a preliminary study of the effect of seven crude extracts of wild plants on Tomato Mosaic Virus (ToMV).

Extracts of *Amaranthus caudatus* , *Chenopodium amaranticolor*, *C. murale* , *Convolvulus arvensis* , *Datura innoxia* , *D. stramonium* and *Portulaca oleracea* were prepared by grinding the fresh leaves with distilled water by mortar and pestle, the extract was strained through four layers of cheesecloth then centrifuged and the resulting supernatant was used in the following investigations. The activity of extracts determined by mixing these extracts in a different concentrations with the inoculum (1:1) and then inoculated on tobacco leaves (*Nicotiana glutinosa*) by using opposite half-leaf inoculation technique as local lesion assay for antiviral activity test.

The leaves extracts of *Chenopodium amaranticolor* and *C. murale* showed a high inhibitory activity. This was a high as 100% for concentrated and diluted juices. While the inhibitory activity of the another extracts were less.

المقدمة

إن للأمراض الفايروسية أهمية بالغة نظراً لما تسببه من خسائر إقتصادية كبيرة ولاسيما فايروس موزائيك الطماطة الذي يكتسب أهمية متميزة نظراً لإنتشاره الواسع في كثير من دول العالم (1،2،3) ، وثباتيته العالية في التربة مع الإحتفاظ بقابلية العدوى (4،5) وسهولة نقله ميكانيكياً بمختلف الوسائل (3،6،7) إذ إنه يهاجم نباتات الطماطة في البيوت الزجاجية والبلاستيكية فيؤثر تأثيراً مباشراً في الأوراق والأزهار فيقلل بذلك من كمية ونوعية الثمار الناتجة (8،9).

لقد حاول الكثير من الباحثين إستعمال المستخلصات النباتية الخام أو المركبات المعزولة منها ومنتجات طبيعية أخرى في تثبيط الفايروسات النباتية وتقليل إنتشارها (10،11،12).

وبسبب تنوع الغطاء النباتي في العراق فقد كان من الطبيعي دراسة تأثير المستخلصات الخام لبعض النباتات البرية على الفايروسات النباتية فكان فايروس موزائيك الطماطة من الفايروسات التي تستحق الاهتمام ، وعليه تم انتخاب سبعة أنواع من الأعشاب البرية على أساس استخداماتها العلاجية المؤكدة في المراجع العلمية ووفرتها في البيئة العراقية على أمل العثور على بعض المركبات ذات التأثير الفعّال على مرض موزائيك الطماطة.

المواد وطرائق العمل

جمع وزراعة النباتات المستخدمة للاستخلاص

إن قسماً من النباتات التي اختبر تأثير مستخلصاتها في تثبيت فايروس موزائيك الطماطة يتواجد طبيعياً بشكل أعشاب منتشرة في الحقول ، أما القسم الأخر فتم زراعته في ظروف ملائمة في بيت زجاجي بدرجة حرارة تتراوح 25-35 ْم إذ وضعت بذور *Chenopodium amaranticolor* ، *Datura stramonium* و *D. innoxia* في المجمدة لمدة أسبوع واحد لغرض كسر طور السكون ثم زرعت بشكل دايات ، بعدها نقلت البادرات Seedlings بعمر ثلاثة أسابيع إلى أصص بلاستيكية لغرض تنميتها ووصول النبات إلى مرحلة التزهير.

تشخيص النباتات

لقد جمعت الأنواع النباتية وتم تهيئتها لغرض التشخيص ، وقد تم التشخيص من قبل المعشب التابع إلى كلية الزراعة/جامعة بغداد، وقد تم حفظ عينة من كل نوع وسجلت عليها المعلومات النباتية التي تخص كل منها .

تحضير المستخلصات النباتية

تم تحضير المستخلصات النباتية بتقطيع الأوراق النباتية مع سويقاتها لتسحق في هاون خزفي ، بعد ذلك تم ترشيح العصارة الناتجة خلال أربع طبقات من الشاش الطبي ، ثم وضع الراشح الناتج في جهاز الانتباذ Centrifuge بسرعة 300 دورة/دقيقة لمدة 20 دقيقة، أهمل الراسب، وتم تركيز الطافي لتُحضر منه التراكيز المستخدمة في الاختبارات اللاحقة .

تهيئة نبات الاختبار

زرعت بذور النبات *Nicotiana glutinosa* بشكل دايات ثم نقلت البادرات بعمر ثلاثة أسابيع إلى أصص بلاستيكية ذات قطر 15 سم تحتوي على تربة رملية مزيجية Sandy loam مخلوطة مع بتموس Peat moss وسماد عضوي بنسبة 2 :1 :1 على الترتيب ، وعُقمت التربة بجهاز الموصدة Autoclave ثم وضعت الشتلات في بيت زجاجي معقم ومحكم الغلق مع استمرار المكافحة بالمبيدات الحشرية ، وكانت درجة الحرارة 25-35 °م والرطوبة النسبية 40-70% ، وقد لقحت النباتات بعمر 5-10 أوراق ، علماً بان هذه الأنواع من النباتات تظهر عليها أعراض الإصابة بفايروس موزائيك الطماطة بشكل بقع موضعية Local lesions .

الحصول على عزلة الفايروس

تم الحصول على عزلة الفايروس من نباتات الطماطة المصابة بمرض الموزائيك طبيعياً في الحقل التي عوملت عصارتها بحمام مائي بدرجة 90 °م لمدة 10 دقائق ، ومن ثم لقحت على نبات *C. amaranticolor* بالعصارة المعاملة بالتسخين ، للحصول على بقع منفردة للفايروس Single lesions التي استعملت فيما بعد لتلقيح عدد من نباتات الطماطة ذات الصنف Pearson (J.E. Ohlsens Enke A/S, Odense, Denmark) لتكون مصدر اللقاح الفايروسي عند ظهور أعراض الإصابة عليها .

تحضير اللقاح الفايروسي

سحقت أوراق نباتات الطماطة التي تحمل أعراض الموزائيك في هاون خزفي بوجود الماء المقطر بحجم 5 مللتر لكل 1 غرام من أوراق الطماطة ، وقد تم ترشيح العصير باستخدام أربع طبقات من الشاش المعقم ، بعدها تم توزيع الراشح (اللقاح) في أنابيب اختبار ليحوي كل منها 3 مللتر من هذا الراشح ، تم سد فوهة الأنابيب بقطن طبي معقم ، ثم حفظت الانابيب في المجمدة لتكون مصدر اللقاح الفايروسي .

دراسة تأثير المستخلصات النباتية الممزوجة مع اللقاح الفايروسي على عدد البقع الناتجة على الورقة الملقحة

استعملت في هذه الدراسة طريقة F.O.Holmes (13) في تلقيح نصف الورقة Half-leaf treatment من أوراق نبات الاختبار Test plant وذلك لتلافي الاختلاف في حساسية الأوراق المختلفة للإصابة بالفايروس ، وكذلك الاختلاف في مساحة الأوراق ، إذ عومل النصف الأيسر للورقة بمزيج اللقاح الفايروسي والمستخلص النباتي المراد اختبار فعاليته على الفايروس وبمختلف التراكيز المستعملة 2 و5 و10 و20 و40 % وبنسبة خلط 1:1 حيث أضيف 1 مللتر من التراكيز المراد اختبارها من المستخلص إلى 1 مللتر من اللقاح الفايروسي ، وبذلك أصبحت التراكيز كالآتي: 1 و 2.5 و 5 و10 و20% ثم أُجري التلقيح بعد الخلط مباشرة وذلك بعد رش ورقة تبغ *Nicotiana glutinosa* المراد تلقيحها بمسحوق الكربورندم Carborundum ، وتمت عملية التلقيح بغمس أصبع السبابة في خليط اللقاح والمستخلص النباتي ،ومسح على النصف الأيسر من السطح العلوي لورقة نبات التبغ لتمثيل عينة المعاملة Treatment ، أما النصف الأيمن منها فقد تم تلقيحه بخليط اللقاح والماء المقطر بنسبة الخلط وطريقة التلقيح نفسهما ليمثل عينة السيطرة Control .

لقد كررت المعاملة لكل تركيز من المستخلص على ثلاثة أوراق من نبات الاختبار وكانت الأوراق تغسل بالماء المقطر بعد التلقيح مباشرة ، وقد ظهرت الأعراض بعد 3-7 أيام من التلقيح ، وتم حساب عدد البقع الموضعية للمعاملة والسيطرة على نصفي الورقة .

إن فعالية المستخلص النباتي تم التعبير عنها بالنسبة المئوية للاختزال في عدد البقع الناتجة وقد حُسبت من المعادلة الآتية:

$$\text{النسبة المئوية للاختزال \%} = 100 - \left(\frac{\text{عدد البقع الناتجة من عينة المعاملة}}{\text{عدد البقع الناتجة من عينة السيطرة}} \times 100 \right) \%$$

النتائج والمناقشة

بينت نتائج هذه الدراسة إن المستخلص المائي لأوراق النباتين *Chenopodium amaranticolor* و *C. murale* قد أظهرت فعالية تثبيطية عالية جداً ، إذ بلغت نسبة التثبيط 100 % لجميع التراكيز المستخدمة من هذين المستخلصين (كما موضح في الجدول رقم 1) . وهذا يشير إلى إمكانية تخفيف المستخلص الخام لهذين النباتين إلى تراكيز أدنى مع احتفاظها بمستوى الفعالية نفسه أو ما يقاربه .

وهذا يتلائم مع ما ذكره مورينو (14) الذي درس تأثير عصارات 28 نوع نباتي على فايروس TMV كان من ضمنها عصارات *Chenopodium amaranticolor* ، *C. quinoa* و *Datura stramonium* ووجد بأنها مثبطة للفايروس عندما مزجت معه واختبرت على تبغ *N. glutinosa* ، وما ذكره علام وجماعته (15) الذين درسوا فعالية عصارات 29 نوع نباتي ينتمي إلى 15 عائلة في تثبيط فايروس TMV و Cucumber Mosaic Virus فوجدوا بان أغلب المكونات الفعالة كانت موجودة في أطراف النبات والأوراق العليا من نباتات *Chenopodium amaranticolor* ، *C. murale* و *C. album* .

إن الفعالية التثبيطية للنوعين *C. amaranticolor* و *C. murale* قد تعود للمادة نفسها لكونهما ينتميان إلى الجنس نفسه ، فقد يكون الفعل التثبيطي عائدا إلى مادة Chenopodin المتوفرة في هذا الجنس ، أو إلى مادة Glycine betaine الموجودة بتركيزٍ عالٍ في هذين النوعين والأنواع الأخرى التي تعود إلى العائلة Chenopodiaceae (16) .

أما بالنسبة لمستخلص أوراق *Amaranthus caudatus* ، *Convolvulus arvensis* ، *Datura innoxia* ، *D. stramonium* و *Portulaca oleracea* فقد أظهرت فعالية تثبيطية أقل ، فعند استخدام هذه المستخلصات بتركيز 20% كانت النسبة المئوية للاختزال 82% ، 71% ، 89% ، 92% ، 87% على الترتيب (كما موضح في الجدول رقم 1) .

وقد تعود الفعالية التثبيطية لهذه المستخلصات إلى ما تحتويه من مركبات تؤثر تأثيرا مباشراً على الفايروس بعد مزجها مع اللقاح الفايروسي ، أو إن هذه المركبات أحدثت تغييراً في حساسية النبات للإصابة من خلال إشغالها مناطق دخول الفايروس على النبات العائل أو من خلال تدخلها في عملية التضاعف الفايروسي بارتباطها مع بروتينات الفايروس مما يحول دون تكون الغلاف البروتيني Protein coat للفايروس .

ولابد من الإشارة هنا إلى إن جميع المستخلصات التي استخدمت لم تظهر أي تأثير سمي على نبات التبغ *N. glutinosa* عند معاملة الأوراق بها حتى عند تجريح الأوراق بالكاربورندم .

جدول رقم- 1: تأثير بعض المستخلصات النباتية في اختزال عدد البقع الموضعية الناتجة بفعل فايروس موزانيك الطماطة (1)

مصدر المستخلص	النسبة المئوية للاختزال (2)				
	التركيز1%	%2.5	% 5	% 10	% 20
Chenopodium amaranticolor	100	100	100	100	100
C. murale	100	100	100	100	100
Datura stramonium	41	47	66	81	92
D. innoxia	33	39	59	72	89
Portulaca oleracea	36	54	61	79	87
Amaranthus caudatus	29	38	51	67	82
Convolvulus arvensis	16	30	48	70	71

(1) اجري الاختبار على نبات تبغ *Nicotiana glutinosa* والذي يعطي أعراض بشكل بقع موضعية وقد مزج المستخلص مع اللقاح الفايروسي .

(2) النسبة المئوية للاختزال = $\left(100 \times \frac{T}{C}\right) - 100$

حيث أن C = عدد البقع الموضعية في المقارنة Control

T = عدد البقع الموضعية في المعاملة Treatment

المصادر

1. Scholthof, K. G.; Shaw, J. G., and Zaitlin, M.. Tobacco Mosaic Virus: One Hundred Years of Contributions to Virology. Trends in Plant Science,5(6): 268(2000).
2. Scholthof, K. G.. Tobacco Mosaic Virus: A Model System for Plant Biology. Annual Review of Phytopathology, 42: 13-34(2004).
3. Ssekyewa, C.. Incidence, Distribution and Characteristics of Major Tomato Leaf Curl and Mosaic Virus Diseases in Uganda. Ph.D. thesis, Faculty of Bioscience Engineering, Ghent University, Ghent, Belgium. 233 (2006).
4. Pares, R. D. ; Gunn, L. V. and Cresswell, G. C.. Tomato mosaic virus infection in a recirculating nutrient solution. Journal of phytopathology, 135: 192-198(1999).

5. Gülser, C. ; Yilmaz, N. K. and Candemir, F.. Accumulation of Tobacco mosaic virus (TMV) at different depths clay and loamy sand textural soils due to tobacco waste application. Environ. Monit. Assess., 146(1-3):235-242 (2008).
6. Park, W. M.; Lee, G.P.; Ryu, K. H. and Park, K. W.. Transmission of tobacco mosaic virus in recirculating hydroponic system. Scientia Horticulturae, 79(3-4): 217-226(1999).
7. EL-Dougdoug, Kh. A.; Gomaa, H. A. and Abo-El-Maaty, S. The Impact of Interference Between Tomato Yellow Leaf Curl and Tomato Mosaic Viruses on Tomato Plants. Journal of Applied Sciences Research, 2(12): 1151-1155 (2006).
8. Nelson, R. S.; McCormick, Sh. M.; Delannay, X.; Dubé, Ph.; Layton, J.; Anderson, E. J.; Kaniewska, M.; Proksch, R. K.; Horsch, R. B.; Rogers, S. G.; Fraley, R. T. and Beachy, R. N.. Virus Tolerance, Plant Performance of Transgenic Tomato Plants Expressing Coat Protein from Tobacco Mosaic Virus. Biotechnology, 6: 403-409(1988).
9. Sikora,E.J.;Gudauskas, R.T.;Murphy,J.F.;Porch, D.W.;Andrianifahanana, M. ; Zehnder, G. W.; Bauske, E. M.; Kemble, J. M.and Lester, D. F.. A multivirus epidemic of tomatoes in Alabama. Plant disease, 82: 117-120 (1998).
10. EL-Dougdoug,Kh.A.;Gomaa,H.A.and Daoud, R. A. Elimination of Some Viruses Infecting Tomato Plants by Phyto-antivirus. Research Journal of Agriculture and Biological Sciences, 3(6): 994-1001(2007).
11. Lehtonen, P. T.; Helander, M.; Siddiqui,Sh. A.; Lehto,K. and Saikkonen, K.. Endophytic fungus decreases plant virus infections in meadow ryegrass (Lolium pratense). Biol. Lett., 22; 2(4): 620–623(2006).
12. Farnsworth, N. R.; Svoboda, G. H. and Blomster, R. N.. Antiviral activity of selected Catharanthus alkaloids. Journal of Pharmaceutical Sciences,57 (12): 2174 – 2175(2006).
13. دميرداغ ، إحسان شفيق ؛ التميمي، كامل مهدي. الفايروسات (الرواشح) مطابع جامعة الموصل، مديرية مطبعة الجامعة ، جامعة صلاح الدين – اربيل(1982).
14. Moreno, C. M.. Inhibitory effect of plant saps on tobacco mosaic virus (TMV) .Turrialba, 30(3):262-267.(Review of plant pathology, 61,P,9) (1980).
15. Allam, E. K.; Morsy, A. A.; Ali, M.D. and Abo-El-Ghar, A.I.. Inhibitors from some higher plants for inhibiting TMV and CMV infection. Egypt. J.Phytopathology,10(1):9-20.(Review of plant pathology,61,:332) (1979).
16. Weigel, P. and Lather, F.Occurrence of high concentration of glycine betaine in the glygophytic Chenopodiaceae. C.R. Acad.Sci.Ser.,3,300(2): 65-70. (Chemical Abstract, 102, :377). (1985)

التقدير الحصين لمعامل الارتباط

نادية هاشم النور وهدى عبد الله رشيد واحمد نجم عبد الله
الجامعة المستنصرية / كلية العلوم / قسم الرياضيات

ABSTRACT

This paper interested in assessment of correlation coefficient between random variables when away from the normal distribution of data through one of the two variables contain the contaminated values (outliers) , as was the comparison between the performance of Pearson's and Spearman's correlation coefficients, with the methods of the modified Pearson's correlation coefficient depending on the robust estimator (the median, Gastwirth's estimator) for the location parameter instead of the mathematical mean.

By using the Mean Square Error (MSE) as criterion for comparison between the estimates for different samples (n=10,24,50,100) and different distributional situations generated by the application of the Monte Carlo simulation (with 1000 replications) with correlation coefficient $\rho = 0, 0.9$, we found the adoption of an robust estimator for the location parameter instead of the mathematical mean has added a significant improvement on the performance of the Pearson's correlation coefficient

الخلاصة

اهتم البحث بمعالجة تقدير معامل الارتباط بين متغيرين عشوائيين عند ابتعاد البيانات عن التوزيع الطبيعي من خلال احتواء احد المتغيرين على الشواذ ، إذ تمت المقارنة بين بعض اداء معاملي ارتباط بيرسون والرتب لسبيرمان وبعض الطرائق المحورة عن معامل بيرسون للارتباط وذلك بالإعتماد على المقدر الحصين لمعلمة الموقع (الوسيط ، مقدر *Gastwirth*) بدلاً عن الوسط الحسابي .

وباستخدام متوسط مربعات الخطأ *Mean Square Error (MSE)* معياراً للمقارنة بين التقديرات ولإحجام عينات مختلفة (n=10,24,50,100) ولحالات توزيعية مختلفة تم توليدها من خلال تطبيق طريقة مونت كارلو للمحاكاة (بتكرار 1000 تجربة لكل حالة) ولمعاملات ارتباط $\rho = 0, 0.9$ تم التوصل الى ان إعتماد المقدر الحصين بدلاً عن الوسط الحسابي قد اضاف تحسناً ملحوظاً على اداء معامل بيرسون للارتباط .

المقدمة

يعرف معامل الارتباط *Correlation Coefficient* أنه مقياس احصائي يبين درجة العلاقة ونوعها بين متغيرين عشوائيين او أنه مقياس يبين التغير الاقتراني بين متغيرين ، وتتراوح قيمته بين (-1) و (+1) .

يعد معامل ارتباط بيرسون من اكثر معاملات الارتباط شيوعاً الا انه شديد الحساسية تجاه المشاهدات الشاذة (*Outliers*) في مجموعة البيانات (1) . تعرف تلك المشاهدات بكونها اما مشاهدات مخالفة (*Discordant*) او مشاهدات ملوثة (*Contaminant*) ويقصد بالمخالفة تلك المشاهدة التي تظهر بشكل غير منسجم مع بقية البيانات اما الملوثة فهي المشاهدة التي لا تكون ضمن المجتمع المحدد (2) .

من هنا ظهرت الحاجة الى ايجاد مقدرات/اساليب اكثر حصانة لا تتأثر بوجود تلك المشاهدات . ان مصطلح الحصانة (*Robustness*) (1) استعمل ولاول مرة عام 1953 من قبل *Box* ليشير الى ان الطريقة الاحصائية تعد من الطرائق الحصينة اذا كانت ذات اداء قريب من اداء الطرائق التقليدية عند تحقق الافتراضات المحددة "منها خلو البيانات من المشاهدات الشاذة" وافضل منها في حالة الانحراف عن تلك الافتراضات .

في عام 1975 اقترح كل من *Devlin , Gnanadesikan* و *Kettenring* (3) طرائق بيانية لتشخيص المشاهدات الثنائية التي من الممكن ان تؤثر على قيمة معامل الارتباط للعينة كما قدموا تقديرات حصينة لمعامل الارتباط بالاعتماد على تجربة المحاكاة للمقارنة بين الطرائق المقترحة والطرائق التقليدية المعروفة .

فـي عـام 1987 درس كـل مـن *Gideon* و *Hollister* (4) معامـل ارتبـاط الرتـب ومقاومتـه للمشاهدات الشاذة (الملوثة) .

فـي عـام 1997 اعتمـد *Shevlyakov* (5) علـى تجربـة المحاكـاة للمقارنـة بـين مجموعـة مـن التقديرات المعروفة لمعامل الارتباط وبعض التقديرات الحصينة المقترحة وبالتالي التوصل الى تقدير عالي الحصانة عند التعامل مع التوزيع الطبيعي الثنائي الملوث اسماه بوسيط معامل الارتباط *Median Correlation Coefficient* ويكون بالصيغة :

$$r_{\text{med}} = \left(\text{med}^2\,|u| - \text{med}^2\,|v|\right) \Big/ \left(\text{med}^2\,|u| + \text{med}^2\,|v|\right)$$

اذ ان :

$$u = \frac{x - \text{med}\,x}{\text{MAD}\,x} + \frac{y - \text{med}\,y}{\text{MAD}\,y}, \qquad v = \frac{x - \text{med}\,x}{\text{MAD}\,x} - \frac{y - \text{med}\,y}{\text{MAD}\,y}$$

$$\text{MAD}\,z = \text{med}\,|z - \text{med}\,z|$$

فـي عـام 2002 درس *Shevlyakov* و *Vilchevski* (6) تقـدير تبـاين معامـل الارتبـاط عنـد التعامل مع التوزيعات الطبيعية الثنائية الملوثة .

في عام 2006 اهتم *Ebd El-Salam* (7) بايجاد تقدير بديل لمعامل الارتباط البسيط في حالة احتواء البيانات على مشاهدات شاذة وتوصل من خلال اعتماده تجربة المحاكاة الى ان المقياس البديل المقترح وفي حالة وجود تلك المشاهدات قد تميز بخصائص احصائية افضل من المعاملات المعروفة للارتباط.

في عام 2008 وضع كل من *Bansal* و *Bhandary* (8) اشتقاقات تتعلق بموضوع مقدرات M الحصينة لمعلمتي الموقع والقياس مع معامل الارتباط واوضحا ان تلك المقدرات تكون عالية الاتساق .

اهتم بحثنا هذا بمقارنة اداء معاملي ارتباط بيرسون والرتب لسبيرمان وبعض الطرائق المحورة عن معامل بيرسون للارتباط والمبنية على اعتماد المقدرات الخطية *Linear Estimators* الحصينة لمعلمة الموقع المتمثلة بالوسيط ومقدر *Gastwirth* بدلاً عن الوسط الحسابي وذلك بالاعتماد على متوسط مربعات الخطأ (*MSE*) كمعيار للمقارنة بين التقديرات المدروسة.

تقدير معامل الارتباط

هنالك مقاييس عدّة لتقدير معامل الإرتباط (ρ) بين متغيرين عشوائيين أهمها معامل بيرسون للإرتباط *Pearson's Correlation Coefficient* والذي يُعرف على النحو الآتي :

ليكن $(x_1,y_1),(x_2,y_2),.....,(x_n,y_n)$ ازواج من المشاهدات المستقلة التي تتبع التوزيع الطبيعي الثنائي *Bivariate Normal Distribution* ، فأن الصيغة الرياضية التي وضعها بيرسون لتقدير معلمة الارتباط تتمثل بالاتي :

$$r_p = \frac{\sum_{i=1}^{n}(x_i-\bar{x})(y_i-\bar{y})}{\sqrt{\sum_{i=1}^{n}(x_i-\bar{x})^2\sum_{i=1}^{n}(y_i-\bar{y})^2}} \qquad .....(1)$$

اذ ان :

$\bar{x}$: الوسط الحسابي لقيم المتغير x .

$\bar{y}$: الوسط الحسابي لقيم المتغير y .

ورغم كفاءة معامل بيرسون في تقدير معامل الإرتباط إلا أنه شديد الحساسية نحو ابتعاد البيانات عن التوزيع الطبيعي الثنائي وبخاصة عندما تكون ملوثة بالمشاهدات الشاذة ، بمعنى آخر أنه تقدير غير حصين عند اختراق البيانات لشرط التوزيع الطبيعي ، من هنا توجه الباحثون نحو التقديرات اللامعلمية وبخاصة الرتبية منها كتقديرات حصينة بدلاً عن معامل بيرسون للإرتباط أهمها معامل ارتباط الرتب

لسبيرمان *Spearman's Ordinal Correlation Coefficient* ، المبني على اساس رتب البيانات والمعرف وفق الصيغة الاتية :

$$r_s = 1 - \frac{6\sum d^2}{n(n^2-1)} \qquad \ldots\ldots(2)$$

اذ ان :

d : الفرق بين رتب مستويات المتغيرالاول x ومستويات المتغير الثاني y ، $d = R_x - R_y$.

الطرائق المحورة

لإيجاد تقدير حصين لمعامل الإرتباط يقاوم إلى حدٍ ما حالة اختراق البيانات لشرط التوزيع الطبيعي فقد وجدنا من المناسب تحوير معامل بيرسون للإرتباط من خلال اعتماد المقدرات الخطية (*Linear Estimators (L.E.)*) الحصينة لمعلمة الموقع كالوسيط ومقدر *Gastwirth* بدلاً عن الوسط الحسابي .

تعرف المقدرات الخطية لمعلمة الموقع بكونها تراكيب خطية موزونة لمشاهدات العينة المرتبة فاذا كانت $x_{(1)} \le x_{(2)} \le \ldots \le x_{(n)}$ مشاهدات مرتبة لعينة بحجم (n) ، وكانت $a_1, a_2 \ldots a_n$ اعداد حقيقية إذ ان $(0 \le a_i \le 1;\ i=1,\ldots,n)$ تمثل اوزان تقترن مع المشاهدة $x_{(i)}$ ، فالصيغة العامة للمقدرات الخطية لمعلمة الموقع تتمثل في (9) :

$$\hat{\mu} = \sum_{i=1}^{n} a_i\, x_{(i)} \qquad \ldots\ldots(3)$$

ويشترط في الاوزان (a_i) عادةً ان تحقق القيد $(\sum_{i=1}^{n} a_i = 1)$ لضمان تمتع المقدر بخاصية ثبات الموقع (*Location Invariance*) وان تكون $a_i = a_{(n+1-i)}$ عند افتراض ان توزيع المتغير العشوائي متماثل حول معلمة الموقع μ كما تكون صغيرة للقيم المتطرفة (والتي يمكن ان تكون ضمنها المشاهدات الشاذة) بينما تكون كبيرة للقيم الأخرى وذلك للتقليل من تأثير المشاهدات الشاذة وبالتالي ضمان الحصول على مقدر حصين .

يبنى الوسيط على اساس المشاهدة المرتبة المركزية او المشاهدتين المرتبتين المركزيتين اعتماداً على كون حجم العينة عدداً فردياً او زوجياً على التوالي اما مقدر *Gastwirth* فيبنى على أساس الوسيط واثنين من مشاهدات العينة المرتبة وبالتالي فأنه يحوي معلومات تخص العينة المدروسة اكثر من الوسيط ، ويكون وفق الصيغة الاتية (10) :

$$G = 0.3\, x_{[n/3+1]} + 0.4\, med + 0.3\, x_{(n-[n/3])} \qquad \ldots\ldots(4)$$

اذ ان :

$[n/3+1]$: الجزء الصحيح من العدد الحقيقي $(n/3+1)$.

$[n/3]$: الجزء الصحيح من العدد الحقيقي $(n/3)$.

الجانب التجريبي

تم اعتماد اسلوب المحاكاة وفق طريقة *Monte Carlo* للمقارنة بين تقديرات معامل الإرتباط الآتية :

1. معامل بيرسون للارتباط ، r_P (الصيغة (1)).
2. معامل بيرسون للارتباط باعتماد الوسيط بدلاً عن الوسط الحسابي وسنرمز له بالرمز r_M.
3. معامل بيرسون للارتباط باعتماد مقدر *Gastwirth* (الصيغة (4)) بدلاً عن الوسط الحسابي وسنرمز له بالرمز r_G.
4. معامل سبيرمان للارتباط ، r_S (الصيغة (2)).

تم تحليل النتائج بالاعتماد على قيمة متوسط مربعات الخطأ (MSE) والذي يساوي مربع التحيز (B) مضافاً اليه تباين التقدير $\text{var}(\hat{\rho})$ ، بمعنى آخر :

$$MSE = B^2 + \text{var}(\hat{\rho}) \qquad .....(5)$$

اذ ان :

$$B = E(\hat{\rho}) - \rho \quad ; \quad E(\hat{\rho}) = \frac{\sum_{i=1}^{I} \hat{\rho}_i}{I} \quad ; \quad \text{var}(\hat{\rho}) = \frac{\sum_{i=1}^{I} (\hat{\rho}_i - \rho)^2}{I-1}$$

I : عدد مرات تكرار تجربة المحاكاة ، وكان خلال بحثنا هذا يساوي 1000 تجربة.
وقد تم دراسة سلوك التقديرات المقارن بينها من خلال توليد عينات عشوائية على وفق التوزيعات الآتية :

1. التوزيع الطبيعي الثنائي القياسي ، أي وفق المعلمات الخاصة بالمتغيرين X ، Y وكالآتي :
$X \sim N(0,1)\ ,\ Y \sim N(0,1)$
2. التوزيع الطبيعي الثنائي الملوث من جهة واحدة بنسبة 20% للمتغير العشوائيY وكالاتي :
$X \sim N(0,1)\ ,\ 20\%\ Y \sim N(5,1) + 80\%\ Y \sim N(0,1)$
3. التوزيع الطبيعي الثنائي الملوث من جهة واحدة بنسبة 20% للمتغير العشوائيY وكالاتي :
$X \sim N(0,1)\ ,\ 20\%\ Y \sim N(15,1) + 80\%\ Y \sim N(0,1)$
4. التوزيع الطبيعي الثنائي الملوث من جهة واحدة مع زيادة التباين لكلا المتغيرين وكالاتي :
$X \sim N(0,10)\ ,\ 20\%\ Y \sim N(5,10) + 80\%\ Y \sim N(0,10)$

وتم تطبيق الحالات الاربعة المذكورة عندما يكون $\rho = 0$ و $\rho = 0.9$ اما احجام العينات فتراوحت مابين الصغيرة ($n = 10\ ,\ 24$) ، المتوسطة ($n = 50$) والكبيرة ($n = 100$) .

النتائج والمناقشة

يمكن تحليل النتائج التي توصلنا اليها خلال الجانب التجريبي بالنقاط الآتية :

1. في حالة اتباع كلا المتغيرين للتوزيع الطبيعي وعندما ($\rho = 0$) ، كما مبين في جدول (1) ، نلاحظ تفوق اداء r_M يليه بالمرتبة الثانية r_G لتقدير معامل الأرتباط ولأحجام العينات الصغيرة والمتوسطة (n=10,24,50) اذ تنخفض قيمة MSE مقارنة بالتقديرات الأخرى اما عند (n=100) فنلاحظ تفوق اداء r_S ليكون r_M بالمرتبة الثانية . اما عند زيادة معامل الارتباط ($\rho = 0.9$) ، كما مبين في جدول (2) ، فأن التقدير وفق طريقة بيرسون r_P يفوق كافة التقديرات الاخرى ولجميع احجام العينات يليه بالمرتبة الثانية r_G .
2. عند التعامل مع التوزيع الطبيعي الثنائي الملوث من جهة واحدة بنسبة 20% للمتغير العشوائي Y وعندما ($\rho = 0$) ، كما مبين في جدول (3)، نلاحظ تفوق اداء r_M و r_G على بقية المعاملات مع بعض التذبذب في التفوق اعتماداً على حجم العينة فعند حجم العينة الصغير (n=10,24) يتفوق r_M على r_G في حين يتفوق r_G على r_M عند حجوم العينات المتوسطة والكبيرة (n=50,100) . اما عند زيادة معامل الارتباط ($\rho = 0.9$) ، كما مبين في جدول (4) ، فنلاحظ ثبات التفوق لـ r_S عند جميع احجام العينات يليه r_G عند احجام العينات الصغيرة والمتوسطة .
3. عند التعامل مع التوزيع الطبيعي الثنائي الملوث من جهة واحدة بنسبة 20% للمتغير العشوائي Y وبزيادة قيمة معلمة الموقع لتكون (15) بدلاً من (5) ولـ ($\rho = 0$) ، كما مبين في جدول (5)، نلاحظ ثبات تفوق اداء r_G يليه r_M على بقية المعاملات عند جميع احجام العينات . اما عند زيادة معامل الارتباط

($\rho = 0.9$)، كما مبين في جدول (6) ، فنلاحظ ثبات التفوق لـ r_S عند جميع احجام العينات يليه r_G عند احجام العينات الصغيرة والمتوسطة .

4. عند التعامل مع التوزيع الطبيعي الثنائي الملوث من جهة واحدة مع زيادة التباين لكلا المتغيرين وعندما ($\rho = 0$) ، كما مبين في جدول (7)، نلاحظ تفوق اداء r_M و r_G على التوالي عند حجم العينة الصغير (n=10,24) ويتراجع اداء r_M ليتفوق عليه r_G عند حجم العينة المتوسط (n=50) كما يتراجع اداء r_G ليكون في المرتبة الثانية يسبقه اداء r_S . اما عند زيادة معامل الارتباط ($\rho = 0.9$) ، كما مبين في جدول (8) ، فنلاحظ تفوق r_G و r_P على التوالي عند (n=10) وينعكس الترتيب عند بقية حجوم العينات.

5. عند التعامل مع التوزيع الطبيعي الثنائي الملوث من جهة واحدة بنسبة 20% للمتغير العشوائي الثاني لا نجد اي تفوق لاداء r_P ليكون في المرتبة الاولى اما عند التعامل مع التوزيع الطبيعي الثنائي الملوث من جهة واحدة مع زيادة التباين لكلا المتغيرين وعند ($\rho = 0.9$) فنلاحظ تفوقه وبالاخص عند حجوم العينات ($n \geq 24$) ولعل السبب في ذلك يعود الى ان زيادة التباين وزيادة حجم العينة وزيادة معامل الارتباط قد ادى الى تقليل تأثير المشاهدات الشاذة .

6. ادناه عرض موجز لافضل طريقتين لتقدير معامل الارتباط من بين الطرائق الاربعة المدروسة موزعة حسب الحالة التوزيعية وحجم العينة والذي يتبين من خلاله تفوق اداء r_M و r_G لجميع الحالات المدروسة عند $\rho = 0$ و n=10,24,50 مع بعض التذبذب في الاولوية كما يتبين ان اعتماد المقدر الحصين لمعلمة الموقع بدلا عن الوسط الحسابي عند التعامل مع معامل ارتباط بيرسون قد اضاف تحسناً على اداءه خصوصاً عند $\rho = 0$ وان اعتماد مقدر *Gastwirth* قد تفوق على اعتماد الوسيط عند $\rho = 0.9$ لجميع حجوم العينات ولجميع الحالات المدروسة كذلك الحال عند $\rho = 0$ لحالتي التلويث الاولى والثانية ولحجوم العينات المتوسطة والكبيرة .

	X ~ N(0,1) , Y ~ N(0,1)		X ~ N(0,1) 20%Y~N(5,1)+80%Y~N(0,1)		X ~ N(0,1) 20%Y~N(15,1)+80%Y~N(0,1)		X ~ N(0,10) 20%Y~N(5,10)+80%Y~N(0,10)	
n	$\rho = 0$	$\rho = 0.9$	$\rho = 0$	$\rho = 0.9$	$\rho = 0$	$\rho = 0.9$	$\rho = 0$	$\rho = 0.9$
10	r_M	r_P	r_M	r_S	r_G	r_S	r_M	r_G
	r_G	r_G	r_G	r_G	r_M	r_G	r_G	r_P
24	r_M	r_P	r_M	r_S	r_G	r_S	r_M	r_P
	r_G	r_G	r_G	r_G	r_M	r_G	r_G	r_G
50	r_M	r_P	r_G	r_S	r_G	r_S	r_M	r_P
	r_G	r_G	r_M	r_G	r_M	r_G	r_G	r_G
100	r_S	r_P	r_G	r_S	r_G	r_S	r_S	r_P
	r_M	r_G	r_M	r_P	r_M	r_P	r_G	r_G

يمكن تلخيص أهم الإستنتاجات التي تم التوصل اليها بما يلي:

1. عدم كفاءة معامل r_P في تقدير معامل الارتباط عندما $\rho = 0$ للبيانات ذات التوزيع الطبيعي الثنائي إذ أن المعامل r_M هو الأكثر كفاءة للعينات الصغيرة والمتوسطة (n=10,24,50) بينما كان المعامل r_S هو الأكثر كفاءة للعينات الكبيرة (n=100) وتزداد كفاءة r_P ليكون هو الافضل عند اقتراب ρ من 1 ($\rho = 0.9$) .

2. عند احتواء البيانات على 20% من الشواذ حسب الموقع فإن r_G و r_M هما التقديران الأكثر كفاءة عندما $\rho = 0$ بينما r_S هو الأكثر كفاءة عند اقتراب ρ من 1 .

3. عند اقتراب ρ من 1 ، يقل تأثير المشاهدات الشاذة على اداء المعامل r_P في حالة التعامل مع حجوم العينات الكبيرة (n=100) كذلك الحال عند زيادة تباين المتغير الملوث .

على ضوء ماورد آنفاً نوصي عند التعامل مع الحالات التوزيعية الملوثة او عند $\rho = 0$ باعتماد المقدرات الحصينة لمعلمة الموقع بدلاً عن الوسط الحسابي عند تطبيق معامل بيرسون للارتباط .

جدول -1: قيم MSE : $\rho=0$ ، $X \sim N(0,1)$, $Y \sim N(0,1)$

n	*Method*	r_P	$_M r$	r_G	$_S r$
10	$\hat{\rho}$	0.00589	0.00746	0.00634	0.00383
	B	0.00589	0.00746	0.00634	0.00383
	$Var(\hat{\rho})$	12.56627	11.70170	12.03040	12.57320
	MSE	12.56630	11.70176	12.03044	12.57321
24	$\hat{\rho}$	-0.00227	-0.00268	-0.00253	-0.00179
	B	0.00227	0.00268	0.00253	0.00179
	$Var(\hat{\rho})$	1.92634	1.86600	1.88722	1.91270
	MSE	1.92635	1.86600	1.88723	1.91270
50	$\hat{\rho}$	-0.00532	-0.00465	-0.00507	-0.00450
	B	0.00532	0.00465	0.00507	0.00450
	$Var(\hat{\rho})$	0.42161	0.41532	0.41654	0.41869
	MSE	0.42164	0.41534	0.41657	0.41871
100	$\hat{\rho}$	-0.00390	-0.00389	-0.00397	-0.00396
	B	0.00390	0.00389	0.00397	0.00396
	$Var(\hat{\rho})$	0.10513	0.10419	0.10460	0.10047
	MSE	0.10514	0.10421	0.10461	0.10049

جدول-2:قيم MSE : $\rho=0.9$ ، $X \sim N(0,1)$, $Y \sim N(0,1)$

n	*Method*	r_P	$_M r$	r_G	$_S r$
10	$\hat{\rho}$	0.88980	0.87320	0.88160	0.84210
	B	0.01020	0.02680	0.01840	0.05790
	$Var(\hat{\rho})$	0.78525	0.95566	0.85429	1.65880
	MSE	0.78535	0.95638	0.85463	1.66215
24	$\hat{\rho}$	0.89693	0.88680	0.89311	0.87165
	B	0.00307	0.01320	0.00689	0.02835
	$Var(\hat{\rho})$	0.07528	0.09231	0.07965	0.14482
	MSE	0.07529	0.09248	0.07970	0.14563
50	$\hat{\rho}$	0.89874	0.89342	0.89701	0.88262
	B	0.00126	0.00658	0.00299	0.01738
	$Var(\hat{\rho})$	0.01550	0.01744	0.01586	0.02790
	MSE	0.01550	0.01748	0.01587	0.02820
100	$\hat{\rho}$	0.89939	0.89658	0.89849	0.88680
	B	0.00061	0.00342	0.00151	0.01320
	$Var(\hat{\rho})$	0.00382	0.00407	0.00389	0.00627
	MSE	0.00382	0.00408	0.00389	0.00644

جدول -3: قيم MSE : $\rho=0$ ، $X \sim N(0,1)$, 20% $Y \sim N(5,1)$ + 80% $Y \sim N(0,1)$

n	Method	r_P	$_M r$	r_G	$_S r$
10	$\hat{\rho}$	0.00393	0.00489	0.00492	0.00147
	B	0.00393	0.00489	0.00492	0.00147
	$Var(\hat{\rho})$	11.40533	10.18084	10.30061	12.23166
	MSE	11.40535	10.18086	10.30063	12.23166
24	$\hat{\rho}$	-0.00987	-0.00697	-0.00828	-0.00583
	B	0.00987	0.00697	0.00828	0.00583
	$Var(\hat{\rho})$	1.76199	1.65921	1.66048	1.78987
	MSE	1.76209	1.65926	1.66055	1.78990
50	$\hat{\rho}$	-0.00612	-0.00643	-0.00645	-0.00700
	B	0.00612	0.00643	0.00645	0.00700
	$Var(\hat{\rho})$	0.44839	0.42524	0.42057	0.44730
	MSE	0.44843	0.42528	0.42061	0.44735
100	$\hat{\rho}$	-0.00023	-0.00040	-0.00011	-0.00146
	B	0.00023	0.00040	0.00011	0.00146
	$Var(\hat{\rho})$	0.10299	0.09976	0.09716	0.10150
	MSE	0.10299	0.09976	0.09716	0.10150

جدول-4:قيم MSE : $\rho=0.9$ ، $X \sim N(0,1)$, 20% $Y \sim N(5,1)$ + 80% $Y \sim N(0,1)$

n	Method	r_P	$_M r$	r_G	$_S r$
10	$\hat{\rho}$	0.34997	0.33097	0.33332	0.54511
	B	0.55003	0.56903	0.56668	0.35489
	$Var(\hat{\rho})$	8.82554	7.98782	7.96061	6.96108
	MSE	9.12806	8.31162	8.28173	7.08702
24	$\hat{\rho}$	0.39835	0.38422	0.38524	0.61327
	B	0.50165	0.51578	0.51476	0.28673
	$Var(\hat{\rho})$	1.14760	1.09606	1.08101	0.83390
	MSE	1.39925	1.36209	1.34599	0.91611
50	$\hat{\rho}$	0.38814	0.36921	0.37171	0.59046
	B	0.51186	0.53079	0.52829	0.30955
	$Var(\hat{\rho})$	0.30092	0.28682	0.28246	0.24192
	MSE	0.56291	0.56855	0.56155	0.33774
100	$\hat{\rho}$	0.39941	0.38058	0.38298	0.60173
	B	0.50059	0.51942	0.51702	0.29827
	$Var(\hat{\rho})$	0.06711	0.06570	0.06342	0.05331
	MSE	0.31770	0.33550	0.33073	0.14227

جدول-5: قيم MSE : ρ =0 ، X ~ N(0,1) , 20% Y ~ N(15,1) + 80% Y ~ N(0,1)

n	Method	r_P	M^r	r_G	S^r
10	$\hat{\rho}$	0.00228	0.00266	0.00337	0.00141
	B	-0.00228	-0.00266	-0.00337	-0.00141
	$Var(\hat{\rho})$	11.41890	9.70830	9.64154	12.23703
	MSE	11.41891	9.70831	9.64155	12.23703
24	$\hat{\rho}$	-0.01006	-0.00571	-0.00758	-0.00580
	B	0.01006	0.00571	0.00758	0.00580
	$Var(\hat{\rho})$	1.77946	1.62931	1.59600	1.79063
	MSE	1.77956	1.62934	1.59606	1.79066
50	$\hat{\rho}$	-0.00512	-0.00553	-0.00550	-0.00696
	B	0.00512	0.00553	0.00550	0.00696
	$Var(\hat{\rho})$	0.43414	0.39341	0.37982	0.44730
	MSE	0.43417	0.39344	0.37985	0.44735
100	$\hat{\rho}$	0.00146	0.00057	0.00091	-0.00148
	B	-0.00146	-0.00057	-0.00091	0.00148
	$Var(\hat{\rho})$	0.10197	0.09547	0.09045	0.10150
	MSE	0.10197	0.09547	0.09045	0.10150

جدول -6:قيم MSE : ρ =0.9 ، X ~ N(0,1) , 20% Y ~ N(15,1) + 80% Y ~ N(0,1)

n	Method	r_P	M^r	r_G	S^r
10	$\hat{\rho}$	0.12545	0.11437	0.11556	0.54459
	B	0.77455	0.78563	0.78444	0.35541
	$Var(\hat{\rho})$	11.18781	9.52312	9.42553	6.99714
	MSE	11.78774	10.14033	10.04088	7.12346
24	$\hat{\rho}$	0.13892	0.13224	0.13089	0.61295
	B	0.76108	0.76776	0.76911	0.28705
	$Var(\hat{\rho})$	1.68671	1.55083	1.51299	0.83609
	MSE	2.26595	2.14028	2.10452	0.91849
50	$\hat{\rho}$	0.13870	0.12569	0.12624	0.59026
	B	0.76130	0.77431	0.77376	0.30974
	$Var(\hat{\rho})$	0.41216	0.37353	0.36096	0.24218
	MSE	0.99174	0.97308	0.95966	0.33812
100	$\hat{\rho}$	0.14786	0.13432	0.13507	0.60141
	B	0.75214	0.76568	0.76493	0.29860
	$Var(\hat{\rho})$	0.09643	0.09040	0.08562	0.05349
	MSE	0.66215	0.67667	0.67074	0.14265

جدول-7: قيم MSE : ρ =0، X ~ N(0,10) , 20% Y ~ N(5,10) + 80% Y ~ N(0,10)

n	Method	r_P	M^r	r_G	S^r
10	$\hat{\rho}$	0.00657	0.00707	0.00719	0.00452
	B	0.00657	0.00707	0.00719	0.00452
	$Var(\hat{\rho})$	12.17708	11.34230	11.60240	12.07278
	MSE	12.17712	11.34235	11.60245	12.07280
24	$\hat{\rho}$	-0.00656	-0.00619	-0.00642	-0.00414
	B	0.00656	0.00619	0.00642	0.00414
	$Var(\hat{\rho})$	1.81940	1.76075	1.78396	1.81510
	MSE	1.81944	1.76078	1.78401	1.81512
50	$\hat{\rho}$	-0.00639	-0.00629	-0.00649	-0.00569
	B	0.00639	0.00629	0.00649	0.00569
	$Var(\hat{\rho})$	0.44753	0.44202	0.44238	0.44708
	MSE	0.44757	0.44206	0.44242	0.44711
100	$\hat{\rho}$	-0.00205	-0.00236	-0.00217	-0.00259
	B	0.00205	0.00236	0.00217	0.00259
	$Var(\hat{\rho})$	0.10474	0.10439	0.10417	0.10150
	MSE	0.10474	0.10440	0.10418	0.10151

جدول-8:قيم MSE : ρ=0.9 ، X ~ N(0,10) , 20% Y ~ N(5,10) + 80% Y ~ N(0,10)

n	Method	r_P	M^r	r_G	S^r
10	$\hat{\rho}$	0.72559	0.70617	0.71420	0.68713
	B	0.17441	0.19383	0.18580	0.21287
	$Var(\hat{\rho})$	2.80772	2.83370	2.79605	3.95556
	MSE	2.83814	2.87127	2.83057	4.00087
24	$\hat{\rho}$	0.76360	0.75258	0.75817	0.74447
	B	0.13640	0.14742	0.14183	0.15553
	$Var(\hat{\rho})$	0.27797	0.29412	0.28596	0.38559
	MSE	0.29657	0.31586	0.30608	0.40978
50	$\hat{\rho}$	0.75292	0.74655	0.75005	0.73634
	B	0.14708	0.15345	0.14995	0.16366
	$Var(\hat{\rho})$	0.07386	0.07570	0.07428	0.10569
	MSE	0.09549	0.09925	0.09676	0.13248
100	$\hat{\rho}$	0.75793	0.75399	0.75604	0.74503
	B	0.14207	0.14601	0.14396	0.15497
	$Var(\hat{\rho})$	0.01632	0.01671	0.01635	0.02347
	MSE	0.03650	0.03803	0.03708	0.04749

المصادر

1. Huber, P. J. "Robust Statistics". (1981): John Wiley & Sons, New York.
2. Beckman, R.J. and Cook, R.D. "Outlier....s". Technometrics, 25: 119-149, (1983)
3. Devlin,S.J.; Gnanadesikan, R. and Kettenring, J. R. "Robust Estimation and Outlier Detection with Correlation Coefficients".Biometrika,62:531-545 , (1975).
4. Gideon, R.A. and Hollister, R.A. "A Rank Correlation Coefficient Resistant to Outliers". J.Amer.Statist.Assn, 94: 656-666, (1987).
5. Shevlyakov, G. L. "On Robust Estimation of a Correlation Coefficient". Journal of Mathematical Sciences, 83: 434 - 438, (1997).
6. Shevlyakov, G. L. and Vilchevski, N. O. "Minimax Variance Estimation of a Correlation Coefficient for ε-Contaminated Bivariate Normal Distributions". Statistics & Probability Letters, 57: 91-100, (2002).
7. Ebd El-Salam, M.E. "A Robust Measure for the Correlation Coefficient". J. Kin Saud Univ., 19: 41-50, (2006).
8. Bansal, N.K. and Bhandary, M. "Robust M-Estimation of the Intraclass Correlation Coefficient". Australian & New Zealand Journal of Statistics, 36: 287 – 301, (2008).
9. Hoaglin, D.C.; Mosteller, F. and Tukey, J.W. "Understanding Robust and Exploratory Data Analysis": John Wiley & Sons, New York. (1983).
10. Gastwirth, J.L. "On Robust Procedures".J.Amer.Statist.Assn, 61: 929-948, (1966).

مقارنة بعض الاختبارات الحصينة لتحليل التباين المتعدد المتغيراتMANOVA بأستخدام تقديرات- MCD

[1]سامي داود كبارة و ظافر حسين رشي[2] و[3] سداد خليل ابراهيم
[1]جامعة صلاح الدين/ كلية العلوم/ قسم الرياضيات
[2]جامعة بغداد /كلية الادارة والاقتصاد/قسم الاحصاء
[3] الجامعة المستنصرية/ كلية العلوم/قسم الرياضيات

ABSTRICT

There are many widely used statistics to test the hypothesis of equal means of multivariate populations of a general linear model. One of these is Wilks statistic which is used in this paper. In the case ,when the assumption normality distribution is violated of random error matrix ,then the Wilks statistic leads to a wrong decision. For this reason , Wilks robust statistic (RFMCD*) has been modified using robust estimations
(RFMCD,RMCD,MCD), with changing the cut-off-values. In the case of multi-normal distribution, a cut-off-value is suggested to get a right decision, also cut-off-value is suggested for one and two sided for contaminated multi-normal distribution for the same reason. The method of simulation has been used to generate a random error matrix, that have non– normal distribution, that follow the multi – contaminated normal distribution of one side and the multi – contaminated normal distribution of the two sides.

It has been shown, that through using simulation, that the modified robust statistics (**RFMCD***) is better than the Classical Wilks statistic presence of outliers from both sides and in some cases, when the outliers are presented in one side, particularly at contamination ratio ($\epsilon = 0.2$) , and at any significant level .

الخلاصة

هنالك العديد من الاحصاءات الشائعة الاستخدام لاختبارفرضية تساوي متوسطات مجتمعات متعددة المتغيرات لنموذج خطي عام, منها احصاءة ولكس والتي استخدمت ضمن هذا البحث. في حالة اختلال شرط التوزيع الطبيعي المتعدد لمصفوفة الاخطاء العشوائية فان احصاءة ولكس تؤدي الى قرار خاطىء. وعليه تم تحويراحصاءة ولكس الحصنية (**RFMCD***) بأستخدام التقديرات الحصينة (**RFMCD, RMCD, MCD**) مع تغيرات في قيم ثوابت القطع. في حالة التوزيع الطبيعي المتعدد تم اقتراح ثابت قطع للحصول على قرار صائب,كما تم اقتراح ثابت قطع للتوزيع الطبيعي المتعدد الملوث من جهة واحدة ومن جهتين وذلك لنفس السبب. وقد استخدم أسلوب المحاكاة لتوليد بيانات لمصفوفة الاخطاء العشوائية تتبع توزيعات غير التوزيع الطبيعي المتعدد، كالتوزيع الطبيعي المتعدد الملوث من جهة واحدة والتوزيع الطبيعي المتعدد الملوث من جهتين. وقد أتضح من خلال دراسة المحاكاة ان الاحصاءة الحصينة المعدلة (**RFMCD***) أفضل من احصاءة ولكس الكلاسيكية في حالة وجود شواذ من جهتين وكذلك في بعض حالات وجود شواذ من جهة واحدة وخصوصا عند نسبة تلوث (ε=0.2) وعند إي مستوى معنوية.

المقدمة

يعتبر استخدام النماذج الخطية من اكثر الطرائق الاحصائية استخداما في مختلف العلوم, لانها تصف العلاقة بين المتغيرات على شكل معادلة خطية . ويستخدم تحليل النماذج الخطية لعدة اغراض اهمها التنبؤ حيث يمكن تقدير معلمة الاستجابة والتنبؤ بها بما يفيد كثيرا في التخطيط واتخاذ القرارات . وللحصول على تنبؤ جيد حول ظاهرة معينة يجب ان نعرف المعالم الغير معلومة في النموذج قيد الدراسة لتمثيل تلك الظاهرة , حيث يتم تقدير هذه المعالم. واكثر الطرائق استخداما في التقدير هما طريقة المربعات الصغرى وطريقة الامكان الاعظم (1) .

ومما لاشك فيه ان عملية الحصول على تقديرات تكون قريبة جدا من قيم معلماتها هو طموح اي باحث او جهد بغية الحصول على افضل تمثيل للمجتمع او المشكلة قيد البحث. وحتى وقت قريب كانت هاتان الطريقتان من اكثر الطرائق انتشارا واستخداما لما تمتاز به مقدراتها من مزايا جيدة. الا ان وجود بعض القيم الشاذة في المشاهدات الناشئة من توزيعات غير التوزيع الطبيعي قد يكون لها تاثير على المربعات الصغرى وبالتالي فان تلك المقدرات تفقد مزاياها الجيدة. وبما ان تحليل التباين المتعدد (2)الذي يستخدم في اختبار فرضيات متعددة لمجاميع جزئية كثيرة من المعلمات , يعتمد على مقدرات المربعات الصغرى . وبما ان الصيغ في تحليل التباين

المتعدد تكون صيغا تربيعية بهذه المقدرات , لهذا السبب فان هذا الاجراء الاستدلالي مشكوك فيه حيث ان حساسية المقدرات للانحرافات ستنتقل الى الاختبارات .

في عام (1932) تمكن Wilks (3) من ايجاد احصاءة اختبار فرضية تساوي متوسطات مجتمعات متعددة المتغيرات على اساس شروط هي ان البيانات التي تم تقسيمها الى مجموعتين مختلفتين لها توزيع طبيعي متعدد المتغيرات بمعلمتي موقع مختلفتين وان مصفوفتي التباين المشترك للجموعتين متساوية وغير معلومة وتكون موجبة تماما.

طريقة ولكس تتطلب توزيع البيانات توزيعا طبيعيا متعدد المتغيرات. ان اختلال التوزيع الطبيعي بسبب وجود الشواذ يدعو إلى ضرورة إيجاد طرائق بديلة تكون اكثر كفاءة وهذا مايسمى بالطرائق الحصينة. على الرغم من كثرة الدراسات والبحوث في مجال الحصانة (Robust) خلال العقودالاربعة الأخيرة, إلا إن الحصول على المقدرات الحصينة للمعالم في النماذج الخطية بداءت بعد عام (1970). و يعد Box أول من أعطى الحصانة المعنى الإحصائي وذلك عام (1953) (4). تعتبر التقديرات الحصينة من المواضيع الحديثة والمهمة في الاحصاء حيث تتصف بان تقديراتها قريبة من تقديرات المربعات الصغرى عند عدم وجود الشواذ وتكون افضل منها عند وجود الشواذ. وتعرف المشاهدة الشاذة بانها قيمة منحرفة عن بقية مشاهدات العينة .وتوجد اسباب كثيرة لنشوء القيم الشاذة منها اخطاء القياس ,التسجيل , اخطاء المعاينة.

بالرغم من كثرة الطرائق الحصينة (5) إلا أنها تشترك في نقطتين هما:إعطاء اهمية (وزن) اقل للمشاهدات الشاذة وذلك للتقليل من تأثيرهاوثانيا استخدام أسلوب التكرار في الحساب.

وان اهم الطرائق الحصينة المستخدمة في تقدير معلمات النموذج الخطي المتعدد المتغيرات يمكن تصنيفها الى:

1- طريقة مقدر اصغر محدد تباين مشترك **(MCD)**.

2- طريقة مقدر اصغر محدد تباين مشترك معاد الأوزان **(RMCD)**.

استخدم (Stahel –Donho) صيغة دالة لايجاد المقدرات الحصينة الموزونة بثوابت قطع معينة . في هذا البحث تم تحوير الصيغة مع استخدام ثوابت قطع مختلفة لكل توزيع طبيعي وغير طبيعي متعدد المتغيرات . وهذا الاجراء مناقش في البند(4).

كما تم في هذا البحث المقارنة بين الطرائق المشار اليها في اعلاه باستخدام معدلات الخطا من النوع الاول (α)وقوة الاختبار $(1-\beta)$ من خلال توليد مجاميع كبيرة ومختلفة من البيانات باستخدام اسلوب المحاكاة(Simulation).

هدف البحث : إن الهدف الأساسي من هذا البحث هو أجراء اختبارتساوي متوسطات q من المجتمعات المتعددة المتغيرات والمقارنة بينها حيث إن كل مجتمع يمتلك p من الصفات, أي إن :

$$H_0 : \underline{\mu}_1 = \underline{\mu}_2 = \dots = \underline{\mu}_q \qquad (1)$$

حيث إن μ_j يمثل متوسط المجتمع j ($j = 1,\dots, q$). هنالك العديد من الإحصاءات لاختبار الفرضية (1) منها أحصاءة ولكس التي تعتمد على مقدرات طريقة المربعات الصغرى، في حالة اختلال شرط التوزيع الطبيعي فان هذه الاحصاءة تؤدي إلى اتخاذ قرار خاطئ .

الجانب النظري

1- النماذج الخطية المتعددة المتغيرات

ليكن لدينا N من الوحدات التجريبية (Experiment Units) والتي يمكن ان نقيس لها p من متغيرات الاستجابة ($p \geq 2$) ، فانه بامكاننا صياغة نموذج خطي متعدد المتغيرات بالشكل الأتي (6)

$$Y = X\beta + E \qquad (2)$$

حيث ان:

Y : مصفوفة مشاهدات لمتغيرات الاستجابة من الدرجة $(N\times p)$.

X : مصفوفة التصميم (Design Matrix) من الدرجة $(N\times q)$ وتحتوي على قيم المتغيرات المصاحبة (المستقلة) (Independent Variables).

β : مصفوفة من الدرجة $(q\times p)$ تتضمن المعلمات غيرالمعروفة (Unknown Parameters).

E : مصفوفة الأخطاء العشوائية من الدرجة $(N\times p)$ وتتكون من N من المتجهات الصفية المستقلة (Independent Random Vectors) التي يفترض ان كل متجه صفي يتبع التوزيع الطبيعي متعدد المتغيرات (Multivariate Normal Distribution) بمتوسط $\underline{0}$ من الدرجة $(p\times 1)$ ومصفوفة تباين مشترك (Covariance Matrix) Σ من الدرجة $(p\times p)$ غير معلومة وتكون موجبة تماما (Positive Definite), أي إن :

$$E' = (\underline{E}_1, \underline{E}_2, ..., \underline{E}_N), \qquad \underline{E}'_i = (E_{i1}, E_{i2}, ..., E_{ip})$$

وعليه فان

$$\underline{E}_i \sim N_p(\underline{0}, \Sigma), \qquad E(\underline{E}_i, \underline{E}_j) = \begin{cases} \Sigma & i = j \\ 0 & o.w. \end{cases} \qquad (3)$$

ولتقدير مصفوفة المعلمات β للنموذج (2) نستخدام طريقة المربعات الصغرى.

ويمكن تقسيم النموذج الخطي المتعدد المتغيرات العام الى نماذج الانحداروالتي تكون فيها مصفوفة مشاهدات المتغيرات التوضيحية X ذات رتبة كاملة أي إن رتبة المصفوفة تساوي عدد الأعمدة q . وبذلك يمكن إيجاد معكوس المصفوفة $(X'X)$. وعندئذ فان مقدرات المربعات الصغرى يمكن الوصول اليها من خلال الصيغة $\hat{\beta} = (X'X)^{-1}X'Y$ ويسمى النموذج في هذه الحالة بنموذج تام الرتبة.

اما النوع الاخر من النماذج فهي نماذج التصميم حيث ان مصفوفة مشاهدات المتغيرات التوضيحية X تحتوي على الاعداد 0 ، 1 فقط كما أنها تكون ذات رتبة غير تامة ، أي ان رتبة المصفوفة ولتكن افتراضيا تساوي $q > r$ ، وبذلك لايمكن إيجاد المعكوس للمصفوفة $(X'X)$ ويسمى النموذج في هذه الحالةبنموذج الرتبة غير التامة (Less than Full Rank) ويمكن الحصول تقديرات المربعات الصغرى بعدة أساليب منها:

إعادة النمذجة (Reparameterization) حيث يتم ايجاد المصفوفة L التي تحقق الشروط الاتية:

1- $X(L')^c L' = X$

2- $rank\ (X(L')^c) = r$.

3- $L'(L')^c = I$.

في هذه الحالة نحصل على النموذج

$$y = V\mu + E \qquad (4)$$

حيث إن V هي مصفوفة من الدرجة $(N\times r)$ ذات رتبة r ونحصل عليها من العلاقة $V = X(L')^c$

μ: هي مصفوفة من الدرجة $(r\times P)$ ونحصل عليها من العلاقة $\mu = L'\beta$.

في هذه الحالة أصبح النموذج (4) تام الرتبة, لذلك تكون مقدرات المربعات الصغرى بالصيغة $\hat{\mu} = (V'V)^{-1}V'Y$ وعليه فانه وبشكل عام نستطيع القول بان نماذج التصميم يمكن ان تعامل من ناحية التقدير والاختبار كما تعامل نماذج الانحدار.

2 - اختبار الفرضية الخطية العامة في تحليل التباين المتعدد المتغيرات (*MANOVA*) (2)

يتضمن هذا البند اختبار الفرضية الخطية التي صيغتها

$$H_o : C\beta D = 0 \quad \text{VS} \quad H_1 : C\beta D \neq 0 \qquad (5)$$

اذ تمثل كل من C و D مصفوفة من الدرجة $(p\times d)$ و $(c\times q)$ وبرتب d و c على التوالي. تستخدام احصاءة ولكس لاختبارالفرضية (5) والتي تكون باحدى الصيغ الاتية :

$$U_0 = \frac{|S_E|}{|S_E + S_H|} = |I + S_H S_E^{-1}|^{-1} \qquad (6)$$

حيث ان

$$S_E = D'Y'\{I_N - X(X'X)^{-1}X'\}YD, \qquad S_H = (C\hat{\beta}D)'\{C(X'X)^{-1}C'\}^{-1}(C\hat{\beta}D).$$

وبذلك ترفض الفرضية $H_\circ$ بمستوى معنوية α إذا كانت $U_0 < U(u, \upsilon_h, \upsilon_e; \alpha)$

إذ تمثل $U(u, \upsilon_h, \upsilon_e; \alpha)$ القيمة الجدولية لاحصاءة ولكس بالقيم u و υ_h وبدرجة حرية الخطأ υ_e وبمستوى معنوية α.

اختبار الفرضيات الخطية العامة بالاعتماد على المقدرات الحصينة

1- اختبار الفرضيات الخطية العامة بالاعتماد على مقدر MCD الحصين

ان الفرضية الخطية لنموذج خطي متعدد المتغيرات والتي صيغتها

$$H_\circ : C\hat{\beta}_{MCD}D = 0 \quad \textbf{VS} \quad H_1 : C\hat{\beta}_{MCD}D \neq 0 \qquad (7)$$

حيث إن $\hat{\beta}_{MCD}$ مصفوفة من الدرجة (q×p) و D مصفوفة أحادية من الدرجة (p×p) وC مصفوفة التصميم من الدرجة (q×1-q) تختبر بأستخدام احصاءة ولكس التي تعتمد على الاحصاءتين $\underline{\mu}_{MCD}$ و S_{MCD} واللتان تتوزعان طبيعيا تقاربيا (7) وعليه فانه يمكن تطبيق احصاءة ولكس الحصينة للاحصاءة U_{MCD} والتي صيغتها

$$U_{MCD} = \frac{|S_E|}{|S_E + S_{HMCD}|} \overset{app.}{\sim} (Wilks) \qquad (8)$$

حيث ان

$$S_E = D'Y'\{I_N - X(X'X)^{-1}X'\}YD, \qquad S_{HMCD} = (C\hat{\beta}_{MCD}D)'\{C(X'X)^{-1}C'\}^{-1}(C\hat{\beta}_{MCD}D)$$

2 - اختبار الفرضيات الخطية العامة بالاعتماد على مقدر RMCD الحصين

ان الفرضية الخطية لنموذج خطي متعدد المتغيرات والتي صيغتها:

$$H_\circ : C\hat{\beta}_{RMCD}D = 0 \quad \textbf{VS} \quad H_1 : C\hat{\beta}_{RMCD}D \neq 0 \qquad (9)$$

حيث ان $\hat{\beta}_{RMCD}$ مصفوفة من الدرجة (q×p) و D مصفوفة أحادية من الدرجة (p×p) وC مصفوفة التصميم من الدرجة (q×1-q) تختبر بأستخدام احصاءة ولكس التي تعتمد على الاحصاءتين $\underline{\mu}_{RMCD}$ و S_{RMCD} واللتان تتوزعان توزيعا طبيعيا تقاربيا (7) وعليه فانه يمكن تطبيق احصاءة ولكس الحصينة الموزونة بالأوزان (0,1) بالشكل الأتي:

$$U_{RMCD} = \frac{|S_E|}{|S_E + S_{HRMCD}|} \overset{APP.}{\sim} (Wilks) \qquad (10)$$

حيث ان

$$S_E = D'Y'\{I_N - X(X'X)^{-1}X'\}YD, \; S_{HRMCD} = (C\hat{\beta}_{RMCD}D)'\{C(X'X)^{-1}C'\}^{-1}(C\hat{\beta}_{RMCD}D).$$

الطريقة المحورة

لغرض الحصول على نتائج افضل لاختبار الفرضية تم استبدال الأوزان (0,1) من دالة (RMCD) والتي هي

$$w(r)=\begin{cases}\dfrac{\exp(-k(1-r/c^2))-\exp(-k)}{1-\exp(-k)} & if \quad r<c\\ 1 & if \quad r\geq c\end{cases} \qquad (11)$$

حيث ان c هي قيمة القطع (cut-off Value) حيث $0<c\leq 1$ (8) وقد استخدم قيم مختلفة للثابت k محصورة بين 3 و 50 وبذلك يمكن ان نعرف مقدرات (**RFMCD**) كالأتي:

$$t_j=\frac{\sum_{i=1}^{N} w_i y_{ij}}{\sum_{i=1}^{N} w_i} \qquad (12)$$

$$C_j=\frac{\sum_{i=1}^{N} w_i (y_{ij}-t_j)(y_{ij}-t_j)'}{\sum_{i=1}^{N} w_i-1}$$

$$\sum_{i=1}^{N} w_i \neq 1 \qquad (13)$$

في هذا البحث تم استخدام دالة وزن محورة من دالة (Stahel-Donho) بعد ان تم استبدال دالة البواقي r (Residuals) بدالة مسافة مهالونبيس و كالأتي:

$$w(d_i)=\begin{cases}\dfrac{\exp(-k(1-d_i/c^2))-\exp(-k)}{1-\exp(-k)} & if \quad d_i<c\\ 1 & if \quad d_i\geq c\end{cases} \qquad (14)$$

حيث ان c هي قيمة القطع (cut-off Value) المقترحة بالصيغ آلاتية:

1- في حالة التوزيع الطبيعي المتعدد المتغيرات

$$C_1^*=0.0255+(p-2)/12 \qquad (15)$$

2- اما حالة التوزيع الطبيعي المتعدد المتغيرات الملوث من جانب واحد ومن جانبين

$$C_2^*=0.162+(p-2)/2 \qquad (16)$$

حيث إن P تمثل عدد الصفات (المتغيرات) وان (P=2,3,4), كما تم اقتراح **(k=7)** وبذلك يمكن إن نعرف مقدرات (RFMCD*) كالأتي:

$$t_j^*=\frac{\sum_{i=1}^{N} w_i^* y_{ij}}{\sum_{i=1}^{N} w_i^*}, \qquad (17)$$

$$C_j^*=\frac{\sum_{i=1}^{N} w_i^* (y_{ij}-t_j^*)(y_{ij}-t_j^*)}{\sum_{i=1}^{N} w_i^*-1} \qquad \sum_{i=1}^{N} w_i^* \neq 1 \qquad (18)$$

خوارزمية حساب الطريقة المحورة

1- بعد الحصول على القيم الابتدائية (t_i°, c_i°) للتقديرات بطريقة (MCD) يتم سحب عينة عشوائية (J) ذات حجم $(P+1)$ من العينة المكونة من (N) من المشاهدات و (p) من المتغيرات .

2- لكل عينة جزئية (J) يجري استخراج المفاتيح المقومة لها والممثلة لمتجه الاوساط $\mu_{(J)}$ ومصفوفة التباين $\Sigma_{(J)}$ المسماة t_j^*, c_j^* في (17)،(18) على التوالي .

3- بعد حساب مصفوفات التباين المشترك لكافة العينات الجزئية ذات الحجم (P+1) وبعد تحديد قيمة المحددة لكل مصفوفة ، يتم اختيار العينة الجزئية التي لها اصغر محدد لمصفوفة التباين المشترك أي $\min\left|\Sigma_{(J)}\right|$.

4 - بعد ان حدد في الخطوة (3) أعلاه أفضل مجموعة جزئية (التي تكون محددة مصفوفة التباين المشترك لها هي الأصغر) يتم استخراج المسافات التربيعية لكافة المشاهدات (N من المشاهدات) وفق $\mu_{(J)}$ و $\Sigma_{(J)}$ المختارة وفق (3).

5- نحسب قيمة $hp = \text{int}(N + P + 1)/2$ التي تمثل عدد المشاهدات الذي سوف يعتمد لحساب مقدرات (RFMCD*).

6- يتم اختيار hp من المشاهدات التي لها اصغر المسافات المستخرجة وفق الخطوة (4).

7- للمصفوفة الجديدة والتي تحتوي على hp من المشاهدات الناتجة من الخطوة (6) اعلاه يتم حساب متجه الأوساط الحسابية لها $\mu_{(hp)}$ ومصفوفة التباين $\Sigma_{(hp)}$.

8- يتم اختيار hp من المشاهدات التي تمتلك اصغر قيم للمسافات حيث يتم لهذه المجموعة الجديدة حساب مقدر الأوساط معاد الوزن (Reweighed Mean Estimate (μ_{RFMCD*})) ومصفوفة التباين المشترك معاد الوزن ((Reweighed Covariance Matrix ($\sum_{RFMCD*}$)).

9- أخيرا وفق ما قدر في الخطوة (8) أعلاه يتم استخراج المسافات الحصينة للمشاهدات كافة ، حيث يتم تشخيص تلك النقاط من خلال هذه المسافات الحصينة. وبعد ذلك نجد $\hat{\beta}_{RFMCD*}$ وكالاتي :

$$\hat{\beta}_{RFMCD^*} = \begin{bmatrix} \hat{\mu}_{1RFMCD^*} \\ \hat{\mu}_{2RFMCD^*} \\ \vdots \\ \hat{\mu}_{KRFMCD^*} \end{bmatrix} \qquad (19)$$

بعد ذلك يتم حساب احصاءة ولكس الحصينة بالاعتماد على هذه المقدرات ومن ثم يتم حساب الخطأ من النوع الأول وقوة الاختبار.

ونتيجة للتحوير الذي تم في هذا البحث فان الفرضية الخطية العامة تكون بالشكل

$$H_0 : C\hat{\beta}_{RFMCD*}D = 0 \qquad \textbf{vs} \qquad H_1 : C\hat{\beta}_{RFMCD*}D \neq 0 \qquad (20)$$

حيث ان $\hat{\beta}_{RFMCD*}$ مصفوفة من الدرجة (q×p) و D مصفوفة أحادية من الدرجة (p×p) وC مصفوفة التصميم من الدرجة (q-1×q) وان الفرضية (20) تختبر باستخدام احصاءة ولكس والتي تعتمد على الاحصاءتين $\underline{\mu}_{RFMCD*}$ و $\sum_{RFMCD*}$ اللتان تتوزعان توزيعا طبيعيا تقاربيا [7]وعليه فانه يمكن تطبيق احصاءة ولكس الحصينة الموزونة بدوال الأوزان بالشكل الأتي:

$$U_{RFMCD*} = \frac{\left|S_E\right|}{\left|S_E + S_{HRFMCD*}\right|} \overset{APP.}{\sim} (Wilks) \qquad (21)$$

حيث ان

$$S_E = D'Y'\{I_N - X(X'X)^{-1}X'\}YD, \qquad S_{HRFMCD*} = (C\hat{\beta}_{RFMCD*}D)'\{C(X'X)^{-1}C'\}^{-1}(C\hat{\beta}_{RFMCD*}D)$$

الجانب التجريبي

تم خلال بحثنا هذا صياغة نموذج المحاكاة المستخدم وفق طريقة مونت كارلو ليحاكي عددا كبيرا من الحالات التي يمكن وجودها في الواقع العملي , حيث تم افتراض اجراء تجارب باستخدام عدد من الحالات التي تكون بمساس مع واقع البيانات، تبعا لما يأتي :

1- حجم العينة ليشمل ذلك على عينات بالإحجام (n=20,30,40) وذلك لقياس تأثير تغير حجوم العينات على الترتيب النسبي للطرائق المدروسة، لاسيما مشكلة الحجوم الصغيرة.
2- تم افتراض أجراء تجارب تستخدم إعداد مختلفة من المتغيرات (p=2,3,4) وذلك لمعرفة سلوك الطرائق المدروسة في حالة تغير المتغيرات.
3- تم افتراض عدد من المجاميع (q=2,3) لمعرفة سلوك الطرائق المدروسة في حالة تغيير عدد المجاميع وتوسيعها .
4- درجة الارتباط بين المتغيرات وقد تضمنت الحالات آلاتية $\rho = 0.000001,0.5,0.9$
5- عددا من المستويات المختلفة لدرجة التجانس داخل البيانات المتعددة المتغيرات وكما هي موضحة في الجدول رقم (1)
6- تم عمل حصانة كلية للاحصاءة (MCD) بدلا من حصانة على كل مجموعة كما قمنا بالتغيير من قيمة العدد الثابت h الذي يمثل مجموعة اصغر قيم المسافات ($h = 0.9 * N$)
7- تم افتراض قيم ابتدائية لمتجهات متوسطات المجتمعات المتعددة المتغيرات وكذلك لمصفوفة التباين المشترك وكما هي موضحة في الجدول رقم (1).

جدول -1 : يبين التشكيلات المدروسة لمتجهات متوسطات المجتمعات المتعددة المتغيرات ودرجة التجانس لكل من المتغيرات المرتبطة

عدد المجاميع q	عدد المتغيرات p	متجه متوسط المجتمع الأول	متجه متوسط المجتمع الثاني	متجه متوسط المجتمع الثالث	درجة التجانس σ_i^2 $i=1,...,p$
2	2	(3 10)	(3 10)	--	1 1
	3	(3 10 4)	(3 10 4)	---	1 1 1
	4	(3 10 4 11)	(3 10 4 11)	----	1 1 1 1
3	2	(3 10)	(3 10)	(3 10)	1 1
	3	(3 10 4)	(3 10 4)	(3 10 4)	1 1 1
	4	(3 10 4 11)	(3 10 4 11)	(3 10 4 11)	1 1 1 1
2	2	3 10)	(3 10)	--	1 4
	3	3 10 4)	(3 10 4)	---	1 4 8
	4	3 10 4 11)	(3 10 4 11)	----	1 4 8 12
3	2	3 10)	(3 10)	(3 10)	1 4
	3	3 10 4)	(3 10 4)	(3 10 4)	1 4 8
	4	3 10 4 11)	(3 10 4 11)	(3 10 4 11)	1 4 8 12
2	2	(3 10)	(4 12)	--	1 1
	3	(3 10 4)	(4 12 5)	---	1 1 1
	4	(3 10 4 11)	(4 12 5 13)	----	1 1 1 1
3	2	(3 10)	(4 12)	(5 13)	1 1
	3	(3 10 4)	(4 12 5)	(5 13 6)	1 1 1
	4	(3 10 4 11)	(4 12 5 13)	(5 13 6 14)	1 1 1 1
2	2	(3 10)	(4 12)	--	1 4
	3	(3 10 4)	(4 12 5)	---	1 4 8
	4	(3 10 4 11)	(4 12 5 13)	----	1 4 8 12
3	2	(3 10)	(4 12)	(5 13)	1 4
	3	(3 10 4)	(4 12 5)	(5 13 6)	1 4 8
	4	(3 10 4 11)	(4 12 5 13)	(5 13 6 14)	1 4 8 12

تم تكرار تجربة المحاكاة لكل حالة من الحالات المدروسة (1000) تجربة كما تم تطبيق جميع التشكيلات التي اشرنا اليها في الجدول (1) ضمن التوزيعات الثلاثة الاتية :
1-التوزيع الطبيعي القياسي المتعدد المتغيرات .
2- التوزيع الطبيعي المتعدد الملوث من جهة واحدة.

3- التوزيع الطبيعي المتعدد الملوث من جهتين. وبنسب تلوث($\varepsilon = 0.20,0.40$) ولمستوى معنوية ($\alpha = 0.01,0.05$)والجدول رقم (2) يوضح الحالات التي جرت دراستها .

جدول -2 : تشكيلات الحالات التي افترضت في عملية المحاكاة

	$\varepsilon = 0.0$	$\varepsilon = 0.2$	$\varepsilon = 0.4$
P	N	N	N
2	20,30,40	20,30,40	20,30,40
3	20,30,40	20,30,40	20,30,40
	20,30,40	20,30,40	20,30,40

النتائج والمناقشة

1- الجدولين(3),(4) والتي هي جزء من مجموعة الجداول في (9) التي تعبر عن النتائج المستخلصة لكافة بيانات التوزيع الطبيعي المتعدد المتغيرات, نرى من خلالها ان معدلات الخطا من النوع الاول للاحصاءة الكلاسيكية كانت مقاومة تحت فرضية H_0 وعند مستوى معنوية تليها الاحصاءة الحصينة المحورة (RFMCD*) رغم تساويها في اغلب الاحيان مع الحالة الكلاسيكية بل اقترابها الى حد ما منها تليها بعد ذلك الاحصاءة الحصينة (**RMCD**).

2- ان معدلات الخطا من النوع الاول لاي طريقة من الطرائق المدروسة للتوزيع الطبيعي المتعدد المتغيرات وعند حالة معينة سوف تبقى ثابتة بعد تغير درجة التجانس داخل المتغيرات.

3- وجود علاقة طردية قوية بين كل من احتمالات الخطا من النوع الاول وقوة الاختبار للطريقة الكلاسيكية والطريقة المحورة للتوزيع الطبيعي المتعدد المتغيرات والتوزيعات الملوثة.

4- قوة الاختبار للتوزيع الطبيعي المتعدد المتغيرات تزداد طرديا مع زيادة عدد المجاميع أي ان قوة الاختبارللطرائق المدروسة عندما(q=3) اكبر من قوة الاختبار عندما(q=2) ولكل حجوم العينات وعند أي درجة تجانس.

5- قوة الاختبار لجميع الطرائق المدروسة تزداد طرديا بزيادة حجم العينة (n) وعند أي درجة تجانس ولكافة التوزيعات.

6- قوة الاختبار وعند درجة تجانس مختلفة تقل كثيرا عن قوة الاختبار عند درجة تجانس متساوية ولكافة التوزيعات.

7- سجلت الاحصاءة الحصينة المحورة (**RFMCD***) أفضل النتائج وخصوصا للتوزيع الطبيعي المتعدد الملوث من جهتين وعند نسبة تلوث ($\varepsilon = 0.2$).

8- قوة الاختبار للتوزيعات الملوثة للطريقة المحورة تتفوق على قوة الاختبار للطريقة الكلاسيكية ولجميع حجوم العينات وعند أي درجة تجانس وعند ($q = 2,3$) و ($p = 2,3,4$).

جدول- 3:احتمال الخطا من النوع الاول لكل طريقة موزع حسب درجة الارتباط (ρ) وحجم العينة(N) وعدد المتغيرات(p) وعدد المجاميع (q) للتوزيع الطبيعي المتعدد عند درجة تجانس متساوية

q = 2	α	0.01									0.05								
	N	20			30			40			20			30			40		
	Stat.	1×10^{-5}	.5	.9	1×10^{-5}	.5	.9	1×10^{-5}	.5	.9	1×10^{-5}	.5	.9	1×10^{-5}	.5	.9	1×10^{-5}	.5	.9
	Λ classic	.008	.008	.008	.01	.01	.01	.014	.014	.014	.041	.041	.041	.04	.04	.04	.051	.051	.051
	Λ MCD	.002	.002	.002	.007	.007	.007	.001*	.001*	.001*	.027*	.027*	.027*	.031*	.031*	.031*	.022*	.022*	.022*
	Λ RMCD	.007	.007	.007	.01	.01	.01	.014	.014	.014	.04	.04	.04	.036	.036	.036	.051	.051	.051
	Λ RFCD*	.009	.009	.009	.011	.011	.011	.016	.016	.016	.043	.043	.043	.043	.043	.043	.053	.053	.053
	Λ classic	.01	.01	.01	.006	.006	.006	.007	.007	.007	.042	.042	.042	.051	.051	.051	.051	.051	.051
	Λ MCD	.006	.006	.006	.005	.005	.005	.002	.002	.002	.035*	.035*	.035*	.03*	.03*	.03*	.023*	.023*	.023*
	Λ RMCD	.01	.01	.01	.006	.006	.006	.007	.007	.007	.039	.039	.039	.048	.048	.048	.05	.05	.05
	Λ RFCD*	.01	.01	.01	.008	.008	.008	.008	.008	.008	.044	.044	.044	.051	.051	.051	.052	.052	.052
	Λ classic	.015	.015	.015	.008	.008	.008	.01	.01	.01	.048	.048	.048	.047	.047	.047	.046	.046	.046
	Λ MCD	.007	.007	.007	.009	.009	.009	.005	.005	.005	.039	.039	.039	.037	.037	.037	.034*	.034*	.034*
	Λ RMCD	.014	.014	.014	.008	.008	.008	.01	.01	.01	.047	.047	.047	.045	.045	.045	.045	.045	.045
	Λ RFCD*	.015	.015	.015	.008	.008	.008	.01	.01	.01	.048	.048	.048	.047	.047	.047	.048	.048	.048

من النوع الاول لايقع في الفترة [.064,.036] عندما تكون (α=.05) ولايقع خلال الفترة [.018,.002] عندما تكون (α=.01)

جدول -4:احتمال الخطا من النوع الاول لكل طريقة موزع حسب درجة الارتباط (ρ) وحجم العينة(N) وعدد المتغيرات(p) وعدد المجاميع (q) للتوزيع الطبيعي المتعدد عند درجة تجانس متساوية

q=3	α	0.01									0.05								
	N	20			30			40			20			30			40		
p	Stat. ρ	1×10^{-5}	.5	.9	1×10^{-5}	.5	.9	1×10^{-5}	.5	.9	1×10^{-5}	.5	.9	1×10^{-5}	.5	.9	1×10^{-5}	.5	.9
2	Λ classic	.009	.009	.009	.015	.015	.015	.011	.011	.011	.043	.043	.043	.054	.054	.054	.054	.054	.054
	Λ MCD	.006	.006	.006	.004	.004	.004	.003	.003	.003	.026*	.026*	.026*	.029*	.029*	.029*	.024*	.024*	.024*
	Λ RMCD	.009	.009	.009	.014	.014	.014	.011	.011	.011	.04	.04	.04	.052	.052	.052	.054	.054	.054
	Λ RFCD*	.01	.01	.01	.015	.015	.015	.011	.011	.011	.045	.045	.045	.058	.058	.058	.059	.059	.059
3	Λ classic	.007	.007	.007	.01	.01	.01	.011	.011	.011	.046	.046	.046	.043	.043	.043	.05	.05	.05
	Λ MCD	.005	.005	.005	.005	.005	.005	.006	.006	.006	.025*	.025*	.025*	.031*	.031*	.031*	.034*	.034*	.034*
	Λ RMCD	.007	.007	.007	.01	.01	.01	.011	.011	.011	.044	.044	.044	.043	.043	.043	.05	.05	.05
	Λ RFCD*	.007	.007	.007	.01	.01	.01	.011	.011	.011	.046	.046	.046	.048	.048	.048	.056	.056	.056
4	Λ classic	.015	.015	.015	.009	.009	.009	.007	.007	.007	.057	.057	.057	.057	.057	.057	.055	.055	.055
	Λ MCD	.01	.01	.01	.004	.004	.004	.007	.007	.007	.041	.041	.041	.035*	.035*	.035*	.039	.039	.039
	Λ RMCD	.009	.009	.009	.009	.009	.009	.006	.006	.006	.055	.055	.055	.056	.056	.056	.05	.05	.05
	Λ RFCD*	.015	.015	.015	.009	.009	.009	.007	.007	.007	.058	.058	.058	.057	.057	.057	.059	.059	.059

* احتمال الخطا من النوع الاول لايقع في الفترة [.064,.036] عندما تكون (α=.05) ولايقع خلال الفترة [.018,.002] عندما تكون (α=.01)

المصادر

1. كاظم,اموري هادي , "طرق القياس الاقتصادي ", مطبعة التعليم العالي ,بغداد,(1988).
2. Morrison, D.F., "Multivariate Statistical Methods", Printed and Bound by & Jo Enterprise PTELTD, sing a pore,(1988) .
3. 3-Wilks,S.S.,"Certain Generalizations in The Analysis of Variance", Biometrika, 24: 471-494 (1932) .
4. Scheffe, H.,"The Analysis of Variance"John Wiley & Sons,New York (1959).
5. الدباغ، ظافر عاصم، " تحليل تباين حصين للنماذج الخطية " ، اطروحة دكتوراه في الاحصاء، كلية الادارة والاقتصاد، جامعة بغداد، (1999).
6. سرار، محمد علي ، " دراسة نموذج التباين العمومي التام متعدد المتغيراتGMANOVA مع تطبيق عملي" ، رسالة ماجستير في الاحصاء، كلية الادارة والاقتصاد، جامعة بغداد، (2000).
7. Rousseeuw, P.J.,Stefan Van Aelst and Katrien Van Driessen,"Robust Multivariate Regression", (2000).
8. http://citeseer.ist.psu.edu/cache/papers/cs/rousseeuw00robust.pdf .
9. Yuun Zuo, Hengjian Cui & Dennis Young, "In Fluence Function and Maximum Bias of Projection Depth Based Estimators "32(1):189-218 (2004).
10. العزاوي, سداد خليل , "مقارنة بعض الاختبارات الحصينة لتحليل التباين المتعدد المتغيرات MANOVA في مجال تصميم التجارب", اطروحة دكتوراه فلسفة في الرياضيات, كلية العلوم, الجامعة المستنصرية, (2006).

مجلة علوم المستنصرية
المجلد 21، العدد 5، 2010

نمذجة انتشار الملوثات

حنين حاكم عبدالرضا عباس
الجامعة المستنصرية- كلية العلوم- قسم علوم الجو

ABSTRACT

This paper was deal with the study and analysis the effect of some effective meteorological elements on pollutants concentration by using Gaussian diffusion theory, matlab program was used to make the relevant computation.

In this paper were showed the relationship between the pollutants concentration and selected surface wind velocity after matched it with atmospheric stability type according to Pasqual classification, as well study the effect of the effective height of pollution source(in the paper select a stack as pollution source) at pollutants concentration in addition to the effect of the source's site on pollutants concentration value.

The results showed that the received pollutants concentration at 1000m horizontal distance were inversely proportion with wind velocity in instability condition wherein the convection current and eddies act to be lessen the pollutants concentration near the surrounding areas from pollution source especially at daytime.

As to the changing of effective height of pollution source it found that when the source's height was increasing lead to decreasing the received pollutants concentration at horizontal distance from the source, and it showed the pollutants concentration gradual decreasing with going far towards (y) that is from the central line of pollutants diffusing , while in the direct (z) it's not necessary the increasing in height from central line giving the same intensity of decreasing pollutants concentration especially at instability condition as to the higher pollutants concentration was at 50m height at stability condition that is in the effective height of pollution source.

الخلاصة

تناول هذا البحث دراسة وتحليل تأثير العوامل الأ نوائية المؤثره على قيم تراكيز الملوثات باستخدام نظرية الأنتشار لكاوس حيث استخدم برنامج حاسوب الـ (MATLAB) للأيفاء بالحسابات المطلوبة.

تم توضيح العلاقة بين تراكيز الملوثات وسرع منتخبة للرياح السطحية بعد تولفيها مع نوع الاستقرارية الجوية باستخدام جدول باسكويل, كذلك تم دراسة تاثير الارتفاع المؤثر لمصدر التلوث (تم في البحث اختيار المدخنة كمصدر للتلوث) على تراكيز الملوثات بالاضافة الى تاثير موقع مصدر التلوث على قيم تراكيز الملوثات.

بينت النتائج ان تراكيز الملوثات المستلمة على مسافة افقية مقدارها 1000m تتناسب عكسيا مع سرعة الرياح في الظروف الجوية الغير مستقرة حيث تعمل تيارات الحمل والدوامات الهوائية على تقليل تراكيز الملوثات على المناطق القريبة من مصدر التلوث وخاصة خلال النهار.

اما تغير الارتفاع المؤثر لمصدر التلوث فوجد انه كلما ازداد ارتفاع المصدر تقل تراكيز الملوثات المستلمة على مسافة افقية من المصدر, كذلك توضح ان قيم التراكيز السطحية تتناقص تدريجيا مع الابتعاد باتجاه (y) اي عن الخط المركزي لانتشار الملوثات بينما في الاتجاه(z) قد لاتعطي الزيادة في الارتفاع عن الخط المركزي نفس الشدة في تناقص تراكيز الملوثات خاصة في الظروف الجوية الغير مستقرة اما الظروف الجوية المستقرة فكانت اعلى قيمة لتركيز الملوثات هو عند ارتفاع 50m اي عند الارتفاع المؤثر لمصدر التلوث.

المقدمة

يعد التلوث من اهم المواضيع التي بدأت تأخذ حيزا متزايدا من الأهتمام نظرا لما له من تأثيرات مباشرة على صحة الانسان وبيئته، إذ له علاقة وثيقة بتلوث المياه والأتربة وهي كلها مترابطة بشكل واضح عبر العمليات الحيوية للكائنات الحية والسلسلة الغذائية من ناحية وكذلك بواسطة تأثيراتها المتبادلة على الطقس والمناخ لاسيما في المناطق المعرضة للتلوث بشكل حاد ومستمر.

وتنقسم مصادر التلوث الى قسمين الاول المصادر الطبيعية مثل الغازات والأتربة الناتجة من ثورات البراكين ومن حرائق الغابات والاتربة الناتجة من العواصف وهذه المصادر عادة ماتكون محدودة في مناطق معينة تحكمها العوامل الجغرافية والجيولوجيا ويعد التلوث من هذه المصادر متقطعا او موسميا، اما المصدر الثاني

فهو نتيجة انشطة الأنسان على سطح الأرض فاستخدام الوقود في الصناعة ووسائل النقل وتوليد الكهرباء يؤدي الى انبعاث غازات مختلفة وجسيمات دقيقة الى الهواء وهذا النوع من التلوث مستمر باستمرار أنشطة الأنسان ومنتشر بأنتشارها على سطح الارض في التجمعات السكانية وهذا التلوث هو الذي يثير الأهتمام والقلق، والحقيقة انه يمكن النظر الى قدرة الغلاف الجوي في اي مكان على استيعاب التلوث البيئي باعتباره نظام مفتوح يسمح للتلوث بالدخول اليه لكنه يقوم بنشره في جميع الأتجاهات ثم يتخلص منه بعد ذلك وإذا حدث اي عائق يحد من قدرة الغلاف الجوي على نشر التلوث هذا يجعله يتركز في البيئة المحلية الضيقة بمصادر التلوث مباشرة ويلحق اضرارا فادحة بالأرواح والممتلكات.

بعض المفاهيم الأنوائية المتعلقة بالتلوث

الانقلاب الحراري:

من المعلوم انه في طبقة التروبوسفير تقل درجة الحرارة مع الارتفاع غير انه أحيانا يحدث العكس، حيث تزداد درجة الحرارة مع الارتفاع لاسباب مختلفة، اما بسبب التبريد الاشعاعي او التبريد التبخيري او بسبب الحركة الافقية للهواء وغير ذلك من الاسباب وتسمى هذه الحالة بالانقلاب الحراري (1) وتقترن حالة الانقلاب الحراري بوجود استقرارية في الجو، وذلك لان بوجود الانقلاب الحراري لايستطيع الهواء البارد الثقيل ان يرتفع الى اعلى، لذا فان مع انتهاء الانقلاب الحراري سيكون الجو اكثر ملائما لانتشار الملوثات بعيدا عن السطح. (2)

الاستقرارية وعدم الأستقرارية:

انتشار الملوثات عادة ماتكون في ثلاث إتجاهات (x ,y, z) وفي حالات الانقلاب الحراري فأن الحركة تكاد تكون مقتصرة على المستوى (x ,y) اي تكون افقية فيما تضمحل الحركة في الاتجاه العمودي (z) ويدعى الجو في هذه الحاله بالجوالمستقر، اما في حالة كون مقدار الانحدار الحراري اكبر من الانحدار الحراري الاديباتيكي تكون الحركة العمودية نشطة ويدعى الجو هنا بالجو غير المستقر (1) ، لذلك فان الحركة العمودية للملوثات في الطبقة المتاخمة تتأثر بصورة كبيرة بعوامل الأستقرارية والأنحدار الحراري لدرجة الحرارة Laps rate حيث ان تيارات الحمل مهمة في نشر المواد الى مساحة اكبر، لذلك أفضل الظروف لأنتشار الملوثات يحدث عند وجود عدم استقرارية جوية في الطبقة المتاخمة (3) .

الأنتقال والتشتت:

حركة الهواء الأفقية تعمل على نقل الملوثات من مصادرها، اما الحركة العمودية فتعمل على تشتيت (diffusion) الملوثات، ويمكن توضيح ذلك بحالتين: حالة انقلاب حراري قوي ورياح هادئة فيكون الأنتشار العمودي للملوثات عندها

مهملا فيما تنتقل الملوثات افقيا بفعل الرياح، اما الحالة الاخرى هي حالة التسخين الشمسي القوي مع رياح افقية خفيفة عندها تنشط الحركة العمودية للهواء وتسبب أنتشار الملوث (3) . من أهم العومل الجوية التي تؤثر على الأستقرارية الجوية هي سرعة الرياح السطحية وكمية الفيض الحراري (heat flux)، ولقد اقترح باسكويل طريقة لتصنيف الأستقرارية الجوية لأجل حساب تشتت الملوثات حيث اعتمد في تصنيفه على السطوع الشمسي معتمدا على زاوية ارتفاع الشمس وكذلك على سرع الرياح السطحية كما موضح في الجدول التالي:

جدول -1: يوضح أنواع الأستقرارية حسب تصنيف باسكويل(4)

Surface wind speed (at 10m) m/sec	Day			Night	3/8 ≤ cloud
	Incoming solar radiation			Thinly overcast or >4/8 low cloud	
	strong	Moderate	slight		
<2	A	A-B	B	-	-
2-3	A-B	B	C	E	F
3-5	B	B-C	C	D	E
5-6	C	C-D	D	D	D
>6	C	D	D	D	D

نظرية الانتشار لكاوس

هي معادلة رياضية تستخدم لحساب تركيز الملوثات المنبعثة من مصدر منفرد مثل مدخنة وتعتبر دالة للتركيز الكلي للملوثات باتجاه (x ,y, z) وتأخذ الصيغة التالية(2) :

$$C(x,y,z,H) = \frac{Q}{2\pi\sigma y\sigma zU} \exp\left[-\frac{1}{2}\left(\frac{y}{\sigma y}\right)^2\right]\left[\exp\left(-\frac{1}{2}\left(\frac{z-H}{\sigma z}\right)^2\right) + \exp\left(-\frac{1}{2}\left(\frac{z+H}{\sigma z}\right)^2\right)\right] \quad \text{---- (1)}$$

حيث ان:

C : تركيز الملوثات بـ (ppm of kg).

Q :معدل تدفق الملوثات الخارجة من المصدر بـ (kg/sec) .

U : سرعة الرياح عند الارتفاع المؤثر للمدخنة بـ (m/sec).

H : الأرتفاع المؤثر للمدخنة (effective height) بـ(m) ويعطى بالعلاقة التالية:

$$H = h + \Delta h \quad \text{------- (2)}$$

حيث ان:

h: ارتفاع المدخنة .

Δh: ارتفاع ريش المدخنة .

x : المسافة الافقية باتجاه مهب الريح بـ (m) .

y :المسافة عن الخط المركزي لانتشار الملوث بـ (m) .

z :المسافة العمودية فوق سطح الارض بـ (m) .

$\sigma y, \sigma z$: معاملي التشتت باتجاه (z ,y) بالامتار وتتغير حسب نوع الاستقرارية وتحسب من المعادلات الموضحة في الجدول التالي:

جدول -2: يبين معادلات حساب σy, σz كدوال لكل من x وصنف الاستقرارية حسب تصنيف باسكويل(6)

CLASS	σy	σ z
A	$0.22x(1+10^{-4})^{-0.5}$	0.2x
B	$0.16x(1+10^{-4})^{-0.5}$	0.12x
C	$0.11x(1+10^{-4})^{-0.5}$	$0.08(1+0.0002x)^{-0.5}$
D	$0.08x(1+10^{-4})^{-0.5}$	$0.06x(1+0.0015x)^{-1}$
E	$0.06x(1+10^{-4})^{-0.5}$	$0.03(1+0.0003x)^{-1}$
F	$0.04x(1+10^{-4})^{-0.5}$	$0.016(1+0.0003x)^{-1}$

النتائج والمناقشة

في هذا البحث تم عمل موديل رياضي لمعادلة كاوس باستخدام برنامج الـ (MATLAB) حيث يقوم البرنامج بحساب تركيز الملوثات وذلك بأدخال قيم للمتغيرات الأنوائية الموجودة في معادلة (1) ، وفي البحث تم دراسة اربع حالات لحساب تركيز الملوثات, ولحساب سرع الرياح عند الارتفاع المؤثر للمدخنة تم تطبيق معادلة سرعة الرياح الاسية(7) وكما يلي:

$$u_2 = u(z_1)\left(\frac{z^2}{z_1}\right)^p$$

حيث ان :

$u(z)$: سرعة الرياح عند مستوى z . $u(z_1)$: سرعة الرياح عند الارتفاع z_1 .
p : معامل القوى ويعتمد على الخشونة السطحية ، الاستقرارية الجوية والارتفاع .
وتتراح قيم p حسب نوع الاستقرارية من 0.06 في حالة عدم الاستقرارية العالية الى 0.33 عندما يكون الجو مستقرا بشكل كبير (7) .

دراسة تاثير سرعة الرياح على قيمة تراكيز الملوثات:
لدراسة تأثير سرعة الرياح تم تثبيت قيمة كل من Q معدل تدفق الملوثات ,الارتفاع المؤثر والموقع حيث اعتبرت القيم : (Q=15kg/sec ,H=50 m ,x=1000m ,y=0m , z=0m) ، تم أختيار قيمة z=0 لان التراكيز السطحية هي هي غالبا محط الأهتمام ، اما y=0 لأن هذه القيمة تمثل الخط المركزي لأنتشار الملوث.
وتم اختيار سلسلة من سرع الرياح السطحية تتراوح من 1- 7 m/sec في ظروف تسخين مختلفة اخذت هذه القيم لسرع الرياح السطحية وذلك من خلال بيانات الراديوسوند لسطح مدينة بغداد والتي لاتتجاوز 7m/sec نهارا و 3m/sec ليلا (8), و اخذت جميع حالات التسخين الموجودة في جدول باسكويل, حيث يلحظ في الشكل (1) وجود تذبذب في قيم التراكيز ولكن مع زيادة سرعة الرياح السطحية حيث تقل تراكيز الملوثات المستلمة على مسافة 1000m بينما تزداد تراكيز الملوثات لاي سرعة سطحية كلما قل السطوع الشمسي واصبح الجو اكثر استقرارا.
التأثير المشترك لسرعة الرياح والأرتفاع المؤثر:
لدراسة علاقة التراكيز السطحية للملوثات مع سرعة الرياح لقيم مختلفة من الارتفاع المؤثر وفي حالات مختلفة من معدلات التسخين حيث تم تثبيت كل من قيم التدفق Q واحداثيات الموقع التالي: (Q=15 kg/sec x=1000m, y=0m ,z=0m) ، بينما أخذت كافة حالات التسخين الموجودة في جدول باسكويل وأخذت اربع قيم مختلفة للارتفاع المؤثر وهي: (50m ,100m, 150m, 200m) ، وكانت النتائج كما موضحة في الاشكال (2) و(3) و(4) ، يتضح من هذه الاشكال وبشكل عام ان زيادة الارتفاع المؤثر تؤدي الى تناقص في قيم التراكيز السطحية الا ان هذا التناقص يتباين تبعا لقوة التسخين الشمسي اذ يزداد كلما قل معدل التسخين الشمسي, من ناحية اخرى ان زيادة سرع الرياح تؤدي غالبا الى تناقص التراكيز ويكون هذا التناقص اوضح مايكون في السرع الاكبر من 5 m/sec.

تأثير الارتفاع المؤثر :

لدراسة تغيرات قيم التراكيز السطحية مع زيادة الارتفاع المؤثر في حالات استقرارية مختلفة ، تم توليف قيم سرع الرياح وحالات التسخين لتعطي فئات استقرارية مختلفة مماثلة لفئات باسكويل واخذت سلسلة لقيم الارتفاع المؤثر من 50m الى 200m فيما ثبتت قيمة التدفق Q والموقع كالتالي: (Q=15kg/sec x=1000m , y=0m, z=0m), والنتائج المستحصلة من الحسابات تم عرضها في الشكل (5) ، حيث يبين تاثير الارتفاع المؤثر للمدخنة على تركيز الملوثاتلحالات الاستقرارية الجوية .

بما ان الزيادة في الارتفاع المؤثر تؤدي الى تناقص في قيم التراكيز السطحية الا ان هذه الزيادة تتباين تبعا لحالة الاستقرارية ، ففي الشكل (5) اصناف A ,B ,C ويتضح ان الزيادة في الارتفاع المؤثر للمدخنة لها تاثير اقل في تقليل كمية الملوثات السطحية للمنطقة مقارنتا بتاثير الاستقرارية الجوية ، وهذا اوضح مايكون في الفئة A المقترنة بعدم استقرارية عالية حيث تتناقص قيم التراكيز ببطأ مع ازدياد الارتفاع المؤثر للمصدر, اما عند حالات عدم الاستقرارية المتوسطة B والخفيفة C فان التناقص في قيم التراكيز يكون واضح مع ازدياد ارتفاع المصدر.

يعزى السبب في ذلك هو ان الدوامات الهوائية النشطة الناشئة عن التسخين الشمسي والتي تؤدي الى تعميق طبقة الخلط بحيث يغطي عمقها الارتفاع المؤثر للمدخنة .

تأثير الموقع:

لدراسةتاثير الموقع على قيم التراكيز تم تثبيت قيم x اذ ان من المعلوم انه كلما زاد الابتعاد في الاتجاه x كلما قلت قيم التراكيز، وتم تغير كل من y , z لحالات استقرارية مختلفة تم توليفها مع قيم سرع رياح وحالات تسخين لتعطي الفئة المطلوبة في جدول باسكويل، فيما وضعت قيم التدفق Q والمسافة الافقية x كالتالي: Q=15 kg/sec , x=1000m.

الرسومات البيانية في الشكلين (6) و (7) تعطي تصورا لحجم المنطقة التي ينتشر فيها الملوث وتوزيعه فيها . أكبر حجم لهذه المنطقة يظهر في الظروف الجوية الغير مستقرة اي عند الصنف A,B,C حيث تتناقص قيم التراكيز السطحية تدريجيا مع الابتعاد في الاتجاه y عن الخط المركزي لانتشار الملوث، بينما في الاتجاه z لاتعطي الزيادة في الارتفاع فوق الخط المركزي لانتشار الملوث (y=0) نفس الشدة في التناقص وهذا ما يوضحه الشكل (6)، وهذا يعني حجما كبيرا جدا تشغلة الملوثات المتشتته.

من ناحية اخرى ان الفئات ذات الاستقرار ية العالية كالفئات F, E تحصر الملوثات في حزام ضيق تتركز فية كمية الملوثات المنبعثة ضمن طبقة الارتفاع المؤثر.

ان الظروف غير المستقرة تفضل عن الظروف المستقرة بسبب الحركات الاضطرابية التي تساهم بشكل اكبر في تشتيت الملوثات وتلاشيها.

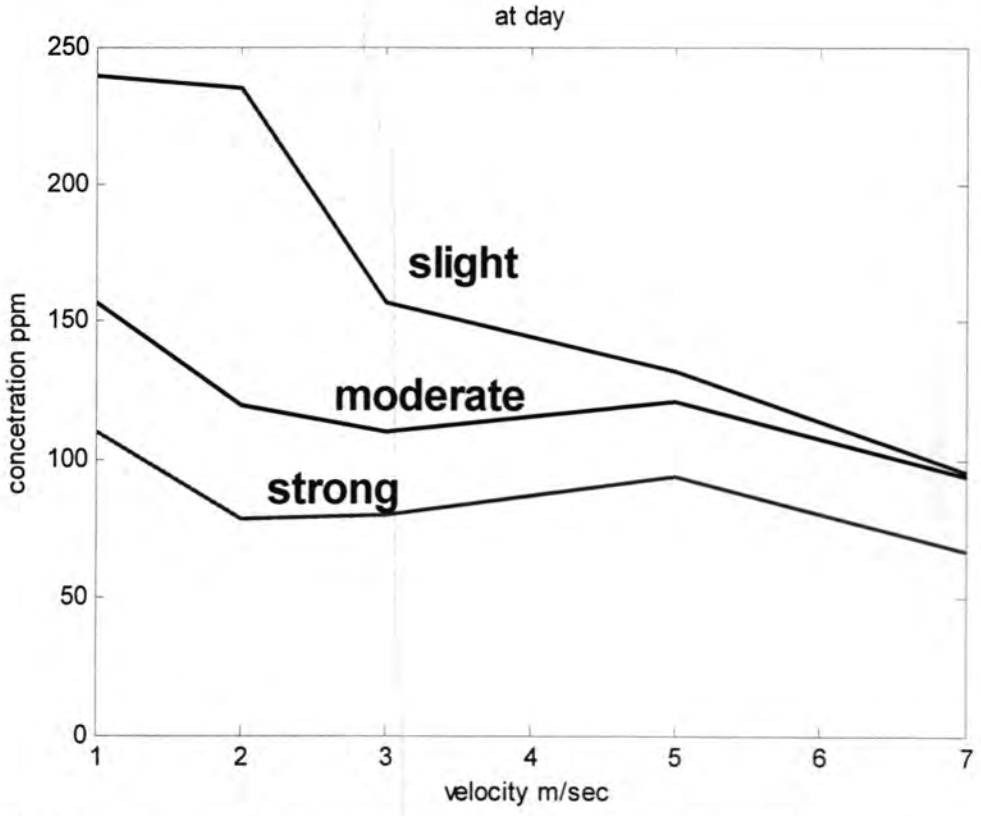

شكل -1: يوضح علاقة سرعة الرياح السطحية مع قيم تراكيز الملوثات في ظروف تسخين مختلفة خلال النهار

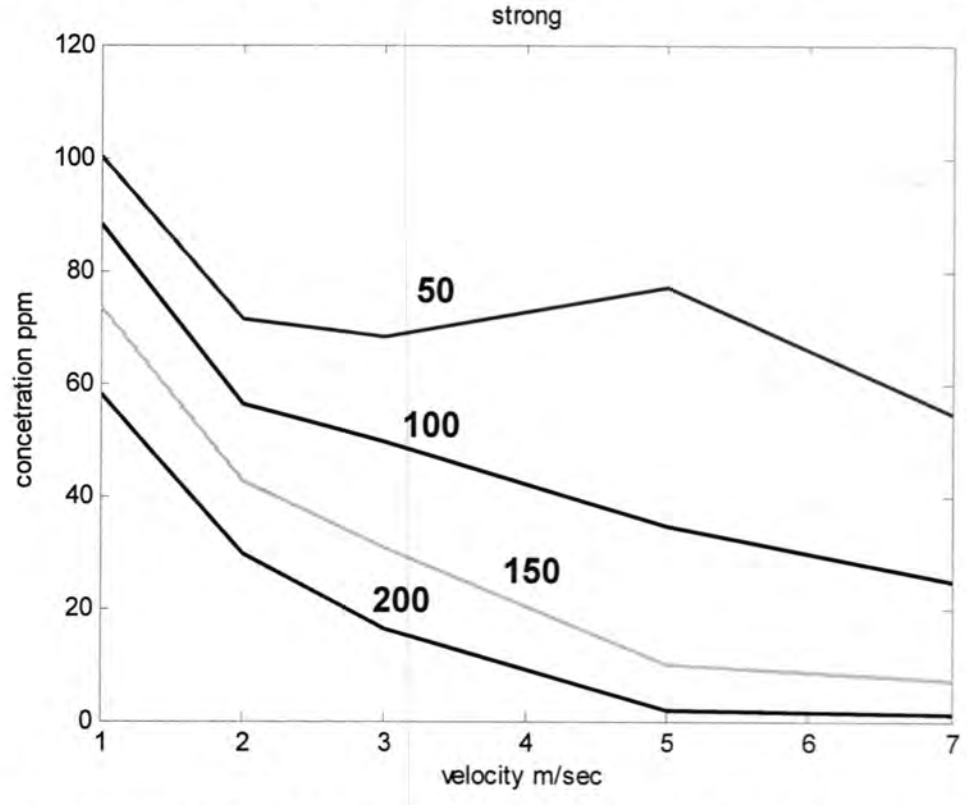

شكل -2: يوضح التاثير المشترك لسرعة الرياح والارتفاع المؤثر في ظروف تسخين عالية والحالات الاربع تمثل ارتفاع المدخنة بالامتار

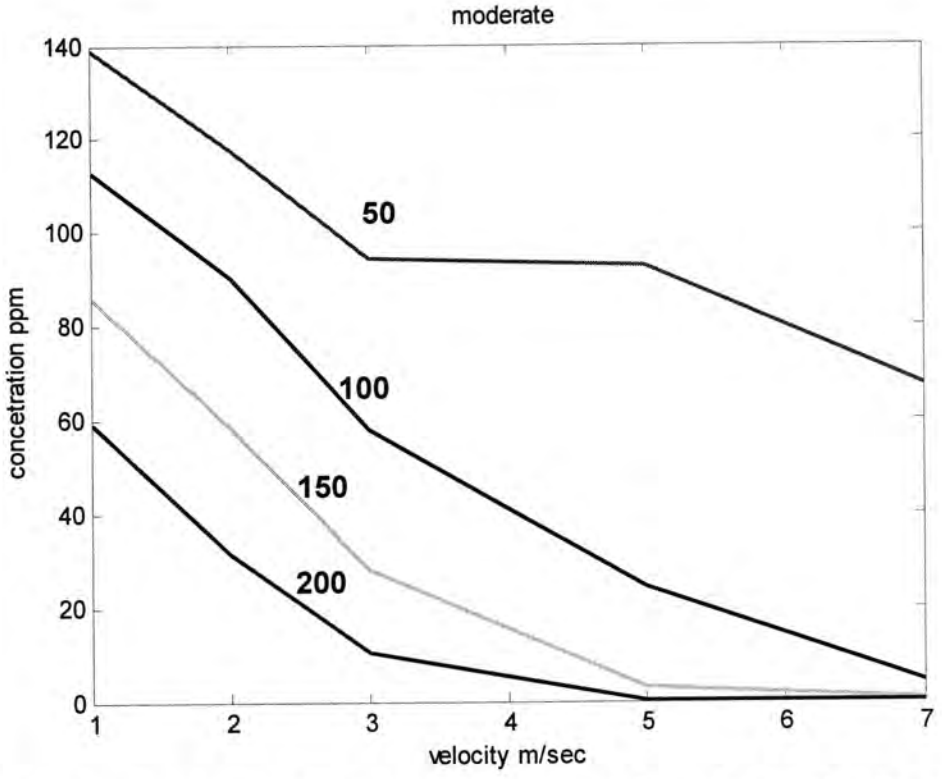

شكل-3: يوضح التاثير المشترك لسرعة الرياح السطحية والارتفاع المؤثر في ظروف تسخين متوسطة والحالات الاربع تمثل ارتفاع المدخنة بالامتار

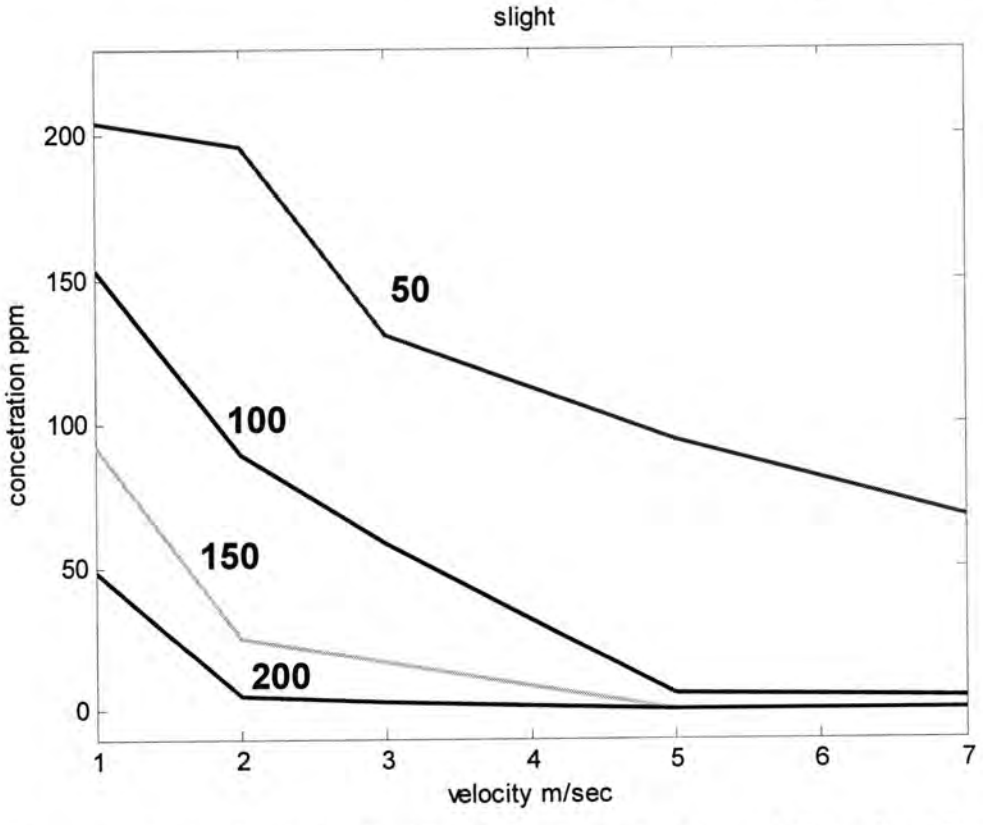

شكل-4: يوضح التاير المشترك لسرعة الرياح السطحية والارتفاع المؤثر في ظروف تسخين خفيفة والحالات الاربع تمثل ارتفاع المدخنة بالامتار

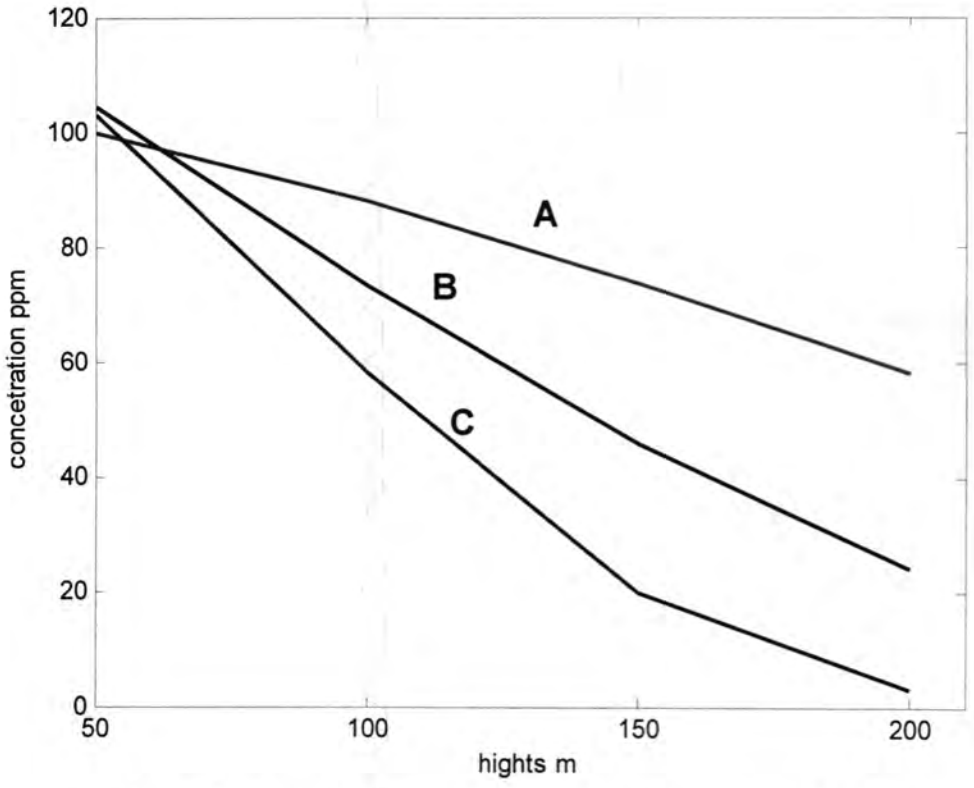

شكل -5: يبين علاقة الارتفاع المؤثر مع فئات الاستقرار ية الجوية

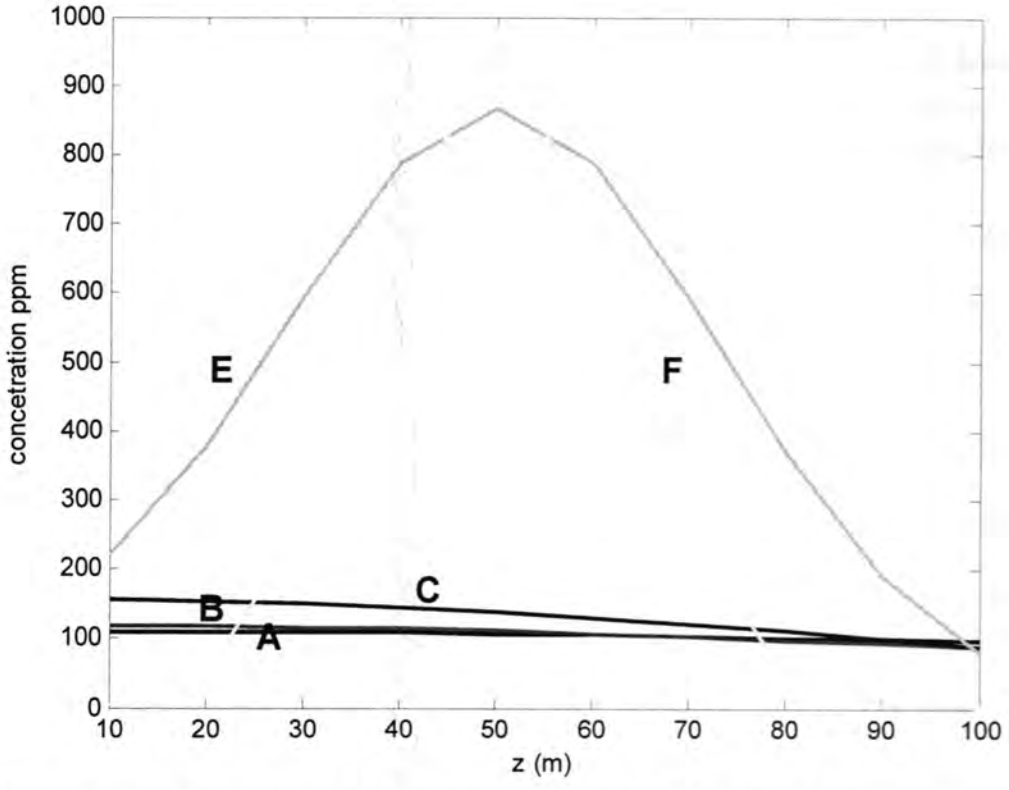

شكل-6 : يبين علاقة تراكيز الملوثات بالاتجاه العمودي z وتوليفها مع حالات الاستقرارية

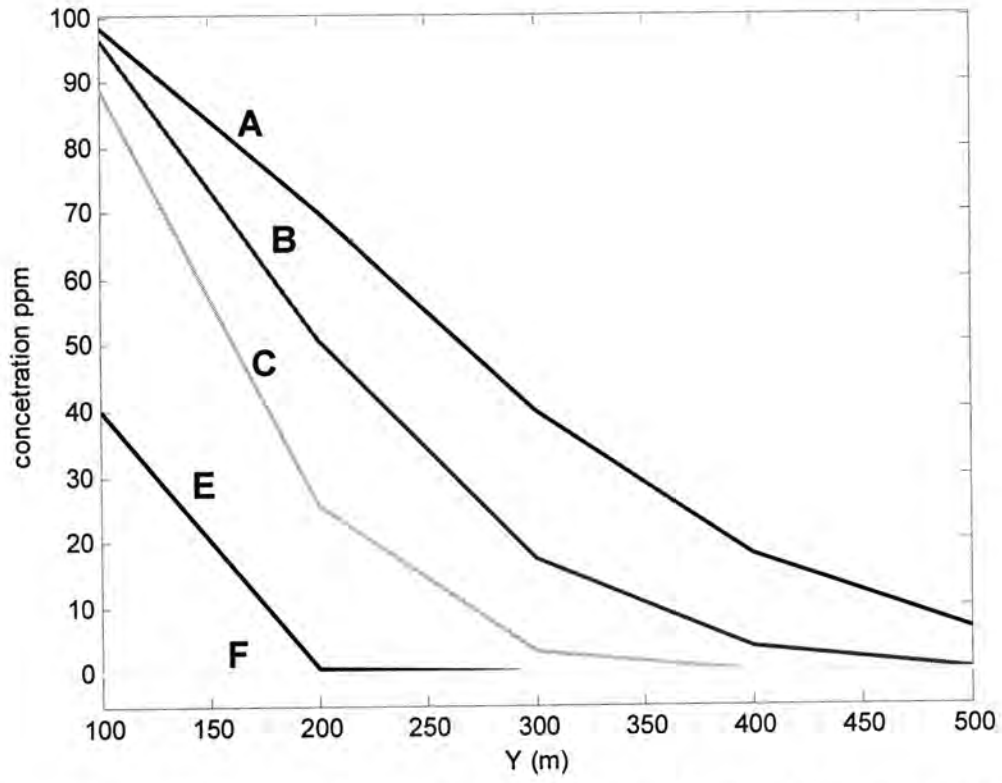

شكل-7 : يبين علاقة تراكيز الملوثات بالاتجاه الافقي y وتوليفها مع حالات الاستقرا رية

ان من اهم العوامل الانوائية التي تؤثر على انتشار الملوثات هي التسخين الشمسي، لذا فان الاوقات المفضلة لتشغيل المصانع او المنشات ذات التلويث المستمر يستحسن ان تبدا من بداية اشتداد التسخين الشمسي حتى بعد غروب الشمس اي مع بداية تكون الانقلاب الحراري وتتوقف بعد ان يصبح الانقلاب الحراري يشمل الطبقة السطحية ويصبح الجو في حالة استقرارية تامة ليلا.
كلما زاد الارتفاع المؤثر لمدخنة المصنع او المنشاة كلما قلت التراكيز السطحية للملوثات خصوصا في الاجواء المستقرة.
تلعب الرياح دورا مزدوجا في حالات التلوث الجوي اذ تعمل على نقل الملوثات وفي نفس الوقت تعمل على تشتيتها بفعل الدوامات الهوائية (eddies) التي تولدها لاسيما عند السرع العالية بالاشتراك مع الدوامات التي يولدها التسخين الشمسي.
ان احسن الظروف لتشتت الملوثات هي حالات التسخين الشمسي القوي المقترن بسرع رياح عالية ، فيما تكون اسوأ الظروف هي تلك الليلية الخالية من الغيوم المقترنة بسرع رياح اقل من 2 m/sec .

المصادر

1. التمييمي، باسم ابراهيم وهاب، انموذج لتقدير ملوثات الهواء في مدينة بغداد، رسالة دكتوراه منشورة، الجامعة المستنصرية، كلية العلوم، قسم الفيزياء : 17-18 ،(2006).
2. شحاذة، نعمان، الجغرافية المناخية، الجامعة الاردنية، قسم الجغرافية، دار المسقبل للنشر والتوزيع:112(1992).
3. Oke,T.R.,Bundary layer clamite,methue and coltd press,London,:274-279 (1978).
4. التميمي، سحر حسين جاسم، حساب وتشخيص سرعة الرياح الافقية مع الارتفاع فوق مدينة بغداد، رسالة ماجستير منشورة، الجامعة المستنصرية، كلية العلوم، قسم علوم الجو : 19(2008).
5. Perkins, H.C., Air pollution, Aerospace and mechanical engineering department, University of Arizona, international student edition, (1984).
6. Blackadar, Alfred, Estimation smokestack pollution concentrations, Jun:40-43, USA (1991).
7. ZHANG, S.F., A statistical analysis of the power law and the logarithmic law using wind data from a 164m lower, research ,department of meteorology ,university of Nanjing, china,(1980).